
Advances in **ORGANOMETALLIC CHEMISTRY**

VOLUME **57**

Editors

ANTHONY F. HILL
*Research School of Chemistry
Institute of Advanced Studies
Australian National University
Canberra, Act
Australia*

MARK J. FINK
*Department of Chemistry
Tulane University
New Orleans, Louisiana, USA*

Founding Editors

F. GORDON A. STONE
ROBERT WEST



Amsterdam • Boston • Heidelberg • London
New York • Oxford • Paris • San Diego
San Francisco • Singapore • Sydney • Tokyo
Academic Press is an imprint of Elsevier



Academic Press is an imprint of Elsevier
Linacre House, Jordan Hill, Oxford OX2 8DP, UK
32 Jamestown Road, London NW1 7BY, UK
Radarweg 29, PO Box 211, 1000 AE Amsterdam, The Netherlands
30 Corporate Drive, Suite 400, Burlington, MA 01803, USA
525 B Street, Suite 1900, San Diego, CA 92101-4495, USA

First edition 2008

Copyright © 2008 Elsevier Inc. All rights reserved

No part of this publication may be reproduced, stored in a retrieval system or transmitted in any form or by any means electronic, mechanical, photocopying, recording or otherwise without the prior written permission of the publisher

Permissions may be sought directly from Elsevier's Science & Technology Rights Department in Oxford, UK: phone (+44) (0) 1865 843830; fax (+44) (0) 1865 853333; email: permissions@elsevier.com. Alternatively you can submit your request online by visiting the Elsevier web site at <http://www.elsevier.com/locate/permissions>, and selecting *Obtaining permission to use Elsevier material*

Notice

No responsibility is assumed by the publisher for any injury and/or damage to persons or property as a matter of products liability, negligence or otherwise, or from any use or operation of any methods, products, instructions or ideas contained in the material herein. Because of rapid advances in the medical sciences, in particular, independent verification of diagnoses and drug dosages should be made

ISBN: 978-0-12-374465-4
ISSN: 0065-3055

For information on all Academic Press publications
visit our website at books.elsevier.com

Printed and bound in USA

08 09 10 11 12 10 9 8 7 6 5 4 3 2 1

Working together to grow
libraries in developing countries

www.elsevier.com | www.bookaid.org | www.sabre.org

ELSEVIER

BOOK AID
International

Sabre Foundation

CONTRIBUTORS

Numbers in parenthesis indicate the pages on which the authors' contributions begins.

Chrysostomos Chatgililoglu (117)

ISOF, Consiglio Nazionale delle Ricerche, 40129 Bologna, Italy

Frank T. Edelmann (183)

Chemisches Institut der Otto-von-Guericke-Universität Magdeburg,
Universitätsplatz 2, D-39106 Magdeburg, Germany

Tiziana Fiore (353)

Dipartimento di Chimica Inorganica e Analitica "Stanislao Cannizzaro",
Università di Palermo, Viale delle Scienze, Parco d'Orleans, 90128 Palermo, Italy

Paul D. Lickiss (1)

Chemistry Department, Imperial College, London SW7 2AZ, UK

László Nagy (353)

Department of Inorganic and Analytical Chemistry, University of Szeged, H-6701
Szeged, Hungary

Enikő Nagy (353)

Biological Research Center of Hungarian Academy of Sciences, Szeged, Hungary

Lorenzo Pellerito (353)

Dipartimento di Chimica Inorganica e Analitica "Stanislao Cannizzaro",
Università di Palermo, Viale delle Scienze, Parco d'Orleans, 90128 Palermo, Italy

Claudia Pellerito (353)

Dipartimento di Chimica Inorganica e Analitica "Stanislao Cannizzaro",
Università di Palermo, Viale delle Scienze, Parco d'Orleans, 90128 Palermo, Italy

Franck Rataboul (1)

Chemistry Department, Imperial College, London SW7 2AZ, UK

Michelangelo Scopelliti (353)

Dipartimento di Chimica Inorganica e Analitica “Stanislao Cannizzaro”,
Università di Palermo, Viale delle Scienze, Parco d’Orleans, 90128 Palermo, Italy

Attila Szorcsik (353)

Bioinorganic Research Group of Hungarian Academy of Sciences, Department of
Inorganic and Analytical Chemistry, University of Szeged, Szeged, Hungary

Vitaliy I. Timokhin (117)

Department of Chemistry and Biochemistry, Florida State University, Tallahassee,
FL 32306-4390, USA

PREFACE

Volume 57 of *Advances in Organometallic Chemistry* sees Robert West assume the status of Founding Editor, some 44 years after he joined F. Gordon A. Stone in inaugurating what quickly became and remains the pre-eminent review series in organometallic chemistry. At that time organometallic chemistry was an emerging field, where rules were broken as quickly as they were formulated. Perhaps a series combining both main group and transition organometallic chemistry might have then appeared incongruous — certainly transition metal alkyls and main group alkyls seemed, were even deemed, to have little in common. Time has proven that the stewardship of this series was safe in the hands of two world leaders from distinct organometallic realms; Robert in main group chemistry, Gordon in transition metal chemistry.

Despite the ever broadening of our field in all manner of previously unimagined directions, the confluence of main group and transition metal organometallic chemistries has been as remarkable as its diversity. Not only has main group organometallic chemistry played a functional role in the design of ligands for use in transition metal chemistry, parallels have emerged in terms of bonding and reactivity. Both fields have gravitated to the concept of “unsaturation,” be it in the form of low-coordinate species, or species which feature element–element multiple bonding. In these respects, within main group chemistry Robert has been a pioneer. His strategies employed to isolate the first divalent silicon compounds and the first compound with a Si=Si bond presaged an entire subdiscipline. This approach has, in the interim, afforded access to many kinetically or thermodynamically stabilized low-coordinate derivatives of the heavier main group elements. Robert has also been a champion of the principle of fundamental chemistry first, with a longer-term view to applications.

Recently, Mark J. Fink joined us as Editor. His perspective on main group chemistry and the interface with transition metal chemistry and applications ideally places him to maintain the synergy between main group and transition metal organometallic chemistry that *Advances in Organometallic Chemistry* has endeavored to chronicle.

It is a pleasure to welcome Mark and to acknowledge the enormous contributions that Robert has made to the success of this series.

Anthony F. Hill
Canberra, Act, Australia

Fully Condensed Polyhedral Oligosilsesquioxanes (POSS): From Synthesis to Application

Paul D. Lickiss* and Franck Rataboul

Contents		
I.	Introduction	2
II.	T ₂ Compounds	4
III.	T ₄ Compounds	5
	A. Synthesis	5
	B. Structural and physical properties	6
	C. Reactions and applications	7
IV.	T ₆ Compounds	7
	A. Synthesis	7
	B. Structural and physical properties	9
	C. Reactions and applications	11
V.	T ₈ Compounds	13
	A. General comments	13
	B. Synthesis, properties, and reactions of T ₈ H ₈ and its derivatives	15
	C. Synthesis, properties, and reactions of T ₈ Ph ₈ and its derivatives	30
	D. Synthesis, properties, and reactions of T ₈ [CH=CH ₂] ₈ and its derivatives	36
	E. Synthesis, properties, and reactions of T ₈ [O ⁻] ₈ and its derivatives	48
	F. Synthesis, properties, and reactions of T ₈ [OSiMe ₂ H] ₈ and its derivatives	52
	G. Synthesis, properties, and reactions of T ₈ [OSiMe ₂ CH=CH ₂] ₈ and its derivatives	61
	H. Synthesis, properties, and reactions of T ₈ [(CH ₂) ₃ NH ₃ Cl] ₈ and its derivatives	64
	I. Miscellaneous T ₈ R ₈ , T ₈ R ₇ R', T ₈ R ₆ R' ₂ , T ₈ R ₅ R' ₃ , and T ₈ R ₄ R' ₄ species	72
	J. The solid-state structures of T ₈ R ₈ compounds	88

Chemistry Department, Imperial College, London SW7 2AZ, UK

*Corresponding author.

E-mail address: p.lickiss@imperial.ac.uk

Advances in Organometallic Chemistry, Volume 57
ISSN 0065-3055, DOI 10.1016/S0065-3055(08)00001-4

© 2008 Elsevier Inc.
All rights reserved

VI. Syntheses, Properties, and Reactions of T_{10} Derivatives	92
A. Synthesis	92
B. Structural and physical properties	95
C. Reactions and applications	97
VII. T_{12} , T_{14} , and T_{16} Derivatives and Larger POSS Compounds	99
A. $T_{12}R_{12}$ species	99
B. $T_{14}R_{14}$ and $T_{16}R_{16}$ species	102
C. Larger polyhedra	103
VIII. Concluding Remarks	104
Abbreviations	104
Acknowledgments	105
References	106

I. INTRODUCTION

The widespread applications of compounds containing Si–O–Si linkages in both inorganic compounds such as silicates and aluminosilicates, and in organometallic compounds such as silicone polymers have been known for many years and have formed the basis of significant industrial effort. In addition to these well-known compounds, the last couple of decades have seen a rapid increase in interest in discrete molecular oligosiloxane species, often formed from the hydrolytic condensation reactions of trifunctional silicon monomers $RSiX_3$ (where X is usually a halide or alkoxide group). The year 2006 saw the 60th anniversary of the first publication by Scott reporting the isolation of a volatile silsesquioxane, probably $Si_8O_{12}Me_8$, from the thermal rearrangement of products derived from the cohydrolysis of Me_2SiCl_2 and $MeSiCl_3$.¹ Much earlier work on the hydrolysis of trichlorosilanes had probably led to some polyhedral oligomeric silsesquioxanes type products being formed as components of complicated mixtures but these were generally wrongly identified as silicon analogs of carboxylic acids or their anhydrides.² Work by Kipping³ did however, recognize the polymeric nature of these compounds and he identified them as “anhydrides” with formulae such as $[(C_6H_{11}SiO)_2O]_n$. Soon after the report by Scott on a volatile silsesquioxane, Barry and Gilkey⁴ correctly identified the polyhedral nature of some of the volatile silsesquioxanes derived from hydrolysis of $RSiCl_3$ compounds ($R = Et, Pr, Bu$) and a more detailed examination of a range of crystalline polyhedral silsesquioxanes was published in 1955.⁵ Detailed studies on the condensation reactions of $c\text{-}C_6H_{11}SiCl_3$ ⁶ and $PhSiCl_3$ ⁷ showed that condensation reactions of trifunctional organosilicon species can give rise to a wide range of products of general formula $(RSiO_{3/2})_n$ including random polymeric networks, **1**, and ladder polymers, **2**,⁸ incompletely condensed polyhedral species, **3**,⁹ and fully condensed polyhedral species, for example, structure **4** as shown in Figure 1.

The random structures, **1**, have no long-range order and the ladder polymers, **2**, contain no polyhedra as do the oligomeric species, **4**, but the incompletely

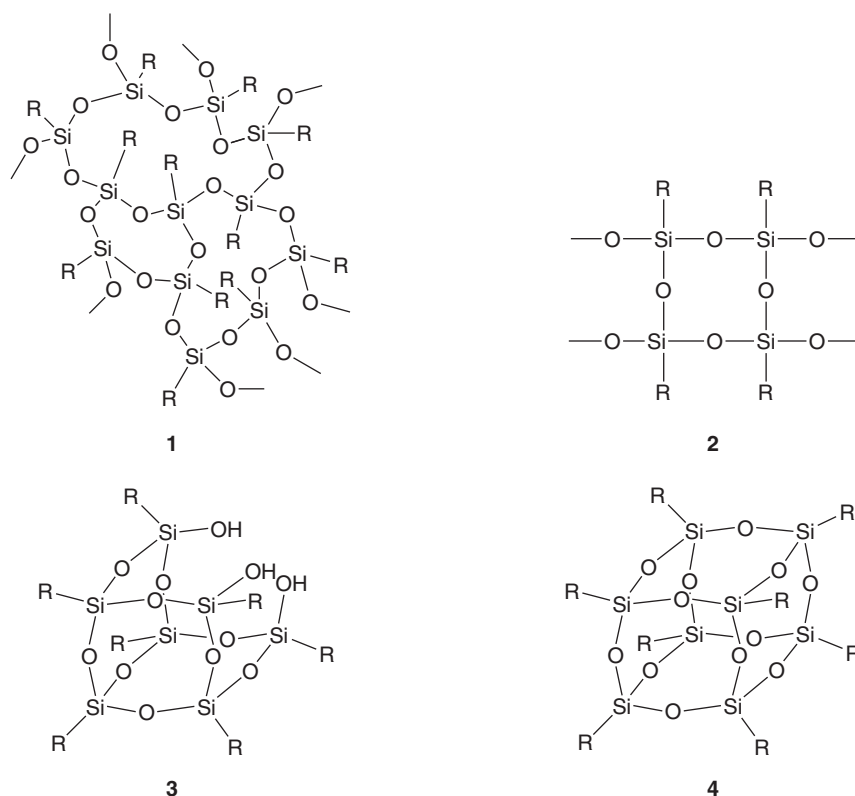


Figure 1 Different structures of compounds $(\text{RSiO}_{3/2})_n$.

condensed compounds, **3**, can readily be seen as precursors to the fully condensed compounds. Significant early work on the organometallic derivatives of species such as **3** ($\text{R} = \text{cyclohexyl}$) was carried out by Feher and coworkers⁹ and led to widespread studies involving the use of the reactive silanol functions as models for such groups at solid silica surfaces.¹⁰ Early work on the synthesis of silsesquioxanes was reviewed in 1982¹¹ and so this chapter will concentrate on work since then. More recent work has concentrated on the study of compounds, **4**, which have been found to have many applications utilizing their highly symmetrical, three-dimensional nature and their potential to act as nano-sized building blocks for the assembly of ordered two- and three-dimensional structures. This review will concentrate on compounds of type **4**, for reviews of the chemistry of compounds of type **1**, **2**, and **3** see Refs. (9, 10c, and 10g). In keeping with the title of this book this chapter also concentrates on organometallic compounds of type **4**; the many inorganic silicates and zeolites containing T_n rings will only be mentioned briefly. The nomenclature to describe structures such as **4** is complicated, for example, the full Chemical Abstracts name for **4** ($\text{R} = \text{H}$) is pentacyclo[9.5.1.13,9.15,15.17,13]octasiloxane. Fortunately, the nomenclature for describing siloxane polymers is convenient for describing

the polyhedra, a “T” unit denoting a silicon atom with three siloxane oxygen atoms attached to it, such that structure 4 ($R = H$) may be labeled as T_8H_8 . The general stoichiometry of these compounds is $(RSiO_{3/2})_n$ and they are usually thus called silsesquioxanes, although this term has largely been superseded in recent years by the term Polyhedral Oligosilsesquioxanes, abbreviated as POSS by those working in this area and trademarked by Hybrid Plastics.¹² These compounds, having a $SiO_{3/2}$ stoichiometry, can be seen as intermediate between the inorganic SiO_2 formula for silica and the SiO repeat unit for the backbone in polysiloxanes or silicones.

The format of this review is based on the number of T units in the polyhedral structure and looks at methods for POSS synthesis, structure, reactivity, and their relatively recent applications in technology. The recent surge in interest in POSS chemistry has been enabled by new syntheses to replace the original, lengthy, and sometimes erratic preparations. The majority of work in the area of POSS chemistry has been carried out on T_8 derivatives (at the end of 2006, a Chemical Abstracts substructure search revealed 23 T_4 derivatives in 26 publications, 87 T_6 derivatives in 87 publications, 1826 T_8 derivatives in 1186 publications, 50 T_{10} derivatives in 74 publications, and 23 T_{12} derivatives in 33 publications) and these compounds will be described in groups according to the nature of the pendent group at the silicon vertices. There are now a very large number of studies on POSS molecules and some discretion has been required in what to include in the review. Many details of the syntheses and physical data are tabulated for convenience and discussion has been limited to the most important compounds. Reviews of the uses of POSS molecules in polymers, copolymers, and nanocomposites have been published¹³ and so have computational simulations of POSS organic/inorganic hybrid materials.¹⁴

II. T_2 COMPOUNDS

The smallest possible fully condensed silsesquioxanes are the hypothetical T_2R_2 species (Figure 2). Such compounds have not been isolated and they would be expected to be extremely reactive toward oligomerization and addition reactions as are the monocyclic compounds containing a single Si_2O_2 ring.¹⁵ The T_2H_2 structure has, however, been the subject of *ab initio* calculations that show it to have an unusually short $Si \cdots Si$ distance of 2.060 Å and an $Si-O-Si$ angle of 74.7° .¹⁶

It is unlikely that T_2R_2 compounds can be prepared by the usual hydrolytic routes to siloxanes, but it might be possible to prepare one by dehydration of a very sterically hindered silanetriol, $RSi(OH)_3$ which can readily be isolated,¹⁷



Figure 2 The structure of hypothetical T_2R_2 species.

using a powerful dehydrating agent. This route has, however, been found previously to give T_6R_6 species for $R = t\text{Bu}$ or $t\text{Hexyl}$,¹⁸ but even larger substituents may promote the formation of smaller rings.

III. T_4 COMPOUNDS

A. Synthesis

The smallest synthetically accessible POSS compounds are the T_4 species based on just four Si atoms in an approximately tetrahedral arrangement. There are few of these compounds that have been well described, the problem being that the obvious synthetic routes to them, for example hydrolysis of RSiCl_3 , much more readily give rise to compounds containing Si_4O_4 rings, that is, T_8 species rather than the more strained Si_3O_3 rings required in T_4 compounds. Although the subject of several computational studies (see below) $T_4\text{H}_4$ has not been isolated, the hydrolysis of HSiCl_3 being well known to provide polymeric materials and low yields of $T_8\text{H}_8$ (see Section V.B). Attempts to prepare T_4R_4 with $R = \text{Me}$, Et , $i\text{Pr}$, or $t\text{Bu}$ by hydrolysis of RSiCl_3 (Figure 3) depend very much on the size of the substituent R , the larger groups giving good yields of polyhedral product.

This formation of smaller polyhedra when larger substituents are present is not surprising when the stability of intermediate silanols formed in these reactions toward polycondensation is taken into account. The methylsilanols condense rapidly and simple methylsilanols are difficult to isolate,¹⁷ whereas $t\text{BuSi}(\text{OH})_3$,²⁰ and $[t\text{BuSi}(\text{OH})_2]_2\text{O}$ ²¹ can both be readily isolated. This bulk effect is clearly consistent with the well-known ability of bulky group to stabilize small rings and low coordination numbers in other areas of organometallic chemistry. Attempts to prepare T_4 derivatives by using intramolecular hydrolysis/condensation reactions of a suitable precursor, such as $\text{MeSi}(\text{OSiMeX}_2)_3$ ($X = \text{Cl}$ or OEt), already containing the four silicon atoms, have also been unsuccessful leading only to T_8 POSS derivatives being isolated.²² Adamantanoid structures of Si with larger chalcogens and small substituents have however, been known for many years, the reaction between alkylsilanes or alkyltrichlorosilanes and H_2S or H_2Se giving, for example, $\text{Si}_4\text{S}_6\text{Me}_4$ or $\text{Si}_4\text{Se}_6\text{Et}_4$.²³ It should be noted that no equivalent carbon-oxygen polyhedral compounds are known, however the anion $[\text{Ge}_4\text{O}_6\text{Te}_4]^{4-}$, with

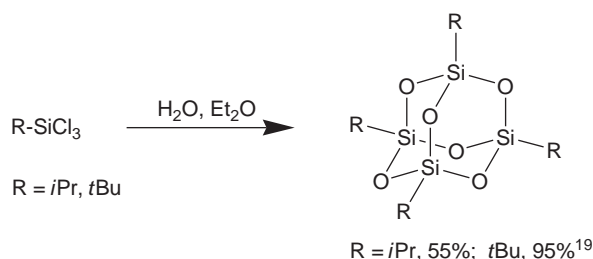


Figure 3 General scheme for the preparation of T_4R_4 species.¹⁹

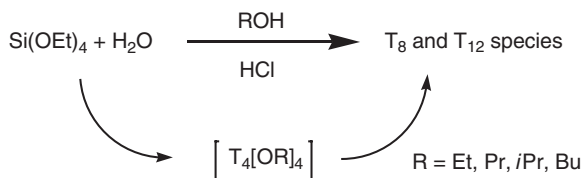


Figure 4 Hydrolysis of Si(OEt)_4 in the presence of alcohols.

an adamantanoid central Ge_4O_6 core has recently been prepared by solvothermal reaction of elemental Ge and Te with $\text{Mn(OAc)}_2 \cdot 4\text{H}_2\text{O}$ in the presence of $[\text{Me}_4\text{N}]\text{I}$ as a mineralizer in superheated ethylene diamine (EDA).²⁴ Tin analogs containing an Sn_4O_6 core are also known and can be prepared, for example, either by reaction of $n\text{BuSnCl}_3$ with $\text{NH}_4\text{OH}/\text{EtOH}/\text{H}_2\text{O}$ to give $\text{Sn}_4\text{O}_6\text{Bu}_4$ ²⁵ or by reaction of $(\text{Me}_3\text{Si})_3\text{CSnBr}_3$ with Na_2O in liquid ammonia to give $\text{Sn}_4\text{O}_6[(\text{Me}_3\text{Si})_3\text{Cl}]_4$.²⁶ The hydrolysis of pyridinium(2,3-naphthalendiolo)-4-(trimethylsilylethynyl)phenyl-silicate gives a mixture of POSS molecules including $\text{T}_4[\text{C}_6\text{H}_4\text{-C}\equiv\text{C-SiMe}_3]_4$, identified within the mixture by matrix-assisted laser desorption ionization time of flight (MALDI-TOF) mass spectrometry but not separated as a single compound.²⁷ The unambiguous synthesis of halogen-substituted T_4 species has not been achieved although the possibility of T_4Cl_4 formation in the reaction between SiCl_4 and O_2 at high temperature has been discussed.²⁸ The isolation of $\text{T}_4[\text{OR}]_4$ species has similarly so far been unsuccessful, any simple hydrolytic methods of synthesis presumably leading to hydrolysis of the Si-OR bonds in any product. However, several alkoxy-substituted compounds $\text{T}_4[\text{OR}]_4$ (R = Et, Pr, *i*Pr, *n*Bu, $\text{C}_6\text{H}_4\text{Me}$, $\text{C}_{18}\text{H}_{37}$) have been reported as intermediates in the hydrolysis of Si(OEt)_4 in the presence of higher alcohols, ROH (Figure 4)²⁹ and the formation of $\text{T}_4[\text{OH}]_4$ at high temperature from Si(OH)_4 dehydration has been investigated computationally.³⁰

Calculations on the ^{29}Si NMR chemical shifts of silicate anions,³¹ including $\text{T}_4[\text{O}^-]_4$, suggest that an initial tentative assignment³² for its presence in solutions of silica/ H_2O - D_2O /alkali-metal hydroxide is incorrect. Laser ablation of a variety of porous siliceous materials gives gas-phase clusters, which mass spectrometry shows contains the anion $[\text{T}_4(\text{OH})_3\text{O}]^-$; density functional theory (DFT) calculations³³ confirm that this ion and the related neutral $\text{T}_4[\text{OH}]_4$ are magic number species for such silicon-dioxide-based clusters but their isolation remains elusive.

B. Structural and physical properties

No detailed structural studies have been carried out experimentally on T_4 derivatives but a number of computational studies have been undertaken as part of the drive to understand the fundamental nature of silicate structures, many of which are made up of small polyhedral units.

It can be seen that although the Si-O bond distances within the polyhedral skeleton are not unusually long (cf. an average distance of 1.629 Å for four-coordinate Si attached to two coordinate O)³⁴ the Si-O-Si angles, varying from about 114.5 to 118.5°, are much sharper than is common in unstrained systems

(averaging 132.8° for simple $(R_2SiO)_3$ species),³⁴ and well below the values of about 140 – 150° found in T_8 derivatives (see Section V). The accommodation of strain by deforming Si–O–Si bond angles is also seen in monocyclic Si_3O_3 rings compared to Si_4O_4 rings in simple siloxane chemistry.³⁴ The E_4O_6 adamantanoid core is well known for group 15 elements with P_4O_6 having a P–O–P angle of 127° ³⁵ and P_4O_{10} having a P–O–P angle of ca. 122.8° .³⁶ The related germanium-containing anion $[Ge_4O_6Te_4]^{4-}$ has a Ge–O–Ge angle of about 119 – 120° (data taken from the Cambridge Crystallographic Data Centre, Version 5.27, May 2006 Update, for structures FIHKUD and FIHKOX).²⁴ The Sn–O–Sn angle in $Sn_4O_6[(Me_3Si)_3Cl]_4$ has a similar value of 120.0° .²⁶

Calculations on T_4H_4 with T_d symmetry show it to be less stable per Si atom by 7.3 or 10 kcal mol^{-1} , respectively, by DFT (nonlocal density approximation),³⁷ or Hartree–Fock (HF; at the 6-31G(d)//6-31G(d) level)³⁸ than O_h symmetry T_8H_8 . Similarly, calculations on C_{2v} symmetry T_4Me_4 show it to be 7.4 and 7.8 kcal mol^{-1} less stable per Si atom, respectively, than C_s and C_{4v} symmetry T_8Me_8 .³⁹

The ^{29}Si NMR chemical shift of $T_4[O^-]_4$ had been tentatively assigned a value of -97.3 ppm ³² but more recent calculations suggest that the correct value for this ion is -78.7 ppm .³¹

C. Reactions and applications

The reactivity of T_4R_4 species remains largely unexplored because of the lack of compounds available for study but the $T_4[OR]_4$ ($R = Et, Pr, iPr, nBu, C_6H_4Me, C_{18}H_{37}$) compounds are reported to be reactive under the hydrolysis conditions under which they are prepared, probably to give T_8 and T_{12} species (Figure 4).²⁹ The reactions of T_4 derivatives with functionalized substituents are likely to be dominated by the reactivity of the substituents as has been found in the case of the T_8 derivatives described in Section V.

IV. T_6 COMPOUNDS

A. Synthesis

The synthesis of T_6R_6 compounds by simple hydrolysis of, for example $RSiCl_3$ precursors, is, as was described above for the T_4 analogs, similarly hampered by the preference to form more stable compounds containing all Si_4O_4 rather than some Si_3O_3 rings. Thus, although the chemistry of T_6 derivatives is much better developed than the T_4 species it is still restricted to a relatively small number of compounds when compared with T_8 derivatives. It should be noted that there are a range of inorganic silicates containing T_6 polyhedra, for example, $(NEt_4)_6Si_6O_{15} \cdot 40.8H_2O$,⁴⁰ $Cs_2ZrSi_6O_{15}$,⁴¹ $Na_3YSi_6O_{15}$,⁴² and $[Ni(en)_3]_3Si_6O_{15} \cdot 26H_2O$ ⁴³ but these will not be considered in detail here.

The synthetic routes to T_6R_6 compounds are outlined in Figure 5. Simple hydrolysis of $RSiCl_3$ or $RSi(OMe)_3$ precursors does not give good yields of T_6 derivatives as they tend to be formed as by-products in the presence of higher

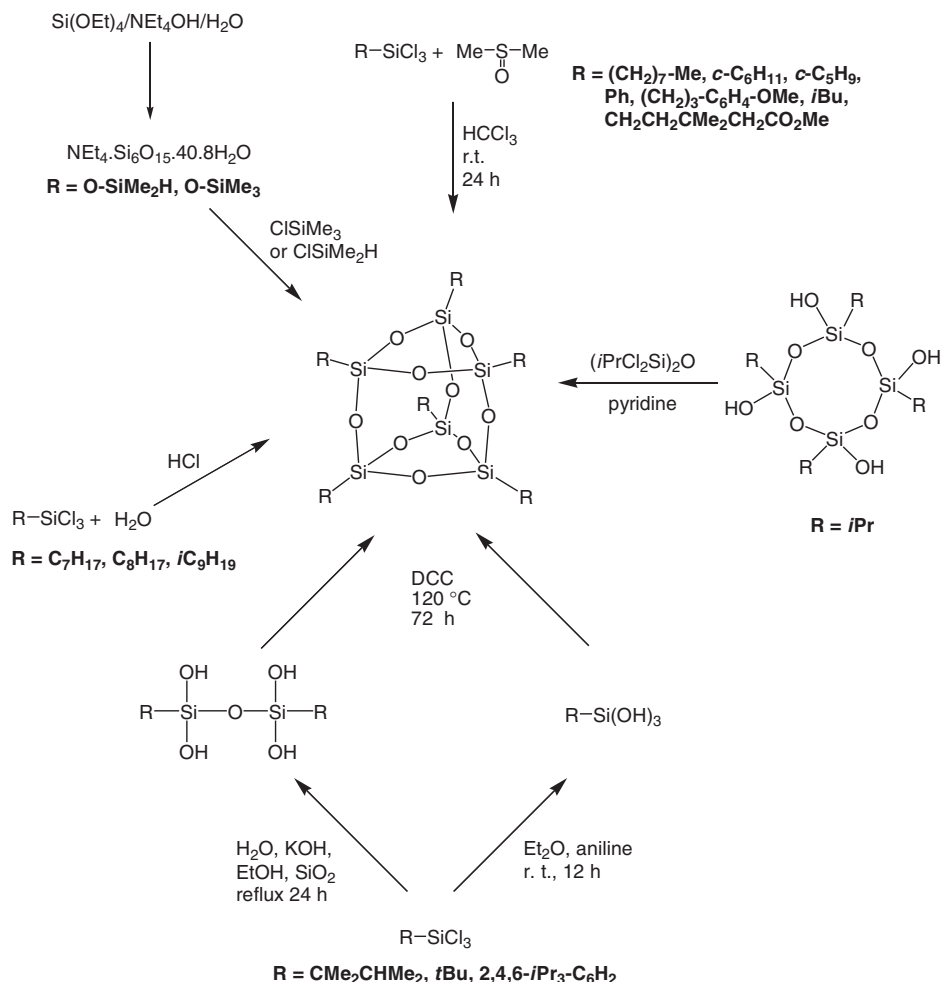


Figure 5 General scheme for the synthesis of T_6R_6 species.

silsesquioxanes but $\text{T}_6[c\text{-C}_6\text{H}_{11}]_6$ can be formed in 10–13% yield^{6,44} and low yields of simple alkyl derivatives T_6Me_6 ⁴⁵ and T_6Et_6 ⁴⁶ are available by hydrolysis of triethoxysilane precursors. Hydrolysis of trichlorosilane precursors with larger alkyl substituents in organic solvents tends to give incompletely condensed materials containing Si–OH groups but if the reaction is carried out in the absence of a cosolvent, using just aqueous HCl as hydrolysis medium, then mixtures of fully condensed species including $\text{T}_6[\text{C}_7\text{H}_{15}]_6$,⁴⁷ $\text{T}_6[\text{C}_8\text{H}_{17}]_6$, and $\text{T}_6[i\text{C}_9\text{H}_{19}]_6$ ⁴⁸ can be prepared. Vacuum distillation of these mixtures leads to thermal rearrangements and pure T_6 derivatives can be isolated.⁴⁸

As mentioned above, hydrolysis of bulky RSiCl_3 precursors tends to give a variety of silanols, these may be isolated and used for the preparation of T_6 derivatives. Thus, simple silanetriols RSi(OH)_3 or disiloxanetetraols $[\text{RSi(OH)}_2]_2\text{O}$ ($\text{R} = t\text{Bu}, t\text{Hexyl}, \text{or } 2,4,6\text{-}i\text{Pr}_3\text{C}_6\text{H}_2$) may be dehydrated^{18,49} and

the cyclotetrasiloxane $[i\text{Pr}(\text{OH})\text{SiO}]_4$ reacts with the tetrachlorodisiloxane $(i\text{PrCl}_2\text{Si})_2\text{O}^{50}$ to give T_6R_6 where $\text{R} = t\text{Bu}$, $t\text{Hexyl}$, or $i\text{Pr}$, respectively. A “non aqueous” hydrolysis in which trichlorosilanes are treated with $\text{Me}_2\text{S}=\text{O}$ in CHCl_3 gives T_6R_6 compounds ($\text{R} = \text{C}_8\text{H}_{17}$, $c\text{-C}_6\text{H}_{11}$, $c\text{-C}_5\text{H}_9$, $i\text{Bu}$, C_6H_5 , $(\text{CH}_2)_3\text{C}_6\text{H}_4\text{-}p\text{-OMe}$, or $\text{CH}_2\text{CH}_2\text{CMe}_2\text{CH}_2\text{CO}_2\text{Me}$) in 6–25% yield, comparable to many yields of POSS syntheses.⁵¹ The silicate anion $\text{T}_6[\text{O}^-]_6$ is present in Et_4N^+ solutions of silicate anions prepared from aqueous NEt_4OH and $\text{Si}(\text{OEt})_4$, and it may be derivatized using a $(\text{RMe}_2\text{Si})_2\text{O}/\text{RMe}_2\text{SiCl}$ mixture to give $\text{T}_6[\text{OSiMe}_2\text{R}]_6$ ($\text{R} = \text{H}$ or Me).⁵² This method would presumably work for a range of other element halides to give a variety of O-substituted T_6 derivatives, as has been the case for the T_8 analogs (Section V), but the chemistry of T_6 derivatives, has, so far, not been developed in this area. The general low-yielding routes to T_6 compounds when compared with some of the higher yielding routes to T_8 compounds will probably mean that T_6 chemistry will remain relatively unexplored.

B. Structural and physical properties

Relatively few T_6 derivatives have been subjected to X-ray crystallographic analysis, some structural data are given in Table 1. The average Si–O bond distances in T_6 derivatives are very similar to the value of 1.629 Å found in a wide range of other Si–O containing compounds³⁴ and are generally unexceptional. It should, however, be noted that the Si–O bond distances in the Si_3O_3 rings are slightly longer than those in Si_4O_4 rings, the same trend for longer bond lengths at smaller Si–O–Si angles being found in other siloxanes.⁵³ The Si–O–Si angles fall into two distinct ranges, a narrower angle of about 130–132° at oxygen atoms involved in both the trisiloxane and tetrasiloxane rings, and a wider angle of about 138–141° for oxygen atoms involved in only tetrasiloxane rings (the silicate $\text{Na}_3\text{YSi}_6\text{O}_{15}$ seems to be an exception having a much narrower range of angles overall⁴²). This significant difference in angles is consistent with that found in simpler cyclosiloxanes $(\text{R}_1\text{R}_2\text{SiO})_n$, 132.8 and 148° for $n = 3$ and 4, respectively,³⁴ and reflects the greater degree of strain and hence greater reactivity in cyclo-trisiloxanes when compared to cyclotetrasiloxanes. The very bulky $\text{T}_6[2,4,6\text{-}i\text{Pr}_3\text{C}_6\text{H}_2]_6$ crystallizes as a racemate, restricted rotation of the aryl groups causing propeller-like enantiomers to be stable at room temperature.⁴⁹ Calculated values for T_6 structural parameters tend to agree well with those found experimentally but, unfortunately, no direct comparisons have yet been made; the small substituents used for computational ease not being compatible with synthetic accessibility. The angles at silicon are generally near to the tetrahedral value.

The ^{29}Si NMR chemical shifts for several T_6 derivatives are shown in Table 2. The alkyl derivatives fall in the range –54 to –57 ppm, while the aryl derivatives are more upfield from –66.9 to –68.9 ppm, as expected for aryl versus alkyl substituents.⁵⁴ Bassindale et al.⁵¹ have derived a relationship, $\delta_{\text{T}_6} = 0.82 \times \delta_{\text{T}_8}$, allowing an estimation of the chemical shift for unknown T_6 derivatives from the known values for the much more common T_8 analogs. The solid-state ^{29}Si NMR spectrum for $\text{T}_6[\text{OSiMe}_3]_6$ shows five signals for the silsesquioxane silicon atoms,

Table 1 Structural data for T_6R_6 compounds

Compound	Si–O (Å) both ring types		Si–O–Si (°) Si_4O_4 rings		Si–O–Si (°) Si_3O_3/Si_4O_4 rings		Method	Reference
	Range	Mean	Range	Mean	Range	Mean		
T_6H_6	1.634–1.643	1.638	139		131		Calc.	38
T_6Cl_6	–		136.6		126.9		Calc.	28
$T_6[OH]_6^a$	1.627		135.7		135.7		Calc.	31
$T_6[OH]_6^b$	1.628		134.9		134.9		Calc.	31
T_6Me_6	1.633–1.642	1.637	141.278		131.321		Calc.	60
T_6iPr_6	1.617(4)–1.641(5)	1.631	138.9(2)–139.4(3)	139.1	130.1(2)–130.6(3)	130.4	X-ray	50
$T_6[CM_2CHMe_2]_6$	1.601(9)–1.656(9)	1.626	137.9(5)–139.7(5)	139.0	130.6(5)–132.5(5)	131.6	X-ray	18
$T_6[C-C_6H_{11}]_6$	1.625(6)–1.649(6)	1.640	139.3(4)–144.7(5)	141.1	128.8(4)–130.8(5)	129.5	X-ray	44
$T_6[(CH_2)_3C_6H_4-p-OMe]_6^d$	1.622–1.642	1.631	137.69–142.37	139.3	130.04–132.15	130.82	X-ray	51
$T_6[2,4,6-iPr_3C_6H_2]_6^c$	1.622(2)–1.646(4)	1.634	138.3(3)–141.7(3)	139.8	131.8(2)–134.0(2)	132.0	X-ray	49
$T_6[OSiMe_3]_6$	1.56(1)–1.63(1)	1.61	136.8(8)–138.6(6)	137.9	128.9(8)–131.7(9)	130.3	X-ray	52a,66
$Na_3YT_6(O^-)_6$	1.623(2)–1.651(1)	1.641	132.8(2)–135.8(2)	134.8	130.3(2)–134.1(1)	132.8	X-ray	42
$(NEt_4)_6T_6(O^-)_6 \cdot 40.8H_2O$	1.630(4)–1.647(4)	1.638	137.8(3)–146.0(3)	141.3	129.6(2)–132.5(3)	131.0	X-ray	40

^a D_{3h} isomer.
^b C_{3v} isomer.
^c For the right-handed enantiomer.
^d CCDC deposition number 217979.

Table 2 ^{29}Si NMR data for T_6R_6 compounds

Compound	^{29}Si NMR chemical shift (ppm from Me_4Si)	Solvent	Reference
T_6H_6 (D_{3h})	−90.7	Calc. value	31
T_6H_6 (C_{3v})	−90.0	Calc. value	31
$\text{Na}_6\text{T}_6(\text{O}^-)_6$	ca. −88	H_2O	32
$(\text{Et}_4\text{N})_6\text{T}_6(\text{O}^-)_6$	−88.2	H_2O	55
$(n\text{Pr}_4\text{N})_6\text{T}_6(\text{O}^-)_6$	−88.2	H_2O	56
$\text{T}_6[\text{OSiMe}_3]_6$	−98.84 ^a	Heptane	52a
$\text{T}_6[\text{OSiMe}_3]_6$	−98.9, −99.2, −100.0, −100.1, −100.6 ^b	Solid	52a
$\text{T}_6[\text{iBu}]_6$	−55.4	CDCl_3	51
$\text{T}_6[\text{tBu}]_6$	−54.3	C_6D_6	18
$\text{T}_6[\text{tHexyl}]_6$	−55.1	C_6D_6	18
$\text{T}_6[\text{C}_8\text{H}_{17}]_6$	−54.2	CDCl_3	51
$\text{T}_6[(\text{CH}_2)_3\text{--C}_6\text{H}_4\text{--4--MeO}]_6$	−54.4	CDCl_3	51
$\text{T}_6[\text{c--C}_5\text{H}_9]_6$	−54.4	CDCl_3	51
$\text{T}_6[\text{c--C}_6\text{H}_{11}]_6$	−56.6	CDCl_3	51
$\text{T}_6[\text{c--C}_6\text{H}_{11}]_6$	−56.72	THF	57
$\text{T}_6[\text{c--C}_6\text{H}_{11}]_6$	−56.23	$\text{CDCl}_3/\text{Et}_3\text{N}$	58
$\text{T}_6[\text{C}_6\text{H}_5]_6$	−66.9	CDCl_3	51
$\text{T}_6[2,4,6\text{-iPr}_3\text{C}_6\text{H}_2]_6$	−68.91	CDCl_3	49

^a13.5 ppm for the SiMe_3 groups.^b15.0, 14.7, 13.7, 13.1, 12.4, 12.3 ppm for the SiMe_3 groups.

one of double intensity, consistent with the asymmetry found for its X-ray crystallographic structure.^{52a} Again, as for the structural data, there appear to be no directly comparable calculated values for ^{29}Si NMR chemical shifts to compare with experimental values.

There have been very few measurements made on the physical properties of T_6 derivatives, their relative greater difficulty of preparation when compared with the T_8 analogs has meant little interest in their properties. However, $\text{T}_6[\text{OSiMe}_3]_6$ has been found to show photoluminescence in the blue region of the spectrum,⁵⁹ third-order nonlinear optical properties for T_6Me_6 ⁶⁰ have been modeled, and electronic properties for T_6H_6 ³⁷ and T_6Me_6 ³⁹ have been calculated.

C. Reactions and applications

The reactions of POSS molecules fall into two categories, those involving the silsesquioxane core of the molecule and those involving reactions of the peripheral substituents. The silsesquioxane core in POSS compounds is fairly unreactive to many reaction conditions and this inertness has led to the successful application of POSS species in many materials (see Section V for further

discussion). The hydrolysis of T_6H_6 ³⁷ and T_6Me_6 ³⁹ has been calculated to be endothermic and POSS compounds are generally air-stable and easy to handle. The silsesquioxane framework is however, like most siloxane linkages, susceptible to attack by both strongly basic and strongly acidic species.

The treatment of T_6R_6 ($R = n\text{-C}_6\text{H}_{11}$ or OSiMe_3) with Et_4NOH proceeds readily and causes cleavage of both of the Si_3O_3 rings in the POSS core to give the silanols **5** as shown in Figure 6.⁶¹ The cyclohexyl derivative slowly reacts further to give the heptasiloxane **6** which can also be produced more rapidly if the initial reaction is carried out in the presence of $n\text{-C}_6\text{H}_{11}\text{Si}(\text{OMe})_3$ which can generate the reactive silanetriol $n\text{-C}_6\text{H}_{11}\text{Si}(\text{OH})_3$ as an intermediate.

In a manner similar to the reactions with Et_4NOH the T_6 polyhedron is also cleaved by fluoride, which in the presence of difunctional ethoxysilanes generates octasiloxanes **7** (Figure 7) (both enantiomers are formed) if the reaction is carried out with a 4:2:1 ratio of alkoxy silane/POSS/fluoride. If an 8:2:1 ratio of alkoxy silane/POSS/fluoride is used the singly cleaved product **8** (Figure 7) and the heptasiloxane **9** (Figure 7) can also be isolated, again, cleavage of the more reactive Si_3O_3 rings predominates.⁶²

The cleavage of the T_6 ring in $T_6[\text{OSiMe}_3]_6$ by acid has been studied in detail. In the presence of Amberlite 15 cation exchange resin/ $\text{Me}_3\text{SiOSiMe}_3/\text{Cl}_3\text{CCO}_2\text{H}$ the siloxane $T_6[\text{OSiMe}_3]_6$, undergoes a complicated series of ring-opening reactions followed by silylations (with either Amberlyst-SiMe₃ or $\text{Cl}_3\text{CCO}_2\text{SiMe}_3$

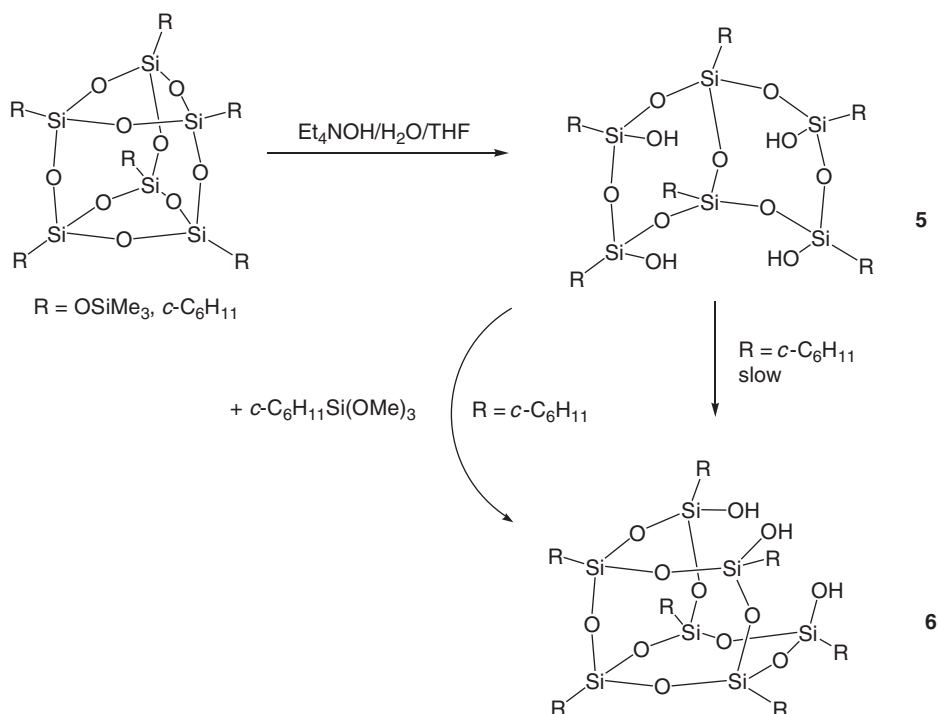


Figure 6 Ring opening of T_6R_6 by NEt_4OH .

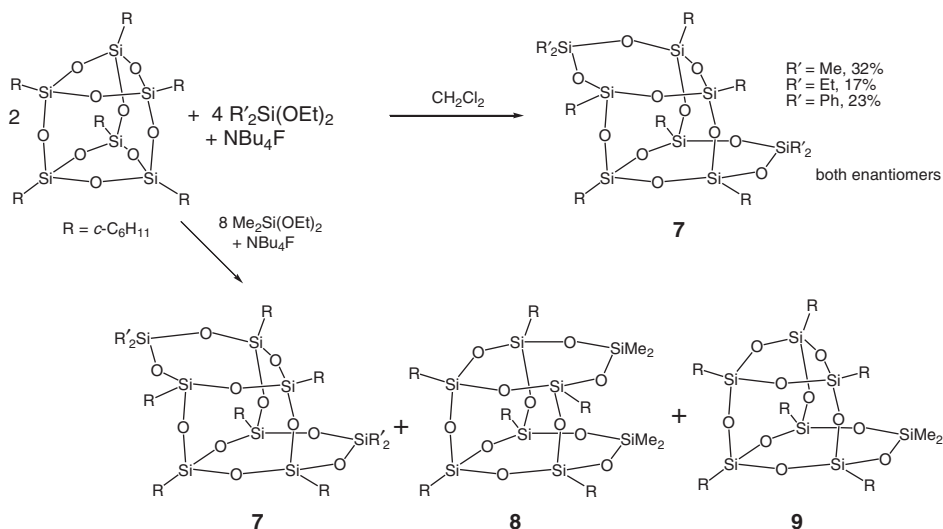


Figure 7 Ring opening of T_6R_6 by NBu_4F .

as silylating agents) to give products with structures similar to those shown in Figure 7, but in which all the substituents are OSiMe_3 . Again, products containing Si_4O_4 rings predominate.⁶³

Relatively few reactions of the peripheral groups in T_6 derivatives have been investigated. Perhaps the most useful reaction described so far is the silylation of $\text{T}_6[\text{O}^-]_6$, which readily reacts with chlorosilanes RMe_2SiCl ($\text{R} = \text{H}$, Me or $\text{CH}=\text{CH}_2$) to give $\text{T}_6[\text{OSiMe}_2\text{R}]_6$.^{52,61a} The vinyl-substituted $\text{T}_8[\text{CH}=\text{CH}_2]_8$ undergoes H_2PtCl_6 catalyzed hydrosilylation with $\text{T}_6[\text{OSiMe}_2\text{H}]_6$ to give a polymer of T_6 and T_8 cages connected by $\text{OSiMe}_2\text{CH}_2\text{CH}_2$ linkages,⁶⁴ while hydrolysis of $\text{T}_6[\text{OSiMe}_2\text{Br}]_6$ (derived from bromination of $\text{T}_6[\text{OSiMe}_2\text{H}]_6$) gives a siloxane polymer in which T_6 cages are linked by $\text{OSiMe}_2\text{OSiMe}_2\text{O}$ units.⁶⁴ Both these polymers have mesoporous properties but little application of these or other T_6 derivatives has been reported. The silicates $\text{Na}_3\text{YSi}_6\text{O}_{15}$ ⁴² and $\text{K}_3\text{NdSi}_6\text{O}_{15}$ ⁶⁵ have been investigated as possible fast-ion conductors but the related $\text{Cs}_2\text{ZrSi}_6\text{O}_{15}$ lacks channels that could be used for migration of cesium ions.⁴¹ This lack of application for T_6 derivatives is likely to continue until higher yielding, more specific syntheses are available and become competitive with the T_8 analogs. Even if convenient syntheses do become available, it is likely that the higher reactivity of the Si_3O_3 rings in T_6 compounds will preclude much of the work carried out for the related T_8 compounds.

V. T_8 COMPOUNDS

A. General comments

The field of POSS chemistry is dominated by the cube-like T_8 derivatives which are becoming important compounds with a wide range of technological

applications. The reasons for this dominance are the practical ones of convenient synthesis and ease of handling, coupled with their useful properties, such as thermal stability, high symmetry, ease of chemical modification, and nano-sized dimensions. There are polyhedral structures other than the well-known cube hypothetically available for eight T-type silicon centers but they have not yet been prepared. The cubic T_8 arrangement forms spontaneously from hydrolysis/condensation reactions of many simple $RSiCl_3$ or $RSi(OR')_3$ silanes described below, and contains only stable, Si_4O_4 rings. However, as will be seen, only a minority of the known T_8R_8 compounds have been prepared in this way. Indeed, the syntheses of the majority of new T_8R_8 compounds arise from chemical modifications of a few simple precursors having reactive sites that allow the preparation of a wide range of compounds, sometimes highly functionalized. These starting materials are T_8H_8 , T_8Ph_8 , $T_8[CH=CH_2]_8$, $T_8[ONMe_4]_8$, $T_8[OSiMe_2H]_8$, $T_8[OSiMe_2CH=CH_2]_8$, and $T_8[(CH_2)_3NH_2]_8$, and, because of their importance, their chemistry will be described in separate sections.

In the case of products prepared from hydrolysis/condensation reactions, the time of reaction varies from a few hours to more than 3 months. Generally, the crude products precipitate from the reaction mixture and pure compound can be obtained by simple filtration followed by washing or recrystallization. However, the yields are often low and rarely exceed 50%.

About 90 POSS compounds with T_8 cores have been structurally characterized using diffraction methods, about 50 of them are of T_8R_8 composition. A list of such studies is given at the end of this section (see Table 34). One of the other main techniques used for the characterization of these compounds is NMR spectroscopy, particularly ^{29}Si NMR spectroscopy, which can give quick information on compound purity, usually with a single signal in the range of -65 to -80 ppm when the silicon corner is linked to a carbon atom, and in the range of -100 to -110 ppm when linked to an oxygen atom. In partially substituted compounds such as $T_8R_6R'_2$ the position of the substituents can also be determined by the pattern of the ^{29}Si NMR spectroscopy signals. Mass spectrometry can also be used to determine the degree of substitution in POSS derivatization reactions.

The POSS core in T_8R_8 species is generally stable under ambient conditions and they can be handled without special requirements. However, they are susceptible to cage cleavage in the presence of strong basic media by nucleophilic attack on the silicon atoms giving rise to degradation. Nevertheless, it has been shown that controlled reactions with base can afford a ring expansion to the $T_{10}R_{10}$ and $T_{12}R_{12}$ analogs (see Table 35 and Figure 11).

As seen below, T_8R_8 compounds have found a broad range of applications. First, these compounds are now important building blocks for the preparation of nanocomposites due to the three-dimensional, highly symmetrical nature of the POSS core. Indeed, the easy introduction of polymerizable or reactive functions allows the preparation of three-dimensional copolymers. Moreover, the variation of the length of the pendant arms can allow the control of the porosity of the polymeric material. Alternatively, hydrophobic $T_8[alkyl]_8$ species have been used as inorganic components for the blending of organic polymers matrices to give homogeneous hybrid polymers. In this case they are an alternative to silica

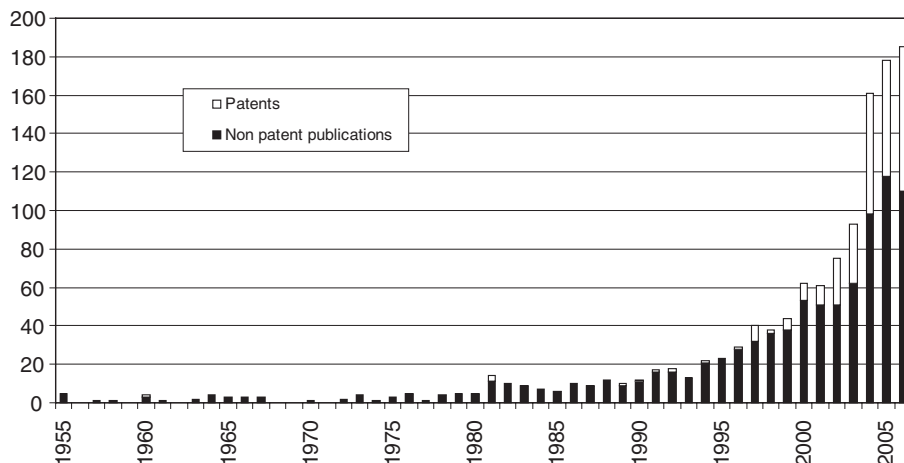


Figure 8 Patent and nonpatent publications concerning compounds containing the T_8 substructure.

nanoparticles which are generally used for this application. The presence of such thermally robust POSS molecules imparts greater thermal stability to the polymer matrix and allows the tailoring of the polymer glass transition temperature by tuning the POSS concentration. Moreover, incorporation of POSS molecules improves the mechanical properties of the final material and reduces its flammability, acting as flame retardants by formation of SiO_2 on heating. Second, catalysis has become an interesting area of application for T_8R_8 compounds. The introduction of coordinating functions such as $-PPh_2$ has enabled the preparation of several three-dimensional ligands for use in preparing metal complexes for reactions such as hydroformylation. The most useful POSS compounds for catalysis have the formula $T_8R_7(OH)$, as they can be seen as molecular models for isolated silanols of silica surface and therefore as models for the characterization of heterogeneous catalysts. Other applications have been found in the fields of optics, electrochemistry, lithography, and dendrimers. For a recent review of many applications of POSS materials see Ref. (13h).

The growth in interest in compounds having the T_8 core structure can be seen when looking at the number of publications on such compounds. Figure 8 shows publications found from a Chemical Abstracts search for the T_8 substructure showing both patent and nonpatent literature. It is clear that both the overall interest and the interest in patented applications have grown rapidly in the last 5–10 years and it is likely to continue as the properties of many new derivatives are explored.

B. Synthesis, properties, and reactions of T_8H_8 and its derivatives

1. Synthesis

The simplest T_8 compound, T_8H_8 , is a white solid that was initially obtained fortuitously and in a very small yield by Müller et al. (1959) while studying the

Table 3 Preparative routes to T_8H_8

Entry	Starting materials and conditions	Yield (%)	Reference
1	$HSiCl_3 + H_2O + (Me_3Si)_2O$, 80% H_2SO_4	< 1	73
2	$HSi(OMe)_3 + H_2O$, HCl, cyclohexane/acetic acid, 9 h	13.3	74
3	$HSiCl_3 + H_2O$, $FeCl_3 \cdot nH_2O$, MeOH/hexanes/PhMe, 9 h	17.5	67
4	$HSiCl_3 + H_2O$, $FeCl_3 \cdot nH_2O$, petroleum ether, 9 h	19	75

preparation of the polymer $Me_3SiO-[SiH(OSiMe_3)O]_n-SiMe_3$ by the hydrolysis of $HSiCl_3$ in presence of H_2SO_4 (Table 3, entry 1). Later, Frye and Collins reported a new method based on the careful hydrolysis of $HSi(OMe)_3$ catalyzed by HCl which gives T_8H_8 , isolated by sublimation and further recrystallization, in 13.3% yield. More recently, Agaskar has developed an improved method based on a “scarce-water” hydrolysis of $HSiCl_3$ in a biphasic system in the presence of partially hydrated $FeCl_3$ for a more controlled hydrolysis. This method gives a mixture of T_8H_8 and $T_{10}H_{10}$ that can be easily separated by washing with hexane to give pure T_8H_8 in 17.5% yield.⁶⁷ Later, this procedure was slightly modified by Frey and coworkers by changing the solvent system but without improving significantly the yield. Table 3 gives details of the preparations of T_8H_8 . The purification of T_8H_8 and the separation of a range of hydridosilsesquioxanes, $(HSiO_{1.5})_{8-18}$ can be achieved by size-exclusion chromatography.⁶⁸ Despite the importance of T_8H_8 as a synthetic precursor to many other POSS species and the poor yields for its synthesis, relatively little is understood about the precise mechanism(s) for its formation. However, the hydrolysis of $HSiCl_3$ and initial condensation reactions have been the subject of calculations and the formation of T_8H_8 from $HSi(OH)_3$ *via* multiple condensation reactions has been studied computationally.⁶⁹ It is found to be overall $[HSi(OH)_3 \text{ to } T_8H_8]$ exothermic by $11.5 \text{ kcal mol}^{-1}$ and to be significantly affected by intramolecular hydrogen bonding. Although the barrier to each condensation reaction is high, the inclusion of one molecule of water in the calculations to represent solvent reduces these barriers significantly.⁷⁰ The conformations, stability, and flexibility of partially condensed silsesquioxanes that can be seen as precursors to fully condensed species have also been calculated.⁷¹

The synthesis of the deuteriated analog, T_8D_8 , by bubbling D_2 into a pentane solution of T_8H_8 in presence of Pd/C (Table 8, entry 1), was described by Calzaferri and coworkers.⁷²

2. Structure and physical properties from experiment and theory

There are 78 vibrational degrees of freedom for T_8H_8 and it has been shown that the molecule has 33 different fundamental modes under O_h symmetry, 6 are IR active, 13 are Raman active, and 14 vibrations are inactive.⁷⁶ The experimental fundamental IR active vibrational frequencies have been assigned as follows: 2277 (ν Si-H), 1141 (ν_{as} Si-O-Si), 881 (δ O-Si-H), 566 (δ_{as} O-Si-O), 465 (ν_s O-Si-O), and 399 cm^{-1} (δ_s O-Si-O). These generally agree well with calculated values.^{74,76a,77} The IR spectrum recorded in the solid state shows bands at 2300 and 2293 cm^{-1}

(ν Si–H), 1178 and 1119 cm^{-1} (ν Si–O–Si), and 887 and 858 cm^{-1} (δ O–Si–H). These data are different to those observed in CCl_4 solution^{74,77} for the major vibrational modes, and this has been attributed to the associated nature of the molecules in the solid state.⁷⁸ A more recent solid-state IR study investigated the solid-state effects on the spectrum in more detail and concluded that some of the former vibrational assignments were probably incorrect.⁷⁹ The Raman spectrum of T_8H_8 has also been recorded^{76a,77,78} and a quantitative correlation of the IR and Raman fundamentals for T_8H_8 and $\text{T}_{10}\text{H}_{10}$ has been carried out *via* a normal coordinate analysis.⁸⁰ Infrared and Raman spectra of T_8D_8 have also been recorded and compared with those from T_8H_8 .^{72b,77}

After the first single-crystal X-ray determination by Larsson in 1960⁸¹ who confirmed the structure proposed by Müller,⁷³ Auf der Heyde et al.⁸² reported a full X-ray structural characterization of T_8H_8 at 100 K. Törnroos⁸³ then reported both an X-ray study at 9.5 K and a neutron diffraction study at 29 K, and Harrison and Hall⁷⁸ reported the powder X-ray diffraction (XRD) pattern. These various structural data together with calculated values for comparison are shown in Table 4. The various bond angles and lengths shown fall in the expected ranges for silicon compounds and are, in themselves, unexceptional. However, the highly symmetrical molecule deviates from ideal O_h symmetry in the solid state, instead having T_h symmetry. The distortions present can be seen by inspection of the geometrical data in Table 4 and can be seen most clearly in different values found for $\text{Si} \cdots \text{Si}$ distances across the face of the cube. The origin of the distortion away from ideal symmetry has been investigated and is thought to be due to four relatively short (ca. 3.63 Å), intermolecular $\text{Si} \cdots \text{O}$ distances between pairs of adjacent molecules.⁸² An investigation into the packing and orientation of T_8H_8 physisorbed onto a graphite surface has provided direct images of the molecules using high resolution scanning tunneling microscopy (STM). The T_8H_8 forms ordered arrays on the surface and may be in contact with the surface either *via* contact with a face (four hydrogen atoms), or an edge (two hydrogen atoms) of the POSS molecule. The STM tip has also been used to provide a measure of the dimensions of the POSS molecule, giving values of 7.7 and 9.6 Å for the total “thickness” of the molecules when viewed along an edge and across a face, respectively, values that agree well with calculated data.⁸⁴ The chemisorption of T_8H_8 on the $\text{Si}(1\ 0\ 0)\text{-}2 \times 1$ surface allows individual molecules to be imaged, and binding through a single vertex is found in this case.⁸⁵ The nature of the binding of T_8H_8 to the $\text{Si}(1\ 0\ 0)\text{-}2 \times 1$ surface has also been studied by reflection absorption IR spectroscopy⁸⁶ and X-ray photoemission spectroscopy.⁸⁷ Interactions of T_8H_8 with gold surfaces have also been studied by the same methods and show that chemisorption occurs to form a single Au–Si bond at a vertex of the POSS molecule.⁸⁸

The structure of T_8H_8 has been the subject of numerous computational studies,^{14,37,38,71a,77,89} not only because it is the parent compound for the increasingly popular T_8 POSS molecules, but also because it is analogous to the well-known double four ring (D4R) found in A-type zeolites.⁹⁰ Some selected computational data are given in Table 4. [The structures of the analogous carbon and germanium compounds $\text{C}_8\text{O}_{12}\text{H}_8$ and $\text{Ge}_8\text{O}_{12}\text{H}_8$ have also been calculated for

Table 4 Selected structural parameters for T_8H_8

Bond or angle	X-ray diffraction ^a		Neutron diffraction ^b		Calculated	
	Range	Mean	Range	Mean	Value	Method and software
Si–O (Å)	1.6168(11)– 1.6195(7)	1.618 1.621 ^c	1.623(2)– 1.628(2)	1.625	1.599–1.607 1.620 1.630 1.640 1.592 1.620	DFT ^d DFT LDA PP ^e HF 6-31G(d) ^f DFT MP2 ^g MM, UFF ^h
					CTR ⁱ	
Si–H (Å)	–	–	1.459(5)– 1.463(3)	1.461 1.36(2) ^c	1.451–1.455 1.510 1.457 1.460 1.470 1.4760	DFT ^d DFT LDA PP ^e HF 6-31G(d) ^f DFT MP2 ^g MM, UFF ^h
						CTR ⁱ
Si–O–Si (°)	147.49(6)– 147.60(7)	147.54 147.18 ^c	147.25(13)– 147.45(13)	147.35	147.8–149.3 148.6 149.0 148.2 146.8 146.80	DFT ^d DFT LDA PP ^e HF 6-31G(d) ^f DFT MP2 ^g MM, UFF ^h
						CTR ⁱ
O–Si–O (°)	109.41(5)– 109.66(5)	109.5 109.39 ^c	109.14(10)– 109.53(10)	109.38	107.0–112.2 109.4 109.0 109.6 110.0 109.73	DFT ^d DFT LDA PP ^e HF 6-31G(d) ^f DFT MP2 ^g MM, UFF ^h
						CTR ⁱ
O–Si–H (°)	–	–	109.07(14)– 109.86(14)	109.56	108.6–110.2 109.3	DFT ^d DFT MP2 ^e
Si...Si body diagonal of cube (Å)	5.381(1)– 5.390(2)	5.386 5.389 ^c	5.401(3)– 5.408(5)	5.405		
Si...Si across face of cube (Å)	3.575(1)– 3.883(1)	3.729 3.727 ^c	3.546(2)– 3.927(2)	3.736		
Si...Si cube edge (Å)	3.109(1)– 3.108(1)	3.108 3.109 ^c	3.117(2)– 3.121(2)	3.119		

^aAt 100 K, Ref. (82).^bAt 9.5 K, Ref. (83).^cAt 29 K, Ref. (83).^dDFT GGA-PW91 ultrasoft PP-PW, CASTEP, Ref. (89f).^eDFT LDA PP, Ref. (89c).^fHF 6-31G(d), GAMESS, Ref. (38).^gDFT MP2 B3LYP 6-31G**, Ref. (89e).^hMM, UFF, molecular mechanics, universal force field, Ref. (14).ⁱCharge transfer reactive force field, Ref. (92).

comparison.]^{89,91} A comparison of various computational methods for the calculation of T_8H_8 geometrical parameters has been made¹⁴ which shows that the molecular mechanics (MM) universal force field (UFF) gives results closest to those observed experimentally. A comparison of force fields for the molecular simulation of physical properties (melting points, unit cell parameters, IR spectra) of POSS species has also been made. A variety of force fields gave reasonable results with the best results being obtained for the Hybrid-COMPASS and charge transfer reactive (CTR) methods.⁹² There is also a C_{2v} isomer possible for the T_8H_8 formula but although it has been the subject of a computational study, it does not seem to have been prepared experimentally.³⁷

The electronic nature of T_8H_8 (and other simple alkyl substituted T_8R_8 species) has been investigated experimentally by UV absorption and photoluminescence^{59,93} and by photoelectron spectroscopy.⁹⁴ The photoluminescence spectra show an intense absorption band at about 6 eV and two intense emission bands, one at about 3.7 eV, attributed to an intermolecular interaction and a second at about 4.2 eV attributed to charge transfer from the cage to the substituent.⁹³ The electronic structure of T_8H_8 has also been the subject of several computational studies. The highest occupied molecular orbital (HOMO) for T_8H_8 is calculated to be the only orbital of A_{2g} symmetry and to be an oxygen lone pair, while the lowest unoccupied molecular orbital (LUMO) is a combination of Si, O, and H atomic orbitals, with a HOMO–LUMO gap of about 6.2–7.4 eV (the earlier value given of 12–14 eV is thought to be too large).^{37,38,91,94}

The 1H NMR spectrum for T_8H_8 displays a single peak at 4.20 ppm ($^1J_{H-Si} = 341$ Hz) characteristic of Si–H protons, while the solid state and solution ^{29}Si NMR spectra each show a single peak at –83.86 and –84.73 ppm, respectively, showing that any difference in the environment of the silicon atoms (particularly in the solid state) is not resolvable.⁷⁸ The mass spectrum of T_8H_8 has also been reported.⁷⁸

The transport and thermodynamic properties of T_8H_8 and T_8Me_8 have been calculated using molecular dynamics methods for both polydimethylsiloxane and hexadecane solutions at various temperatures. The results show that both solvents are “poor” and that the POSS species are attracted to each other.⁹⁵ These results have implications in the processing of POSS materials as building blocks in nanocomposites materials. Thermal stability studies have shown that T_8H_8 is quite stable up to 300 °C as shown by ^{29}Si NMR and IR spectroscopic studies and powder XRD. Above 600 °C, it is thought that the cubic structure undergoes cage-opening accompanied by the elimination of H_2 to form an amorphous material.^{78,96}

3. Reactivity and applications

The chemistry of T_8H_8 has been investigated by many research groups as, although its synthesis is low yielding, it is readily available in gram quantities and it provides a convenient precursor to very much more elaborate T_8 derivatives. It should be noted that, although T_8H_8 is conveniently handled in the air, it is thought to undergo slow reaction with atmospheric moisture to give silanol species that can then condense to give dimeric POSS species.⁹⁷ The POSS core in T_8H_8 is stable toward dilute acid but is susceptible to attack by base (MeOLi and

MeONa both attack the POSS core),⁹⁸ the hydrolysis being calculated to be endothermic with a calculated energy significantly dependent on the method of calculation.^{37,38} The reactivity of T_8H_8 appears to be lower than expected when compared with simple silanes such as $(MeO)_3Si-H$ which may be due to the steric bulk and relative rigidity of the POSS cage.⁹⁹

The application of T_8H_8 in hydrosilylation reactions (Figure 9) was first reported by Herren et al. who described the reaction with 1-hexene or methylenecyclohexane in the presence of H_2PtCl_6 in 2-propanol solution giving products in quantitative yields (Table 5, entries 6 and 15).

The preparation of octa-functionalized products was then pursued by Bassindale et al. who used the same catalytic system to hydrosilylate a series of nonfunctionalized alkenes. IR and ^{29}Si NMR spectroscopies showed that the reaction was complete and gave single products. Indeed, since silicon has a very strong directing effect, only α -addition products were obtained (Table 5, entries 7, 12–14). These authors also reported the reaction with alkenyl- and allyl-siloxanes $CH_2=CH(CH_2)_3OSiMe(OSiMe_3)_2$, $CH_2=CHSiMe_2(OSiMe_2)_3Bu$, and $CH_2=CHCH_2SiMe_2(OSiMe_2)_3Bu$, respectively, giving POSS with siloxane arms (Table 5, entries 19–21). However, in the case of the second of these alkenyl-siloxanes ^{29}Si NMR spectroscopy showed that several Si environments were present, indicating that both α - and β -additions occurred along with the formation of a T_8 -dimer arising from H/alkenyl exchange during the hydrosilylation process (Figure 10 and Table 5, entry 20). In the case of the allyl-siloxane, good regioselectivity was observed but some of the corresponding T_8 -dimer was also observed (*via* H/allyl exchange) (Table 5, entry 21).

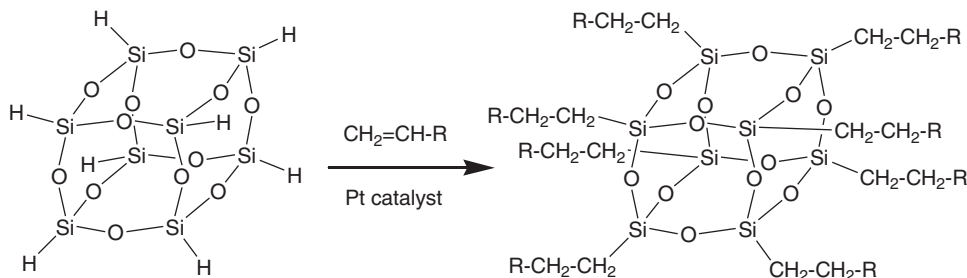


Figure 9 Catalyzed hydrosilylation of T_8H_8 .

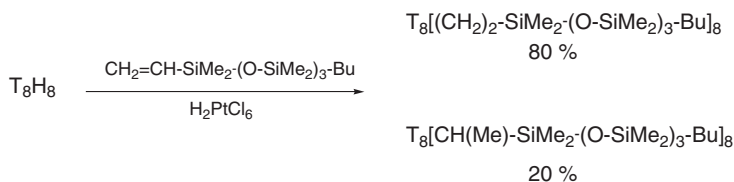


Figure 10 α - and β -additions to T_8H_8 .

Table 5 T₈R₈ compounds obtained from hydrosilylation of T₈H₈

Entry	R	Starting materials	Yield (%)	²⁹ Si NMR ^a	Reference
1	-C ₂ H ₅	T ₈ H ₈ +CH ₂ =CH ₂ , H ₂ PtCl ₆	89	-65.74	104
2	- <i>n</i> -C ₃ H ₇	T ₈ H ₈ +CH ₂ =CHCH ₃ , H ₂ PtCl ₆	76	-66.93	104
3	- <i>n</i> -C ₄ H ₉	T ₈ H ₈ +CH ₂ =CHC ₂ H ₅ , H ₂ PtCl ₆	76	-66.64	104
4	- <i>n</i> -C ₅ H ₁₁	T ₈ H ₈ +CH ₂ =CHC ₃ H ₇ , H ₂ PtCl ₆	87	-66.63	104
5	- <i>n</i> -C ₆ H ₁₃	T ₈ H ₈ +CH ₂ =CHC ₄ H ₉ , H ₂ PtCl ₆	97	-66.63	104
6	- <i>n</i> -C ₆ H ₁₃	T ₈ H ₈ +CH ₂ =CHC ₄ H ₉ , H ₂ PtCl ₆	90	-	105
7	- <i>n</i> -C ₆ H ₁₃	T ₈ H ₈ +CH ₂ =CHC ₄ H ₉ , H ₂ PtCl ₆	-	-66.6	106
8	- <i>n</i> -C ₇ H ₁₅	T ₈ H ₈ +CH ₂ =CHC ₅ H ₁₁ , H ₂ PtCl ₆	92	-66.63	104
9	- <i>n</i> -C ₈ H ₁₇	T ₈ H ₈ +CH ₂ =CHC ₆ H ₁₃ , H ₂ PtCl ₆	87	-66.64	104
10	- <i>n</i> -C ₉ H ₁₉	T ₈ H ₈ +CH ₂ =CHC ₇ H ₁₅ , H ₂ PtCl ₆	87	-66.64	104
11	- <i>n</i> -C ₁₀ H ₂₁	T ₈ H ₈ +CH ₂ =CHC ₈ H ₁₇ , H ₂ PtCl ₆	94	-66.65	104
12	- <i>n</i> -C ₁₀ H ₂₁	T ₈ H ₈ +CH ₂ =CHC ₈ H ₁₇ , H ₂ PtCl ₆	-	-	106
13	- <i>n</i> -C ₁₄ H ₂₉	T ₈ H ₈ +CH ₂ =CHC ₁₂ H ₂₅ , H ₂ PtCl ₆	-	-66.7	106
14	- <i>n</i> -C ₁₈ H ₃₇	T ₈ H ₈ +CH ₂ =CHC ₁₆ H ₃₃ , H ₂ PtCl ₆	-	-	106
15	-CH ₂ - <i>c</i> -C ₆ H ₁₁	T ₈ H ₈ +methylcyclohexane, H ₂ PtCl ₆	90	-	105
16	-(CH ₂) ₂ - <i>c</i> -C ₆ H ₁₁	T ₈ H ₈ +CH ₂ =CH- <i>c</i> -C ₆ H ₁₁ , H ₂ PtCl ₆	74	-	107
17	-(CH ₂) ₃ Ph	T ₈ H ₈ +CH ₂ =CHCH ₂ Ph, H ₂ PtCl ₆	93	-65.96	108
18	-(CH ₂) ₃ SiMe ₃	T ₈ H ₈ +CH ₂ =CHCH ₂ SiMe ₃ , H ₂ PtCl ₆	93	-66.37	108
19	-(CH ₂) ₅ OSiMe(OSiMe ₃) ₂	T ₈ H ₈ +CH ₂ =CH(CH ₂) ₃ -OSiMe(OSiMe ₃) ₂ , H ₂ PtCl ₆	Quantitative	7.1, -57.1, -66.7	109
20	-(CH ₂) ₂ SiMe ₂ (OSiMe ₂) ₃ Bu (80% α -product), -CHMeSiMe ₂ (OSiMe ₂) ₃ Bu (20% β -product)	T ₈ H ₈ +CH ₂ =CHSiMe ₂ (OSiMe ₂) ₃ Bu, H ₂ PtCl ₆	-	-65, -69	106
21	-(CH ₂) ₃ SiMe ₂ (OSiMe ₂) ₃ Bu (100% α -product)	T ₈ H ₈ +CH ₂ =CHCH ₂ SiMe ₂ (OSiMe ₂) ₃ Bu, H ₂ PtCl ₆	-	-67.4	106

^aReferenced to SiMe₄.

This work was followed by Bolln et al. who treated T_8H_8 with a series of nonfunctionalized alkenes in the presence of H_2PtCl_6 as a catalyst, in toluene solutions or directly in bulk in the case of less volatile alkenes. The corresponding $T_8[alkyl]_8$ were obtained with good yields and selectivity (Table 5, entries 1–5, 8–11). This method gives much better yields than the hydrolysis of organotrichloro- or trialkoxy-silanes previously used by Olsson (yields from 37 to 44% for ethyl to *n*-butyl) or later by Bassindale¹⁰⁰ (yields from 44 to 65% for *n*-hexyl and *n*-octyl) for the preparation of $T_8[alkyl]_8$ species, but it does rely on the use of T_8H_8 .¹⁰¹ The thermal properties of these alkyl-based POSS have been studied and it was shown that the melting point tends to decrease with longer alkyl chains (212 °C for $T_8[nC_3H_7]_8$ and 60.5 °C for $T_8[nC_{10}H_{21}]_8$) indicating, that for short chains, the cubic unit determines the packing of the molecules whereas for longer chains the flexibility controls the packing in a layered type. This effect of a gradual increase of the organic chain length on the thermal stability is of interest since this series can act as model compounds for other silsesquioxanes. It should be noted that $T_8[nC_3H_7]_8$ has been used as an inorganic phase in polymer nanocomposites with its introduction into a polystyrene matrix.¹⁰² Rikowski et al. have shown that the preparation of higher cage analogs of most of these $T_8[alkyl]_8$ cubes is possible by partial catalyzed cage rearrangements. For example, $T_8[C_2H_5]_8$ gives a mixture of $T_{10}[C_2H_5]_{10}$ and $T_{12}[C_2H_5]_{12}$ in 55 and 4% yield (41% is unreacted starting material) in the presence of K_2CO_3 in refluxing acetone. Other $T_8[alkyl]_8$ give only their corresponding $T_{10}[alkyl]_{10}$ products in low yields (<18%) (Figure 11).¹⁰³

Hydrosilylation has also been shown to be an efficient way to introduce functionalized arms using vinyl or allyl compounds bearing functions that can be useful for further applications in the field of materials chemistry. For example, Dittmar et al. have treated T_8H_8 with various allyl derivatives, using H_2PtCl_6 or $Pt(cyclooctadiene; COD)Cl_2$ as catalysts, giving alkoxy, epoxy, or cyano functionalized POSS in high yields (Table 6, entries 2–6). Bassindale et al. have studied the reactivity of T_8H_8 with pentenol and found that depending on the catalyst, activation occurs either at the vinyl group, in the presence of H_2PtCl_6 , or at the alcohol function, in the presence of Et_2NOH (the reaction of hydrosilanes with alkenylalcohols is well known to give hydroxyl- and vinyl-terminated products)¹¹⁰ (Table 6, entries 7 and 8). Using this reactivity of the OH group,

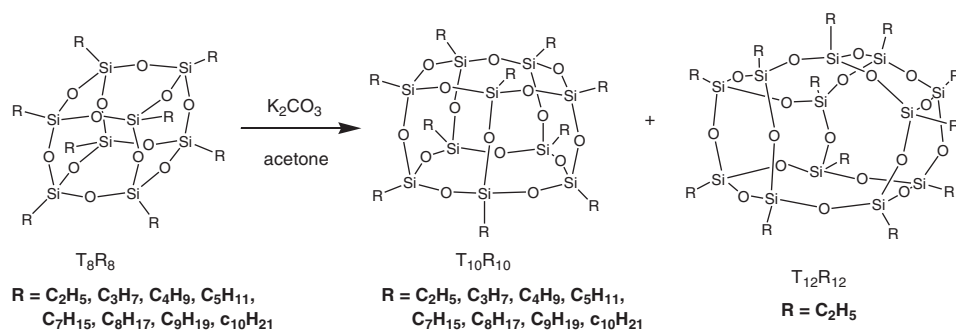


Figure 11 Base-catalyzed cage rearrangement of alkyl silsesquioxanes.

Table 6 Functionalized T₈R₈ compounds obtained from T₈H₈

Entry	R	Starting materials	Yield (%)	²⁹ Si NMR ^a	Reference
1	-(CH ₂) ₂ CMMe ₂ OH	T ₈ H ₈ +CH ₂ =CHCMe ₂ OH, H ₂ PtCl ₆	62	-64.9	111
2	-(CH ₂) ₃ - <i>p</i> -MeOC ₆ H ₄	T ₈ H ₈ +CH ₂ =CH-CH ₂ - <i>p</i> -MeOC ₆ H ₄ , H ₂ PtCl ₆	97	-65.76	108
3	-(CH ₂) ₃ OPh	T ₈ H ₈ +CH ₂ =CH-CH ₂ OPh, Pt(COD)Cl ₂	79	-65.85	108
4	-(CH ₂) ₃ OCH ₂ CH(O)CH ₂	T ₈ H ₈ +allylglycidyl ether, Pt(COD)Cl ₂	24	-65.81	108
5	-(CH ₂) ₃ CN	T ₈ H ₈ +CH ₂ =CHCH ₂ CN, Pt(COD)Cl ₂	93	-67.76	108
6	-(CH ₂) ₃ C ₆ F ₅	T ₈ H ₈ +CH ₂ =CHCH ₂ C ₆ F ₅ , H ₂ PtCl ₆	98	-66.21	108
7	-O-(CH ₂) ₃ CH=CH ₂	T ₈ H ₈ CH ₂ =CH(CH ₂) ₃ OH, Et ₃ NOH	-	-103	109
8	-(CH ₂) ₅ OH	T ₈ H ₈ +CH ₂ =CH(CH ₂) ₃ OH, H ₂ PtCl ₆	-	-	109
9	-(CH ₂) ₄ CH(O)CH ₂	T ₈ H ₈ +CH ₂ =CH(CH ₂) ₃ -CH(O)CH ₂ , Pt(dvs)	100	-66.0, -67.0, -68.5	112,115
10	-(CH ₂) ₅ OC ₆ H ₄ - <i>p</i> -CNC ₆ H ₄	T ₈ H ₈ +CH ₂ =CH-(CH ₂) ₃ OC ₆ H ₄ - C ₆ H ₄ CN, H ₂ PtCl ₆ ·6H ₂ O	52	-66.7	113
11	-(CH ₂) ₅ OC ₆ H ₄ - <i>p</i> -MeOC ₆ H ₄	T ₈ H ₈ +CH ₂ =CH(CH ₂) ₃ OC ₆ H ₄ - <i>p</i> - MeOC ₆ H ₄ , H ₂ PtCl ₆ ·6H ₂ O	66	-66.6	113
12	-(CH ₂) ₅ OC ₆ H ₄ -N=N- <i>p</i> -CNC ₆ H ₄	T ₈ H ₈ +CH ₂ =CH(CH ₂) ₃ OC ₆ H ₄ - N=N- <i>p</i> -CNC ₆ H ₄ , H ₂ PtCl ₆ ·6H ₂ O	50	-66.7	113
13	-(CH ₂) ₆ OH	T ₈ H ₈ +CH ₂ =CH-(CH ₂) ₄ OH, H ₂ PtCl ₆ ·6H ₂ O	49	-65.8	114
14	-(CH ₂) ₂ O(CH ₂) ₂ OCH=CHMe	T ₈ H ₈ +CH ₂ =CHO(CH ₂) ₂ O- CH=CHMe, Pt(dvs)	100	-68.5	115
15	-(CH ₂) ₂ O(CH ₂) ₂ O(CH ₂) ₂ OCH ₂ - 3- <i>c</i> -C ₆ H ₅	T ₈ H ₈ +CH ₂ =CHO(CH ₂) ₂ OCH ₂ -3- <i>c</i> - C ₆ H ₅ , Pt(dvs)	-	-68.5	115
16	-CH ₂ CHMe-C ₆ H ₄ -CMMe ₂ NCO	T ₈ H ₈ +CH ₂ =CMMe-C ₆ H ₄ -CMMe ₂ NCO	-	-	116

^aReferenced to SiMe₄.

$T_8[O(SiMe_2O)_3SiMe_3]_8$ has also been prepared by the reaction of T_8H_8 with the silanol $Me_3Si(OSiMe_2)_3OH$ in the presence of Et_2NOH .¹⁰⁹ Other functionalized products have been prepared in relatively good yields giving materials having liquid crystal properties (Table 6, entries 10–12) or polymer precursor compounds (Table 6, entries 13 and 14).

It is also possible to prepare POSS species with halogen-terminated substituents using hydrosilylation in good-to-excellent yields (see Table 7). For example, Liu and Dare have prepared a wide range of bromo- and chloro-terminated compounds with long alkyl chains using H_2PtCl_6 or Pt/C as catalysts (Table 7, entries 2–7). Dare et al. have studied the hydrosilylation of a chlorohexyne; however, two isomers were obtained which could not be separated (Table 7, entry 8).

Relatively few reactions other than hydrosilylation have been performed on T_8H_8 . Feher et al. found that T_8H_8 reacts with a series of Si, Sb, or Sn reagents to give products having Si–O–M groups (M = Si, Sb, or Sn) that are of fundamental interest in studies of spherosilicates as models for siliceous materials. For example, the reaction with $Me_3SiOSbMe_4$ in benzene gives $T_8[OSiMe_3]_8$, while the reaction with $(Me_3Sn)_2O$ gives $T_8[OSnMe_3]_8$ (Figure 12) that further reacts with $Me_3SiOSbMe_4$ to lead to the antimony-containing $T_8[OSbMe_4]_8$ (Table 8, entries 4, 8, and 9). The first octasilsesquioxane in which eight metals are directly bound to the silicon corners was reported by Rattay et al. who treated T_8H_8 with four equivalents of $Co_2(CO)_8$ to give $T_8[Co(CO)_4]_8$ (Figure 12), which was characterized by single-crystal XRD (Table 8, entry 12). Since this last compound could be seen as a model for silica-supported transition metal catalysts, its catalytic activity in the hydroformylation of 1-hexene in presence of Ph_3P was

Table 7 Halogen-terminated T_8R_8 compounds obtained from T_8H_8

Entry	R	Starting materials	Yield (%)	Reference
1	$-(CH_2)_3-Br$	$T_8H_8 + CH_2=CH-CH_2Br$, H_2PtCl_6	57	117
2	$-(CH_2)_4-Br$	$T_8H_8 + CH_2=CH-(CH_2)_2Br$, Pt/C	90	118
3	$-(CH_2)_5-Br$	$T_8H_8 + CH_2=CH-(CH_2)_3Br$, Pt/C	99	118
4	$-(CH_2)_6-Cl$	$T_8H_8 + CH_2=CH-(CH_2)_4Cl$, H_2PtCl_6	98	118
5	$-(CH_2)_7-Br$	$T_8H_8 + CH_2=CH-(CH_2)_5Br$, H_2PtCl_6	90	118
6	$-(CH_2)_8-Br$	$T_8H_8 + CH_2=CH-(CH_2)_6Br$, H_2PtCl_6	96	118
7	$-(CH_2)_2-O-(CH_2)_2-Cl$	$T_8H_8 + CH_2=CHO(CH_2)_2Cl$, H_2PtCl_6	98	118
8	Mixture of $-CH=CH(CH_2)_4Cl$ and $-C(=CH_2)(CH_2)_4Cl$	$T_8H_8 + CH\equiv C(CH_2)_4Cl$, H_2PtCl_6	–	107

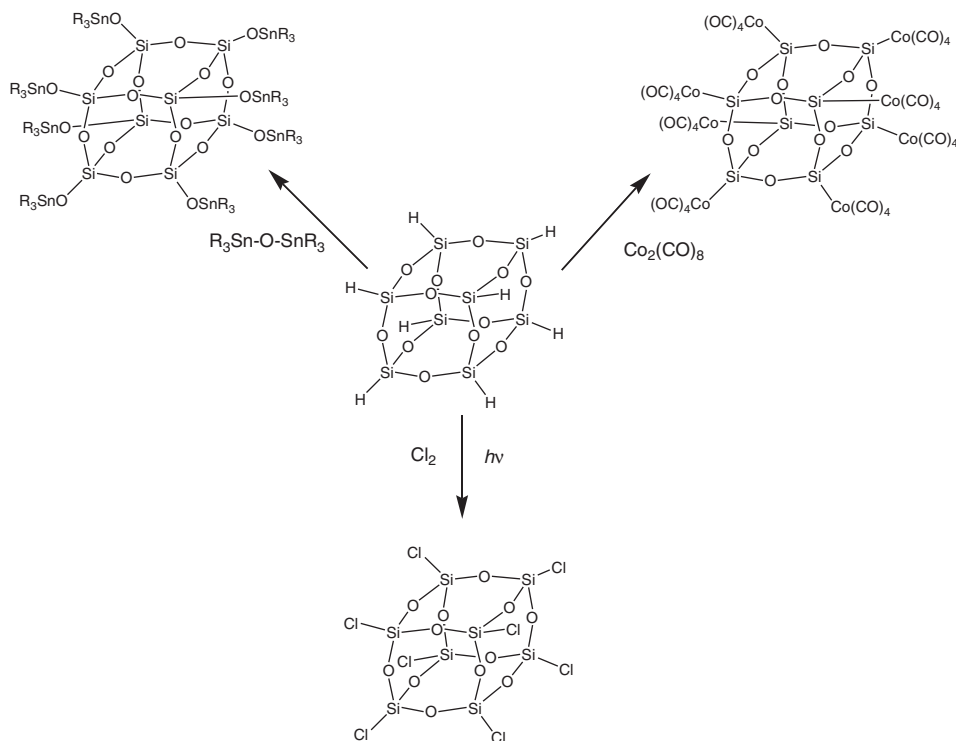


Figure 12 Examples of reactions of T_8H_8 .

assessed and it was shown that a higher chemoselectivity was obtained compared to the case of $Co_2(CO)_8$.¹¹⁹

In the course of the synthesis of building blocks for the preparation of silicas, Day et al. reported the synthesis of $T_8[OMe]_8$ using T_8Cl_8 as an intermediate (Table 8, entries 2 and 3) (attempts to alkylate directly the $T_8[O^-]_8$ silicate anion (see Section V.E) were unsuccessful). The octachloride was prepared by UV irradiation of T_8H_8 in a Cl_2 atmosphere and was obtained in high yield (it appears to be the only Si-halogen T_8 compound known to date). T_8Cl_8 then reacts with $MeNO_2$ or $HC(OMe)_3$ in a sealed tube to give the desired $T_8[OMe]_8$ in 46% yield. This procedure allowed the conversion of the Si-H bonds to Si-OMe without breaking the Si-O bonds of the cube by avoiding high polar reagents. $T_8[OMe]_8$ was used as a precursor for the formation of silica by sol-gel polymerization under neutral conditions. The xerogels obtained have shown to have a much higher surface area ($900\text{ m}^2\text{ g}^{-1}$) than the ones obtained classically from $Si(OEt)_4$ ($500\text{ m}^2\text{ g}^{-1}$). This difference was attributed to the symmetrical, rigid structure of the POSS precursor.¹²⁰ It has also been reported that T_8H_8 undergoes insertion of a carbene, derived from irradiation of a diazoacetate, into the Si-H bond.¹²¹

The vast majority of reactions of T_8H_8 give products in which all eight hydrogen atoms have been substituted to give T_8R_8 type products. Attempts to prepare partially substituted compounds such as T_8H_7R or $T_8H_6R_2$ are fraught

Table 8 Compounds T_8R_8 obtained from T_8H_8 via reactions other than hydrosilylation

Entry	R	Starting materials and conditions	Yield (%)	^{29}Si NMR ^a	Reference
1	-D	$T_8H_8 + D_2$, Pd/C	90	–	72a
2	-Cl	$T_8H_8 + Cl_2$, CCl_4 , UV activation	95	–91.16	98,120
3	-OMe	$T_8[Cl]_8 + MeNO_2$ or $HC(OMe)_3$	46	–101.40	98,120
4	-OSiMe ₃ ^b	$T_8H_8 + Me_3SiOSbMe_4$	Quantitative	–	122
5	-OSi(CD ₃) ₃	$T_8H_8 + (CD_3)_3SiCl \cdot Me_3NO$	–	–	123
6	-OSiMe ₂ CH=CH ₂	$T_8H_8 + CH_2=CHMe_2SiCl \cdot Me_3NO$	87	–109.03	124
7	-OSiMe ₂ CH ₂ Cl	$T_8H_8 + CH_2ClMe_2SiCl \cdot Me_3NO$	46	–109.33	124
8	-OSnMe ₃	$T_8H_8 + (Me_3Sn)_2O$	54	–101.55	122
9	-OSbMe ₄	$T_8[OSnMe_3]_8 + Me_3Si-O-SbMe_4$	60	–104.33	122
10	-OSnBu ₃	$T_8H_8 + (Bu_3Sn)_2O$	95	–101.0	125
11	-OTiClCp ₂	$T_8[OSnMe_3]_8 + Cp_2TiCl_2$	84	–106.34	125
12	-Co(CO) ₄	$T_8H_8 + Co_2(CO)_8$	87	–55	119

^aPOSS cage Si only, referenced to SiMe₄.^bFor an alternative synthesis see Section V.E.

with the problems of the formation of mixtures and the formation of isomers when more than one substituent other than H is present. Despite these problems, some mono-substituted compounds T_8H_7R have been prepared *via* reactions used for preparing octa-substituted compounds, high-dilution methods and chromatographic separation of mixtures. Mono-substituted compounds such as T_8H_7R have been reviewed^{121,126} and T_8H_7Ph and $T_8H_6Ph_2$ have been the subject of computational studies.^{89f} Calzaferri and Imhof¹²⁷ studied the mono-functionalization of T_8H_8 by its reaction with one equivalent of vinylferrocene using catalytic H_2PtCl_6 in refluxing toluene leading to $T_8H_7[(CH_2)_2-C_5H_4-Fe-C_5H_5]$ in 14% yield, which was the first organometallic mono-substituted octanuclear silsesquioxane. The disubstituted metallasilane $T_8H_6[Co(CO)_4]_2$ has been isolated from the reaction between T_8H_8 and $Co_2(CO)_8$.⁹⁹ Sellinger et al. have reported the synthesis of photochemically curable, liquid, epoxy-functionalized cubes by the reaction of T_8H_8 with allylglycidyl ether in toluene and in the presence of $Pt(\text{divinyltetramethyldisiloxane}; \text{dvs})$ as catalyst. The products, $T_8H_4[(CH_2)_3OCH_2CH(O)CH_2]_4$ and $T_8H[(CH_2)_3OCH_2CH(O)CH_2]_7$ were obtained in 95% yield as a mixture, but it was not possible to obtain the octa-substituted product. Photo-induced cationic polymerization of these compounds gave hybrid polymers.¹²⁸

In the field of polymer synthesis, Tsuchida et al. have treated T_8H_8 with 9,10-dibromo-1-decene in the presence of H_2PtCl_6 to give the mono-substituted compound $T_8H_7[(CH_2)_8CHBrCH_2Br]$. Further substitution was realized by reacting this compound with ethylene to give $T_8[C_2H_5]_7[(CH_2)_8CHBrCH_2Br]$. Final debromination by zinc leads to $T_8[C_2H_5]_7[(CH_2)_8CH=CHBrCH_2Br]$, which was then polymerized or copolymerized (with ethylene or propylene) in presence of methylaluminoxane-activated metallocenes to give two-dimensional polymers or copolymers, having pendant octasiloxane cubes, of high molecular weight.⁷⁵ Auner et al. have prepared polymers by reacting T_8H_8 with a diyne, $PhC\equiv C-C_6H_4-C\equiv CPh$, or vinylsiloxane $(CH_2=CHMe_2Si)_2O$ in the presence of a platinum catalyst in toluene. In these polymers, the cubic cores are separated by $PhCH=CH-C_6H_4-CH=CHPh$ or $CH_2CH_2Me_2SiOSiMe_2CH_2CH_2$ linkages.¹²⁹ A model compound (Figure 13) for this kind of unusual structure could be isolated by gel permeation chromatography and was characterized by X-ray

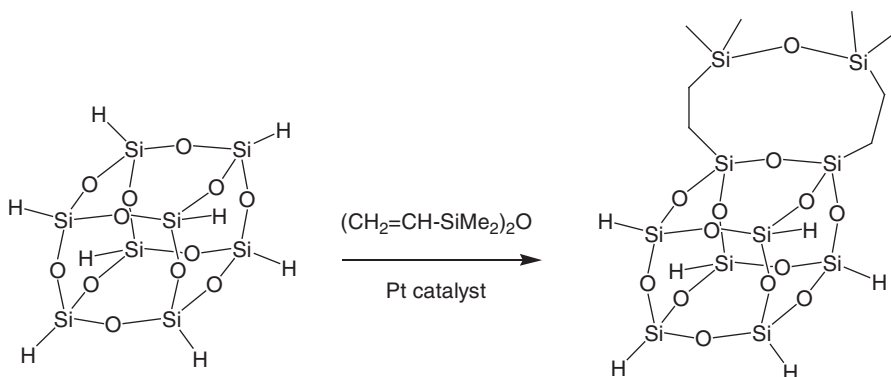


Figure 13 Formation of a disubstituted product by hydrosilylation of T_8H_8 .

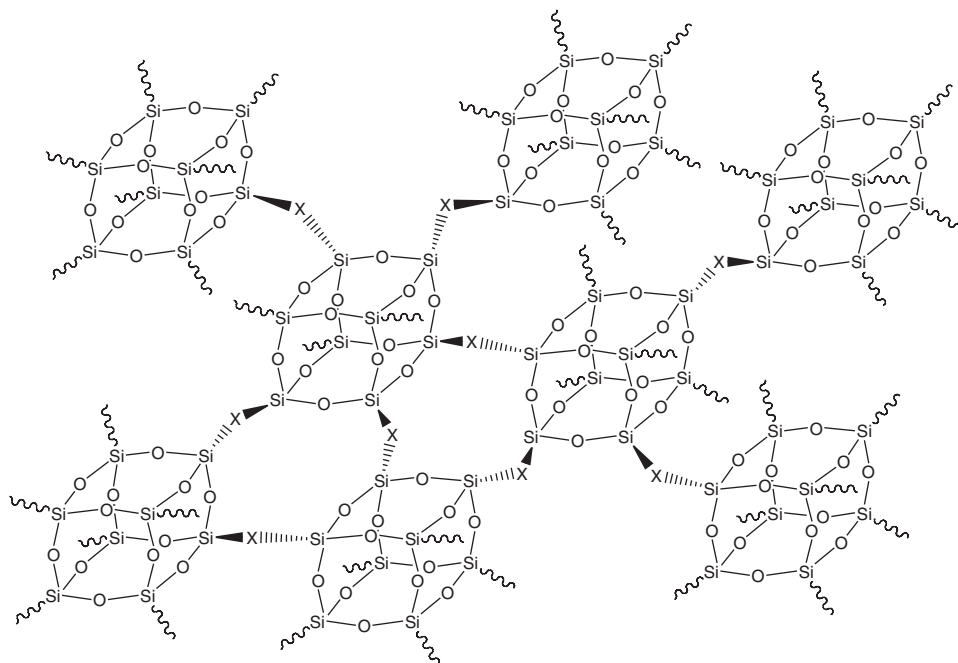


Figure 14 Polymeric three-dimensional network of T_8 cubes.

crystallography.¹²⁹ X-ray crystallographic studies have also been carried out on $T_8H_7[C_6H_{13}]$,¹³⁰ T_8H_7Ph ,¹³¹ and $T_8H_7[Co(CO)_4]$.¹³²

Laine and coworkers have prepared three-dimensional (meso)porous polymers with high surface area by reacting T_8H_8 with stoichiometric amounts of $T_8[CH=CH_2]_8$ or $T_8[OSiMe_2CH=CH_2]_8$ in presence of $Pt(dvs)$ in toluene (Figure 14). The cube moieties were separated by a 2- or 4-atom spacer, depending on the reactants, and the polymers have a degree of cross-linking of 43 and 66%, respectively, a surface area of $529 \text{ m}^2 \text{ g}^{-1}$ and a pore volume of 0.242 mL g^{-1} . It must be noted that the pore volume does not include the pores within the cubes due to their small size (3–4 Å).¹³³

Recently, T_8H_8 has been encapsulated within single-walled (SWNTs) and multiwalled carbon nanotubes (MWNTs) with internal diameters of 0.8–8 nm. It was shown that the best results were obtained when the internal diameters (1.4–1.5 nm for SWNTs and 1.0–3.0 nm for MWNTs) slightly exceeded the diameter of T_8H_8 (1.2 nm). T_8H_8 was introduced in the gas phase and reacted with the nanotubes through van der Waals interactions.¹³⁴

The search for chemical vapor deposition (CVD) precursors to silicon-containing materials in recent decades has led to studies on T_8H_8 which is conveniently volatile and thermally stable at temperatures in the range of 80–140 °C.¹³⁵ High-quality, smooth, amorphous SiO_2 has been deposited on Si using T_8H_8 in an oxygen atmosphere at temperatures in the range 450–525 °C.^{135,136}

A coating of T_8H_8 molecules on chromium, molybdenum, tungsten, iron, and nickel oxide surfaces has also been applied by CVD methods to give hydrophobic layers that are shown to comprise intact POSS cores chemisorbed on the surface.¹³⁷ Heating of T_8H_8 molecules on a silicon surface to 700 °C leads to loss of hydrogen but some Si–H groups are retained even at 850 °C.¹³⁸ Nicholson et al. have reported the chemisorption of T_8H_8 under ultra high vacuum onto a gold surface. The formation of a thick, hydrophobic 6 Å silicon oxide film occurs through a surprising Si–H activation by the gold surface giving Si–Au bonds (with the concomitant elimination of H_2), the cube being attached to the surface by one corner.^{88a} A similar phenomenon was observed in the case of the chemisorption of T_8H_8 onto a clean Si(100) surface.¹³⁹

The thermal degradation of T_8H_8 and other T_8R_8 species ($R = \text{Me}, i\text{Bu}, n\text{C}_8\text{H}_{17}, \text{Ph}$) in air and an inert atmosphere has been studied by thermogravimetric analysis and shows that for T_8H_8 incomplete sublimation tends to occur, and, in air, oxidation competes with volatilization.⁹⁶

Theoretical investigations of the insertion of N_2 and O_2 molecules into T_nH_n ($n = 8, 10, 12$) have been performed using *ab initio* methods (restricted HF theory). It was shown that in the case of T_8H_8 the energy required to overcome the insertion is close to the dissociation enthalpy of the Si–O bonds. However, in the case of $T_{12}H_{12}$, the insertion appears to be feasible. It was also found that T_8H_8 is more permeable toward O_2 than to N_2 and more selective toward permeability than $T_{12}H_{12}$ which has larger Si_5O_5 faces to accommodate incoming molecules.¹⁴⁰ Molecular dynamics studies of the interaction between T_8H_8 and a nearby NaCl to act as a charge dipole have been carried out in order to assess charge distributions in T_8H_8 and to develop a new reactive force field.¹⁴ The potential degradation of T_8H_8 by high- or low-energy impact from atomic oxygen has also been studied by *ab initio* molecular dynamics simulations which found that, unless very high energy atoms are used, the POSS cage remains intact, the predominant reaction being insertion of oxygen atoms into Si–H bonds to give silanol groups.¹⁴

As mentioned above, the structure of T_8H_8 is reminiscent of the D4R in zeolite frameworks and the work carried out on D4R species to investigate whether species can be incorporated inside the cage¹⁴¹ has led to similar studies on T_8H_8 and other POSS compounds. The most studied endohedral complexes of T_8H_8 (and T_8Me_8) are those with hydrogen and deuterium ($H@T_8H_8$ and $D@T_8H_8$) which have been the subject of both experimental and computational studies. The compounds can be prepared *via* ion-implantation methods and have been studied by EPR to investigate both the nature of the endohedral complex itself, and the detrapping mechanism.^{89e,89g,123,142} Although the cavity within a T_8 cage is not large, it is calculated to be large enough to accommodate both ionic and atomic guests other than hydrogen, Li^+ , Na^+ , K^+ , F^- , Cl^- , Br^- , He, Ne, and Ar, with endohedral complexes of both Li^+ and F^- being energetically favorable for T_8H_8 .⁹¹ These calculations also suggest that F^- might be introduced into the cage from outside without destroying it (endohedral complexes of F^- in other T_8 cages have been prepared and characterized, see Sections V.C and V.D).

C. Synthesis, properties, and reactions of T_8Ph_8 and its derivatives

This section concerns T_8Ph_8 and its derivatives formed by reactions on the phenyl rings. For other related compounds prepared from hydrolysis of the corresponding silanes (e.g., $T_8[tolyl]_8$) see the miscellaneous [Section V.I](#).

1. Synthesis

The synthesis of T_8Ph_8 was first described by Olsson in 1958 as a product from refluxing a solution of $PhSiCl_3$ in methanol in the presence of aqueous HCl, giving the product in low yield ([Table 9](#), entry 1). A significant improvement to this was made more recently by Bassindale et al. who developed a synthesis of various T_8R_8 cages from alkoxyisilanes using tetrabutylammonium fluoride (TBAF) as a catalyst, which in the case of T_8Ph_8 , gave 49% yield using $PhSi(OEt)_3$ after 1 day. In the course of this procedure the authors found that if they modified the work-up (evaporation of the solvent instead of precipitation) it was possible to isolate a new cage with different solubility properties to those of T_8Ph_8 . This new product, $[T_8Ph_8F][NBu_4]$, comprised a T_8Ph_8 cage encapsulating a fluoride ion, and a tetrabutylammonium cation, as confirmed by single-crystal XRD.¹⁴³ A more recent procedure described by Dare et al. based on the use of Amberlite IRA 400 resin as basic catalyst (the reaction failed with an acidic resin) gives T_8Ph_8 in 74% yield after an overnight reaction. Further improvements in yield have been achieved using different solvents (see [Table 9](#)), and high yields can be achieved if the initial hydrolysis product is treated with base to cause equilibration ([Table 9](#), entry 5).

2. Structure and physical properties

T_8Ph_8 is usually obtained as a white microcrystalline powder, sparingly soluble in the common solvents but slightly soluble in pyridine and in CH_2Cl_2 .¹⁵⁰ It has high thermal stability, losing 5% weight only on heating to above 436 °C^{147,150} and gives a high yield of ceramic residue when heated in nitrogen.⁹⁶ Thermodynamic properties such as the temperature dependence of the heat capacity, and the entropy of formation of T_8Ph_8 have also been measured.¹⁵¹ The cross-polarization magic angle spinning ^{29}Si NMR spectrum has been variously reported to displays

Table 9 Preparative methods for T_8Ph_8 and $[T_8Ph_8F]^-$

Entry	Starting materials and conditions	Yield (%)	Reference
1	$PhSiCl_3 + H_2O$, HCl, MeOH, 12 h	9	101
2	$PhSi(OEt)_3 + H_2O$, Bu_4NF in THF, CH_2Cl_2 , 1 day	49	100
3	$PhSiCl_3 + H_2O$, EtOAc, 14 h	70	144
4	$PhSiCl_3 + H_2O$, Amberlite IRA 400, EtOH, 12 h	74	145
5	$PhSiCl_3 + H_2O$, C_6H_6 , then $PhCH_2Me_3NOH$	88	146
6	$PhSiCl_3 + H_2O$, then trace KOH	ca. 90	147
7	$PhSi(OEt)_3 + H_2O$, EtOH+KOH	90	148
8	$PhSiCl_3 + H_2O$, C_6H_6 , 12 h	98	149
9	$[NBu_4][T_8Ph_8F]$: $PhSi(OEt)_3 + H_2O$, Bu_4NF in THF, 1 day	46	143

signals at -72.82 and -80.4 ppm,¹⁰⁰ -75.9 ppm,¹⁴⁸ and at -76.5 ppm.¹⁵² The ultraviolet,¹⁵³ infrared, and Raman^{150,154} spectra of T_8Ph_8 have also been reported.

The solid-state structure of T_8Ph_8 has been determined both as an acetone solvate, prepared by allowing a $PhSiCl_3/Me_2C=O/H_2O$ mixture to stand for a few days followed by recrystallization of the resulting solid from $CH_2Cl_2/Me_2C=O$,¹⁵⁵ and as a pyridine/*o*-dichlorobenzene solvate¹⁵⁶ (Figure 15). Early X-ray crystallographic studies of T_8Ph_8 described three forms for the structure, one triclinic ($Z = 1$) and one monoclinic ($Z = 2$),¹⁵⁷ and one rhombohedral,¹⁴⁶ which in the light of more recent studies may be due to differences in the method of crystallization. Pertinent structural data for T_8Ph_8 are presented in Table 10 and show that the Si–O bonds are of normal length, that the geometry at silicon is approximately tetrahedral and the Si–O–Si angles to be similar to those found in other T_8R_8 species (see Figure 15). Although the T_8 cage could be viewed as having an ideal cubic arrangement of Si atoms, the cube is, in fact distorted, the angles at oxygen in the acetone solvate range from $144.7(2)^\circ$ to $151.6(2)^\circ$ and in the aromatic solvent solvate from $143.9(3)^\circ$ to $156.6(4)^\circ$. This distortion is common in T_8 derivatives and is also seen in variations in the nonbonded Si \cdots Si distances, this feature is described in more detail in Section V.J. Lin et al. calculated the structural data for T_8Ph_8 using the DFT CASTEP method which

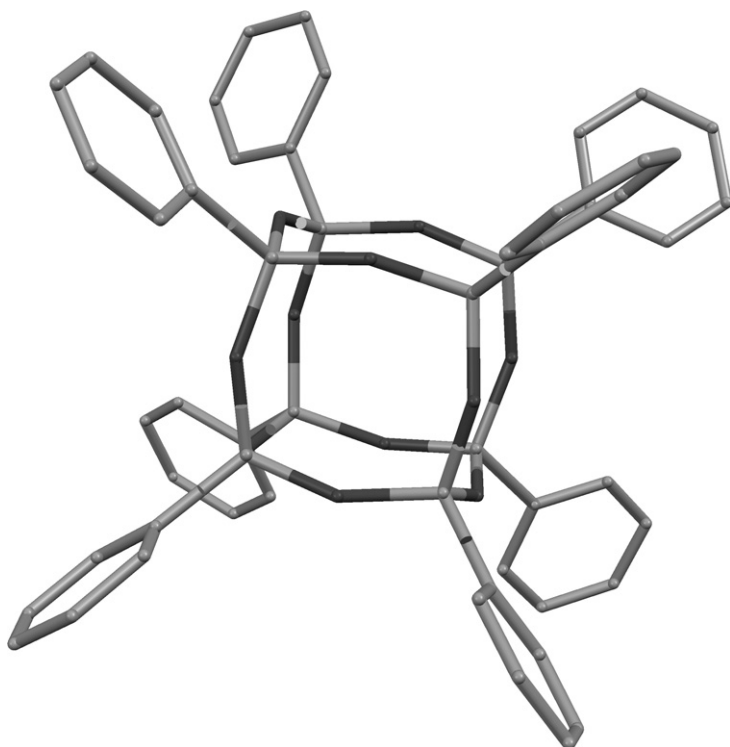
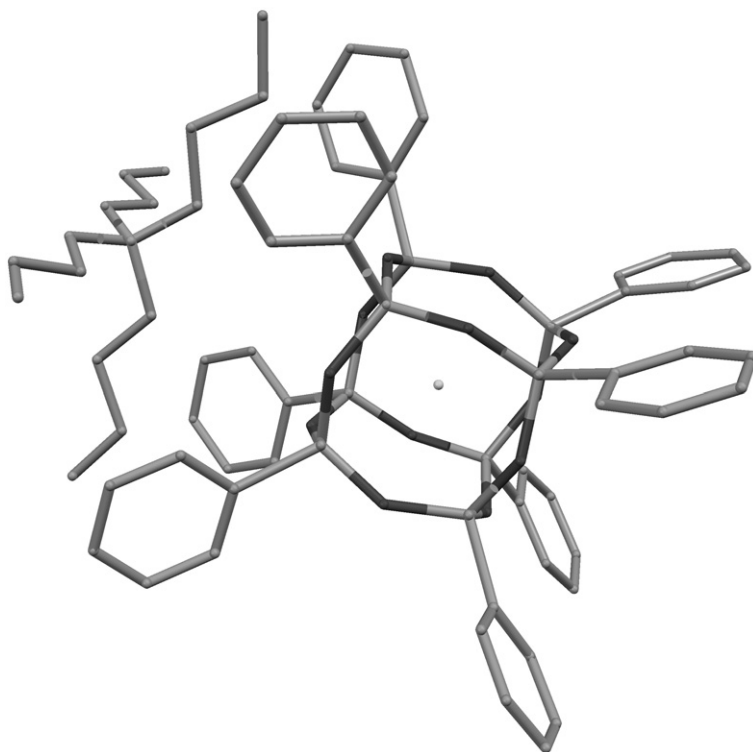


Figure 15 Structure of T_8Ph_8 . (Redrawn using data for structure OPSIOY from the Cambridge Crystallographic Data Centre.) H atoms are omitted for clarity.

Table 10 Selected structural data for T_8Ph_8 and $[T_8Ph_8F]^-$

	Si–O (Å)		Si–O–Si (°)		O–Si–C (°)	
	Range	Mean	Range	Mean	Range	Mean
T_8Ph_8 , acetone solvate ¹⁵⁵	1.606(3)–1.618(3)	1.612	144.7(2)–151.6(2)	149.2	108.3(2)–111.7(2)	109.9
T_8Ph_8 , pyridine/dichlorobenzene solvate ¹⁵⁶	1.606(5)–1.621(5)	1.614	143.9(3)–156.6(4)	149.2	–	–
$[T_8Ph_8F][NBu_4]$ ¹⁴³	1.6198(15)–1.6295(15)	1.6248	138.56(10)–143.88(10)	141.18	103.86(9)–107.00(9)	105.86
T_8Ph_8 , calculated data ^{a,89f}	1.603–1.614	1.609	145.4–152.8	149.5	108.1–111.8	110.1

^aGeometric optimization using CASTEP GGA-PW91.

**Figure 16** Structure of $[T_8Ph_8F][NBu_4]$. (Redrawn using data for structure OJUYIB from the Cambridge Crystallographic Data Centre.) H atoms are omitted for clarity.

reproduces the experimental data well (Table 10). The optimized structure has low symmetry because of the various orientations of the eight phenyl rings.^{89f}

The structural data of $[T_8Ph_8F][NBu_4]$ are also presented in Table 10 (see Figure 16 for the structure). The presence of the encapsulated fluoride ion makes

very little difference to the structure compared to T_8Ph_8 itself. The wider Si–O–Si angles indicate a pushing apart of the oxygen atoms by the fluoride ion. However, other data such as the small difference observed in the ^{29}Si NMR chemical shift (0.9 ppm upfield from T_8Ph_8) and the absence of any measurable Si–F coupling show that the interaction between the fluoride ion and the silicon atoms is small. Studies to evaluate the collision cross section of T_8Ph_8 using Na^+ show that the cation attaches itself to the outside of the POSS cage and does not significantly distort the structure.¹⁵⁸

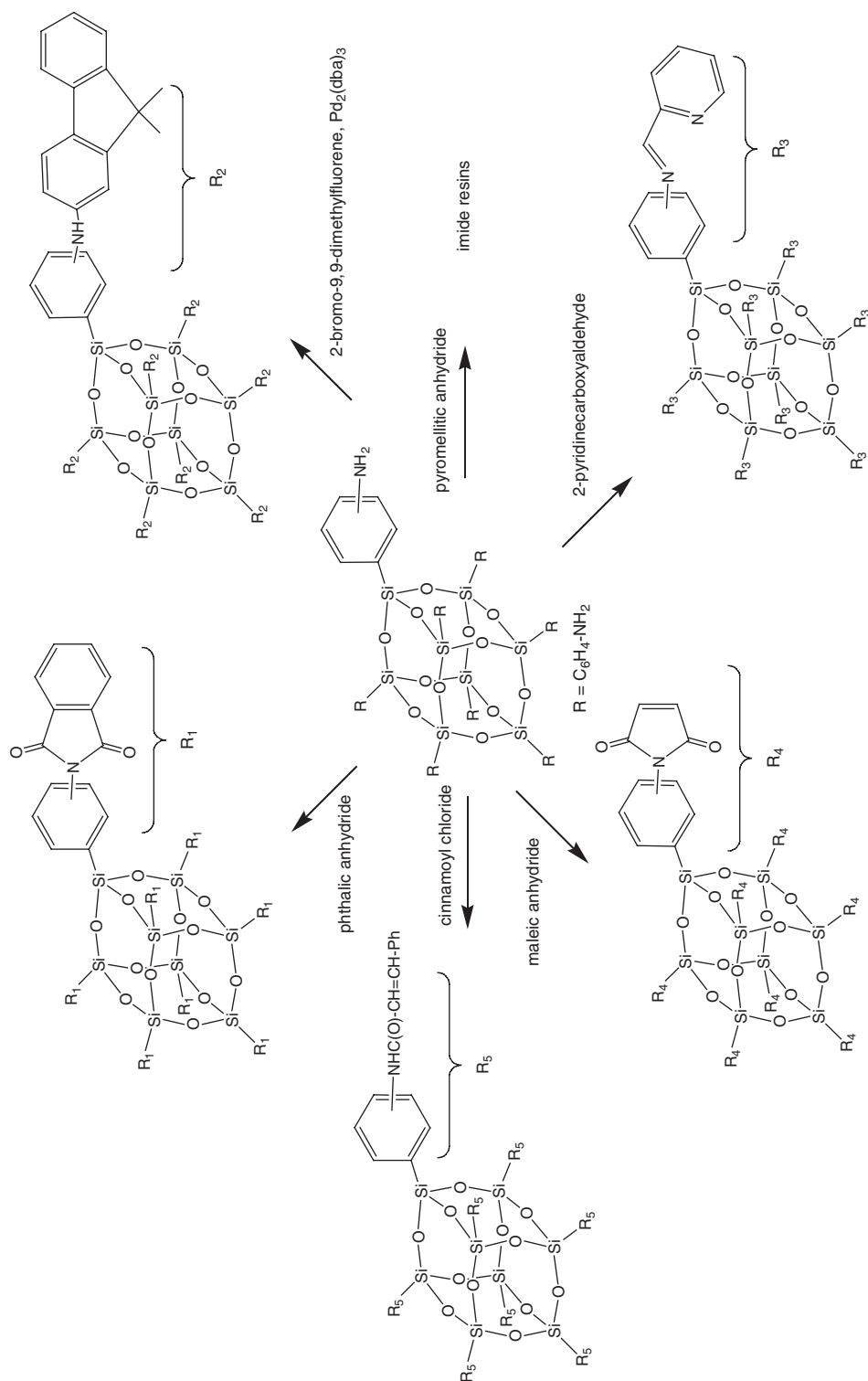
3. Reactivity and applications

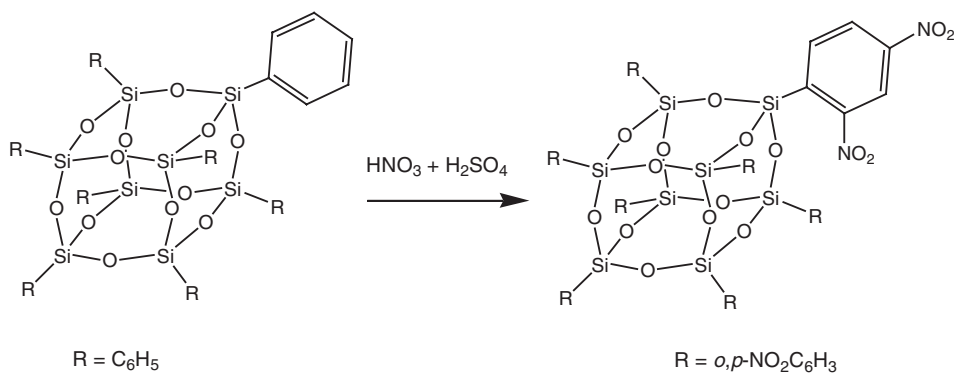
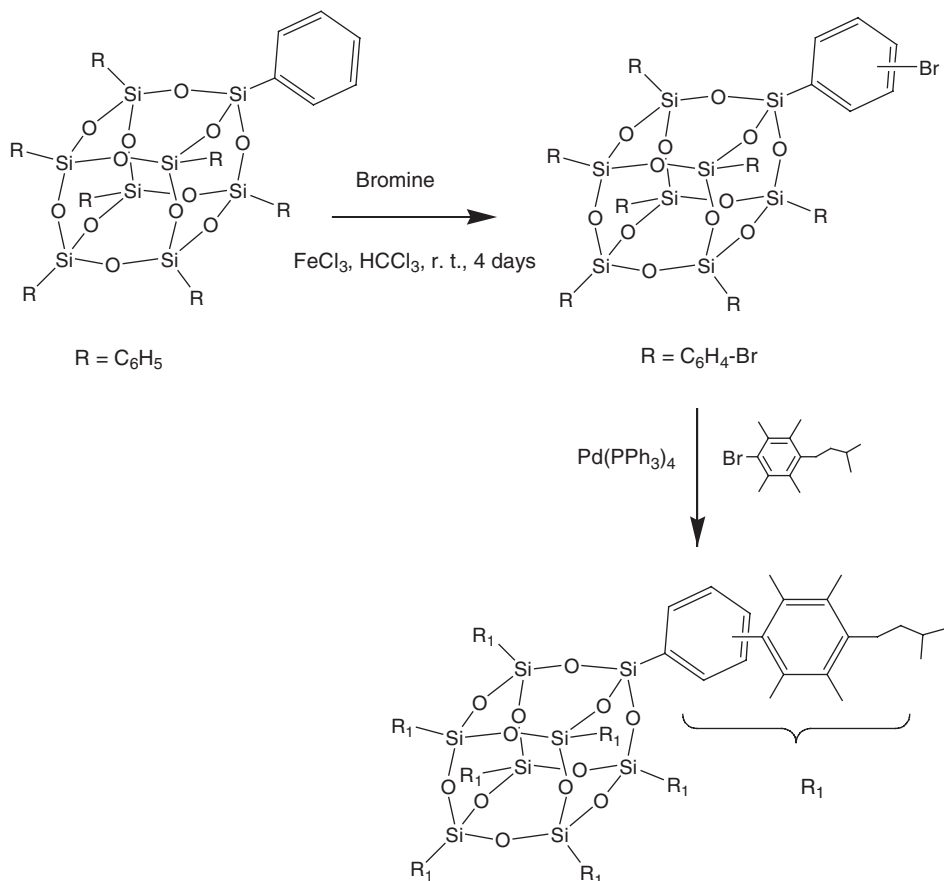
The relative stability of the phenyl ring coupled with the potential for reaction at the siloxane bonds means that few derivatives have been prepared directly from T_8Ph_8 . The most important reaction of the phenyl groups is the nitration of the ring. First observed by Olsson^{101,159} after the dissolution of T_8Ph_8 in cold fuming nitric acid, the formation of $T_8[C_6H_4-NO_2]_8$ was later reinvestigated by Laine and coworkers.^{148,160} This reaction was shown not to be regioselective since a mixture of meta- and para-isomers are formed, nonetheless the nitrated products have become the precursors to a range of new materials. The nitro groups can be quantitatively reduced to NH_2 functions using formic acid in the presence of Pd/C to give a mixture of meta- and para-isomers of $T_8[C_6H_4-NH_2]_8$. Despite the fact that a mixture of isomeric silsesquioxanes derivatives are produced in these reactions the amine groups have been used as precursors to novel materials containing Schiff base, phthalimide, fluorenyl, and cinnamide groups as well as imide resins (Figure 17).^{149,152,160} The nitrophenyl and aminophenyl POSS derivatives have also been used as precursors to epoxy resin-based inorganic/organic polymers¹⁶¹ and polyimide nanocomposites.¹⁶²

The di-nitration of each Ph group in T_8Ph_8 was investigated in detail more recently using a mixture of HNO_3 and H_2SO_4 at 50 °C (Figure 18).^{144,163} Since it was not possible to determine the positions of the nitration on the phenyl directly by 1H NMR spectroscopy, cleavage of the Si–Ph bonds was carried out using aqueous hydrogen peroxide, the organic product was then isolated and shown to be 1,3-dinitrobenzene, suggesting, along with ^{13}C NMR spectroscopy data, that a 2,4-di-nitration (rather than a 3,5-di-nitration) has occurred. This hexadecanitate, obtained in 78% yield has been found to be explosive at 420 °C.^{144,163}

The bromination of the phenyl group in T_8Ph_8 has been reported by He et al. but few characterization data were given. The product, $T_8[C_6H_4-Br]_8$, obtained in a 60% yield was subject to Pd catalyzed arylations to form the first organic-based quantum dot-like materials (Figure 19).¹⁶⁴

Brick et al. have studied this bromination in more detail and showed that the extent of the bromination can be controlled by changing the ratio of the reagents. The first substitution was found to be in the para position but subsequent intramolecular rearrangements allowed the formation of 2-5-dibrominated species. Brick et al.¹⁶⁵ also reported the functionalization of such species using Pd-catalyzed reactions such as Heck and Suzuki couplings to give fully substituted *p*-stilbenes, *p*-biphenyls, diarylamines, and methylcinnamates. Hydrogenation of

Figure 17 Reactions of $T_8[C_6H_4NH_2]_8$.

**Figure 18** Di-nitration of phenyl groups in T_8Ph_8 .**Figure 19** Bromination of phenyl groups in T_8Ph_8 .

T_8Ph_8 using $Pd/C/H_2$ occurs quantitatively, without cleaving the POSS core to give $T_8[C-C_6H_{11}]_8$.¹⁶⁶

Ovchinnikov et al. have reported the synthesis of a cobaltasiloxane anionic framework from the reaction of T_8Ph_8 and $[PhSiO(ONa)]_3 \cdot 3H_2O$ in the presence of $CoCl_2$. The structure of the product $Na_6[(PhSiO_{1.5})_{22}Co_3O_6] \cdot 7H_2O$ has been determined by single-crystal XRD and shows that for each cube, one edge has been opened up and one of the Si atoms has been replaced by a Co atom.¹⁶⁷ Surprisingly, T_8Ph_8 reacts with $(NH_3)_3Cr(CO)_3$ to give a mono-substituted $Cr(CO)_3$ product with coordination to only one Ph group.¹⁶⁸

Applications for T_8Ph_8 have begun to be found, for example, it can be used as a nano-scale filler in a polycarbonate matrix by melt blending to give nanocomposite materials. It was shown that the compatibility between the polymer and the POSS molecule is better when T_8Ph_8 is used compared to POSS with other substituents.¹⁶⁹ However, this compatibility is even better when an incompletely condensed POSS (trisilanol) is used, giving materials with enhanced mechanical properties such as tensile and dynamic mechanical modulus.¹⁶⁹ In a related field, T_8Ph_8 has been introduced into an epoxy resin by intensive mixing. It was found that the adhesion properties, strengthening and toughening of the new formed material can be improved due to the presence of the POSS entity in the polymer.¹⁷⁰ A further application of T_8Ph_8 , along with T_8Me_8 , has been in studies to test the binding properties of peptides. Peptides with high silsesquioxane affinity have been identified and this can be seen as a new technology for the preparation of hybrid materials.¹⁷¹ The convenient synthesis and robust nature of T_8Ph_8 and its derivatives means that new applications in materials science are likely to expand rapidly.

D. Synthesis, properties, and reactions of $T_8[CH=CH_2]_8$ and its derivatives

1. Synthesis

The synthesis of $T_8[CH=CH_2]_8$ was initially attempted by Andrianov et al. with the hydrolysis of vinyltrichlorosilane, but a poor yield was obtained (Table 11, entry 1). Later, up to 20% yield was achieved using aqueous ethanol as the hydrolysis medium (Table 11, entry 2). Vinyltriethoxysilane has also been used as precursor, but after several days the reaction gave only a few percent yield of crystals (Table 11, entry 3). Nevertheless, these crystals were suitable for X-ray characterization (see below). Bassindale et al. attempted the hydrolysis of vinyltriethoxysilane in the presence of Bu_4NF , a method that was successful for other compounds (e.g., T_8Ph_8), but in this case only 1% yield was obtained (Table 11, entry 4). Using this synthetic route, the authors observed the same phenomenon as for T_8Ph_8 (see Section V.C), that is, the encapsulation of a fluoride ion from Bu_4NF in the cage structure.¹⁷² Recently, Dare et al. reported an improved preparation based on the reaction of vinyltrichlorosilane in MeOH in the presence of an acid resin Amberlite IR-120 PLUS which can be reused, giving a 41% yield (Table 11, entry 6), while an even better yield is reported when using Me_4NOH as a phase-transfer catalyst for the reaction (Table 11, entry 7).¹⁷³

Table 11 Preparative routes to $T_8[CH=CH_2]_8$

Entry	Starting materials and conditions	Yield (%)	Reference
1	$CH_2=CH-SiCl_3+H_2O$ /acetone, 4 days	6	174
2	$CH_2=CH-SiCl_3+EtOH/H_2O$	20	78
3	$CH_2=CH-Si(OEt)_3+H_2O$, gives single crystals for crystallography	Low	175
4	$CH_2=CH-Si(OEt)_3+H_2O$, Bu_4NF	1	100
5	$CH_2=CH-SiCl_3+BuOH$, then H_2O	21–33	176
6	$CH_2=CH-SiCl_3+MeOH$, Amberlite IR-120 PLUS, 12 h	41	145
7	$CH_2=CH-Si(OEt)_3+MeOH$, Me_4NOH , 24 h, room temperature; 48 h, 60 °C	80	173

A detailed analysis of the mechanism of formation of $T_8[CH=CH_2]_8$ in butanol/ H_2O showed that intermediates containing 1–8 silicon atoms could be identified showing that the POSS core was built up stepwise rather than occurring by dimerization of a four silicon intermediate.¹⁷⁶

2. Structure and physical properties

The ^{29}Si NMR spectrum of $T_8[CH=CH_2]_8$ has been reported to display a single signal at -81.63 ppm in solution¹⁴⁵ and two signals in 3:1 ratio at -78.98 and -80.42 ppm,⁷⁸ -80.2 and -80.7 ppm,¹⁷⁷ or -79.9 and -80.4 ppm¹⁷⁵ in the solid state. Detailed solid-state 1H , ^{13}C , and ^{29}Si NMR studies,^{175,177–179} calorimetry,^{179a} and IR studies have also been reported.^{154,175} The NMR studies show that the vinyl groups are disordered in the solid state and that a phase change occurs in the solid at 229.6 K. The mass spectrum of $T_8[CH=CH_2]_8$ has been obtained by turbo ion-spray¹⁸⁰ and atmospheric pressure chemical ionization¹⁸¹ methods. The structure of $T_8[CH=CH_2]_8$ has been the subject of two crystallographic studies, the first by Baidina et al.¹⁸² resulting in a final value $R = 0.11$ and the second by Bonhomme et al.¹⁷⁵ with $R = 0.048$. In both cases the CH_2 groups were found to be disordered, the structure is shown in Figure 20. The Si–O distances for the structure determined by Bonhomme et al. are in the range 1.596(6)–1.616(6) Å and the Si–O–Si angles 150.0(4)–150.5(4)°, the small range for these distances and angles indicating a more symmetrical cube than is often found in T_8 derivatives (see Section VJ). In addition, XRD studies of polycrystalline films of vacuum-deposited $T_8[CH=CH_2]_8$ show layers of molecules ideally orientated with the [001] texture axis.¹⁸³ The various ladder and cage structure products obtained from hydrolysis of vinyltrimethoxysilane have been characterized and the structures, including that of O_h symmetry $T_8[CH=CH_2]_8$, been calculated.¹⁸⁴

3. Reactivity and applications

The alkene groups in $T_8[CH=CH_2]_8$ have allowed a wider variety of chemistry to be carried out than for either T_8H_8 or T_8Ph_8 . For example, Feher's group have prepared a variety of unsaturated POSS molecules *via* olefin cross-metathesis

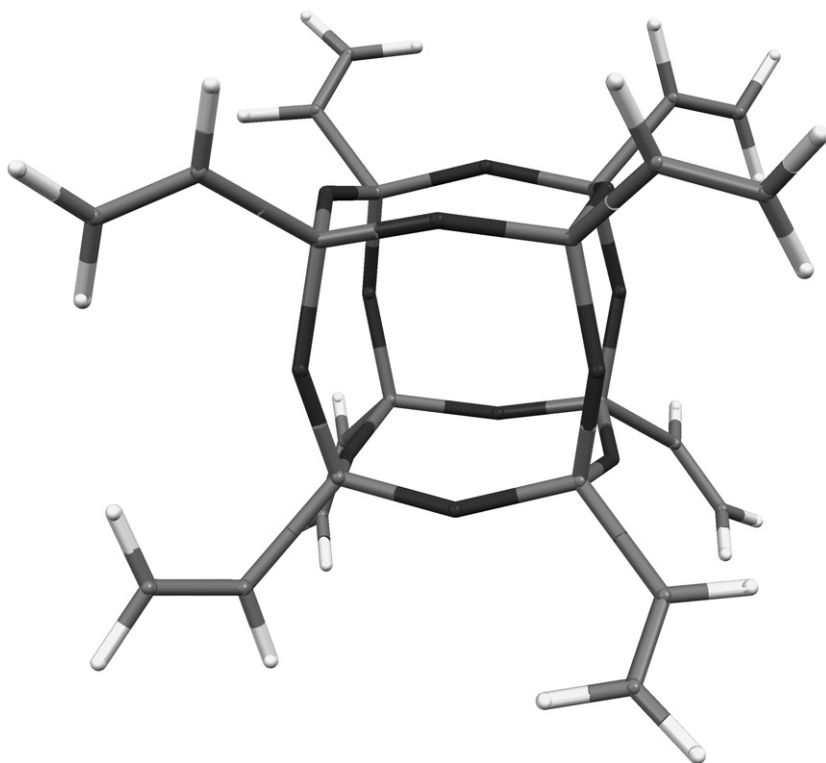


Figure 20 Crystal structure of $T_8[CH=CH_2]_8$. (Redrawn using data for structure VINSIO01 from the Cambridge Crystallographic Data Centre.)

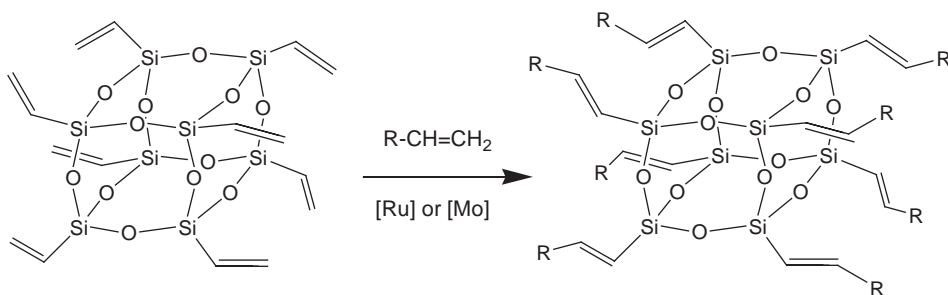


Figure 21 Cross-metathesis reactions using $T_8[CH=CH_2]_8$.

reactions of $T_8[CH=CH_2]_8$ with various alkenes such as 4-octene, pentene, and functionalized alkenes (Figure 21 and Table 12) using either the Grubbs' catalyst, $[(PCy_3)_2Cl_2Ru(=CHPh)]$ ([Ru]), or Schrock's $[(2,6-iPr_2C_6H_3N)Mo(=CHCMe_2Ph)]$ ([Mo]).

The Schrock catalyst has shown to be the most active and it was compatible with a range of functional groups giving good-to-excellent yields (Table 12,

Table 12 Compounds T_8R_8 obtained by cross-metathesis or silylative coupling of $T_8[CH=CH_2]_8$ with alkenes

Entry	R	Starting materials	Yield (%)	^{29}Si NMR ^a	Reference
1	-CH=CHPh	$T_8[CH=CH_2]_8+CH_2=CHPh$, [Mo]	81	–	187
2	-CH=CHPh	$T_8[CH=CH_2]_8+CH_2=CHPh$, [Ru]	96	–78.35	188
3	-CH=CHPh	$T_8[CH=CH_2]_8+CH_2=CHPh$, [Ru-H]	92	–78.35	188
4	-CH=CHSiMe ₃	$T_8[CH=CH_2]_8+CH_2=CHSiMe_3$, [Ru]	Traces	–	188
5	-CH=CHSiMe ₃	$T_8[CH=CH_2]_8+CH_2=CHSiMe_3$, [Ru-H]	95	4 signals	188
6	-CH=CHO- <i>n</i> Bu	$T_8[CH=CH_2]_8+CH_2=CHO-nBu$, [Ru-H]	99	–74.67, –79.10	188
7	-CH=CHO- <i>t</i> Bu	$T_8[CH=CH_2]_8+CH_2=CHO-tBu$, [Ru-H]	99	–76.94	188
8	-CH=CHOSiMe ₃	$T_8[CH=CH_2]_8+CH_2=CHOSiMe_3$, [Ru-H]	99	11 signals	188
9	-CH=CHS- <i>t</i> Bu	$T_8[CH=CH_2]_8+CH_2=CHS-tBu$, [Ru]	95	–80.10	188
10	-CH=CH- <i>c</i> -[N(CH ₂) ₃ -C(O)-]	$T_8[CH=CH_2]_8+N$ -vinylpyrrolidone, [Ru-H]	69	–	188
11	-CH=CHCH ₂ SiMe ₃	$T_8[CH=CH_2]_8+CH_2=CHCH_2SiMe_3$, [Ru]	69	–79.86	188
12	-CH=CHCH ₂ SiMe ₃	$T_8[CH=CH_2]_8+CH_2=CHCH_2SiMe_3$, [Ru-H]	69	–79.86	188
13	-CH=CHCH ₂ -Si(OMe) ₃	$T_8[CH=CH_2]_8+CH_2=CHCH_2Si(OMe)_3$, [Mo]	100	–	187
14	-CH=CH(CH ₂) ₂ CH ₃	$T_8[CH=CH_2]_8+cis-CH_3(CH_2)_2CH=CH-(CH_2)_2CH_3$, [Mo]	100	–	187
15	-CH=CH(CH ₂) ₂ CH ₃	$T_8[CH=CH_2]_8+CH_2=CHC_3H_7$, [Mo]	100	–	187
16	-CH=CH(CH ₂) ₃ CH ₃	$T_8[CH=CH_2]_8+CH_2=CHC_4H_9$, [Ru]	72	–79.10	188
17	-CH=CH(CH ₂) ₃ CH ₃	$T_8[CH=CH_2]_8+CH_2=CHC_4H_9$, [Ru-H]	74	–79.10	188
18	-CH=CH(CH ₂) ₃ Br	$T_8[CH=CH_2]_8+CH_2=CH(CH_2)_3Br$, [Ru]	76	–	187
19	-CH=CH(CH ₂) ₃ OH	$T_8[CH=CH_2]_8+CH_2=CH(CH_2)_3OH$, [Ru]	<10	–	187
20	-CH=CH(CH ₂) ₆ -Si(OMe) ₃	$T_8[CH=CH_2]_8+CH_2=CH(CH_2)_6Si(OMe)_3$, [Mo]	100	–	187
21	-CH=CH(CH ₂) ₈ CO ₂ Et	$T_8[CH=CH_2]_8+CH_2=CH(CH_2)_8CO_2Et$, [Mo]	100	–	187

^aReferenced to SiMe₄.

entries 13, 20, and 21). For each substrate, a mixture of *trans* and *cis* cross-metathesis products was obtained with a majority of the former, except in the case of styrene when only the *trans* product was obtained (Table 12, entry 1). $T_8[CH=CH-Ph]_8$ can be used in the blending of organic polymers.¹⁸⁵ Similar work has been carried out by Itami et al. who treated $T_8[CH=CH_2]_8$ with alkenes using both catalyzed cross-metathesis and silylative coupling¹⁸⁶ with $[(PCy_3)_2Cl_2(Ru=CHPh)]$, $[(Ru)]$, and $[RuHCl(CO)(PCy_3)_2]$, $[(Ru-H)]$, respectively (Table 12). A comparative study showed that when the Grubbs' catalyst was not active, the silylative catalyst gave products in good yields, notably with functionalized substrates such as vinylsilanes, vinyl ethers, and vinylpyrrolidone (Table 12, entries 6, 7, 10, and 12).

König et al. have achieved thioether functionalization of $T_8[CH=CH_2]_8$ via the radical addition of thiols such as thiophenol, cyclohexylthiol, and 2-mercaptopyridine in the presence of azobisisobutyronitrile (AIBN) as a radical initiator (Table 13), while Gao et al.^{189a} have also used this method to prepare very highly functionalized POSS by reacting $T_8[CH=CH_2]_8$ with thiol-terminated glycosides giving glycoclusters in 70% yield (Figure 22).

A related reaction has been reported by Cole-Hamilton and coworkers who treated $T_8[CH=CH_2]_8$ with HPet₂ in the presence of AIBN giving the phosphine $T_8[(CH_2)_2-Pet_2]_8$ (Table 14, entry 1). Previously, Morris and coworkers reported the preparation of chloro- and vinyl-terminated dendrimers (Figure 23) such as $T_8\{(CH_2)_2Si[(CH_2)_2SiCl_3]_3\}_8$ and $T_8\{(CH_2)_2Si[(CH_2)_2Si(CH=CH_2)_3]_3\}_8$ by repetitive hydrosilylation with H-SiCl₃ and alkenylation with $CH_2=CHMgX$ reagents (Table 14, entries 2, 6–8).

Table 13 Compounds T_8R_8 obtained by reaction of $T_8[CH=CH_2]_8$ with thiols

R	Starting materials	Reference
$-CH_2CH_2SPh$	$T_8[CH=CH_2]_8 + PhSH$, AIBN	189b
$-CH_2CH_2S-c-C_6H_{11}$	$T_8[CH=CH_2]_8 + HS-c-C_6H_{11}$, AIBN	189b
$-CH_2CH_2S-2-c-C_5H_5N$	$T_8[CH=CH_2]_8 + HS-2-c-C_5H_5N$, AIBN	189b

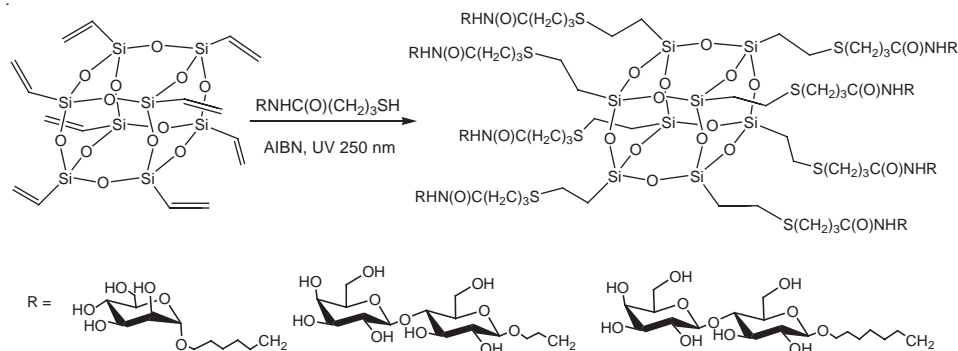


Figure 22 Glycoclusters prepared from $T_8[CH=CH_2]_8$.

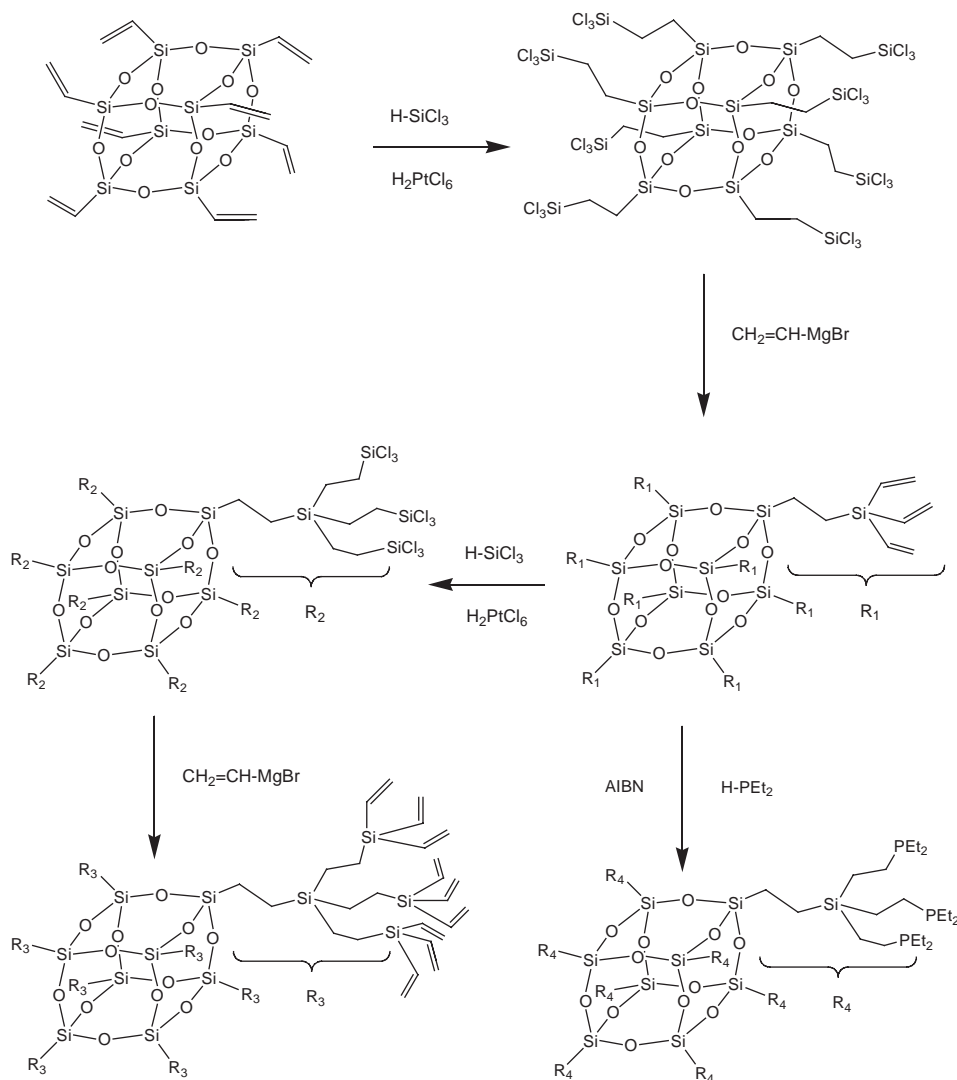


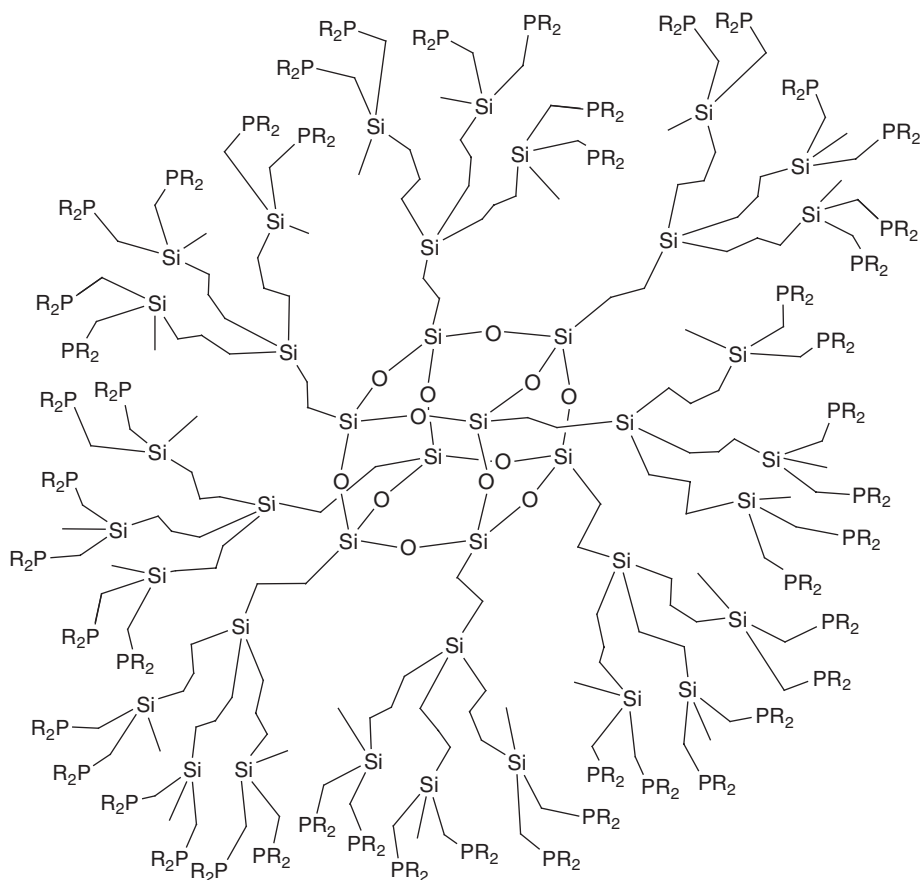
Figure 23 Dendrimers prepared from $T_8[CH=CH_2]_8$.

The dendrimers have been further functionalized to give phosphinated POSS by reacting either the Cl-terminated compounds with $LiCH_2PR_2$ or the alkenyl derivatives with R_2PH (in the presence of AIBN) giving finally an impressive range of POSS-based dendritic materials containing up to 72 phosphine groups (Table 14 and Figure 23). Some of these compounds (Figure 24) were successfully applied as ligands for the Rh-catalyzed hydroformylation reaction (of 1-hexene and 1-octene), in some cases increasing the selectivity while retaining the activity observed for similar nondendritic phosphines. It was shown that the number of functional groups and the length of the bridge between the phosphines were

Table 14 Dendritic compounds T_8R_8 obtained from $T_8[CH=CH_2]_8$

Entry	R	Starting materials	Yield (%)	^{29}Si NMR ^a	Reference
1	$-(CH_2)_2PEt_2$	$T_8[CH=CH_2]_8+HPEt_2$, AIBN	> 90	–	191
2	$-(CH_2)_2SiCl_3$	$T_8[CH=CH_2]_8+HSiCl_3$, H_2PtCl_6	98	12.82, –67.48	191,192
3	$-(CH_2)_2Si(CH_2PMe_2)_3$	$T_8[(CH_2)_2SiCl_3]_8+LiCH_2PMe_2$	97	–	191,193
4	$-(CH_2)_2Si(CH_2PPh_2)_3$	$T_8[(CH_2)_2SiCl_3]_8+LiCH_2PPh_2$	40	–	191,193
5	$-(CH_2)_2Si(CH_2PPh_2)_3$	$T_8[(CH_2)_2SiCl_3]_8+LiCH_2PPh_2$	93	–	191
6	$-(CH_2)_2Si(CH=CH_2)_3$	$T_8[(CH_2)_2SiCl_3]_8+CH_2=CH-MgCl(Br)$	81	–18.2, –67.48	191,192
7	$-(CH_2)_2Si[(CH_2)_2SiCl_3]_3$	$T_8[(CH_2)_2Si(CH=CH_2)_3]_8+HSiCl_3$, H_2PtCl_6	88	3 peaks	191,192
8	$-(CH_2)_2Si[(CH_2)_2Si(CH=CH_2)_3]_3$	$T_8[(CH_2)_2Si((CH_2)_2SiCl_3)_3]_8+CH_2=CH-MgBr$	21	3 peaks	192
9	$-(CH_2)_2Si[(CH_2)_2Si(CH_2PMe_2)_3]_3$	$T_8[(CH_2)_2Si((CH_2)_2SiCl_3)_3]_8+LiCH_2PMe_2$	80	–	191,193
10	$-(CH_2)_2Si[(CH_2)_2PEt_2]_3$	$T_8[(CH_2)_2Si(CH=CH_2)_3]_8+HPEt_2$, AIBN	93	–	191,193
11	$-(CH_2)_2-Si[(CH_2)_2PCy_2]_3$	$T_8[(CH_2)_2Si(CH=CH_2)_3]_8+HPCy_2$, AIBN	95	–	191
12	$-(CH_2)_2-Si[(CH_2)_2PPh_2]_3$	$T_8[(CH_2)_2Si(CH=CH_2)_3]_8+HPPPh_2$, AIBN	95	–	191
13	$-(CH_2)_2Si[(CH_2)_2PCy_2]_3$	$T_8[(CH_2)_2Si(CH=CH_2)_3]_8+HPCy_2$, AIBN	52	–	193
14	$-(CH_2)_2SiMeCl_2$	$T_8[CH=CH_2]_8+HSiMeCl_2$, H_2PtCl_6	98	–	193,194
15	$-(CH_2)_2SiMe(CH=CH_2)_2$	$T_8[(CH_2)_2-SiMeCl_2]_8+CH_2=CH-MgBr$	85	–	193,194
16	$-(CH_2)_2-SiMe((CH_2)_2PEt_2)_2$	$T_8[(CH_2)_2SiMe(CH=CH_2)_2]_8+HPEt_2$, AIBN	95	–	193,194
17	$-(CH_2)_2SiMe((CH_2)_2PPh_2)_2$	$T_8[(CH_2)_2SiMe(CH=CH_2)_2]_8+HPPPh_2$, AIBN	85	–	194
18	$-(CH_2)_2SiMe((CH_2)_2PCy_2)_2$	$T_8[(CH_2)_2SiMe(CH=CH_2)_2]_8+HPCy_2$, AIBN	74	–	193
19	$-(CH_2)_2SiMe(CH_2-CH=CH_2)_2$	$T_8[(CH_2)_2SiMeCl_2]_8+CH_2=CH-CH_2-MgBr$	90	–	193,194
20	$-(CH_2)_2SiMe[(CH_2)_3PPh_2]_2$	$T_8[(CH_2)_2SiMe(CH_2CH=CH_2)_2]_8+HPPPh_2$, AIBN	87	–	193,194
21	$-(CH_2)_2Si(CH_2CH=CH_2)_3$	$T_8[(CH_2)_2SiCl_3]_8+CH_2=CHCH_2MgBr$	81	–	193,194
22	$-(CH_2)_2Si[(CH_2)_3PEt_2]_3$	$T_8[(CH_2)_2-Si(CH_2CH=CH_2)_3]_8+HPEt_2$, AIBN	85	–	193,194
23	$-(CH_2)_2Si[(CH_2)_3-OH]_3$	$T_8[(CH_2)_2Si(CH_2CH=CH_2)_3]_8+H_2O_2$, 9-BBN, NaOH	65	–	195
24	$-(CH_2)_2Si[(CH_2)_3-SiMeCl_2]_3$	$T_8[(CH_2)_2Si(CH_2CH=CH_2)_3]_8+HSiMeCl_2$, H_2PtCl_6	95	–	193,194
25	$-(CH_2)_2Si[(CH_2)_3-SiMe(CH=CH_2)_3]$	$T_8[(CH_2)_2Si[(CH_2)_3SiMeCl_2]_3]_8+CH_2=CHMgBr$	70	–	193,194
26	$-(CH_2)_2Si[(CH_2)_3-SiMe(CH_2)_3]$	$T_8[(CH_2)_2Si[(CH_2)_3SiMe(CH=CH_2)_3]_8+HPEt_2$, AIBN	86	–	193,194
27	$-(CH_2)_2Si[(CH_2)_3-SiMe((CH_2)_2PPh_2)_3]$	$T_8[(CH_2)_2Si[(CH_2)_3SiMe(CH=CH_2)_2]_3]_8+HPPPh_2$, AIBN	63	–	194

^aReferenced to $SiMe_4$.



R = Et or Ph

Figure 24 Phosphine-based dendrimers prepared from $T_8[CH=CH_2]_8$ and used in the hydroformylation reaction.

determining factors and a dendritic effect was observed. The structures of some POSS-based dendrimers have been modeled by molecular dynamics, and show, that for hydroxyl-terminated dendrimers, the hydroxyl groups are found as a shell on the periphery of the molecule.¹⁹⁰

Lücke et al.¹⁹⁶ have prepared other phosphinated POSS compounds $T_8[(CH_2)_2-PMe_2]_8$ and $T_8[(CH_2)_3-PMe_2]_8$ by treating $T_8[CH=CH_2]_8$ or $T_8[CH_2-CH=CH_2]_8$ with H-PMe₂ under UV irradiation. The former compound has shown to have good coordination properties to carbonyl transition metal complexes such as $CpMn(CO)_3$ (Table 15).

Other products have been obtained from $T_8[CH=CH_2]_8$ *via* additions to the double bonds (Table 16 and Figure 25). For example, T_8Et_8 can be prepared by catalytic hydrogenation of $T_8[CH=CH_2]_8$ giving a better yield than from the reaction of T_8H_8 with ethylene (see Section V.B) (Table 16, entries 1–3) and

Table 15 Phosphines and metal complexes T_8R_8 derived from $T_8[CH=CH_2]_8$

R	Starting materials and conditions	Yield (%)	Reference
$-(CH_2)_2PMe_2$	$T_8[CH=CH_2]_8 + HPMe_2$, UV	100	196
$-(CH_2)_2P(S)Me_2$	$T_8[(CH_2)_2PMe_2]_8 + S_8$	100	196
$-(CH_2)_2PMe_2W(CO)_5$	$T_8[(CH_2)_2PMe_2]_8 + W(CO)(THF)$, UV	100	196
$-(CH_2)_2PMe_2MnCp(CO)_2$	$T_8[(CH_2)_2PMe_2]_8 + CpMn(CO)_3$, UV	100	196
$-(CH_2)_2PMe_2CoCp(CO)$	$T_8[(CH_2)_2PMe_2]_8 + CpCo(CO)_2$, UV	100	196
$-(CH_2)_2PMe_2RhCp^*(CO)$	$T_8[(CH_2)_2PMe_2]_8 + Cp^*Rh(CO)_2$, UV	100	196

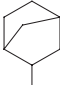
hydrobromination of the double bond was achieved by reaction with HBr using $PhC(O)O-O(O)CPh$ as a radical initiator (Table 16, entry 5). Many other compounds derived from $T_8[CH=CH_2]_8$ can also be found in Table 16 which give a good idea of the wide range of reagents and reaction conditions that can be survived by the POSS core when carrying out reactions at its substituents. It should be pointed out however, that the susceptibility of POSS cages to strongly basic reagents can be seen in the reaction of $T_8[CH=CH_2]_8$ with catalytic amounts of KOH which causes Si-O bond cleavage and the formation of larger silsesquioxanes.¹⁹⁷

It is also possible to carry out reactions of $T_8[CH=CH_2]_8$ in which only some of the double bonds react. Epoxy-functionalized cubes have been prepared *via* epoxidation of $T_8[CH=CH_2]_8$ using *m*-chloroperbenzoic acid (*m*-CPBA), however, only the product arising from partial epoxidation could be isolated, with an average of two epoxy groups per cube when three equivalents of *m*-CPBA were used. Indeed, in the case of 10 equivalents of *m*-CPBA no molecular product could be isolated, instead intractable gels were formed. The epoxides polymerize readily in the presence of a Lewis acid or on reaction with diamines, showing potential as precursors for hybrid materials (Figure 26).²⁰⁷

Monofunctionalized compounds have been prepared by Feher et al. who showed that $T_8[CH=CH_2]_8$ reacts with HOTf to give $T_8[CH=CH_2]_7[(CH_2)_2OTf]$ that can then be hydrolyzed to give $T_8[CH=CH_2]_7[(CH_2)_2OH]$, or treated with 2-mercaptopyridine to give POSS with novel pendant groups (Figure 26). These reactions show that under the right conditions, reactions of $T_8[CH=CH_2]_8$ can be selective for the functionalization of a single vinyl group²⁰⁸ and a variety of $T_8[CH=CH_2]_7R$ species should be available *via* this route that can then undergo further reaction at the vinyl groups. For example, $T_8[CH=CH_2]_7[(CH_2)_2OH]$ can be reduced to give $T_8Et_7[(CH_2)_2OH]$.²⁰⁸ The chlorination of $T_8[CH=CH_2]_8$ by SO_2Cl_2 leads to products $T_8[CH=CH_2]_{8-n}Cl_n$ ($n = 1-4$) derived from cleavage of Si-C bonds as well as a mixture of chloroalkyl-substituted POSS species.²⁰⁹

In the field of materials synthesis, $T_8[CH=CH_2]_8$ has been used to prepare three-dimensional (meso)porous polymers with high surface area *via* reactions with T_8H_8 or $T_8[OSiMe_2H]_8$ in the presence of a Pt catalyst as described in Section V.B.^{64,133,210} Xu et al. prepared a POSS-based monomer by reaction of $T_8[CH=CH_2]_8$ with 4-acetoxystyrene in the presence of AIBN giving rise to partially functionalized POSS species that were then polymerized into

Table 16 Miscellaneous compounds T_8R_8 obtained from $T_8[CH=CH_2]_8$

Entry	R	Starting materials and conditions	Yield (%)	^{29}Si NMR ^a	Reference
1	-Et	$T_8[CH=CH_2]_8+H_2$, Pt/C, 40 °C	Quantitative	-	198
2	-Et	$T_8[CH=CH_2]_8+H_2$, Pt/C, 70 °C, 16 h	89	-65.5	199
3	-CHDCHD ₂ +isomers	$T_8[CH=CH_2]_8+D_2$, Pt/C, 70 °C, 16 h	-	-65.4	199
4	-CH ₂ CH ₂ Br	$T_8[CH=CH_2]_8+HBr$, AlBr ₃	28	-	200
5	-CH ₂ CH ₂ Br	$T_8[CH=CH_2]_8+HBr$, (PhCOO) ₂	48	-70.45	201
6	-CH ₂ CH ₂ CO ₂ Me	$T_8[CH=CH_2]_8+CO+MeOH$, Pd ₂ (dba) ₂	43	-67	201
7	-C ₇ H ₉	$T_8[CH=CH_2]_8$ +dicyclopentadiene	60	-	202
8	-2,2-Cl ₂ -c-C ₃ H ₄	$T_8[CH=CH_2]_8+HCCl_3$, NaOHR ₄ NX (phase transfer catalytic system)	44	-	203
9	-CH ₂ CH ₂ Ph	$T_8[CH=CH_2]_8+C_6H_6+AlCl_3$	73	-	203,225
10		$T_8[CH=CH_2]_8$ +cyclopentadiene, reflux	50–60	-	202
11	-(CH ₂) ₂ SiMe ₂ -C ₆ H ₄ - (4-CH(O-CH ₂ CH ₂ O))	$T_8[CH=CH_2]_8+2-(4\text{-dimethylsilyl})\text{-phenyl})\text{-1,3-dioxalane}$, Pt(dvs)	79	-	204
12	-(CH ₂) ₂ SiMe ₂ -C ₆ H ₄ - (<i>p</i> -CHO)	$T_8[(CH_2)_2\text{-SiMe}_2\text{-C}_6\text{H}_4\text{-(}p\text{-CH(O-CH}_2\text{CH}_2\text{O)-O})]_8$ +pyridinium toluene sulfonate	-	-	204
13	-(CH ₂) ₂ SiMe ₂ -C ₆ H ₄ - (<i>m</i> -CH(O-CH ₂ -CH ₂ -O))	$T_8[CH=CH_2]_8+2-(m\text{-dimethylsilyl})\text{phenyl})\text{-1,3-dioxalane}$, Pt(dvs)	65	-	204
14	-(CH ₂) ₂ SiMe ₂ -C ₆ H ₄ - (<i>m</i> -CHO)	$T_8[(CH_2)_2\text{SiMe}_2\text{-C}_6\text{H}_4\text{-(}m\text{-CH(O-CH}_2\text{CH}_2\text{O)-O})]_8$ +pyridinium toluene sulfonate	92	-	204
15	-(CH ₂) ₂ SiMe ₂ Cl	$T_8[CH=CH_2]_8+HSiMe_2Cl$, H ₂ PtCl ₆	99	-	192
16	-(CH ₂) ₂ SiMe ₂ CH=CH ₂	$T_8[(CH_2)_2\text{SiMe}_2Cl]_8+CH_2=CH\text{-MgBr}$	52	-	192
17	-(CH ₂) ₂ SiMe ₂ H	$T_8[(CH_2)_2\text{SiMe}_2Cl]_8+LiAlH_4$	61	-	205
18	-(CH ₂) ₂ SiMe ₂ OH	$T_8[(CH_2)_2\text{-SiMe}_2\text{-H}]_8+H_2O$, Pd	65	-	205
19	-(CH ₂) ₂ P(O)(OEt) ₂	$T_8[CH=CH_2]_8+(EtO)_2P(O)H$, cyclohexane, AIBN	-	-	195
20	-(CH ₂) ₂ P(O)(OH) ₂	$T_8[(CH_2)_2P(O)(OEt)_2]_8+H_2O$, BrSiMe ₃	-	-	195
21	-(CH ₂) ₂ P(O)(<i>μ</i> -O) ₂ Ti(O <i>i</i> Pr) ₂	$T_8[(CH_2)_2P(O)(OH)_2]_8+TiCl(OiPr)_3$, THF	-	-	195
22	-(CH ₂) ₂ CHO	$T_8[CH=CH_2]_8+CO/H_2$, PCl ₂ (sixantphos), CH ₂ Cl ₂	-	-	206

^aReferenced to SiMe₄.

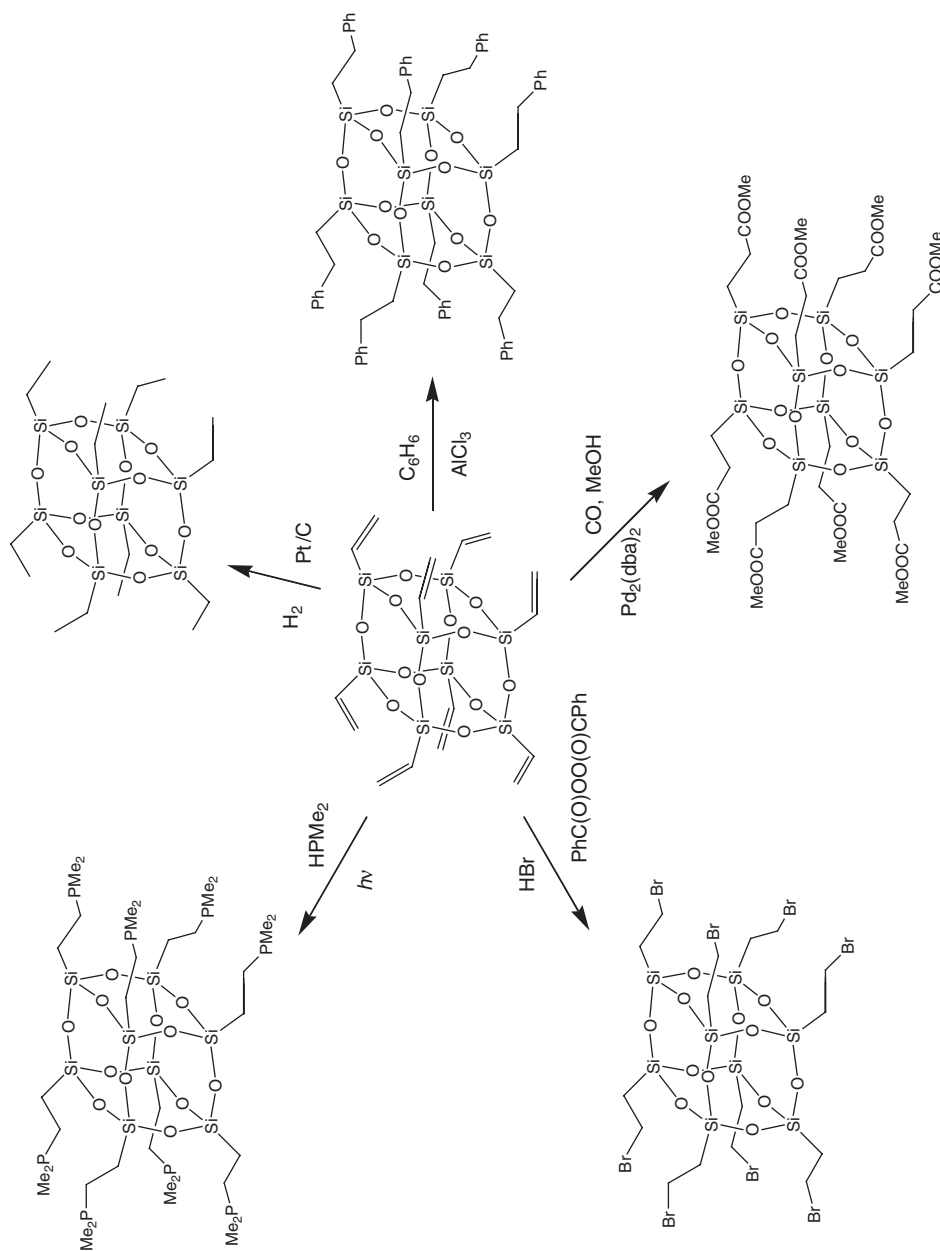


Figure 25 Miscellaneous addition reactions of $T_8[CH=CH_2]_8$.

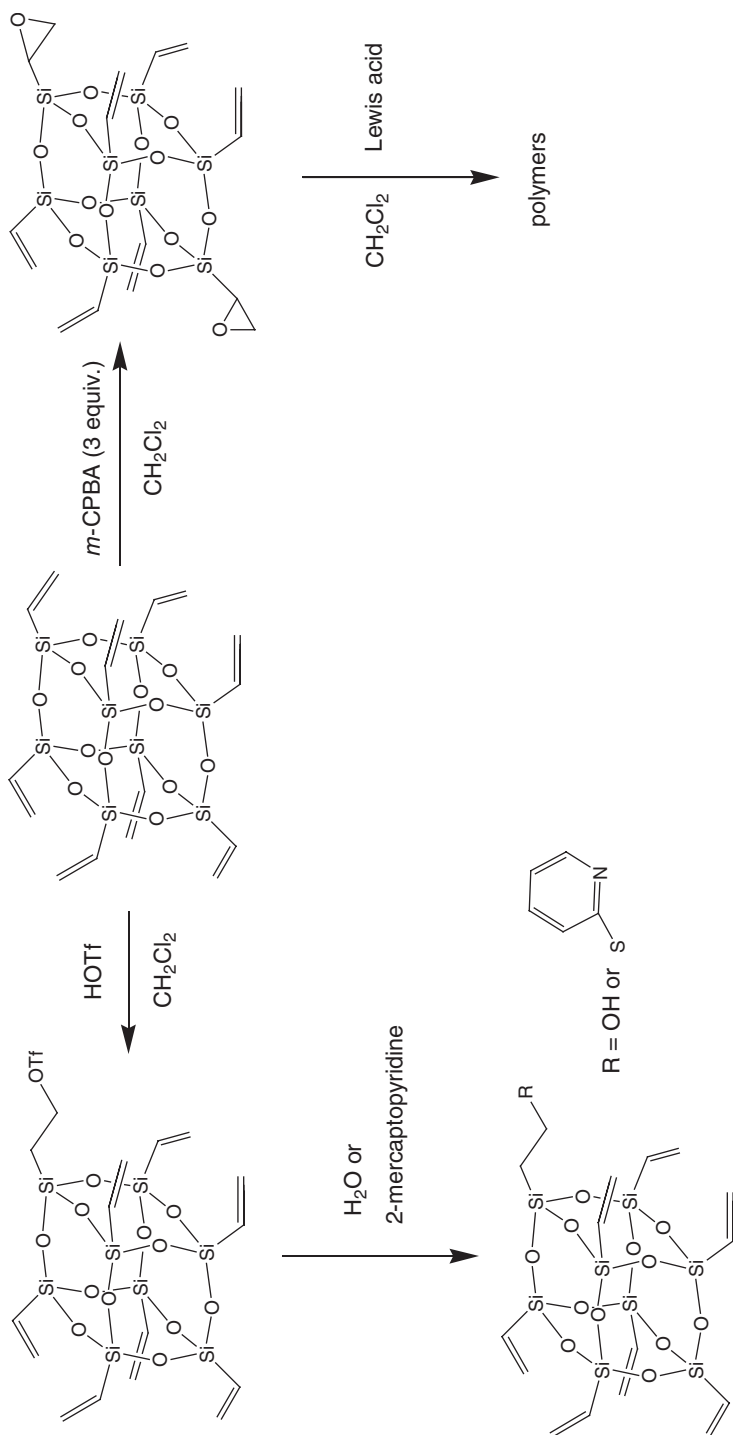


Figure 26 Examples of partial functionalization of $T_8[CH=CH_2]_8$.

poly(acetoxystyrene-co-octavinyl-POSS) materials.²¹¹ The Heck coupling of $T_8[CH=CH_2]_8$ with large, aromatic, hole-transporting compounds gives nano-composite materials that can be used in organic light emitting diode devices that have quantum efficiencies higher than their small-molecule counterparts.²¹² The hydrosilylation reactions of $SiMe_2H$ derivatives of long-chain biphenyl esters with $T_8[CH=CH_2]_8$ leads to inorganic/organic hybrid materials that exhibit smectic C or smectic X phase behavior near room temperature.²¹³

The relatively high volatility of $T_8[CH=CH_2]_8$ has enabled it to be used as a CVD precursor for the preparation of thin films that can be converted by either argon or nitrogen plasma into amorphous siloxane polymer films having useful dielectric properties.²¹⁴ The high volatility also allows deposition of $T_8[CH=CH_2]_8$ onto surfaces for use as an electron resist²¹⁵ and the thin solid films formed by evaporation may also be converted into amorphous siloxane dielectric films *via* plasma treatment.²¹⁴

4. Theoretical studies

Lamm et al. and Sheng et al. have performed Monte Carlo simulations to study nanostructured networks formed by $T_8[CH=CH_2]_8$ and T_8H_8 or $T_8[OSiMe_2H]_8$. In the former study, the effect of the linker length on network properties (porosity, spatial distribution) was explored and a comparison with experimental data¹³³ has been made. It has been shown that the porosity decreases as tether length increases in agreement with the experimental results available from Laine's work.¹³³ In the case of the degree of cross-linking, the theoretical results show that it decreases as the linker length increases (up to six atoms), in contrast with the experimental data. It has been suggested that a six-atom linker is the optimum length for balancing the competition between steric hindrance and tether flexibility.²¹⁶ A study by Sheng et al. using a different models based on a continuous-space Monte Carlo simulation, was consistent with the experimental data.²¹⁷

E. Synthesis, properties, and reactions of $T_8[O^-]_8$ and its derivatives

1. Synthesis

The T_8 -based octa-anion $T_8[O^-]_8$ can be seen as a model for the well-known D4R found in inorganic structures such as zeolite A. Synthesis of $T_8[O^-]_8$ can be achieved more readily than many other POSS species and it can be obtained in quantitative yield from the reaction of a tetra-alkoxysilane with H_2O (10 equiv./Si) in the presence of Me_4NOH (1 equiv./Si) in methanol at room temperature for 1 day (Figure 27).^{173,218} Alcoholysis of $T_8[OSiMe_2H]_8$ causes terminal Si-O bond cleavage and the formation of $T_8[O^-]_8$.²¹⁹ This is, however, not a useful synthetic route as the $T_8[OSiMe_2H]_8$ is prepared by silylation of $T_8[O^-]_8$ (see below). An alternative preparation was reported by Asuncion et al. who used the depolymerization of rice hull ash silica at room temperature in the presence of $[Me_3NCH_2CH_2OH]OH$ in methanol to give a crystalline material suitable for single-crystal XRD (see below).²²⁰ This method is unlike all other methods for preparing simple molecular POSS materials in that it relies on the breakdown of large siloxane materials rather than building up the cage from smaller units and is

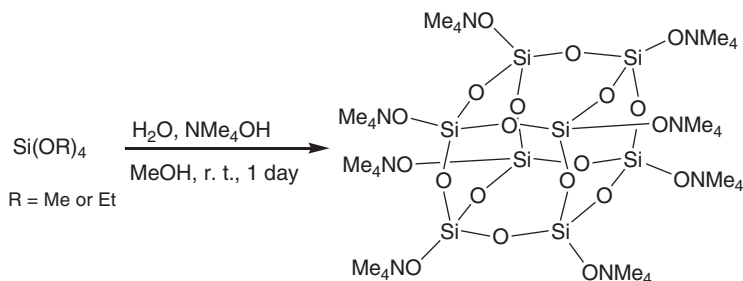


Figure 27 Preparation of $\text{T}_8[\text{ONMe}_4]_8$.

also of low cost. Many studies²²¹ on the effects of concentration, cation, solvent, and temperature on the formation of simple silicate anions, including $\text{T}_8[\text{O}^-]_8$, as precursors to larger structures such as zeolites have been carried out but these are beyond the scope of this review.

2. Structure and physical properties

The octa-anion $\text{T}_8[\text{O}^-]_8$ is almost always used without being isolated from the reaction mixture from which it was prepared and ^{29}Si NMR data have been obtained for $\text{T}_8[\text{ONMe}_4]_8$ in methanolic solutions for which the chemical shift has been reported at -99.2 ppm^{218a} or at -99.4 ppm²²² and for aqueous solutions of $\text{T}_8[\text{O}(\text{NMe}_3\text{CH}_2\text{CH}_2\text{OH})]_8$ $\delta^{29}\text{Si}$ is -98.4 ppm.²²³ The solid-state ^{29}Si chemical shift for $\text{T}_8[\text{O}(\text{NMe}_3\text{CH}_2\text{CH}_2\text{OH})]_8$ is -98.38 ppm¹²⁴ and the ^{17}O chemical shifts for aqueous solution of $\text{T}_8[\text{ONMe}_4]_8$ are 72.0 and 47.5 ppm, respectively, for the bridging and terminal oxygen atoms.²²⁴ A detailed ^{29}Si NMR study of the equilibria between $\text{T}_8[\text{O}^-]_8$ and related silicates in aqueous solution gives a temperature-dependant chemical shift for $\text{T}_8[\text{O}^-]_8$ of ca. -107 ppm.²²⁵ In one study it was shown that at the start of the reaction, $\text{T}_8[\text{ONMe}_4]_8$ was formed along with $\text{T}_6[\text{ONMe}_4]_6$ (^{29}Si NMR chemical shift, -89.6 ppm) and polymeric materials that react further to give selectively the octamer $\text{T}_8[\text{ONMe}_4]_8$ after a few hours.^{218a} Molecular dynamics simulations have been carried out in order to investigate this preferential stabilization and show that the stability of $\text{T}_8[\text{O}^-]_8$ over $\text{T}_6[\text{O}^-]_6$ in aqueous solution is about 70 kcal mol^{-1} . The preferred formation of the T_8 derivative over the prismatic T_6 species is found to be due to the fact that the T_6 species cannot form a protective layer of NMe_4^+ ions around it which makes it vulnerable to hydrolysis, while the T_8 species is able to form a protective coating of cations which prevent further reaction.²²⁶

The structures of several salts of $\text{T}_8[\text{O}^-]_8$ containing different cations and numbers of water molecules have been determined by X-ray crystallography. The first structure determined was of $[\text{Me}_4\text{N}]_8[\text{Si}_8\text{O}_{20}] \cdot 64.8\text{H}_2\text{O}$, which showed Si–O bond distances of 1.558 – 1.619 Å (mean = 1.598 Å) and Si–O–Si angles of 150.03 – 150.70° (mean = 150.34°) indicating a much less distorted cubic arrangement of the Si atoms than is found in many POSS cubes (see Section V.J).²²⁷ More recently, $[\text{Me}_3\text{NCH}_2\text{CH}_2\text{OH}]_8[\text{Si}_8\text{O}_{20}] \cdot 24\text{H}_2\text{O}$ has been found to have a similar structure for the POSS core,²¹⁰ while $[\text{DMPI}]_6\text{H}_2[\text{Si}_8\text{O}_{20}] \cdot 48.5\text{H}_2\text{O}$ (DMPI = 1,

1-dimethylpiperidinium)²²⁸ and $[\text{Bu}_4\text{N}]\text{H}_7[\text{Si}_8\text{O}_{20}] \cdot 5.33\text{H}_2\text{O}$ both have complicated structures in which water has been deprotonated so that there are some Si–OH groups present. The structure and the Raman spectrum for $\text{Na}_8[\text{Si}_8\text{O}_{20}]$ have also been calculated²²⁹ and comparisons of calculated vibrational spectra for $[\text{Si}_8\text{O}_{20}]^{8-}$ with related silicates and aluminosilicates have also been made.²³⁰

3. Reactivity and applications

The reactivity of $\text{T}_8[\text{O}^-]_8$ has been dominated so far by reactions involving chlorosilanes such as RMe_2SiCl , with $\text{R}=\text{H}$, $\text{CH}=\text{CH}_2$, CH_2Cl , Ph , and CH_3 , to form $\text{T}_8[\text{OSiMe}_2\text{H}]_8$, $\text{T}_8[\text{OSiMe}_2\text{CH}=\text{CH}_2]_8$, $\text{T}_8[\text{OSiMe}_2\text{CH}_2\text{Cl}]_8$, $\text{T}_8[\text{OSiMe}_2\text{Ph}]_8$, and $\text{T}_8[\text{OSiMe}_3]_8$, respectively, in methanolic solution and in the presence of 2, 2-dimethoxypropane (to act as a dehydrating agent to aid complete silylation) (Figure 28 and Table 17). The $\text{T}_8[\text{OSiMe}_2\text{H}]_8$ and $\text{T}_8[\text{OSiMe}_2\text{CH}=\text{CH}_2]_8$ species have been used as precursors to a variety of POSS compounds, their reactivity is described below in Sections V.F and V.G. When $\text{T}_8[\text{O}^-]_8$ reacts with the difunctional Me_2SiCl_2 , a three-dimensional network is formed *via* the cross-linking of POSS cages by SiMe_2 units.²³¹

The trimethylsilyl derivative, $\text{T}_8[\text{OSiMe}_3]_8$, shows photoluminescence in the blue spectral region,⁵⁹ and is able both to trap atomic hydrogen or deuterium under γ -irradiation and undergo detrapping processes that may be studied by EPR.^{123,237} It can also be deposited by CVD onto various supports to give layers forming polycrystalline films that have been investigated by XRD.²³⁸ X-ray crystallographic data for $\text{T}_8[\text{OSiMe}_3]_8$ are given in Section V.J. The solid-state ^{13}C and ^{29}Si NMR spectra of $\text{T}_8[\text{OSiMe}_3]_8$ have been recorded using two-dimensional J-resolved and SUPERCOSY experiments, which show the distortion of the T_8 core resulting in chemical shifts of -108.36 , -108.64 , -109.36 , and -109.71 for the POSS cage Si atoms and shifts of 11.77 , 11.72 , and 11.51 ppm for the peripheral Si atoms rather than single signals for each type of silicon. This distortion is consistent with the X-ray structural data.²³⁹ The solution NMR data do, as expected, comprise singlets at -106.0 and 14.2 ppm for the POSS core and Me_3Si , respectively, in the ^{29}Si spectrum and a single signal at 5.0 ppm in the ^{13}C spectrum.¹⁷⁸

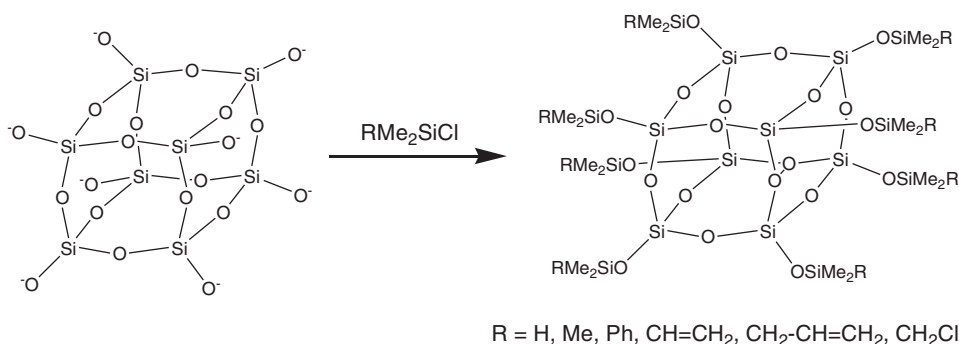


Figure 28 Reactions of $\text{T}_8[\text{O}^-]_8$ with chlorosilanes.

Table 17 Compounds $T_8[OR]_8$ obtained by silylation of $T_8[O^-]_8$

Entry	R	Starting materials and conditions	Yield (%)	^{29}Si NMR ^a	Reference
1	-SiMe ₂ H	$T_8[ONMe_4]_8$ in THF+ClSiMe ₂ H, (MeO) ₂ CMe ₂ , 25 °C, 1 h	88	-2.08, -109.36	232
2	-SiMe ₂ H	$T_8[O^-]_8$ in MeOH+ClSiMe ₂ H in hexane, 0 °C, 1 h	46.5	-	220
3	-SiMe ₂ CH=CH ₂	$T_8[ONMe_4]_8$ in H ₂ O/DMSO+(MeO) ₂ CMe ₂ , ClSiMe ₂ CH=CH ₂ , (CH ₂ =CHMe ₂ Si) ₂ O/DMF	59	-	233
4	-SiMe ₂ CH=CH ₂	$T_8[ONMe_4]_8$ in MeOH+ClSiMe ₂ CH=CH ₂ , (MeO) ₂ CMe ₂ , 25 °C, 1 h	61	0.53, -109.12	234
5	-SiMe ₂ CH ₂ CH=CH ₂	$T_8[ONMe_4]_8$ in MeOH+ClSiMe ₂ CH ₂ CH=CH ₂	52	8.70, -109.41	235
6	-SiMe ₂ CH ₂ Cl	$T_8[ONMe_4]_8$ in H ₂ O/DMSO+(MeO) ₂ CMe ₂ , ClSiMe ₂ CH=CH ₂ , (CH ₂ ClMe ₂ Si) ₂ O/DMF	47	-	233
7	-SiMe ₂ CH ₂ Cl	$T_8[ONMe_4]_8$ in MeOH+ClSiMe ₂ CH ₂ Cl, (MeO) ₂ CMe ₂ , 25 °C, 1 h	53	7.28, -109.41	234
8	-SiMe ₂ Ph	$T_8[ONMe_4]_8$ in MeOH+ClSiMe ₂ Ph, (MeO) ₂ CMe ₂ , 25 °C, 1 h	54	2.18, -109.03	234
9	-SiMe ₃ ^b	$T_8[ONMe_4]_8$ in H ₂ O/DMSO+(MeO) ₂ CMe ₂ , ClSiMe ₂ CH=CH ₂ , (Me ₃ Si) ₂ O/DMF	81	-	233
10	-SiMe ₃ ^b	$T_8[ONMe_4]_8$ in MeOH+ClSiMe ₃ , (MeO) ₂ CMe ₂ , 25 °C, 1 h	72	12.53, -108.95	234
11	-SiMe ₃ ^b	$T_8[ONMe_3(CH_2OH)]_8$ in MeOH+hexane/ClSiMe ₃ , 20 ± 5 °C, 1 h	93	12.53, -108.95	218d
12	-SiMe ₃ ^b	[Cu(en) ₂] ₄ $T_8[O^-]_8$ in DMF/hexane+Me ₃ SiO ₂ CCF ₃ , or Me ₃ SiCl or Me ₃ SiOAc	74–86	-	236

^aReferenced to SiMe₄, the signals at ca. -109 ppm are due to the POSS silicon atoms, the others due to the substituents.

^bFor alternative preparations of the Me₃Si derivative from T_8H_8 and from $T_8[OSiMe_2H]_8$ (see Sections V.B and V.F).

Table 18 Preparative routes to $T_8[OSiMe_2H]_8$

Entry	Starting materials	Yield (%)	^{29}Si NMR ^a	Reference
1	$T_8[ONMe_4]_8 + ClSiMe_2H$, DMF/heptane	88	−2.08, −109.36	232
2	$T_8[ONMe_4]_8 + ClSiMe_2H$, THF	87	−0.8, −103.9	117
3	$T_8[ONMe_4]_8 + ClSiMe_2H$, H_2O /hexane	60	−1.16, −109.43	240
4	$T_8[ONMe_3(C_2H_4OH)]_8 + ClSiMe_2H$, H_2O /hexane	83	−3.00, −110.34	218d

^aReferenced to $SiMe_4$.

F. Synthesis, properties, and reactions of $T_8[OSiMe_2H]_8$ and its derivatives

1. Synthesis

The synthesis of $T_8[OSiMe_2H]_8$ was first reported by Hoebbel et al. from the reaction between $T_8[ONMe_4]_8$ and chlorodimethylsilane in dimethylformamide (DMF)/heptane (Table 18, entry 1). Other authors have modified the procedure by changing the solvents to tetrahydrofuran (THF) or hexane, or by using $T_8[ONMe_3(C_2H_4OH)]_8$ as the silicate anion source, but without significant improvement in the yield (Table 18).

2. Structure and physical properties

Several values for the ^{29}Si NMR spectroscopy chemical shifts for $T_8[OSiMe_2H]_8$ have been reported depending on the NMR solvent used (see Table 18). Noticeable differences were obtained for the $SiMe_2H$ group with a chemical shift of −1.3 ppm in heptane,⁷⁸ −2.08 ppm in heptane, −1.16 ppm in $CDCl_3$, −0.8 ppm in D_2O , and −3.0 ppm in $THF-D_8$, whereas, apart from in THF, for the cage silicon the chemical shifts are mostly around −109 ppm. In the solid-state ^{29}Si NMR spectrum two signals were observed for each type of silicon, −3.04 and −2.18 ppm for $SiMe_2H$ and −109.2 and −109.06 ppm for the cage silicon, both in 3:1 ratio indicating some distortion due to crystal packing effects.⁷⁸ The mass spectrum of $T_8[OSiMe_2H]_8$ has been reported in a study to show that atmospheric pressure chemical ionization mass spectrometry can be used to characterize low molecular weight silsesquioxanes.¹⁸¹

Suitable crystals for a single-crystal XRD study were obtained by slow diffusion of hexane into a THF solution of $T_8[OSiMe_2H]_8$,¹¹⁷ or by slow evaporation of a CH_2Cl_2/CH_3CN mixture.²⁴¹ The Si–O bond distances fall in the range 1.480(5)–1.605(4) Å (mean = 1.560 Å) and the Si–O–Si angles in the range 148.5(3)–167.0(2)° (mean = 154.7°). Both the bond distances and angles for the POSS core vary widely for such an apparently highly symmetrical structure (Figure 29). This is found to be a common feature in many T_8 derivatives with flexible substituents and is discussed further in Section VJ.

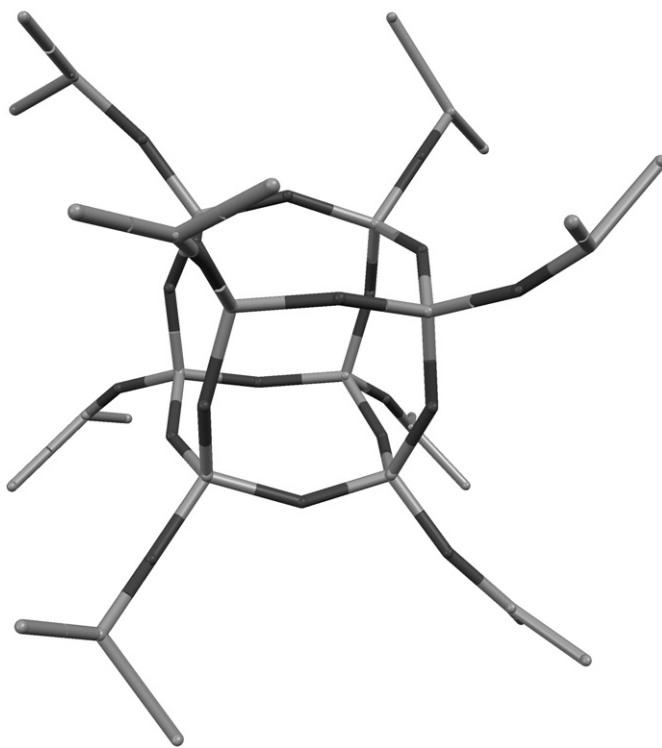


Figure 29 Crystal structure of $T_8[OSiMe_2H]_8$. (Redrawn using data for structure HOKTUW from the Cambridge Crystallographic Data Centre.) H atoms are omitted for clarity.

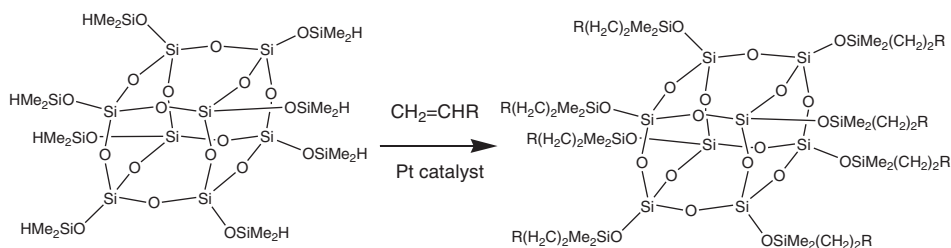
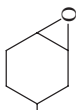
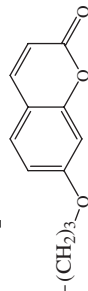


Figure 30 General scheme of hydrosilylation reactions using $T_8[OSiMe_2H]_8$.

3. Reactivity and applications

The reactivity of $T_8[OSiMe_2H]_8$ is dominated by its capacity to undergo hydrosilylation reactions with a wide variety of vinyl and allyl derivatives (Figure 30) that have subsequently mainly been used as precursors to polymers and nanocomposites by the introduction of reactive terminating functions as shown in Table 19. For example, $T_8[OSiMe_2H]_8$ has been modified with allylglycidyl ether, epoxy-5-hexene, and 1,2-cyclohexene-epoxide to give epoxy-terminated POSS. These have then been treated with *m*-phenylenediamine, with polyamic acids or

Table 19 Compounds $T_8[OSiMe_2R]_8$ for hybrid material synthesis obtained from $T_8[OSiMe_2H]_8$

Entry	R	Starting materials	Yield (%)	^{29}Si NMR ^a	Reference
1	$-(CH_2)_3OCH_2CH(O)CH_2$	$T_8[OSiMe_2H]_8 + CH_2 = CHCH_2OCH_2CH(O)CH_2$	–	12.27, –109.8	243–245
2	$-(CH_2)_4CH(O)CH_2$	$T_8[OSiMe_2H]_8 + CH_2 = CH(CH_2)_2CH(O)CH_2$	95	21.3, –101.0	244, 246
3	$-(CH_2)_2$ 	$T_8[OSiMe_2H]_8 + 4\text{-vinyl-1,2-cyclohexene-epoxide}$	90	–	218c, 246, 247
4	$-(CH_2)_3OH$	$T_8[OSiMe_2H]_8 + CH_2 = CHCH_2OH$	86	13.9, –108.3	248–251
5	$-(CH_2)_3O(CH_2)_2OH$	$T_8[OSiMe_2H]_8 + CH_2 = CHCH_2O(CH_2)_2OH$	87	13.6, –108.5	248
6	$-(CH_2)_3OSiMe_3$	$T_8[OSiMe_2H]_8 + CH_2 = CHCH_2OSiMe_3$	82	13.3, 16.5, –108.9	248
7	$-(CH_2)_3O_2CCMe = CH_2$	$T_8[OSiMe_2(CH_2)_3OH]_8 + CH_2 = CHCH_2O_2CCMe = CH_2$	75	14.4, –107.8	248
8	$-(CH_2)_3O_2CCMe_2Br$	$T_8[OSiMe_2(CH_2)_3OH]_8 + Br(O)CCMe_2Br$	60	12.0, –109.8	252
9	$-(CH_2)CH(Me)-C_6H_4-CMe_2NCO$	$T_8[OSiMe_2H]_8 + CH_2 = C(Me)-C_6H_4-CMe_2NCO$	94	11.9, –109.1	116, 253
10		$T_8[OSiMe_2H]_8 + 7\text{-allyloxy coumarin}$	91	–	254
11	$-(CH_2)_3O(CH_2CH_2O)_nH$	$T_8[OSiMe_2H]_8 + CH_2 = CHCH_2-O(CH_2CH_2O)_nH$ ($n = 1-4$)	–	–	255
12	$-(CH_2)_2-C_6H_4-4-O_2CMe$	$T_8[OSiMe_2H]_8 + CH_2 = CH-C_6H_4-4-O_2CMe$	93	–	256
13	$-(CH_2)_3CN$	$T_8[OSiMe_2H]_8 + CH_2 = CH-CH_2CN$	43	–18.4, –118.0	257

^aReferenced to $SiMe_4$.

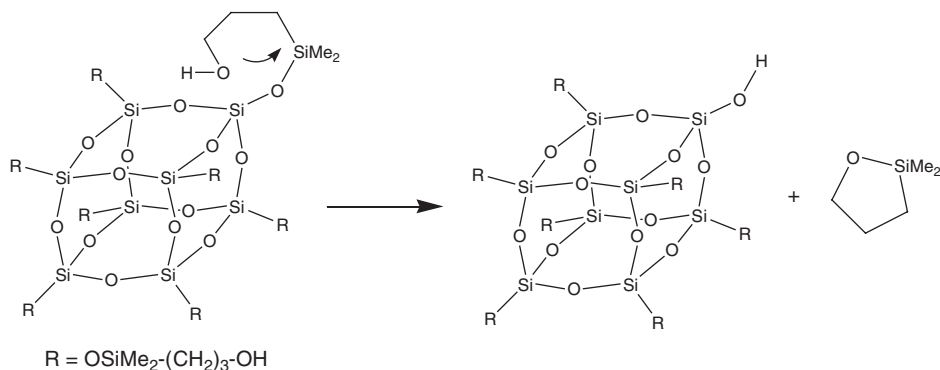


Figure 31 Proposed decomposition pathway of $T_8[\text{OSiMe}_2(\text{CH}_2)_3\text{OH}]_8$.

introduced in the Ciba epoxy resin (Araldite LY5210) to give epoxy resin networks with nanostructures. It has been shown that the improvement of the cross-link densities in these hybrid systems improves the thermal stability with a higher glass transition temperature compared to the standard resins (Table 19, entries 1–3). Polyamic acid also reacts with a more complicated POSS precursor containing both hexafluoroisopropyl and glycidyl termini (both introduced *via* hydrosilylation) to give low dielectric constant polyimides.²⁴²

Alcohol functions have also been introduced *via* hydrosilylation reactions, for example, the reaction of $T_8[\text{OSiMe}_2\text{H}]_8$ with allyl alcohol and allyloxy ethanol (Table 19). In the first case, it has been postulated that the compound $T_8[\text{OSiMe}_2(\text{CH}_2)_3\text{OH}]_8$ is not very stable due to back-biting of the -OH groups on the silicon corners (Figure 31). Nevertheless, it reacts with polymers such as polyvinyl pyrrolidone to give polymer hybrids (Table 19, entries 4 and 5).

A methacrylate function has been introduced using the reaction of $T_8[\text{OSiMe}_2\text{H}]_8$ with allyl alcohol and then methacryloyl chloride. Preliminary studies on polymerization under UV irradiation of the reaction product showed the formation of nanocomposites (Table 19, entries 5 and 7). The bromo-terminated compound formed by the reaction of $T_8[\text{OSiMe}_2(\text{CH}_2)_3\text{OH}]_8$ with 2-bromo-2-methylpropionylbromide undergoes Cu-catalyzed atom transfer radical polymerization to give nanocomposites (Table 19, entry 8). Hybrid polyurethanes have been prepared by reacting the isocyanate-terminated $T_8[\text{OSiMe}_2\text{CH}_2\text{CH}(\text{Me})\text{-C}_6\text{H}_4\text{-CMe}_2\text{NCO}]_8$ with polyethylene glycol (Table 19, entry 9). When $T_8[\text{OSiMe}_2(\text{CH}_2)_2\text{-C}_6\text{H}_4\text{-O}_2\text{CMe}]_8$ is treated with phenolic resins, nanocomposites are formed and stabilized through H-bonding interactions between the phenol groups and the carbonyl or siloxane functions of the POSS moiety (Table 19, entry 12). Another interesting example is the product obtained by reaction between $T_8[\text{OSiMe}_2\text{H}]_8$ and allyloxy coumarin, which can be dimerized under UV to give three-dimensional hybrid materials (Table 19, entry 10).

The synthesis of three-dimensional polymers derived from $T_8[\text{OSiMe}_2\text{H}]_8$ has been also achieved in several ways. For example, by reacting $T_8[\text{OSiMe}_2\text{H}]_8$ with bifunctional vinyl-terminated linkers such as $(\text{CH}_2=\text{CHSiMe}_2)_2\text{O}$,²⁵⁸

vinyl-ferrocenes,²⁵⁹ 1,5-hexadiene,²⁶⁰ or $F_2C=CH_2O_2C-C_6H_4-CO_2CH=CF_2$ giving, in the last case, fluorinated polymers²⁶¹ (Figure 32).

The Si-H-terminated $T_8[OSiMe_2H]_8$ has also been treated with other POSS molecules containing vinyl groups such as $T_8[CH=CH_2]_8$ ^{64,133,210} and $T_8[OSiMe_2CH=CH_2]_8$,^{133,262} as already described in previous sections. Polymers have also been formed by the auto-condensation and cross-linking of $T_8[OSiMe_2H]_8$ in the presence of water.²⁶³ Vinyl-terminated polymers $CH_2=CH(OSiMe_2)_nCH=CH_2$ and $CH_2=CHCH_2(OCH_2CH_2)_nOCH=CH_2$ have also been used as organic linkers for $T_8[OSiMe_2H]_8$ to give membranes.²⁶³ The polymers obtained possess quite high surface areas, up to $500\text{ m}^2\text{ g}^{-1}$, with pore sizes in the range of 1–50 nm, and thermal stability up to 1000°C .

Hasegawa et al. have found a different kind of reactivity for $T_8[OSiMe_2H]_8$ and showed that it undergoes substitution reactions with compounds such as $ClSiMe_2X$ ($X = \text{Me}$, CH_2Cl , and CH_2Br) in hexane/acetic acid solution to give $T_8[OSiMe_3]_8$, $T_8[OSiMe_2CH_2Cl]_8$, and $T_8[OSiMe_2CH_2Br]_8$ with yields greater than 90% (Figure 33; Table 20, entries 1, 3, 4). This is an interesting alternative synthesis for this type of compound, which is readily obtained from $T_8[O^-]_8$ (Section V.E), but, although it gives high yields, it is unlikely to be synthetically useful as $T_8[OSiMe_2H]_8$ is itself also prepared from $T_8[O^-]_8$.

Hasegawa's group has also demonstrated that when $T_8[OSiMe_2H]_8$ reacts with MeOH or H_2O , the silicate core is retained while a cleavage of the SiO–SiMe₂H bond occurs. This does not happen for $T_8[OSiMe_3]_8$ indicating that the reactivity

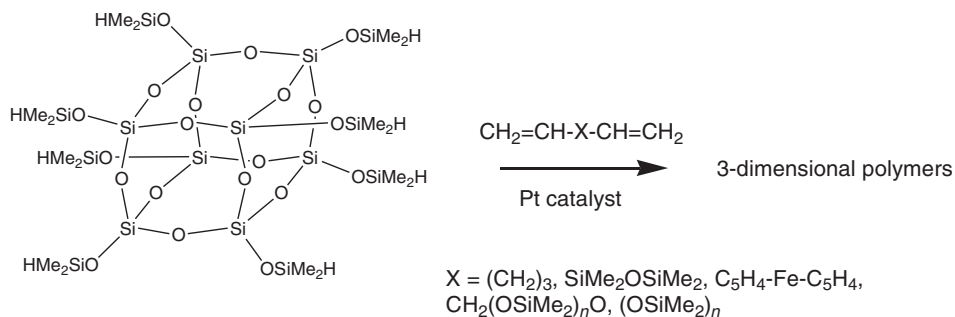


Figure 32 Formation of three-dimensional polymers using $T_8[OSiMe_2H]_8$.

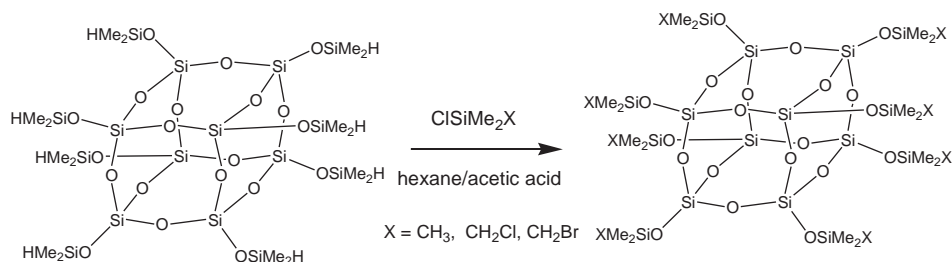


Figure 33 Substitution of dimethylsilyl groups of $T_8[OSiMe_2H]_8$.

Table 20 Compounds $T_8[R]_8$ obtained by Si substitution of $T_8[OSiMe_2H]_8$

Entry	R	Starting materials	Yield (%)	^{29}Si NMR ^a	Reference
1	$-\text{OSiMe}_3$	$T_8[OSiMe_2H]_8 + \text{ClSiMe}_3$, $\text{C}_6\text{H}_{14}/\text{AcOH}$	> 90	–	264
2	$-\text{OSiMe}_2\text{OSiMe}_3$	$T_8[OSiMe_2H]_8 + (\text{Me}_3\text{Si})_2\text{O}$	97	12.5, –21.9, –109.8	219
3	$-\text{OSiMe}_2\text{CH}_2\text{Cl}$	$T_8[OSiMe_2H]_8 + \text{ClSiMe}_2\text{CH}_2\text{Cl}$, $\text{C}_6\text{H}_{14}/\text{AcOH}$	> 90	7.36, –109.31	264
4	$-\text{OSiMe}_2\text{CH}_2\text{Br}$	$T_8[OSiMe_2H]_8 + \text{ClSiMe}_2\text{CH}_2\text{Br}$, $\text{C}_6\text{H}_{14}/\text{AcOH}$	> 90	7.02, –109.36	264

^aReferenced to SiMe_4 .

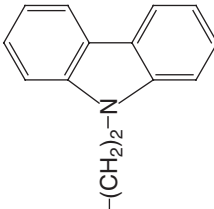
of Si–O–Si bonds depends on the type of groups attached to the pendant Si atoms.²¹⁹

Other compounds with various applications have also been prepared from $T_8[OSiMe_2H]_8$ and are listed in Table 21 (Figure 34). An interesting example is the metallation on reaction with $\text{Co}_2(\text{CO})_8$ (entry 1) giving rise to the formation of Si–Co bonds without the loss of carbonyl ligands. When $T_8[OSiMe_2H]_8$ reacts with vinylferrocene, the product has ferrocenyl-terminated substituents and has been subjected to electrochemical studies (Table 21, entry 7). Polymeric capping agents for Pd and Pt nanoparticles have been prepared by reaction of $T_8[OSiMe_2H]_8$ with polyethylene glycol and $\text{CH}_2=\text{CHCH}_2\text{O}-(\text{CH}_2\text{CH}_2\text{O})_n\text{CH}_3$, respectively (Table 21, entries 15 and 16). The product from the reaction between $T_8[OSiMe_2H]_8$ and 9-vinylcarbazole shows photoluminescent properties, while the one from the reaction with 4-cyano-4'-(5-hexenyloxy)biphenyl shows liquid crystal properties (Table 21, entries 18 and 19). Blue light, electroluminescent nanoparticles can be produced from the hydrosilylation reaction between $T_8[OSiMe_2H]_8$ and an allyl-substituted terfluorene chromophore.²⁶⁵ Only a selection of the wide variety of materials derived from $T_8[OSiMe_2H]_8$ with potentially useful properties are described above, further applications of these materials are being investigated in the fields of nanocomposites,^{217,266} organic–inorganic hybrid gels,²⁶⁷ electrolytes for lithium batteries,²⁶⁸ amperometric biosensors,²⁶⁹ and inclusion complexes.²⁷⁰ It can be expected that many more applications will be realized in the near future.

All of the hydrosilylation reactions described above have been performed using a catalyst, Pt-based compounds being widely used. Karstedt's catalyst, $\text{Pt}(\text{dvs})$, is most popular compared with others such as H_2PtCl_6 because it allows mild reaction conditions, gives reproducible results, and is more regioselective to α -addition (anti-Makovnikov), and if in high concentration, gives the preferred C-silylation versus the O-silylation when allylic alcohols are used (Table 19, entry 4). Interestingly, in the case of allylbromide, when a $\text{Rh}(\text{acac})_3$ catalyst is used, the reaction occurring is a halogenation, giving Si–Br bond formation, whereas when a Pt catalyst is used, the reaction gives a product with $\text{Si}(\text{CH}_2)_3\text{Br}$ groups (Table 21, entries 12 and 13). Huang et al. have shown that the catalyst $\text{Pt}(\text{dvs})$ can

Table 21 Miscellaneous $T_8[\text{OSiMe}_2\text{R}]_8$ compounds obtained from $T_8[\text{OSiMe}_2\text{H}]_8$

Entry	R	Starting materials	Yield (%)	^{29}Si NMR ^a	Reference
1	$-\text{Co}(\text{CO})_4$	$T_8[\text{OSiMe}_2\text{H}]_8 + \text{Co}_2(\text{CO})_8$	99	46.3, –110.6	78
2	$-(\text{CH}_2)_2\text{C}_6\text{H}_9$	$T_8[\text{OSiMe}_2\text{H}]_8 + 4\text{-vinylcyclohexene}$	–	12.4, –109.5	243
3	$-(\text{CH}_2)_{17}\text{CH}_3$	$T_8[\text{OSiMe}_2\text{H}]_8 + \text{CH}_2 = \text{CHC}_{16}\text{H}_{33}$	–	11.9, –109.5	243
4	$-(\text{CH}_2)_2\text{Ph}$ (40% selectivity)	$T_8[\text{OSiMe}_2\text{H}]_8 + \text{CH}_2 = \text{CHPh}$	–	11.9, –109.3	243
5	$-\text{CH}(\text{CH}_3)\text{Ph}$ (60% selectivity)	$T_8[\text{OSiMe}_2\text{H}]_8 + \text{CH}_2 = \text{CHPh}$	–	9.98, –109.6	243
6	$-\text{CH}(\text{Me})\text{CH}_2\text{CO}_2\text{Me}$	$T_8[\text{OSiMe}_2\text{H}]_8 + \text{CH}(\text{Me}) = \text{CHCO}_2\text{Me}$	–	11.9, –109.1	243
7	$-(\text{CH}_2)_2-\text{C}_3\text{H}_4-\text{Fe}-\text{C}_5\text{H}_5$	$T_8[\text{OSiMe}_2\text{H}]_8 + \text{CH}_2 = \text{CH}-\text{C}_3\text{H}_4-\text{Fe}-\text{C}_5\text{H}_5$	57	13.2, –107.9	259
8	$-(\text{CH}_2)_3\text{C} \equiv \text{C}-\text{MeB}_{10}\text{H}_{10}$	$T_8[\text{OSiMe}_2\text{H}]_8 + \text{CH}_2 = \text{CHCH}_2\text{C} \equiv \text{C}-\text{MeB}_{10}\text{H}_{10}$	85	12.7, –108.9	271
9	$-(\text{CH}_2)_2-\text{C}_3\text{H}_3(\text{Me})-\text{Mn}(\text{CO})_3$, 2 isomers	$T_8[\text{OSiMe}_2\text{H}]_8 + \text{CH}_2 = \text{CH}-\text{C}_3\text{H}_3(\text{Me})\text{Mn}(\text{CO})_3$	9	12.8, 10.6, –108.4	271
10	$(\text{CH}_2)_2-\text{CH} = \text{CH}-\text{CH}_2-\text{O}_2\text{C}-\text{CMe} = \text{CH}_2$	$T_8[\text{OSiMe}_2\text{H}]_8 + \text{CH}_2 = \text{CH}-\text{CH} = \text{CH}-\text{CH}_2-\text{O}_2\text{C}-\text{CMe} = \text{CH}_2$	–	–	272
11	$-(\text{CH}_2)_3(\text{CH}_2\text{CMe}_2)_n\text{H}$	$T_8[\text{OSiMe}_2\text{H}]_8 + \text{CH}_2 = \text{CHCH}_2(\text{CH}_2\text{CMe}_2)_n\text{H}$	–	–	273
12	$-(\text{CH}_2)_3\text{Br}$	$T_8[\text{OSiMe}_2\text{H}]_8 + \text{CH}_2 = \text{CHCH}_2\text{Br}$ (Pt catalyst)	50	10.7, –106.9	117
13	$-\text{Br}$	$T_8[\text{OSiMe}_2\text{H}]_8 + \text{CH}_2 = \text{CHCH}_2\text{Br}$ (Rh catalyst)	99	5.4, –110.9	78
14	$-\text{CH}_2\text{CH}(\text{Me})\text{CO}_2-(\text{CH}_2)_2\text{C}_8\text{F}_{17}$	$T_8[\text{OSiMe}_2\text{H}]_8 + \text{CH}_2 = \text{CMeCO}_2(\text{CH}_2)_2-\text{C}_8\text{F}_{17}$	–	11.9, –109.7	274

15	$-(O-CH_2CH_2)_nOH$	$T_8[OSiMe_2H]_8 + \text{polyethylene glycol, Wilkinson's catalyst}$	98	-57.8, -56.2	275
16	$-(CH_2)_3O(CH_2CH_2O)_nCH_3$	$T_8[OSiMe_2H]_8 + CH_2 = CHCH_2O(CH_2CH_2O)_nCH_3$ ($n = 2-12.5$)	-	-	276-278
17	$-(CH_2)_3OSiMe_2tBu$	$T_8[OSiMe_2H]_8 + CH_2 = CHCH_2OSiMe_2tBu$	88	-	249
18		$T_8[OSiMe_2H]_8 + 9\text{-vinylcarbazole}$	70	12.4, -108.9	279
19	$-O-(CH_2)_4-C_6H_4-C_6H_4CN$	$T_8[OSiMe_2H]_8 + 4\text{-cyano-4'-(5-hexenyloxy)biphenyl}$	85	12.3, -108.8	280
20	$-CH(COOEt)_2$	$T_8[OSiMe_2H]_8 + BrCH(COOEt)_2, Na$	27	-	281
21	$-(CH_2)_3Cl$	$T_8[OSiMe_2H]_8 + CH_2 = CHCH_2Cl$	48	-	282
22	$-(CH_2)_3OCH-(CH_2OCH_2Ph)_2$	-	-	-	283

^aReferenced to SiMe₄.

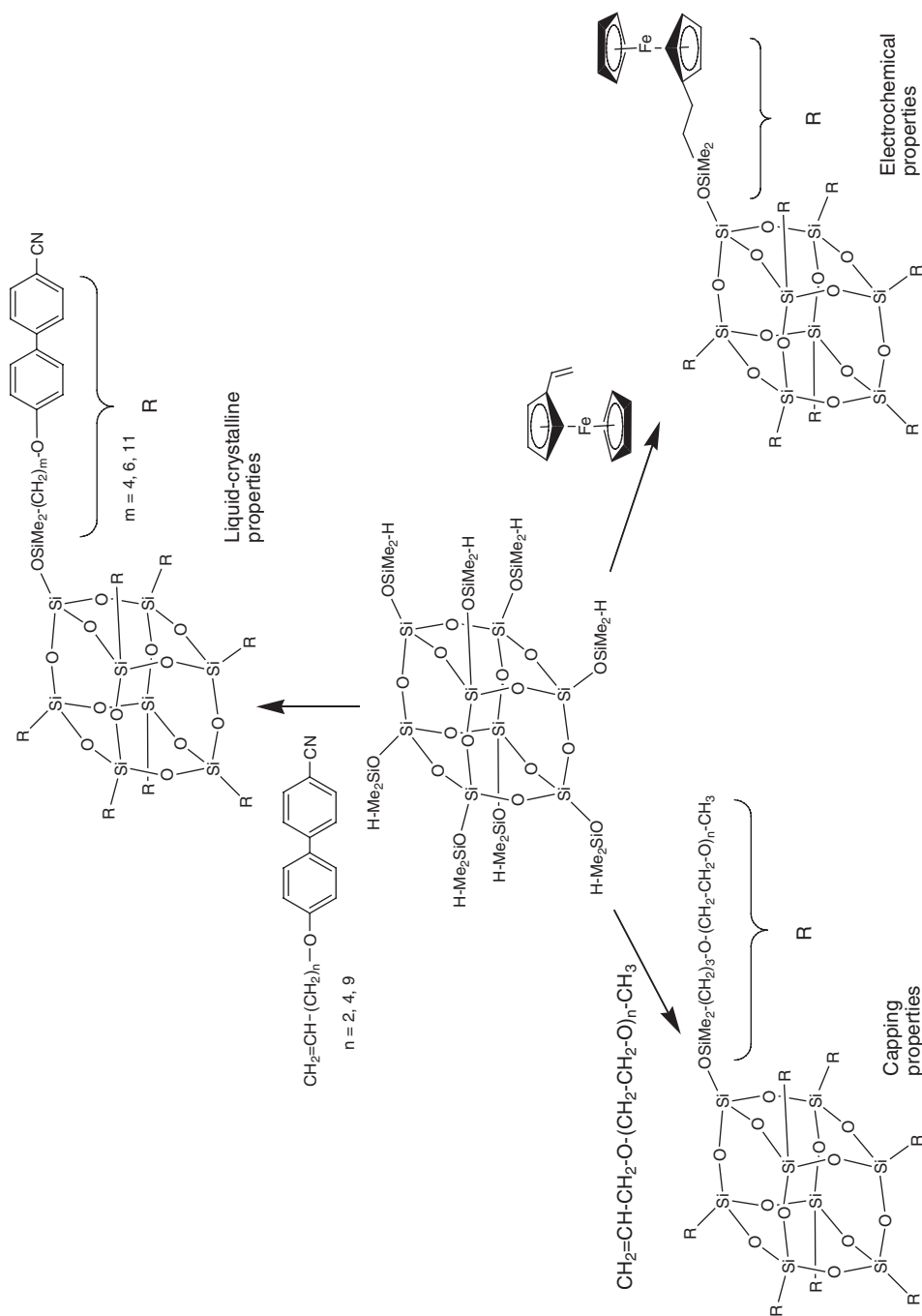


Figure 34 Monomeric functionalized products obtained from $\text{T}_8[\text{OSiMe}_2\text{H}]_8$.

be used as an *in situ* Pt precursor for Pt nanoparticles during the Pt-catalyzed synthesis of $T_8[OSiMe_2(CH_2)_3(CH_2CH_2O)_nCH_3]_8$, this latter compound being then used as a capping agent for the nanoparticles formed during this process (Table 21, entry 16 and Figure 34).

G. Synthesis, properties, and reactions of $T_8[OSiMe_2CH=CH_2]_8$ and its derivatives

1. Synthesis

The synthesis of $T_8[OSiMe_2CH=CH_2]_8$ was first reported in 1989 by Hoebbel et al. using the reaction between the silicate anion $T_8[ONMe_4]_8$ and $CH_2=CHSiMe_2Cl$ in the presence of $(CH_2=CHMe_2Si)_2O$ at room temperature giving a 50% yield. Later, Agaskar described a different synthesis, giving up to 89% yield that required three different solutions to be mixed sequentially. The first, an aqueous solution of $T_8[ONMe_4]_8$ in dimethylsulfoxide (DMSO), the second a 2,2-dimethoxypropane (dehydrating agent) solution of $(CH_2=CHMe_2Si)_2O$ in the presence of concentrated HCl, and the third a solution of $(CH_2=CHMe_2Si)_2O$ and $ClSiMe_2CH=CH_2$ in DMF. Hasegawa et al. and Yuchs et al. also introduced a procedure, using $CH_2=CHMe_2SiCl$ as a single silylation precursor, but without improving the final yield (see Table 22 for details).

2. Structure and physical properties

The ^{29}Si NMR spectrum displays two signals, as expected, at 0.53 and -109.1 ppm in $CDCl_3$ solution;^{218b} the MALDI-TOF mass spectrum and DSC curve for $T_8[OSiMe_2CH=CH_2]_8$ have also been reported.²⁴¹ The single-crystal X-ray structure was reported by Auner et al. in 1999, the Si–O bond distances are in the range 1.597–1.608(3) Å (mean = 1.602 Å) and the Si–O–Si angles in the range 148.1–148.3(3)° (mean = 148.2°). These values fall in much narrower ranges than for the related $T_8[OSiMe_2H]_8$ species and show much less distortion from the ideal cubic arrangement for the core Si atoms (Figure 35).²⁴¹ The structures of T_8R_8 species are described in more detail in Section V.J.

3. Reactivity and applications

The reactivity of $T_8[OSiMe_2CH=CH_2]_8$ is, as expected, often similar to that described for $T_8[CH=CH_2]_8$. Initially, Feher et al. performed olefin cross-metathesis

Table 22 Preparative routes to $T_8[OSiMe_2CH=CH_2]_8$

Entry	Starting materials	Yield (%)	Reference
1	$T_8[ONMe_4]_8 + ClSiMe_2CH=CH_2 + (CH_2=CHSiMe_2O)_2$, HCl, <i>i</i> PrOH/ H_2O	50	235
2	$T_8[ONMe_4]_8 + ClSiMe_2CH=CH_2 + (CH_2=CHSiMe_2O)_2$, HCl, DMSO/ Me_2NCHO/H_2O	89	233,284
3	$T_8[ONMe_4]_8 + ClSiMe_2CH=CH_2$, MeOH/THF/ H_2O	–	218b
4	$T_8[ONMe_4]_8 + ClSiMe_2CH=CH_2$, hexane/DMF	87	281

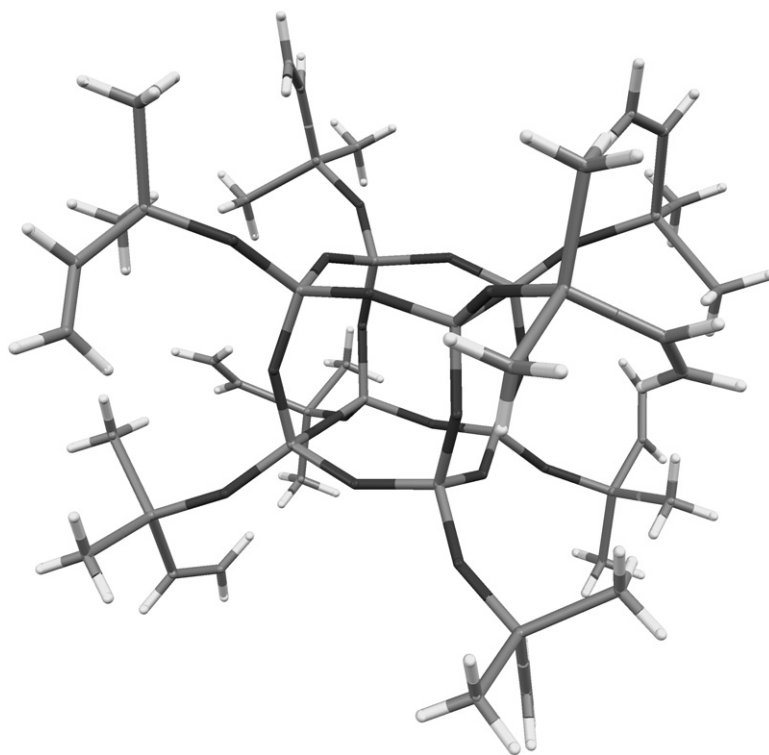


Figure 35 Crystal structure of $T_8[OSiMe_2CH=CH_2]_8$. (Redrawn using data for structure HOKVEI from the Cambridge Crystallographic Data Centre.)

reactions at room temperature with alkenes such as styrene and 1-pentene, in the presence of 6% of the Schrock catalyst $[(2,6\text{-}iPr_2C_6H_3N)Mo(=CHCMe_2Ph)]$ (see Table 23). As already observed in the case of $T_8[CH=CH_2]_8$, only the *trans* product was obtained in the case of styrene (70% yield), while a *cis/trans* mixture was observed for 1-pentene with a majority of the *trans* product (quantitative yield).¹⁸⁷ Subsequently, functionalized products have been prepared by hydrosilylation reactions of $T_8[OSiMe_2CH=CH_2]_8$. For example, Hoebbel et al. have used $HSiMe(OSiMe_3)_2$ and $HSiEt_3$ in toluene at 100 °C in the presence of H_2PtCl_6 giving products following anti-Markovnikov addition (Table 23, entries 1 and 2) and Jutzi et al. have performed a series of hydrosilylations using either the Karstedt's catalyst, $Pt(dvs)$, or Speier's catalyst ($H_2PtCl_6 \cdot 6H_2O$ in toluene or THF) giving products in high yields (Table 23, entries 3–6). Mutluay et al. have reinvestigated the dendrimer synthesis introduced by Morris and Cole-Hamilton (see Section V.D) with the preparation of chloro- and allyl-silsesquioxanes by successive reactions (Table 23, entries 7, 8, and 9). The electrochemistry of a ferrocenyl-substituted compound was studied and showed reversible redox process, indicating that all the 16 ferrocene moieties are independent of each other. Zhang et al. have performed a complete epoxidation of the terminating vinyl groups, in contrast with the case of $T_8[CH=CH_2]_8$, using *m*-CPBA (Figure 36). The resulting compound reacted in the

Table 23 Miscellaneous $T_8[OSiMe_2R]_8$ compounds derived from $T_8[OSiMe_2CH=CH_2]_8$

Entry	R	Starting materials	Yield (%)	^{29}Si NMR ^a	Reference
1	$-(CH_2)_2SiMe(OSiMe_3)_2$	$T_8[OSiMe_2CH=CH_2]_8+HSiMe(OSiMe_3)_2$ H_2PtCl_6	–	12.8, 6.5, –21.3, –108.6	285
2	$-(CH_2)_2SiEt_3$	$T_8[OSiMe_2CH=CH_2]_8+HSiEt_3$, H_2PtCl_6	–	12.2, 7.8, –109.4	285
3	$-(CH_2)_2SiMe_2-Fc^b$	$T_8[OSiMe_2CH=CH_2]_8+HSiMe_2-Fc$, H_2PtCl_6	70	13.5, –0.4, –108.1	271
4	$-(CH_2)_2SiMe_2Cl$	$T_8[OSiMe_2CH=CH_2]_8+HSiMe_2Cl$, Speier's catalyst	97	32.9, 13.3, –108.8	271
5	$-(CH_2)_2SiMeCl_2$	$T_8[OSiMe_2CH=CH_2]_8+HSiMeCl_2$, H_2PtCl_6	86	33.6, 13.3, –109.0	271
6	$-(CH_2)_2Si(OEt)_3$	$T_8[OSiMe_2CH=CH_2]_8+HSi(OEt)_3$, Speier's catalyst	83	13.2, –44.6, –108.8	271
7	$-(CH_2)_2SiMe(CH_2CH=CH_2)_2$	$T_8[OSiMe_2(CH_2)_2-SiMeCl_2]_8+$ $CH_2=CHCH_2MgBr$	–	–	286
8 ^b	$-(CH_2)_2SiMe(CH_2)_3-SiMe_2Fc$	$T_8[OSiMe_2(CH_2)_2SiMe(CH_2-CH=CH_2)_2]_8+$ $HSiMe_2Fc$	–	–	286
9	$-(CH_2)_2SiMe(OCH_2-CH=CH_2)_2$	$T_8[OSiMe_2(CH_2)_2SiMeCl_2]_8+CH_2=CHCH_2OH$	–	–	286
10	$-CH(O)CH_2$	$T_8[OSiMe_2CH=CH_2]_8+m-CPBA$	87	6.98, –109.45	207
11	$-(CH_2)_2Br$	$T_8[OSiMe_2CH=CH_2]_8+HBr$, PhOOPh	79	10.71, –109.43	281
12	$-(CH_2)_2SiCl_3$	$T_8[OSiMe_2CH=CH_2]_8+HSiCl_3$, H_2PtCl_6	95	13.6, 13.1, –109.0	287
13	$-(CH_2)_2Si(CH=CH_2)_3$	$T_8[OSiMe_2(CH_2)_2-SiCl_3]_8+CH_2=CH-MgBr$	78	–	287

^aReferenced to $SiMe_4$.^b $Fc = C_3H_4FeC_5H_5$.

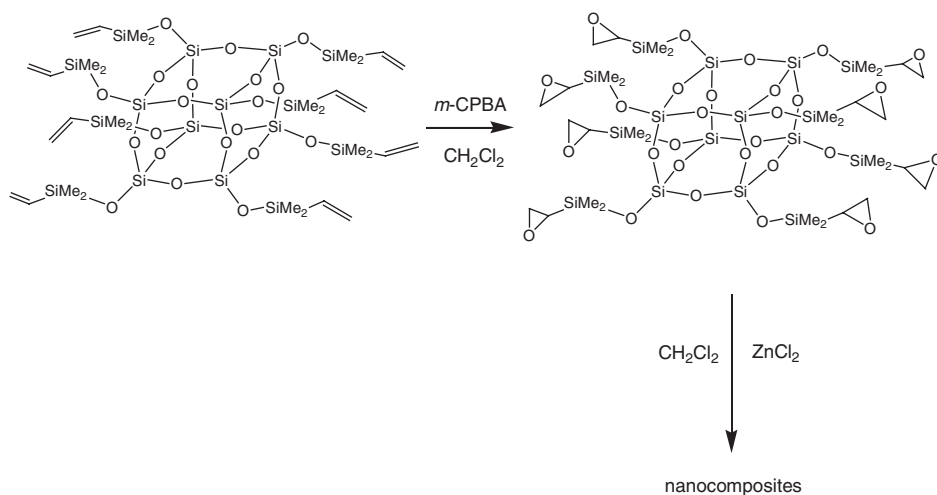


Figure 36 Epoxidation of $\text{T}_8[\text{OSiMe}_2\text{CH}=\text{CH}_2]_8$.

presence of ZnCl_2 or EDA, to give insoluble nanocomposite polymers (Table 23, entry 10).

The copolymerization of $\text{T}_8[\text{OSiMe}_2\text{CH}=\text{CH}_2]_8$ with other POSS species such as $\text{T}_8[\text{OSiMe}_2\text{H}]_8$ and T_8H_8 or with other silanes such as $(\text{HMeSiO})_4$ or $\text{Me}_3\text{SiO}(\text{HMeSiO})_5\text{OSiMe}_3$ gives nanocomposites containing both small intercubic pores and mesopores that have been analyzed by a range of solid-state techniques.^{133,187,258,262,288} The sizes, shapes, and distribution of the pores have also been the subject of a Monte Carlo study in order to determine the effect of the linker length and rigidity.²¹⁷

H. Synthesis, properties, and reactions of $\text{T}_8[(\text{CH}_2)_3\text{NH}_3\text{Cl}]_8$ and its derivatives

1. Synthesis

The synthesis of $\text{T}_8[(\text{CH}_2)_3\text{NH}_2]_8$ was first reported by the Wacker-Chemie company²⁸⁹ but no experimental details or characterization data were provided in this patent. Later work reinvestigated the claims and found that the hydrolytic condensation of $\text{H}_2\text{N}(\text{CH}_2)_3\text{Si}(\text{OEt})_3$ gave, after 6 weeks, a compound that was shown to be the hydrochloride salt $\text{T}_8[(\text{CH}_2)_3\text{NH}_3\text{Cl}]_8$ (Figure 37 and Table 24, entries 1 and 2).

The hydrochloride may be isolated in a 35% yield as a stable and easy to handle white solid. The free amine $\text{T}_8[(\text{CH}_2)_3\text{NH}_2]_8$ can be prepared in a quantitative yield by the reaction of $\text{T}_8[(\text{CH}_2)_3\text{NH}_3\text{Cl}]_8$ in methanol with a basic Amberlite IRA-400 exchange resin (Table 24, entry 3). Alternatively, if the initial solvolysis of $\text{H}_2\text{N}(\text{CH}_2)_2\text{Si}(\text{OEt})_3$ is carried out in a basic medium the free amine is reported to be formed directly in excellent yield (Table 24, entry 4). In this case, decomposition of the resulting amine was not reported (see below).

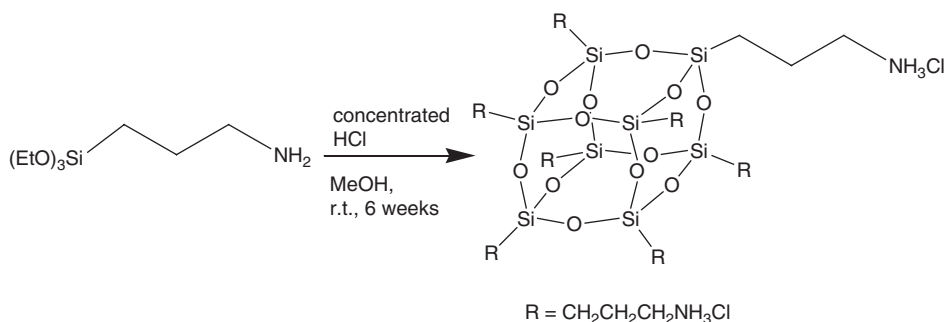


Figure 37 Preparation of T₈[(CH₂)₃NH₃Cl]₈.

Table 24 Preparative routes to T₈[(CH₂)₃NH₃Cl]₈ and T₈[(CH₂)₃NH₂]₈

Entry	Compound T ₈ [(CH ₂) ₃ R] ₈	Starting materials and conditions	Yield (%)	Reference
1	R = -NH ₃ Cl	H ₂ N(CH ₂) ₃ Si(OEt) ₃ +H ₂ O/MeOH, HCl	–	290
2	R = -NH ₃ Cl	H ₂ N(CH ₂) ₃ Si(OEt) ₃ +H ₂ O, HCl, MeOH, 6 weeks	35	291–293
3	R = -NH ₂	T ₈ [(CH ₂) ₃ NH ₃ Cl] ₈ +Amberlite IRA-400 resin, MeOH	35 overall	291–293
4	R = -NH ₂	H ₂ N(CH ₂) ₃ Si(OEt) ₃ +Me ₄ NOH/ MeOH, 24 h room temperature, 48 h, 60 °C	92.7	294

2. Structure and physical properties

The ²⁹Si NMR spectrum for both T₈[(CH₂)₃NH₂]₈ and T₈[(CH₂)₃NH₃Cl]₈ displays a signal at –66.4 ppm (CD₃OD),²⁹² while the solid-state ²⁹Si NMR chemical shift for T₈[(CH₂)₃NH₂]₈ is broad and centered at –68.0 ppm.²⁹⁴ The IR, ¹H, and ¹³C NMR spectra, and the thermal behavior of T₈[(CH₂)₃NH₂]₈ have also been reported²⁹⁴ as has the mass spectrum of T₈[(CH₂)₃NH₃Cl]₈.¹⁸⁰ The structure of neither compound has been determined by single-crystal X-ray diffraction but an X-ray powder diffraction study of T₈[(CH₂)₃NH₂]₈ reveals a rhombohedral unit cell with *a* = 11.527 Å and α = 94.97°.²⁹⁵

While T₈[(CH₂)₃NH₂]₈ is soluble in many solvents, the solubility of T₈[(CH₂)₃NH₃Cl]₈ is very poor. It is only highly soluble in water and DMSO, and in methanol at low concentration only (1 g in 50 mL), this limits its use as a starting material as will be described below. T₈[(CH₂)₃NH₂]₈ has been shown to be unstable in the solid state as well as in solution at room temperature.²⁹² Nevertheless it can be stored for several months in dilute methanol solution (30 mg mL^{–1}) at –35 °C.²⁹² Feher et al. have suggested that the reason for the instability is that the amine nitrogen can attack the POSS core leading to decomposition products (Figure 38).

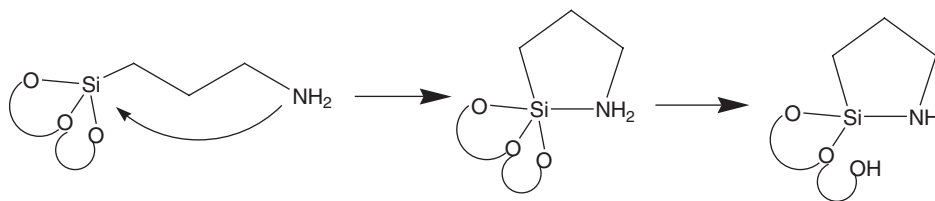


Figure 38 Proposed decomposition pathway for $T_8[(CH_2)_3NH_2]_8$.

Table 25 Compounds $T_8[(CH_2)_3NR_1R_2]_8$ obtained from the reaction of $T_8[(CH_2)_3NH_3Cl]_8$ with Z-protected amino acids and peptides

R_1, R_2	Starting materials	Yield (%)	^{29}Si NMR ^a	Reference
-H, -Gly-Z	$T_8[(CH_2)_3NH_3Cl]_8$ +glycine	91	–	296
-H, -Ala-Z	$T_8[(CH_2)_3NH_3Cl]_8$ +alanine	98	–	296
-H, -Pro-Z	$T_8[(CH_2)_3NH_3Cl]_8$ +proline	44	–66.2	296
-H, -Phe-Leu-Z	$T_8[(CH_2)_3NH_3Cl]_8$ +phenylalanine-leucine	94	–	296
-H, -Phe-Leu-Ala-Z	$T_8[(CH_2)_3NH_3Cl]_8$ +phenylalanine-leucine-alanine	73	–	296
-H, -Ala-Pro-Z	$T_8[(CH_2)_3NH_2-H-Pro]_8$ +alanine	100	–	296

^aReferenced to SiMe_4 .

3. Reactivity and applications

The amine hydrochloride, $T_8[(CH_2)_3NH_3Cl]_8$, and the free amine, $T_8[(CH_2)_3NH_2]_8$, are both interesting starting materials that can be readily functionalized through reactions at the amine group with electrophilic reagents. For example, biologically relevant species were introduced into POSS compounds in high yields using reactions with amino acids such as glycine, alanine, and proline, and peptides such as phenylalanine-leucine or phenylalanine-leucine-alanine or by iteratively coupling and deprotecting Z-protected amino acids (Table 25).

The free amine $T_8[(CH_2)_3NH_2]_8$ has also been coupled with a range of lactones to afford a variety of useful compounds (Table 26 and Figure 39). In the cases of the reactions with δ -lactonolactone and δ -maltonolactone, the highly functionalized products, having lactose-derived and maltose-derived substituents, possess biological binding affinities with the asialoglycoprotein receptor and *Concanavalin A*, respectively (Table 26, entries 1 and 2).

Reactions with anhydrides afford interesting compounds having a carboxylic acid function (Table 26, entries 5 and 7 and Figure 40). It is notable that in the case of succinic anhydride, if the reaction is carried out at 25 °C, only one substitution occurs on the nitrogen atom, if the temperature is increased to 180 °C, there is a second substitution giving rise to a heterocyclic substituent (Table 26, entries 5–8).

Table 26 Compounds $T_8[(CH_2)_3NR_1R_2]_8$ obtained from the reaction of $T_8[(CH_2)_3NH_2]_8$ with lactones and anhydrides

Entry	R_1, R_2	Starting materials and conditions	Yield (%)	^{29}Si NMR ^a	Reference
1	See Figure 39	$T_8[(CH_2)_3NH_2]_8$ + δ -lactonolactone	53	−65.9, −66.9	292,297
2	See Figure 39	$T_8[(CH_2)_3NH_2]_8$ + δ -maltonolactone	26	−65.9, −66.9	292,297
3	See Figure 39	$T_8[(CH_2)_3NH_2]_8$ + δ -gluconolactone	30	−66.1, −66.8	292
4	See Figure 39	$T_8[(CH_2)_3NH_2]_8$ + ϵ -caprolactone	23	−66.4	292
5	−H, −C(O)(CH ₂) ₂ CO ₂ H	$T_8[(CH_2)_3NH_2]_8$ +succinic anhydride, 25 °C	58	−66.2	292
6	−C(O)(CH ₂) ₂ C(O)−	$T_8[(CH_2)_3NH_2]_8$ +succinic anhydride, 180 °C	61	−67.3	298
7	−H, −C(O)CH=CHCO ₂ H	$T_8[(CH_2)_3NH_2]_8$ + maleic anhydride	64	−66.2	292
8	−C(O)CH ₃	$T_8[(CH_2)_3NH_3Cl]_8$ +acetic anhydride	–	–	298

^aReferenced to SiMe₄.

For all the reactions with anhydrides it is preferable to use the free amine rather than the hydrochloride salt in order to reduce the amount of external base in the reaction mixture and thus obtain clean products.

When $T_8[(CH_2)_3NH_2]_8$ reacts with aromatic dianhydrides, it forms hyper-branched polyimide nanocomposite networks having a high thermal stability (up to 500 °C) as shown recently by Seçkin et al.²⁹³ (Figure 41).

Further molecular compounds have been prepared from $T_8[(CH_2)_3NH_3Cl]_8$ and $T_8[(CH_2)_3NH_2]_8$ using reactions involving olefins (Table 27, entries 1, 4, and 8), acid chlorides (Table 27, entries 3 and 7), and phosphines (Table 27, entries 9 and 10). Further elaboration of the resulting compounds can also be carried out without the POSS core being degraded (Table 27, entries 2 and 6).

There are also applications, both for $T_8[(CH_2)_3NH_3Cl]_8$ and $T_8[(CH_2)_3NH_2]_8$ in the field of materials synthesis. For example, Cassagneau et al. have stabilized 6–8 nm Ag nanoparticles using $T_8[(CH_2)_3NH_2]_8$ in the preparation of metallo-dielectric materials with optical properties.²⁹⁹ The same group has also used $T_8[(CH_2)_3NH_2]_8$ as a building block for the preparation of ultra-thin films, by a layer-by-layer assembly with poly(styrene-4-sulfonate) onto silica or polystyrene particles as supports. The calcination of these films leads to ultra-thin silica coatings and hollow silica spheres.³⁰⁰ Chujo and coworkers have prepared aggregates of 4 nm Pd nanoparticles stabilized by $T_8[(CH_2)_3NH_3Cl]_8$. Here, the advantages of $T_8[(CH_2)_3NH_3Cl]_8$ as capping agent are that the cubic core is rigid, the eight functional groups appended to the cube are unable to attach to the same nanoparticle due to steric hindrance, and that its combination with metal ions in solution forms stable and spherical colloids.³⁰¹ They were also able to form a

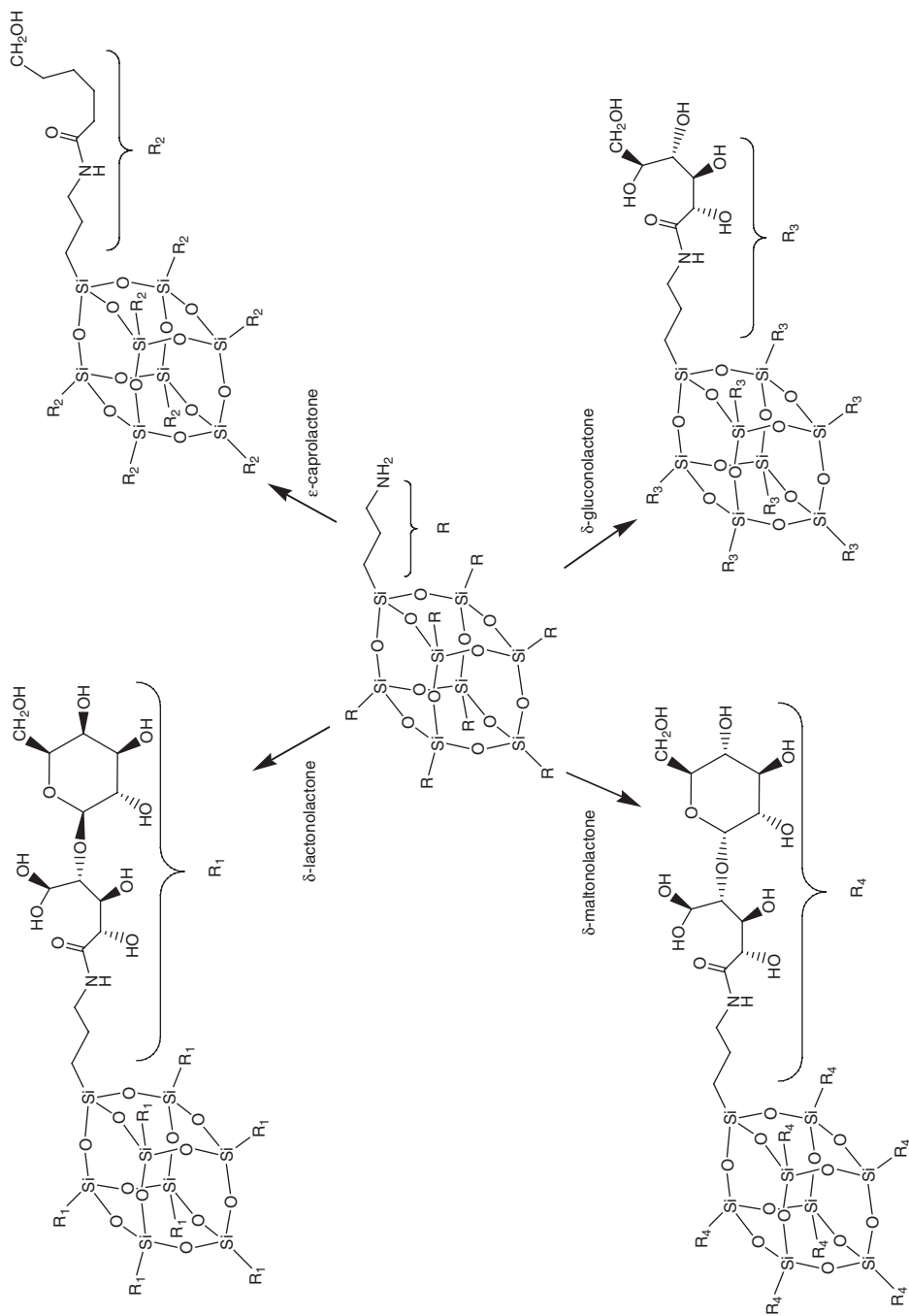


Figure 39 Reactions of $T_8[(CH_2)_3NH_2]_8$ with lactones.

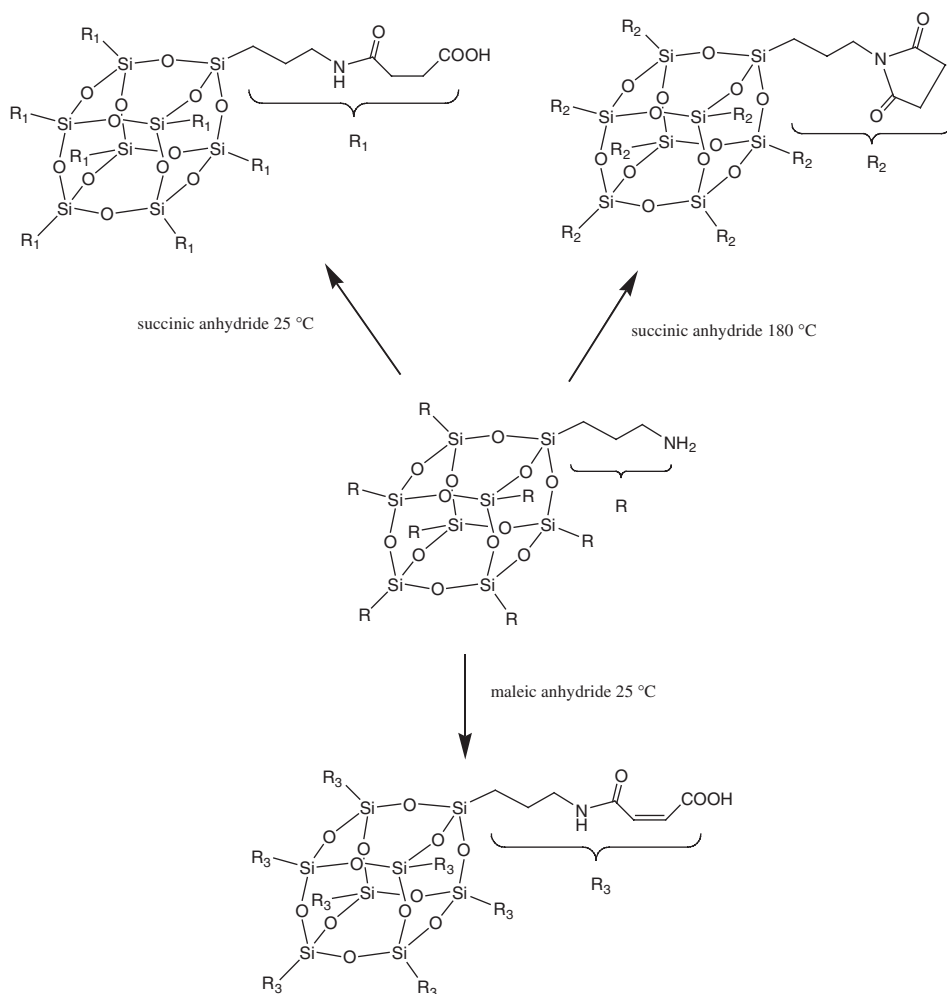


Figure 40 Reactions of $T_8[(CH_2)_3NH_2]_8$ with anhydrides.

network of 3 nm Au nanoparticles stabilized by dodecanethiol acid and separated by $T_8[(CH_2)_3NH_3Cl]_8$. In the presence of a base, deprotonation of the ammonium groups occurs and amido covalent bonds are formed from the acid and the amine groups which then stabilize the system (Figure 42).³⁰²

Studies on the use of $T_8[(CH_2)_3NH_3Cl]_8$ as an intercalating agent to modify smectite clays such as montmorillonite have also been carried out. In this case, the POSS compound carries out a cation exchange reaction with the Na^+ ions of the clay to obtain, by interaction of the NH_3^+ sites with the negative charges of the silica-alumina sheets, an intercalated layered silicate with POSS molecules.³⁰³ Silica-pillared phosphates may also be prepared by intercalation of POSS species into layered phosphates followed by calcinations.³⁰⁴ Kim et al. have mixed $T_8[(CH_2)_3NH_3Cl]_8$ with various organic polymers [poly(2-methyl-2-oxazoline),

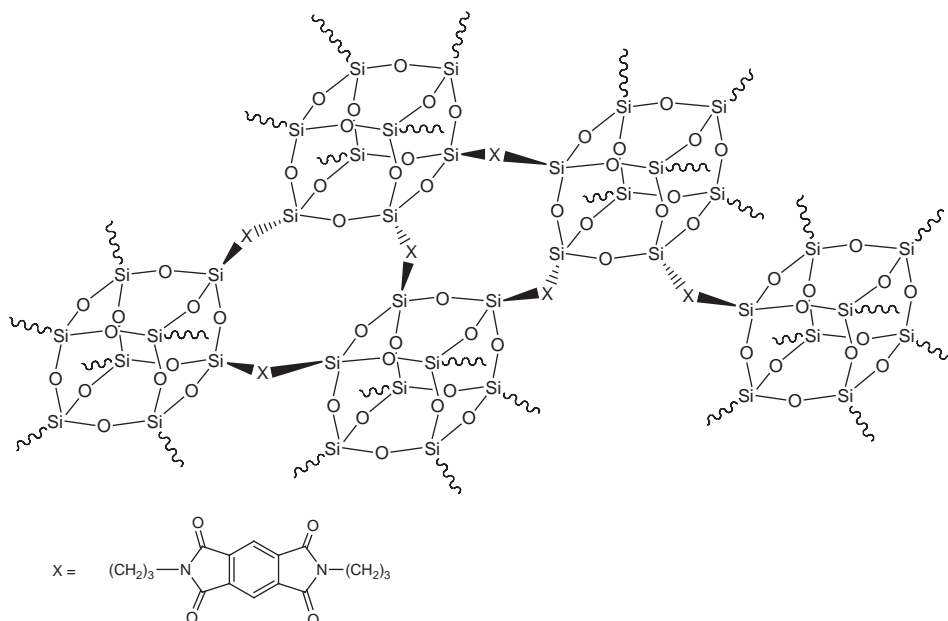


Figure 41 Polymeric three-dimensional polyimide derived from $T_8[(CH_2)_3NH_2]_8$.

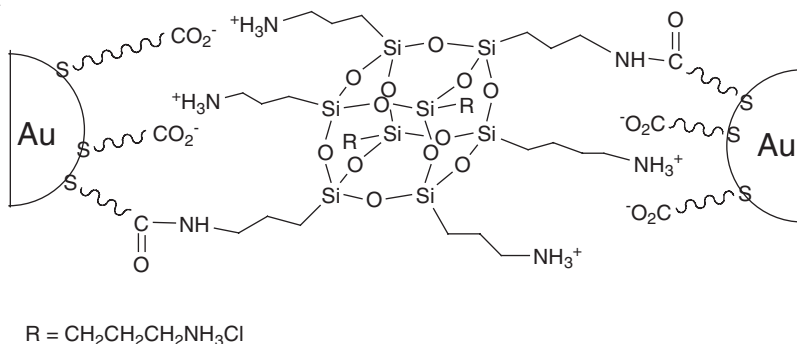


Figure 42 Stabilization of gold nanoparticles using $T_8[(CH_2)_3NH_3Cl]_8$.

polyvinylalcohol, etc.] in the presence of $Si(OMe)_4$ in a MeOH/HCl solution. The sol-gel reaction yields hybrid polymers that are optically transparent with a higher elastic modulus and ultimate elongation than those of simpler polymer analogs.³⁰⁵ Polymer hybrid materials have been prepared from $T_8[(CH_2)_3NH_3Cl]_8$ and polymers such as poly(*N*-vinylpyrrolidone) or poly(vinylalcohol). The resulting materials are optically transparent and soluble in water or methanol.³⁰⁶ The hydrochloride $T_8[(CH_2)_3NH_3Cl]_8$ has been neutralized using Et_3N and then labeled with a fluorescent dye for studies on the potential for POSS species to be used as biocompatible drug carriers. The resulting compound was found to have

Table 27 Miscellaneous compounds $T_8[(CH_2)_3NR_1R_2]_8$ obtained from $T_8[(CH_2)_3NH_2]_8$ or $T_8[(CH_2)_3NH_3Cl]_8$

Entry	R_1, R_2	Starting materials	Yield (%)	^{29}Si NMR ^a	Reference
1	$-(CH_2)_2CO_2Me$ ($R_1 = R_2$)	$T_8[(CH_2)_3NH_2]_8 + CH_2 = CHCO_2CH_3$	73	-66.0	291
2	$-(CH_2)_2C(O)NH-(CH_2)_2NH_2$ ($R_1 = R_2$)	$T_8[(CH_2)_3-N[(CH_2)_2-CO_2Me]_2]_8 + H_2N(CH_2)_2NH_2$	100	-66.2	291
3	$-H, -C(O)Ph$	$T_8[(CH_2)_3NH_3Cl]_8 + PhC(O)Cl$	49	-66.5	292
4	$-H, -C(O)NHCH_2-CH=CH_2$	$T_8[(CH_2)_3NH_2]_8 + CH_2 = CHCH_2NCO$	90	-66.0	292
5	$-H, -C(O)NH-tBu$	$T_8[(CH_2)_3NH_2]_8 + CH_3(CH_2)_3NCO$	65	-66.0	292
6	$-H, -C(O)NH-tBu$	$T_8[(CH_2)_3N = C = O]_8 + tBuNH_2$	18	-66.1	292
7	$=C=O$	$T_8[(CH_2)_3NH_2]_8 + C(O)Cl_2$	11-47	-67.0	292
8	$-H, -CH_2CH_2CO_2CH_3$	$T_8[(CH_2)_3NH_2]_8 + CH_2 = CHCO_2CH_3$	73	-66.0	292
9	$-H, -CH_2PPh_2$	$T_8[(CH_2)_3NH_2]_8 + H_2CO/Ph_2PH$	37	-66.3	292
10	$-H, -CH_2PPh_2HCl$	$T_8[(CH_2)_3NH_3Cl]_8 + H_2CO/Ph_2PH$	-	-67.6	292

^aReferenced to $SiMe_4$.

low toxicity, high solubility, and efficient cellular uptake indicating that POSS derivatives may be useful as drug carriers for compounds insoluble in water.³⁰⁷

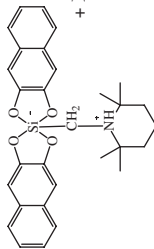
I. Miscellaneous T_8R_8 , T_8R_7R' , $T_8R_6R'_2$, $T_8R_5R'_3$, and $T_8R_4R'_4$ species

This section deals with the many POSS species that are not simple derivatives of the main compounds described in the sections above. For clarity, these compounds have been divided and listed in tables depending on the structure of the pendant arm. As there are a very large number of compounds of this type and many publications describing applications and properties of these compounds, the discussion has had to be limited to the most important ones. Some of these compounds have been reported only in patent literature and the synthetic and characterization data are included only if specifically described in the patent. This section also describes compounds in which not all eight pendant groups are the same. Many such compounds have been prepared but they are usually formed in complicated mixtures and are often not isolated as pure compounds. This highlights one of the problems in the synthesis of POSS derivatives, that is, the efficient synthesis of compounds in which several different pendant groups are present in well-defined positions. This is an area still in relative infancy but it will be seen below that there are useful syntheses available, especially for T_8R_7R' compounds.

1. T_8R_8 where R is a simple linear or branched alkyl, benzyl, or related group

The synthesis of T_8R_8 compounds of this type is, as might be expected from the discussion in earlier sections, usually achieved *via* hydrolysis of simple $RSiCl_3$ or $RSi(OEt)_3$ precursors. There are also variations on this theme involving the thermal treatment of intermediate gels or condensation of oligomeric siloxanes. The synthesis of T_8Me_8 was reported by Olsson using the acid hydrolysis of $MeSiCl_3$ (Table 28, entry 1) along with other $T_8[alkyl]_8$ species (Et, *n*Pr, *n*Bu, *i*Pr, Table 28). Despite the improved syntheses of the higher alkyl species (see Section V.B) it has proven more difficult to obtain good yields of T_8Me_8 , but recent syntheses involving carrying out the hydrolysis within a polymer matrix (Table 28, entry 3) and using a more complicated hydrolysis medium (Table 28, entry 4) have led to significant improvements. Computational studies have been performed on compounds T_nMe_n ($n = 4$ –16) to give structural data⁶⁰ and show an increasing stability of T_nMe_n (except for $T_{14}Me_{14}$) with size against fragmentation meaning, for example, that $T_{10}Me_{10}$ is more stable than T_8Me_8 .³⁹ The crystal structure of T_8Me_8 has been reported³⁰⁸ and shows Si–O bond lengths of 1.615(2)–1.617(2) (mean = 1.614) Å, and Si–O–Si angles of 148.9(1)–149.6(5) (mean = 149.2)°. The ethyl derivative T_8Et_8 may be prepared by hydrolysis/rearrangement (Table 28, entry 5) or reduction of $T_8[CH=CH_2]_8$ (see Section V.D). T_8iPr_8 has, unusually, been prepared from $(iPrOHSiO)_4$, the relatively bulky *i*Pr groups allowing the isolation of the half-cube silanol, using dicyclohexylcarbodiimide (DCC) as a dehydrating agent to give the product in 45% yield, while the synthesis of $T_8[iOct]_8$ has been reported using the base-catalyzed hydrolysis of $RSi(OEt)_3$ developed by Bassindale and coworkers. Preparations of other simple alkyl-based species are

Table 28 Synthesis of compounds T_{8g} : R = alkyl and substituted alkyl groups, and silyl group

Entry	R	Starting materials and conditions	Yield (%)	^{29}Si NMR ^a	Reference
1	-Me	MeSiCl ₃ +H ₂ O, HCl, MeOH, 10 days	5	-	101
2	-Me	MeSi(OEt) ₃ +KOH/H ₂ O, MeOH followed by heating of resulting gel to 325–400 °C	25–80	-	310
3	-Me	MeSi(OEt) ₃ in poly(2-hydroxyethylmethacrylate)+H ₂ O/NH ₃ /MeOH	23	-	311
4	-Me	MeSi(OEt) ₃ +H ₂ O/acetone/MeCN+Et ₃ N, HCl, AcOH, 50 °C	88	-	312
5	-Et	(EtHSiO) ₄ +(EtHSiO) ₄ (9:1), MeOH/KOH, 120 h	37	-	313
6	-Et	EtSiCl ₃ +EtSi(OEt) ₃ in C ₆ H ₆ /H ₂ O	<1	-	46
7	-iPr	(iPrOHSiO) ₄ +DCC, 180 °C, 3 days	45	-66.26	314
8	-iBu	iBuSi(OEt) ₃ +H ₂ O, NBu ₄ F, THF/CH ₂ Cl ₂ , 1 day	26	-67.9	100,103,315
9	-nHex	nHexSi(OEt) ₃ +NBu ₄ F, H ₂ O/THF/CH ₂ Cl ₂ , 1 day	44	-66.6	100
10	-iHex	-	-	-	316
11	-iOct	iOctSi(OMe) ₃ +NBu ₄ F, H ₂ O/THF/CH ₂ Cl ₂ , 2 days	43	-68.20	317
12	-(CH ₂) ₁₀ CH(OH)HSO ₃	-	-	-	318
13	-CH ₂ Ph	PhCH ₂ SiCl ₃ +H ₂ O, EtOH, reflux, 2 days	31	-71.28	166
14	-CHMe-C ₆ H ₄ OH	-	-	-	319
15	-CH ₂ CH=CH ₂	CH ₂ =CH-CH ₂ -Si(OMe) ₃ +H ₂ O, HNO ₃ , 10 days	1.75	-70.77	320
16	-CH ₂ -CH(O)CH ₂	T ₈ [CH ₂ -CH=CH ₂] ₈ +m-CPBA	75	-69.7	320
17	-CH(O)CH-Ph	-	-	-	185
18	-CH ₂ (NC ₅ H ₆ -2,2,6,6-Me ₄)	 + H ₂ O, CH ₂ Cl ₂ , 2 h	43	-70.8	321
19	-SiMe ₂ tBu	1,1,1-tribromo-2- <i>t</i> -butyl-2,2-dimethyldisilane, Na, toluene	72	5.60, -35.03	322,323

^aReferenced to SiMe₄.

given in Table 28. POSS species containing longer alkyl chains T_8R_8 ($R = C_6H_{11}$, $C_{10}H_{20}$, $C_{14}H_{28}$, $C_{18}H_{36}$) have been prepared by hydrosilylation reactions between T_8H_8 and terminal alkenes¹⁰⁶ (see Section V.B). Photoluminescence spectra for a range of simple alkyl POSS species T_8R_8 ($R = Me$, Et, Pr, Bu etc.) have been recorded.^{59,93} Applications have been found for T_8Me_8 and T_8Bu_8 as inorganic components in polymer nanocomposites as already seen for $T_8[nC_3H_7]_8$ (Section V.B)^{112,113,309} and for $T_8[CH(O)CHPh]_8$, which can be cross-linked into cured epoxy networks.

2. Other alkyl derivatives $T_8[(CH_2)_2R]_8$

A variety of more complicated compounds having a CH_2CH_2 linkage to the POSS core have been prepared using methods outlined in Table 29. Thus, epoxides have been made from cyclohexene-terminated POSS (Table 29, entries 1 and 2) and are precursors for the preparation of nanocomposite polymers under ultraviolet irradiation (Figure 43).^{115,247}

The phosphine derivative $T_8[(CH_2)_2PPh_2]_8$ has been used for the preparation of dendrimers (Table 29, entry 12) and the highly fluorinated species, $T_8[(CH_2)_2(CF_2)_nCF_3]_8$, prepared by a base hydrolysis of $(EtO)_3Si(CH_2)_2(CF_2)_nCF_3$ ($n = 0, 5$, or 7) has been used for the blending of fluorinated polymers (Table 29, entry 16).

3. Species containing a propyl pendant arm, $T_8[(CH_2)_3R]_8$

Compounds containing a $(CH_2)_3$ linkage to the POSS core have become more widely studied than many of the alkyl derivatives because of their ready preparation and because the propyl arm is the shortest linker that usually prevents the reactivity of functional groups being enhanced by the nearby silicon

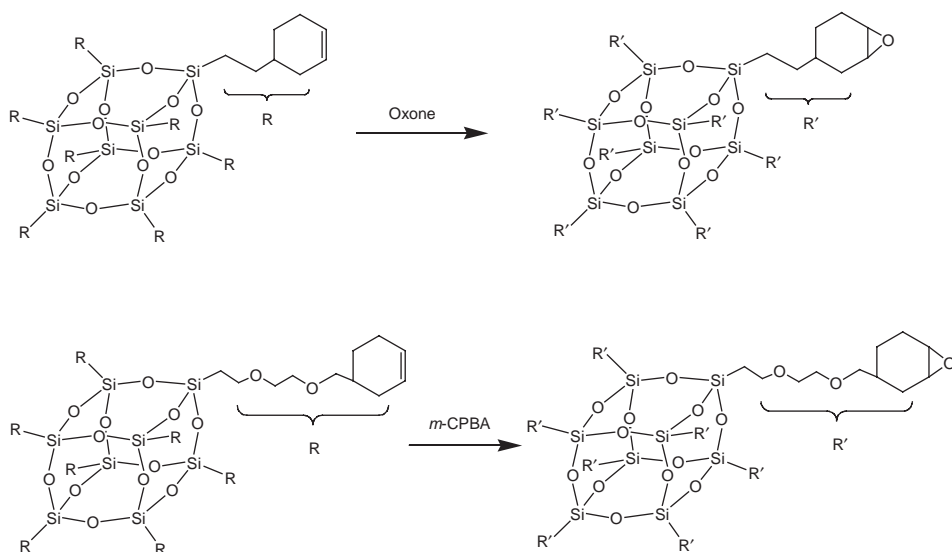


Figure 43 Preparation of POSS compounds containing epoxide groups.

Table 29 Other compounds $T_8[(CH_2)_2R]_8$

Entry	R	Starting materials and conditions	Yield (%)	^{29}Si NMR ^a	Reference
1	-cyclohexane-3,4-epoxide	$T_8[(CH_2)_2\text{-3-cyclohexene}]_8 + \text{Oxone}^{\text{®}}$	Quantitative	-65.3, -66.3, -68	115
2	$-\text{O}[(CH_2)_2\text{OCH}_2\text{-cyclohexane-3,4-epoxide}]_8$	$T_8[(CH_2)_2\text{O}[(CH_2)_2\text{OCH}_2\text{-3-cyclohexene}]_8 + m\text{-CPBA}]$	Quantitative	-68.5	115
3	$-C_6H_9$	–	–	–	324
4	-3-norbornenyl	Norbornenylethyltriethoxysilane + NBu_4OH , $i\text{Bu}(\text{CO})\text{Me}$, 3 days	64	–	324
5	-Ph	$T_8[\text{CH}=\text{CH}_2]_8 + C_6H_6$, AlCl_3	75	–	325
6	$-\text{Si}(\text{OMe})_3$	$T_8[\text{CH}_2\text{CH}_2\text{SiCl}_3]_8 + \text{MeOH}/\text{THF}/\text{Et}_3\text{N}$	–	–	326
7	$-\text{SiMe}(\text{OMe})_2$	$T_8[\text{CH}_2\text{CH}_2\text{SiMeCl}_2]_8 + \text{MeOH}/\text{THF}/\text{Et}_3\text{N}$	–	–	326
8	$-\text{SiMe}_2\text{OMe}$	$T_8[\text{CH}_2\text{CH}_2\text{SiMe}_2\text{Cl}]_8 + \text{MeOH}/\text{THF}/\text{Et}_3\text{N}$	–	–	326
9	$-\text{SiMe}[(CH_2)_2\text{SiMe}_2\text{Cl}]_2$	–	–	–	192,205
10	$-\text{SiMe}[(CH_2)_2\text{SiMe}_2\text{H}]_2$	$T_8[(CH_2)_2\text{-SiMe}[(CH_2)_2\text{-SiMe}_2\text{Cl}]_8 + \text{LiAlH}_4]$	40	–	205
11	$-\text{SiMe}[(CH_2)_2\text{SiMe}_2\text{OH}]_2$	$T_8[(CH_2)_2\text{-SiMe}[(CH_2)_2\text{-SiMe}_2\text{H}]_8 + \text{H}_2\text{O}]$ Pd	96	–	205
12	$-\text{PPh}_2$	–	–	–	327–329
13	$-\text{CF}_3$	$\text{CF}_3[(CH_2)_2\text{SiCl}_3 + \text{H}_2\text{O}]$, $i\text{BuOH}$, 100 days	32	-67.5, -68.4	330
14	$-\text{Cl}$	–	–	–	331
15	$-\text{CMe}_2\text{CH}_2\text{CO}_2\text{Me}$	$\text{MeO}_2\text{CCH}_2\text{CMe}_2\text{-(CH}_2)_2\text{Si}(\text{OEt})_3 + \text{H}_2\text{O}$, TBAF, CH_2Cl_2 , 1 day	20	-65.9	100
16	$-(\text{CF}_2)_n\text{CF}_3$ ($n = 0, 5$, or 7)	$\text{CF}_3\text{-(CF}_2)_n\text{-(CH}_2)_2\text{-Si}(\text{OR})_3 + \text{H}_2\text{O}$, base catalyst ($n = 0, 5$, or 7)	–	–	332

^aReferenced to SiMe_4 .

atom leading to Si–C bond cleavage. The synthesis of $T_8[(CH_2)_3Cl]_8$ has been reported by two different procedures, acid hydrolysis of $Cl(CH_2)_3Si(OMe)_3$ with or without a Lewis acid catalyst ($FeCl_3$), giving up to 32% yield (Table 30, entries 1 and 2). This compound is a precursor to a wide range of other POSS species *via* nucleophilic substitutions (Figure 44). For example, halogen exchange with NaI gives the iodide $T_8[(CH_2)_3I]_8$ that can react further, for example, with $AgNO_3$ to give the nitrate $T_8[(CH_2)_3ONO_2]_8$ which can be reduced to the hydroxy derivative $T_8[(CH_2)_3OH]_8$ (Table 30, entries 4–7). The alcohol can also be prepared by the direct reaction of $T_8[(CH_2)_3Cl]_8$ with H_2O in presence of Ag_2O (Table 30, entry 8). $T_8[(CH_2)_3Cl]_8$ can react directly with alkali salts to give phosphorus- or sulphur-based compounds in good yields (Table 30, entries 10–12; Figure 44).

As previously seen for other POSS derivatives, compounds $T_8[(CH_2)_3X]_8$ ($X = Cl, Br, I, \text{ or } SCN$) react in the presence of base to give T_{10} and T_{12} homologs by cage rearrangement.¹⁰³ The iodide, $T_8[(CH_2)_3I]_8$, reacts with 2-methyl-2-oxazoline to give a precursor that can be used for polymer blending (Figure 45).³³³

The thiol, $T_8[(CH_2)_3SH]_8$, reacts with the ruthenium cluster $[Ru_3(CO)_{10}(NCMe)_2]$ to give, depending on the stoichiometry employed, partial or full substitution at the S–H groups *via* oxidative addition to give $T_8[(CH_2)_3SH]_6[\mu_2-(CH_2)_3SRu_3(\mu-H)(CO)_{10}]_2$ or $T_8[\mu_2-(CH_2)_3SRu_3(\mu-H)(CO)_{10}]_8$ (Figure 46).³³⁴ Compounds $T_8[(CH_2)_3OSiMe_3]_8$ and $T_8[(CH_2)_3OSiMe_2OSiMe_3]_8$ have been used for the preparation of inks (Table 30, entries 18 and 19).

4. T_8R_8 compounds where R is a cycloalkyl or substituted aryl group

Two compounds of this type, $T_8[c-C_5H_9]_8$ and $T_8[c-C_6H_{11}]_8$ (Table 31, entries 1–4) are of particular interest not because of the nature of their pendant groups which are difficult to functionalize (a few examples of the use of such compounds as polymer nanofillers have been reported),³⁴¹ but because they are the precursors to compounds with T_8R_7R' structures ($R = c-C_5H_9$ or $c-C_6H_{11}$) as described at the end of this section.

The majority of compounds in this section contain substituted phenyl rings directly attached to the silicon atoms (Table 31), they are generally prepared either by hydrolysis of a suitable trifunctional precursor or by modification of an aryl group within a POSS molecule (the synthesis and derivatization of T_8Ph_8 is described in Section V.C). For example, a series of methyl-substituted compounds has been prepared by the hydrolysis of the corresponding trichlorosilanes (Table 31, entries 5, 7, 9), while the corresponding saturated products are obtained by the catalytic hydrogenation of the aromatic ring in excellent yields (Table 31, entries 6, 8, 10). Interestingly, $T_8[C_6H_4-2-NMe_2]_8$ has been prepared by two methods: firstly by the classical acid hydrolysis of a trimethoxysilane giving a 84% yield after 3 weeks (Table 31, entry 15), second by the hydrolysis of bis[2,3-naphthalenediolato(2-)] [2-(dimethylamino)phenyl]silicate over 30 h giving the product with a slightly better yield (Table 31, entry 16).

A series of functionalized compounds have been prepared from $T_8[C_6H_4-4-CH_2Cl]_8$, obtained from the hydrolysis of $4-ClCH_2-C_6H_4SiCl_3$ (Table 31, entry 18). An initial nucleophilic substitution gives the corresponding iodo derivative $T_8[C_6H_4-4-CH_2I]_8$ (Table 31, entry 19) that can then readily undergo other

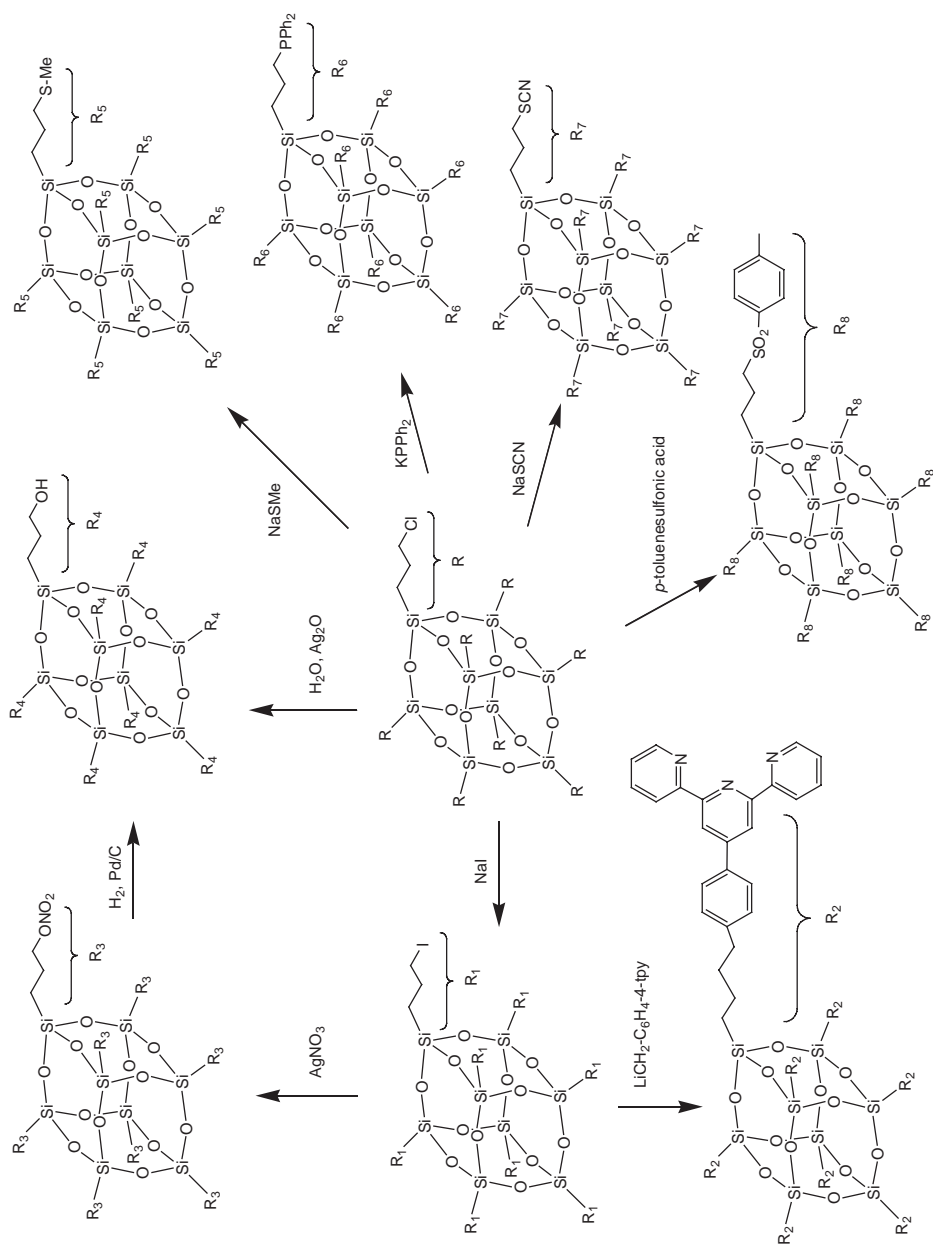


Figure 44 Reactions of $\text{T}_8[(\text{CH}_2)_3\text{Cl}]_8$.

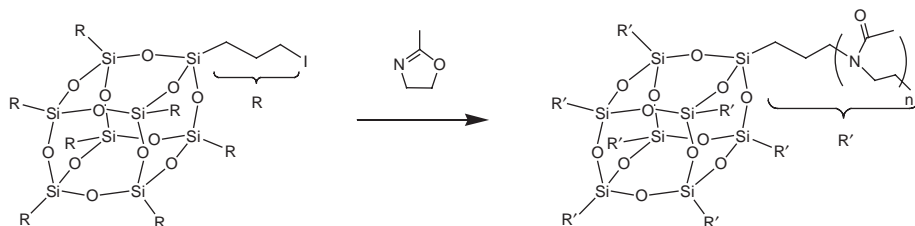


Figure 45 Formation of polymer from $T_8[(CH_2)_3I]_8$.

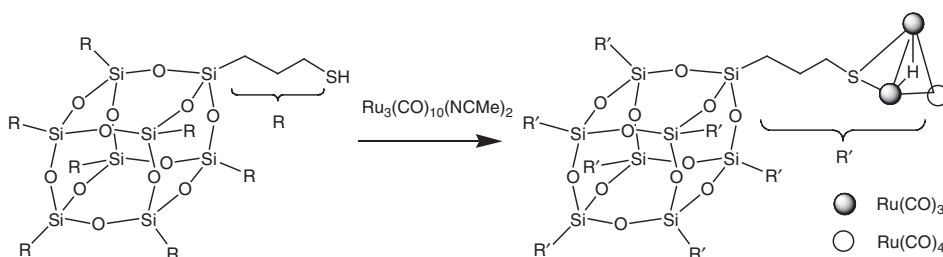


Figure 46 Formation of a POSS-based ruthenium cluster.

nucleophilic substitutions to give, in very good yields, hydroxy-, nitrate-, or phosphine-derivatives (Table 31, entries 20–27 and Figure 47).

As well as phenyl derivatives, other products have been prepared by hydrolysis of alkoxyisilanes such as cyclohexenyl or naphthyl derivatives as well as heterocyclic compounds based on thienyl rings (Table 31, entries 28–33). Few practical applications have been reported for this type of compound, except for the styryl compound $T_8[C_6H_4-4-CH=CH_2]_8$, and the fluorinated $T_8[C_6F_5]_8$ which have been used in polymer blending (Table 31, entries 13 and 28).³³²

5. Silanol, silylether, and siloxane derivatives, $T_8[OR]_8$

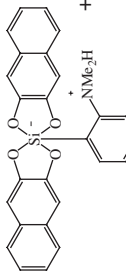
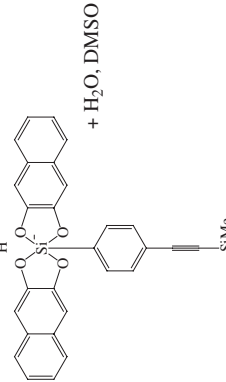
The most widely studied POSS species with oxygen substituents, $T_8[O^-]_8$, $T_8[OSiMe_2CH=CH_2]_8$, and $T_8[OSiMe_2H]_8$ have been described in detail in sections above, less common species are described here. $T_8[OH]_8$ has been subject to computational studies only and can be seen as a silicate cluster involved in the chemistry of silica in solution. Geometric parameters have been calculated using *ab initio* methods which show that there are two different conformations for the structure differing in the arrangement of the Si_4O_4 rings forming the six faces of the cage. Calculations showed no intramolecular hydrogen bonds interactions because the hydroxyl groups are too far apart.³⁴⁸ *Ab initio* studies on vibrational values for $T_8[OH]_8$ gave of 1114 cm^{-1} for $\nu_{as}(Si-O-Si)$ and $736, 707, 555\text{ cm}^{-1}$ for $\nu_s(Si-O-Si)$, which are in agreement with those observed for silicates.³⁴⁹ Few silylether POSS derivatives have found use but $T_8[OCH_2CH_2OH]_8$ and $T_8[OCH_2CH_2OCH_2CH_2OH]_8$ have been used for the synthesis of photocurable resins.³⁵⁰

Table 30 Synthesis of compounds $T_8[(CH_2)_3R]_8$ containing a substituted propyl group

Entry	R	Starting materials and conditions	Yield (%)	^{29}Si NMR ^a	Reference
1	-Cl	$\text{Cl}[(CH_2)_3\text{Si}(\text{OMe})_3 + \text{H}_2\text{O}, \text{HCl}, \text{methanol}, 5 \text{ weeks}]$	28–31	–67.11	108,295,335
2	-Cl	$\text{Cl}[(CH_2)_3\text{SiCl}_3 + \text{H}_2\text{O}, \text{FeCl}_3, \text{HCl}, \text{methanol/pentane/toluene}, 13 \text{ h}]$	14	–66.8	336
3	-Br	$\text{Br}[(CH_2)_3\text{SiCl}_3 + \text{H}_2\text{O}, \text{FeCl}_3, \text{HCl}, \text{methanol/pentane/toluene}, 13 \text{ h}]$	3	–	336
4	-I	$\text{I}_8[(CH_2)_3\text{Cl}]_8 + \text{NaI}, \text{acetone}$	97	–67.93	108
5	-C ₆ H ₄ -4-tpy	$\text{I}_8[(CH_2)_3\text{I}]_8 + \text{LiCH}_2\text{-C}_6\text{H}_4\text{-4-tpy}, \text{THF}$	–	–	337
6	-ONO ₂	$\text{I}_8[(CH_2)_3\text{I}]_8 + \text{AgNO}_3, \text{CH}_3\text{CN}$	100	–66.7	292
7	-OH	$\text{I}_8[(CH_2)_3\text{ONO}_2]_8 + \text{H}_2, \text{Pd/C}, \text{methanol}$	85	–65.9	292
8	-OH	$\text{I}_8[(CH_2)_3\text{Cl}]_8 + \text{Ag}_2\text{O}, \text{H}_2\text{O}, \text{THF}, \text{EtOH}$	91	–67.2	335
9	-SO ₂ -C ₆ H ₄ -Me	$\text{I}_8[(CH_2)_3\text{Cl}]_8 + p\text{-toluenesulfonic acid}, \text{CH}_3\text{CN}$	–	–	338
10	-PPh ₂	$\text{I}_8[(CH_2)_3\text{Cl}]_8 + \text{KPPPh}_2, \text{THF}$	83	–66.41	108
11	-SMe	$\text{I}_8[(CH_2)_3\text{Cl}]_8 + \text{NaSMe}, \text{toluene}$	55	–66.25	108
12	-SCN	$\text{I}_8[(CH_2)_3\text{Cl}]_8 + \text{NaSCN}, \text{acetone}$	90	–66.62	108
13	-OCOMe	$\text{I}_8[(CH_2)_3\text{OH}]_8 + \text{MeCOCl}$	Quantitative	–	318
14	-Cp	$\text{Cp}-(CH_2)_3\text{Si}(\text{OEt})_3 + \text{H}_2\text{O}/\text{acetone} + \text{HCl}$	59	–68.51	339
15	-CH(COOEt) ₂	–	–	–	318
16	-CHO	$\text{I}_8[(CH_2)_3\text{CH}(\text{COOEt})_2]_8 + \text{HCl}$	Quantitative	–	318
17	-SH	$\text{HS}[(CH_2)_3\text{Si}(\text{OMe})_3 + \text{H}_2\text{O}, \text{HCl}, \text{methanol}, 5 \text{ weeks}]$	17	–66.16	108
18	-OSiMe ₃	–	–	–	340
19	-OSiMe ₂ OSiMe ₃	–	–	–	340

^aReferenced to SiMe₄.

Table 31 Synthesis of compounds T_{8R_8} where R is a cycloalkyl, cycloalkenyl, or substituted aryl group

Entry	R	Starting materials and conditions	Yield (%)	^{29}Si NMR ^a	Reference
1	- <i>c</i> -C ₃ H ₆	<i>c</i> -C ₅ H ₉ Si(OEt) ₃ +H ₂ O, TBAF, acetone/THF, 1 day	95	-66.6	100
2	- <i>c</i> -C ₃ H ₆	<i>c</i> -C ₅ H ₉ Si(OEt) ₃ +H ₂ O, acetone, Me ₃ N, CH ₃ (CH ₂) ₂ CN, HCl, AcOH, 70 °C, 18 h	85.5	-	312
3	- <i>c</i> -C ₆ H ₁₁	<i>c</i> -C ₆ H ₁₁ Si(OEt) ₃ +H ₂ O, MeC(O)(CH ₂) ₂ Pr ⁱ , Et ₃ N, MeCN, HCl, D-aspartic acid, 65 °C, 18 h	87	-	312
4	- <i>c</i> -C ₆ H ₁₁	<i>c</i> -C ₆ H ₁₁ Si(OEt) ₃ +H ₂ O, TBAF, acetone/THF, 1 day	84	-68.7	100
5	-C ₆ H ₄ -4-Me	4-Me-C ₆ H ₄ SiCl ₃ +H ₂ O, ethanol, reflux, 2 days	19	-	159
6	-C ₆ H ₁₀ -4-Me	T ₈ [C ₆ H ₄ -4-Me] ₈ +H ₂ , Pd/C	93	-70.3	166
7	-C ₆ H ₄ -3-Me	3-Me-C ₆ H ₄ SiCl ₃ +H ₂ O, ethanol, 3 days	25	-71.8	166
8	-C ₆ H ₁₀ -3-Me	T ₈ [C ₆ H ₄ -3-Me] ₈ +H ₂ , Pd/C	95	-68.8	166
9	-C ₆ H ₁₃ -3,5-Me ₂	3,5-Me ₂ -C ₆ H ₄ SiCl ₃ +H ₂ O, ethanol, 3 days	22	-78.1	166
10	-C ₆ H ₉ -3,5-Me ₂	T ₈ [C ₆ H ₃ -3,5-Me ₂] ₈ +H ₂ , Pd/C	88	-67.6	166
11	-C ₆ H ₄ -2-Me	2-Me-C ₆ H ₄ Si(OMe) ₃ +PhCH ₂ Me ₃ NOH H ₂ O/C ₆ H ₆ , reflux 4 h	82	-	150
12	-C ₆ H ₄ -2-Et	2-Et-C ₆ H ₄ Si(OMe) ₃ +PhCH ₂ Me ₃ NOH H ₂ O/C ₆ H ₆ , reflux 4 h	>70	-78.8	150
13	-C ₆ H ₄ -4-CH=CH ₂	-	-	-	341b
14	-C ₆ H ₄ -4-Cl	4-Cl-C ₆ H ₄ SiCl ₃ +H ₂ O, benzene, BnMe ₃ NOH, 72 h	-	-	342
15	-C ₆ H ₄ -2-NMe ₂	2-NMe ₂ -C ₆ H ₄ Si(OMe) ₃ +H ₂ O, HCl, CH ₃ CN, 21 days	84	-79.5	343
16	-C ₆ H ₄ -2-NMe ₂	 + H ₂ O, CH ₃ CN, 30 h	90	-79.5	343
17	-C ₆ H ₄ -C≡C-SiMe ₃	 + H ₂ O, DMSO	88	-17.2, -78.2	27

18		4-ClCH ₂ -C ₆ H ₄ SiCl ₃ +H ₂ O, acetone, 2 days	15	-78.4	344
19		T ₈ [C ₆ H ₄ -4-CH ₂ Cl] ₈ +NaI, THF	100	-77.5	344
20		T ₈ [C ₆ H ₄ -4-CH ₂] ₈ +H ₂ O, AgClO ₄ , acetone	95	-78.5	344
21		T ₈ [C ₆ H ₄ -4-CH ₂] ₈ +AgNO ₃ , MeCN	93	-78.6	344
22		T ₈ [C ₆ H ₄ -4-CH ₂ OH] ₈ +acetic anhydride	100	-78.3	344
23		T ₈ [C ₆ H ₄ -4-CH ₂ OH] ₈ +4-NO ₂ C ₆ H ₄ COCl, pyridine	80	-78.5	344
24		T ₈ [C ₆ H ₄ -4-CH ₂ OH] ₈ +4-ClCOC ₆ H ₄ COCl+MeOH, pyridine	91	-78.35	344
25		T ₈ [C ₆ H ₄ -4-CH ₂ OH] ₈ +Ph ₂ POCl, THF	70	-	345
26		T ₈ [C ₆ H ₄ -4-CH ₂] ₈ +Ph ₂ P(O)Et, HCCl ₃	83	-	345
27		T ₈ [C ₆ H ₄ -4-CH ₂ P(O)Ph ₂] ₈ +AlH ₃ , THF	64	-77.11	345
28		C ₆ F ₅ Si(OR) ₃ +H ₂ O, base catalyst	-	-	332
29		2-bicycloheptenyl-Si(OEt) ₃ +H ₂ O, Bu ₄ NF, CH ₂ Cl ₂ , 1 day	56	-68.72	100
30		2-(<i>c</i> -C ₆ H ₉)-SiCl ₃ +H ₂ O, methanol, BnMe ₃ NOH	80	-67.4	346
31		1-naphthyl-Si(OMe) ₃ +H ₂ O, Et ₃ N, methanol, reflux, 3 h	52	-	159
32		2-Thienyl-Si(OMe) ₃ +H ₂ O, MeOH, 2 h	13	-	347
33		T ₈ [2-C ₄ H ₃ S] ₈ +bromine	90	-	347

^aReferenced to SiMe₄.

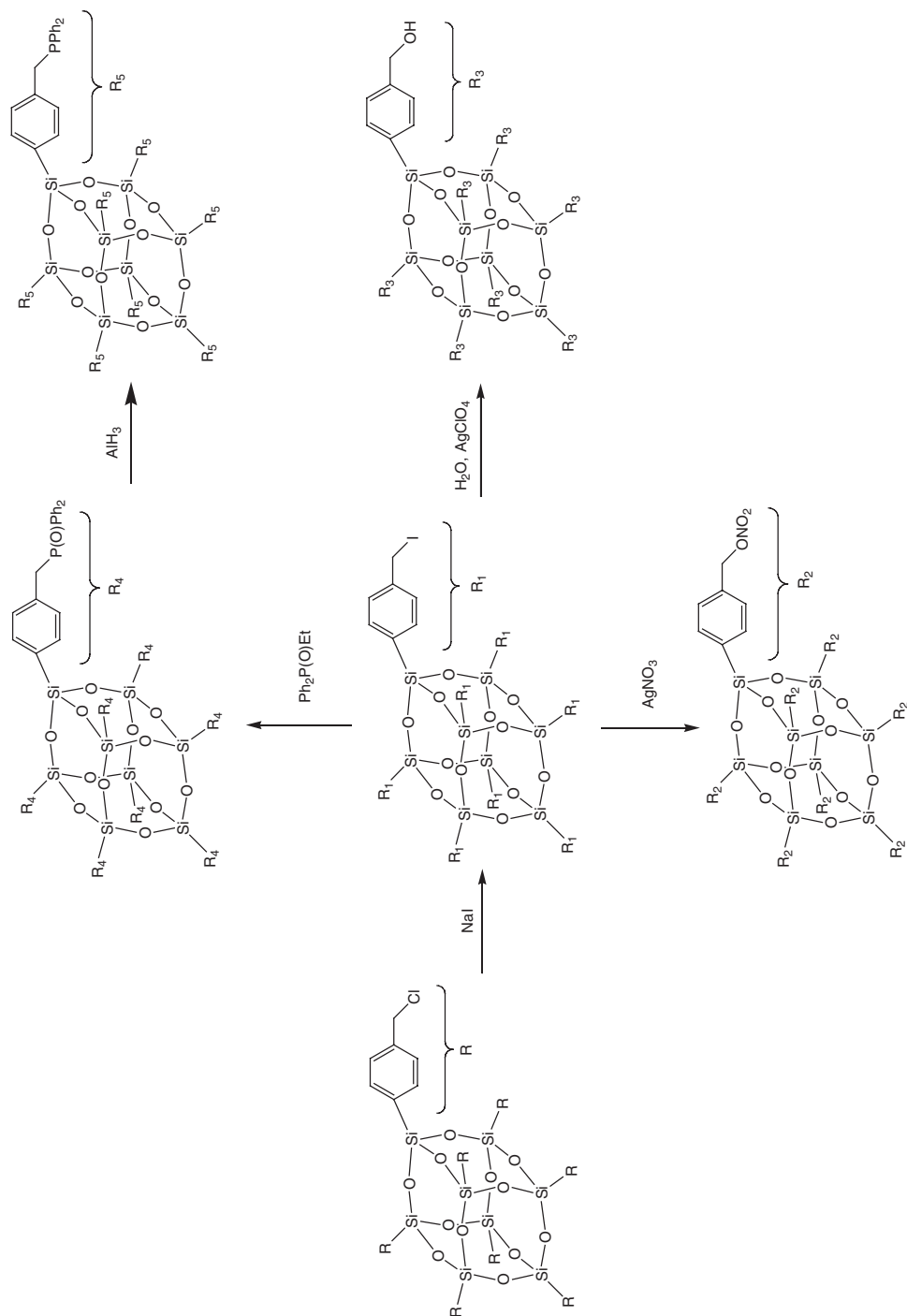


Figure 47 Reactions of $T_8[C_6H_4-4-CH_2]_8$.

Several siloxane derivatives $T_8[\text{OSiMe}_2\text{R}]_8$ other than those mentioned in Sections V.F and V.G containing more complicated R groups, for example, $\text{R}=(\text{CH}_2)_2\text{C}_6\text{H}_4-4\text{-OH}$,³⁵¹ polycyclic groups,^{351a} and $\text{CH}_2\text{CH}_2\text{CO}_2-t\text{Bu}$, which is photosensitive,³⁵² have also been prepared.

6. POSS containing different substituents: $T_8\text{R}_7\text{R}'$, $T_8\text{R}_6\text{R}'_2$, $T_8\text{R}_5\text{R}'_3$, and $T_8\text{R}_4\text{R}'_4$
The most widely studied POSS derivatives in which there are different substituents on the siloxane core are $T_8[\text{c-C}_5\text{H}_9]_7\text{R}$ and $T_8[\text{c-C}_6\text{H}_{11}]_7\text{R}$ species which are usually derived from silanols (see Figure 48 and Tables 32 and 33). The trisilanol species, which can be viewed as a T_8 cube minus one corner, can be prepared either as shown in Figure 48 by base-mediated cleavage giving the pure products in 23% yield,¹¹⁴ or by direct hydrolysis of $\text{c-C}_n\text{H}_{2n+1}\text{SiCl}_3$ precursors, and can also be seen as molecular models for silica surfaces. The chemistry of the trisilanol has been studied extensively over recent years and many metal complexes of types 14 and 15 have been prepared.^{10g,353}

Attempts to prepare T_8 derivatives with more than one type of substituent, other than $T_8[\text{c-C}_5\text{H}_9]_7\text{R}$ and $T_8[\text{c-C}_6\text{H}_{11}]_7\text{R}$, as pure species, are hampered by the lack of suitable trisilanol precursors. Clearly, the cohydrolysis of mixed trifunctional species, RSiX_3 and R'SiX_3 , is likely to give POSS products bearing different substituents, but they form as mixtures that are difficult to separate. The cohydrolysis of HSiCl_3 with PhSiCl_3 gives mixture from which $T_8\text{H}_7\text{Ph}$ can be isolated by HPLC and recrystallized in 0.5% yield. Despite the low yield, this compound is one of the few that has been isolated pure and fully characterized, including by X-ray crystallography, from the cohydrolysis route.¹³¹ The cohydrolysis of MeSiX_3 and EtSiX_3 ($\text{X} = \text{Cl}$ or OAc) gives nine products $T_8\text{Me}_n\text{Et}_{8-n}$ ($n = 0-8$), the effects on the product ratio of time, concentration, and reactant ratio have been reviewed.³⁶¹ An attempt to prepare $T_8\text{R}_7\text{R}'$ by the cohydrolysis method was also made by Lavrent'ev who hydrolyzed a mixture of $\text{CH}_2=\text{CHSiCl}_3$ and $\text{PhCH}_2\text{SiCl}_3$ in a 6:2 ratio in organic solvents in the presence of HCl at 40°C . The reaction products, characterized by GC-MS, were a complicated mixture of $T_8[\text{CH}=\text{CH}_2]_8$, $T_8[\text{CH}=\text{CH}_2]_7[\text{CH}_2\text{Ph}]$, and $T_8[\text{CH}=\text{CH}_2]_6[\text{CH}_2\text{Ph}]_2$, along with compounds containing hydroxy and alkoxy substituents.³⁶² A related reaction, performed in aqueous 2-propanol, used $\text{CH}_2=\text{CHSiCl}_3$ and PhSiCl_3 in a 5:3 ratio, to give $T_8[\text{CH}=\text{CH}_2]_7\text{Ph}$ and $T_8[\text{CH}=\text{CH}_2]_6\text{Ph}_2$ as the main products, the expected $T_8[\text{CH}=\text{CH}_2]_5\text{Ph}_3$ being obtained in a 13% yield.³⁶³ A detailed study of the cohydrolysis of mixtures of chloro- or methoxy-silanes $\text{RSiX}_3/\text{R'SiX}_3$ in a 7:1 ratio ($\text{R} = \text{Pr}$, $\text{R}' = 3\text{-ClC}_3\text{H}_6$, $3\text{-IC}_3\text{H}_6$, $3\text{-HSC}_3\text{H}_6$, C_3H_5 ; $\text{R} = \text{Et}$, $\text{R}' = \text{C}_2\text{H}_3$) gives mixtures $T_8\text{R}_{8-n}\text{R}'_n$ ($n = 0, 1$ or 2 , three isomers) that can be separated by HPLC. The three isomers of the disubstituted products can be readily distinguished both from each other and from other products by ^{29}Si NMR spectroscopy but in all cases the product mixture is complicated.³⁶⁴ A heteronetwork clathrate $[\text{DMPI}]_6[\text{T}_8(\text{O}^-)_6(\text{OH})_2]$ in which the two silanol groups are on diagonally opposed silicon atoms is formed as crystals from an aqueous solution of $[\text{DMPI}]\text{OH}/\text{SiO}_2$.²²⁸ Unfortunately this is not likely to be a useful precursor to other $T_8\text{R}_6\text{R}'_2$ species.

An elegant alternative to the simple hydrolysis method is to use precursors already containing several of the required siloxane linkages. Thus, $T_8\text{R}_6\text{R}'_2$

Table 32 Synthesis of $T_8[c-C_3H_9]_7[R]$ compounds

Entry	R	Starting materials	Yield (%)	^{29}Si NMR ^a	Reference
1	-Cl	(10)+SiCl ₄ , NEt ₃ , Et ₂ O	92	-66.85, -66.98, -90.20	354
2	-OH	T ₈ [c-C ₃ H ₉] ₇ [Cl]+H ₂ O, THF	80	-64.18, -97.75	354
3 ^b	-TiCl ₂ Cp'	T ₈ [c-C ₃ H ₉] ₇ [OH]+Cp'TiCl ₃ , BuLi, hexane	51	-65.92, -66.66, -111.76	354
4	-CH ₂ Cl	(10)+Cl ₃ SiCH ₂ Cl, NEt ₃ , THF	78	-65.83, -66.41, -77.01,	355
5 ^c	-CH ₂ -9-FluH	(10)+(EtO) ₃ SiCH ₂ -9-FluH, toluene	58	-65.73, -65.77, -65.82, -70.17	355
6 ^{b,c}	-CH ₂ -9-FluZrCl ₂ Cp'	T ₈ [c-C ₃ H ₉] ₇ [CH ₂ -9-FluH]+Cp'ZrCl ₃ , BuLi, THF/hexane	73	10.1, -66.76, -66.92, -67.30, -70.62	355

^aReferenced to SiMe₄.^bCp' = 1,3-bis(trimethylsilyl)cyclopentadienyl.^cFluH₂ = fluorene.

Table 33 Synthesis of $T_8[c-C_6H_{11}]_7[R]$ compounds

Entry	R	Starting materials	Yield (%)	^{29}Si NMR ^a	Reference
1	-H	(11)+HSiCl ₃ , NEt ₃ , Et ₂ O	88	-68.05, -68.12, -68.15, -83.16	356
2	-OSiMe ₃	$T_8[c-C_6H_{11}]_7[H]+ClSiMe_3$, Me ₃ NO, THF	Quantitative	11.29, -67.54, -68.09, -68.12, -107.81	356
3	-OSnMe ₃	$T_8[c-C_6H_{11}]_7[H]+ClSnMe_3$, Me ₃ NO, THF	87	-68.00, -68.09, -68.14, -102.99	356
4	-OSbMe ₄	$T_8[c-C_6H_{11}]_7[H]+ClSbMe_4$, Me ₃ NO, THF	83	-68.08, -68.16, -68.58, -108.93	356
5	-Cl	(11)+SiCl ₄ , NEt ₃ , Et ₂ O	-	-	357
6	-OH	$T_8[c-C_6H_{11}]_7[Cl]+H_2O$	-	-	358
7	-NH ₂	$T_8[c-C_6H_{11}]_7[Cl]+NH_3$, CH ₂ Cl ₂	Quantitative	-	357
8	-NHSiMe ₃	$T_8[c-C_6H_{11}]_7[NH_2]+ClSiMe_3$, NEt ₃ , Et ₂ O	87	-	357
9	-N=C(NMe ₂) ₂	$T_8[c-C_6H_{11}]_7[Cl]+$ tetramethylguanidine, Et ₂ O	85	-	357
10	-N=C(NH- <i>o</i> -Tol) ₂	$T_8[c-C_6H_{11}]_7[Cl]+$ di- <i>o</i> -tolylguanidine, Et ₂ O	80	-	357
11	-SiCl ₃	(11)+Si ₂ Cl ₆ , NEt ₃ , toluene	43	-	359
12	-OSiCl ₃	(11)+O(SiCl ₃) ₂ , NEt ₃ , toluene	62	-	359
13	-(CH ₂) ₃ NH ₂	(11)+(MeO) ₃ Si(CH ₂) ₃ NH ₂ , THF	78	-	360
14	-OLi	$T_8[c-C_6H_{11}]_7OH+MeLi$	> 68	-	358
15	-OSmCp [*] ₂ bridged species	$T_8[c-C_6H_{11}]_7OLi+Cp^*Sm(\mu-Cl)_2Li(THF)_2$	68	-	358
16	-OSc(acac) ₂ bridged species	$T_8[c-C_6H_{11}]_7OH+Cp^*Sc(acac)_2$	61	-	358

^aReferenced to SiMe₄.

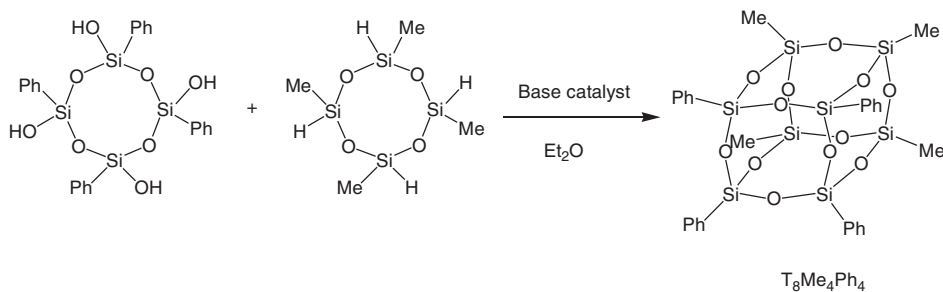


Figure 49 Formation of $T_8Me_4Ph_4$.

compounds with the R' substituents diagonally opposite to each other, could, in theory be formed from hydrolysis of $R'Si(OSiRX_2)_3$ precursors. This has been carried out for $CH_2=CHSi[OSiMeX_2]_3$ ($X = Cl$ or OEt) but few details have been reported.³⁶⁵ Another synthetic route using oligomeric precursors is to condense two “halves” of a cube together. Thus, a rare example of $T_8R_4R'_4$ species has been prepared in 95% yield by the reaction between two cyclotetrasiloxanes in low concentrations (2.5%) in ether (Figure 49) in the presence of basic catalysts.³⁶⁶ This looks an attractive synthetic route but it is unlikely to be general as it is difficult to prepare the cyclotetrasilanol precursors. Attempts have also been made to cohydrolyze a cyclotetrasiloxane as one “half” of a cube with a simple chlorosilane. Unfortunately, cohydrolysis of $[MeClSiO]_4$ with $CH_2=CHSiCl_3$ gives $T_8Me_n[CH=CH_2]_{8-n}$ ($n = 4-6$), the main product after sublimation being $T_8Me_6[CH=CH_2]_2$. This shows that Si–O bond cleavage and rearrangement of intermediates must occur and that the divinyl compound is probably the most thermodynamically stable.³⁶¹

The alternative to the synthetic routes involving the building up of the POSS core with the different substituents already present is to modify an existing T_8R_8 species as shown in Figure 48. This undoubtedly often occurs accidentally when trying to convert one T_8R_8 species into a different $T_8R'_8$, but the partially substituted products are then usually regarded as nuisance by-products. The synthetic problem is to modify the T_8R_8 species into, for example, a single one of the three isomers of $T_8R_6R'_2$, cleanly and in high yield. Apart from the method shown in Figure 48, this ideal has been found hard to realize. Size-exclusion HPLC is useful in separating the mono-substituted products $T_8H_7[Co(CO)_4]$ in 10% yield and $T_8H_7[C_6H_{13}]$ from the reaction of T_8H_8 with $[Co_2(CO)_8]$ and with 1-hexene, respectively.^{130,132,367} In each case the mono-substituted compound can be isolated in pure form and has been the subject of X-ray crystallographic studies. In an attempt to prepare $T_8[OC(=CH_2)Me]_8$ from the $[Co_2(CO)_8]$ catalyzed reaction between T_8H_8 and acetone the partially substituted product $T_8[OC(=CH_2)Me]_6[OH]_2$ was surprisingly isolated as a single isomer in 35% yield. X-ray crystallography showed the two silanol groups to be on diagonally opposite silicons and the ^{29}Si NMR spectrum showed only two resonances, at -103.0 and -103.3 ppm, also indicative of this isomer.¹¹¹ The reasons for this relatively high-yielding reaction leading to a single isomer being readily isolated are unclear but

it does illustrate that syntheses of useful amounts of single isomers of $T_8R_6R'_2$ compounds should be possible. One method by which disubstitution at silicon atoms along an edge of the POSS core can be achieved is by treatment of T_8R_8 with a small difunctional reagent. Thus, T_8H_8 reacts with $(CH_2=CHSiMe_2)_2O$ according to Figure 13 to give a disubstituted compound, which has been crystallographically characterized, as one of several compounds in the product mixture.¹²⁹ Hasegawa has treated a methanolic solution of $T_8[ONMe_4]_8$ (see Section V.E) with $MeSi(OEt)_3$ and, after trimethylsilylation of the reaction mixture, gas chromatography showed the formation of $T_8[OSiMe_3]_8$ as the main product along with the heterosubstituted products $T_8[OSiMe_3]_7Me$ and $T_8[OSiMe_3]_6Me_2$. The formation of the latter products was explained by exchange of $Si(O^-)_4$ units in the silicate species $T_8[O^-]_8$.³⁶⁸ The chlorination of $T_8[CH=CH_2]_8$ using SO_2Cl_2 gives a mixture of $T_8Cl_n[CH=CH_2]_{8-n}$ (mainly $n = 1$ or 2) and UV initiated chlorination of T_8Et_8 with SO_2Cl_2 gives $T_8Cl_nEt_{8-n}$ (mainly $n = 1-7$).²⁰⁹ Addition of dichlorocarbene to $T_8[CH=CH_2]_8$ gives dichlorocyclopropyl derivatives $T_8[C_3H_3Cl_2]_4[CH=CH_2]_4$ of unknown isomeric mixture in 33% yield.³⁶⁹

Despite the problems outlined above, increasing efforts are being made to design synthetic routes to compounds that have, for example, the $T_8R_6R'_2$ formula with the R' groups either adjacent to each other or on diagonally opposite corners of the cube, or $T_8R_4R'_4$ compounds in which two halves of the cube are differently substituted. The synthesis of unsymmetrical compounds is likely to be driven by their potentially useful materials properties and considerable growth in this area can be expected.

J. The solid-state structures of T_8R_8 compounds

A wide range of T_8R_8 structures have been determined by X-ray crystallography in addition to those less symmetrical structures described earlier in Section V. Selected structural data are given in Table 34 which shows both the range of compounds characterized and bond lengths and angles for the POSS core. The Si–O bond lengths are generally unexceptional and most fall in the range 1.60–1.63 Å, as found in other siloxanes.³⁴

Perhaps the most striking feature of the data shown in Table 34 is that although the compounds T_8R_8 are, ideally, highly symmetrical, and their mean Si–O–Si angles mostly fall in a fairly narrow range, 147–150°, the spread of Si–O–Si angles within a single POSS structure may be large. This significant distortion of the POSS core has often been hidden in X-ray data reports where average Si–O–Si angles are discussed, but recently this feature has been described in more detail with reference to the particularly distorted $T_8[OSnMe_3]_8 \cdot 4H_2O$ (Table 34, entry 51) in which the range of siloxane angles spreads over nearly 36°. This large distortion is probably attributable to the water molecules that are also present in the lattice as the anhydrous analog $T_8[OSnMe_3]_8$ has a Si–O–Si angle range of about 12.5° (Table 34, entry 50). The distortion of the Si atoms in the POSS core away from an ideal cubic structure can also be seen in differences in nonbonded Si...Si distances along the edges, across faces, and across the body diagonals of the polyhedron. These features have been tabulated and discussed for a range of

Table 34 Selected structural data for T_8R_8 compounds

Entry	R	Si-O (Å)		Si-O-Si (°)		Reference
		Range	Mean	Range	Mean	
1	-H	1.578	1.578	-	-	81
2	-H	1.6168(11)-1.6195(7)	1.618	147.49(6)-147.60(7)	147.54	82
3	-CH ₃	1.603(25)-1.620(25)	1.610	144.2(30)-146.3(30)	145.25	308
4	-C ₂ H ₅	1.55(1)-1.66(1)	1.61	148.4(9)-150.3(9)	149.3	370
5 ^a	-C ₂ H ₅	-	-	-	-	157
6 ^a	- <i>n</i> -C ₃ H ₇	-	-	-	-	157
7 ^a	- <i>i</i> -C ₃ H ₇	-	-	-	-	157
8	- <i>i</i> -C ₃ H ₇	1.607(4)-1.613(4)	1.610	149.4(2)-149.6(3)	149.5	50,314
9 ^a	- <i>n</i> -C ₄ H ₉	-	-	-	-	157
10	- <i>n</i> -C ₈ H ₁₇	1.615-1.628	1.621	141.13-159.78	149.27	317
11	-CH ₂ - <i>i</i> -C ₃ H ₇	1.611(5)-1.622(5)	1.617	143.7(3)-152.3(3)	149.62	100
12	-CH ₂ CH=CH ₂	1.51(3)-1.73(3)	1.63	146.8-156.3	150.7	371
13	-CH ₂ C ₆ H ₅	1.600(5)-1.627(5)	1.616	141.0(4)-154.5(4)	147.75	166
14	-CH ₂ -(2,2,6,6-Me ₄ C ₃ H ₂ N)	1.6044(11)-1.6197(10)	1.613	146.27-150.57	148.81	321
15	-(CH ₂) ₂ Br	1.603(10)-1.629(10)	1.615	145.9(7)-152.8(7)	149.2	201
16	-(CH ₂) ₂ PMe ₂	1.588(2)-1.598(2)	1.594	145.44(17)-152.37(17)	148.96	196
17	-(CH ₂) ₂ Si(CH=CH ₂) ₃	1.54(3)-1.65(3)	1.602	146.55-157.21	150.36	192
18	-(CH ₂) ₂ -SiMe(CH=CH ₂) ₂	1.5(2)-1.7(2)	1.6	148(10)-158(10)	150	193
19	-(CH ₂) ₂ -CO ₂ Me	1.601(10)-1.650(10)	1.627	143.7(8)-148.7(8)	148.2	201
20	-(CH ₂) ₂ CMe ₂ CH ₂ -CO ₂ Me	1.611(2)-1.632(2)	1.620	139.61-155.88	149.14	100
21	-(CH ₂) ₂ CMe ₂ OH, THF/H ₂ O	1.619(2)-1.628(2)	1.624	142.28-152.26	148.51	111
22	-(CH ₂) ₂ O(CH ₂) ₂ Cl	1.604-1.632	1.616	142.92-159.32	149.22	118,372
23	-(CH ₂) ₃ Br	1.597(7)-1.633(7)	1.619	141.7(4)-153.8(5)	148.8	336
24	-(CH ₂) ₃ I	1.604(5)-1.622(7)	1.615	147.3(3)-150.6(4)	149.3	108
25	-(CH ₂) ₃ - <i>p</i> -MeOC ₆ H ₄	1.604-1.627	1.614	145.59-156.56	149.53	317
26 ^b	-CH=CH ₂	1.57-1.63	1.60	148.8-151.7	150.2	182
27 ^c	-CH=CH ₂	1.596(6)-1.616(6)	1.603	150.0(4)-150.5(4)	150.2	175
28	-CH=CH ₂ , NMe ₄ F	1.618-1.630	1.625	138.67-143.06	141.10	172
29	-CH=CHC ₆ H ₅	1.598-1.627	1.617	145.89-150.31	148.11	188
30	-CH=CHCH ₂ SiMe ₃	1.620-1.629	1.624	142.4(16)-154.6(17)	148.8	188
31 ^d	- <i>c</i> -C ₆ H ₁₁	1.586(6)-1.635(6)	1.603	149.9(4)-151.7(4)	150.8	317

Table 34 (Continued)

Entry	R	Si-O (Å)		Si-O-Si (°)		Reference
		Range	Mean	Range	Mean	
32 ^e	- <i>c</i> -C ₆ H ₁₁	1.539(2)–1.6705(17)	1.613	140.76(8)–160.68(11)	150.52	317
33 ^f	- <i>c</i> -C ₆ H ₁₁	1.613(2)–1.625(2)	1.618	144.82(16)–151.82(17)	149.32	317
34	- <i>c</i> -C ₅ H ₉	1.615(3)–1.630(3)	1.623	141.51–156.06	148.53	100
35	-C ₆ H ₅ pyridine, <i>o</i> -Cl ₂ -C ₆ H ₄ solvate	1.606(5)–1.621(5)	1.614	143.9(3)–156.6(4)	149.2	156
36	-C ₆ H ₅ acetone solvate	1.607–1.614	1.612	144.6–151.4	149.2	155
37	-C ₆ H ₅ · TBAF	1.6213–1.6284	1.6250	139.11–143.36	141.19	143
38	- <i>p</i> -MeC ₆ H ₄ · NMe ₄ F	1.623–1.629	1.625	140.50–142.47	141.20	172
39	- <i>o</i> -NMe ₂ C ₆ H ₄	1.611(1)–1.626(2)	1.617	143.5(1)–155.2(1)	148.42	343
40 ^a	-1-Naphthyl	–	–	–	–	157
41	-ONMe ₄ , H ₂ O	1.558–1.619	1.598	150.03–150.70	150.34	373
42	-OCu(EDA) ₂ , H ₂ O	1.559–1.653	1.613	143.17–163.26	150.97	374
43	-O ⁻ , 4TMP	1.579–1.632	1.614	148.11–154.69	150.61	375
44	-ONMe ₃ Ph, H ₂ O	1.570–1.638	1.607	144.65–156.54	150.12	376
45	-OMe	1.592–1.609	1.604	145.42–151.92	148.15	98
46	-OSiMe ₃	1.585–1.616(9)	1.600	147.2–150.5(6)	148.8	241
47 ^g	-OSiMe ₂ H	1.599–1.607(5)	1.603	148.1–148.3(3)	148.2	241
48 ^h	-OSiMe ₂ H	1.480(5)–1.605(4)	1.560	148.5(3)–167(2)	154.7	117
49	-OSiMe ₂ CH=CH ₂	1.597–1.608(3)	1.602	148.1–148.3(3)	148.2	241
50	-OSnMe ₃	1.580(3)–1.629(4)	1.608	148.8(2)–161.2(2)	149.3	125
51	-OSnMe ₃ , 4H ₂ O	1.5872(16)–1.6277(17)	1.6121	136.35(10)–172.13(12)	149.50	125
52	-OTiClCp ₂ , 3CH ₂ Cl ₂	1.579(2)–1.612(2)	1.601	145.36(14)–151.21(16)	148.70	125
53	-Cl	1.595(4)–1.610(4)	1.601	148.0(3)–148.8(3)	148.4	377
54	-Co(CO) ₄	1.610(4)–1.637(4)	1.623	147.6(2)–154.1(3)	150.8	119
55	-SiMe ₂ tBu	1.620(7)–1.630(6)	1.625	148.5(4)–152.2(4)	150.2	323

^aUnit cell and space group only.^bStructure VINSIO from the CCDC.^cStructure VINSIO01 from the CCDC.^dStructure ZZZVUY01 from the CCDC.^eStructure ZZZVUY02 from the CCDC.^fStructure ZZZVUY03 from the CCDC.^gStructure HOKTUW from the CCDC.^hStructure HOKTUW01 from the CCDC.

T_8 derivatives^{125,317} and can be useful in describing the nature of the distortion present. One of the $T_8[\text{OSiMe}_2\text{H}]_8$ structure determinations (Table 34, entry 48) also appears to show a siloxane angle variation of about 19° but the other (Table 34, entry 47) has a less than one degree range. This difference may be due to the different temperatures at which the structures were recorded, 295 and 200 K for entries 48 and 47, respectively, the higher temperature structure being significantly disordered. The flexibility of the POSS core can also be seen in the three polymorphs of $T_8[\text{c-C}_6\text{H}_{11}]_8$ (Table 34, entries 31–33), one of which has an approximate range of 20° for the Si–O–Si angles, while the other two have much smaller ranges of about 2 and 7° .

A further aspect of interest in the structures of T_8R_8 species is the arrangement of the substituents around the POSS core. In an idealized structure, the eight substituents would point to the vertices of a cube, such a packing arrangement would, however, lead to large spaces between the substituents. To avoid this, if relatively flexible substituents are present, then molecules may distort in one of two ways, either the substituents on two opposite faces of the POSS core close up toward each other to form a more disk-like structure, or the substituents around a pair of opposite faces close up around these faces to provide a more rod-like geometry. The rod-like structure can be clearly seen in $T_8[n\text{C}_8\text{H}_{17}]_8$ (Figure 50), where the octyl arms do not interdigitate with neighboring molecules and the arrangement has been pointed out to be reminiscent of some mesogenic silsesquioxane compounds.³¹⁷ The rod-like nature of $T_8[n\text{C}_8\text{H}_{17}]_8$ allows a closest cage-center to cage-center distance of 8.519 Å, which is only a little longer than the shortest analogous distance in $T_8\text{Me}_8$, 8.441 Å (data calculated using structures HALJEK and OCMSIO01 from the Cambridge Crystallographic Database). This shows how effectively the substituents can distort away from pointing toward the vertices of a cube in order to minimize the free space in the lattice.

The more disk-like structure can be seen in $T_8[(\text{CH}_2)_2\text{Si}(\text{CH}=\text{CH}_2)_3]_8$ and is shown in Figure 51.

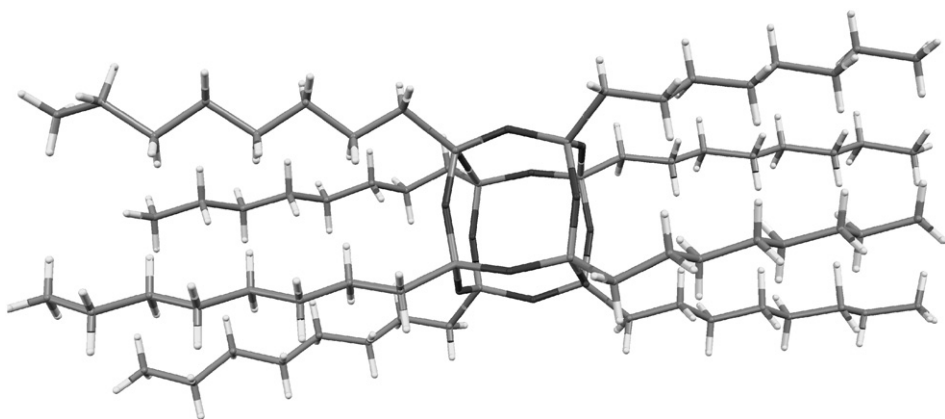


Figure 50 Structure of $T_8[n\text{C}_8\text{H}_{17}]_8$. (Redrawn using data for structure HALJEK from the Cambridge Crystallographic Data Centre.)

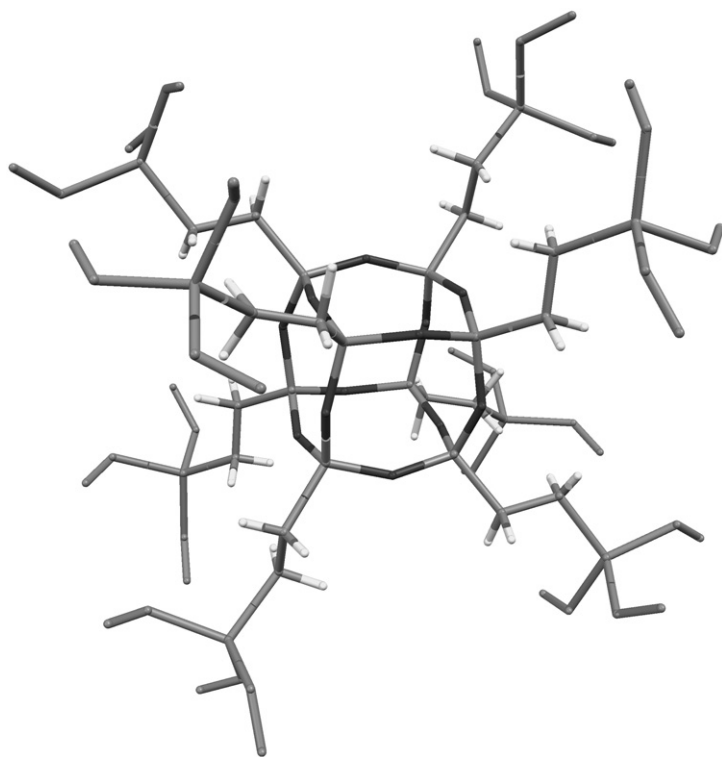


Figure 51 Structure of $T_8[(CH_2)_2Si(CH=CH_2)_3]_8$. (Redrawn using data for structure PUTTON from the Cambridge Crystallographic Data Centre.) Vinylic H atoms are omitted for clarity.

VI. SYNTHESSES, PROPERTIES, AND REACTIONS OF T_{10} DERIVATIVES

A. Synthesis

There are far fewer T_{10} derivatives known than there are T_8 species and their applications, have, so far, been limited. This is due to difficulties with their efficient preparation in good yield and the fact that T_8 derivatives are easier to prepare and can generally be expected to have similar chemistry to the more difficult to access T_{10} analogs. The synthetic routes to T_8 derivatives described in the previous sections usually lead to a mixture of POSS compounds in which T_{10} species often form a small component, for example, the synthesis of T_8H_8 by hydrolysis of $HSiCl_3$ gives $T_{10}H_{10}$ as a by-product in low yield (Table 35, entries 1, 2). The silicate anion $T_{10}[O^-]_{10}$ may be prepared as for the T_8 derivative, from strongly alkaline solutions of silica (Table 35, entry 25)^{221b,378} and it can be separated from other silicate anions by gel-filtration chromatography.³⁷⁹ The routes to T_{10} derivatives are summarized in Figure 52 and details are given in Table 35. These routes are generally the same as those for T_8 derivatives but the synthesis is usually followed by extensive purification *via* crystallization, sublimation, HPLC, or size-exclusion chromatography to provide the small percentage of T_{10} derivative formed in a

Table 35 Synthetic routes $T_{10}R_{10}$ compounds

Entry	R	Starting materials and conditions	Yield (%)	$^{29}\text{SiNMR}^a$	Reference
1	-H	$\text{HSiCl}_3 + \text{H}_2\text{O}$, HCl, FeCl_3 , $\text{MeOH}/\text{C}_6\text{H}_{14}/\text{PhMe}$, 9 h	—	—	67
2	-H	$\text{HSiCl}_3 + \text{H}_2\text{O}$, $\text{C}_6\text{H}_6 + \text{H}_2\text{SO}_4$	ca. 1–2	—	74
3	-H	$\text{HSiCl}_3 + c\text{-C}_6\text{H}_{12}/\text{PhMe} + \text{H}_2\text{SO}_4$	3.6	–86.255	381
4	-CH ₃	$c\text{-(CH}_3\text{HSiO)}_n$, $\text{H}_2\text{O}/\text{NaOH}$, sublimation giving crystals suitable for X-ray studies	—	—	382
5	-C ₂ H ₅	$\text{T}_8\text{Et}_8 + \text{K}_2\text{CO}_3$, acetone	55	–67.56	103
6	- <i>n</i> -C ₃ H ₇	$\text{T}_{8n}\text{Pr}_{18} + \text{K}_2\text{CO}_3$, acetone	12	–69.16	103
7	- <i>n</i> -C ₄ H ₉	$\text{T}_{8n}\text{Bu}_8 + \text{K}_2\text{CO}_3$, acetone	18	–68.61	103
8	- <i>n</i> -C ₅ H ₁₁	$\text{T}_{8n}\text{Pent}_8 + \text{K}_2\text{CO}_3$, acetone	10	–68.61	103
9	- <i>n</i> -C ₇ H ₁₅	$\text{T}_{8n}\text{Hept}_8 + \text{K}_2\text{CO}_3$, acetone	4	–68.56	103
10	- <i>n</i> -C ₈ H ₁₇	$\text{T}_{8n}\text{Hex}_8 + \text{K}_2\text{CO}_3$, acetone	15	–68.68	103
11	- <i>n</i> -C ₉ H ₁₉	$\text{T}_{8n}\text{Non}_8 + \text{K}_2\text{CO}_3$, acetone	8	–68.62	103
12	- <i>n</i> -C ₁₀ H ₂₁	$\text{T}_{8n}\text{Dec}_8 + \text{K}_2\text{CO}_3$, acetone	7	–68.55	103
13	- <i>c</i> -C ₅ H ₉	$c\text{-C}_5\text{H}_9\text{SiCl}_3 + \text{H}_2\text{O}$, acetone, 65 h, then NBu_4F , THF/ CH_2Cl_2 , 2 days	12	–69.20	383
14	-Cp	$\text{CpSiCl}_3 + \text{H}_2\text{O}$, THF/ $(\text{NH}_4)_2\text{CO}_3$, 7 days	67	–71.50, –74.39, –77.04 ^b	339
15	-C ₆ H ₅	$\text{PhSiCl}_3 + \text{H}_2\text{O}$, toluene, KOH, 9 h, then recrystallization from benzene/hexane	—	—	146
16	-CH=CH ₂	$[\text{CH}_2 = \text{CHSi}(\text{OEt})_2\text{O} + \text{H}_2\text{O}]$, NBu_4F , THF/ CH_2Cl_2 , 2 days	26	–81.48	383
17	-(CH ₂) ₂ CF ₃	$\text{CF}_3\text{CH}_2\text{CH}_2\text{SiCl}_3 + \text{H}_2\text{O}$, acetone, 40 days, not isolated, by-product in synthesis of T_8R_8	—	—	330
18	-(CH ₂) ₃ C ₆ F ₅	$\text{T}_8[(\text{CH}_2)_3\text{C}_6\text{F}_5]_8 + \text{Na}_2\text{SiF}_6 + 18\text{-crown-6}$, acetonitrile	52	–69.11	103
19	-(CH ₂) ₃ I	$\text{T}_8[(\text{CH}_2)_3\text{I}]_8 + \text{NaOH}$, acetone	12	–68.85	103
20	-(CH ₂) ₃ Br	$\text{T}_8[(\text{CH}_2)_3\text{Br}]_8 + \text{NaOH}$, acetone	36	–69.31	103
21	-(CH ₂) ₃ Cl	$\text{T}_8[(\text{CH}_2)_3\text{Cl}]_8 + \text{Na}_2\text{SiF}_6 + 18\text{-crown-6}$, acetonitrile	61	–68.97	103
22	-(CH ₂) ₃ SCN	$\text{T}_8[(\text{CH}_2)_3\text{SCN}]_8 + \text{Na}_2\text{SiF}_6 + 18\text{-crown-6}$, acetonitrile	62	–69.56	103
23	-(CH ₂) ₃ O–C(=O)C(=CH ₂)Me	$(\text{MeO})_3\text{Si}[(\text{CH}_2)_3\text{OC}(=\text{O})\text{C}(=\text{CH}_2)\text{Me}] + \text{PrOH}$, Me_4NOH , then reflux in PhMe, Me_4NOH	—	—	384

Table 35 (Continued)

Entry	R	Starting materials and conditions	Yield (%)	$^{29}\text{SiNMR}^a$	Reference
24	$-\text{O}^-[\text{NBu}_4]^+$	$\text{Si}(\text{OEt})_4 + \text{H}_2\text{O}$, $n\text{Bu}_4\text{N}^+\text{OH}^-$, not isolated	–	–	241,378a
25	$-\text{O}^-$	$\text{Si}(\text{OMe})_4 + \text{Et}_4\text{NOH} / \text{H}_2\text{O}$ or $\text{Bu}_4\text{NOH} + \text{SiO}_2 + \text{H}_2\text{O}$	–	-99 ± 1	221b,378a,378b
26	$-\text{OSi}(\text{CH}_3)_3$	$\text{T}_{10}[\text{ON}n\text{Bu}_4]_{10} + \text{Me}_3\text{SiCl} / (\text{Me}_3\text{Si})_2\text{O}$, $i\text{PrOH}$	–	12.4, -110.2	221b,241,378a
27	$-\text{OSiMe}_2\text{H}$	$\text{T}_{10}[\text{ON}n\text{Bu}_4]_{10} + \text{HMMe}_2\text{SiCl}$, 2-propanol	–	–	241
28	$-\text{OSiMe}_2\text{CH}=\text{CH}_2$	$\text{T}_{10}\text{H}_{10} + \text{CH}_2=\text{CHMe}_2\text{SiCl} \cdot \text{Me}_3\text{NO}$, THF	65	0.0, -110.36	124
29	$-\text{OSiMe}_2\text{CH}_2\text{Cl}$	$\text{T}_{10}\text{H}_{10} + \text{ClCH}_2\text{Me}_2\text{SiCl} \cdot \text{Me}_3\text{NO}$, THF	52	6.9%, -110.82	124
30	$-\text{OSiMe}_2\text{CH}_2^-$ $\text{CH}_2\text{SiMe}_2\text{C}_6\text{H}_4\text{O}_{1/2}$ polymer	$\text{T}_{10}\text{H}_{10} + (\text{HSiMe}_2\text{C}_6\text{H}_4)_2\text{O} + \text{PtCl}_2(\text{PhCN})_2$ catalyst	–	-109.1^c	286,385
31	$-\text{OSn}(\text{CH}_3)_3 \cdot 4\text{H}_2\text{O}$	$(\text{Me}_3\text{Sn})_2\text{O} + \text{T}_{10}\text{H}_{10}$, toluene	93	-101.9	125

^aReferenced to SiMe_4 .^bThree isomers present.^cSolid state for POSS core Si.

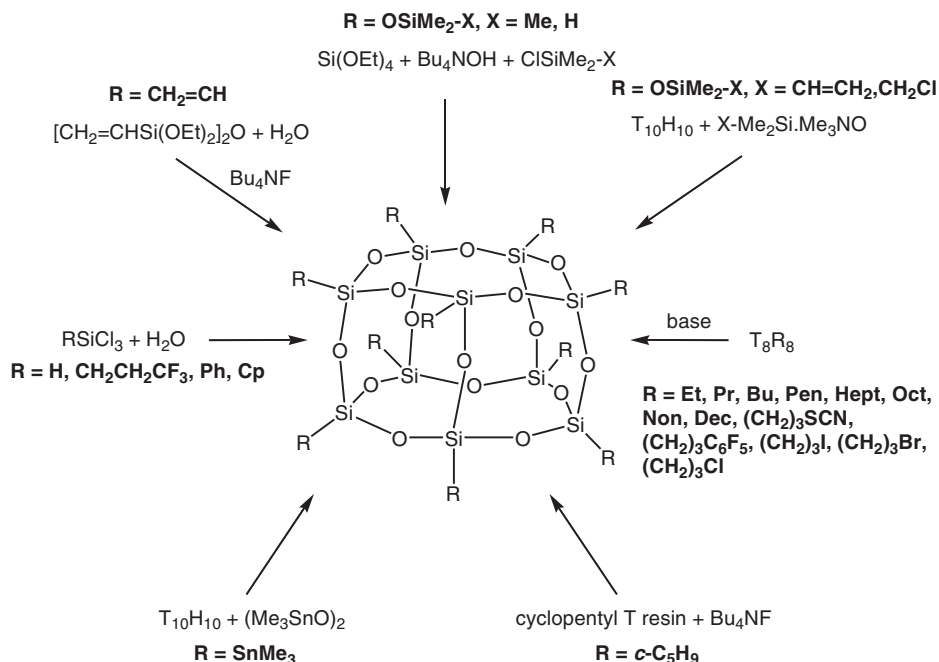


Figure 52 Summary of synthetic routes to T_{10} derivatives.

pure form. Good yields are, as expected, obtained for syntheses involving the modification of one T_{10} derivative to give another (Table 35, entries 28–30). Exceptions to the low-yielding routes to the T_{10} core are the surprising 67% yield for the hydrolysis of CpSiCl_3 to give $\text{T}_{10}\text{Cp}_{10}$ (Table 35, entry 14) and the fragmentation/rearrangement reactions of T_8 POSS cores to give T_{10} species (Table 35, entries 4–12 and 18–22). However, although the fragmentation/rearrangement reactions give good yields of the T_{10} species from T_8 analogs there is also present in the product mixture, some T_8 precursor and T_{12} species which need to be separated by HPLC. Rare examples of T_{10} derivatives containing two different substituents are also available by this method. Thus, a redistribution/rearrangement occurs between $\text{T}_8[(\text{CH}_2)_3\text{Cl}]_8$ and $\text{T}_8[n\text{C}_3\text{H}_7]_8$ to give a complicated mixture of products from which it is possible to separate, $\text{T}_{10}[(\text{CH}_2)_3\text{Cl}][n\text{C}_3\text{H}_7]_9$ and $\text{T}_{10}[(\text{CH}_2)_3\text{Cl}]_9[n\text{C}_3\text{H}_7]$.³⁸⁰ The mixed substituent species $\text{T}_{10}\text{H}_9\text{Ph}$ has also been prepared, in 0.5% yield, but using the cohydrolysis of HSiCl_3 with PhSiCl_3 and separation of the product mixture by HPLC.¹³¹

B. Structural and physical properties

The $\text{T}_{10}\text{R}_{10}$ compounds are generally air-stable white solids and their physical properties are similar in many ways to their T_8R_8 counterparts although much fewer data are available. The ^{29}Si NMR chemical shift data for a range of $\text{T}_{10}\text{R}_{10}$ compounds are given in Table 36, data for compounds containing more than one

Table 36 ^{29}Si NMR data for $\text{T}_{10}\text{R}_{10}$ compounds

Compound	^{29}Si NMR chemical shift (ppm from SiMe_4)	Solvent	Reference
$\text{T}_{10}[\text{CH}=\text{CH}_2]_{10}$	−81.48	CDCl_3	383
$\text{T}_{10}\text{Et}_{10}$	−67.56	CDCl_3	103
$\text{T}_{10}[\text{C}_3\text{H}_7]_{10}$	−69.16	CDCl_3	103
$\text{T}_{10}[\text{C}_3\text{H}_6\text{Cl}]_{10}$	−68.97	CDCl_3	103
$\text{T}_{10}[\text{C}_3\text{H}_6\text{Br}]_{10}$	−69.31	CDCl_3	103
$\text{T}_{10}[\text{C}_3\text{H}_6\text{I}]_{10}$	−69.85	CDCl_3	103
$\text{T}_{10}[\text{C}_3\text{H}_6\text{SCN}]_{10}$	−69.56	CDCl_3	103
$\text{T}_{10}[\text{C}_3\text{H}_6(\text{C}_6\text{F}_5)]_{10}$	−69.11	CDCl_3	103
$\text{T}_{10}[\text{C}_4\text{H}_9]_{10}$	−68.61	CDCl_3	103
$\text{T}_{10}[\text{c-C}_5\text{H}_9]_{10}$	−69.20	CDCl_3	383
$\text{T}_{10}[\text{C}_5\text{H}_{11}]_{10}$	−68.61	CDCl_3	103
$\text{T}_{10}[\text{C}_7\text{H}_{15}]_{10}$	−68.56	CDCl_3	103
$\text{T}_{10}[\text{C}_8\text{H}_{17}]_{10}$	−68.68	CDCl_3	103
$\text{T}_{10}[\text{C}_9\text{H}_{19}]_{10}$	−68.62	CDCl_3	103
$\text{T}_{10}[\text{C}_{10}\text{H}_{21}]_{10}$	−68.55	CDCl_3	103
$\text{T}_{10}[\text{OSiMe}_2\text{CH}_2\text{Cl}]_{10}$	−110.82 ^a	CDCl_3	124
$\text{T}_{10}[\text{OSiMe}_2\text{H}]_{10}$	ca. −110 ^b	Solid	241
$\text{T}_{10}[\text{OSiMe}_2\text{CH}=\text{CH}_2]_{10}$	−110.36 ^c	CDCl_3	124
$\text{T}_{10}[\text{OSiMe}_3]_{10}$	−110.2 ^d	Unknown	378a
$\text{T}_{10}[\text{OSiMe}_2\text{CH}_2\text{CH}_2\text{C}_6\text{H}_4\text{O}]_{10}$	−109.1	Solid	385
polymer			
$\text{T}_{10}[\text{OSnMe}_3]_{10}$	−101.9	Unknown	125

^a6.96 ppm for $\text{SiMe}_2\text{CH}_2\text{Cl}$ group.^bApproximately −2 ppm for SiMe_2H group.^c0.00 ppm for SiMe_2 vinyl group.^d12.4 ppm for SiMe_3 group.

type of substituent can be found in Refs. (103, 380). The NMR data are as might be anticipated and are close in value to those obtained for the T_8 analogs, for example, the ^{29}Si NMR chemical shifts for $\text{T}_8[\text{CH}=\text{CH}_2]_8$ and $\text{T}_{10}[\text{CH}=\text{CH}_2]_{10}$ are −81.63 and −81.48 ppm, respectively. A detailed study of the inelastic neutron scattering, IR and Raman spectra of $\text{T}_{10}\text{H}_{10}$ has been made and comparisons with the spectra from T_8H_8 are made.^{72b,76b,80} The main IR bands are 2270, 1147 and 881 cm^{-1} for ν Si–H, ν_{as} Si–O–Si, and δ O–Si–H, respectively,³⁸⁶ similar to those for T_8H_8 . The X-ray photoemission spectra for T_8H_8 and $\text{T}_{10}\text{H}_{10}$ chemisorbed on a Si surface have also been compared^{386,387} as have the photoluminescence spectra for $\text{T}_{10}\text{R}_{10}$ [$\text{R} = \text{H}$, $(\text{CH}_2)_3\text{Cl}$, and OSiMe_3] species with other POSS analogs.⁵⁹ Gas-phase conformational studies on various POSS compounds, including $\text{T}_{10}[\text{CH}=\text{CH}_2]_{10}$, to measure collision cross sections show that the cage structures maintain the same conformations in the gas phase as in the solid state determined by X-ray crystallography.¹⁵⁸

The structural and electronic properties of $\text{T}_{10}\text{H}_{10}$ have been calculated^{37,38} and the structural data show significant differences to those obtained experimentally

(see Table 37). More recent calculations on $T_{10}Me_{10}$ ^{39,60} give better correlations with the experimentally determined structure.^{382a} The main structural difference between T_{10} derivatives and the smaller T_8 analogs is that they contain two different ring sizes, Si_4O_4 and Si_5O_5 , some oxygen atoms being in only Si_4O_4 rings and some in both Si_4O_4 and Si_5O_5 ; structural parameters are given for both ring types in Table 37. The Si–O bond distances are similar to those found in T_8 derivatives and, as might be expected the Si–O–Si angles in the Si_4O_4 rings only are usually smaller than those bounding both an Si_4O_4 and Si_5O_5 ring. The range of bond angles in the Si_4O_4 only rings is generally larger than that found for analogous T_8 derivatives but there are only a small number of directly comparable examples and more data are needed before general conclusions can be made when comparing structures.

C. Reactions and applications

The chemistry of T_{10} derivatives is much less well developed than for the analogous T_8 compounds for the reasons given at the head of this section, and the reactions reported are, as might be expected, generally very similar to those for the T_8 analogs. Thus, $T_{10}H_{10}$ reacts in a similar manner to T_8H_8 with $Me_3NO \cdot ClSiMe_2R$ reagents ($R = CH=CH_2$ or CH_2Cl) to give $T_{10}[OSiMe_2R]_{10}$ compounds in good yield,^{124,385} and with $(Me_3Sn)_2O$ to give $T_{10}[OSnMe_3]_{10}$,¹²⁵ while $T_{10}[OSiMe_2H]_{10}$ undergoes hydrosilylation with terminal alkenes,³⁸⁹ and $T_{10}[O^-]_{10}$ can be silylated to give $T_{10}[OSiMe_2H]_{10}$ ²⁴¹ or $T_{10}[OSiMe_3]_{10}$.^{378a} In a reaction that does not seem to have a direct analog in T_8 chemistry, $T_{10}Cp_{10}$ undergoes polymerization *via* Diels–Alder reaction of the Cp groups on reflux in THF solution.³³⁹

The difficulties associated with preparing T_{10} derivatives pure and in large amounts have precluded much study of their potential applications. However, as for T_8H_8 , $T_{10}H_{10}$ has been used to form useful monolayer coatings on gold³⁹⁰ and has also been cross-linked with $(CH_2=CHCMe_2O)_2SiMe_2$ to give a hydrolyzable silsesquioxane polymer with good thermal and chemical stability.³⁹¹ A $T_8H_8/T_{10}H_{10}$ mixture has also been used as a precursor to high-quality SiO_2 thin films by CVD methods.¹³⁶ In an attempt to prepare a microporous solid, the platinum catalyzed hydrosilylation of $T_{10}[OSiMe_2CH=CH_2]_{10}$ with $(HMe_2SiC_6H_4)_2O$ was carried out. A thermally stable polymer was formed but it was not microporous and was thought to comprise interpenetrating networks.³⁸⁵ Copolymers between $T_{10}Ph_9[styryl]$ and styrene have been studied by molecular dynamics in order to investigate the property changes occurring on incorporation of a POSS molecule as a pendant group along the polymer chain. The polymers themselves do not, however, seem to have been prepared.³⁹² The incorporation of $T_{10}Me_{10}$ into dielectric films has been investigated³⁹³ while $T_{10}[CH=CH_2]_{10}$ may be copolymerized with a polyphenylene ether to give cross-linked composite materials with good chemical and thermal stability³⁹⁴ and has also been used in porous gas-permeable materials.³⁹⁵ The vinyl-substituted $T_{10}[CH=CH_2]_{10}$ also undergoes an amine-catalyzed Michael addition with $HS(CH_2)_2CO_2Bu$ in a 1:6 ratio to give $T_{10}[CH=CH_2]_4[(CH_2)_2S(CH_2)_2CO_2Bu]_6$, which can be photopolymerized with thiols to give coatings.³⁹⁶ Resin films with potentially useful properties are also

Table 37 Selected structural data for $T_{10}R_{10}$ and related compounds

Compound	Si–O (Å) both ring types		Si–O–Si (°) Si_4O_4 rings		Si–O–Si (°) Si_5O_5 rings		Reference
	Range	Mean	Range	Mean	Range	Mean	
$T_{10}H_{10}$ ^a	1593(2)–1.616(2)	1.606	147.43(13)–150.64(12)	149.5	151.51(14)–159.53(15)	154.7	388
$T_{10}H_{10}$ ^b	1.591(3)–1.615(3)	1.602	147.8(2)–150.2(2)	149.3	152.8(2)–157.9(2)	154.9	388
$T_{10}H_{10}$ (calc.)	–	1.67	–	153.3	–	149.0	37
$T_{10}Cl_{10}$ (calc.)	–	–	–	151.6	–	150.6	28
$T_{10}Me_{10}$	1.582–1.626	1.604	147.3–152.7	149.3	148.0–160.5	154.97	382a
$T_{10}Me_{10}$ (calc.)	1.624–1.627	1.625	–	153.449	–	155.703	60
$T_{10}[OSiMe_3]_{10}$	1.574–1.609(8)	1.589	149.25–154.99	151.74	149.31–157.89	153.75	241
$T_{10}[OSiMe_2H]_{10}$	1.585–1.613(6)	1.599	149.49–154.94	152.05	142.18–156.05	151.55	241
$T_{10}[OSnMe_3]_{10} \cdot 4H_2O$	1.588(6)–1.636(6)	1.615	140.3(4)–151.8(4)	145.34	137.4(4)–159.7(4)	148.59	125
$T_{10}H_9Ph$	1.571(4)–1.620(3)	1.602	145.2(2)–150.9(2)	148.26	150.5(2)–162.7(3)	155.53	131

^a180 K.^b295 K.

available from polymerization of $T_{10}[\text{OSiMe}_2\text{CH}=\text{CH}_2]_{10}$ with polyphenylene ethers.³⁹⁷ The silane $T_{10}[\text{OSiMe}_2\text{H}]_{10}$ can undergo platinum catalyzed hydrosilylation with a mesogen to give a compound with potential liquid crystalline properties.³⁹⁸

The potentially useful materials described above have similar properties; good thermal stability, good chemical resistance, porosity, etc., to the related T_8 -based materials. Their formation also relies on the same type of chemistry, usually hydrosilylation reactions involving either Si-H or Si-CH=CH₂ containing POSS derivatives, and given the difficulties in preparing most T_{10} derivatives compared to their T_8 counterparts, it is unlikely that they will have significant applications.

VII. T_{12} , T_{14} , AND T_{16} DERIVATIVES AND LARGER POSS COMPOUNDS

A. $T_{12}R_{12}$ species

The structure of $T_{12}R_{12}$ compounds can, unlike the smaller POSS species readily adopt either of two different geometries; one, of ideal D_{6h} symmetry based on 12-membered rings linked by 6 oxygen atoms, and a second of ideal D_{2d} symmetry, based on four 10-membered rings and four 8-membered rings as shown in Figure 53. The D_{6h} structure appears to be rare for molecular species but is well known as a building unit in silicates.³⁴⁹

The synthesis of $T_{12}R_{12}$ compounds has mainly been achieved by the methods used for the synthesis of T_{10} derivatives, that is, either by hydrolysis of RSiX_3 ($\text{X} = \text{Cl}$ or alkoxide) or by cage-opening reactions from the corresponding T_8R_8 as seen in the previous section. The synthetic routes are summarized in Figure 54 and details are given in Table 38.

As has been seen for smaller POSS compounds, synthesis of the POSS core itself is often a low-yield procedure but modification of existing POSS derivatives to give new compounds usually proceeds in high yield. The formation of $T_{12}H_{12}$ (D_{2d}) occurs during the synthesis of the T_8H_8 along with other lower and higher analogs (as seen in earlier sections). It can be isolated in 3.5% yield by preparative

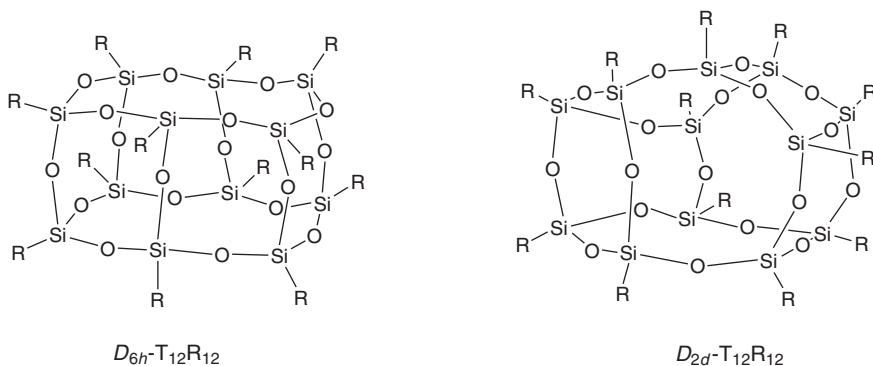


Figure 53 Possible isomeric structures for $T_{12}R_{12}$.

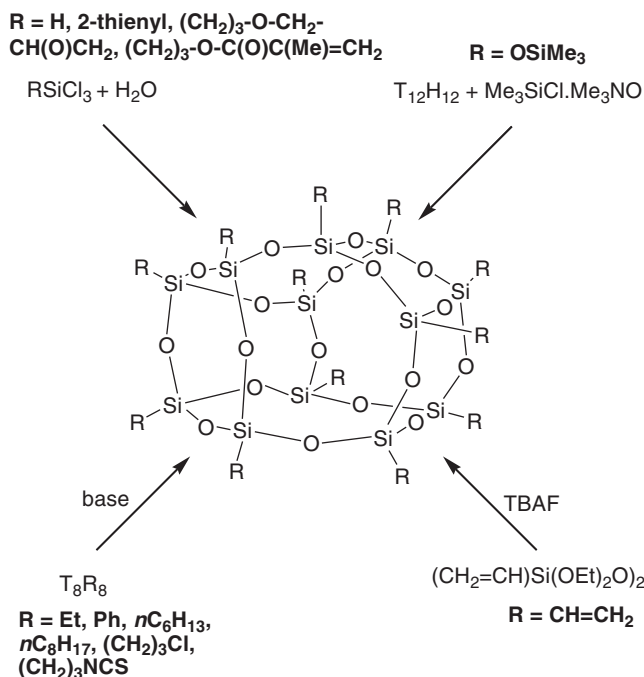


Figure 54 Synthetic routes to $\text{T}_{12}\text{R}_{12}$ compounds.

gas chromatography³⁸¹ or size-exclusion chromatography⁶⁸ (Table 38, entry 1) and has been characterized on a silicon surface using soft X-ray photoemission spectra in order to model the Si/SiO₂ interface.^{87b} Other $\text{T}_{12}\text{R}_{12}$ species can be obtained directly *via* hydrolysis (Table 38), for example, the preparation of $\text{T}_{12}\text{Ph}_{12}$ was reported by Brown et al. during the study of equilibrated phenylsilsesquioxane solutions. If THF was used as a solvent, the hydrolysis of PhSiCl_3 gave $\text{T}_{12}\text{Ph}_{12}$ after 4–6 months at room temperature or after 2–3 days at reflux. A more recent patent described the preparation of $\text{T}_{12}\text{Ph}_{12}$ by the hydrolysis of PhSiCl_3 with NaHCO_3 in toluene (9% yield) and considered this product as a useful starting material to ladder polymers.³⁹⁹ The Pd/C catalyzed hydrogenation of $\text{T}_{12}\text{Ph}_{12}$ gives $\text{T}_{12}[\textit{c}\text{-C}_6\text{H}_{11}]_{12}$ (Table 38, entry 7). Nitration of $\text{T}_{12}\text{Ph}_{12}$ can be achieved, as in the case of T_8Ph_8 , using HNO_3 , to give $\text{T}_{12}[\text{C}_6\text{H}_4\text{NO}_2]_{12}$ which, followed by reduction, affords $\text{T}_{12}[\text{C}_6\text{H}_4\text{NH}_2]_{12}$ (Table 38, entries 8 and 9). $\text{T}_{12}\text{Ph}_{12}$ has been used as a monomer for the preparation of cross-linked polysiloxanes with excellent thermal stability, by an anionic ring-opening polymerization with $(\text{Me}_2\text{SiO})_4$ and $(\text{Ph}_2\text{SiO})_4$ as comonomers.⁴⁰⁰

Several $\text{T}_{12}\text{R}_{12}$ species have been obtained by cage rearrangement as seen for the preparation of $\text{T}_{10}\text{R}_{10}$ compounds. Here, the range of T_{12} compounds obtained is smaller than for the T_{10} analogs and all have D_{2d} symmetry as shown by the two different chemical shifts in the ²⁹Si NMR spectrum (Table 38). $\text{T}_{12}[\text{CH}=\text{CH}_2]_{12}$ has also been prepared *via* a base-catalyzed cage rearrangement of $\text{T}_8[\text{CH}=\text{CH}_2]_8$ in the presence of KOH in MeOH/ CHCl_3 with an estimated yield of 12%.¹⁹⁷

Table 38 Synthetic routes to T₁₂R_n compounds

Entry	R	Starting materials and conditions	Yield (%)	²⁹ Si NMR ^a	Reference
1	-H	HSiCl ₃ +H ₂ O, H ₂ SO ₄ , cyclohexane/toluene, 6 h	3.5	-85.78, -87.76	381
2	-CH ₃	(MeHSiO) ₆ , hydrogenation in presence of alkali	-	-	39,401
3	-C ₂ H ₅	T ₈ (C ₂ H ₅) ₈ +K ₂ CO ₃ , acetone	4	-67.53, -69.79	103
4	- <i>n</i> C ₈ H ₁₇	T ₈ (C ₈ H ₁₇) ₈ +base catalyst	-	-	315
5	-CH=CH ₂	[CH ₂ =CH(EtO) ₂ Si] ₂ O, TBAF/THF, CH ₂ Cl ₂ , 2 days	15	-81.34, -83.35 (1:2)	383
6	-C ₆ H ₅	PhSiCl ₃ +H ₂ O, KOH, THF, reflux, 3 days	50-70	-	146
7	- <i>c</i> -C ₆ H ₁₁	T ₁₂ Ph ₁₂ +H ₂ , Pd/C, EtOAc/AcOH	93	-71.29, -74.29	166
8	-C ₆ H ₄ NO ₂	T ₁₂ Ph ₁₂ +HNO ₃	90	-79.9	148
9	-C ₆ H ₄ NH ₂	T ₁₂ Ph ₁₂ +HCO ₂ H, Et ₃ N, Pd/C, THF	87	-76.7	148
10	-OSiMe ₃	T ₈ [OSiMe ₃] ₈ +base catalyst	-	-	315
11	-2-C ₄ H ₃ S	2-thienyltrimethoxysilane+H ₂ O, Et ₃ N, in methanol, 24 h	55	-	347
12	-2-C ₄ Br ₃ S	T ₁₂ [2-C ₄ H ₃ Si] ₁₂ +Br ₂ , in bromine, 2 h	90	-	347
13	-(CH ₂) ₂ CF ₃	CF ₃ (CH ₂) ₂ SiCl ₃ +H ₂ O, acetone, 40 days	-	-	330
14	-(CH ₂) ₃ Cl	T ₈ [(CH ₂) ₃ Cl] ₈ +NaOCN, acetone	17	-68.73, -71.37	103
15	-(CH ₂) ₃ NCS	T ₈ [(CH ₂) ₃ NCS] ₈ +NaOCN	26	-69.27, -72.07	103
16	-(CH ₂) ₃ OCH ₂ -CH(O)CH ₂	CH ₂ (O)CHCH ₂ O(CH ₂) ₃ Si(OMe) ₃ +H ₂ O, Me ₄ NOH, 2-propanol	-	-	384
17	-(CH ₂) ₃ -OC(O)-CMe=CH ₂	CH ₂ =CMeCO ₂ (CH ₂) ₃ Si(OMe) ₃ +H ₂ O, Me ₄ NOH, 2-propanol	-	-	384
18	-OSi(CH ₃) ₃	T ₁₂ H ₁₂ +Me ₃ SiCl·Me ₃ NO, THF	95	-	124,402

^aReferenced to SiMe₄.

Table 39 Selected structural data for $T_{12}H_{12}$

Bond or angle	X-ray diffraction ^a		Calculated values ³⁷	
	Range	Mean	Range (D_{2d})	Range (D_{6h})
Si–O (Å)				
4R/4R ^b	1.608(3)–1.616(3)	1.611	1.68	1.67 1.67 (4R/6R)
4R/5R	1.582(4)–1.617(4)	1.601	1.68	
5R/5R	1.587(3)–1.608(4)	1.595	1.68	
Si–O–Si (°)				
4R/4R	149.4(2)–154.0(2)	151.7	147.5	162.8 143.3 (4R/6R)
4R/5R	142.9(2)–164.2(3)	154.7	136.7, 145	
5R/5R	152.2(3)–163.0(3)	157.7	143.8	

^a D_{2d} structure.⁴⁰³^bNotation denotes the size of the rings that the oxygen atoms are part of, i.e., 4R/4R is an oxygen atom on an edge between two Si_4O_4 rings.

The structures of few T_{12} derivatives have been determined but $T_{12}H_{12}$ has been investigated by XRD⁴⁰³ and its structure compared with that of $T_{12}Ph_{12}$,⁴⁰⁴ (the structure of a DMSO solvate of $T_{12}Ph_{12}$ has also been determined)⁴⁰⁵ both having distorted D_{2d} symmetry. Selected structural data for $T_{12}H_{12}$ are presented in Table 39 along with calculated values obtained by DFT methods. More recent calculations using DFT (Becke's three-parameter hybrid exchange and the nonlocal correction functional of Lee, Yang, and Parr; B3LYP) showed Si–O: 1.63–1.64 Å, Si–O–Si: 147–150° for the D_{6h} symmetry structure.^{71a} The experimental structural data in Table 39 show smaller ring sizes have smaller bond angles and that there is an inverse correlation with the bond length, that is, smaller angles comprise longer bonds. The calculated data do not correspond well with the experimental data which may be due to the POSS core being significantly distorted from its ideal D_{2d} symmetry in the crystal lattice. As for the case of T_8H_8 , theoretical studies on the insertion of N_2 and O_2 molecules into $T_{12}H_{12}$ have been performed (see Section V.B for further comments).¹⁴⁰ The structures of $T_{12}[OH]_{12}$,^{31,230b,349,106} $T_{12}Me_{12}$,³⁹ and $T_{12}Cl_{12}$ ²⁸ have also been subject to computational studies. The calculations comparing both the two possible structures of $T_{12}Me_{12}$ ³⁹ and of $T_{12}H_{12}$ ³⁷ conclude that the lowest energy is for the D_{2d} structure, as found experimentally for molecular $T_{12}R_{12}$ species. Infrared spectra³⁴⁹ have also been calculated for T_{12} species and photoluminescence⁵⁹ recorded in order for comparisons to be made with smaller POSS compounds.

B. $T_{14}R_{14}$ and $T_{16}R_{16}$ species

Only a small number of compounds with the formula $T_{14}R_{14}$ or $T_{16}R_{16}$ have been reported and synthetic details of their preparation are listed in Table 40. As seen for smaller T_nH_n species, $T_{14}H_{14}$ and $T_{16}H_{16}$ are obtained during the synthesis of T_8H_8 and can be isolated in a very low yield after several purification steps^{68,381} to separate the lower analogs. Few experimental data for these larger POSS

Table 40 Synthetic routes to $T_{14}R_{14}$ and $T_{16}R_{16}$ compounds

Entry	Product	Starting materials and conditions	Yield (%)	Reference
1	$T_{14}H_{14}$, $T_{16}H_{16}$	$HSiCl_3 + H_2O$, H_2SO_4 , $c\text{-}C_6H_{12}/PhMe$, 6 h	1.1 for $T_{14}H_{14}$	381
2	$T_{14}Me_{14}$	$(MeHSiO)_6$, hydrogenation in presence of alkali	–	401
3	$T_{14}Et_{14}$	$(EtHSiO)_6$, hydrogenation in presence of alkali	–	401
4	$T_{14}[CH=CH_2]_{14}$, $T_{16}[CH=CH_2]_{16}$	$CH_2=CHSi(OMe)_3 + H_2O$, HCO_2H , $EtOH$, 7 days	–	184
5	$T_{14}[OSiMe_3]_{14}$	$T_{14}H_{14} + Me_3SiCl \cdot Me_3NO$, THF	95	124

compounds are available but $T_{14}H_{14}$ has been characterized on a silicon surface, as have been smaller T_nH_n species, using soft X-ray photoemission spectra in order to model the Si/SiO₂ interface.^{87b} $T_{14}[CH=CH_2]_{14}$ and $T_{16}[CH=CH_2]_{16}$ were not isolated but were detected using MALDI-TOF mass spectrometry in a complex mixture of oligomers arising from the hydrolysis of $CH_2=CHSi(OMe)_3$ in ethanol in presence of formic acid.

Computational studies have been carried out on $T_{14}H_{14}$, $T_{16}H_{16}$,³⁷ $T_{14}Me_{14}$, $T_{16}Me_{16}$,³⁹ and $T_{14}Cl_{14}$ ²⁸ which have been used not only to determine bond lengths and distances as has been the case for smaller POSS species but also to determine which of the several possible structural isomers for each species is the most stable. For the silylated compound, $T_{14}[OSiMe_3]_{14}$, crystal structures of two isomers have been determined⁴⁰² containing the D_{3h} and C_{2v} polyhedral cores **16** and **17** shown schematically in Figure 55. The D_{3h} symmetry isomer was the most abundant isolated experimentally and this is consistent with computational studies of $T_{14}H_{14}$ ³⁷ and $T_{14}Me_{14}$ which both determined this isomer to be the most stable. The ²⁹Si NMR spectrum of the major isomer of $T_{14}H_{14}$ contains three signals at –87.89, –88.03, and –89.71 ppm in a 3:3:1 ratio, also consistent with a D_{3h} symmetry structure.³⁸¹

There are few experimental details available for T_{16} derivatives but NMR spectra of $T_{16}H_{16}$ suggest that it has the idealized D_{4d} structure, **18**,³⁸¹ shown schematically in Figure 55. In this case the calculations on $T_{16}H_{16}$ ³⁷ do not suggest this isomer to be the most stable but calculations on $T_{16}Me_{16}$ ³⁹ do indicate that the D_{4d} isomer is the most stable.

C. Larger polyhedra

The separation of $T_{18}H_{18}$ from mixtures of other smaller POSS species has been attempted by gas chromatography and size-exclusion chromatography,^{68,381} but it has not been characterized. There is very little experimental evidence for well-decried POSS species with large numbers of silicon atoms but such compounds have been the subject of computational studies. The structure of I_h symmetry $T_{20}Cl_{20}$ has been calculated²⁸ and the O_h symmetry $T_{24}[OH]_{24}$ structure has been used as a model for the sodalite cage which is an important secondary building unit in zeolite structures.⁴⁰⁶ The structures of much larger chlorinated polyhedra

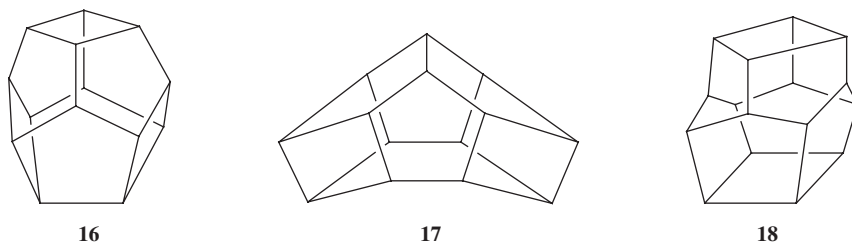


Figure 55 Line drawing of structurally characterized D_{3h} and C_{2v} isomers **16** and **17** of $T_{14}H_{14}$, and D_{4d} isomer **18** of $T_{16}H_{16}$. Each vertex represents an Si-H unit and each edge contains the linking O atoms.

such as $T_{36}Cl_{36}$, $T_{48}Cl_{48}$, and $T_{60}Cl_{60}$, which are analogous to C_{60} , have also been calculated in a study looking at the growth patterns for chlorosiloxanes²⁸ and the analogous $T_{36}H_{36}$, $T_{48}H_{48}$, and $T_{60}H_{60}$ have been modeled to investigate the preferred distribution of ring sizes in large polyhedra,^{89d} but none of the compounds have been prepared. Finally it should be noted that large, tubular POSS-like species such as $T_{72}H_{72}$, $T_{144}H_{144}$, and $T_{240}H_{240}$ have been studied using the MSINDO method and are found to have structures similar to the well-known carbon nanotubes.⁴⁰⁷

VIII. CONCLUDING REMARKS

The data presented in Figure 8 graphically illustrate the tremendous and rapid growth in interest in POSS chemistry, especially for patented applications. This looks set to continue with current applications in areas as diverse as dendrimers, composite materials, polymers, optical materials, liquid crystal materials, atom scavengers, and cosmetics, and, no doubt, many new areas to come. These many applications derive from the symmetrical nature of the POSS cores which comprise relatively rigid, near-tetrahedral vertices connected by more flexible siloxane bonds. The compounds are usually thermally and chemically stable and can be modified by conventional synthetic methods and are amenable to the usual characterization techniques. The recent commercial availability of a wide range of simple monomers on a multigram scale will help to advance research in the area more rapidly.

The use of POSS polyhedra as models for silica surfaces or as secondary building units in inorganic materials such as zeolites or other porous solids is likely to increase rapidly as more is understood about the mechanisms by which the polyhedra may be constructed. It will be of particular interest to see if the larger structures such as $T_{60}H_{60}$ or $T_{240}H_{240}$ or their derivatives (Section VII.C) and analogous to carbon structures such as C_{60} or nanotubes, can be prepared.

ABBREVIATIONS

AIBN	azobisisobutyronitrile
9-BBN	9-boracyclo[3.3.1]nonane

B3LYP	Becke's three-parameter hybrid exchange and the nonlocal correction functional of Lee, Yang, and Parr
CCDC	Cambridge Crystallographic Data Centre
COD	cyclooctadiene
Cp [*]	pentamethylcyclopentadienyl
Cp	cyclopentadienyl
CP/MAS	cross-polarisation magic angle spinning
CTR	Charge transfer reactive
CVD	chemical vapor deposition
dba	dibenzylidene acetate
DCC	dicyclohexylcarbodiimide
DFT	density functional theory
DMF	dimethylformamide
DMPI	1,1-dimethylpiperidinium
DMSO	dimethylsulfoxide
dvs	divinyltetramethyldisiloxane
EDA	ethylene diamine
Fc	ferrocenyl, C ₅ H ₄ FeC ₅ H ₅
GAMESS	general atomic and molecular electronic structure system
GGA	generalized gradient approximation
HF	Hartree–Fock
HOMO	highest occupied molecular orbital
LDA PP	local density approximation pseudo-potential
LUMO	lowest unoccupied molecular orbital
MALDI-TOF	matrix-assisted laser desorption ionization time of flight
<i>m</i> -CPBA	<i>meta</i> -chloroperbenzoic acid
MM	molecular mechanics
MP2	second-order Møller–Plesset perturbation theory
MWNTs	multi-walled carbon nanotubes
OLED	organic light emitting diode
POSS	polyhedral oligosilsesquioxanes
PP-PW	pseudo-potential plane wave
Sixantphos	4,6-bis(diphenylphosphino)-10,10-dimethylphenoxasilin
STM	scanning tunneling microscopy
SWNTs	single-walled carbon nanotubes
TBAF	tetrabutylammonium fluoride
THF	tetrahydrofuran
TMP	1,1,4,4-tetramethylpiperazinium
UFF	universal force field

ACKNOWLEDGMENTS

Franck Rataboul thanks the UK Energy Research Center for funding. We would also like to thank Prof. C. McCabe, Prof. F. T. Edelmann, and Prof. P. G. Harrison for supplying information, and Mr. S. Gazard for helpful discussions.

REFERENCES

- (1) Scott, D. W. *J. Am. Chem. Soc.* **1946**, 68, 356.
- (2) (a) Buff, H.; Wohler, F. *Ann. Chem. Pharm.* **1857**, 104, 94. (b) Friedel, C.; Ladenburg, A. *Ann. Chem. Phys.* **1871**, 23, 430. (c) Ladenburg, A. *Ber. Dtsch. Chem. Ges.* **1873**, 6, 379. (d) Gatterman, L. *Ber. Dtsch. Chem. Ges.* **1889**, 22, 186. (e) Stock, A.; Zeidler, F. *Ber. Dtsch. Chem. Ges.* **1923**, 56, 986.
- (3) (a) Meads, J. A.; Kipping, F. S. *J. Chem. Soc. Trans.* **1914**, 105, 679. (b) Palmer, K. W.; Kipping, F. S. *J. Chem. Soc.* **1930**, 1020.
- (4) Barry, A. J.; Gilkey, J. W. US Patent 2465188, **1949**.
- (5) Barry, A. J.; Daudt, W. H.; Domicone, J. J.; Gilkey, J. W. *J. Am. Chem. Soc.* **1955**, 77, 4248.
- (6) Brown, J. F.; Vogt, L. H. Jr. *J. Am. Chem. Soc.* **1965**, 87, 4313.
- (7) Brown, J. F. Jr. *J. Am. Chem. Soc.* **1965**, 87, 4317.
- (8) For a review see: Baney, R. H.; Itoh, M.; Sakakibara, A.; Suzuki, T. *Chem. Rev.* **1995**, 95, 1409.
- (9) Feher, F. J.; Budzichowski, T. A. *Polyhedron* **1995**, 14, 3239.
- (10) (a) Lorenz, V.; Fischer, A.; Gießmann, S.; Gilje, J. W.; Gun'ko, Y.; Jacob, K.; Edelmann, F. T. *Coord. Chem. Rev.* **2000**, 206–207, 321. (b) Pescarmona, P. P.; Maschmeyer, T. *Aust. J. Chem.* **2001**, 54, 583. (c) Duchateau, R. *Chem. Rev.* **2002**, 102, 3525. (d) Edelmann, F. T. In: Jutzi, P.; Schubert, U. (Eds.), *Silicon Chemistry*, Wiley-VCH, Weinheim, **2003**; p. 383. (e) Lorenz, V.; Gießmann, S.; Gun'ko, Y. K.; Fischer, A. K.; Gilje, J. W.; Edelmann, F. T. *Angew. Chem. Int. Ed.* **2004**, 43, 4603. (f) Hanssen, R. W. J. M.; van Santen, R. A.; Abbenhuis, H. C. L. *Eur. J. Inorg. Chem.* **2004**, 675. (g) Lorenz, V.; Edelmann, F. T. *Adv. Organomet. Chem.* **2005**, 53, 101.
- (11) Voronkov, M. G.; Lavrent'yev, V. I. *Top. Curr. Chem.* **1982**, 102, 199.
- (12) Registered trademark #2,548,048 of Hybrid Plastics Inc. <http://www.hybridplastics.com/>. Hybrid Plastics supply a wide range of POSS products.
- (13) (a) Lichtenhan, J. D. *Comments Inorg. Chem.* **1995**, 17, 115. (b) Provatas, A.; Matison, J. G. *Trends Polym. Sci.* **1997**, 5, 327. (c) Schwab, J. J.; Lichtenhan, J. D. *Appl. Organomet. Chem.* **1998**, 12, 707. (d) Li, G.; Wang, L.; Ni, H.; Pittman, C. U. Jr. *J. Inorg. Organomet. Polym.* **2002**, 11, 123. (e) Pittman, C. U. Jr.; Li, G.-Z.; Ni, H. *Macromol. Symp.* **2003**, 196, 301. (f) Phillips, S. H.; Haddad, T. S.; Tomczak, S. J. *Curr. Opin. Solid State Mater. Sci.* **2004**, 8, 21. (g) Joshi, M.; Butola, B. S. *J. Macromol. Sci. Polym. Rev.* **2004**, C44, 389. (h) Li, G.; Pittman, C. U. Jr. *Macromolecules Containing Metal and Metal-Like Elements*, **2005**, 4(Group IVA Polymers), 79; (i) Laine, R. M. J. *Mater. Chem.* **2005**, 15, 3725. (j) Kannan, R. Y.; Salacinski, H. J.; Butler, P. E.; Seifalian, A. M. *Acc. Chem. Res.* **2005**, 38, 879. (k) Bourbigot, S.; Duquesne, S.; Jama, C. *Macromol. Symp.* **2006**, 233, 180.
- (14) McCabe, C.; Glotzer, S. C.; Kieffer, J.; Neurock, M.; Cummings, P. T. *J. Comp. Theor. Nanosci.* **2004**, 1, 265.
- (15) Sohn, H.; Tan, R. P.; Powell, D. R.; West, R. *Organometallics* **1994**, 13, 1390.
- (16) Nagase, S.; Kudo, T.; Kurakake, T. *J. Chem. Soc. Chem. Commun.* **1988**, 1063.
- (17) (a) Lickiss, P. D. *Adv. Inorg. Chem.* **1995**, 42, 147. (b) Lickiss, P. D. In: Rappoport, Z.; Apeloig, Y. (Eds.), *The Chemistry of Organic Silicon Compounds*, Wiley, Chichester, **2001**; Vol. 3, p. 695.
- (18) Unno, M.; Alias, S. B.; Saito, H.; Matsumoto, H. *Organometallics* **1996**, 15, 2413.
- (19) Wiberg, E.; Simmler, W. Z. *Anorg. Allg. Chem.* **1955**, 282, 330.
- (20) Winkhofer, N.; Roesky, H. W.; Noltemeyer, M.; Robinson, W. T. *Angew. Chem. Int. Ed. Engl.* **1992**, 31, 599.
- (21) Lickiss, P. D.; Litster, S. A.; Redhouse, A. D.; Wisener, C. A. *J. Chem. Soc. Chem. Commun.* **1991**, 173.
- (22) Rebrov, E. A.; Tebenva, N. A.; Mouzafarov, A. M.; Ovchinnikov, Yu. E.; Struchkov, Yu. T.; Strelkova, T. V. *Russ. Chem. Bull.* **1995**, 44, 1332.
- (23) Forstner, J. A.; Muetterties, E. L. *Inorg. Chem.* **1966**, 5, 552.
- (24) van Almsick, T.; Kromm, A.; Sheldrick, W. S. Z. *Anorg. Allg. Chem.* **2005**, 631, 19.
- (25) Pereira, A. G.; Porto, A. O.; Silva, G. G.; de Lima, G. M.; Siebald, H. G. L.; Neto, J. L. *Phys. Chem. Chem. Phys.* **2002**, 4, 4528.
- (26) Wraage, K.; Pape, T.; Herbst-Irmer, R.; Noltemeyer, M.; Schmidt, H.-G.; Roesky, H. W. *Eur. J. Inorg. Chem.* **1999**, 869.
- (27) Rattay, M.; Jutzi, P.; Fenske, D. In: Auner, N.; Weis, J. (Eds.), *Organosilicon Chemistry IV: From Molecules to Materials*, Wiley-VCH, Weinheim, **2000**; p. 526.
- (28) Jug, K.; Wichmann, D. *Theochem* **1997**, 398–399, 365.

- (29) Rinse, J. US 3177238, **1965**, CA **1965**, 63, 2978.
- (30) Timoshkin, A. Y. *Proc. Electrochem. Soc.* **2001**, 12, 262.
- (31) Moravetski, V.; Hill, J.-R.; Eichler, U.; Cheetham, A. K.; Sauer, J. *J. Am. Chem. Soc.* **1996**, 118, 13015.
- (32) Kinrade, S. D.; Swaddle, T. W. *J. Am. Chem. Soc.* **1986**, 108, 7159.
- (33) (a) Xu, C.; Wang, W.; Zhang, W.; Zhuang, J.; Liu, L.; Kong, Q.; Zhao, L.; Long, Y.; Fan, K.; Qian, S.; Li, Y. *J. Phys. Chem. A* **2000**, 104, 9518. (b) Kong, Q.; Zhao, L.; Wang, W.; Wang, C.; Xu, C.; Zhang, W.; Liu, L.; Fan, K.; Li, Y.; Zhuang, J. *J. Comp. Chem.* **2005**, 26, 584.
- (34) Kaftory, M.; Kapon, M.; Botoshansky, M. In: Rappoport, Z.; Apeloig, Y. (Eds.), *The Chemistry of Organic Silicon Compounds*, Wiley, Chichester, **1998**; Vol. 2, p. 181.
- (35) Jansen, M.; Moebs, M. *Inorg. Chem.* **1984**, 23, 4486.
- (36) Jansen, M.; L  r, B. Z. *Kristallogr.* **1986**, 177, 149.
- (37) Xiang, K.-H.; Pandey, R.; Pernisz, U. C.; Freeman, C. *J. Phys. Chem. B* **1998**, 102, 8704.
- (38) Earley, C. W. *J. Phys. Chem.* **1994**, 98, 8693.
- (39) Franco, R.; Kandalam, A. K.; Pandey, R.; Pernisz, U. C. *J. Phys. Chem. B* **2002**, 106, 1709.
- (40) Wiebcke, M.; Felsche, J. *Microporous Mesoporous Mater.* **2001**, 43, 289.
- (41) Jolcart, G.; Leblanc, M.; Morel, B.; Dehaudt, Ph.; Dubois, S. *Eur. J. Sol. St. Inorg. Chem.* **1996**, 33, 647.
- (42) Haile, S. M.; Maier, J.; Wuensch, B. J.; Laudise, R. A. *Acta Crystallogr. B* **1995**, 51, 673.
- (43) Smolin, Yu. I. *J. Chem. Soc. Chem. Commun.* **1969**, 395.
- (44) Behbehani, H.; Brisdon, B. J.; Mahon, M. F.; Molloy, K. C. *J. Organomet. Chem.* **1994**, 469, 19.
- (45) Sprung, M. M.; Guenther, F. O. *J. Am. Chem. Soc.* **1955**, 77, 3990.
- (46) Sprung, M. M.; Guenther, F. O. *J. Am. Chem. Soc.* **1955**, 77, 3996.
- (47) Andrianov, K. A.; Izmailov, B. A. *Russ. J. Gen. Chem.* **1966**, 36, 350.
- (48) Andrianov, K. A.; Izmailov, B. A. *Russ. J. Gen. Chem.* **1976**, 46, 328.
- (49) Unno, M.; Imai, Y.; Matsumoto, H. *Silicon Chem.* **2003**, 2, 175.
- (50) Unno, M.; Suto, A.; Takada, K.; Matsumoto, H. *Bull. Chem. Soc. Jpn.* **2000**, 73, 215.
- (51) Bassindale, A. R.; MacKinnon, I. A.; Maesano, M. G.; Taylor, P. G. *Chem. Commun.* **2003**, 1382.
- (52) (a) Hoebbel, D.; Engelhardt, G.; Samoson, A.;   jsz  szi, K.; Smolin, Yu. I. *Z. Anorg. Allg. Chem.* **1987**, 552, 236. (b) Weidner, R.; Zeller, N.; Deubzer, B.; Frey, V. US Patent 5047492, **1991**; (c) Harrison, P. G.; Kannengiesser, R.; Hall, C. J. *Main Group. Met. Chem.* **1997**, 20, 137.
- (53) Gejji, S. P.; Hermansson, K.; Lindgren, J. *J. Phys. Chem.* **1994**, 98, 8687.
- (54) Williams, E. A. In: Patai, S.; Rappoport, Z. (Eds.), *The Chemistry of Organic Silicon Compounds*, Wiley, Chichester, **1989**; p. 511.
- (55) Hasegawa, I.; Sakka, S. In: Occelli, M. L.; Robson, H. E. (Eds.), *Zeolite Synthesis (ACS Symposium Series 398)*, ACS, Washington, DC, **1989**; p. 140.
- (56) Hoebbel, D.; Garz  , G.; Engelhardt, G.; Ebert, R.; Lippmaa, E.; Alla, M. Z. *Anorg. Allg. Chem.* **1980**, 465, 15.
- (57) Pescarmona, P. P.; Van der Wall, J. C.; Maschmeyer, T. *Eur. J. Inorg. Chem.* **2004**, 978.
- (58) Feher, F. J.; Neuman, D. A.; Walzer, J. F. *J. Am. Chem. Soc.* **1989**, 111, 1741.
- (59) Ossadnik, C.; Vepřek, S.; Marsmann, H. C.; Rikowski, E. *Monatsh. Chem.* **1999**, 130, 55.
- (60) Shen, J.; Cheng, W.-D.; Wu, D.-S.; Li, X.-D.; Lan, Y.-Z.; Gong, Y.-J.; Li, F.-F.; Huang, S.-P. *J. Chem. Phys.* **2005**, 122, 204709.
- (61) (a) Feher, F. J.; Terroba, R.; Jin, R.-Z. *J. Chem. Soc. Chem. Commun.* **1999**, 2513. (b) Feher, F. J.; Terroba, R.; Jin, R.-Z.; Wyndham, K. D.; L  cke, S.; Brutchey, R.; Nguyen, F. *Polym. Mater. Sci. Eng.* **2000**, 82, 301.
- (62) Bassindale, A. R.; Liu, Z.; Parker, D. J.; Taylor, P. G.; Horton, P. N.; Hursthouse, M. B.; Light, M. E. *J. Organomet. Chem.* **2003**, 687, 1.
- (63) (a) Garz  , G.; Vargha, A.; Sz  kely, T.; Hoebbel, D. *J. Chem. Soc. Dalton Trans.* **1980**, 2068. (b) Garz  , G.; Hoebbel, D.; Vargha, A.; Ujs  szi, K. *J. Chem. Soc., Dalton Trans.* **1984**, 1857.
- (64) Harrison, P. G.; Kannengiesser, R. *Chem. Commun.* **1996**, 415.
- (65) Haile, S. M.; Wuensch, B. J.; Siegrist, T.; Laudise, R. A. *Solid State Ionics* **1992**, 53–56, 1292.
- (66) Smolin, Y. I.; Shepelev, Y. F.; Hobb  l, D. *Kristallografiya* **1994**, 39, 558.
- (67) Agaskar, P. A. *Inorg. Chem.* **1991**, 30, 2707.
- (68) B  rgy, H.; Calzaferri, G. *J. Chromatogr.* **1990**, 507, 481.
- (69) (a) Kudo, T.; Gordon, M. S. *J. Am. Chem. Soc.* **1998**, 120, 11432. (b) Kudo, T.; Gordon, M. S. *J. Phys. Chem. A* **2000**, 104, 4058.

- (70) Kudo, T.; Machida, K.; Gordon, M. S. *J. Phys. Chem. A* **2005**, *109*, 5424.
- (71) (a) Ribeiro-Claro, P. J. A.; Amado, A. M. *Theochem* **2000**, 528, 19. (b) Hillson, S. D.; Smith, E.; Zeldin, M.; Parish, C. A. *J. Phys. Chem. A* **2005**, *109*, 8371.
- (72) (a) Bürgy, H.; Calzaferri, G. *Helv. Chim. Acta* **1990**, *73*, 698. (b) Marcolli, C.; Lainé, P.; Bühler, R.; Calzaferri, G.; Tomkinson, J. *J. Phys. Chem. B* **1997**, *101*, 1171.
- (73) Müller, R.; Kohne, R.; Sliwinski, S. *J. Prakt. Chem.* **1959**, *9*, 71.
- (74) Frye, C. L.; Collins, W. T. *J. Am. Chem. Soc.* **1970**, *92*, 5586.
- (75) Tsuchida, A.; Bolln, C.; Sernetz, F. G.; Frey, H.; Mülhaupt, R. *Macromolecules* **1997**, *30*, 2818.
- (76) (a) Bornhauser, P.; Calzaferri, G. *Spectrochim. Acta [A]* **1990**, *46*, 1045. (b) Bärtsch, M.; Calzaferri, G.; Marcolli, C. *Res. Chem. Intermed.* **1995**, *21*, 577.
- (77) Bärtsch, M.; Bornhauser, P.; Calzaferri, G.; Imhof, R. *J. Phys. Chem.* **1994**, *98*, 2817.
- (78) Harrison, P. G.; Hall, C. *Main Group Met. Chem.* **1997**, *20*, 515.
- (79) Chomel, A. D.; Jayasooriya, U. A.; Babonneau, F. *Spectrochim. Acta [A]* **2004**, *60*, 1609.
- (80) Bärtsch, M.; Bornhauser, P.; Calzaferri, G.; Imhof, R. *Vib. Spectrosc.* **1995**, *8*, 305.
- (81) Larsson, K. *Ark. Kemi* **1960**, *16*, 215.
- (82) Auf der Heyde, T. P. E.; Bürgy, H. B.; Tönroos, K. W. *Chimia* **1991**, *45*, 38.
- (83) Törnroos, K. W. *Acta Crystallogr. C* **1994**, *50*, 1646.
- (84) Shieh, D.-L.; Chen, F.-C.; Lin, J.-L. *Appl. Surf. Sci.* **2006**, *252*, 2171.
- (85) Chen, Y.; Schneider, K. S.; Banaszak Holl, M. M.; Orr, B. G. *Phys. Rev. B* **2004**, *70*, 085402.
- (86) Greeley, J. N.; Meeuwenberg, L. M.; Banaszak Holl, M. M. *J. Am. Chem. Soc.* **1998**, *120*, 7776.
- (87) (a) Banaszak Holl, M. M.; McFeely, R. R. *Phys. Rev. Lett.* **1993**, *71*, 2441. (b) Lee, S.; Makan, S.; Banaszak Holl, M. M.; McFeely, F. R. *J. Am. Chem. Soc.* **1994**, *116*, 11819.
- (88) (a) Nicholson, K. T.; Zhang, K. Z.; Banaszak Holl, M. M. *J. Am. Chem. Soc.* **1999**, *121*, 3232. (b) Nicholson, K. T.; Zhang, K. Z.; Banaszak Holl, M. M.; McFeely, F. R.; Pernisz, U. C. *Langmuir* **2000**, *16*, 8396. (c) Schneider, K. S.; Nicholson, K. T.; Fosnacht, D. R.; Orr, B. G.; Banaszak Holl, M. M. *Langmuir* **2002**, *18*, 8116. (d) Schneider, K. S.; Nicholson, K. T.; Fosnacht, D. R.; Orr, B. G.; Banaszak Holl, M. M. *Langmuir* **2004**, *20*, 2250.
- (89) See for example: (a) Earley, C. W. *Inorg. Chem.* **1992**, *31*, 1250. (b) Xiang, K.-H.; Pandey, R.; Pernisz, U.; Freeman, C. *J. Phys. Chem.* **1994**, *98*, 1238. (c) Pasquarello, A.; Hybertsen, M. S.; Car, R. *Phys. Rev. B* **1996**, *54*, R2339. (d) Wichmann, D.; Jug, K. *J. Phys. Chem. B* **1999**, *103*, 10087. (e) Mattori, M.; Mogi, K.; Sakai, Y.; Isobe, T. *J. Phys. Chem. A* **2000**, *104*, 10868. (f) Lin, T.; He, C.; Xiao, Y. *J. Phys. Chem. B* **2003**, *107*, 13788. (g) Päch, M.; Macrae, R. M.; Carmichael, I. *J. Am. Chem. Soc.* **2006**, *128*, 6111.
- (90) Uzunova, E. L.; St. Nikolov, G. *J. Phys. Chem. B* **2000**, *104*, 7299.
- (91) Hagelberg, F.; Hossain, D.; Pittman, C. U.; Saebo, S. *J. Phys. Chem. A* **2004**, *108*, 11260.
- (92) Ionescu, T. C.; Qi, F.; McCabe, C.; Striolo, A.; Kieffer, J.; Cummings, P. T. *J. Phys. Chem. B* **2006**, *110*, 2502.
- (93) Azinović, D.; Cai, J.; Eggs, C.; König, H.; Marsmann, H. C.; Vepřek, S. *J. Lumin.* **2002**, *97*, 40.
- (94) Calzaferri, G.; Hoffmann, R. *J. Chem. Soc., Dalton Trans.* **1991**, 917.
- (95) (a) Striolo, A.; McCabe, C.; Cummings, P. T. *Macromolecules* **2005**, *38*, 8950. (b) Striolo, A.; McCabe, C.; Cummings, P. T. *J. Phys. Chem. B* **2005**, *109*, 14300.
- (96) Fina, A.; Tabuani, D.; Carniato, F.; Frache, A.; Boccaleri, E.; Camino, G. *Thermochim. Acta* **2006**, *440*, 36.
- (97) Falkenhagen, J.; Jancke, H.; Krüger, R.-P.; Rikowski, E.; Schulz, G. *Rapid. Commun. Mass Spectrom.* **2003**, *17*, 285.
- (98) Day, V. W.; Klemperer, W. G.; Mainz, V. V.; Millar, D. M. *J. Am. Chem. Soc.* **1985**, *107*, 8262.
- (99) Harrison, P. G.; Kannengiesser, R. *J. Chem. Soc., Chem. Commun.* **1995**, 2065.
- (100) Bassindale, A. R.; Liu, Z.; MacKinnon, I. A.; Taylor, P. G.; Yang, Y.; Light, M. E.; Horton, P. N.; Hursthouse, M. B. *Dalton. Trans.* **2003**, 2945.
- (101) Olsson, K. *Ark. Kemi* **1958**, *13*, 367.
- (102) Kramer, T.; Schweins, R.; Huber, K. *Macromolecules* **2005**, *38*, 151.
- (103) Rikowski, E.; Marsmann, H. C. *Polyhedron* **1997**, *16*, 3357.
- (104) Bolln, C.; Tsuchida, A.; Frey, H.; Mülhaupt, R. *Chem. Mater.* **1997**, *9*, 1475.
- (105) Herren, D.; Bürgy, H.; Calzaferri, G. *Helv. Chim. Acta* **1991**, *74*, 24.
- (106) Bassindale, A. R.; Gentle, T. E. *J. Mater. Chem.* **1993**, *3*, 1319.

- (107) Dare, E. O.; Olatunji, G. A.; Ogunniyi, D. S. *Pol. J. Chem.* **2005**, 79, 101.
- (108) Dittmar, U.; Hendan, B. J.; Flörke, U.; Marsmann, H. C. *J. Organomet. Chem.* **1995**, 489, 185.
- (109) Bassindale, A. R.; Gentle, T. J. *Organomet. Chem.* **1996**, 521, 391.
- (110) Eaborn, C. *Organosilicon Compounds*, Butterworths Scientific, London, **1960**.
- (111) Said, M. A.; Roesky, H. W.; Rennekamp, C.; Andruh, M.; Schmidt, H.-G.; Noltemeyer, M. *Angew. Chem. Int. Ed.* **1999**, 38, 661.
- (112) Joshi, M.; Butola, B. S. *Polymer* **2004**, 45, 4953.
- (113) Kim, K.-M.; Chujo, Y. *Polym. Bull.* **2001**, 46, 15.
- (114) Feher, F. J.; Terroba, R.; Ziller, J. W. *Chem. Commun.* **1999**, 2309.
- (115) Crivello, J. V.; Malik, R. J. *Polym. Sci. A* **1997**, 35, 407.
- (116) Constantopoulos, K.; Clarke, D.; Markovic, E.; Uhrig, D.; Clarke, S.; Matisons, J. G.; Simon, G. *Polym. Prepr.* **2004**, 45, 668.
- (117) Provatas, A.; Luft, M.; Mu, J. C.; White, A. H.; Matisons, J. G.; Skelton, B. W. *J. Organomet. Chem.* **1998**, 565, 159.
- (118) Liu, L.-K.; Dare, E. O. *J. Chin. Chem. Soc.* **2004**, 51, 175.
- (119) Rattay, M.; Fenske, D.; Jutzi, P. *Organometallics* **1998**, 17, 2930.
- (120) Brevett, C. S.; Cagle, P. C.; Klemperer, W. G.; Millar, D. M.; Ruben, G. C. *J. Inorg. Organomet. Polym.* **1991**, 1, 335.
- (121) Maitland, J. Jr. Private communication 1996, cited in Marcolli, C.; Calzaferri, G. *Appl. Organomet. Chem.* **1999**, 13, 213.
- (122) Feher, F. J.; Weller, K. *Inorg. Chem.* **1991**, 30, 880.
- (123) Päch, M.; Stösser, R. *J. Phys. Chem. A* **1997**, 101, 8360.
- (124) Agaskar, P. A. *Synth. React. Inorg. Met-Org. Chem.* **1990**, 20, 483.
- (125) Clark, J. C.; Saengerkerdsub, S.; Eldridge, G. T.; Campana, C.; Barnes, C. E. *J. Organomet. Chem.* **2006**, 691, 3213.
- (126) (a) Calzaferri, G. *Nachr. Chem. Tech. Lab.* **1992**, 40, 1111. (b) Calzaferri, G. In: Corriu, R.; Jutzi, P. (Eds.), *Tailor-Made Silicon-Oxygen Compounds: From Molecules to Materials*, Vieweg, Wiesbaden, **1996**; p. 149.
- (127) Calzaferri, G.; Imhof, R. *J. Chem. Soc. Dalton Trans.* **1992**, 3391.
- (128) Sellinger, A.; Laine, R. M. *Chem. Mater.* **1996**, 8, 1592.
- (129) Auner, N.; Bats, J. W.; Katsoulis, D. E.; Suto, M.; Tecklenburg, R. E.; Zank, G. A. *Chem. Mater.* **2000**, 12, 3402.
- (130) Calzaferri, G.; Imhof, R.; Törnroos, K. W. *J. Chem. Soc. Dalton Trans.* **1994**, 3123.
- (131) Calzaferri, G.; Marcolli, C.; Imhof, R.; Törnroos, K. W. *J. Chem. Soc. Dalton Trans.* **1996**, 3313.
- (132) Calzaferri, G.; Imhof, R.; Törnroos, K. W. *J. Chem. Soc. Dalton Trans.* **1993**, 3741.
- (133) Zhang, C.; Babonneau, F.; Bonhomme, C.; Laine, R. M.; Soles, C. L.; Hristov, H. A.; Yee, A. F. *J. Am. Chem. Soc.* **1998**, 120, 8380.
- (134) Wang, J.; Kuimova, M. K.; Poliakov, M.; Briggs, G. A. D.; Khlobystov, A. N. *Angew. Chem. Int. Ed.* **2006**, 45, 5188.
- (135) Nyman, M. D.; Desu, S. B.; Peng, C. H. *Chem. Mater.* **1993**, 5, 1636.
- (136) Desu, S. B.; Peng, C. H.; Shi, T.; Agaskar, P. A. *J. Electrochem. Soc.* **1992**, 139, 2682.
- (137) Greeley, J. N.; Lee, S.; Banaszak Holl, M. M. *Appl. Organomet. Chem.* **1999**, 13, 279.
- (138) Nicholson, K. T.; Zhang, K. Z.; Banaszak Holl, M. M.; McFeely, F. R. *J. Appl. Phys.* **2002**, 91, 9043.
- (139) Eng, J. Jr.; Raghavachari, K.; Struck, L. M.; Chabal, Y. J.; Bent, B. E.; Banaszak-Holl, M. M.; McFeely, F. R.; Michaels, A. M.; Flynn, G. W.; Christman, S. B.; Chaban, E. E.; Williams, G. P.; Radermacher, K.; Mantl, S. *J. Chem. Phys.* **1998**, 108, 8680.
- (140) Tejerina, B.; Gordon, M. S. *J. Phys. Chem. B* **2002**, 106, 11764.
- (141) See for example: (a) George, A. R.; Catlow, C. R. A. *Chem. Phys. Lett.* **1995**, 247, 408. (b) Tossell, J. A. *J. Phys. Chem. A* **1998**, 102, 3368.
- (142) Dinse, K.-P. *Phys. Chem. Chem. Phys.* **2002**, 4, 5442.
- (143) Bassindale, A. R.; Pourny, M.; Taylor, P. G.; Hursthouse, M. B.; Light, M. E. *Angew. Chem. Int. Ed.* **2003**, 42, 3488.
- (144) Takahashi, K.; Sulaiman, S.; Katzenstein, J. M.; Snoblen, S.; Laine, R. M. *Aust. J. Chem.* **2006**, 59, 564.

- (145) Dare, E. O.; Liu, L.-K.; Peng, J. *Dalton Trans.* **2006**, 3668.
- (146) Brown, J. F. Jr.; Vogt, L. H.; Prescott, P. I. *J. Am. Chem. Soc.* **1964**, 86, 1120.
- (147) Du, J.-K.; Yang, R.-J. *Jingxi Huagong* **2005**, 22, 409. CAN 144:293211.
- (148) Kim, S. G.; Choi, J.; Tamaki, R.; Laine, R. M. *Polymer* **2005**, 46, 4514.
- (149) Krishnan, P. S. G.; He, C. J. *Polym. Sci. A* **2005**, 43, 2483.
- (150) Pakjamsai, C.; Kawakami, Y. *Design. Monom. Polym.* **2005**, 8, 423.
- (151) Bykova, T. A.; Lebedev, B. V. *Russ. J. Gen. Chem.* **2003**, 73, 1077.
- (152) Ni, Y.; Zheng, S. *Chem. Mater.* **2004**, 16, 5141.
- (153) Brown, J. F.; Prescott, P. I. *J. Am. Chem. Soc.* **1964**, 86, 1402.
- (154) Kolesov, B. A.; Martynova, T. N.; Chupakhina, T. I. *J. Struct. Chem.* **1989**, 29, 888.
- (155) Hossain, M. A.; Hursthouse, M. B.; Malik, K. M. A. *Acta Crystallogr. B* **1979**, 35, 2258.
- (156) Shklover, V. E.; Struchkov, Yu. T.; Makarova, N. N.; Andrianov, K. A. *J. Struct. Chem.* **1978**, 19, 944.
- (157) Larsson, K. *Ark. Kemi* **1960**, 16, 209.
- (158) Gidden, J.; Kemper, P. R.; Shammel, E.; Fee, D. P.; Anderson, S.; Bowers, M. T. *Int. J. Mass Spectrom.* **2003**, 222, 63.
- (159) Olsson, K.; Gröwall, C. *Ark. Kemi* **1961**, 17, 529.
- (160) Tamaki, R.; Tanaka, Y.; Asuncion, M. Z.; Choi, J.; Laine, R. M. *J. Am. Chem. Soc.* **2001**, 123, 12416.
- (161) Ni, Y.; Zheng, S.; Nie, K. *Polymer* **2004**, 45, 5557.
- (162) Huang, J.-C.; He, C.-B.; Xiao, Y.; Mya, K. Y.; Dai, J.; Siow, Y. P. *Polymer* **2003**, 44, 4491.
- (163) Chen, H.-J. *Chem. Res. Chin. Univ.* **2004**, 20, 42.
- (164) He, C.; Xiao, Y.; Huang, J.; Lin, T.; Mya, K. Y.; Zhang, X. J. *Am. Chem. Soc.* **2004**, 126, 7792.
- (165) Brick, C. M.; Tamaki, R.; Kim, S.-G.; Asuncion, M. Z.; Roll, M.; Nemoto, T.; Ouchi, Y.; Chujo, Y.; Laine, R. M. *Macromolecules* **2005**, 38, 4655.
- (166) Feher, F. J.; Budzichowski, T. A. *J. Organomet. Chem.* **1989**, 373, 153.
- (167) Ovchinnikov, Yu. E.; Shklover, V. E.; Struchkov, Yu. T.; Levitsky, M. M.; Zhdanov, A. A. *J. Organomet. Chem.* **1988**, 347, 253.
- (168) Kaganovich, V. S.; Rybinskaya, M. I.; Zhdanov, A. A.; Levitskii, M. M.; Lavrukhin, B. D. *Bull. Acad. Sci. USSR* **1987**, 1911.
- (169) Zhao, Y.; Schiraldi, D. A. *Polymer* **2005**, 46, 11640.
- (170) Dodiuk, H.; Kenig, S.; Blinsky, I.; Dotan, A.; Buchman, A. *Int. J. Adhes. Adhes.* **2004**, volume date 2005, 25: 211.
- (171) Codina, A.; Bassindale, A.; Murray, C.; Taylor, P. *Polym. Prepr.* **2004**, 45, 654.
- (172) Bassindale, A. R.; Parker, D. J.; Pourny, M.; Taylor, P. G.; Horton, P. N.; Hursthouse, M. B. *Organometallics* **2004**, 23, 4400.
- (173) Gao, J.-G.; Wang, S.-C.; Zhang, X.-J.; Run, M.-T. *Youjigui Cailiao* **2005**, 19, 5. CAN 145:167319.
- (174) Andrianov, K. A.; Petrovnina, N. M.; Vasil'eva, T. V.; Shklover, V. E.; D'yachenko, B. I. *Russ. J. Gen. Chem.* **1978**, 48, 2442.
- (175) Bonhomme, C.; Tolédano, P.; Maquet, J.; Livage, J.; Bonhomme-Courty, L. *J. Chem. Soc. Dalton. Trans.* **1997**, 1617.
- (176) Kovrigin, V. M.; Lavrent'ev, V. I. *Russ. J. Gen. Chem.* **1989**, 59, 332.
- (177) Gorsh, L.É.; Shubin, A. A.; Nekipelov, V. M.; Kanev, A. N. *J. Struct. Chem.* **1982**, 23, 345.
- (178) Yan, F.; Lu, B.-Z.; Hu, G.-F.; Guo, C.; Xu, J.-H. *Bopuxue Zazhi (Chinese J. Mag. Res.)* **2004**, 21, 57. CAN 141:190845.
- (179) (a) Panich, A. M.; Kozlova, S. G.; Berezovskii, G. A.; Gorsh, L. E. *J. Struct. Chem.* **1985**, 26, 639.
(b) Bonhomme, C.; Coelho, C.; Azaïs, T.; Bonhomme-Courty, L.; Babonneau, F.; Maquet, J.; Thouvenout, R. C. R. *Chimie* **2006**, 9, 466.
- (180) Bakhtiar, R.; Feher, F. J. *Rapid. Commun. Mass Spectrom.* **1999**, 13, 687.
- (181) Bakhtiar, R. *Rapid Commun. Mass Spectrom.* **1999**, 13, 87.
- (182) Baidina, I. A.; Podbereskaya, N. V.; Alekseev, V. I.; Martynova, T. N.; Borisov, S. V.; Kanev, A. N. *J. Struct. Chem.* **1980**, 20, 550.
- (183) Gromilov, S. A.; Prokhorova, S. A.; Baidina, I. A. *J. Struct. Chem.* **1996**, 37, 786.
- (184) Zhang, X.; Hu, L.; Huang, Y.; Sun, D.; Sun, Y. *Sci. China, Ser. B* **2004**, 47, 388.
- (185) Baker, E. S.; Gidden, J.; Anderson, S. E.; Haddad, T. S.; Bowers, M. T. *Nano Lett.* **2004**, 4, 779.

- (186) Marciniak, B.; Pietraszuk, C. *Curr. Org. Chem.* **2003**, *7*, 691.
- (187) Feher, F. J.; Soulivong, D.; Eklund, A. G.; Wyndham, K. D. *Chem. Commun.* **1997**, 1185.
- (188) Itami, Y.; Marciniak, B.; Kubicki, M. *Chem. Eur. J.* **2004**, *10*, 1239.
- (189) (a) Gao, Y.; Eguchi, A.; Kakehi, K.; Lee, Y. C. *Org. Lett.* **2004**, *6*, 3457. (b) Koenig, H. J.; Marsmann, H. C.; Letzel, M. C. In: Auner, N.; Weis, J. (Eds.), *Organosilicon Chemistry V: From Molecules to Materials*, Wiley-VCH, Weinheim, **2003**; p. 425.
- (190) Zhang, X.; Haxton, K. J.; Ropartz, L.; Cole-Hamilton, D. J.; Morris, R. E. *J. Chem. Soc. Dalton Trans.* **2001**, 3261.
- (191) Ropartz, L.; Morris, R. E.; Schwarz, G. P.; Foster, D. F.; Cole-Hamilton, D. J. *Inorg. Chem. Commun.* **2000**, *3*, 714.
- (192) Jaffrès, P.-A.; Morris, R. E. *J. Chem. Soc. Dalton Trans.* **1998**, 2767.
- (193) Ropartz, L.; Foster, D. F.; Morris, R. E.; Slawin, A. M. Z.; Cole-Hamilton, D. J. *J. Chem. Soc. Dalton Trans.* **2002**, 1997.
- (194) Ropartz, L.; Morris, R. E.; Foster, D. F.; Cole-Hamilton, D. J. *J. Mol. Catal. A* **2002**, 182–183, 99.
- (195) Stengel, B. F.; Ridland, J.; Hearshaw, M.; Cole-Hamilton, D. J.; Tooze, R.; Morris, R. E. WO 2004022231, **2004**. CAN 140:271389.
- (196) Lücke, S.; Stoppek-Langner, K.; Kuchinke, J.; Krebs, B. *J. Organomet. Chem.* **1999**, 584, 11.
- (197) Martynova, T. N.; Korchkov, V. P.; Semyannikov, P. P. *Russ. J. Gen. Chem.* **1983**, *53*, 1431.
- (198) Kovrigin, V. M.; Lavrent'ev, V. I.; Sinegubova, N. V. *Russ. J. Gen. Chem.* **1987**, *57*, 995.
- (199) Poliski, G. M.; Hadda, T. S.; Blanski, R. L.; Gleason, K. K. *Thermochim. Acta* **2005**, 438, 116.
- (200) Lavrent'ev, V. I.; Moroz, T. Y. *Russ. J. Gen. Chem.* **1993**, *63*, 109.
- (201) Drylie, E. A.; Andrews, C. D.; Hearshaw, M. A.; Jimenez-Rodriguez, C.; Slawin, A.; Cole-Hamilton, D. J.; Morris, R. E. *Polyhedron* **2006**, *25*, 853.
- (202) Kovrigin, V. M.; Lavrent'ev, V. I.; Moralev, V. M. *Russ. J. Gen. Chem.* **1986**, *56*, 2049.
- (203) Dare, E. O.; Olatunji, G. A.; Oggunniyi, D. S.; Lasisi, A. A. *Pol. J. Chem.* **2005**, *79*, 109.
- (204) Manson, B. W.; Morrison, J. J.; Coupar, P. I.; Jaffrès, P.-A.; Morris, R. E. *J. Chem. Soc. Dalton Trans.* **2001**, 1123.
- (205) Coupar, P. I.; Jaffrès, P.-A.; Morris, R. E. *J. Chem. Soc. Dalton Trans.* **1999**, 2183.
- (206) Kuehnle, A.; Jost, C.; Abbenhuis, H. C. L.; Gerritsen, G. WO 2006027074, **2006**.
- (207) Zhang, C.; Laine, R. M. *J. Organomet. Chem.* **1996**, 521, 199.
- (208) Feher, F. J.; Wyndham, K. D.; Baldwin, R. K.; Soulivong, D.; Lichtenhan, J. D.; Ziller, J. W. *Chem. Commun.* **1999**, 1289.
- (209) Chupakhina, T. I.; Martynova, T. N.; Semyannikov, P. P.; Kolesov, B. A. *Bull. Acad. Sci. USSR* **1990**, 384.
- (210) (a) Harrison, P. G.; Hall, C. J. *Sol-Gel Sci. Tech.* **1998**, *13*, 391. (b) Morrison, J. J.; Love, C. J.; Manson, B. W.; Shannon, I. J.; Morris, R. E. *J. Mater. Chem.* **2002**, *12*, 3208.
- (211) Xu, H.; Yang, B.; Wang, J.; Guang, S.; Li, C. *Macromolecules* **2005**, *38*, 10455.
- (212) Sellinger, A.; Tamaki, R.; Laine, R. M.; Ueno, K.; Tanabe, H.; Williams, E.; Jabbour, G. E. *Chem. Commun.* **2005**, 3700.
- (213) Elsasser, R.; Mehl, G. H.; Goodby, J. W.; Photinos, D. J. *Chem. Commun.* **2000**, 851.
- (214) Korchkov, V. P.; Martynova, T. N.; Belyi, V. I. *Thin Solid Films* **1983**, *101*, 373.
- (215) (a) Litvin, L. V.; Gavrilova, T. A.; Plotnikov, A. E.; Gutakovskii, A. K.; Nastaushchev, Yu. V.; Assev, A. L.; Dul'tsev, F. N.; Mogilnikov, K. P.; Baklanov, M. R.; Prokhorova, S. A.; Nikulina, L. D.; Volkova, S. M.; Liskovskaya, T. I.; Danilovich, V. S.; Spangenberg, B.; Altmeyer, S. *Russ. Microelect.* **1997**, *26*, 387. (b) Schmidt, A.; Babin, S.; Boehmer, K.; Koops, H. W. P. *Microelectron. Eng.* **1997**, *35*, 129. (c) Foglietti, V.; Cianci, E.; Gianni, G. *Microelectron. Eng.* **2001**, 57–58, 807.
- (216) Lamm, M. H.; Chen, T.; Glotzer, S. C. *Nano Lett.* **2003**, *3*, 989.
- (217) Sheng, Y.-J.; Lin, W.-J.; Chen, W.-C. *J. Chem. Phys.* **2004**, *121*, 9693.
- (218) (a) Hasegawa, I.; Sakka, S.; Sugahara, Y.; Kuroda, K.; Kato, C. *J. Chem. Soc. Chem. Commun.* **1989**, 208. (b) Hasegawa, I.; Motojima, S. *J. Organomet. Chem.* **1992**, *441*, 373. (c) Choi, J.; Yee, A. F.; Laine, R. M. *Macromolecules* **2003**, *36*, 5666. (d) Hasegawa, I.; Ino, K.; Ohnishi, H. *Appl. Organomet. Chem.* **2003**, *17*, 287. (e) do Carmo, D. R.; Guinesi, L. S.; Dias Filho, N. L.; Stradiotto, N. R. *Appl. Surf. Sci.* **2004**, *235*, 449.
- (219) Hasegawa, I.; Imamura, W.; Takayama, T. *Inorg. Chem. Commun.* **2004**, *7*, 513.

- (220) Asuncion, M. Z.; Hasegawa, I.; Kampf, J. W.; Laine, R. M. *J. Mater. Chem.* **2005**, *15*, 2114.
- (221) See for example: (a) Hoebbel, D.; Vargha, A.; Fahlke, B.; Englehardt, G. Z. *Anorg. Allg. Chem.* **1985**, 521, 61. (b) Groenen, E. J. J.; Kortbeek, A. G. T. G.; Mackay, M.; Sudmeijer, O. *Zeolites* **1986**, *6*, 403. (c) Thouvenot, R.; Hervé, G.; Guth, J. L.; Wey, R. *Nouv. J. Chim.* **1986**, *10*, 479.
- (222) Frasch, J.; Lebeau, B.; Soulard, M.; Patatin, J.; Zana, R. *Langmuir* **2000**, *16*, 9049.
- (223) Hasegawa, I. *Zeolites* **1992**, *12*, 720.
- (224) Knight, C. T. G.; Thompson, A. R.; Kunwar, A. C.; Gutowsky, H. S.; Oldfield, E.; Kirkpatrick, R. J. *J. Chem. Soc. Dalton Trans.* **1989**, 275.
- (225) Kinrade, S. D.; Knight, C. T. G.; Pole, D. L.; Syvitski, R. T. *Inorg. Chem.* **1998**, *37*, 4272.
- (226) (a) Caratzoulas, S.; Vlachos, D. G.; Tsapatsis, M. *J. Phys. Chem. B* **2005**, *109*, 10429. (b) Caratzoulas, S.; Vlachos, D. G.; Tsapatsis, M. *J. Am. Chem. Soc.* **2006**, *128*, 596.
- (227) Smolin, Y. I.; Shepelev, Y. F.; Pomes, R.; Khobbel, D.; Viker, V. *Soviet Phys. Crystallogr.* **1979**, *24*, 19.
- (228) Wiebcke, M.; Emmer, J.; Felsche, J. *J. Chem. Soc. Chem. Commun.* **1993**, 1604.
- (229) You, J.-L.; Jiang, G. C.; Hou, H.-Y.; Chen, H.; Wu, Y.-Q.; Xu, K.-D. *Chin. Phys. Lett.* **2004**, *21*, 640.
- (230) (a) Tossell, J. A. *J. Phys. Chem.* **1996**, *100*, 14828. (b) Mozgawa, W.; Handke, M.; Jastrzębski, W. *J. Mol. Struct.* **2004**, *704*, 247.
- (231) (a) Hasegawa, I. *J. Sol-Gel Sci. Tech.* **1995**, *5*, 93. (b) Hasegawa, I.; Nakane, Y.; Takayama, T. *Appl. Organomet. Chem.* **1999**, *13*, 273.
- (232) Hoebbel, D.; Pitsch, I.; Grimmer, A. R.; Jancke, H.; Hiller, W.; Harris, R. K. *Z. Chem.* **1989**, *29*, 260.
- (233) Agaskar, P. A. *Inorg. Chem.* **1990**, *29*, 1603.
- (234) Hasegawa, I.; Ishida, M.; Motojima, S. *Synth. React. Inorg. Met.-Org. Chem.* **1994**, *24*, 1099.
- (235) Hoebbel, D.; Pitsch, I.; Reiher, T.; Hiller, W.; Jancke, H.; Müller, D. *Z. Anorg. Allg. Chem.* **1989**, 576, 160.
- (236) Kalmychkov, G. V.; Rakhlin, V. I.; Gostevskii, B. A.; Mirskov, R. G.; Voronkov, M. G. *Dokl. Akad. Nauk.* **1998**, 362, 359.
- (237) (a) Sasamori, R.; Okaue, Y.; Isobe, T.; Matsuda, Y. *Science* **1994**, 265, 1691. (b) Dilger, F.; Roduner, E.; Scheuermann, R.; Major, J.; Schefzik, M.; Stosser, R.; Pach, M.; Fleming, D. G. *Physica B Condens. Matter.* **2000**, 289 and 290, 482. (c) Hayashino, Y.; Isobe, T.; Matsuda, Y. *Chem. Phys. Chem.* **2001**, *2*, 748.
- (238) (a) Gromilov, S. A.; Emel'yanov, D. Yu.; Kuzmin, A. V.; Prokhorova, S. A. *J. Struct. Chem.* **2003**, *44*, 704. (b) Gromilov, S. A.; Basova, T. V.; Emel'yanov, D. Yu.; Kuzmin, A. V.; Prokhorova, S. A. *J. Struct. Chem.* **2004**, *45*, 471.
- (239) (a) Englehardt, G.; Zeigan, D.; Hoebbel, D.; Samoson, A.; Lippmaa, E. *Z. Chem.* **1982**, *22*, 314. (b) Kolodziejski, W.; Klinowski, J. *Solid State Nucl. Magn. Res.* **1992**, *1*, 41.
- (240) Holzinger, D.; Kickelbick, G. *J. Polym. Sci. A* **2002**, *40*, 3858.
- (241) Auner, N.; Ziemer, B.; Herrschaft, B.; Ziche, W.; John, P.; Weis, J. *Eur. J. Inorg. Chem.* **1999**, *7*, 1087.
- (242) Ye, Y.-S.; Chen, W.-Y.; Wang, Y.-Z. *J. Polym. Sci. A* **2006**, *44*, 5391.
- (243) Pitsch, I.; Hoebbel, D.; Jancke, H.; Hiller, W. *Z. Anorg. Allg. Chem.* **1991**, 596, 63.
- (244) Mya, K. Y.; He, C.; Huang, J.; Xiao, Y.; Dai, J.; Slow, Y.-P. *J. Polym. Sci. A* **2004**, *42*, 3490.
- (245) Chen, W.-Y.; Wang, Y.-Z.; Kuo, S.-W.; Huang, C.-F.; Tung, P.-H.; Chang, F.-C. *Polymer* **2004**, *45*, 6897.
- (246) Huang, J.; Xiao, Y.; Mya, K. Y.; Liu, X.; He, C.; Dai, J.; Siow, Y. P. *J. Mater. Chem.* **2004**, *14*, 2858.
- (247) Huang, J.; He, C.; Liu, X.; Xu, J.; Tay, C. S. S.; Chow, S. Y. *Polymer* **2005**, *46*, 7018.
- (248) Zhang, C.; Laine, R. M. *J. Am. Chem. Soc.* **2000**, *122*, 6979.
- (249) Chan, S.-C.; Kuo, S.-W.; Chang, F.-C. *Macromolecules* **2005**, *38*, 3099.
- (250) Toepfer, O.; Neumann, D.; Choudhury, N. R.; Whittaker, A.; Matisons, J. *Chem. Mater* **2005**, *17*, 1027.
- (251) Kim, K.-M.; Inakura, T.; Chujo, Y. *Polymer Bull.* **2001**, *46*, 351.
- (252) Costa, R. O.; Vasconcelos, W. L.; Tamaki, R.; Laine, R. M. *Macromolecules* **2001**, *34*, 5398.
- (253) Neumann, D.; Fisher, M.; Tran, L.; Matisons, J. G. *J. Am. Chem. Soc.* **2002**, *124*, 13998.
- (254) Fujiwara, M.; Shikawa, K.; Kawasaki, N.; Tanaka, Y. *Adv. Funct. Mater.* **2003**, *13*, 371.
- (255) Markovic, E.; Clarke, D.; Constantopoulos, K.; Uhrig, D.; Clarke, S.; Matisons, J. G.; Simon, G. *Polym. Prepr.* **2004**, *45*, 655.
- (256) Kuo, S.-W.; Lin, H.-C.; Huang, W.-J.; Huang, C.-F.; Chang, F.-C. *J. Polym. Sci. [B]* **2005**, volume date 2006, *44*, 673.

- (257) Ribeiro do Carmo, D.; Paim, L. L.; Dias Filho, N. L.; Stradiotto, N. R. *Appl. Surf. Sci.* **2007**, 253, 3683.
- (258) Hoebbel, D.; Pitsch, I.; Heidemann, D. Z. *Anorg. Allg. Chem.* **1991**, 592, 207.
- (259) Morán, M.; Casado, C. M.; Cuadrado, I.; Losada, J. *Organometallics* **1993**, 12, 4327.
- (260) Su, R. Q.; Müller, T. E.; Procházka, J.; Lercher, J. A. *Adv. Mater.* **2002**, 14, 1369.
- (261) Fujiwara, H.; Narita, T.; Hamana, H. J. *Fluorine Chem.* **2004**, 125, 1279.
- (262) Hoebbel, D.; Endres, K.; Reinert, T.; Pitsch, I. J. *Non-Cryst. Solids* **1994**, 176, 179.
- (263) Isayeva, I. S.; Kennedy, J. P. J. *Polym. Sci. A* **2004**, 42, 4337.
- (264) Hasegawa, I.; Niwa, T.; Takayama, T. *Inorg. Chem. Commun.* **2005**, 8, 159.
- (265) Cho, H.-J.; Hwang, D.-H.; Lee, J.-I.; Jung, Y.-K.; Park, J.-H.; Lee, J.; Lee, S.-K.; Shim, H.-K. *Chem. Mater.* **2006**, 18, 3780.
- (266) Lee, Y.-J.; Kuo, S.-W.; Huang, C.-F.; Chang, F.-C. *Polymer* **2006**, 47, 4378.
- (267) Naga, N.; Oda, E.; Toyota, A.; Horie, K.; Furukawa, H. *Mol. Chem. Phys.* **2006**, 207, 627.
- (268) Zhang, H.; Kulkarni, S.; Wunder, S. L. J. *Electrochem. Soc.* **2006**, 153, A239.
- (269) Losada, J.; Garcia Armada, M. P.; Cuadrado, I.; Alonso, B.; Gonzalez, B.; Casado, C. M.; Zhang, J. *J. Organomet. Chem.* **2004**, 689, 2799.
- (270) Huang, J.; Li, X.; Lin, T.; He, C.; Mya, K. Y.; Xiao, Y.; Li, J. J. *Polym. Sci. [B]* **2004**, 42, 1173.
- (271) Jutzi, P.; Batz, C.; Mutluay, A. Z. *Naturforsch.* **1994**, 49b, 1689.
- (272) Sellinger, A.; Laine, R. M. *Macromolecules* **1996**, 29, 2327.
- (273) Majoros, I.; Marsalko, T. M.; Kennedy, J. P. *Polymer Bull.* **1997**, 38, 15.
- (274) Hoebbel, D.; Weber, C.; Schmidt, H.; Krüger, R.-P. J. *Sol-Gel Sci. Tech.* **2002**, 24, 121.
- (275) Chauhan, B. P. S.; Latif, U. *Macromolecules* **2005**, 38, 6231.
- (276) Maitra, P.; Wunder, S. L. *Chem. Mater.* **2002**, 14, 4494.
- (277) Huang, J.; He, C.; Liu, X.; Xiao, Y.; Mya, K. Y.; Chai, J. *Langmuir* **2004**, 20, 5145.
- (278) Mya, K. Y.; Li, X.; Chen, L.; Ni, X.; Li, J.; He, C. J. *Phys. Chem. B* **2005**, 109, 9455.
- (279) Imae, I.; Kawakami, Y. J. *Mater. Chem.* **2005**, 15, 4581.
- (280) Mehl, G. H.; Goodby, J. W. *Angew. Chem. Int. Ed. Engl.* **1996**, 35, 2641.
- (281) Yuchs, S. E.; Carrado, K. A. *Inorg. Chem.* **1996**, 35, 261.
- (282) Ribeiro do Carmo, D.; Dias Filho, N. L.; Stradiotto, N. R. *Mater. Res.* **2004**, 7, 499.
- (283) Neumann, D.; Matisons, J. G. *Polym. Mater. Sci. Eng.* **2001**, 84, 1025.
- (284) Agaskar, P. A. *Colloids Surf.* **1992**, 63, 131.
- (285) Hoebbel, D.; Pitsch, I.; Heidemann, D.; Jancke, H.; Hiller, W. Z. *Anorg. Allg. Chem.* **1990**, 583, 133.
- (286) Mutluay, A.; Jutzi, P. In: Auner, N.; Weis, J. (Eds.), *Organosilicon Chemistry IV: From Molecules to Materials*, Wiley-VCH, Weinheim, **2000**; p. 531.
- (287) Muller, E.; Edelmann, F. T. *Main Group Met. Chem.* **1999**, 22, 485.
- (288) Laine, R. M.; Zhang, C.; Sellinger, A.; Viculis, L. *Appl. Organomet. Chem.* **1998**, 12, 715.
- (289) Weidner, R.; Zeller, B.; Deubzer, B.; Frey, V. US Patent 5047492, **1990**.
- (290) Gravel, M.-C.; Laine, R. M. *Polymer Prepr.* **1997**, 38, 155.
- (291) Feher, F. J.; Wyndham, K. D. *Chem. Commun.* **1998**, 323.
- (292) Feher, F. J.; Wyndham, K. D.; Soulivong, D.; Nguyen, F. J. *Chem. Soc. Dalton Trans.* **1999**, 1491.
- (293) Seçkin, T.; Gültek, A.; Köytepe, S. *Turk. J. Chem.* **2005**, 29, 49.
- (294) Gao, J.; Zhang, X.; Wang, S.; Run, M. *Chem. J. on Internet*, <http://www.chemistrymag.org/cji/2005/077048ne.htm>. CAN 145:271839.
- (295) Gültek, A.; Seçkin, T.; Adigüzel, H. I. *Turk. J. Chem.* **2005**, 29, 391.
- (296) Feher, F. J.; Wyndham, K. D.; Scialdone, M. A. *Chem. Commun.* **1998**, 1469.
- (297) Feher, F. J.; Wyndham, K. D.; Knauer, D. J. *Chem. Commun.* **1998**, 2393.
- (298) Gravel, M. C.; Zhang, C.; Dinderman, M.; Laine, R. M. *Appl. Organomet. Chem.* **1999**, 13, 329.
- (299) Cassagneau, T.; Caruso, F. *Adv. Mater.* **2002**, 14, 732.
- (300) Cassagneau, T.; Caruso, F. J. *Am. Chem. Soc.* **2002**, 124, 8172.
- (301) (a) Naka, K.; Itoh, H.; Chujo, J. *Nano Lett.* **2002**, 2, 1183. (b) Wang, X.; Naka, K.; Zhu, M.; Itoh, H.; Chujo, Y. *Langmuir* **2005**, 21, 12395.
- (302) (a) Naka, K.; Itoh, H.; Chujo, Y. *Bull. Chem. Soc. Jpn.* **2004**, 77, 1767. (b) Wang, X.; Naka, K.; Itoh, H.; Chujo, Y. *Chem. Lett.* **2004**, 33, 216. (c) Li, W.; Zhu, M.; Wang, X.; Zhou, X.; Naka, K.; Chujo, Y. *J. Macromol. Sci., Part B: Phys.* **2006**, 45, 549.

- (303) (a) Coche-Guerente, L.; Cosnier, S.; Desprez, V.; Labbe, P.; Petridis, D. *J. Electroanal. Chem.* **1996**, 401, 253. (b) Petridis, D.; Gournis, D.; Karakasides, M. A. *Mol. Cryst. Liq. Cryst. Sci. Technol. Sect. A; Mol. Cryst. Liq. Cryst.* **1998**, 311, 753. (c) Szabo, A.; Gournis, D.; Karakasides, M. A.; Petridis, D. *Chem. Mater.* **1998**, 10, 639. (d) Liu, H.; Zhang, W.; Zheng, S. *Polymer* **2005**, 46, 157.
- (304) (a) Cassagneau, T.; Jones, D. J.; Roziere, J. *J. Phys. Chem.* **1993**, 97, 8678. (b) Cassagneau, T.; Hix, G. B.; Jones, D. J.; Mairles-Torres, P.; Rhomari, M.; Roziere, J. *J. Mater. Chem.* **1994**, 4, 189.
- (305) Kim, K.-M.; Adachi, K.; Chujo, Y. *Polymer* **2001**, volume date 2002, 43, 1171.
- (306) Adachi, K.; Tamaki, R.; Chujo, Y. *Bull. Chem. Soc. Jpn.* **2004**, 77, 2115.
- (307) McCusker, C.; Carroll, J. B.; Rotello, V. M. *Chem. Commun.* **2005**, 996.
- (308) (a) Larsson, K. *Ark. Kemi* **1960**, 16, 203. (b) Koellner, G.; Müller, U. *Acta cryst.* **1989**, C45, 1106.
- (309) (a) Fu, B. X.; Yang, L.; Somali, R. H.; Zong, S. X.; Hsiao, B. S.; Phillips, S.; Blanski, R.; Ruth, P. *J. Polym. Sci. [B]* **2001**, 39, 2727. (b) Li, G. Z.; Wang, L.; Toghiani, H.; Daulton, T. L.; Pittman, C. U. *Polymer* **2002**, 43, 4167. (c) Fu, B. X.; Gelfer, M. Y.; Hsiao, B. S.; Phillips, S.; Viers, B.; Blanski, R.; Ruth, P. *Polymer* **2003**, 44, 1499. (d) Kopesky, E. T.; Haddad, T. S.; Cohen, R. E.; McKinley, G. H. *Macromolecules* **2004**, 37, 8992. (e) Pracella, M.; Chionna, D.; Fina, A.; Yabuani, D.; Frache, A.; Camino, G. *Macromol. Symp.* **2006**, 234, 59. (f) Chen, J.-H.; Chiou, Y.-D. *Polym. Phys.* **2006**, 44, 2122.
- (310) Vogt, L. H.; Brown, J. F. *Inorg. Chem.* **1963**, 2, 189.
- (311) Luo, Q.; Tang, D.; Li, X.; Wang, Q.; Wang, Z.; Zhen, Z.; Liu, X. *Chem. Lett.* **2006**, 35, 278.
- (312) Gu, Y.; Liang, G.; Zhang, Z.; Wang, J.; Lu, T. *Faming Zhuanli Shenqing Gongkai Shuomingshu* **2006**, CN 1803808 A 20060719, CAN 145:377464.
- (313) Voronkov, M. G.; Lavrentyev, V. I.; Kovrigin, V. M. *J. Organomet. Chem.* **1981**, 220, 285.
- (314) Unno, M.; Takada, K.; Matsumoto, H. *Chem. Lett.* **1998**, 6, 489.
- (315) Kruger, R.-P.; Much, H.; Schulz, G.; Rikowski, E. In: Auner, N.; Weis, J. (Eds.), *Organosilicon Chemistry IV: From Molecules to Materials*, Wiley-VCH, Weinheim, **2000**; p. 545.
- (316) Lichtenhan, J. D.; Schwab, J. J.; Reinerth, W.; Carr, M. J.; An, Y.-Z.; Feher, F. J.; Terroba, R. WO 2001010871, **2001**.
- (317) Bassindale, A. R.; Chen, H.; Lui, Z.; MacKinnon, I. A.; Parker, D. J.; Taylor, P. G.; Yang, Y.; Light, M. E.; Horton, P. N.; Hursthouse, M. B. *J. Organomet. Chem.* **2004**, 689, 3287.
- (318) Bassindale, A. R.; Gentle, T. E.; Taylor, P. G.; Watt, A. In: Corriu, R.; Jutzi, P. (Eds.), *Tailor-Made Silicon-Oxygen Compounds: From Molecules to Materials*, Vieweg, Wiesbaden, **1996**; p. 171.
- (319) Lin, Q.; Sooriyakumaran, R. US 2004137241, **2004**.
- (320) Lee, L.-H.; Chen, W.-C. *Polymer* **2005**, 46, 2163.
- (321) Richter, I.; Burschka, C.; Tacke, R. *J. Organomet. Chem.* **2002**, 646, 200.
- (322) Matsumoto, H.; Higuchi, K.; Hoshino, Y.; Koite, H.; Naoi, Y.; Nagai, Y. *J. Chem. Soc. Chem. Commun.* **1988**, 1083.
- (323) Unno, M.; Matsumoto, T.; Mochizuki, K.; Higuchi, K.; Goto, M.; Matsumoto, H. *J. Organomet. Chem.* **2003**, 685, 156.
- (324) Lichtenhan, J. D.; Schwab, J. D.; An, Y.-Z.; Reinerth, W.; Feher, F. J. WO 2001046295, **2001**.
- (325) Voronkov, M. G.; Kovrigin, V. M.; Lavrent'ev, V. I.; Moralev, V. M. *Doklady Acad. Sci. USSR, Chem. Ser.* **1985**, 281, 126.
- (326) Lyu, Y. Y.; Yim, J. H.; Mah, S. K.; Nah, E. J.; Hwang, S. I.; Jeong, H. D.; Kim, J. H. US 2003065123, **2003**.
- (327) Murfee, H. J.; Thoms, T. P. S.; Greaves, J.; Hong, B. *Inorg. Chem.* **2000**, 39, 5209.
- (328) Hong, B.; Thoms, T. P. S.; Murfee, H. J.; Lebrun, M. J. *Inorg. Chem.* **1997**, 36, 6146.
- (329) Murfee, H. J.; Hong, B. *Polymer Prepr.* **2000**, 41, 431.
- (330) Lavrent'ev, V. I. *Russ. J. Gen. Chem.* **2004**, 74, 1188.
- (331) Waite, M. S.; Burden, A. P.; Lee, W.; Tuck, R. A. WO 2004029326, **2004**.
- (332) Mabry, J. M.; Vij, A.; Viers, B. D.; Blanski, R. L.; Gonzales, R. I.; Schlaefer, C. E. *Polymer Prepr.* **2004**, 45, 648.
- (333) Shen, J.; Zheng, S. *J. Polym. Sci. [B]* **2006**, 44, 942.
- (334) Braunstein, P.; Galsworthy, J. R.; Hendan, B. J.; Marsmann, H. C. *J. Organomet. Chem.* **1998**, 551, 125.
- (335) Liu, Y.; Yang, X.; Zhang, W.; Zheng, S. *Polymer* **2006**, 47, 6814.
- (336) Lucke, S.; Stoppek-Langner, K.; Krebs, B.; Lage, M. *Z. Anorg. Allg. Chem.* **1997**, 623, 1243.

- (337) Murfee, H. J.; Hong, B. *Polymer Prepr.* **1999**, 40, 412.
- (338) Kim, K.-M.; Ouchi, Y.; Chujo, Y. *Polymer Bull.* **2003**, 49, 341.
- (339) (a) Bent, M.; Gun'ko, Y. J. *Organomet. Chem.* **2005**, 690, 463. (b) Bent, M.; Gun'ko, Y. J. *Organomet. Chem.* **2006**, 691, 1320.
- (340) Nguyen, M. T. US Patent 6270561, **2001**.
- (341) (a) Fu, B. X.; Hsiao, B. S.; Pagola, S.; Stephens, P.; White, H.; Rafailovich, M.; Sokolov, J.; Mather, P. T.; Jeon, H. G.; Phillips, S.; Lichtenhan, J.; Schwab, J. *Polymer* **2000**, 42, 599. (b) Blanski, R. L.; Phillips, S. H.; Chaffee, K.; Lichtenhan, J.; Lee, A.; Geng, H. P. *Polymer Prepr.* **2000**, 41, 585. (c) Hosaka, N.; Tanaka, K.; Otsuka, H.; Takahara, A. *Compos. Interfaces* **2004**, 11, 297. (d) Capaldi, F. M.; Rutledge, G. C.; Boyce, M. C. *Macromolecules* **2005**, 38, 6700. (e) Kopesky, E. T.; McKinley, G. H.; Cohen, R. E. *Polymer* **2006**, 47, 299.
- (342) Marissen, R.; Lange, R. F. M.; Coussens, B. B.; Put, J. A.; Van Dijk, J.; Loontjens, J. A. WO 2004092253, **2004**.
- (343) Tacke, R.; Lopez-Mras, A.; Sheldrick, W. S.; Sebal, A. Z. *Anorg. Allg. Chem.* **1993**, 619, 347.
- (344) Feher, F. J.; Budzichowski, A. *J. Organomet. Chem.* **1989**, 379, 33.
- (345) Feher, F. J.; Schwab, J. J.; Phillips, S. H.; Eklund, A.; Martinez, E. *Organometallics* **1995**, 14, 4452.
- (346) Lichtenhan, J. D.; Schwab, J. J.; Reinerth, W.; Carr, M. J.; An, Y.-Z.; Feher, F. J. WO 2001010871, **2001**. CAN 134:179001.
- (347) Olsson, K.; Axen, C. *Ark. Kemi* **1964**, 22, 237.
- (348) Pereira, J. C. G.; Catlow, C. R. A.; Price, G. D. *J. Phys. Chem. A* **1999**, 103, 3252.
- (349) Handke, M.; Jastrzębski, W. *J. Mol. Struct.* **2005**, 744, 671.
- (350) Nguyen, M. T.; Nazarov, V. **2002**. CAN 2324794.
- (351) (a) Allen, R. D.; Huang, S.-W.; Khojasteh, M.; Lin, Q.; Pfeiffer, D.; Sooriyakumaran, R.; Truong, H. D. US 2005112382, **2005**; (b) Huang, W.-S.; Angelopoulos, M.; Brunner, T. A.; Pfeiffer, D.; Sooriyakumaran, R. US 2006063103, **2006**.
- (352) Sato, M.; Hanahata, M.; Kitajima, S.; Katayama, J.; Ueda, M. JP 2004189602, **2004**.
- (353) For some examples see: (a) Duchateau, R.; Cremer, U.; Harmsen, R. J.; Mohamud, S. I.; Abbenhuis, H. C. L.; Van Santen, R. A.; Meetsma, A.; Thiele, S. K.-H.; Van Tol, M. F. H.; Kranenburg, M. *Organometallics* **1999**, 18, 5447. (b) Chabanas, M.; Quadrelli, E. A.; Fenet, B.; Copéret, C.; Thivolle-Cazat, J.; Basset, J.-M.; Lesage, A.; Emsley, L. *Angew. Chem. Int. Ed.* **2001**, 40, 4493. (c) Fraile, J. M.; Garcia, J. I.; Mayoral, J. A.; Vispe, E. *J. Catal.* **2005**, 233, 90. (d) Blanc, F.; Copéret, C.; Thivolle-Cazat, J.; Basset, J.-M.; Lesage, A.; Emsley, L.; Sinha, A.; Schrock, R. R. *Angew. Chem. Int. Ed.* **2006**, 45, 1216. (e) Cho, H. M.; Weissman, H.; Wilson, S. R.; Moore, J. S. *J. Am. Chem. Soc.* **2006**, 128, 14742. (f) Rhers, B.; Quadrelli, E. A.; Baudoin, A.; Taoufik, M.; Copéret, C.; Lefebvre, F.; Basset, J.-M.; Fenet, B.; Sinha, A.; Schrock, R. R. *J. Organomet. Chem.* **2006**, 691, 5448.
- (354) Duchateau, R.; Abbenhuis, H. C. L.; Van Santen, R. A.; Thiele, S. K.-H.; Van Tol, M. F. H. *Organometallics* **1998**, 17, 5222.
- (355) Severn, J. R.; Duchateau, R.; Van Santen, R. A.; Ellis, D. D.; Spek, A. L. *Organometallics* **2002**, 21, 4.
- (356) Feher, F. J.; Weller, K. J. *Organometallics* **1990**, 9, 2638.
- (357) Fei, Z.; Ibrom, K.; Edelmann, F. T. Z. *Anorg. Allg. Chem.* **2002**, 628, 2109.
- (358) Lorenz, V.; Fisher, A.; Edelmann, F. T. *J. Organomet. Chem.* **2002**, 647, 245.
- (359) Giessmann, S.; Fischer, A.; Edelmann, F. T. Z. *Anorg. Allg. Chem.* **2004**, 630, 1982.
- (360) Pescarmona, P. P.; Masters, A. F.; van der Waal, J. C.; Maschmeyer, T. *J. Mol. Catal. A* **2004**, 220, 37.
- (361) Martynova, T. N.; Chupakhina, T. I. *J. Organomet. Chem.* **1988**, 345, 11.
- (362) Lavrent'ev, V. I. *Russ. J. Gen. Chem.* **1997**, 67, 239.
- (363) Lavrent'ev, V. I.; Sheludyakova, L. A. *Bull. Acad. Sci. USSR* **1983**, 1707.
- (364) Hendan, B. J.; Marsmann, H. C. *J. Organomet. Chem.* **1994**, 483, 33.
- (365) (a) Rebrov, E. A.; Tebeneva, N. A.; Muzafarov, A. M.; Ovchinikov, Y. E.; Struchkov, Y. T.; Strelkova, T. V. *Russ. Chem. Bull.* **1995**, 44, 1286. (b) Tebeneva, N. G.; Rebrov, E. A.; Muzafarov, A. M. *Polymer Prepr.* **1998**, 39, 503.
- (366) Andrianov, K. A.; Tikhonov, V. S.; Makhneva, G. P.; Chernov, G. S. *Izv. Akad. Nauk., Ser. Khim.* **1973**, 4, 956.
- (367) Calzaferri, G.; Herren, D.; Imhof, R. *Helv. Chim. Acta* **1991**, 74, 1278.
- (368) Hasegawa, I. *Polyhedron* **1991**, 10, 1097.

- (369) Dare, E. O.; Olatunji, G. A.; Ogunnuyi, D. S.; Lasisi, A. A. *Pol. J. Chem.* **2005**, 79, 109.
- (370) Podberezskaya, N. V.; Magarill, S. A.; Baidina, I. A.; Borisov, S. V.; Gorsh, L. E.; Kanev, A. N.; Martynova, T. N. *J. Struct. Chem.* **1982**, 23, 422.
- (371) Podberezskaya, N. V.; Baidina, I. A.; Alekseev, V. I.; Borisov, S. V.; Martynova, T. N. *J. Struct. Chem.* **1982**, 22, 737.
- (372) Dare, E. O.; Olatunji, G. A.; Ogunniyi, D. S. *Bull. Chem. Soc. Ethiop.* **2004**, 18, 37.
- (373) Smolin, Yu. I.; Shepelev, Yu. F.; Pomes, R.; Hoebbel, D.; Wiker, V. *Kristallografiya* **1979**, 24, 38.
- (374) Smolin, Yu. I.; Shepelev, Yu. F.; Butikova, I. K. *Kristallografiya* **1972**, 17, 15.
- (375) Wiebcke, M.; Emmer, J.; Felsche, J.; Hoebbel, D.; Engelhardt, G. Z. *Anorg. Allg. Chem.* **1994**, 620, 757.
- (376) Emmer, J.; Wiebcke, M. *J. Chem. Soc. Chem. Commun.* **1994**, 2079.
- (377) Törnroos, K. W.; Calzaferri, G.; Imhof, R. *Acta Crystallogr. C* **1995**, 51, 1732.
- (378) (a) Hoebbel, D.; Wieker, W.; Franke, P.; Otto, A. Z. *Anorg. Allg. Chem.* **1975**, 418, 35. (b) Boxhoorn, G.; Sudmeijer, O.; Van Kasteren, P. H. G. *J. Chem. Soc. Chem. Commun.* **1983**, 1416.
- (379) Fitzgerald, J. J.; Hoffman, J. A.; Nebo, C. O. *J. Chromatogr. Sci.* **1989**, 27, 186.
- (380) Rikowski, E. In: Auner, N.; Weis, J. (Eds.), *Organosilicon Chemistry IV: From Molecules to Materials*, Wiley-VCH, Weinheim, **2000**; p. 540.
- (381) Agaskar, P. A.; Klemperer, W. G. *Inorg. Chim. Acta* **1995**, 229, 355.
- (382) (a) Baidina, I. A.; Podberezskaya, N. V.; Borisov, S. V.; Alekseev, V. I.; Martynova, T. N.; Kanev, A. N. *J. Struct. Chem.* **1980**, 21, 352. (b) Martynova, T. N.; Korchkov, V. P. *Izvestiya Sibirskogo Otdeleniya Akademii Nauk SSSR, Seriya Khimicheskikh Nauk* **1984**, 62. CAN 101:23569.
- (383) Liu, Z.-H.; Bassindale, A. R.; Taylor, P. G. *Chem. Res. Chin. Univ.* **2004**, 20, 433.
- (384) Saito, T.; Isozaki, M.; Ando, H. JP 2004143449, **2004**. CAN 140:423827.
- (385) Agaskar, P. A. *J. Am. Chem. Soc.* **1989**, 111, 6858.
- (386) Greeley, J. N.; Banaszak Holl, M. M. *Inorg. Chem.* **1998**, 37, 6014.
- (387) Zhang, K. Z.; Meeuwenberg, L. M.; Banaszak Holl, M. M.; McFeely, F. R. *Jpn. J. Appl. Phys., Part 1* **1997**, 36(3B), 1622.
- (388) Bürgi, H.-B.; Törnroos, K. W.; Calzaferri, G.; Bürgy, H. *Inorg. Chem.* **1993**, 32, 4914.
- (389) Mehl, G. H.; Saez, I. M. *Appl. Organomet. Chem.* **1999**, 13, 261.
- (390) Nicholson, K. T.; Zhang, K. Z.; Holl, M. B. *Polym. Mater. Sci. Eng.* **2000**, 83, 329.
- (391) Kabeta, K. JP 11071462 **1999**. CAN 130:267915.
- (392) Patel, R. R.; Mohanraj, R.; Pittman, C. U. Jr. *J. Polym. Sci. [B]: Polym. Phys.* **2006**, 44, 234.
- (393) Kevwitch, R.; Hansen, B.; Toma, D. I.; Zhu, J. US 2005215072, **2005**. CAN 143:358450.
- (394) Kato, A.; Ogiya, S. JP 2003012820, **2003**. CAN 138:91058.
- (395) Sammons, J.; Goddard, D. M. WO 2000076634, **2000**. CAN 134:73334.
- (396) Pan, B.; Clark, T.; Hoyle, C. E.; Lichtenhan, J. D. *Polymer Prepr.* **2004**, 45, 170.
- (397) Kato, A.; Ikeda, M. JP 2002363414, **2002**. CAN 138:40075.
- (398) Spes, P.; Kreuzer, F. H.; Freyer, C.; Hessling, M. EP 446912, **1991**. CAN 116:6737.
- (399) Shin-Etsu Chemical Industry Co. JP 55145694, **1980**. CAN 95:25258.
- (400) Li, H.; Yu, D.; Zhang, J. *Polymer* **2005**, 46, 5317.
- (401) Martynova, T. N., USSR **1981**. CAN 97:39136.
- (402) Agaskar, P. A.; Day, V. W.; Klemperer, W. G. *J. Am. Chem. Soc.* **1987**, 109, 5554.
- (403) Törnroos, K. W.; Bürgi, H.-B.; Calzaferri, G.; Bürgy, H. *Acta Crystallogr. B* **1995**, 51, 155.
- (404) Clegg, W.; Sheldrick, G. M.; Vater, N. *Acta Crystallogr. B* **1980**, 36, 3162.
- (405) Shklover, V. E.; Ovchinnikov, Yu. E.; Struchkov, Yu. T.; Levitskii, M. M.; Zhdanov, A. A. *Metallorg. Khim.* **1988**, 1, 1273.
- (406) Ahlrichs, R.; Baer, M.; Haeser, M.; Koelmel, C.; Sauer, J. *Chem. Phys. Lett.* **1989**, 164, 199.
- (407) Jug, K.; Wichmann, D. *J. Comp. Chem.* **2000**, 21, 1549.

CHAPTER 2

Silyl Radicals in Chemical Synthesis

Chrysostomos Chatgililoglu^{a,*} and Vitaliy I. Timokhin^b

Contents	I. Introduction	117
	II. Silyl Radicals	118
	A. Methods of generation and kinetic data	118
	B. Bond dissociation enthalpies	121
	C. Structural properties	122
	III. Silanes as Radical-Based Reducing Agents	124
	A. <i>Tris</i> (trimethylsilyl)silane	125
	B. Other silanes	134
	C. The silicon hydride/thiol couple	136
	IV. Silanes as Mediators of Consecutive Radical Reactions	138
	A. Intramolecular reactions	139
	B. Intermolecular reactions	148
	C. Tandem and cascade radical reactions	153
	V. Radical Chemistry of Poly(hydrosilane)s	158
	VI. Radical Chemistry on the Silicon Surfaces	162
	A. Radical reactions on H–Si(111) surfaces	164
	B. Radical reactions on H–Si(100)-2 × 1 surfaces	169
	C. Radical reactions on pSi and Si _{scr} surfaces	172
	D. Oxidation of hydrogen-terminated silicon surfaces	173
	VII. Conclusions	176
	References	176

I. INTRODUCTION

The synthetic application of free-radical reactions has steadily increased with time. Nowadays, radical reactions can often be found driving the key steps of

^aISOF, Consiglio Nazionale delle Ricerche, 40129 Bologna, Italy

^bDepartment of Chemistry and Biochemistry, Florida State University, Tallahassee, FL 32306-4390, USA

*Corresponding author.

E-mail address: chrys@isof.cnr.it

Advances in Organometallic Chemistry, Volume 57
ISSN 0065-3055, DOI 10.1016/S0065-3055(08)00002-6

© 2008 Elsevier Inc.
All rights reserved

complex synthetic procedures oriented toward the construction of natural products as well as of densely packed monolayer fabrication of silicon surfaces. The purpose of this chapter is to review the recent advancement of chemical synthesis in diverse areas based on the role of silyl radicals.

Twenty years ago, Chatgililoglu and coworkers introduced *tris*(trimethylsilyl)silane, $(\text{TMS})_3\text{SiH}$, as a radical-based reducing agent for functional group modifications and as a mediator of sequential radical reactions. Today, the majority of radical reactions using silanes as mediators for the C–C bond formation deal with $(\text{TMS})_3\text{SiH}$. The entire radical chemistry of $(\text{TMS})_3\text{SiH}$ has been the subject of periodical reviews^{1–5} and summarized in the book *Organosilanes in Radical Chemistry*.⁶ Some of its recent uses of as reagent have been highlighted.⁷ Furthermore, based on $(\text{TMS})_3\text{SiH}$ flexibility and applicability in several synthetic transformations, a recent concept article has also indicated its future potential.⁸ Sections III and IV of this chapter deal mainly with recent application of $(\text{TMS})_3\text{SiH}$ in organic synthesis. Where necessary, however, some related work published in the early 1990s is discussed in the light of the recent results.

In Section V, a general discussion of how silicon surfaces can be used to obtain monolayers is presented. The functionalization of silicon surfaces using radical chemistry is an area of intense and active investigation because of the potential for a myriad of practical applications.^{9,10} In order to help those readers who are not familiar with silyl radical chemistry, we discuss some general aspects of silyl radicals in Section II,^{2,4} together with some recent findings.

II. SILYL RADICALS


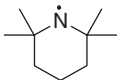
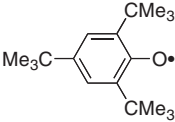
A. Methods of generation and kinetic data

The reaction of radicals with silicon hydrides is the most important methodology for generating silyl radicals in solution. In Reaction (1) radicals X^\bullet could be centered at carbon, nitrogen, oxygen, or sulfur atoms depending on the applications. A large number of kinetic data are available, as well as the reactivity ranges within a few orders of magnitude, depending on the substituent on the Si–H moiety and on the attacking radical.^{2,4}



Table 1 shows the kinetic data available for the $(\text{TMS})_3\text{SiH}$, which was chosen because the majority of radical reactions using silanes in organic synthesis deal with this particular silane (see Sections III and IV). Furthermore, the monohydride terminal surface of H–Si(111) resembles $(\text{TMS})_3\text{SiH}$ and shows similar reactivity for the organic modification of silicon surfaces (see Section V). Rate constants for the reaction of primary, secondary, and tertiary alkyl radicals with $(\text{TMS})_3\text{SiH}$ are very similar in the range of temperatures that are useful for chemical transformations in the liquid phase. This is due to compensation of entropic and enthalpic effects through this series of alkyl radicals. Phenyl and fluorinated alkyl radicals show rate constants two to three orders of magnitude

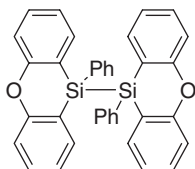
Table 1 Kinetic data for the reactions of a variety of radicals with (TMS)₃SiH

Radical	<i>T</i> (°C)	<i>k</i> (M ⁻¹ s ⁻¹)	Log <i>A</i> (M ⁻¹ s ⁻¹)	<i>E</i> _a (kJ mol ⁻¹)	References
RCH ₂ CH ₂ •	25	3.8 × 10 ⁵	8.9	18.8	11
RCH ₂ •CHCH ₃	25	1.4 × 10 ⁵	8.3	18.0	11
RCH ₂ -C(CH ₃) ₂ •	25	2.6 × 10 ⁵	7.9	14.2	11
	20	~3 × 10 ⁸			4
R-C(=O)•	23	1.6 × 10 ⁴	8.2	29.3	12
R _f CF ₂ CF ₂ •	30	5.1 × 10 ⁷			13
PhCH ₂ N(CH ₃)•	76	~3 × 10 ⁵			14
	25	34.4	4.8	18.4	15
Ph ₂ N•	25	4.4	5.2	25.9	16
CH ₃ -C(CH ₃) ₂ -O•	24	1.1 × 10 ⁸			17
Ph-C(CH ₃) ₂ -OO•	73	66.3			18
	25	4.8 × 10 ⁻⁴	4.4	43.8	16
O ₂	70	~3.5 × 10 ⁻⁵			19

higher, and acyl radicals at least one order of magnitude lower than alkyl radicals. For a comparison of the rate constants of hydrogen abstraction from a variety of reducing agents by primary alkyl radicals see Figure 1 in Section III.

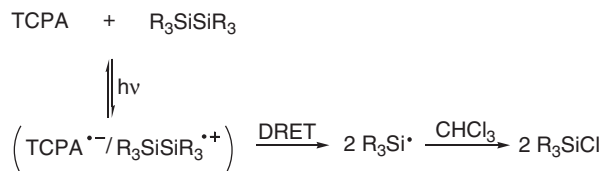
Nitrogen- and oxygen-centered radicals offer some specific features. The rate constant of the reaction of dialkylaminyl radicals with $(\text{TMS})_3\text{SiH}$ is close to the analogous reaction of secondary alkyl radicals. In the reactions of 2,2,6,6-tetramethylpiperidiny and $\text{Ph}_2\text{N}\cdot$ radicals with $(\text{TMS})_3\text{SiH}$ a common characteristic is represented by the low preexponential factor, due to steric effects in the transition state that demand a very specific orientation between the abstracting aminyl radical and the hydrogen-silicon bond in $(\text{TMS})_3\text{SiH}$. The rate constants of reaction of a variety of oxygen species with $(\text{TMS})_3\text{SiH}$ are known and it can be seen that the reactivity of *tert*-butoxyl, cumylperoxyl, and 2,4,6-tri-*tert*-butylphenoxyl radicals change as much as 12 orders of magnitude. It is worth underlining that molecular oxygen reacts spontaneously with $(\text{TMS})_3\text{SiH}$ to give $(\text{TMS})_3\text{Si}\cdot$ and $\text{HOO}\cdot$ radicals.¹⁹

Photolytical methods of generation of silyl radicals are known, though none of which is of general applicability (Reaction 2). For example, the photochemistry of aryldisilanes consists essentially of three principal photoprocesses depending on the substituents and polarity of the solvent: Silylene extrusion, 1,3-Si shift to the *ortho* position of the aryl group to afford silatrienes, and homolytic cleavage of Si-Si bond to give silyl radicals.²⁰⁻²² However, UV photolysis (266 nm) of **1** is found to cleave selectively the Si-Si bond, being the dissociation quantum yield close to 1 and the quantum yield for the silyl radical production close to 2. The photoinitiation activity of **1** in the polymerization of methyl acrylate is also found to be highly effective. By replacing the two Ph groups with Me, the efficiency decreases substantially.²³

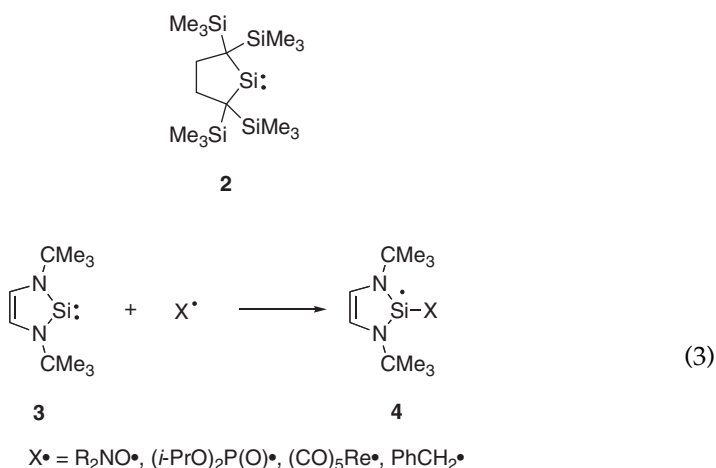


1

The photo-oxidation of 1,1,2,2-tetra-*tert*-butyl-1,2-diphenyldisilane by the triplet sensitizer tetrachlorophthalic anhydride (TCPA) in $\text{CHCl}_3/\text{CCl}_4$ solutions can give the corresponding chlorosilane in high chemical yield (Scheme 1). The quantum yield for formation of chlorosilane depends on the energy of the ion radical pair formed following the initial electron transfer. Dissociative return electron transfer (DRET) is proposed as the mechanism for the highly efficient Si-Si bond cleavage in disilanes.²⁴ DRET can be a useful strategy for the fragmentation of other such bonds in di-, oligo-, and polysilanes using a variety of sensitizers with different spectral properties.

**Scheme 1**

Developments in the synthesis and characterization of stable silylenes ($\text{R}_2\text{Si:}$) open a new route for the generation of silyl radicals.^{25,26} For example, dialkylsilylene **2** is monomeric and stable at 0 °C, whereas *N*-heterocyclic silylene **3** is stable at room temperature under anaerobic conditions. The reactions of silylene **3** with a variety of free radicals have been studied by product characterization, EPR spectroscopy, and DFT calculations (Reaction 3).²⁷ EPR studies have shown the formation of several radical adducts **4**, which represent a new type of neutral silyl radicals stabilized by delocalization. The products obtained by addition of 2,2,6,6-tetramethyl-1-piperidinyloxy (TEMPO) to silylenes **2** and **3** has been studied in some detail.^{28,29}



B. Bond dissociation enthalpies

Kinetic studies of chemical equilibrium (Reaction 4) have provided very accurate thermodynamic information about the series $\text{Me}_{3-n}\text{SiH}_{n+1}$ (with n having values from 0 to 3).^{30–32} In particular, the rate constants k_4 and k_{-4} , obtained by time-resolved experiments, allow the determination of the reaction enthalpy (ΔH_r) either by second or third law method. In Table 2 the $\text{DH}(\text{R}_3\text{Si-H})$ values obtained by Equation (5) are reported.

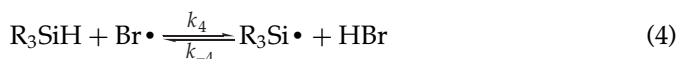


Table 2 Bond dissociation enthalpies of silanes (kJ mol^{-1})

Silane (R_3SiH)	$DH(\text{R}_3\text{Si-H})$	Silane ($\text{Me}_3\text{Si-X}$)	$DH(\text{Me}_3\text{Si-X})$
$\text{H}_3\text{Si-H}$	384.1 ± 2	$\text{Me}_3\text{Si-CH}_3$	396
$\text{MeSiH}_2\text{-H}$	388 ± 5	$\text{Me}_3\text{Si-SiMe}_3$	336
$\text{Me}_2\text{SiH-H}$	392 ± 5	$\text{Me}_3\text{Si-SBu}$	457
$\text{Me}_3\text{Si-H}$	397.4 ± 2	$\text{Me}_3\text{Si-Cl}$	491
$\text{Me}_3\text{SiSiMe}_2\text{-H}$	378	$\text{Me}_3\text{Si-Br}$	426
$(\text{Me}_3\text{Si})_3\text{Si-H}$	351.5	$\text{Me}_3\text{Si-I}$	345

$$DH(\text{R}_3\text{Si-H}) = -\Delta H_r + DH(\text{H-Br}) \quad (5)$$

Considering the homolytic cleavage of silicon–hydrogen bond (Reaction 6), the $DH(\text{R}_3\text{Si-H})$ is related to the enthalpy of formation of silyl radicals, $\Delta H_f^\circ(\text{R}_3\text{Si}\cdot)$, by Equation (7). A value of $16 \pm 6 \text{ kJ mol}^{-1}$ is obtained for $\Delta H_f^\circ(\text{Me}_3\text{Si}\cdot)$, which increases by a fixed amount of approximately 60 kJ mol^{-1} , per methyl group—hydrogen atom replacement.



$$DH(\text{R}_3\text{Si-H}) = \Delta H_f^\circ(\text{R}_3\text{Si}\cdot) + \Delta H_f^\circ(\text{H}\cdot) - \Delta H_f^\circ(\text{R}_3\text{SiH}) \quad (7)$$

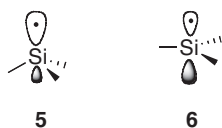
Similar values have been obtained for $\Delta H_f^\circ(\text{Me}_3\text{Si}\cdot)$ from two independent studies.^{33,34} The bond dissociation enthalpy $DH(\text{Me}_3\text{Si-SiMe}_3) = 332 \pm 12 \text{ kJ mol}^{-1}$ was obtained from a kinetic study on the very low pressure pyrolysis of hexamethyldisilane³³ and the enthalpy of formation of trimethylsilyl ion, $\Delta H_f^\circ(\text{Me}_3\text{Si}^+) = 617.3 \pm 2.3 \text{ kJ mol}^{-1}$, was determined using threshold photoelectron-photoion coincidence spectroscopy (TPEPICO).³⁴ Both data are related to $\Delta H_f^\circ(\text{Me}_3\text{Si}\cdot)$.

A few bond dissociation enthalpies of silanes have been measured by photoacoustic calorimetry in solution.^{2,35} Table 2 reports two of these values, which show the substantial decrease in silicon–hydrogen bond strength by replacing methyl with Me_3Si groups. From Table 2 it emerges that when the Me group progressively replaces the H atom, the Si–H bond strength in the silane increases of ca. 4 kJ mol^{-1} , the effect being cumulative. On the other hand, when the Me group progressively is replaced by Me_3Si group, the Si–H bond strength in the silane significantly decreases ($16\text{--}18 \text{ kJ mol}^{-1}$), the effect being again cumulative. The rationalization of these data is reported elsewhere.^{2,6} Table 2 shows also a set of $\text{Me}_3\text{Si-X}$ bond dissociation enthalpies calculated using $\Delta H_f^\circ(\text{Me}_3\text{Si}\cdot) = 16 \text{ kJ mol}^{-1}$.

C. Structural properties

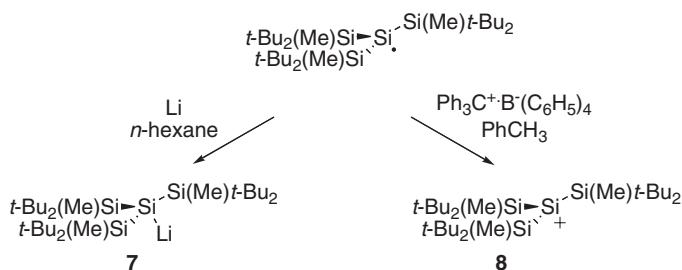
Trialkylsilyl radicals are known to be strongly bent out of the plane (σ -type structure 5). The pyramidal structure of trialkylsilyl radicals ($\text{R}_3\text{Si}\cdot$) was first indicated by chirality studies on optically active compounds containing

asymmetric silicon. However, α -substituents can have a profound influence on the geometry of silyl radicals as indicated by the ^{29}Si hfs constants of EPR spectra. When Me_3Si groups progressively replace methyl groups the ^{29}Si hfs constants decrease from 181 G in the $\text{Me}_3\text{Si}\cdot$ radical to 64 G in the $(\text{Me}_3\text{Si})_3\text{Si}\cdot$ radical, mainly due to the decrease in the degree of pyramidalization at the radical center.^{2,6} Bulkier trialkylsilyl substituents, like *i*- Pr_3Si or *t*- Bu_2MeSi groups, considerably increase the persistency of silyl radicals. Indeed, the half-lives of the radicals increase within the series and the $(t\text{-Bu}_2\text{MeSi})_3\text{Si}\cdot$ radical is found to be stable and isolable in a crystal form. Thus, the radicals $(\text{Et}_3\text{Si})_3\text{Si}\cdot$, $(i\text{-Pr}_3\text{Si})_3\text{Si}\cdot$, $(t\text{-BuMe}_2\text{Si})_3\text{Si}\cdot$, and $(t\text{-Bu}_2\text{MeSi})_3\text{Si}\cdot$ have a practically planar structure **6** due to the steric repulsions among the bulky silyl substituents.^{36,37}

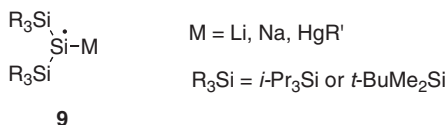


The stable $(t\text{-Bu}_2\text{MeSi})_3\text{Si}\cdot$ radical reacts with lithium in hexane at room temperature affording the silyllithium **7**, with the central anionic silicon atom almost planar,³⁸ whereas the one-electron oxidation with triphenylmethyl ion produces the corresponding silylium ion **8** (Scheme 2).^{39,40}

Considerable efforts have been made for the formation and characterization of α -metalsilyl radicals **9**, potentially useful intermediates in chemical synthesis. The first example of α -lithiumsilyl radical has been obtained from the photolytic cleavage of Si–Hg bond of a symmetrically substituted mercury compound.⁴¹ EPR spectra are consistent with a planar geometry around the central Si atom. α -Lithium-substituted silyl radicals were also detected by photolysis of aggregated 1,1-dilithiosilane.⁴² α -Lithium- and α -sodium-silyl radicals were chemically generated by stirring a fluorosilylenoid derivative with lithium or sodium powder in THF.⁴³ Furthermore, photolysis or thermolysis of $(t\text{-BuHgSiR}_2)_2\text{Hg}$, where $\text{R} = i\text{-Pr}_3\text{Si}$ or *t*- BuMe_2Si , leads to the formation of a α -mercurysilyl radical which has been detected by EPR and trapped with nitroxide radical (TEMPO).⁴⁴



Scheme 2

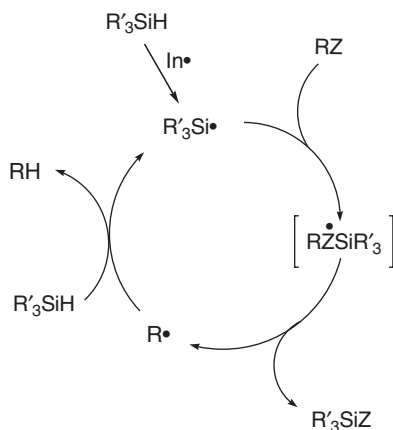


III. SILANES AS RADICAL-BASED REDUCING AGENTS

The majority of radical reactions of interest to synthetic chemists are chain processes under reductive conditions. The reduction of a functional group by silicon hydride is shown in [Scheme 3](#) as an example of a chain process. Initially, $\text{R}'_3\text{Si} \cdot$ radicals are generated by some initiation process. In the propagation steps, the removal of the functional group Z in the organic substrate (RZ) takes place by action of $\text{R}'_3\text{Si} \cdot$ radical *via* a reactive intermediate or a transition state represented by $[\text{RZ}(\cdot)\text{SiR}'_3]$. A site-specific radical ($\text{R} \cdot$) is generated, which then reacts with the silicon hydride and gives the reduced product (RH), together with “fresh” $\text{R}'_3\text{Si} \cdot$ radicals to continue the chain. The chain reactions terminate by radical–radical combination or disproportionation reactions.

The hydrogen abstraction from the Si–H moiety of silanes is fundamentally important for these reactions. Kinetic studies have been performed with many types of silicon hydrides and with a large variety of radicals and been reviewed periodically.^{2,4,6} The data can be interpreted in terms of the electronic properties of the silanes imparted by substituents for each attacking radical. In brevity, we compared in [Figure 1](#) the rate constants of hydrogen abstraction from a variety of reducing systems by primary alkyl radicals at ca. 80 °C.⁴⁵

The upper part of the diagram shows that primary alkyl radicals abstract a H atom from silylated cyclohexadiene, $(\text{EtO})_2\text{P}(\text{O})\text{H}$, $n\text{-Bu}_3\text{GeH}$, $n\text{-Bu}_3\text{SnH}$, and $(\text{TMS})_3\text{GeH}$ with rate constants of ca. 1×10^5 , 1.2×10^5 , 3.8×10^5 , 6.4×10^6 , and $1.5 \times 10^7 \text{ M}^{-1} \text{ s}^{-1}$, respectively, at 80 °C. In the lower part of the diagram, the reactivities of a few organosilanes and $(\text{TMS})_3\text{SiH}$ /thiols are reported. The rate



Scheme 3

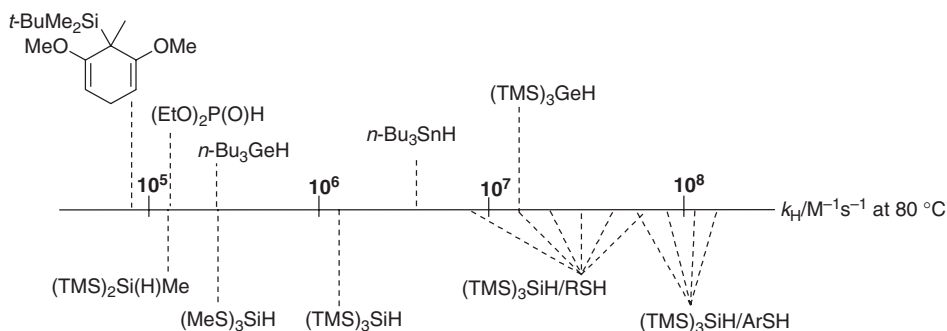
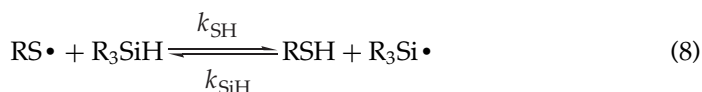


Figure 1 Rate constants for H-atom abstraction from a variety of reducing systems by primary alkyl radicals at 80 °C.

constants cover a range of a few orders of magnitude that indicate how the hydrogen donor abilities of reducing system can be modulated. Primary alkyl radicals will abstract a H atom from $(\text{TMS})_2\text{Si}(\text{H})\text{Me}$, $(\text{MeS})_3\text{SiH}$, and $(\text{TMS})_3\text{SiH}$ with a rate constant of 1.5×10^5 , 3.9×10^5 , and $1.2 \times 10^6 \text{ M}^{-1} \text{ s}^{-1}$, respectively. The alkyl and/or phenyl substituted silicon hydrides are not shown (for left of scale) which indicates their poor ability of hydrogen donation. As we will see, $(\text{TMS})_3\text{SiH}$ is the most efficient reducing agent among the silane family under free-radical conditions and, most importantly, $(\text{TMS})_3\text{SiH}$ is a very good mediator for consecutive radical reactions.

The reaction of thiyl radicals with silicon hydrides (Reaction 8) is the key step of the so-called *polarity-reversal catalysis* in the radical chain reduction.⁴⁶ The reaction is strongly endothermic and reversible with alkyl-substituted silanes (Reaction 8). For example, the rate constants k_{SH} and k_{SiH} for the couple triethylsilane/1-adamantanethiol are 3.2×10^4 and $5.2 \times 10^7 \text{ M}^{-1} \text{ s}^{-1}$, respectively, at 60 °C. The equilibrium constant $K_{\text{eq}} = k_{\text{SH}}/k_{\text{SiH}}$ being 6.2×10^{-4} and hence $\Delta_r G$ is $+20.4 \text{ kJ mol}^{-1}$.⁴⁷



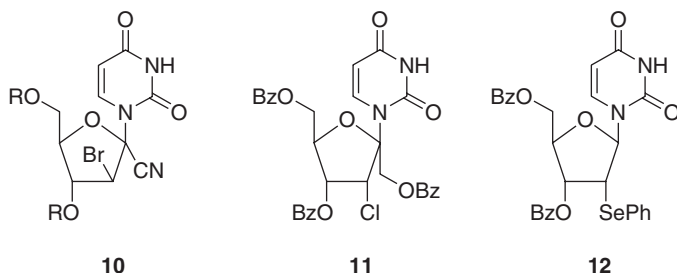
The couple $\text{RSH}/(\text{TMS})_3\text{SiH}$ functions as a free-radical reducing system.⁴⁵ The role of thiol is to modulate the hydrogen donor ability of the system and allow the fast reaction of carbon-centered radicals with the thiols to be studied. Rate constants of primary alkyl radicals vary over two orders of magnitude in the range of 10^6 – $10^8 \text{ M}^{-1} \text{ s}^{-1}$ depending on the thiol substituent. Figure 1 shows that $(\text{TMS})_3\text{SiH}/\text{RSH}$ and $(\text{TMS})_3\text{SiH}/\text{ArSH}$ are in the range of 0.9 – 8×10^7 and 0.75 – $1.5 \times 10^8 \text{ M}^{-1} \text{ s}^{-1}$, respectively, at 80 °C.

A. *Tris(trimethylsilyl)silane*

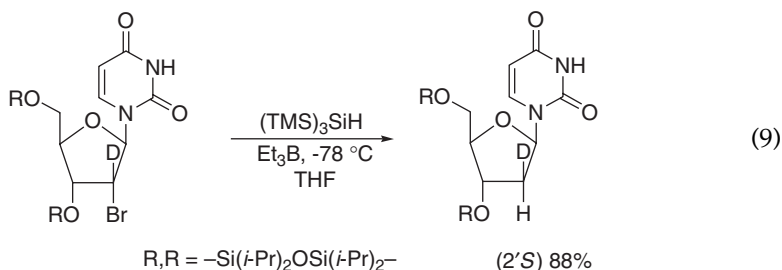
$(\text{TMS})_3\text{SiH}$ is an effective reducing agent for the removal of a variety of functional groups, including halides, selenides, xanthates, and isocyanides.^{1,3,6}

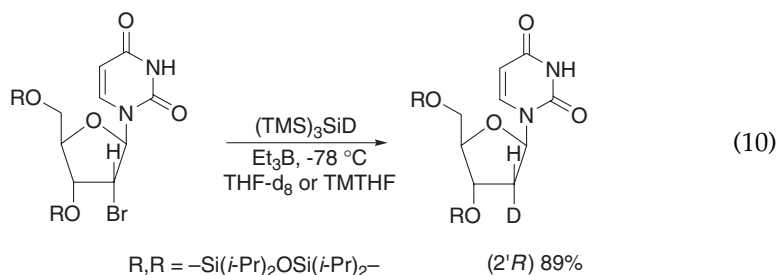
The reactions are radical chain processes (Scheme 3) and, therefore, the initial silyl radicals are generated by some initiation. The most popular thermal initiator is azobisisobutyronitrile (AIBN), with a half-life of 1 h at 81 °C. Other azo-compounds are used from time to time depending on the reaction conditions. Et₃B in the presence of very small amounts of oxygen is an excellent initiator for lower temperature reactions (down to −78 °C). The procedures and examples for reductive removal of functional groups by (TMS)₃SiH are numerous and have recently been summarized in the book *Organosilanes in Radical Chemistry*.⁶

Some examples in the area of nucleoside chemistry are the reductions of bromide **10**, chloride **11**, and selenide **12** in 94, 92, and 87% yields, respectively, at 80 °C using AIBN as the radical initiator.^{48–50} Multiple dehalogenations are possible in a one-pot procedure by using the corresponding equivalents of (TMS)₃SiH.^{51,52}

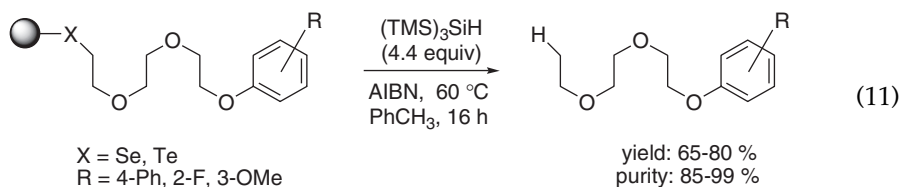


A highly diastereoselective and efficient method for the synthesis of (2'S)- and (2'R)-2'-deoxy[2'-²H]ribonucleoside derivatives starting from the corresponding bromide at the 2'-position has been developed.⁵³ Reactions (9) and (10) show the flexibility of this methodology in obtaining a single diastereoisomer, (2'S) or (2'R), respectively. The high stereoselectivity in these reactions is due to the transfer of hydrogen or deuterium atoms from the less-hindered side of the ring. It is worth mentioning that the solvent employed in Reaction (10) was either THF-d₈ or 2,2,5,5,-tetramethyltetrahydrofuran (TMTHF), in order to eliminate a small percentage of hydrogen donation from the reaction medium.

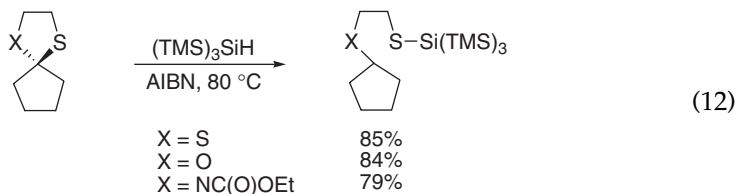




A novel protocol for traceless cleavage from resin-bound selenium and tellurium using $(\text{TMS})_3\text{SiH}$ has been reported (Reaction 11).⁵⁴ The six alkyl aryl ethers below were obtained after column chromatography in good yields and excellent purities. Beside the formation of products, the reaction led to the formation of resin-bound $\text{Se-Si}(\text{TMS})_3$ and $\text{Te-Si}(\text{TMS})_3$, which were characterized by the use of high-resolution magic-angle spinning (HR-MAS) two-dimensional (2D) $^{29}\text{Si}/^1\text{H}$ NMR spectroscopy. Previously, this technology has only been accomplished through the use of highly toxic reagents, thus suffering significant drawbacks due to serious environmental problems and reliability problems with screening results, in particular for the synthesis of large libraries.

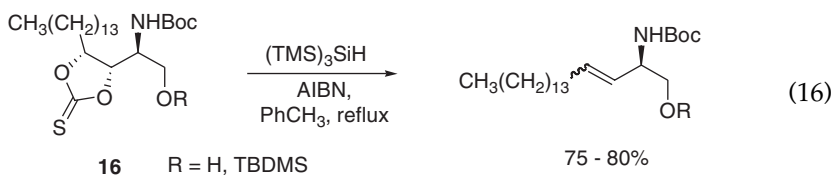
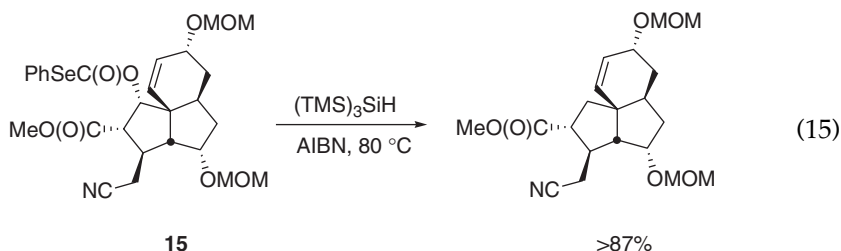
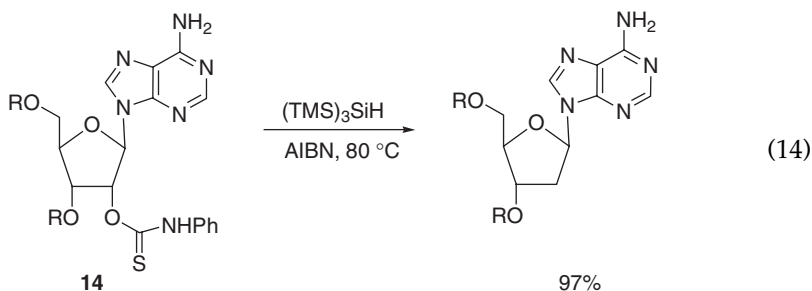
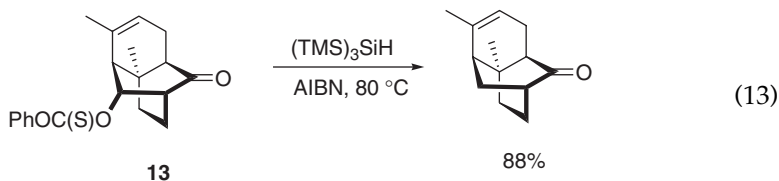


The reaction with sulfides occurs efficiently only when the resulting carbon-centered radicals are further stabilized by a α -heteroatom. Indeed, $(\text{TMS})_3\text{SiH}$ can induce the efficient radical chain monoreduction of 1,3-dithiolane, 1,3-dithiane, 1,3-oxathiolane, 1,3-oxathiolanone, and 1,3-thiazolidine derivatives.⁵⁵ Three examples are outlined in Reaction (12). The reaction of benzothiazole sulfenamide with $(\text{TMS})_3\text{SiH}$, initiated by the decomposition of AIBN at 76°C , is an efficient chain process producing the corresponding dialkylamine quantitatively.¹⁴ However, the mechanism of this chain reaction is complex as it is also an example of a degenerate-branched chain process.



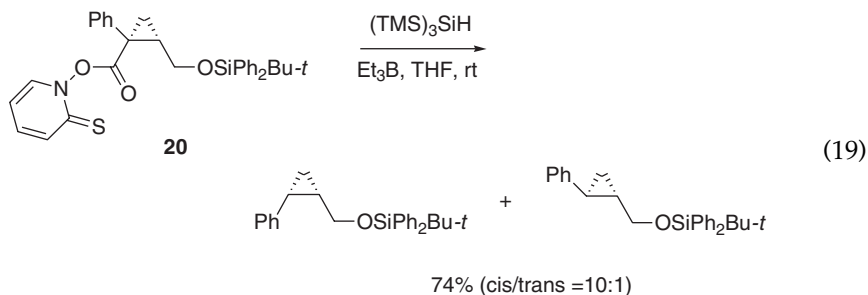
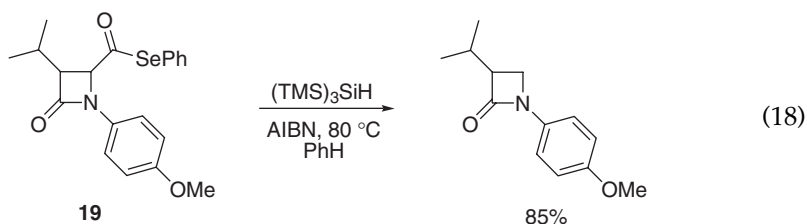
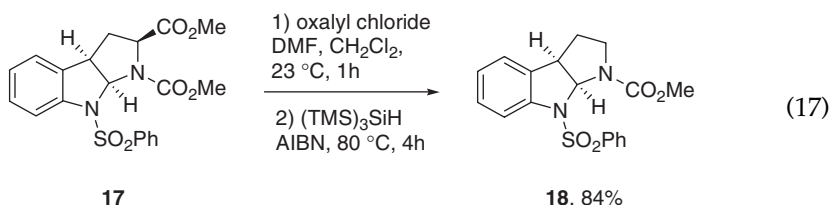
The removal of the hydroxy group is easily achieved by radical chemistry starting from the appropriate thiocarbonyl derivative or selenocarbonate.

Two examples of deoxygenations are reported in sugar and nucleoside chemistry using the *O*-phenylthiocarbonate **13** (Reaction 13) and *O*-thioxocarbamate **14** (Reaction 14), giving the reduced products with 88 and 97% yields, respectively.^{56,57} On the other hand, by heating the selenocarbonate **15** (Reaction 15) in the presence of $(\text{TMS})_3\text{SiH}$, the deoxygenation was achieved in good yield.⁵⁸ 1,2-Diols can be transformed into olefins using the cyclic thiocarbonates or bisdithiocarbonate derivatives. Reaction (16) shows the olefination transformation from cyclic thiocarbonate **16** where the *E*-isomer is more favored in the presence of bulky TBDMS group.⁵⁹

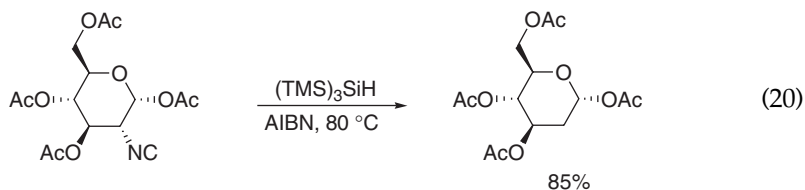


Reductive decarbonylation and decarboxylation can be carried out by $(\text{TMS})_3\text{SiH}$ using acyl chlorides, phenylseleno esters, or *N*-hydroxypyridine-2-thione esters. Examples are shown in Reactions (17)–(19). Hydrolysis of the methyl ester followed by decarbonylation at the C2 position of hexahydropyrroloindole (+)-**17** afforded the desired tricycle (+)-**18** in 84% yield and >99% *ee*.⁶⁰

The acyl selenide **19** affords the decarbonylated β -lactam in good yield.⁶¹ A *N*-hydroxypyridine-2-thione ester **20** is used in the key step to construct the chiral *cis*-cyclopropane structure in compounds designed as antidopaminergic agents.⁶² The observed high *cis* selectivity is due to the hydrogen abstraction from the sterically demanding (TMS)₃SiH, which occurs from the less-hindered side of the intermediate cyclopropyl radical.

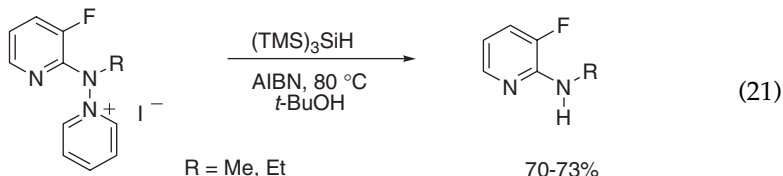


Isocyanides can be reduced to the corresponding hydrocarbons by (TMS)₃SiH.⁶³ The reaction can be considered as a smooth route for the deamination of primary amines. An example is given in Reaction (20). The key step for these chain reactions is expected to be the fragmentation of the intermediate radical derived from the fast addition of (TMS)₃Si• radical to the terminal carbon atom.

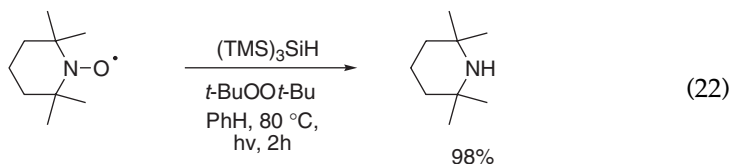


Synthesis of secondary amines can be achieved by replacement of a pyridinium moiety with hydrogen.⁶⁴ Two examples are given in Reaction (21),

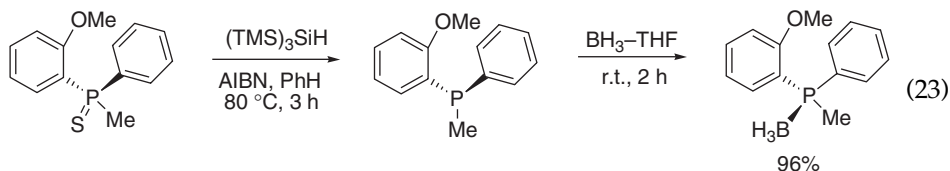
where the formation of 3-fluoro-2-aminopyridine derivatives are obtained in good yields with $(\text{TMS})_3\text{SiH}$ under standard radical chain conditions.



Another methodology is the deoxygenation of nitroxides by $(\text{TMS})_3\text{SiH}$, shown in Reaction (22).¹⁵ Indeed, the reaction of this silane with TEMPO, in the presence of thermal or photochemical radical initiators, afforded the corresponding amine in quantitative yield, together with the siloxane $(\text{TMS})_2\text{Si}(\text{H})\text{OTMS}$.

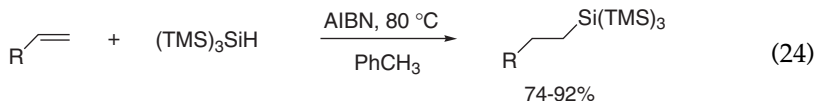


$(\text{TMS})_3\text{SiH}$ reacts with phosphine sulfides and phosphine selenides under free-radical conditions to give the corresponding phosphines or, after treatment with $\text{BH}_3\text{-THF}$, the corresponding phosphine-borane complex in good to excellent yields.⁶⁵ Stereochemical studies on P-chiral phosphine sulfides have shown that these reductions proceed with retention of configuration (Reaction 23). This protocol has also been applied for the desulfidation of bulky phosphine sulfides in high yields⁶⁶ as well as of (Z)-1,2-bis(diphenylthiophosphinyl)-1-alkenes.⁶⁷

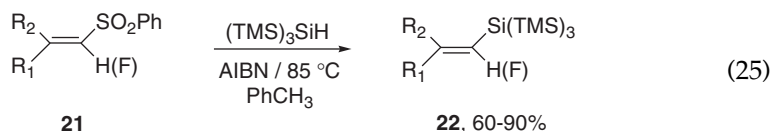


The radical-based hydrosilylation of carbon-carbon, carbon-heteroatom, or heteroatom-heteroatom multiple bonds by $(\text{TMS})_3\text{SiH}$ is an important class of reactions. The initially generated $\text{R}_3\text{Si}\cdot$ radical adds to the double bond to give a radical adduct, which then reacts with the silicon hydride and gives the addition product, together with "fresh" $\text{R}_3\text{Si}\cdot$ radicals to continue the chain. Rate constants for the reaction of $(\text{TMS})_3\text{Si}\cdot$ radical with a variety of monosubstituted olefins have been measured by laser flash photolysis techniques.^{63,68} Hydrosilylation of monosubstituted (Reaction 24) and *gem*-disubstituted olefins is an efficient process that occurs with high regioselectivity (anti-Markovnikov) in the case of both electron-rich and electron-poor olefins.⁶⁹ Analogous reactions are performed using tetrahydropyran as the solvent and 2,2'-azobis(dimethyl valeronitrile) at 70 °C as the initiator,⁷⁰ as well as in water using 1,1'-azobis(cyclohexane carbonitrile) (ACCN) at 100 °C (see *infra*).⁷¹ For *cis* or

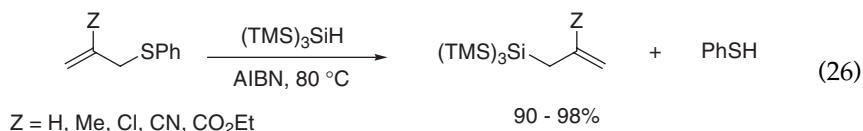
trans disubstituted double bonds, hydrosilylation is still an efficient process, although it requires slightly longer reaction times and an activating substituent.⁶⁹



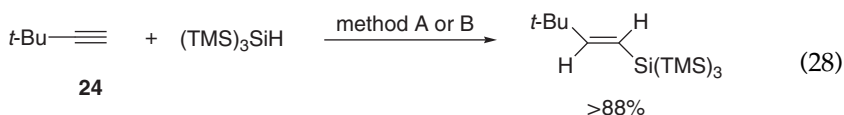
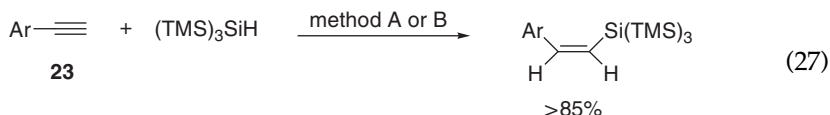
Radical-mediated silyldesulfonylation of various vinyl and (α -fluoro)vinyl sulfones **21** with $(\text{TMS})_3\text{SiH}$ (Reaction 25) provide access to vinyl and (α -fluoro)vinyl silanes **22**.⁷² These reactions presumably occur *via* a radical addition of $(\text{TMS})_3\text{Si}\cdot$ radical followed by β -scission with the ejection of $\text{PhSO}_2\cdot$ radical. Hydrogen abstraction from $(\text{TMS})_3\text{SiH}$ by $\text{PhSO}_2\cdot$ radical completes the cycle of these chain reactions. Such silyldesulfonylation provides a flexible alternative to the hydrosilylation of alkynes with $(\text{TMS})_3\text{SiH}$ (see below). On oxidative treatment with hydrogen peroxide in basic aqueous solution, compound **22** undergoes Pd-catalyzed cross-couplings with aryl halides.



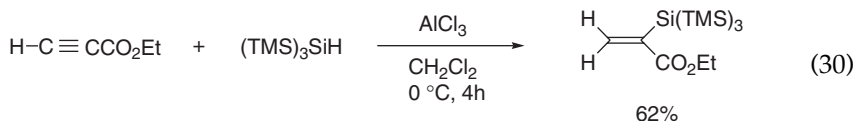
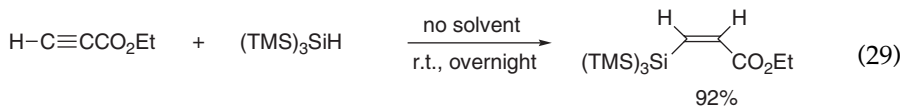
In an analogous process, the reactions of unsubstituted and 2-substituted allyl phenyl sulfides with $(\text{TMS})_3\text{SiH}$ give a facile entry to allyl *tris*(trimethylsilyl) silanes in high yields (Reaction 26). In this case, the addition of $(\text{TMS})_3\text{Si}\cdot$ radical to the double bond is followed by the β -scission with ejection of a thiyl radical, thus affording the transposed double bond. Hydrogen abstraction from $(\text{TMS})_3\text{SiH}$ by $\text{PhS}\cdot$ radical completes the cycle of these chain reactions.⁷³



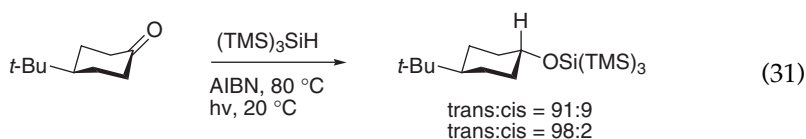
The addition of $(\text{TMS})_3\text{SiH}$ to a number of monosubstituted acetylenes has also been studied in some detail.^{69,74} These reactions are highly regioselective (anti-Markovnikov) and give terminal $(\text{TMS})_3\text{Si}$ -substituted alkenes in good yields. High *cis* or *trans* stereoselectivity is also observed, depending on the nature of the substituents at the acetylenic moiety. For example, the reaction of the alkynes **23** and **24** with $(\text{TMS})_3\text{SiH}$, initiated either by Et_3B at room temperature (method A)^{69,74} or by thermal decomposition of di-*tert*-butyl peroxide at 160 °C (method B),⁷⁵ gave the same results (Reactions 27 and 28).



These reactions proceed without solvent as well (Reaction 29).⁷⁶ On the other hand, reaction in the presence of AlCl_3 in CH_2Cl_2 gave exclusively *gem*-disubstituted olefins (Reaction 30).⁷⁶ The presence of Lewis acid shifts the reaction mechanism from radical to ionic, affording a complementary regioselectivity.



Reaction (31) shows an example of hydrosilylation of ketones, i.e., the reduction of 4-*tert*-butyl-cyclohexanone affording mainly the *trans* isomer, indicating that the axial H-abstraction is favored.⁷⁷

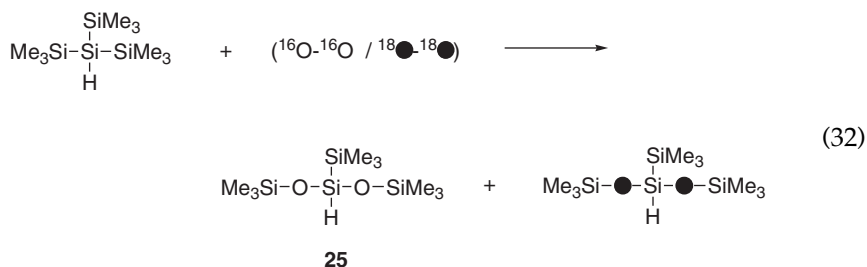


It has been reported that $(\text{TMS})_3\text{SiCl}$ can be used for the protection of primary and secondary alcohols.⁷⁸ *Tris*(trimethylsilyl)silyl ethers are stable to the usual conditions employed in organic synthesis for the deprotection of other silyl groups and can be deprotected using photolysis at 254 nm, in yields ranging from 62 to 95%. Combining this fact with the hydrosilylation of ketones and/or aldehydes, a radical pathway can be drawn, which is formally equivalent to the ionic reduction of carbonyl moieties to the corresponding alcohols (see *infra*).

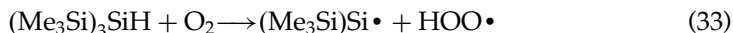
$(\text{TMS})_3\text{SiH}$ is not soluble in water and does not suffer from any significant reaction with water at 100°C for a few hours. Taking advantage of this observation, reduction, or hydrosilylation of hydrophobic substrates (like organohalides, thiocarbonyl derivatives, alkenes, alkynes, and aldehydes) were successfully carried out in good yields, using $(\text{TMS})_3\text{SiH}$ and ACCN as the initiator at 100°C in water.⁷¹ These results show that the nature of the reaction medium does not play an important role neither in influencing the efficiency of the radical transformation nor in the ability to dissolve the reagents. It was suggested that all water-insoluble materials (substrate, $(\text{TMS})_3\text{SiH}$, and initiator) suspended in the aqueous medium can interact, due to the vigorous stirring that creates an efficient vortex and dispersion.

$(\text{TMS})_3\text{SiH}$ as a pure material or in solution reacts spontaneously and slowly at ambient temperature with molecular oxygen from air, to form the siloxane 25.⁷⁹ When $(\text{TMS})_3\text{SiH}$ was treated with a mixture of $^{16}\text{O}_2$ and $^{18}\text{O}_2$ (Reaction 32) and the crude products were analyzed by mass spectrometry, similar label

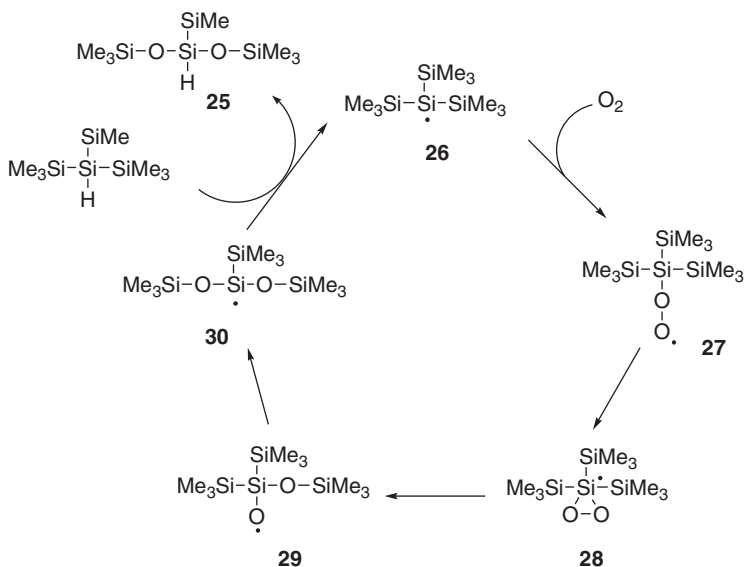
distributions were observed in the products as in the reactants for both cases, indicating an *intramolecular* mechanism, i.e., two oxygen atoms in the final product arise from the same oxygen molecule.



The mechanism of this unusual process has been studied in some detail.¹⁹ Absolute rate constants for the spontaneous reaction of (TMS)₃SiH with molecular oxygen (Reaction 33) has been determined to be $\sim 3.5 \times 10^{-5} \text{ M}^{-1} \text{ s}^{-1}$ at 70 °C and theoretical studies elucidate the reaction coordinates.^{19,76}



The propagation sequence shown in [Scheme 4](#) is in accord with all the experimental and theoretical findings.^{19,76} Silyl radical **26** adds to oxygen to form the peroxy radical **27**. This silylperoxy radical undergoes three consecutive unimolecular steps: **27** → **28** → **29** → **30**. In the end, hydrogen abstraction from the silane by radical **30** gives the observed product **25** and another silyl radical **26**, thus completing the cycle of this chain reaction. There is strong

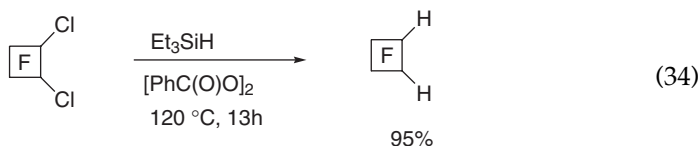


Scheme 4

evidence that the rate-determining step ($\sim 10^3 \text{ s}^{-1}$ at 70°C) of three consecutive unimolecular steps is the formation of the dioxirane-like pentacoordinated silyl radical **28**.

B. Other silanes

Trialkylsilanes are not capable of donating their hydrogen atom at a sufficient rate to propagate the chain. Therefore, chain reactions are not supported under normal conditions, although trialkylsilyl radicals are among the most reactive species toward various organic functional groups. For example, the reduction of thiocarbonyl derivatives by Et_3SiH can be described as a chain process under “forced” conditions.⁸⁰ However, Et_3SiH reacts with polyfluorinated halocarbons under free-radical conditions when initiated by thermal decomposition of peroxides.⁸¹ One example is 1,2-dichlorohexafluorocyclobutane which reacts with an excess of Et_3SiH , affording the dihydro derivative in excellent yield (Reaction 34).



Phenyl or mixed alkyl/phenyl substituted silicon hydrides show similar reactivities to trialkylsilanes. Indeed, by replacing one alkyl by a phenyl group the effect on the hydrogen donating ability of SiH moiety increases only slightly.^{2,6}

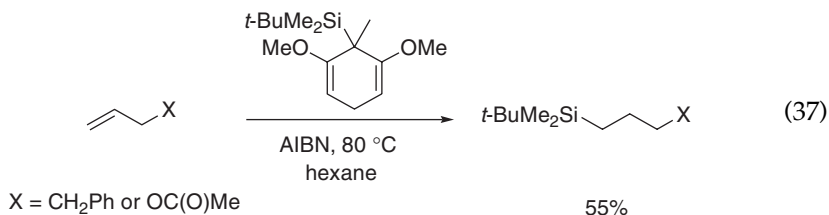
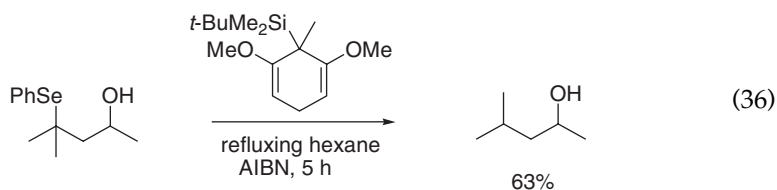
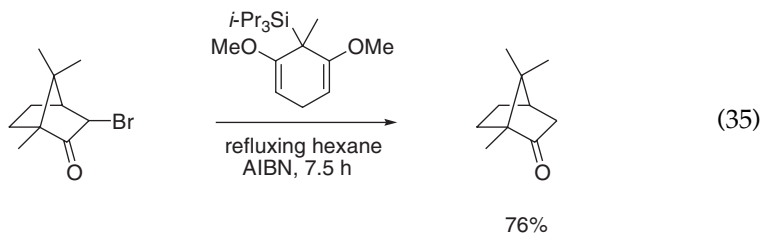
Although under canonical radical chain conditions these silanes are poor reducing agents, there are some interesting applications, in particular using Ph_2SiH_2 .⁸² A variety of arylsilanes with hydrophilic groups have been prepared for testing radical dehalogenations in aqueous media.⁸³ Yields varied from poor to good depending on the substrate and the silicon hydride. 9,10-Disilaanthracenes as an alternative silane for the reduction of halides and a Barton–McCombie type deoxygenation have also been proposed.^{84,85}

A systematic investigation of organosilanes having different silyl substituents at the SiH moiety has been carried out with the aim of testing how to tune the reactivity by the choice of substituents. Reductions of a variety of organic derivatives were carried out using RSi(H)Me_2 , where $\text{R} = \text{SiMe}_3$, $\text{SiMe}_2\text{SiMe}_3$, or $\text{Si(SiMe}_3)_3$, and the initiation was provided by benzoyl peroxide or *tert*-butyl perbenzoate (AIBN was found not to be efficient in these cases).⁸⁶ Reduction of a variety of organic derivatives was carried out by using $(\text{TMS})_2\text{Si(H)Me}$ under normal conditions, i.e., AIBN at 80°C .⁸⁷ Although $(\text{TMS})_2\text{Si(H)Me}$ does not react spontaneously with oxygen at room temperature, a reaction takes place at 80°C similar to the one described for $(\text{TMS})_3\text{SiH}$ in Scheme 4.⁸⁸ Poly(phenylsilane)s of the type $\text{H(RSiH)}_n\text{H}$, where $\text{R} = n$ -hexyl or phenyl, rival the effectiveness of $(\text{TMS})_3\text{SiH}$ in radical chain dehalogenation reactions.⁸⁹ $\text{Ph}_2\text{Si(H)SiPh}_2\text{(H)}$ has

been used in the reductions of alkyl bromides, phenyl chalcogenides, and xanthates with AIBN in refluxing ethanol or $\text{Et}_3\text{B}/\text{O}_2$ at room temperature. Yields varied from moderate to excellent, depending on the experimental conditions.⁹⁰

Substitution at the SiH moiety has been carried out with alkylthio groups, such as MeS and *i*-PrS. *Tris*(alkylthio)silanes, $(\text{RS})_3\text{SiH}$, are radical-based reducing agents which can effect the reduction of bromides, iodides, xanthates, phenylselenides, and isocyanides in toluene, using AIBN as the initiator at 85 °C.⁹¹

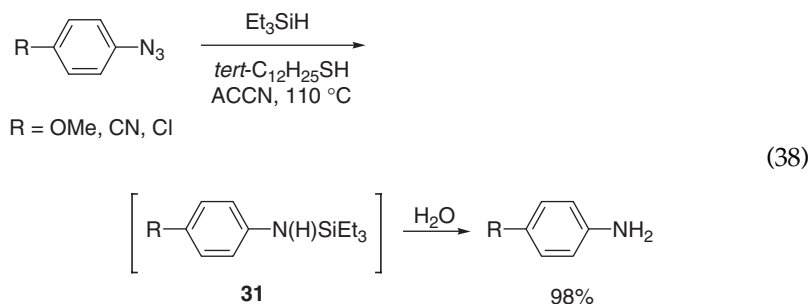
Silylated cyclohexadienes have been prepared and utilized as radical transfer agents. Silylated 1,4-cyclohexadienes were introduced as reducing agents in radical chain reactions such as dehalogenation, deoxygenation *via* thionocarbonate ester, and deselenization, as well as hydrosilylating agents for some alkenes and alkynes.^{92–94} Two examples are given in Reactions (35) and (36), which show that these reactions also work well with different substituted silyl moieties.⁹³ The CH_2 moiety of cyclohexadiene acts as the H-donor with formation of cyclohexadienyl radical as the intermediate, which rapidly ejects the silyl radical on rearomatization. The silyl radical is able to propagate the chain by reaction with a starting halide. Reaction (37) shows that the silane-addition products of terminal alkenes are obtained in moderate yields.⁹⁴



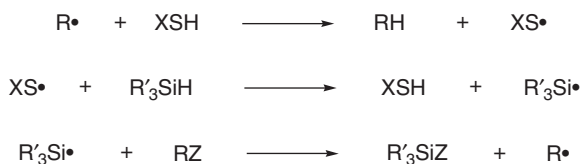
C. The silicon hydride/thiol couple

The low reactivity of alkyl and/or phenyl substituted organosilanes in reduction processes can be ameliorated in the presence of a catalytic amount of alkanethiols. The reaction mechanism is reported in [Scheme 5](#) and shows that alkyl radicals abstract hydrogen from thiols and the resulting thiyl radical abstracts hydrogen from the silane. This procedure, which was coined polarity-reversal catalysis, has been applied to dehalogenation, deoxygenation, and desulfurization reactions.⁴⁶ For example, 1-bromoadamantane is quantitatively reduced with 2 equiv of triethylsilane in the presence of a catalytic amount of *tert*-dodecanethiol.

This approach has been recently extended to the reduction of aromatic azides using Et_3SiH , which afford anilinosilanes and hence the corresponding anilines in virtually quantitative yields (Reaction 38).⁹⁵ The $\text{Et}_3\text{Si}\cdot$ radical adds to the aromatic azido group to give an *N*-silylarylaminy radical presumably through loss of nitrogen. Eventual reduction of the silylarylaminy radical by *tert*-dodecanethiol affords *N*-silylaniline **31**, the hydrolytic precursors of the final anilines.

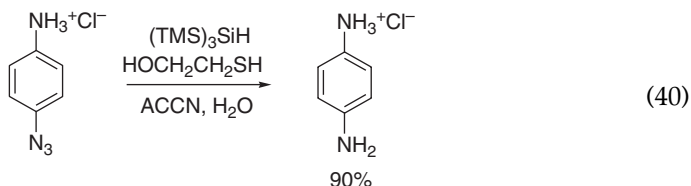
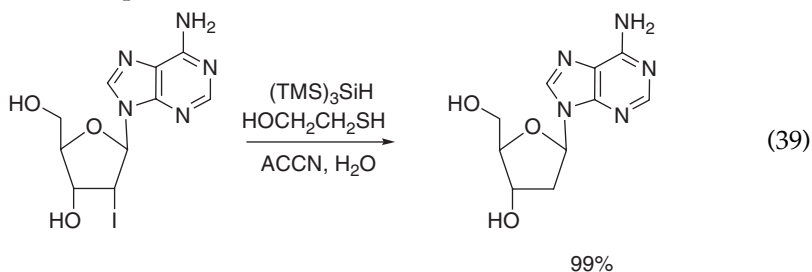


The reduction of different water-soluble organohalides was successfully carried out in very good yields using $(\text{TMS})_3\text{SiH}$ in a heterogeneous system with water as solvent.^{71,96} This procedure, employing amphiphilic 2-mercaptoethanol as the catalyst and the hydrophobic ACCN as the initiator as shown in Reaction (39), illustrates that $(\text{TMS})_3\text{SiH}$ can be the radical-based reducing agent of choice in aqueous medium with additional benefits, such as ease of purification and environmental compatibility. This protocol has successfully been extended to the reduction of water-soluble aliphatic and aromatic azides to the corresponding primary amines, in yields ranging from 90% to quantitative (an example is shown in Reaction 40).⁷¹ The reaction mechanism is analogous to that described in Reaction (38), i.e., after the addition of $(\text{TMS})_3\text{Si}\cdot$ radical to the azide moiety,

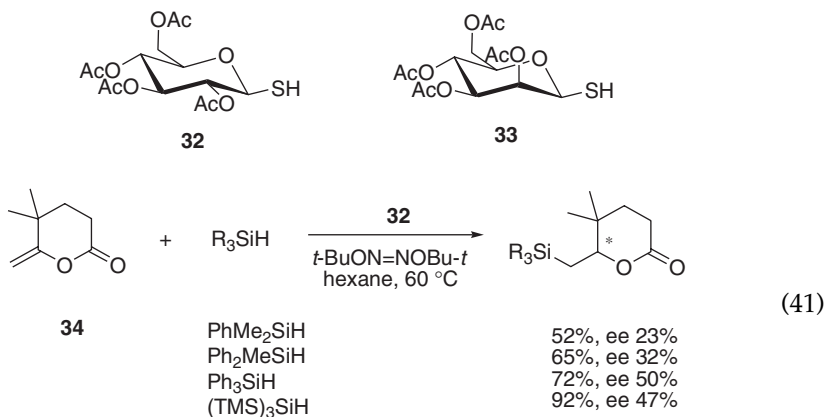


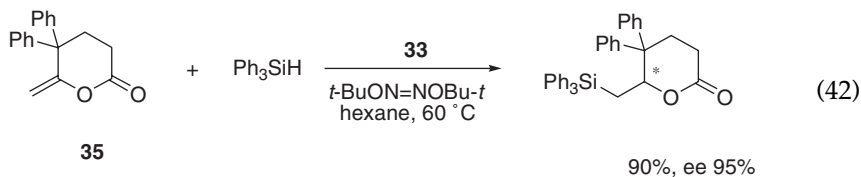
Scheme 5

liberation of nitrogen, and formation of a silyl-substituted aminyl radical, the thiol serves as the hydrogen atom donor. Hydrolysis of the silylamine afforded the amine as the final product.



Radical chain hydrosilylation of alkenes has been investigated in some detail.⁴⁶ Poor to moderate yields were obtained for the reaction of Et_3SiH with alkenes at 60°C .⁹⁷ Thiol catalysis is more effective for the addition of arylsilanes than trialkylsilanes, presumably because the hydrogen abstraction by thiyl radical is more rapid from aromatic silanes. This methodology has been extended to enantioselective hydrosilylation using optically active thiols as catalysts, like the thioglucose tetraacetate **32** or the β -mannose thiol **33**.⁹⁸ Reaction (41) shows the hydrosilylation of methylenelactone **34** with various silicon hydrides and thioglucose tetraacetate **32** as the catalyst. Both yields and enantiomeric purities increase with the degree of phenyl substitution at silicon. Thiols have also been shown to catalyse the addition of $(\text{TMS})_3\text{SiH}$ to alkenes. Higher enantioselectivities were generally found when β -mannose thiol **33** was used as hydrogen donor. The extra bulkiness provided by the *gem*- β -diphenyl groups in the alkene **35** compared to the alkene **34** is responsible for the high enantiomeric purity observed (Reaction 42).

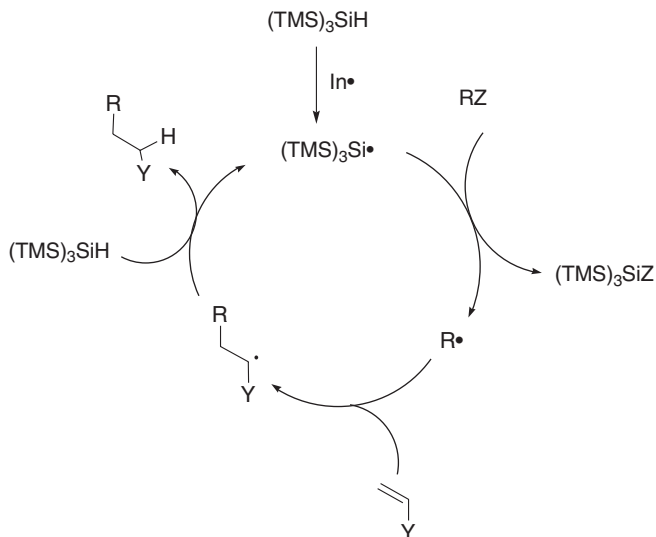




IV. SILANES AS MEDIATORS OF CONSECUTIVE RADICAL REACTIONS

Synthetic strategies based on multistep radical reactions have steadily grown in popularity with time. The knowledge of radical reactivity has increased to such a level as to aid in making the necessary predictions for performing sequential transformations.^{99,100} Silanes, and in particular $(\text{TMS})_3\text{SiH}$, as mediators have contributed substantially in this area, with interesting results in terms of reactivity and stereoselectivity.⁶

The carbon-centered radical $\text{R}\cdot$, resulting from the initial atom (or group) removal by a silyl radical or by addition of a silyl radical to an unsaturated bond, can be designed to undergo a number of consecutive reactions prior to H-atom transfer. The key step in these consecutive reactions generally involves the intra- or inter-molecular addition of $\text{R}\cdot$ to a multiple-bonded carbon acceptor. As an example, the propagation steps for the reductive alkylation of alkenes by $(\text{TMS})_3\text{SiH}$ are shown in Scheme 6.

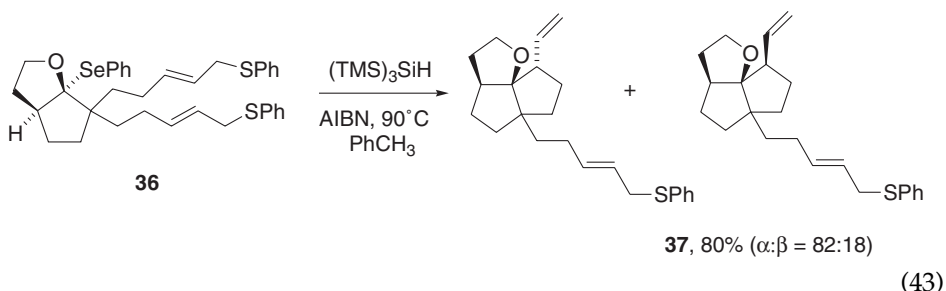


Scheme 6

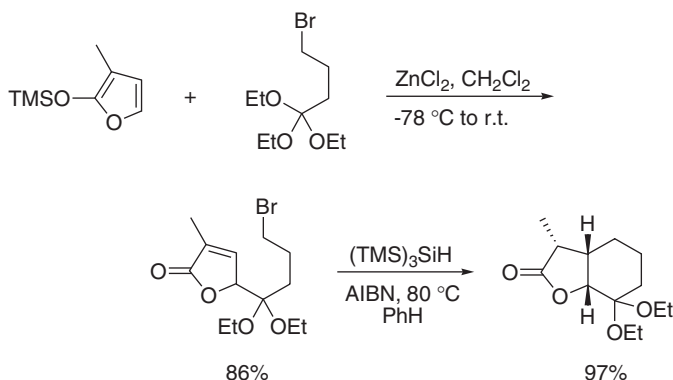
A. Intramolecular reactions

The majority of sequential radical reactions deal with cyclizations as the key steps. The constructions of carbocycles, oxygen, and nitrogen heterocycles using $(\text{TMS})_3\text{SiH}$ as a mediator are many and represents the expansion and importance of these synthetic approaches. For example, Nicolaou and coworkers found that $(\text{TMS})_3\text{SiH}$ serves as a superior reagent in the radical-based approach toward the synthesis of azadirachtin, an antifeedant agent currently used as an insecticide, and in other related systems.^{101,102} Here below we collected a number of reactions mostly from the recent work in the area of intramolecular reactions.

In the construction of carbocycles, five-membered ring formation has been used for preparing fused cyclic compounds, such as functionalized diquinanes.¹⁰³ The reaction of **36** with $(\text{TMS})_3\text{SiH}$ furnished the expected product **37** in 80% yield and in a $\alpha:\beta$ ratio of 82:18, as the result of a kinetic controlled reaction (Reaction 43).

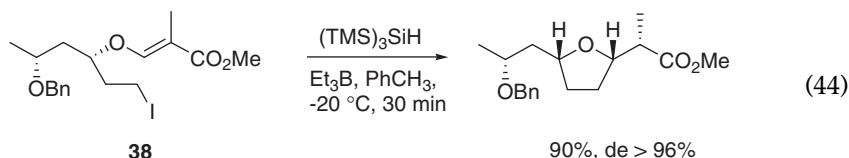


An efficient two-step annelation of functionalized orthoesters with trimethylsilyloxyfuran derivatives has been reported that produces bicyclo[3.n.0]lactones.¹⁰⁴ The reaction in Scheme 7 shows an example in which the initial condensation between silyl enol ether and orthoester is followed by the radical cyclization reaction under standard conditions. It is worth underlining the complete diastereocontrol in which three contiguous stereocenters are generated in one step with >95% stereoselectivity.

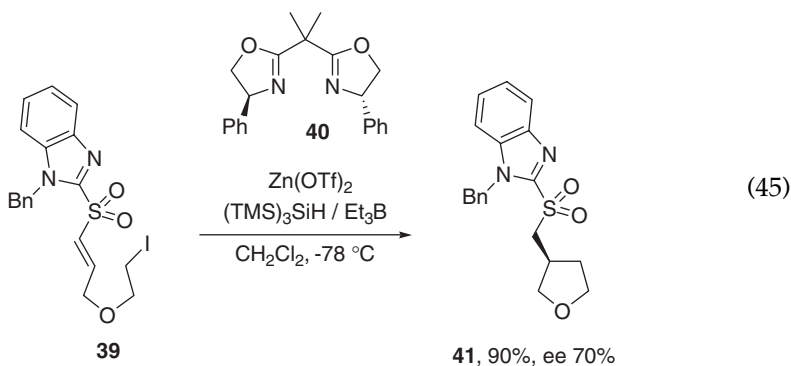


Scheme 7

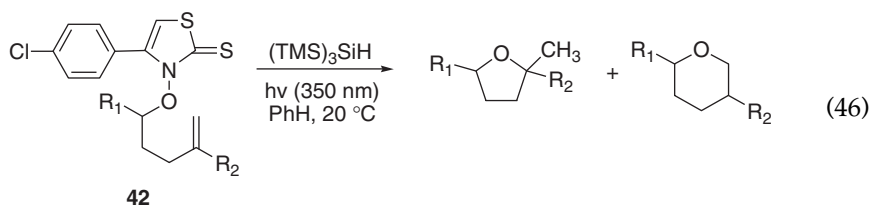
As a strategy for the construction of cyclic ethers, the radical cyclization of β -alkoxyacrylates was used for the preparation of *cis*-2,5-disubstituted tetrahydrofurans and *cis*-2,6-disubstituted tetrahydropyrans. An example is given with β -alkoxymethacrylate **38** as precursor of the optically active benzyl ether of (+)-methyl nonactate, exclusively formed as the *threo* product (Reaction 44).¹⁰⁵



Enantioselective radical cyclizations have been performed by using chiral Lewis acids together with $(\text{TMS})_3\text{SiH}$ as a reducing agent. An example with 70% *ee* is given in Reaction (45).¹⁰⁶ The selective coordination of one of the enantiotopic sulfonyl oxygen in ω -iodoalkenyl sulfone **39** is achieved using $\text{Zn}(\text{OTf})_2$ -bis(oxazoline)-Ph **40**. After the 5-*exo-trig* cyclization, the hydrogen atom transfer from silane proceeds with high enantioselectivity to give **41** in 90% yield. Similar asymmetric reactions were extended to 6-*exo-trig* cyclization as well as to 5-*exo-trig* cyclization of vinyl radicals with good yields and enantioselectivity.¹⁰⁶

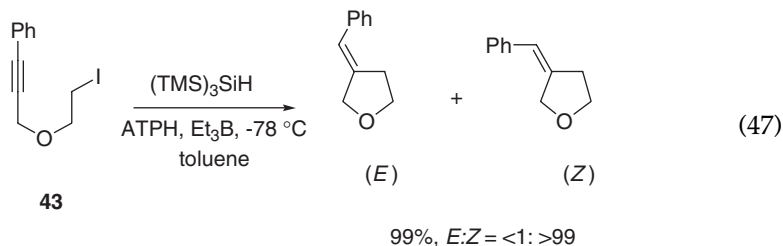


Cyclic ethers were also obtained by cyclization of alkoxy radicals, generated in a radical chain reaction by reacting the thione **42** with $(\text{TMS})_3\text{SiH}$ under photochemical conditions at 20°C (Reaction 46). Regioselectivities of cyclization have been investigated and a progressive increase of the 6-*endo-trig* selectivity along the series $\text{R}_2 = \text{H} < \text{CH}_3 < \text{C}(\text{CH}_3)_3 < \text{Ph}$ was found.¹⁰⁷

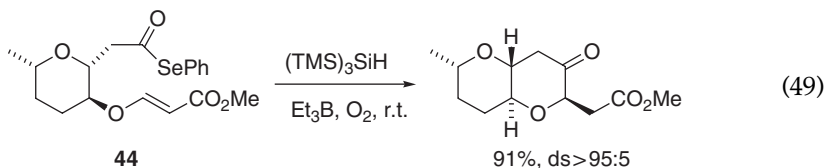
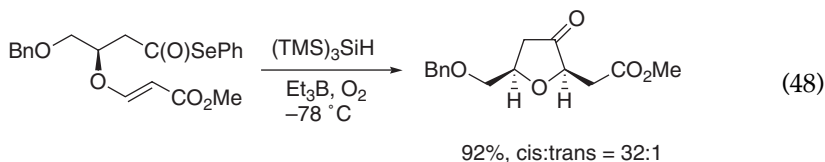


Radical cyclization to triple bonds is used as the key step for the synthesis of oxygen heterocycles.¹⁰⁸ This methodology can benefit from a Lewis acid, such as aluminum *tris*(2,6-diphenyl phenoxide) (ATPH), which forms a complex with the

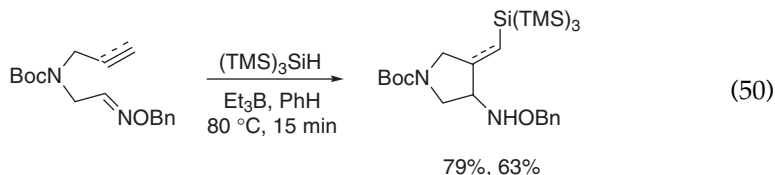
alkyne and assists in the radical cyclization.¹⁰⁹ The β -iodoether **43** can be complexed by 2 equiv of ATPH, to achieve a relevant template effect, facilitating the subsequent radical intramolecular addition and orienting the $(\text{TMS})_3\text{SiH}$ approach from one face (Reaction 47). The resulting quantitatively formed cyclization products show a preferential *Z* configuration.



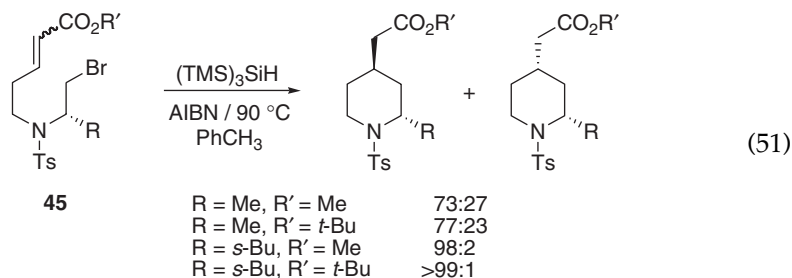
Using $(\text{TMS})_3\text{SiH}$ as the mediator, phenylseleno esters can be conveniently used as precursors of acyl radicals. An example is the key step for the enantioselective synthesis of nonisoprenoid sesquiterpene (–)-kumausallene, obtained by radical cyclization at low temperature in a 32:1 mixture in favor of the 2,5-*cis* diastereoisomer (Reaction 48).¹¹⁰ Another example of acyl radical cyclization is given in Reaction (49).¹¹¹ The careful choice of the configuration of the double bond, combined with conformational features of the preexisting ring in the starting material **44**, can improve the poor diastereoselectivity of 6-*exo-trig* cyclizations.



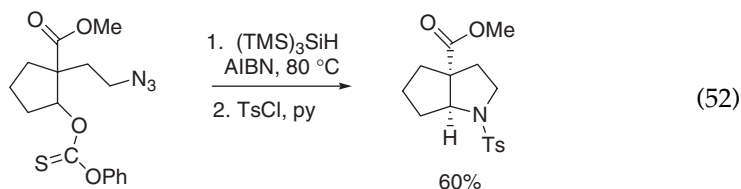
The $(\text{TMS})_3\text{Si}\cdot$ radical addition to terminal alkenes or alkynes, followed by radical cyclization to oxime ethers, were also studied (Reaction 50).¹¹² The radical reactions proceeded effectively by the use of triethylborane as a radical initiator to provide the functionalized pyrrolidines *via* a carbon–carbon bond-forming process. Yields of 79 and 63% are obtained for oxime ethers connected with an olefin or propargyl group, respectively.



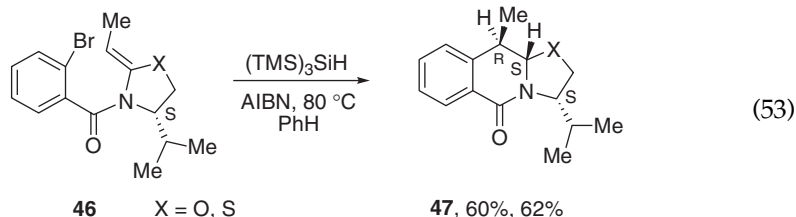
A diastereoselective radical route to 2,4-disubstituted piperidines has been achieved in good yields (60–90%) by cyclization of 7-substituted-6-aza-8-bromooct-2-enoates (**45**), using $(\text{TMS})_3\text{SiH}$ as the reducing agent.^{113,114} Four examples are given in Reaction (51), where the *trans*/*cis* diastereomeric ratios range from 73:27 for $\text{R} = \text{R}' = \text{Me}$ (90% yield) to approaching >99:1 selectivity for $\text{R} = s\text{-Bu}$ and $\text{R}' = t\text{-Bu}$ (60% yield). Although the bulkiness of the ester does not appear to have a significant effect on the stereoselectivity, the bulkiness of the 2-substituent increases the pseudo A^{1,3} strain and favors the *trans* product.



The inertia of $(\text{TMS})_3\text{SiH}$ toward azides allows this functionality to be used as a radical acceptor.¹¹⁵ An example is given in Reaction (52) where the amine product was tosylated before work-up.

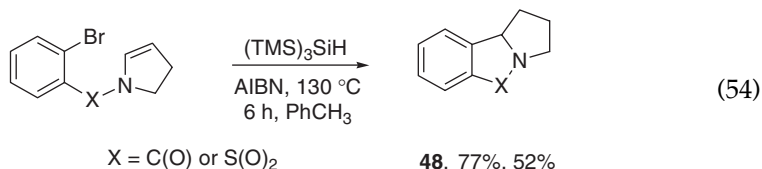


The *N,O*- and *N,S*-heterocyclic fused ring products **47** were also synthesized under radical chain conditions (Reaction 53). Ketene acetals **46** readily underwent stereocontrolled aryl radical cyclizations on treatment with $(\text{TMS})_3\text{SiH}$ under standard conditions to afford the central six-membered rings.¹¹⁶ The tertiary *N,O*- and *N,S*-radicals formed on aryl radical reaction at the ketene-*N,X* ($\text{X} = \text{O}, \text{S}$)-acetal double bond appear to have reasonable stability. The stereoselectivity in hydrogen abstractions by these intermediate radicals from $(\text{TMS})_3\text{SiH}$ was investigated and found to provide higher selectivities than Bu_3SnH .

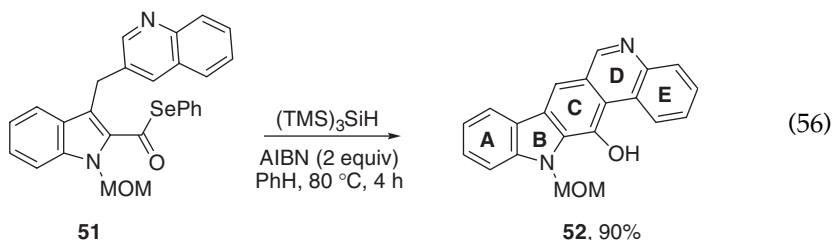
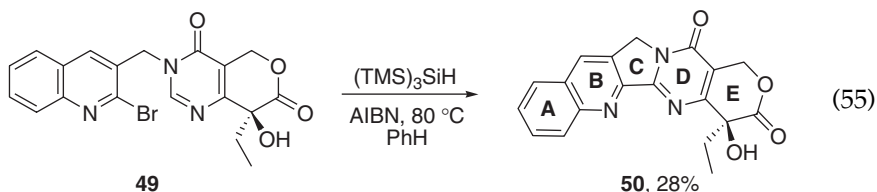


Starting from readily available substrates, a new one-pot procedure has been devised to prepare polycyclic lactams and sultams. 2-Pyrrolines **48** were obtained

from *N,N*-bisallylamides or *N,N*-bisallylsulfonamides by ring-closure metathesis and subsequent isomerization promoted by ruthenium hydride complexes, which then underwent radical cyclization to furnish tricyclic lactams or sultams in good yields (Reaction 54).¹¹⁷

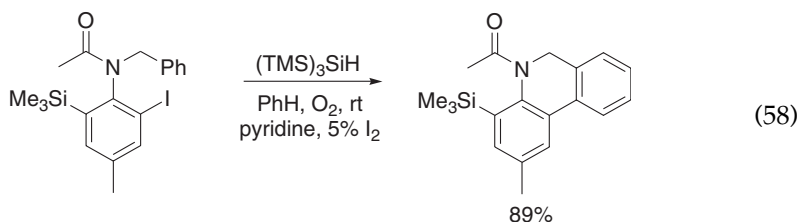
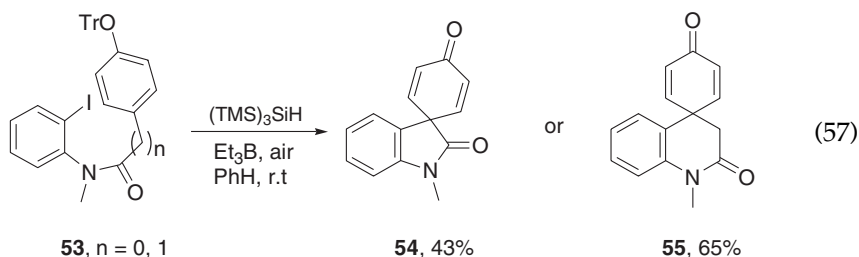


The (TMS)₃SiH-mediated radical cyclization has been applied in the formation of ring **C** in two pentacyclic alkaloids (Reactions 55 and 56).^{118,119} After condensation of the **AB** and **DE** rings, the appropriate precursors bromide **49** and seleno ester **51** were treated with (TMS)₃SiH and AIBN in benzene to give the pentacycles **50** and **52**, respectively. In Reaction (55) AIBN was used in catalytic amounts,¹¹⁸ whereas in Reaction (56) the initiator was in large excess.¹¹⁹ The reactions are not radical chain reactions, being the radical derived from the decomposition of AIBN is involved in some way in the oxidation or rearomatization of the intermediate radical after cyclization.

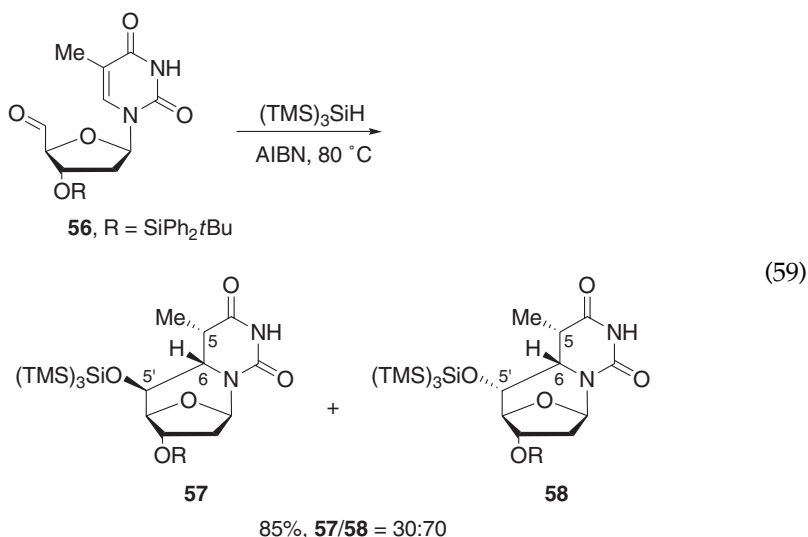


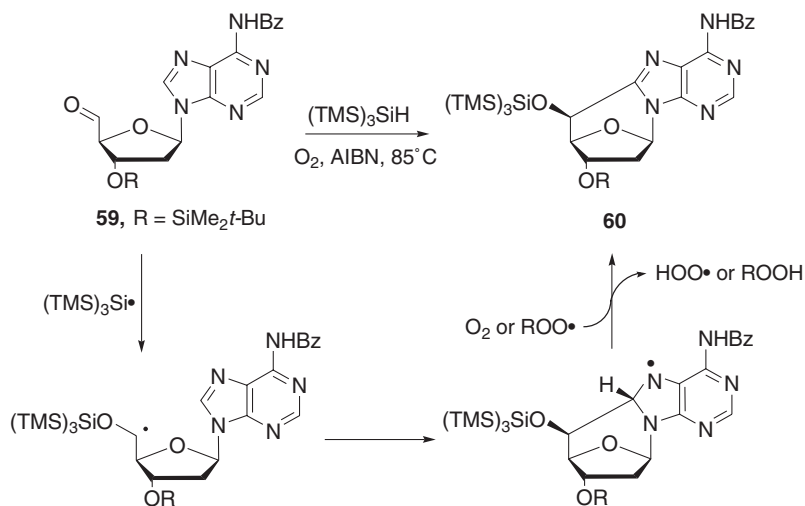
The (TMS)₃SiH/AIBN in toluene at 90 °C was used with an aryl iodide for a radical-induced transannular ring contraction, which is a featured as a key step in the first total synthesis of cavicularin.¹²⁰ Cyclization of an aryl radical to the adjacent arene has further developed to the target of spirocyclohexadienone, a moiety common to various biologically active compounds.¹²¹ Two examples are shown in Reaction (57) for the synthesis of spirooxindole **54** and spirodihydroquinolone **55**. A solution of the appropriate trityl precursor **53** in benzene (0.15 M) was treated with 1.2 equiv of (TMS)₃SiH and 1.2 equiv of Et₃B, and the resulting mixture was stirred at room temperature open to air until the starting material was consumed (typically 3 h). The reactions proceed *via ipso* cyclization of aryl radicals to oxygen substituted aromatic ring, followed by β-fragmentation of the trityl substituent to give the desired products. The (TMS)₃SiH-mediated

intramolecular addition of aryl iodides to arenes are facilitated by oxidative rearomatization with oxygen (Reaction 58).¹²² Actually the AIBN is not necessary for the good performance of the reaction (see below for a mechanistic proposal).



The reaction of aldehyde **56** with $(\text{TMS})_3\text{SiH}$ under radical conditions affords the two diastereoisomers of cyclonucleoside **57** and **58** as the only products in 25 and 60% yield, respectively (Reaction 59). Subsequent exposure to UV irradiation for 30 min at room temperature in an 8:3 $\text{CH}_2\text{Cl}_2/\text{CH}_3\text{OH}$ mixture gave the quantitative deprotection of $(\text{TMS})_3\text{SiO}$ group.¹²³ Although a simple hydrosilylation/deprotection combination is formally equivalent to the ionic reduction of carbonyl moieties, the use of an aldehyde functional group in consecutive radical reactions followed by photo-deprotection could be a new approach for the formation of new stereogenic centers based on the hindered properties of $(\text{TMS})_3\text{Si}$ -group.

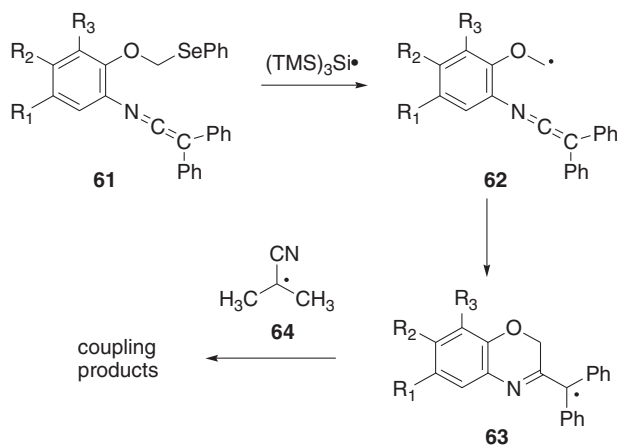


**Scheme 8**

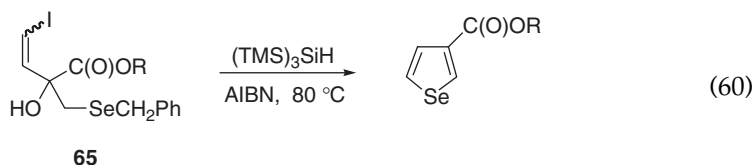
The analogous aldehyde **59** (Scheme 8), under reaction conditions identical to Reaction (59), showed a low conversion of the starting aldehyde. However, when aldehyde **59** was treated with 5 equiv of $(\text{TMS})_3\text{SiH}$ and stoichiometric amounts of AIBN at 85°C under air, it was converted quantitatively in 2 h to the cyclonucleoside **60** as the sole product in a 75% yield.¹²³ From a mechanistic point of view, the addition of $(\text{TMS})_3\text{Si}\cdot$ radical to aldehyde **59** affords the C5' radical which then attacks intramolecularly the adenine moiety. The cyclization occurs with defined stereochemistry, affording exclusively the chair conformation in the forming rings. Oxygen has been suggested to facilitate subsequent rearomatization.

The number of reported reactions in which the radical derived from the decomposition of AIBN plays a role in the termination process has increased considerably. Often these reactions are not radical chain reactions, since the initiator is used in stoichiometric amounts. A few examples of rearomatization of cyclohexadienyl radicals by disproportionation have been reported herein. Below are some other examples, where the phenyl selenide **61** reacts with $(\text{TMS})_3\text{SiH}$ (3 equiv), AIBN (1.2 equiv) in refluxing benzene for 24 h to give the coupling product of radicals **63** and **64** in good yields (Scheme 9).^{124,125} In all of these cases, after cyclization (**62** \rightarrow **63**), the very low reactivity of radical **63** with $(\text{TMS})_3\text{SiH}$ is overcome by the radical combination. In these reactions, the role of radicals derived from the decomposition of AIBN is twofold, i.e., to generate silyl radicals and intercept the desired radical after cyclization.

The C–Se and C–Te bonds are formed by an internal homolytic substitution of vinyl or aryl radicals at selenium or tellurium with the preparation of selenophenes and tellurophenes, respectively.¹²⁶ An example is shown below, where $(\text{TMS})_3\text{SiH}$ was used in the cyclization of vinyl iodide **65** that affords

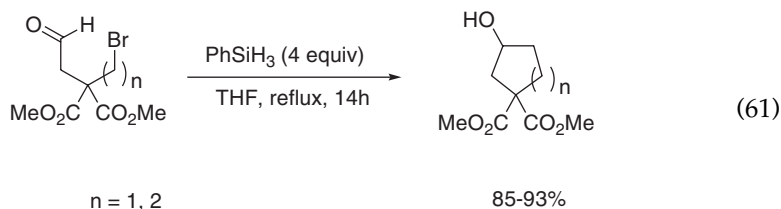
**Scheme 9**

(after concomitant dehydration) the selenophene-3-carboxylate (Reaction 60).

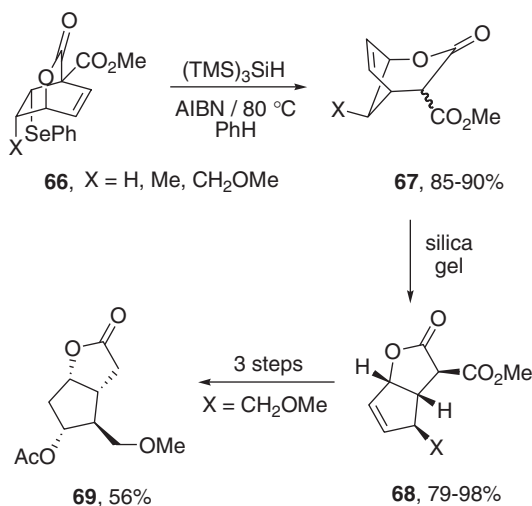


Treatment of bicyclic lactones **66**, derived from Diels–Alder reaction of 3-carboxy-2-pyrone under standard radical conditions using $(TMS)_3SiH$, leads to bridged lactones **67**, which can smoothly be converted to bicyclo[3.3.0]-lactones **68** (Scheme 10).¹²⁷ For $X = CH_2OMe$, this cascade of rearrangements took place in a 78% overall yield, providing **68** in diastereomerically pure form.¹²⁸ Three additional steps provided a novel route toward Corey's lactone **69**.

The use of silanes other than $(TMS)_3SiH$ in sequential reactions have been limited. A few selected examples are reported below. Taking advantage of the high reactivity of alkoxy radicals toward organosilanes, which is two to three orders of magnitude higher than that of primary alkyl radicals, cyclization can start from halocarbonyl compounds using $PhSiH_3$ or $(TMS)_3SiH$ (Reaction 61).¹²⁹ Both 6-*exo-trig* and 5-*exo-trig* cyclizations of alkyl radicals to the carbonyl moieties can be accomplished, with aldehydes working better than ketones.

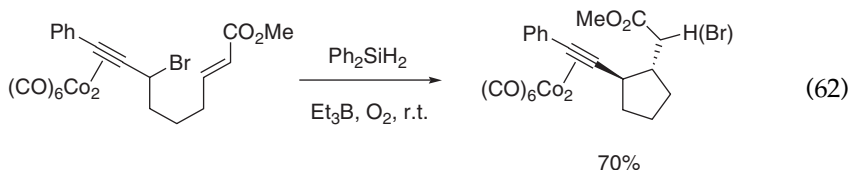


Reaction (62) reports the cyclization of a thermally unstable propargyl bromide cobalt complex mediated by Ph_2SiH_2 at room temperature and Et_3B/O_2 as the

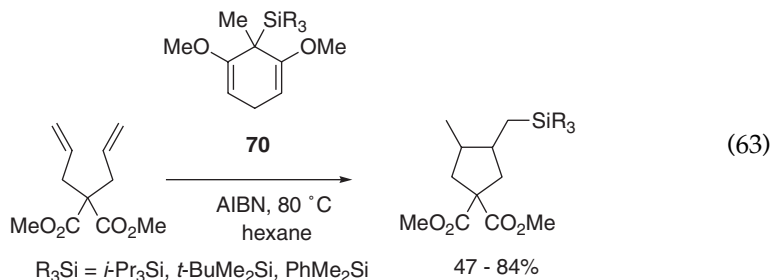


Scheme 10

radical initiator. However, a mixture of reduced and bromine atom transfer products (1:1.8 ratio) are also isolated due to the low hydrogen donating ability of the employed silane.¹³⁰

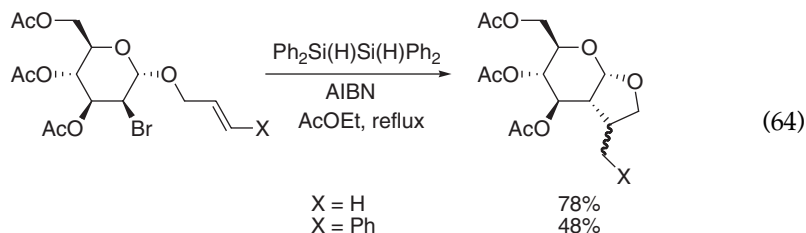


A few examples of the hydrosilylation/cyclization of dienes are given by using the silylated cyclohexadienes **70** as reagents. Reaction (63) shows the cyclization of a 1,6-diene and how flexible this methodology is to introduce any type of silyl group in reaction products.¹³¹ Yields are moderate to good and the *cis:trans* ratio of ca. 4:1 does not change substantially by the nature of the silylating group as expected.



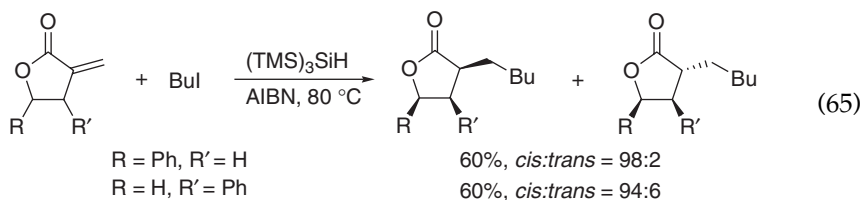
Fused cyclic ethers can be derived from appropriately substituted sugars. An example is given with the stereoselective 5-*exo* radical cyclization of allylic

2-bromo-2-deoxysugars, in the presence of 1,1,2,2-tetraphenyldisilane as the radical mediator and AIBN in refluxing ethyl acetate. The corresponding *cis*-fused bicyclic sugars have been prepared in moderate to good yields (Reaction 64).¹³²

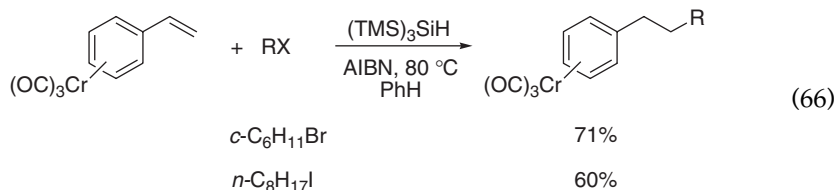


B. Intermolecular reactions

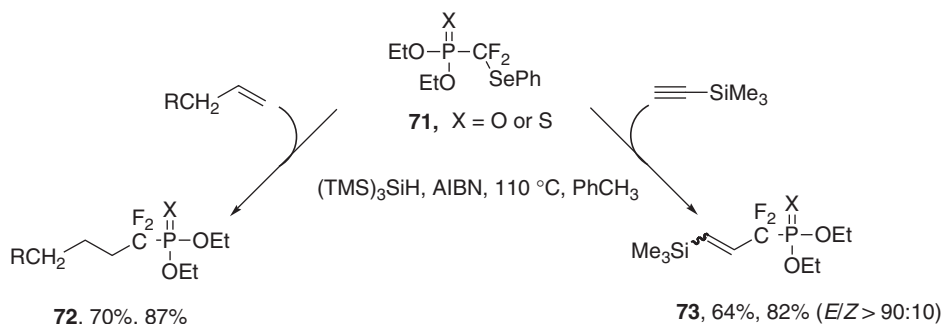
The intermolecular C–C bond formation mediated by $(\text{TMS})_3\text{SiH}$ has been the subject of several synthetically useful investigations. The effect of the bulky $(\text{TMS})_3\text{SiH}$ can be appreciated in the example of β - or γ -substituted α -methylenebutyrolactones with *n*-BuI (Reaction 65).¹³³ The formation of α,β - or α,γ -disubstituted lactones was obtained in good yields and diastereoselectivity, when one of the substituents is a phenyl ring.



Alkyl radical addition reactions to styrene chromium tricarbonyl can be accomplished using alkyl halides (10 equiv) and $(\text{TMS})_3\text{SiH}$ (5 equiv) in the presence of AIBN in refluxing benzene, for 18 h (Reaction 66).¹³⁴ These reactions are believed to proceed through intermediates in which the unpaired electron is interacting with the adjacent arene chromium tricarbonyl moiety since the analogous reaction with styrene affords only traces of addition products.



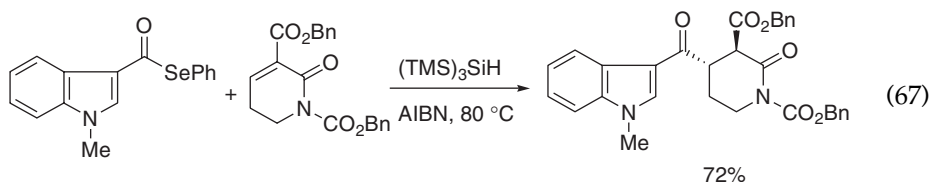
Phenylseleno derivatives **71** are found to be good precursors of phosphonodifluoromethyl and phosphonothiodifluoromethyl radicals (Scheme 11). Moreover, when generated by the $(\text{TMS})_3\text{Si}^\bullet$ attack on **71** and in the presence of alkenes or



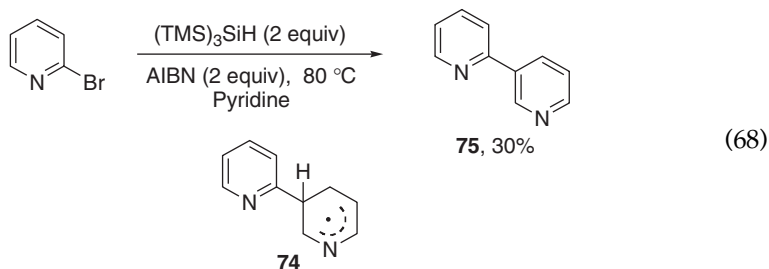
Scheme 11

alkynes, they gave access to α,α -difluorinated derivatives **72** and β,γ -unsaturated adducts **73**, *via* carbon–carbon bond formation. The phosphonothio derivatives are obtained in higher yields than phosphonates (**72** and **73**).¹³⁵

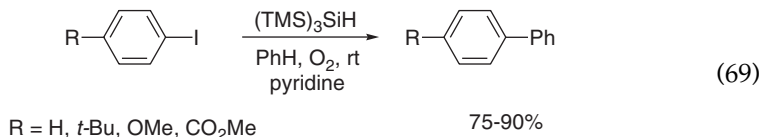
The use of $(\text{TMS})_3\text{SiH}$ with acyl selenides can also yield new C–C bond formation, as shown with the α,β -unsaturated lactam ester (Reaction 67). The resulting ketone can be envisaged as potentially useful for the synthesis of 2-acylindole alkaloids.¹³⁶ Both the effects of H-donating ability and steric hindrance by the silicon hydride are evident.



Homolytic aromatic substitution often requires high temperatures, high concentrations of initiator, long reaction times and typically occurs in moderate yields.¹³⁷ Such reactions are often conducted under reducing conditions with $(\text{TMS})_3\text{SiH}$, even though the reactions are not reductions and often finish with oxidative rearomatization. Reaction (68) shows an example where a solution containing silane (2 equiv) and AIBN (2 equiv) is slowly added (8 h) in heated pyridine containing 2-bromopyridine (1 equiv).¹³⁸ The synthesis of 2,3'-bipyridine **75** presumably occurs *via* the formation of cyclohexadienyl radicals **74** and its rearomatization by disproportionation with the alkyl radical from AIBN.¹³⁷

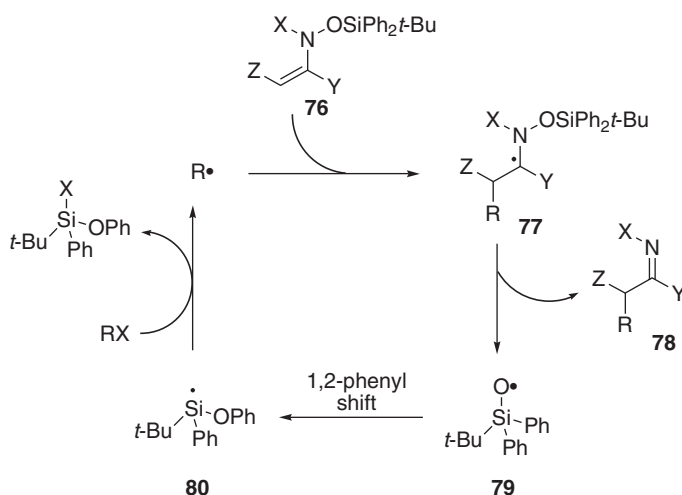


More recently, Curran and Keller found that the $(\text{TMS})_3\text{SiH}$ -mediated addition of aryl iodides to arenes are facilitated by oxidative rearomatization with oxygen (Reaction 69).¹²² Here, AIBN is not necessary for good performance of the reaction. The reaction proceeds well in both inter- and intra-molecular (see above) versions.

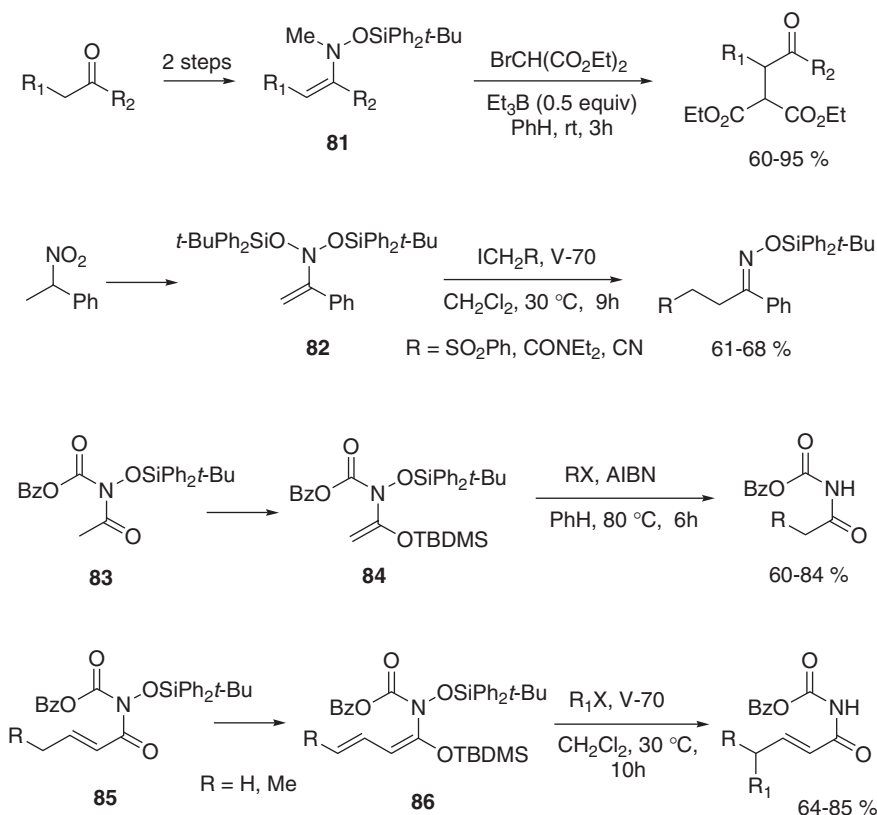


Kim and coworkers introduced silyl radical mediated addition of alkyl radical to silyloxy enamine **76**. The silyloxy enamine moiety is readily accessible from a variety of functionalities.^{139–142} The mechanistic concept is illustrated in the Scheme 12 and involves the addition of R^\bullet radical to **76** to give the radical adduct **77** and the subsequent homolytic cleavage of N–O bond to yield the desired product **78** and a silyloxy radical **79**. The latter undergoes 1,2-phenyl migration to give the silyl radical **80** that abstracts halogen from the alkyl halide to regenerate the R^\bullet radical.

The radical alkylation of ketones is achieved by their conversion into the desired *N*-silyloxy enamines **81** (Scheme 13). The reaction of **81** with diethyl bromomalonate in the presence of Et_3B (0.5 equiv) in benzene was performed in open air and stirred at room temperature for 3 h.¹³⁹ With nitro compounds it is achieved by their conversion into the desired *N*-bis(silyloxy)enamines (**82**) (Scheme 13). When the reaction is carried out with **82** and alkyl iodides with an electron-withdrawing substituent at the α -position, using V-70 as radical initiator (2,2'-azobis(4-methoxy-2,4-dimethylvaleronitrile)), it underwent a clean radical alkylation reaction to yield an oxime ether.¹⁴⁰ Successful radical alkylation of



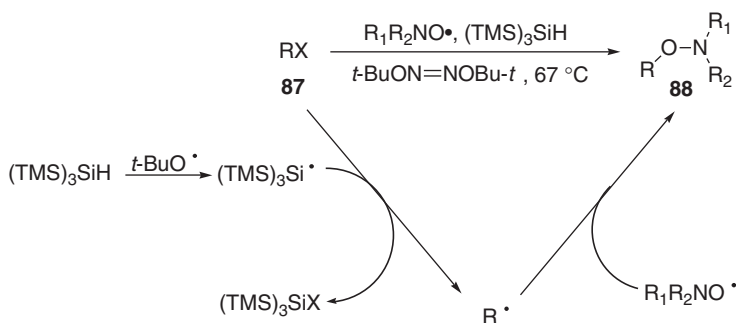
Scheme 12



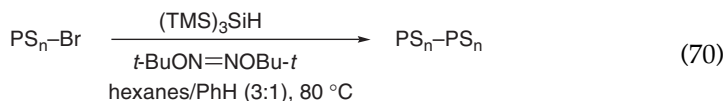
Scheme 13

carboxylic imides was obtained by an analogous approach. The imide **83** is the precursor of ketene *O,N*-acetal **84** (Scheme 13). Reaction of **84** with a variety of alkyl bromides or iodides using AIBN (0.1 equiv) as the initiator in benzene at 80 °C for 6 h afforded the alkylated imides in 60–84% yields.¹⁴¹ The last approach was extended to unsaturated carboxylic amides. The diene *O,N*-acetal **86** was prepared from the amide **85** in high yields and subsequently treated with azoinitiator V-70 to afford the desired products (Scheme 13).¹⁴²

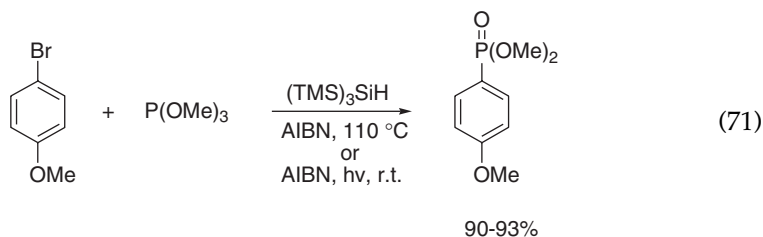
N-Alkoxyamines **88** are a class of initiators in “living” radical polymerization (Scheme 14). A new methodology for their synthesis mediated by $(TMS)_3SiH$ has been developed.¹⁴³ The method consists of the trapping of alkyl radicals generated *in situ* by stable nitroxide radicals. To accomplish this simple reaction sequence, an alkyl bromide or iodide **87** was treated with $(TMS)_3SiH$ in the presence of thermally generated *t*-BuO• radicals. The reaction is not a radical chain process and stoichiometric quantities of the radical initiator are required. This method allows the generation of a variety of carbon-centered radicals such as primary, secondary, tertiary, benzylic, allylic, and α -carbonyl, which can be trapped with various nitroxides.

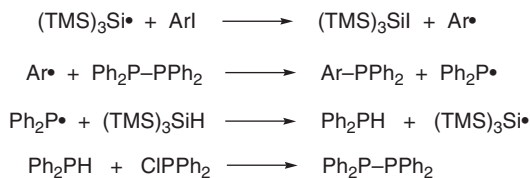
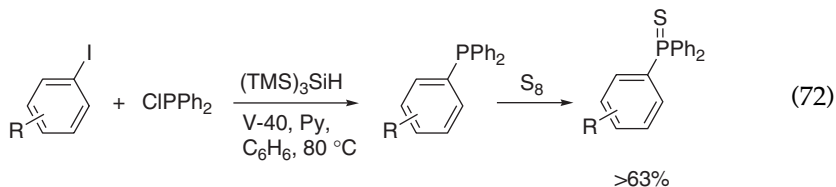
**Scheme 14**

Silane radical atom transfer (SRAA) was demonstrated as an efficient, metal-free method to generate polystyrene of controllable molecular weight and low polydispersity index values.¹⁴⁴ $(TMS)_3Si^\bullet$ radicals were generated *in situ* by reaction of $(TMS)_3SiH$ with thermally generated $t-BuO^\bullet$ radicals as depicted in Scheme 14. $(TMS)_3Si^\bullet$ radicals in the presence of polystyrene bromide (PS_n-Br), effectively abstract the bromine from the chain terminus and generate macroradicals that undergo coupling reactions (Reaction 70).

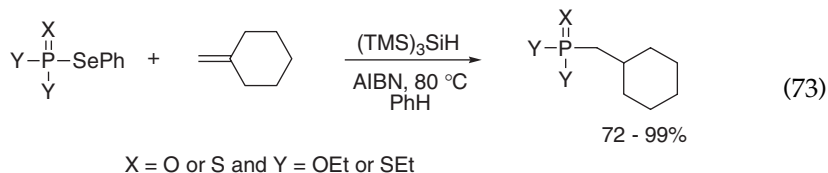


Examples of the intermolecular C–P bond formation by means of radical phosphonation¹⁴⁵ and phosphination¹⁴⁶ have been achieved by reaction of aryl halides with trialkyl phosphites and chlorodiphenylphosphine, respectively, in the presence of $(TMS)_3SiH$ under standard radical conditions. The phosphonation reaction (Reaction 71) worked well either under UV irradiation at room temperature or in refluxing toluene. The radical phosphination (Reaction 72) required pyridine in boiling benzene for 20 h. Phosphinated products were handled as phosphine sulfides. Scheme 15 shows the reaction mechanism for the phosphination procedure that involves *in situ* formation of tetraphenylbiphosphine. This approach has also been extended to the phosphination of alkyl halides and sequential radical cyclization/phosphination reaction.¹⁴⁶



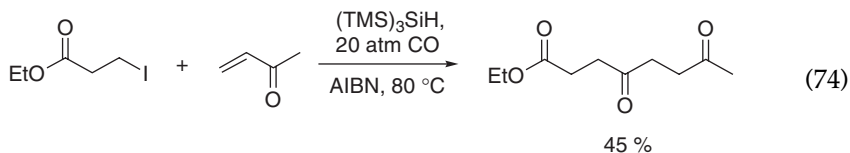
**Scheme 15**

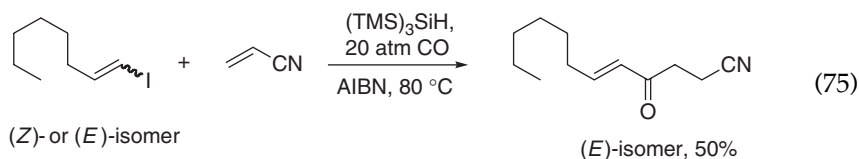
The $(\text{TMS})_3\text{SiH}$ mediated addition of phosphorus-centered radicals to a number of alkenes has been investigated in some detail. Reaction (73) is an example of phosphorous–carbon bond formation using four structurally different phenylseleno derivatives with 3 equiv of $(\text{TMS})_3\text{SiH}$ and AIBN in refluxing benzene for 2 h. Comparative studies on the reaction of the four phosphorus-centered radicals have been obtained. Although the reaction with 1-methylene cyclohexane is efficient with all four derivatives,¹⁴⁷ different selectivity is observed with electron-rich or electron-poor alkenes.



C. Tandem and cascade radical reactions

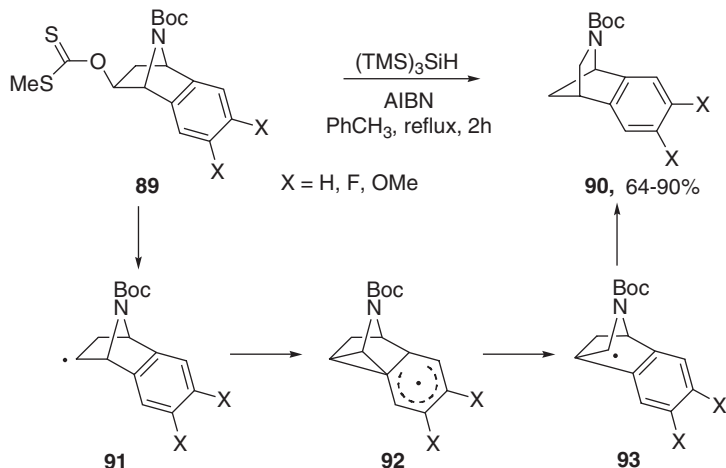
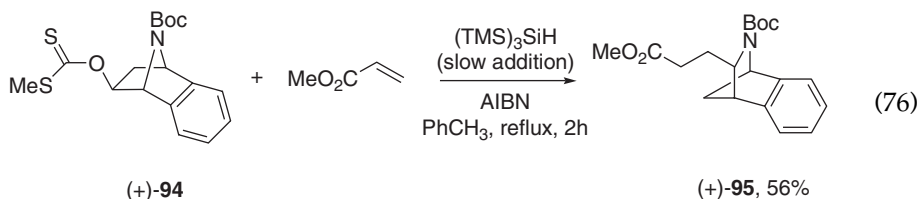
Radical-based carbonylation procedures can be advantageously mediated by $(\text{TMS})_3\text{SiH}$. Examples of three-component coupling reactions are given in Reactions (74) and (75). The cascade proceeds by the addition of an alkyl or vinyl radical onto carbon monoxide with formation of an acyl radical intermediate, which can further react with electron-deficient olefins to lead to the polyfunctionalized compounds.^{148,149}





Another reaction sequence can start from Barton–McCombie deoxygenation as in the case of 7-azabenzonorbornanols *via* xanthate derivatives **89**, using $(\text{TMS})_3\text{SiH}$ in refluxing toluene, which affords the corresponding 2-azabenzonorbornanes **90** in 64–90% yields.^{150–153} These compounds cannot be readily accessible by other means. The reaction proceeds through the neophyl-type radical rearrangement **91** \rightarrow **92** \rightarrow **93** with a rate constant of ca. 10^5 s^{-1} at 111°C for $\text{X} = \text{H}$ (Scheme 16).¹⁵¹ It was also found that the slow addition of silane in the presence of methyl acrylate (or other electron-deficient alkenes) gave good yields of rearranged trapped azacycle.

Extension of these processes to provide enantio-enriched products was successfully applied after desymmetrization of the starting materials. An example is shown below (Reaction 76), where silane-mediated xanthate deoxygenation-rearrangement-electrophile trapping afforded the conversion of (+)-**94** to (+)-**95** in 56% yield.¹⁵²

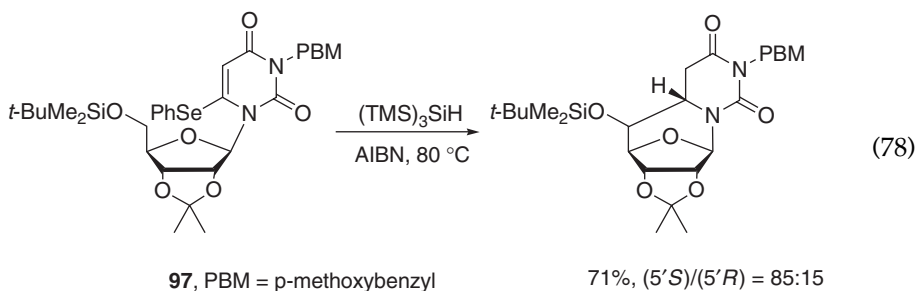


Scheme 16

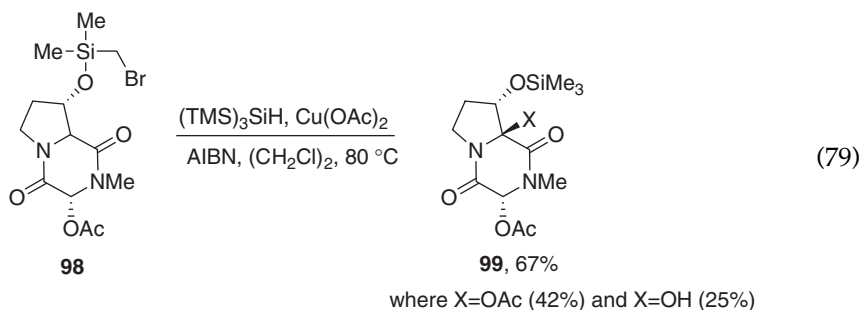
96, R = SiMe₂Bu-*t*

86%, (5'*S*)/(5'*R*) = 90:10

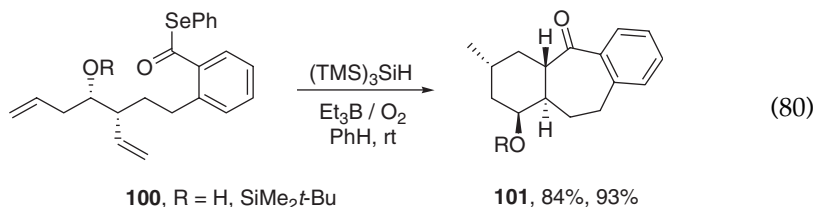
(77)



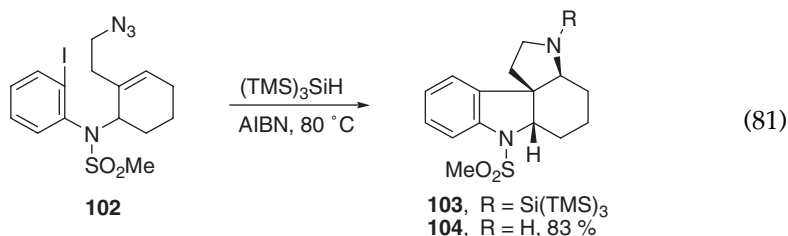
Another interesting example of radical translocation followed by oxidation, where (TMS)₃SiH proved to be the best radical mediator, is illustrated in Reaction (79).¹⁵⁶ In particular, the radical-promoted functionalization of the angular carbon was developed with the readily available bromomethylsilyl acetal **98**. Large excess of Cu(OAc)₂ (10 equiv) and AIBN (3 equiv) are required together with (TMS)₃SiH (3 equiv). The electron-rich captodative radical produced on 1,5-hydrogen atom transfer is readily oxidized by Cu(OAc)₂ to afford the desired acetate **99** in 42% yield, together with the corresponding alcohol in 25% yield. Such procedure for selective oxidation of the angular methane carbon of hydroxyproline-derivatives should be useful for oxidative elaboration of analogous molecules.



Radical cascades that feature a 7-*exo* acyl radical cyclization followed by a 6-*exo* or 5-*exo* alkyl radical cyclization proceed with very good yields and diastereoselectivities.¹⁵⁷ Two examples are shown in Reaction (80), where treatment of **100** with E_3B , air, and $(\text{TMS})_3\text{SiH}$ provided the tricycle **101** in excellent yields as a single diastereomer. Interestingly, the bulky silyl ether moiety is not required to achieve stereoselectivity in this process.

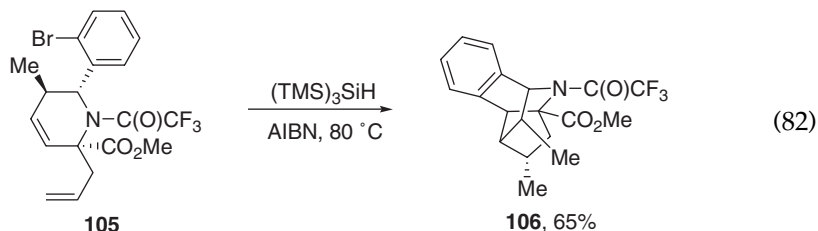


The field of alkaloid synthesis *via* tandem cyclizations favors the application of $(\text{TMS})_3\text{SiH}$ over other radical-based reagents, due to its very low toxicity and high chemoselectivity. For example, cyclization of the iodoarylazide **102**, mediated by $(\text{TMS})_3\text{SiH}$ under standard experimental conditions, produced the N-Si(TMS)₃ protected alkaloid **103** that after washing with dilute acid afforded the amine **104** in an overall 83% yield from **102** (Reaction 81).^{158–160} The formation of the labile N-Si(TMS)₃ bond was thought to arise from the reaction of the product amine **104** with the by-product $(\text{TMS})_3\text{SiI}$. The skeletons of (±)-horsfiline, (±)-aspidospermidine and (±)-vindoline have been achieved by this route.^{158–160}

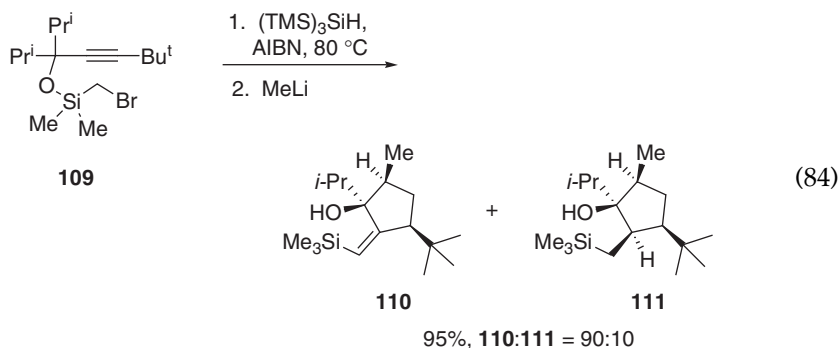
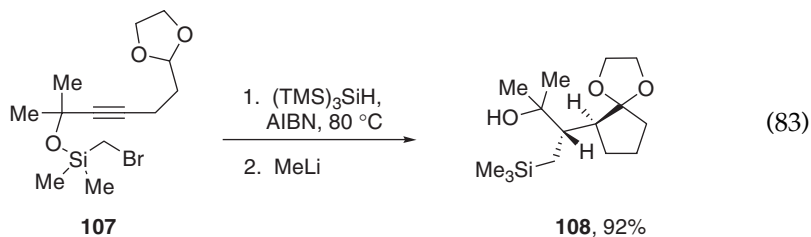


Radical cyclizations of tetrahydropyridine scaffolds have been used to access diverse skeletal frameworks.¹⁶¹ An example of tandem radical cyclizations with two C–C bond formation is shown in Reaction (82). Treatment

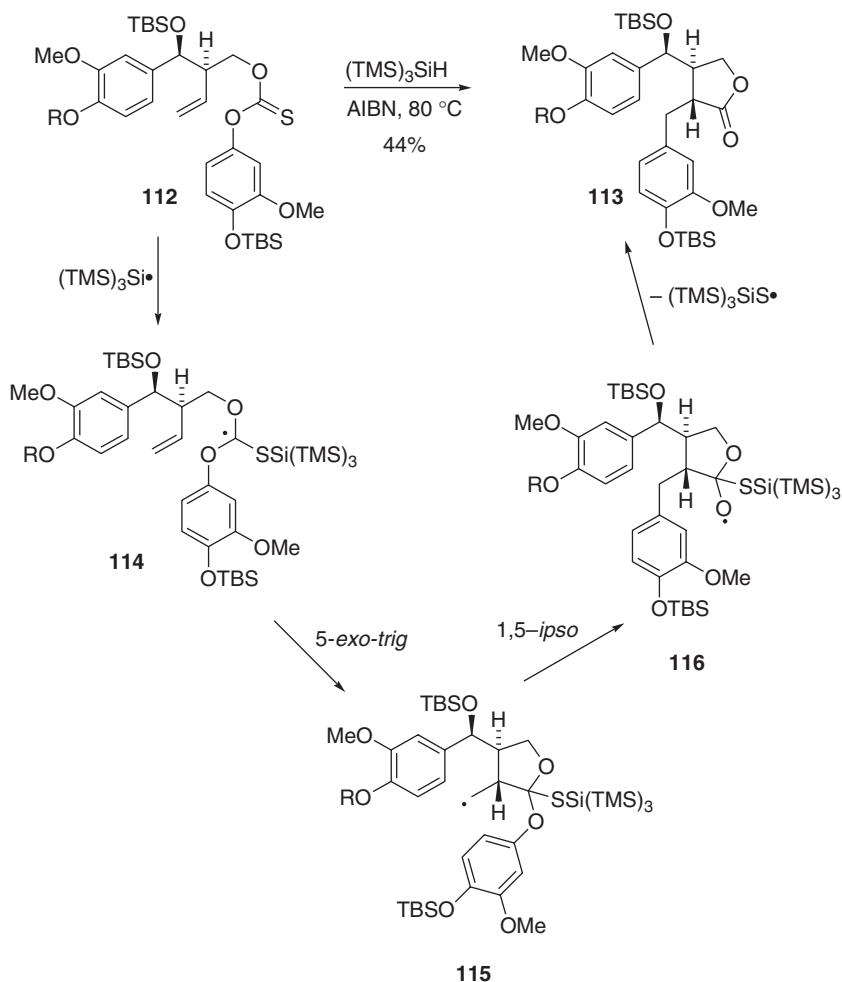
of the allylated tetrahydropyridine **105** with $(\text{TMS})_3\text{SiH}$ and AIBN in benzene at 80°C for 4 h resulted in a single diastereomer **106** in a 65% isolated yield.



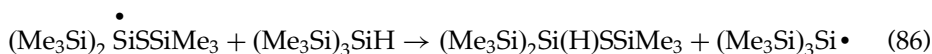
Another effective radical cascade strategy started from bromomethyltrimethylsilyl propargyl ethers.^{162–164} The synthesis of functionalized cyclopentanone **108** was achieved as a single diastereomer, starting from the reduction of bromoderivative **107** in the presence of $(\text{TMS})_3\text{SiH}$ (Reaction 83). When different substituents are used in the skeleton, as in compound **109**, a completely different reaction pattern resulted (Reaction 84).



A radical carboxyarylation approach was introduced as the key step in the total synthesis of several biologically important natural products (Scheme 17).^{165,166} Treatment of thiocarbonate derivatives **112** ($\text{R} = \text{Me}$ or TBS) with 1.1 equiv of $(\text{TMS})_3\text{SiH}$ in refluxing benzene and in the presence of AIBN (0.4 equiv added over 6 h) as radical initiator, produced compound **113** in 44% yield. This remarkable transformation resulted from a radical cascade, involving $(\text{TMS})_3\text{Si}\cdot$ radical addition to a thiocarbonyl function (**112** \rightarrow **114**), 5-*exo* cyclization (**114** \rightarrow **115**) and intramolecular 1,5-*ipso* substitution (**115** \rightarrow **116**) with the final ejection of $(\text{TMS})_3\text{SiS}\cdot$ radical.

**Scheme 17**

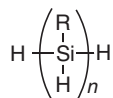
We suggest that the ejected thiyl radical undergoes a fast 1,2-migration of silyl group from silicon to sulfur (Reaction 85), affording a new silyl radical that either reacts with $(\text{TMS})_3\text{SiH}$ (Reaction 86) which completes the reaction cycle, or replaces the $(\text{TMS})_3\text{Si}\cdot$ radical in the above described reaction sequence.¹⁶⁷



V. RADICAL CHEMISTRY OF POLY(HYDROSILANE)S

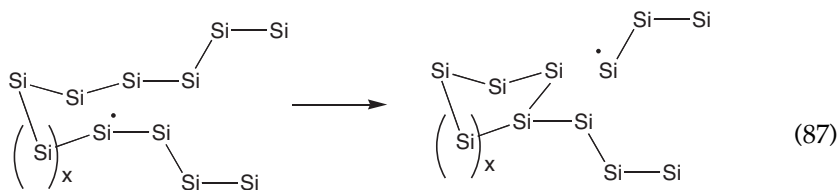
Polysilanes (or polysilylenes) consist of a silicon-catenated backbone with two substituents on each silicon atom. The two groups attached to the silicon chain

can be of a large variety.¹⁶⁸ Among the various synthetic procedures for formation of polysilanes is the dehydrogenative coupling of RSiH_3 in the presence of Group 4 metallocenes.¹⁶⁹ One of the characteristics of the products obtained by this procedure is the presence of Si–H moieties, which exhibit a rich radical-based chemistry.



117

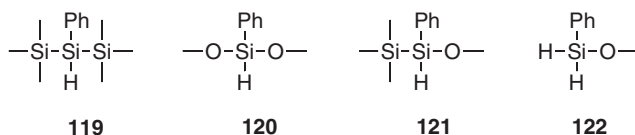
Direct evidence that a hydrogen abstraction from poly(hydrosilane)s affords the silyl radical was obtained by EPR spectroscopy.⁸⁹ Polysilane **117**, where $\text{R} = \text{Ph}$, was found to be stable on heating at 140°C for a few hours. However, in the presence of radical initiators, they decompose to give low molecular weight species, being mainly cyclic. Reaction (87) is proposed to be the key step for this radical-based degradation, in which the silyl radical **118** attacks another silicon atom in the same backbone to give a cyclic polysilane that contains an acyclic chain and another silyl radical. The last silyl radical can either cyclize or abstract a hydrogen atom from another macromolecule, thus propagating the chain degradation.⁶



where $x = 1, 2$ or 3

118

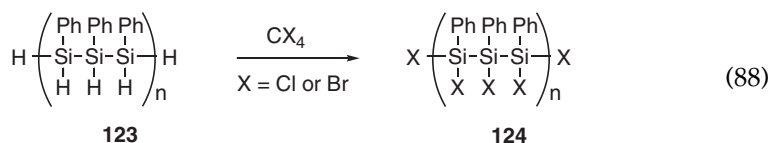
Poly(hydrosilane)s are stable compounds and can be manipulated in the air only for a short period since they are oxygen-sensitive. The oxidized products obtained from poly(phenylhydrosilane) exposed to the air contain the units **119–122** without the formation of silyl hydroperoxides and peroxides.⁸⁸ In particular, units **119**, **120**, and **121+122** were present in the relative percentages of 27, 54, and 19%, respectively, which means that more than 70% of the catenated silicons are altered.



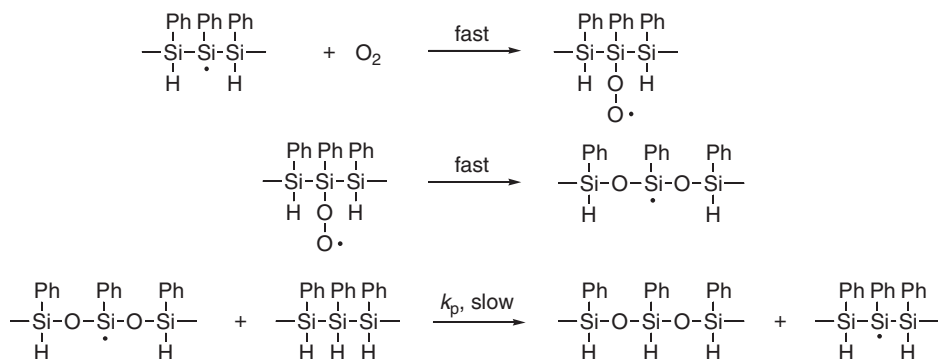
Two different kinetic approaches have been used to obtain mechanistic information about this phenomenon.^{88,170} Oxidizability values, $k_p/(2k_t)^{1/2}$, are in

the range of $(0.6\text{--}1.8) \times 10^{-2} \text{ M}^{-1/2} \text{ s}^{-1/2}$ (referring to each SiH moiety) depending on the experimental conditions and approach. The reaction rates show the following dependences: a first-order on polysilane, a zero-order on oxygen, and a half-order on the radical initiator. The chain length of oxidation is found to be relatively long ($\nu > 10$). Based on these investigations, the radical chain reactions for the oxidation of poly(phenylhydrosilane) can be described by the reaction sequence shown in **Scheme 18**, which parallels the reaction mechanism of $(\text{TMS})_3\text{SiH}$ oxidation (see **Scheme 4**). In the propagation steps, the reaction of silyl radical with oxygen should be a *fast* step and the resulting silyl peroxy radical is expected to rearrange to disilyloxysilyl radical *fast* as well, whereas the *slow* step is expected to be the hydrogen abstraction from the starting polysilane by the disilyloxysilyl radical.

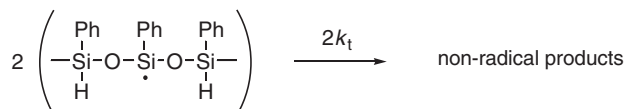
The reaction of **123** with CCl_4 or CBr_4 with room light affords the polyhalo derivative **124** (Reaction 88). For example, the replacement of Si–H moieties by Si–Cl is found to be >84 or $>95\%$ for reaction periods of 28 h and 5 days, respectively.¹⁷¹ The reactions of **124** with MeOH or MeMgBr afforded polysilanes containing Si–OMe or Si–Me moieties, respectively, whereas its reaction with LiAlH_4 regenerated the starting poly(phenylhydrosilane).



Propagation steps:



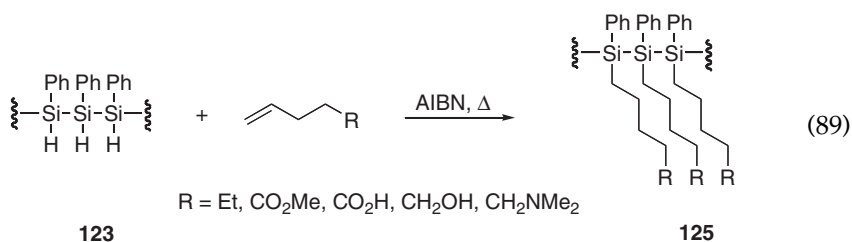
Termination steps:



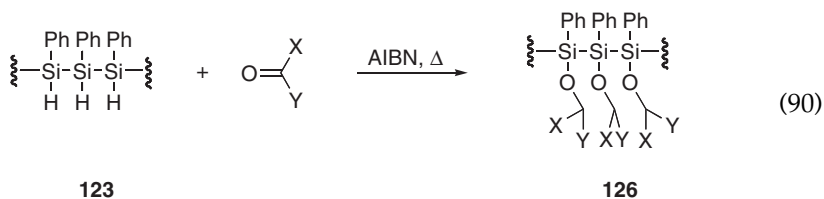
Scheme 18 The reaction mechanism for the radical chain oxidation of poly(phenylhydrosilane).

Poly(hydrosilane)s have been used as radical-based reducing agents for organic halides (RX, where X = Cl, Br, I), rivaling the effectiveness of the (TMS)₃SiH. A rate constant (k_H referring to each SiH moiety) in the range of $(5\text{--}60) \times 10^4 \text{ M}^{-1} \text{ s}^{-1}$ is estimated for the reaction of primary alkyl radicals with **123**.⁸⁹

The addition of a variety of monosubstituted olefins on poly(hydrosilane) **123** was carried out in refluxing toluene or 2,5-dimethyl-THF by using AIBN as the radical initiator.¹⁷² These reactions allowed the synthesis of functional polysilanes **125** derived from the addition of a silyl radical to the less crowded end of the double bond and with a high degree of substitution (Reaction 89). Indeed, the replacement of Si–H moieties ranged from 84 to 93%. The incorporation of polar side groups renders some of these polysilanes also soluble in water and alcohols. No examples of hydrosilylation of poly(hydrosilane)s with electron-poor olefins are reported. Probably such reactions suffer from competitive polymerization of the olefin counterpart. The addition of *gem*-disubstituted olefins, CH₂=CXY, on polysilane **123** also worked well.¹⁷² For example, the addition of 2-methoxypropene and methylenecyclohexane afforded the expected adducts with 73 and 77% degree of substitution, although a greater loss of molecular weight with respect to the hydrosilylation of monosubstituted olefins is observed.



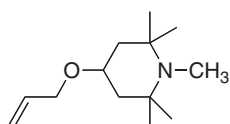
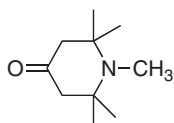
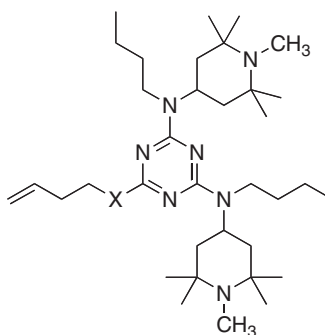
Analogous to terminal alkenes, the reaction of **123** with valeraldehyde and cyclohexanone under radical-based conditions allowed for the preparation of the corresponding functional polysilanes **126** (Reaction 90). The efficiency of Si–H bond replacement was 80–85%.¹⁷²



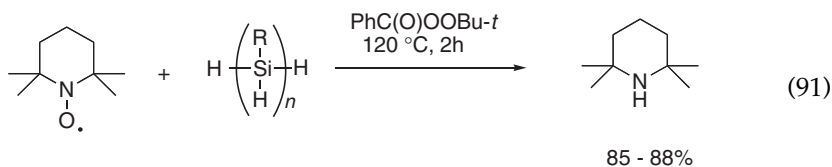
Silyl radicals generated from both phenyl and *n*-hexyl substituted poly(hydrosilane)s add readily to a variety of compounds containing C=C and O=C moieties to give the corresponding radical adducts for which EPR spectra have been recorded.⁸⁹

Poly(hydrosilane)s have been successfully applied as processing stabilizers for organic polymeric materials subject to oxidative degradation.¹⁷³ The degradation of polyolefins during processing takes place by a widely accepted

free-radical mechanism. In particular, the ability of poly(phenylhydrosilane) to stabilize polypropylene during multiple extrusion is an important finding. It is believed to be due to the combined action of the effectiveness of hydrogen donation of these polysilanes together with their capabilities to scavenge traces of oxygen present during the extrusion process. On the other hand, the introduction of sterically hindered amine groups through radical hydrosilylation of olefins or ketones allowed for the preparation of polysilanes as the stabilizer of polyolefins during their life.¹⁷⁴ The hydrosilylation was carried out with simple molecules like olefin **127** or ketone **128**, as well as with larger olefins like **129**. The degree of Si-H substitution was as high as 90%, depending on the experimental conditions. In this context, the free-radical chemistry associated with poly(hydrosilane) domains is used in conjunction with the well-known activity of hindered amines light stabilizer (HALS) in a synergistic effect.

**127****128****129**, X = O, NH

Poly(hydrosilane)s reacted with nitroxides (TEMPO) under free-radical conditions and in the absence of molecular oxygen to give the corresponding amine in good yields (Reaction 91).⁸⁸ The propagation steps for these radical chain processes are thought to be similar to those reported for the analogous reduction using (TMS)₃SiH (see Reaction 22).



VI. RADICAL CHEMISTRY ON THE SILICON SURFACES

The understanding and control of silicon surfaces is of great importance for technological applications, since the fraction of atoms residing on or near the surface becomes significant. In the last decade, much attention has been directed

toward the synthesis of organic monolayers, which can be modified on demand for specific requirements. For example, the assembly of biomolecules on silicon surfaces is of growing interest for applications in biochips and biomaterials. Several methods for preparing organic films on silicon surfaces have been developed, involving wet chemical, gas-phase, and ultrahigh vacuum approaches. Among these, radical reactions has been found to be the most convenient method for organic modifications of hydrogen-terminated silicon surfaces.^{9,10}

Structural properties of hydrogen-terminated silicon surfaces are of critical importance for their chemical behavior. Although the porous silicon (pSi) is terminated with SiH, SiH₂, and SiH₃ moieties in a variety of different local orientations and environments, the Si(111) and Si(100) are flat (single crystal) with specific orientations (Figure 2).⁹ Under ultrahigh vacuum conditions and exposure to hydrogen atoms it is possible to produce from Si(100) the so-called H-Si(100)-2 × 1 dimer surface, in which the Si-H surface bonds decrease from two per silicon to only one.^{10,175} These materials can be prepared and manipulated in air for tens of minutes as well as in a number of organic solvents. However, by prolonged exposure to air, single crystal silicon becomes coated with a thin, native oxide that can be removed chemically from Si(111) using 40% aqueous NH₄F or from Si(100) and pSi using dilute aqueous HF.

The H-Si(111) and H-Si(100)-2 × 1 have 2D rhombic and square lattices, respectively. Surface sites array in an isotropic style on H-Si(111) but adopt the anisotropic distribution on H-Si(100)-2 × 1, these properties influence

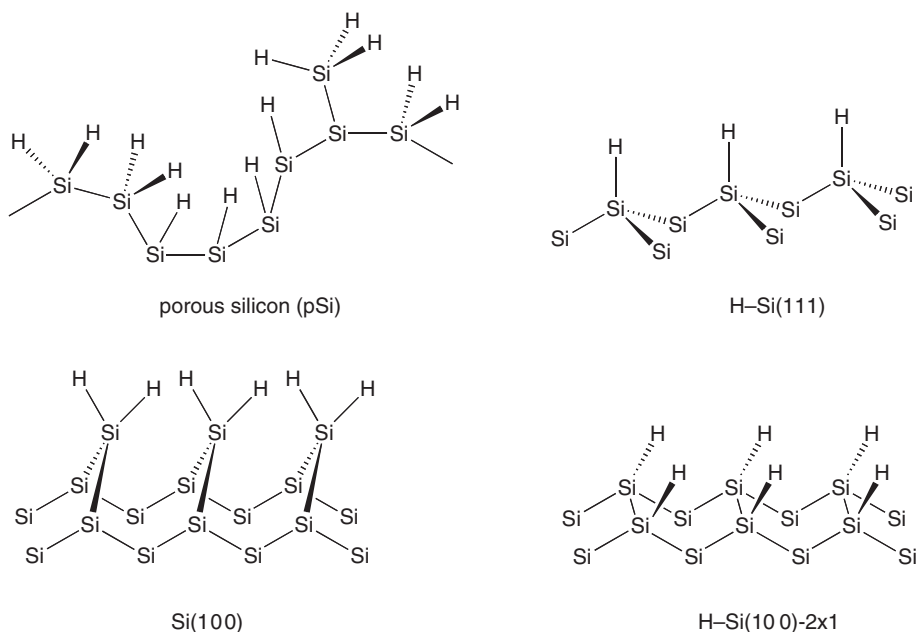


Figure 2 Hydrogen-terminated pSi, Si(111), Si(100), and Si(100)-2 × 1 surfaces.

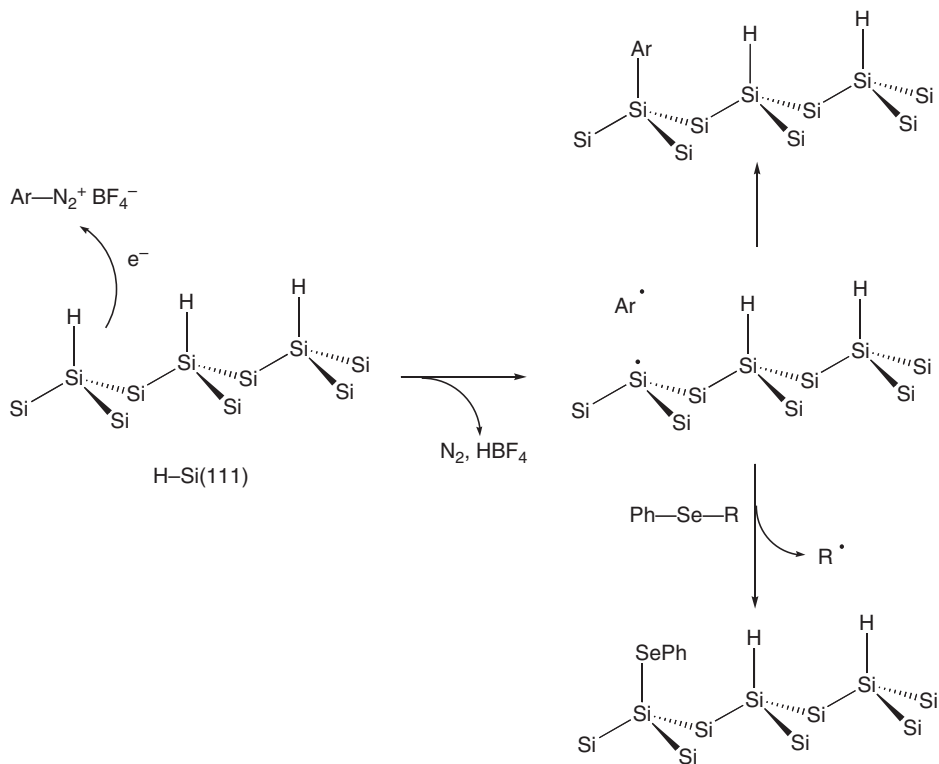
profoundly the various film structures and, consequently, the reaction outcome.¹⁷⁶ Both H-Si(111) and H-Si(100)-2 × 1 resemble (Me₃Si)₃SiH in a way that three silicon atoms are attached at the SiH moieties. For example, the H-Si(111) surface has a sharp peak at 2084 cm⁻¹ with p-polarized infrared light due to Si-H stretching absorption,¹⁷⁵ which is comparable with the $\nu_{\text{Si-H}}$ of 2052 and 2075 cm⁻¹ for (Me₃Si)₃Si-H and (Me₃Si)₂MeSi-H, respectively.⁸⁷ Therefore, it is not surprising that several of (Me₃Si)₃SiH reactions have been adopted and applied to surfaces, and that mechanistic schemes are often proposed in analogy with radical chemistry of organosilane molecules. Despite some structural similarities, the H-Si(111) has a band gap of about 1.1 eV while the highest occupied molecular orbital–lowest unoccupied molecular orbital (HOMO–LUMO) gap in the (Me₃Si)₃SiH is within 8–11 eV, which leads to significant consequences for the reactions with nucleophilic and electrophilic species.¹⁰

A. Radical reactions on H-Si(111) surfaces

The radical-based functionalization of H-Si(111) surfaces with formation of Si-heteroatom or Si-C bonds is an area of intense and active investigations. Crystalline H-Si(111) surfaces have been alkylated in a two-step chlorination/alkylation process using sterically bulky alkyl groups. The Cl-Si(111) surface was prepared by treating H-Si(111) with PCl₅ in chlorobenzene under free-radical conditions using either thermal decomposition of dibenzoyl peroxide^{177,178} or UV illumination under reflux.¹⁷⁹ The Cl-Si(111) was characterized by several spectroscopic methods and has been further used in reactions with organolithium^{177,179} or alkyl Grignard¹⁷⁸ reagents to obtain monolayer films R-Si(111). Analogously, H-Si(111) surfaces were brominated by reaction with *N*-bromosuccinimide or BrCCl₃ to give Br-Si(111) using radical initiating conditions.¹⁸⁰

When a cleaned silicon surface is exposed to 0.5 mM solution of an aryldiazonium salt in CH₃CN in the dark, over 2 h under an inert atmosphere, it afforded the grafting of the aryl group onto the silicon surface. The method is proposed to involve a 1 *e*⁻ reduction of the aryldiazonium salt to the corresponding aryl radical, which then combines with the surface-isolated silyl radical on Si(111) to yield the surface-bound aryl as shown in Scheme 19.¹⁸¹ This reaction has been successfully used as the radical initiation step for chemically binding alkyl- or arylseleno derivatives on H-Si(111) surface in a manner analogous to the chemistry of (Me₃Si)₃SiH.¹⁸² Scheme 19 also shows the proposed mechanism in the presence of a phenylseleno derivative, that allows the grafting of the PhSe group onto the silicon surface. The aryl radical derived from the diazonium salt or the alkyl radical derived from the homolytic substitution at selenium could abstract another hydrogen from the H-Si(111) surface, leading to a new silyl radical.

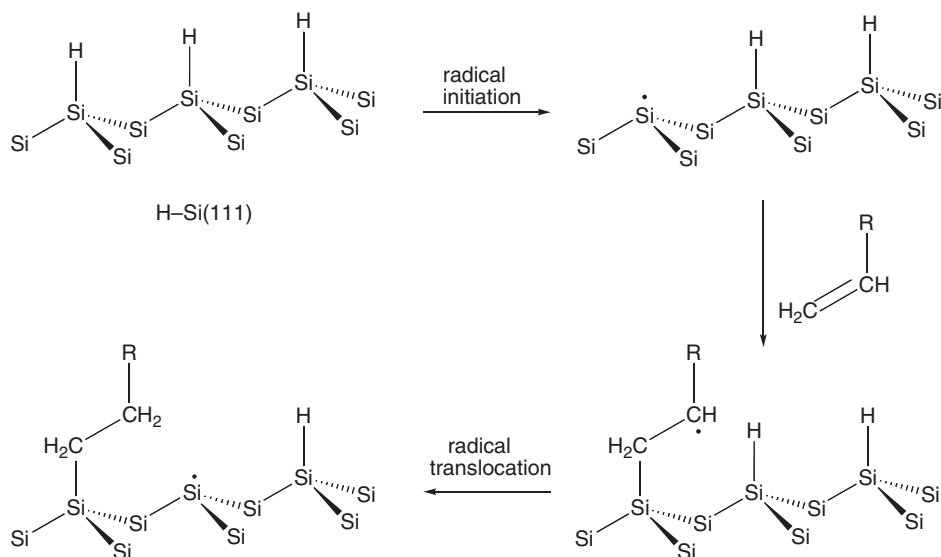
Chidsey and coworkers made pioneering works in preparing covalently bonded monolayer films on silicon surfaces by the radical-initiated reaction of 1-alkenes with the H-Si(111) surfaces.^{175,183} Reactions were carried out in neat deoxygenated alkenes using thermal decomposition of diacyl peroxides as the



Scheme 19 Aryldiazonium salt reacts spontaneously with H-Si(111) to afford modified Si(111) surfaces depending from the reaction conditions.

radical initiation. In the absence of radical initiation, it was found that the hydrosilylation process occurs either by heating at temperatures $>150^\circ\text{C}$ or by UV irradiation. Spectroscopic evidence for densely packed monolayers through Si-C linkages is provided. The modified surface, R-Si(111), could withstand exposure to boiling water, boiling CHCl_3 and sonication in CH_2Cl_2 , which also suggests chemisorption and not physisorption of the monolayer to the silicon.^{175,184} The reaction is formally a hydrosilylation process (Scheme 20).¹⁷⁵ The initially formed surface silyl radical reacts with an alkene to form a secondary alkyl radical that abstracts hydrogen from a vicinal Si-H bond thus creating another surface silyl radical. The best candidate for the radical translocation from the carbon atom of the alkyl chain to a silicon surface is the 1,5-hydrogen shift, which is also supported theoretically.¹⁷⁶ The lack of significant polymerization when styrene is used as 1-alkene, indicates the efficiency of the 1,5-hydrogen shift with respect to carbon-carbon bond formation.¹⁷⁵

Electrons from a scanning tunneling microscope (STM) in ultrahigh vacuum have been used to create surface-isolated silyl radicals on Si(111), and their exposure to styrene leads to the formation of compact islands containing multiple

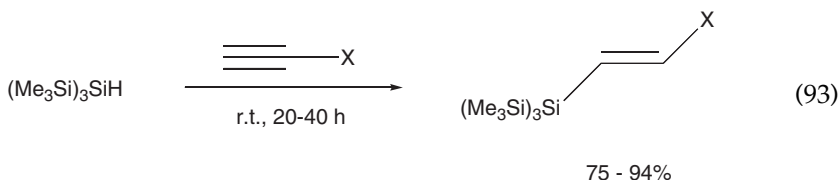
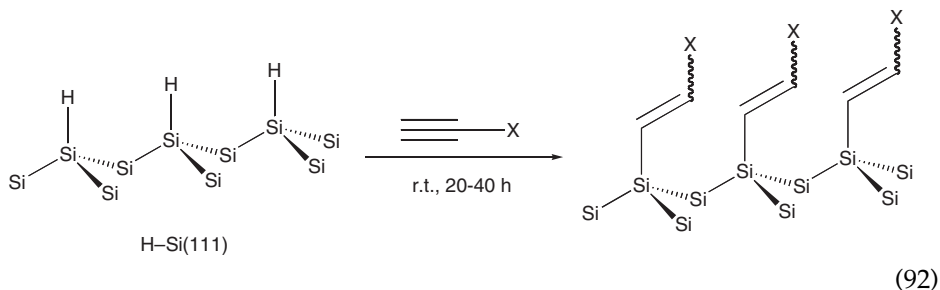


Scheme 20 Hydrosilylation of an alkene by hydrogen-terminated Si(111) surface.

styrene adsorbates bonded to the surface through individual C–Si bonds.¹⁸⁵ The formation of cluster-shaped aggregation of styrene molecules on H–Si(111) results from unidirectional chain reactions, due to the isotropic hexagonal arrangement of surface sites, and support the radical chain reaction mechanism of Scheme 20.¹⁷⁶ Molecular monolayers on H–Si(111) surfaces utilizing gas-phase photochemical reactions (UV light from a mercury lamp) were also reported. Monolayer growth can occur through either a radical chain reaction mechanism or through direct radical attachment to the silicon dangling bonds.¹⁸⁶

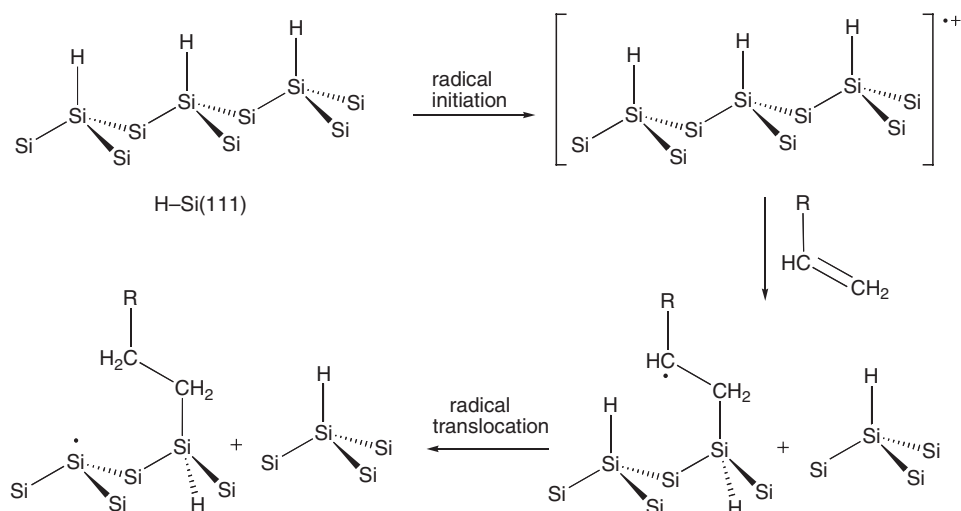
Terminal acetylenes, like 1-octyne or phenylacetylene, also form monolayers on H–Si(111) when initiated by diacyl peroxide decomposition or UV irradiation.^{175,183} Spectroscopic evidence that a vinyl group is attached on the Si surface is obtained. In this case, the proposed mechanism is a surface propagation chain reaction in which a vinyl radical, formed by the addition of alkyne to a surface silyl radical, abstracts a hydrogen atom from an adjacent site of the silicon backbone. More recently, modification of H–Si(111) surfaces by hydrosilylation of activated alkenes and alkynes has been reported in comparison with $(\text{Me}_3\text{Si})_3\text{SiH}$ under milder conditions.^{187,188} When freshly prepared H–Si(111) surfaces are immersed in neat alkene or alkyne, or $(\text{Me}_3\text{Si})_3\text{SiH}$ is mixed with neat alkene or alkyne, the hydrosilylation proceed smoothly under room light and ambient temperature. Similar results were also obtained in the dark, which suggests that the radical initiation step in both systems is caused by traces of molecular oxygen (*vide infra*). The coverage ratio of organic monolayer is estimated by X-ray photoelectron spectroscopy analysis to be from 16 to 58% for alkenes and from 31 to 56% for alkynes (Reaction 92, where $\text{X} = \text{CO}_2\text{R}$ or CN), whereas the reaction yields with $(\text{Me}_3\text{Si})_3\text{SiH}$ varied from 50 to 87% for alkene and from 75 to 94% for alkynes (Reaction 93, where

X = CO₂R or CN). Theoretical calculation at B3LYP/6-31G*//HF/STO-3G* level showed that the Si–H bond dissociation energies of H–Si(111) and (Me₃Si)₃Si–H are very similar, which further justifies the use of the well-established radical-based reactivity of (Me₃Si)₃SiH as a model for surface reactions.¹⁸⁷



To date, numerous radical-induced hydrosilylations of terminal olefins or acetylenes have been reported for the H-terminated Si(111) surfaces. These reactions are mainly performed by using thermal conditions, UV irradiation, or electrochemistry. More recently, a very mild method was developed for the attachment of high-quality organic monolayers on crystalline silicon surfaces.^{189–191} By using visible light sources, a variety of 1-alkenes and 1-alkynes were attached to H–Si(111) surfaces at room temperature. The reaction is rather flexible with regard to the wavelength of irradiation (371 to > 650 nm) and light source, and thus can avoid any light absorption by the agent that needs to be attached. The proposed mechanism for the initiation step involves a nucleophilic attack on the delocalized radical cations at the silicon surface formed on excitation (Scheme 21). Such a reaction may result in a Si–Si bond cleavage in a concerted manner, with formation of a Si-centered cation at the surface, stabilized by the neighboring Si atoms.¹⁹¹ A series of mixed monolayers derived from the mixed solutions of a 1-alkene and an ω-fluoro-1-alkene were also investigated to reveal that the composition of the mixed monolayers is directly proportional to the molar ratio of the two compounds in solutions. These extremely mild conditions are compatible with a very large variety of biologically active moieties that can be covalently linked to the reactive alkene or alkyne functionality. This method thus allows the development of patterned, (bio)active monolayers,¹⁹² via the combination of (bio)organic chemistry, surface science, and (nano)lithographic techniques.

The functionalization of H–Si(111) surface has been extended to the reaction with aldehydes. The reaction of H–Si(111) with octadecanal activated by irradiation with 150W mercury vapor lamp (21 h at 20–50 °C) afforded a well-ordered



Scheme 21 Proposed mechanism for the initiation of the light-induced hydrosilylation of an alkene.

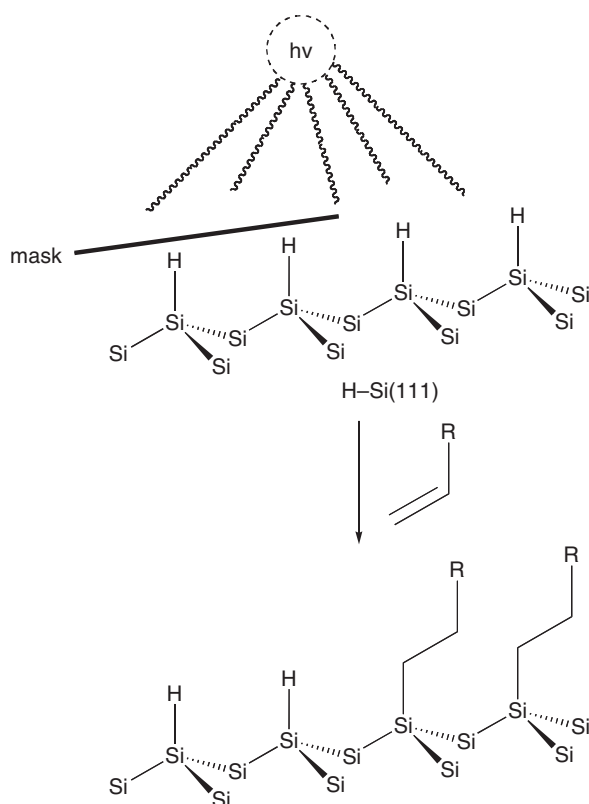


Figure 3 Schematic representation of light-promoted hydrosilylation of an alkene through masking procedure.

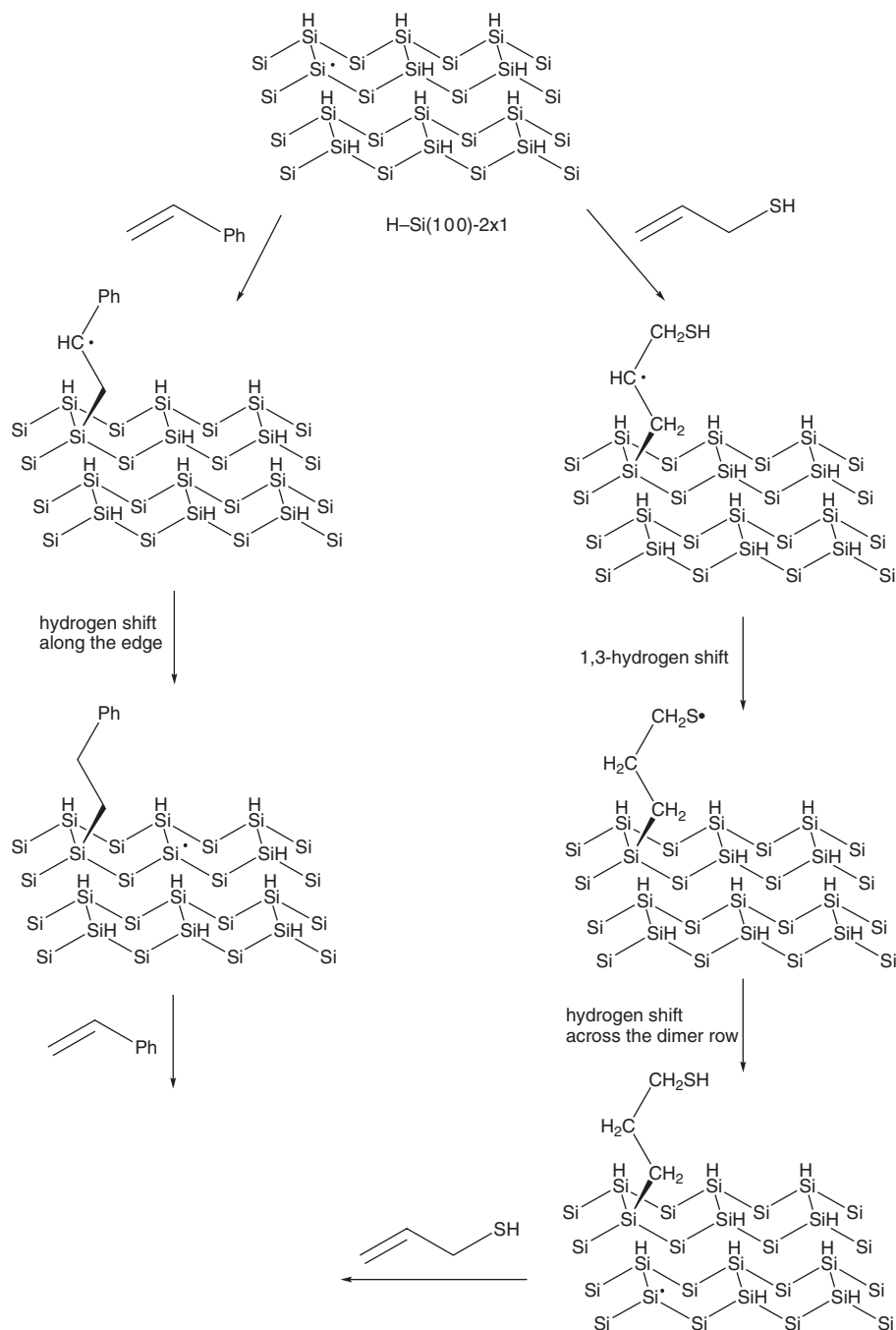
monolayer with surprisingly high coverage (97%).¹⁷⁵ Using periodic DFT calculations, the radical chain reaction mechanism has been studied for different aldehydes (formaldehyde, benzaldehyde, propanaldehyde, propenaldehyde) interacting with the H-Si(111) surface where one H vacancy is present.¹⁹³ In the case of benzaldehyde and propenaldehyde, the conjugation was found to play a crucial role in the viability of the reaction, by controlling the delocalization of the spin density of the reaction intermediate.

The ability to photoinitiate the reaction of unsaturated compounds with H-Si(111) opened the possibility of direct photopatterning of organics on the surface. Figure 3 shows schematically the light-promoted hydrosilylation with 1-alkene in the presence of a mask that can pattern the surface. The first photolithographic accomplishment to write $>100\mu\text{m}$ features, is obtained by exposure of the Si(111) surface to octadecanal and to 385 nm light through a structured mask.¹⁹⁴ It was further demonstrated that the unexposed areas, containing SiH moieties, remained completely reactive toward other radical reactions.

B. Radical reactions on H-Si(100)- 2×1 surfaces

Reactions of alkenes with H-Si(100)- 2×1 surfaces have been shown to yield films with one-dimensional (1D) molecular lines through Si-C linkages,^{195–202} contrary to formation of the islands observed on H-Si(111). The reaction can be initiated from isolated surface silyl radicals created using the tip of the STM. The STM images showed molecular lines running along and across the dimer rows depending on the chemical constituent of R in the $\text{CH}_2=\text{CH-R}$ molecules.

The proposed reaction mechanism for chain reaction along and across the dimer rows is schematically shown in Scheme 22 for styrene and allyl mercaptan, respectively.^{195,199} The first step of the reaction involves the addition of a surface silyl radical to a C=C double bond with the creation of a C-centered radical. For styrene, this radical translocates to the surface by a 1,5-hydrogen shift within the same row.¹⁹⁵ The new silicon dangling bond is now ready to accept another styrene molecule leading to the reaction along the dimer rows. The preferential growth along one edge of the silicon dimer row is also observed for vinyl ferrocene,¹⁹⁷ and long-chain alkenes (C_nH_{2n} ; $n\geq 8$).¹⁹⁸ However, evidence for reversible chain reactions in this system has been obtained by increasing the temperature from 300 to 400 K, leading to the complete desorption of the styrene line.²⁰¹ Interestingly, the reversed chain reaction was observed even at 300 K for 2,4-dimethylstyrene.²⁰¹ These results suggest that the rate of desorption plays an important role and a molecular line in an STM image is determined by the competing rates of the forward and reversed chain reactions at a given temperature. Indeed, 1-heptene, and vinyl cyclohexene did not show any line growth at 300 K,¹⁹⁸ while 1-hexene and 1-heptene have been found to undergo chain reaction with formation of a 1D molecular lines at 180 K.²⁰¹ For allyl mercaptan, the line grows across the rows.¹⁹⁹ The C-centered radical is thought initially to rearrange to a S-centered radical *via* a 1,3-hydrogen shift, followed by a radical translocation from sulfur to the silicon surface on the neighboring row. The abstraction of a H-atom from



Scheme 22 Mechanism of radical chain reactions of the growth of styrene line along the edge of a dimer (left side) and of the growth of allyl mercaptan line across the dimer rows (right side) of a $\text{H-Si}(100)\text{-}2 \times 1$ surface.

the neighboring row results in a dangling bond, which can now accept another allyl mercaptan molecule leading to the cross-row chain reaction. This cross-row line is found to be stable even at 659 K.²⁰¹ In analogy with these findings, it is worth mentioning that trimethylene sulfide produces structures that grow along dimer rows.²⁰² It was suggested that surface silyl radicals react with trimethylene sulfide leading to the formation of a Si-S bond and carbon-centered radical *via* a ring-opening.²⁰²

Thus, with variation of R in the $\text{CH}_2=\text{CH-R}$ molecules, the chain reaction can be directed along or across the dimer rows on the H-Si(100)- 2×1 surface. This strong directional preference is due to the H-Si(100)- 2×1 anisotropic type. The growth direction of chain reaction depends on the degree of delocalization of the C-centered radical, on the dispersion interactions between long alkyl chains and surface, and on the distance of the intermediate radical site from the anchoring point of the molecule.^{195–202} There are several possible H-abstraction pathways, through formation of transition states containing five-, six-, and even eight-membered ring structures were investigated with the aid of surface cluster models and density functional theory (DFT) calculations.^{176,203}

The hydrosilylation methodology of a H-Si(100)- 2×1 surface has been extended to aldehydes and ketones. The derived nanostructures bind these molecules to the surface through a strong Si-O covalent bond.²⁰⁴ For benzaldehyde and acetaldehyde, the self-directed growth allows for the formation of organic-silicon nanostructures composed of single and double lines of molecules, which suggests that the intermediate C-centered radical can reach and abstract both the nearest H-atom within the same row and the H-atom of the neighboring row. On the other hand, the acetone molecules undergo the chain reaction with a dangling-bond site resulting exclusively in single molecular lines, in which molecules are bonded to one of the Si-Si dimer atoms lying on the same side of a row, i.e., the chain reaction does not flip onto the other side in a dimer row.²⁰⁵ The cyclopropyl methyl ketone reacted at single dangling bonds to form an adduct radical, followed by ring-opening of the cyclopropyl ring prior to hydrogen abstraction from one of a variety of surface sites within the range of the radical.²⁰⁶ The surface dangling bond created by abstraction allows the process to repeat, leading to the creation of a contiguous string of molecules attached to the surface.

The rapid fabrication of covalently bonded 1D functional molecular lines with predefined location, direction, and length provides a means to make a predesigned interconnection of molecular lines running along and across the dimer rows. Indeed, the perpendicularly connected allyl mercaptan and styrene lines or allyl mercaptan and acetone lines have been fabricated on the H-Si(100)- 2×1 surface.^{200,205}

The ultrahigh vacuum STM was used to investigate the addition of the 2,2,6,6-tetramethyl-1-piperidinyloxy (TEMPO) radical to the dangling bond of Si(100)- 2×1 surface.^{207–209} The TEMPO can bond with a single dangling bond to form stable Si-O coupling products, in contrast to the thermal decomposition of TEMPO-silicon compounds. Semiempirical and DFT calculations of TEMPO bound to a three-dimer silicon cluster model yielded

occupied state density isosurfaces below the HOMO and unoccupied state densities isosurfaces above the LUMO, which is in qualitative agreement with the bias dependent STM topography. The placement of TEMPO molecules on dangling bonds was controlled with atomic precision on the surface *via* electron stimulated desorption of H atoms, demonstrating the compatibility of nitroxyl free-radical binding chemistries with nanopatterning techniques such as feedback controlled lithography.²⁰⁸ Furthermore, it was shown that the STM can be used to reform the terminal dangling bond at select molecular lines by removing TEMPO caps with local control. The ease of removal of TEMPO molecules from the surface is related to the weak covalent bond formed between TEMPO and the surface radical.

C. Radical reactions on pSi and Si_{scr} surfaces

Radical reactions on silicon surfaces have been applied for the preparation of terminal monolayers on both pSi and scribed silicon (Si_{scr}) surfaces. The Si_{scr} is believed to be similar to the reconstructed silicon surface H-Si(1 0 0)-2 × 1.²¹⁰

Monolayers on Si_{scr} have been produced by scribing in the presence of 1-alkenes, 1-alkynes, aldehydes, alkyl halides, and acid chlorides.²¹⁰ Although 1-alkenes, 1-alkynes, and aldehydes are believed to react with Si_{scr} through a [2+2] addition to produce four-membered rings,²¹⁰ alkyl halides probably react in a two-step mechanism consisting of halogen abstraction by the surface, followed by condensation of the resulting alkyl radicals with the surface to form one carbon-silicon bond.²¹¹ Similarly, Si_{scr} is proposed first to react with acid chlorides by chlorine abstraction to form Si-Cl bonds. The acyl radical formed in this process then returns to the surface to condense with a silicon radical.²¹²

Monolayers on pSi have recently been produced by radical-initiated reactions of 1-bromoalkanes and 1-alkenes. Both end-functionalized (α -bromo and ω -carboxy) compounds were assembled on the hydrogen-terminated pSi surface under microwave irradiation.²¹³ The radical coupling reaction of alkyl bromides to hydrogen-terminated pSi can be enhanced by increasing the concentration of reactants and by the involvement of initiators. This grafting strategy can be potential applicable in the fabrication of biosensors and protein chips. Indeed, the resulting carboxylic acid monolayers were converted to an amino-reactive linker, *N*-hydroxysuccinimide ester, terminated monolayers, and two proteins of bovine serum albumin and lysozyme were immobilized through amide bonds. The formation of Si-C bonded monolayers by reaction of 1-undecene with hydrogen-terminated pSi surfaces has been studied in some details.²¹⁴ The results of reactions carried out with strict control over the conditions (atmosphere, light, water) and point to the initiation of this reaction by trace amounts of oxygen. The monolayer formation occurs *via* the same radical chain process as on single-crystal surfaces: a silyl radical attacks 1-alkene to form both the Si-C bond and radical center on the β -carbon atom. This carbon-centered radical may then abstract a hydrogen atom from a neighboring Si-H bond to propagate the chain. Highly deuterated pSi and FTIR spectroscopy were used to provide evidence for this mechanism. The spontaneous reaction of

aryldiazonium salt with H-Si(111) for grafting of the aryl group onto a silicon surface¹⁸¹ (see Scheme 19) has been extended to the hydride-terminated pSi.¹⁸² This process has been also used as radical initiation step for the reaction of pSi surface with a variety reagents such as alkyl/arylselenoethers, alkenes, alkynes, and alkylbromide groups to generate covalently bound functionalities.¹⁸² Scheme 19 also shows the proposed mechanism in the presence of a phenylseleno derivative that allows for the grafting of the PhSe group onto pSi.

D. Oxidation of hydrogen-terminated silicon surfaces

It has been observed that the H-Si(111) and H_x-Si(100) surfaces develop a submonolayer oxide when exposed to an average sitting time of 1 h prior to gate oxidation in typical room air and room lighting conditions. Furthermore, the oxidation of the H-Si(111) and H_x-Si(100) surfaces occurs when they are exposed to UV light in the presence of dry air or humid air.^{175,215} Analogous experiments are reported for the photo-oxidation of pSi.²¹⁶

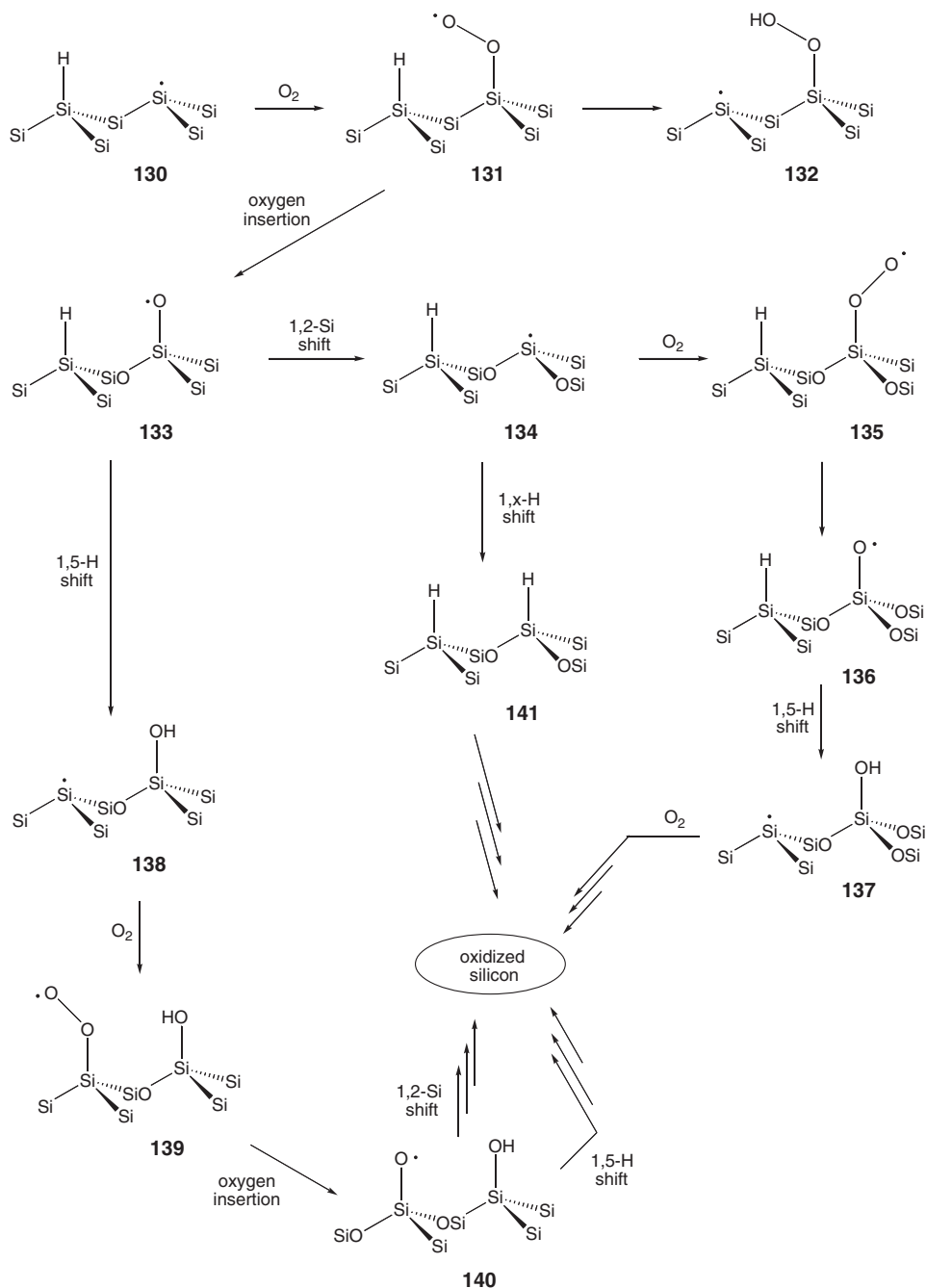
The room temperature photo-oxidation of the H-Si(111) and H_x-Si(100) indicates that both surfaces oxidize when exposed to UV light in the presence of O₂ only, H₂O only, or humid air (both O₂ and H₂O).²¹⁵ Dry air experiments show that both surfaces oxidize in UV light to an order of magnitude more than when they are exposed to 447 nm wavelength or when they are exposed to no light. It was proposed that UV light assists in the oxidation process by cleaving the H-Si surface bond, because the photon-stimulated hydrogen desorption occurs around 351 nm, which corresponds to the energy required to cleave the H-Si bond. Oxidation also occurs to both surfaces when exposed to H₂O in the presence of UV light. Experiments show that the photo-oxidation of the silicon surfaces exposed to UV light and humid air is approximately one order of magnitude greater than the photo-oxidation at similar light conditions in dry air or in water. It was proposed that the Si surface radicals, generated by UV light, can be scavenged by H₂O or O₂.

The FTIR spectra show that the photo-oxidation of H-Si(111) and pSi surfaces behave differently.^{175,216} For example, in the photolysis of H-Si(111) after 30 min with Hg lamp, the area of the $\nu_{\text{Si-H}}$ band decreases to 14%.¹⁷⁵ In case of pSi, there is a tremendous increase in $\nu_{\text{Si-O}}$, without a correspondingly large loss of $\nu_{\text{Si-H}}$ peak intensity. The decrease of the $\nu_{\text{Si-H}}$ band is offset by an increase in the $\nu_{\text{OSi-H}}$ band, resulting in no net loss of hydride species on the surface during the course of the photo-oxidation reaction. These data apparently suggest that oxidation does not result in the removal of H atoms, implying that Si-Si bonds are attacked directly.²¹⁶ However, the exposure of hydrogen-terminated silicon surfaces either to dry molecular oxygen or to deoxygenated water gives low oxide growth rates, whereas the combination of water and oxygen results in a significantly faster oxide growth rate. Indeed, infrared studies have shown that the half-life of the Si-H stretch in air of H-Si(111) surface is humidity dependent. It was suggested that the oxidation of Si-H to Si-OH by H₂O is the rate-limiting step in the native oxide formation.²¹⁷

The mechanism for the photo-oxidation of silicon surfaces is not well understood. It was suggested that surface silyl radicals (**130**), formed by UV irradiation of H-Si(111), react with oxygen to form a peroxy radical (**131**) that can abstract a neighboring hydrogen to produce a new surface dangling bond (**132**) (Scheme 23).^{175,215} How the migration of oxygen into the Si-Si backbone of the lattice occurs and how the regeneration of surface silyl radical or Si-H bond arises is not yet understood.

The mechanism reported in Scheme 23 has been proposed by Chatgililoglu in analogy with the oxidation of $(\text{Me}_3\text{Si})_3\text{Si-H}$ and poly(hydrosilane)s described earlier in this chapter.⁶ The peroxy radical **131** rearranges to silyloxy radical **133** by the oxygen insertion step, which is found to be ca. 10^4 s^{-1} for the analogous reaction in $(\text{Me}_3\text{Si})_3\text{Si-H}$. The alternative neighboring hydrogen abstraction to give **132** is expected to be much slower, as it is analogous with cumylperoxy radical hydrogen abstraction from $(\text{Me}_3\text{Si})_3\text{Si-H}$ occurring with a rate constant of $66 \text{ M}^{-1} \text{ s}^{-1}$ at 73°C . In turn radical **133** is expected to undergo a fast 1,2-silyl shift to give silyl radical **134**, which can add to oxygen to give peroxy radical **135**, followed by oxygen insertion to the remaining $\gamma(\text{Si-Si})$ bond. The resulting silyloxy radical **136** is ready to undergo 1,5-hydrogen shift to give another surface silyl radical (**137**). Radical **133** can also abstract neighboring hydrogen *via* a 6-membered transition state from the side that already inserted an oxygen atom, to give another surface silyl radical (**138**). The latter could add to oxygen to give **139** and continue the chain, eventually until there is complete oxidation of the surface. Both 1,5-hydrogen and 1,2-silyl shifts from radical **133** are expected to be very fast. The bimolecular rate constant for hydrogen abstraction from $(\text{Me}_3\text{Si})_3\text{SiH}$ by alkoxy radical is $1 \times 10^8 \text{ M}^{-1} \text{ s}^{-1}$, which suggests that the intramolecular version could be even two orders of magnitude faster. On the other hand, a rate constant $> 10^8 \text{ s}^{-1}$ is estimated for the 1,2-silyl shift in the oxidation of $(\text{Me}_3\text{Si})_3\text{SiH}$. Therefore, it is likely that the preferred path will strongly depend on entropic factors determined by the rigidity of the surface. It should also be noticed that the silyl radical **134** has two silyloxy substituents and a 1, x -H shift from a $(\text{Si})_3\text{Si-H}$ moiety is expected to be strongly exothermic. When favorable transition states are formed such 1, x -H shifts should be quite fast to give **141** (the silyl radical moiety is not shown). Therefore, the reaction mechanism for the surface oxidation given in Scheme 23 could lead to Si-OH or Si-H as terminal groups depending on the type of silicon surface.

This mechanistic proposal is also in agreement with the various spectroscopic measurements that provided evidence for a peroxy radical species on the surface of silicon during thermal oxidation.²¹⁸ The oxidation of hydrogen-terminated silicon surfaces by molecular oxygen also occurs without irradiation. The STM investigation showed that the exposure of H-Si(111) to O_2 induces surface modification that is assigned to the insertion of oxygen atom into Si-Si backbone.²¹⁹ It is not clear how silicon surface radicals can be scavenged by H_2O to form silanols (Si-OH). Results also showed that photo-oxidation is most significant when the surface is exposed to both O_2 and H_2O in the presence of UV light. This is probably due to the presence of two parallel reaction schemes that can have a synergic effect. In analogy with the proposed mechanism for the



Scheme 23 Possible mechanism for the oxidation of silicon surfaces by molecular oxygen.

light-induced hydrosilylation of terminal olefins reported in [Scheme 21](#), perhaps a nucleophilic attack by H_2O onto the delocalized radical cations at the silicon surface formed on excitation can play a role. Such a reaction may result in the formation of Si–O–Si and/or Si–OH moieties, as well as Si-centered radicals ready to add to oxygen and propagate the oxidation. Evidences that support a spontaneous reaction of O_2 with hydrogen-terminated silicon surfaces to afford surface radicals and $\text{HOO}\cdot$, in analogy with the reaction of O_2 with $(\text{Me}_3\text{Si})_3\text{SiH}$, have been reported.^{187,220}

VII. CONCLUSIONS

The synthetic application of silyl radical reactivity in the last decade has expanded considerably. Silyl radicals play an important role in diverse areas of research such as organic synthesis, material science, and polymer chemistry. Synthetic strategies using $(\text{TMS})_3\text{SiH}$ as a radical-based reducing agent have become popular among organic chemists since a wide selection of functional groups can now be used to generate carbon-centered radicals under mild conditions. Unique transformations are possible, allowing one to generate structures that would otherwise be very difficult to synthesize. The scope and breadth of $(\text{TMS})_3\text{SiH}$ utility as a mediator of consecutive radical reactions is spectacular and we are convinced that much more diverse applications are yet to come. It seems pertinent to suggest a significant role of $(\text{TMS})_3\text{SiH}$ or the $(\text{TMS})_3\text{SiH}$ /thiol couple in aqueous or heterogeneous media in future research.

The radical-based functionalization of silicon surfaces is a growing area because of the potential practical applications. Although further knowledge is needed, the scope, limitations, and mechanism of these reactions are sufficiently well understood that they can be used predictably and reliably in the modification of hydrogen-terminated silicon surfaces. The radical chemistry of $(\text{TMS})_3\text{SiH}$ has frequently served as a model in reactions of both hydrogen-terminated porous and flat silicon surfaces. We trust that the survey presented here will serve as a platform to expand silicon radical chemistry with new and exciting discoveries.

REFERENCES

- (1) Chatgililoglu, C. *Acc. Chem. Res.* **1992**, 25, 188.
- (2) Chatgililoglu, C. *Chem. Rev.* **1995**, 95, 1229.
- (3) Chatgililoglu, C.; Ferreri, C.; Gimisis, T. Tris(trimethylsilyl)silane in organic synthesis. In: Rappoport, Z.; Apeloig, Y. (Eds.), *The Chemistry of Organic Silicon Compounds*, Wiley, Chichester, **1998**; Vol. 2, Chapter 25, pp. 1539–1579.
- (4) Chatgililoglu, C.; Newcomb, M. *Adv. Organomet. Chem.* **1999**, 44, 67.
- (5) Chatgililoglu, C.; Schiesser, C. H. Silyl radicals. In: Rappoport, Z.; Apeloig, Y. (Eds.), *The Chemistry of Organic Silicon Compounds*, Wiley, Chichester, **2001**; Vol. 3, Chapter 4, pp. 341–390.
- (6) Chatgililoglu, C. *Organosilanes in Radical Chemistry*, Wiley, Chichester, **2004**.
- (7) Brazeau, J.-F. *Synlett* **2007**, 1972.
- (8) Chatgililoglu, C. *Chem. Eur. J.* **2008**, 14, 2310.

- (9) Buriak, J. M. *Chem. Rev.* **2002**, *102*, 1271.
- (10) Wayner, D. D. M.; Wolkow, R. A. *J. Chem. Soc., Perkin Trans. 2* **2002**, 23.
- (11) Chatgililoglu, C.; Dickhaut, J.; Giese, B. *J. Org. Chem.* **1991**, *56*, 6399.
- (12) Chatgililoglu, C.; Ferreri, C.; Lucarini, M.; Pedrielli, P.; Pedulli, G. F. *Organometallics* **1995**, *14*, 2672.
- (13) Rong, X. X.; Pan, H.-Q.; Dolbier, W. R. Jr.; Smart, B. E. *J. Am. Chem. Soc.* **1994**, *116*, 4521.
- (14) Varlamov, V. T.; Ferreri, C.; Chatgililoglu, C. *J. Organomet. Chem.* **2005**, *690*, 1756.
- (15) Lucarini, M.; Marchesi, E.; Pedulli, G. F.; Chatgililoglu, C. *J. Org. Chem.* **1998**, *63*, 1687.
- (16) Varlamov, V. T.; Denisov, E. T.; Chatgililoglu, C. *J. Org. Chem.* **2001**, *66*, 6317.
- (17) Chatgililoglu, C.; Rossini, S. *Bull. Soc. Chim. Fr.* **1988**, 298.
- (18) Chatgililoglu, C.; Timokhin, V. I.; Zaborovskiy, A. B.; Lutsyk, D. S.; Prystansky, R. E. *J. Chem. Soc., Perkin Trans. 2* **2000**, 577.
- (19) Zaborovskiy, A. B.; Lutsyk, D. S.; Prystansky, R. E.; Kopylets, V. I.; Timokhin, V. I.; Chatgililoglu, C. *J. Organomet. Chem.* **2004**, *689*, 2912.
- (20) Leigh, W. J.; Sluggett, G. W. *J. Am. Chem. Soc.* **1993**, *115*, 7531.
- (21) Leigh, W. J.; Sluggett, G. W. *Organometallics* **1994**, *13*, 269.
- (22) Sluggett, G. W.; Leigh, W. J. *Organometallics* **1994**, *13*, 1005.
- (23) Lalevée, J.; El-Roz, M.; Morlet-Savary, F.; Graff, B.; Allonas, X.; Fouassier, J. P. *Macromolecules* **2007**, *40*, 8527.
- (24) Al-Kaysi, R. O.; Goodman, J. L. *J. Am. Chem. Soc.* **2005**, *127*, 1620.
- (25) Hill, N. J.; West, R. *J. Organomet. Chem.* **2004**, *689*, 4165.
- (26) Haaf, M.; Schmedake, T. A.; West, R. *Acc. Chem. Res.* **2000**, *33*, 704.
- (27) Tumanskii, B.; Pine, P.; Apeloig, Y.; Hill, N. J.; West, R. *J. Am. Chem. Soc.* **2004**, *126*, 7786.
- (28) Iwamoto, T.; Masuda, H.; Ishida, S.; Kabuto, C.; Kira, M. *J. Am. Chem. Soc.* **2003**, *125*, 9300.
- (29) Naka, A.; Hill, N. J.; West, R. *Organometallics* **2004**, *23*, 6330.
- (30) Seetula, J. A.; Feng, Y.; Gutman, D.; Seakins, P. W.; Pilling, M. J. *J. Phys. Chem.* **1991**, *95*, 1658.
- (31) Kalinowski, I. J.; Gutman, D.; Krasnoperov, L. N.; Goumri, A.; Yuan, W.-J.; Marshall, P. *J. Phys. Chem.* **1994**, *98*, 9551.
- (32) Ding, L.; Marshall, P. *J. Chem. Soc., Faraday Trans.* **1993**, *89*, 419.
- (33) Bullock, W. J.; Walsh, R.; King, K. D. *J. Phys. Chem.* **1994**, *98*, 2595.
- (34) Davalos, J. Z.; Baer, T. *J. Phys. Chem. A* **2006**, *110*, 8572.
- (35) Kanabus-Kaminska, J. M.; Hawari, J. A.; Griller, D.; Chatgililoglu, C. *J. Am. Chem. Soc.* **1987**, *109*, 5267.
- (36) Kira, M.; Obata, T.; Kon, I.; Hashimoto, H.; Ichinohe, M.; Sakurai, H.; Kyushin, S.; Matsumoto, H. *Chem. Lett.* **1998**, *27*, 1097.
- (37) Sekiguchi, A.; Fukawa, T.; Nakamoto, M.; Lee, V. Y.; Ichinohe, M. *J. Am. Chem. Soc.* **2002**, *124*, 9865.
- (38) Nakamoto, M.; Fukawa, T.; Lee, V. Y.; Sekiguchi, A. *J. Am. Chem. Soc.* **2002**, *124*, 15160.
- (39) Nakamoto, M.; Fukawa, T.; Sekiguchi, A. *Chem. Lett.* **2004**, *33*, 38.
- (40) Lee, V. Y.; Sekiguchi, A. *Acc. Chem. Res.* **2007**, *40*, 410.
- (41) Bravo-Zhivotovskii, D.; Yuzefovich, M.; Sigal, N.; Korogodsky, G.; Klinkhammer, K.; Tumanskii, B.; Shames, A.; Apeloig, Y. *Angew. Chem. Int. Ed.* **2002**, *41*, 649.
- (42) Bravo-Zhivotovskii, D.; Ruderfer, I.; Melamed, S.; Botoshansky, M.; Tumanskii, B.; Apeloig, Y. *Angew. Chem. Int. Ed.* **2005**, *44*, 739.
- (43) Molev, G.; Bravo-Zhivotovskii, D.; Karni, M.; Tumanskii, B.; Botoshansky, M.; Apeloig, Y. *J. Am. Chem. Soc.* **2006**, *128*, 2784.
- (44) Bravo-Zhivotovskii, D.; Ruderfer, I.; Yuzefovich, M.; Kosa, M.; Botoshansky, M.; Tumanskii, B.; Apeloig, Y. *Organometallics* **2005**, *24*, 2698.
- (45) Chatgililoglu, C. *Helv. Chim. Acta* **2006**, *89*, 2387.
- (46) Roberts, B. P. *Chem. Soc. Rev.* **1999**, *28*, 25.
- (47) Cai, Y.; Roberts, B. P. *J. Chem. Soc., Perkin Trans. 2* **2002**, 1858.
- (48) Chatgililoglu, C.; Gimisis, T. *Chem. Commun.* **1998**, 1249.
- (49) Chatgililoglu, C.; Costantino, C.; Ferreri, C.; Gimisis, T.; Romagnoli, A.; Romeo, R. *Nucleosides Nucleotides* **1999**, *18*, 637.

- (50) Gimisis, T.; Ialongo, G.; Zamboni, M.; Chatgililoglu, C. *Tetrahedron Lett.* **1995**, 36, 6781.
- (51) Wahl, F.; Wörth, J.; Prinzbach, H. *Angew. Chem. Int. Ed. Engl.* **1993**, 32, 1722.
- (52) Snyder, S. A.; Zografos, A. L.; Lin, Y. *Angew. Chem. Int. Ed.* **2007**, 46, 8186.
- (53) Kawashima, E.; Uchida, S.; Miyahara, M.; Ishido, Y. *Tetrahedron Lett.* **1997**, 38, 7369.
- (54) Ruhland, T.; Torang, J.; Pedersen, H.; Madsen, J. C.; Bang, K. S. *Synthesis* **2005**, 1635.
- (55) Lesage, M.; Arya, P. *Synlett* **1996**, 237.
- (56) Kraft, P.; Weymuth, C.; Nussbaumer, C. *Eur. J. Org. Chem.* **2006**, 1403.
- (57) Oba, M.; Nishiyama, K. *Tetrahedron* **1994**, 50, 10193.
- (58) Paquette, L. A.; Friedrich, D.; Pinard, E.; Williams, J. P.; St. Laurent, D.; Roden, B. A. *J. Am. Chem. Soc.* **1993**, 115, 4377.
- (59) Song, B. G.; Son, B. S.; Seo, M. J.; Kim, J. K.; Lee, G.; No, Z.; Kim, H. R. *Bull. Korean Chem. Soc.* **2005**, 26, 375.
- (60) Movassaghi, M.; Schmidt, M. A. *Angew. Chem. Int. Ed.* **2007**, 46, 3725.
- (61) Alcaide, B.; Rodriguez-Vicente, A.; Sierra, M. A. *Tetrahedron Lett.* **1998**, 39, 163.
- (62) Yamaguchi, K.; Kazuta, Y.; Abe, H.; Matsuda, A.; Shuto, S. *J. Org. Chem.* **2003**, 68, 9255.
- (63) Ballestri, M.; Chatgililoglu, C.; Clark, K. B.; Griller, D.; Giese, B.; Kopping, B. *J. Org. Chem.* **1991**, 56, 678.
- (64) García de Viedma, A.; Martínez-Barrasa, V.; Burgos, C.; Luisa Izquiedro, M.; Alvarez-Builla, J. *J. Org. Chem.* **1999**, 64, 1007.
- (65) Romeo, R.; Wozniak, L. A.; Chatgililoglu, C. *Tetrahedron Lett.* **2000**, 41, 9899.
- (66) Kondoh, A.; Yorimitsu, H.; Oshima, K. *J. Am. Chem. Soc.* **2007**, 129, 4099.
- (67) Kondoh, A.; Yorimitsu, H.; Oshima, K. *J. Am. Chem. Soc.* **2007**, 129, 6996.
- (68) Lalevée, J.; Allonas, X.; Fouassier, J. P. *J. Org. Chem.* **2007**, 72, 6434.
- (69) Kopping, B.; Chatgililoglu, C.; Zehnder, M.; Giese, B. *J. Org. Chem.* **1992**, 57, 3994.
- (70) Yasuda, H.; Uenoyama, Y.; Nobuta, O.; Kobayashi, S.; Ryu, I. *Tetrahedron Lett.* **2008**, 49, 367.
- (71) Postigo, A.; Kopsov, S.; Ferreri, C.; Chatgililoglu, C. *Org. Lett.* **2007**, 9, 5159.
- (72) Wnuk, S. F.; Garcia, P. I.; Wang, Z. *Org. Lett.* **2004**, 6, 2047.
- (73) Chatgililoglu, C.; Ballestri, M.; Vecchi, D.; Curran, D. P. *Tetrahedron Lett.* **1996**, 37, 6383.
- (74) Miura, K.; Oshima, K.; Utimoto, K. *Bull. Chem. Soc. Jpn.* **1993**, 66, 2356.
- (75) Naka, A.; Ohnishi, H.; Ohshita, J.; Ikadai, J.; Kunai, A.; Ishikawa, M. *Organometallics* **2005**, 24, 5356.
- (76) Liu, Y.; Yamazaki, S.; Yamabe, S. *J. Org. Chem.* **2005**, 70, 556.
- (77) Kulicke, K. J.; Giese, B. *Synlett* **1990**, 91.
- (78) Brook, M. A.; Balduzzi, S.; Mohamed, M.; Gottardo, C. *Tetrahedron* **1999**, 55, 10027.
- (79) Chatgililoglu, C.; Guarini, A.; Guerrini, A.; Seconi, G. *J. Org. Chem.* **1992**, 57, 2207.
- (80) Chatgililoglu, C.; Ferreri, C. *Res. Chem. Intermed.* **1993**, 19, 755.
- (81) Petrov, V. A. *J. Org. Chem.* **1998**, 63, 7294.
- (82) Barton, D. H. R.; Jang, D. O.; Jaszberenyi, J. C. *Tetrahedron* **1993**, 49, 7193.
- (83) Yamazaki, O.; Togo, H.; Nogami, G.; Yokoyama, M. *Bull. Chem. Soc. Jpn.* **1997**, 70, 2519.
- (84) Gimisis, T.; Ballestri, M.; Ferreri, C.; Chatgililoglu, C.; Boukherroub, R.; Manuel, G. *Tetrahedron Lett.* **1995**, 36, 3897.
- (85) Oba, M.; Kawahara, Y.; Yamada, R.; Mizuta, H.; Nishiyama, K. *J. Chem. Soc., Perkin Trans. 2* **1996**, 1843.
- (86) Ballestri, M.; Chatgililoglu, C.; Guerra, M.; Guerrini, A.; Lucarini, M.; Seconi, G. *J. Chem. Soc., Perkin Trans. 2* **1993**, 12, 421.
- (87) Chatgililoglu, C.; Guerrini, A.; Lucarini, M. *J. Org. Chem.* **1992**, 57, 3405.
- (88) Chatgililoglu, C.; Guerrini, A.; Lucarini, M.; Pedulli, G. F.; Carrozza, P.; Da Roit, G.; Borzatta, V.; Lucchini, V. *Organometallics* **1998**, 17, 2169.
- (89) Chatgililoglu, C.; Ferreri, C.; Vecchi, D.; Lucarini, M.; Pedulli, G. F. *J. Organomet. Chem.* **1997**, 545/546, 475.
- (90) Togo, H.; Matsubayashi, S.; Yamazaki, O.; Yokoyama, M. *J. Org. Chem.* **2000**, 65, 2816.
- (91) Chatgililoglu, C.; Guerra, M.; Guerrini, A.; Seconi, G.; Clark, K. B.; Griller, D.; Kanabus-Kaminska, J.; Martinho-Simoes, J. A. *J. Org. Chem.* **1992**, 57, 2427.
- (92) Walton, J. C.; Studer, A. *Acc. Chem. Res.* **2005**, 38, 794.

- (93) Studer, A.; Amrein, S.; Schlegel, F.; Schulte, T.; Walton, J. C. *J. Am. Chem. Soc.* **2003**, *125*, 5726.
- (94) Amrein, S.; Studer, A. *Helv. Chim. Acta* **2002**, *85*, 3559.
- (95) Benati, L.; Bencivenni, G.; Leardini, R.; Minozzi, M.; Nanni, D.; Scialpi, R.; Spagnolo, P.; Zanardi, G. *J. Org. Chem.* **2006**, *71*, 5822.
- (96) Postigo, A.; Ferreri, C.; Navacchia, M. L.; Chatgililoglu, C. *Synlett* **2005**, 2854.
- (97) Dang, H.-S.; Roberts, B. P. *Tetrahedron Lett.* **1995**, *36*, 2875.
- (98) Haque, M. B.; Roberts, B. P.; Tocher, D. A. *J. Chem. Soc., Perkin Trans. 1* **1998**, 2881.
- (99) Renaud, P.; Sibi, M. P. (Eds.), *Radicals in Organic Synthesis*, Wiley-VCH, Weinheim, **2001**.
- (100) Curran, D. P.; Porter, N. A.; Giese, B. *Stereochemistry of Radical Reactions: Concepts, Guidelines, and Synthetic Applications*, VCH, Weinheim, **1996**.
- (101) Nicolaou, K. C.; Sasmal, P. K.; Roecker, A. J.; Sun, X.-W.; Mandal, S.; Converso, A. *Angew. Chem. Int. Ed.* **2005**, *44*, 3443.
- (102) Nicolaou, K. C.; Sasmal, P. K.; Koftis, T. V.; Converso, A.; Loizidou, E.; Kaiser, F.; Roecker, A. J.; Dellios, C. C.; Sun, X.-W.; Petrovic, G. *Angew. Chem. Int. Ed.* **2005**, *44*, 3447.
- (103) Usui, S.; Paquette, L. A. *Tetrahedron Lett.* **1999**, *40*, 3495.
- (104) Maulide, N.; Markó, I. E. *Chem. Commun.* **2006**, 1200.
- (105) Lee, E.; Choi, S. J. *Org. Lett.* **1999**, *1*, 1127.
- (106) Sugimoto, H.; Kobayashi, M.; Nakamura, S.; Toru, T. *Tetrahedron Lett.* **2004**, *45*, 4213.
- (107) Hartung, J.; Kneuer, R.; Rumme, C.; Bringmann, G. *J. Am. Chem. Soc.* **2004**, *126*, 12121.
- (108) Sasaki, K.; Kondo, Y.; Maruoka, K. *Angew. Chem. Int. Ed.* **2001**, *40*, 411.
- (109) Ooi, T.; Hokke, Y.; Maruoka, K. *Angew. Chem. Int. Ed. Engl.* **1997**, *36*, 1181.
- (110) Evans, P. A.; Murthy, V. S.; Roseman, J. D.; Rheingold, A. L. *Angew. Chem. Int. Ed.* **1999**, *38*, 3175.
- (111) Evans, P. A.; Roseman, J. D.; Garber, L. T. *J. Org. Chem.* **1996**, *61*, 4880.
- (112) Miyabe, H.; Tanaka, H.; Naito, T. *Chem. Pharm. Bull.* **2004**, *52*, 74.
- (113) Gandon, L. A.; Russell, A. G.; Snaith, J. S. *Org. Biomol. Chem.* **2004**, *2*, 2270.
- (114) Gandon, L. A.; Russell, A. G.; Guveli, T.; Brodewolf, A. E.; Kariuki, B. M.; Spencer, N.; Snaith, J. S. *J. Org. Chem.* **2006**, *71*, 5198.
- (115) Kim, S. *Pure Appl. Chem.* **1996**, *68*, 623.
- (116) Zhou, A.; Njogu, M. N.; Pittman, C. U. *Tetrahedron* **2006**, *62*, 4093.
- (117) Bressy, C.; Menant, C.; Piva, O. *Synlett* **2005**, 12, 577.
- (118) Rahier, N. J.; Cheng, K.; Gao, R.; Eisenhauer, B. M.; Hecht, S. M. *Org. Lett.* **2005**, *7*, 835.
- (119) Bennasar, M.-L.; Roca, T.; Ferrando, F. *Org. Lett.* **2006**, *8*, 561.
- (120) Harrowven, D. C.; Woodcock, T.; Howes, P. D. *Angew. Chem. Int. Ed.* **2005**, *44*, 3899.
- (121) de Turiso, F. G.-L.; Curran, D. P. *Org. Lett.* **2005**, *7*, 151.
- (122) Curran, D. P.; Keller, A. I. *J. Am. Chem. Soc.* **2006**, *128*, 13706.
- (123) Navacchia, M. L.; Manetto, A.; Montevicchi, P. C.; Chatgililoglu, C. *Eur. J. Org. Chem.* **2005**, 4640.
- (124) Alajarin, M.; Vidal, A.; Ortin, M.-M.; Bautista, D. *New J. Chem.* **2004**, *28*, 570.
- (125) Alajarin, M.; Vidal, A.; Ortin, M.-M.; Bautista, D. *Synlett* **2004**, 991.
- (126) Schiesser, C. H. *Chem. Commun.* **2006**, 4055.
- (127) Markó, I. E.; Warriner, S. L.; Augustyns, B. *Org. Lett.* **2000**, *2*, 3123.
- (128) Augustyns, B.; Maulide, N.; Markó, I. E. *Tetrahedron Lett.* **2005**, *46*, 3895.
- (129) Batey, R. A.; MacKay, D. B. *Tetrahedron Lett.* **1998**, *39*, 7267.
- (130) Salazar, K. L.; Nicholas, K. M. *Tetrahedron* **2000**, *56*, 2211.
- (131) Amrein, S.; Timmermann, A.; Studer, A. *Org. Lett.* **2001**, *3*, 2357.
- (132) Yamazaki, O.; Yamaguchi, K.; Yokoyama, M.; Togo, H. *J. Org. Chem.* **2000**, *65*, 5440.
- (133) Urabe, H.; Kobayashi, K.; Sato, F. *J. Chem. Soc., Chem. Commun.* **1995**, 1043.
- (134) Byers, J. H.; Janson, N. J. *Org. Lett.* **2006**, *8*, 3453.
- (135) Pignard, S.; Lopin, C.; Gouhier, G.; Piettre, S. R. *J. Org. Chem.* **2006**, *71*, 31.
- (136) Bennasar, M.-L.; Roca, T.; Grier, R.; Bassa, M.; Bosch, J. *J. Org. Chem.* **2002**, *67*, 6268.
- (137) Beckwith, A. L. J.; Bowry, V. W.; Bowman, W. R.; Mann, E.; Parr, J.; Storey, J. M. D. *Angew. Chem. Int. Ed.* **2004**, *43*, 95.
- (138) Nunez, A.; Sanchez, A.; Burgos, C.; Alvarez-Builla, J. *Tetrahedron* **2004**, *60*, 6217.
- (139) Song, H.-J.; Lim, C. J.; Lee, S.; Kim, S. *Chem. Commun.* **2006**, 2893.

- (140) Lee, J. Y.; Hong, Y.-T.; Kim, S. *Angew. Chem. Int. Ed.* **2006**, *45*, 6182.
- (141) Kim, S.; Lim, C. J.; Song, C.; Chung, W. J. *Am. Chem. Soc.* **2002**, *124*, 14306.
- (142) Kim, S.; Lim, C. J. *Angew. Chem. Int. Ed.* **2004**, *43*, 5378.
- (143) Braslau, R.; Tsimelzon, A.; Gewandter, J. *Org. Lett.* **2004**, *6*, 2233.
- (144) Thakur, S.; Tillman, E. S. J. *Polym. Sci. [A]* **2007**, *45*, 3488.
- (145) Jiao, X.-Y.; Bentrude, W. G. J. *Org. Chem.* **2003**, *68*, 3303.
- (146) Sato, A.; Yorimitsu, H.; Oshima, K. J. *Am. Chem. Soc.* **2006**, *128*, 4240.
- (147) Lopin, C.; Gouhier, G.; Gautier, A.; Piettre, S. R. J. *Org. Chem.* **2003**, *68*, 9916.
- (148) Ryu, I.; Sonoda, N. *Angew. Chem. Int. Ed. Engl.* **1996**, *35*, 1050.
- (149) Chatgililoglu, C.; Crich, D.; Komatsu, M.; Ryu, I. *Chem. Rev.* **1999**, *99*, 1991.
- (150) Hodgson, D. M.; Bebbington, M. W. P.; Willis, P. *Org. Lett.* **2002**, *4*, 4353.
- (151) Hodgson, D. M.; Bebbington, M. W. P.; Willis, P. *Org. Biomol. Chem.* **2003**, *1*, 3787.
- (152) Hodgson, D. M.; Winning, L. H. *Synlett* **2006**, 2476.
- (153) Hodgson, D. M.; Winning, L. H. *Org. Biomol. Chem.* **2007**, *5*, 3071.
- (154) Navacchia, M. L.; Chatgililoglu, C.; Montevecchi, P. M. J. *Org. Chem.* **2006**, *71*, 4445.
- (155) Yoshimura, Y.; Yamazaki, Y.; Wachi, K.; Satoh, S.; Takahata, K. *Synlett* **2007**, 111.
- (156) Overman, L. E.; Sato, T. *Org. Lett.* **2007**, *9*, 5267.
- (157) Grant, S. W.; Zhu, K.; Zhang, Y.; Castle, S. L. *Org. Lett.* **2006**, *8*, 1867.
- (158) Kizil, M.; Patro, B.; Callaghan, O.; Murphy, J. A.; Hursthouse, M. B.; Hibbs, D. J. *Org. Chem.* **1999**, *64*, 7856.
- (159) Zhou, S.; Bommeziijn, S.; Murphy, J. A. *Org. Lett.* **2002**, *4*, 443.
- (160) Lizos, D. E.; Murphy, J. A. *Org. Biomol. Chem.* **2003**, *1*, 117.
- (161) Dandapani, S.; Duduta, M.; Panek, J. S.; Porco, J. A. Jr. *Org. Lett.* **2007**, *9*, 3849.
- (162) Bogen, S.; Journet, M.; Malacria, M. *Synlett* **1994**, 958.
- (163) Bogen, S.; Malacria, M. J. *Am. Chem. Soc.* **1996**, *118*, 3992.
- (164) Bogen, S.; Gulea, M.; Fensterbank, L.; Malacria, M. J. *Org. Chem.* **1999**, *64*, 4920.
- (165) Reynolds, A. J.; Scott, A. J.; Turner, C. I.; Sherburn, M. S. J. *Am. Chem. Soc.* **2003**, *125*, 12108.
- (166) Fischer, J.; Reynolds, A. J.; Sharp, L. A.; Sherburn, M. S. *Org. Lett.* **2004**, *6*, 1345.
- (167) Ballestri, M.; Chatgililoglu, C.; Seconi, G. J. *Organomet. Chem.* **1991**, *408*, C1.
- (168) West, R. "Polysilanes: Conformations, chromotropism and conductivity". In: Rappoport, Z.; Apeloig, Y. (Eds.), *The Chemistry of Organic Silicon Compounds*, Wiley, Chichester, **2001**; Vol. 3, pp. 541–563.
- (169) Tilley, T. D. *Acc. Chem. Res.* **1993**, *26*, 22.
- (170) Zaborovskiy, A. B.; Timokhin, V. I.; Chatgililoglu, C. *Polym. Sci. A* **2003**, *45*, 612.
- (171) Banovetz, J. P.; Hsiao, Y.-L.; Waymouth, R. M. J. *Am. Chem. Soc.* **1993**, *115*, 2540.
- (172) Hsiao, Y.-L.; Waymouth, R. M. J. *Am. Chem. Soc.* **1994**, *116*, 9779.
- (173) Carrozza, P.; Borzatta, V.; Chatgililoglu, C. US Patent 6005036, 1999.
- (174) Carrozza, P.; Borzatta, V.; Da Roit, G.; Chatgililoglu, C. US Patent 6538055, 2003.
- (175) Cicero, R. L.; Linford, M. R.; Chidsey, C. E. D. *Langmuir* **2000**, *16*, 5688.
- (176) Pei, Y.; Ma, J. *Langmuir* **2006**, *22*, 3040.
- (177) Bansal, A.; Li, X.; Lauermaann, I.; Lewis, N. S.; Yi, S. I.; Weinberg, W. H. J. *Am. Chem. Soc.* **1996**, *118*, 7225.
- (178) Nemanick, E. J.; Hurley, P. T.; Brunschwig, B. S.; Lewis, N. S. J. *Phys. Chem. B* **2006**, *110*, 14800.
- (179) Okubo, T.; Tsuchiya, H.; Sadakata, M.; Yasuda, T.; Tanaka, K. *Appl. Surf. Sci.* **2001**, *171*, 252.
- (180) He, J.; Patitsas, S. N.; Preston, K. F.; Wolkow, R. A.; Wayner, D. D. M. *Chem. Phys. Lett.* **1998**, *286*, 508.
- (181) Stewart, M. P.; Maya, F.; Kosynkin, D. V.; Dirk, S. M.; Stapleton, J. J.; McGuinness, C. L.; Allara, D. L.; Tour, J. M. J. *Am. Chem. Soc.* **2004**, *126*, 370.
- (182) Wang, D.; Buriak, J. M. *Langmuir* **2006**, *22*, 6214.
- (183) Linford, M. R.; Fenter, P.; Eisenberger, P. M.; Chidsey, C. E. D. J. *Am. Chem. Soc.* **1995**, *117*, 3145.
- (184) Terry, J.; Linford, M. R.; Wigren, C.; Cao, R.; Pianetta, P.; Chidsey, C. E. D. *Appl. Phys. Lett.* **1997**, *71*, 1056.
- (185) Cicero, R. L.; Chidsey, C. E. D.; Lopinski, G. P.; Wayner, D. D. M.; Wolkow, R. A. *Langmuir* **2002**, *18*, 305.
- (186) Eves, B. J.; Lopinski, G. P. *Langmuir* **2006**, *22*, 3180.

- (187) Liu, Y.; Yamazaki, S.; Yamabe, S.; Nakato, Y. *J. Mater. Chem.* **2005**, *15*, 4906.
- (188) Liu, Y.; Yamazaki, S.; Izuhara, S. *J. Organomet. Chem.* **2006**, *691*, 5821.
- (189) Sun, Q.-Y.; de Smet, L. C. P. M.; van Lagen, B.; Wright, A.; Zuilhof, H.; Sudhölter, E. J. R. *Angew. Chem. Int. Ed.* **2004**, *43*, 1352.
- (190) Eves, B. J.; Sun, Q.-Y.; Lopinski, G. P.; Zuilhof, H. J. *Am. Chem. Soc.* **2004**, *126*, 14318.
- (191) Sun, Q.-Y.; de Smet, L. C. P. M.; van Lagen, B.; Giesbers, M.; Thüne, P.; van Engelenburg, J.; de Wolf, F. A.; Zuilhof, H.; Sudhölter, E. J. R. *J. Am. Chem. Soc.* **2005**, *127*, 2514.
- (192) de Smet, L. C. P. M.; Stork, G. A.; Hurenkamp, G. H. F.; Sun, Q.-Y.; Topal, H.; Vronen, P. J. E.; Sieval, A. B.; Wright, A.; Visser, G. M.; Zuilhof, H.; Sudhölter, E. J. R. *J. Am. Chem. Soc.* **2003**, *125*, 13916.
- (193) Kanai, Y.; Takeuchi, N.; Car, R.; Selloni, A. *J. Phys. Chem. B* **2005**, *109*, 18889.
- (194) Effenberger, F.; Götz, G.; Bidlingmaier, B.; Wezstein, M. *Angew. Chem. Int. Ed.* **1998**, *37*, 2462.
- (195) Lopinski, G. P.; Wayner, D. D. M.; Wolkow, R. A. *Nature* **2000**, *406*, 48.
- (196) Piva, P. G.; DiLabio, G. A.; Pitters, J. L.; Zikovsky, J.; Rezeq, M.; Dogel, S.; Hofer, W. A.; Wolkow, R. A. *Nature* **2005**, *435*, 658.
- (197) Kruse, P.; Johnson, E. R.; DiLabio, G. A.; Wolkow, R. A. *Nano Lett.* **2002**, *2*, 807.
- (198) DiLabio, G. A.; Piva, P. G.; Kruse, P.; Wolkow, R. A. *J. Am. Chem. Soc.* **2004**, *126*, 16048.
- (199) Md. Hossain, Z.; Kato, H. S.; Kawai, M. *J. Am. Chem. Soc.* **2005**, *127*, 15030.
- (200) Md. Hossain, Z.; Kato, H. S.; Kawai, M. *J. Phys. Chem. B* **2005**, *109*, 23129.
- (201) Md. Hossain, Z.; Kato, H. S.; Kawai, M. *J. Am. Chem. Soc.* **2007**, *129*, 3328.
- (202) Dogel, S. A.; DiLabio, G. A.; Zikovsky, J.; Pitters, J. L.; Wolkow, R. A. *J. Phys. Chem. C* **2007**, *111*, 11965.
- (203) Pei, Y.; Ma, J. *J. Phys. Chem. C* **2007**, *111*, 5486.
- (204) Pitters, J. L.; Dogel, I.; DiLabio, G. A.; Wolkow, R. A. *J. Phys. Chem. B* **2006**, *110*, 2159.
- (205) Md. Hossain, Z.; Kato, H. S.; Kawai, M. *J. Am. Chem. Soc.* **2007**, *129*, 12304.
- (206) Tong, X.; DiLabio, G. A.; Clarkin, O. J.; Wolkow, R. A. *Nano Lett.* **2004**, *4*, 357.
- (207) Pitters, J. L.; Piva, P. G.; Tong, X.; Wolkow, R. A. *Nano Lett.* **2003**, *3*, 1431.
- (208) Greene, M. E.; Guisinger, N. P.; Basu, R.; Baluch, A. S.; Hersam, M. C. *Surf. Sci.* **2004**, *559*, 16.
- (209) Pitters, J. L.; Wolkow, R. A. *J. Am. Chem. Soc.* **2005**, *127*, 48.
- (210) Yang, L.; Lua, Y.-Y.; Lee, M. V.; Linford, M. R. *Acc. Chem. Res.* **2005**, *38*, 933.
- (211) Jiang, G.; Niederhauser, T. L.; Fleming, S. A.; Asplund, M. C.; Linford, M. R. *Langmuir* **2004**, *20*, 1772.
- (212) Lua, Y.-Y.; Fillmore, W. J. J.; Yang, L.; Lee, M. V.; Savage, P. B.; Asplund, M. C.; Linford, M. R. *Langmuir* **2005**, *21*, 2093.
- (213) Guo, D.-J.; Xiao, S.-J.; Xia, B.; Wei, S.; Pei, J.; Pan, Y.; You, X.-Z.; Gu, Z.-Z.; Lu, Z. *J. Phys. Chem. B* **2005**, *109*, 20620.
- (214) de Smet, L. C. P. M.; Zuilhof, H.; Sudhölter, E. J. R.; Lie, L. H.; Houlton, A.; Horrocks, B. R. *J. Phys. Chem. B* **2005**, *109*, 12020.
- (215) Morse, K. A.; Pianetta, P. *J. Appl. Phys.* **2004**, *96*, 6851.
- (216) Harper, J.; Sailor, M. J. *Langmuir* **1997**, *13*, 4652.
- (217) Miura, T.; Niwano, M.; Shoji, D.; Miyamoto, N. *J. Appl. Phys.* **1996**, *79*, 4373.
- (218) Vezenov, D. V.; Golubev, V. B.; Melnikov, V. P. *Macromolecules* **2003**, *36*, 1819.
- (219) Hamers, R. J.; Wang, Y. *Chem. Rev.* **1996**, *96*, 1261.
- (220) Woods, M.; Carlsson, S.; Hong, Q.; Patole, S. N.; Lie, L. H.; Houlton, A.; Horrocks, B. R. *J. Phys. Chem. B* **2005**, *109*, 24035.

Advances in the Coordination Chemistry of Amidinate and Guanidinate Ligands [☆]

Frank T. Edelman ^{*}

Contents		
I.	Introduction	184
II.	General Aspects of Amidinate and Guanidinate Complexes	186
III.	Coordination Chemistry of Amidinate and Guanidinate Ligands	188
A.	Amidinate and guanidinate complexes of main group metals	188
B.	Amidinate and guanidinate complexes of the early transition metals	226
C.	Amidinate and guanidinate complexes of the middle and late transition metals	268
IV.	Special Aspects of Amidinate and Guanidinate Coordination Chemistry	292
A.	Complexes containing chiral amidinate ligands	292
B.	Complexes containing cyclic guanidinate ligands	296
C.	Complexes containing functionalized amidinate ligands	299
D.	Complexes containing bis(amidinate) ligands	307
E.	Dinuclear “lantern” and “paddlewheel”-type amidinate and guanidinate complexes	325
F.	Phosphaguanidinate complexes	327
V.	Amidinate and Guanidinate Complexes in Catalysis	328
A.	Polymerization reactions catalyzed by amidinate and guanidinate complexes	331
B.	Hydroamination/cyclization reactions catalyzed by amidinate and guanidinate complexes	336
C.	Miscellaneous reactions catalyzed by amidinate and guanidinate complexes	336
VI.	Amidinate and Guanidinate Complexes in Materials Science	339

[☆]Dedicated to Professor Josef Takats on the occasion of his 65th birthday.

Chemisches Institut der Otto-von-Guericke-Universität Magdeburg, Universitätsplatz 2, D-39106 Magdeburg, Germany

^{*}Corresponding author.

E-mail address: frank.edelmann@ovgu.de

Advances in Organometallic Chemistry, Volume 57
ISSN 0065-3055, DOI 10.1016/S0065-3055(08)00003-8

© 2008 Elsevier Inc.
All rights reserved

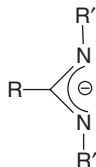
VII. Future Outlook	342
Acknowledgments	343
References	343

I. INTRODUCTION

The quest for alternatives to cyclopentadienyl-based ligands has led to a recent renaissance of *N*-centered donor ligands in various fields of organometallic and coordination chemistry. Among these alternative ligands, the highly versatile and readily accessible amidinate and guanidinate anions play a major role. Metal amidinate and guanidinate complexes are well established for various elements throughout the Periodic Table and, more important, diverse applications in catalysis and materials science are beginning to emerge. The most recent publications that comprehensively covered this field were published in 1994. Thus this review is intended to give a comprehensive account of the rapidly expanding field, thereby focussing on the results published after 1994. Earlier review articles can be found in Ref. (1) Amidinate anions of the general formula $[\text{RC}(\text{NR}')_2]^-$ (Scheme 1) are the nitrogen analogs of the carboxylate anions. They have been widely employed as ligands in main group and transition metal coordination chemistry, with the latter covering both early and late transition metals as well as the lanthanides and actinides.¹ As illustrated in Scheme 1, amidinate ligands offer a large degree of variability, which allows for an effective tuning of the steric and electronic requirements.

In addition to the substituents listed in Scheme 1, chiral groups may be introduced and unsymmetrically substituted amidinate anions are also possible. The amidinate anions may also contain additional functional groups, or two such anions can be linked with or without a suitable spacer unit. Yet another variety comprises the amidinate ligands being part of an organic ring system. All these aspects will be covered in the present review.

Historically, the amidinate story begins with the discovery of *N,N,N'*-tris(trimethylsilyl)benzamidine, $\text{PhC}(=\text{NSiMe}_3)[\text{N}(\text{SiMe}_3)_2]$, by Sanger.² The compound was prepared by the reaction of benzonitrile with $\text{LiN}(\text{SiMe}_3)_2$ followed by treatment with chlorotrimethylsilane. The method was later



R = H, alkyl, aryl

R' = H, alkyl, cycloalkyl, aryl, trimethylsilyl

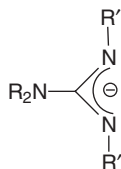
Scheme 1

improved by Oakley et al. In their 1987 paper, these authors also reported a series of *p*-substituted derivatives.³ In the following years, these *N*-silylated ligands were extensively employed in main group and transition metal chemistry, and the first review article covering the field was published by Dehnicke in 1990.^{1a} Since 1994 an incredible variety of differently substituted amidinate ligands has been developed and employed in the coordination of various elements throughout the Periodic Table. The main advantages of these ligands are twofold. Amidinate anions are generally readily accessible using commercially available or easily prepared starting materials. Furthermore, their steric and electronic properties can be readily modified in a wide range through variation of the substituents on the carbon and nitrogen atoms. These properties combined make the amidinate anions clearly almost as versatile as the ubiquitous cyclopentadienyl ligands. Metal amidinato complexes are generally accessible through several synthetic routes. The most prevalent of them include:

- (i) insertion of carbodiimides into an existing metal-carbon bond;
- (ii) deprotonation of an amidine using a metal alkyl;
- (iii) salt-metathesis reactions between a metal halide substrate and an alkali metal amidinate (with the latter normally being generated by one of the routes (i) or (ii));
- (iv) reaction of metal halides with *N,N,N'*-tris(trimethylsilyl)amidines.

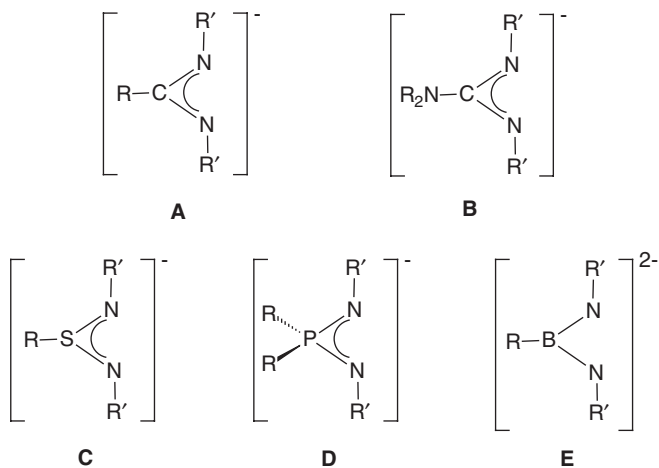
Closely related to the amidinate anions are the guanidinate ligands (Scheme 2), which differ only in that they contain a tertiary amino group at the central carbon atom of the NCN unit. The beginning of their coordination chemistry dates back to the year 1970, when Lappert et al. reported the first transition metal guanidinate complexes.⁴ Like the amidinates, these anions too make attractive ligands because of the similar steric and electronic tunability through systematic variations of the substituents at the carbon and nitrogen atoms. The general synthetic methods for preparing metal amidinato complexes can in part be applied to the corresponding guanidates and include the following:

- (i) insertion of carbodiimides into an existing metal-nitrogen bond;
- (ii) deprotonation of a guanidine using a metal alkyl;
- (iii) salt-metathesis reactions between a metal halide substrate and an alkali metal guanidinate (with the latter normally being generated by one of the routes (i) or (ii)).



R = alkyl, trimethylsilyl
R' = H, alkyl, cycloalkyl, aryl, trimethylsilyl

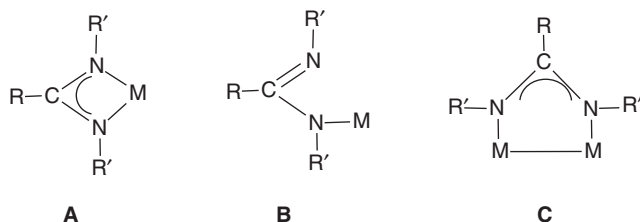
Scheme 2

**Scheme 3**

“The coordination chemistry of guanidines and guanidates” has been reviewed in 2001 by Bailey and Pace,^{5a} and more recently, Coles published a comprehensive review on “Application of neutral amidines and guanidines in coordination chemistry”.^{5b} Besides the amidinate and guanidinate anions, depicted in Scheme 3 as **A** and **B**, there are several isoelectronic chelating ligands which have been reported in the literature. Apparently the least investigated among these ligands are the diiminosulfinate anions **C**^{6–8} although they are readily accessible through addition of organolithium compounds to sulfur diimides.^{9–13} Diiminophosphinate anions **D** are accessible with different substituents at phosphorus (e.g., Bu^t, Ph). Lithium salts and transition metal complexes of these anions are known, and they have been shown to be important building blocks in the synthesis of cyclic metallaphosphenes.^{14–19} The first metal compound formally derived from a dianionic boraamidinate anion **E** was reported as early as 1979,²⁰ and lithium salts of these anions were first reported in 1990.^{21,22} Since then these dianionic ligands have become increasingly popular. Various main group and transition metal complexes are known,^{23–26} and a comprehensive review was published very recently by Chivers et al.²⁷ Thus the coordination chemistry of the ligands **C–E** has been excluded from this review.

II. GENERAL ASPECTS OF AMIDINATE AND GUANIDINATE COMPLEXES

The general coordination modes of amidinate and guanidinate ($R = NR'_2$) ligands are shown in Scheme 4. Both ligands display a rich coordination chemistry in which both chelating and bridging coordination modes can be achieved. By far the most common coordination mode is the chelating type **A**.

**Scheme 4**

In contrast, there are only rare examples of monodentate metal coordination (**B**). This type of bonding can be the result of severe steric crowding in certain amidinate or guanidinate ligands containing very bulky substituents. Also very common in transition metal chemistry is the bridging coordination mode **C**. The Group 11 metal copper, silver, and gold strongly tend to form dinuclear complexes containing two amidinate or guanidinate bridging ligands. The bridging coordination mode is often found in dinuclear transition metal complexes with short metal–metal distances. In some cases, these contain three bridging ligands. The majority of these complexes, however, belong to the class of “paddlewheel”-type compounds with the general formula $M_2(\text{amidinate})_4$ or $M_2(\text{guanidinate})_4$. The fascinating chemistry of these complexes has been extensively investigated mainly by Cotton and Murillo et al. These compounds have also been utilized for the construction of exciting supramolecular architectures. This chemistry differs largely from that of the chelating amidinate and guanidinate complexes and will thus be considered only briefly in [Section IV.E](#). For further information on the “lantern”- or “paddlewheel”-type compounds the reader is referred to the original literature.^{28–45}

The factors governing the formation of either chelating or bridging coordination modes in amidinate and guanidinate complexes have been analyzed in detail.⁴⁶ Perhaps the greatest advantage of these ligands besides their easy availability is the possibility of tuning their steric demand in a wide range by variation of the substituents at carbon and nitrogen. To some extent, the electronic properties can also be influenced by introduction of suitable substituents. Amidinate and guanidinate ligands have small N–M–N bite angles typically in the range of 63–65°. The balance between the bridging and chelating coordination modes of amidinate and guanidinate ligands is governed by the substitution pattern on the N–C–N unit. The orientation of the lone pairs at nitrogen is greatly influenced by steric interactions between the substituents on the carbon and nitrogen atoms. Formation of chelate complexes is favored when large substituents are present on the central carbon atom, as they induce a convergent orientation of the lone pairs of electron at nitrogen. The bridging coordination mode is more often observed for small substituents, which lead to a more parallel orientation of the lone pairs. Tuning of the steric demand of the ligand by varying the substituents at nitrogen can also influence the coordination geometry of the metal center in bis(amidinato) complexes. Steric hindrance imparted by substituents on the nitrogen atoms has its main effects mainly within

the N–M–N plane. Terphenyl substituents on the amidinate carbon atom have been successfully employed to effect steric shielding above and below the N–M–N plane, although this shielding is fairly remote from the metal center.^{47–52} Another approach to provide steric protection of the N–M–N coordination plane is the use of *ortho*-disubstituted aryl substituents on the nitrogen atoms. Especially useful in this respect is the 2,6-diisopropylphenyl group.^{53–55} Also notable is that in *N,N'*-bis(trimethylsilyl)-benzamidinate and related ligands the orientation of the phenyl ring on the central carbon atom with respect to the N–C–N unit is normally nearly perpendicular. This conformation accounts for the fact that such amidinate anions are not “flat” ligands such as the isoelectronic carboxylate anions, but also extend above and below the N–C–N plane. It was first pointed out by us that these ligands can be regarded as “steric cyclopentadienyl equivalents”.^{56–58} The concept of “steric cyclopentadienyl equivalents” was developed by Wolczanski et al. in connection with a series of tri-*t*-butylmethoxide (tritox) complexes.⁵⁹

III. COORDINATION CHEMISTRY OF AMIDINATE AND GUANIDINATE LIGANDS

In this review only complexes containing formally anionic amidinate or guanidinate ligands are considered. Complexes of coordinated *neutral* amidines or guanidines have thus been excluded. The area was previously compiled in several excellent review articles, most of which though cover only special aspects of the coordination chemistry of amidinate and guanidinate ligands. “The coordination chemistry of guanidines and guanidates” has been reviewed by Bailey and Pace^{5a}, and more recently, Coles reviewed the “Application of neutral amidines and guanidines in coordination chemistry.”^{5b} Coordination compounds of amidinate and aminopyridinate ligands have been discussed in a review by Schareina and Kempe entitled “Amido ligands in coordination chemistry.”⁶⁰

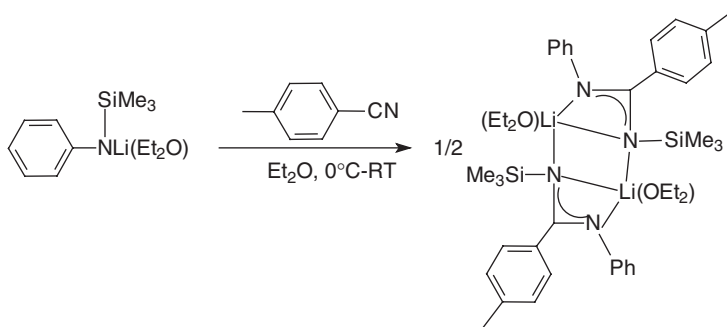
A. Amidinate and guanidinate complexes of main group metals

1. Group 1 metal complexes: useful starting materials

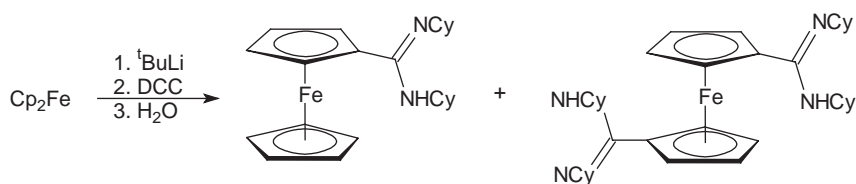
The general route leading to lithium amidinates can also be adapted to prepare asymmetrically substituted derivatives as illustrated in Scheme 5.⁶¹

The lithium benzamidinates $\text{Li}[\text{PhC}(\text{NR})_2]$ ($\text{R} = \text{Cy}, \text{Pr}^i$) and $\text{Li}[2,4,6\text{-(CF}_3)_3\text{C}_6\text{H}_2\text{C}(\text{NCy})_2]$ have been prepared analogously.⁶² Reaction of FcLi ($\text{Fc} = \text{ferrocenyl}$) with 1,3-dicyclohexylcarbodiimide (= DCC, Scheme 6), followed by addition of water, afforded the ferrocene-substituted amidine $\text{Fc}(\text{NCy})\text{NHCy}$ in 50% yield. The amidine is readily deprotonated by $\text{LiN}(\text{SiMe}_3)_2$ or $\text{NaN}(\text{SiMe}_3)_2$ to yield the alkali metal amidinates, $\text{Li}[\text{FcC}(\text{NCy})_2]$ and $\text{Na}[\text{FcC}(\text{NCy})_2]$ in high yields.⁶³

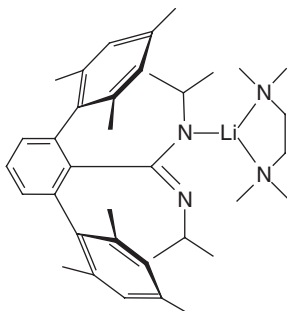
The frequently used starting material $\text{Li}(\text{TMEDA})[\text{PhC}(\text{NSiMe}_3)_2]$ was found to be monomeric in the solid state.⁶⁴ Monomeric molecular structures were also established for lithium amidinates containing very bulky terphenyl or triptycenyl



Scheme 5



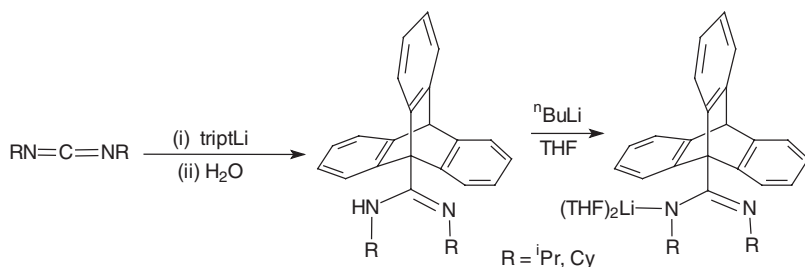
Scheme 6



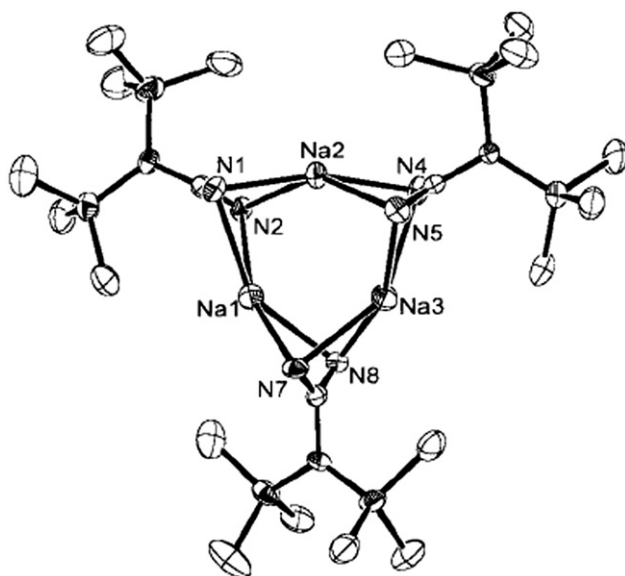
Scheme 7

substituents at the central carbon atom. Among them are the first examples of monodentate amidinate coordination to lithium (Schemes 7 and 8).^{49,52}

Dimeric molecular structures have been established by X-ray crystallography for $[\text{Li}\{\text{PhC}(\text{NPr}^{\text{ii}})(\text{NSiMe}_3)\}(\text{Et}_2\text{O})]_2$,⁶⁵ $[\text{Li}\{\text{MeC}(\text{NCy})_2\}(\text{THF})]_2$,⁶⁶ $[\text{Li}\{\text{PhN}(\text{NPr}^i)_2\}(\text{THF})]_2$,⁶² $[\text{FcC}(\text{NCy})_2\text{Li}(\text{Et}_2\text{O})]_2$ (Fc = ferrocenyl),⁶⁷ and the solvent-free alkali metal guanidates $[\text{M}\{(\text{Me}_3\text{Si})_2\text{NC}(\text{NCy})_2\}]_2$ (M = Li, K).⁶⁸ The trimeric sodium guanidinate $[\text{Na}\{(\text{Me}_3\text{Si})_2\text{NC}(\text{NCy})_2\}]_3$ represents a new mode of aggregation for species containing an anionic N–C–N linkage. Its structure is depicted in Figure 1.⁶⁸ The synthesis and structural chemistry of lithium fluoroarylamidates have also been thoroughly investigated. This family of lithium amidinates gives rise to a large number of different types of structures.⁶⁹



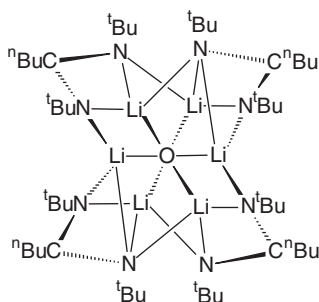
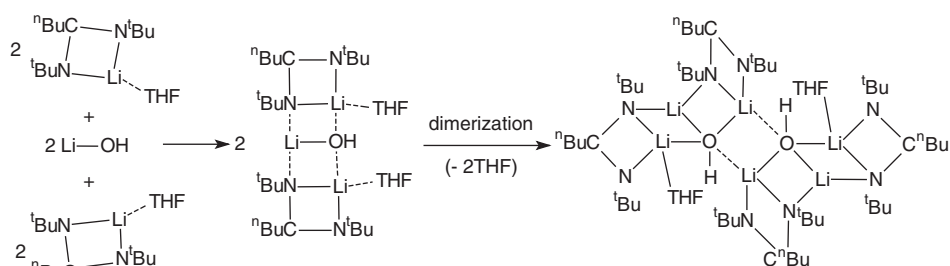
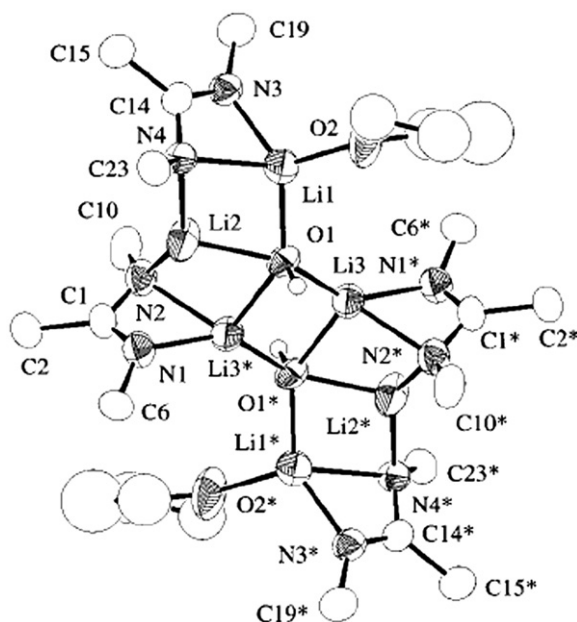
Scheme 8

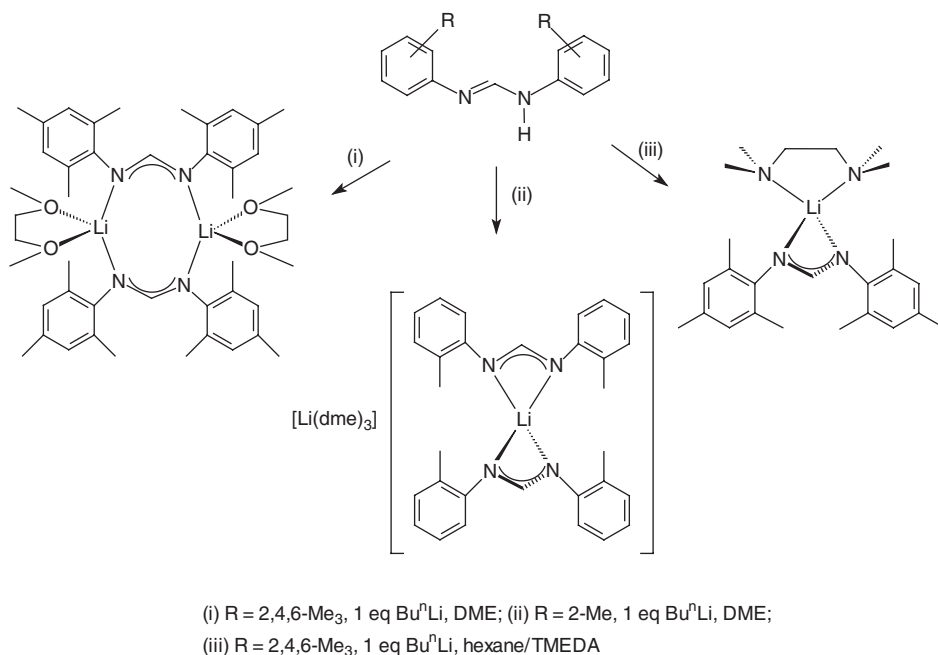
Figure 1 Molecular structure of $[\text{Na}\{(\text{Me}_3\text{Si})_2\text{NC}(\text{NCy})_2\}]_3$.⁶⁸

The entrapment of lithium oxide and lithium halides by the lithium amidinate $\text{Li}[\text{Bu}^n\text{C}(\text{NBu}^t)_2]$ has been studied in detail by X-ray crystallography. Interesting polycyclic molecular structures have been obtained, as exemplified by the unusual sandwich complex of lithium oxide made from $\text{Li}[\text{Bu}^n\text{C}(\text{NBu}^t)_2]$ in toluene (Scheme 9).⁷⁰

Addition of anhydrous LiX ($\text{X} = \text{OH}, \text{Cl}, \text{Br}, \text{I}$) to $\text{Li}[\text{Bu}^n\text{C}(\text{NBu}^t)_2]$ in THF afforded laddered aggregates in which two neutral lithium amidinates chelate one LiX unit. When the added salt is LiI , the monomeric laddered aggregate is isolated as a bis-THF adduct. In the case of LiOH , LiCl , and LiBr , the ladders dimerize about their external LiX edges. This process is highlighted in Scheme 10 for LiOH . The molecular structure of the resulting dimeric ladder complex is depicted in Figure 2.⁷⁰

Alkali metal derivatives of N,N' -diarylformamidines form a particularly well investigated class of compounds. Most recently, in 2007, the fascinating structural

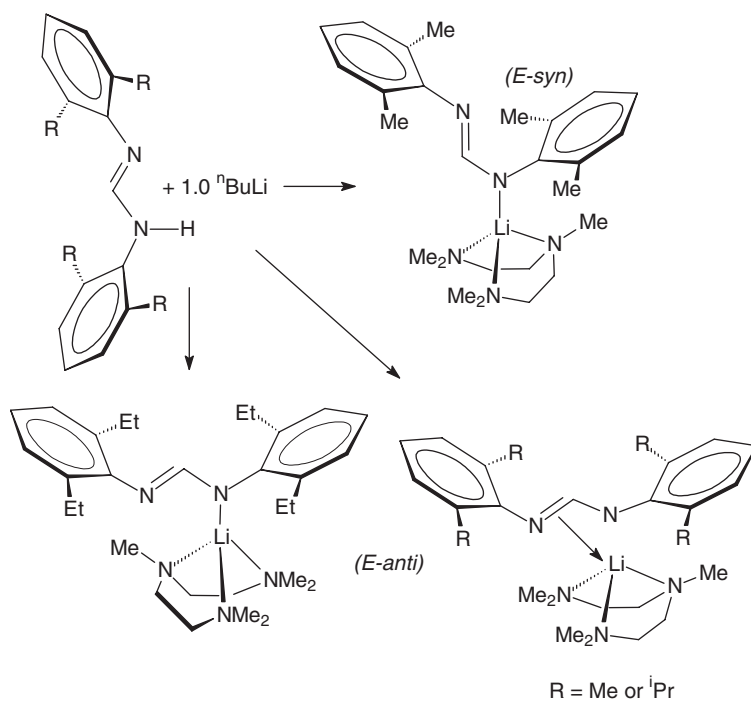
**Scheme 9****Scheme 10****Figure 2** Molecular structure of $[(\text{Bu}^n\text{C}(\text{NBu}^t)_2)_2\text{Li}_2(\text{THF})(\text{LiOH})]_2$.⁷⁰

**Scheme 11**

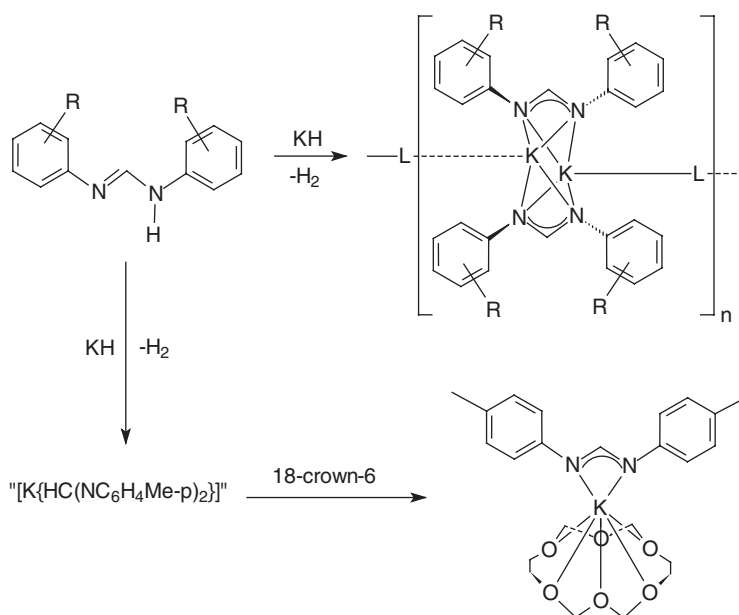
chemistry and coordinative versatility of these compounds has been highlighted in an excellent review article by Junk and Cole.⁷¹ Thus only selected cases will be described here in more detail. An interesting structural variety has been observed when studying the aryl substituent and solvent donor effects on *N,N'*-diaryldiethylenetriamine complexes of lithium. The synthetic procedures and three different structural types are outlined in Scheme 11.^{72a}

In the presence of *N,N,N',N'',N'''*-pentamethyldiethylenetriamine (= PMDETA), monomeric lithium complexes of bulky formamidinate ligands can be isolated. The compounds (Scheme 12) comprise a Li(PMDETA) center coordinated by a bulky formamidinate in either the *E-syn*- or *E-anti*-isomeric form. Two of the structures display coordination of the pendant amidinate imine, and can therefore be considered the first examples of $\eta^2:\eta^1\text{-C}=\text{N},\text{N}'$ metal amidinate coordination.^{72b}

FT-IR spectroscopy was employed to investigate the structures of the 1:1 complexes between Li⁺ and the guanidine-substituted azo compounds pyridine-2-azo-*p*-phenyltetramethylguanidine and 4,4'-bis(tetramethylguanidine)azobenzene. Both Li⁺ complexes exist as dimers in acetonitrile solution.⁷³ The structural chemistry of potassium *N,N'*-di(tolyl)formamidinate complexes has been investigated in detail. These compounds were prepared by deprotonation of the parent *N,N'*-di(tolyl)formamidines with potassium hydride (Scheme 13). The resulting adducts with either THF or DME display one-dimensional polymeric solid-state structures that exhibit $\mu\text{-}\eta^2:\eta^2$ -coordinated formamidinates.



Scheme 12



Scheme 13

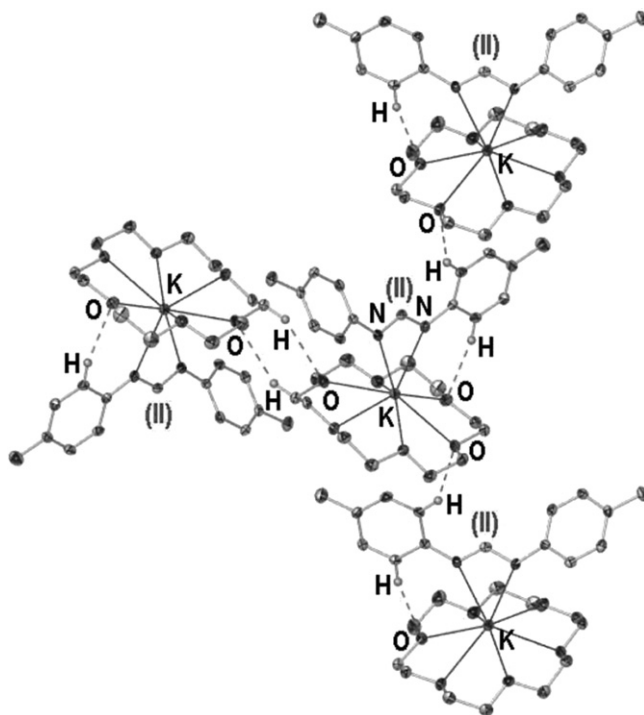


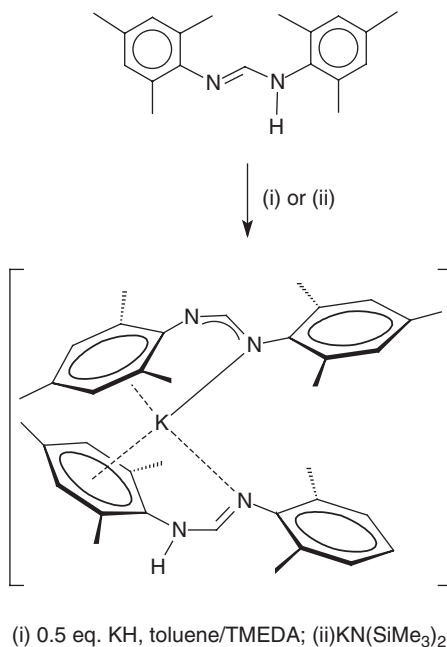
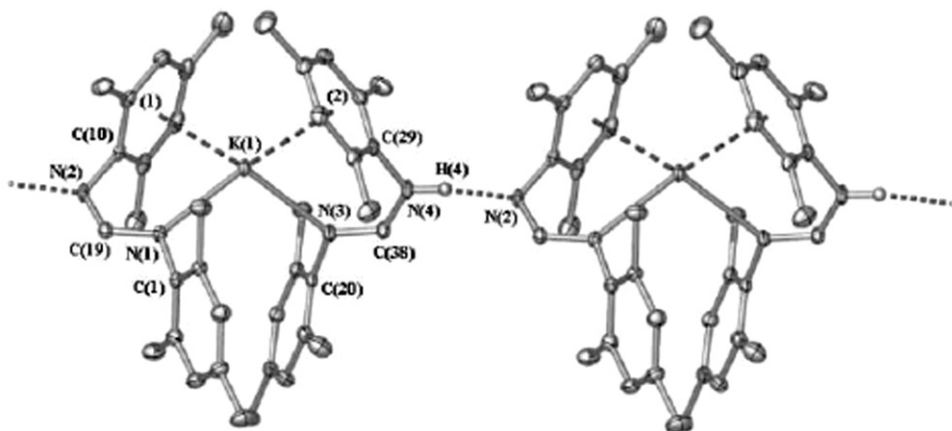
Figure 3 Extended lattice structure of $K[HC(NC_6H_4Me-p)_2](18\text{-crown-6})$ with hydrogen bonding contacts.⁷⁴

The crown-ether adduct shown in Scheme 13 exhibits both inter- and intramolecular $C-H \cdots O$ hydrogen bonding in the solid state (Figure 3).⁷⁴

In a similar manner, the potassium complex of the very bulky formamidinate anion $[HC(NMes)_2]^-$ was prepared as depicted in Scheme 14 by treatment of the free formamidine with either potassium hydride or $KN(SiMe_3)_2$. Unlike most other potassium formamidinates the molecular structure of this compound is monomeric and incorporates a protonated formamidine ligand. Furthermore, the diarylformamidinate ligand coordinates in an unconventional nearly symmetrical $NCN \eta^1$ -amide mode with additional η^6 -arene group ligation. Hydrogen bonding leads to formation of a polymeric structure in the solid state (Figure 4).⁷⁵

The structural investigations have been extended to potassium derivatives of the "super" formamidine $HC(NC_6H_3Pr^i-2,6)(NHC_6H_3Pr^i-2,6)$ (= HDippForm). Treatment of the free formamidine with $KN(SiMe_3)_2$ yielded the formamidinate species $[K(DippForm)_2K(THF)_2]_n(THF)_m$, which exhibits a macromolecular structure of alternating η^6 -arene: η^1 -amidinate bound potassium di-amidinate and potassium di-THF units in a one-dimensional polymeric array (Figure 5). Addition of a further equivalent of HDippForm afforded hydrogen-bonded $[K(DippForm)(THF)_3](HDippForm)$.⁷⁶

Structural studies have also been carried out on related alkali metal complexes of N,N' -di(*o*-fluorophenyl)formamidine (= HFPhF). Preparations

**Scheme 14****Figure 4** Molecular structure of $[\text{K}\{\text{HC}(\text{NMe}_2)_2\}\{\text{HC}(\text{NMe}_2)(\text{NHMe})\}]_n$.⁷⁵

according to [Scheme 15](#) afforded the colorless crystalline formamidinate complexes $\text{Li}(\text{FPhF})(\text{THF})$, $\text{Na}(\text{FPhF})(\text{THF})$, and $\text{K}(\text{FPhF})$ as well as the diethylether adducts $\text{Na}(\text{FPhF})(\text{Et}_2\text{O})$ and $\text{Na}_3(\text{FPhF})(\text{Et}_2\text{O})(\text{NaF})$. The coordination in the potassium derivative involves both potassium–fluoride interactions and η^2 -arene coordination ([Figure 6](#)). In the crystal, the resulting dimeric units are associated to result in a polymeric solvent-free structure ([Figure 7](#)).⁷⁷

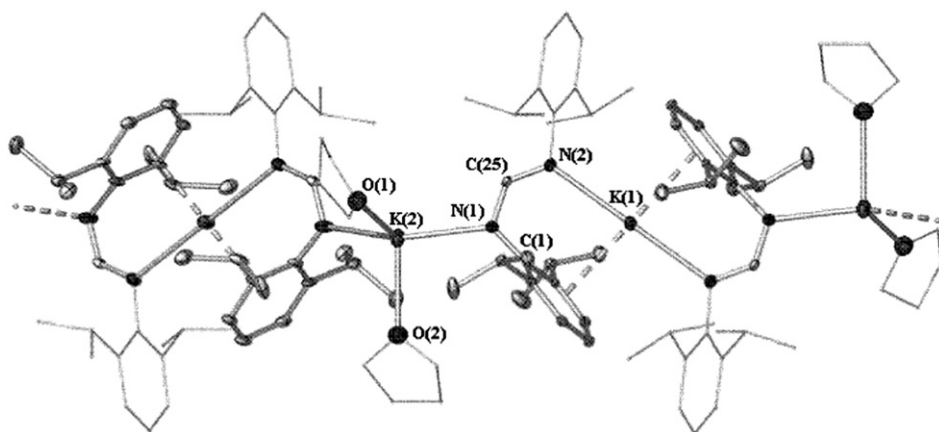
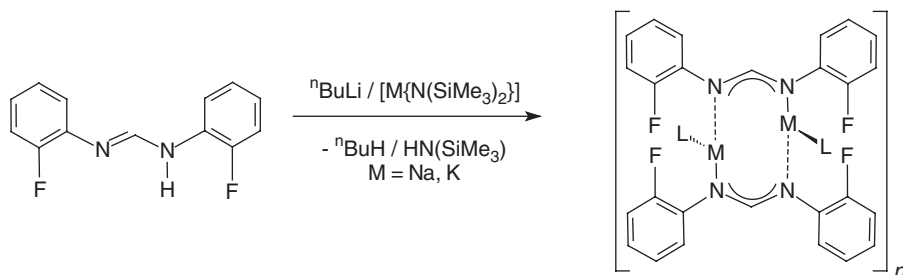


Figure 5 Molecular structure of $[K(\text{DippForm})_2K(\text{THF})_2]_n(\text{THF})_n$.⁷⁶



Scheme 15

In closely related studies, the molecular and crystal structures of lithium, sodium and potassium N,N' -di(*p*-tolyl)formamidinate and N,N' -di(2,6-dialkylphenyl)formamidinate complexes have been elucidated. These showed the anions to be versatile ligands for alkali metals, exhibiting a wide variety of binding modes.^{78,79}

2. Group 2 metal complexes

The chemistry of amidinate and guanidinate complexes of the alkaline earth metals has made significant progress since 1994. Two major trends can be identified. Less bulky amidinate ligands were employed in magnesium chemistry with the aim of obtaining volatile complexes suitable for MOCVD or ALD processes (cf. Section VI). On the other hand, very bulky amidinate and guanidinate ligands are used to stabilize novel compounds of the heavier alkaline earth metals. Not surprisingly, beryllium amidinato complexes are rare, and guanidates of Be have not been reported until now. Two beryllium complexes containing the sterically encumbered $[\text{PhC}(\text{NSiMe}_3)_2]^-$ ligand have been prepared and structurally characterized. Reaction of BeCl_2 with a 1:1 mixture of $\text{LiN}(\text{SiMe}_3)_2$ and PhCN afforded the six-membered ring

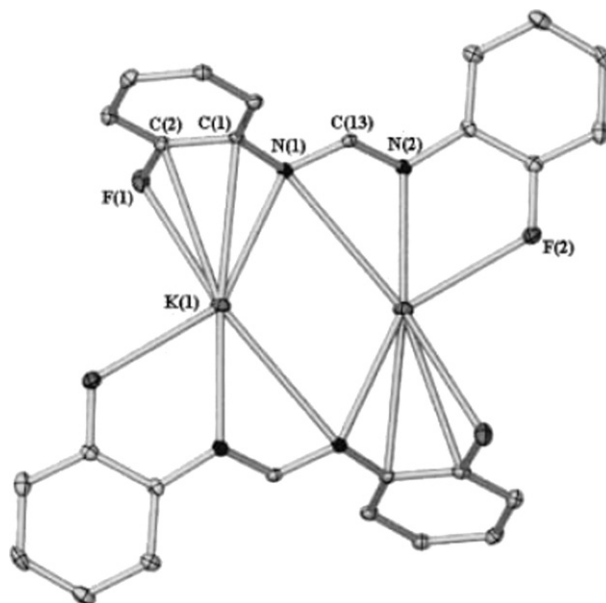


Figure 6 Molecular structure of the dimeric $[K(FPhF)]_2$ units.⁷⁷

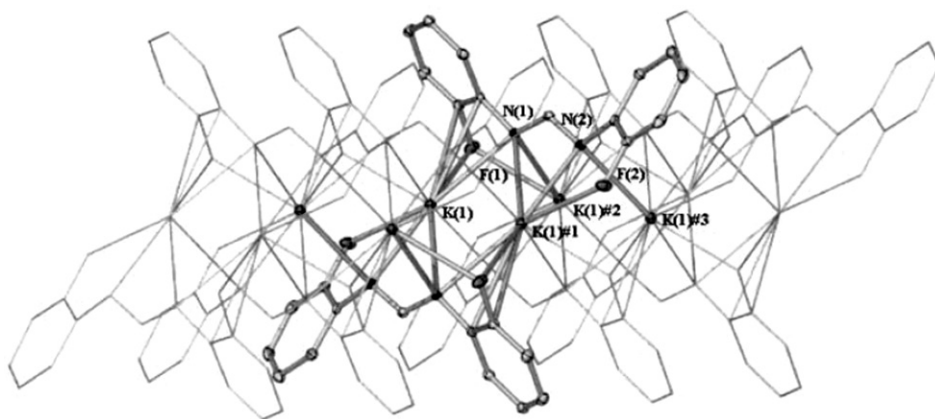


Figure 7 Polymeric structure of $[K(FPhF)]_n$ units.⁷⁷

compound $PhC(NSiMe_3)_2(BeCl)_2N(SiMe_3)_2$ (Figure 8) and the four-coordinate monomer $[PhC(NSiMe_3)_2]_2Be$ which could be separated by fractional crystallization.⁸⁰

A series of magnesium amidinate complexes, $[RC(NPr^i)_2]_2Mg(THF)_2$ ($R = Et, Pr^i, Ph$) and $[EtC(NBu^i)_2]_2Mg(THF)_2$, have been prepared by the stoichiometric reaction between MgR_2 ($R = Et, Pr^i, Ph$) and carbodiimides in THF solution. The 1:1 reaction between diisopropylmagnesium gave a dinuclear μ -amido complex, $[(Pr^iC(NPr^i)_2)Mg(\mu-NPr^i_2)]_2$, and a mononuclear complex, $[Pr^iC(NPr^i)_2]_2$

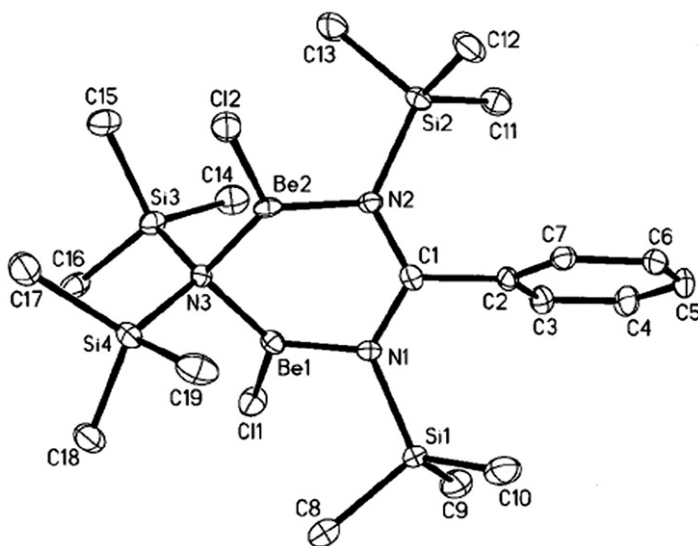


Figure 8 Molecular structure of $\text{PhC}(\text{NSiMe}_3)_2(\text{BeCl}_2)_2\text{N}(\text{SiMe}_3)_2$.⁸⁰

$\text{Mg}(\text{THF})$, when the stoichiometry was 1:2.⁸¹ Monomeric and dimeric amidinate complexes of magnesium have been studied in detail with respect to potential applications of these compounds in the chemical vapor deposition of magnesium-doped Group 13 compound semiconductor films. The reactions and products are summarized in [Scheme 16](#).⁸²

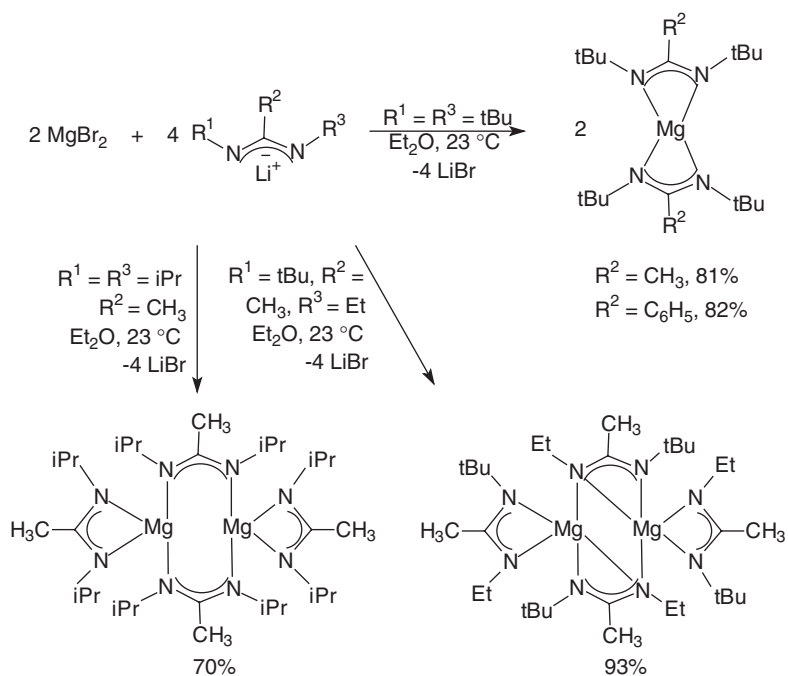
Two independent routes to magnesium amidinates containing very bulky terphenyl substituents have been developed, yielding both mono- and bis(amidinate) magnesium complexes. As shown in [Scheme 17](#), the free amidine reacted cleanly with 0.5 equivalents of dibutylmagnesium in toluene to form the bis(amidinate) in moderate yield. The highly soluble compounds were recrystallized from hexanes as clear, colorless crystalline blocks.⁴⁹

By using an alternate synthetic route, a mono(amidinate) magnesium complex was obtained. In this case, the Grignard reagent formed by treatment of the terphenyliodide with Mg was allowed to react directly with 1 equivalent of 1,3-diisopropylcarbodiimide, yielding the amidinate ([Scheme 18](#)).⁴⁹

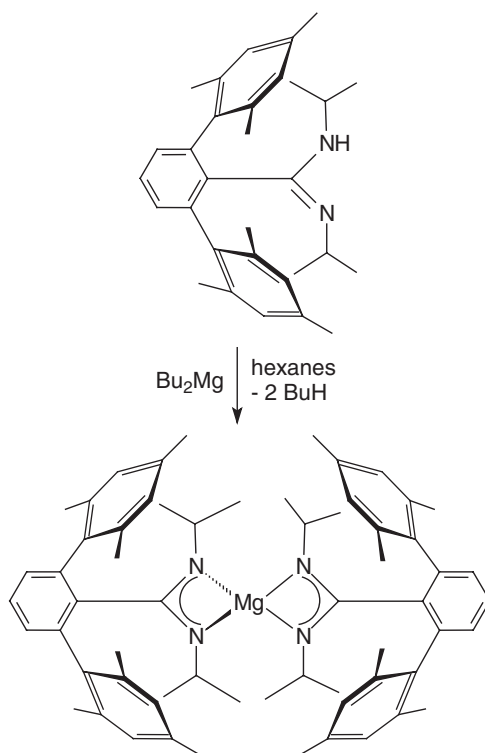
Another set of very bulky amidinate ligands has been successfully employed in the synthesis of mono(cyclopentadienyl) magnesium amidinates. Reaction of the free amidine with $[\text{CpMgMe}(\text{Et}_2\text{O})]_2$ in diethyl ether gave a product containing one diethyl ether ligand, which was readily lost on solvent removal and vacuum drying ([Scheme 19](#)).⁸³

Dissolution of the reaction product with $\text{R} = \text{mesityl}$ in THF , followed by workup, afforded $\text{CpMg}[\text{Bu}^t\text{C}(\text{NC}_6\text{H}_2\text{Me}_3-2,4,6)_2](\text{THF})$ as a white crystalline solid that was stable to loss of tetrahydrofuran at room temperature ([Scheme 20](#)).⁸³

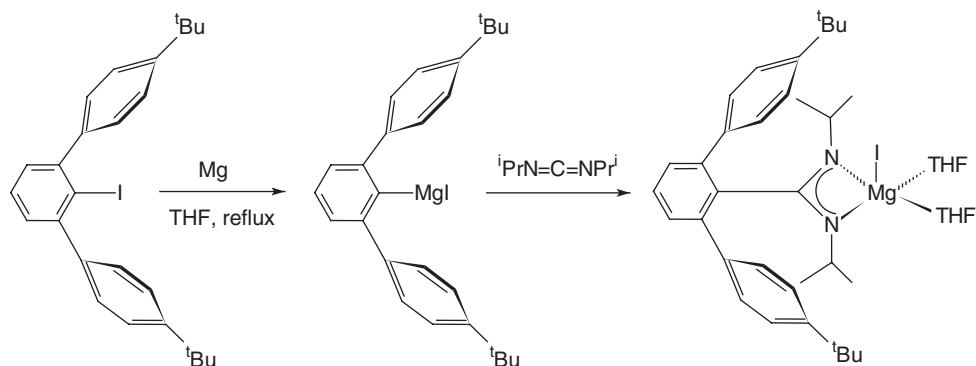
Volatility studies revealed that the unsolvated complex $\text{CpMg}[\text{Bu}^t\text{C}(\text{NC}_6\text{H}_3\text{Pr}_2-2,6)_2]$ sublimed unchanged at $180^\circ\text{C}/0.05\text{ Torr}$, and was recovered



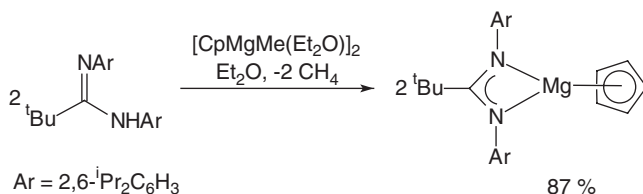
Scheme 16



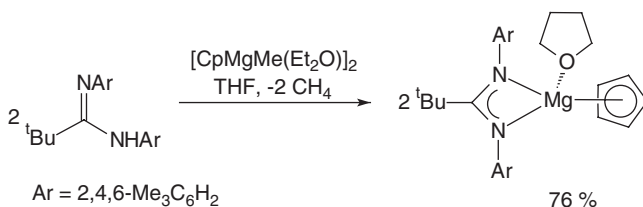
Scheme 17



Scheme 18

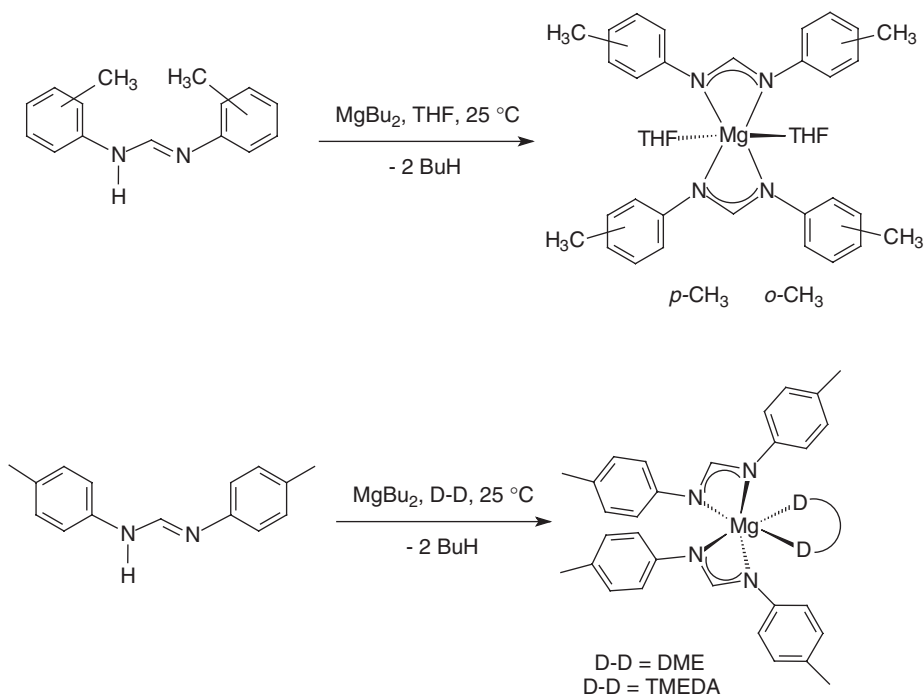


Scheme 19



Scheme 20

in 80% yield in a preparative sublimation. However, the THF solvate $\text{CpMg}[\text{Bu}^t\text{C}(\text{NC}_6\text{H}_2\text{Me}_3\text{-2,4,6})_2](\text{THF})$ decomposed under similar sublimation conditions to afford Cp_2Mg and the corresponding homoleptic magnesium bis(amidinate) $[\text{Bu}^t\text{C}(\text{NC}_6\text{H}_2\text{Me}_3\text{-2,4,6})_2]_2\text{Mg}$. Cp_2Mg was collected at the cold end of the sublimation apparatus, while the bis(amidinate) remained at the heated end.⁸³ The functionalized magnesium amidinate complex $[\text{Bu}^n\text{C}(\text{NCy})_2]\text{Mg}[\text{Ph}(\text{Bu}^n)\text{PNC}_6\text{H}_3\text{Pr}_2\text{-2,6}](\text{Et}_2\text{O})$ was obtained on treatment of the acyclic NPNCN ligand 2,6- $\text{Pr}_2\text{C}_6\text{H}_3\text{N}(\text{H})\text{P}(\text{Ph})\text{NCyC}(\text{Bu}^n)\text{NCy}$ with dibutylmagnesium.⁸⁴ A series of magnesium tolylformamidinate complexes have been prepared as depicted in Scheme 21. THF, DME, or TMEDA were employed as supporting donor ligands. In the solid state, all these compounds display monomeric octahedral bis(η^2 -formamidinate) metal centers.⁸⁵

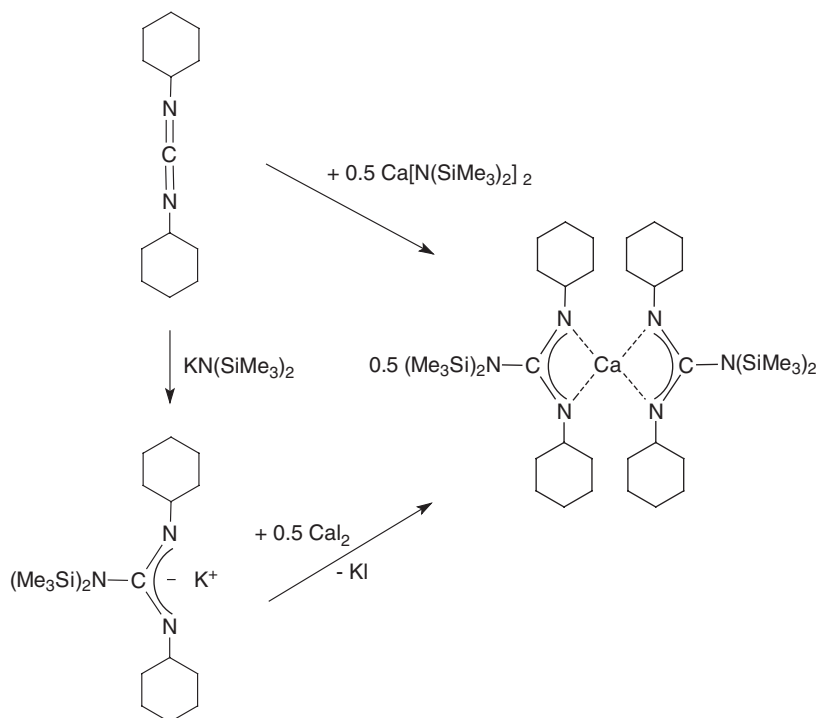
**Scheme 21**

The reaction of $[(\text{Me}_3\text{Si})_2\text{N}]_2\text{Ca}(\text{THF})_2$ with benzonitrile in THF afforded $[\text{PhC}(\text{NSiMe}_3)_2]\text{Ca}(\text{THF})_2$ in nearly quantitative yield. The coordination geometry around Ca is distorted octahedral with the two THF ligands occupying the *trans* positions. Similar treatment of $[(\text{Me}_3\text{Si})_2\text{N}]_2\text{Ca}(\text{THF})_2$ with pivalonitrile did not afford the corresponding amidinate derivative.⁸⁶ The preparation of calcium guanidates can be achieved by employing the two most general routes, i.e., carbodiimide insertion into the Ca–N bond of suitable calcium amides or the reaction of calcium diiodide with preformed lithium guanidates. Scheme 22 illustrates these different synthetic routes.⁸⁷

The heavy alkaline earth metals Ca, Sr, and Ba react with 2 equivalents of *N,N'*-bis(2,6-diisopropylphenyl)formamidine in the presence of bis(pentafluorophenyl)-mercury to afford the bis(formamidinato) species as THF adducts in good to moderate yield (Scheme 23). When the same reactions are carried out in a 1:1 molar ratio, *N-p*-tetrafluorophenyl-*N,N'*-bis(2,6-diisopropylphenyl)formamidine is isolated as the sole product in all cases (Scheme 23).⁵³ Other substituted *N,N'*-bis(aryl)formamidinate complexes of the heavy alkaline earth metals were synthesized accordingly.⁸⁸

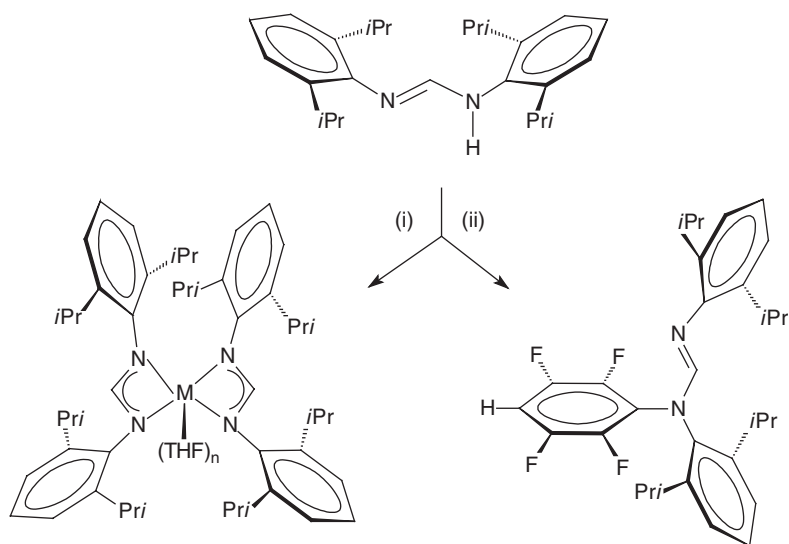
3. Group 13 metal complexes

Amidinate- and guanidinate-substituted boron halides are normally prepared using the two standard synthetic routes, i.e., salt-metathesis between suitable

**Scheme 22**

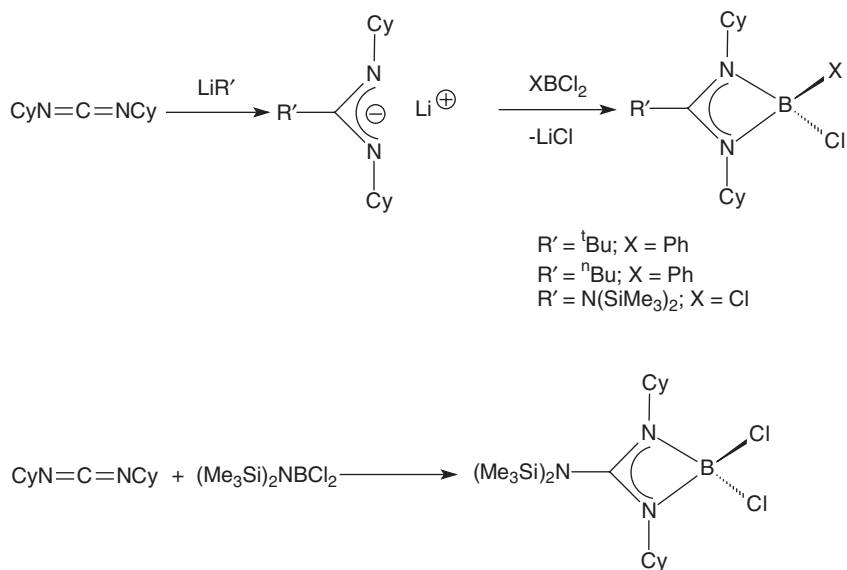
organoboron halides with lithium amidinates and carbodiimide insertion into B–N bonds (Scheme 24).⁸⁹ The structurally characterized four-membered BN_2C heterocycle $\text{Ph}(\text{Cl})\text{B}(\mu\text{-N}^t\text{Bu})_2\text{CBu}^n$ was obtained analogously using the standard metathetical route by allowing PhBCl_2 to react with $\text{Li}[\text{Bu}^n\text{C}(\text{N}^t\text{Bu})_2]$.⁹⁰

A third method involves elimination of chlorotrimethylsilane. This has been employed in the preparation of the bis(amidinate)-substituted boron halides $1,3\text{-C}_6\text{H}_4[\text{C}\{\text{N}(\text{SiMe}_3)_2\text{BCl}_2\}_2]$, $1,4\text{-C}_6\text{H}_4[\text{C}\{\text{N}(\text{SiMe}_3)_2\text{BCl}_2\}_2]$, and $1,4\text{-C}_6\text{H}_4[\text{C}\{\text{N}(\text{SiMe}_3)_2\text{B}(\text{Ph})\text{Cl}\}_2]$, while the analogous cyclohexyl-substituted derivatives $1,4\text{-C}_6\text{H}_4[\text{C}(\text{NCy})_2\text{B}(\text{Ph})\text{Cl}]_2$ and $1,4\text{-C}_6\text{H}_4[\text{C}(\text{NCy})_2\text{B}(\text{Ph})\text{Cl}]_2$ were made *via* salt-metathesis reactions of the appropriate dilithium bis(amidinates) with BCl_3 or PhBCl_2 .⁹¹ A 1:1 Lewis acid–base complex between $\text{CyN}=\text{C}=\text{NCy}$ and PhBCl_2 was isolated in 96% yield and structurally characterized. Heating of this material in refluxing toluene resulted in the amidinate $[\text{PhC}(\text{NCy})_2]\text{BCl}_2$, which had already been prepared independently *via* the salt-metathesis reaction of $\text{Li}[\text{PhC}(\text{NCy})_2]$ and BCl_3 . The overall reaction has been modeled by DFT calculations.⁹² Other amidinate-substituted boron halides that have been reported include $[\text{PhC}(\text{NSiMe}_3)_2]\text{BX}_2$ ($\text{X} = \text{Cl}, \text{Br}$), $[\text{RC}(\text{NCy})_2]\text{BCl}_2$ ($\text{R} = \text{Me}, \text{C}_6\text{H}_2\text{Bu}_3^t\text{-2,4,6}$), $[\text{MeC}(\text{N}^i\text{Pr})_2]\text{BCl}_2$, and $[\text{FcC}(\text{NCy})_2]\text{BBr}_2$. Scheme 25 illustrates the preparation of the ferrocenyl-substituted derivative, which was isolated in good yield (71%) as an orange, crystalline solid. An X-ray analysis confirmed the proposed structure (Figure 9).⁹³

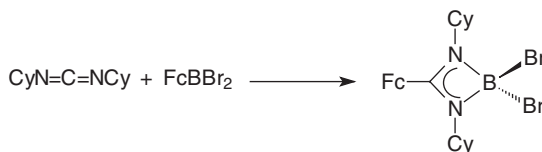


- (i) 0.5 eq M, 0.5 eq $\text{Hg}(\text{C}_6\text{F}_5)_2$, THF ($\text{M} = \text{Ca}$: $n = 1$; $\text{M} = \text{Sr}, \text{Ba}$: $n = 2$);
(ii) 1 eq M, 1 eq $\text{Hg}(\text{C}_6\text{F}_5)_2$, THF

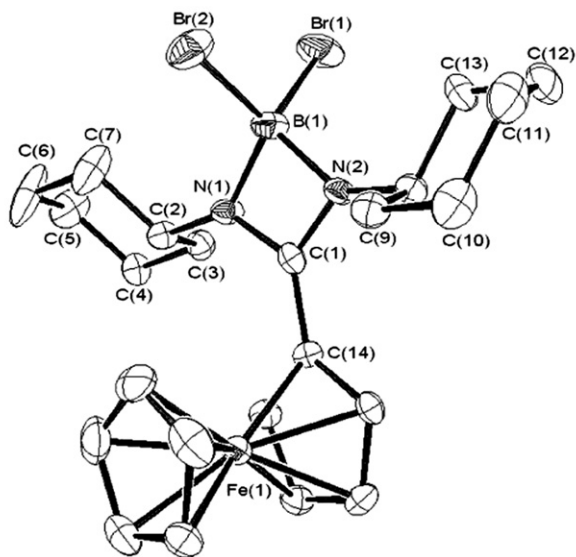
Scheme 23



Scheme 24



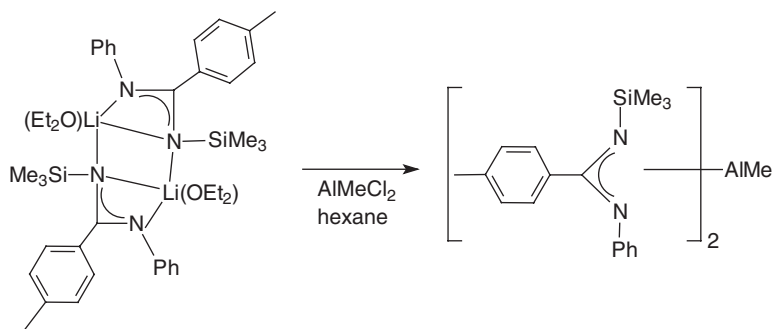
Scheme 25

Figure 9 Molecular structure of $[\text{FcC}(\text{NCy})_2]\text{BBr}_2$.⁹³

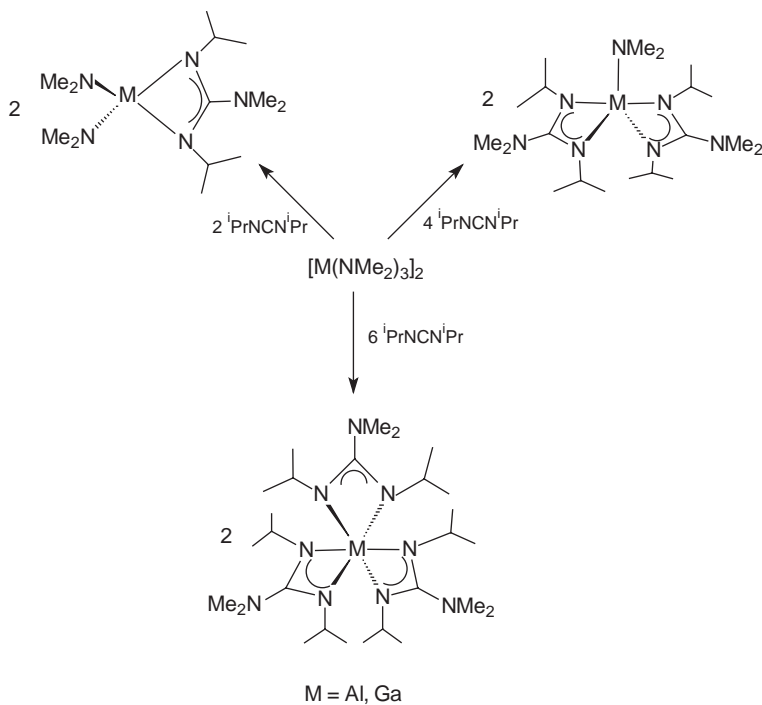
A monomeric aluminum amidinate containing asymmetrically substituted ligands has been synthesized as shown in Scheme 26 and isolated in 60% yield as colorless crystals.⁶¹

This metathetical route was recently extended to the synthesis of amidinato complexes of Al, Ga, and In containing very bulky amidinate ligands with 2,6- $\text{Pr}_2\text{C}_6\text{H}_3$, adamantyl, *m*-terphenyl or 9-triptycenyl substituents at the central carbon atom.^{94–96}

The insertion of carbodiimides into existing metal–heteroatom bonds^{95,97} has been demonstrated to be an important preparative route for the synthesis of Group 13 metal amidinates and guanidinates.^{98–100} For example, starting from the metal tris(dimethylamides) of Al and Ga, mono-, bis-, and tris(guanidinates) are readily accessible simply by adjusting the stoichiometry of the starting materials (Scheme 27).⁹⁸ Aluminum chloro-alkyl and -dialkyl complexes containing guanidinate ligands are accessible in an analogous manner starting from AlR_3 or through salt-elimination reactions between lithium guanidinates and AlCl_3 or AlMe_2Cl , respectively.¹⁰⁰ In one of these studies,^{99b} it was shown

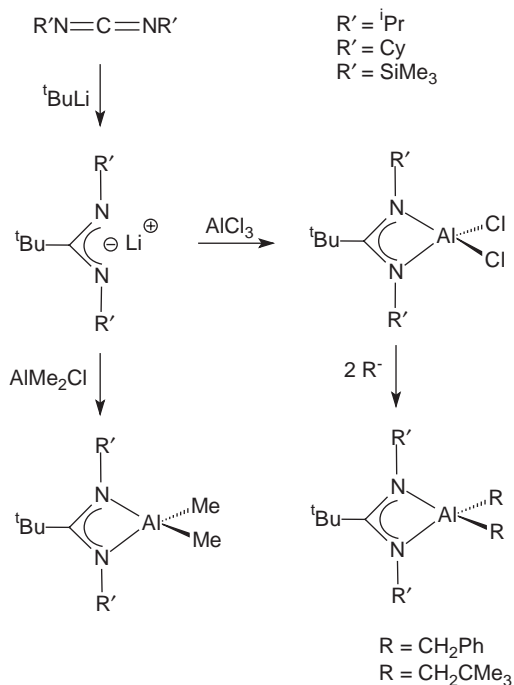


Scheme 26



Scheme 27

that ligand exchange of guanidinate ligands between aluminum centers plays an important role and will form dimeric intermediates, demonstrated by the synthesis and characterization of the dimer [Me₂NC(NPr^{*i*})₂]₂Al₂Cl₄. According to an X-ray diffraction study, the eight-membered dimer ring in this molecule adopts a twisted boat conformation. The compound decomposes to monomers at room temperature over 4 days, or within 18 h at 90 °C. A detailed computational characterization of the reaction pathway supporting

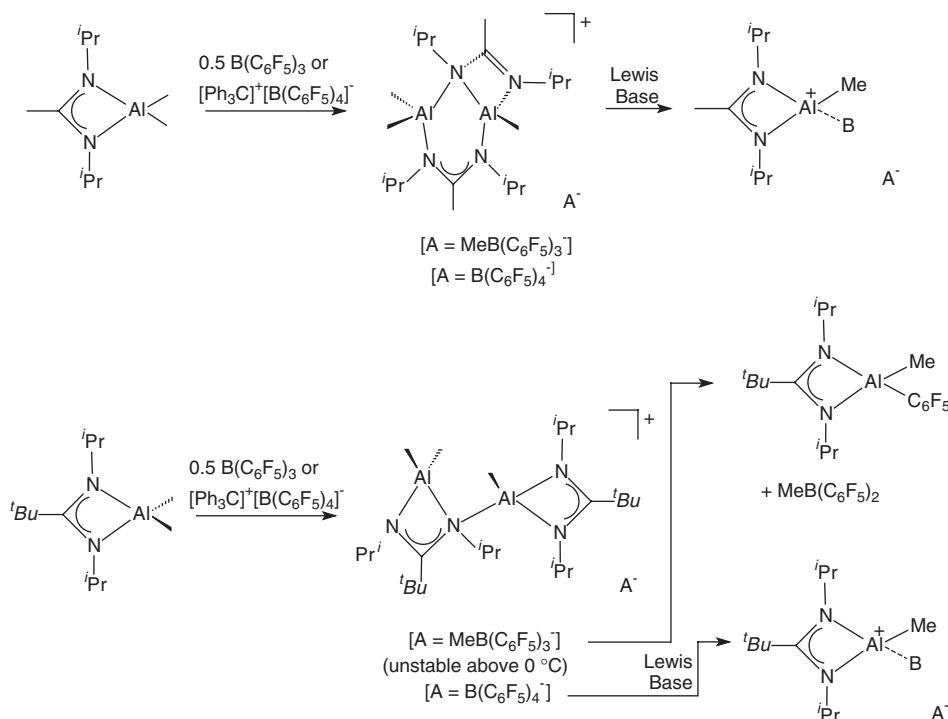
**Scheme 28**

the dimer structure and subsequent monomer formation was also carried out.^{99b}

Aluminum amidinates were made analogously starting from AlR_3 ($R = Me, Et$)^{95,101,102} or through metathetical route from $AlCl_3$ and 1 or 2 equivalents of lithium amidinates. Scheme 28 depicts typical synthetic methods leading to mono(amidinato) aluminum dichlorides and dialkyls.^{95,102}

The metathetical route has also been employed to prepare bis(amidinato) aluminum chloride derivatives. The compounds $[RC(NR')_2]_2AlCl$ ($R = Me, Bu^t$; $R' = Pr^i, Cy$) were made that way from $AlCl_3$ and 2 equivalents of the corresponding lithium amidinate.¹⁰²

Olefin polymerization catalyzed by cationic and neutral aluminum benzamidinate alkyl complexes has been studied by theoretical methods.¹⁰³ In the course of developing new amidinate-based catalysts for the polymerization of methylacrylate and other polar monomers, the activation of dimethylaluminum complexes bearing amidinate ligands was thoroughly investigated. It was found that aluminum (and gallium) (amidinate) MMe_2 complexes react with the "cationic activators" $[Ph_3C][B(C_6F_5)_4]$ and $B(C_6F_5)_3$ to yield cationic Al and Ga alkyl species whose structures are strongly influenced by the steric properties of the amidinate ligand. Scheme 29 illustrates typical examples for the formation and interconversion of mono- and dinuclear species depending of the steric bulk of the amidinate ligand.^{104–107}



Scheme 29

N,N'-unsubstituted amidinato metallacycle complexes of Group 13 metal alkyls have been prepared and studied by X-ray crystallography. The amidinato complexes $[\text{Me}_2\text{ML}]$ ($\text{L} = \text{PhC}(\text{NH})_2$, $\text{M} = \text{Al}, \text{Ga}, \text{In}$; $\text{L} = \text{Bu}^t\text{C}(\text{NH})_2$, $\text{M} = \text{Ga}$) result from the reaction of the metal trialkyls with an equimolar amount of the amidine. An X-ray structural investigation on $[\text{Me}_2\text{Al}[\text{PhC}(\text{NH})_2]]_3$ revealed a novel trimeric structure in the solid state, with bridging benzamidinato ligands, and a 12-membered metallacycle (Figure 10).¹⁰⁸

The opposite side of the steric demand scale is represented by some amidinate ligand containing very bulky organosilicon substituents. For this purpose, the sterically encumbered carbodiimide $[(\text{Ph}_2\text{MeSiCH}_2\text{CH}_2)_3\text{Si}]\text{N}=\text{C}=\text{N}[\text{Si}(\text{CH}_2\text{CH}_2\text{SiMePh}_2)_3]$ was synthesized. Subsequent reaction with AlMe_3 in toluene at elevated temperature (Scheme 30) resulted in formation of a neutral dimethylaluminum mono(amidinate) complex. Reaction of the latter with 1 equivalent of $\text{B}(\text{C}_6\text{F}_5)_3$ formed the neutral complex $[\text{MeC}\{\text{NSi}(\text{CH}_2\text{CH}_2\text{SiMePh}_2)_3\}_2\text{AlMe}(\text{C}_6\text{F}_5)]$ and $\text{BMe}(\text{C}_6\text{F}_5)_2$. Treatment of the silyl-substituted carbodiimide with Cp^*TiMe_3 failed to afford the corresponding amidinate complex.¹⁰⁹

In a related study, sterically bulky amidinate ligands containing terphenyl substituents on the backbone carbon atoms have been utilized in organoaluminum chemistry. Mono(amidinate) dialkyl complexes were generated as shown in

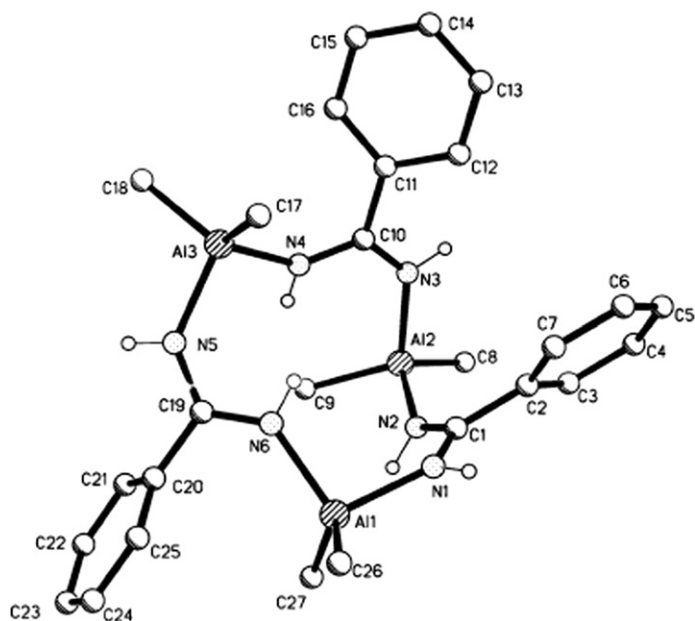
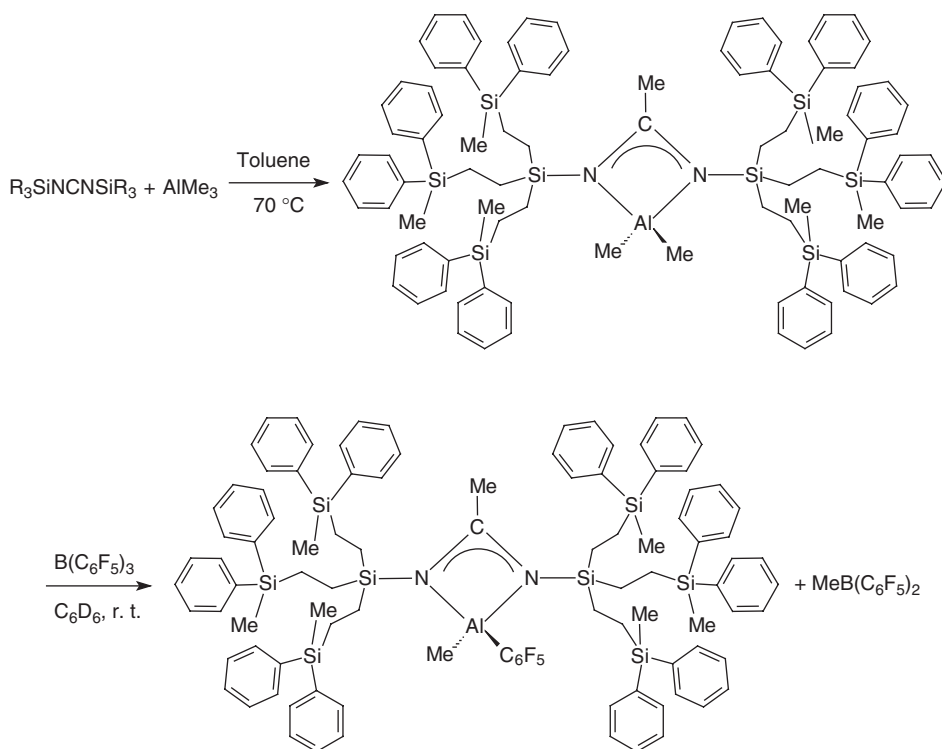
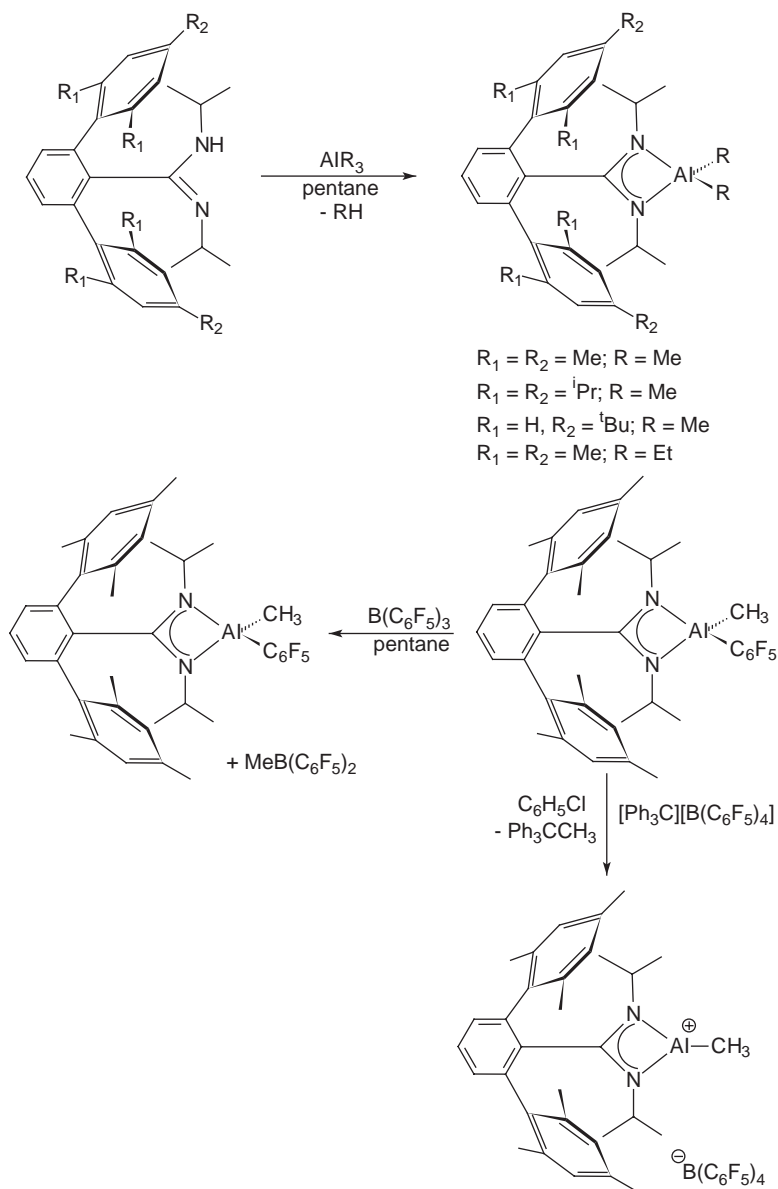


Figure 10 Molecular structure of $[\text{Me}_2\text{Al}\{\text{PhC}(\text{NH})_2\}]_3$.¹⁰⁸



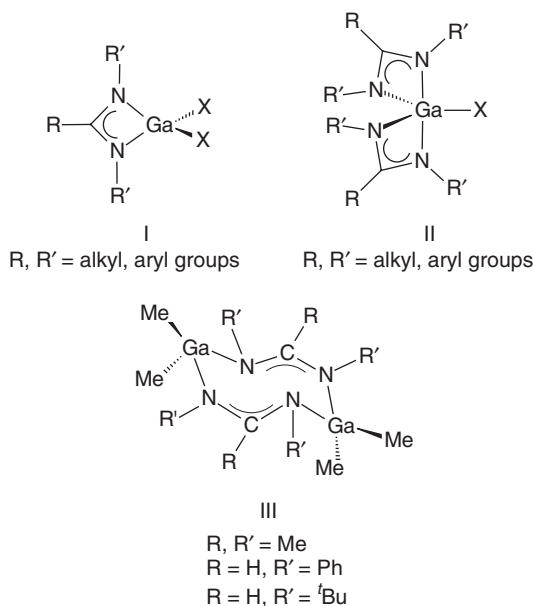
Scheme 30



Scheme 31

Scheme 31, and their reactions with methide abstraction reagents to yield cationic aluminum alkyl species were studied.⁴⁸

Gallium compounds that incorporate amidinate ligands have been studied because of their potential use as volatile precursors to nitride materials.¹¹⁰ The two most common classes of Ga amidinate compounds, however, are $[\text{RC}(\text{NR}')_2]\text{GaX}_2$ species, $\text{X} = \text{Cl}, \text{alkyl}$; I in Scheme 32), in which one amidinate

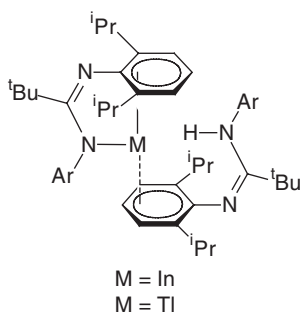
**Scheme 32**

ligand chelates the metal center, and $[\text{RC}(\text{NR}')_2]\text{GaX}$ species ($\text{X} = \text{Cl}$, alkyl; **II** in Scheme 32), which contain two chelating amidinates. There are also a few examples of dinuclear complexes in which two Ga centers are linked by two bridging amidinate ligands (**III** in Scheme 32).¹¹⁰

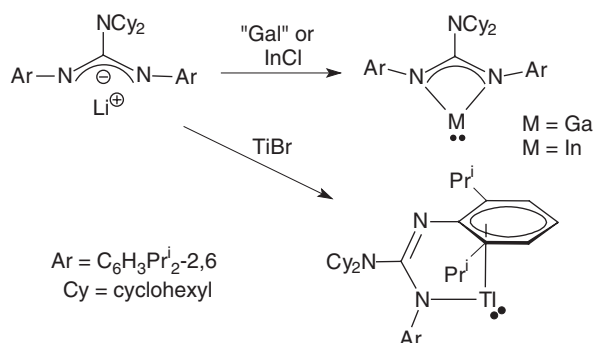
The sterically crowded gallium amidinato complexes $[\text{Bu}^t\text{C}(\text{NR}')_2]\text{GaX}_2$ ($\text{X} = \text{Cl}$, Me, Et, CH_2Ph ; $\text{R}' = \text{Pr}^i$, Bu^t , Cy) have been synthesized in good yield. X-ray crystallographic analyses showed that the steric interactions between the Bu^t and R' groups influence the $\text{R}'\text{-N-Ga}$ angle and the steric environment at gallium.¹¹⁰

The synthesis and characterization of the monomeric amidinato-indium(I) and thallium(I) complexes $[\text{Bu}^t\text{C}(\text{NAr})_2]\text{M}[\text{Bu}^t\text{C}(\text{NAr}(\text{NHAr}))]$ ($\text{M} = \text{In}$, Tl; $\text{Ar} = 2,6\text{-Pr}_2\text{C}_6\text{H}_3$) have been reported. Both compounds were isolated as pale yellow crystals in 72–74% yield. These complexes, in which the metal center is chelated by the amidinate ligand in an N, η^3 -arene-fashion (Scheme 33), can be considered as isomers of four-membered Group 13 metal(I) carbene analogs. Theoretical studies have compared the relative energies of both isomeric forms of a model compound, $\text{In}[\text{HC}(\text{NPh})_2]$.¹¹¹

A major recent achievement in this field was the successful synthesis of four-membered Group 13 metal(I) *N*-heterocyclic carbene (NHC) analogs. A bulky guanidinate ligand was designed especially for this purpose. Treatment of Group 13 metal(I) halides with the lithium guanidinate $\text{Li}[\text{Cy}_2\text{NC}(\text{NAr})_2]$ ($\text{Ar} = \text{C}_6\text{H}_3\text{Pr}_2^{i-2,6}$) as highlighted in Scheme 34 afforded mono(guanidinate) metal(I) complexes. In the cases of the gallium and indium complexes, N, N' -chelation was found to be preferred over N, η^3 -arene-coordination, which was the observed



Scheme 33



Scheme 34

structural motif for the thallium complex. Figure 11 depicts the molecular structure of the gallium complex. These compounds represent the first Group 13 metal(I) analogs of the NHCs. Preliminary theoretical studies suggested that they will make novel ligands and that the corresponding Al(I) heterocycle may be experimentally accessible.^{112–114}

Recently the first examples of complexes between the four-membered amidinato-Group 13 metal(I) heterocycles and transition metal fragments were reported. Complexes of the type CpFe(CO)₂[M(X){Bu^tC(NR)₂}] (M = Al, Ga, In; X = Cl, Br; R = Pri, Cy) were formed in salt-elimination reactions between Na[CpFe(CO)₂] and [Bu^tC(NR)₂]MX₂.¹¹³ A series of complexes between the four-membered amidinato-Group 13 metal(I) heterocycles and Group 10 metal(0) fragments have been prepared according to Scheme 35.¹¹⁴

Reaction of InMe₃ with two moles of benzamidine yielded a cyclic imidoamidinato derivative with a six-membered [InNCNCN] ring. The reaction pathway leading to the formation of the benzimidoylbenzamidonato group remains obscure.¹⁰⁸ Bis(*N,N'*-diphenylacetamidinato)-ethylindium(III), [MeC(NPh)₂]₂InEt, contains an In^{III} atom in a square-pyramidal geometry.¹¹⁵ Reactions of indium trichloride with lithium amidinates in a molar ratio of 1:2 afford the bis(amidinato) indium chlorides which can subsequently be alkylated,

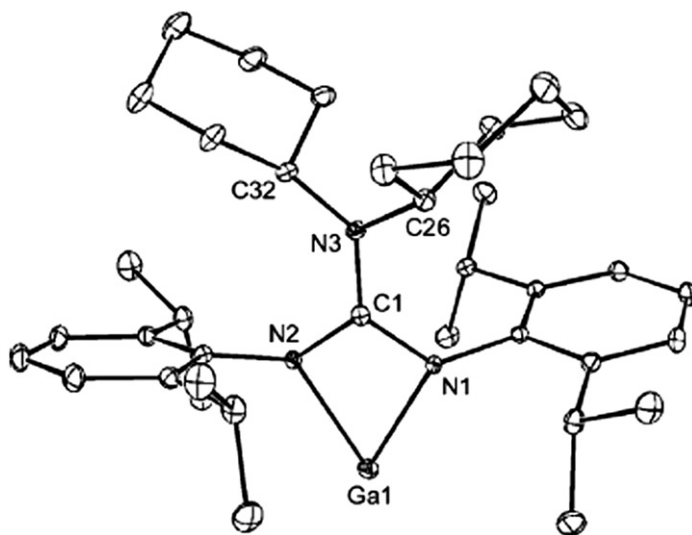
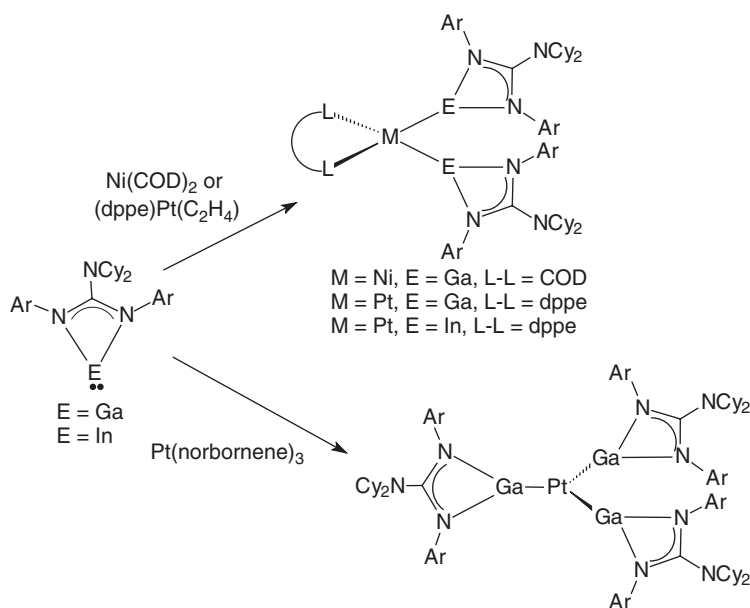
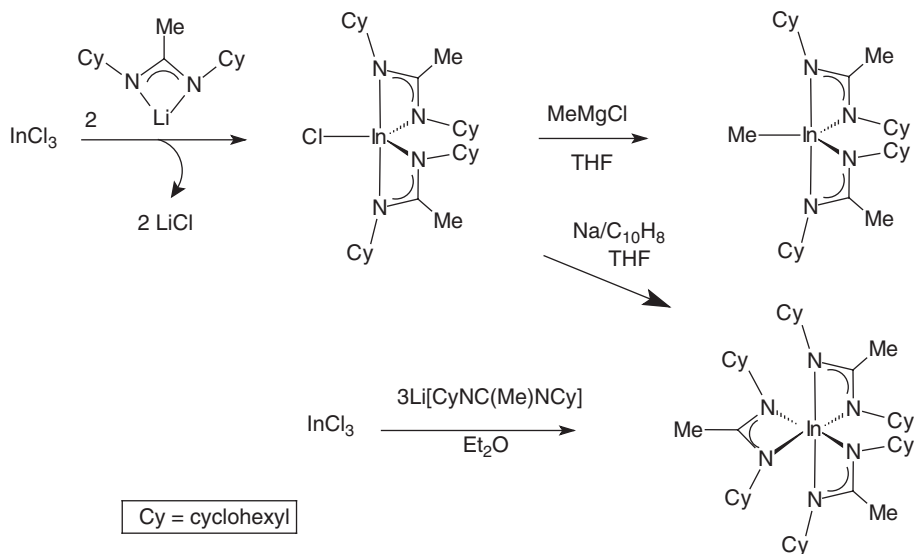


Figure 11 Molecular structure of $[\text{C}_2\text{NC}(\text{NAr})_2]\text{Ga}$.¹¹²

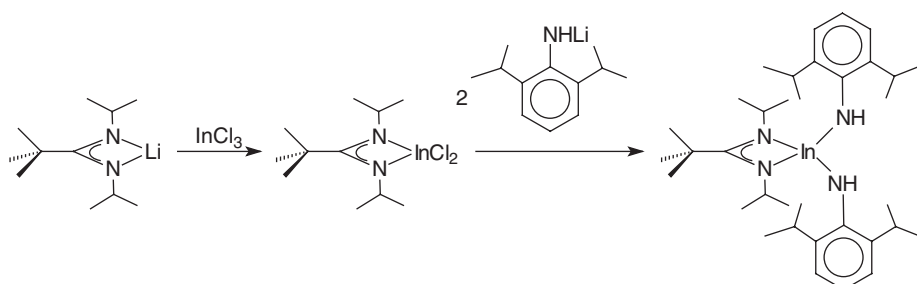


Scheme 35

for example using Grignard reagents. In the case of the less bulky acetamidinates homoleptic indium tris(amidinate) complexes are also accessible. When the methyl group at the central carbon atom is replaced by *t*-butyl the reaction stops at the disubstitution stage. Scheme 36 summarizes typical reactions leading to the various types of indium amidinate complexes.¹¹⁶



Scheme 36



Scheme 37

Scheme 37 shows a reaction sequence leading to a mono(amidinato) indium bis(arylimido) complex. Subsequent treatment of the latter with $\text{Ti}(\text{NMe}_2)_4$ resulted in formation of the heterobimetallic In/Ti complex $[\text{Bu}^t\text{C}(\text{NPr}^i)_2]\text{In}\{\mu\text{-NC}_6\text{H}_3\text{Pr}_2\text{-2,6}\}_2\text{Ti}(\text{NMe}_2)_2$ (cf. Sections III.B.2 and V.A.1).¹¹⁷

In contrast, reactions of trimethylindium with free amidines led to formation of dinuclear amidinate-bridged indium complexes. These reactions are illustrated in Scheme 38.¹¹⁸

Treatment of an ethereal solution of LiInH_4 with 2 equivalents of the bulky formamidine $\text{HC}(\text{NC}_6\text{H}_3\text{Pr}_2\text{-2,6})(\text{NHC}_6\text{H}_3\text{Pr}_2\text{-2,6})$ led to elimination of H_2 and LiH and formation of the unprecedented bis(formamidinato) indium hydride $[\text{HC}(\text{NC}_6\text{H}_3\text{Pr}_2\text{-2,6})_2]_2\text{InH}$. An X-ray structure analysis showed that the complex is monomeric in the solid state and that it has a heavily distorted trigonal-bipyramidal indium coordination environment (Figure 12). Solid $[\text{HC}(\text{NC}_6\text{H}_3\text{Pr}_2\text{-2,6})_2]_2\text{InH}$

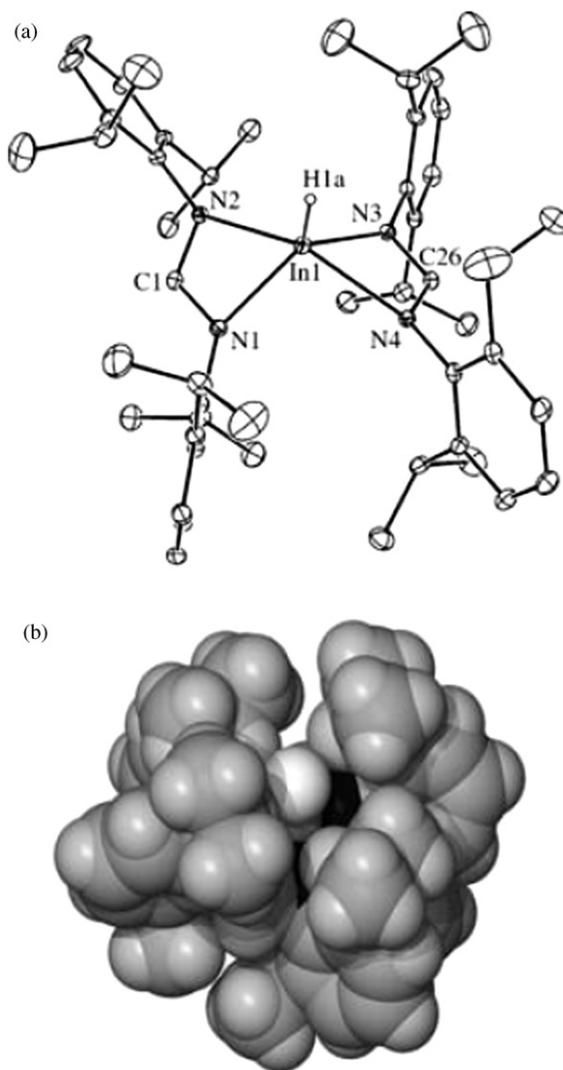
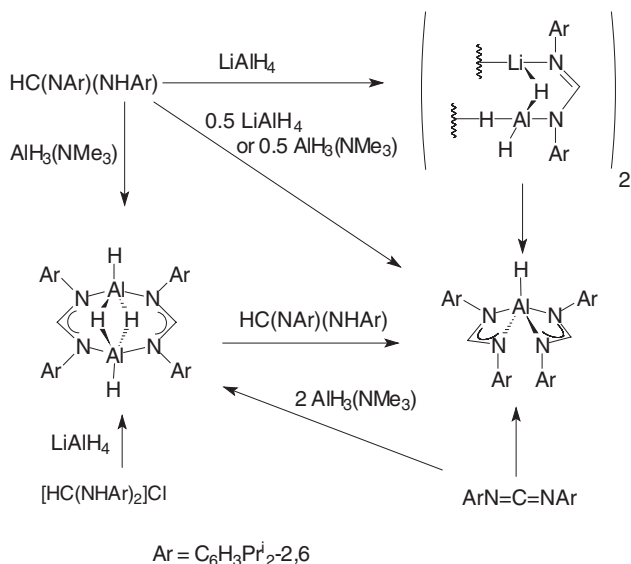


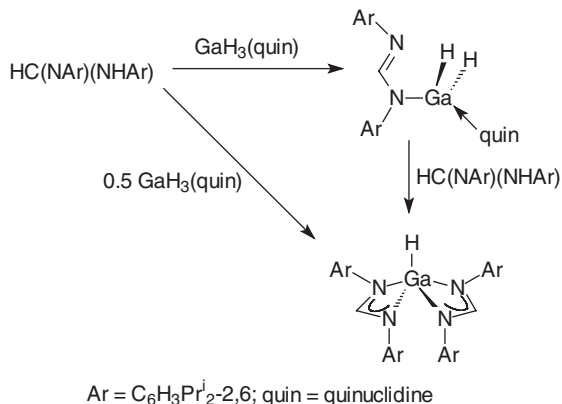
Figure 12 Molecular structure of $[\text{HC}(\text{NC}_6\text{H}_3\text{Pr}_2^{i-2,6})_2]\text{InH}$.¹¹⁹

compounds.”¹²¹ The bonding properties of amidinate complexes of the Group 14 elements silicon, germanium, tin, and lead in their divalent and tetravalent oxidation states have been studied with quantum chemical methods.¹²²

A series of four-, six-, and eight-membered SiNC inorganic heterocycles containing dianionic amidinate ligands was prepared by allowing the lithium amidinates $\text{Li}[\text{PhC}(\text{NR})(\text{NH})]$ ($\text{R} = \text{Me}, \text{Pr}^i$) to react with SiCl_4 or Me_2SiCl_2 .^{123a} The first pentacoordinated silanol has been synthesized according to Scheme 41 by adding traces of water to the starting silaheterocycle and isolated in the form of colorless needles.^{123b}



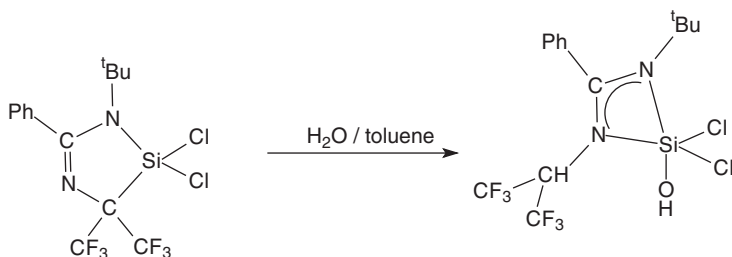
Scheme 39



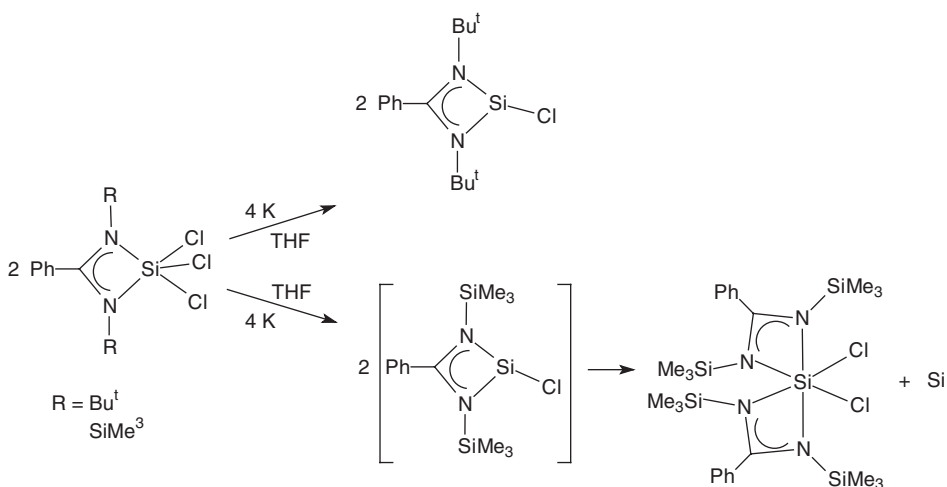
Scheme 40

Notable among the major achievements in this field is the successful synthesis and structural characterization of novel heteroleptic silylenes based on amidinate ligands. Reaction of the benzamidinato silicon trichlorides $[\text{PhC}(\text{NR})_2]\text{SiCl}_3$ ($\text{R} = \text{Bu}^t$, SiMe_3) with 2 equivalents of potassium metal in THF afforded the mononuclear chlorosilylene $[\text{PhC}(\text{NBu}^t)_2]\text{SiCl}$ and the dichlorosilane derivative $[\text{PhC}(\text{NSiMe}_3)_2]\text{SiCl}_2$, with the latter presumably being formed through disproportionation of the unstable chlorosilylene $[\text{PhC}(\text{NSiMe}_3)_2]\text{SiCl}$ (Scheme 42).¹²⁴

Other members of this new class of heteroleptic silylenes could be synthesized by the preparative route outlined in Scheme 43. The colorless



Scheme 41

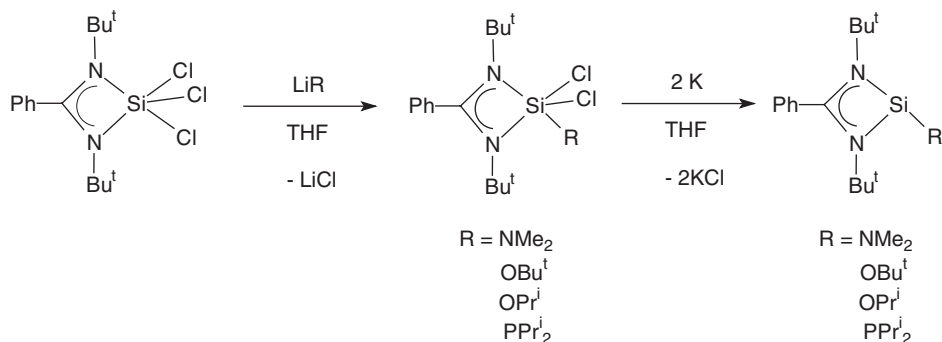


Scheme 42

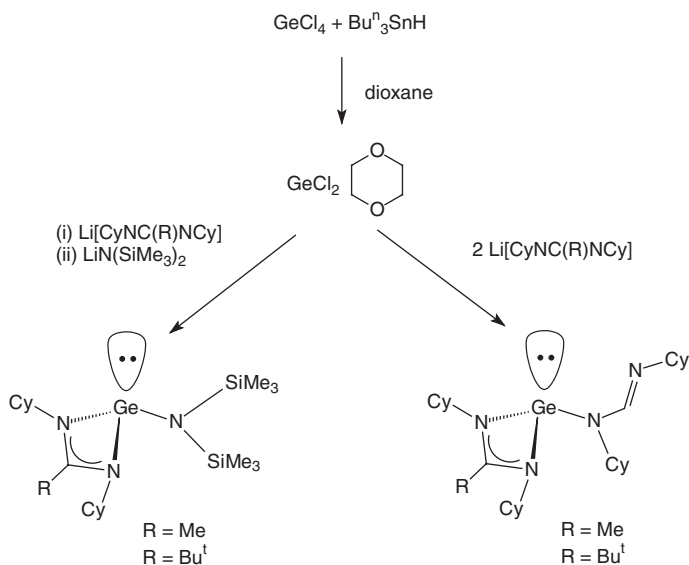
compounds with $\text{R} = \text{NMe}_2$ and PPr_2^i were structurally characterized by single-crystal X-ray analyses.¹²⁴

The first characterized amidinate complexes of Ge were $[\text{MeC}(\text{NCy})_2]_2\text{Ge}$ and $[\text{ButC}(\text{NCy})_2]_2\text{Ge}$, which were both prepared through metathetical reactions between $\text{GeCl}_2(\text{dioxane})$ and the respective lithium amidinates (Scheme 44). The coordination geometry around germanium is distorted tetrahedral with one of the vertices being occupied by a lone pair of electrons. Both molecules exhibit one chelating and one monodentate (dangling) amidinate ligand. Mixed amidinato-amido analogs were similarly obtained as outlined in Scheme 44.¹²⁵

A bis(chelate) structure was found for the closely related gerylene $[\text{MeC}(\text{NPr}^i)_2]_2\text{Ge}$, which was also made from $\text{GeCl}_2(\text{dioxane})$ and 2 equivalents of the lithium amidinate (colorless crystals, 81%). The same synthetic approach was used to make bis(amidinato) metal dichlorides of silicon and germanium in high yields (83–95%).¹²⁶ Rapid oxidative addition of chalcogen atom sources (styrene sulfide and elemental Se) to the gerylene derivatives resulted in a series



Scheme 43



Scheme 44

of rare terminal chalcogenido complexes with the formulas $[\text{RC}(\text{NCy})_2]_2\text{Ge}=\text{E}$ ($\text{R} = \text{Me}, \text{Bu}^t$; $\text{E} = \text{S}, \text{Se}$). In a similar manner the amidinato-amido analogs $[\text{RC}(\text{NCy})_2][\text{N}(\text{SiMe}_3)_2]\text{Ge}=\text{Se}$ ($\text{R} = \text{Me}, \text{Bu}^t$) have been obtained. An X-ray structure determination of the acetamidinate derivative (Figure 13) confirmed the presence of a terminal $\text{Ge}=\text{Se}$ bond.¹²⁵

Oxidative addition of diphenyldichalcogenides, PhEEPh ($\text{E} = \text{S}, \text{Se}$) to $\text{Ge}(\text{II})$ bis(amidinate) complexes was found to occur rapidly, resulting in formation of the corresponding $\text{Ge}(\text{IV})$ bis(phenylchalcogenolato) derivatives as shown in Scheme 45. Diphenylditelluride did not react even at elevated temperatures.¹²⁷

Different coordination modes of the amidinate ligands were observed when the mixed-ligand amidinato-amido complexes of $\text{Ge}(\text{II})$ and $\text{Sn}(\text{II})$ were treated

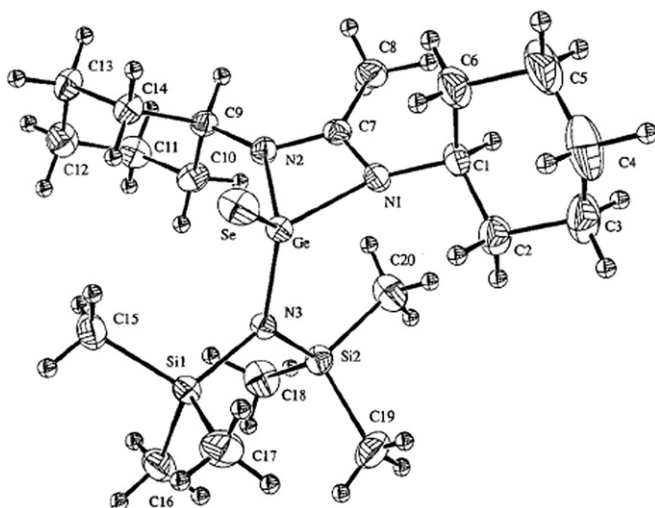
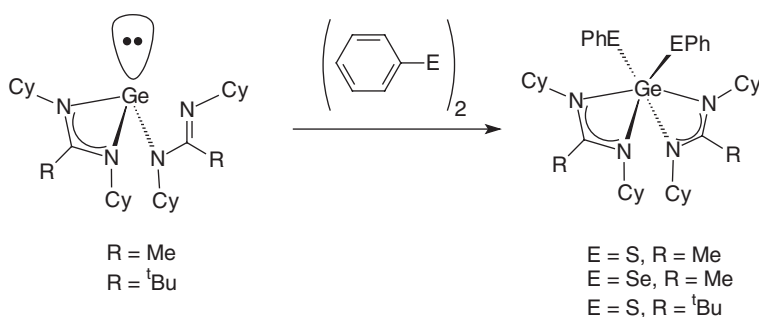


Figure 13 Molecular structure of $[\text{MeC}(\text{NCy})_2][\text{N}(\text{SiMe}_3)_2]\text{Ge}=\text{Se}$.¹²⁵



Scheme 45

similarly with diphenyldichalcogenides (Scheme 46). While the amidinate unit remains chelating in the resulting Sn(IV) bis(phenylchalcogenolates), it becomes “dangling” in the tetrahedrally coordinated germanium products.¹²⁷

The most remarkable recent result in this area was certainly the synthesis of novel germanium(I) dimers, which are stabilized by bulky amidinate or guanidinate ligands. Reactions of the lithium amidinate and guanidinate salts $\text{Li}[\text{Bu}^t\text{C}(\text{NAr})_2]$ and $\text{Li}[\text{Pr}_2^i\text{NC}(\text{NAr})_2]$ ($\text{Ar} = \text{C}_6\text{H}_3\text{Pr}_2^{i,2,6}$) with GeCl_2 (dioxane) yielded the chlorogermanium(II) precursors in good yields. X-ray crystal structure analyses (Figure 14) confirmed the monomeric structure with a chelating, delocalized amidinate ligand, and a Cl-heterocycle plane angle of 104.6° in the amidinate and 102.8° in the guanidinate. Reductions of the chloro precursors with potassium mirrors in toluene at room temperature over 3–4 h afforded deeply colored solutions of the germanium(I) dimers (Scheme 47).

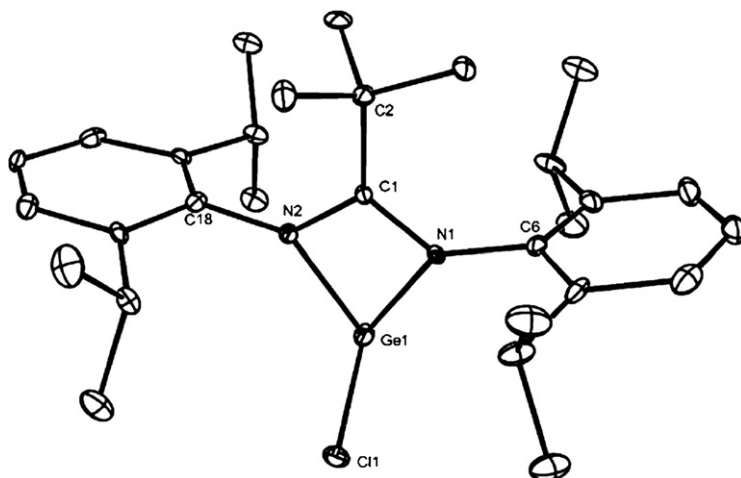
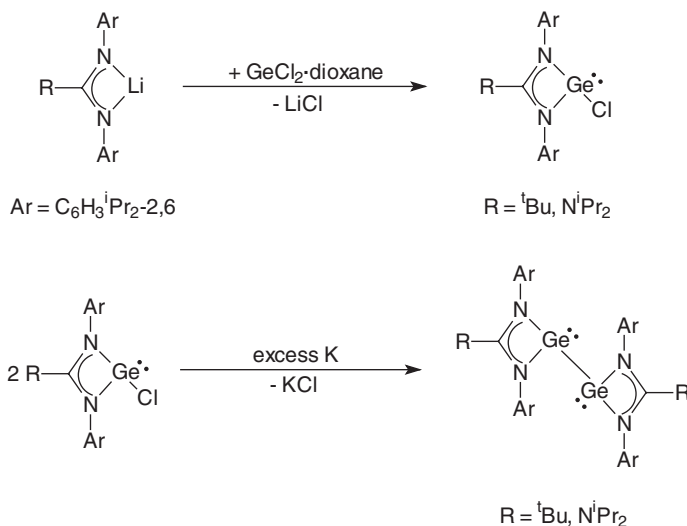


Figure 14 Molecular structure of $[\text{Bu}^t\text{C}(\text{NAr})_2]\text{GeCl}$.¹²⁸

**Scheme 47**

Recrystallization of the crude products from these reactions afforded dichroic, green-red crystals of the amidinate and lime-green crystals of the guanidinate in low yield. Both compounds are remarkably thermally stable, with decomposition temperatures above 200 °C, but are extremely sensitive toward oxygen and moisture. The molecular structure of the amidinate dimer is shown in Figure 15. With 2.6380(8) Å the Ge–Ge bond length is in the normal region for single Ge–Ge interactions but significantly longer than what is typical for digermenes $\text{R}_2\text{Ge}=\text{GeR}_2$ (2.21–2.51 Å). Theoretical studies on a model complex suggested that the Ge–Ge bonds show no multiple bond character but their LUMOs are π -bonding in nature, as is the case for distannynes.¹²⁸

Tin amidinates display a rich coordination chemistry with the metal in both the di- and tetravalent oxidation states. The first results in this area were mainly obtained with *N*-silylated benzamidinate ligands. Typical reactions are summarized in Scheme 48.^{61,129} A stannylene containing unsymmetrically substituted amidinate ligands, $[o\text{-MeC}_6\text{H}_4\text{C}(\text{NSiMe}_3)(\text{NPh})]_2\text{Sn}$, has been prepared accordingly and isolated in the form of colorless crystals in 75% yield.⁶¹

High-yield syntheses of the bulky tin(IV) amidinate complexes $[\text{RC}(\text{NCy})_2]_2\text{SnCl}_2$ (R = H, Me) and $[\text{Bu}^t\text{C}(\text{NSiMe}_3)_2]_2\text{SnCl}_2$ have been reported.¹³⁰ The fluorinated benzamidinate ligand $[2,4,6\text{-(CF}_3)_3\text{C}_6\text{H}_2\text{C}(\text{NSiMe}_3)_2]^-$ forms the stable tin(II) and lead(II) bis(amidinates) $[2,4,6\text{-(CF}_3)_3\text{C}_6\text{H}_2\text{C}(\text{NSiMe}_3)_2]_2\text{M}$ (M = Sn, Pb).¹³¹ More recently, the tin(II) coordination chemistry of two *N,N'*-bis(2,6-diisopropylphenyl)alkylamidinate ligands was investigated.¹³² Complexation studies with the acetamidinate ligand $[\text{MeC}(\text{NAr})_2]^-$ (Ar = $\text{C}_6\text{H}_3\text{Pr}_2^i\text{-2,6}$) were found to be complicated by the side formation of the bis(amidinate) tin(II) compound $[\text{MeC}(\text{NAr})_2]_2\text{Sn}$ (Scheme 49).¹³²

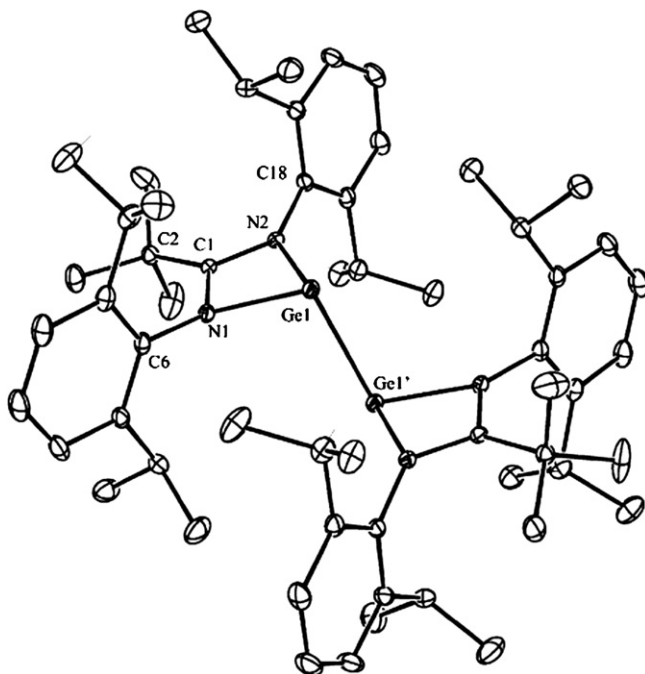
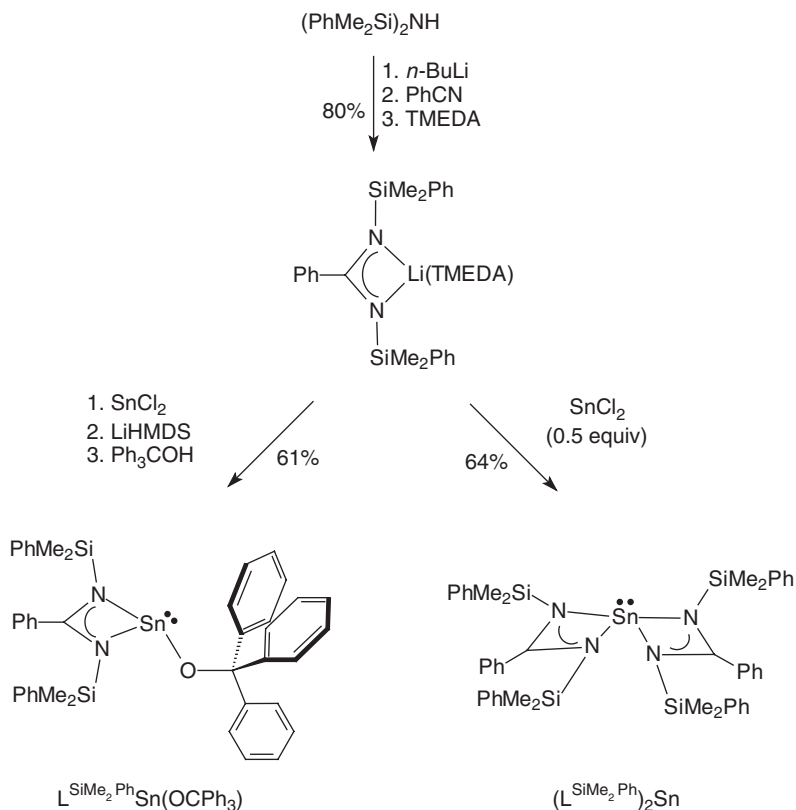


Figure 15 Molecular structure of $[(\text{Bu}^t\text{C}(\text{NAr})_2)\text{Ge}]_2$.¹²⁸

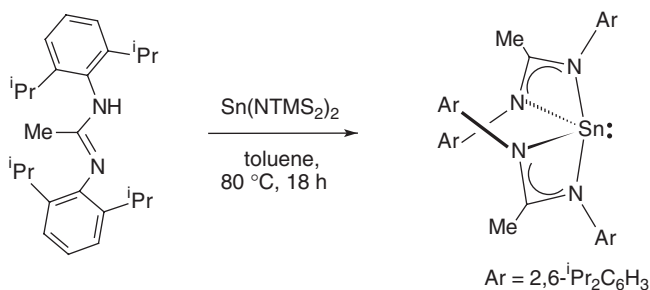
In contrast, the bulkier *tert*-butylamidinate $[\text{Bu}^t\text{C}(\text{NAr})_2]^-$ allowed tin(II) mono-halide, -alkoxide, and -amide complexes to be isolated cleanly in high yields. The preparative routes are summarized in [Scheme 50](#).¹³²

Interesting new sulfido complexes of tin have been prepared by the reaction of styrene sulfide with the *N*-alkylated tin(II) amidinate complexes $\text{Sn}[\text{RC}(\text{NCy})_2]_2$ (Cy = cyclohexyl; R = Me, Bu^t). The products exhibit two very different bonding modes for the sulfido ligands: in one case, $\text{S}=\text{Sn}[\text{RC}(\text{NCy})_2]_2$, a terminal $\text{Sn}=\text{S}$ moiety was found while in the other case the bridging sulfido dimer $[\text{RC}(\text{NCy})_2]_2\text{Sn}(\mu\text{-S})_2$ was formed.^{130,133} Unusual cyclic tin tetrasulfido complexes have been prepared by the reaction of elemental sulfur with the amidinato tin amides $[\text{RC}(\text{NCy})_2]\text{Sn}[\text{N}(\text{SiMe}_3)_2]$ (R = Me, Bu^t ; [Scheme 51](#)). The tetrasulfide derivatives were further converted to dimeric sulfido complexes, which can also be derived from the oxidative addition of sulfur atom sources (e.g., propylene sulfide) to the stannylene precursors $[\text{RC}(\text{NCy})_2]\text{Sn}[\text{N}(\text{SiMe}_3)_2]$.^{130,134}

The first guanidinate complexes of tin have been prepared using *N,N',N''*-trialkylguanidates, $[\text{RNHC}(\text{NR})_2]^-$ (R = Cy, Pr^i), as ligands. The direct reaction between triisopropylguanidine and SnCl_4 according to [Scheme 52](#) provided the complex $[\text{Pr}^i\text{NHC}(\text{NPr}^i)_2]\text{SnCl}_3$ along with concomitant formation of the guanidinium salt $[\text{C}(\text{NHPr}^i)_3][\text{SnCl}_5(\text{THF})]$. The Sn(II) guanidinate complex $[\text{CyNHC}(\text{NCy})_2]_2\text{Sn}$ was prepared from SnCl_2 and $\text{Li}[\text{CyNHC}(\text{NCy})_2]$.¹³⁵



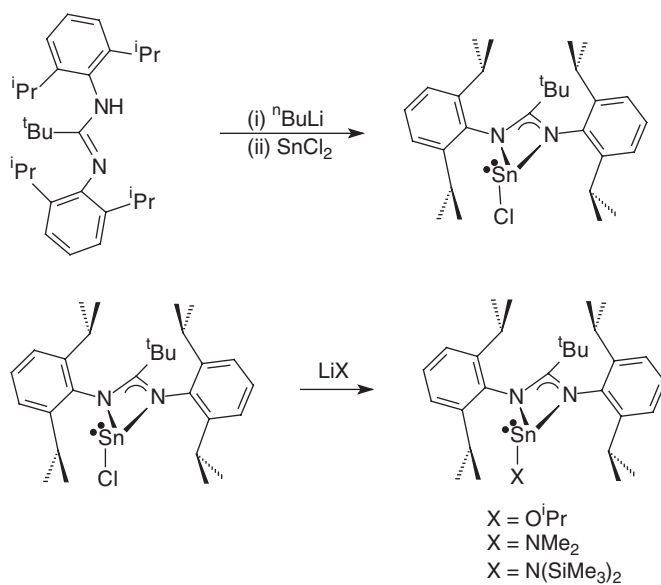
Scheme 48



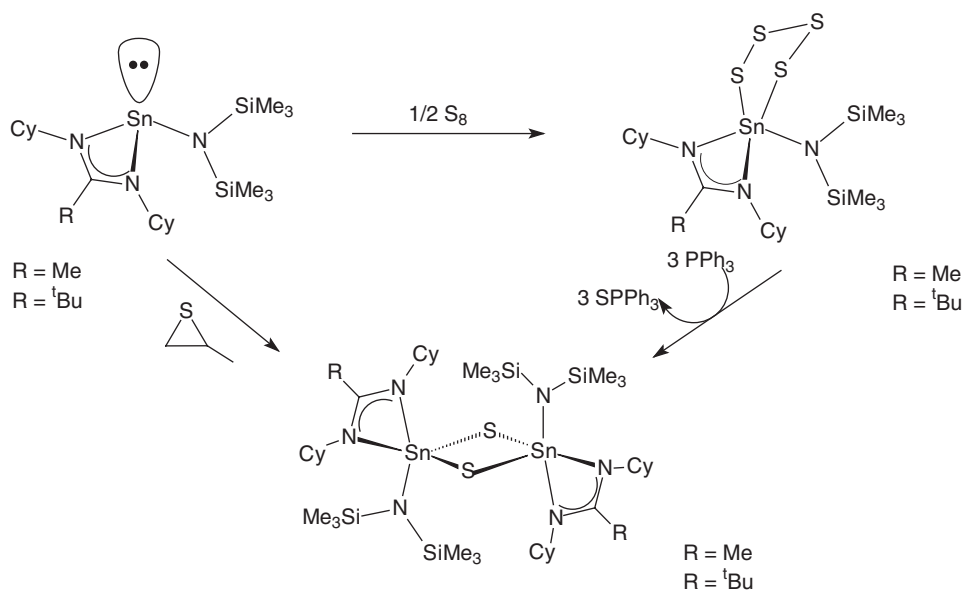
Scheme 49

5. Group 15 metal complexes

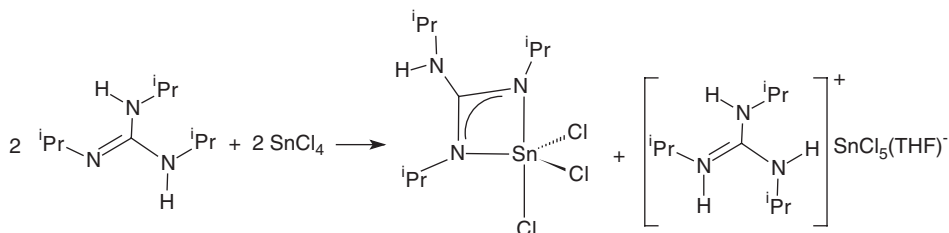
Little progress has been made in the field of Group 15 metal amidinate and guanidinate derivatives. Only very recently some exciting results have been reported which demonstrate that this area may hold some real surprises and merits further exploration. It was found that amidinato ligands are capable to stabilize novel amidodiarsenes. Reduction of the four-membered ring As(III)



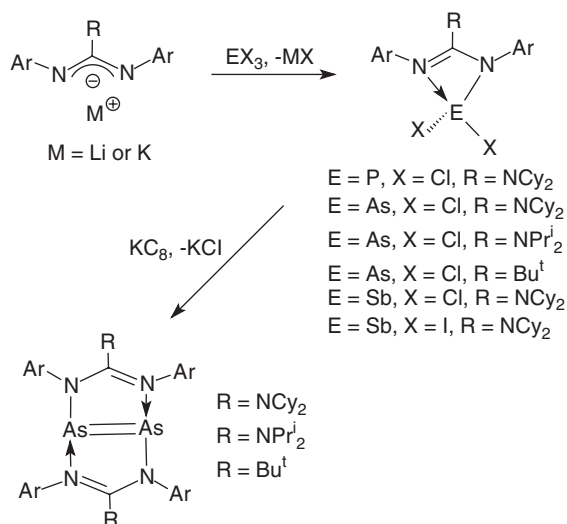
Scheme 50



Scheme 51



Scheme 52



Scheme 53

precursors $[\text{RC}(\text{NAr})_2]\text{AsCl}_2$ with KC_8 in toluene (Scheme 53) afforded the guanidinato- or amidinato-bridged diarsenes $[\text{As}\{\mu\text{-RC}(\text{NAr})_2\}]_2$ ($\text{R} = \text{NCy}_2$, NPr_2 , Bu^t ; $\text{Ar} = \text{C}_6\text{H}_3\text{Pr}_2\text{-2,6}$). The corresponding P and Sb precursors did not afford isolable double-bonded species. Figure 16 depicts the molecular structure of the guanidinate derivative $[\text{As}\{\mu\text{-Cy}_2\text{NC}(\text{NAr})_2\}]_2$. The As–As distance in this compound is 2.2560(5) Å. Theoretical studies suggest that the As–As bonds of the dimers have significant double-bond character, the σ and π components of which are derived mainly from As p orbital overlaps.¹³⁶

Especially notable is also the synthesis and structural characterization of an unusual antimony(III) guanidinate.^{137a} 1,2,3-Triisopropylguanidine, $\text{Pr}^i\text{N}=\text{C}(\text{NHP}^i)_2$, was found to react with 1 molar equivalent of $\text{Sb}(\text{NMe}_2)_3$ in toluene under formation of a yellow solution, from which the novel compound $\text{Sb}[\text{Pr}^i\text{NC}(\text{NPr}^i)_2][\text{Pr}^i\text{NHC}(\text{NPr}^i)_2]$ could be isolated in 10% yield as highly air-sensitive crystals. In the solid state, the complex adopts a heavily distorted trigonal-bipyramidal molecular structure in which the Sb is chelated by a $[\text{C}(\text{NPr}^i)_3]^{2-}$ dianion and a $[\text{Pr}^i\text{NHC}(\text{NPr}^i)_2]^-$ monoanion (Figure 16). Supramolecular

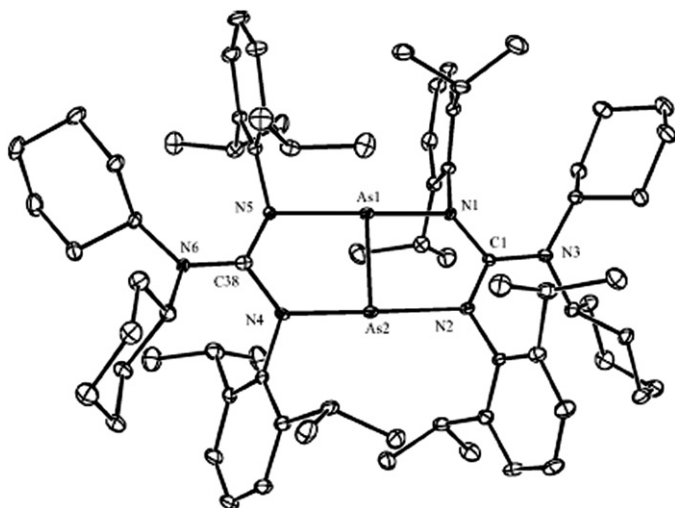


Figure 16 Molecular structure of $[\text{As}\{\mu\text{-Cy}_2\text{NC}(\text{NAr})_2\}]_2$.¹³⁶

association leads to formation of a helical N–H···N hydrogen-bonded network (Figure 17).^{137a}

A series of novel homoleptic and heteroleptic bismuth(III) formamidinate complexes has been prepared and structurally characterized.^{137b} Using formamidinate ligands L of differing steric bulk ($\text{L} = [\text{HC}(\text{NAr})_2]^-$, Ar = substituted aryl) it was possible to isolate and characterize stable complexes of the types $[(\text{L})\text{BiBr}(\mu\text{-Br})(\text{THF})]_2$, $[(\text{L})\text{BiCl}_2(\text{THF})]_2\text{Bi}(\text{L})\text{Cl}_2$, L_2BiX (X = Cl, Br), and BiL_3 . In one instance, an analogous organometallic complex, L_2BiBu^n , was also isolated as a side-product. The complexes of the form L_2BiX (X = Cl, Br, Bu^n) and BiL_3 all have monomeric structures, but the BiL_3 species show marked asymmetry of the formamidinate binding suggesting that they have reached coordination saturation.^{137b}

B. Amidinate and guanidinate complexes of the early transition metals

1. Group 3 metal complexes (Sc, Y, La, and the lanthanides and actinides)

For decades, the most important ancillary ligands in organo-*f*-element chemistry have been the derivatives of cyclopentadienyl anions, since lanthanocene complexes have shown highly efficient catalytic activity for various olefin transformations such as hydrogenation, polymerization, hydroboration, hydrosilylation, and hydroamination. However, in this chemistry the steric saturation of the coordination sphere around the large *f*-element ions is much more important than the number of valence electrons. Thus current research in this area is increasingly focussed on the development of alternative ligand sets. Amidinate and guanidinate play a central role in this area of research. An early account of lanthanide amidinate chemistry can be found in a 1995 review article by Edelmann entitled “Cyclopentadienyl-free organolanthanide chemistry.”¹³⁸

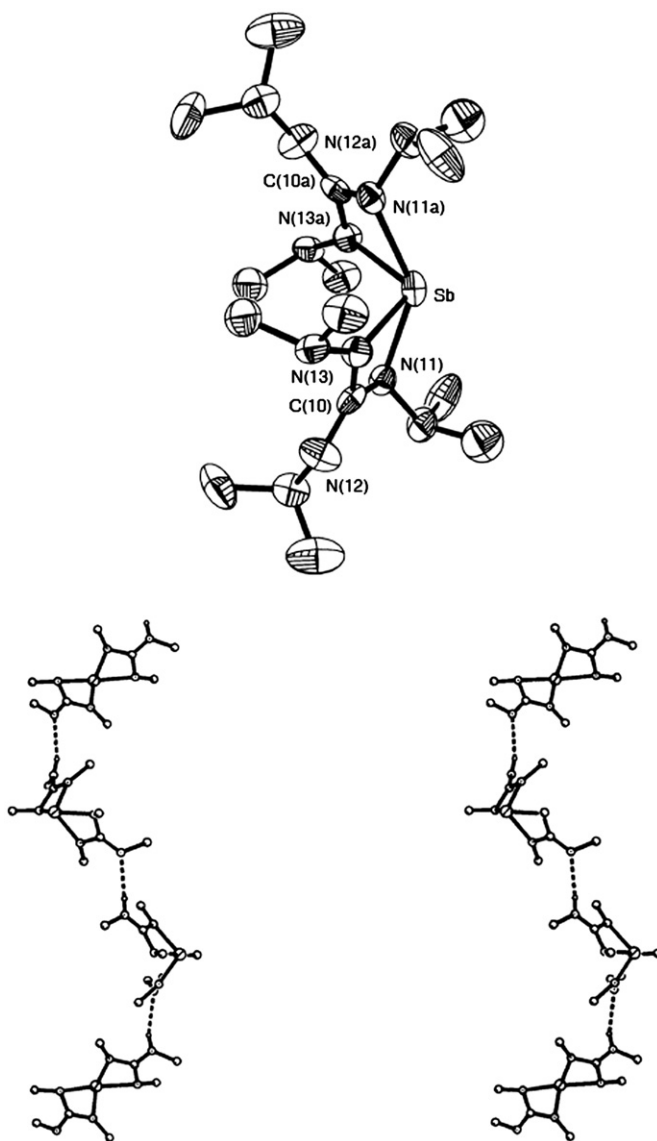
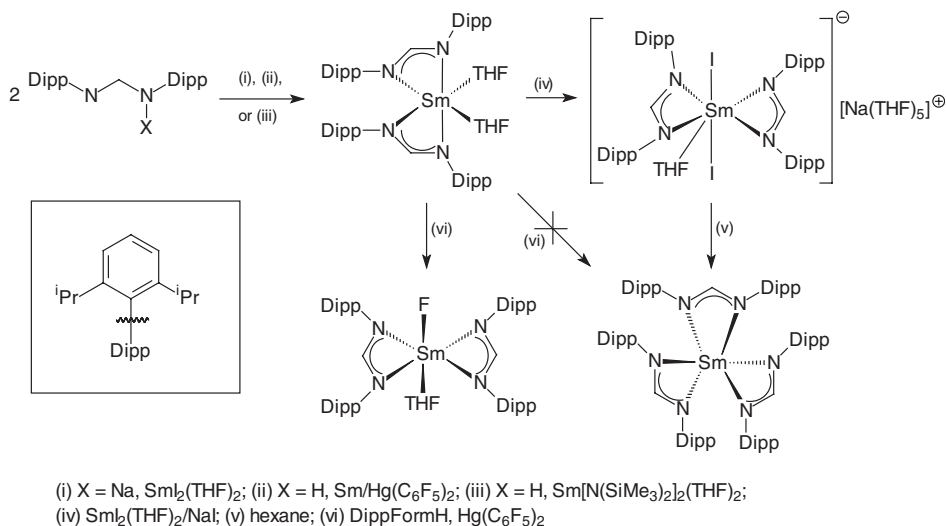


Figure 17 Molecular structure of $\text{Sb}[\text{Pr}^i\text{NC}(\text{NPr}^i)_2][\text{Pr}^i\text{NHC}(\text{NPr}^i)_2]$ (top) and stereoview showing the association of molecules of $\text{Sb}[\text{Pr}^i\text{NC}(\text{NPr}^i)_2][\text{Pr}^i\text{NHC}(\text{NPr}^i)_2]$ via N–H...N hydrogen bond into helices (bottom).^{137a}

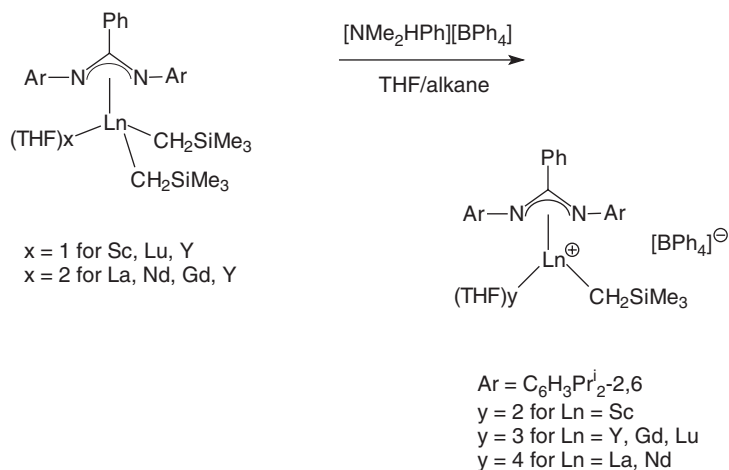
While ytterbium(II) benzamidinate complexes have been known for many years,¹ the synthesis of the first divalent samarium bis(amidinate) required the use of a sterically hindered amidinate ligand, $[\text{HC}(\text{NDipp})_2]^-$ (Dipp = $\text{C}_6\text{H}_3\text{Pr}_2$ -2,6).^{139a} As illustrated in Scheme 54, the dark green compound $\text{Sm}(\text{DippForm})_2(\text{THF})_2$ (DippForm = $[\text{HC}(\text{NDipp})_2]^-$) can be prepared by three different synthetic routes. Structural data indicated that hexacoordinated

**Scheme 54**

$\text{Sm}(\text{DippForm})_2(\text{THF})_2$ is isomorphous with the related strontium and barium amidinates. The trivalent samarate complex $[\text{Na}(\text{THF})_5][\text{SmI}_2(\text{DippForm})_2(\text{THF})_2]$ was isolated in small quantities as a colorless by-product. Dissolution of this compound in hexane led to ligand redistribution to give homoleptic $\text{Sm}(\text{DippForm})_3$ with concomitant precipitation of NaI and $\text{SmI}_3(\text{THF})_{3.5}$. The monofluoro-bis(amidinate) $\text{SmF}(\text{DippForm})_2(\text{THF})$ could also be isolated from $\text{Sm}(\text{DippForm})_2(\text{THF})_2$.^{139a}

In 2007 the first homoleptic lanthanide(II) guanidinate complexes, $\text{Ln}(\text{Giso})_2$ ($\text{Ln} = \text{Sm}, \text{Eu}, \text{Yb}$; $\text{Giso} = \text{Cy}_2\text{NC}(\text{NAr})_2$; $\text{Ar} = \text{C}_6\text{H}_3\text{Pr}_2\text{-}2,6$), were reported and shown to have differing coordination geometries (including unprecedented examples of planar 4-coordination). In particular, X-ray studies revealed planar 4-coordinate coordination geometries for Sm and Eu derivatives, while the ytterbium(II) species is distorted tetrahedral. In the case of Yb , two iodo-bridged dimeric lanthanide(II) guanidinate complexes were also isolated from the reaction mixtures.^{139b} The reaction of equimolar amounts of $\text{Na}[(\text{Me}_3\text{Si})_2\text{NC}(\text{NCy})_2]$ (which was prepared *in situ* from $\text{NaN}(\text{SiMe}_3)_2$ and N,N' -dicyclohexylcarbodiimide) and $\text{YbI}_2(\text{THF})_2$ in THF gave the closely related ytterbium(II) guanidinate complex $\{[(\text{Me}_3\text{Si})_2\text{NC}(\text{NCy})_2]\text{Yb}(\mu\text{-I})(\text{THF})_2\}_2$ with bridging iodo ligands.¹⁴⁰

A review article entitled “Bulky amido ligands in rare-earth chemistry: Syntheses, structures, and catalysis” has been published by Roesky. Benzamidinate ligands are briefly mentioned in this context.¹⁴¹ The use of bulky benzamidinate ligands in organolanthanide chemistry was also briefly mentioned in a review article by Okuda et al. devoted to “Cationic alkyl complexes of the rare-earth metals: Synthesis, structure, and reactivity.” Particularly mentioned in this article are reactions of neutral bis(alkyl) lanthanide benzamidinates with $[\text{NMe}_2\text{HPh}][\text{BPh}_4]$ which result in the formation of thermally robust ion pairs (Scheme 55).^{142,143}

**Scheme 55**

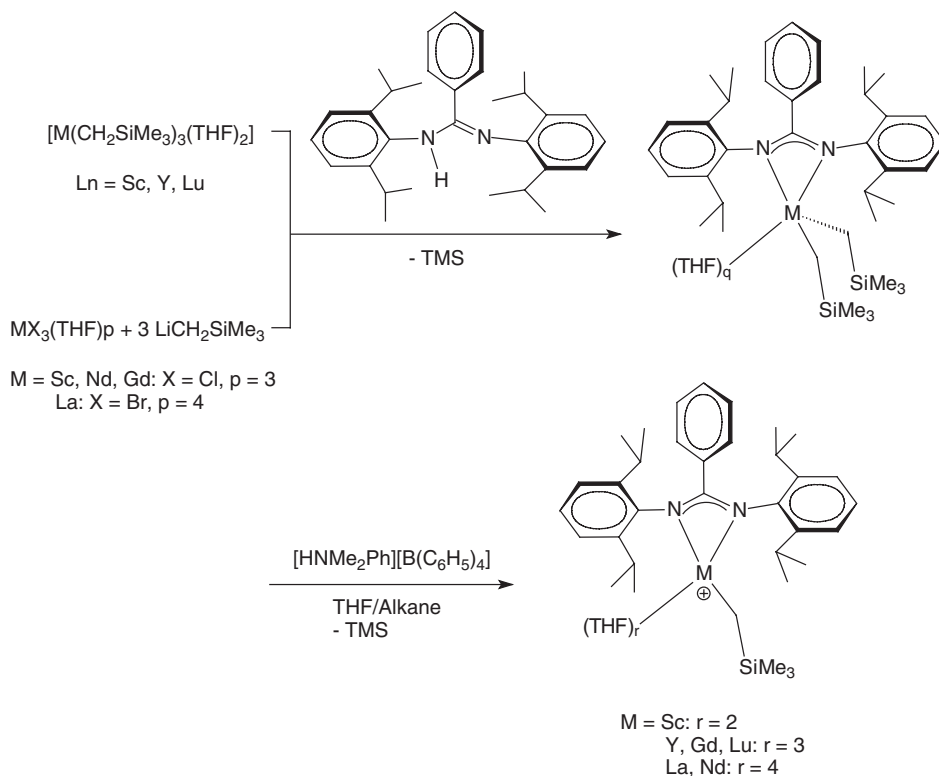
In a systematic study, it was demonstrated that, using a specially designed bulky benzamidinate ligand, it is possible to isolate mono(amidinato) dialkyl complexes over the full size range of the Group 3 and lanthanide metals, i.e., from scandium to lanthanum. The synthetic methods leading to the neutral and cationic bis(alkyls) are summarized in Scheme 56. Figure 18 displays the molecular structures of the cations obtained with Sc, Gd, and La.¹⁴⁴

A novel amidinate ligand incorporating a bulky terphenyl group has been synthesized by the reaction sequence outlined in Scheme 57. The ligand was used to prepare unusual, low-coordinate lithium and yttrium mono-amidinate complexes.⁴⁷

A mono(amidinato) dialkyl yttrium complex, $[\text{Bu}^t\text{C}(\text{NPr}^i)_2]\text{Y}[\text{CH}(\text{SiMe}_3)_2]_2(\mu\text{-Cl})\text{Li}(\text{THF})_3$, has also been prepared by the sequential reaction of $\text{YCl}_3(\text{THF})_{3.5}$ with $\text{Li}[\text{Bu}^t\text{C}(\text{NPr}^i)_2]$ and 2 equivalents of $\text{LiCH}(\text{SiMe}_3)_2$. Coordination of LiCl to the yttrium center results in a five-coordinated molecule (Figure 19).¹⁴⁵

Mono(guanidinate) complexes of lanthanum^{146a} and yttrium^{146b} have been synthesized as illustrated in Scheme 58.^{146a} The lanthanum compounds were made starting from $\text{La}[\text{N}(\text{SiMe}_3)_2]_3$ and dicyclohexylcarbodiimide. Both mono(guanidinate) derivatives are monomeric in the solid state with a four-coordinate La center.^{146a}

In the case of yttrium, it was recently reported that even the less bulky guanidinate ligand $[(\text{Me}_3\text{Si})\text{NC}(\text{NPr}^i)_2]^-$ stabilizes mono(guanidinato) complexes such as $[(\text{Me}_3\text{Si})\text{NC}(\text{NPr}^i)_2]\text{YCl}_2(\text{THF})_2$, $[(\text{Me}_3\text{Si})\text{NC}(\text{NPr}^i)_2]\text{Y}(\text{CH}_2\text{SiMe}_3)_2(\text{THF})_2$, and $[(\text{Me}_3\text{Si})\text{NC}(\text{NPr}^i)_2]\text{Y}(\text{Bu}^t)_2(\text{THF})$.^{146b} Closely related mono(guanidinato) lanthanide borohydride complexes of the type $[(\text{Me}_3\text{Si})_2\text{NC}(\text{NCy})_2]\text{Ln}(\text{BH}_4)_2(\text{THF})_2$ (Ln = Nd, Sm, Er, Yb) were prepared by the reactions of the corresponding borohydrides $\text{Ln}(\text{BH}_4)_3(\text{THF})_3$ with the sodium guanidinate $\text{Na}[(\text{Me}_3\text{Si})_2\text{NC}(\text{NCy})_2]$ in a 1:1 molar ratio in THF,¹⁴⁷ while two scandium mono(benzamidinates) containing tetradentate diamino-bis(phenolate) ligands (Scheme 59) were synthesized from ScCl_3 by subsequent reaction with the respective alkali metal salts of the two ligand systems.^{148a} The formation of dianionic benzamidinate ligands has



Scheme 56

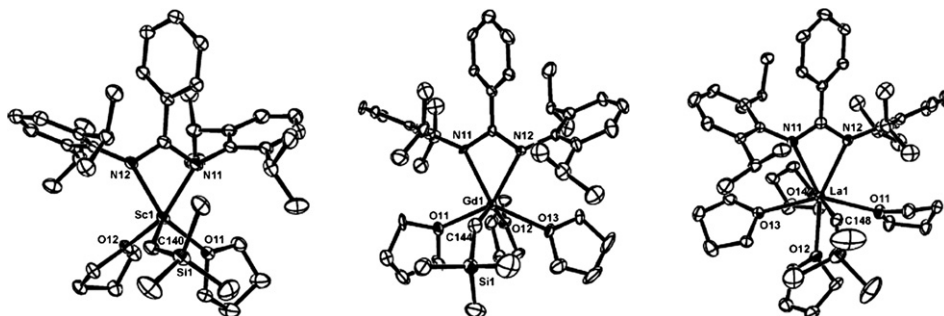
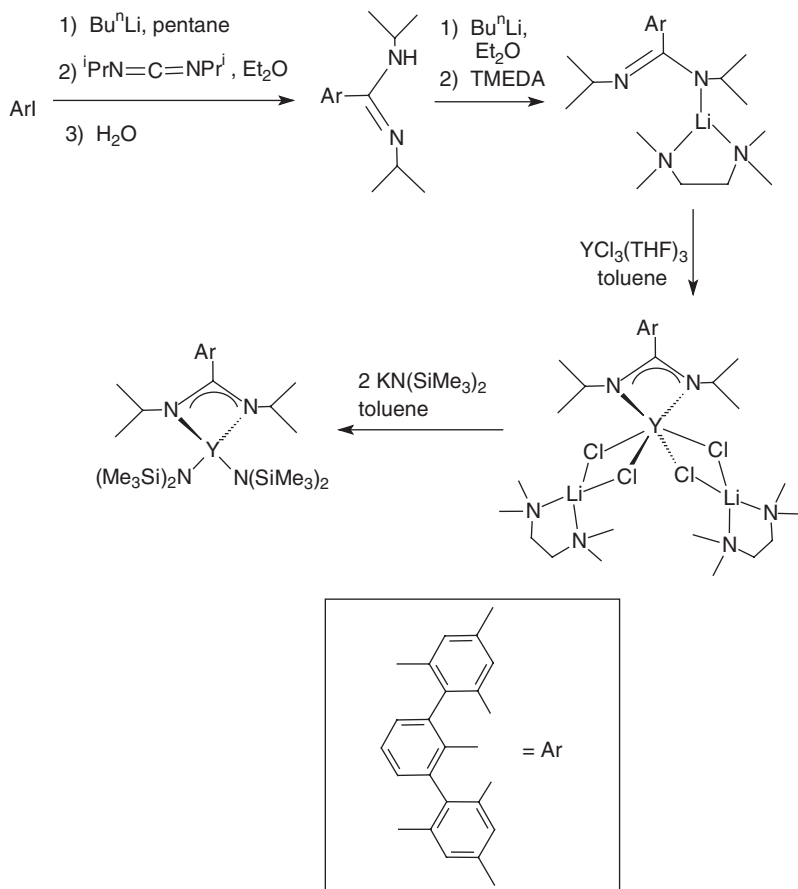


Figure 18 Molecular structure of $[\text{PhC}(\text{NAr})_2]\text{Ln}(\text{CH}_2\text{SiMe}_3)(\text{THF})_n$ cations ($\text{Ln} = \text{Sc}$, $n=2$; $\text{Ln} = \text{Gd}$, $n=3$; $\text{Ln} = \text{La}$, $n=4$).¹⁴⁴

been reported for reactions of lanthanide-imido cluster complexes with benzonitrile.^{148b}

Bis(phenolate) ligands are also present in two new lanthanide guanidinate complexes shown in Scheme 60, which were prepared by insertion of diisopropylcarbodiimide into the $\text{Ln}-\text{N}$ bonds of appropriate neutral lanthanide amide precursors.¹⁴⁹

**Scheme 57**

A series of highly colored mono(benzamidinato) cyclooctatetraenyl lanthanide(III) complexes was prepared as shown in [Scheme 61](#) by reactions of either $[(\text{C}_8\text{H}_8)\text{Ln}(\mu\text{-Cl})(\text{THF})_2]$ or $[(\text{C}_8\text{H}_8)\text{Ln}(\mu\text{-O}_3\text{SCF}_3)(\text{THF})_2]_2$ with the sodium benzamidinate derivatives $\text{Na}[\text{RC}_6\text{H}_4\text{C}(\text{NSiMe}_3)_2]$ ($\text{R} = \text{H}, \text{OMe}, \text{CF}_3$). According to X-ray structural analyses of $[\text{PhC}(\text{NSiMe}_3)_2]\text{Tm}(\text{C}_8\text{H}_8)(\text{THF})$ and $[\text{MeOC}_6\text{H}_4\text{C}(\text{NSiMe}_3)_2]\text{Lu}(\text{C}_8\text{H}_8)(\text{THF})$, the compounds are monomeric in the solid state.¹⁵⁰

The scandium and yttrium bis(benzamidinates) $[\text{RC}_6\text{H}_4\text{C}(\text{NSiMe}_3)_2]_2\text{LnCl}(\text{THF})$ ($\text{Ln} = \text{Sc}, \text{Y}$; $\text{R} = \text{H}, \text{MeO}, \text{CF}_3$) were prepared from $\text{ScCl}_3(\text{THF})_3$ or $\text{YCl}_3(\text{THF})_{3.5}$ by treatment with 2 equivalents of the corresponding lithium benzamidinates. A similar approach using yttrium triflate as starting material has been used to prepare the first bis(amidinato) lanthanide triflate complexes ([Scheme 62](#)).¹⁵¹

Metathetical routes using bulky lithium guanidinates as starting materials have also been employed to synthesize bis(guanidinato) lanthanide halides as well as reactive alkyls and hydrides. [Scheme 63](#) shows as a typical example the formation of the lutetium chloro precursor, which was isolated in 76% yield.^{152–156}

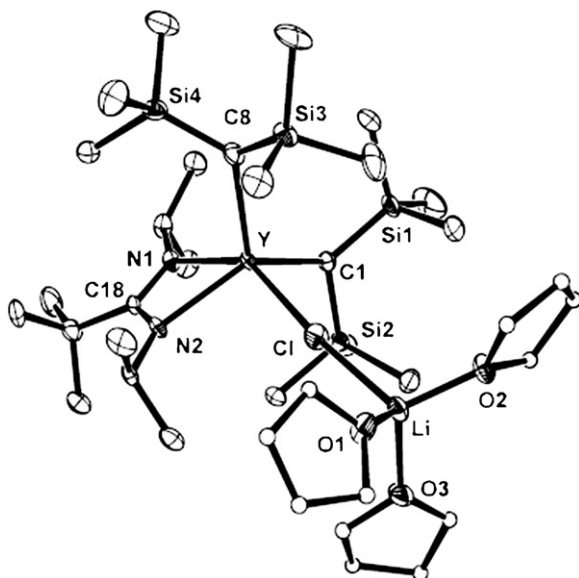
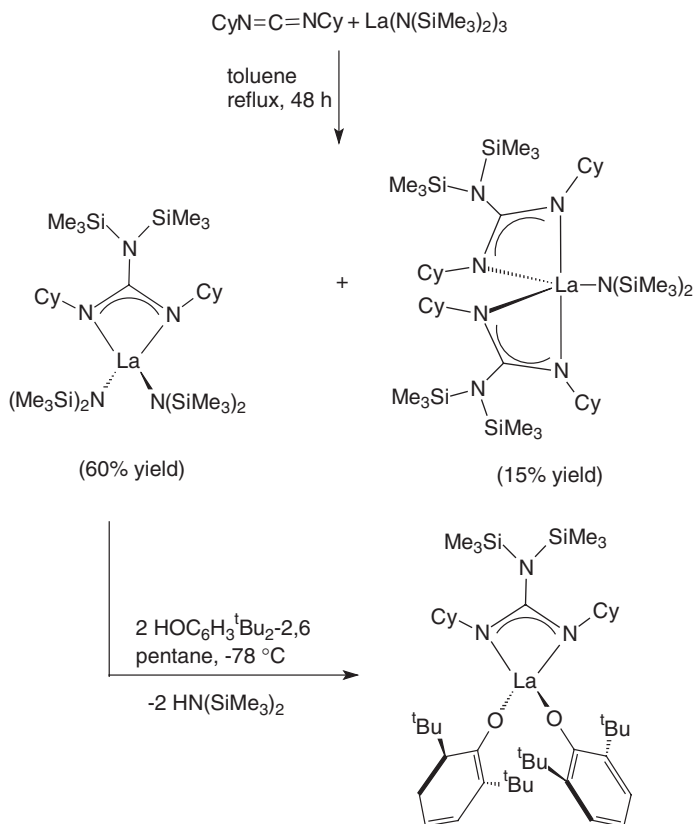


Figure 19 Molecular structure of $[\text{Bu}^t\text{C}(\text{NPr}^i)_2]\text{Y}[\text{CH}(\text{SiMe}_3)_2](\mu\text{-Cl})\text{Li}(\text{THF})_3$.¹⁴⁵

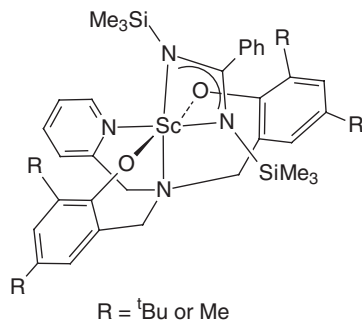
Treatment of $[(\text{Me}_3\text{Si})_2\text{NC}(\text{NPr}^i)_2]_2\text{Ln}(\mu\text{-Cl})_2\text{Li}(\text{THF})_2$ with 2 equivalents of methyllithium in the presence of TMEDA afforded the methyl bridged “ate” complexes $[(\text{Me}_3\text{Si})_2\text{NC}(\text{NPr}^i)_2]_2\text{Ln}(\mu\text{-Me})_2\text{Li}(\text{THF})_2$ ($\text{Ln} = \text{Nd}, \text{Yb}$).¹⁵³ With $\text{Ln} = \text{Y}$ and Nd the unsolvated, chloro-bridged dimers $[(\text{Me}_3\text{Si})_2\text{NC}(\text{NPr}^i)_2]_2\text{Ln}(\mu\text{-Cl})_2$ were also synthesized. Amination of these complexes with 2 equivalents of LiNPr^i gave $[(\text{Me}_3\text{Si})_2\text{NC}(\text{NPr}^i)_2]_2\text{LnNPr}^i_2$ in good isolated yields.¹⁵⁶ The alkyl lutetium derivative $[(\text{Me}_3\text{Si})_2\text{NC}(\text{NPr}^i)_2]_2\text{Lu}(\text{CH}_2\text{SiMe}_3)$ was synthesized through a metathesis reaction of the chloro precursor with $\text{LiCH}_2\text{SiMe}_3$ in toluene. Treatment of the alkyl with an equimolar amount of PhSiH_3 in hexane led to formation of the first known dimeric lanthanide hydride in a bis(guanidinato) coordination environment (Scheme 64).¹⁵²

Closely related bis(guanidinate) samarium and ytterbium^{157a} as well as yttrium^{157b} alkyls and amides of the type $[(\text{Me}_3\text{Si})\text{NC}(\text{NCy})_2]_2\text{LnE}(\text{SiMe}_3)_2$ ($\text{Ln} = \text{Sm}, \text{Yb}$; $\text{E} = \text{CH}, \text{N}$) were prepared analogously. Mutual ligand arrangement in binuclear lanthanide guanidinate complexes of types $[(\text{guanidinate})_2\text{Ln}(\mu\text{-Cl})_2]$, $[(\text{guanidinate})_2\text{Ln}(\mu\text{-H})_2]$, and $(\text{guanidinate})_2\text{Ln}(\mu\text{-Cl})_2\text{Li}(\text{THF})_2$ was quantitatively analyzed based on the ligand solid-state angle approach.¹⁵⁸ In complexes of the larger lanthanides Nd , Sm , and Gd the guanidinate ligands shield up to 87% of the metal, and the bidentate ligands on opposite metal centers are in the eclipsed arrangement. In complexes of lanthanides with smaller ionic radii such as Y , Yb , and Lu the guanidinate ligands shield over 88.3% of the metal surface, and their staggered conformation is observed.¹⁵⁸

Reaction of lanthanum with $\text{Hg}(\text{C}_6\text{F}_5)_2$ and bulky N,N' -bis(2,6-diisopropylphenyl)-formamidine (HDippForm) in THF (Scheme 65) afforded $(\text{DippForm})_2\text{LaF}(\text{THF})$ with a rare terminal La-F bond (colorless crystals, 77% yield). A novel

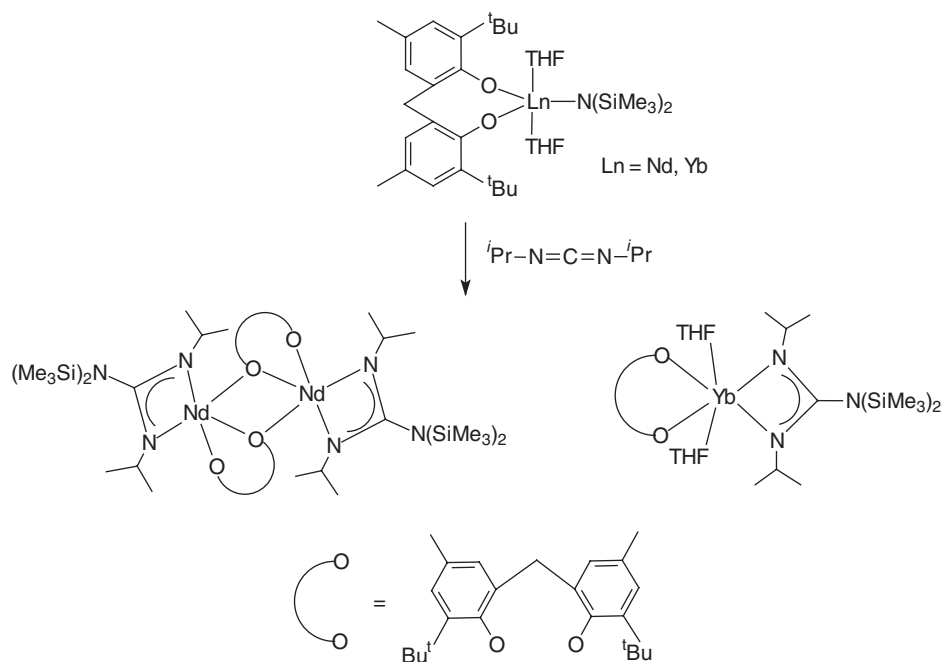


Scheme 58



Scheme 59

functionalized formamidine, resulting from ring-opening of THF, was formed as a by-product in this reaction.^{54a} More recently these studies have been extended to other lanthanide elements such as Ce, Nd, Sm, Ho, Er, and Yb in order to gain a better understanding of the steric modulation of coordination number and reactivity in the synthesis of lanthanide(III) formamidinates.^{54b}

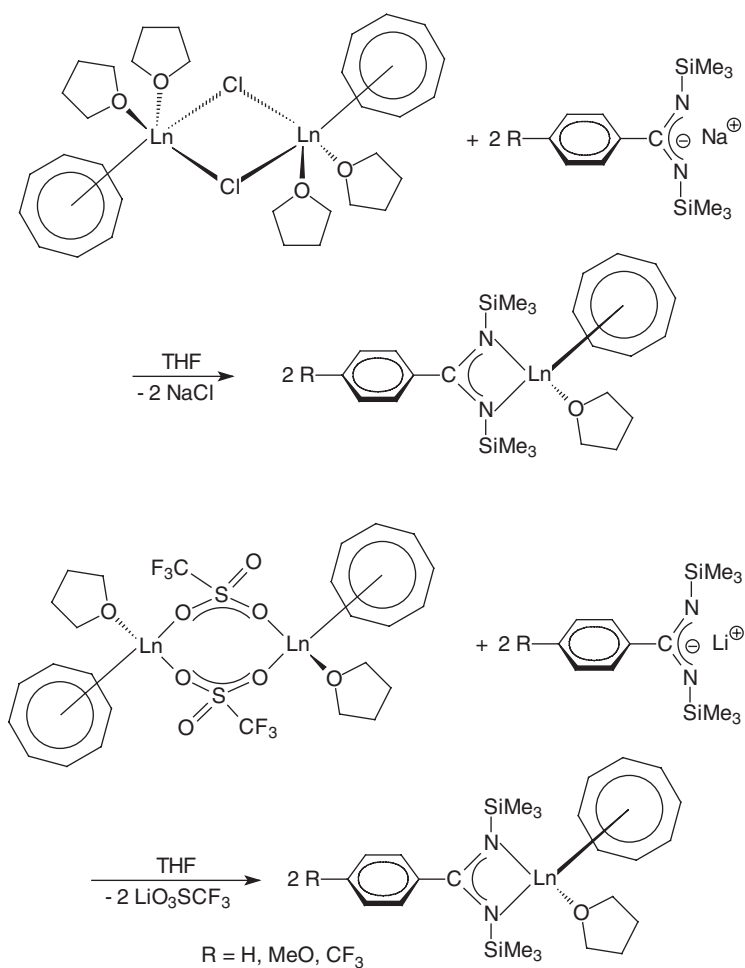
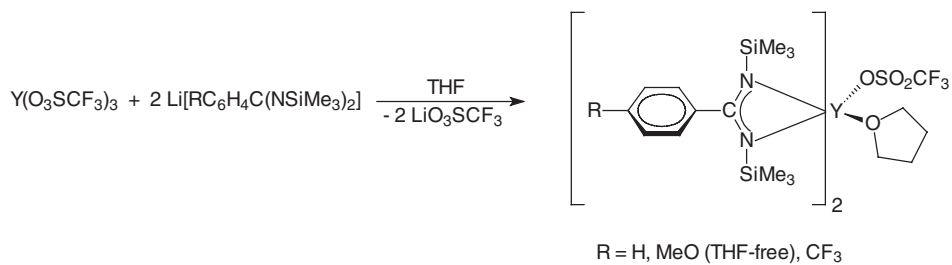


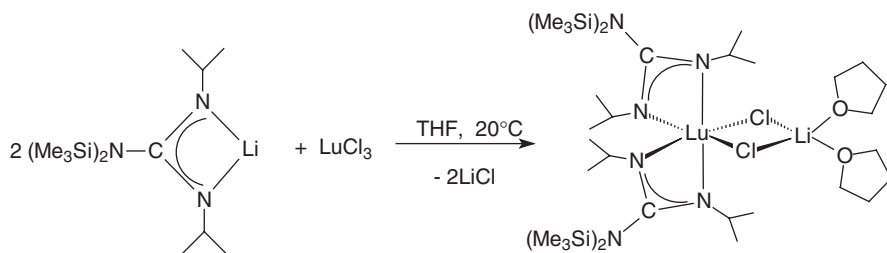
Scheme 60

Insertion of carbodiimides into the Ln–C σ -bond of organolanthanide complexes provides a straightforward access to organolanthanide amidinates. For example, insertion of *N,N'*-dicyclohexylcarbodiimide into one of the Y–N bonds of $\text{Y}[\text{N}(\text{SiMe}_3)_2]_3$ in toluene at 70 °C afforded the monoguanidinate diamide derivative $[(\text{Me}_3\text{Si})_2\text{NC}(\text{NCy})_2]\text{Y}[\text{N}(\text{SiMe}_3)_2]_2$ in 72% yield.¹⁴⁰ The complexes $\text{Cp}_2\text{Ln}[\text{Bu}^n\text{C}(\text{NBu}^t)_2]$ (Ln = Y, Gd, Er) were prepared following the same route from Cp_2LnBu^n and *N,N'*-di-*tert*-butylcarbodiimide.¹⁵⁹ The analogous insertion of carbodiimides into Ln–N bonds has been shown to be an effective way of making lanthanide guanidinate complexes.^{160–162} Complexes of the type $\text{Cp}_2\text{Ln}[\text{Pr}^i\text{NC}(\text{NPr}^i)_2]$ (Ln = Y, Gd, Dy, Yb) have been prepared this way,^{161,162} and even more exotic derivatives such as carbazolate,¹⁶³ pyrazolate,¹⁶³ and the phenothiazine derivatives shown in Scheme 66 are accessible using this route.¹⁶⁰

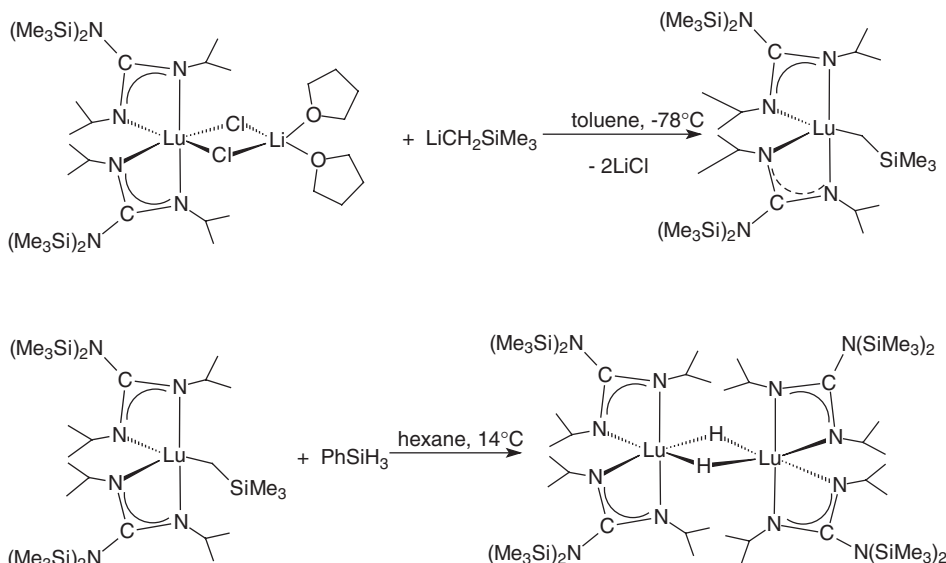
Related organolanthanide complexes containing bridging guanidinate ligands were obtained through direct reactions of Cp_2LnCl with $\text{LiN}=\text{C}(\text{NMe}_2)_2$ according to Scheme 67. The scheme also depicts the outcome of phenyl isocyanate insertion reactions into the Ln–N bonds of the bridging guanidinate complexes.¹⁶⁴

Homoleptic lanthanide(III) tris(amidinates) and guanidinates are among the longest known lanthanide complexes containing these chelating ligands. In this area the carbodiimide insertion route is usually not applicable, as simple, well-defined lanthanide tris(alkyls) and tris(dialkylamides) are not readily available. A notable exception is the formation of homoleptic lanthanide guanidinates from

**Scheme 61****Scheme 62**



Scheme 63

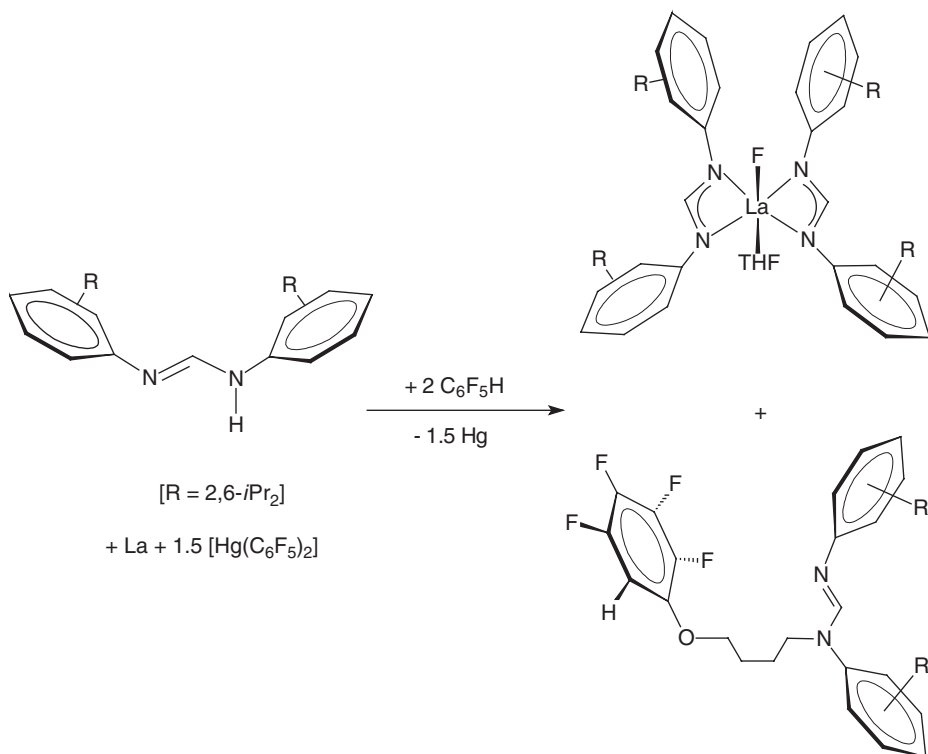


Scheme 64

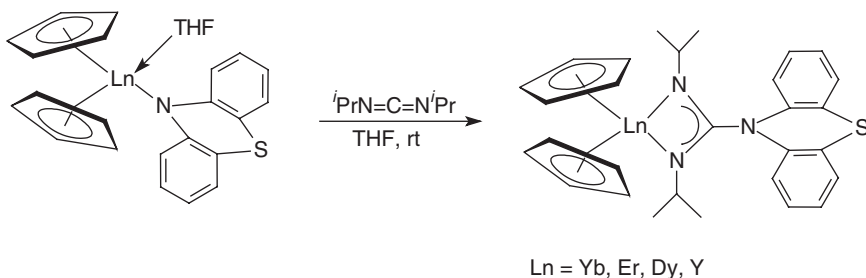
anionic lanthanide amido complexes and carbodiimides. Scheme 68 shows the preparation of a samarium complex as an example.¹⁶⁵

The major synthetic route leading to homoleptic lanthanide tris(amidates) and guanidates, however, is the metathetical reaction between anhydrous lanthanide trichlorides and preformed lithium amidates or guanidates, respectively, in a molar ratio of 1:3. This is outlined in Scheme 69, showing a samarium(III) guanidate as a typical example.^{62,66,154,165,166}

In a similar manner, treatment of anhydrous rare-earth chlorides with 3 equivalents of lithium 1,3-di-*tert*-butylacetamidate (prepared *in situ* from di-*tert*-butylcarbodiimide and methyllithium) in THF at room temperature afforded $\text{Ln}[\text{MeC}(\text{N}(\text{Me})_2)_2]_3$ ($\text{Ln} = \text{Y}, \text{La}, \text{Ce}, \text{Nd}, \text{Eu}, \text{Er}, \text{Lu}$) in 57–72% isolated yields. X-ray crystal structures of these complexes demonstrated monomeric formulations with distorted octahedral geometry about the lanthanide(III) ions (Figure 20, $\text{Ln} = \text{La}$). The new complexes are thermally stable at $>300^\circ\text{C}$, and sublime



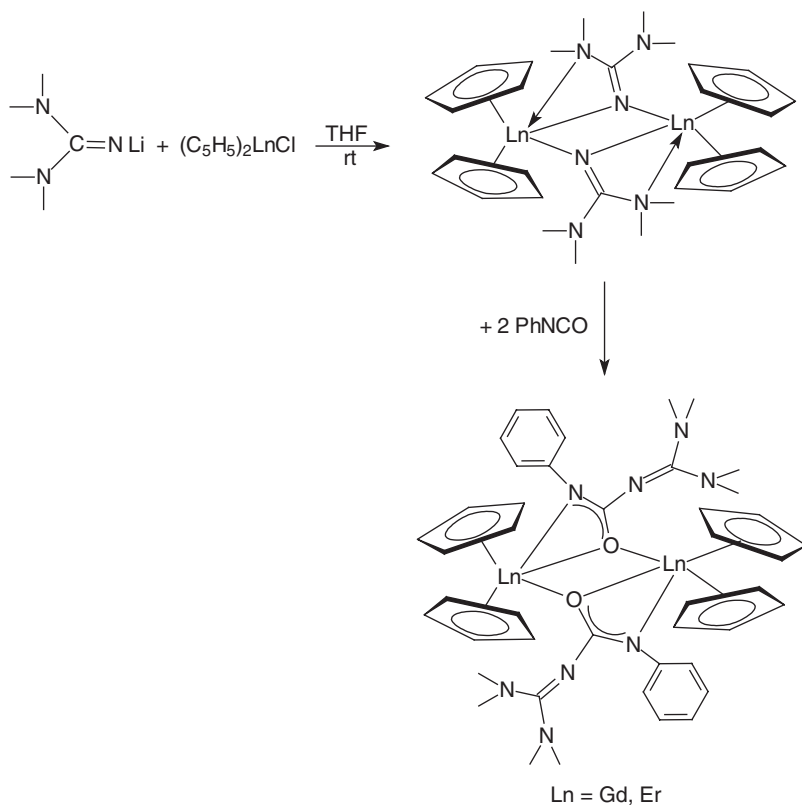
Scheme 65



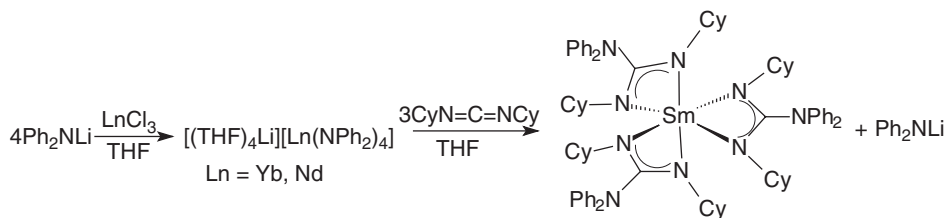
Scheme 66

without decomposition between 180 and 220 °C/0.05 Torr.¹⁶⁷ A series of homoleptic lanthanide amidinate complexes with the general formula $\text{Ln}[\text{RC}(\text{NCy})_2]_3(\text{THF})_n$ ($R = \text{Me}$, $\text{Ln} = \text{La, Nd, Gd, Yb}$, $n = 0$; $R = \text{Ph}$, $\text{Ln} = \text{Y, Nd, Yb}$, $n = 2$) was obtained analogously.^{66,168}

A sterically hindered homoleptic samarium(III) tris(amidinate), $\text{Sm}[\text{HC}(\text{NC}_6\text{H}_3\text{Pr}_2\text{-2,6})_2]_3$, was obtained by oxidation of the corresponding Sm(II) precursor (cf. Scheme 54).¹³⁹ Magnetic data and the results of low temperature absorption, luminescence, and magnetic circular dichroism spectra have been

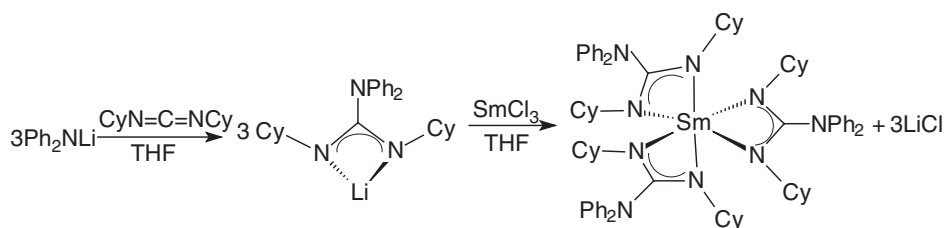


Scheme 67

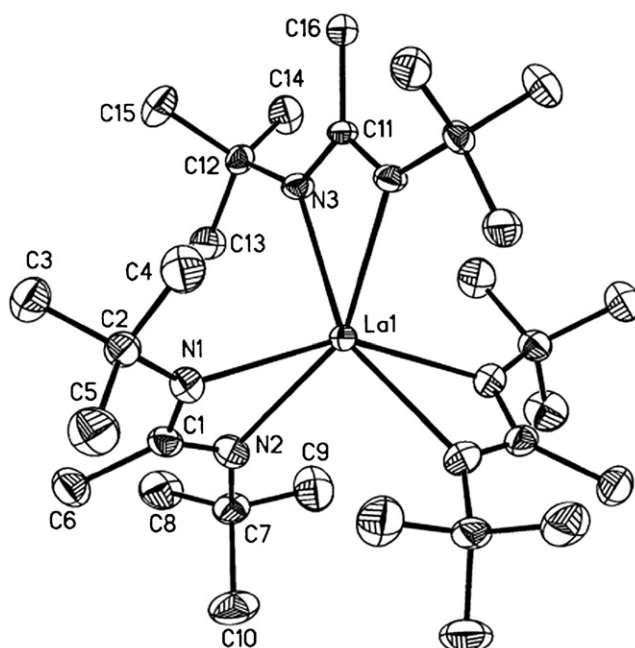
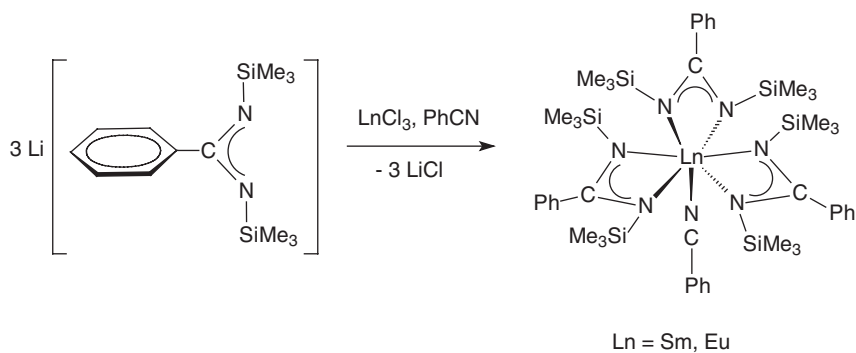


Scheme 68

reported for the homoleptic tris(amidates) $[p\text{-MeOC}_6\text{H}_4\text{C(NSiMe}_3)_2]_2\text{Ln}$ (Ln = Pr, Nd, Eu) and compared with the data of related η^3 -allyl and cyclopentadienyl complexes of these lanthanide elements.¹⁶⁹ Six-coordinate lanthanide tris(benzamidates) of the type $\text{Ln}[\text{PhC(NSiMe}_3)_2]_3$ form 1:1 adducts with donor ligands such as THF, MeCN, or PhCN. In the case of benzonitrile, it was possible to isolate and structurally characterize two of these seven-coordinate nitrile-adducts. They are most readily isolated when the original preparation is directly carried out in the presence of 1 equivalent of benzonitrile (Scheme 70).⁶²

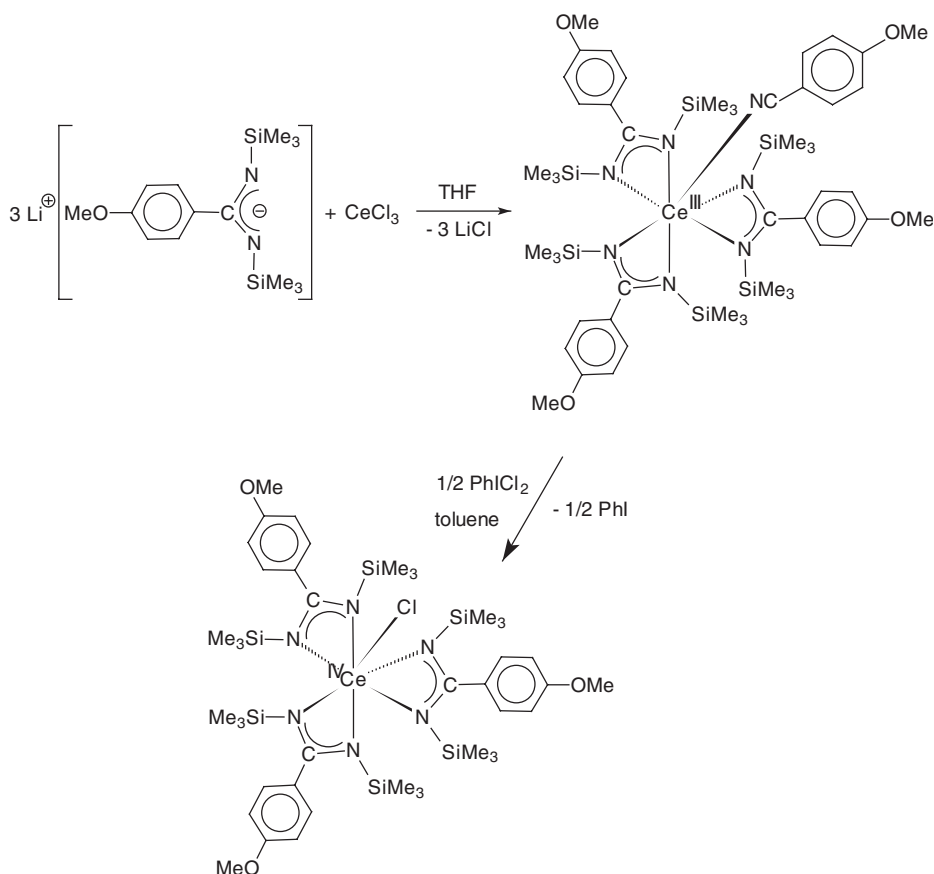


Scheme 69

Figure 20 Molecular structure of $[\text{MeC}(\text{NBu}^t)_2]_3\text{La}$.¹⁶⁷

Scheme 70

In recent years homoleptic lanthanide(III) tris(amidates) and guanidates have been demonstrated to exhibit extremely high activity for the ring-opening polymerization of polar monomers such as ϵ -caprolactone¹⁶⁶ and trimethylene carbonate¹⁶⁵ (cf. Section V.A.2). Another promising field of application is their use in MOCVD and ALD processes (cf. Section VI). Most recently it was discovered in our lab that benzamidinate ligands are also capable of stabilizing novel cerium(IV) species.¹⁷⁰ In analogy to the reaction shown in Scheme 70, treatment of anhydrous cerium(III) trichloride with 3 equivalents of the lithium amidinate precursor $\text{Li}[p\text{-MeOC}_6\text{H}_4\text{C}(\text{NSiMe}_3)_2]$ first afforded the bright yellow *p*-anisonitrile adduct of the homoleptic cerium(III) amidinate (Scheme 71). Oxidation to the corresponding cerium(IV) amidinate $[p\text{-MeOC}_6\text{H}_4\text{C}(\text{NSiMe}_3)_2]_3\text{CeCl}$ was readily achieved using the reagent phenyliodine(III) dichloride. The advantage of this method is that iodobenzene is formed as the only by-product. Thus the almost black cerium(IV) species could be isolated by simple crystallization directly from the concentrated



Scheme 71

reaction mixture. A single-crystal X-ray analysis clearly established the presence of the first amidinate complex of tetravalent cerium (Figure 21).¹⁷⁰

The chemistry of actinide amidinate and guanidinate complexes remains largely unexplored despite the large variety of possible coordination modes and reaction patterns. The reaction of the bis(benzamidinato)uranium(IV) dichloride complex $[\text{PhC}(\text{NSiMe}_3)_2]_2\text{UCl}_2$ with 2 equivalents of NaBH_4 afforded the bis(borohydride) complex $[\text{PhC}(\text{NSiMe}_3)_2]_2\text{U}(\mu_3\text{-BH}_4)_2$ (green crystals, 75% yield). An X-ray crystal structure determination unequivocally proved the μ_3 coordination of the BH_4 moieties (Figure 22).¹⁷¹

Reactions of UCl_4 with $[\text{Li}[\text{RC}(\text{NCy})_2](\text{THF})]_2$ ($\text{R} = \text{Me}, \text{Bu}^t$) in THF gave the tris(amidinate) compounds $[\text{RC}(\text{NCy})_2]_3\text{UCl}$ that could be reduced with lithium powder in THF to the dark-green homoleptic uranium(III) complexes $[\text{RC}(\text{NCy})_2]_3\text{U}$. Comparison of the crystal structure of $[\text{MeC}(\text{NCy})_2]_3\text{U}$ with those of the lanthanide analog showed that the average U–N distance is shorter than expected from a purely ionic bonding model.⁶⁶

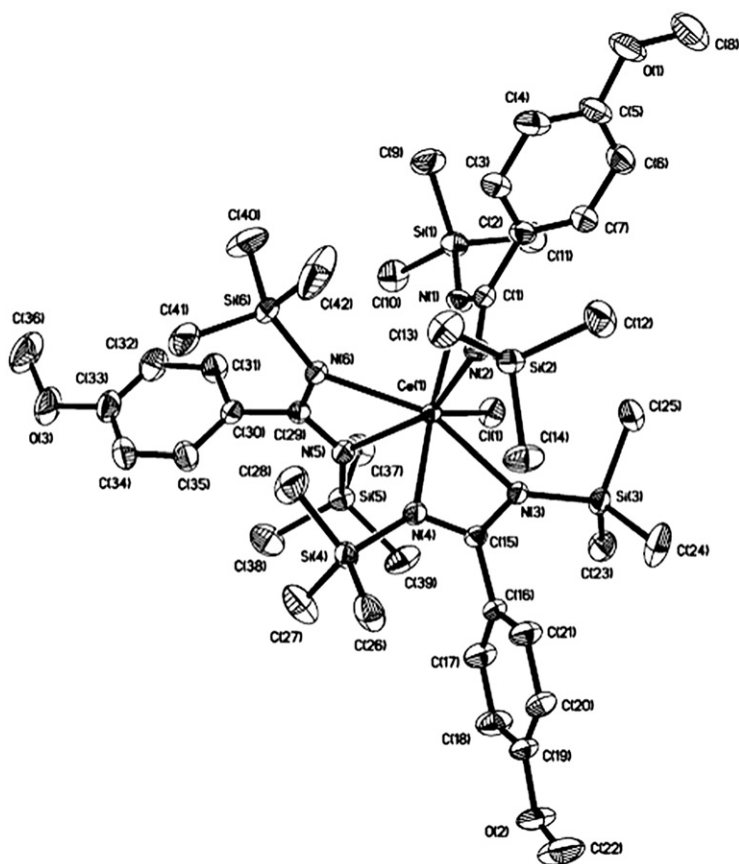


Figure 21 Molecular structure of $[\text{p-MeOC}_6\text{H}_4\text{C}(\text{NSiNe}_3)_2]_3\text{CeCl}$.¹⁷⁰

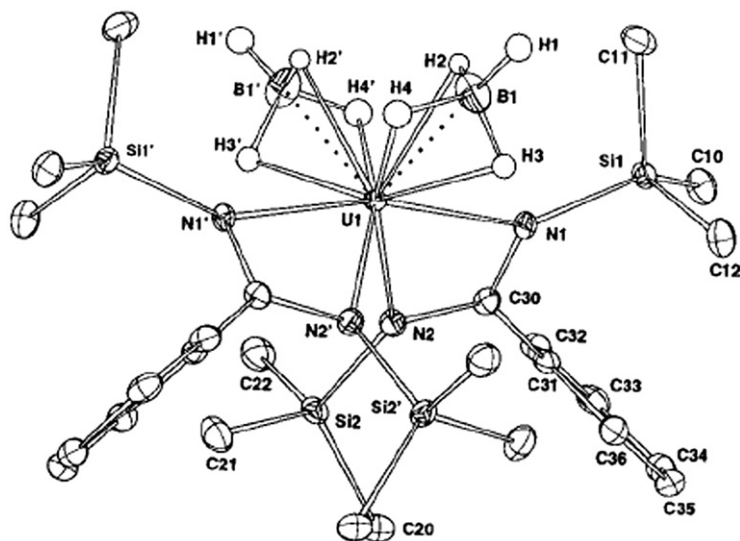


Figure 22 Molecular structure of $[\text{PhC}(\text{NSiMe}_3)_2]_2\text{U}(\mu_3\text{-BH}_4)_2$.¹⁷¹

2. Group 4 metal complexes

Especially in Group 4 metal chemistry, where possible catalytic applications play a major role, the development of amidinate and guanidinate complexes has largely been driven by the quest for alternatives to cyclopentadienyl-based ligands. Titanium(IV) bis(amidinates) were among the first amidinate complexes ever reported,¹ and by now a large variety of amidinato and guanidinato complexes of the Group 4 metals have been reported.

The synthesis of a series of bis(alkylamidinato) Group 4 metal complexes of the general formula $[\text{MeC}(\text{NCy})_2]_2\text{MCl}_2$ ($\text{M} = \text{Ti}, \text{Zr}, \text{Hf}$; $\text{Cy} = \text{cyclohexyl}$), $[\text{Bu}^t\text{C}(\text{NCy})_2]\text{ZrCl}_2$, and $[\text{MeC}(\text{NCy})_2]_2\text{ZrMe}_2$ has been reported.^{172–174} Bis[*N,N'*-trimethylsilyl]benzamidinato]dimethyltitanium(IV) was obtained as an intensely red solid by allowing freshly prepared tetramethyltitanium in diethyl ether to react with the free amidine $\text{PhC}(=\text{NSiMe}_3)(\text{NHSiMe}_3)$.¹⁷⁵ The first structurally characterized hafnium amidinate complex, $[\text{Bu}^n\text{C}(\text{NPr}^i)_2]_2\text{HfCl}_2$, has been prepared analogously by a metathetical reaction between HfCl_4 and 2 equivalents of $\text{Li}[\text{Bu}^n\text{C}(\text{NPr}^i)_2]$. The central hafnium atom in the monomeric molecule displays a highly distorted octahedral coordination geometry.¹⁷⁶ Zirconium chloride and methyl complexes with the sterically demanding amidinate and guanidinate ligands $[\text{PhC}(\text{NAr})_2]^-$ (**A**), $[\text{PhC}(\text{NAr})\text{NAr}']^-$ (**B**), and $[\text{ArNC}(\text{NMe}_2)\text{NSiMe}_3]^-$ ($\text{Ar} = \text{C}_6\text{H}_3\text{Pr}^i\text{-2,6}$; $\text{Ar}' = \text{C}_6\text{H}_3\text{Me}_2\text{-2,6}$) have been prepared and structurally characterized.¹⁷⁷ The steric demand of ligand **A** induces the unusual *trans* geometry in *trans*-(**A**)₂ZrCl₂ (Figure 23 above), whereas (**A**)₂ZrMe₂ and (**B**)₂ZrX₂ ($\text{X} = \text{Cl}, \text{Me}$) adopt the more common *cis*-X₂ geometry (Figure 23 below).^{177a}

Another type of sterically demanding benzamidinate ligands contains the 2,4,6-tris(trifluoromethyl)phenyl substituent at the central carbon atom of the

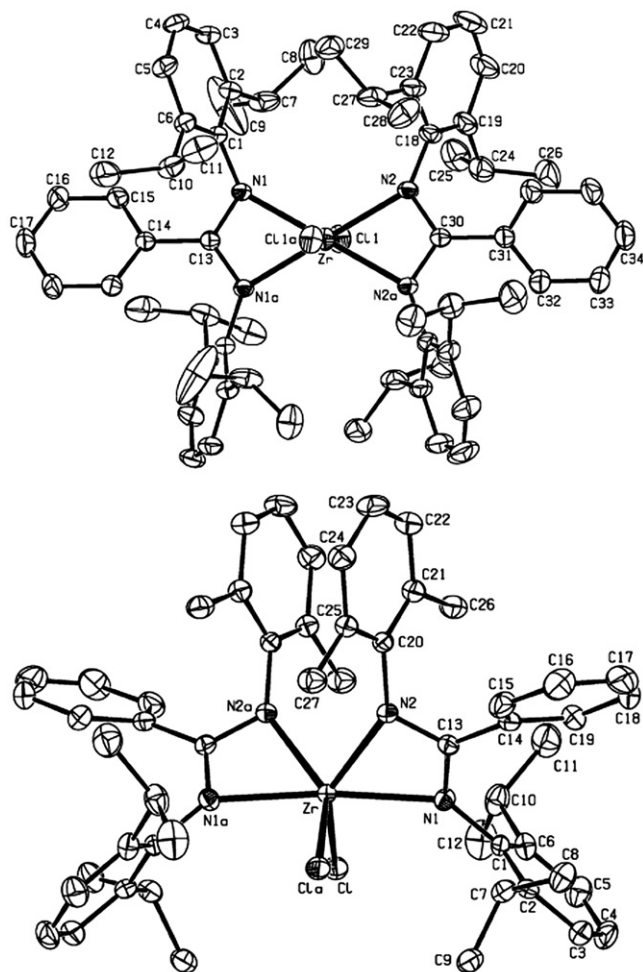
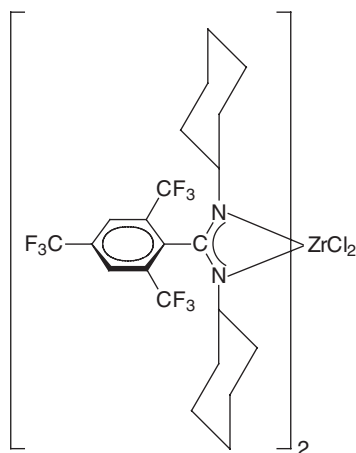


Figure 23 Molecular structures of *trans*-(A)ZrCl₂ (top) and *cis*-(B)ZrCl₂ (bottom).^{177a}

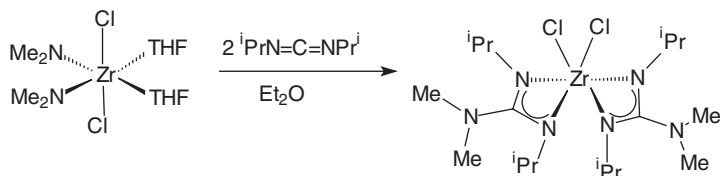
NCN unit. The zirconium complex [2,4,6-(CF₃)₃C₆H₂C(NCy)₂]₂ZrCl₂ (Scheme 72) was obtained by treatment of ZrCl₄ with 2 equivalents of Li[2,4,6-(CF₃)₃C₆H₂C(NCy)₂].¹³²

The synthesis, structures, and reactivity of neutral and cationic mono- and bis(guanidinato)zirconium(IV) complexes have been studied in detail. Either salt-metathesis using preformed lithium guanidates or carbodiimide insertion of zirconium amides can be employed. Typical examples for these two main synthetic routes are illustrated in Schemes 73 and 74. Various σ -alkyl complexes and cationic species derived from these precursors have been prepared and structurally characterized.^{178–181}

In certain cases, free guanidines can also serve as precursors to Group 4 metal guanidinate complexes. The bis(guanidinato) bis(benzyl)zirconium complex [Pr^{*i*}NHC(NPr^{*i*})₂]₂Zr(CH₂Ph)₂ was obtained by addition of 2 equivalents of



Scheme 72



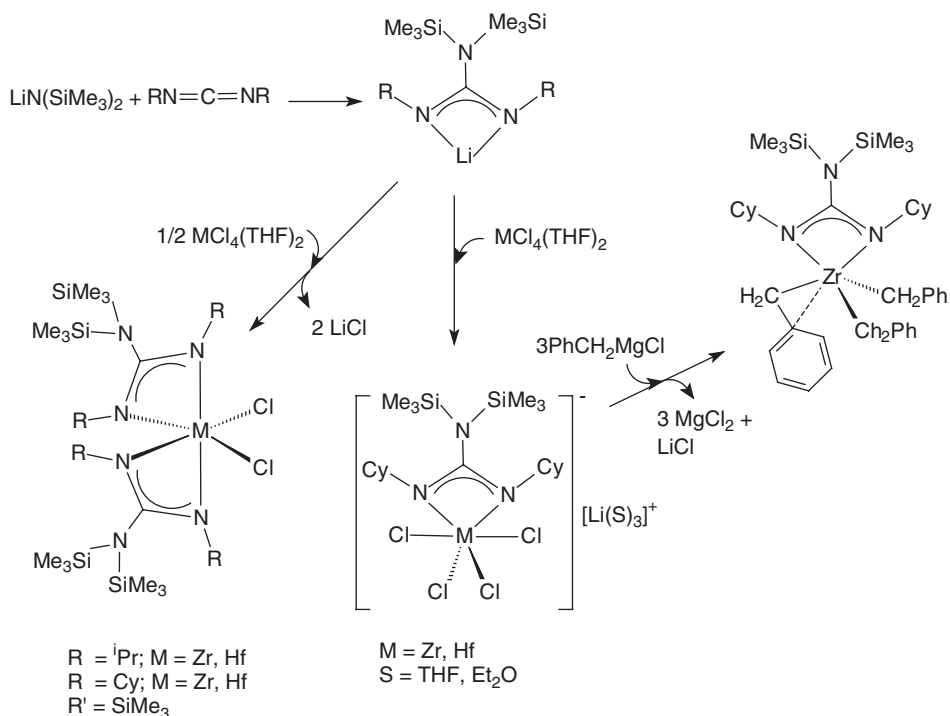
Scheme 73

N,N',N'' -triisopropylguanidine to $\text{Zr}(\text{CH}_2\text{Ph})_4$ (Scheme 75) while treatment of ZrCl_4 with the same guanidine precursor produced the mono(guanidinato) complex $[\text{Pr}^i\text{NHC}(\text{NPr}^i)_2]\text{ZrCl}_3$.¹⁸²

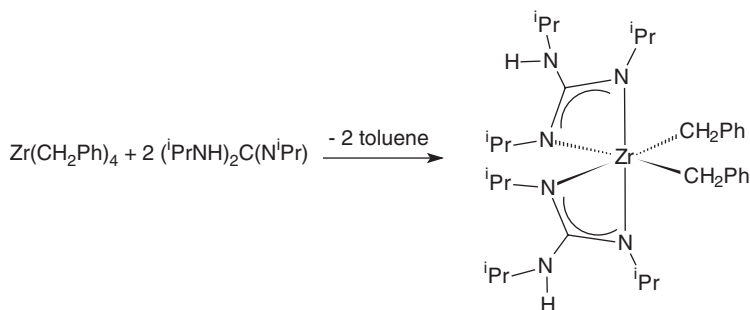
$\text{Zr}(\text{CH}_2\text{Ph})_4$ also served as starting material for the mono(guanidinato)zirconium tribenzyl complex $[(\text{Me}_3\text{Si})_2\text{NC}(\text{NCy})_2]\text{Zr}(\text{CH}_2\text{Ph})_3$.¹⁸³ While the same compound made by the salt-elimination route and crystallized from toluene showed η^2 -coordination of one benzyl group in the solid state, no such interaction was found in the crystal structure of $[(\text{Me}_3\text{Si})_2\text{NC}(\text{NCy})_2]\text{Zr}(\text{CH}_2\text{Ph})_3$ made from $\text{Zr}(\text{CH}_2\text{Ph})_4$. It appears that this difference can be traced back to crystal packing effects resulting from slight differences in crystallization conditions.¹⁸³

Several series of mono(cyclopentadienyl) amidinato complexes of titanium, zirconium, and hafnium were reported already in 1995. The chloro derivatives are normally prepared *via* metathetical reactions of suitable cyclopentadienyl metal trichlorides with 1 or 2 equivalents of lithium benzamidinates. Scheme 76 illustrates typical synthetic routes. In some cases, the formation of oxo-bridged hydrolysis products was observed. Most of the chloro complexes could be converted to the corresponding σ -methyl or benzyl derivatives by treatment with the corresponding alkylating agents (MeMgCl , PhCH_2MgCl , KCH_2Ph , etc.).^{184,185}

Facile insertion of carbodiimides $\text{R}^1\text{N}=\text{C}=\text{NR}^3$ (R^1 , $\text{R}^3 = \text{Et}$, Pr^i , Bu^t , Cy , $\text{C}_6\text{H}_3\text{Me}_2$ -2,6) into a $\text{Ti}-\text{C}_{\text{Me}}$ bond of $(\text{C}_5\text{R}_5)\text{TiMe}_3$ ($\text{R} = \text{H}$, Me) in pentane



Scheme 74

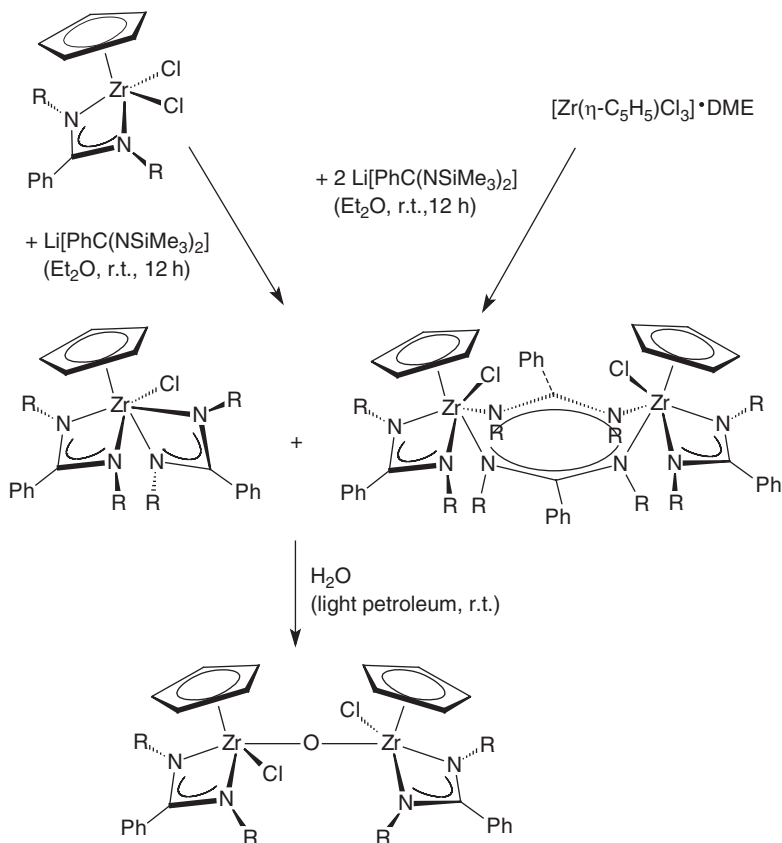


Scheme 75

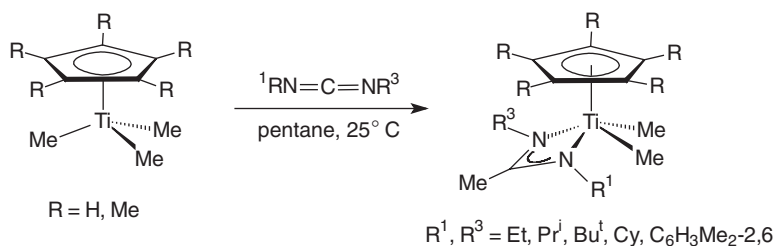
solutions at 25°C provided a wide range of derivatives of $(\text{C}_5\text{R}_5)\text{TiMe}_2$ (amidinate) complexes in high yield (Scheme 77).¹⁸⁶ The reaction has been extended to the insertion of optically pure (*R,R*)- and *meso*-(*R,S*)-1,3-bis(1-phenylethyl)carbo-diimide.¹⁸⁷

Synthetic routes to mixed cyclopentadienyl/guanidinato complexes of Group 4 metals have also been developed. Scheme 78 illustrates two typical reactions leading to such compounds.¹⁸²

Also known are the bis(cyclopentadienyl) zirconium formamidates $\text{Cp}_2\text{ZrCl}[\text{HN}(\text{NR})_2]$ and $\text{Cp}_2\text{ZrMe}[\text{HN}(\text{NR})_2]$ ($\text{R} = \text{Cy}, \text{Ph}$). The latter could be



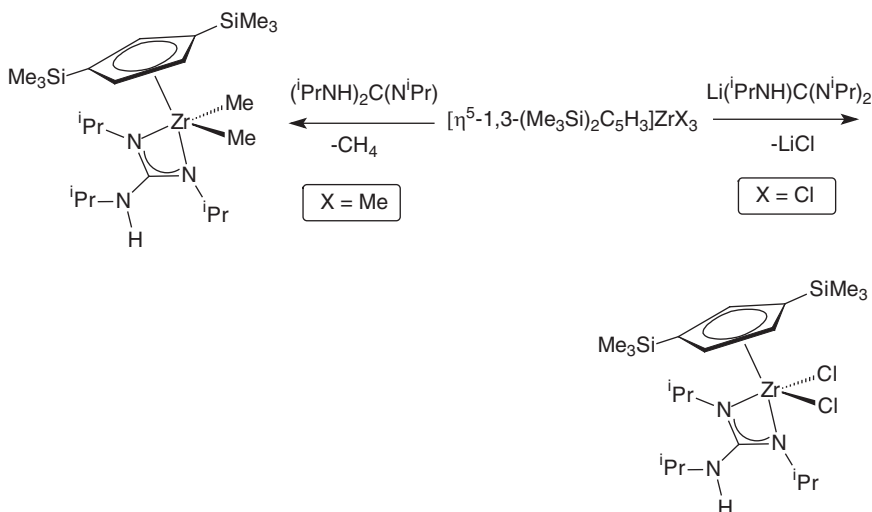
Scheme 76



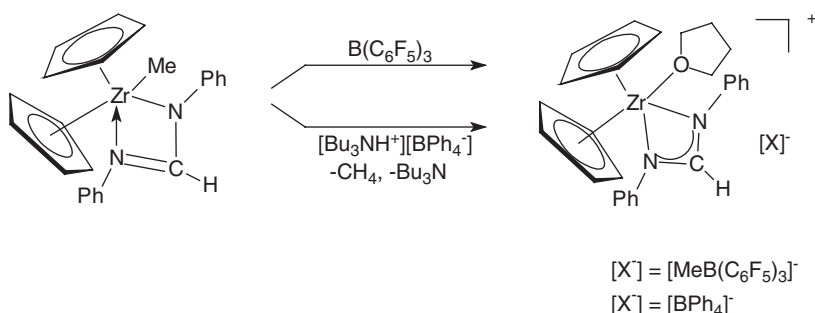
Scheme 77

transformed into cationic species according to the methods shown in [Scheme 79](#).¹⁸⁸

Several mono(amidinato) complexes of titanium containing the *N,N'*-bis(trimethylsilyl)benzamidinato ligand have been prepared either by metathetical routes or ligand substitution reactions as outlined in [Schemes 80 and 81](#). Trialkoxides are accessible as well as the dimeric trichloride, which can be



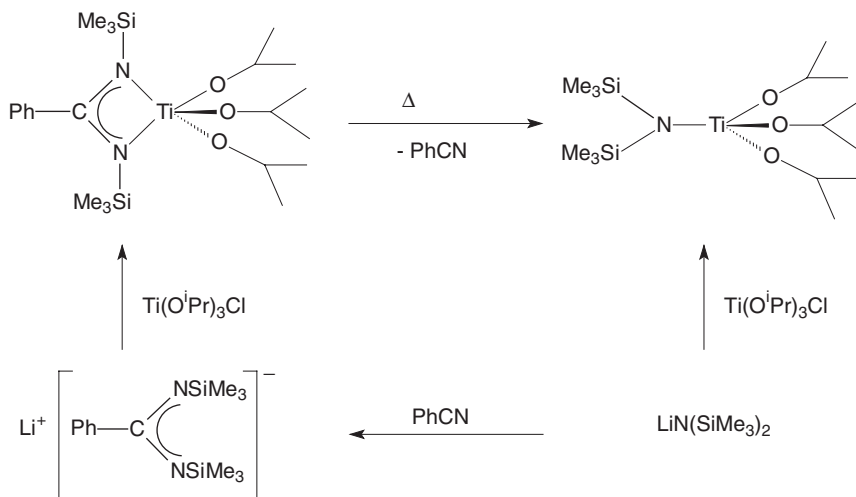
Scheme 78



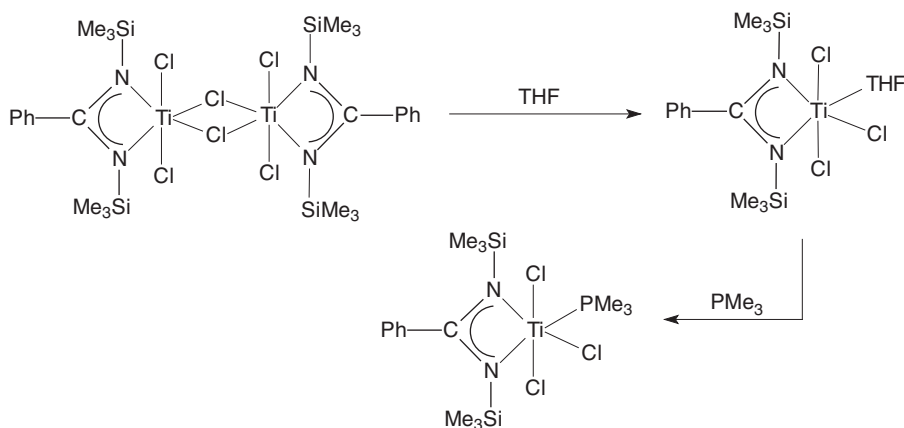
Scheme 79

split into monomeric complexes on treatment with donor ligands such as THF and trimethylphosphine.^{173,174}

Particularly rich is the chemistry of titanium bis(benzamidinate) complexes containing the silylated $[\text{PhC}(\text{NSiMe}_3)_2]^-$ ligand.^{173,189} Numerous complexes with titanium in the oxidation states +2, +3, and +4 have been prepared and in most cases structurally characterized by X-ray diffraction. These include dinuclear μ -oxo and μ -dinitrogen-bridged species as well as terminal oxo, sulfido, and imido complexes, σ -alkyls and a peroxo derivative. Scheme 82 highlights some typical reaction sequences. These studies demonstrated that the $[\text{PhC}(\text{NSiMe}_3)_2]^-$ ligand is capable of supporting a wide range of unusual titanium chemistry in a variety of oxidation states. In several instances, the $[\text{PhC}(\text{NSiMe}_3)_2]_2\text{Ti}$ compounds show reactivity comparable to that of related Cp_2Ti derivatives but with some notable differences. Most of these may be attributed to the less electron-rich nature of the bis(benzamidinate) series of



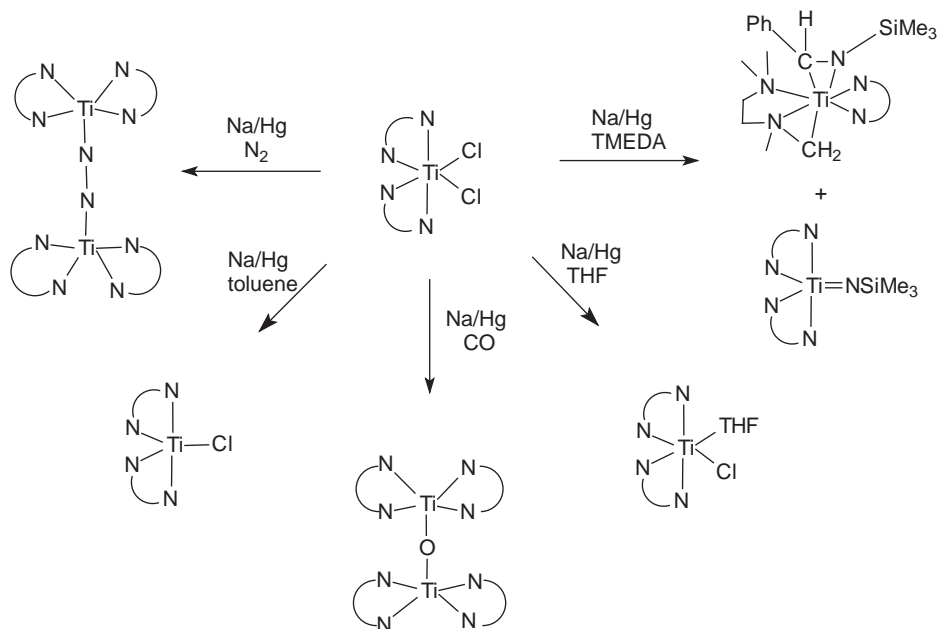
Scheme 80



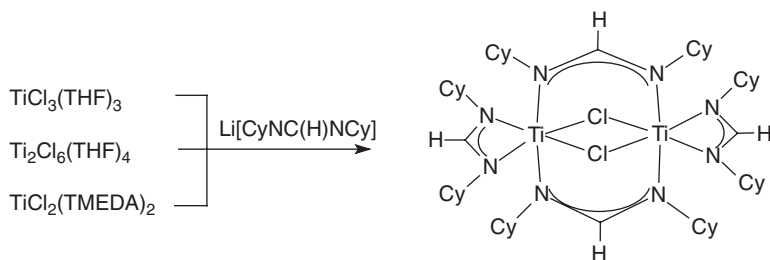
Scheme 81

compounds relative to the Cp systems.¹⁸⁹ A mixed-ligand bis(benzamidinato)-hydrazido titanium(IV) complex, $[\text{PhC}(\text{NSiMe}_3)_2\text{TiCl}(\text{MeNNMe}_2)]$, was prepared in the form orange-red crystals by the reaction of $[\text{PhC}(\text{NSiMe}_3)_2\text{TiCl}_2]$ with $\text{LiN}(\text{Me})\text{NMe}_2$.⁶⁴

A closely related titanium dinitrogen complex supported by guanidinate ligands, $(\mu\text{-N}_2)[\{(\text{Me}_2\text{N})\text{C}(\text{NPr}^i)_2\}_2\text{Ti}]_2$, was synthesized by reduction of the dichloride precursor $[(\text{Me}_2\text{N})\text{C}(\text{NPr}^i)_2\text{TiCl}_2]$ with Mg powder. The reactivity of the dark purple dinitrogen complex toward phenyl azide (*vide infra*), pyridine N-oxide, and propylene sulfide has been investigated.¹⁹⁰ As part of a search for compounds containing Ti-Ti bonds, the diamagnetic and dinuclear titanium(III) formamidinate complex $\text{Ti}_2\text{Cl}_2[\text{HC}(\text{NCy})_2]_4 \cdot 2\text{THF}$ was prepared according to



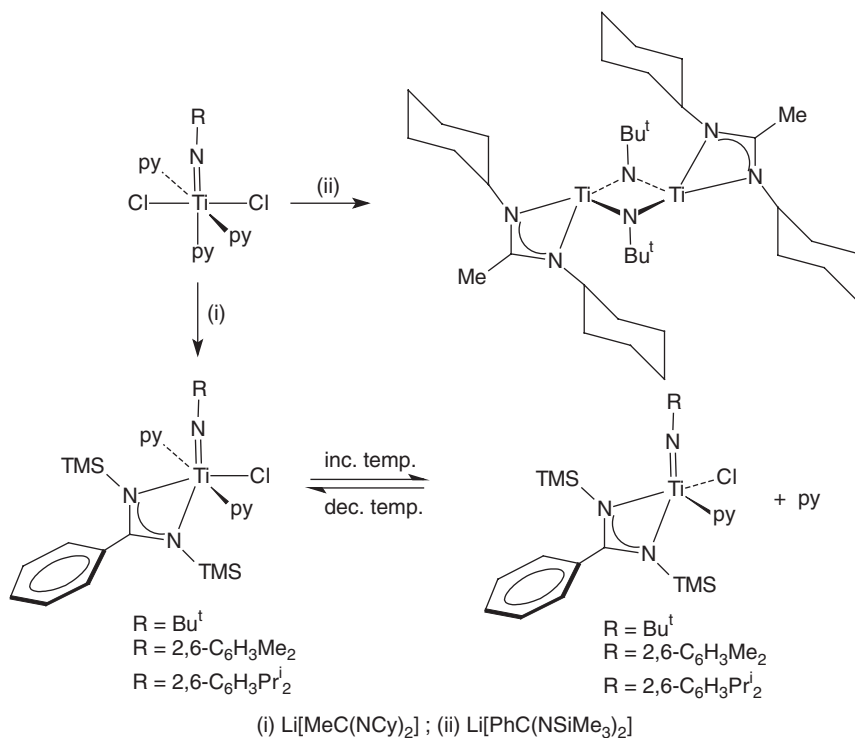
Scheme 82



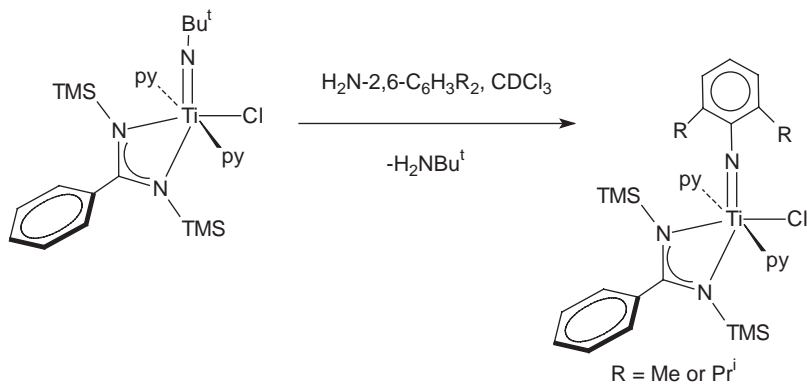
Scheme 83

Scheme 83 and crystallographically characterized. With $2.942(2) \text{ \AA}$ the Ti–Ti distance in the molecule is fairly short, and *ab initio* unrestricted Hartree–Fock calculations suggested the presence of a Ti–Ti bonding interaction.¹⁹¹

Titanium imido complexes supported by amidinate ligands form an interesting and well-investigated class of early transition metal amidinato complexes. Metathetical reactions between the readily accessible titanium imide precursors $\text{Ti}(=\text{NR})\text{Cl}_2(\text{py})_3$ with lithium amidinates according to Scheme 84 afforded either terminal or bridging imido complexes depending on the steric bulk of the amidinate anion. In solution, the mononuclear bis(pyridine) adducts exist in temperature-dependent, dynamic equilibrium with their mono(pyridine) homologs and free pyridine.¹⁹²



Scheme 84



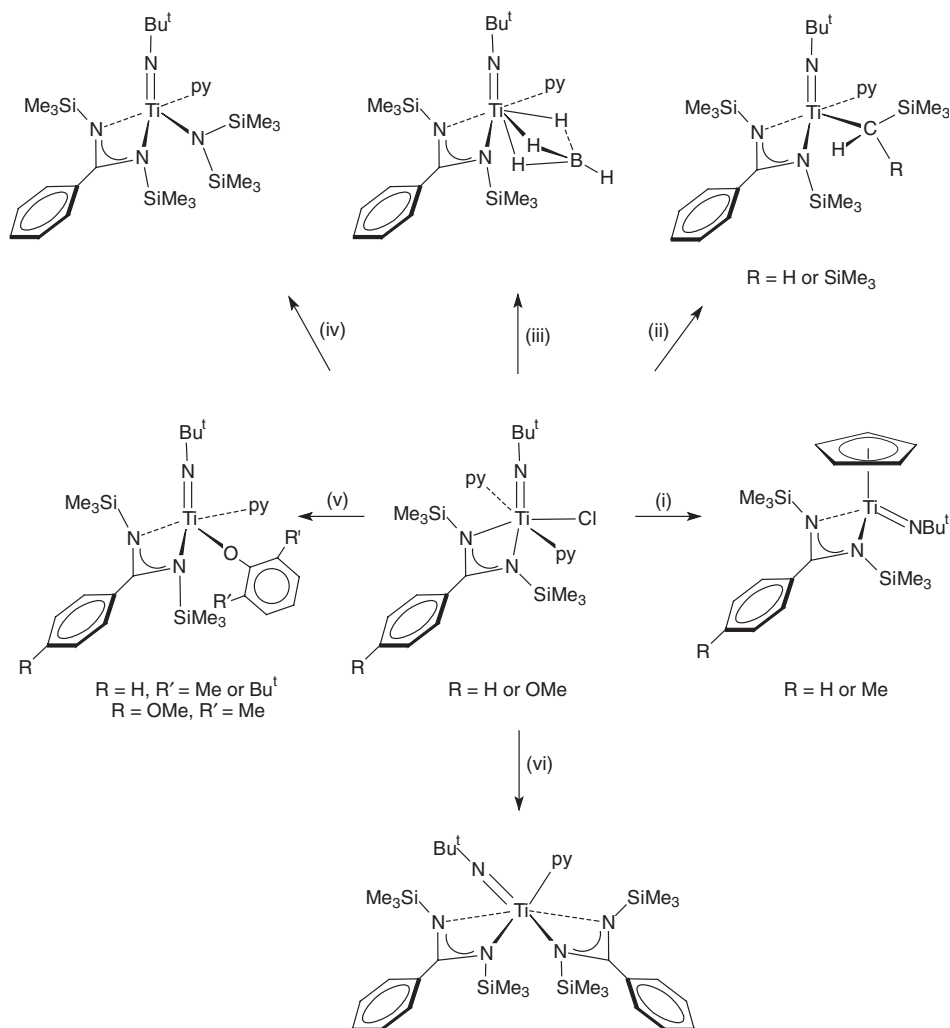
Scheme 85

As depicted in [Scheme 85](#), the terminal arylimido titanium amidinates may also be prepared by treating $[\text{PhC}(\text{NSiMe}_3)_2]\text{Ti}(=\text{NBu}^t)\text{Cl}(\text{py})_2$ with the appropriate arylamine.¹⁹²

A range of chloride metathesis reactions of the monomeric titanium *N,N'*-bis(trimethylsilyl)benzamidinato-imido complexes have been described. These

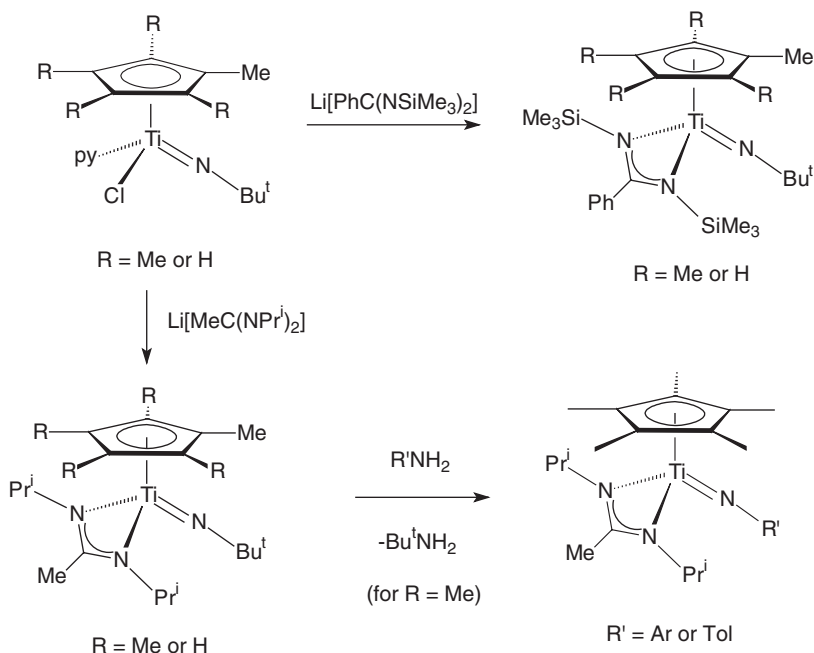
are illustrated in [Scheme 86](#) and include the preparation of the corresponding aryloxides, borohydrides, alkyls, bis(trimethylsilyl)amides, cyclopentadienyl complexes, and bis(amidinate)s.¹⁹³

The Cp^{*}Ti(amidinate) fragment provides a particularly useful platform for the synthesis of novel titanium imido complexes and the study of their unusual reactivity. Numerous single-, double-, and cross-coupling and imido-transfer reactions were investigated using these compounds. The synthetic routes leading to CpTi and Cp^{*}Ti amidinate derivatives are outlined in [Scheme 87](#).^{193,194}



- (i) LiCp, toluene; (ii) LiCH₂SiMe₃ or LiCH(SiMe₃)₂, benzene; (iii) LiBH₄, toluene;
 (iv) LiN(SiMe₃)₂(OEt)₂, toluene; (v) LiOC₆H₃Me₂-2,6 or LiOC₆H₃Bu^t-2,6; (vi) Li[PhC(NSiMe₃)₂], toluene.

Scheme 86

**Scheme 87**

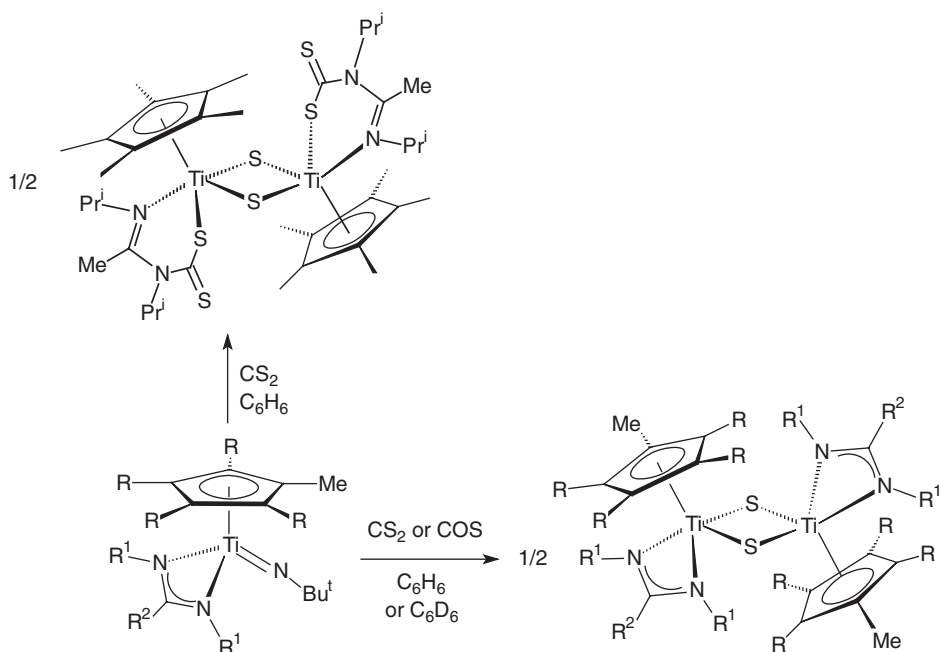
As representative examples for the reactivity of the $\text{Cp}^*\text{Ti}(\text{amidinate})$ complexes some reactions with CS_2 and COS are shown in [Scheme 88](#). Other reagents that have been investigated in this study include carbodiimides, isocyanates, CO_2 , PhNO as well as aldehydes, ketones, and imines.¹⁹⁴

Reactions of the cyclopentadienyl-amidinate-supported imidotitanium complexes with CO_2 proceed *via* initial cycloaddition reactions, but depending on the imido *N*-substituent go on to yield products of either isocyanate extrusion or unprecedented double CO_2 insertion ([Scheme 89](#)).¹⁹⁵

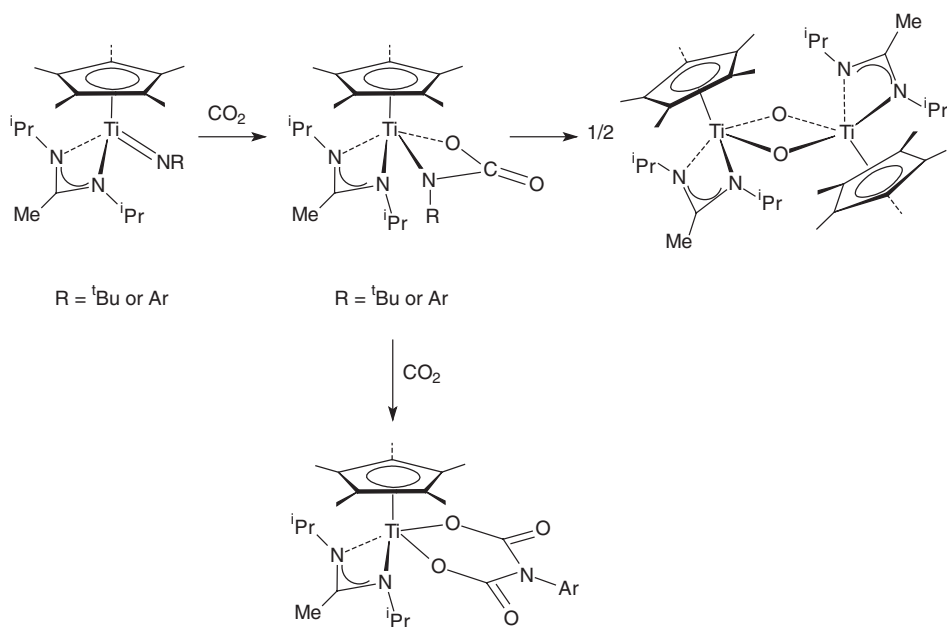
The formation of a bis(guanidinate)-supported titanium imido complex has been achieved in different ways, two of which are illustrated in [Scheme 90](#). The product is an effective catalyst for the hydroamination of alkynes (cf. [Section V.B](#)). It also undergoes clean exchange reactions with other aromatic amines to afford new imide complexes such as $[\text{Me}_2\text{NC}(\text{NPr}^i)_2]_2\text{Ti}=\text{NC}_6\text{F}_5$.^{196,197}

Yet another preparation of titanium imido complexes supported by guanidinate ligands involves reaction of the dinitrogen complex $(\mu\text{-N}_2)[\{(\text{Me}_2\text{N})\text{C}(\text{NPr}^i)_2\}_2\text{Ti}]_2$ (*vide supra*) with phenyl azide.¹⁹⁰ Transformations of aryl isocyanides on guanidinate-supported organozirconium complexes have been studied in detail and found to give rise to terminal imido, iminoacyl, and enediamido ligands. The latter originate from intramolecular coupling of two iminoacyl groups. [Scheme 91](#) summarizes these reactions.^{196,197}

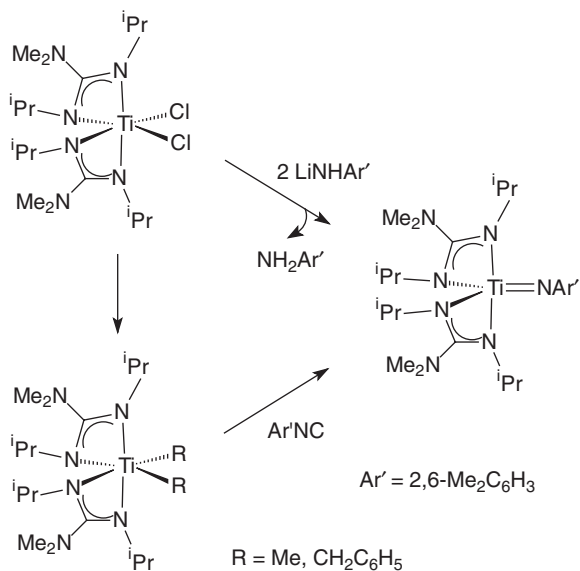
Diazametallacycles of the type $\text{Cp}_2\text{Zr}[\text{Bu}^t\text{NC}(=\text{NR}'\text{NR}')]_2$ have been prepared according to [Scheme 92](#) from terminal zirconium imides and carbodiimides. A second series of analogous compounds was synthesized starting



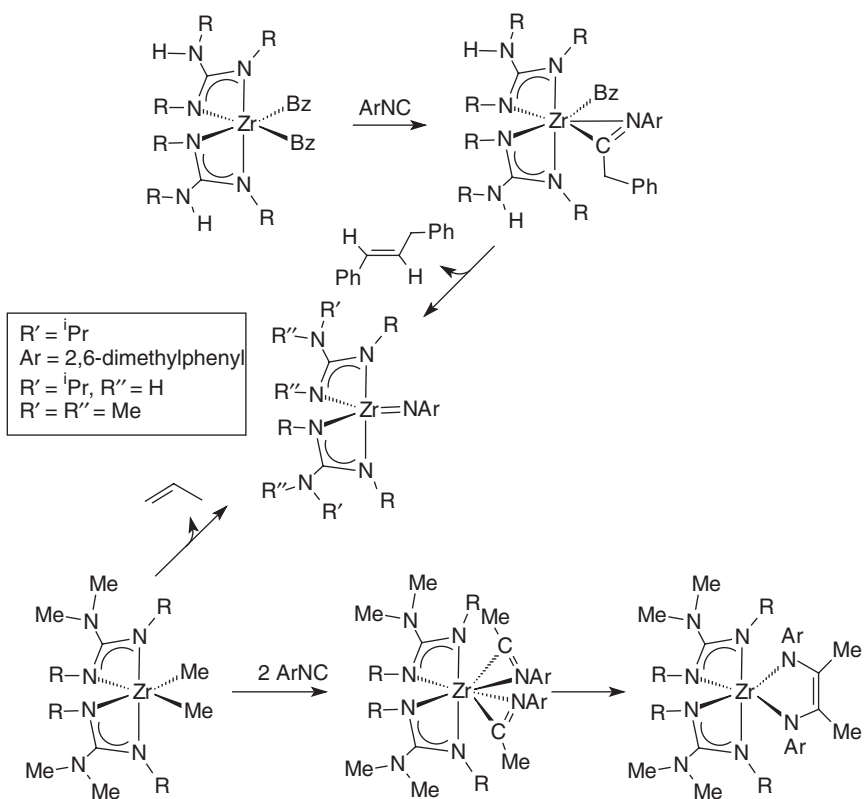
Scheme 88



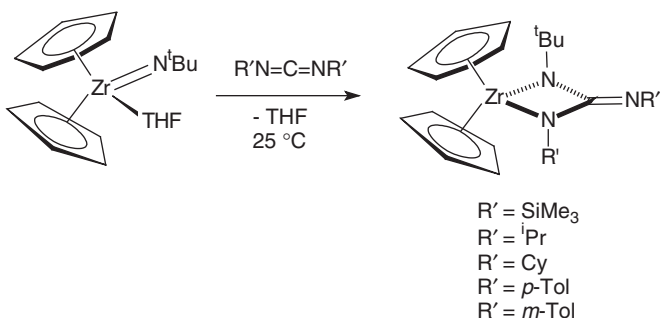
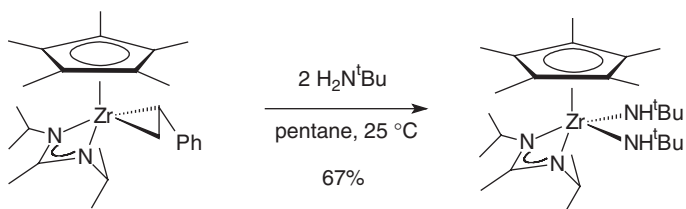
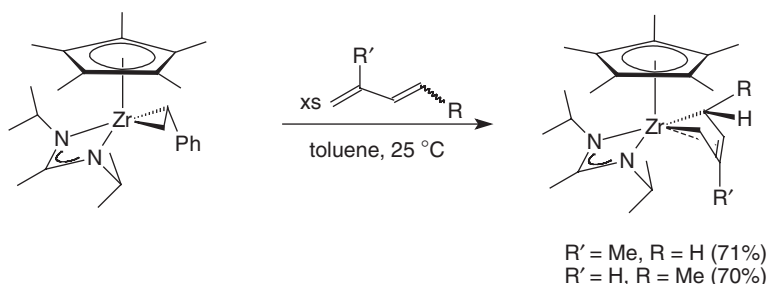
Scheme 89



Scheme 90



Scheme 91

**Scheme 92****Scheme 93****Scheme 94**

from $\text{Cp}_2\text{Zr}(=\text{NAr})(\text{THF})$ ($\text{Ar} = 2,6\text{-Me}_2\text{C}_6\text{H}_3$). The ligands in the resulting diazametallacycles can be regarded as doubly deprotonated guanidinate anions. The products display a rich derivative chemistry with unsaturated organic substrates.¹⁹⁸

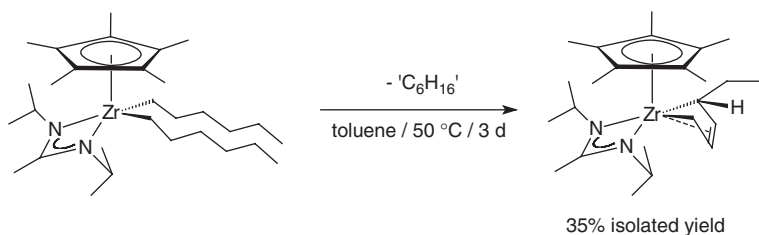
Protonolysis of the η^2 -styrene zirconium complex $\text{Cp}^*\text{Zr}(\eta^2\text{-PhCHCH}_2)[\text{MeC}(\text{NPr}^i)_2]$ with 2 equivalents of Bu^tNH_2 provided a high yield of a novel bis(amido) complex according to Scheme 93.^{199a}

As shown in Scheme 94, the η^2 -styrene zirconium complex $\text{Cp}^*\text{Zr}(\eta^2\text{-PhCHCH}_2)[\text{MeC}(\text{NPr}^i)_2]$ also served as starting material in the synthesis of alkyl-substituted 1,3-diene complexes of (pentamethylcyclopentadienyl)zirconium amidinates. NMR spectroscopy as well as single-crystal X-ray analyses of these complexes revealed that they are best described by the Zr(IV) σ^2, π -metallacyclopent-3-ene limiting resonance form rather than as Zr(II) η^4 -diene complexes.^{199b}

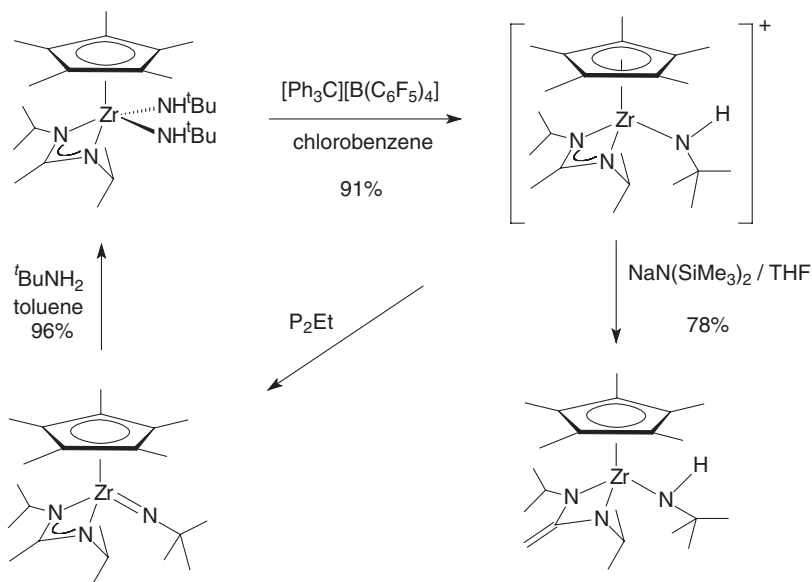
One of these 1,3-diene complexes, a 1,3-hexadiene derivative, was also obtained in a less straightforward manner by thermally induced loss of “C₆H₁₆” from a bis(*n*-hexyl) precursor (Scheme 95).^{199b}

Treatment of Cp^{*}Zr[MeC(NPr^{*i*})₂](NHBu^{*t*})₂ with [Ph₃C][B(C₆F₅)₄] led to amide abstraction and formation of the corresponding cationic zirconium amido complex in high yield. Subsequent deprotonation with NaN(SiMe₃)₂ in THF surprisingly afforded the neutral enolamide Cp^{*}Zr(NHBu^{*t*})[CH₂=C(NPr^{*i*})₂]. The originally desired imido complex Cp^{*}Zr(=NBu^{*t*})[MeC(NPr^{*i*})₂] was only accessible when commercially available EtNP(NMe₂)₂NP(NMe₂)₃ (abbreviated as P₂Et) was used as deprotonating agent (Scheme 96). With 1.839(2) Å the Zr–N distance is typical for zirconium imido complexes.^{199a}

The (pentamethylcyclopentadienyl)zirconium amidinate unit also served as a platform for the synthesis and characterization of remarkable cationic and zwitterionic allyl zirconium complexes derived from trimethylenemethane (TMM). A direct synthetic route to the neutral precursors was found in the



Scheme 95

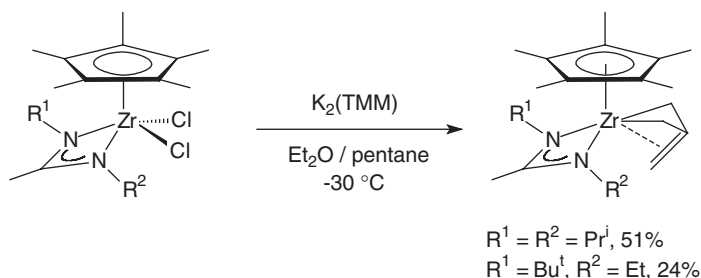


Scheme 96

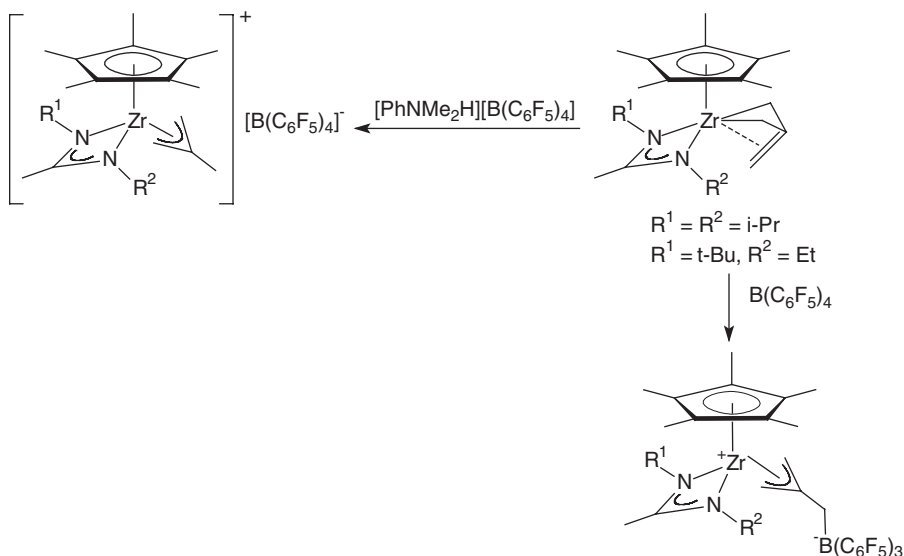
reaction of dichloro (pentamethylcyclopentadienyl)zirconium acetamidates with the dipotassium salt of the trimethylenemethane dianion, $K_2(\text{TMM})$, as depicted in Scheme 97.^{200,201}

Protonation of the TMM complexes with $[\text{PhNMe}_2\text{H}][\text{B}(\text{C}_6\text{F}_5)_4]$ in chlorobenzene at -10°C provided cationic methallyl complexes which are thermally robust in solution at elevated temperatures as determined by ^1H NMR spectroscopy. In contrast, addition of $\text{B}(\text{C}_6\text{F}_5)_3$ to the neutral TMM precursors provided zwitterionic allyl complexes (Scheme 98). Surprisingly, it was found that neither the cationic nor the zwitterionic complexes are active initiators for the Ziegler–Natta polymerization of ethylene and α -olefins.²⁰⁰

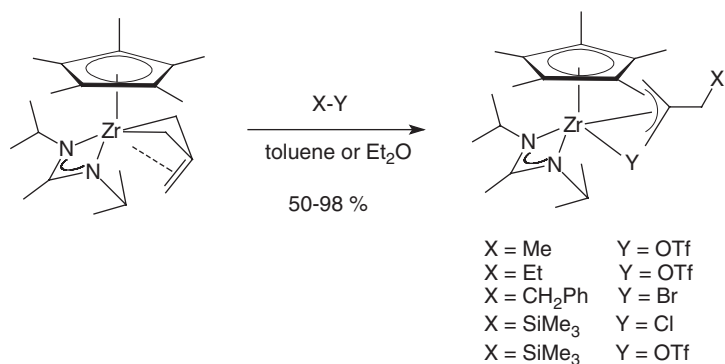
The zirconium TMM complexes also react with organic electrophiles, including unactivated ones, according to Scheme 99 under formation of the corresponding substituted allyl complexes.^{202a}



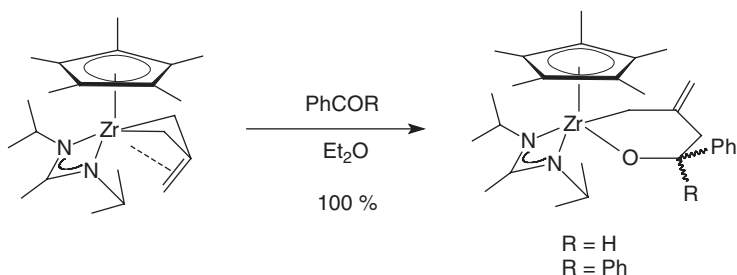
Scheme 97



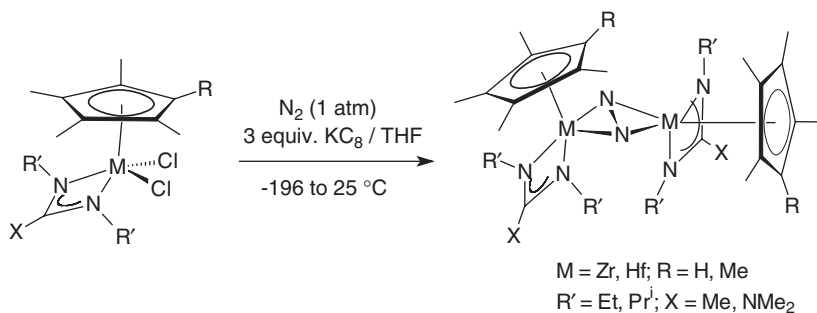
Scheme 98



Scheme 99



Scheme 100



Scheme 101

It was also found that $Cp^*Zr[MeC(NPr^i)_2](TMM)$ readily reacts with benzaldehyde and benzophenone to provide the heterocyclic insertion products shown in [Scheme 100](#).^{202a}

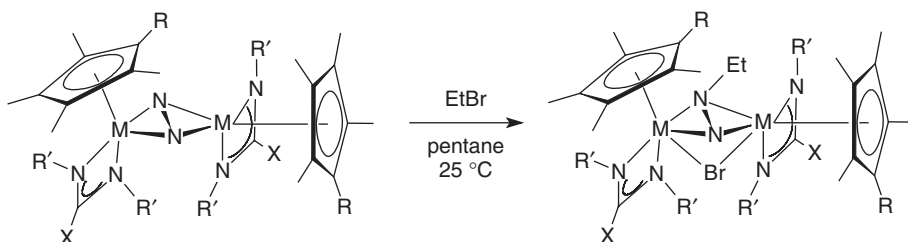
Potassium graphite reduction of the dichloro precursors under an atmosphere of N_2 in THF according to [Scheme 101](#) allowed access to new families of Group 4 bimetallic “side-on-bridged” dinitrogen complexes.^{202b}

Six members of this series could be isolated in modest yields as highly air-sensitive, dark blue or dark purple crystalline solids for which analytical, spectroscopic, and single-crystal X-ray analyses were fully consistent with the side-on-bridged N_2 structures shown in Scheme 102. These complexes show unusual structural features as well as a unique reactivity. An extreme degree of $N\equiv N$ bond elongation was manifested in $d(N-N)$ values of up to 1.64 Å, and low barriers for N-atom functionalization allowed functionalization such as hydrogenation, hydrosilylation, and, for the first time, alkylation with alkyl bromides at ambient temperature.^{202b}

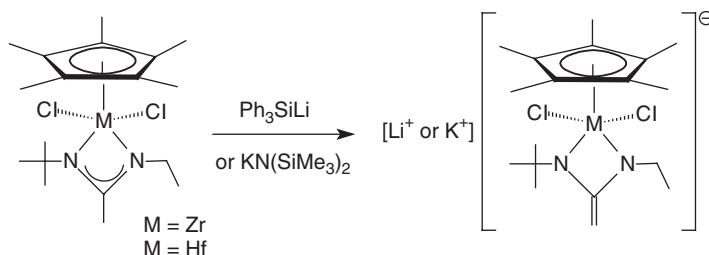
Deprotonation of Group 4 mono(pentamethylcyclopentadienyl) metal acetamidinates can be achieved in high yield using sterically encumbered bases (Scheme 103) to provide anionic enolate complexes as purple powders. These can subsequently be allowed to react with electrophiles (e.g., $PhCH_2Cl$, CH_2Cl_2 , Me_2SiCl_2) to produce several new classes of metal amidinates that are not accessible by conventional routes (Scheme 104).²⁰³

An unusual porphyrin-supported hafnium guanidinate was obtained from the reaction of $(TTP)Hf=NAr$ (TTP = *meso*-tetra-*p*-tolylporphyrinato dianion, Ar = 2,6-diisopropylphenyl) with 1,3-diisopropylcarbodiimide. The molecular structure of the product, $(TTP)Hf[Pr^iNC(NPr^i)(NAr)]$ is shown in Figure 24.²⁰⁴

The heterobimetallic In/Ti complex $[Bu^tC(NPr^i)_2]In\{\mu-NC_6H_3Pr_2^{i-2,6}\}_2Ti(NMe_2)_2$ (Scheme 105) has been prepared as a yellow crystalline material by



Scheme 102



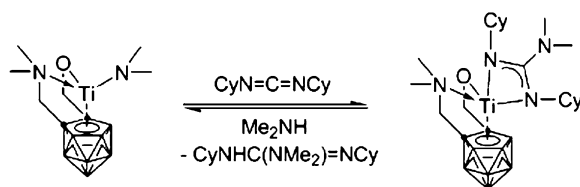
Scheme 103

allowing the mono(amidinato)indium bis(amide) precursor $[\text{Bu}^t\text{C}(\text{NPr}^i)_2]\text{In}\{\text{NHC}_6\text{H}_3\text{Pr}_2^i\text{-2,6}\}_2$ (cf. Section III.A.3) to react with $\text{Ti}(\text{NMe}_2)_4$.¹¹⁷

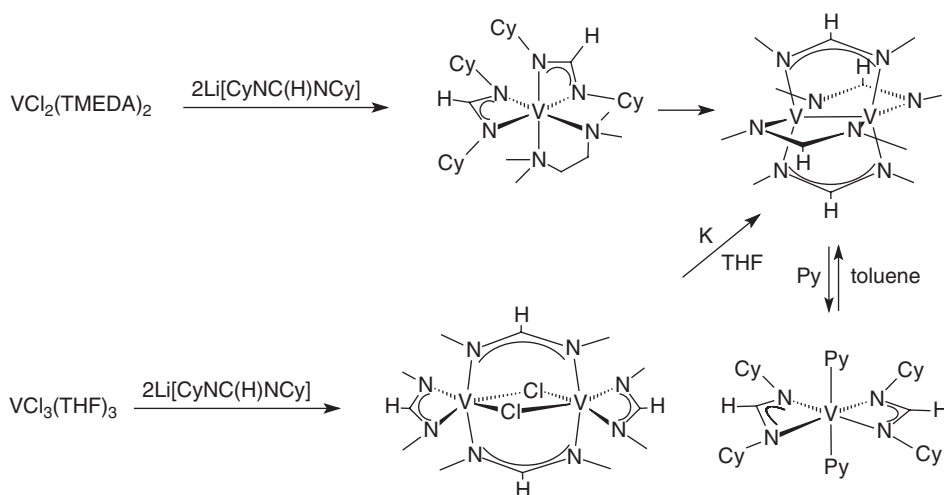
A half-sandwich titanacarborane guanidinate complex is formed on treatment of the corresponding amide precursor with 1,3-dicyclohexylcarbodiimide (Scheme 106). The compounds have been employed as catalysts for the guanylation of amines (cf. Section V.C).²⁰⁵

3. Group 5 metal complexes

The role of steric influences on the formation of various vanadium amidinate complexes in the oxidation states +2 and +3 has been studied in detail. The reaction of $\text{VCl}_2(\text{TMEDA})_2$ and of $\text{VCl}_3(\text{THF})_3$ with 2 equivalents of formamidinate salts afforded dimeric $\text{V}_2[\text{HC}(\text{NCy})_2]_4$ (cf. Section IV.E) with a very short V–V multiple bond and $[\{\text{HC}(\text{NCy})_2\}\text{V}(\mu\text{-Cl})_2]$ which is also dimeric (Scheme 107). The formation of $\text{V}_2[\text{HC}(\text{NCy})_2]_4$ was shown to proceed through the intermediate monomeric $[\text{HC}(\text{NCy})_2]_2\text{V}(\text{TMEDA})$, which was isolated and fully characterized. The dinuclear structure was reversibly cleaved by treatment with pyridine forming the monomeric $[\text{HC}(\text{NCy})_2]_2\text{V}(\text{py})_2$.^{206,207}



Scheme 106



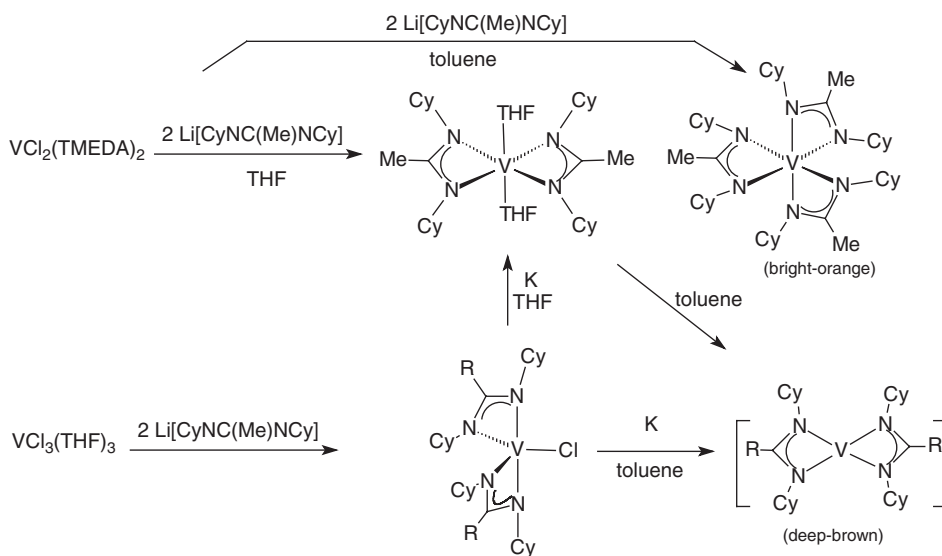
Scheme 107

Similar reactions with the corresponding acetamidinate anion gave only the monomeric $[\text{MeC}(\text{NCy})_2]_2\text{V}(\text{THF})_2$ and $[\text{MeC}(\text{NCy})_2]_2\text{VCl}$, respectively (Scheme 108). Removal of THF from $[\text{MeC}(\text{NCy})_2]_2\text{V}(\text{THF})_2$ or reduction of $[\text{MeC}(\text{NCy})_2]_2\text{VCl}$ led to formation of the homoleptic V(III) complex $[\text{MeC}(\text{NCy})_2]_3\text{V}$ instead of a metal–metal-bonded dimer.^{206,207}

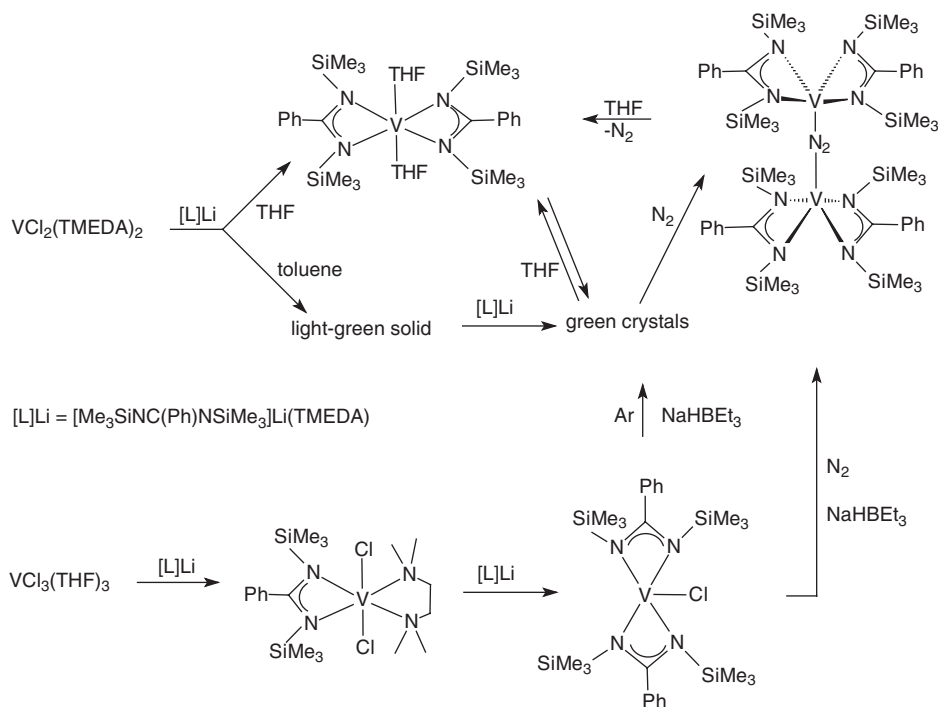
In the case of the very bulky *N*-silylated benzamidinate ligand $[\text{PhC}(\text{NSiMe}_3)_2]^-$ similar monomeric complexes were obtained (Scheme 109). However, attempts to form a dinuclear structure either *via* THF dissociation from $[\text{PhC}(\text{NSiMe}_3)_2]_2\text{V}(\text{THF})_2$ or reduction of $[\text{PhC}(\text{NSiMe}_3)_2]_2\text{VCl}$ gave a novel dinitrogen complex, $(\mu\text{-N}_2)[\{\text{PhC}(\text{NSiMe}_3)_2\}_2\text{V}]_2$.^{206–208}

Amidinate ancillary ligands were also found to stabilize vanadium(III) allyl complexes. Chloro complexes of the types $(\text{amidinate})_2\text{VCl}$ and $(\text{amidinate})\text{VCl}_2(\text{THF})$ were prepared using the amidinate ligands $[\text{PhC}(\text{NSiMe}_3)_2]^-$ and $[\text{Bu}^t\text{C}(\text{NPr}^i)_2]^-$. These served as precursors for amidinate V(III) alkyl and allyl derivatives on treatment with alkyl and allyl Grignard reagents. The allyl ligand in $(\text{amidinate})_2\text{V}(\text{allyl})$ is η^3 -bound. The bis(allyl) complex $[\text{Bu}^t\text{C}(\text{NPr}^i)_2]\text{V}(\eta^3\text{-allyl})_2$ was prepared and structurally characterized (Figure 25), but its analog with the $[\text{PhC}(\text{NSiMe}_3)_2]^-$ ligand already decomposes around -30°C . This shows that the substituent pattern of the amidinate ancillary ligand can strongly affect the stability of organometallic derivatives.²⁰⁸

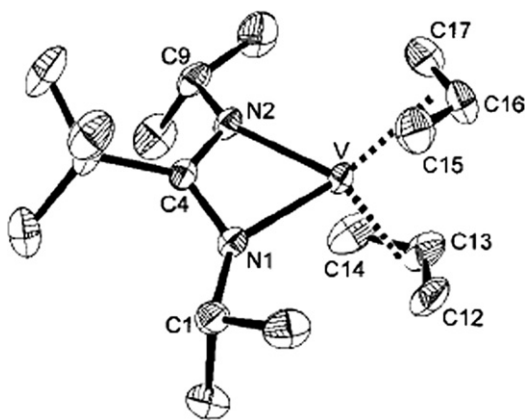
Closely related vanadium(III) complexes have been synthesized using the *N,N'*-bis(trimethylsilyl)pentafluorobenzamidinate ligand, which was obtained in the form of its lithium salt by allowing $\text{LiN}(\text{SiMe}_3)_2$ to react with $\text{C}_6\text{F}_5\text{CN}$. The fully characterized vanadium(III) complexes include $[\text{C}_6\text{F}_5\text{C}(\text{NSiMe}_3)_2]_2\text{VCl}(\text{L})$ ($\text{L} = \text{THF}, \text{PhCN}$) as well as the orange base-free chloride $[\text{C}_6\text{F}_5\text{C}(\text{NSiMe}_3)_2]_2\text{VCl}$ and the alkyl derivatives $[\text{C}_6\text{F}_5\text{C}(\text{NSiMe}_3)_2]_2\text{VMe}(\text{THF})$ and $[\text{C}_6\text{F}_5\text{C}(\text{NSiMe}_3)_2]_2\text{VMe}$



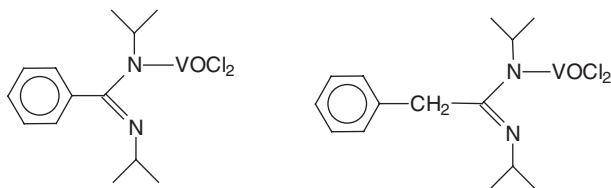
Scheme 108



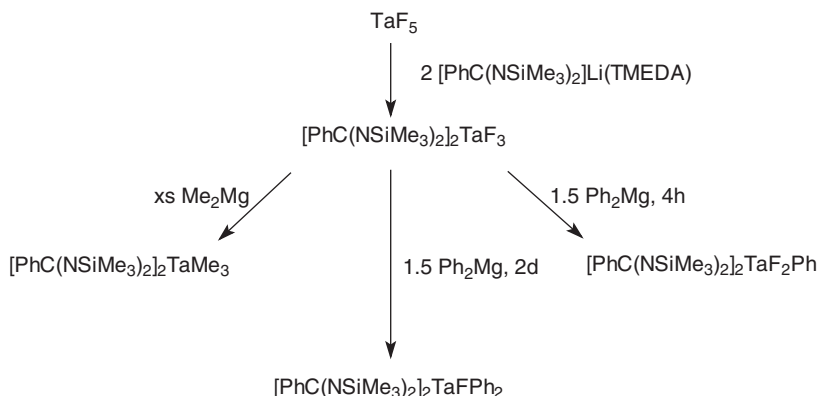
Scheme 109

Figure 25 Molecular structure of bis(allyl) complex $[\text{Bu}^t\text{C}(\text{NPr}^i)_2]\text{V}(\eta^3\text{-allyl})_2$.²⁰⁸

(cf. Section V.A.1).²⁰⁹ The molecular structure of the *p*-tolylimido bis(benzamido)vanadium(V) complex $[\text{PhC}(\text{NSiMe}_3)_2]_2\text{V}(=\text{NC}_6\text{H}_4\text{Me-}p)\text{Cl}$ has been determined by X-ray diffraction.²¹⁰ Two new vanadyl(V) amidinates (Scheme 110) have been synthesized and characterized by single-crystal X-ray diffraction. In the solid state, both complexes are dimeric with Cl bridges and monodentate coordination of the amidinate to the *pseudo*-octahedrally coordinated vanadium.²¹¹



Scheme 110

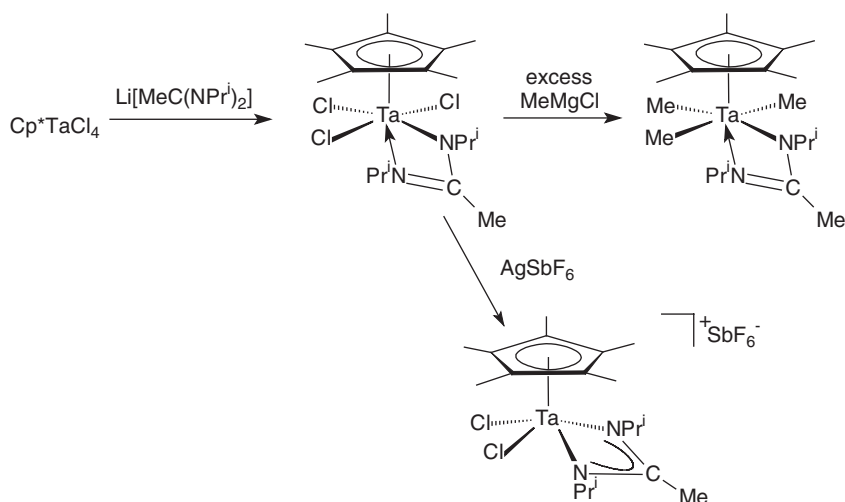


Scheme 111

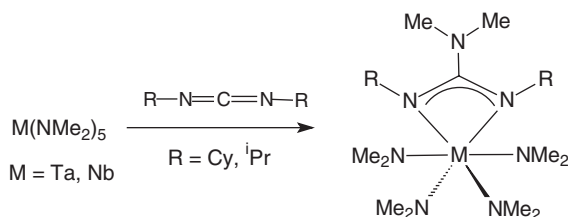
The reaction of $[\text{PhC}(\text{NSiMe}_3)_2]\text{Li}(\text{TMEDA})$ with TaF_5 afforded $[\text{PhC}(\text{NSiMe}_3)_2]_2\text{TaF}_3$ in 40% isolated yield. The solid-state structure shows a pentagonal-bipyramidal coordination geometry. Reactions of the trifluoride with Me_2Mg or Ph_2Mg (Scheme 111) produced $[\text{PhC}(\text{NSiMe}_3)_2]_2\text{TaMe}_3$ and $[\text{PhC}(\text{NSiMe}_3)_2]_2\text{TaF}_2\text{Ph}$ or $[\text{PhC}(\text{NSiMe}_3)_2]_2\text{TaFPh}_2$, respectively, which all adopt a similar ligand arrangement as the starting material.²¹²

Orange-yellow $\text{Cp}^*[\text{MeC}(\text{NPr}^i)_2]\text{TaCl}_3$ was prepared in a 60% yield by the reaction of Cp^*TaCl_4 with 1 equivalent of $\text{Li}[\text{MeC}(\text{NPr}^i)_2]$ in THF (Scheme 112). The structure is *pseudo*-octahedral with a plane of symmetry containing the amidinate ligand and bisecting the Cp^* . Reaction of $\text{Cp}^*[\text{MeC}(\text{NPr}^i)_2]\text{TaCl}_3$ with excess MeMgCl yielded the corresponding trimethyl derivative, while treatment with AgSbF_6 afforded a deep red cationic complex as shown in Scheme 112. In the latter, the amidinate orientation is changed with respect to the starting material such that the amidinate and the Cp^* are nearly co-planar.²¹³

Metathetical reactions between $\text{NbCl}_4(\text{THF})_2$, NbCl_5 , TaCl_5 , $[(\text{Et}_2\text{N})_2\text{TaCl}_3]_2$, or $(\text{R}_2\text{N})_3\text{Ta}(=\text{N}^i\text{Bu})$ ($\text{R} = \text{Me}, \text{Et}$) with various amounts of lithium amidinates have been employed to synthesize the corresponding heteroleptic niobium and tantalum amidinate complexes. The products were investigated as potential precursors to metal nitrides (cf. Section VI).^{214–216} Carbodiimide insertion routes have been employed for the preparation of guanidinate-containing complexes of Nb and Ta. The mono(guanidinate) complexes $[\text{Me}_2\text{NC}(\text{NR})_2]\text{M}(\text{NMe}_2)_4$ were smoothly formed at room temperature on treatment $\text{M}(\text{NMe}_2)_5$ with either dicyclohexylcarbodiimide or diisopropylcarbodiimide (Scheme 113).²¹⁷



Scheme 112

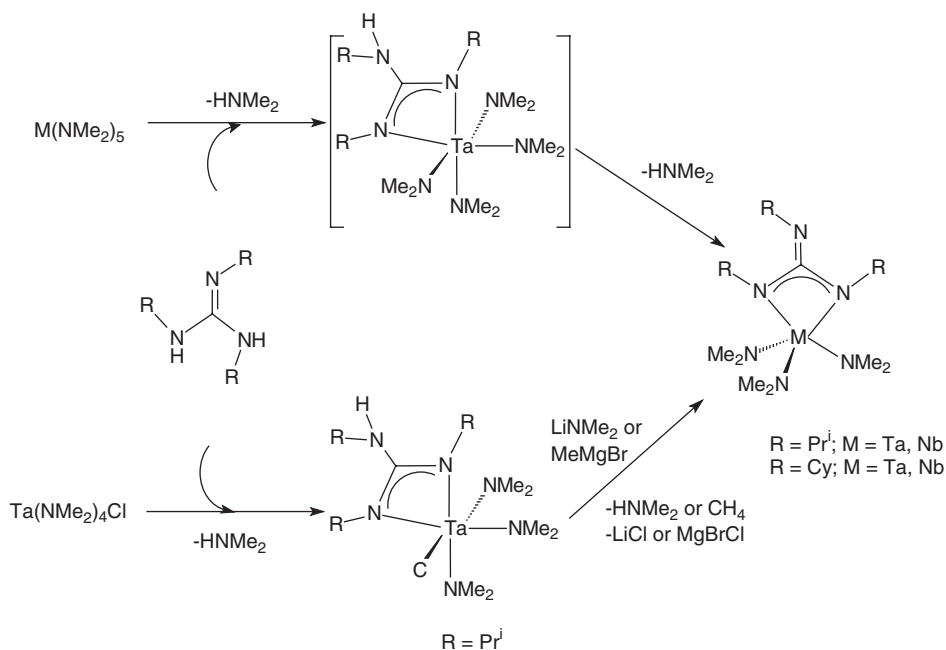


Scheme 113

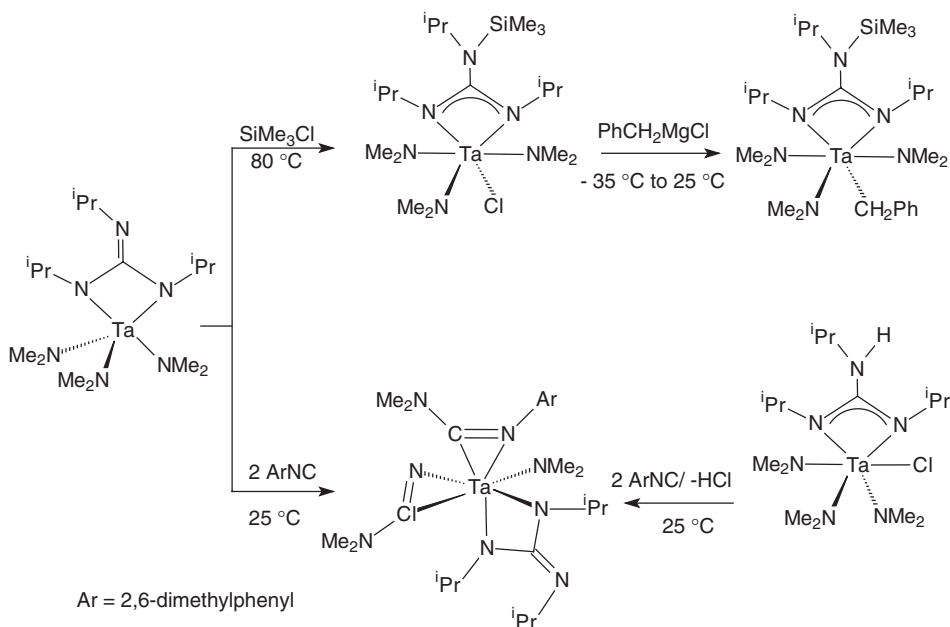
An alternative route to niobium and tantalum guanidinate complexes involves deprotonation of tricyclohexylguanidine or triisopropylguanidine by the homoleptic amido complexes $\text{M}(\text{NMe}_2)_5$ ($\text{M} = \text{Nb}, \text{Ta}$). In this case, however, dianionic N,N',N'' -trialkylguanidinate ligands are formed. The reaction, shown in Scheme 114, also proceeds smoothly at room temperature and provides the mono(guanidinato) complexes in good yield. In contrast, protonation of the amido groups of $\text{Ta}(\text{NMe}_2)_4\text{Cl}$ with triisopropylguanidine gave the six-coordinated $[\text{Pr}^i\text{NHC}(\text{NPr}^i)_2]\text{Ta}(\text{NMe}_2)_3\text{Cl}$ containing a regular bidentate monoanionic guanidinate ligand. Further deprotonation of this intermediate can be achieved by reaction with either LiNMe_2 or MeMgBr (Scheme 114).^{218,219}

The reactivity of the dianionic guanidinate complex $[\text{Pr}^i\text{N}=\text{C}(\text{NPr}^i)_2]\text{Ta}(\text{NMe}_2)_3$ and the monoanionic guanidinate complex $[\text{Pr}^i\text{NHC}(\text{NPr}^i)_2]\text{Ta}(\text{NMe}_2)_3\text{Cl}$ toward Me_3SiCl and ArNC ($\text{Ar} = 2,6\text{-Me}_2\text{C}_6\text{H}_3$) has been investigated. These reactions are summarized in Scheme 115.^{220a,b}

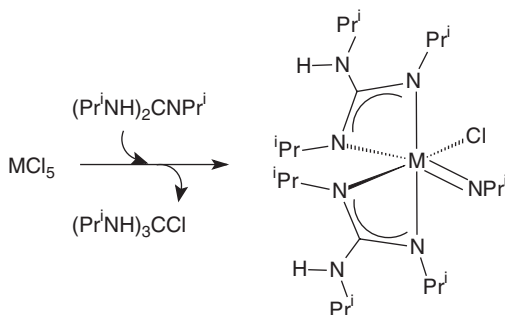
Unique examples of N,N',N'' -tri(isopropyl)guanidinate complexes of Nb(V) and Ta(V) bearing additional terminal imido ligands have been obtained as depicted in Scheme 116. Depending on the reaction conditions, these reactions may also lead to the formation of compounds containing dianionic guanidinate



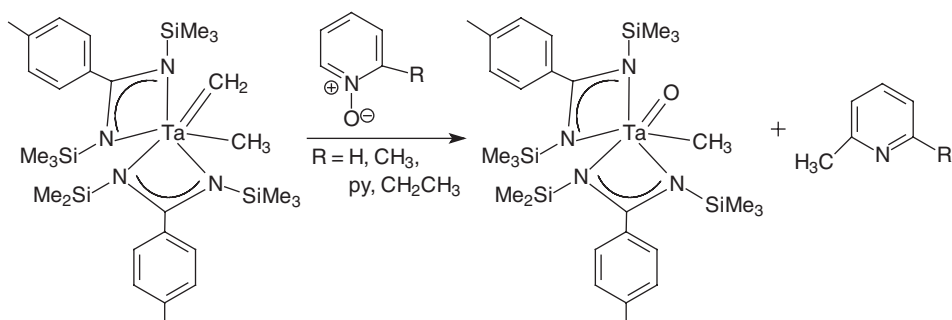
Scheme 114



Scheme 115



Scheme 116



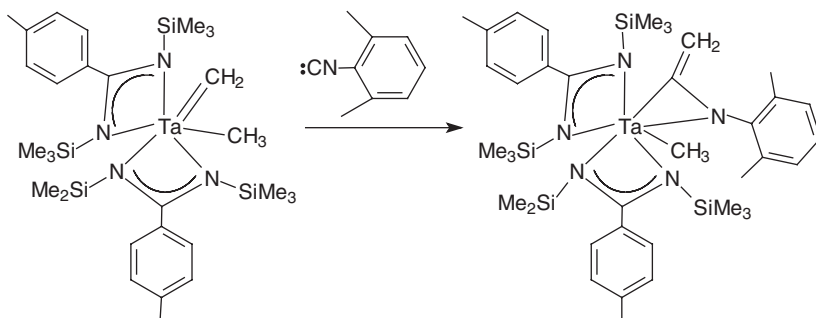
Scheme 117

ligands, which exhibit unusual bonding modes involving all of the nitrogen centers of the ligand.^{220a,b}

Closely related mixed amido/imido/guanidinato tantalum complexes of the type $\text{Ta}(\text{NR}^1\text{R}^2)[(\text{R}^1\text{R}^2\text{N})\text{C}(\text{NR}^3)_2](=\text{NR}^4)$ ($\text{R}^1, \text{R}^2 = \text{Me}, \text{Et}$; $\text{R}^3 = \text{Cy}, \text{Pr}^i$; $\text{R}^4 = \text{Pr}^n, \text{Bu}^t$) were synthesized by the insertion of carbodiimides into to tantalum-amide bonds in imidotantalum triamide precursors, and the effects of ligand substitution on thermal properties were studied by TGA/DTA measurements. In addition, selected compounds were pyrolyzed at 600°C and the decomposition products were studied by GC-MS and ^1H NMR spectroscopy.^{220c}

The reactivity of a remarkable electronically unsaturated tantalum methyldene complex, $[p\text{-MeC}_6\text{H}_4\text{C}(\text{NSiMe}_3)_2]_2\text{Ta}(=\text{CH}_2)\text{CH}_3$, has been investigated. Electrophilic addition and olefination reactions of the $\text{Ta}=\text{CH}_2$ functionality were reported. The alkylidene complex participates in group-transfer reactions not observed in sterically similar but electronically saturated analogs. Reactions with substrates containing unsaturated $\text{C}-\text{X}$ ($\text{X} = \text{C}, \text{N}, \text{O}$) bonds yield $[\text{Ta}] = \text{X}$ compounds and vinylated organic products. Scheme 117 shows the reaction with pyridine N -oxide, which leads to formation of a tantalum oxo complex.²²¹

The reaction of $[p\text{-MeC}_6\text{H}_4\text{C}(\text{NSiMe}_3)_2]_2\text{Ta}(=\text{CH}_2)\text{CH}_3$ with 2,6-dimethylphenyl isocyanide afforded an η^2 -ketenimine complex (Scheme 118). Carbon-sulfur cleavage reactions produced tantalum thioformaldehyde and tantalum sulfido complexes.²²¹



Scheme 118

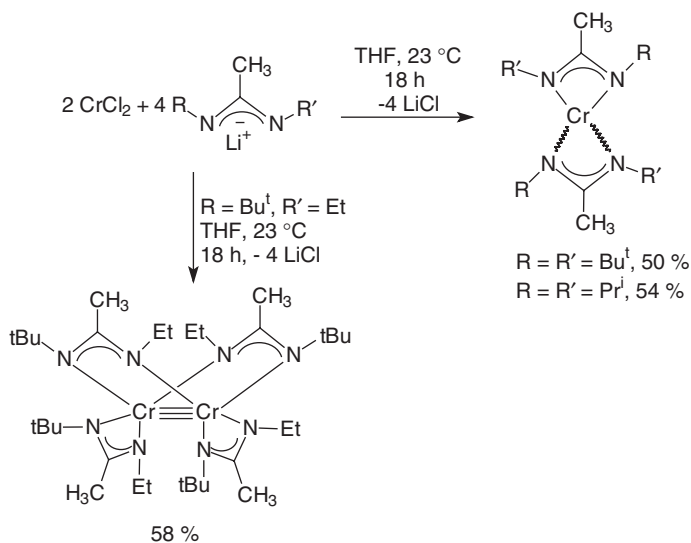
C. Amidinate and guanidinate complexes of the middle and late transition metals

1. Group 6 metal complexes

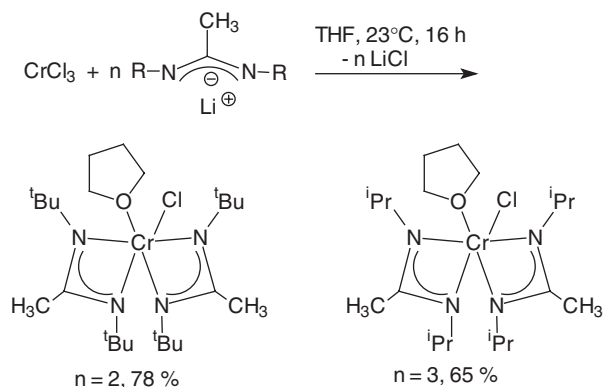
Homoleptic tris(amidinato) complexes of the type $\text{Cr}[\text{HC}(\text{NC}_6\text{H}_4\text{Me-}p)_2]_3$ and $\text{Cr}[\text{HC}(\text{NPh})_2]_3$ were prepared from either CrCl_2 or CrCl_3 using the standard metathetical route and structurally characterized by X-ray diffraction.²²² $\text{CrCl}_2(\text{THF})_2$ was the starting material for the synthesis of chromium bis(amidinates) containing bulky amidinate ligands. The complexes $[\text{MeC}(\text{NCy})_2]_2\text{Cr}$, $[o\text{-Me}_2\text{NCH}_2\text{C}_6\text{H}_4\text{C}(\text{NCy})_2]_2\text{Cr}(\text{THF})_2$, and $[\text{PhC}(\text{NSiMe}_3)_2]_2\text{Cr}$ were made by metathetical reactions using this THF-adduct as precursor.²⁹ A related bis(amidinato) chromium(II) complex was prepared using a bulky terphenyl-substituted amidinate ligand (cf. Scheme 7),⁵⁰ as was the compound $\text{Cr}[\text{Bu}^t\text{C}(\text{NAr})(\text{NHAr})]$ ($\text{Ar} = 2,6\text{-Pr}_2\text{C}_6\text{H}_3$).⁴⁶ As illustrated in Scheme 119, the outcome of reactions of chromium(II) chloride with differently substituted lithium acetamidinates depends on the substitution pattern of the amidinate ligands. When $\text{R} = \text{R}' = \text{Pr}^i$ or Bu^t , monomeric complexes result. However, metallic green crystals of a dimeric complex were obtained when $\text{R} = \text{Bu}^t$ and $\text{R}' = \text{Et}$. Despite the presence of a short chromium–chromium bond (1.9601(12) Å), NMR spectra and solution molecular weight experiments demonstrated that this dimeric complex dissociates to monomers in cyclohexane and benzene solutions. This was the first example of chromium–chromium bond cleavage in the absence of an added Lewis base and implies that the chromium–chromium bond in the dimeric complex is weak.^{223a}

A series of chromium(III) amidinates containing additional pyrazolato, triazolato, or tetrazolato ligands have recently been reported. Treatment of anhydrous chromium(III) chloride with 2 or 3 equivalents of $\text{Li}[\text{MeC}(\text{NBu}^t)_2]$ or $\text{Li}[\text{MeC}(\text{NPr}^i)_2]$ in THF at room temperature afforded $[\text{MeC}(\text{NBu}^t)_2]_2\text{CrCl}(\text{THF})$ and $[\text{MeC}(\text{NPr}^i)_2]_3\text{Cr}$ in 78 and 65% yields, respectively (Scheme 120).^{223b}

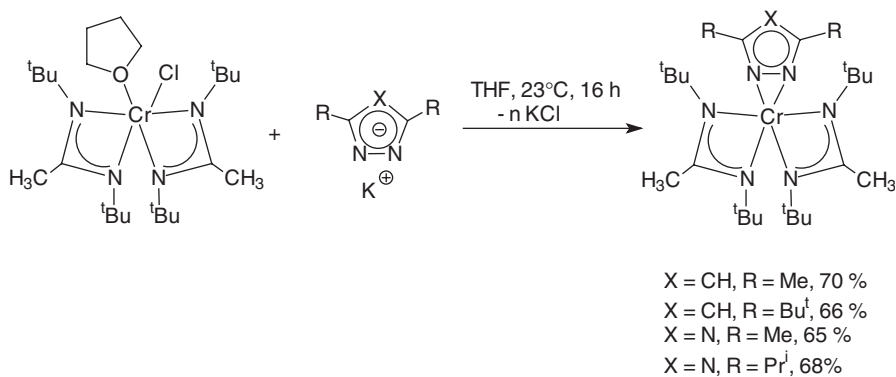
Treatment of $[\text{MeC}(\text{NBu}^t)_2]_2\text{CrCl}(\text{THF})$ with the potassium salts derived from pyrazoles and 1,2,4-triazoles as outlined in Scheme 121 afforded the corresponding derivatives with 3,5-disubstituted pyrazolato or 3,5-disubstituted 1,2,4-triazolato ligands in 65–70% yields. X-ray structural analyses revealed η^2 -coordination of the heterocyclic ligands.^{223b}



Scheme 119



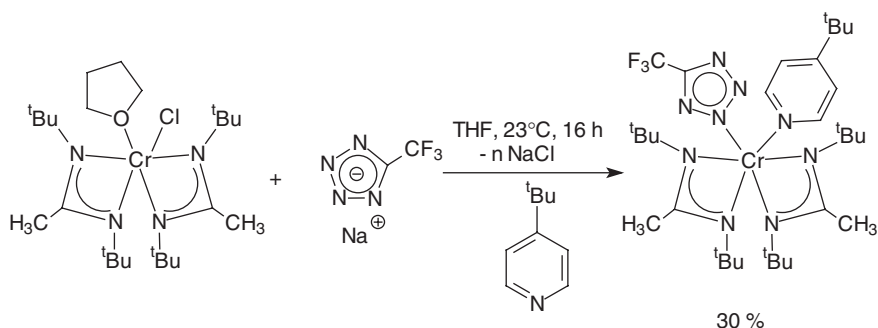
Scheme 120



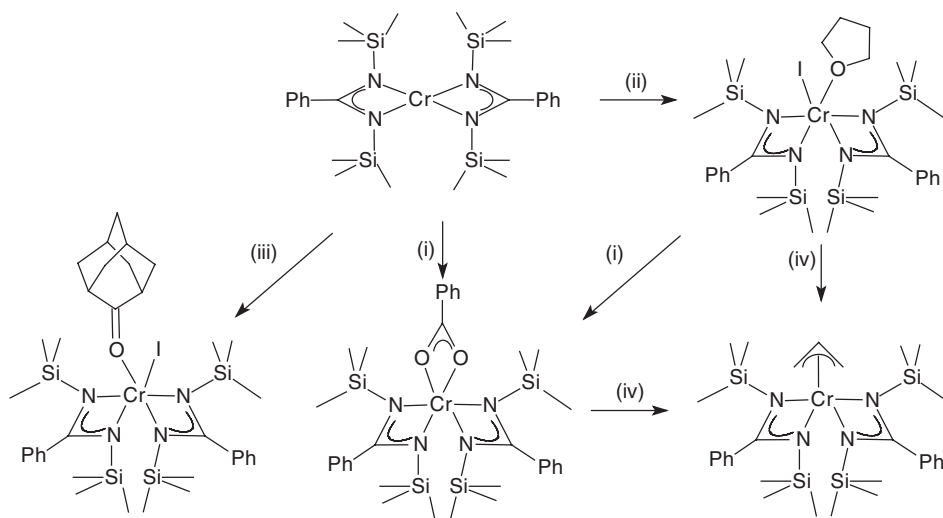
Scheme 121

Similar treatment of $[\text{MeC}(\text{N}^t\text{Bu})_2]_2\text{CrCl}(\text{THF})$ with sodium trifluoromethyl-tetrazolate (NaCF_3tetz) in the presence of 4-*tert*-butylpyridine afforded $[\text{MeC}(\text{N}^t\text{Bu})_2]_2\text{Cr}(\text{CF}_3\text{tetz})(4\text{-}t\text{Bupy})$ as red crystals in 30% yield (Scheme 122).^{223b}

Recently it was shown that single-electron oxidation of the longer known Cr(II) bis(amidinate) complex $\text{Cr}[\text{PhC}(\text{NSiMe}_3)_2]_2$ ^{1c} provides straightforward synthetic access to neutral Cr(III) amidinate complexes.²²⁴ The new complexes $[\text{PhC}(\text{NSiMe}_3)_2]_2\text{CrX}$ were prepared by reaction of $\text{Cr}[\text{PhC}(\text{NSiMe}_3)_2]_2$ with AgO_2CPh ($\text{X} = \text{O}_2\text{CPh}$), with iodine in THF ($\text{X} = \text{I/THF}$), or with iodine in pentane, followed by addition of 2-adamantanone ($\text{X} = \text{I/2-adamantanone}$) (Scheme 123). Quite remarkably, treatment of either the benzoate derivative $[\text{PhC}(\text{NSiMe}_3)_2]_2\text{Cr}(\text{O}_2\text{CPh})$ or the iodide $[\text{PhC}(\text{NSiMe}_3)_2]_2\text{Cr}(\text{THF})$ with $\text{C}_3\text{H}_5\text{MgCl}$ resulted in formation of the thermally stable allyl complex $[\text{PhC}(\text{NSiMe}_3)_2]_2\text{Cr}(\eta^3\text{-C}_3\text{H}_5)$.²²⁴



Scheme 122



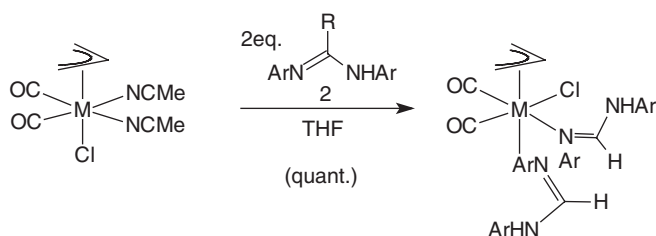
Scheme 123 Experimental conditions: (i) AgO_2CPh , THF; (ii) I_2 , THF; (iii) (a) I_2 , pentane, (b) 2-adamantanone; (iv) $\text{C}_3\text{H}_5\text{MgCl}$, THF.²²⁴

Treatment of bis(pyridine) complexes of molybdenum and tungsten, $M(\eta^3\text{-allyl})\text{Cl}(\text{CO})_2(\text{py})_2$ ($M = \text{Mo}, \text{W}$) with equimolar amounts of lithium amidinates $\text{Li}[\text{RC}(\text{NPh})_2]$ ($R = \text{H}, \text{Me}$) afforded amidinato complexes of the type $M(\eta^3\text{-allyl})[\text{RC}(\text{NPh})_2](\text{CO})_2(\text{py})$ ($M = \text{Mo}, \text{W}$). Reactions of the latter with acetonitrile, PEt_3 , and $\text{P}(\text{OMe})_3$ have been investigated.²²⁵ Free amidines react with $M(\eta^3\text{-allyl})\text{Cl}(\text{CO})_2(\text{NCMe})_2$ according to Scheme 124 to give the corresponding bis(amidine) complexes.²²⁶

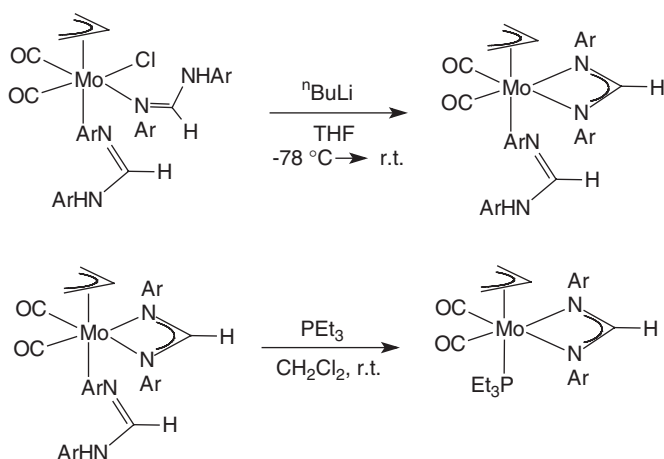
Treatment of the bis(amidine) derivatives with a strong base such as Bu^nLi leads to conversion to the corresponding amidinato(amidine) complexes which on further reaction with triethylphosphine loose the coordinated free amidine as illustrated in Scheme 125.^{226,227}

Closely related pyridine adducts were prepared as shown in Scheme 126 by treatment of the corresponding chloro precursor with lithium amidinates.²²⁷

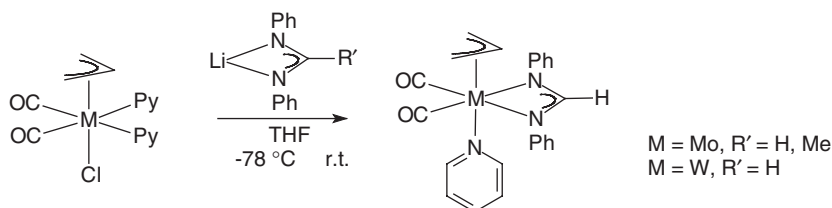
The pyridine ligand in the products shown in Scheme 126 is labile and can be readily replaced by bidentate ligands such as 1,10-phenanthroline (phen) or 1,2-bis(diphenylphosphino)ethane (dppe). Scheme 127 illustrates the reaction with phen.²²⁸



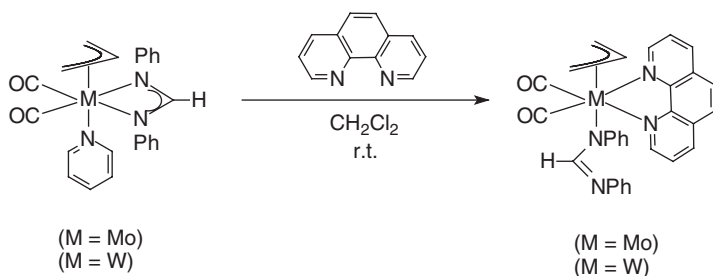
Scheme 124



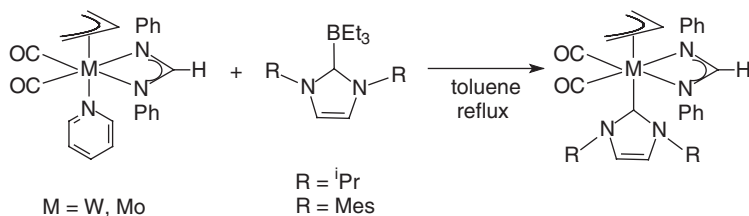
Scheme 125



Scheme 126



Scheme 127

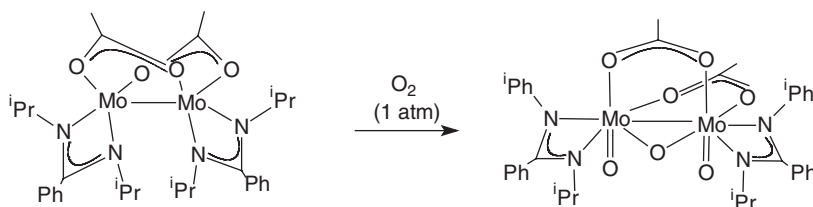


Scheme 128

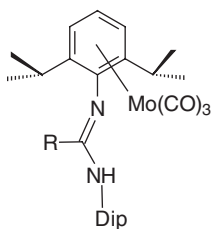
The amidinato(pyridine) complexes also react with the triethylborane adduct of the NHC 1,3-diisopropylimidazol-2-ylidene in toluene at reflux temperature to give the corresponding carbene complexes (Scheme 128).²²⁹

The 16 valence-electron molybdenum(IV) formamidinate complexes $\text{CpMoCl}_2[\text{HC}(\text{NPh})_2]$ and $(\text{Ind})\text{MoCl}_2[\text{HC}(\text{NPh})_2]$ are synthesized by allowing the respective trichloro precursors, CpMoCl_3 or $(\text{Ind})\text{MoCl}_3$, to react with $\text{AgCH}(\text{NPh})_2$ in dichloromethane.²³⁰ A multiply bonded dimolybdenum complex containing bridging acetate and terminal amidinate ligands has been reported to react readily with dry oxygen to give the dimolybdenum(V) complex $(\mu\text{-O})(\mu\text{-OAc})_2[\text{Mo}(\text{O})(\text{PhC}(\text{NPr}^t)_2)_2]$ as a red solid (Scheme 129).²³¹

A unique pair of stereoisomeric dimolybdenum amidinate complexes has been prepared and structurally characterized. The reaction of $\text{Li}[\text{PhC}(\text{NSiMe}_3)_2]$ with dimolybdenum tetraacetate afforded *trans*- and *cis*- $\text{Mo}_2(\text{O}_2\text{CMe})_2[\text{PhC}(\text{NSiMe}_3)_2]_2$. While the acetates coordinate to the Mo_2 core *via* a bridging mode in both compounds, the benzamidinates are bridging in the *trans* complex and



Scheme 129



R = Me, C₆H₄Me-*p*, C₆H₄OMe-*p*

Dip = C₆H₃Pr^{*i*}_{2-2,6}

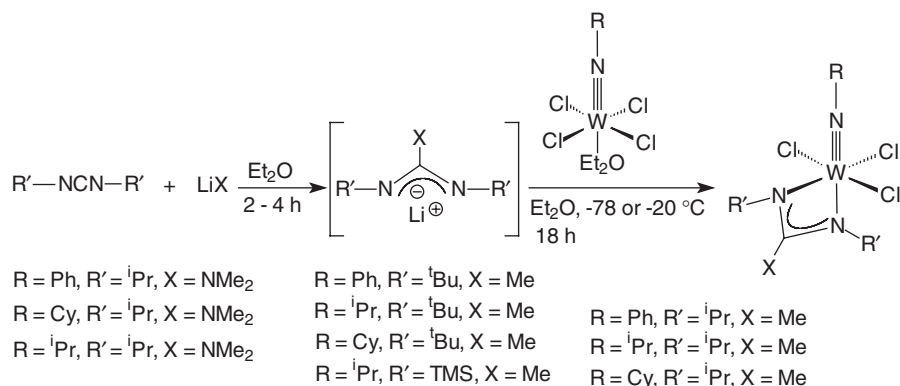
Scheme 130

chelating in the *cis* isomer. The Mo–Mo bond lengths are 2.0692(4) and 2.1241(3), respectively.²³² Very bulky *N,N'*-disubstituted amidines containing 2,6-diisopropylphenyl substituents at nitrogen have been found to react with Mo(CO)₆ at elevated temperatures under formation of η^6 -arene-coordinated complexes as exemplified in Scheme 130.⁵⁵

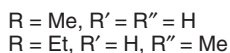
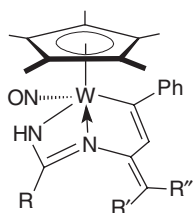
The reaction of (ArN=)₂MoCl₂(DME) (Ar = C₆H₃Pr^{*i*}_{2-2,6}) with lithium amidinates or guanidinates resulted in molybdenum(VI) complexes of the type (ArN=)₂[RN(NR')₂][MoCl] (R = Me, R' = Cy; R = NPr^{*i*}₂, R' = Cy; R = N(SiMe₃)₂, R' = Cy; R = Ph, R' = SiMe₃) with five-coordinated molybdenum atoms. Methylation of these compound with MeLi afforded the corresponding methyl derivatives (ArN=)₂[RN(NR')₂][MoMe].²³³ A series of tungsten imido guanidinate and amidinate complexes were synthesized according to Scheme 131 by treatment of the corresponding imido complexes W(=NR)Cl₄(OEt)₂ with the appropriate lithium amidinate or guanidinate. Crystallographic structure determination of [MeC(NPr^{*i*})₂]W(=NPr^{*i*})Cl₃ and [Me₂NC(NPr^{*i*})₂]W(=NPr^{*i*})Cl₃ allowed comparison of structural features between the guanidinate and amidinate ligand in the presence of an identical ligand set.²³⁴

Thermolysis of the tungsten vinyl complex Cp^{*}W(NO)(CH₂SiMe₃)(CPh=CH₂) in RCN (R = Me, Et) yielded the unusual vinyl amidinate complexes Cp^{*}W(NO)[η^3 -NHC(R)=NC(=C(R¹)(R²))CH=CPh] as shown in Scheme 132.²³⁵

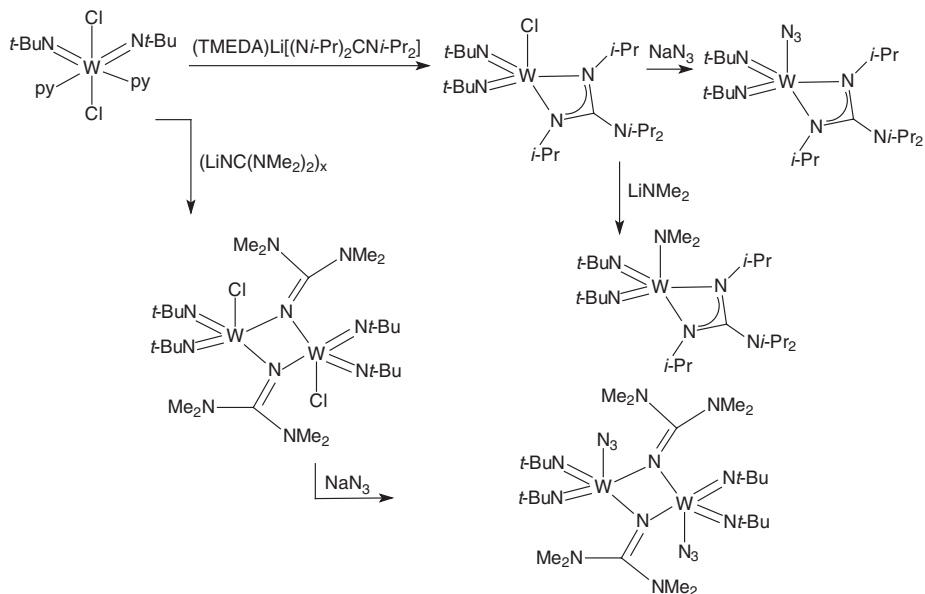
A unique series of mixed guanidinato/alkylimido/azido tungsten(VI) complexes has been synthesized and structurally characterized. As illustrated in Scheme 133, the syntheses start with the readily accessible imido precursor WCl₂(NBu^{*t*})₂py₂, which is treated successively with either appropriate lithium



Scheme 131



Scheme 132



Scheme 133

guanidates, sodium azide, or lithium dimethylamide. The azido derivative $[\text{Pr}^i_2\text{NC}(\text{NPr}^i)_2]\text{W}(\text{N}_3)(\text{NBu}^t)_2$ can be sublimed at $80^\circ\text{C}/1\text{ Pa}$.²³⁶

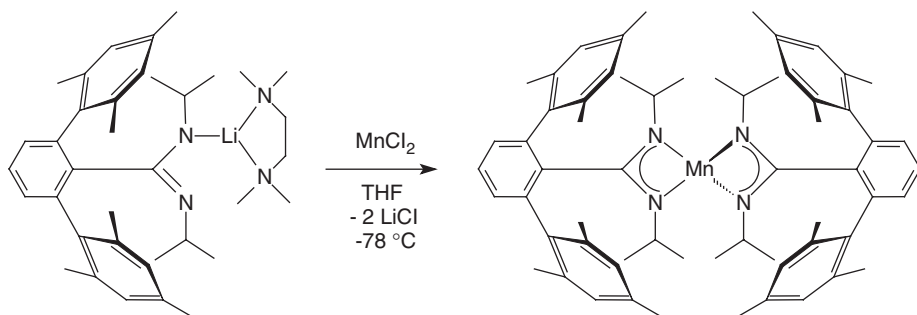
2. Group 7 metal complexes

Amidinate and guanidinate complexes of the Group 7 metals have not been extensively studied. Technetium derivatives are not known at all, and especially the interesting (amidinato)rhenium trioxides still await further investigation. Attempts to prepare an imido-bridged dimer $[\text{CpMn}\{\mu\text{-N}=\text{C}(\text{NMe}_2)_2\}]_2$ by the reaction of Cp_2Mn with 1,1,3,3-tetramethylguanidine, $\text{HN}=\text{C}(\text{NMe}_2)_2$, resulted only in formation of the bis-adduct $\text{Cp}_2\text{Mn}[\text{HN}=\text{C}(\text{NMe}_2)_2]_2$.²³⁷ Treatment of $\text{MnI}_2(\text{THF})_2$ with 2 equivalents of $[\text{PhC}(\text{NSiMe}_3)_2]_2\text{Mg}(\text{THF})_2$ in THF followed by addition of elemental iodine afforded the crystalline black-violet manganese(III) complex $[\text{PhC}(\text{NSiMe}_3)_2]_2\text{MnI}$ in good yields.²³⁸ A bis(amidinato) manganese(II) complex was prepared using a bulky terphenyl-substituted amidinate ligand (Scheme 134).⁵⁰

The monomeric manganese bis(amidinate) $\text{Mn}[\text{Bu}^t\text{C}(\text{NAr}(\text{NHAr}))]$ ($\text{Ar} = 2,6\text{-Pr}^i_2\text{C}_6\text{H}_3$) was made accordingly.⁴⁶ The cationic rhenium formamidinato complex $[\text{Re}\{\text{HC}(\text{NC}_6\text{H}_4\text{Me-}p)_2\}(\text{NO})\text{P}_3][\text{BPh}_4]$ ($\text{P} = \text{PPh}_2\text{OEt}$) was prepared by allowing the hydride $\text{ReH}_2(\text{NO})\text{P}_3$ to react first with triflic acid and then with $p\text{-MeC}_6\text{H}_4\text{N}=\text{C}=\text{NC}_6\text{H}_4\text{Me-}p$ followed by treatment with $\text{Na}[\text{BPh}_4]$.²³⁹ Using $[\text{PhC}(\text{NSiMe}_3)_2]_2\text{Zn}$ and Re_2O_7 as starting materials, the rhenium(VII) complex $[\text{PhC}(\text{NSiMe}_3)_2]\text{ReO}_3$ was synthesized and isolated as colorless diamagnetic crystals, which are stable in air for a short time. In solution, $[\text{PhC}(\text{NSiMe}_3)_2]\text{ReO}_3$ is light-sensitive and decomposes above 10°C . The ReN_2O_3 polyhedron in $[\text{PhC}(\text{NSiMe}_3)_2]\text{ReO}_3$ shows considerable irregularity compared with a trigonal-bipyramidal structure.²³⁸

3. Group 8 metal complexes

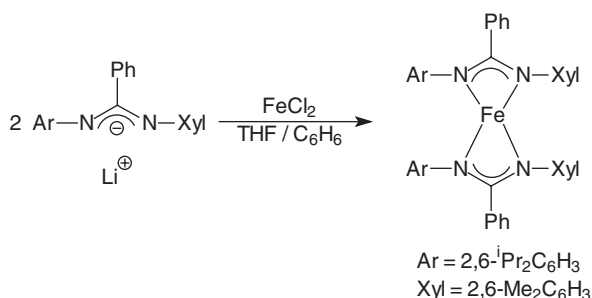
Treatment of FeCl_2 with 2 equivalents of the lithium ferrocenyl amidinate $\text{FcC}(\text{NCy})_2\text{Li}(\text{Et}_2\text{O})$ in THF followed by crystallization from $\text{CH}_2\text{Cl}_2/\text{Et}_2\text{O}$ afforded orange crystals of the trimetallic iron(II) complex $[\text{FcC}(\text{NCy})_2]_2\text{Fe}$ in good yield.^{63,67} A related bis(amidinato) iron(II) complex was also prepared using a bulky terphenyl-substituted amidinate ligand (cf. Scheme 7),⁵⁰ and the monomeric iron bis(amidinate) $\text{Fe}[\text{Bu}^t\text{C}(\text{NAr}(\text{NHAr}))]$ ($\text{Ar} = 2,6\text{-Pr}^i_2\text{C}_6\text{H}_3$)



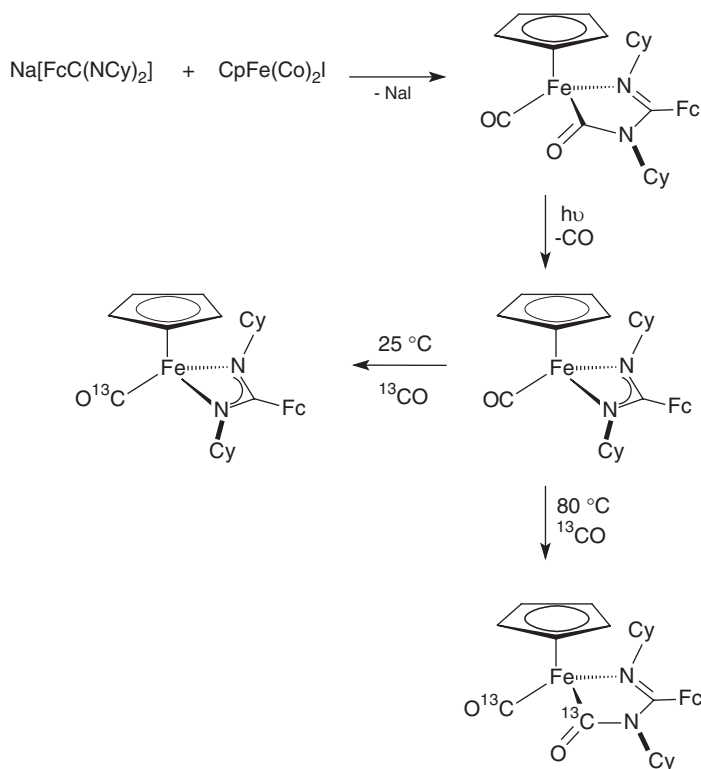
Scheme 134

was made accordingly.⁴⁶ A slight decrease in ligand steric demand as illustrated in [Scheme 135](#) also resulted in the formation of monomeric iron(II) complexes which still adopt a distorted square-planar geometry.⁴⁶

Reaction of $\text{Na}[\text{FcC}(\text{NCy})_2]$ with $\text{CpFe}(\text{CO})_2\text{I}$ afforded the carbamoyl derivative $\text{CpFe}(\text{CO})[\text{FcC}(\text{NCy})\text{N}(\text{Cy})\text{C}(\text{O})]$ ([Scheme 136](#)). Although not thermally labile, a CO ligand is readily lost on UV irradiation to give the amidinate derivative $\text{CpFe}(\text{CO})[\text{FcC}(\text{NCy})_2]$. The addition of ^{13}CO (50 psig) to a solution of



Scheme 135



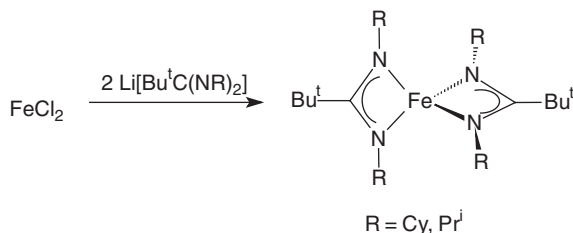
Scheme 136

$\text{CpFe(CO)[FcC(NCy)}_2]$ results in rapid exchange of CO at 25 °C. Heating this solution to 80 °C results in the partial formation of the carbamoyl species by a formal CO insertion into an Fe–N bond (Scheme 136).⁶³

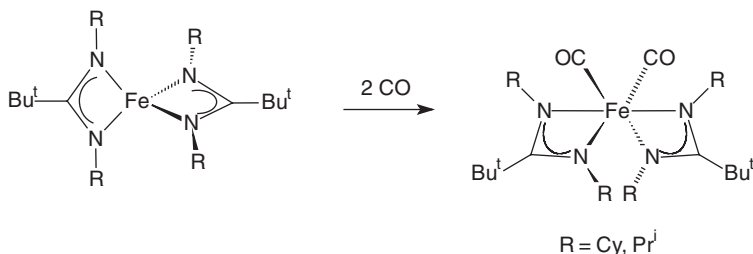
Other paramagnetic bis(amidinate) iron(II) complexes of the type $[\text{Bu}^t\text{C(NR)}_2]_2\text{Fe}$ ($\text{R} = \text{Cy}, \text{Pr}^i$) have been prepared analogously from the lithium amidinate salts and FeCl_2 . The coordination geometry around Fe is distorted tetrahedral (Scheme 137).

Both Fe(II) amidinates depicted in Scheme 137 react readily with CO to give the new diamagnetic Fe(II) dicarbonyls $[\text{Bu}^t\text{C(NR)}_2]_2\text{Fe(CO)}_2$ (Scheme 138). The compound with $\text{R} = \text{Pr}^i$ was structurally characterized, which showed it to have a strongly distorted octahedral structure with the carbonyls in a *cis* arrangement.²⁴⁰

The mono(amidinato) iron(II) complex $[\text{PhC(NAr)}_2]\text{Fe}(\mu\text{-Cl})\text{Li}(\text{THF})_3$ ($\text{Ar} = \text{C}_6\text{H}_3\text{Pr}^i\text{-2,6}$) was prepared and found to undergo ligand redistribution in noncoordinating solvents to give the homoleptic $[\text{PhC(NAr)}_2]_2\text{Fe}$ as the only isolable product. Reactions of $[\text{PhC(NAr)}_2]\text{Fe}(\mu\text{-Cl})\text{Li}(\text{THF})_3$ with alkylating agents also induced this redistribution, but the presence of pyridine allowed isolation of the four-coordinate $14 e^-$ -monoalkyl complex $[\text{PhC(NAr)}_2]\text{FeCH}_2\text{SiMe}_3(\text{py})$, which was isolated in the form of orange crystals.²⁴¹ The formation of a novel dinuclear iron(II) species with a dianionic $\mu\text{-}\eta^2\text{:}\eta^2$ (biguanidinate) ligand has also been reported. Reaction of the lithium salt of *N,N',N''*-triisopropylguanidinate with Fe(III) or Fe(II) halides led to isolation of the new species $[\text{Pr}^i\text{NHC(NPr}^i)_2]_2\text{FeCl}$ and $[\mu\text{-}\eta^2\text{-Pr}^i\text{NHC(NPr}^i)_2]_2\text{Fe}_2[\text{Pr}^i\text{NHC(NPr}^i)_2]_2$ which was also formed on attempted alkylation of $[\text{Pr}^i\text{NHC(NPr}^i)_2]_2\text{FeCl}$ with a variety of



Scheme 137

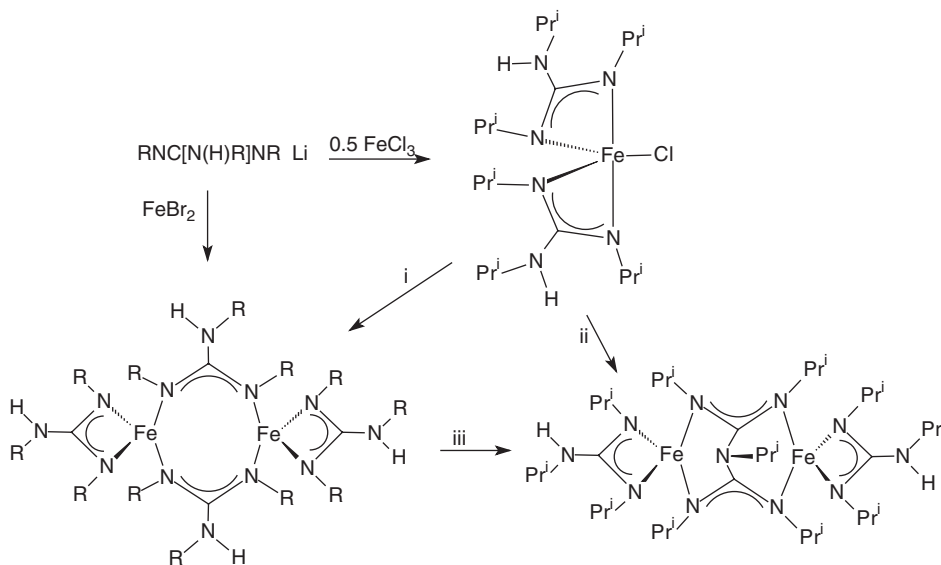


Scheme 138

alkylating reagents (Scheme 139). However, treatment of the dinuclear Fe(II) complex with $\text{LiCH}_2\text{SiMe}_3$ resulted in a coupling reaction between the two bridging ligands to yield $(\mu\text{-}\eta^2\text{:}\eta^2\text{-Pr}^i\text{N}\{\text{C}(\text{NPr}^i)_2\}_2)[\text{Fe}\{\text{Pr}^i\text{NHC}(\text{NPr}^i)_2\}]_2$.^{242,243}

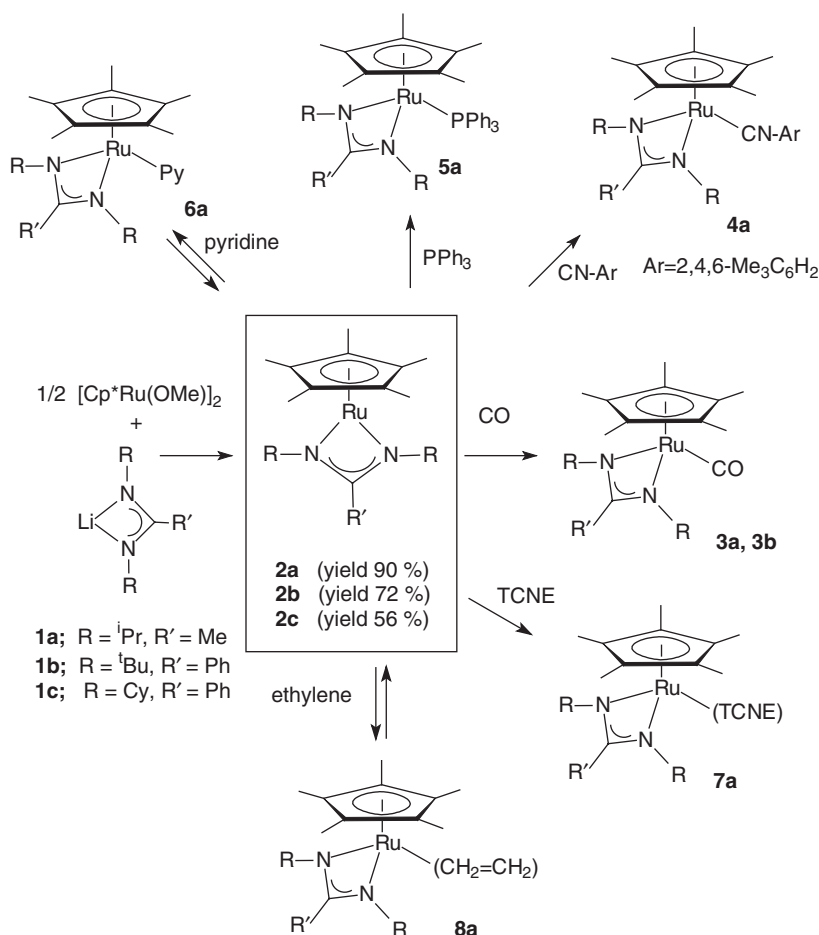
Homoleptic tris(amidinato) complexes of the type $\text{Fe}[\text{HC}(\text{NC}_6\text{H}_4\text{Me-}p)_2]_3$, $\text{Fe}[\text{HC}(\text{NPh})_2]_3$, and $\text{Ru}[\text{HC}(\text{NC}_6\text{H}_4\text{Me-}p)_2]_3$ were prepared from the metal trichlorides using the standard metathetical route and structurally characterized by X-ray diffraction.²²² Treatment of $[\text{Ru}(\eta^6\text{-C}_6\text{H}_6)\text{Cl}_2]_2$ with N,N',N'' -triphenylguanidine also resulted in formation of the tris-chelate $[\text{PhNHC}(\text{NPh})_2]_3\text{Ru}$.¹⁸¹ Insertion reactions of the nonclassical hydrides $[\text{MH}(\eta^2\text{-H}_2)\text{P}_4]^+$ ($\text{M} = \text{Ru}, \text{Os}$; $\text{P} = \text{P}(\text{OEt})_3$, $\text{PPh}(\text{OEt})_2$) with di- p -tolylcarbodiimide, $p\text{-MeC}_6\text{H}_4\text{N}=\text{C}=\text{NC}_6\text{H}_4\text{Me-}p$, afforded the cationic formamidinato complexes $[\{\text{HC}(\text{NC}_6\text{H}_4\text{Me-}p)_2\}\text{MP}_4]^+$, which were isolated as tetraphenylborates. Reactions of these products with CO and p -tolylisocyanide have also been reported.²⁴⁴

The "Chemistry of coordinatively unsaturated organoruthenium amidinates as entry to homogeneous catalysis" was comprehensively reviewed in 2003 by Nagashima et al.²⁴⁵ $\text{Cp}^*\text{Ru}(\text{amidinate})$ complexes (amidinate = $[\text{MeC}(\text{NPr}^i)_2]^-$ and $[\text{PhC}(\text{NBU}^t)_2]^-$), which show signs of coordinative unsaturation, are readily accessible by a standard metathetical route outlined in Scheme 140. Instead of $[\text{CpRu}(\text{OMe})_2]$ the tetrameric chloro complex $[\text{Cp}^*\text{RuCl}]_4$ can also be employed as precursor.^{246,247} The complexes exist as monomers in both solution and solid state and are highly reactive toward two-electron ligands, including pyridine, triphenylphosphine, isonitriles, carbon monoxide, tetracyanoethylene (TCNE), or ethylene (Scheme 140).²⁴⁷



Reagents and conditions: i, MeLi , $\text{LiCH}_2\text{SiMe}_3$, ZnEt_2 , or PhCH_2MgCl ;
ii, $2 \text{ LiCH}_2\text{SiMe}_3$; iii, $\text{LiCH}_2\text{SiMe}_3$.

Scheme 139

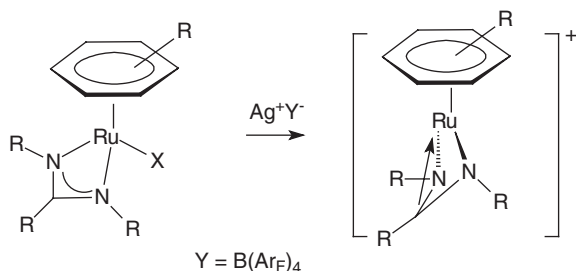


Scheme 140

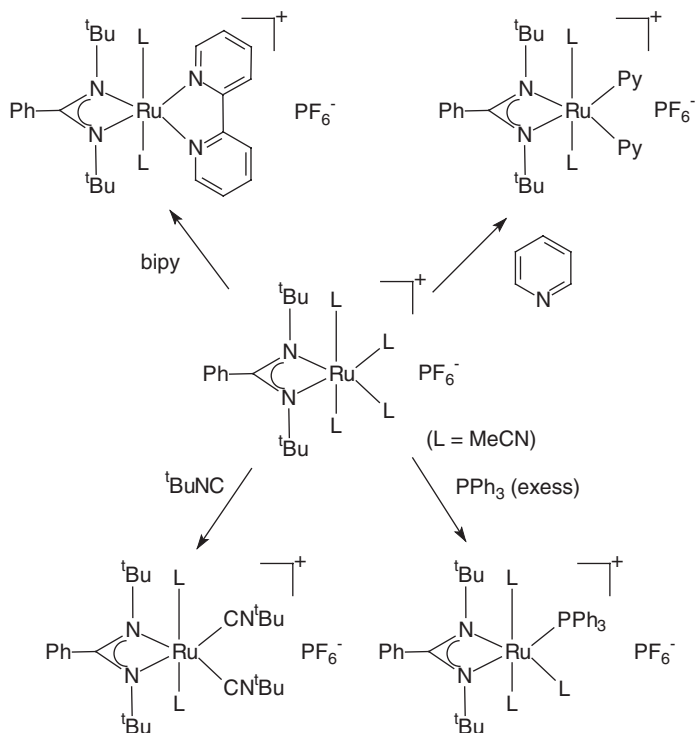
Scheme 141 illustrates the preparation of related cationic π -arene ruthenium amidinates.²⁴⁶

Novel ruthenium–amidinate complexes of the type $(\eta^6\text{-C}_6\text{H}_5\text{R})\text{Ru}(\text{amidinate})\text{X}$ (R = Me, OMe, F; X = Cl, Br, OTf) and $[\text{Ru}(\text{amidinate})(\text{MeCN})_4][\text{PF}_6]$ have been synthesized by photochemical displacement of the benzene ligand in $(\eta^6\text{-C}_6\text{H}_6)\text{Ru}(\text{amidinate})\text{X}$ by substituted arenes or MeCN. The acetonitrile ligands of $[\text{Ru}(\text{amidinate})(\text{MeCN})_4][\text{PF}_6]$ are easily replaceable by other σ -donor ligands (L) such as pyridines, phosphines, and isocyanides to afford the corresponding derivatives $[\text{Ru}(\text{amidinate})(\text{MeCN})_n(\text{L})_{4-n}][\text{PF}_6]$ ($n = 1, 2$). These reactions are summarized in Scheme 142.²⁴⁸

Chlorination of the $\text{Cp}^*\text{Ru}(\text{amidinate})$ complexes is readily achieved by treatment with CHCl_3 , while oxidative addition of allylic halides results in formation of cationic π -allyl ruthenium(IV) species (Scheme 143).^{246,249,250}

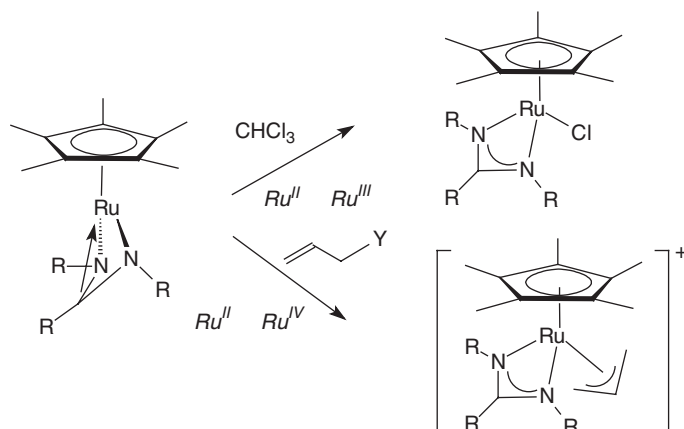
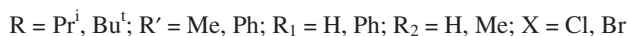
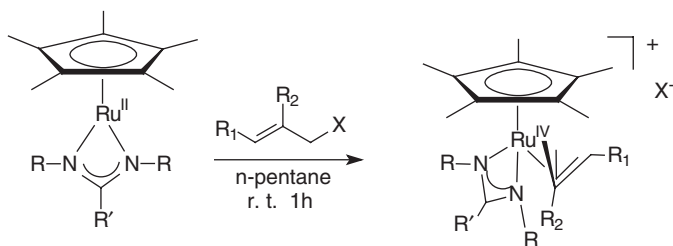
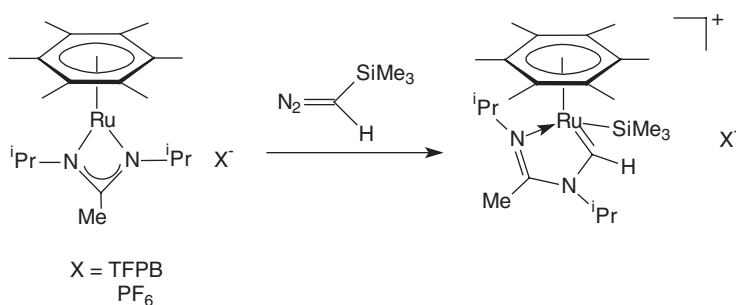


Scheme 141



Scheme 142

The addition of allyl halides can be extended to various substituted derivatives (Scheme 144). The compounds $[\text{Cp}^*\text{Ru}(\eta^3\text{-allyl})(\eta^2\text{-amidinate})]\text{X}$ were isolated by anion exchange of the products ($\text{X} = \text{PF}_6, \text{BF}_4, \text{BPh}_4$). Addition of nucleophiles such as PhLi , dimethyl methylsodiummalonate, and piperidine to the salt-like $\text{Ru}(\text{IV})$ species gave rise to allylation of these nucleophiles and regeneration of $\text{Cp}^*\text{Ru}(\text{amidinate})$.^{246,249,250} A series of organoruthenium amidinates bearing η^4 -diene ligands such as η^4 -cyclooctadiene (COD) or η^4 -norbornadiene (NBD) ligands has been prepared by treatment of either $(\eta^4\text{-COD})\text{Ru}(\text{MeCN})_2\text{Cl}_2$ or $(\eta^4\text{-NBD})\text{Ru}(\text{pyridine})_2\text{Cl}_2$ with the disilver amidinate

**Scheme 143****Scheme 144****Scheme 145**

$\text{Ag}_2[\text{HC}(\text{NPh})_2]_2$. Alternatively the lithium amidinate $\text{Li}[\text{MeC}(\text{NPr}^i)_2]$ can be employed as starting material.²⁵¹

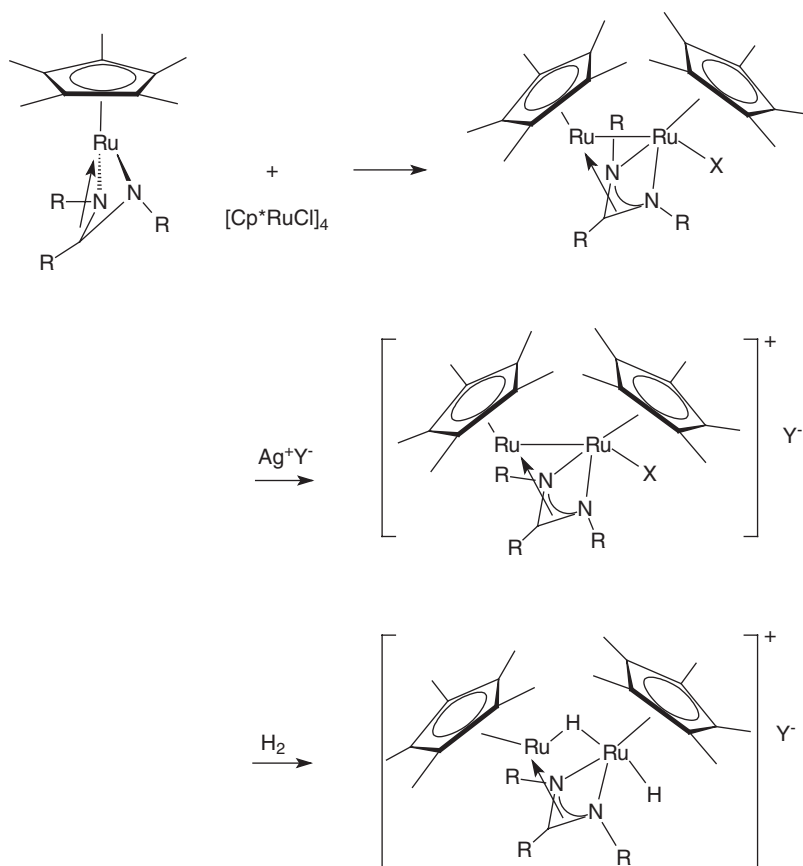
An unprecedented carbene insertion reaction was observed on reaction of the cationic π-arene ruthenium amidinates with trimethylsilyldiazomethane (Scheme 145, TFPB = tetrakis[3,5-bis(trifluoromethyl)phenyl]borate).

The resulting complexes comprise a novel amidinato-carbene ligand as well as a Ru–Si bond.^{246,252}

The reaction of the coordinatively unsaturated ruthenium amidinates with $[\text{Cp}^*\text{RuCl}]_4$ tetramer or $[\text{CpRu}(\text{MeCN})_3]\text{PF}_6$ provides access to novel amidinate-bridged dinuclear ruthenium complexes (Scheme 146), which in turn can be transformed into cationic complexes or hydride derivatives. In these complexes, a bridging amidinate ligand perpendicular to the metal–metal axis effectively stabilizes the highly reactive cationic diruthenium species.^{246,253–255}

Related organoruthenium amidinates bearing a Ru–C σ -bond were prepared by treating the halogenoruthenium amidinate precursor $(\eta^6\text{-C}_6\text{H}_6)\text{Ru}[\text{PhC}(\text{N}^t\text{Bu})_2]\text{Cl}$ with Grignard reagents to form the thermally and air-stable alkyl ruthenium complexes $(\eta^6\text{-C}_6\text{H}_6)\text{Ru}[\text{PhC}(\text{N}^t\text{Bu})_2]\text{R}$ ($\text{R} = \text{Me}, \text{Et}, \text{CH}_2\text{Ph}$). C_s -symmetric “piano stool” structures of these complexes were confirmed by NMR data and crystallographic studies.²⁵⁶

N,N',N'' -triphenylguanidine reacts with $\text{Ru}(\text{O}_2\text{CCF}_3)_2(\text{CO})(\text{PPh}_3)_2$ in boiling toluene to yield the lemon-yellow bis(guanidinate) complex



Scheme 146

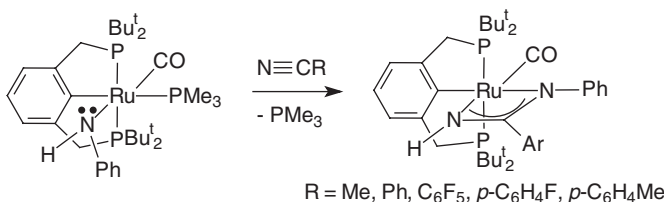
$[\text{PhNHC}(\text{NPh})_2]_2\text{Ru}(\text{CO})(\text{PPh}_3)$.²⁵⁷ The Ru(II) amido complex $(\text{PCP})\text{Ru}(\text{CO})(\text{PMe}_3)(\text{NHPh})$ ($\text{PCP} = \text{C}_6\text{H}_3(\text{CH}_2\text{P}^t\text{Bu}_2)_2$ -2,6) reacts with nitriles under formation of amidinate complexes (48–52% yield) as shown in Scheme 147.^{258,259}

In refluxing toluene, N,N',N'' -triphenylguanidine reacts with $\text{RuH}_2(\text{CO})(\text{PPh}_3)_3$ and with $\text{OsH}_2(\text{CO})(\text{PPh}_3)_3$ in refluxing *o*-xylene to yield the guanidinate complexes $[\text{PhNHC}(\text{NPh})_2]\text{RuH}(\text{CO})(\text{PPh}_3)_2$ and $[\text{PhNHC}(\text{NPh})_2]\text{Os}(\text{CO})(\text{PPh}_3)_2$, respectively. The reaction of N,N',N'' -triphenylguanidine with $\text{RuCl}_3(\text{PPh}_3)_3$ in refluxing toluene provided a new route to the known complex $[\text{PhNHC}(\text{NPh})_2]_2\text{Ru}(\text{CO})(\text{PPh}_3)$.^{260,261} Another series of ruthenium(II) amidinato complexes has been obtained from reactions of N,N' -diphenylamidines $\text{PhC}(\text{R})\text{NHPh}$ ($\text{R} = \text{H}, \text{Me}, \text{Et}, \text{Ph}$) with $[\text{RuCl}_2(\text{C}_7\text{H}_8)]_n$, $[\text{RuCl}_2(\text{CO})_2]_n$, and $\text{RuCl}_2(\text{Me}_2\text{SO})_4$ in the presence of a base (NEt_3 or Na_2CO_3).²⁶²

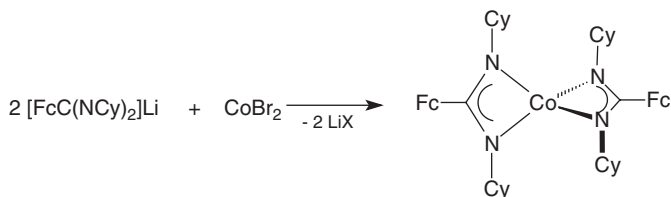
4. Group 9 metal complexes

A reaction of CoCl_2 with 2 equivalents of the lithium ferrocenyl amidinate $\text{FcC}(\text{NCy})_2\text{Li}(\text{Et}_2\text{O})$ in THF gave the trimetallic complex $[\text{FcC}(\text{NCy})_2]_2\text{Co}$ (Scheme 148, Figure 26) in good yield.^{63,67}

A related bis(amidinato) cobalt(II) complex was also prepared using a bulky terphenyl-substituted amidinate ligand (cf. Scheme 7);⁵⁰ and the monomeric cobalt bis(amidinate) $\text{Co}[\text{Bu}^t\text{C}(\text{NAr})(\text{NHAr})]$ ($\text{Ar} = 2,6\text{-Pr}_i^2\text{C}_6\text{H}_3$) was prepared analogously.⁴⁶ The homoleptic tris(amidinato) complex $[\text{HC}(\text{NC}_6\text{H}_4\text{Me-}p)_2]_3\text{Co}$ was obtained by treatment of CoCl_2 with $\text{Li}[\text{HC}(\text{NC}_6\text{H}_4\text{Me-}p)_2]$ and structurally characterized by X-ray diffraction.²²² Rhodium amidinate and guanidinate complexes are rare. The synthesis of a unique N,S -bonded N,N' -bis(*tert*-butylbutanesulfinyl)amidinate rhodium(I) complex has been reported (Scheme 149). The compound was isolated as a fluorescent orange powder.²⁶³



Scheme 147



Scheme 148

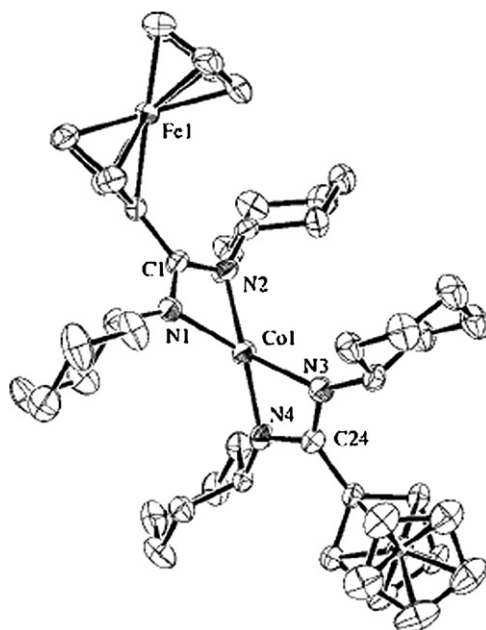
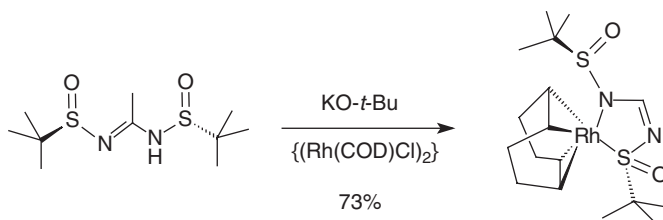


Figure 26 Molecular structure of $[\text{FcC}(\text{NCy})_2]_2\text{Co}$.⁶⁷

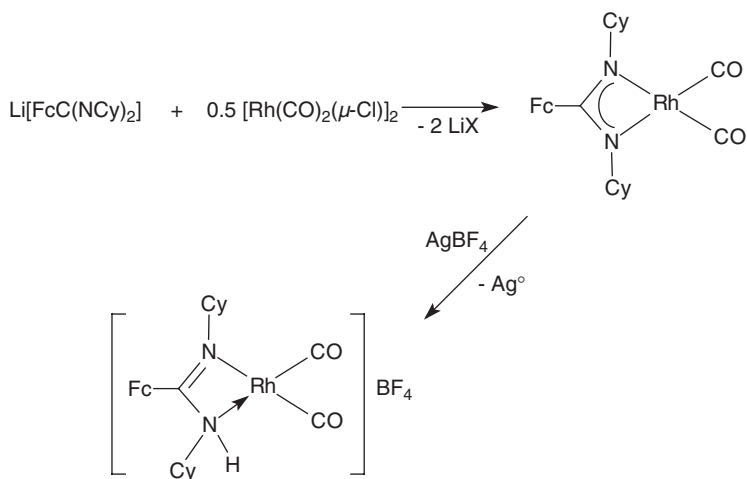


Scheme 149

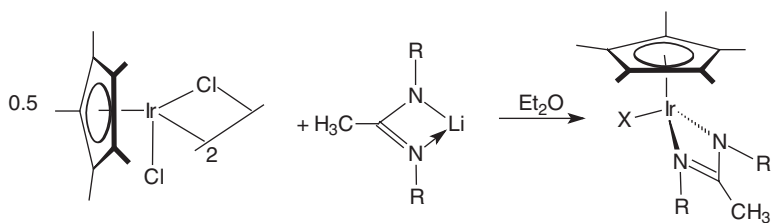
Reaction of $\text{Li}[\text{FcC}(\text{NCy})_2]$ with 0.5 equivalents of $[\text{Rh}(\text{CO})_2(\mu\text{-Cl})_2]$ formed orange $[\text{FcC}(\text{NCy})_2]\text{Rh}(\text{CO})_2$ in good yield. Chemical oxidation of $[\text{FcC}(\text{NCy})_2]\text{Rh}(\text{CO})_2$ with AgBF_4 generated the amidine-containing product $[\{\text{FcC}(\text{NCy})\text{NHCy}\}\text{Rh}(\text{CO})_2][\text{BF}_4]$ (Scheme 150).⁶³

Reaction of $[\text{Cp}^*\text{IrCl}_2]_2$ with lithium amidinates provided an entry into a series of $\text{Cp}^*\text{Ir}[\text{MeC}(\text{NR})_2]\text{X}$ ($\text{X} = \text{Cl}, \text{Br}$; $\text{R} = \text{Bu}^t, \text{Cy}$) complexes as depicted in Scheme 151. The bromide derivative is formed when lithium amidinates containing LiBr are used as starting materials. All halide derivatives are bright orange, crystalline solids that may be stored in air for several weeks without noticeable decomposition.²⁶⁴

Alkyl or hydride derivatives are formed by addition of a variety of Grignard reagents or sodium isopropoxide to the halide precursors. Cationic complexes may be obtained by the interaction with AgSbF_6 in the presence of an appropriate



Scheme 150

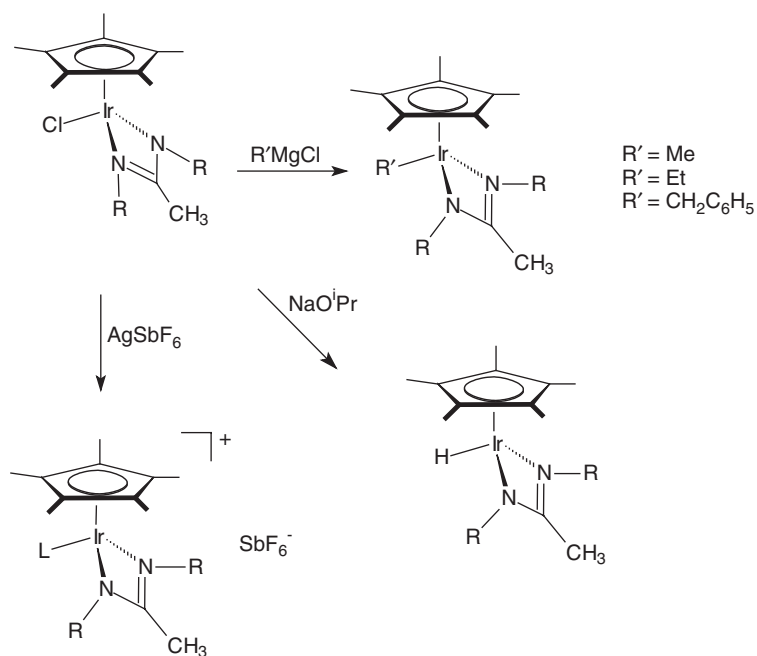


Scheme 151

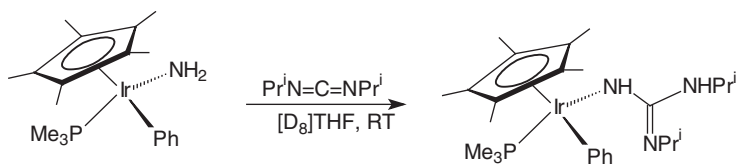
ligand (Scheme 152). In all of these compounds, the amidinate ligand adopts a symmetrical, bidentate coordination geometry.²⁶⁴

Iridium chemistry also holds a rare example of a monodentate guanidinate ligand. The monomeric parent amido complex $\text{Cp}^*\text{Ir}(\text{PMe}_3)(\text{Ph})(\text{NH}_2)$ cleanly undergoes an insertion reaction on treatment with diisopropylcarbodiimide (Scheme 153). Spectroscopic data and an X-ray structural analysis revealed the presence of a nonchelating guanidinate ligand.²⁶⁵

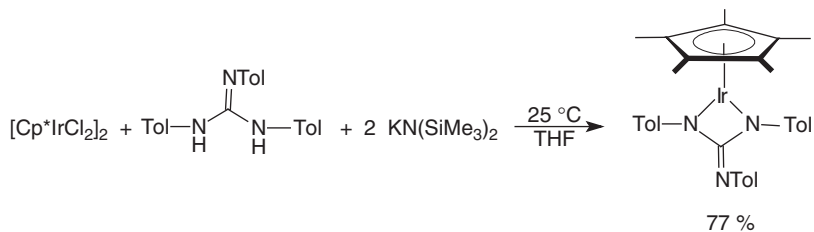
A (pentamethylcyclopentadienyl)iridium chelating guanidinate complex has been conveniently prepared by treatment of $[\text{Cp}^*\text{IrCl}_2]_2$ with *N,N',N''*-tri-*p*-tolylguanidine and base in THF at room temperature followed by recrystallization of the green product from toluene and pentane (Scheme 154). Insertion reactions of the product with heterocumulenes (diaryl carbodiimides, aryl isocyanates) have been investigated. It was found that the complex serves as highly active catalyst for the metathesis of diaryl carbodiimides with each other and for the more difficult metathesis of diaryl carbodiimides with aryl isocyanates (cf. Section V.C).²⁶⁶



Scheme 152



Scheme 153



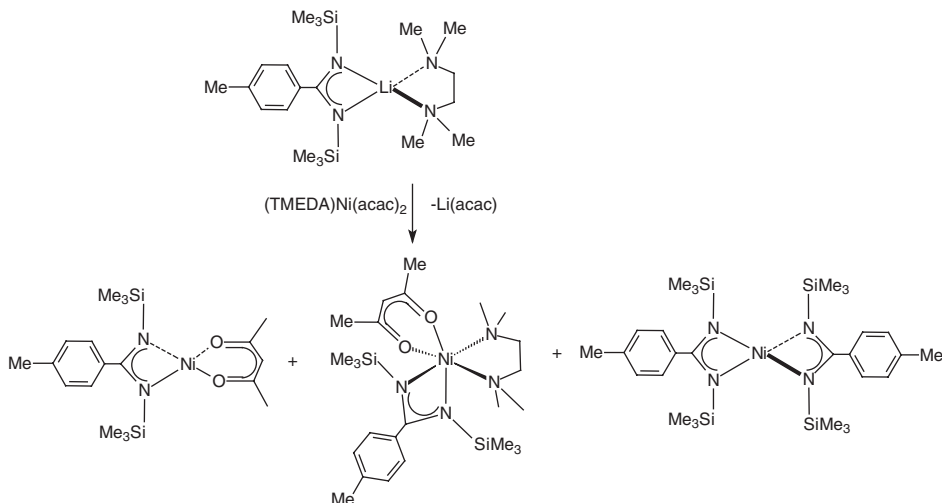
Scheme 154

Treatment of *mer*-IrH₃(PPh₃)₃ with *N,N',N''*-triphenylguanidine in refluxing toluene afforded the iridium(III) dihydride complex [PhNHC(NPh)₂]IrH₂(PPh₃)₂.^{260,261}

5. Group 10 metal complexes

The unsolvated bis(benzamidinates) [PhC(NSiMe₃)₂]₂M (M = Ni, Pd) have been prepared by metathetical routes from NiBr₂(THF)₂ or (MeCN)₂PdCl₂ and [PhC(NSiMe₃)₂]₂Mg(THF)₂ in diethyl ether solution. In the presence of an equimolar amount of water, the same reactions afford [PhC(NSiMe₃)₂][PhC(NSiMe₃)(NHSiMe₃)]MX (M = Ni, X = Br; M = Pd, X = Cl) containing a monodentate amidine ligand.²³⁸ A related bis(amidinato) nickel(II) complex was prepared using a bulky terphenyl-substituted amidinate ligand (cf. Scheme 7),⁵⁰ and the red, monomeric nickel bis(amidinate) Ni[BuⁱC(NAr)(NHAr)](DME) (Ar = 2,6-Prⁱ₂C₆H₃) was made accordingly.⁴⁶ Salt-metathesis routes have also been employed for the synthesis of a series of neutral nickel(II) amidinato complexes such as [PhC(NSiMe₃)₂]Ni(acac), [PhC(NSiMe₃)₂]Ni(acac)(TMEDA), and [PhC(NSiMe₃)₂]₂Ni. In some cases, the reactions produce mixtures of compounds, which can be separated in low yields by continuous fractional crystallizations. Scheme 155 shows such a reaction from which three different products have been successfully isolated and structurally characterized.²⁶⁷

Palladium(II) acetate reacts with *N,N',N''*-triphenylguanidine (= HTpg) in warm benzene to form a bis-adduct which, under more forcing conditions, converts to the novel dinuclear guanidinate-bridged complex [Pd(μ-Tpg)]₂(Tpg)₂.^{257,268} When the same ligand was allowed to react with Pt(PhCN)₂Cl₂, the square-planar bis-chelate complex [PhNHC(NPh)₂]₂Pt was formed.^{181,268} Treatment of Pd(MeCN)₂Cl₂ with HDpyF (HDpyF = bis(2-pyridyl)formamidine) in acetonitrile afforded a yellow product, Pd₂Cl₂(DpyF)₂, which was



Scheme 155

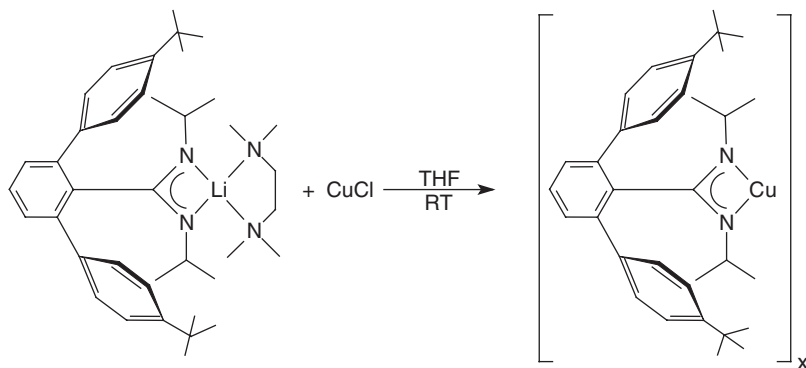
characterized by X-ray crystallography. The DpyF[−] ligand coordinates to the Pd atoms in a new tridentate fashion, forming a chelating and a bridging bonding mode. The molecules are chiral due to the ligand constraints. Spontaneous resolution of the racemic product could be achieved by crystallization of the product from MeCN/diethylether, and a CD spectrum could be obtained.²⁶⁹

6. Group 11 metal complexes

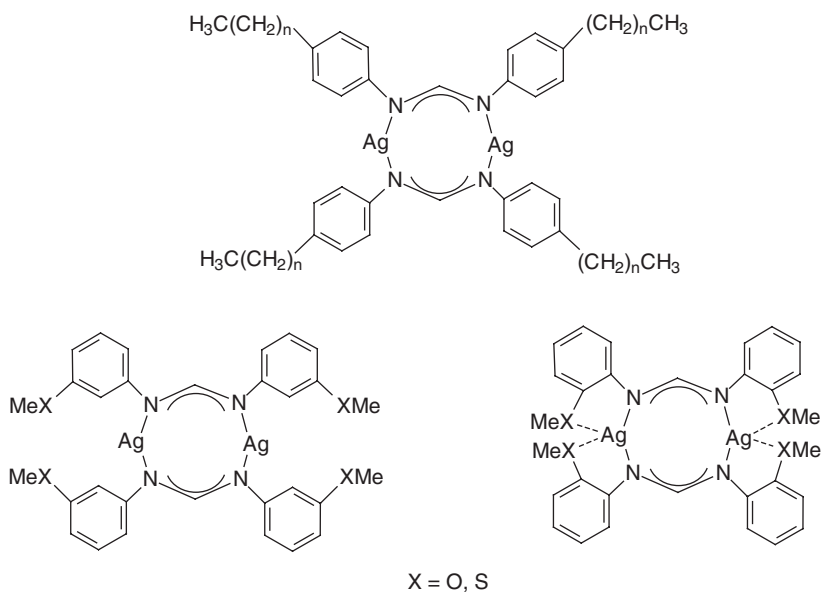
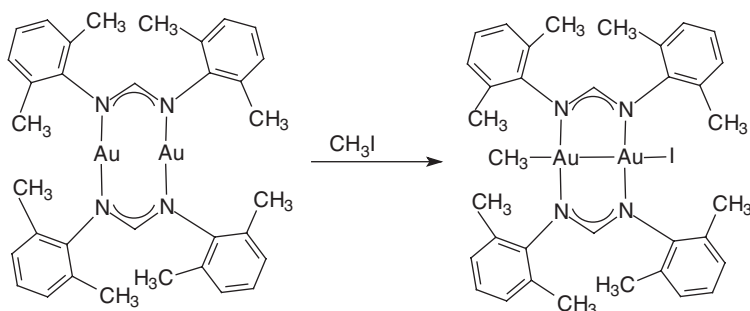
The question of steric bulk of benzamidinate ligands has been addressed using the formation of dimeric and tetrameric copper(I) complexes as a model system.²⁷⁰ The quasitetrahedral compound Cu(PhPyF)₂ (PhPyF = phenylpyridylformamidinate) has been prepared. It involves coordination of the pyridyl N-atoms to give six-membered chelate rings.²⁷¹ A mono(amidinato) copper complex was synthesized according to Scheme 156 by using a bulky terphenyl-derived amidinate ligand. The molecular structure of the product is not yet known, as X-ray quality crystals of this compound proved elusive, but a polymeric or cluster-type arrangement seems likely for this material.⁵⁰

Other amidinate anions normally form dinuclear copper(I) complexes with bridging amidinate ligands, although tetracopper(I) complexes have also been reported.^{272,273} Silver(I) forms dimeric complexes with functionalized *N,N'*-diphenylformamidines (Scheme 157). In the case of donor substituents in the *ortho*-positions these dimers exhibit tetra-coordination at silver with additional longer interactions with the ether oxygens or thioether sulfurs.^{274,275}

Gold in the oxidation state +1 also tends to form dinuclear complexes with bridging amidinate ligands. A typical example is Au₂[HC(NC₆H₃Me₂-2,6)₂]₂ (cf. Section IV.E).^{276,277} Oxidative addition of iodomethane to the dinuclear gold(I) amidinate complex Au₂[HC(NC₆H₃Me₂-2,6)₂]₂ in THF under nitrogen at 0 °C (Scheme 158) and in the absence of light generated a metal–metal bonded Au(II) product, formulated as Au₂[HC(NC₆H₃Me₂-2,6)₂]₂(Me)I, in quantitative yield. The Au–Au distance is 2.711(3) Å, and the N–Au–N angle is 170.2(3)°. ²⁷⁶ Au₂[HC(NC₆H₃Me₂-2,6)₂]₂ reacts with Hg(CN)₂ to give a 2-D coordination polymer.^{277a} Most recently, the oxidative addition of small molecules such as Cl₂, Br₂, I₂, CH₃I, and benzoyl peroxide to Au₂[HC(NC₆H₃Me₂-2,6)₂]₂ has also been



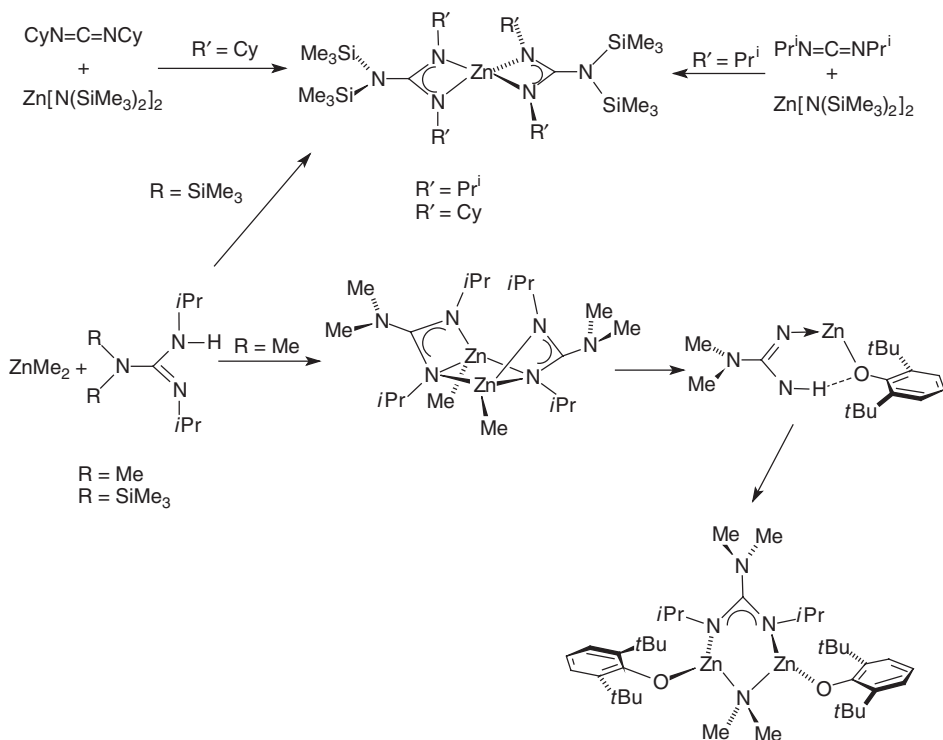
Scheme 156

**Scheme 157****Scheme 158**

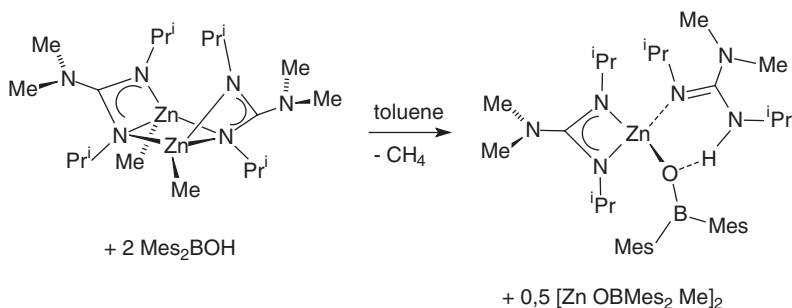
investigated and found to yield again Au(II) metal–metal bonded complexes which are stable as solids at room temperature.^{277b}

7. Group 12 metal complexes

For many years, the Group 12 metals have been largely ignored in amidinate and guanidinate coordination chemistry. Only recently efficient preparative routes to different types of zinc amidinates and guanidinates have been devised. They are mainly based either on the insertion of a carbodiimide into an existing zinc–amide bond or deprotonation of guanidines by dimethylzinc. The reactions and products are illustrated in [Scheme 159](#).^{278a} Related reactions employing



Scheme 159



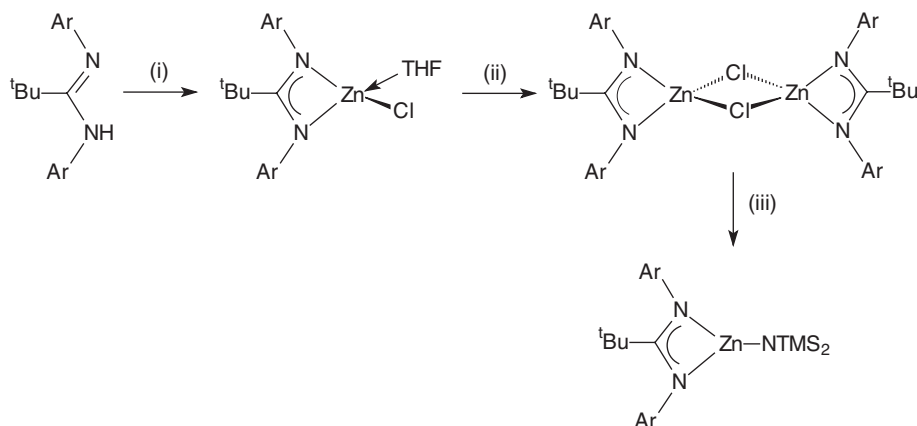
Scheme 160

di(*p*-tolyl)formamidinium led to formation of oxygen-centered tetranuclear cluster compounds resulting from partial oxidation and/or hydrolysis.⁸⁵

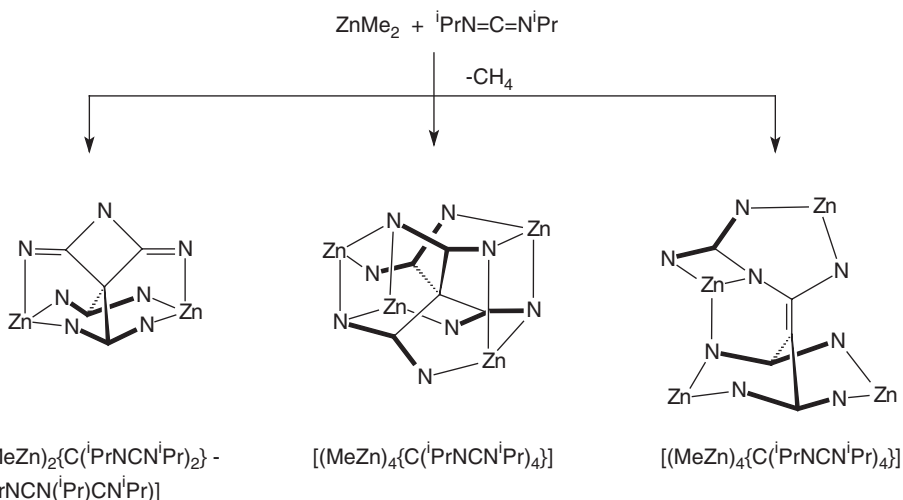
The dimethylzinc route has also been extended to aminopyridinato ligands (cf. Section IV.B).¹⁰⁰ Scheme 160 depicts the reaction of a dimeric zinc guanidinate with dimesityl borinic acid, which leads to formation of a mononuclear complex as a result of protonation at the guanidinate ligand in addition to the Zn–Me bond.^{278b}

Scheme 161 illustrates the synthetic pathway leading to heteroleptic zinc amidinates containing the sterically highly demanding $[\text{Bu}^t\text{C}(\text{NAr})_2]^-$ ligand ($\text{Ar} = \text{C}_6\text{H}_3\text{Pr}_2\text{-2,6}$). Interestingly, this ligand was found to exclusively promote mono-chelation.^{278c}

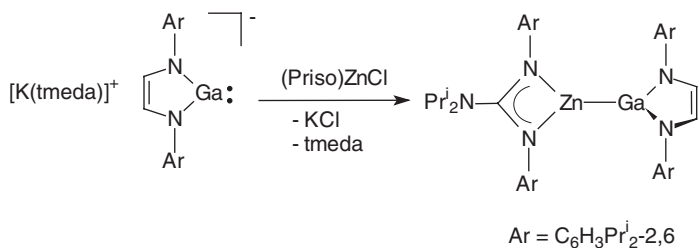
The reaction of diisopropylcarbodiimide with ZnMe_2 (90 °C, 60 h) was recently reported to yield a product mixture, from which three unusual compounds could be isolated and structurally characterized, including two tetranuclear zinc amidinate clusters (**Scheme 162**).^{278d}



Scheme 161



Scheme 162 (Me and Pr^i groups omitted for clarity).

**Scheme 163**

One of the most exciting results in this area was the successful synthesis and characterization of an unprecedented (guanidinato)zinc gallyl complex which enabled the first structural elucidation of an unsupported Zn–Ga bond.²⁷⁹ Scheme 163 illustrates the synthetic routes. The anionic gallium heterocycle employed in this reaction is a valence isoelectronic analog of the well-known NHC class of ligands. The zinc chloride reagent (Priso)ZnCl contains the very bulky guanidinate ligand $[\text{Pr}_2\text{NC}(\text{NAr})_2]^-$ (= Priso, Ar = $\text{C}_6\text{H}_3\text{Pr}_2^{i-2,6}$). The Zn–Ga species was isolated in the form of yellow crystals in 96% yield. Figure 27 illustrates the molecular structure of the (amidinato)zinc gallyl complex as determined by X-ray diffraction. The Ga–Zn bond length is 2.3230(7) Å.²⁷⁹

Reactions of $\text{Cd}(\text{NO}_3)_2 \cdot 4\text{H}_2\text{O}$ with bis(2-pyridyl)formamidine (HDpyF) and bis(6-methyl-2-pyridyl)formamidine (HDMepyF) in methanol afforded the dinuclear products $[\text{Cd}_2(\text{DpyF})_3][\text{Cd}(\text{NO}_3)_4]_{0.5}$ and $[\text{Cd}_2(\text{DMepyF})_3](\text{NO}_3)$, respectively. Both the DpyF^- and DMepyF^- ligands are coordinated to the Cd atoms in new tetradentate fashions, forming two chelating and four bridging bonding modes. Each cadmium metal center of the cations is tris-chelated and strongly distorted from octahedral coordination due to the small bite of the DpyF^- and DMepyF^- ligands.^{280a} Similar preparations have been performed with the potentially polydentate *N,N'*-bis(pyrimidine-2-yl)formamidinate ligand (= pmf[−]). Various salts of Zn(II), Cd(II), and Hg(II) react instantaneously with Kpmf in THF, thereby producing bimetallic complexes of the types $[\text{M}_2(\text{pmf})_3]\text{X}$ (M = Zn, Cd; X = I_3^- , NO_3^- , ClO_4^-) and $\text{Hg}_2(\text{pmf})_3\text{X}_2$ (X = Cl^- , Br^- , I^-) in which new tridentate and tetradentate coordination modes were observed for the pmf[−] ligands.^{280b}

IV. SPECIAL ASPECTS OF AMIDINATE AND GUANIDINATE COORDINATION CHEMISTRY

A. Complexes containing chiral amidinate ligands

The facile insertion of carbodiimides into a Ti–C_{Me} bond of $(\text{C}_5\text{R}_5)\text{TiMe}_3$ (R = H, Me) (cf. Section III.B.2) has been extended to the insertion of optically pure (*R,R*)- and *meso*-(*R,S*)-1.3-bis(1-phenylethyl)carbodiimide.¹⁸⁷ Treatment of $\text{Cp}^*\text{M}(\text{NMe}_2)_3$ (M = Zr, Hf) with both achiral and optically pure aminooxazoline proligands HL yielded metastable aminooxazoline half-sandwich diamide

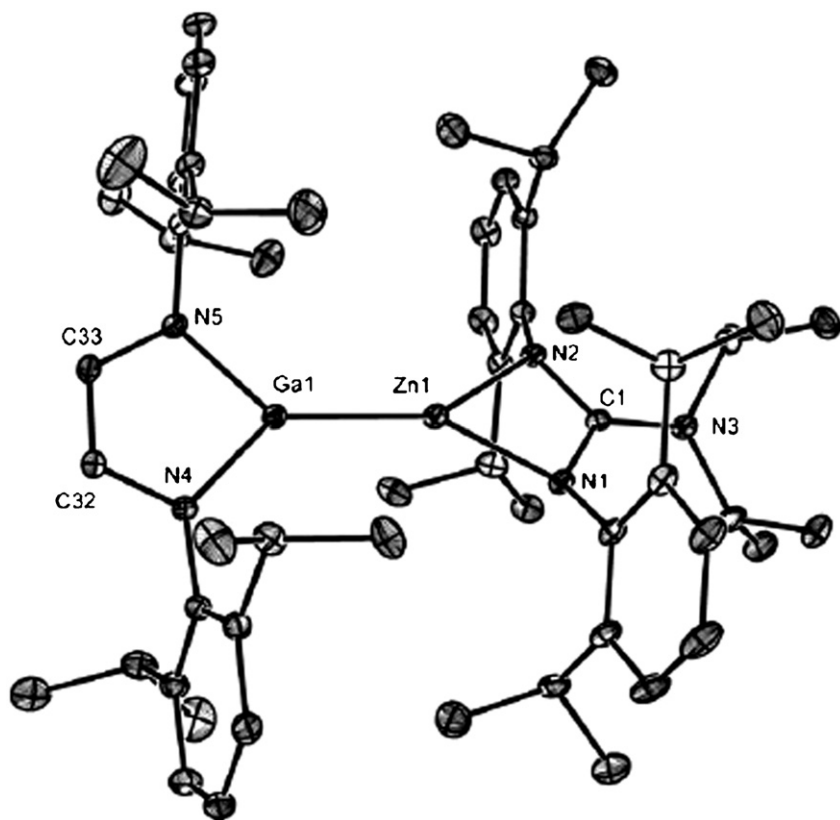


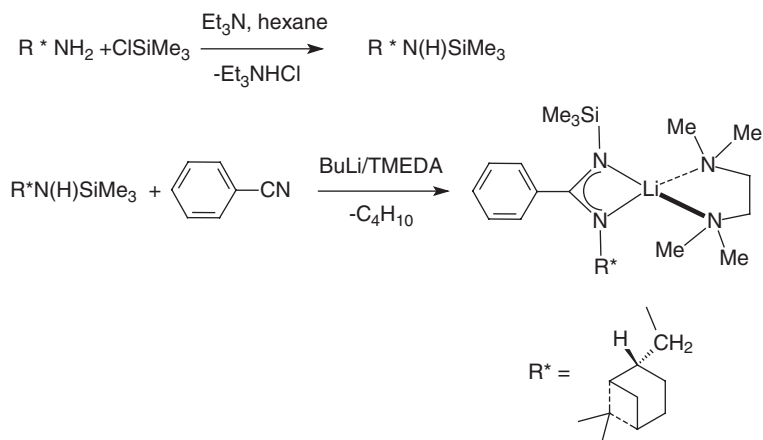
Figure 27 Molecular structure of $[(\text{ArNCH})_2]\text{GaZn}(\text{Priso})$.²⁷⁹

complexes $\text{Cp}^*\text{ML}(\text{NMe}_2)_2$. These species undergo clean rearrangement *via* oxazoline ring-opening to carbodiimides followed by amide migratory insertion. The resulting chiral-at-metal products contain novel tridentate alkoxide-functionalized guanidinate ligands, as confirmed by X-ray diffraction.²⁸¹

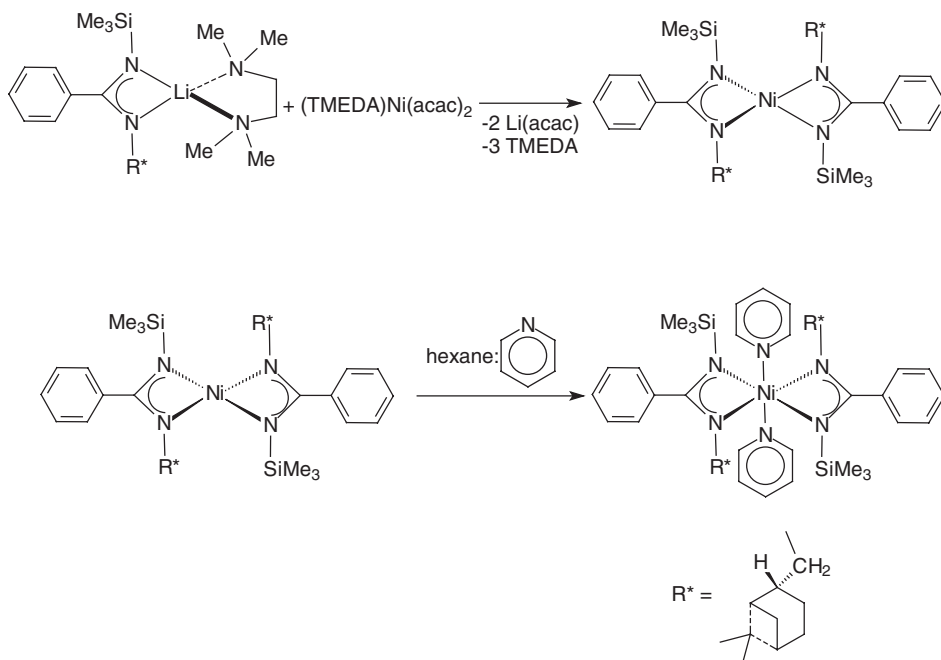
The chiral benzamidinate ligand $[\text{PhC}(\text{NSiMe}_3)(\text{N}'\text{-myrtanyl})]^-$ was obtained according to [Scheme 164](#) from the silylated chiral amine and isolated as the TMEDA-coordinated lithium salt $[\text{Li}(\text{TMEDA})][\text{PhC}(\text{NSiMe}_3)(\text{N}'\text{-myrtanyl})]$.²⁸²

A related nickel complex containing the chiral benzamidinate ligand $[\text{PhC}(\text{NSiMe}_3)(\text{N}'\text{-myrtanyl})]^-$ was prepared and structurally characterized. The first synthetic route is a metathetical reaction between the lithium salt of the ligand and $(\text{TMEDA})\text{Ni}(\text{acac})_2$ according to [Scheme 165](#). The initially formed tetrahedral complex $[\text{PhC}(\text{NSiMe}_3)(\text{N}'\text{-myrtanyl})]_2\text{Ni}$ proved to be difficult to crystallize. Only in the presence of a strongly coordinating polar solvent, pyridine (hexane:pyridine = 1:1), it was possible to obtain the bis(pyridine) solvate in the form of green single crystals in 54% yield ([Scheme 165](#)).²⁸²

The same compound was also obtained from a reaction of $(\text{TMEDA})\text{NiMe}_2$ with the neutral ligand as illustrated in [Scheme 166](#). The initially formed monomethyl complex could not be isolated in a pure state.²⁸²

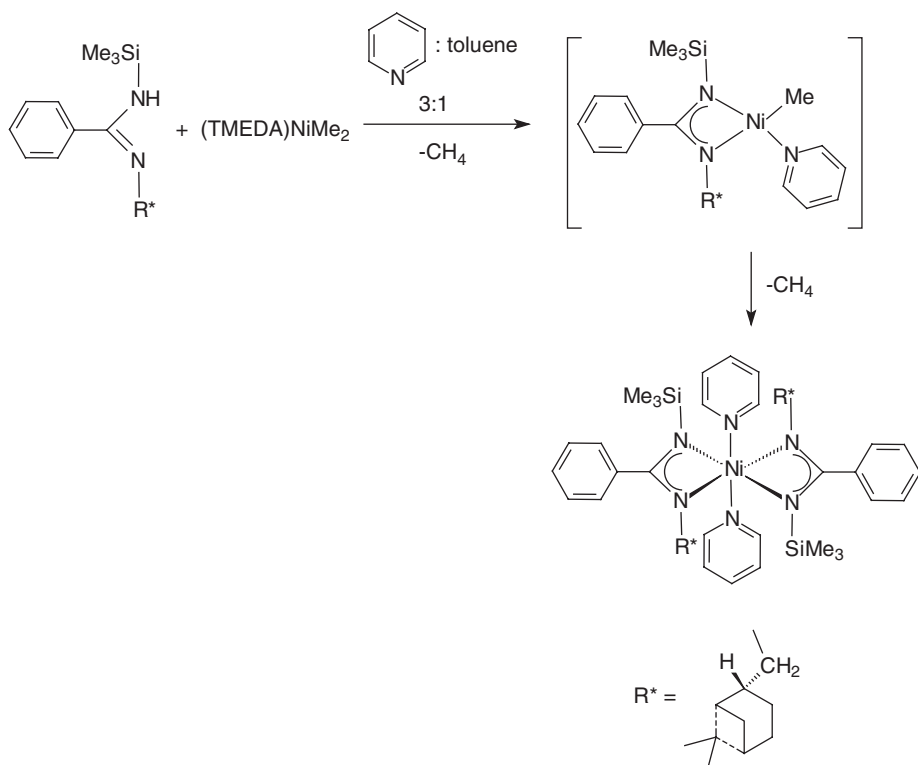


Scheme 164

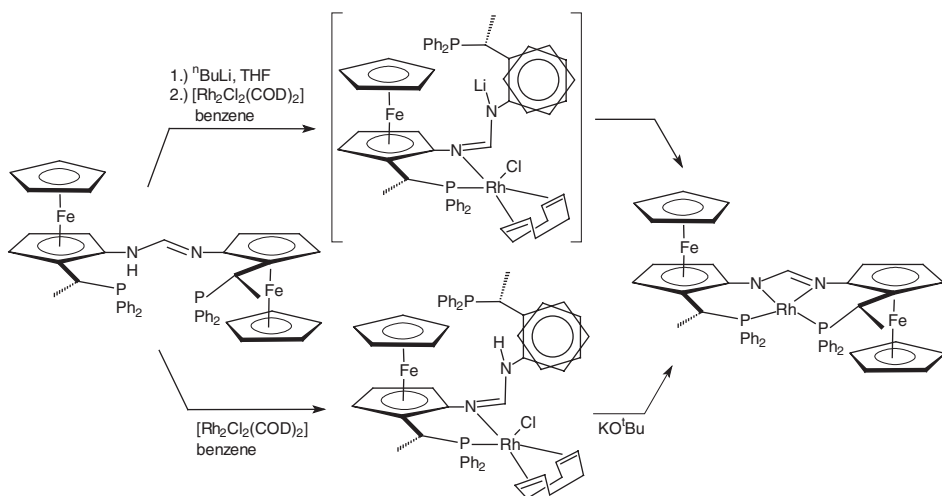


Scheme 165

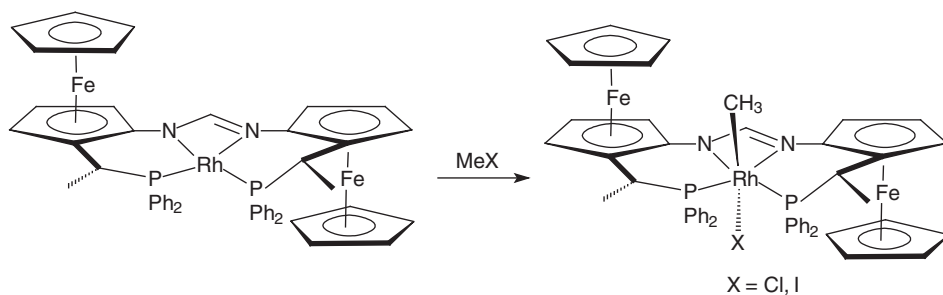
Recently a novel chiral ferrocene-based amidinato ligand and its rhodium complexes have been described. The chiral *N,N'*-bis(ferrocenyl)-substituted formamidine (*N,N'*-bis[(*S*)-2-[(1*R*)-1-(diphenylphosphino)ethyl]ferrocen-1-yl]formamidine) was prepared from commercially available [(1*R*)-1-(dimethylamino)ethyl]ferrocene by a multistep procedure in an overall yield of 29%. Deprotonation of the ligand with *n*-butyllithium followed by addition of $[\text{RhCl}_2(\text{COD})_2]$ as illustrated in [Scheme 167](#) yielded the corresponding (formamidinato)rhodium(I)



Scheme 166



Scheme 167

**Scheme 168**

complex. Direct reaction of the bis(ferrocenyl)-substituted formamidine with $[\text{RhCl}_2(\text{COD})_2]$ led to formation of a chloro-COD intermediate, which could be converted into the chloride-free complex on treatment with a base (e.g., KOBU^t).²⁸³

As shown in [Scheme 168](#), oxidative addition reactions with either methyl chloride or methyl iodide proved successful and yielded the corresponding octahedral rhodium(III) complexes.²⁸³

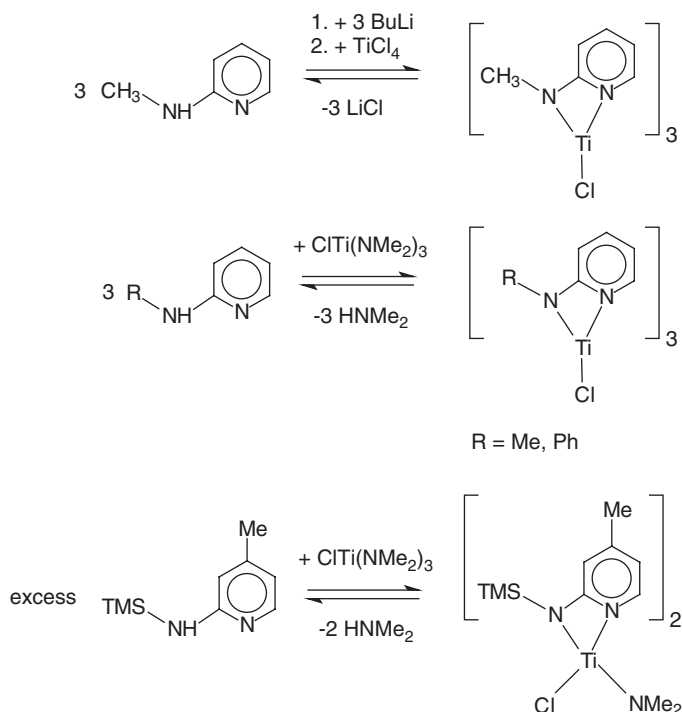
B. Complexes containing cyclic guanidinate ligands

Aminopyridinato ligands form a special class of anionic ligands in which an aromatic ring is part of an amidinate system. These ligands have frequently been employed in early transition metal and lanthanide coordination chemistry. Their diverse and interesting chemistry has been described in detail by Kempe et al.^{60,284} and will thus be covered here only briefly. Typical reaction pathways leading to titanium aminopyridinato complexes are outlined in [Scheme 169](#). Metathetical as well as salt-free routes have been developed.^{284b}

Alkali metal derivatives of 2-(trimethylsilyl)aminopyridines can be further derivatized by insertion of 1,3-dicyclohexylcarbodiimide. Functionalized guanidates are formed in this reaction *via* a 1,3-silyl shift. [Scheme 170](#) illustrates the reaction sequence as well as the preparation of an aluminum complex of the modified ligand, which exhibits *pseudo* β -diketiminato binding of the metal center, thus exemplifying the coordinative versatility of this new multi-*N*-donor system.²⁸⁵

A promising recent extension of the aminopyridinato ligand concept involves the use of potentially tridentate amidinato-cyclopentadienyl ligands. Typical complexes with $\text{M} = \text{Ti}, \text{Zr}$ are depicted in [Scheme 171](#). Other heterocycles can be incorporated in the ligand system instead of the pyridine ring.²⁸⁶

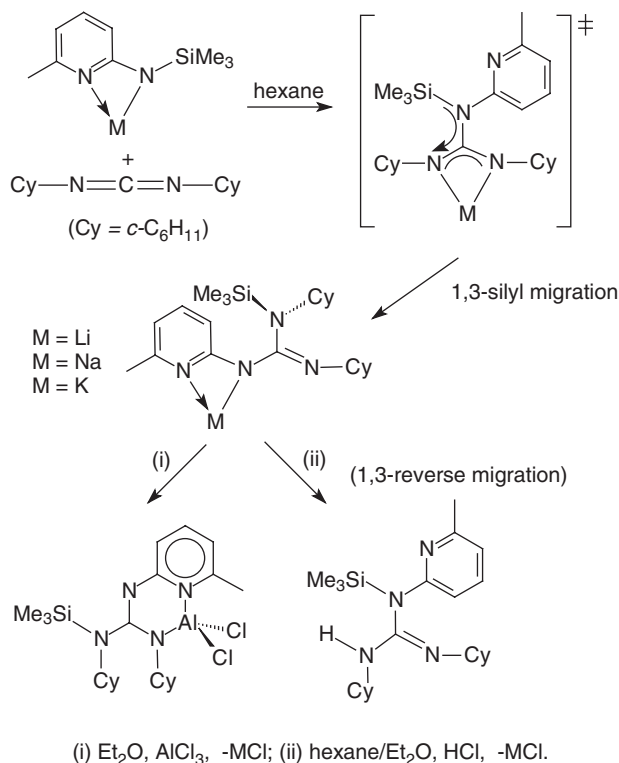
The bicyclic anion 1,3,4,6,7,8-hexahydro-2*H*-pyrimido[1,2-*a*]pyrimidine (= [hpp][−]) has become a popular ligand in both main group and transition metal chemistry. It contains a guanidinate ligand system as part of the bicyclic ring system. The monomeric 1:1 borane adduct $\text{H}_3\text{B} \cdot \text{hppH}$ was synthesized by a reaction of hppH with equimolar quantities of H_3BNMe_3 .²⁸⁷ This compound was used as a precursor to new dinuclear boron(II) compounds featuring a B–B single

**Scheme 169**

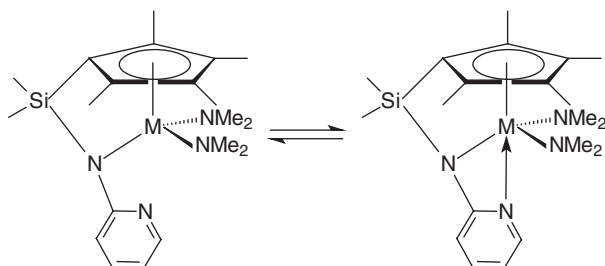
bond. Thus H₂ elimination followed by dimerization of H₃B·hppH led to formation of [(hpp)BH]₂ with two bridging hpp units.²⁸⁷ Scheme 172 highlights the preparation of an Sn(II) complex in which the [hpp][−] anion acts either as a chelating or a bridging ligand.¹³⁵

Synthetic routes to titanium complexes incorporating the bicyclic guanidinate 1,3,4,6,7,8-hexahydro-2*H*-pyrimido[1,2-*a*]pyrimidine (= [hpp][−]) have been described. This report includes the first example of a chelating coordination mode for the [hpp][−] anion and synthesis of the trimetallic complex Me₂Al(hpp)₂TiCl₂(AlMe₃) containing [hpp][−] ligands that chelate to titanium and, in addition, bridge to an AlMe₂ unit *via* nitrogen. The synthetic routes are outlined in Scheme 173.²⁸⁸ The related bis(benzyl) complex (hpp)₂Ti(CH₂Ph)₂ was synthesized from an alkane elimination reaction between the neutral ligand precursor, hppH, and Ti(CH₂Ph)₄. Also reported was the synthesis of the titanium *t*-butylimido complexes [(hpp)Ti(μ-NBu^{*t*})Cl]₂ and [(hpp)Ti(=NBu^{*t*})(μ-hpp)]₂ from the salt-metathesis reaction of 1 and 2 equivalents of (hppLi)_{*n*}, respectively, with Ti(=NBu^{*t*})Cl₂(py)₃.²⁸⁸

Several high oxidation-state complexes of niobium containing the [hpp][−] ligand have been synthesized. The reagents and products, including the seven-coordinate bis-ligand compound Nb(hpp)₂Cl₃, are summarized in Scheme 174. The compounds represent the first examples of guanidinate complexes in which



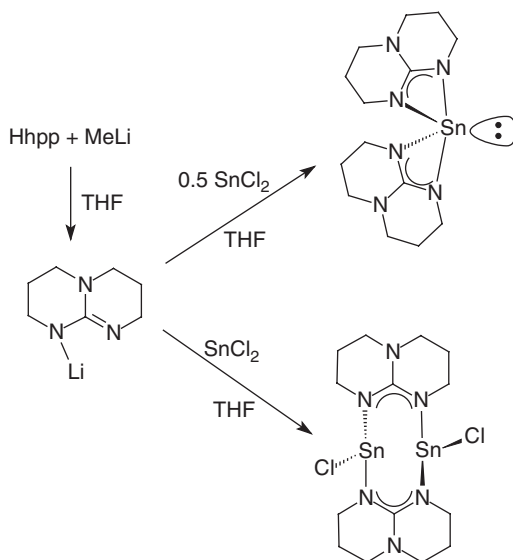
Scheme 170



Scheme 171

niobium is stable in the +5 oxidation state, believed to result from enhanced electron donation caused by the bicyclic framework of the ligand.²⁸⁹

Attempts to prepare related hpp complexes of tantalum were only partially successful. Reaction of 2 equivalents of either (hpp)SiMe₃ or *in situ* generated Li[hpp] with TaCl₅ afforded a solid that analyzed correctly for the compound (hpp)₂TaCl₃. X-ray structural analysis of the crystallized product identified the coordination isomer [Ta(hpp)₄][TaCl₆], with a distorted dodecahedral cation and a regular octahedral anion (Figure 28).²⁹⁰

**Scheme 172**

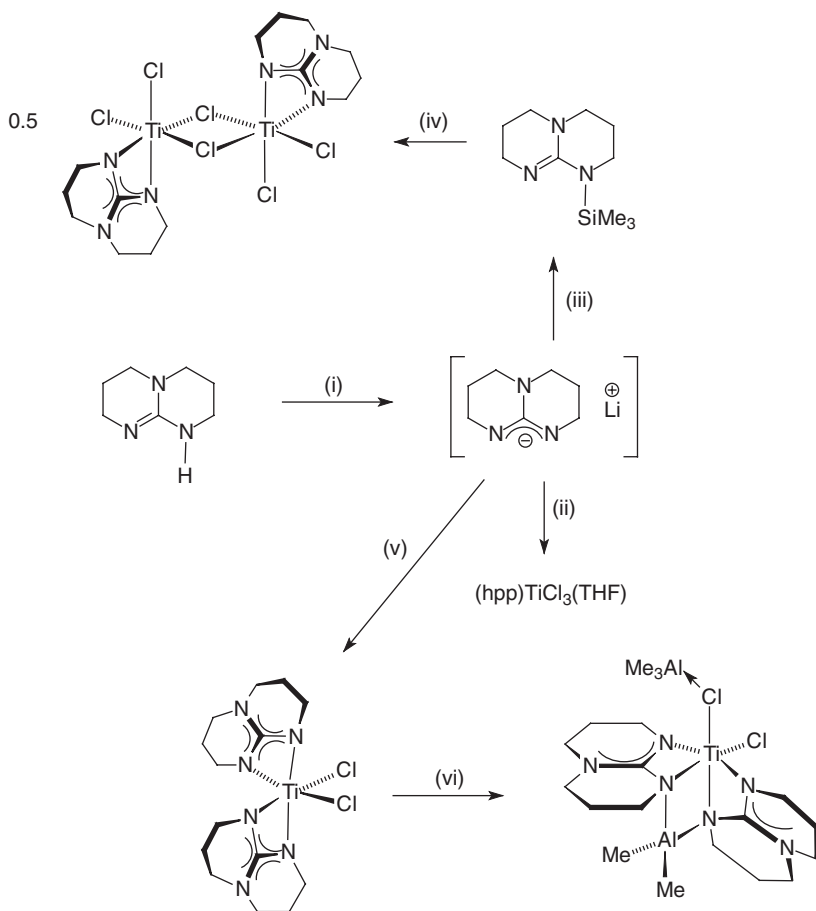
Complexation *via* amidinate units was found in ruthenium complexes containing tri- and pentacyclic trifluoromethylaryl-substituted quinoxalines. The complex fragment $[(\text{tbbpy})_2\text{Ru}]^{2+}$ (tbbpy = bis(4,4'-di-*tert*-butyl-2,2'-bipyridine)) has been employed in these compounds which have all been structurally characterized by X-ray diffraction.²⁹¹

Zinc complexes containing aminopyridinato ligands or a bicyclic guanidinate ligand derived from 1,3,4,6,7,8-hexahydro-2H-pyrimido[1,2-a]pyrimidine (=hppH) were prepared through deprotonation of the free ligands by dimethylzinc.¹⁰⁰ The analogous reaction of this ligand with AlMe₃ generated $[\text{AlMe}_2(\mu\text{-hpp})]_2$.²⁷⁹

C. Complexes containing functionalized amidinate ligands

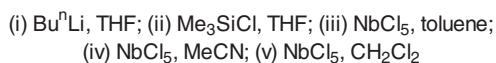
Various amino-functionalized amidinate ligands have been synthesized with the aim of mimicking the well-known pendant-arm half-metallocene catalysts. Lithium derivatives of benzamidinate anions incorporating a pendant amine functional group were prepared according to the reaction sequence shown in Scheme 175. Instead of using Me₃SiCl/NEt₃ in the first step, the starting amine can also be converted into the monosilylated derivative by successive reaction with Bu_nLi followed by treatment with Me₃SiCl. This variant has been employed in the preparation of the trimethylene-bridged homolog.^{292–294}

The lithium derivatives $\text{Li}[\text{Me}_3\text{SiNC}(\text{Ph})\text{N}(\text{CH}_2)_n\text{NMe}_2]$ ($n = 2, 3$) crystallize as dimers with each of the Li atoms bonding to two N atoms of an amidinate fragment in one ligand and to two N atoms of the other ligand in the dimer. The coordination geometry around the Li atoms is distorted tetrahedral (Scheme 176).^{292,294}



Scheme 173 (i) Bu^nLi , 0°C , THF; (ii) $\text{TiCl}_4(\text{THF})_2$, THF; (iii) Me_3SiCl ; (iv) TiCl_4 , CH_2Cl_2 ; (v) $0.5 \text{ TiCl}_4(\text{THF})_2$, THF; (vi) 2 AlMe_3 , toluene.

Reactions of $\text{Li}[\text{Me}_3\text{SiNC}(\text{Ph})\text{N}(\text{CH}_2)_3\text{NMe}_2]$ ($= \text{LiL}$) with MCl_3 in appropriate stoichiometry led to the mononuclear $(\text{L})\text{MCl}_2$ ($\text{M} = \text{Al}, \text{Ga}$) and the dinuclear $[(\text{L})_2\text{M}(\mu\text{-Cl})_2]$ ($\text{M} = \text{La}, \text{Ce}$) complexes.²⁹⁴ The potentially tridentate ligands $[\text{Me}_3\text{SiNC}(\text{Ph})\text{N}(\text{CH}_2)_n\text{NMe}_2]^-$ ($n = 2$; **B**, $n = 3$; **C**) have also been utilized in the synthesis of yttrium alkyl and benzyl complexes. Scheme 177 summarizes the results of this study. While the dialkyl complexes $[\text{Me}_3\text{SiNC}(\text{Ph})\text{N}(\text{CH}_2)_n\text{NMe}_2]\text{Y}[\text{CH}(\text{SiMe}_3)_2]_2$ could be isolated salt-free, attempts to prepare analogous benzyl or trimethylsilylmethyl complexes with ligand **B** yielded the *ate*-complexes $\text{Li}[\text{Me}_3\text{SiNC}(\text{Ph})\text{N}(\text{CH}_2)_2\text{NMe}_2]\text{YR}_2$ ($\text{R} = \text{CH}_2\text{Ph}, \text{CH}_2\text{SiMe}_3$) in which the Li ion is encapsulated by two amidinate and two amine nitrogens. The increased spacer length between the amidinate and amine functionalities in ligand **C** prevented encapsulation of the Li ion, but still produced a bis(amidinate) yttrium benzyl complex, $[\text{Me}_3\text{SiNC}(\text{Ph})\text{N}(\text{CH}_2)_3\text{NMe}_2]_2\text{YCH}_2\text{Ph}$. In this compound only one of the two dimethylamino functionalities is coordinated to the metal center.¹⁴⁵



Scheme 174

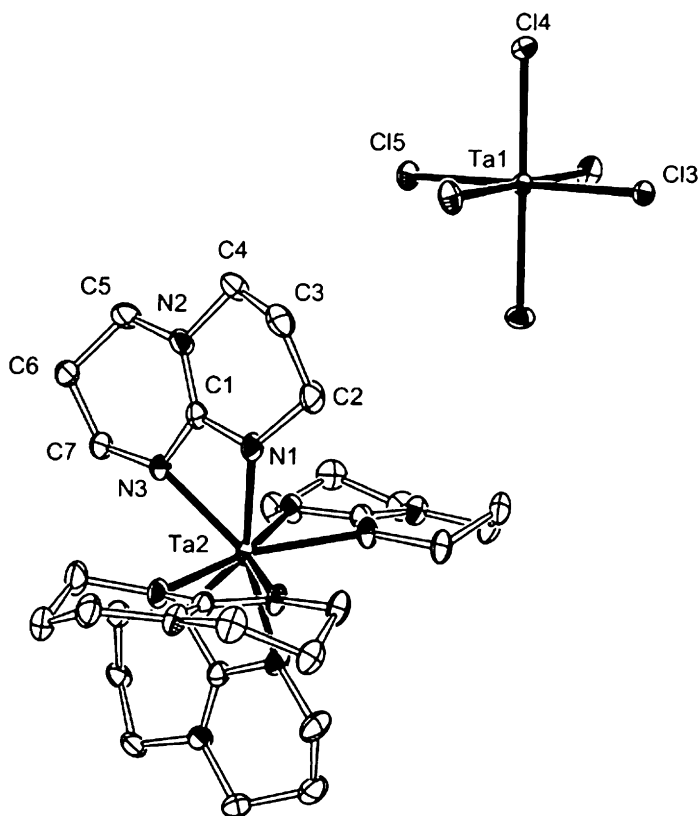
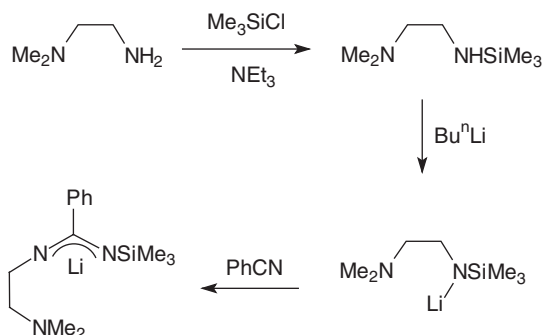
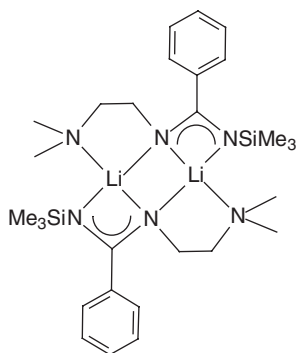


Figure 28 Molecular structure of $[\text{Ta}(\text{hpp})_4][\text{TaCl}_6]$.²⁹⁰



Scheme 175



Scheme 176

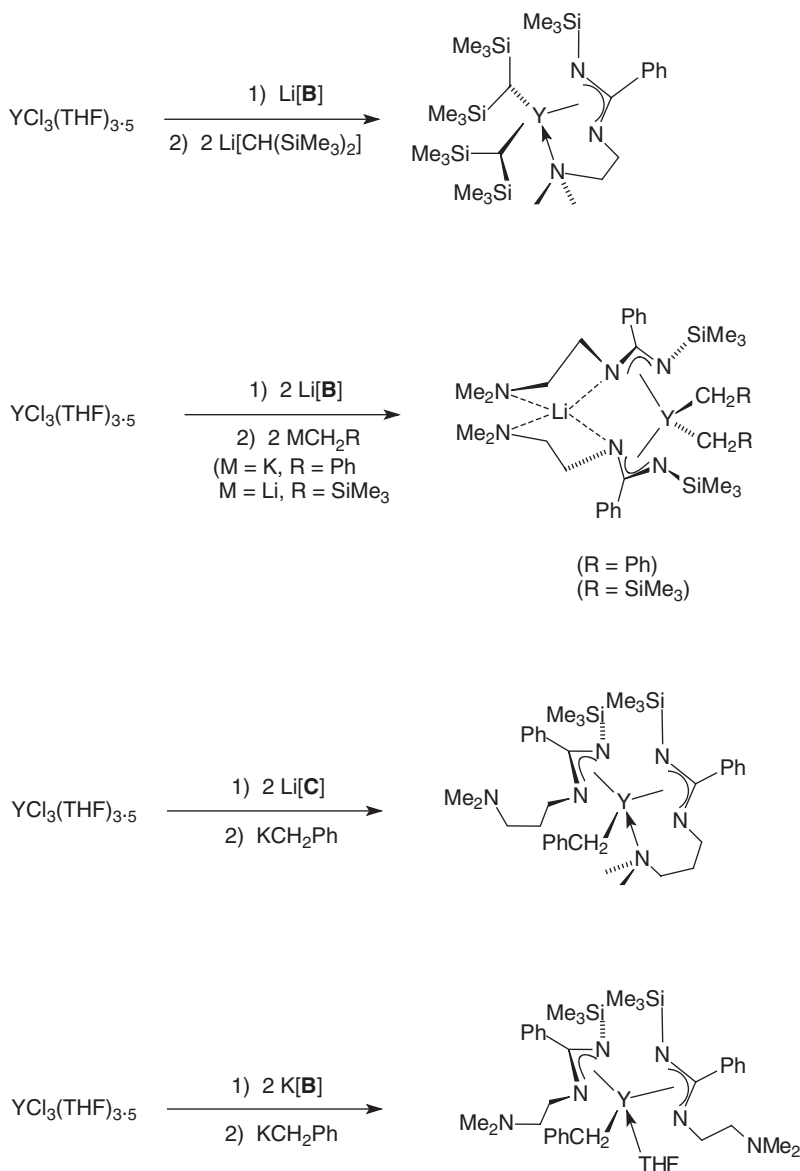
A closely related lithium amidinate with a pendant methyl(trimethylsilyl) amine functionality was prepared by the straightforward route outlined in [Scheme 178](#) (55% yield).²⁹⁵

The lithium derivative was found to react with $\text{TiCl}_4(\text{THF})_2$ to give an orange-red titanium amidinate-amide dichloride complex ([Scheme 179](#)) by elimination of LiCl and Me_3SiCl . The elimination of Me_3SiCl from the corresponding cyclopentadienyl complex $\text{Cp}[\text{Me}_3\text{SiNC}(\text{Ph})\text{N}(\text{CH}_2)_3\text{N}(\text{SiMe}_3)\text{Me}]\text{TiCl}_2$ to give $\text{Cp}[\text{Me}_3\text{SiNC}(\text{Ph})\text{N}(\text{CH}_2)_3\text{NMe}]\text{TiCl}$ is much less favorable, and was found to be readily reversible ([Scheme 179](#)).²⁹⁵

The ligand was shown to stabilize dialkyltitanium complexes of the type $[\text{Me}_3\text{SiNC}(\text{Ph})\text{N}(\text{CH}_2)_3\text{NMe}]\text{Ti}(\text{CH}_2\text{R})_2$ ($\text{R} = \text{Ph}, \text{SiMe}_3$) ([Scheme 180](#)), but these could not be activated for catalytic ethylene polymerization.²⁹⁵

Tridentate amido-amidinate ligands have also been constructed starting from (1*R*,2*R*)-diaminocyclohexane (cf. [Section IV.D](#)). [Scheme 181](#) illustrates the use of such ligand in the preparation of novel amidinato-titanium alkoxide complexes.²⁹⁶

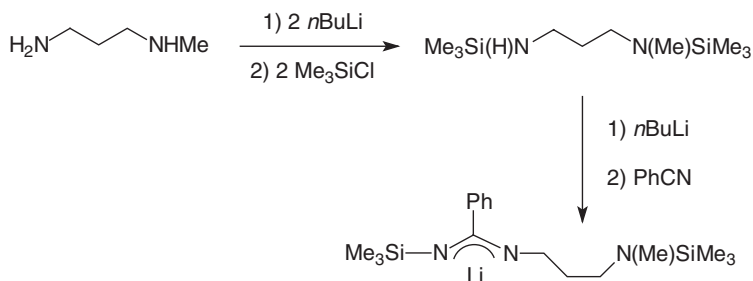
The lithiated amino-benzamidinate $\text{Li}[\text{Me}_3\text{SiNC}(\text{Ph})\text{NCH}_2\text{CH}_2\text{NMe}_2]$ as well as its homolog containing a trimethylene pendant arm have been used to prepare

**Scheme 177**

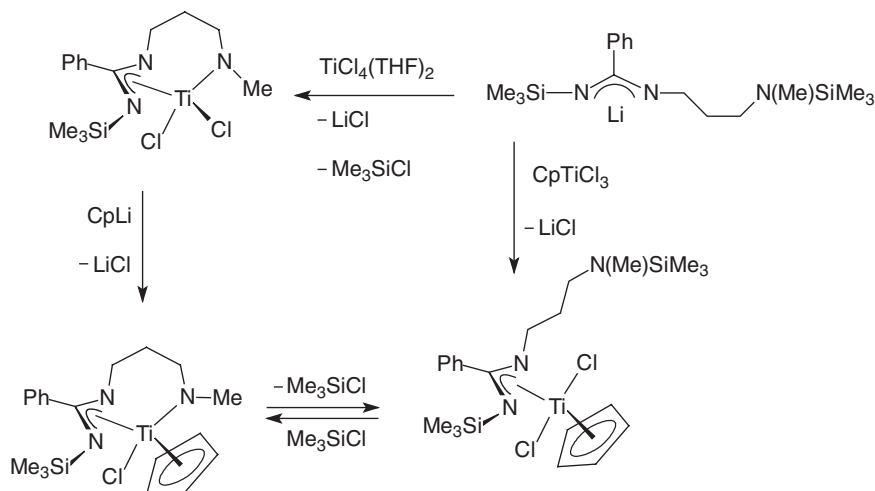
imidotitanium complexes by reaction with $\text{Ti}(=\text{NR})\text{Cl}_2(\text{py})_3$ (R = Bu^t , $\text{C}_6\text{H}_3\text{Me}_2$ -2,6) (Scheme 182).²⁹⁷

The resulting imidotitanium chlorides served as useful starting materials for the synthesis of a series of alkyl, aryl, aryloxo, and amide derivatives. The reagents and products are depicted in Scheme 183.²⁹⁷

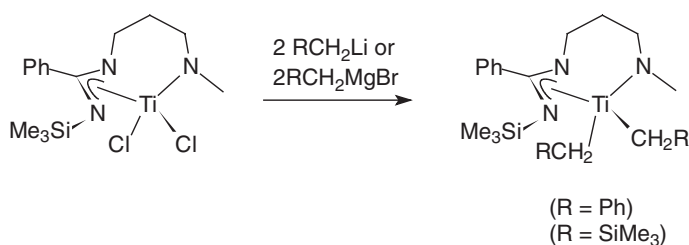
In a related study the synthesis of half-sandwich cyclopentadienyl titanium *t*-butylimido complexes containing pendant-arm-functionalized amidinate ligands



Scheme 178



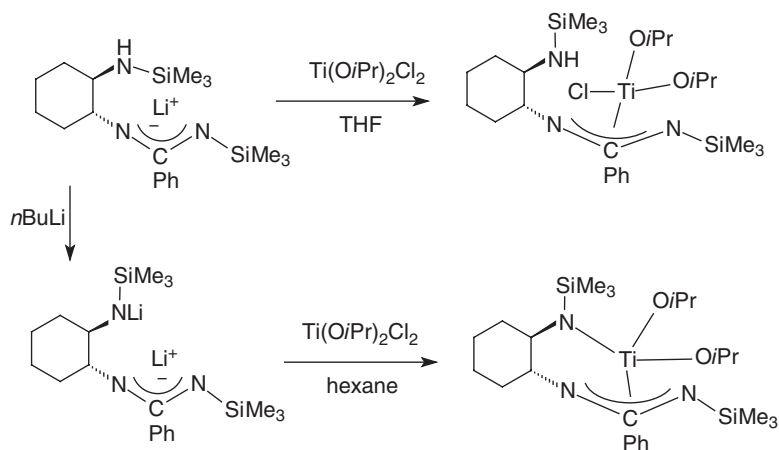
Scheme 179



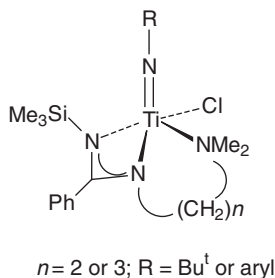
Scheme 180

was reported, together with their reaction with CO_2 . Mechanistic and DFT computational studies have also been described. [Scheme 184](#) summarizes the synthetic procedures leading to such complexes.²⁹⁸

All these complexes react further with CO_2 to form the corresponding *N,O*-bound carbamate complexes, which, in turn, extrude Bu^tNCO (above -25°C for the methylcyclopentadienyl complexes and at room temperature in the case of the



Scheme 181

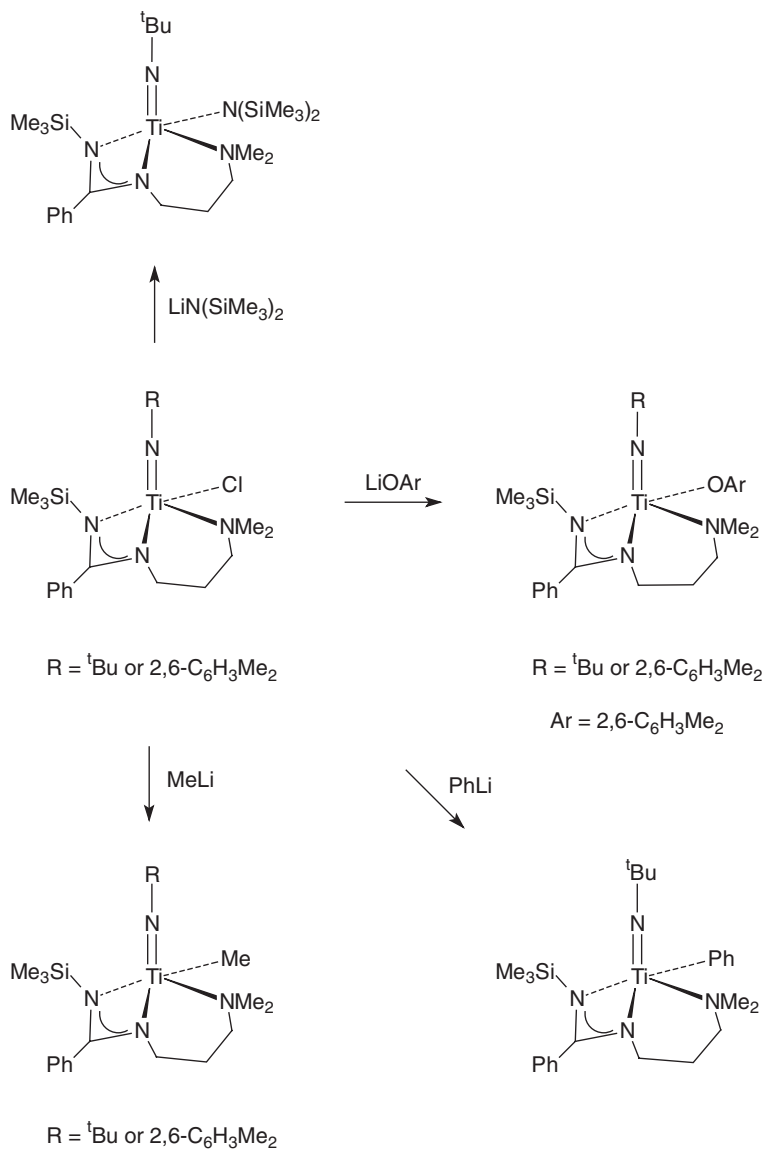


Scheme 182

Cp^* derivatives (Scheme 185) to form μ -oxo-bridged dimeric complexes. The stabilities of the N,O -bound carbamate intermediates depend mainly on the cyclopentadienyl ring substituents, but there is also a small dependence on the nature of the length of the (dimethylamino)alkyl chain for the $\text{C}_5\text{H}_4\text{Me}$ systems.²⁹⁸

The amidinate ligand containing a pendant tertiary amine functionality has also been used to prepare a monomeric vanadium(III) complex. The crystal structure of $[\text{Me}_3\text{SiNC}(\text{Ph})\text{NCH}_2\text{CH}_2\text{NMe}_2]\text{VCl}_2(\text{THF})$ showed that the ligand can adopt a facial geometry, with an unusual distortion of the amidinate nitrogen bearing the pendant functionality (Figure 29). This amidinate nitrogen, N(2), is distinctly nonplanar, the sum of the angles around N(2) being 336.4° as compared to 359.9° for N(1). This is unusual for metal amidinates, and may suggest that the ligand has partial amido-imine character.²⁹³

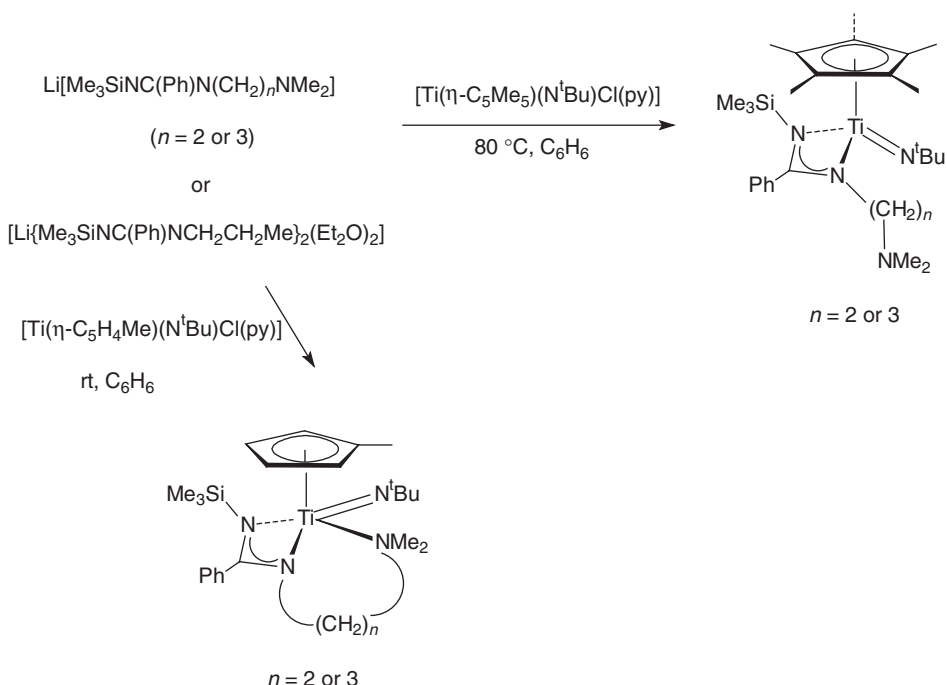
The coordination chemistry of ancillary amidinate ligands with a pyridine functionality has been described. Magnesium, aluminum, zirconium, and lanthanum complexes have been prepared in which the amidinate anions act as tridentate, six-electron-donor ligands.^{299a} Amidinate ligands containing quinolyl substituents were constructed in the coordination sphere of lanthanide

**Scheme 183**

ions as illustrated in [Scheme 186](#). The compounds were obtained *via* double N–H addition of bridging amide functionalities to carbodiimides.^{299b}

A similar approach, i.e., carbodiimide insertion into M–N bonds was used to prepare unusual zirconacarboranes containing guanidinate ligands. In an alternative approach, these compounds were also synthesized by the route outlined in [Scheme 187](#).^{299c}

Very recently, yet another interesting approach to novel-functionalized amidinate ligands has been reported. It involves the combination of amidinate

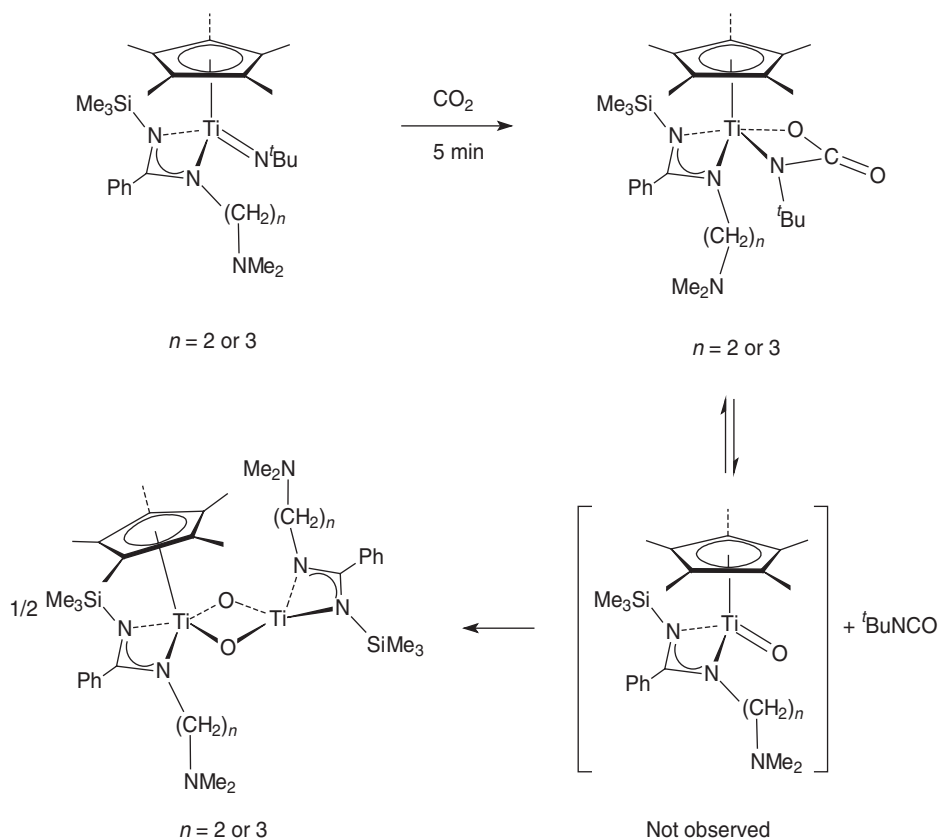
**Scheme 184**

and scorpionate functionalities in one ligand system.^{299d} Lithium salts of the new polyfunctional anionic ligands were prepared by the reaction of bis(3,5-dimethylpyrazol-1-yl)methane with Bu^nLi followed by treatment of the lithiated intermediates with different carbodiimides as outlined in Scheme 188.^{299d}

These lithium derivatives were found to be excellent reagents for the introduction of the new amidinate scorpionate ligands into Group 4 metal complexes, and a series of neutral titanium and zirconium complexes were prepared according to Scheme 189 and fully characterized.^{299d}

D. Complexes containing bis(amidinate) ligands

Oxalamidinate anions represent the most simple type of bis(amidinate) ligands in which two amidinate units are directly connected *via* a central C–C bond. Oxalamidinate complexes of *d*-transition metals have recently received increasing attention for their efficient catalytic activity in olefin polymerization reactions. Almost all the oxalamidinate ligands have been synthesized by deprotonation of the corresponding oxalic amidines [pathway (a) in Scheme 190]. More recently, it was found that carbodiimides, $\text{RN}=\text{C}=\text{NR}$, can be reductively coupled with metallic lithium into the oxalamidinate dianions $[(\text{RN})_2\text{C}=\text{C}(\text{NR})_2]^{2-}$ [route (c)] which are clearly useful for the preparation of dinuclear oxalamidinato complexes. The lithium complex obtained this way from *N,N'*-di(*p*-tolyl)carbodiimide was crystallized from pyridine/pentane and



Scheme 185

structurally characterized by X-ray diffraction. Figure 30 depicts the molecular structure containing a planar C_2N_4 unit.^{300a}

Treatment of UCl_4 with the lithium complex obtained from dicyclohexylcarbodiimide followed by crystallization from pyridine afforded a dinuclear uranium(IV) oxalamidinate complex in the form of dark green crystals in 94% yield (Scheme 191). The same compound could also be obtained by first reducing UCl_4 to LiUCl_4 (or $\text{UCl}_3 + \text{LiCl}$) followed by reductive dimerization of di(cyclohexyl)carbodiimide as shown in Scheme 191. The molecular structure of this first oxalamidinato complex of an actinide element is depicted in Figure 31.^{300a}

The reductive coupling of carbodiimides was also achieved very recently with the use of samarium(II) bis(trimethylsilyl)amides. The reaction of $\text{Sm}[\text{N}(\text{SiMe}_3)_2]_2(\text{THF})_2$ with carbodiimides $\text{RN}=\text{C}=\text{NR}$ ($\text{R} = \text{Cy}$, $\text{C}_6\text{H}_3\text{Pr}_2^{i-2,6}$) led to the formation of dinuclear Sm(III) complexes. For $\text{R} = \text{Cy}$ (Scheme 192), the product has an oxalamidate $[\text{C}_2\text{N}_4\text{Cy}_4]^{2-}$ ligand resulting from coupling at the central C atoms of two $\text{CyN}=\text{C}=\text{NCy}$ moieties. The same product was obtained when the Sm(II) "ate" complex $\text{Na}[\text{Sm}\{\text{N}(\text{SiMe}_3)_2\}_3]$ was used as divalent samarium precursor.^{300b}

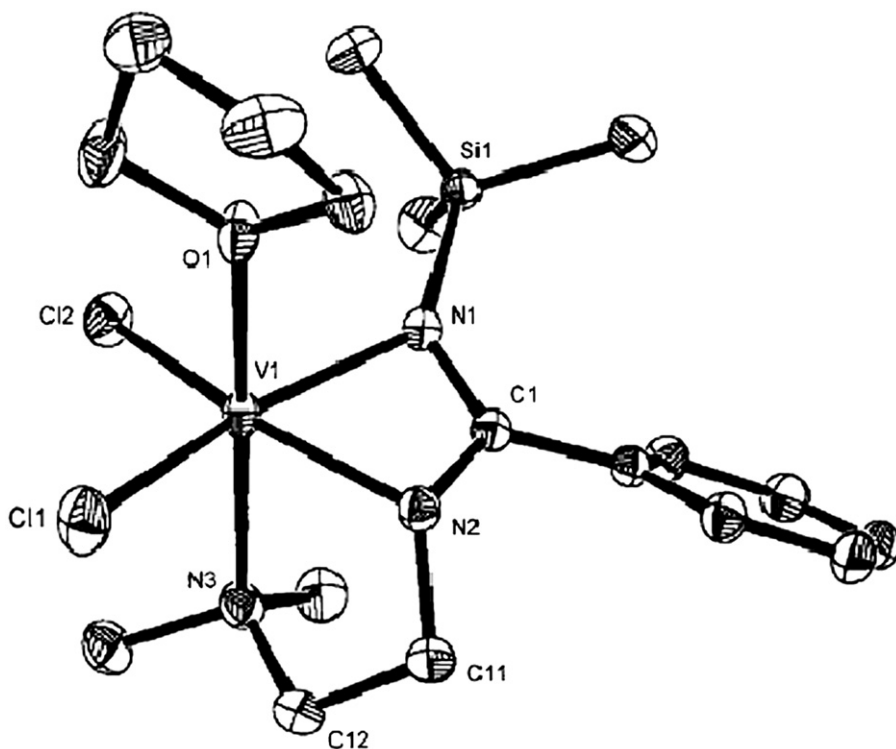
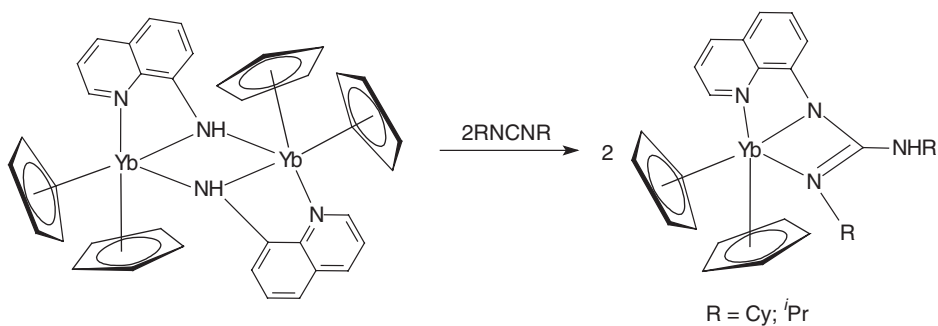


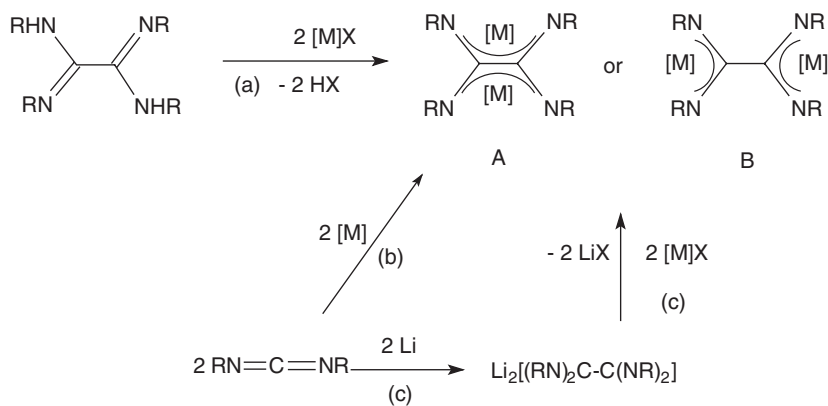
Figure 29 Molecular structure of $[\text{Me}_3\text{SiNC(Ph)NCH}_2\text{CH}_2\text{NMe}_2]\text{VCl}_2(\text{THF})$.²⁹³



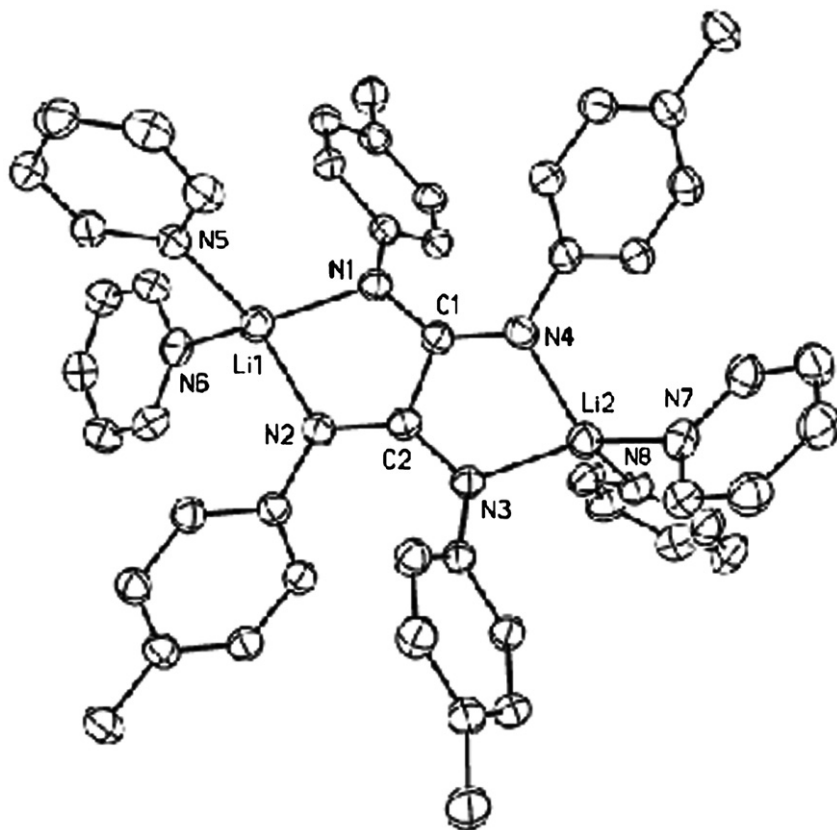
Scheme 186

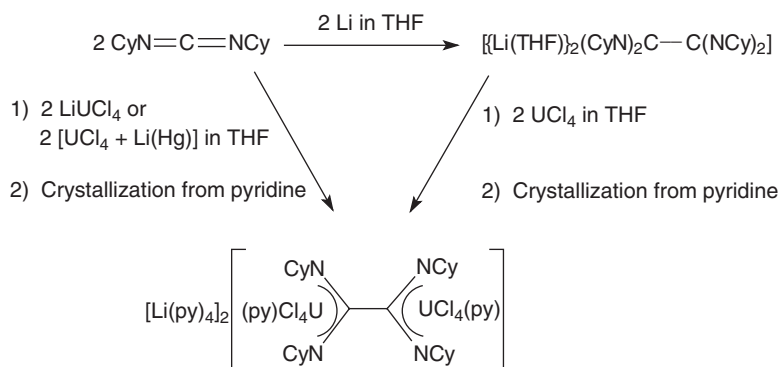
In contrast, for $\text{R} = \text{C}_6\text{H}_3\text{Pr}_2\text{-2,6}$, H transfer and an unusual coupling of two Pr^i methine C atoms resulted in a linked formamidinate complex as illustrated in Scheme 193.^{300b}

In this case the use of the Sm(II) “ate” complex $\text{Na}[\text{Sm}[\text{N}(\text{SiMe}_3)_2]_3]$ as starting material afforded yet another novel C-substituted amidinate complex resulting from γ C–H activation of a $\text{N}(\text{SiMe}_3)_2$ ligand (Scheme 194). All new

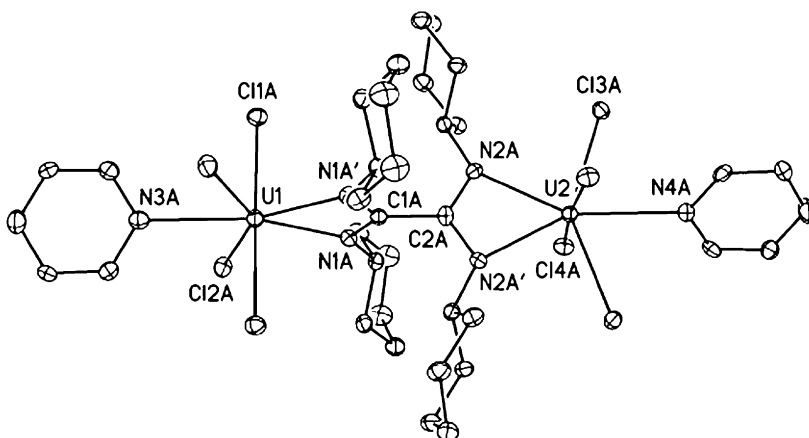


Scheme 190

Figure 30 Molecular structure of $[\mu\text{-C}_2(\text{NTol})_4][\text{Li}(\text{THF})_2]_2$.^{300a}



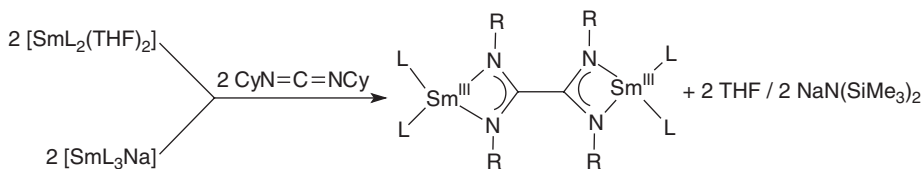
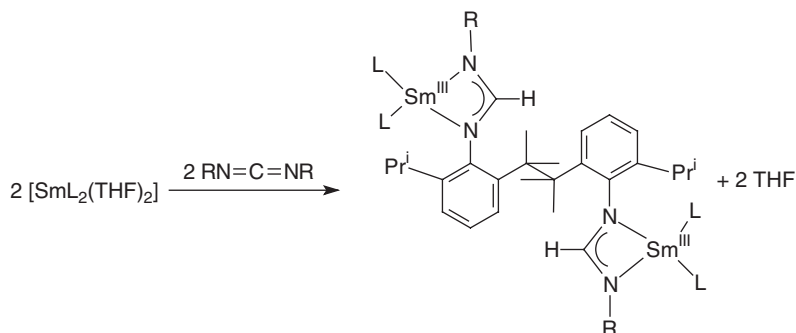
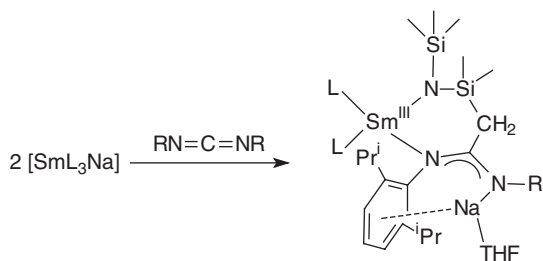
Scheme 191

Figure 31 Molecular structure of $[\mu\text{-C}_2(\text{NCy})_4][\text{UCl}_4(\text{py})]_2$.^{300a}

samarium amidinate complex reported in this paper were structurally characterized by X-ray diffraction.^{300b}

The readily accessible oxalamidine derivative $\text{PhN}=\text{C}(\text{NHBu}^t)\text{C}(\text{NHBu}^t)=\text{NPh}$ provides another useful entry into the coordination chemistry of oxalamidinato ligands. Scheme 195 summarizes the results of an initial study. Mono- and dinuclear complexes of Ti, Zr, and Ta have been isolated and fully characterized. Silylation of both N–H functions was achieved by subsequent treatment with 2 equivalents of *n*-butyllithium and Me_3SiCl . The preparation of a nickel(II) complex failed and gave a hydrobromide salt instead.³⁰¹

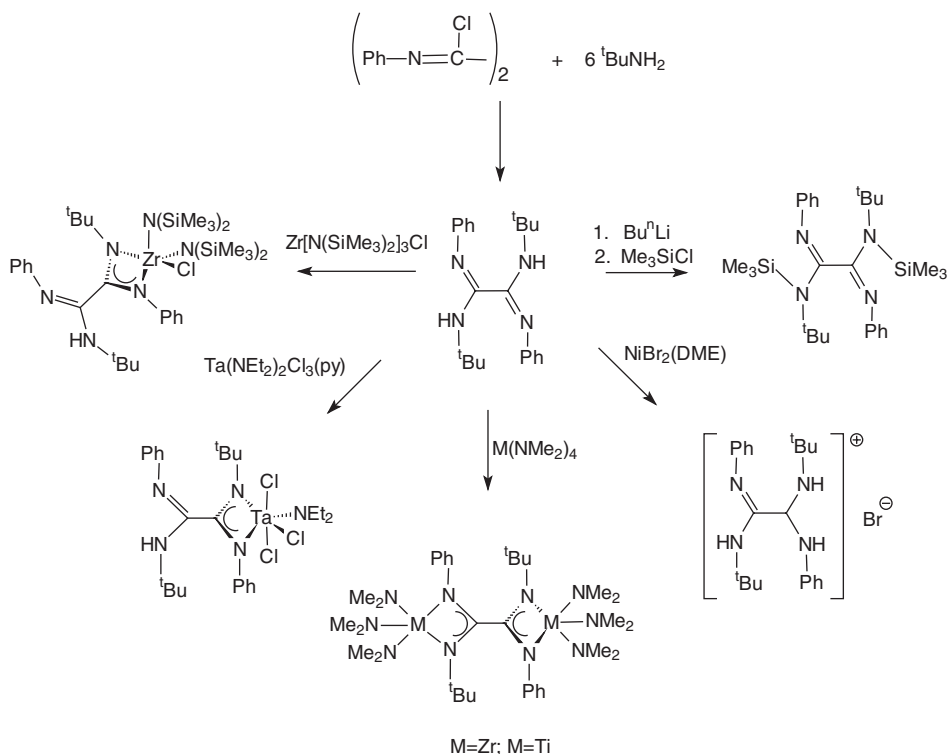
A family of di-, tri-, and tetranuclear Ni(II) complexes containing oxalamidinate as bridging ligands has been described. They were prepared by allowing nickel(II) acetylacetonate, $\text{Ni}(\text{acac})_2$, to react with a variety of aryl-substituted oxalamidines (Scheme 196). The products were isolated as red-brown diamagnetic crystalline solids in 35–60% yields. Heterobimetallic Ni_2Zn and Ni_2Zn_2

**Scheme 192****Scheme 193****Scheme 194**

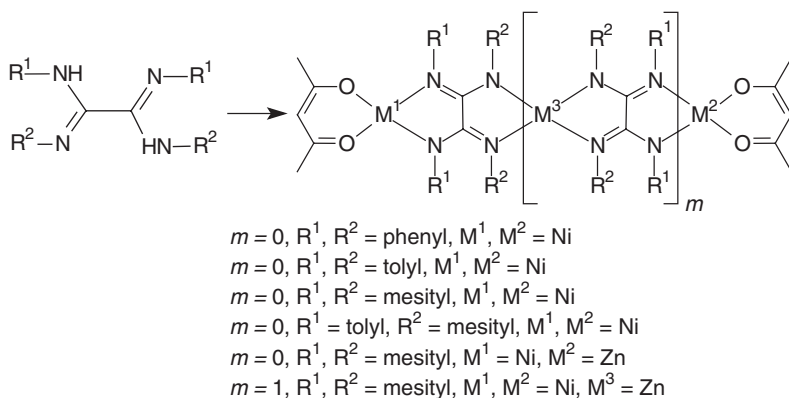
complexes of this type were obtained by treating the oxalamidines first with ZnEt_2 , followed by addition of $\text{Ni}(\text{acac})_2$.^{302,303}

The palladium(II) and heterobimetallic palladium(II)/zinc oxalamidinate complexes depicted in [Scheme 197](#) have been prepared analogously from the free ligands and $\text{Pd}(\text{acac})_2$ or $\text{ZnEt}_2/\text{Pd}(\text{acac})_2$, respectively.³⁰³

The oxalamidinate ligand system can even be further modified by attaching pendant donor functionalities. Two pendant oxalamidine compounds have been synthesized as shown in [Scheme 198](#). Reactions of the new oxalamidines with 2 molar equivalents of AlMe_3 in toluene produced the corresponding bimetallic AlMe_2 complexes, while Grignard type dimagnesium complexes were obtained on treatment with 2 molar equivalents of MeMgBr in THF.³⁰⁴

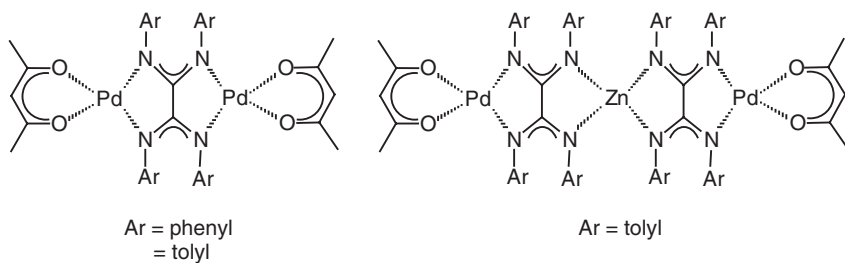


Scheme 195

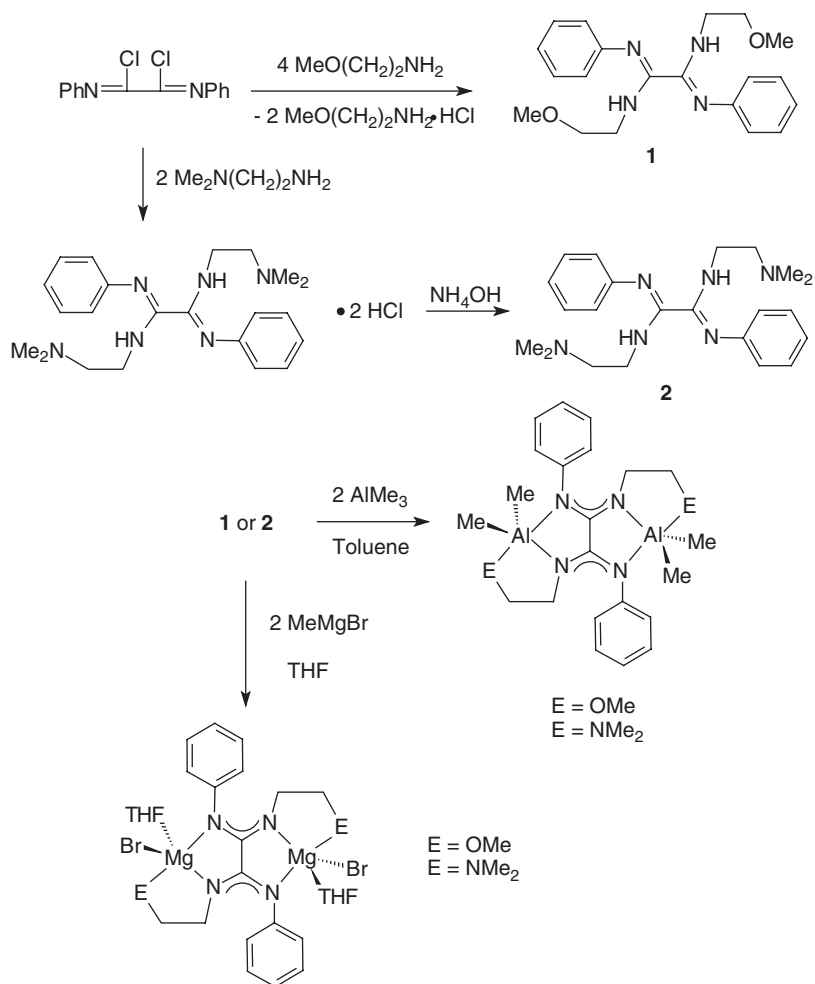


Scheme 196

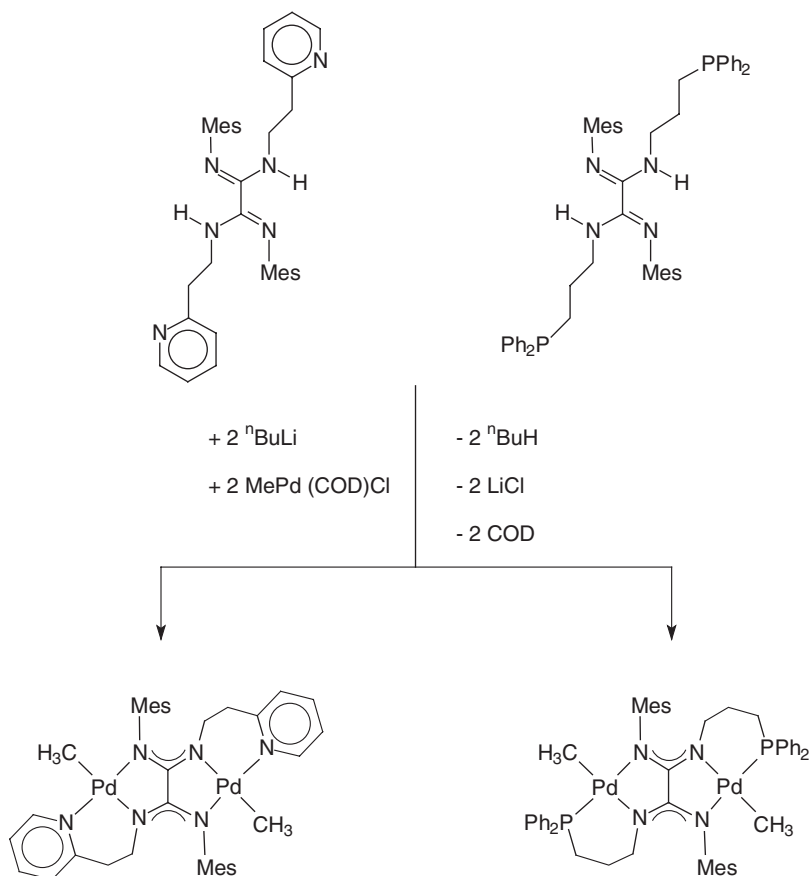
Attachment of pyridine- and phosphine-functionalities to oxalamidine ligands has also been achieved. Scheme 199 exemplifies the use of such ligands in the synthesis of novel organopalladium oxalamidinate complexes.^{305,306}



Scheme 197



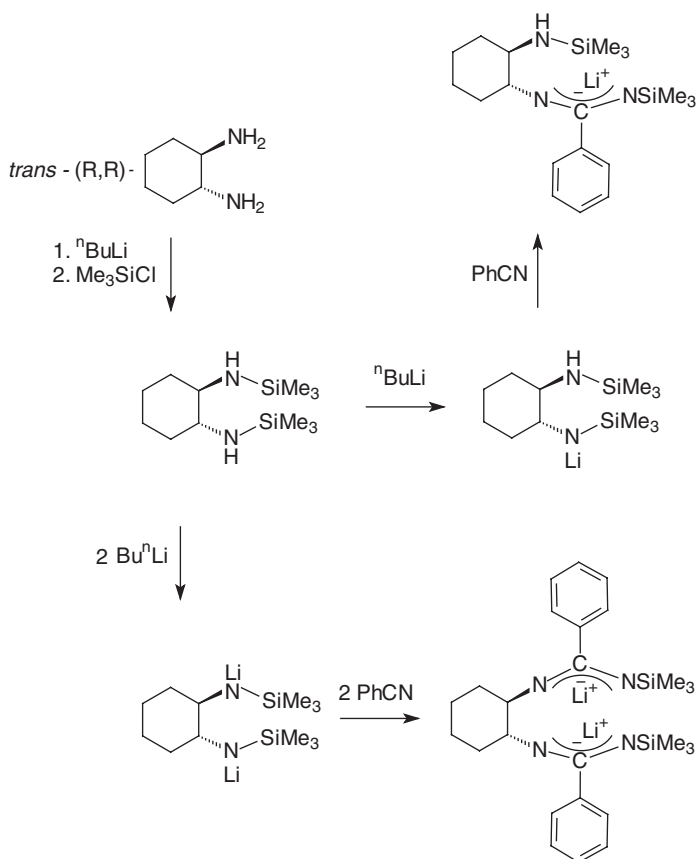
Scheme 198

**Scheme 199**

A series of lithium amidinates derived from (1*R*,2*R*)-*trans*-1,2-diaminocyclohexane has been synthesized and structurally characterized. The synthetic routes are summarized in [Scheme 200](#).³⁰⁷

The bis(amidinate) ligand obtained by successive metallation with 2 equivalents of *n*-butyllithium followed by treatment with 2 equivalents of benzonitrile was employed in the synthesis of novel iron(II) amidinate complexes. A dinuclear iron(II) complex was obtained on reaction of the dilithium salt with FeCl_2 in THF and isolated as yellow crystals in 47% yield ([Scheme 201](#)). Further reaction of this complex with carbon monoxide has been investigated. The compound reacts readily with 1 atm of CO even in the solid state as well as in diethylether to afford a paramagnetic orange dicarbonyl derivative ([Scheme 201](#)). According to X-ray analysis, the homochiral binuclear frame was retained during the reaction with both carbonyl ligands being coordinated to a single iron atom.³⁰⁸

Another series of diamidines based on *trans*-1,2-diaminocyclohexane has been prepared by metallation of the neutral precursors with either $^n\text{BuLi}$ or alkali

**Scheme 200**

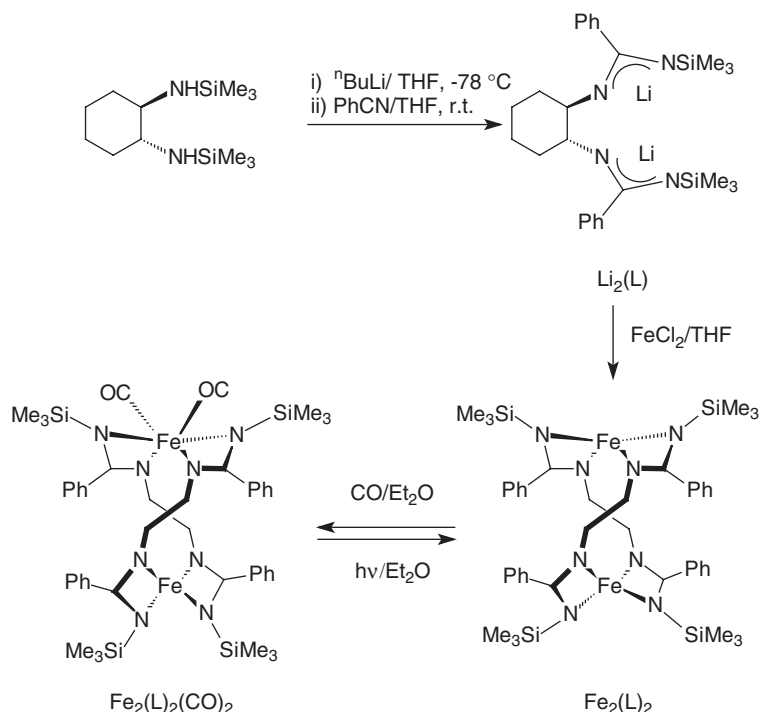
metal bis(trimethylsilyl)amides affording the corresponding crystalline alkali metal derivatives (Scheme 202).³⁰⁹

Reactions of the protonated *trans*-1,2-diaminocyclohexane-derived diaminides $\text{L}^{\text{X}}\text{H}_2$ with tetrabenzyltitanium have also been investigated. The dibenzyl derivatives $(\text{L}^{\text{X}})\text{Ti}(\text{CH}_2\text{Ph})_2$ were obtained as red crystals in high yields. The dibenzyl complex $(\text{L}^{\text{Me}})\text{Ti}(\text{CH}_2\text{Ph})_2$ reacts with H_2 (1.7 bar) in C_6D_6 under formation of the unusual η^6 -toluene complex $(\text{L}^{\text{Me}})\text{Ti}(\eta^6\text{-C}_6\text{H}_5\text{Me})$ (Figure 32).³⁰⁹

The crystal structure of a mono(cyclopentadienyl)zirconium complex containing a novel Me_2Si -linked bis(amidinate) ligand was reported (Scheme 203). In this compound the central Zr atom is octahedrally coordinated with the bis(amidinate) acting as a tridentate ligand.³¹⁰

The dilithium salt of a linked bis(amidinate) dianionic ligand, $\text{Li}_2[\text{Me}_3\text{SiNC}(\text{Ph})\text{N}(\text{CH}_2)_3\text{NC}(\text{Ph})\text{NSiMe}_3]$ ($= \text{Li}_2\text{L}$) was prepared in 69% yield according to Scheme 204 by reaction of dilithiated *N,N'*-bis(trimethylsilyl)-1,3-diaminopropane with benzonitrile.³¹¹

Reaction of the resulting dilithium salt of the linked bis(amidinate) dianionic ligand $[\text{Me}_3\text{SiNC}(\text{Ph})\text{N}(\text{CH}_2)_3\text{NC}(\text{Ph})\text{NSiMe}_3]^{2-}$ ($= \text{Li}_2\text{L}$) with YCl_3

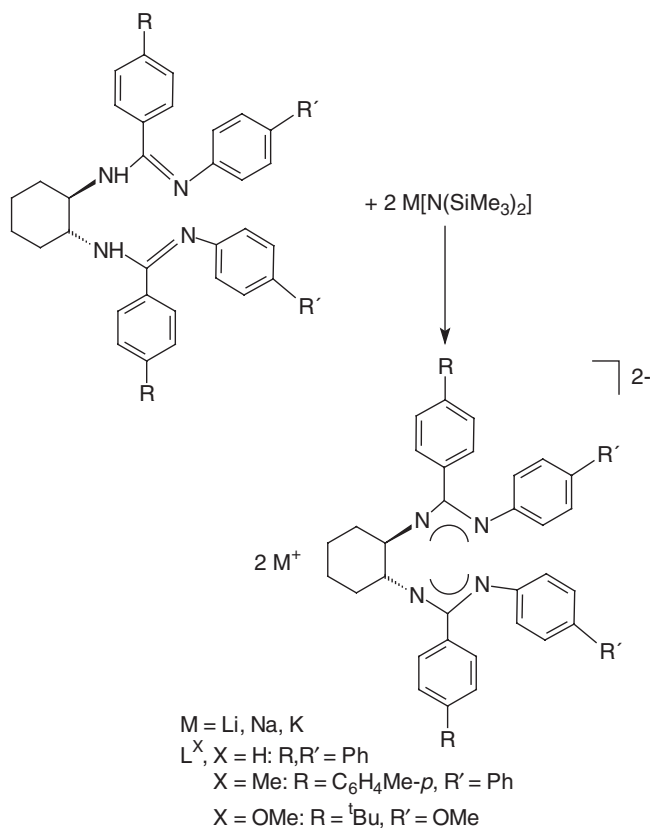


Scheme 201

$(\text{THF})_{3.5}$ gave $[\text{Me}_3\text{SiNC}(\text{Ph})\text{N}(\text{CH}_2)_3\text{NC}(\text{Ph})\text{NSiMe}_3]\text{YCl}(\text{THF})_2$, which, by reaction with $\text{LiCH}(\text{SiMe}_3)_2$, was converted to the alkyl complex $[\text{Me}_3\text{SiNC}(\text{Ph})\text{N}(\text{CH}_2)_3\text{NC}(\text{Ph})\text{NSiMe}_3]\text{-Y}[\text{CH}(\text{SiMe}_3)_2](\text{THF})$ (Scheme 205). A structure determination of this compound (Figure 33) showed that linking together the amidinate functionalities opens up the coordination sphere to allow for the bonding of an additional molecule of THF not present in the unbridged bis(amidinate) analog $[\text{PhC}(\text{NSiMe}_3)_2]_2\text{Y}[\text{CH}(\text{SiMe}_3)_2]$.³¹¹

An analogous reaction of $\text{Li}_2[\text{Me}_3\text{SiNC}(\text{Ph})\text{N}(\text{CH}_2)_3\text{NC}(\text{Ph})\text{NSiMe}_3]$ ($= \text{Li}_2\text{L}$) with anhydrous YbCl_3 in THF in a 1:1 molar ratio afforded the linked bis(amidinato) ytterbium chloride $\text{LYb}(\mu\text{-Cl})_2\text{YbL}(\text{THF})$. The chloro-bridges in this compound are easily cleaved on treatment with THF. Further reaction of the resulting monomeric chloro complex with NaCp in DME gave $\text{LYbCp}(\text{DME})$ in high yield (Scheme 206).^{312a}

In an extension of this work the steric effect of an amide group on the synthesis, molecular structures and reactivity of ytterbium amides supported by the linked bis(amidinate) ligand was investigated. Reactions of the chloro precursor with sodium arylamides afforded the corresponding monometallic amide complexes in which the linked bis(amidinate) is coordinated to the ytterbium center as a chelating ligand (Scheme 207). In contrast, the similar reaction with $\text{NaN}(\text{SiMe}_3)_2$ gave a bimetallic amide complex in which two linked

**Scheme 202**

bis(amidinate)s act as bridging ancillary ligands connecting two $\text{YbN}(\text{SiMe}_3)_2$ fragments in one molecule.^{312b}

A surprisingly simple and straightforward access to a bis(guanidinate) ligand involves the direct reaction of 2 equivalents of diisopropylcarbodiimide with ethylenediamine in toluene at 100 °C (1, Scheme 208). The direct synthesis of this bis(amidinate) ligand from commercial reagents and the ready availability of other diamines with a variety of tethers should allow considerable flexibility for modifications of this bis(amidinate) ligand. Treatment of the free ligand with the homoleptic tetra(benzyl) complexes of Ti and Zr afforded the bis(benzyl) derivatives, the reactivity of which toward 2,6-dimethylphenyl isocyanide was studied.³¹³

Other interesting bis(amidinate) ligands are, for example, those featuring dibenzofuran or 9,9-dimethylxanthene spacers. This new class of bis(amidinates) has been used to prepare structurally characterized dizirconium species. The parent bis(amidines) are highlighted in Scheme 209. Organozirconium derivatives of these ligands were made by treatment with $\text{Zr}(\text{CH}_2\text{Ph})_4$.³¹⁴

Reactions of the free ligands with trimethylaluminum in toluene solution afforded the bis(amidinates) as shown in Scheme 210.³¹⁵

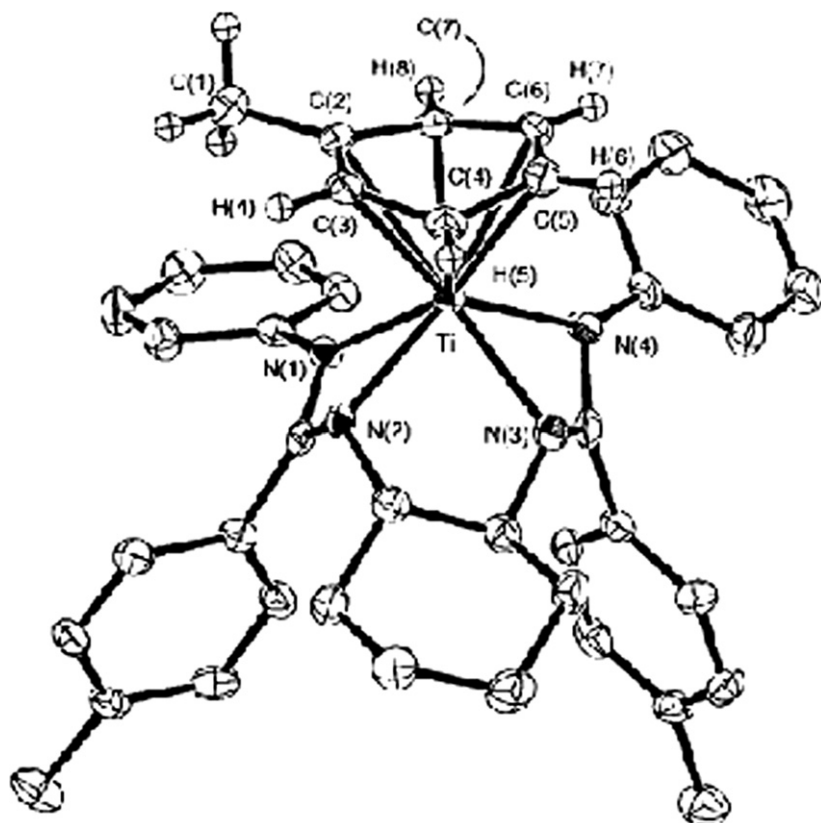
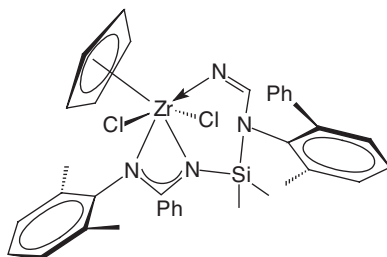
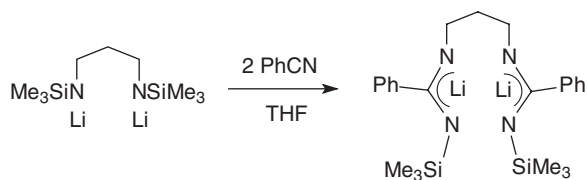


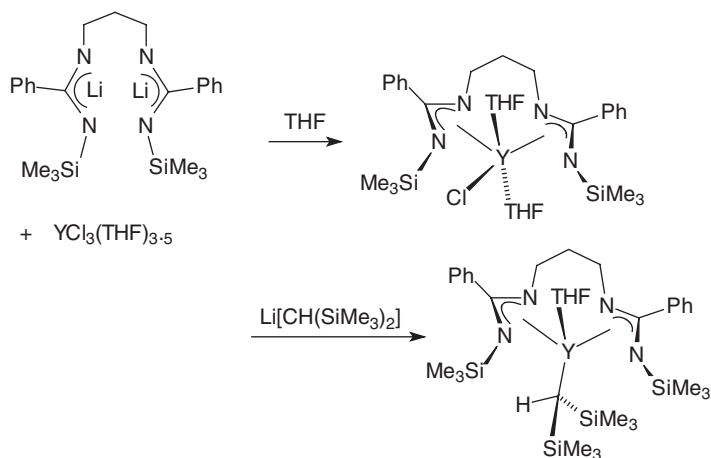
Figure 32 Molecular structure of $(L^{\text{Me}})\text{Ti}(\eta^6\text{-C}_6\text{H}_5\text{Me})$.³⁰⁹



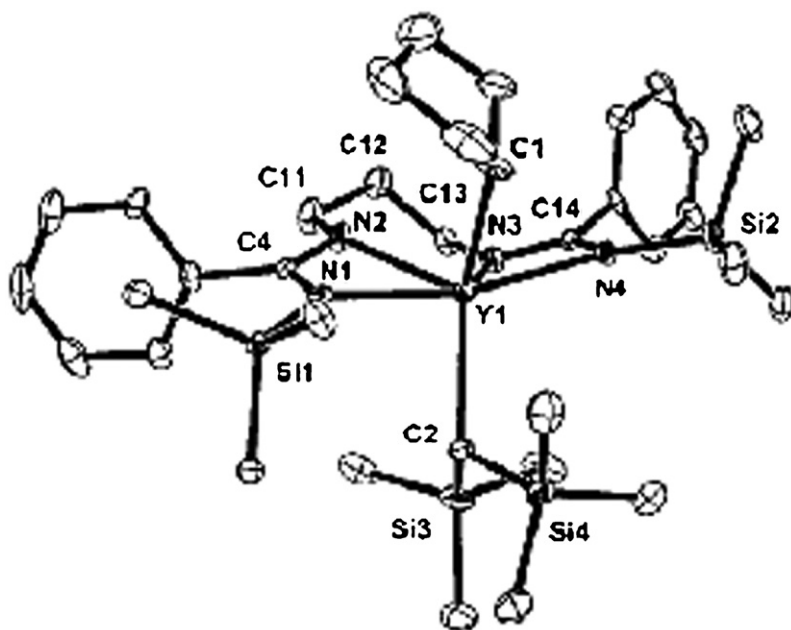
Scheme 203



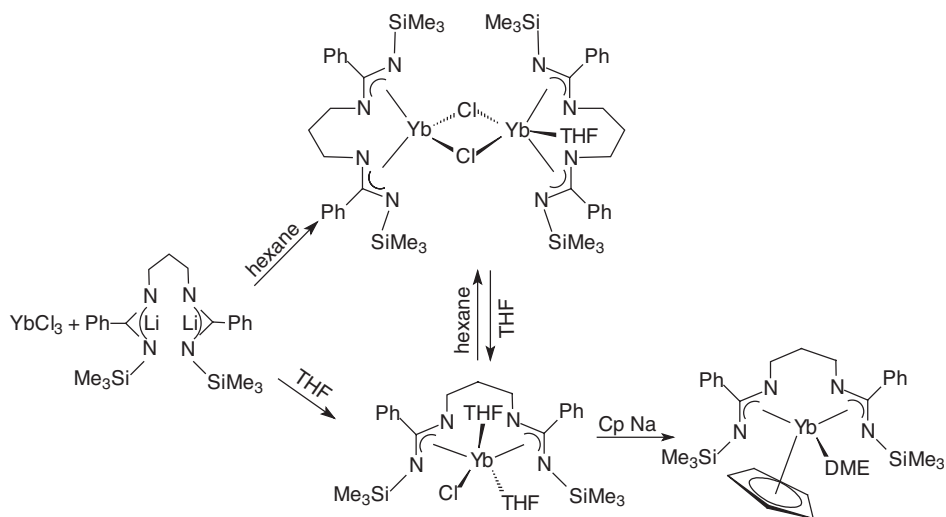
Scheme 204



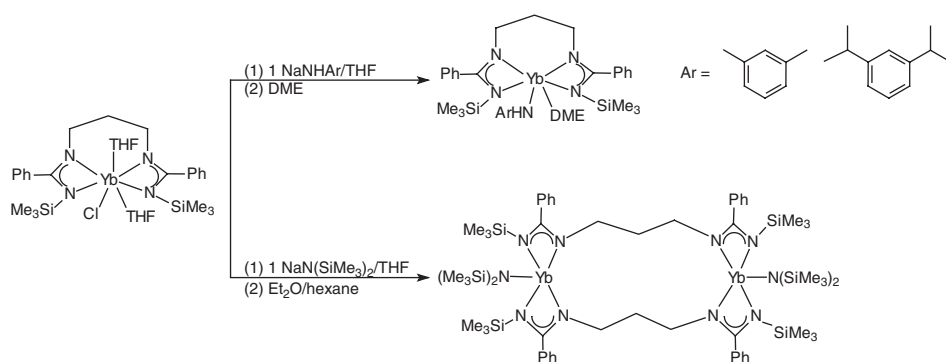
Scheme 205

Figure 33 Molecular structure of $[\text{Me}_3\text{SiNC}(\text{Ph})\text{N}(\text{CH}_2)_3\text{NC}(\text{Ph})\text{NSiMe}_3]\text{Y}[\text{CH}(\text{SiMe}_3)_2](\text{THF})$.³¹¹

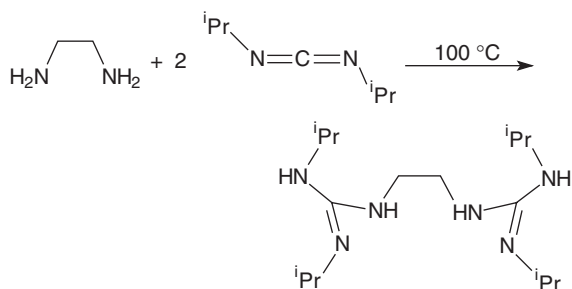
The binucleating bis(amidinate) ligands based on the 9,9-dimethylxanthene backbone have also been used to prepare new dititanium(IV) complexes of the general formula $[\text{bis}(\text{amidinate})]\text{Ti}_2\text{Cp}_2\text{R}_4$ ($\text{R} = \text{CH}_3$, $^{13}\text{CH}_3$, CD_3). Reaction of these methyl derivatives with H_2 as exemplified in Scheme 211 afforded the dititanium(III) μ -methyl- μ -hydrido derivatives $[\text{bis}(\text{amidinate})]\text{Ti}_2\text{Cp}_2(\mu\text{-R})(\mu\text{-H})$



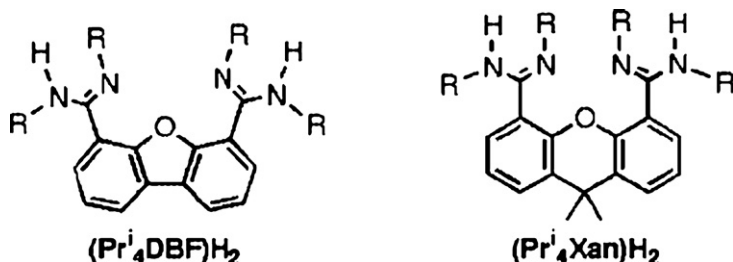
Scheme 206



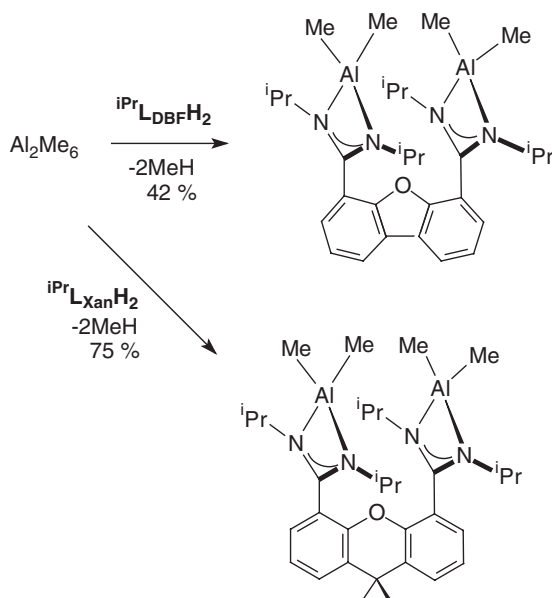
Scheme 207



Scheme 208



Scheme 209

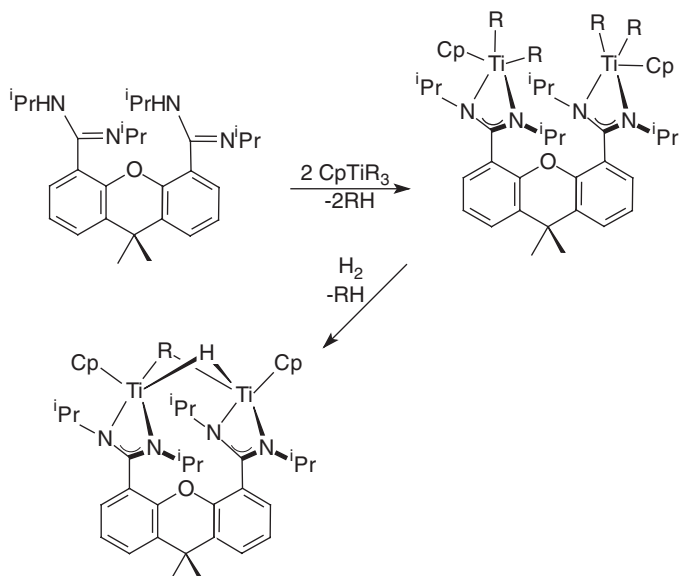


Scheme 210

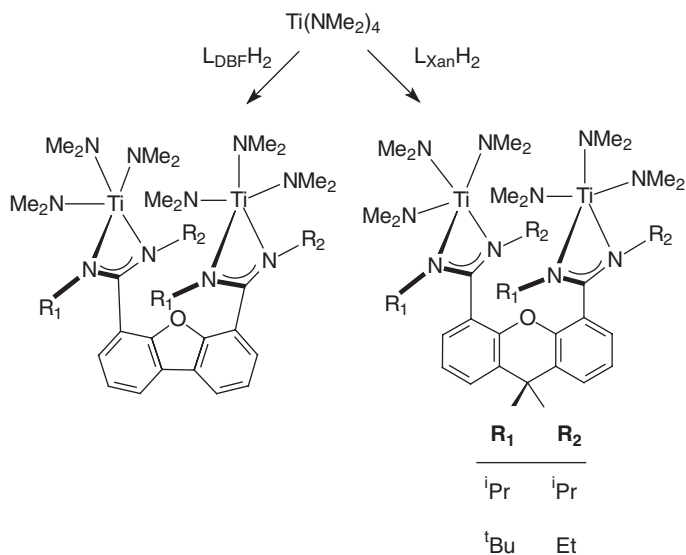
($\text{R} = \text{CH}_3$, $^{13}\text{CH}_3$, CD_3), which were characterized by single-crystal X-ray diffraction and NMR and IR spectroscopy. These complexes are rare examples of first-row transition metal alkyl-hydrido species.³¹⁶

Using the preorganized bis(amidinate) ligands featuring 9,9-dimethylxanthene backbones, several new dizirconium complexes have been prepared. For example, hexa(amido) complexes were obtained by reaction of the ligands with 2 equivalents of $\text{Zr}(\text{NMe}_2)_4$ (Scheme 212).³¹⁷

Reactions leading to a series of remarkable dizirconium alkyls and hydrides are outlined in Scheme 213. In solution, the tetrahydride undergoes a rapid fluxional process (observed by ^1H NMR spectroscopy) that exchanges the four hydrides. At low temperature three distinct hydrides can be observed, which is consistent with either a dibridged structure, or a tri-bridged species undergoing



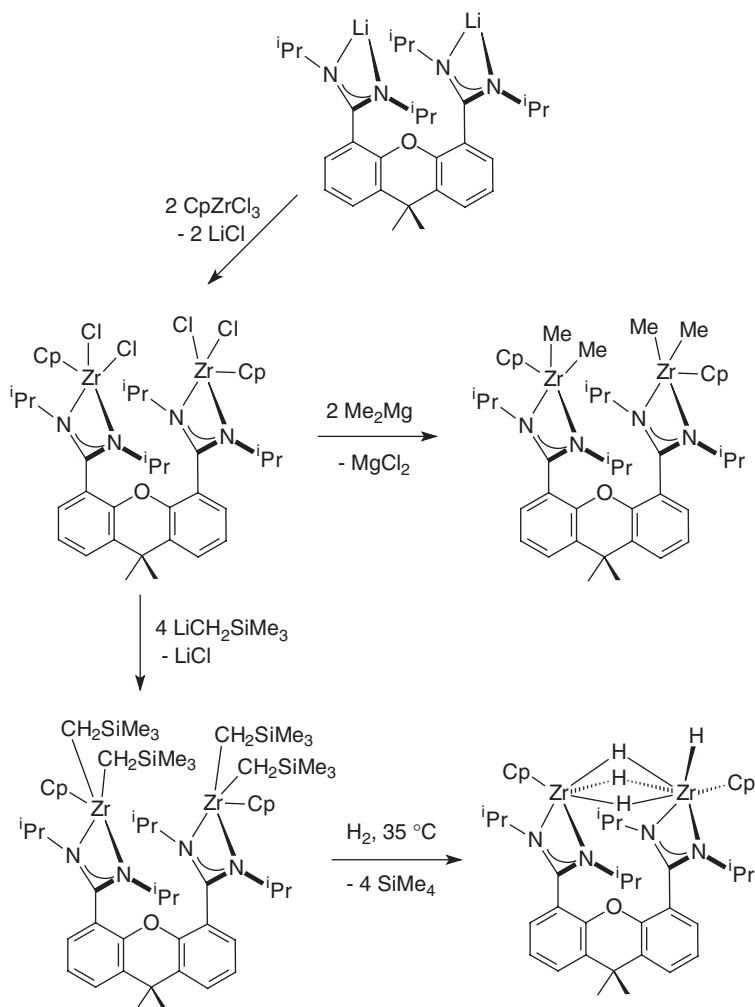
Scheme 211



Scheme 212

rapid exchange of the terminal hydride with only one of the three bridging hydrides.³¹⁷

Bis(amidinate) ligands derived from bulky terphenyl systems were prepared and used for the preparation of dialkylaluminum bis(amidinate) complexes.⁵¹ In a

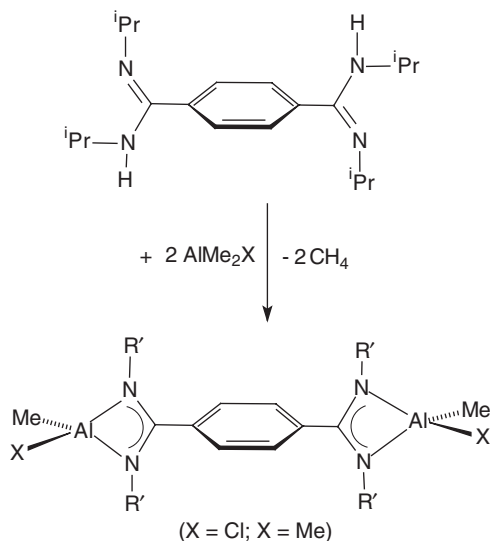
**Scheme 213**

closely related study, 1,4-benzene-bis(amidinate) dianions have been generated and used for the preparation of bimetallic aluminum complexes (Scheme 214).³¹⁸

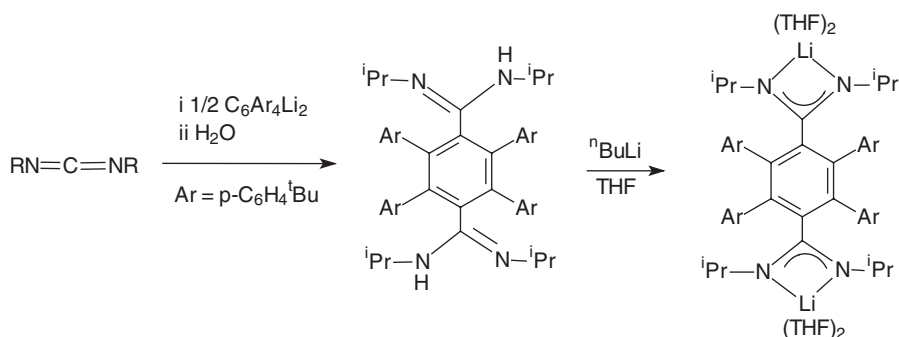
A closely related bis(amidine) ligand and the corresponding dilithium bis(amidinate) complex containing a sterically bulky tetraarylphenylene spacer unit have also been synthesized (Scheme 215).⁵²

E. Dinuclear “lantern” and “paddlewheel”-type amidinate and guanidinate complexes

In 1994 a remarkable new type of amidinate complex having a strongly M–M bonded Fe_2^{3+} core bridged by three *N,N*-diphenylformamidinato anions was



Scheme 214



Scheme 215

reported.³¹⁹ Further investigation of this compound showed that it has an Fe–Fe bond of the order of 1.5, consistent with the short Fe–Fe distance of 2.232(1) Å and at the same time an electron configuration with seven unpaired electrons. There are mainly two different synthetic routes leading to complexes of this type. The first (A) involves reduction of halide precursors such as MCl₂[amidinate]₂ (M = transition metal) using reducing agents such as Na[BEt₃H] or methyl-lithium. Alternatively (Route B) low-valent transition metal complexes can be allowed to react directly with the appropriate amounts of alkali metal amidinates or guanidines. In some cases one-electron oxidation, for example, with AgPF₆ affords the corresponding cationic species. For example, the tri-bridged “lantern”-type dicobalt complex Co₂[PhC(NPh)₂]₃ · 0.5 toluene can be oxidized on treatment with AgPF₆ in acetonitrile to give the cationic species [Co₂{μ-PhC(NPh)₂}(MeCN)₂]⁺PF₆[−] which does not possess a metal–metal bond but contains

two distorted tetrahedrally coordinated Co^{2+} ions bridged by three amidinate groups.³²

There are numerous reports on tetra-bridged “paddlewheel” type amidinate and guanidinate complexes of transition metals. The general synthetic routes leading to such complexes are principally the same as those leading to the tri-bridged dinuclear species, i.e., the first method (A) involves reduction of halide precursors such as $\text{MCl}_2[\text{amidinate}]_2$ (M = transition metal) using reducing agents such as $\text{Na}[\text{BET}_3\text{H}]$ or methyllithium. Alternatively (Route B) low-valent transition metal complexes can be treated with the appropriate amounts of alkali metal amidinates or guanidinates. In some cases, one-electron oxidation, for example, with AgPF_6 affords the corresponding cationic species (Method C). For example, treatment of $\text{Co}_2[\text{PhC}(\text{NPh})_2]_4$ with AgPF_6 afforded $[\text{Co}_2\{\text{PhC}(\text{NPh})_2\}_4]\text{PF}_6$.³²⁰ On the other hand, one-electron reduction has been achieved in some cases, for example by using KC_8 as strong reductant (Method D) (Table 1).³²¹ The nature of the chemical bond in dinuclear complexes of the type $\text{M}_2(\text{formamidinate})_4$ (M = Nb, Mo, Tc, Ru, Rh, Pd) has been investigated by analysis of the electron localization function.³²²

F. Phosphaguanidinate complexes

A little investigated though highly promising variation of the guanidinate ligand system is the replacement of an amino substituent by a phosphine unit to give phospho(III)guanidinate anions $[\text{R}_2\text{PC}(\text{NR}')_2]^-$. In contrast to their conventional nitrogen analogs where delocalization across the central CN_3 core of the molecule is normally observed, retention of the lone-pair at phosphorus is predicted, due to unfavorable overlap with the sp^2 -hybridized carbon. Thus in addition to regular N,N' -bonding (Scheme 216, type I), participation of the P -center in either an N,P -(type II), or ambidentate (type III) coordination mode should be possible.³³¹

Reaction of Ph_2PLi with $\text{Pr}^i\text{N}=\text{C}=\text{NPr}^i$ in THF proceeds *via* insertion of the carbodiimide into the Li-P bond, affording the lithium phosphaguanidinate salt $\text{Li}[\text{Ph}_2\text{PC}(\text{NPr}^i)_2]$ in 72% yield. The preparation and reactivity of this new ligand are summarized in Scheme 217. An X-ray crystal structure analysis of the product obtained after removal of the solvent from the reaction mixture revealed the presence of a mono-solvated, centrosymmetric dimer in the solid state (Figure 34).^{331,332}

Addition of TMEDA to a toluene solution of $\text{Li}[\text{Ph}_2\text{PC}(\text{NPr}^i)_2]$ afforded colorless crystals of the monomeric 1:1 adduct $(\text{TMEDA})\text{Li}[\text{Ph}_2\text{PC}(\text{NPr}^i)_2]$. Both lithium derivatives reacted with AlMe_2Cl to generate the aluminum dimethyl compound $\text{Me}_2\text{Al}[\text{Ph}_2\text{PC}(\text{NPr}^i)_2]$. An X-ray analysis revealed a monomeric complex incorporating type I bonding of the phospho(III)guanidinate ligand and the presence of a planar, four-membered metallacycle as shown in Figure 35.^{331,332}

The versatility of the phospho(III)guanidinate ligands was further demonstrated by the synthesis of a mixed Pt/Al compounds according to Scheme 218.³³¹

Table 1 Representative examples of “paddlewheel” type amidinate and guanidinate complexes^a

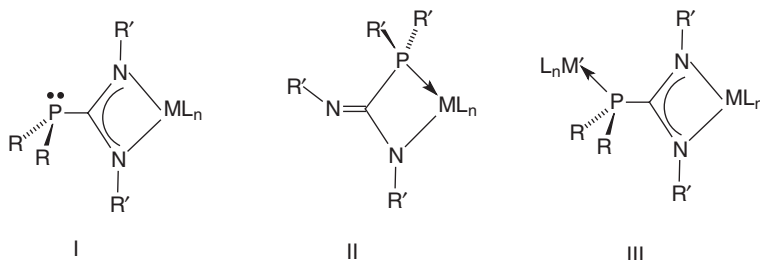
Compound	Synthetic route	M-M distance (Å)	References
V ₂ [HC(NCy) ₂] ₄	B	1.968(2)	206,207,321
V ₂ [HC(NC ₆ H ₄ R- <i>p</i>) ₂] ₂ (R = H, Cl, OMe)	B	1.974(1)–1.9876(5)	321
V ₂ [PhNHC(NPh) ₂] ₄	B	1.9521(7)	321
V ₂ (anilinopyridinate) ₄	B	1.9425(4)	321
V ₂ (hpp) ₄	B	1.9521(7)	321
[K(THF) ₃][V ₂ {HC(NPh) ₂] ₄]	D	1.9295(8)	321
[K(18-crown-6)(THF) ₂][V ₂ {HC(NPh) ₂] ₄]	D	1.924(2)	321
Cr ₂ [HC(NCy) ₂] ₄ · toluene	B	1.913(3)	29
Cr ₂ [(CH ₂) ₄ NC(NPh) ₂] ₄	B	1.904(1)	323
[Cr ₂ [(CH ₂) ₄ NC(NPh) ₂] ₄][PF ₆]	C	1.9249(9)	323
Mo ₂ [HC(NC ₆ H ₄ X) ₂] ₄	B	2.085(1)–2.0964(5)	324
(X = H, <i>p</i> -OMe, <i>m</i> -OMe, <i>p</i> -Cl, <i>m</i> -Cl, <i>p</i> -CF ₃ , <i>m</i> -CF ₃ , <i>p</i> -C(O)Me, or 3,5-Cl ₂ C ₆ H ₃)			
Mo ₂ (μ-OAc)[MeC(NPr ⁱ) ₂] ₃	B	2.0702(3)	231
Mo ₂ (μ-OAc) ₂ [PhC(NPr ⁱ) ₂] ₂	B	2.0677(4)	231
Mo ₂ (hpp) ₄	B	2.067(1)	325
Mo ₂ (hpp) ₄ Cl	C	2.128(2)	325
Mo ₂ (hpp) ₄ Cl(BF ₄)	C	2.1722(9)	325
W ₂ (hpp) ₄ · 2NaHBEt ₃	A	2.1608(5)	326,327
W ₂ (hpp) ₄ Cl	B	2.2131(8)	326,327
W ₂ (hpp) ₄ Cl ₂	B	2.250(2)	326,327
W ₂ (hpp) ₄ (TFPB) ₂	C	2.1920(3)	326
Fe ₂ [HC(NPh) ₂] ₃	A	2.2318(8)	319
Fe ₂ [HC(NPh) ₂] ₄	A	2.462(2)	31,36,328
Co ₂ [HC(NPh) ₂] ₃	A	2.385(1)	31,32
Co ₂ [PhC(NPh) ₂] ₃	A	2.3201(9)	31,32
Co ₂ [HC(NPh) ₂] ₄	A	2.3735(9)	320
Co ₂ [PhC(NPh) ₂] ₄ (PF ₆)	A	2.322(2)	320
Rh ₂ (hpp) ₄ Br	B	2.430(3)	329
Pd ₂ [HC(NC ₆ H ₄ OMe- <i>p</i>) ₂] ₄	B	2.6486(8)	268
Ag ₄ (hpp) ₄	B	2.8614(6)	330
Au ₂ [HC(NC ₆ H ₃ Me ₂ -2,6) ₂] ₂	B	2.7	277
Au ₂ (hpp) ₂ Cl ₂	B	2.4752(9)	330

[hpp][−] = 1,3,4,6,7,8-hexahydro-2*H*-pyrimido[1,2-*a*]pyrimidine; TFPB = tetrakis[3,5-bis(trifluoromethyl)phenyl]borate.

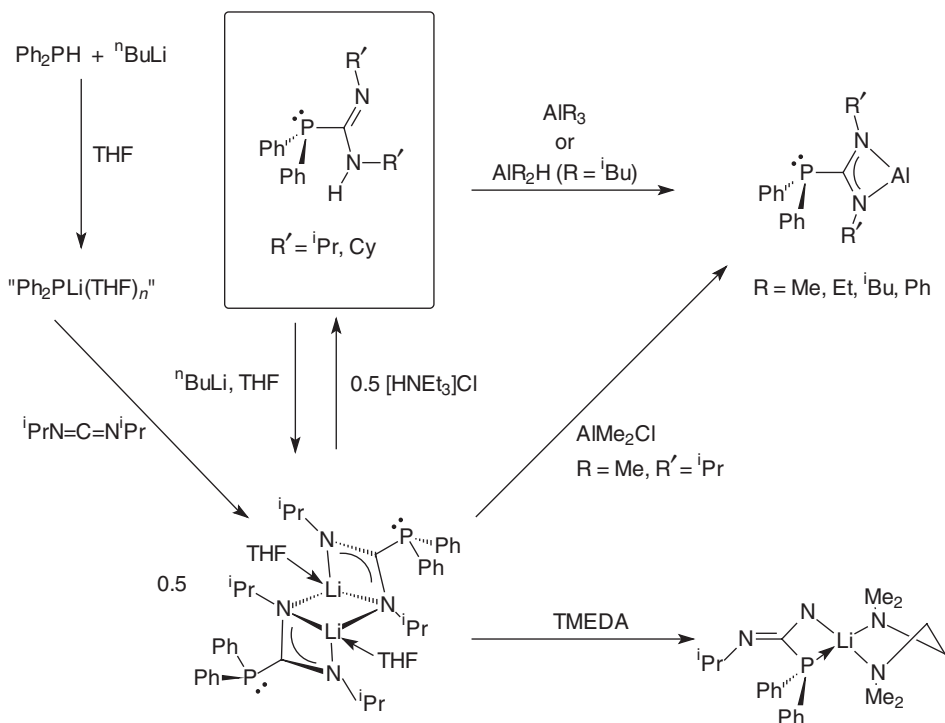
^aTable 1 lists only a small selection of the compounds known in this area.

V. AMIDINATE AND GUANIDINATE COMPLEXES IN CATALYSIS

Certain aspects of catalytic applications of transition metal amidinate complexes have already been summarized in review articles. The “Chemistry of



Scheme 216



Scheme 217

coordinatively unsaturated organoruthenium amidinates as entry to homogeneous catalysis" was reviewed in 2003 by Nagashima et al.²⁴⁵ A 2005 review on "Cationic alkyl complexes of the rare-earth metals: Synthesis, structure, and reactivity" by Arndt and Okuda covered some organolanthanide amidinates.¹⁴² In 2007, Smolensky and Eisen published a review entitled "Design of organometallic group IV heteroallylic complexes and their catalytic properties for polymerizations and olefin centered transformations."³³³ In this article a strong emphasis was placed on various synthetic and catalytic aspects of group IV metal amidinate complexes. It was clearly pointed out that such amidinate

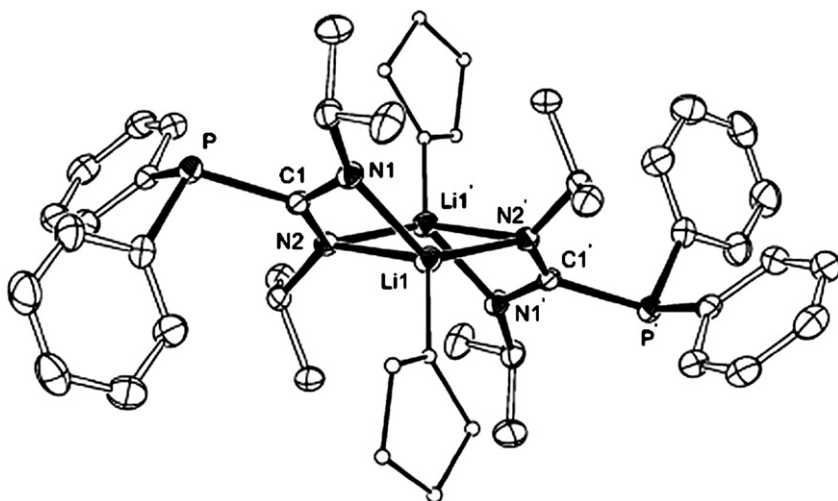


Figure 34 Molecular structure of $[\text{Li}\{\text{Ph}_2\text{PC}(\text{NPr}^i)_2\}(\text{THF})]_2$.^{331,332}

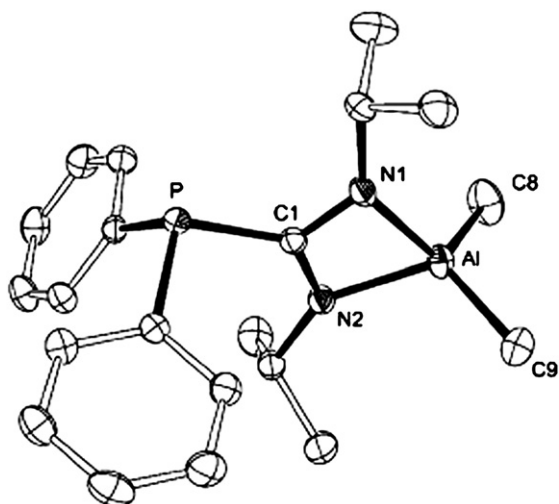
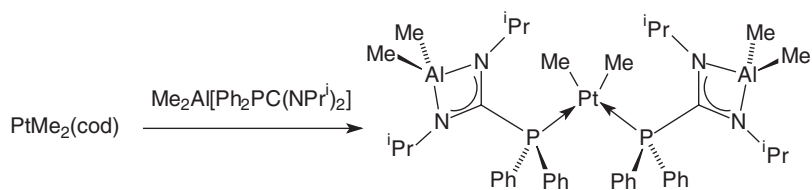


Figure 35 Molecular structure of $\text{Me}_2\text{Al}[\text{Ph}_2\text{PC}(\text{NPr}^i)_2]$.^{331,332}



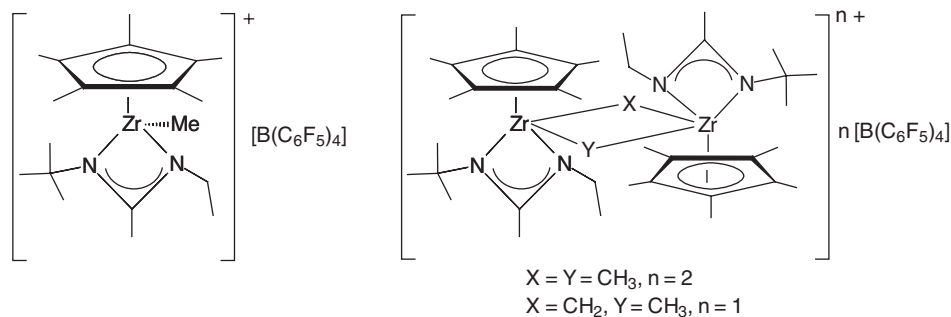
Scheme 218

complexes not only promote the polymerization of propylene but are also effective homogeneous catalysts for the polymerization of dienes and the dehydrogenative coupling of silanes.³³³

A. Polymerization reactions catalyzed by amidinate and guanidinate complexes

1. Olefin polymerization

The use of amidinato catalyst systems for the polymerization of olefins has first been reported in a patent application by us in cooperation with BASF company.³³⁴ Since then various other patents dealing with the use of amidinato metal complexes as catalysts for olefin polymerizations have appeared.^{334–341} The effect of substituent variation on olefin insertion and chain transfer in cationic aluminum amidinate alkyls¹⁰³ as well as in nickel amidinates³⁴² was studied by theoretical methods. Atactic polystyrene has been produced with a calcium guanidinate as catalyst.⁸⁷ The dimeric bis(guanidinato) lutetium hydride complex $[(\text{Me}_3\text{Si})_2\text{NC}(\text{NPr}^i)_2]_2\text{Lu}(\mu\text{-H})_2$ was found to catalyze the polymerization of ethylene, propylene, and styrene.¹⁵² Moderate activity in the polymerization of both styrene and ethylene has been reported for the mono(benzamidinato)titanium trichloride complex $[\{p\text{-MeC}_6\text{H}_4\text{C}(\text{NSiMe}_3)_2\}\text{TiCl}_2(\mu\text{-Cl})]_2$ when activated with methylaluminoxane.¹⁷⁴ In the presence of methylaluminoxane (MAO) as a cocatalyst, the bis(alkylamidinate) Group 4 metal complexes of the general formula $[\text{MeC}(\text{NCy})_2]_2\text{MCl}_2$ ($\text{M} = \text{Ti}, \text{Zr}, \text{Hf}$; $\text{Cy} = \text{cyclohexyl}$), $[\text{Bu}^t\text{C}(\text{NCy})_2]_2\text{ZrCl}_2$, and $[\text{MeC}(\text{NCy})_2]_2\text{ZrMe}_2$ are active ethylene polymerization catalysts.¹⁷² The activity of four racemic mixtures of bis(benzamidinato) Group 4 complexes, $[p\text{-R}'\text{C}_6\text{H}_4\text{C}(\text{NR})_2]_2\text{MX}_2$ ($\text{M} = \text{Ti}, \text{Zr}$; $\text{X} = \text{Cl}, \text{Me}$; $\text{R}' = \text{H}, \text{Me}$; $\text{R} = \text{Pr}^i, \text{SiMe}_3$) as precatalysts for the stereoregular polymerization of propylene has been investigated. It was found that these complexes catalyze the stereoregular polymerization of propylene only under pressure in CH_2Cl_2 , producing polypropylene with very large isotacticities ($\text{mmmm} \% = \sim 95\text{--}98$) and high melting points ($140\text{--}154^\circ\text{C}$).³⁴³ Using the mono(pentamethylcyclopentadienyl)-zirconium acetamidinates $\text{Cp}^*\text{ZrMe}_2[\text{MeC}(\text{NR})(\text{NR}')]$ ($\text{R}, \text{R}' = \text{cyclohexyl}$; $\text{R} = \text{Bu}^t$, $\text{R}' = \text{Et}$) the stereospecific living polymerization of 1-hexene was achieved to provide highly isotactic, high molecular weight materials possessing low polydispersities. This was the first catalyst system for the stereospecific living Ziegler–Natta polymerization of an α -olefin. In the closely related series of cationic zirconium amidinates, $[\text{Cp}^*\text{ZrMe}_2\{\text{RC}(\text{NEt})(\text{NBu}^t)\}][\text{B}(\text{C}_6\text{F}_5)_4]$ ($\text{R} = \text{H}, \text{Me}, \text{Bu}^t, \text{Ph}$) a marked influence of the substituent at the central amidinate carbon on the activity in the stereoselective living Ziegler–Natta polymerization of 1-hexene was found. While the compound with $\text{R} = \text{Me}$ is highly active, the species with $\text{R} = \text{H}$ and Ph display a significant loss of stereocontrol. In the case of $\text{R} = \text{Bu}^t$ the polymerization is no longer living. Some of the zirconium cations involved in these systems have been structurally characterized. Addition of trace amounts of diethyl ether to $[\text{Cp}^*\text{ZrMe}_2\{\text{MeC}(\text{NEt})(\text{NBu}^t)\}][\text{B}(\text{C}_6\text{F}_5)_4]$ (Scheme 219) provided the bright yellow 1:1 diethyl ether adduct. Figure 35 shows the molecular structure of the cation. In the absence of a Lewis base, it was



Scheme 219

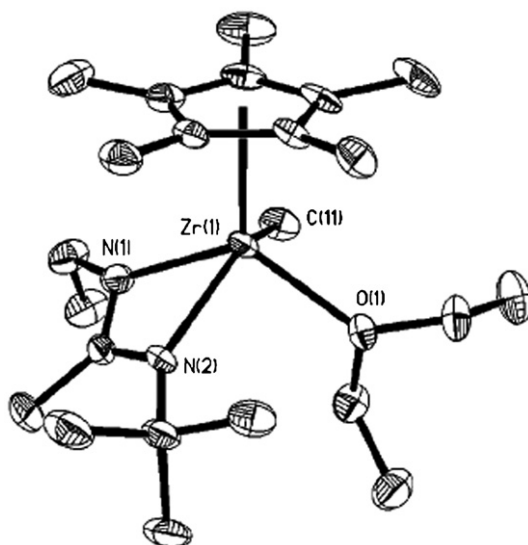
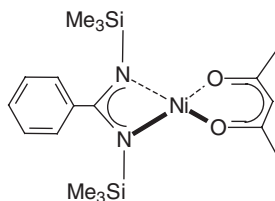


Figure 36 Molecular structure of the cation in $[\text{Cp}^*\text{ZrMe}_2\{\text{MeC}(\text{NEt})(\text{NBU}^t)\}][\text{B}(\text{C}_6\text{F}_5)_4]$.^{344–346}

possible to isolate the $\mu\text{-CH}_3$, $\mu\text{-CH}_3$ dinuclear dication as well as the $\mu\text{-CH}_2$, $\mu\text{-CH}_3$ dinuclear monocation in the form of their $[\text{B}(\text{C}_6\text{F}_5)_4]^-$ salts (Scheme 219). All these species have been structurally characterized by X-ray diffraction (Figure 36).^{344–346}

The bis(benzamidinato) zirconium dimethyl complex $[\text{PhC}(\text{NSiMe}_3)_2]\text{ZrMe}_2$ has been activated by a mixture of $[\text{Ph}_3\text{C}][\text{B}(\text{C}_6\text{F}_5)_4]$ and a small amount of methylalumoxane (MAO) ($\text{Zr}:\text{B}:\text{Al} = 1:1:50$), forming an extremely active catalytic system for the polymerization of olefins, producing high-density polyethylene and elastomeric polypropylene with a narrow molecular weight distribution. This system rivals the activity of the best metallocene complexes.³⁴⁷

Two chloro-bridged dimeric vanadyl(V) amidinates, $[\{\text{PhC}(\text{NPr}^i)_2\}\text{VOCl}_2]_2$ and $[\{\text{PhCH}_2\text{C}(\text{NPr}^i)_2\}\text{VOCl}_2]_2$ have been reported to promote the polymerization

**Scheme 220**

of propene and 1,3-butadiene in the presence of organometallic compounds of aluminum.²¹¹ The nickel(II) amidinate complex $[\text{PhC}(\text{NSiMe}_3)_2]\text{Ni}(\text{acac})$ (Scheme 220) activated with MAO was shown to be an efficient catalyst system for the norbornene vinyl-type polymerization. The activity of the catalyst and the molecular weights of the resulting polynorbornenes were found to be dependent on the reaction time, the MAO/precatalyst ratio, and the reaction temperature. In addition, this catalyst system was found to dimerize propylene to a mixture of hexenes with a high turnover frequency and oligomerize ethylene to either a mixture of C4–C6 or/and C4–C14 products.²⁶⁷ When activated with MAO the related nickel complex $[\text{PhC}(\text{NSiMe}_3)(N'\text{-myrtanyl})]_2\text{Ni}(\text{py})_2$ also showed a good activity for the vinyl-type polymerization of norbornene.²⁸²

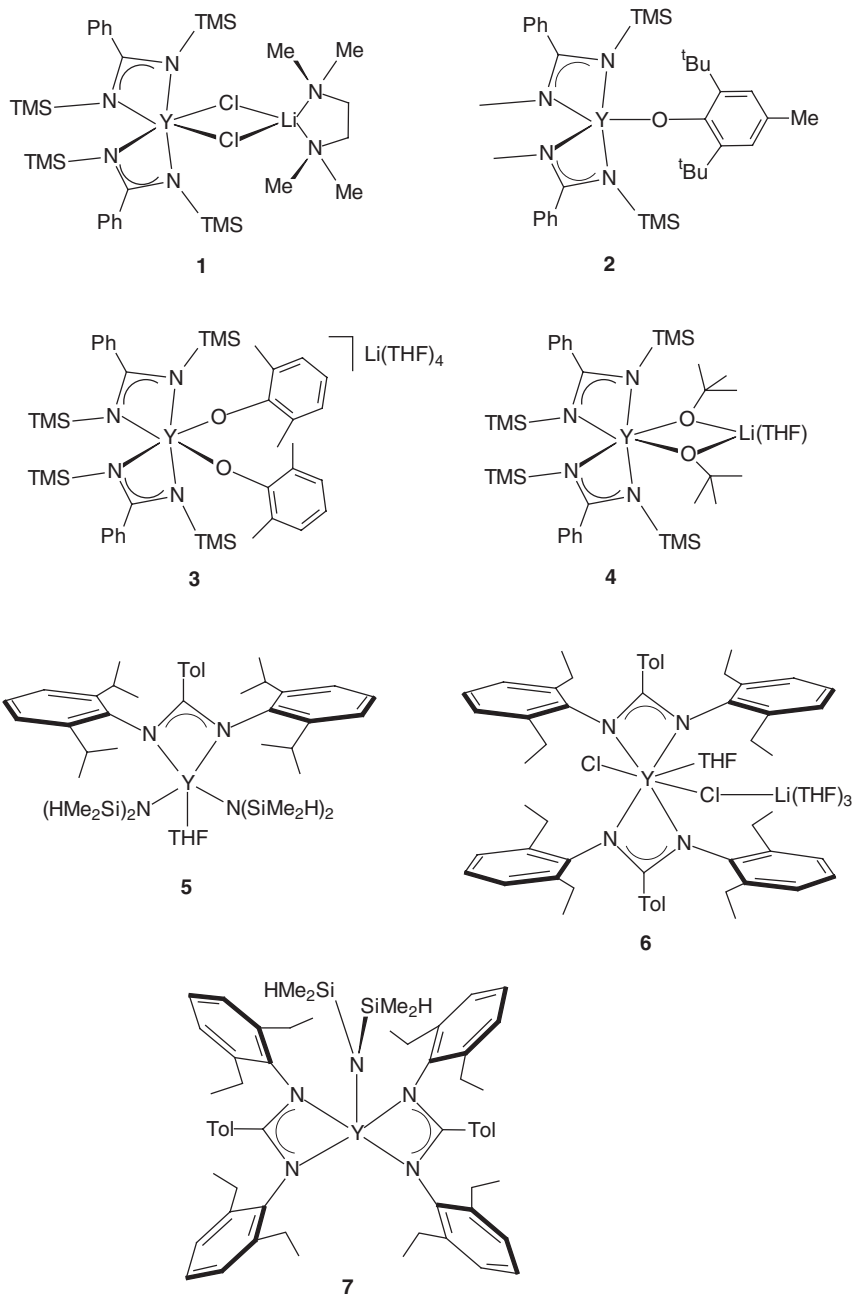
Other metal amidinates and guanidates for which catalytic activity in olefin polymerization or oligomerization (normally on activation with MAO or other aluminum alkyls) has been found include $[\text{Bu}^i\text{C}(\text{NPr}^i)_2]\text{In}\{\mu\text{-NC}_6\text{H}_3\text{Pr}^i_2\text{-2,6}\}_2$, $\text{Ti}(\text{NMe}_2)_2$,¹¹⁷ various bis(benzamidinato) complexes of titanium and zirconium,³⁴⁸ $\text{CpTiMe}_2(\text{amidinate})$ and $\text{Cp}^*\text{TiMe}_2(\text{amidinate})$ complexes,^{184–186} Group 4 metal amidinates and guanidates such as $[\text{PhC}(\text{NSiMe}_3)_2]\text{Ti}(\text{OPr}^i)_3$ ³³⁶ and $[\text{Zr}\{\text{ArNC}(\text{NMe}_2)\text{NSiMe}_3\}(\mu\text{-Cl})\text{Cl}_2]_2$,^{177b} $[\text{C}_6\text{F}_5\text{C}(\text{NSiMe}_3)_2]_2\text{VMe}$,²⁰⁹ vanadium amidinates,³³⁵ $\text{Cp}^*[\text{MeC}(\text{NPr}^i)_2]\text{TaCl}_3$,¹⁸⁷ Ni(II) complexes with bridging oxalamidinato ligands (cf. Section IV.D),³⁰² and copper amidinates.³³⁴

2. Polymerization of polar monomers

Dimethylaluminum complexes (cf. Scheme 29) bearing amidinate ligands have been investigated as catalysts for the polymerization of methyl methacrylate, ϵ -caprolactone, and propylene oxide. The neutral complexes generally did not carry out polymerization, but the polymerization/oligomerization of all three monomers was achieved when the precatalysts were activated with $\text{B}(\text{C}_6\text{F}_5)_3$ or $[\text{Ph}_3\text{C}]^+[\text{B}(\text{C}_6\text{F}_5)_4]^-$.¹⁰⁴

In quest of new single-site catalysts for polymerizations of cyclic esters, a series of mononuclear yttrium(III) complexes have been synthesized which are depicted in Scheme 221.³⁴⁹

Coordination numbers ranging from five to seven were observed, and they appeared to be controlled by the steric bulk of the supporting amidinate and coligands. Complexes 2–5 and 7 were found to be active catalysts for the polymerization of D,L-lactide (e.g., with 2 and added benzyl alcohol, 1000 equiv of D,L-lactide were polymerized at room temperature in <1 h). The neutral complexes 2, 5, and 7 were more effective than the anionic complexes 3 and 4.³⁴⁹

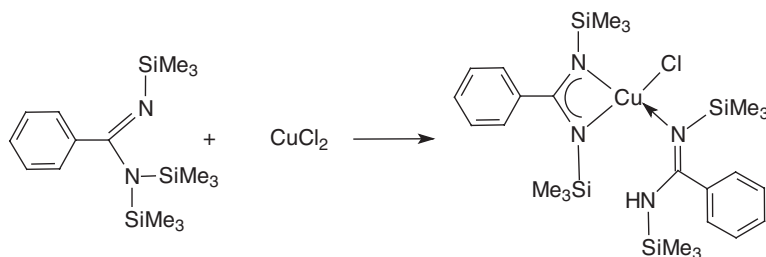


Scheme 221

Polymerization of D,L-lactide to polylactide was also achieved using monomeric tin(II) amidinates (cf. Schemes 48 and 49)^{129,132} and the mono (guanidinate) lanthanum complex $[(\text{Me}_3\text{Si})_2\text{NC}(\text{NCy})_2]\text{La}[\text{N}(\text{SiMe}_3)_2]_2$. Although a high molecular weight polymer was obtained, polydispersities were broad and no control over the stereochemistry of the polymer was observed.¹⁴⁶ Recently ytterbium amide complexes stabilized by linked bis(amidinate) ligands (cf. Scheme 207) were reported to be efficient initiators for the polymerization of L-lactide. The catalytic performance was found to be highly dependent on the amido groups and molecular structures.^{312b} The methyl bridged "ate" complexes $[(\text{Me}_3\text{Si})_2\text{NC}(\text{NPr}^i)_2]_2\text{Ln}(\mu\text{-Me})_2\text{Li}(\text{THF})_2$ ($\text{Ln} = \text{Nd}, \text{Yb}$) exhibited extremely high activity for the ring-opening polymerization of ϵ -caprolactone to give high molecular weight polymers. The Nd derivative also showed good catalytic activity for the syndiotactic polymerization of methylmethacrylate.¹⁵³ Other metal amidinates and guanidinates, for which high activity in the polymerization of polar monomers such as ϵ -caprolactone, lactide, and methylmethacrylate (MMA) have been reported, include the homoleptic lanthanide amidinates $\text{Ln}[\text{RC}(\text{NCy})_2]_3(\text{THF})_n$ ($\text{R} = \text{Me}, \text{Ln} = \text{Nd}, \text{Gd}, \text{Yb}, n = 0$; $\text{R} = \text{Ph}, \text{Ln} = \text{Y}, \text{Nd}, \text{Yb}, n = 2$),¹⁶⁸ the bis(guanidinato) lanthanide amides $[(\text{Me}_3\text{Si})_2\text{NC}(\text{NPr}^i)_2]_2\text{LnN}(\text{Pr}^i)_2$ ($\text{Ln} = \text{Y}, \text{Nd}$),¹⁵⁶ the borohydrides $[(\text{Me}_3\text{Si})_2\text{NC}(\text{NCy})_2]\text{Ln}(\text{BH}_4)_2(\text{THF})_2$ ($\text{Ln} = \text{Nd}, \text{Sm}, \text{Er}, \text{Yb}$),¹⁴⁷ $[\text{MeC}(\text{NCy})_2]_3\text{U}$, $[\text{MeC}(\text{NCy})_2]_3\text{Nd}$,⁶⁶ and cationic dinuclear ruthenium amidinates.^{337,350}

The ring-opening polymerization of trimethylene carbonate (TMC) using homoleptic lanthanide guanidinate complexes $[\text{R}'_2\text{NC}(\text{NR})_2]_3\text{Ln}$ has been investigated in detail. The metal centers and the substituents on the guanidinate ligands showed a marked effect on the catalytic activities with $[\text{Ph}_2\text{NC}(\text{NCy})_2]_3\text{Yb}$ being the most active catalyst. The copolymerization of TMC with ϵ -caprolactone initiated by $[\text{Ph}_2\text{NC}(\text{NCy})_2]_3\text{Yb}$ was also tested.^{165,351} The other members of this series of homoleptic lanthanide(III) guanidinates also exhibited extremely high activity for the ring-opening polymerization of ϵ -caprolactone giving polymers with high molecular weights. In this case, too, the different substituents at the guanidinate ligands have a great effect on the catalytic activity.¹⁶⁶

The polymerization of methyl methacrylate (MMA) by Cu(II) amidinate complexes (Scheme 222) in combination with alkyl aluminum complexes has been reported. The preferred alkylating agent is methylalumoxane (MAO) in



Scheme 222

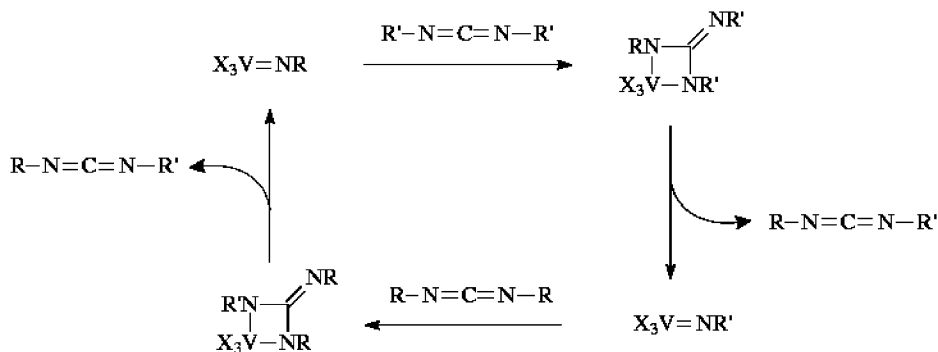
terms of improved yield and catalyst activity. Mechanistic studies indicated that the active species is a copper(I) complex.³³⁴

B. Hydroamination/cyclization reactions catalyzed by amidinate and guanidinate complexes

The guanidinate-supported titanium imido complex $[\text{Me}_2\text{NC}(\text{NPr}^i)_2]_2\text{Ti}=\text{NAr}$ ($\text{Ar} = 2,6\text{-Me}_2\text{C}_6\text{H}_3$) (cf. Section III.B.2) was reported to be an effective catalyst for the hydroamination of alkynes.¹⁹⁶ The catalytic activity of bulky amidinato bis(alkyl) complexes of scandium and yttrium (cf. Section III.B.1) in the intramolecular hydroamination/cyclization of 2,2-dimethyl-4-pentenylamine has been investigated and compared to the activity of the corresponding cationic mono(alkyl) derivatives.¹⁴³

C. Miscellaneous reactions catalyzed by amidinate and guanidinate complexes

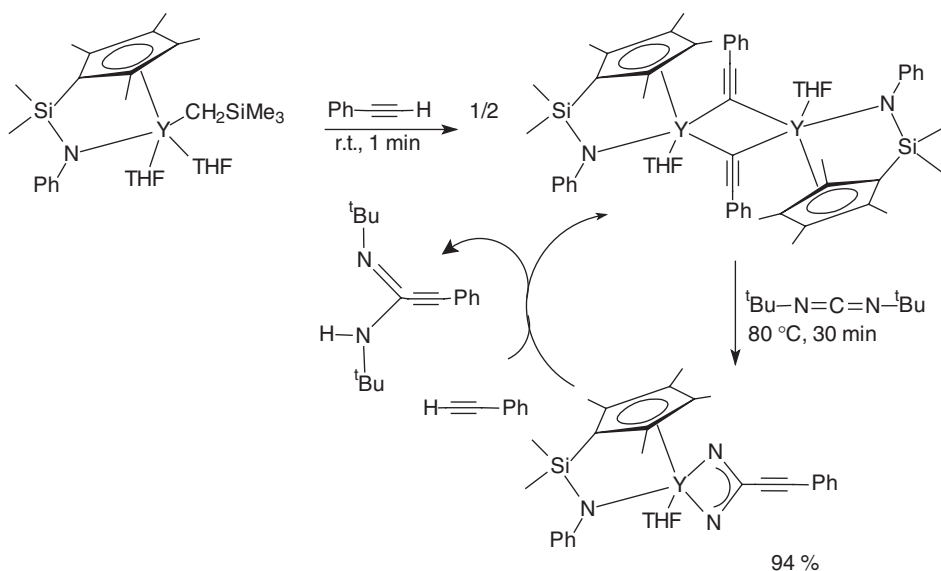
Amidinate complexes were included in a computational study of the catalytic synthesis of arylisocyanates from nitroaromatics.³⁵² Fixation of carbon dioxide has been achieved by oxalamidinato magnesium complexes. The reaction of oxalamidines with MeMgBr followed by uptake of CO_2 resulted in the formation of trimeric carbamate complexes.³⁵³ The bis(guanidinate)-supported titanium imido complex $[\text{Me}_2\text{NC}(\text{NPr}^i)_2]_2\text{Ti}=\text{NAr}$ ($\text{Ar} = 2,6\text{-Me}_2\text{C}_6\text{H}_3$) has been reported to be an effective catalyst for the guanylation of amines as well as the transamination of guanidines.¹⁹⁷ The catalytic guanylation of amines was achieved using a half-sandwich titanacarborane amide complex which forms a guanidinate derivative on treatment with 1,3-dicyclohexylcarbodiimide (cf. Section III.B.2).²⁰⁵ The formation of guanidines by coupling of carbodiimides and aromatic amines using imido vanadium complexes as catalysts has been investigated. The results demonstrated that the complex $\text{V}(=\text{NC}_6\text{H}_3\text{Pr}_2\text{-2,6})\text{Cl}_3$ is an effective catalyst for this process. As can be seen in Scheme 223, the catalytic cycle involves the formation of vanadium guanidinate intermediates.³⁵⁴



Scheme 223

The catalytic addition of various terminal alkynes to carbodiimides has been achieved with the use of an yttrium half-sandwich complex. This compound, shown in the catalytic cycle in [Scheme 224](#), reacts with 1 equivalent of phenylacetylene (or various ring-substituted derivatives thereof) in toluene to give the corresponding dimeric phenylacetylide in quantitative yield. Nucleophilic addition of the latter to 1,3-di-*tert*-butylcarbodiimide takes place rapidly at 80 °C to yield the propiolamidinate complex. Catalytic formation of propiolamidine was achieved when excess phenylacetylene and 1,3-di-*tert*-butylcarbodiimide (1:1) were added at 80 °C. A wide range of terminal alkynes could be used for this catalytic cross-coupling reaction.³⁵⁵

The cyclic tin tetrasulfido complexes $[\text{RC}(\text{NCy})_2][\text{N}(\text{SiMe}_3)_2]\text{SnS}_4$ ($\text{R} = \text{Me}$, Bu^t) have been found to be outstanding catalysts for the cyclotrimerization of aryl isocyanates to perhydro-1,3,5-triazine-2,4,6-triones (isocyanurates) at room temperature.^{134,131} Another good catalyst for the cyclotrimerization of phenyl isocyanate was found in the organoyttrium amidinate complex $\text{Cp}_2\text{Y}[\text{Bu}^t\text{C}(\text{NBU}^t)_2]$.¹⁵⁹ The catalytic $\text{C}=\text{N}$ metathesis of carbodiimides is effectively catalyzed by Group 4 (Ti, Zr) and Group 5 (Ta) terminal imido complexes supported by guanidinate ligands. Evidence suggests that this reaction proceeds *via* a sequential addition/elimination pathway.³⁵⁶ It was also found that the iridium guanidinate complex $\text{Cp}^*\text{Ir}[\text{ToI}\text{N}=\text{C}(\text{NToI})_2]$ ($\text{ToI} = p\text{-tolyl}$) serves as highly active catalyst for the metathesis of diaryl carbodiimides with each other and for the more difficult metathesis of diaryl carbodiimides with aryl isocyanates.²⁶⁶ The dinuclear palladium(II) oxalamidinate complex shown in [Scheme 197](#) ($\text{Ar} = \text{Ph}$) acts as highly selective precatalyst in the copper-free Sonogashira reaction between *p*-bromoacetophenone and phenylacetylene. In addition, the

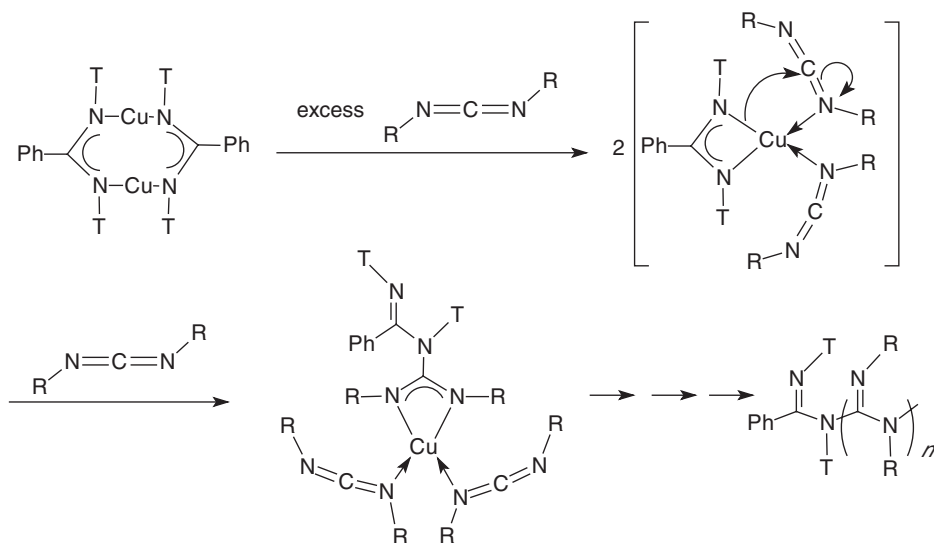


Scheme 224

analogous complex with $R = \text{tolyl}$ (Scheme 197) is an active and extremely selective precatalyst for the Negishi reaction between 3,5,6,8-tetrabromophenanthroline and $R-C\equiv C-ZnCl$ ($R = \text{Ph}, \text{SiPr}_3^i$) to form tetra-alkyne-substituted derivatives.³⁰³

Amidinate complexes of copper(I) and copper(II) have been found to catalyze the polymerization of carbodiimides. The copper catalysts are highly active even under air and oxygen. It was shown that the catalytic activity of an air-stable copper(II) amidinato complex is almost equal to that of reported air-sensitive titanium(IV) amidinate initiators. Scheme 225 illustrates the proposed reaction mechanism.^{357,358}

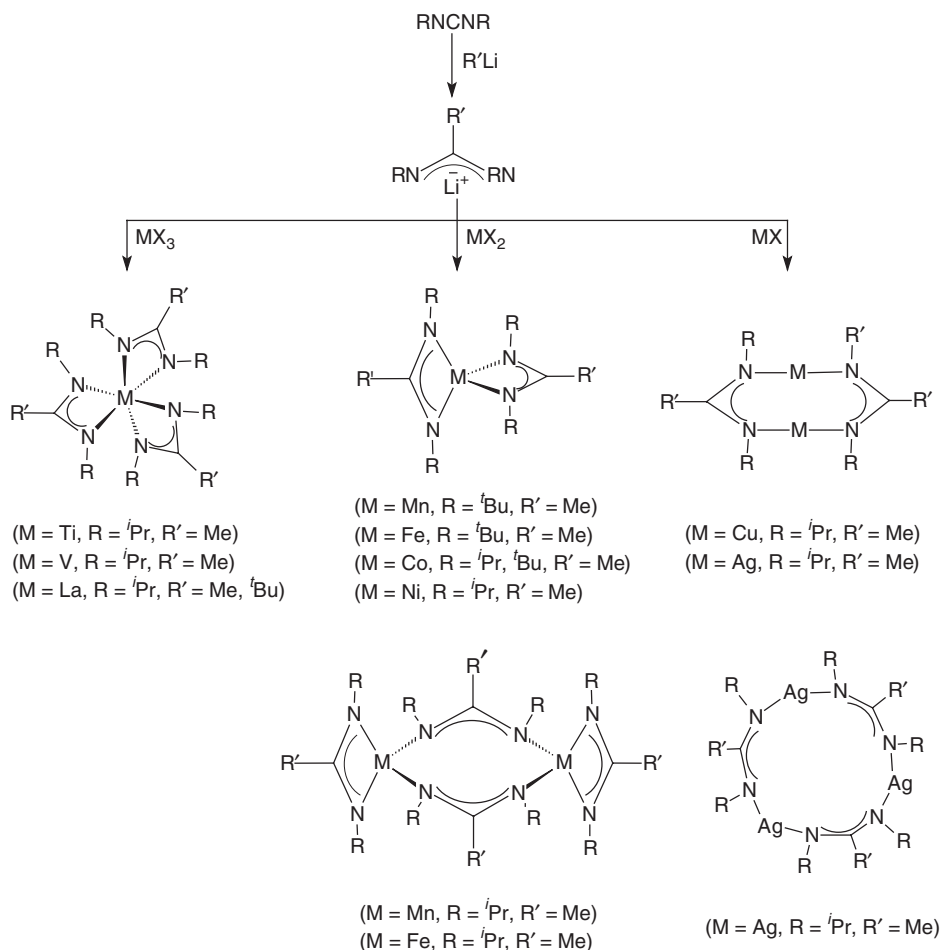
The manufacture of polysilanes using metal amidinate catalysts has been patented. For example, PhSiH_3 was polymerized in the presence of $\text{Cp}[\text{PhC}(\text{NSiMe}_3)_2]\text{ZrCl}_2$ and BuLi to give a syndiotactic polysilane in 77% yield.³⁵⁹ Dinuclear organopalladium complexes containing donor-functionalized oxalamidinate ligands (cf. Scheme 199) were found to be highly active, selective and long-living catalysts in the Heck reaction of *p*-bromoacetophenone and *n*-butylacrylate.^{305a} Dinuclear and mononuclear palladium complexes having *N,N'*-bis[2-(diphenylphosphino)phenyl]amidinate as a ligand were reported to catalyze the cross-addition of triisopropylsilylacetylene to unactivated internal alkynes, giving enynes selectively. Several terminal alkynes also gave cross-adducts selectively, although the yields were moderate.^{305b} Atom-transfer radical cyclization (ATRC) and addition (ATRA) catalyzed by a coordinatively unsaturated diruthenium amidinate complex (cf. Scheme 146) have been investigated. As an example of ATRC, the cationic diruthenium amidinate was found to exhibit excellent catalytic reactivity for the cyclization of *N*-allyl α -halogenated acetamides including an alkaloid skeleton at ambient temperature.³⁵⁰



Scheme 225

VI. AMIDINATE AND GUANIDINATE COMPLEXES IN MATERIALS SCIENCE

Several patents dealing with the use of volatile metal amidinate complexes in MOCVD or ALD processes have appeared in the literature.^{167,360–364} The use of volatile amidinato complexes of Al, Ga, and In in the chemical vapor deposition of the respective nitrides has been reported. For example, $[\text{PhC}(\text{NPh})_2]_2\text{GaMe}$ was prepared in 68% yield from GaMe_3 and N,N' -diphenylbenzamidine in toluene. Various samples of this and related complexes could be heated to 600 °C in N_2 to give GaN.³⁶¹ A series of homoleptic metal amidinates of the general type $[\text{M}(\text{RC}(\text{NR}')_2)_n]_x$ ($\text{R} = \text{Me}, \text{Bu}^t$; $\text{R} = \text{Pr}^i, \text{Bu}^t$) has been prepared for the transition metals Ti, V, Mn, Fe, Co, Ni, Cu, Ag, and La. The types of products are summarized in Scheme 226. The new compounds were found to have properties well-suited for use as precursors for atomic layer deposition (ALD) of thin films.



Scheme 226

They have high volatility, high thermal stability, and high and properly self-limited reactivity with molecular hydrogen, depositing pure metals, or water vapor, depositing metal oxides.^{365,366} The chromium(III) amidinate complexes shown in Schemes 121 and 122 have been found to be volatile and to sublime with <1% residue between 120 and 165 °C at 0.05 Torr. In addition, these complexes are thermally stable at >300 °C under an inert atmosphere such as nitrogen or argon. Due to the good volatility and high thermal stability, these compounds are promising precursors for the growth of chromium-containing thin films using ALD.^{223b} A highly volatile asymmetric iron(II) amidinate, $\text{Fe}[\text{MeC}(\text{NEt})(\text{NBU}^t)]_2$, was isolated starting from different iron(II) precursors such as acetylacetonate, acetate, and chloride.^{366b}

ALD of Er_2O_3 films has been demonstrated using $\text{Er}[\text{MeC}(\text{NBU}^t)]_3$ and ozone with substrate temperatures between 225–300 °C. The growth rate increased linearly with substrate temperature from 0.37 Å per cycle at 225 °C to 0.55 Å per cycle at 300 °C (Figure 37). The as-deposited films were amorphous below 300 °C, but showed reflections due to cubic Er_2O_3 at 300 °C.¹⁶⁷

Titanium(IV) guanidinato complexes, which are easily accessible by the standard synthetic routes (cf. Section III.B.2), have been studied as precursors to titanium carbonitride. Thin films of titanium carbonitride were obtained by low-pressure chemical vapor deposition of either $[(\text{Me}_3\text{Si})_2\text{NC}(\text{NPr}^i)_2]\text{TiCl}(\text{NMe}_2)_2$ or $[\text{Me}_2\text{NC}(\text{NPr}^i)_2]_2\text{TiCl}_2$ at 600 °C.¹⁷⁹ Most recent developments in this field comprise the synthesis of novel guanidinate-stabilized monomeric amide complexes of zirconium and hafnium and their use as promising precursors of

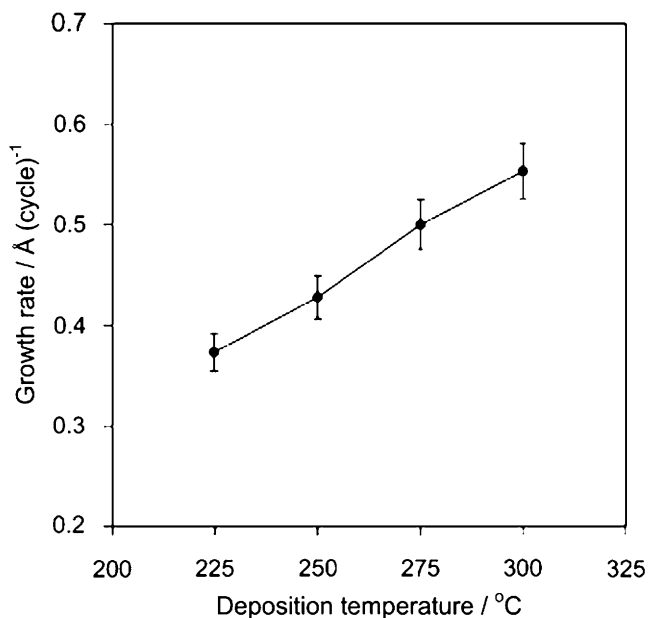


Figure 37 Growth rate of Er_2O_3 films deposited from $\text{Er}[\text{MeC}(\text{NBU}^t)]_3$.¹⁶⁷

MOCVD for ZrO_2 and HfO_2 , respectively.^{367,368} For example, the new bis(guanidinato)zirconium diamide $[\text{MeEtNC}(\text{NPr}^i)_2]_2\text{Zr}(\text{NMeEt})_2$ was synthesized *via* double insertion of $\text{Pr}^i\text{N}=\text{C}=\text{NPr}^i$ into the $\text{Zr}-\text{N}$ bonds of $\text{Zr}(\text{NMeEt})_4$ and isolated in the form of colorless crystals (m.p. 128°C) which are highly soluble in toluene and diethyl ether. This compound is thermally stable and can be sublimed quantitatively that renders it promising for thin film growth using vapor deposition techniques like CVD or ALD. The use of this complex for CVD of ZrO_2 on $\text{Si}(000)$ substrates was attempted in combination with oxygen as the oxidant. Stoichiometric ZrO_2 films with preferred orientation at lower temperatures were obtained, and the films were almost carbon-free. Preliminary electrical characterization of the ZrO_2 films showed encouraging results for possible applications in dielectric oxide structures.³⁶⁷ The same synthetic route, i.e., carbodiimide insertion into $\text{M}-\text{N}$ bonds, was employed in the preparation of the closely related bis(guanidinato)hafnium diamides $[\text{R}_2\text{NC}(\text{NPr}^i)_2]_2\text{Hf}(\text{NR}_2)_2$ ($\text{R}_2 = \text{Me}_2$; Me, Et ; Et_2). The thermal characteristics of these compounds too were found to be promising for the production of HfO_2 thin films by vapor deposition techniques. MOCVD experiments with $[\text{MeEtNC}(\text{NPr}^i)_2]_2\text{Hf}(\text{NMeEt})_2$ resulted in smooth, uniform, and stoichiometric HfO_2 thin films at relatively low deposition temperatures.³⁶⁸ Metal(IV) tetrakis(N, N' -dialkylamidinates) and their use in vapor deposition processes were claimed in a recent patent application. Exemplary metals include Zr, Hf, Nb, Ta, Mo, W, and U. These compounds are volatile, thermally highly stable, and suitable for vapor deposition of metals and their oxides, nitrides and other compounds.³⁶⁹

Metathetical reactions between $\text{NbCl}_4(\text{THF})_2$, NbCl_5 , TaCl_5 , $[(\text{Et}_2\text{N})_2\text{TaCl}_3]_2$ or $(\text{R}_2\text{N})_3\text{Ta}(=\text{NBu}^t)$ ($\text{R} = \text{Me}, \text{Et}$) with various amounts of lithium amidinates have been employed to synthesize the corresponding heteroleptic niobium and tantalum amidinate complexes such as $[(\text{Me}_3\text{Si})_2\text{NC}(\text{NCy})_2]_2\text{NbCl}_2$. The products have been investigated as potential precursors to metal nitrides. Volatility was reached for some of the new species either for Ta(V) or Nb(IV) but the rate of sublimation was too slow for applications *via* conventional MOCVD.^{214,215} Volatile amidinato complexes of Cu, Ag, and Au have been employed in the chemical vapor deposition of the respective metals, for example for the manufacture of integrated circuits.^{360,364} A full series of copper(I) amidinates of the general type $[\{\text{RC}(\text{NR}')_2\}\text{Cu}]_2$ ($\text{R} = \text{Me}, \text{Bu}''$; $\text{R}' = \text{Pr}''$, Pr' , Bu'' , Bu^i , Bu^s , Bu^t) have been synthesized and characterized. These compounds are planar dimers, bridged by nearly linear $\text{N}-\text{Cu}-\text{N}$ bonds. Their properties (volatility, low melting point, high thermal stability, and self-limited surface reactivity) are well-suited for ALD of copper metal films that are pure, highly conductive, and strongly adherent to substrates.²⁷² Related copper(I) guanidinate dimers $[\{\text{MR}_2\text{NC}(\text{NPr}^i)_2\}\text{Cu}]_2$ ($\text{R}_2\text{N} = \text{Me}_2\text{N}$, $\text{Pr}^i(\text{H})\text{N}$) were generated by a salt-metathesis route from lithium guanidinates and CuCl and structurally characterized.³⁷⁰ The guanidinates differ from the known amidinate dimers²⁷² because of a large torsion angle of the dimer ring. This was found to have a direct effect on their thermal chemistry. The copper guanidinates underwent carbodiimide deinsertion to produce copper metal at temperatures between 225 and 250°C in the gas phase and at 125°C in solution. The guanidinate compounds deposited

crystalline copper at 225 °C in a simple chemical vapor deposition experiment.³⁷⁰ A patent application also claims the use of copper(I) amidinates and guanidines for forming copper thin films using CVD, ALD, and rapid vapor deposition processes.³⁷¹

VII. FUTURE OUTLOOK

During the past 20 years, amidinate and guanidinate anions have emerged as an extremely versatile class of ligands for numerous metals spanning the entire Periodic Table. The elements, for which amidinate and guanidinate complexes have been reported, range from lithium to the actinides. Both ligand systems can be regarded as “steric cyclopentadienyl equivalents” and, in fact, their versatility rivals that of the cyclopentadienyl derivatives. This results from the fact that numerous different substituents can be introduced at the carbon as well as the nitrogen atoms of the N–C–N unit. By varying the substitution pattern, the steric as well as the electronic properties of amidinate and guanidinate ligands can be tuned by a large degree. Especially the steric bulk of these anions can be varied to such an extent, that either chelating or bridging coordination modes can be enforced. Other variations of the amidinate and guanidinate ligands include the attachment of pendant functional groups or the incorporation of amidinate or guanidinate units into bicyclic ring systems. Interesting results were also obtained using bis(amidinate) ligands.

The first decade of research in amidinate and guanidinate coordination chemistry was dominated by the search for novel compounds and structural types containing numerous main group and transition metals. The “Periodic Table of amidinate and guanidinate complexes” is now well filled and shows only a small number of white spots. Some groups of elements may have been somewhat neglected, but amidinate and guanidinate complexes are now known for almost every naturally occurring metallic or semimetallic element. Thus it can be foreseen, that the simple search for new compounds will not be the most important task in the future. One synthetic aspect that merits further investigation is the stabilization of unusually high or low oxidation states using amidinate and guanidinate ligands. The syntheses of divalent lanthanide and trivalent titanium complexes containing such ligands (cf. [Section III.B.1](#)) are promising examples for this approach. On the other hand, the stabilization of unusually high oxidation states (e.g., cerium+4, manganese +3, etc.) with the use of amidinate and guanidinate ligands is far from being well explored. Furthermore, there is no doubt that the upcoming years will witness a shift of research activities in this area from pure preparative chemistry to applications in various fields. Among these activities, catalysis involving amidinate and guanidinate complexes is expected to play the most important role. Olefin polymerization catalyzed by such complexes is already well established. A major goal in this area would certainly be the establishment of industrially applicable metal amidinate or guanidinate catalysts for olefin polymerizations. As outlined in [Section V](#), certain amidinate and guanidinate exhibit high catalytic activities

not only in olefin polymerization but also in the polymerization of polar monomers as well as various other catalytic reactions. Future research in this area will certainly be directed toward broadening the scope of synthetically useful reactions catalyzed by metal amidinate or guanidinate complexes. The second main area, for which increased research activities can be expected for the future, is the application of metal amidinates and guanidinates in materials science. As shown in Section VI, such compounds have already found interesting applications especially as volatile precursors for the MOCVD or ALD production of thin films. In this respect the potential of metal amidinate and guanidinate complexes is far from being exhausted.

ACKNOWLEDGMENTS

The author thanks Ms. Petra Kuske, Dr. Volker Lorenz, and Dr. Stephan Gießmann for their tremendous help in drawing the Schemes for this manuscript. I also thank Prof. Tristram Chivers, University of Calgary, for valuable comments. Our own work described in this report was generously supported by the Deutsche Forschungsgemeinschaft. This support is most gratefully acknowledged. Special thanks are also due to my coworkers, whose names appear in the list of references, and to the Georg-August-Universität Göttingen, the Otto-von-Guericke-Universität Magdeburg, and the Fonds der Chemischen Industrie for financial support.

REFERENCES

- (1) Most recent review articles: (a) Dehnicke, K. *Chem.-Ztg.* **1990**, 114, 295. (b) Barker, J.; Kilner, M. *Coord. Chem. Rev.* **1994**, 133, 219. (c) Edelmann, F. T. *Coord. Chem. Rev.* **1994**, 137, 403. (d) Edelmann, F. T. *Top. Curr. Chem.* **1996**, 179, 113. (e) Nagashima, H.; Kondo, H.; Hayashida, T.; Yamaguchi, Y.; Gondo, M.; Masuda, S.; Miyazaki, K.; Matsubara, K.; Kirchner, K. *Coord. Chem. Rev.* **2003**, 245, 177.
- (2) Sanger, A. R. *Inorg. Nucl. Chem. Lett.* **1973**, 9, 351.
- (3) Boéré, R. T.; Oakley, R. T.; Reed, R. W. *J. Organomet. Chem.* **1987**, 331, 161.
- (4) Chandra, G.; Jenkins, A. D.; Lappert, M. F.; Srivastava, R. C. *J. Chem. Soc.* **1970**, 2550.
- (5) (a) Bailey, P. J.; Pace, S. *Coord. Chem. Rev.* **2001**, 214, 91. (b) Coles, M. P. *Dalton Trans.* **2006**, 985.
- (6) Vrieze, K.; van Koten, G. *Recl. Trav. Chim. Pays-Bas* **1980**, 99, 145.
- (7) Roesky, H. W.; Mainz, B.; Noltemeyer, M. *Z. Naturforsch.* **1990**, 45b, 53.
- (8) Knösel, F.; Noltemeyer, M.; Edelmann, F. T. *Z. Naturforsch.* **1989**, 44b, 1171.
- (9) Steiner, A.; Zacchini, S.; Richards, P. I. *Coord. Chem. Rev.* **2002**, 227, 193.
- (10) Scherer, O. J.; Schmitt, R. *J. Organomet. Chem.* **1969**, 16, P11.
- (11) (a) Kuyper, J.; Keijzer, P. C.; Vrieze, K. *J. Organomet. Chem.* **1976**, 116, 1. (b) Kuyper, J.; Vrieze, K. *J. Chem. Soc., Chem. Commun.* **1976**, 64.
- (12) Hänssgen, D.; Steffens, R. *J. Organomet. Chem.* **1982**, 236, 53.
- (13) Hänssgen, D.; Plum, R. *Chem. Ber.* **1987**, 120, 1063.
- (14) Roesky, H. W.; Katti, K. V.; Seseke, U.; Witt, M.; Egert, E.; Herbst, R.; Sheldrick, G. M. *Angew. Chem.* **1986**, 98, 447. Roesky, H. W.; Katti, K. V.; Seseke, U.; Witt, M.; Egert, E.; Herbst, R.; Sheldrick, G. M. *Angew. Chem. Int. Ed.* **1986**, 25, 477.
- (15) Roesky, H. W.; Katti, K. V.; Seseke, U.; Schmidt, H.-G.; Egert, E.; Herbst, R.; Sheldrick, G. M. *J. Chem. Soc., Dalton Trans.* **1987**, 847.
- (16) Katti, K. V.; Roesky, H. W.; Rietzel, M. *Inorg. Chem.* **1987**, 26, 814.
- (17) Witt, M.; Roesky, H. W.; Noltemeyer, M.; Sheldrick, G. M. *Angew. Chem.* **1988**, 100, 852. Witt, M.; Roesky, H. W.; Noltemeyer, M.; Sheldrick, G. M. *Angew. Chem. Int. Ed.* **1989**, 27, 851.

- (18) Roesky, H. W.; Olms, P.; Witt, M.; Keller, K.; Stalke, D.; Henkel, T.; Sheldrick, G. M. *J. Chem. Soc., Chem. Commun.* **1989**, 366.
- (19) Recknagel, A.; Witt, M.; Edelmann, F. T. *J. Organomet. Chem.* **1989**, 371, C40.
- (20) Fußstetter, H.; Nöth, H. *Chem. Ber.* **1979**, 112, 3672.
- (21) Heine, A.; Fest, D.; Habben, C. D.; Meller, A.; Sheldrick, G. M. *J. Chem. Soc., Chem. Commun.* **1990**, 742.
- (22) Fest, D.; Habben, C. D.; Meller, A.; Sheldrick, G. M.; Stalke, D.; Pauer, F. *Chem. Ber.* **1990**, 123, 703.
- (23) Brask, J. K.; Chivers, T.; Schatte, G. *Chem. Commun.* **2000**, 1805.
- (24) Manke, D. R.; Nocera, D. G. *Inorg. Chem.* **2003**, 42, 4431.
- (25) Chivers, T.; Eisler, D. J.; Fedorchuk, C.; Schatte, G.; Tuononen, H. M.; Boéré, R. T. *Chem. Commun.* **2005**, 3930.
- (26) Chivers, T.; Eisler, D. J.; Fedorchuk, C.; Schatte, G.; Tuononen, H. M.; Boéré, R. T. *Inorg. Chem.* **2006**, 45, 2119.
- (27) Fedorchuk, C.; Copsey, M. C.; Chivers, T. *Coord. Chem. Rev.* **2007**, 251, 897.
- (28) Cotton, F. A.; Daniels, L. M.; Murillo, C. A. *Angew. Chem.* **1992**, 104, 795. Cotton, F. A.; Daniels, L. M.; Murillo, C. A. *Angew. Chem. Int. Ed.* **1992**, 31, 737.
- (29) Hao, S.; Gambarotta, S.; Bensimon, C.; Edema, J. J. H. *Inorg. Chim. Acta* **1993**, 213, 65.
- (30) Cotton, F. A.; Daniels, L. M.; Murillo, C. A. *Inorg. Chem.* **1993**, 32, 2881.
- (31) Cotton, F. A.; Daniels, L. M.; Maloney, D. J.; Murillo, C. A. *Inorg. Chim. Acta* **1996**, 249, 9.
- (32) Cotton, F. A.; Daniels, L. M.; Maloney, D. J.; Matonic, J. H.; Murillo, C. A. *Inorg. Chim. Acta* **1997**, 256, 283.
- (33) Cotton, F. A.; Daniels, L. M.; Feng, X.; Maloney, D. J.; Matonic, J. H.; Murillo, C. A. *Inorg. Chim. Acta* **1997**, 256, 291.
- (34) Cotton, F. A.; Feng, X.; Murillo, C. A. *Inorg. Chim. Acta* **1997**, 256, 303.
- (35) Cotton, F. A.; Daniels, L. M.; Falvello, L. R.; Matonic, J. H.; Murillo, C. A. *Inorg. Chim. Acta* **1997**, 256, 269.
- (36) Cotton, F. A.; Daniels, L. M.; Matonic, J. H.; Murillo, C. A. *Inorg. Chim. Acta* **1997**, 256, 277.
- (37) Cotton, F. A.; Murillo, C. A.; Pascual, I. *Inorg. Chem.* **1999**, 38, 2182.
- (38) Cotton, F. A.; Daniels, L. M.; Murillo, C. A.; Pascual, I.; Zhou, H.-C. *J. Am. Chem. Soc.* **1999**, 121, 6856.
- (39) Cotton, F. A.; Dalal, N. S.; Liu, C. Y.; Murillo, C. A.; North, J. M.; Wang, X. *J. Am. Chem. Soc.* **2003**, 125, 12945.
- (40) Cotton, F. A.; Lin, C.; Murillo, C. A. *Inorg. Chem.* **2001**, 40, 478.
- (41) Cotton, F. A.; Lin, C.; Murillo, C. A. *Inorg. Chem.* **2001**, 40, 472.
- (42) Cotton, F. A.; Lin, C.; Murillo, C. A. *Inorg. Chem.* **2001**, 40, 6413.
- (43) Cotton, F. A.; Donahue, J. P.; Lin, C.; Murillo, C. A. *Inorg. Chem.* **2001**, 40, 1234.
- (44) Cotton, F. A.; Daniels, L. M.; Lin, C.; Murillo, C. A.; Yu, S.-Y. *Dalton Trans.* **2001**, 502.
- (45) Cotton, F. A.; Liu, C. Y.; Murillo, C. A. *Inorg. Chem.* **2004**, 43, 2267.
- (46) Nijkuis, C. A.; Jellema, E.; Sciarone, T. J. J.; Meetsma, A.; Budzelaar, P. H. M.; Hessen, B. *Eur. J. Inorg. Chem.* **2005**, 2089.
- (47) Schmidt, J. A. R.; Arnold, J. *Chem. Commun.* **1999**, 2149.
- (48) Schmidt, J. A. R.; Arnold, J. *Organometallics* **2002**, 21, 2306.
- (49) Schmidt, J. A. R.; Arnold, J. *Dalton Trans.* **2002**, 2890.
- (50) Schmidt, J. A. R.; Arnold, J. *Dalton Trans.* **2002**, 3454.
- (51) Jenkins, H. A.; Abeysekera, D.; Dickie, D. A.; Clyburne, J. A. C. *Dalton Trans.* **2002**, 3919.
- (52) Baker, R. J.; Jones, C. J. *Organomet. Chem.* **2006**, 691, 65.
- (53) Cole, M. L.; Junk, P. C. *New J. Chem.* **2005**, 29, 135.
- (54) (a) Cole, M. L.; Deacon, G. B.; Junk, P. C.; Konstas, K. *Chem. Commun.* **2005**, 1581. (b) Cole, M. L.; Deacon, G. B.; Forsyth, C. M.; Junk, P. C.; Konstas, K.; Wang, J. *Chem. Eur. J.* **2007**, 13, 8092.
- (55) Boéré, R. T.; Klassen, V.; Wolmershäuser, G. *Dalton Trans.* **1998**, 4147.
- (56) Wedler, M.; Knösel, F.; Pieper, U.; Stalke, D.; Edelmann, F. T.; Amberger, H.-D. *Chem. Ber.* **1992**, 125, 2171.
- (57) Hagen, C.; Reddmann, H.; Amberger, H.-D.; Edelmann, F. T.; Pegelow, U.; Shalimoff, G. V.; Edelstein, N. M. *J. Organomet. Chem.* **2005**, 690. Hagen, C.; Reddmann, H.; Amberger, H.-D.; Edelmann, F. T.; Pegelow, U.; Shalimoff, G. V.; Edelstein, N. M. *J. Organomet. Chem.* **1993**, 462, 69.

- (58) Wedler, M.; Knösel, F.; Edelmann, F. T.; Behrens, U. *Chem. Ber.* **1992**, 125, 1313.
- (59) Lubben, T. V.; Wolczanski, P. T.; Van Duyne, G. D. *Organometallics* **1984**, 3, 977.
- (60) Schareina, T.; Kempe, R. *Synth. Meth. Organomet. Inorg. Chem.* **2002**, 1.
- (61) Hitchcock, P. B.; Lappert, M. F.; Merle, P. G. *Phosphorus, Sulfur Silicon* **2001**, 169, 39.
- (62) Richter, J.; Feiling, J.; Schmidt, H.-G.; Noltemeyer, M.; Brüser, W.; Edelmann, F. T. *Z. Anorg. Allg. Chem.* **2004**, 630, 1269.
- (63) Hagadorn, J. R.; Arnold, J. J. *Organomet. Chem.* **2001**, 637–639, 521.
- (64) Pietryga, J. M.; Jones, J. N.; Macdonald, C. L. B.; Moore, J. A.; Cowley, A. H. *Polyhedron* **2006**, 25, 259.
- (65) Boyd, C. L.; Tyrrell, B. R.; Mountford, P. *Acta Cryst.* **2002**, E58, m597.
- (66) Villiers, C.; Thuéry, P.; Ephritikhine, M. *Eur. J. Inorg. Chem.* **2004**, 4624.
- (67) Hagadorn, J. R.; Arnold, J. *Inorg. Chem.* **1997**, 36, 132.
- (68) Giesbrecht, G. R.; Shafir, A.; Arnold, J. *Dalton Trans.* **1999**, 3601.
- (69) Knapp, C.; Lork, E.; Watson, P. G.; Mews, R. *Inorg. Chem.* **2002**, 41, 2014.
- (70) Chivers, T.; Downard, A.; Parvez, M. *Inorg. Chem.* **1999**, 38, 4347.
- (71) Junk, P. C.; Cole, M. L. *Chem. Commun.* **2007**, 1579.
- (72) (a) Baldamus, J.; Berghof, C.; Cole, M. L.; Hey-Hawkins, E.; Junk, P. C.; Louis, L. M. *Eur. J. Inorg. Chem.* **2002**, 2878. (b) Cole, M. L.; Davis, A. J.; Jones, C.; Junk, P. C. *New J. Chem.* **2005**, 29, 1404.
- (73) Brzezinski, B.; Jarczewski, A.; Stanczyk, M.; Zundel, G. J. *Mol. Struct.* **1993**, 297, 81.
- (74) Baldamus, J.; Berghof, C.; Cole, M. L.; Evans, D. J.; Hey-Hawkins, E.; Junk, P. C. *Dalton Trans.* **2002**, 4185.
- (75) Baldamus, J.; Berghof, C.; Cole, M. L.; Evans, D. J.; Hey-Hawkins, E.; Junk, P. C. *Dalton Trans.* **2002**, 2802.
- (76) Cole, M. L.; Junk, P. C. *J. Organomet. Chem.* **2003**, 666, 55.
- (77) Cole, M. L.; Evans, D. J.; Junk, P. C.; Smith, M. K. *Chem. Eur. J.* **2003**, 9, 415.
- (78) (a) Cole, M. L.; Junk, P. C.; Louis, L. M. *Dalton Trans.* **2002**, 3906. (b) Cole, M. L.; Davies, A. J.; Jones, C.; Junk, P. C. *J. Organomet. Chem.* **2004**, 689, 3093.
- (79) Cole, M. L.; Davies, A. J.; Jones, C.; Junk, P. C. *J. Organomet. Chem.* **2007**, 692, 2508.
- (80) Niemeyer, M.; Power, P. *Inorg. Chem.* **1997**, 36, 4688.
- (81) Srinivas, B.; Chang, C.-C.; Chen, C.-H.; Chiang, M. Y.; Chen, I.-T.; Wang, Y.; Lee, G.-H. *Dalton Trans.* **1997**, 957.
- (82) Sadique, A. R.; Heeg, M. J.; Winter, C. H. *Inorg. Chem.* **2001**, 40, 6349.
- (83) Xia, A.; El-Kaderi, H.; Heeg, M. J.; Winter, C. H. *J. Organomet. Chem.* **2003**, 682, 224.
- (84) Chivers, T.; Copsey, M. C.; Fedorchuk, C.; Parvez, M.; Stubbs, M. *Organometallics* **2005**, 24, 1919.
- (85) Cole, M. L.; Evans, D. J.; Junk, P. C.; Louis, L. M. *New J. Chem.* **2002**, 26, 1015.
- (86) Westerhausen, M.; Schwarz, W. Z. *Naturforsch.* **1992**, 47b, 453.
- (87) Feil, F.; Harder, S. *Eur. J. Inorg. Chem.* **2005**, 4438.
- (88) Cole, M. L.; Deacon, G. B.; Forsyth, C. M.; Konstas, K.; Junk, P. C. *Dalton Trans.* **2006**, 3360.
- (89) (a) Findlater, M.; Hill, N. J.; Cowley, A. H. *Polyhedron* **2006**, 25, 983. (b) Pierce, G. A.; Coombs, N. D.; Willock, D. J.; Day, J. K.; Stasch, A.; Aldridge, S. *Dalton Trans.* **2007**, 4405.
- (90) (a) Blais, P.; Chivers, T.; Downard, A.; Parvez, M. *Can. J. Chem.* **2000**, 78, 10. (b) Chivers, T.; Fedorchuk, C.; Parvez, M. *Inorg. Chem.* **2004**, 43, 2643.
- (91) Lu, Z.; Hill, N. J.; Findlater, M.; Cowley, A. H. *Inorg. Chim. Acta* **2007**, 360, 1316.
- (92) Hill, N. J.; Moore, J. A.; Findlater, M.; Cowley, A. H. *Chem. Commun.* **2005**, 5462.
- (93) Hill, N. J.; Findlater, M.; Cowley, A. H. *Dalton Trans.* **2005**, 3229.
- (94) Jones, C.; Junk, P. C.; Kloth, M.; Proctor, K. M.; Stasch, A. *Polyhedron* **2006**, 25, 1592.
- (95) Coles, M. P.; Swenson, D. C.; Jordan, R. F.; Young, V. G. Jr. *Organometallics* **1998**, 17, 4042.
- (96) Abeysekera, D.; Robertson, K. N.; Cameron, T. S.; Clyburne, J. A. C. *Organometallics* **2001**, 20, 5532.
- (97) Rowley, C. N.; DiLabio, G. A.; Barry, S. T. *Inorg. Chem.* **2005**, 44, 1983.
- (98) Kenney, A. P.; Yap, G. P. A.; Richeson, D. S.; Barry, S. T. *Inorg. Chem.* **2005**, 44, 2926.

- (99) (a) Chang, C.-C.; Hsiung, C.-S.; Su, H.-L.; Srinivas, B.; Chiang, M. Y.; Lee, G.-H.; Wang, Y. *Organometallics* **1998**, *17*, 1595. (b) Brazeau, A. L.; DiLabio, G. A.; Kreisel, K. A.; Monillas, W.; Yap, G. P. A.; Barry, S. T. *Dalton Trans.* **2007**, 3297.
- (100) Aeilts, S. L.; Coles, M. P.; Swenson, D. C.; Jordan, R. F.; Young, V. G. Jr. *Organometallics* **1998**, *17*, 3265.
- (101) Brazeau, A. L.; Wang, Z.; Rowley, C. N.; Barry, S. T. *Inorg. Chem.* **2006**, *45*, 2276.
- (102) Coles, M. P.; Swenson, D. C.; Jordan, R. F.; Young, V. G. Jr. *Organometallics* **1997**, *16*, 5183.
- (103) (a) Talarico, G.; Budzelaar, P. H. M. *Organometallics* **2000**, *19*, 5691. (b) Meier, R. J.; Koglin, E. *J. Phys. Chem. A* **2001**, *105*, 3867.
- (104) Baugh, L. S.; Sussano, J. A. *J. Polym. Sci.* **2002**, *40*, 1663.
- (105) Ihara, E.; Young, V. G.; Jordan, R. F. *J. Am. Chem. Soc.* **1998**, *120*, 8277.
- (106) Coles, M. P.; Jordan, R. F. *J. Am. Chem. Soc.* **1997**, *119*, 8125.
- (107) Dagorne, S.; Guzei, I. A.; Coles, M. P.; Jordan, R. F. *J. Am. Chem. Soc.* **2000**, *122*, 274.
- (108) Barker, J.; Aris, D. R.; Blacker, N. C.; Errington, W.; Phillips, P. R.; Wallbridge, M. G. H. *J. Organomet. Chem.* **1999**, *586*, 138.
- (109) Amo, V.; Andrés, R.; de Jesús, E.; de la Mata, F. J.; Flores, J. C.; Gómez, R.; Gómez-Sal, M. P.; Turner, J. F. C. *Organometallics* **2005**, *24*, 2331.
- (110) Dagorne, S.; Jordan, R. F.; Young, V. G. Jr. *Organometallics* **1999**, *18*, 4619.
- (111) Jones, C.; Junk, P. C.; Platts, J. A.; Rathmann, D.; Stasch, A. *Dalton Trans.* **2005**, 2497.
- (112) Jones, C.; Junk, P. C.; Platts, J. A.; Stasch, A. *J. Am. Chem. Soc.* **2006**, *128*, 2206.
- (113) Jones, C.; Aldridge, S.; Gans-Eichler, T.; Stasch, A. *Dalton Trans.* **2006**, 5357.
- (114) Green, S. P.; Jones, C.; Stasch, A. *Inorg. Chem.* **2007**, *46*, 11.
- (115) Aris, D. R.; Barker, J.; Errington, W.; Wallbridge, M. G. H. *Acta Cryst.* **2004**, *E60*, m302.
- (116) Zjou, Y.; Richeson, D. S. *Inorg. Chem.* **1996**, *35*, 2448.
- (117) Patton, J. T.; Bokota, M. M.; Abboud, K. A. *Organometallics* **2002**, *21*, 2145.
- (118) Zjou, Y.; Richeson, D. S. *Inorg. Chem.* **1996**, *35*, 1423.
- (119) Baker, R. J.; Jones, C.; Junk, P. C.; Cloth, M. *Angew. Chem.* **2004**, *116*, 3940. Baker, R. J.; Jones, C.; Junk, P. C.; Cloth, M. *Angew. Chem. Int. Ed.* **2004**, *43*, 3852.
- (120) Cole, M. L.; Jones, C.; Junk, P. C.; Kloth, M.; Stasch, A. *Chem. Eur. J.* **2005**, *11*, 4482.
- (121) Kühl, O. *Coord. Chem. Rev.* **2004**, *248*, 411.
- (122) (a) Schoeller, W. W.; Sundermann, A.; Reiher, M. *Inorg. Chem.* **1999**, *38*, 29. (b) Schoeller, W. W.; Sundermann, A.; Reiher, M.; Rozhenko, A. *Eur. J. Inorg. Chem.* **1999**, 1155.
- (123) (a) Segmüller, T.; Schlüter, P. A.; Drees, M.; Schier, A.; Nogai, S.; Nitzel, N. W.; Straßner, T.; Karsch, H. H. *J. Organomet. Chem.* **2007**, *692*, 2789. (b) Karsch, H. H.; Bienlein, F.; Sladek, A.; Heckel, M.; Burger, K. *J. Am. Chem. Soc.* **1995**, *117*, 5160.
- (124) So, C.-W.; Roesky, H. W.; Gurubasavaraj, P. M.; Ostwald, R. B.; Gamer, M. T.; Jones, P. G.; Blarrock, S. J. *J. Am. Chem. Soc.* **2007**, *129*, 12049.
- (125) Foley, S. R.; Bensimon, C.; Richeson, D. S. *J. Am. Chem. Soc.* **1997**, *119*, 10359.
- (126) Karsch, H. H.; Schlüter, P. A.; Reisky, M. *Eur. J. Inorg. Chem.* **1998**, 433.
- (127) Foley, S. R.; Yap, G. P. A.; Richeson, D. S. *Dalton Trans.* **2000**, 1663.
- (128) Green, S. P.; Jones, C.; Junk, P.; Lippert, K.-A.; Stasch, A. *Chem. Commun.* **2006**, 3978.
- (129) Aubrecht, K. B.; Hillmeyer, M. A.; Tolman, W. B. *Macromolecules* **2002**, *35*, 644.
- (130) (a) Zhou, Y.; Richeson, D. S. *Inorg. Chem.* **1997**, *36*, 501. (b) Foley, S. R.; Zhou, Y.; Yap, G. P. A.; Richeson, D. S. *Inorg. Chem.* **2000**, *39*, 924.
- (131) Richter, J.; Belay, M.; Brüser, W.; Edelman, F. T. *Main Group Met. Chem.* **1997**, *20*, 191.
- (132) Nimitsiriwat, N.; Gibson, V. C.; Marshall, E. L.; White, A. J. P.; Dale, S. H.; Elsegood, M. R. *J. Dalton Trans.* **2007**, 4464.
- (133) Zhou, Y.; Richeson, D. S. *J. Am. Chem. Soc.* **1996**, *118*, 10850.
- (134) Foley, S. R.; Yap, G. P. A.; Richeson, D. S. *Organometallics* **1999**, *18*, 4700.
- (135) Foley, S. R.; Yap, G. P. A.; Richeson, D. S. *Polyhedron* **2002**, *21*, 619.
- (136) Green, S. P.; Jones, C.; Jin, G.; Stasch, A. *Inorg. Chem.* **2007**, *46*, 8.
- (137) (a) Bailey, P. J.; Gould, R. O.; Harmer, C. N.; Pace, S.; Steiner, A.; Wright, D. S. *Chem. Commun.* **1997**, 1161. (b) Brym, M.; Forsyth, C. M.; Jones, C.; Junk, P. C.; Rose, R. P.; Stasch, A.; Turner, D. R. *Dalton Trans.* **2007**, 3282.

- (138) Edelmann, F. T. *Angew. Chem.* **1995**, 107, 2647. Edelmann, F. T. *Angew. Chem. Int. Ed.* **1995**, 34, 2467.
- (139) (a) Cole, M. L.; Junk, P. C. *Chem. Commun.* **2005**, 2695. (b) Heitmann, D.; Jones, C.; Junk, P. C.; Lippert, K.-A.; Stasch, A. *Dalton Trans.* **2007**, 187.
- (140) Trifonov, A. A.; Lyubov, D. M.; Fedorova, E. A.; Skvortsov, G. G.; Fukin, G. K.; Kurskii, Yu. A.; Bochkarev, M. N. *Russ. Chem. Bull. Int. Ed.* **2006**, 55, 435.
- (141) Roesky, P. W. Z. *Anorg. Allg. Chem.* **2003**, 629, 1881.
- (142) Arndt, S.; Okuda, J. *Adv. Synth. Catal.* **2005**, 347, 339.
- (143) Bambirra, S.; Bouwkamp, M. W.; Meetsma, A.; Hessen, B. J. *Am. Chem. Soc.* **2004**, 126, 9182.
- (144) Bambirra, S.; Tsurugi, H.; van Leusen, D.; Hessen, B. *Dalton Trans.* **2006**, 1157.
- (145) Bambirra, S.; Brandsma, M. J. R.; Brussee, E. A. C.; Meetsma, A.; Hessen, B.; Teuben, J. H. *Organometallics* **2000**, 19, 3197.
- (146) (a) Giebrecht, G. R.; Whitener, G. D.; Arnold, J. *Dalton Trans.* **2001**, 923. (b) Lyubov, D. M.; Fukin, G. K.; Trifonov, A. A. *Inorg. Chem.* **2007**, 46, 11450.
- (147) (a) Yuan, F.; Zhu, Y.; Xiong, L. J. *Organomet. Chem.* **2006**, 691, 3377. (b) Skvortsov, G. G.; Yakovenko, M. V.; Castro, P. M.; Fukin, G. K.; Cherkasov, A. V.; Carpentier, J.-F.; Trifonov, A. A. *Eur. J. Inorg. Chem.* **2007**, 3260.
- (148) (a) Boyd, C. L.; Toupance, T.; Tyrrell, B. R.; Ward, B. D.; Wilson, C. R.; Cowley, A. R.; Mountford, P. *Organometallics* **2005**, 24, 309. (b) Cui, D.; Nishiura, M.; Hou, Z. *Angew. Chem.* **2005**, 117, 981. Cui, D.; Nishiura, M.; Hou, Z. *Angew. Chem. Int. Ed.* **2005**, 44, 959.
- (149) Xu, X.; Zhang, Z.; Yao, Y.; Zhang, Y.; Shen, Q. *Inorg. Chem.* **2007**, 46, 9379.
- (150) Schumann, H.; Winterfeld, J.; Hemling, H.; Hahn, F. E.; Reich, P.; Brzezinka, K.-W.; Edelmann, F. T.; Kilimann, U.; Schäfer, M.; Herbst-Irmer, R. *Chem. Ber.* **1995**, 128, 395.
- (151) Edelmann, F. T.; Richter, J. *Eur. J. Solid State Inorg. Chem.* **1996**, 33, 157.
- (152) Trifonov, A. A.; Fedorova, E. A.; Fukin, G. K.; Bochkarev, M. N. *Eur. J. Inorg. Chem.* **2004**, 4396.
- (153) Luo, Y.; Yao, Y.; Shen, Q.; Weng, L. *Eur. J. Inorg. Chem.* **2003**, 318.
- (154) Pang, X.; Sun, H.; Zhang, Y.; Shen, Q.; Zhang, H. *Eur. J. Inorg. Chem.* **2005**, 1487.
- (155) Yao, Y.-M.; Luo, Y.-J.; Shen, Q.; Yu, K.-B. *Jiegou Huaxue* **2004**, 23, 391.
- (156) Yao, Y.; Luo, Y.; Chen, J.; Zhang, Z.; Zhang, Y.; Shen, Q. *J. Organomet. Chem.* **2003**, 679, 229.
- (157) (a) Thou, Y.; Yap, G. P. A.; Richeson, D. S. *Organometallics* **1998**, 17, 4387. (b) Lu, Z.; Yap, G. P. A.; Richeson, D. S. *Organometallics* **2001**, 20, 706.
- (158) Fukin, G. K.; Guzei, I. A.; Baranov, E. V. *J. Coord. Chem.* **2007**, 60, 937.
- (159) Zhang, J.; Ruan, R.; Shao, Z.; Cai, R.; Weng, L.; Zhou, X. *Organometallics* **2002**, 21, 1420.
- (160) Ma, L.; Zhang, J.; Cai, R.; Chen, Z.; Weng, L.; Zhou, X. *J. Organomet. Chem.* **2005**, 690, 4926.
- (161) Zhang, J.; Cai, R.; Weng, L.; Zhou, X. *J. Organomet. Chem.* **2003**, 672, 94.
- (162) Zhang, J.; Cai, R.; Weng, L.; Zhou, X. *Organometallics* **2004**, 23, 3303.
- (163) Zhang, J.; Cai, R.; Weng, L.; Zhou, X. *Organometallics* **2003**, 22, 5385.
- (164) Zhang, J.; Zhou, X.; Cai, R.; Weng, L. *Inorg. Chem.* **2005**, 44, 716.
- (165) Zhou, L.; Yao, Y.; Zhang, Y.; Xue, M.; Chen, J.; Shen, Q. *Eur. J. Inorg. Chem.* **2004**, 2167.
- (166) Chen, J.-L.; Yao, Y.-M.; Luo, Y.-J.; Zhou, L.-Y.; Zhang, Y.; Shen, Q. *J. Organomet. Chem.* **2004**, 689, 1019.
- (167) Päiväsaari, J.; Dezelah, C. L.; Back, D.; El-Kaderi, H. M.; Heeg, M. J.; Putkonen, M.; Niinistö, L.; Winter, C. H. *J. Mater. Chem.* **2005**, 15, 4224.
- (168) Luo, Y.; Yao, Y.; Shen, Q.; Sin, J.; Weng, L. *J. Organomet. Chem.* **2002**, 662, 144.
- (169) (a) Amberger, H.-D.; Reddmann, H.; Unrecht, B.; Edelmann, F. T.; Edelstein, N. M. *J. Organomet. Chem.* **1998**, 566, 125. (b) Hagen, C.; Reddmann, H.; Amberger, H.-D.; Edelmann, F. T.; Pegelow, U.; Shalimoff, G. V.; Edelstein, N. M. *J. Organomet. Chem.* **1993**, 462, 69.
- (170) Dröse, P.; Gottfriedsen, J.; Blaurock, S.; Edelmann, F. T., unpublished.
- (171) Müller, M.; Williams, V. C.; Doerrer, L. H.; Leech, M. A.; Mason, S. A.; Green, M. L. H.; Prout, K. *Inorg. Chem.* **1998**, 37, 1315.
- (172) Littke, A.; Sleiman, N.; Bensimon, C.; Richeson, D. S.; Yap, G. P. A.; Brown, S. J. *Organometallics* **1998**, 17, 446.
- (173) Flores, J. C.; Chien, J. C. W.; Rausch, M. D. *Organometallics* **1995**, 14, 1827.

- (174) Flores, J. C.; Chien, J. C. W.; Rausch, M. D. *Organometallics* **1995**, *14*, 2106.
- (175) Thiele, K.-H.; Windisch, H.; Windisch, H.; Edelmänn, F. T.; Kilimann, U.; Noltemeyer, M. Z. *Anorg. Allg. Chem.* **1996**, *622*, 713.
- (176) Milanov, A. P.; Bhakta, R.; Winter, M.; Merz, K.; Devi, A. *Acta Cryst.* **2005**, *C61*, m370.
- (177) (a) Otten, E.; Dijkstra, P.; Visser, C.; Meetsma, A.; Hessen, B. *Organometallics* **2005**, *24*, 4374.
(b) Zhou, M.; Zhang, S.; Tong, H.; Sun, W.-H.; Liu, D. *Inorg. Chem. Commun.* **2007**, *10*, 1262.
- (178) Duncan, A. P.; Mullins, S. M.; Arnold, J.; Bergman, R. G. *Organometallics* **2001**, *20*, 1808.
- (179) Carmalt, C. J.; Newport, A. C.; O'Neill, S. A.; Parkin, I. P.; White, A. J. P.; Williams, D. J. *Inorg. Chem.* **2005**, *44*, 615.
- (180) Wood, D.; Yap, G. P. A.; Richeson, D. S. *Inorg. Chem.* **1999**, *38*, 5788.
- (181) Bailey, P. J.; Grant, K. J.; Mitchell, L. A.; Pace, S.; Parkin, A.; Parsons, S. *Dalton Trans.* **2000**, 1887.
- (182) Bazinet, P.; Wood, D.; Yap, G. P. A.; Richeson, D. S. *Inorg. Chem.* **2003**, *42*, 6225.
- (183) Giesbrecht, G. R.; Whitener, G. D.; Arnold, J. *Organometallics* **2000**, *19*, 2809.
- (184) Gómez, R.; Duchateau, R.; Chernega, A. N.; Teuben, J. H.; Edelmänn, F. T.; Green, M. L. H. *J. Organomet. Chem.* **1995**, *491*, 153.
- (185) Gómez, R.; Duchateau, R.; Chernega, A. N.; Meetsma, A.; Edelmänn, F. T.; Teuben, J. H.; Green, M. L. H. *Dalton Trans.* **1995**, 217.
- (186) Sita, L. R.; Babcock, J. R. *Organometallics* **1998**, *17*, 5228.
- (187) Koterwas, L. A.; Fettingner, J. C.; Sita, L. R. *Organometallics* **1999**, *18*, 4183.
- (188) Cornelißen, C.; Erker, G.; Kehr, G.; Fröhlich, R. Z. *Naturforsch.* **2004**, *59b*, 1246.
- (189) Hagadorn, J. R.; Arnold, J. *Organometallics* **1998**, *17*, 1355.
- (190) Mullins, S. M.; Duncan, A. P.; Bergman, R. G.; Arnold, J. *Inorg. Chem.* **2001**, *40*, 6952.
- (191) Hao, S.; Feghali, K.; Gambarotta, S. *Inorg. Chem.* **1997**, *36*, 1745.
- (192) Stewart, P. J.; Blake, A. J.; Mountford, P. *Inorg. Chem.* **1997**, *36*, 3616.
- (193) Stewart, P. J.; Blake, A. J.; Mountford, P. *Organometallics* **1998**, *17*, 3271.
- (194) Guiducci, A. E.; Boyd, C. L.; Mountford, P. *Organometallics* **2006**, *25*, 1167.
- (195) Guiducci, A. E.; Cowley, A. R.; Skinner, M. E. G.; Mountford, P. *Dalton Trans.* **2001**, 1392.
- (196) (a) Ong, T.-G.; Wood, D.; Yap, G. P. A.; Richeson, D. S. *Organometallics* **2002**, *21*, 1. (b) Ong, T.-G.; Yap, G. P. A.; Richeson, D. S. *Organometallics* **2002**, *21*, 2839.
- (197) Ong, T.-G.; Yap, G. P. A.; Richeson, D. S. *J. Am. Chem. Soc.* **2003**, *125*, 8100.
- (198) Zuckerman, R. L.; Bergman, R. G. *Organometallics* **2001**, *20*, 1792.
- (199) (a) Kissounko, D. A.; Epshteyn, A.; Fettingner, J. C.; Sita, L. R. *Organometallics* **2006**, *25*, 1076.
(b) Fontaine, P. P.; Epshteyn, A.; Zavalij, P. Y.; Sita, L. R. *J. Organomet. Chem.* **2007**, *692*, 4683.
- (200) Kissounko, D. A.; Fettingner, J. C.; Sita, L. R. *J. Organomet. Chem.* **2003**, *683*, 29.
- (201) Keaton, R. J.; Koterwas, L. A.; Fettingner, J. C.; Sita, L. R. *J. Am. Chem. Soc.* **2002**, *124*, 5932.
- (202) (a) Kissounko, D. A.; Sita, L. R. *J. Am. Chem. Soc.* **2004**, *126*, 5946. (b) Hirotsu, M.; Fontaine, P. P.; Zavalij, P. Y.; Sita, L. R. *J. Am. Chem. Soc.* **2007**, *129*, 12690.
- (203) Zhang, Y.; Kissounko, D. A.; Fettingner, J. C.; Sita, L. R. *Organometallics* **2003**, *22*, 21.
- (204) Thorman, J. L.; Guzei, I. A.; Young, V. G.; Woo, L. K. *Inorg. Chem.* **1999**, *38*, 3814.
- (205) Shen, H.; Chan, H.-S.; Xie, Z. *Organometallics* **2006**, *25*, 5515.
- (206) Hao, S.; Berno, P.; Minhas, R. K.; Gambarotta, S. *Inorg. Chim. Acta* **1996**, *244*, 37.
- (207) Berno, P.; Hao, S.; Minhas, R.; Gambarotta, S. *J. Am. Chem. Soc.* **1994**, *116*, 7417.
- (208) Brussee, E. A. C.; Meetsma, A.; Hessen, B.; Teuben, J. H. *Organometallics* **1998**, *17*, 4090.
- (209) Brussee, E. A. C.; Meetsma, A.; Hessen, B.; Teuben, J. H. *Chem. Commun.* **2000**, 497.
- (210) Ellis, D. D.; Spek, A. L. *Acta Cryst.* **2001**, *C57*, 147.
- (211) Liguori, D.; Centore, R.; Csok, Z.; Tuzi, A. *Macromol. Chem. Phys.* **2004**, *205*, 1058.
- (212) Mullins, S. M.; Hagadorn, J. R.; Bergman, R. G.; Arnold, J. *J. Organomet. Chem.* **2000**, *607*, 227.
- (213) Decker, J. M.; Geib, S. J.; Meyer, T. Y. *Organometallics* **1999**, *18*, 4417.
- (214) Hubert-Pfalzgraf, L. G.; Decams, J.-M.; Daniele, S. J. *Phys. IV France* **1999**, *9*, 953.
- (215) Baunemann, A.; Rische, D.; Milanov, A.; Kim, Y.; Winter, M.; Gemel, C.; Fischer, R. A. *Dalton Trans.* **2005**, 3051.
- (216) Decams, J. M.; Hubert-Pfalzgraf, L. G.; Vaissermann, J. *Polyhedron* **1999**, *18*, 2885.
- (217) Tin, M. K. T.; Yap, G. P. A.; Richeson, D. S. *Inorg. Chem.* **1999**, *38*, 998.
- (218) Tin, M. K. T.; Yap, G. P. A.; Richeson, D. S. *Inorg. Chem.* **1998**, *37*, 6728.

- (219) Tin, M. K. T.; Thirupathi, N.; Yap, G. P. A.; Richeson, D. S. *Dalton Trans.* **1999**, 2947.
- (220) (a) Thirupathi, N.; Yap, G. P. A.; Richeson, D. S. *Chem. Commun.* **1999**, 2483. (b) Thirupathi, N.; Yap, G. P. A.; Richeson, D. S. *Organometallics* **2000**, 19, 2573. (c) Baunemann, A.; Winter, M.; Csapek, K.; Gemel, C.; Fischer, R. A. *Eur. J. Inorg. Chem.* **2006**, 4665.
- (221) Mullins, S. M.; Bergman, R. G.; Arnold, J. *Dalton Trans.* **2006**, 203.
- (222) Cotton, F. A.; Daniels, L. M.; Maloney, D. J.; Murillo, C. A. *Inorg. Chim. Acta* **1996**, 242, 31.
- (223) (a) Sadique, A. R.; Heeg, M. J.; Winter, C. H. *J. Am. Chem. Soc.* **2003**, 125, 7774. (b) El-Kadri, O. M.; Heeg, M. J.; Winter, C. H. *Dalton Trans.* **2006**, 4506.
- (224) Dykerman, B. A.; Smith, J. J.; McCarvill, E. M.; Gallant, A. J.; Doiron, N. D.; Wagner, B. D.; Jenkins, H. A.; Patrick, B. O.; Smith, K. M. *J. Organomet. Chem.* **2007**, 692, 3183.
- (225) Yamaguchi, Y.; Ogata, K.; Kobayashi, K.; Ito, T. *Inorg. Chim. Acta* **2004**, 357, 2657.
- (226) Yamaguchi, Y.; Ogata, K.; Kobayashi, K.; Ito, T. *Bull. Chem. Soc. Jpn.* **2004**, 77, 303.
- (227) Yamaguchi, Y.; Ogata, K.; Kobayashi, K.; Ito, T. *Organomet. News* **2004**, 124.
- (228) Yamaguchi, Y.; Ogata, K.; Kobayashi, K.; Ito, T. *Dalton Trans.* **2004**, 3982.
- (229) Ogata, K.; Yamaguchi, Y.; Kashiwabara, T.; Ito, T. *J. Organomet. Chem.* **2005**, 690, 5701.
- (230) Romao, C. C.; Royo, B. *J. Organomet. Chem.* **2002**, 663, 78.
- (231) Yamaguchi, Y.; Ozaki, S.; Hinago, H.; Kobayashi, K.; Ito, T. *Inorg. Chim. Acta* **2005**, 358, 2363.
- (232) Zhou, G.; Ren, T. *Inorg. Chim. Acta* **2000**, 304, 305.
- (233) Hao, H.; Cui, C.; Bai, G.; Roesky, H. W.; Noltemeyer, M.; Schmidt, H.-G.; Ding, Y. Z. *Anorg. Allg. Chem.* **2000**, 626, 1660.
- (234) Wilder, C. B.; Reitfort, L. L.; Abboud, K. A.; McElwee-White, L. *Inorg. Chem.* **2006**, 45, 263.
- (235) Legzdins, P.; Lumb, S. A.; Young, V. G. Jr. *Organometallics* **1998**, 17, 854.
- (236) Rische, D.; Baunemann, A.; Winter, M.; Fischer, R. A. *Inorg. Chem.* **2006**, 45, 269.
- (237) Alvarez, C. S.; Ross, S. R.; Burley, J. C.; Humphry, S. M.; Layfield, R. A.; Kowenicki, R. A.; McPartlin, M.; Rawson, J. M.; Wheatley, A. E. H.; Wood, P. T.; Wright, D. S. *Dalton Trans.* **2004**, 3481.
- (238) Walther, D.; Gebhardt, P.; Fischer, R.; Kreher, U.; Görls, H. *Inorg. Chim. Acta* **1998**, 281, 181.
- (239) Albertin, G.; Antoniutti, S.; Roveda, G. *Inorg. Chim. Acta* **2005**, 358, 3093.
- (240) Vendemiati, B.; Prini, G.; Meetsma, A.; Hessen, B.; Teuben, J. H.; Traverso, O. *Eur. J. Inorg. Chem.* **2001**, 707.
- (241) Sciarone, T. J. J.; Nijhuis, C. A.; Meetsma, A.; Hessen, B. *Dalton Trans.* **2006**, 4896.
- (242) Foley, S. R.; Yap, G. P. A.; Richeson, D. S. *Chem. Commun.* **2000**, 1515.
- (243) Foley, S. R.; Yap, G. P. A.; Richeson, D. S. *Inorg. Chem.* **2002**, 41, 4149.
- (244) Albertin, G.; Antoniutti, S.; Bordignon, E. *Gazz. Chim. Ital.* **1994**, 124, 355.
- (245) Nagashima, H.; Kondo, H.; Hayashida, T.; Yamaguchi, Y.; Gondo, M.; Masuda, S.; Miyazaki, K.; Matsubara, K.; Kirchner, K. *Coord. Chem. Rev.* **2003**, 245, 177.
- (246) Hayashida, T.; Nagashima, H. *Organomet. News* **2002**, 32.
- (247) Yamaguchi, Y.; Nagashima, H. *Organometallics* **2000**, 19, 725.
- (248) (a) Hayashida, T.; Nagashima, H. *Organometallics* **2002**, 21, 3884. (b) Hayashida, T.; Kondo, H.; Terasawa, J.-I.; Kirchner, K.; Sunada, Y.; Nagashima, H. *J. Organomet. Chem.* **2007**, 692, 382.
- (249) Kondo, H.; Kageyama, A.; Yamaguchi, Y.; Haga, M.; Kirchner, K.; Nagashima, H. *Bull. Chem. Soc. Jpn.* **2001**, 74, 1927.
- (250) Kondo, H.; Yamaguchi, Y.; Nagashima, H. *Chem. Commun.* **2000**, 1075.
- (251) Hayashida, T.; Miyazaki, K.; Yamaguchi, Y.; Nagashima, H. *J. Organomet. Chem.* **2001**, 634, 167.
- (252) Hayashida, T.; Nagashima, H. *Organometallics* **2001**, 20, 4996.
- (253) Kondo, H.; Yamaguchi, Y.; Nagashima, H. *J. Am. Chem. Soc.* **2001**, 123, 500.
- (254) Terasawa, J.; Kondo, H.; Matsumoto, T.; Kirchner, K.; Motoyama, Y.; Nagashima, H. *Organometallics* **2005**, 24, 2713.
- (255) Kondo, H.; Matsubara, K.; Nagashima, H. *J. Am. Chem. Soc.* **2002**, 124, 534.
- (256) Hayashida, T.; Nagashima, H. *Reports Inst. Adv. Mater Study (Kyushu Univ.)* **2001**, 15, 31.
- (257) Holman, K. T.; Robinson, S. D.; Sahajpal, A.; Steed, J. W. *Dalton Trans.* **1999**, 15.
- (258) Zhang, J.; Gunnoe, T. B.; Petersen, J. L. *Inorg. Chem.* **2005**, 44, 2895.
- (259) Zhang, J.; Gunnoe, T. B.; Boyle, P. D. *Organometallics* **2004**, 23, 3094.
- (260) Robinson, S. D.; Sahajpal, A.; Steed, J. *Inorg. Chim. Acta* **2000**, 303, 265.

- (261) Robinson, S. D.; Sahajpal, A.; Steed, J. *Inorg. Chim. Acta* **2000**, 306, 205.
- (262) Clark, T.; Cochrane, J.; Colson, S. F.; Malik, K. Z.; Johnson, S. D.; Steed, J. W. *Polyhedron* **2001**, 20, 1875.
- (263) Souers, A. J.; Owens, T. D.; Oliver, A. G.; Hollander, F. J.; Ellman, J. A. *Inorg. Chem.* **2001**, 40, 5299.
- (264) Simpson, R. D.; Marshall, W. J. *Organometallics* **1997**, 16, 3719.
- (265) Rais, D.; Bergman, R. G. *Chem. Eur. J.* **2004**, 10, 3970.
- (266) Holland, A. W.; Bergman, R. G. *J. Am. Chem. Soc.* **2002**, 124, 9010.
- (267) Nelkenbaum, E.; Kapon, M.; Eisen, M. S. *Organometallics* **2005**, 24, 2645.
- (268) Berry, J. F.; Cotton, F. A.; Ibragimov, S. A.; Murillo, C. A.; Wang, X. *Inorg. Chem.* **2005**, 44, 6129.
- (269) Su, C.-W.; Chen, J.-D.; Keng, T.-C.; Wang, J.-C. *Inorg. Chem. Commun.* **2001**, 4, 201.
- (270) Jiang, X.; Bollinger, J. C.; Lee, D. J. *Am. Chem. Soc.* **2005**, 127, 15678.
- (271) Cotton, F. A.; Lei, P.; Murillo, C. A.; Wang, L.-S. *Inorg. Chim. Acta* **2003**, 349, 165.
- (272) Li, Z.; Barry, S. T.; Gordon, R. G. *Inorg. Chem.* **2005**, 44, 1728.
- (273) Jiang, X.; Bollinger, J. C.; Baik, M.-H.; Lee, D. *Chem. Commun.* **2005**, 1043.
- (274) Archibald, S. J.; Alcock, N. W.; Busch, D. H.; Whitcomb, D. R. *Inorg. Chem.* **1999**, 38, 5571.
- (275) Radak, S.; Ni, Y.; Xu, G.; Shaffer, K. L.; Ren, T. *Inorg. Chim. Acta* **2001**, 321, 200.
- (276) Abdou, H. E.; Mohamed, A. A.; Fackler, J. P. Jr. *Z. Naturforsch.* **2004**, 59b, 1480.
- (277) (a) Abdou, H. E.; Mohamed, A. A.; Fackler, J. P. Jr. *Inorg. Chem.* **2006**, 45, 11. (b) Abdou, H. E.; Mohammed, A. A.; Fackler, J. P. Jr. *Inorg. Chem.* **2007**, 46, 9692. (c) Abdou, H. E.; Mohamed, A. A.; Fackler, J. P. Jr. *Inorg. Chem.* **2007**, 46, 141.
- (278) (a) Coles, M. P.; Hitchcock, P. B. *Eur. J. Inorg. Chem.* **2004**, 2662. (b) Birch, S. J.; Ross, S. R.; Cole, S. C.; Coles, M. P.; Haigh, R.; Hitchcock, P. B.; Wheatley, A. E. H. *Dalton Trans.* **2004**, 3568. (c) Nimitsiriwat, N.; Gibson, V. C.; Marshall, E. L.; Takolpuckdee, P.; Tomov, A. K.; White, A. J. P.; Williams, D. J.; Elsegood, M. R. J.; Dale, S. H. *Inorg. Chem.* **2007**, 46, 9988. (d) Münch, M.; Flörke, U.; Bolte, M.; Schulz, S.; Gudat, D. *Angew. Chem.* **2008**, 120, 1535.
- (279) Jones, C.; Rose, R. P.; Stasch, A. *Dalton Trans.* **2007**, 2997.
- (280) (a) Lin, W. B.; Liang, H.-C.; Chen, J.-D.; Keng, T.-C. *Inorg. Chim. Acta* **2002**, 336, 157. (b) Chan, Z.-K.; Chen, T.-R.; Chen, J.-D.; Wang, J.-C.; Liu, C. W. *Dalton Trans.* **2007**, 3450.
- (281) Scott, A. L.; Coles, S. R.; Clarke, A. J.; Clarkson, G. J.; Scott, P. *Organometallics* **2007**, 26, 136.
- (282) Nelkenbaum, E.; Kapon, M.; Eisen, M. S. *J. Organomet. Chem.* **2005**, 690, 3154.
- (283) Bertogg, A.; Togni, A. *Organometallics* **2006**, 25, 622.
- (284) (a) Kempe, R.; Arndt, P. *Inorg. Chem.* **1996**, 35, 2644. (b) Kempe, R. *Eur. J. Inorg. Chem.* **2003**, 791.
- (285) Cole, M. L.; Junk, P. C. *Dalton Trans.* **2003**, 2109.
- (286) Bertolasi, V.; Boaretto, R.; Cherotti, M. R.; Gobetto, R.; Sostero, S. *Dalton Trans.* **2007**, 5179.
- (287) (a) Ciobanu, O.; Roquette, P.; Leingang, S.; Wadepohl, H.; Mautz, J.; Himmel, H.-J. *Eur. J. Inorg. Chem.* **2007**, 4530. (b) Ciobanu, O.; Leingang, S.; Wadepohl, H.; Himmel, H.-J. *Eur. J. Inorg. Chem.* **2008**, 322.
- (288) (a) Coles, M. P.; Hitchcock, P. B. *Dalton Trans.* **2001**, 1169. (b) Coles, M. P.; Hitchcock, P. B. *Organometallics* **2003**, 22, 5201.
- (289) Soria, D. B.; Grundy, J.; Coles, M. P.; Hitchcock, P. B. *J. Organomet. Chem.* **2005**, 690, 2278.
- (290) Soria, D. B.; Grundy, J.; Coles, M. P.; Hitchcock, P. B. *Polyhedron* **2003**, 22, 2731.
- (291) Schramm, F.; Walther, D.; Görls, H.; Käpplinger, C.; Beckert, R. *Z. Naturforsch.* **2005**, 60b, 843.
- (292) Tong, H.-B.; Wei, X.-H.; Liu, D.-S.; Huang, S.-P. *Acta Cryst.* **2004**, E60, m825.
- (293) Brandsma, M. J. R.; Brussee, E. A. C.; Meetsma, A.; Hessen, B.; Teuben, J. H. *Eur. J. Inorg. Chem.* **1998**, 1867.
- (294) Doyle, D.; Gun'ko, Yu. K.; Hitchcock, P. B.; Lappert, M. F. *Dalton Trans.* **2000**, 4093.
- (295) van Meerendonk, W. J.; Schröder, K.; Brussee, E. A. C.; Meetsma, A.; Hessen, B.; Teuben, J. H. *Eur. J. Inorg. Chem.* **2003**, 427.
- (296) Li, J.-F.; Huang, S.-P.; Weng, L.-H.; Liu, D.-S. *Eur. J. Inorg. Chem.* **2003**, 810.
- (297) Croft, A. C. R.; Boyd, C. L.; Cowley, A. R.; Mountford, P. *J. Organomet. Chem.* **2003**, 683, 120.
- (298) Boyd, C. L.; Clot, E.; Guiducci, A. E.; Mountford, P. *Organometallics* **2005**, 24, 2347.
- (299) (a) Kincaid, K.; Gerlach, C. P.; Giesbrecht, G. R.; Hagadorn, J. R.; Whitener, G. D.; Shafir, A.; Arnold, J. *Organometallics* **1999**, 18, 5360. (b) Pi, C.; Zhang, Z.; Pang, Z.; Zhang, J.; Luo, J.; Chen, Z.; Weng, L.; Zhou, X. *Organometallics* **2007**, 26, 1934. (c) Shen, H.; Chan, H. S.; Xie, Z. *J. Am. Chem. Soc.*

- 2007, 129, 12934. (d) Otero, A.; Fernández, J.; Antinolo, A.; Tejada, J.; Lara-Sánchez, A.; Sánchez-Barba, L. F.; López-Soler, I.; Rodríguez, A. M. *Inorg. Chem.* **2007**, 46, 1760.
- (300) (a) Villiers, C.; Thuéry, P.; Ephritikhine, M. *Chem. Commun.* **2006**, 392. (b) Deacon, G. B.; Forsyth, C. M.; Junk, P. C.; Wang, J. *Inorg. Chem.* **2007**, 46, 10022.
- (301) Chen, C.-T.; Rees, L. H.; Cowley, A. R.; Green, M. L. H. *Dalton Trans.* **2001**, 1761.
- (302) Döhler, T.; Görls, H.; Walther, D. *Chem. Commun.* **2000**, 945.
- (303) Rau, S.; Lamm, K.; Görls, H.; Schöffel, J.; Walther, D. *J. Organomet. Chem.* **2004**, 689, 3582.
- (304) Chen, C.-T.; Huang, C.-A.; Tzeng, Y.-R.; Huang, B.-H. *Dalton Trans.* **2003**, 2585.
- (305) (a) Lamm, K.; Stollenz, M.; Meier, M.; Görls, H.; Walther, D. *J. Organomet. Chem.* **2003**, 681, 24. (b) Tsukada, N.; Ninomiya, S.; Aoyama, Y.; Inoue, Y. *Org. Lett.* **2007**, 9, 2919.
- (306) Stollenz, M.; Walther, D.; Böttcher, L.; Görls, H. *Z. Anorg. Allg. Chem.* **2004**, 630, 2701.
- (307) Li, J.-F.; Weng, L.-H.; Wei, X.-H.; Liu, D.-S. *Dalton Trans.* **2002**, 1401.
- (308) Kawaguchi, H.; Matsuo, T. *Chem. Commun.* **2002**, 958.
- (309) (a) Whitener, G. D.; Hagadorn, J. R.; Arnold, J. *Dalton Trans.* **1999**, 1249. (b) Hagadorn, J. R.; Arnold, J. *Angew. Chem.* **1998**, 110, 1813. Hagadorn, J. R.; Arnold, J. *Angew. Chem. Int. Ed.* **1998**, 37, 1729.
- (310) Li, J.; Bai, S.-D. *Acta Cryst* **2007**, E63, m3111.
- (311) Bambirra, S.; Meetsma, A.; Hessen, B.; Teuben, J. H. *Organometallics* **2001**, 20, 782.
- (312) (a) Wang, J.; Yao, Y.; Cheng, J.; Pang, X.; Zhang, Y.; Shen, Q. *J. Mol. Struct.* **2005**, 743, 229. (b) Wang, J.; Cai, T.; Yao, Y.; Zhang, Y.; Shen, Q. *Dalton Trans.* **2007**, 5275.
- (313) Ong, T. G.; Yap, G. P. A.; Richeson, D. S. *Organometallics* **2003**, 22, 387.
- (314) Hagadorn, J. R. *Chem. Commun.* **2001**, 2144.
- (315) Clare, B.; Sarker, N.; Shoemaker, R.; Hagadorn, J. R. *Inorg. Chem.* **2004**, 43, 1159.
- (316) Hagadorn, J. R.; McNevin, M. J. *Organometallics* **2003**, 22, 609.
- (317) (a) McNevin, M. J.; Hagadorn, J. R. *Inorg. Chem.* **2004**, 43, 8547. (b) Hagadorn, J. R.; McNevin, M. J.; Wiedenfeld, G.; Shoemaker, R. *Organometallics* **2003**, 22, 4818.
- (318) Grundy, J.; Coles, M. P.; Hitchcock, P. B. *J. Organomet. Chem.* **2002**, 662, 178.
- (319) Cotton, F. A.; Daniels, L. M.; Falvello, L. R.; Murillo, C. A. *Inorg. Chim. Acta* **1994**, 219, 7.
- (320) Cotton, F. A.; Daniels, L. M.; Feng, X.; Maloney, D. J.; Matonic, J. H.; Murillo, C. A. *Inorg. Chim. Acta* **1997**, 256, 291.
- (321) Cotton, F. A.; Hillard, E. A.; Murillo, C. A.; Wang, X. *Inorg. Chem.* **2003**, 42, 6063.
- (322) Andrés, J.; Berski, S.; Feliz, M.; Llusar, R.; Sensato, F.; Silci, B. C. R. *Chim.* **2005**, 8, 1400.
- (323) Cotton, F. A.; Daniels, L. M.; Huang, P.; Murillo, C. A. *Inorg. Chem.* **2002**, 41, 317.
- (324) Lin, C.; Protasiewicz, J. D.; Smith, E. T.; Ren, T. *Chem. Commun.* **1995**, 2257.
- (325) (a) Cotton, F. A.; Daniels, L. M.; Murillo, C. A.; Timmons, D. J.; Wilkinson, C. C. J. *Am. Chem. Soc.* **2002**, 124, 9249. (b) Cotton, F. A.; Murillo, C. A.; Wang, X.; Wilkinson, C. C. *Dalton Trans.* **2007**, 3943.
- (326) Cotton, F. A.; Donahue, J. P.; Gruhn, N. E.; Lichtenberger, D. L.; Murillo, C. A.; Timmons, D. J.; Van Dorn, L. O.; Villagrán, D.; Wang, X. *Inorg. Chem.* **2006**, 45, 201.
- (327) Cotton, F. A.; Huang, P.; Murillo, C. A.; Timmons, D. J. *Inorg. Chem. Commun.* **2002**, 5, 501.
- (328) Cotton, F. A.; Daniels, L. M.; Murillo, C. A. *Inorg. Chim. Acta* **1994**, 224, 5.
- (329) Berry, J. F.; Cotton, F. A.; Huang, P.; Murillo, C. A.; Wang, X. *Dalton Trans.* **2005**, 3713.
- (330) Irwin, M. D.; Abdou, H. E.; Mohamed, A. A.; Fackler, J. P. Jr. *Chem. Commun.* **2003**, 2882.
- (331) Coles, M. P.; Hitchcock, P. B. *Chem. Commun.* **2002**, 2794.
- (332) Mansfield, N. E.; Coles, M. P.; Hitchcock, P. B. *Dalton Trans.* **2005**, 2833.
- (333) Smolensky, E.; Eisen, M. S. *Dalton Trans.* **2007**, 5623.
- (334) Schlund, R.; Lux, M.; Edelmann, F.; Reissmann, U.; Rohde, W. US Patent 5707913, **1998**.
- (335) (a) Koichi, S. US Patent, Appl. Publ. No. 2002026031, **2002**. (b) Shibayama, K. *Polym. J.* **2003**, 35, 711. (c) Yamashita, J. JP 2001064316, **2001**.
- (336) Flores, J. C.; Rausch, M. D. US Patent 5502128, **1996**.
- (337) Nagashima, H.; Motoyama, Y. JP 2005272817, **2005**.
- (338) Hessen, B.; Bambirra, S. WO 2004000894, **2003**.
- (339) Jordan, R. F.; Coles, M. P. US 5777120, **1998**.
- (340) Inoue, A.; Tsukada, N. JP 2003212886, **2003**.

- (341) Jordan, R. F.; Coles, M. P. WO 9840421, **1998**.
- (342) Collins, S.; Ziegler, T. *Organometallics* **2007**, 26, 6612.
- (343) Volkis, V.; Shmulinson, M.; Averbuj, C.; Lisovskii, A.; Edelmann, F. T.; Eisen, M. S. *Organometallics* **1998**, 17, 3155.
- (344) Jayaratne, K. C.; Sita, L. R. *J. Am. Chem. Soc.* **2000**, 122, 958.
- (345) Keaton, R. J.; Jayaratne, K. C.; Fettingner, J. C.; Sita, L. R. *J. Am. Chem. Soc.* **2000**, 122, 12909.
- (346) Zhang, Y.; Reeder, E. K.; Keaton, R. J.; Sita, L. R. *Organometallics* **2004**, 23, 3512.
- (347) Volkis, V.; Tumanskii, B.; Eisen, M. S. *Organometallics* **2006**, 25, 2722.
- (348) Richter, J.; Edelmann, F. T.; Noltemeyer, M.; Schmidt, H.-G.; Shmulinson, M.; Eisen, M. S. *J. Mol. Catal. A: Chemical* **1998**, 130, 149.
- (349) Aubrecht, K. B.; Chang, K.; Hillmyer, M. A.; Tolman, W. B. *J. Polym. Sci. [A]* **2001**, 39, 284.
- (350) Motoyama, Y.; Hanada, S.; Niibayashi, S.; Shimamoto, K.; Takaoka, N.; Nagashima, H. *Tetrahedron* **2005**, 61, 10216.
- (351) Zhou, L.; Sun, H.; Chen, J.; Yao, Y.; Shen, Q. *J. Polym. Sci. [A]* **2005**, 43, 1778.
- (352) Kazi, A. B.; Cundari, T. R.; Baba, E.; DeYonker, N. J.; Dinescu, A.; Spaine, L. *Organometallics* **2007**, 26, 910.
- (353) Ruben, M.; Walther, D.; Knake, R.; Görls, H.; Beckert, R. *Eur. J. Inorg. Chem.* **2000**, 1055.
- (354) Montilla, F.; Pastor, A.; Galindo, A. *J. Organomet. Chem.* **2004**, 689, 993.
- (355) Zhang, W.-X.; Nishiura, M.; Hou, Z. *J. Am. Chem. Soc.* **2005**, 127, 16788.
- (356) Ong, T.-G.; Yap, G. P. A.; Richeson, D. S. *Chem. Commun.* **2003**, 2612.
- (357) Shibayama, K.; Seidel, S. W.; Novak, B. M. *Polym. Prepr.* **1996**, 37, 202.
- (358) Shibayama, K.; Seidel, S. W.; Novak, B. M. *Macromolecules* **1997**, 30, 3159.
- (359) Ohara, K.; Tanaka, M. JP 2000095869, **2000**.
- (360) Denk, M.; Fournier, S. US 2005042372, **2005**.
- (361) Wallbridge, M. G. H.; Philips, P. R.; Barker, J. GB 2295393, **1996**.
- (362) (a) Abrams, M. B.; Aubart, M. A.; Russo, D. A.; Bruce-Gerz, L. B. WO 2006012052, **2006**. (b) Lee, J.-H.; Choi, J.-S.; Cho, J.-H.; Chon, S.-M. US Patent 2005277223, **2005**.
- (363) Thenappan, A.; Lao, J.; Nair, H. K.; Devi, A.; Bhakta, R.; Milanov, A. WO 2007005088, **2007**.
- (364) Xu, C.; Borovik, A.; Baum, T. H. US 2005281952, **2005**.
- (365) Lim, B. S.; Rahtu, A.; Park, J.-S.; Gordon, R. G. *Inorg. Chem.* **2003**, 42, 7951.
- (366) (a) Wu, J.; Li, J.; Zhou, C.; Li, X.; Gaffney, T.; Norman, J. A. T.; Gordon, R.; Cheng, H. *Organometallics* **2007**, 26, 2803. (b) Li, X.-G.; Li, Z.; Gordon, R. G. *Eur. J. Inorg. Chem.* **2007**, 1135.
- (367) Devi, A.; Bhakta, R.; Milanov, A.; Hellwig, M.; Barreca, D.; Tondello, E.; Thomas, R.; Ehrhart, P.; Winter, M.; Fischer, R. *Dalton Trans.* **2007**, 1671.
- (368) Milanov, A.; Bhakta, R. R.; Baumann, A.; Becker, H.-W.; Thomas, R.; Ehrhart, P.; Winter, M.; Devi, A. *Inorg. Chem.* **2006**, 45, 11008.
- (369) Gordon, R. G.; Lehn, J.-S.; Li, H. PCT Int. Appl. WO 2008002546, **2008**.
- (370) Coyle, J. P.; Monillas, W. H.; Yap, G. P. A.; Barry, S. T. *Inorg. Chem.* **2008**, 47, 683.
- (371) Chen, T.; Xu, C.; Baum, T. H.; Hendrix, B. C.; Cameron, T.; Roeder, F. F.; Stender, M. PCT Int. Appl. WO 2007142700, **2007**.

Equilibrium, Structural and Biological Activity Studies on [Organotin(IV)]ⁿ⁺ Complexes

László Nagy^{a,*}, Lorenzo Pellerito^b, Tiziana Fiore^b,
Enikő Nagy^c, Claudia Pellerito^b, Attila Szorcsik^d and
Michelangelo Scopelliti^b

Contents	I. Introduction	354
	II. Physicochemical and Biological Methods for Study of Organotin(IV) Compounds	355
	A. pH-metric titration	355
	B. Analysis	355
	C. ¹¹⁹ Sn NMR spectroscopy	356
	D. ¹¹⁹ Sn Mössbauer spectroscopy	356
	E. XAFS (EXAFS and XANES) methods	356
	F. X-ray diffraction method	357
	G. Biological investigations	357
	III. Hydrolysis of [Organotin(IV)] ⁿ⁺ Cations	360
	IV. Interactions of [Organotin(IV)] ⁿ⁺ with Biological Molecules	365
	A. Interactions of [organotin(IV)] ⁿ⁺ with amino acids and peptides	365
	B. Interactions of [organotin(IV)] ⁿ⁺ with carbohydrates and their derivatives	369
	C. Interaction of [organotin(IV)] ⁿ⁺ with nucleic acids and DNA	380
	D. Interaction of [organotin(IV)] ⁿ⁺ with other bioligands	385
	E. Some results of biological studies	415
	V. Applications	429

^a Department of Inorganic and Analytical Chemistry, University of Szeged, H-6701 Szeged, Hungary

^b Dipartimento di Chimica Inorganica e Analitica "Stanislao Cannizzaro", Università di Palermo, Viale delle Scienze, Parco d'Orleans, 90128 Palermo, Italy

^c Biological Research Center of Hungarian Academy of Sciences, Szeged, Hungary

^d Bioinorganic Research Group of Hungarian Academy of Sciences, Department of Inorganic and Analytical Chemistry, University of Szeged, Szeged, Hungary

*Corresponding author.

E-mail address: laci@chem.u-szeged.hu

Advances in Organometallic Chemistry, Volume 57

ISSN 0065-3055, DOI 10.1016/S0065-3055(08)00004-X

© 2008 Elsevier Inc.

All rights reserved

VI. Conclusions	431
Abbreviations	431
Acknowledgments	432
References	432

I. INTRODUCTION

Organotin(IV) compounds are characterized by the presence of at least one covalent C–Sn bond. The compounds contain tetravalent {Sn} centers and are classified as mono-, di-, tri-, and tetraorganotin(IV), depending on the number of alkyl (R) or aryl (Ar) moieties bound. The anions are usually Cl^- , F^- , O^{2-} , OH^- , $-\text{COO}^-$, or $-\text{S}^-$. It seems that the nature of the anionic group has only secondary importance in biological activity.

The rapid rise in the industrial (catalyst in PVC and foam production), agricultural (fungicides and acaricides), and biological applications (wood, stone, and glass preservatives) of organotin(IV) compounds during the last few decades has led to their accumulation in the environment and, consequently, in biological systems.

It is well known that organotin(IV) compounds display strong biological activity. Most organotin(IV) compounds are generally very toxic, even at low concentration. The biological activity is essentially determined by the number and nature of the organic groups bound to the central {Sn} atom. The $[\text{R}_3\text{Sn(IV)}]^+$ and $[\text{Ar}_3\text{Sn(IV)}]^+$ derivatives exert powerful toxic action on the central nervous system. Within the series of $[\text{R}_3\text{Sn(IV)}]^+$ compounds, the lower homologs (Me, Et) are the most toxic when administrated orally, and the toxicity decreases progressively from propyl (Pr) to octyl (Oc), the latter being not toxic at all towards humans.

Several surveys of organotin(IV) compounds have been published. Saxena and Huber¹ covered the literature dealing with the biological activities, including the anticancer of the most part of the compounds studied until 1989. Melnik and Holloway² compiled the list of X-ray structures of organotin(IV) compounds with different coordination numbers. Another work summarizing the results obtained in the wide field of bioorganotin(IV) compounds was produced by Molloy.³ Later, Tsangaris and Williams⁴ published a paper on organotin(IV) compounds in pharmacy and nutrition. A full listing of reports concerning the evaluation of organotin(IV) compounds in agriculture is found in the two-part review by Crowe.^{5,6} In 1985, two independently published reviews demonstrated the utility of organotin(IV) derivatives of (poly)alcohols in regioselective manipulations involving indirect acylation, alkylation, and oxidation,^{7,8} while a work by Grindley⁹ dealt with the applications of tin-containing intermediates in carbohydrate chemistry. Strong carbohydrate–organotin(IV) cation complexation has been discussed by Burger and Nagy,¹⁰ Gyurcsik and Nagy,¹¹ Verchère et al.¹² in English, and Nagy¹³ in Hungarian, while Barbieri et al.¹⁴ dealt mainly with the interactions of organotin(IV) cations and complexes with deoxyribonucleic acid (DNA) and their derivatives. Gielen¹⁵ compiled the results obtained in Vrije University during the last 20 years. Recent works by Nath et al.¹⁶ or Pellerito and

Nagy¹⁷ covered a large number of publications on the amino acids and peptides and on the other complexes discussed.

The aim of the present work is to survey the results obtained by means of different equilibrium and structural measurements on the complexes formed with the various organotin(IV) cations. The biological activities of parent organotin(IV) and some of the complexes in object are also discussed. In the rest of the chapter, complexes of the organotin(IV) cations will be discussed — in most cases — in the following order:

- (i) the results of equilibrium studies on the systems in question;
- (ii) coordination compounds of mono-, di-, or trialkyltin(IV) cations;
- (iii) complexes of organotin(IV) cations with oxygen, nitrogen, sulphur, or other (mixed) donor atoms.

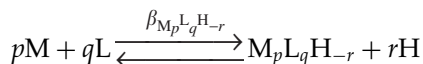
II. PHYSICOCHEMICAL AND BIOLOGICAL METHODS FOR STUDY OF ORGANOTIN(IV) COMPOUNDS

A. pH-metric titration

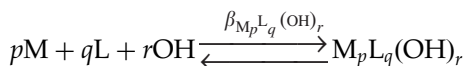
Coordination equilibria were investigated by pH and potentiometric titration in aqueous solution. The measured e.m.f. values (E) are converted into hydrogen-ion concentrations using the modified Nernst equation:

$$E = E_0 + K \cdot \log[H^+] + J_H \cdot [H^+] + \frac{J_{OH} \cdot K_w}{[H^+]}$$

where J_H and J_{OH} are fitting parameters in acidic and alkaline media for the correction of experimental errors, mainly due to the liquid junction and to the alkaline and acidic errors of the glass electrode; K_w is the autoprotolysis constant of water: $10^{-13.75}$ at 298 K. The used parameters were calculated with a nonlinear least squares method. The species formed in the studied systems are characterized by general equilibrium processes, while formation constants for these generalized species are given by equations:



or



$$\beta_{M_p L_q H_{-r}} = \frac{[M_p L_q H_{-r}][H]^r}{[M]^p [L]^q} = \frac{[M_p L_q (OH)_r](K_w)^r}{[M]^p [L]^q [OH]^r} = \beta_{M_p L_q (OH)_r} (K_w)^r$$

Charges are omitted for simplicity; M denotes $[R_{-en}Sn(IV)]^{(4-n)+}$ ($n = 1-3$) and L the ligand molecule deprotonated on its coordinating groups and H the protonation.

B. Analysis

In most cases, the composition of the complexes is determined by standard microanalytical method, but sometimes this gives a relatively large negative error

in the carbon content. This may be due to the formation of volatile organotin(IV) compounds, or of carbides.

To avoid these phenomena, according to our experience, it is necessary to use the so-called Finel–Burell method. The {Sn} content could be measured by slurry nebulization of the sample in inductively coupled plasma-atomic emission spectrometry (ICP-AES).¹⁸ The slurries were prepared by first dissolving the organotin(IV) compounds in a proper solvent (MeOH, pyridine, or acetone) well-miscible with H₂O, and then by adding this solution dropwise to a 0.005% TX-100 tenside solution while maintaining intensive mixing. Typically, 70 µg dm⁻³ detection limit and 1–5% relative standard deviation on five replicates can be achieved by this method.

C. ¹¹⁹Sn NMR spectroscopy

The most convenient technique used to study organotin(IV) derivatives in solution and in solid state is ¹¹⁹Sn NMR spectroscopy. The ¹¹⁹Sn nucleus has a spin of 1/2 and a natural abundance of 8.7%; looking only at the isotopic abundance, it is about 25.5 times more sensitive than ¹³C. The isotope ¹¹⁷Sn is slightly less sensitive (natural abundance 7.7%) but it has not been used as much. Both nuclei have negative gyromagnetic ratios, and, as a consequence, the nuclear Overhauser enhancements are negative. Some examples of the applications of this method are mentioned later, in different sections.

D. ¹¹⁹Sn Mössbauer spectroscopy

The effect discovered by R. Mössbauer in 1957, the “nuclear resonance fluorescence of γ radiation,” is analogous to the atomic fluorescence of UV–vis light. The effect is now generally termed as recoil-free emission and resonant absorption of nuclear γ -rays.¹⁹ The characteristic quantities measured are the Mössbauer isomer shift (δ), the Mössbauer quadrupole splitting (Δ), and the full width at half the maximum of the observed resonance line (Γ) in mm s⁻¹. The information extracted from the ¹¹⁹Sn Mössbauer spectroscopy of {Sn} compounds are essentially: (1) the valence state in the inorganic derivative, (2) the structure and bonding in the metal environment [mainly in organotin(IV)], and (3) the dynamics of the {Sn} nuclei, which possibly correlates with the nature of the substrate (mono- or polymeric). Measurements may be made on solids, gels, and quickly frozen solutions. As usual, this method has both advantages and disadvantages.¹⁷

E. XAFS (EXAFS and XANES) methods

The X-ray absorption fine structure (XAFS) methods (EXAFS and X-ray absorption near-edge structure (XANES)) are suitable techniques for determination of the local structure of metal complexes. Of these methods, the former provides structural information relating to the radial distribution of atom pairs in systems studied: the number of neighboring atoms (coordination number) around a central atom in the first, second, and sometimes third coordination spheres; the

interatomic distances; and their root mean square deviations (Debye–Waller factor, σ , in pm). For analysis of the EXAFS spectra, however, additional and independently obtained spectroscopic data on the metal-ion binding sites and suitable structural models are needed.

XANES method gives useful information of effective electron occupation (oxidation state) of the studied element.

Both techniques use a very high flux X-rays; synchrotron radiation is needed for this kind of measurements.

Some structural data obtained by these methods are also discussed in the following sections. The XANES spectra of organotin(IV) are usually not so informative. The advantages and disadvantages of EXAFS as a structural probe are discussed.^{20,21}

F. X-ray diffraction method

X-ray crystallographic findings for compounds containing a ligand and a metal ion in stoichiometric proportions do not constitute evidence of complex formation in solution. The well-defined crystal structure merely indicates that — in the solid state — the ligands, the metal ion, and the anion are regularly packed in the space, usually held together by coordination, electrostatic, and hydrogen bonding. When crystals are dissolved, solvation can break bonds — both hydrogen bonds or coordination bonds, depending on the nature of the solvent — changing drastically the coordination sphere of the metal ion. Thus, on the basis of the crystal structures only, it is not possible to predict complex formation in solution. On the other hand, when complex formation is known to occur in solution from independent equilibrium measurements, or there are other spectroscopic evidences, it is very likely that the main binding sites are the same in the crystal and in solution. In the crystal, additional weak binding sites may also be present.

G. Biological investigations

Sublethal effects of organotin(IV) compounds, used as biocides toward several organisms, have been extensively investigated. Even if effects are defined as sublethal, there are evidences of critical long-term consequences, eventually affecting metabolism and survival of contaminated species. For this reason there is considerable interest in understanding their toxic action mechanism. Very few agents are able to break DNA directly; rather, damage occurs as a result of metabolic transformation in cells, DNA recombination, replication, repair, or compaction–relaxation (during mitosis) processes.²² Beside affecting the primary structure of DNA, damaging agents induce a complex, prolonged, and unpredictable response in cells. The resulting actions of protective mechanisms provide the cell with ways to survive. Repair, tolerance, cycle delay, or death *via* apoptosis or necrosis are the alternatives.

Apoptosis is known as programmed cell death and represents also a control mechanism within the cell that reacts to the changes in its environment. This active cellular death process is characterized by distinctive morphological changes

which include condensation of nuclear chromatin, cell shrinkage, nuclear disintegration, plasma membrane blebbing, and the formation of membrane-bound apoptotic bodies.²³ In contrast to apoptosis, necrosis is an accidental cell death, often caused by toxic agents.²⁴ Necrosis differs from apoptosis morphologically and biochemically.²⁵ Necrosis is characterized by swelling and bursting of the cell, leading to release of cytoplasmic materials into the extracellular space, as well as by random cleavage of DNA. Furthermore, plasma membrane integrity, which is maintained during apoptosis, is lost during necrosis.

Although toxic agents have the potential to cause necrosis, some of them can interfere with intracellular signaling pathways and induce apoptosis instead of necrosis. It seems that organotin(IV) compounds exert their toxic effects involving all these processes. The precise balance of these actions and their outcomes may differ radically from one cell type to another and among different organisms.

Biological investigations on organotin(IV) compounds are based on evaluation of cell viability. Cell death could be evaluated by diffusion of trypan blue, a common staining used to distinguish between viable and nonviable cells. Cultures are incubated on plates in a growth medium added with test substance. After addition of trypan blue, cells are counted by light microscopy. The only cells positive to the stain are those for which membrane permeability has been lost due to toxic effect. Results are generally presented as percentage respect to an untreated control. Flow cytometry is often chosen as a tool of investigation for its power, not only for cell viability, but also to probe membrane and chromosomal damage, cell-cycle analysis, and morphological alterations.

The DNA content of each cell in any living organism is generally highly uniform. In the resting phase of the cell-cycle, a human somatic cell contains approximately 6–7 pg of DNA (diploid DNA content). This stage is occupied by noncycling cells (G_0 phase) as well as those recovering from the previous division or preparing for the next cycle (G_1 phase). At the beginning, in the process of replication, a cell enters DNA synthesis (S phase). Cellular DNA content progressively increases until replication is complete: the cell enters the G_2 phase with a DNA content twice that of G_1 (tetraploid). After repairing damaged DNA and organizing the chromosomes, the cell enters mitosis (M phase) dividing into two diploid daughter cells and completing the cycle.²⁶ The DNA flow histograms represent snapshots of the distribution of nuclei in the various phases of the cell-cycle at the time of fixation. Because organotin(IV) toxicity in cell cultures evolves over 24–48 h,²⁷ these are, usually, chosen as incubation times before harvesting. By comparing the normal cell-cycle DNA content distribution of appropriate cell lines with that of cells incubated with 10^{-5} M concentration of the various potential toxicants for 24 h, it is possible to observe effects on the DNA content distributions. The appearance of distinct subpopulations, characterized by reduction of PI-fluorescence (DNA content; PI = propidium iodide) and reduction of forward angle light scatter (1–19°; this angle is function of the mean cell size) is indicative of apoptotic cells.

Another morphological assay of apoptosis is done with acridine orange, a nuclear staining that reveals chromatin condensation under light and fluorescent microscope.

Annexin V FLUOS staining is another procedure which allows to label the cells by allowing the observation of the morphological features of apoptosis.

One of the early events of the apoptotic process involves the translocation of phosphatidylserine on the surface of cell membranes; annexin V binding and propidium iodide uptake reveals various cellular states. After treatment with organotin(IV) compounds the cells could be categorized into populations; vital cells (annexin V⁻/P⁻), early apoptotic cells (annexin V⁺/P⁻), late apoptotic cells (annexin V⁺/P⁺), and necrotic cells (annexin V⁻/P⁺). Cells are observed with a fluorescence microscope and it is possible to observe translocation of phosphatidylserine (PS) from the inner side of the plasma membrane to the outer one and to see a green stain for annexin V FLUOS bound to PS, and a red stain for propidium iodide.

The terminal dUTP nick end labeling assay (TUNEL reaction) and electrophoretic analysis of DNA/organotin(IV) mixtures allowed the investigation of DNA fragmentation.

Two main apoptotic pathways have been identified in mammalian cells: the extrinsic pathway that is activated by the binding of ligands to cell-surface death receptors,²⁸ and the intrinsic pathway that involves the mitochondrial release of cytochrome c.²⁹ The activation of extrinsic and intrinsic apoptotic pathways promotes the cleavage into the active form of the pro-caspase-8 and pro-caspase-9, respectively, that mainly determine the activation of effector caspase-3.³⁰ The intrinsic pathway is the main apoptotic pathway activated by chemotherapeutic drugs, while the cytotoxic drug-induced activation of the extrinsic pathway is a more controversial issue.³¹

Active effector caspases, such as caspase-3, mediate the cleavage of an overlapping set of protein substrates, resulting in the morphological features of apoptosis and the demise of the cell. Therefore, it could be crucial to determine if organotin(IV) compounds could induce the activation of caspases. The proteolytic processing of caspase-9 and -3 could be examined by Western blotting experiments using appropriate antibodies (anticaspase), to determine if compounds induce apoptosis *via* the mitochondrial pathway.

Developmental systems represent a suitable field of study because they share certain fundamental features that include:

1. storage and transfer of developmental information;
2. molecular, cell, or organism growth;
3. morphogenesis; and
4. differentiation, the emergence of a functionally speedised state.

The genotoxicity studies of organotin(IV) compounds and mutagenicity test are widely developed and used mainly in aquatic developing embryos such as *Truncatella subcylindrica* (Mollusca, Mesogastropoda), *Anilocra physodes* (Crustacea, Isopoda), *Aphanius fasciatus*, *Rutilus rubilio* (Pisces, Teleostei), and *Paracentrotus lividus* (Echinodermata). At ultrastructural level, biological investigations include the observation by transmission electron microscopy (TEM) of fertilized eggs and embryos at different development stages. Specimens in the TEM are examined by passing the electron beam through them, revealing structural lesions: breakages,

bridging, irregular outline, and light areas after staining. As the electron beam passes through the specimen, some electrons are scattered, while the remaining are focused by the objective lens either onto a phosphorescent screen or photographic film to form an image. Unfocused electrons are blocked out by the objective aperture, resulting in an enhancement of the image contrast. Contrast in the TEM depends on the atomic number of the atoms in the specimen; the higher the atomic number, the more electrons are scattered and thus greater is the contrast. Biological molecules are composed of atoms of very low atomic number ($\{C\}$, $\{N\}$, $\{H\}$, $\{P\}$ and $\{S\}$). Thin sections of biological material are made visible by selective staining.³²

It is possible to observe effects of organotin(IV) compounds exposure such as inhibition of cleavage of fertilized eggs, interference with the formation of the mitotic spindle, damages affecting chromosome structure, and electron-dense precipitate formation in organelles.

To correlate embryonic arrests with the metabolic pathways, and especially to understand why cellular organelles first undergo chemical damages, biological investigations include evaluation of DNA, RNA, protein, glucose, lipid, and adenosine-5'-triphosphate (ATP) contents, whose fractions are extracted and isolated by modified Schneider methods. In particular,

- (a) DNA, RNA, and lipid contents are determined according to standard methods described by Dische and Schwarz,³³ Brown,³⁴ Marsh and Weinstein,³⁵ respectively.
- (b) Protein content determinations are carried out according to the Lory³⁶ modified method, after precipitation with 5% TCA and collection of the insoluble material as pellet with a 10,000g centrifugation.
- (c) Finally, Gluc and ATP contents are, usually, determined according to the GOD-POD-PAP method.

III. HYDROLYSIS OF [ORGANOTIN(IV)]ⁿ⁺ CATIONS

In order to understand the activity of organotin(IV) in water environments (both fresh and seawater), equilibrium and speciation studies are very important. Moreover, characterizing the structures of hydrolyzed species could be helpful to assess the toxicity mechanism.

The species [organotin(IV)]⁽⁴⁻ⁿ⁾⁺ ($n = 1-3$) are considered to be Lewis acids of different strength, depending on the groups bound to the tin atom.³⁷ As a consequence, they promptly hydrolyze in aqueous solution, as first demonstrated by Tobias.³⁸ Later studies on the interactions of [Me₂Sn(IV)]²⁺ with ligands containing different donor atoms ($\{O\}$, $\{N\}$, $\{S\}$, etc.) necessitated determination of the hydrolysis constants; the evaluation of such complex formation constants was based on the data obtained earlier from independent measurements. Some data are compared in Table 1.

Most of the reported thermodynamic parameters refer to a single ionic medium and a single ionic strength. Hydrolysis of [Me₂Sn(IV)]²⁺ was performed

Table 1 Stability constants of species formed in the hydrolysis of [Me₂Sn(IV)]²⁺ at 298 K in different media

(p,r)	Log β _{pr}				
	0.1 M NaClO ₄	0.1 M NaNO ₃	0.1 M KNO ₃	0.1 M NaCl	3 M NaClO ₄
(1,-1)	-3.17	-3.18	-3.12	-3.25	-3.54
(1,-2)	-8.42	-8.42	-8.43	-8.54	-8.98
(1,-3)	-19.45	—	-19.45	—	—
(2,-2)	-4.96	-4.69	-5.05	-5.05	-4.60
(2,-3)	-9.71	-9.64	-9.74	-9.81	-9.76
(2,-4)	—	-15.44	—	—	—
(3,-2)	—	-3.21	—	—	—
(3,-4)	—	—	—	-11.52	-10.40
(4,-5)	—	-11.72	—	—	—
(4,-6)	—	-16.36	—	—	—
Reference	39	40	41	42	42

p = [Me₂Sn(IV)]²⁺, r = OH⁻.

in different aqueous media [NaCl or (Me)₄NCl, NaNO₃, NaClO₄, and Na₂SO₄], in a wide range of ionic strength at 298 K. The dependence on the ionic strength for different salt solutions was taken into account by using a Debye–Hückel equation. Medium effects were explained considering the formation of chloride and sulfate complexes too.⁴³

According to Rizzarelli et al.⁴¹ there is no significant difference in the acidities of [Me₂Sn(IV)]²⁺ and [Et₂Sn(IV)]²⁺. This result is in contrast with earlier findings by Tobias, which pointed to an acidity increase in the series [Me₂Sn(IV)]²⁺, [Et₂Sn(IV)]²⁺, and [Pr₂Sn(IV)]²⁺, with log K values of -3.54, -3.40, and -2.92, respectively.³⁷ This trend, which is opposite to that observed for [Me₃Sn(IV)]⁺ and [Et₃Sn(IV)]⁺, and to that expected simply on the basis of inductive effects, was explained by invoking a decreasing degree of solvation of the acid with increase in size of the R groups. It is likely that the difference between these results and the published results³⁷ is attributable to an incomplete model that considers only the formation of [R₂Sn(OH)]⁺ and [(R₂Sn)₂(OH)₂]²⁺ hydroxo species.

Recently, these reactions were reinvestigated by Gharib et al.⁴⁴ They have found the same species with similar stabilities as was discussed above.

Despite their environmental relevance, relatively few studies have been performed on the solution chemistry of [R₃Sn(IV)]⁺, though their structures have been extensively investigated both in the solid state and in solution. In natural waters, they can originate also from bioalkylation processes.^{45,46} Tributyltin(IV) derivatives are also used as “antifouling” additives in paints for ships. Therefore, they are often present in the marine environments, with a higher concentration in sediments, especially in harbor areas where naval traffic is more intense. The distribution of organotin(IV) compounds between water and sediments strongly depends on their solubility in aqueous media. For example, the solubility of

Table 2 Comparison of literature data on the hydrolysis constants of $[\text{Me}_3\text{Sn(IV)}]^+$

Ionic medium	Methods	$-\text{Log } \beta_{11}$	Reference
KNO_3 , 0.5 M	NMR	6.35	47
KCl , 0.5 M	NMR	6.38	47
NaClO_4 , 3 M	pH-metry	6.59	37
KCl , 2 M	pH-metry	6.40	48
NaNO_3 , 0.5 M	pH-metry	6.21	50
NaCl , 0.5 M	pH-metry	6.25	50
NaClO_4 , 0.3 M	pH-metry	6.26	49

All measurements were performed at 298 K.

Me_3SnCl in seawater is estimated to be around to $15,000 \text{ mg dm}^{-3}$, while the solubility of Pr_3SnCl and of Bu_3SnCl are lower, 50 and 25 mg dm^{-3} , respectively. Studies of the hydrolysis on aqueous solutions of $[\text{Me}_3\text{Sn(IV)}]^+$ have been performed by ^{119}Sn NMR measurements⁴⁷ and by pH-metric titrations, in NaClO_4 medium (3 and 0.3 mol dm^{-3}).^{37,48} Investigations of the interactions of $[\text{Me}_3\text{Sn(IV)}]^+$ with carboxylic and amino acids were measured in aqueous solution (total ionic strength adjusted to 0.3 mol dm^{-3}).⁴⁹ Cannizzaro reinvestigated the system in different ionic media (NaNO_3 and NaCl), at different ionic strengths ($0\text{--}1.5 \text{ mol dm}^{-3}$) and at different temperatures ($5\text{--}45^\circ\text{C}$). Only two species could be detected throughout the whole pH range: Me_3SnOH and $[\text{Me}_3\text{Sn(OH)}_2]^-$. At higher Cl^- ion concentrations, the cation also forms a weak chloro complex.⁵⁰ For purpose of comparison, the $-\log \beta_{11}$ values are collected in Table 2.

A recent work by Sammartano et al.⁵¹ demonstrated that the $[\text{Me}_3\text{Sn(IV)}]^+$, $[\text{Et}_3\text{Sn(IV)}]^+$, and $[\text{Pr}_3\text{Sn(IV)}]^+$ in synthetic seawater form the mononuclear hydrolytic species $[\text{M(OH)}]^0$, whose formation is relevant at the pH of natural fluids (between 6 and 8) for all the trialkyltin(IV) cations. Dependence on the medium (NaNO_3 , NaCl , Na_2SO_4) was interpreted both in terms of ion pair formation between $[\text{R}_3\text{Sn(IV)}]^+$ cation and chloride or sulfate anions, and in terms of specific interactions. In addition to the equilibrium studies on the hydrolysis of $[\text{Me}_2\text{Sn(IV)}]^{2+}$, the structures of the main species formed have also been determined. In ethanol solution the *trans*- Me_2 species are formed, with composition $\text{Me}_2\text{SnCl}_2(\text{EtOH})_2$. This species has an octahedral (O_h) structure.^{52,53} In aqueous solution, the gradual hydrolysis of $[\text{Me}_2\text{Sn(IV)}]^{2+}$ has been followed by potentiometric titration and Mössbauer spectroscopic measurements. The results show that the structure varies from O_h in the aquo species $\text{Me}_2\text{Sn(H}_2\text{O)}_4$ to T_d in $\text{Me}_2\text{Sn(OH)}_2$.

The ^1H NMR spectra of Me_2SnCl_2 ⁵⁴ and Et_2SnCl_2 ⁵⁵ solutions present a sharp signal with satellite peaks, as a result of heteronuclear couplings [$^2J\text{--}(^{117}\text{Sn--}^1\text{H})$ and $^2J\text{--}(^{119}\text{Sn--}^1\text{H})$] with the two NMR active isotopes of Sn. In the $[\text{Me}_2\text{Sn(IV)}]^{2+}$ system, both the chemical shift and the coupling constants decrease with increasing pH. The $^2J\text{--}(^{119}\text{Sn--}^1\text{H})$ values can be used to determine the C–Sn–C angle, providing information on the structure of the species formed in solution.⁵⁶

Table 3 Individual NMR parameters (δ , 2J) calculated for different hydrolytic species of [Me₂Sn(IV)]²⁺ (Ref. 54) and [Et₂Sn(IV)]²⁺ (Ref. 55)

Species	$\delta(\text{CH}_3)$ (ppm)	$\delta(\text{CH}_2)$ (ppm ²)	$J(\text{Sn-H})$ (Hz)	C-Sn-C°
[Me ₂ Sn(IV)] ²⁺	0.89	–	106	175
[Me ₂ Sn(OH)] ⁺	0.87	–	95	154
Me ₂ Sn(OH) ₂	0.64	–	81	175
[Me ₂ Sn(OH) ₃] [–]	0.41	–	81	132
[Me ₂ Sn ₂ (OH) ₂] ²⁺	0.74	–	80	132
[Me ₂ Sn ₂ (OH) ₃] ⁺	0.79	–	82	132
[Et ₂ Sn(IV)] ²⁺	1.244	1.582	90.8	146
[Et ₂ Sn(OH)] ⁺	1.289	1.536	73.5	123
Et ₂ Sn(OH) ₂	1.213	1.320	71.0	120
[Et ₂ Sn(OH) ₃] [–]	1.205	1.153	70.7	120
[Et ₂ Sn ₂ (OH) ₂] ²⁺	1.143	1.319	88.2	142
[Et ₂ Sn ₂ (OH) ₃] ⁺	1.188	1.343	70.3	120

From the ¹H NMR spectra of Me₂SnCl₂ solutions recorded at different values of pH, considering the known species distribution of hydroxo complexes in fast mutual exchange, it is possible to calculate the individual NMR parameters (δ , 2J) for the different species. The values calculated for the different hydrolytic species are collected in Table 3. These data suggest an *O_h* structure for the aqua ion, a trigonal bipyramidal (*Tbp*) structure for the complexes M(OH)₂, M(OH)₃, M₂(OH)₂, and M₂(OH)₃, {where M = [Me₂Sn(IV)]²⁺ or [Et₂Sn(IV)]²⁺}, for M(OH)₂, more probably a *T_d*,⁵⁷ while for MOH an intermediate value is determined, probably as results of: (1) the coexistence of both *O_h* and *Tbp* structures in fast mutual exchange; or (2) a very distorted structure.

A rhombic crystal of the perchlorate of [(Me₂Sn)₂(OH)₃]⁺ was obtained.⁴⁰ The results of crystal structure analysis showed that the polymer structure consists of pentacoordinate {Sn} units with di- and monohydroxo bridging. The coordination geometry of the {Sn} unit is a distorted *Tbp* with two Me groups and one μ -hydroxo group in *eq* positions (equatorial position in the geometry) and the other two μ -hydroxo groups in *ax* positions (axial position in the geometry). Each di- μ -hydroxo bridge has two different Sn–O bond lengths, 203.0 and 222.0 pm for Sn(1)–O(3) and Sn(1)–O(3'), and 201.9 and 223.6 pm for Sn(2)–O(2) and Sn(2)–O(2'). The shorter and longer bonds correspond to the *eq* (Sn–O_{eq}) and *ax* bonds (Sn–O_{ax}), respectively. This di- μ -hydroxo structure is quite similar to that of the nitrate dimer, di- μ -hydroxo-bis[dimethylnitratotin(IV)],⁵⁸ in which the two bridging bond lengths are 206 and 218 pm. On the other hand, the mono- μ -hydroxo O(1) bridges Sn(1) and Sn(2), *via* their *ax* positions, with similar bond lengths, 213.9 and 213.2 pm, respectively.

Mono-organotin(IV) compounds, considered the least toxic among organotin(IV) derivatives [R₃Sn(IV)⁺ > R₂Sn(IV)²⁺ > RSn(IV)³⁺ > Sn⁴⁺, toxicity scale], have not achieved as much commercial application as diorgano- and triorganotin(IV) derivatives. However, they are often used as hydrophobic agents for building

materials and cellulose-derived materials⁶ and may be present in the aquatic environment as a first step in the alkylation of inorganic Sn.⁴⁵

The behavior of $[\text{RSn(IV)}]^{3+}$ compounds in aqueous solution has not been widely investigated. Most of the studies, performed many years ago, concern the complex formation with N-donor containing molecules⁵⁹ and with Cl^- (Ref. 60–62) and F^- ions.^{63,64} Raman spectroscopic measurements showed the formation of the species $[\text{CH}_3\text{SnCl}_2(\text{OH})_2]^-$ in the presence of a high concentration of Cl^- . The results of NMR measurements in very concentrated solutions of $[\text{CH}_3\text{Sn(IV)}]^{3+}$ (from 210 up to 830 mmol dm^{-3}) indicated the formation of mixed chloro-hydroxo complexes $[\text{CH}_3\text{SnCl}_x(\text{OH})_y]$, with x decreasing in dilute solutions. Analogous behavior was found by Tobias³⁸ and more recently by Gianguzza et al.⁴³ in the interactions of $[\text{Me}_2\text{Sn(IV)}]^{2+}$ in Cl^- -containing solutions. Luijten⁶⁵ investigated the hydrolysis products of Et-, Bu-, and Oct SnCl_3 and reported their properties and preparation in the solid state. Some potentiometric studies on the hydrolysis^{66–68} and complex formation with S^{2-} (Ref. 69) of EtSnCl_3 in mixed water/methanol solutions have been performed by Devaud et al., in the concentration range 6–60 mmol dm^{-3} . The results obtained by these authors are partially in contrast with the earlier findings on MeSnCl_3 , probably because of the different solvent and concentration ranges used. Results of ^1H and ^{119}Sn NMR and ^{119}Sn Mössbauer spectroscopic studies on the hydrolysis of Me- and Bu SnCl_3 (0.5 mol dm^{-3}) have been reported by Blunden et al.^{70,71} In the very recent and detailed publication of De Stefano et al.⁷² it was found that at low MeSnCl_3 concentration only five different species could be detected (with metal to OH^- ion ratios 1:1, 1:2, 1:3, 1:4, and 2:5). The first hydrolysis step takes place at very low pH. The obtained equilibrium constants are given in Table 4. According to the species distribution curves, the amount of the dimeric species gradually increases along with the concentration of $[\text{MeSn(IV)}]^{3+}$. Among the triply charged cations, $[\text{MeSn(IV)}]^{3+}$ is the most hydrolyzed: it undergoes hydrolysis at lower pH values than those for Fe(III) and Al(III).

Table 4 Equilibrium constants and standard deviations for the hydrolysis of $[\text{MeSn(IV)}]^{3+}$ at 25 °C and $I = 0 \text{ mol dm}^{-3}$ (Ref. 72)

Reactions	Log β
$\text{MeSn(IV)}^{3+} + \text{H}_2\text{O} \rightleftharpoons [\text{MeSn(IV)(OH)}]^{2+} + \text{H}^+$	-1.5 ± 0.5
$\text{MeSn(IV)}^{3+} + 2\text{H}_2\text{O} \rightleftharpoons [\text{MeSn(IV)(OH)}_2]^+ + 2\text{H}^+$	-3.36 ± 0.05
$\text{MeSn(IV)}^{3+} + 3\text{H}_2\text{O} \rightleftharpoons [\text{MeSn(IV)(OH)}_3]^0 + 3\text{H}^+$	-8.99 ± 0.04
$\text{MeSn(IV)}^{3+} + 4\text{H}_2\text{O} \rightleftharpoons [\text{MeSn(IV)(OH)}_4]^- + 4\text{H}^+$	-20.27 ± 0.06
$2\text{MeSn(IV)}^{3+} + 5\text{H}_2\text{O} \rightleftharpoons \{[\text{Me}_2(\text{Sn(IV)})_2(\text{OH})_5]^+ + 5\text{H}^+$	-7.61 ± 0.08
$\text{MeSn(IV)}^{3+} + \text{OH}^- \rightleftharpoons [\text{MeSn(IV)(OH)}]^{2+}$	-1.5 ± 0.5
$\text{MeSn(IV)}^{3+} + 2\text{OH}^- \rightleftharpoons [\text{MeSn(IV)(OH)}_2]^+$	22.64
$\text{MeSn(IV)}^{3+} + 3\text{OH}^- \rightleftharpoons [\text{MeSn(IV)(OH)}_3]^0$	33.01
$\text{MeSn(IV)}^{3+} + 4\text{OH}^- \rightleftharpoons [\text{MeSn(IV)(OH)}_4]^-$	35.73
$2\text{MeSn(IV)}^{3+} + 5\text{OH}^- \rightleftharpoons \{[\text{MeSn(IV)}]_2(\text{OH})_5\}^+$	62.38

IV. INTERACTIONS OF [ORGANOTIN(IV)]ⁿ⁺ WITH BIOLOGICAL MOLECULES

A. Interactions of [organotin(IV)]ⁿ⁺ with amino acids and peptides

The most widely studied interactions between biologically active ligands and organotin(IV) cations relate to the amino acids and their derivatives (N- or S-protected amino acids and peptides), though new data on several of the most commonly occurring amino acids are still being published. This is specially true for aqueous speciation studies. Nice and very detailed reviews were published in this area by Molloy³ and Nath.¹⁶

In aqueous solutions at pH 7, there is little evidence of complex formation between [Me₃Sn(IV)]⁺ and Gly.^{49,73} Potentiometric determination of the formation constants for L-Cys, DL-Ala, and L-His with the same cation indicates that L-Cys binds more strongly than other two amino acids (pK₁ ca. 10, 6, or 5, respectively).⁷⁴ Equilibrium and spectroscopic studies on L-Cys and its derivatives (S-methylcystein (S-Me-Cys), N-Ac-Cys) and the [Et₂Sn(IV)]²⁺ system showed that these ligands coordinate the metal ion *via* carboxylic {O} and the thiolic {S} donor atoms in acidic media. In the case of S-Me-Cys, the formation of a protonated complex MLH was also detected, due to the stabilizing effect of additional thioether coordination.⁷⁵

A number of equilibrium data, among them data on amino acids, were published on [R₂Sn(IV)]²⁺ complexes.^{39,41,76–79} These studies also revealed the “chameleon” nature of the [R₂Sn(IV)]²⁺, since strong affinity was reported toward ligands containing {O}, {S, O, N}, or {O, N} donor sites. The formation constants and the thermodynamic quantities of the [Me₂Sn(IV)]²⁺ complexes of Gly, DL-Ala and DL-Met were determined in the pH range 3.5–5.5.⁸⁰ Complex formation equilibria of [divinyln(IV)]²⁺ with amino acids, oligopeptides, and dicarboxylic acids were also investigated. The results showed the formation of ML, MLH, and ML₂ species with amino acids, while peptides form ML and MLH_{–1} complexes; the latter species contains deprotonated amide nitrogen.⁸¹ Several organotin(IV) complexes of L-Cys were prepared and characterized by ¹H NMR, UV–vis, FT-IR, and Mössbauer spectroscopic techniques. One of the dimeric compounds was obtained as a single crystal, after recrystallization from DMSO/methanol 2:1 solution.⁸²

In the solid state, the di- and triorganotin(IV)-amino acid compounds are readily formed by reaction between the free ligand and an organotin(IV) oxide or hydroxide.⁸³ FT-IR [$\nu_a(\text{COO})$] and Mössbauer spectroscopic data showed that organotin(IV) derivatives of Gly are N-bridged polymers.^{84,85} This structure has been confirmed crystallographically and extensively evaluated by Mössbauer spectroscopy.^{63,86} The N–Sn interaction apparently occurs in Gly derivatives, because the carbonyl oxygen atom is involved in the hydrogen bonding network –C = O...H–N. In N-protected Gly complexes, polymerization occurs through bidentate –COO[–] groups, or by bridging through the amide oxygen atom.^{87–89} [Me₃Sn(IV)]⁺ and [Me₂Sn(IV)]²⁺ complexes of *N*-benzoylglycine (N-Bz-Gly) display antitumor activity against the leukemia P-388 cell line.⁹⁰

Several alkyltin(IV) complexes of peptides have been prepared and studied in the solid state (or dissolved in different solvents),^{91–94} for example, Me-N-Bz-Leu-His was found to be a useful model to mimic alkyltin(IV) binding of proteins through imidazolic {N}. The metal binding by amidic {N} is particularly important in peptide complexes. X-ray diffraction (XRD) studies of some crystalline $R_2Sn(IV)$ -peptide complexes and NMR measurements on the same complexes dissolved in H_2O solution, provided definite evidence for formation of the $Sn-N^-$ bond.^{92,95} The pH-metric and spectroscopic results have confirmed that the $[Me_2Sn(IV)]^{2+}$ does not interact with histamine (Histm) and Gly-Histm which contain only {N} donor atoms. Hydrolyzed species of the $[Me_2Sn(IV)]^{2+}$ always predominate over the complexes with Gly-Histm, imidazole-4-acetic acid, Gly and β -Ala-His, while the glycyl-glycine (Gly-Gly) and glycyl-histidine (Gly-His) coordinate through $\{-COO^-, N^-, NH_2\}$ donor sites at neutral pH and *Thp* species are formed.⁵⁴ Very similar species are formed between $[Me_2Sn(IV)]^{2+}$ and Gly-Asp and Asp-Gly as ligands as mentioned above.⁹⁶ Continuing this work, the coordination properties of Ala-Gly and its mercapto analog *N*-(2-mercapto-propionyl) glycine (MPGly) toward $[Me_2Sn(IV)]^{2+}$ were compared.⁹⁷ The considerably higher stability of the MPGly complexes is due to the outstanding affinity of the $[Me_2Sn(IV)]^{2+}$ cation toward {S} donor atoms. In the MLH and ML species, formed in acidic region, monodentate carboxylate, and thiolate coordination have been observed for Ala-Gly and MPGly, respectively. Therefore, different donor groups assist the metal-promoted deprotonation of amide nitrogen.

In consequence of their structural variability, organotin(IV) derivatives of *N*-substituted amino acids and peptides have been extensively studied in recent decades. It is of particular interest to examine the structural variations caused by organic substituents on the {Sn} and protecting groups on the amino {N} of the ligand. The spectroscopic data have revealed that in $[R_3Sn(IV)]^+$ derivatives of *N*-Ac dipeptides the $-COO^-$ groups of the latter are bound in a monodentate manner.^{83,90} The amide $-C=O$ group coordinates to another $[R_3Sn(IV)]^+$ unit in these compounds, resulting in a polymeric structure. In contrast, $[R_3Sn(IV)]^+$ derivatives of *N*-acetyl-glycine (*N*-Ac-Gly) and *N*-acetyl-cysteine are believed to contain bidentate $-COO^-$ donor groups.⁹⁸

In the *N*-Bz derivatives of Gly^{87,88} and Gly-Gly,⁹⁹ the planar $[R_3Sn(IV)]^+$ moieties are bridged by $-COO^-$ groups. Because of the negative inductive effect of the Ph group, which reduces the donor ability of oxygen atoms, coordination of the amide $-C=O$ in the latter compounds could be ruled out.

The influence of the length of the peptide chain on the coordination mode in $[R_3Sn(IV)]^+$ complexes has recently been studied.¹⁰⁰ The Gly-Gly-Gly moiety proved to be long enough to shade the $-I$ effect of the Bz group in its *N*-Bz derivatives: $[R_3Sn(IV)]^+$ complexes of *N*-Bz-Gly-Gly-Gly were considered to be polymeric, with monodentate carboxylate and $-C=O$ coordination similar to that in the corresponding complexes of *N*-acetylated peptides.^{83,100,101}

$[R_2Sn(IV)]^+$ derivatives of *N*-Bz-Gly-Gly⁹⁹ and *N*-Bz-Gly-Gly-Gly¹⁰⁰ were found to involve both dicarboxylate binding to yield hexacoordinated {Sn} centers, and dimeric tetraorganodistannoxanes in which the carboxylates bind

alternatively as monodentate and bridging bidentate groups. In these compounds, the involvement of amide groups in the coordination has been totally excluded. On the other hand, in triorganotin(IV) derivatives of N-Bz-Gly-Gly⁹⁹ and N-Bz-Gly,^{87,88} planar [R₃Sn(IV)]⁺ units are bridged by -COO⁻ groups. A different coordination mode is observed in triorganotin(IV) derivatives of amino acids and N-acetylated dipeptides: XRD studies on trimethyltin(IV) glycinate¹⁰⁶ and vibrational and Mössbauer spectroscopic data for the other derivatives^{83,101} showed that the -COO⁻ group acts essentially as a monodentate ligand, and that the amino¹⁰⁷ or amide C=O group^{83,101} coordinates to another [R₃Sn(IV)]⁺ unit. In this way pentacoordination of the {Sn} and polymeric structure resulted. The amide, C=O, group not seems to be able to coordinate to the central {Sn} atom in N-Bz derivatives, presumably as a consequence of the reduced donor power of the {O} atom, due to the inductive effect (-I) of the Ph group. On the other hand, in the [R₃Sn(IV)]⁺ derivatives of N-Bz-Gly-Gly-Gly and N-Ac-Gly-Gly-Gly the {Sn} atom is in a *Tbp* environment, where the planar [R₃Sn(IV)]⁺ unit is bound by a monodentate -COO⁻ and presumably the amide -C=O. The diorganotin(IV) compounds gave both dicarboxylates R₂SnL₂, containing hexacoordinated {Sn}, and dimeric tetraorganodistannoxanes {[R₂SnL]₂O}₂, in which the {Sn} atoms are essentially pentacoordinated.¹⁰⁰

Recent work demonstrated that in R₂SnL (R=Bu, L = the dianion of glycylytyrosine, glycylytryptophane, leucyltyrosine, leucylleucine, valylvaline, and alanylvaline) complexes, all the ligands act as dianionic tridentate ligands coordinating through the -COO⁻, NH₂, and peptidic {N} groups, whereas in Ph₃SnHL the ligand acts as a bidentate coordinating by -COO⁻ and NH₂ groups. The R₂SnL complexes are monomeric, and the polyhedron around the {Sn} is a *Tbp* with Bu groups and N_{peptide} in the *eq* positions, while the *ax* positions are occupied by a carboxylic {O} and an amide {N} atom. In Ph₃Sn(HL) the structure is intermediate between pseudotetrahedral and *cis-Tbp*, with the N-amino and two phenyl groups in *ax* positions. All the complexes were tested against seven cancer cell lines of human origin, *viz.* MCF-7, EVSA-T, WiDr, IGROV, M19, MEL A498, and H226. Ph₃Sn(HL) displays the lowest ID₅₀ values of the compounds tested and reported in this publication. Its activity is comparable to those of methotrexate and 5-fluorouracil. All the [Bu₂Sn(IV)]²⁺ compounds exhibit lower *in vitro* activities than [Ph₃Sn(IV)]⁺ derivatives; however, they do provide significantly higher activities than etoposide and cisplatin (see Table 5).¹⁰² Some of the aforementioned complexes were tested a wide spectrum of bacteria (*Escherichia coli*, *Rhizobium meliloti*, *Pseudomonas putida*, and *Aeromonas formicans*) and fungi (*Aspergillus niger*, *Penicillium chrysogenum*, *Aureobasidium pullulans*, and *Verticillium dahliae*) and were found to be active. The LD₅₀ values are >500 mg kg⁻¹ for albino rats. Some of the complexes also exhibit very high anti-inflammatory activity.¹⁰³ The same authors published a paper on the structure-activity relationship of the di- and triorganotin(IV) derivatives of amino acids and peptides.¹⁰⁴ Some triorganotin(IV) complexes exhibit good anti-inflammatory activities comparable to that of phenylbutazone.

[Ph₃Sn(IV)]⁺ complexes of N-Ac-Gly, N-acetyl-leucine, N-acetyl-asparagine, and N-Ac-L-Tyr were prepared by two procedures and characterized by means

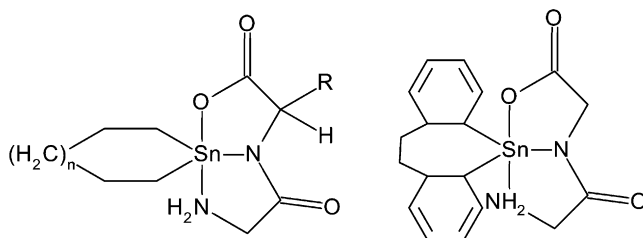
Table 5 *In vitro* antitumor activity (LD_{50} , $ng\ ml^{-1}$) values of compounds 1–7, in comparison with some reference compounds used clinically¹⁰²

Cell line	1	2	3	4	5	6	7	DOX	TAX	MTX	DDPt	5FU	ETO
MEL A498	138	196	336	155	134	332	30	90	<3	37	2253	143	1314
EVSA-T	21	64	74	56	32	84	7	8	<3	5	422	475	317
H226	57	133	177	108	78	105	11	199	<3	2287	3269	340	3934
IGROV	25	72	118	90	46	199	6	60	<3	7	169	7	580
M19	73	182	205	150	89	139	16	16	<3	23	558	23	505
MCF-7	40	93	150	96	51	478	10	10	<3	18	699	18	2594
WiDr	284	424	420	295	265	332	8	11	<3	<3	967	<3	150

MEL A498, renal cancer; EVSA-7, mammary cancer; H226, lung cancer; IGROV, ovarian cancer; M19, melanoma; MCF-7, mammary cancer; WiDr, colon cancer.

1, Bu_2Sn -Gly-Tyr; 2, Bu_2Sn -Gly-Trp; 3, Bu_2Sn -Leu-Tyr; 4, Bu_2Sn -Leu-Leu; 5, Bu_2Sn -Val-Val; 6, Bu_2Sn -Ala-Val; 7, Ph_3Sn -Gly-Leu.

DOX, doxorubicine; TAX, taxol; MTX, methotrexate; DDPt, cisplatin; 5FU, flurouracil; ETO, etoposide.

**Figure 1** Structures of stannacyclohexyl and stannacycloheptyl derivatives (AA).¹⁰⁶

of different spectroscopic methods (FT-IR, multinuclear, 1H , ^{13}C , and ^{119}Sn NMR and ^{119}Sn Mössbauer spectroscopy). The data indicated that the N-Ac-Gly complex adopts a *Tbp* structure in which the monodentate carboxylate and the amide, $-C=O$, group are bound to the same organotin(IV) moiety. The other three complexes are linear oligomers in which the planar $[Ph_3Sn(IV)]^+$ is coordinated axially by a monodentate $-COO^-$ and an amide $-C=O$ from two different ligands. At the C-terminal end of the oligomer chain there is a tetracoordinated Sn(IV) with a monodentate $-COO^-$ as donor group.¹⁰⁵

Stannacyclohexyl and stannacycloheptyl derivatives of dipeptides (AA) were prepared and investigated by Barbieri et al. In these compounds, {Sn} is a member of a ring system (Figure 1). IR and ^{119}Sn Mössbauer spectroscopic data on the solid compounds indicate that the AA acts as a tridentate {O, N, N} ligand and the {Sn} has a *Tbp* environment. An analogous structure has been found for the undissociated molecules in methanol solution.¹⁰⁶ This work clearly demonstrated that there are no basic restrictions for Sn(IV) to extend its coordination sphere (at least to attain pentacoordination) when it is part of a cycloalkyl system. These results are confirmed by an X-ray structure determination of the Schiff base complex H_2SAT [$=2$ -(*O*-hydroxyphenyl)benzothiazolidine] in which the {Sn} is pentacoordinated.

B. Interactions of [organotin(IV)]ⁿ⁺ with carbohydrates and their derivatives

Organotin(IV) compounds have been used widely in synthetic carbohydrate chemistry,^{108–110} because of the regioselective directing power of the organometallic cation toward further reactivity of the sugar substrate. They provide reliable, high-yielding methods for obtaining monosubstituted derivatives of diols or polyols, often with high selectivity. Moreover, the reactions occur under milder conditions or at rates that are much higher than those for the parent alcohols. For further reading, extended references for such applications can be found in several reviews and books.^{7,111,112}

Literature contains only a few reports on equilibrium studies on the interactions of organotin(IV)–carbohydrates or carbohydrate derivatives. ¹³C NMR spectroscopy and mass spectrometry measurements showed that D-glucopyranosiduronic acid (GlupA) forms complexes Ar₃Sn(IV)–GlupA upon reaction with [(Bu₃Sn(IV))₂O] but surprisingly not with Bu₃SnCl or Me₃SnCl in Me₂SO or with Me₃SnCl in H₂O. Primarily the O-4 –OH and to a lesser extent the ring {O} at C-1 are coordinated to the organotin(IV) cation.¹¹³ It was also shown that the interactions of [Et₂Sn(IV)]²⁺ and 2-polyhydroxyalkylthiazolidine-4-carboxylic acid (PHTAc; formed by the reaction of L-Cys and aldoses under mild conditions) led to formation of the complexes MLH, ML, and MLOH [where M = Et₂Sn(IV)²⁺], including the hydrolysis products of the latter one.⁷⁸ Furthermore, [Et₂Sn(IV)]²⁺ coordinated the N-D-gluconyl-α-amino acids (formed in the reactions between D-gluconic acid-δ-lactone and amino acids) *via* –COO[–], amine and deprotonated alcoholic –OH groups, while the β-amino acid derivatives were coordinated through –COO[–] and deprotonated sugar –OH groups only. ¹³C NMR measurements have confirmed that the amine group does not participate in complex formation.⁷⁹

To study the effect of the conformation of the sugar –OH groups on metal complexation processes, the complex formation of eight saccharides with [Me₂Sn(IV)]²⁺ was investigated in aqueous solution by pH-metric measurements, ¹³C NMR, polarimetry, and Mössbauer spectroscopy. The experimental results revealed that deprotonation of D-fructose and L-sorbose is caused by the coordination of [Me₂Sn(IV)]²⁺ in the unusually low pH interval 4–6, in contrast with the other saccharides, which are deprotonated in an analogous way at pH > 8. Increase of the pH of the solution resulted in the formation of further complexes that differed from each other only in deprotonation state. ¹³C NMR measurements led to the assignment of the sugar –OH groups participating in the processes. Mössbauer spectroscopic investigations of the quick-frozen solutions permitted determination of the stereochemistry of {Sn} in the complexes.³⁹ Evaluation of the pH-metric and ¹³C-NMR titration curves of [Me₂Sn(IV)]²⁺ polyhydroxyalkyl carboxylic acids revealed that the equilibria in aqueous solutions are also rather complicated. In the acidic region the formation of 1:1 and 1:2 –COO[–] coordinated species dominate; however, the deprotonation of the alcoholic –OH also starts at very low pH. In the pH range from 5 to 9, several ligand exchange reactions take place, without pH-metrically detectable proton

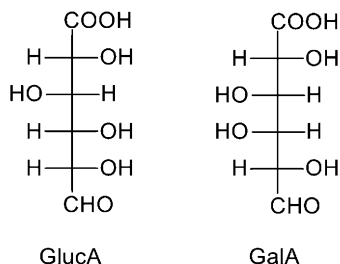


Figure 2 Structures of D-glucuronic (GlucA 1), D-galacturonic (GalA 2), and D-gluconic (GluA 3) acids.

release, but well expressed in the NMR spectra. At alkaline pH, further deprotonation processes occur either due to the deprotonation of alcoholic -OH groups or due to the partial hydrolysis of the complexes resulting in mixed hydroxo species,¹¹⁴ similarly as in the carbohydrate- $[\text{Me}_2\text{Sn(IV)}]^{2+}$ systems already shown.²⁰

Complex formation of D-glucuronic acid (GlucA) (Figure 2) with mono-, di-, and trimethyltin(IV) cations has been investigated by pH-metric titration in a wide range of ionic strength ($I = 0.1\text{--}1\text{ mol dm}^{-3}$, NaCl medium). The following complex species have been found: $[\text{MeSn(GlucA)(OH)}]^+$, $[\text{MeSn(GlucA)(OH)}_2]^0$, and $[(\text{MeSn})_2(\text{GlucA})(\text{OH})_5]^0$ for monomethyltin(IV) $^-$; $[\text{Me}_2\text{Sn(GlucA)}]^+$ and $[\text{Me}_2\text{Sn(GlucA)(OH)}]^0$ for dimethyltin(IV) $^-$; and $[\text{Me}_3\text{Sn(GlucA)}]^0$ for $[\text{Me}_3\text{Sn(IV)}]^+$ –glucoseA system. As expected, the formation of a parent 1:1 species was only found in the $[\text{Me}_3\text{Sn(IV)}]^+$ –GlucA system. In the other systems, in particular in $[\text{MeSn(IV)}]^{3+}$, mixed hydroxo complexes are always formed, owing to the very strong tendency to hydrolysis of the double or triply charged organotin(IV) cation. Mössbauer spectroscopic investigations enable to propose a structure for each species, and also confirm the formation of the dimeric hydroxo species $[(\text{MeSn})_2(\text{OH})_5]^+$ with Tbp {Sn} geometry.¹¹⁵

Dialkylstannylene acetals (or, more properly, 2,2-dialkyl-1,3,2-dioxastannolanes, if the ring is five-membered; 2,2-dialkyl-1,3,2-dioxastannanes, if the ring is six-membered; and 2,2-dialkyl-1,3,2-dioxastannapanes, if the ring is seven-membered) are easily prepared by the reactions of vicinal diols with R_2SnO or $\text{R}_2\text{Sn(OH)}_2$, or $\text{R}_2\text{Sn(IV)}$ diethoxide¹¹⁷ under conditions of azeotropic dehydration in benzene, methanol, or toluene. Molecular weight measurements in solution indicated that the main reaction product is a dimeric species.^{118,119} Where more than one unprotected -OH group is available for reaction, both partially and fully stannylated products are formed.^{120–123} Early work established the regioselectivity of tributylstannylation of carbohydrates, which is related to the easy reaction with which {Sn} can coordinate a neighboring {O} atom. Thus, C-6(O) is the most reactive, followed by the secondary -OH groups, all of which are capable of coordinating to {Sn} by a second, *cis*-O.¹²⁴ $[\text{R}_3\text{Sn(IV)}]^+$ –carbohydrate complexes are easily distilled as oils, which are rapidly hydrolyzed upon exposure to air, though the aerobic stability increases if free hydroxy groups are retained in the product.¹²⁵

In general, the carbohydrate–organotin(IV) complexes have been studied by ¹H and ¹³C NMR,^{120,126} or, especially by multinuclear NMR (¹¹⁹Sn, ¹H, and ¹³C) spectroscopy.^{121,127–129} A series of papers by Grindley et al.^{128,129} demonstrated that these compounds are present in solution as dimers and/or higher oligomers in which the central {Sn} atoms are penta- or hexacoordinated. ¹¹⁹Sn NMR chemical shift ranges have also been established for the {Sn} nuclei in 2,2-dibutyl-1,3,2-dioxastannolanes; pentacoordinate {Sn} nuclei absorb in the region from –115 to –150 ppm with respect to Me₄Sn, while hexacoordinate {Sn} nuclei absorb between –220 and –300 ppm in solution. The ¹¹⁹Sn NMR spin-lattice relaxation rates in solution for a number of 1,3,2-dioxastannolanes in which the central {Sn} atoms are in either penta- or hexacoordinate environments have also been measured.¹²⁹ The relaxation times in these compounds were found to be very short, and the major mechanism of spin-lattice relaxation at 8.48 T was due to chemical shift anisotropy. In solution, the chemical shift anisotropies for the hexacoordinate sites are approximately 1.6 times higher than those for the pentacoordinate sites. It was subsequently shown that these observations also held true for solid compounds.^{130,131} These results supported the previous conclusion¹²⁸ that the antisymmetric terms of the chemical shift tensor give only a small or negligible contribution to the rate of ¹¹⁹Sn spin-lattice relaxation in these compounds.

The solid-state structure of tetrabutylbis(2,3:4,6-diisopropylidene-2-keto-L-gulonato)distannoxane has been determined.¹³² The [Bu₂Sn(IV)]²⁺ complex of D-lactobionic acid also proved to be oligomeric, containing octa- (within the chain) and pentacoordinated (at the end of the chain) {Sn} centers in a ratio of 2:4.¹³³

A number of organotin(IV) complexes of polyhydroxyalkyl carboxylic acids were prepared in solid state. The compositions of the complexes were determined by ICP method. The bonding sites of the ligands were measured by means of FT-IR, Raman and in some cases ¹³C NMR spectroscopy. On the basis of partial quadrupole splitting (pqs) calculations, the coordination geometry around {Sn} center was determined by Mössbauer measurements. The results showed that oligomeric complexes are formed where the –COO[–] group made a bridge between the organometallic cations. The {Sn} atoms are in *Tbp* and *O_h* surroundings. These observations were confirmed by EXAFS measurements.¹¹⁴ In the D-galacturonic acid (GalA) dialkyltin(IV) (Me, Bu) complexes, the ligand (Figure 2), acts as a dianionic species, coordinating the tin(IV) atom through and ester-type carboxylate and deprotonated alcoholic OH groups, whereas a bridging carboxylate occurs in the Ph₂Sn(IV) complex. *O_h* and *Tbp* local geometries on tin(IV) atoms are proposed on the basis of Mössbauer spectroscopy. In D₂O and DMSO-d₆ solution the R₂Sn(IV) moieties are mainly coordinated by the GalA^{2–} in the β-furanosidic form.¹¹⁶

In some cases, when partially protected sugars were used as ligands, single crystals suitable for XRD measurements were obtained. In 1979, David et al.¹³⁴ found that dibutylstannylene derivative of methyl-4,6-di-*O*-benzylidene-α-D-glucopyranoside has a dimeric structure, in which every tin atom exhibits *Tbp* geometry (Figure 3). The structure of the same complex was redetermined by Cameron et al.¹³⁵ XRD data were collected at –70 °C because the previous assignment had involved a large R (fitting parameter) value. The results

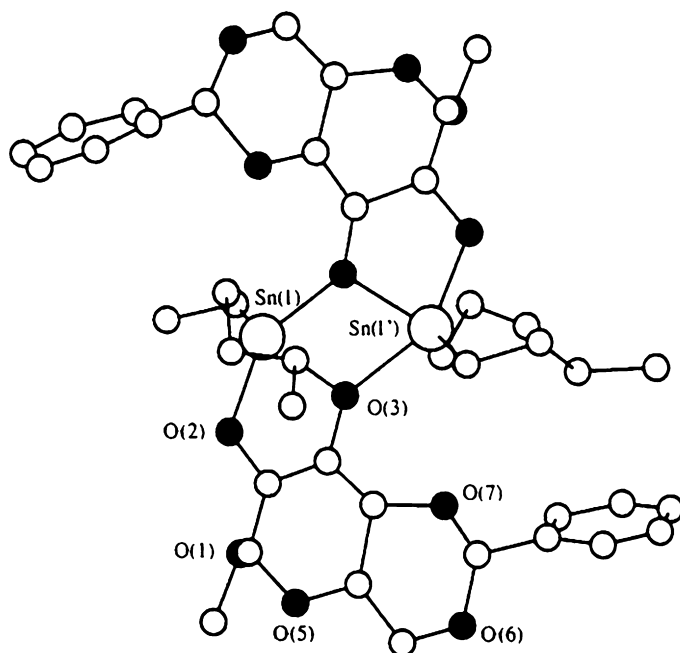


Figure 3 The dimeric structure of the dibutylstannylene derivative of methyl-4,6-di-O-benzylidene- α -D-glucopyranoside.¹³⁴

showed, similarly to the previous findings, that the {Sn} atom is pentacoordinated in a severely distorted *Tbp* geometry. The butyl {C} atoms are *eq*, but the average C–Sn–C bond angle is large, 131.0°. The two butyl groups adopt different conformations and are still significantly disordered even at –70 °C. The Sn–O bond lengths inside the monomer units are shorter (average 207 pm) than those between the monomer units (average 223.7 pm).

In contradiction with the results discussed above, Holzapfel et al.¹³⁶ reported that methyl-4,6-O-benzylidene-2,3-O-dibutylstannylene- α -D-mannopyranoside has a pentameric structure containing two penta- and three hexacoordinated central {Sn} atoms. The intramolecular Sn–O distances are similar (209 pm), and the intermolecular Sn–O distances (223 pm) in this dimer (both {Sn} atoms are pentacoordinated) are equivalent to 223 and 227 pm that separate the two terminal {Sn} atoms from their respective neighboring {O} atoms in the pentamer. The average intermolecular Sn–O distance in hexacoordinated {Sn} moieties is 248 pm. The reasons for oligomerization have been elegantly discussed in terms of steric interaction between the sugar residues (Figure 4) shown in the structure of the pentamer. Finally, Davies et al.¹³⁷ indicated, on the basis of the Mössbauer spectroscopic measurements on 2,2-dibutyl-D-mannose-stannolane, that this compound contains both penta- and hexacoordinated {Sn} atoms in a ratio of 2:3. The XRD measurements demonstrated an average Sn–O bond length of 204 pm within each monomer unit, and of 251 pm between different units. The endocyclic and exocyclic O–Sn–O observed angles were 79.9 and 138.6°, respectively.

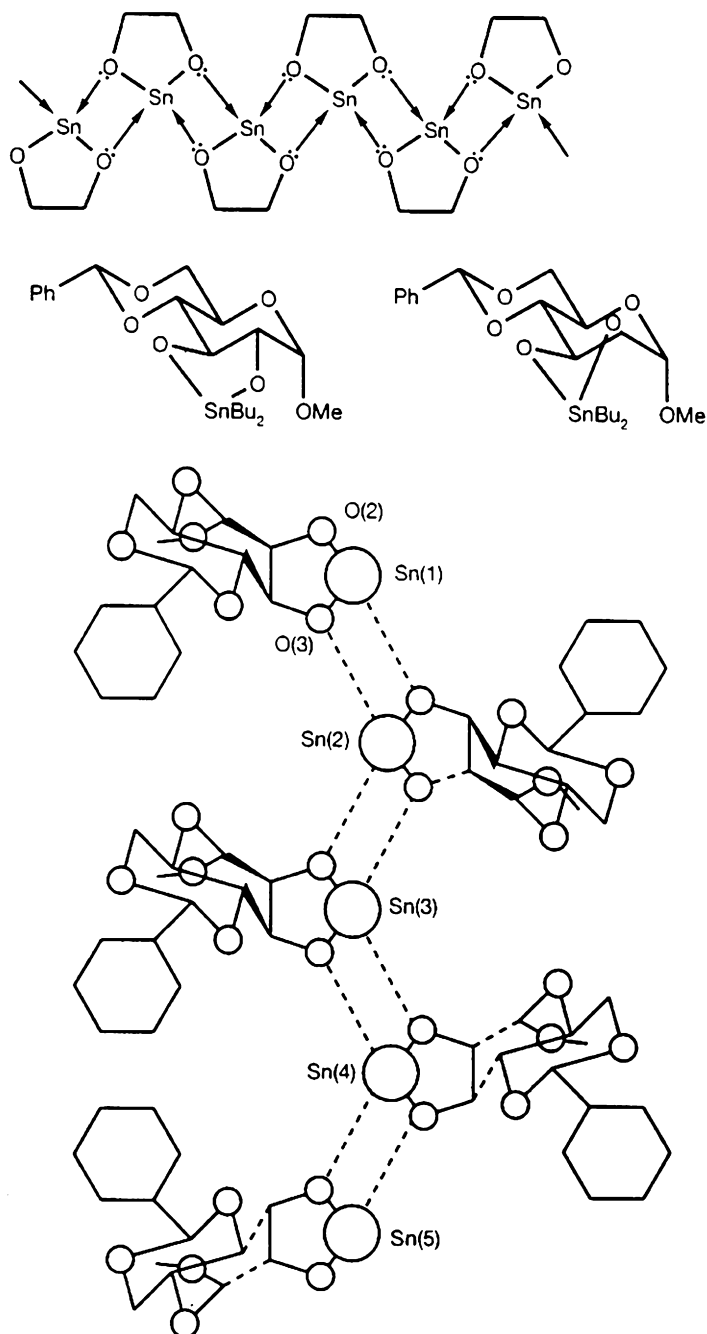


Figure 4 The structure of pentameric methyl-4,6-O-benzylidene-2,3-O-dibutylstannylene- α -D-mannopyranoside.¹³⁶

The two –OH groups in 1,2:5,6-di-*O*-cyclohexylidene-*myo*-inositol and its di-*O*-isopropylidene analog are *trans*. The X-ray crystal structure¹³⁸ of the latter compound suggests that the ring is in a skew conformation with the O-3 and O-4 –OH groups both in *ax* positions, but NMR studies¹³⁹ and *ab initio* calculations¹⁴⁰ indicate that a mixture of the skew and chair conformations, with O-3 and O-4 both in *eq* positions, is present. Formation of a dibutylstannylene acetal presumably locks these two compounds in the latter conformation.

Mössbauer spectroscopy has also been widely used to investigate the structures of dialkylstannylene derivatives of carbohydrates in the solid state.^{113,137,141–147} The usual magnitude of $\Delta = 2.78\text{--}3.07\text{ mm s}^{-1}$ indicated a coordination number larger than four, with {Sn} centers in a penta- or hexacoordinated environment.

Comparison for these type of complexes of the $|\Delta_{\text{exp}}|$ values with those calculated on the basis of the pqs concept revealed that the complexes formed are of three types, with central $[\text{Et}_2\text{Sn(IV)}]^{2+}$ or $[\text{Bu}_2\text{Sn(IV)}]^{2+}$ present (a) in a purely *Tbp cis*- R_2SnO_3 unit within a polymeric framework, (b) in a purely *O_h*, and (c) in both *O_h* and *Tbp* arrangements in a ratio of approximately 1:1.^{142,143} For $[\text{Bu}_2\text{Sn(IV)}]^{2+}$, a *T_d* complex of D-mannitol is detectable. It was also possible to distinguish between the different structural isomers (*eq* or *ax* arrangements of the two organic substituents) for the complexes $[\text{Et}_2\text{Sn(IV)}]^{2+}$,¹⁴² $[\text{Bu}_2\text{Sn(IV)}]^{2+}$,¹⁴³ and $[\text{Bz}_2\text{Sn(IV)}]^{2+}$ -carbohydrates¹⁴⁶, and $[\text{Bu}_2\text{Sn(IV)}]^{2+}$ -PHTAc.⁷⁸ The formation of different structural isomers has been discussed in terms of different steric requirements of the organic substituents. As discussed above, the organotin(IV) complexes formed with unprotected sugars are oligomeric in the solid state, and it is very difficult, or even impossible, to obtain them as single crystals suitable for XRD measurements. The first structural information on complexes formed with $[\text{Et}_2\text{Sn(IV)}]^{2+}$ was obtained by means of EXAFS method in the solid state.¹⁴⁸ Structural data obtained by XRD^{134,136} and EXAFS¹⁴⁸ are summarized in Table 6. The results demonstrate that the dioxastannolane units are associated into an infinite ribbon polymer, in which the {Sn} is bound by two {C} and three or four {O} atoms. Within each unit, the average Sn–O and Sn–C bond lengths in the first coordination shell are 206–210 and 213 pm, while the intermolecular bond distances display a somewhat larger variation (246–255 pm). The Sn...C and Sn...Sn distances in the third and fourth shells are in the range 277–323 and 324–362 pm, respectively, similarly to XRD data obtained on complexes formed with protected sugars and discussed above. The endocyclic Sn–O–Sn angles fall in the range 80–98° and are comparable with the published value of 79°.¹³⁷ These EXAFS investigations proved the correctness of the structural information derived from Mössbauer studies based on the pqs concept of the symmetry and coordination sphere of diorganotin(IV) complexes.

The complexes of carbohydrate derivatives containing {O, N, S} donor atoms (2,3,4,6-tetra-*O*-acetyl- β -D-thioglucofuranoside, 1-thio- β -D-glucose, 2-amino-mercaptapurine, 4-amino-2-mercaptopyrimidine, and 2-amino-6-mercaptapurine-9-D-riboside) with Bu_2SnO , Ph_2SnO , Bz_3SnCl , and Me_3SnCl contain the organotin(IV) moiety and the ligand in a ratio of 1:1 or 2:1. The vibration spectra clearly demonstrated that the cationic organotin(IV) moieties coordinated to the deprotonated –SH group of the ligands, while Bu_2SnO reacted with the

Table 6 Structural data for [Bu₂Sn(IV)]²⁺ and [Et₂Sn(IV)]²⁺ carbohydrates and related compounds complexes, obtained by X-ray diffraction^{134,136} and EXAFS^{148,165,166} methods

Bond length (pm) and angles (°)	CN	1	2	3 (Ref. 136)	4 (Ref. 148)	5 (Ref. 148)	6 (Ref. 165)	7 (Ref. 166)
Intramolecular		77	79.1		206	208	211	211
	5	82	80.0					
			77.6					
O–Sn–O	6	–		79.0	–	–		
			78.3					
Intermolecular		67						
	5–5		–	–	246	255	224	220
		70						
O–Sn–O	5–6	–	69.6	–	–	–		
			70.6					
			65.5	65.2				
–	6–6	–			–	–		
			69.2	66.8				
Intermolecular	6	–	142.0		–	–		
			149					
			150.5					
O–Sn–O	–	–	–	–	–	–		
		126	124.2		–	–		
Exocyclic	5			–				
		139	127.4					
			134.7					
C–Sn–C	6	–		138.6	–	–		
			142.7					
		213	202					

Table 6 (Continued)

Bond length (pm) and angles (°)	CN	1	2	3 (Ref. 136)	4 (Ref. 148)	5 (Ref. 148)	6 (Ref. 165)	7 (Ref. 166)
Intramolecular	5	209	207	—	—	—	—	—
			206	198				
Sn–O	6	—	213	210	—	—	—	—
		229	223					
Intermolecular	5	217	227	—	—	—	—	—
			243	250				
Sn–O	6	—	260	252	—	—	—	—
		223	204	213				
Exocyclic	5	226	225	214	—	—	—	—
			214					
Sn–C	6	—	—	—	213, 323	213, 307	213	—
			220					
Sn...Sn	1	—	—	—	324	362	—	410

CN, coordination number. A CN of 5–6 means that the compound contains the [Sn] central atom in two different environments. 1, Bu₂SnOCH₂CH₂O; 2, methyl-4,6-O-benzylidene- α -D-glucopyranoside; 3, methyl-4,6-O-benzylidene- α -D-mannopyranoside; 4, D-lactobionic acid; 5, D-galactose; 6, Bu₂Sn-DNA, maleic acid.

deprotonated alcoholic –OH groups. In several cases, the basic part of the ligands may also participate in complex formation. The Mössbauer spectroscopic data revealed the formation of complexes with *Tbp* and in certain cases *T_d* geometry too. Some of the complexes polymerized and contain the organotin(IV) cation in two different surroundings.¹⁴⁹

Several complexes of [Bu₂Sn(IV)]²⁺ with flavonoid glycosides {3-[6-O-(6-deoxy- α -L-mannopyranosyl)-(β -D-glucopyranosyl)oxy]-2-(3,4-dihydroxyphenyl)-5,7-dihydroxy-4-H-1-benzopyran-4-one} (rutin) and 2',4',3-trihydroxy-5',4-dimethoxychalcone 4-rutinoside (hesperidin) and flavonoid aglycones (quercetin, morin, hesperitin, and other flavones) (Figure 5) were prepared.

The analytical data indicated the formation of complexes containing the [R₂Sn(IV)]²⁺ moiety and the ligand in a ratio of 1:1, 2:1, or 3:1. The FT-IR spectra were consistent with the presence of Sn–O vibrations in the compounds. The Mössbauer spectroscopic investigations revealed that the complexes are polymeric with four types of species: with the central {Sn} atoms surrounded by donor atoms in a purely *Tbp*, *O_h+Tbp*, *Tbp+T_d*, or *O_h+T_d* arrangement in different ratios.¹⁵⁰ The pqs calculations also distinguished the different structural isomers of both *Tbp* and *O_h* complexes. These properties are similar to those of the dialkyltin(IV)–carbohydrate complexes discussed above and originate from the polymeric nature of the compounds. In addition, the [Bu₂Sn(IV)]²⁺ complexes of rutin and quercetin in ligand-to-metal ratios of 1:1 and 1:2 was studied by EXAFS. It was found that the Sn–O bond distances in the first coordination sphere are close to the values found in [Et₂Sn(IV)]²⁺ complexes with unprotected carbohydrates.²⁰ The parameters obtained are in Table 6, and the proposed structure is depicted in Figure 6.

A set of six Bu₃Sn(IV) citrates and three Bu₃Sn(IV) 1,2,3-propanetricarboxylates of general formula R₁C(CH₂)₂(COOR₂)₃, where R₁ = OH or H, and R₂ = H, [Bu₂Sn(IV)]⁺, C₆H₁₁NH⁺, (C₆H₁₁)₂NH₂⁺, or (CH₂)₅NH₂⁺, were prepared and their structures were studied in the solid state and in solutions of different types of solvent by IR, ¹H, ¹³C, and ¹¹⁹Sn NMR, ¹³C and ¹¹⁹Sn CP/MAS NMR, and ¹¹⁹Sn Mössbauer spectroscopies. Isolated molecules or “ionic” or “pseudo-ionic” pairs with a pseudotetrahedral {Sn} atom neighborhood were found in solutions of noncoordinating solvents. Similar isolated particles enriched by one solvent molecule bound to each of the {Sn} atoms were present in solutions of coordinating solvents, forming a *trans-Tbp* arrangement around the {Sn} atoms with Bu substituents situated in the *eq* plane and a donor atom of the coordinating solvent and {O} atom of the monodentate –COO[–] group in *ax* positions. A part of the Bu₃Sn(IV) groups, together with some bidentate bridging –COO[–] groups, form polymeric chains in the solid state with citrates and 1,2,3-propanetricarboxylates. Stannadioxacycles with the participation of α -hydroxycarboxylate fragments and one of the Bu₃Sn(IV) groups probably occur in the solid state in some citrates. The molecular structure of one of the complexes is depicted in Figure 7.¹⁵¹ Further structural data obtained by EXAFS on similar complexes are collected in Table 6.

Wardell et al. studied the preparation, reactivities, and structures of C(carbohydrate)–Sn bonded mono-, or di-*O*-isopropylidene or di-*O*-benzylidene triphenylstannyl–carbohydrate derivatives by means of X-ray crystallography,

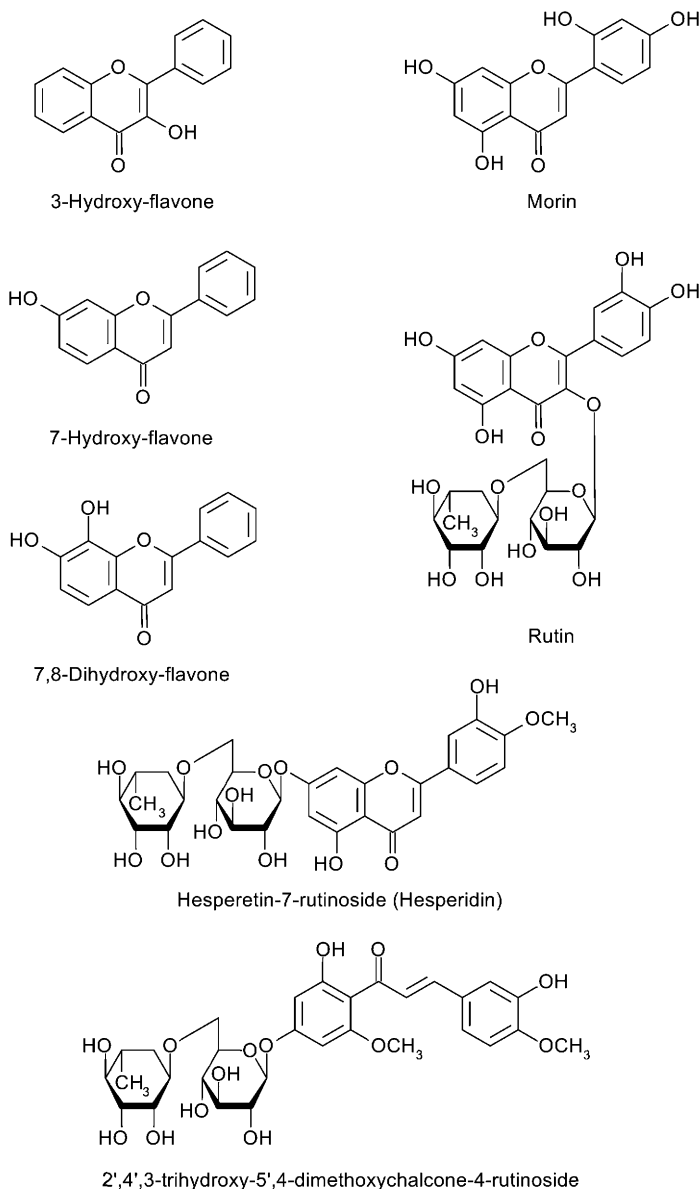


Figure 5 The structure of flavonoid ligands studies.¹⁵⁰

and ^1H , ^{13}C , and ^{119}Sn NMR spectroscopy.^{8,152–155} It was found that in most cases the {Sn} atoms are in a slightly distorted T_d environment,^{8,152,154,155} but a distorted Tbp arrangement with {I} and {O} atoms in ax positions ($\text{Sn}-\text{O} = 268\text{ pm}$) has also been observed.¹⁵³ In cases involving a T_d structure,¹⁵⁹ the shortest $\text{Sn}\cdots\text{O}$ separation is about 335 pm , an interaction that appears to have no effect on the stereochemistry of the metal. In the crystals of the chiral carbohydrates, the $-\text{OH}$

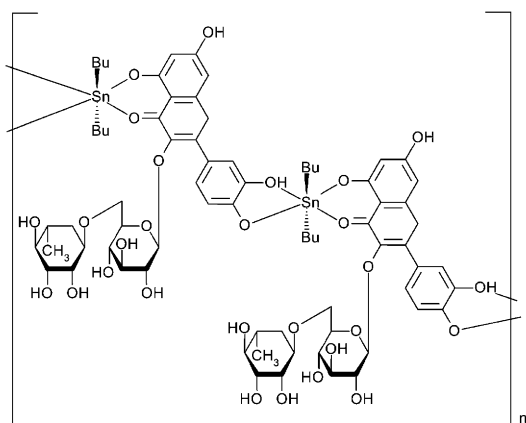


Figure 6 Proposed structure of the $\text{Bu}_2\text{Sn(IV)}$ -rutin complex of 1:1 molar ratio.²⁰

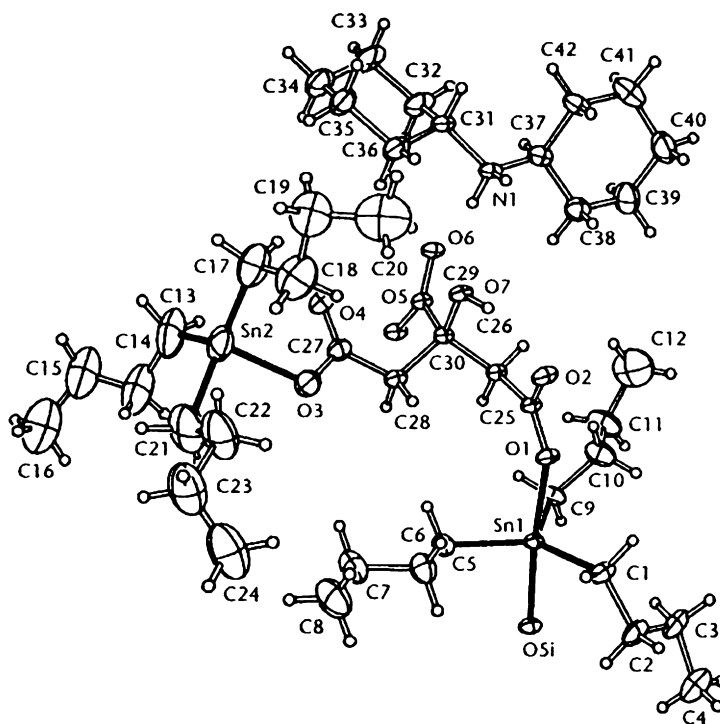


Figure 7 Molecular structure of the tributyltin 1,2,3-propanetricarboxylates.¹⁵¹

groups are held together by an intermolecular hydrogen bonding network. Due to the large number of hydrophilic $-\text{OH}$ groups, this phenomenon is quite characteristic for carbohydrate-metal ion complexes.^{8,9}

The wood preservation properties of $[\text{Bu}_3\text{Sn(IV)}]^+$ compounds are strongly related to the interactions between cellulose and the organotin(IV) cation and are

based on the good fungicidal activity and low mammalian toxicity of these complexes. TBTO-treated wood [TBTO = $(\text{Bn}_2\text{Sn})_2\text{O}$] is effectively preserved for up to 25 years, although there is some concern about the long-term stability of the organotin(IV) toward dealkylation to less effective $[\text{R}_2\text{Sn(IV)}]^{2+}$ compounds.¹⁵⁶ Some fungi which colonize wood, for example, are capable of causing this dealkylation process.^{157,158}

The basic question on the nature of TBTO within the cellulose matrix is still not fully resolved. Early work suggested that the $[\text{Bu}_3\text{Sn(IV)}]^+$ moiety condensates with the terminal OH groups of wood cellulose,¹⁶⁰ but this was inferred on the basis of electron microscopy studies.¹⁶¹ Mössbauer spectra of TBTO-impregnated pine (experimental parameters: $\delta_{\text{TBTO}} = 1.17 \text{ mm s}^{-1}$, $\Delta_{\text{TBTO}} = 1.46 \text{ mm s}^{-1}$) point strongly to the presence of $[(\text{Bu}_3\text{Sn})_2\text{CO}_3]$ (characteristic parameters: $\delta = 1.38$ and 1.43 , $\Delta = 2.70$ and 3.79 mm s^{-1}); formed by reaction with atmospheric CO_2 ,¹⁶² for $(\text{Bu}_3\text{Sn})_2\text{CO}_3$ in wood; $\delta = 1.39$ and 1.44 , $\Delta = 2.64$ and 3.66 mm s^{-1} , while for TBTO in wood $\delta = 1.39$ and 1.46 , $\Delta = 2.84$ and 3.59 mm s^{-1} .¹⁶³

Complexes formed between carboxymethyl cellulose (CMC) (model compound for cellulose) and $[\text{Me}_2\text{Sn(IV)}]^{2+}$ cation have been prepared in the solid state and characterized by FT-IR and Mössbauer spectroscopy. The complexes contained CMC with varying molar weight and degree of carboxylation, and complexes were isolated from acidic and neutral solutions at varying metal:ligand ratios. The characteristic vibration bands of the ligands were identified from their pH-dependent FT-IR spectra. In the organotin(IV) complexes obtained at pH 2, the $-\text{COO}^-$ moieties were found to be coordinated in a monodentate manner and the band characteristic of the protonated (unbound) $-\text{COO}^-$ group was also identified. The broad $-\text{OH}$ band is interpreted as the sum of the contributions of the alcoholic $-\text{OH}$ groups of the sugar units and the mixed organotin(IV) aquo complexes. In complexes obtained at pH 7 the broad OH band significantly sharpens, which is probably due to the metal-ion-induced deprotonation and subsequent coordination of the $-\text{OH}$ groups. At the same time $-\text{COO}^-$ groups are also involved in the coordination of the metal ions, resulting in a complicated network formed through inter- and intramolecular bridges. Mössbauer Δ values revealed that the oxidation state of tin is IV in all of the complexes. The $|\Delta_{\text{exp}}|$ values were compared with theoretically calculated ones, obtained from the pqs theory. From these data, Tbp and tetrahedral (T_d) geometry have been suggested for the complexes obtained. It was concluded that the structure of the complexes prepared depend mainly on the pH of the solution, and are relatively insensitive to the other parameters, like molar mass, carboxylation degree of the ligand, or the metal:ligand ratio in the reaction mixture.¹⁶⁴

C. Interaction of $[\text{organotin(IV)}]^{n+}$ with nucleic acids and DNA

Many organometallic compounds exhibit interesting antitumor activity against several human cancer cell lines.^{167–169} The well-known complex cisplatin, $\text{Pt}(\text{NH}_3)_2\text{Cl}_2$, used clinically in cancer chemotherapy, proved to interact with the N-7 atoms of two adjacent guanines in the same DNA strand.^{170–172} In contrast with platinum compounds, very little is known of the origin of the antitumor activity of organotin(IV) compounds, though the structural similarity to cisplatin

suggests that DNA could be the target.¹⁷³ It was suggested that organotin(IV) compounds exert their effects through binding to thiol groups of proteins.¹⁷⁴ In contrast to this view, but in analogy with the behavior of several antitumor metal complexes, some authors proposed that the DNA is the probable target for cytotoxic activity of organotin(IV) compounds. In this section we survey and compare the most important literature data published to date on this subject.

[R₂Sn(IV)]-bis(adenine) was obtained by reaction performed in N₂ atmosphere. The Mössbauer spectroscopic data ($|\Delta_{\text{exp}}| = 1.91\text{--}2.21 \text{ mm s}^{-1}$) are consistent with *T_d* geometry around the central {Sn} atom, though a *cis*-R₂SnN₄ configuration cannot be excluded.¹⁷⁵ When adenine or 9-methyladenine is refluxed in methanol with Me₂SnCl₂, only simple adducts are formed. Under similar conditions, R₂SnCl₂ does not generally react with guanine, cytosine, thymine, uracil, or theophylline.¹⁷⁶ Crystallization of Me₂SnCl₂ and purine from acetone leads to a product in which hydrated Me₂SnCl₂ is coordinated to four purine molecules *via* a hydrogen bonding network.¹⁷⁷

The interactions between different organotin(IV) compounds and 6-thiopurine, an antitumor metabolite, are more complex. At 0 °C, a polymeric mixture is formed, with {N, S} or {N, N} donor atoms coordinated. At *T* > 0 °C, only {N, N}-bound product is observed.^{178,179}

Complexes of adenosine and related compounds with R₂SnO and/or R₂SnCl₂ were obtained. The complexes contain the organotin(IV) moiety and the ligand in a ratio of 1:1 or 2:1. The FT-IR spectra demonstrated that R₂SnO reacts with the D-ribose (Rib) moiety of the ligands, while R₂SnCl₂ is coordinated by the deprotonated phosphate group. The basic part of the ligands does not participate directly in complex formation. Comparison of the $|\Delta_{\text{exp}}|$ values with those calculated on the basis of the pqs concept revealed that the organotin(IV) moiety has *Tbp*, *O_h*, or in some cases *T_d* geometry. Some of the complexes contain the organotin(IV) cation in two different surroundings.¹⁸⁰ Very similar conclusions were obtained earlier on the complexes formed between Bu₂SnCl₂ or Bu₃SnCl and adenosine-5'-monophosphate (5'-AMP), guanosine-5'-monophosphate (5'-GMP), and their 3'-5' cyclic analogs. The stoichiometry of the compounds of 5'-AMP and 5'-GMP with Bu₃SnCl was 1:2, while that with Bu₂SnCl₂ was 1:1. Only 1:1 compounds were formed with the 3'-5' cyclic nucleotides. Most of the compounds are polymeric and differ in the environments of the two butyl groups. For all the [Bu₃Sn(IV)]⁺ complexes, ³¹P NMR chemical shifts indicate that the Sn is bound to the phosphate group, but probably it is not chelated by it. A much larger ³¹P NMR upfield shift in (Bu₃Sn)₂(5'-GMP) is an indication of phosphate chelation. The Rib conformation is different within the [Bu₃Sn(IV)]⁺ and [Bu₂Sn(IV)]²⁺ complexes.¹⁸¹

Mössbauer spectroscopic titration of [Me₂Sn(IV)]²⁺ and [Me₃Sn(IV)]⁺ hydroxides with ligands mimicking nucleic acid phosphate sites and with native DNA was the aim of work by Barbieri et al.¹⁸² A series of aqueous solutions of each system, formed by the organotin(IV) hydroxides and the phosphate ligands used [H_{*n*}PO₄^{(3-*n*)-} (*n* = 1 or 2, phosphate buffer), D-ribose-5-phosphate (R-5P), dimethylphosphinate, adenosine 3':5'-cyclic monophosphate (Ado-3':5'-P), and

DNA], with varying ligand:organotin(IV) molar ratios, frozen at 77.3 K, were monitored by ^{119}Sn Mössbauer spectroscopy.

On the basis of the point-charge model formalism, applied on the experimental nuclear quadrupole splitting rationalization, $|\Delta_{\text{exp}}|$, the results obtained were interpreted in terms of strong complex formation by either $\text{Me}_2\text{Sn}(\text{OH})_2$ or $\text{Me}_3\text{Sn}(\text{OH})(\text{H}_2\text{O})$ with $\text{H}_n\text{PO}_4^{(3-n)-}$ ($n = 1$ or 2 , obtained in phosphate buffer) and R-5P. Based on the trend of the isomer shift, δ , along the titration, gradual opening of the C–Sn–C was proposed from T_d structure in $\text{Me}_2\text{Sn}(\text{OH})_2$, to O_h *trans*- $\text{Me}_2\text{Sn}(\text{IV})$ in $\text{Me}_2\text{Sn}(\text{OH})_2$ -ligand. As far as the $\text{Me}_3\text{Sn}(\text{OH})(\text{H}_2\text{O})$ -ligand was concerned, the invariance of its δ with respect to that of $\text{Me}_3\text{Sn}(\text{OH})(\text{H}_2\text{O})$ ($\delta = 1.24 \text{ mm s}^{-1}$)¹⁸³ suggested that the distorted *Tbp* configuration of $\text{Me}_3\text{Sn}(\text{OH})(\text{H}_2\text{O})$ was maintained in the complexes $\text{Me}_3\text{Sn}(\text{OH})(\text{H}_2\text{O})$ -ligand. Such distortions were quantified by rationalization of the experimental $|\Delta_{\text{exp}}|$ according to the point-charge model formalism, which permitted estimation of the C–Sn–C angles in the $[\text{Me}_2\text{Sn}(\text{IV})]^{2+}$ derivatives and of the angle C–Sn–A in the Me_3SnA moieties ("A" being a coordinated atom). Quite limited effects were reported for the interactions of $\text{Me}_2\text{Sn}(\text{OH})_2$ and $\text{Me}_3\text{Sn}(\text{OH})(\text{H}_2\text{O})$ with dimethylphosphinate and Ado-3':5'-P. Native DNA did not induce any interaction.

Barbieri et al.^{52,53,184} investigated the interactions between ethanolic diorganotin(IV)²⁺ and triorganotin(IV)⁺ $[\text{R}_2\text{SnCl}_2(\text{EtOH})_2]$ and $\text{R}_3\text{SnCl}(\text{EtOH})$, R = Me, Et, Bu, Oct, or Ph], and aqueous $[\text{Me}_2\text{Sn}(\text{H}_2\text{O})_n]^+$ and $[\text{Me}_3\text{Sn}(\text{H}_2\text{O})_2]^{2+}$ species with aqueous DNA from calf thymus by ^{119}Sn Mössbauer spectroscopy. In particular, the latter data showed that the solids obtained by adding solvated $[\text{R}_2\text{SnCl}_2(\text{C}_2\text{H}_5\text{OH})_n]$ and $\text{R}_3\text{SnCl}(\text{EtOH})$ to DNA (R = Me, Et, Bu) were probably $\text{R}_2\text{Sn}(\text{DNA phosphate})_2$ and $\text{R}_3\text{Sn}(\text{DNA phosphate})$. In these complexes, the environment of the {Sn} atoms would be *trans*- O_h , with a linear $\text{CH}_3\text{--Sn--CH}_3$ skeleton, and *Tbp*, respectively. Possible structures of the {Sn} sites in phosphate-bound $[\text{R}_2\text{Sn}(\text{IV})]^{2+}$ -DNA and $[\text{R}_3\text{Sn}(\text{IV})]^+$ -DNA (R = Me, Et, Bu) are reported in Figure 8.

According to Barbieri et al.,^{52,53} it can not be excluded that some of the coordination sites are occupied by {N} atoms of the nucleic acid constituents. The precipitate obtained from $[\text{Ph}_2\text{Sn}(\text{IV})]^{2+}$ would contain both the $[\text{R}_2\text{Sn}(\text{IV})]^{2+}$ -DNA complex and distannoxane $[(\text{Ph}_2\text{SnCl})_2\text{O}]$. The main products of the

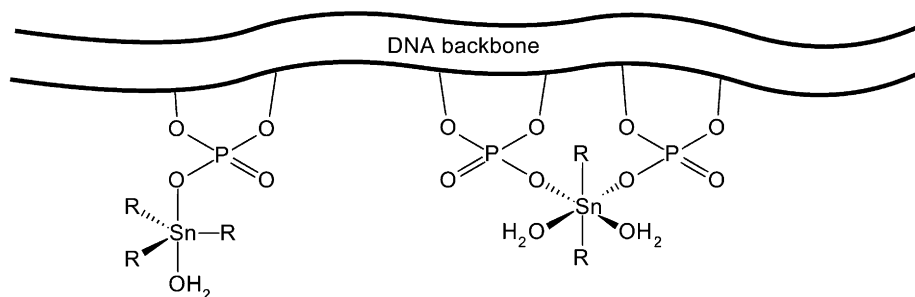


Figure 8 Possible structures of {Sn} sites in phosphate-bound $[\text{R}_2\text{Sn}(\text{IV})]^{2+}$ -DNA, bond distance $r=0.5:1$ and $[\text{R}_3\text{Sn}(\text{IV})]^+$ -DNA, $r=1:1$ (adapted from Ref. (53)).

interactions of aqueous DNA with Oct₂SnCl₂(EtOH)₂ and R₃SnCl(EtOH) [R = Oct, Ph] were possibly stannoxanes [(R₂SnCl)₂O] and hydroxides [R₃SnOH]. Furthermore, no interaction at all was detected when the water-soluble hydrolyzed species [Me₂Sn(OH)(H₂O)_n]⁺, Me₂Sn(OH)₂, and Me₃Sn(OH)(H₂O)₂ were added to native DNA. Such results imply that organotin(IV) moieties may interact *in vivo* with cellular DNA only if they are weakly solvated.⁵² Finally, a Quantitative Structure–Activity Relationship (QSAR)^{185–187} treatment of |Δ_{exp}| data was applied to rationalize the Coulomb interactions in conjunction with effects originating from the R groups.

The interactions between ethanolic solutions of Me₂SnCl(SPy) or Me₂SnCl(SPym) and aqueous calf-thymus DNA have been the subject of a report.¹⁸⁸ They concluded that the 1:1 complex/DNA condensates are derived from an electrostatic interaction between the cations Me₂Sn(SPy)⁺ and Me₂Sn(SPym) and the phosphate (O) of phosphodiester groups. The reactions with DNA of two antitumor-active organotin(IV) compounds, the dimer of bis[(dibutyl-3,6-dioxahaptainato)tin (C₅₂H₁₀₈Sn₄O₁₈·2H₂O)], compound I, and tributyltin 3,6,9-trioxodecaonate (C₁₉H₄₀SnO₅·0.5H₂O), compound II, were investigated by different methods.¹⁸⁹ The main chemical features of the two compounds were also previously published.¹⁹⁰ These complexes are moderately water-soluble and very slowly hydrolyze toward the corresponding tin oxides. Both complexes exhibit strong antitumor activities on several tumor cell lines of human origin, larger than that induced by some classical antitumor drugs. IC₅₀ values in 1–5 nM range were found for compound I, while values in the 50–200 nM range were measured for compound II.¹⁹⁰ It was also shown that both compounds produce slight effects on DNA conformation while affecting significantly the DNA melting behavior (the melting point decreases). No significant effects on gel mobility of plasmidic DNA samples were detected. This work also suggests that the interaction of organotin(IV) parent compounds or complexes with DNA is not sequence- or base-specific and therefore it most likely occurs at the level of external phosphate groups.¹⁸⁹

Semiempirical calculations on the interaction between [Me₂Sn(IV)]²⁺ and a dinucleide triphosphate duplex (DD), mimicking a DNA model system, were performed with the PM3 method and published by Barbieri et al.¹⁹² The results indicate that the [Me₂Sn(IV)]²⁺ moiety binds to two adjacent phosphate groups.

Small-angle X-ray scattering (SAXS), circular dichroism (CD), and UV spectroscopy at different temperatures were used to investigate the nature of calf-thymus DNA in aqueous solution, in the presence of [Me_nSn]^{(4–n)+} (n = 1–3) species.¹⁹³ The results demonstrate that the [MeSn(IV)]³⁺ moiety does not influence the structure and conformation of the DNA double helix, and does not degrade DNA, as indicated by agarose gel electrophoresis. *Inter alia*, the radii of gyration, R_g, of the cross section of native calf-thymus DNA, determined by SAXS in aqueous solution in the presence of [Me_nSn]^{(4–n)+} (n = 1–3) species are constant and independent of the nature and concentration of the [Me_nSn]^{(4–n)+} species.

Model compounds of DNA have also been studied. For example, the coordination of [Me₂Sn(IV)]²⁺ to 5'-GMP, 5'-ATP, 5'-AMP, and 5'-[d(CGCGCG)₂]

and to their sugar constituents (Rib and 2-deoxy-D-ribose) was investigated in aqueous solution by means of pH-metric titration and ^1H and ^{31}P NMR spectroscopic methods. The results showed that the phosphate groups can provide suitable sites for metal ion coordination only in acidic medium, while in the higher pH range the $-\text{OH}$ groups of the studied sugars or the sugar moieties of the two nucleotides play a role in this process. The base moieties of 5'-GMP, 5'-AMP, and 5'-ATP were not coordinated to $[\text{Me}_2\text{Sn}(\text{IV})]^{2+}$. The stability constants of the complexes formed in the above systems were determined by pH-metric titration. The data revealed a stronger coordination ability of the triphosphate compared with that of the monophosphate. The observed chemical shift changes of the ^{31}P NMR resonances, compared with those measured for the metal-free systems, demonstrated that the phosphate groups of the DNA fragment $[\text{5}'\text{-d}(\text{CGCGCG})_2]$ chains act as binding sites for $[\text{Me}_2\text{Sn}(\text{IV})]^{2+}$ between pH 4.5 and 7. The one- and two-dimensional ^1H NMR spectra indicated that the base and sugar moieties do not participate in the coordination process under these conditions.¹⁹⁴ Similar studies were performed on the interactions of $[\text{Me}_2\text{Sn}(\text{IV})]^{2+}$, D-ribose-5-phosphate (R-5P), D-glucose-6-phosphate (G-6P), and D-glucose-1-phosphate (G-1P). It was concluded again that at low pH ($\text{pH} < 4$) the organotin(IV) cations interact with pyrophosphate $\{\text{O}\}$. At intermediate pH values (4–9.5) no interaction takes place (in the systems depending on the concentration of metal ion and the ligand ratio a precipitate is formed), while at $\text{pH} > 9.5$ the sugar O'-2 and O'-3 atoms are the preferred coordination sites. Additionally oligomeric complexes were obtained in the solid state, containing $\{\text{Sn}\}$ centers in Tbp or O_h geometry.¹⁹⁵ Furthermore, evaluation of the pH-metric and ^{13}C NMR titration curves of the β -nicotinamide-adenine-dinucleotide-phosphoric acid (NADP) and $[\text{Me}_2\text{Sn}(\text{IV})]^{2+}$ system revealed that the equilibria in aqueous solutions are fairly complicated. In the acidic region, the formation of 1:1 and 2:1 phosphate-coordinated species dominate in different deprotonated stages together with hydrolysis products of the $[\text{Me}_2\text{Sn}(\text{IV})]^{2+}$ cation. In alkaline solutions further deprotonation processes occur either due to the deprotonation of alcoholic $-\text{OH}$ groups or due to the partial hydrolysis of the complexes resulting in mixed hydroxo complexes. A number of complexes with NADP and related ligands were prepared in the solid state. The binding sites of the ligands were determined by means of FT-IR spectroscopy. Based on pqs calculations, the coordination geometry around the $\{\text{Sn}\}$ center was determined by Mössbauer spectroscopy. The results showed that, in solid-state, oligomeric complexes were formed. $\{\text{Sn}\}$ atoms are mostly in O_h surroundings and in one case Tbp .¹⁹⁶

Formation constants for complex species of mono-, di-, and trialkytin(IV) cations with some nucleotide-5'-monophosphates (AMP, LIMP, IMP, and GMP) are reported by De Stefano et al.¹⁹⁷ The investigation was performed in the light of speciation of organometallic compounds in natural fluids ($I = 0.16\text{--}1\text{ mol dm}^{-3}$). As expected, owing to the strong tendency of organotin(IV) cations to hydrolysis (as already was pointed above) in aqueous solution, the main species formed in the pH-range of interest of natural fluids are the hydrolytic ones.¹⁹⁷

The local structure of these complexes and adducts of calf-thymus DNA with different organotin(IV) moieties were determined by means of EXAFS. The

EXAFS data were analyzed by using multishell models up to 300 pm. These results are the first structural data (bond lengths) on complexes formed with organotin(IV)–DNA and related compounds.¹⁶⁵ Some data are collected in Table 6. The proposed structures are similar to those depicted in Figure 6.

Li et al.¹⁹⁸ investigated the interaction of Et₂SnCl₂(phen) with 5'-dGMP in aqueous medium, using [*trans*-en₂Os(η-H₂)](CF₃SO₃)₂, a versatile ¹H NMR probe. The authors also studied solid mixtures of the same Et₂SnCl₂ complex with 5'-AMP, 5'-CMP, and 5'-GMP dissolved in DMSO, using ¹H and ³¹P NMR, and UV spectroscopy. Recently, Hadjiliadis et al.¹⁹⁹ studied the interactions of purine nucleotides 5'-IMP and 5'-GMP with Et₂SnCl₂, using various techniques. Finally, the interactions of Et₂SnCl₂ with 5'-CMP, 5'-dCMP, and 5'-UMP, using multinuclear (¹¹⁹Sn, ¹⁵N, and ³¹P) one- and two-dimensional NMR techniques have been also carried out.¹⁹¹ These studies were combined with electrospray mass spectrometry, IR spectroscopy, solid-state ¹³C, ³¹P, and ¹¹⁷Sn CP-MAS NMR, and elemental analysis.¹⁹¹ Finally, one paper has dealt with the interactions of Et₂SnCl₂ with 5'-CMP, 5'-dCMP, and 5'-UMP, using multinuclear (¹¹⁹Sn, ¹⁵N, and ³¹P) one- and two-dimensional NMR techniques. These studies were combined with electrospray mass spectrometry, IR spectroscopy, solid-state ¹³C, ³¹P, and ¹¹⁷Sn CP-MAS NMR, and elemental analysis.¹⁹⁸

Summarizing the above results, the basic question of how the organotin(IV) cations interact with DNA and influence the growth of tumor cells is still open. Except for the phosphate group and the sugar moieties in alkaline solution, no specific interactions between the DNA bases and organotin(IV) cations were found under physiological conditions. For further research it is a good challenge to determine which phosphate groups of DNA (terminal or internal one) reacted first with organotin(IV) cation. It seems that the mechanism of antitumor action of organotin(IV) complexes (if the target is the DNA) differs substantially from that of cisplatin.

D. Interaction of [organotin(IV)]ⁿ⁺ with other bioligands

The coordination of [Me₂Sn(IV)]²⁺ to penicillin derivatives (Figure 9) was investigated in H₂O by means of pH-metric titration. The results showed that if there is no electron-withdrawing group on the R substituent of the penicillin derivative (penicillin G and methicillin) the fast opening of the β-lactamic ring and the time-consuming method hinders the investigation of the interaction. In the case of ampicillin and amoxicillin, between pH 2 and 6, the ligand coordinates to the metal ion by its –COO[–] group forming [MLH]⁺ and [MLH₂]⁺ complexes, respectively. In the next step a OH[–] ion may be coordinated or a bonded H₂O molecule may be deprotonated forming mixed hydroxo complexes. Based on the potentiometric measurements no evidence was found for the existence of other hydroxo complexes or participation of other donor groups of the ligands in the coordination at higher pH ranges.²⁰⁰

Equilibrium studies in water were performed for [Me₂Sn(IV)]²⁺ complexes of zwitterion buffers, such as bicine and tricine (L). The results showed the formation of MLH, ML, ML₂, MLH_{–1}, and MLH_{–2} with the hydrolysis products of the

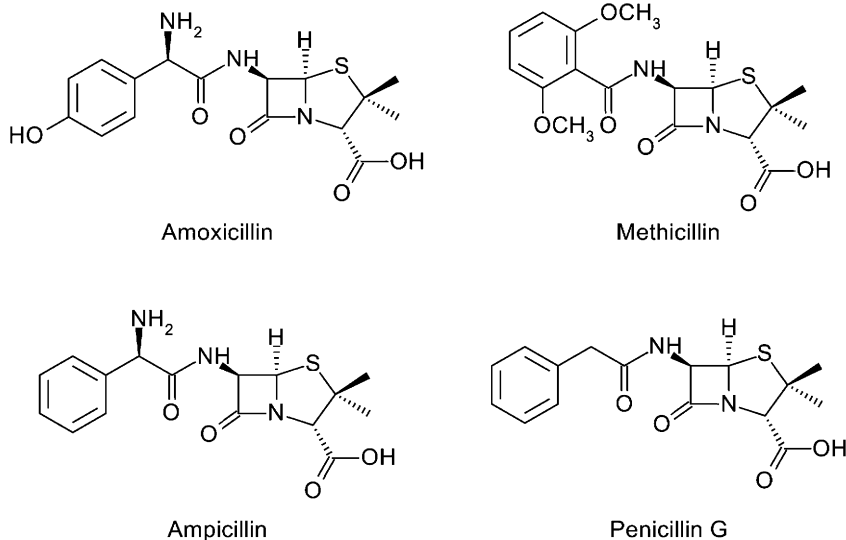


Figure 9 Structure of the penicillin studied.²⁰⁰

organotin(IV) cation. At pH 3, one complex was prepared in the solid state, with formula $[\text{Me}_2\text{SnL}(\text{H}_2\text{O})]\text{Cl}$, while in alkaline media only hydrolytic species are formed.²⁰¹

To date, only a few papers have been published on the structures of organotin(IV) complexes formed with carboxylate compounds containing {O, S} donor sites.^{55,202–206}

The complex formation of $[\text{Et}_2\text{Sn}(\text{IV})]^{2+}$ with glycolic, lactic, succinic, malic, tartaric, mercaptoacetic, 2-mercaptopropionic, mercaptosuccinic, and dimercaptosuccinic acids has been investigated in aqueous solution. The formation constants of the complexes and of the hydrolysis products of $[\text{Et}_2\text{Sn}(\text{IV})]^{2+}$ were determined by pH-metric measurements and (for the thiocarboxylic acids) by spectrophotometry. The thiocarboxylic acids yielded very stable complexes. Complexes displaying slow ligand exchange were detected. In the systems with hydroxycarboxylic acids, both mixed hydroxo complexes and hydrolytic species were observed. The formation of complexes participating in slow ligand exchange and the significant shift of the CH (situated adjacent to the –OH group) signals indicated coordination of the deprotonated alcoholic –OH group. The Mössbauer spectroscopic data on the $[\text{Et}_2\text{Sn}(\text{IV})]^{2+}$ –malic, –thioacetic, –mercaptosuccinic, and –dimercaptosuccinic acid systems demonstrated that dimeric species were formed in which *Tbp* and *O_h* arrangements around the tin atom occurred.⁵⁵

The coordination of $[\text{Me}_2\text{Sn}(\text{IV})]^{2+}$ to captopril (cap) [(2S)-1-[(2S)-2-methyl-3-sulfanyl propanoyl]pyrrolidine-2-carboxylic acid] in aqueous solution was studied by means of pH-metric titration, electrospray mass spectrometry, ¹H NMR, and Mössbauer spectroscopies in the 2–11 pH range. The results obtained proved that only monomeric complexes are formed in solution. In the acidic pH

range, species with a metal-to-ligand ratio of 1:1 do exist. The neutral complex ML, similarly to the complex Me₂Sn(cap) crystallized in the same pH range, adopts a *Tbp* structure with *eq* -S⁻ and *ax* -COO⁻, while, instead of the coordination of the amide -C=O, observed in the solid state, the other *ax* position is occupied by a H₂O molecule. With increasing pH, in the neutral and weakly basic pH range the complexes MLH₋₁ and ML₂ are formed, in which the -COO⁻ group is displaced from the coordination sphere by an OH⁻ and an S⁻ of another ligand, respectively.²⁰⁷ A number of cap complexes formed with Bu₂SnO, ^tBu₂SnO, Me₂SnCl₂, and Ph₃SnCl were prepared in the solid state. The spectroscopic results demonstrated that the organotin(IV) moieties react with the {S} atom of the ligand, while the other coordination sites are the -COO⁻ and the amide C=O groups. Mössbauer |Δ_{exp}| data revealed that the diorganotin(IV) compounds adopt slightly distorted *Tbp* geometry. A single-crystal X-ray study was performed on the Me₂Sn(cap). The {Sn} atom is five-coordinated in a distorted *Tbp* environment, with two {O} atoms in the *ax* positions and the {S} and two {C} atoms in the *eq* plane. Each cap ligand coordinates to two different {Sn} atoms, and infinite zigzag chains are formed (Figure 10). NMR (in CDCl₃) and electrospray ionization mass spectrometry (ESI-MS) studies (in H₂O) of the [R₂Sn(IV)]²⁺ complexes indicate the presence of different oligomeric species.²⁰⁸

Four [Bu₂Sn(IV)]²⁺ complexes have been prepared with mercaptoacetic, 2-mercaptopropionic, mercaptosuccinic, and *m*-2,3-dimercaptosuccinic acid by two different procedures. The IR and Raman spectroscopic measurements indicate the presence of bidentately coordinated -COO⁻ groups, nonlinear C-Sn-C bonds, and Sn-S bonds. The results of Mössbauer spectroscopic measurements revealed the general occurrence of {Sn} in *Tbp* environments. A multinuclear NMR study also suggested {O, S} coordination of the [Bu₂Sn(IV)]²⁺

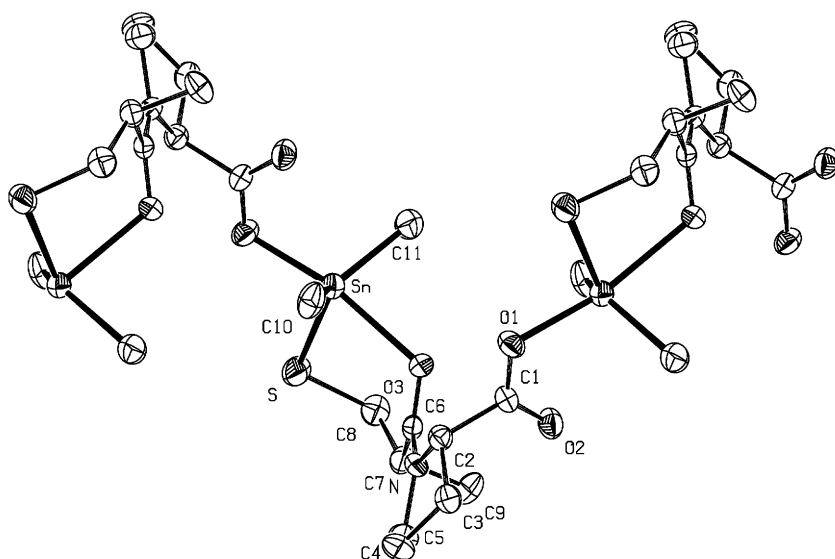


Figure 10 The diagram of the Me₂Sn(IV)-cap complex.²⁰⁸

fragment, within the cyclic oligomeric complexes. In strongly donor solvent (DMSO) depolymerization occurs.²⁰⁶

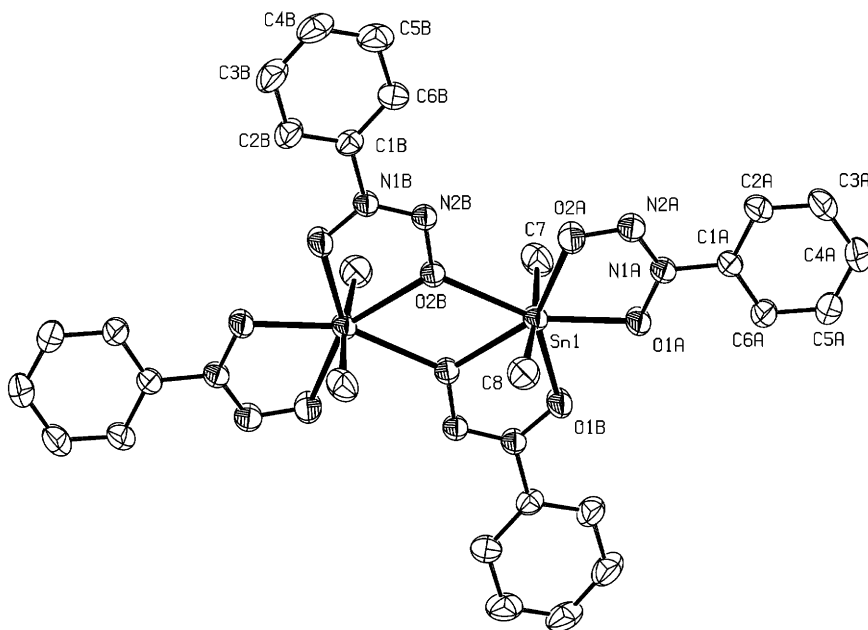
On the other hand, the $[\text{Bu}_2\text{Sn(IV)}]^{2+}$ complexes of the {O} analogs of the above-mentioned ligands are linear oligomers. The FT-IR and Raman spectroscopic data indicated the presence of bidentate and/or monodentate $-\text{COO}^-$ groups, nonlinear C–Sn–C bonds, and Sn–O bonds within the complexes. The results of Mössbauer spectroscopic measurements showed a *Tbp* arrangement around the central {Sn} atom in addition to the O_h and T_d structures.²⁰⁹

Until now only a few papers have been published on the organotin(IV)–hydroxamic acid complexes. A series of air-stable, soluble in alcohols and hydroalcoholic solution and in some cases in water, diorganotin(IV) complexes of 4-X-benzohydroxamic acid are formulated as $[\text{R}_2\text{SnL}_2]$ and $[\text{R}_2\text{Sn(L)(2)O}]$, where $[\text{R} = \text{Me, Et, Bu, or Ph and } \text{X} = \text{NH}_2, (\text{HL}_1)\text{NO}_2(\text{HL}_2), \text{ or F } (\text{HL}_3)]$ and characterized by different spectroscopic methods. The complexes have coordination geometry intermediate between distorted O_h and bicapped T_d . Their *in vitro* antitumor activity against a series of human tumor cell lines is identical, or sometimes higher than that of the cisplatin. For the mononuclear $[\text{R}_2\text{Sn(IV)}]^{2+}$ complexes, the activity generally increases with the length of the carbon chain of the alkyl ligand.^{210,211}

Recently, the synthesis and structural characterization of *N*-nitroso-*N*-phenylhydroxylaminato (PhN_2O_2^-) cupf organotin(IV) complexes, such as $[\text{Me}_3\text{Sn(cupf)}]_4$ (5),²¹² $\text{Ph}_2\text{Sn(cupf)}_2$ (6), $[\text{Me}_2\text{Sn(cupf)}_2]_2$ (1), and Sn(cupf)_4 (7) was reported.²¹³ It was found that, depending on the number (0, 2, 3) and the nature (Me, Ph) of the organotin(IV) moieties, the cupf anion displays various coordination patterns in these molecules: chelating (1, 6, 7), bridging (5), and bridging-chelating (1). As a consequence of this, the central {Sn} atom assumes a penta- (5), hexa- (6), hepta- (1), or octacoordinate (7) state, respectively.^{212,213} Bridging-chelating coordination mode of cupf to $[\text{Me}_2\text{Sn(IV)}]^{2+}$ gives the dimeric species (Scheme 1),²¹³ whereas a bridging coordination afford the tetrameric $[\text{Me}_3\text{Sn(cupf)}]_4$ complex (Scheme 2).²¹²

Compound (5) proved to be an attractive material for building supramolecular structures based upon chains of alternating trigonal planar $[\text{Me}_3\text{Sn(IV)}]^+$ units with rigid linear spacers, such as 4,4'-bipyridine (4,4'-bipy). The reaction of (5) with 4,4'-bipyridine (bipy), pyridine (py), and 2,6-diaminio-4-phenyl-1,3,5-triazine (dpt) afforded three new hepta-coordinated derivatives, $[\mu-(4,4'\text{-bipy})\{\text{Me}_2\text{Sn(cupf)}_2\}_2] \cdot \text{MeOH}$ (2), $\text{Me}_2\text{Sn(cupf)}_2(\text{py})$ (3), and $[\text{Me}_2\text{Sn(cupf)}_2(\text{MeOH})] \cdot \text{dpt}$ (4) (Figure 11),²¹⁴ following Sn–C bond redistribution. Such coordination of N- and O-donor molecules to the $[\text{Me}_2\text{Sn(IV)}]^{2+}$ center of dimeric complex (1) results in the cleavage of the stanoxanic dative Sn←O bonds, and consequently formation of novel heptacoordinated $[\text{Me}_2\text{Sn(IV)}]\text{--cupf}$ complexes (2–4). The crystal structures of the later complexes are shown in Figure 11 (a–c).

In these structures, the cupf assumes its typical chelating coordination pattern and is nearly symmetrically bound to the $[\text{Me}_2\text{Sn(IV)}]^{2+}$ center. In complex (4) a pentagonal bipyramidal (*PBP*) geometry containing C_2SnO_5 moiety was found by XRD method. The $^t\text{Bu}_2\text{Sn(IV)}\text{--cup}$ complex proved to be O_h .²¹⁵



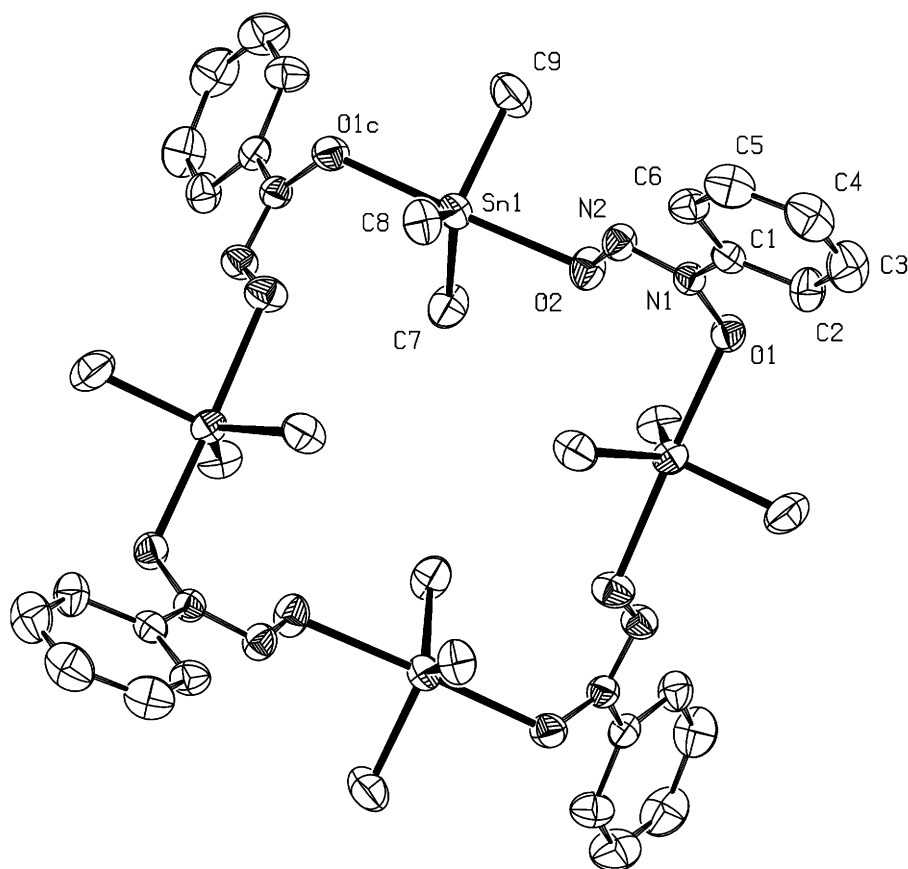
Scheme 1

Organotin(IV) compounds are strong neurotoxins and induce thymus atrophy and bile duct damage. The metabolism involves subsequent dealkylation reactions; accordingly, $[\text{R}_3\text{Sn(IV)}]^+$ or $[\text{R}_4\text{Sn(IV)}]$ exposure results in systematic exposure to the $[\text{RSn(IV)}]^{3+}$, and $[\text{R}_2\text{Sn(IV)}]^{2+}$ compounds. Although dimercaptosuccinic acid did not reduce the $[\text{Bu}_2\text{Sn(IV)}]^{2+}$ -induced mortality in mice, it reduced thymus and bile duct damage more efficiently than did DMP (2,3-dimercaptopropanol) and it was also an antidote in rats.^{216,217}

One woman died after 1 week, with multiorgan failure despite intravenous dimercaptosuccinic acid chelation. The other gradually recovered from severe neuropsychiatric symptoms over several months. She had been chelated for several weeks with oral dimercaptosuccinic acid, which apparently improved her clinical condition.²¹⁸

The complexes of aromatic hydroxy carboxylic acids (salicylic acid and its isomers) with $[\text{Bu}_2\text{Sn(IV)}]^{2+}$ and $[\text{Ph}_3\text{Sn(IV)}]^+$ were obtained. The FT-IR and Raman spectra clearly demonstrated that the organotin(IV) moieties react with the {O, O} atoms of the ligands. It was found that in most cases the $-\text{COO}^-$ group chelated to the central atoms, but monodentate coordination was also observed. The complexes probably have polymeric structures.

Comparison of the Mössbauer $|\Delta_{\text{exp}}|$ values with those calculated on the basis of the pqs formalism revealed that the organotin(IV) moiety has *Tbp* geometry, and in certain cases *T_d* geometry too. Some of the complexes contain the organotin(IV) cation in two different environments. Finally, the local structure of the maleic acid complex formed with $[\text{Bu}_2\text{Sn(IV)}]^{2+}$ was determined by an EXAFS method.¹⁶⁶ The structural data are collected in Table 6. Similar studies



Scheme 2

were performed on the $\text{Bu}_2\text{Sn(IV)}$ complexes formed with quinic acid (phenolic –OH) and gallic acid (alcoholic –OH group) (Figure 12).²¹⁹

The FT-IR spectroscopic measurements shown that in most cases the –COO^- or –O^- groups formed a bridge between two {Sn} central atom, and polymerization occurred. The pqs approximations proved the formation of complexes with O_h , Tbp , and T_d structures. ^1H NMR measurements performed in DMSO solution have shown that the polymeric structure of the complexes does not persist in solution, and depolymerization occurs.²¹⁹

The reaction of $[\text{Me}_2\text{Sn(IV)}]^{2+}$ with pyridoxine [3-hydroxy-4,5-bis(hydroxymethyl)-2-methylpyridine, PN, vitamin B_6] yielded three complexes, one with composition $[\text{Me}_2\text{Sn(PN–H)}]\text{NO}_3 \cdot 2\text{H}_2\text{O}$. This complex is a polymer: each monoprotonated pyridoxine coordinates to one {Sn} *via* the phenolic {O} and a deprotonated CH_2OH group {O}, and to the other *via* the latter group alone. In each dimeric unit, the {Sn} is coordinated to two Me groups, the phenolic {O} atom, the {O} atoms of two deprotonated CH_2OH groups, and the {O} atom of the nondeprotonated CH_2OH group.²²⁰ Further work on the interaction of the same

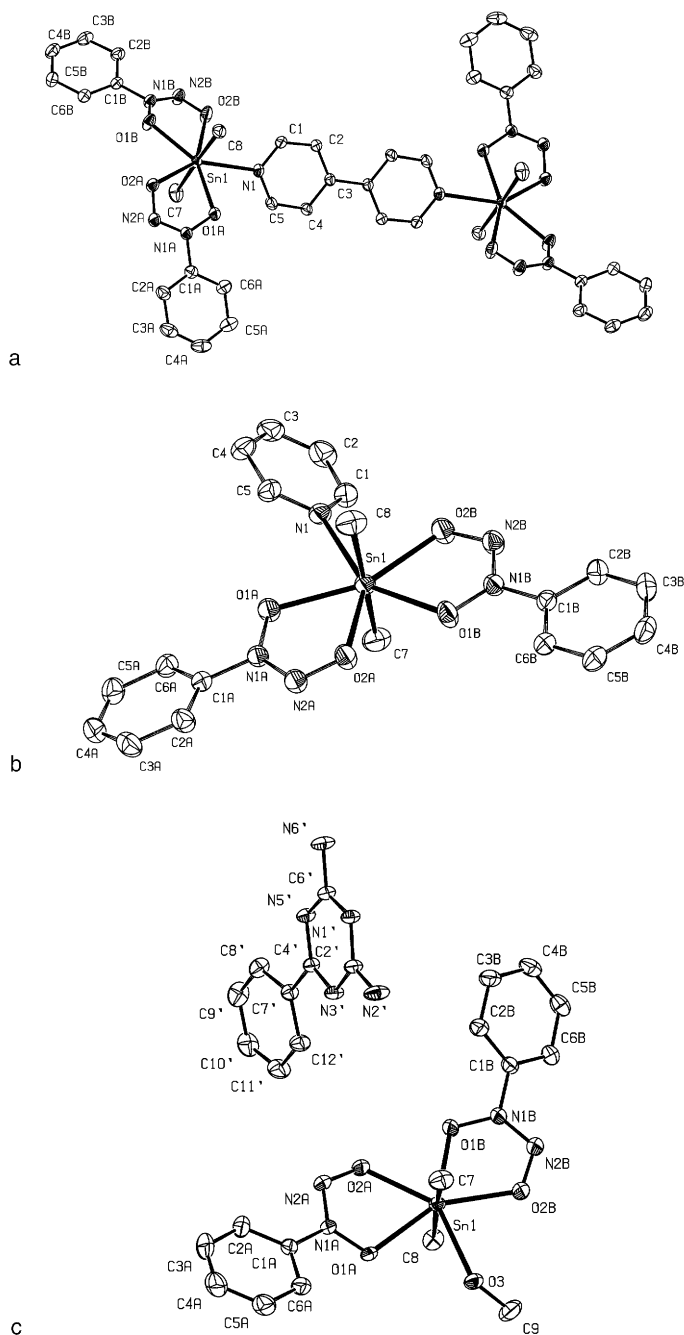


Figure 11 (a) Molecular structure of (2), the distorted MeOH molecules are omitted.²¹⁴
 (b) Molecular structure of (3).²¹⁴ (c) Molecular structure of (4).²¹⁴

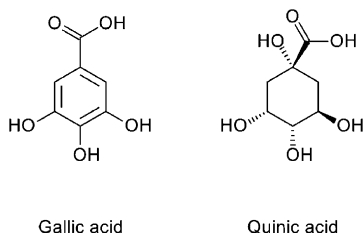


Figure 12 The structure of quinic and gallic acids.²¹⁹

ligand and $[\text{Et}_2\text{Sn(IV)}]^{2+}$ in an 4:1 (v/v) ethanol–water mixture containing different anions in various molar ratios, was published in Ref. (221). In this system, three complexes were formed. The structure of one of the compounds was determined by XRD, and was found to consist of dimeric $[\text{EtSn(PN-H)}]_2^{2+}$ units (in which two bridged-chelating hydrogenpyridoxinate anions link the {Sn} with coordination number five) and hydrogen-bonded Cl^- . This is similar to the system discussed above. Other work on similar systems was reported in Refs. (222,223).

Organotin(IV) compounds are a widely studied class of metal-based antitumor drugs.^{224–227} Their intensive investigation has led to the discovery of compounds with excellent *in vitro* antitumor activity, but, in many cases, disappointingly low *in vivo* activity or high *in vivo* toxicity.^{224–227} The design of improved organotin(IV) antitumor agents is unfortunately hampered by the paucity of information concerning the cellular targets of these compounds and their mechanism of action, although inhibition of mitochondrial oxidative phosphorylation appears to be an important mode of toxicity.^{225,226}

A review of the extensive literature in this field reveals two classes of organotin(IV) compounds with exceptionally high antitumor power. $[\text{Ph}_3\text{Sn(IV)}]^+$ benzoates exhibit an *in vitro* antitumor activity higher than that of cisplatin and comparable with that of mitomycin C.²²⁸ The most active of these compounds have been patented.²²⁹ However, Tranter et al.²³⁰ recently reported that, while $[\text{Ph}_3\text{Sn(IV)}]^+$ esters have a greater *in vitro* activity against four human tumor cell lines, this activity is independent of the structure of the ester moiety and comparable with that of Ph_3SnOH , suggesting that hydrolysis is a common, cytotoxic intermediate. A large number of structurally diverse $[\text{Bu}_2\text{Sn(IV)}]^{2+}$ carboxylates and other Sn–O bound $[\text{Bu}_2\text{Sn(IV)}]^{2+}$ derivatives exhibit consistently high *in vitro* antitumor activity and some possess low mammalian toxicity and greater *in vivo* activity than those of cisplatin (selected examples can be found).^{231–236} This antitumor potency is, in general, structure-dependent, although for some compounds there is evidence of prior hydrolysis to a common $[\text{Bu}_2\text{Sn(IV)}]^{2+}$ equivalent species which is responsible for the comparable activity.²³⁵ It was reported that dibutylstannylene alkoxides also exhibited greater *in vivo* antitumor activity than that of cisplatin in a variety of human tumor cell lines. The first step in the mechanism of action is hydrolysis to a common cytotoxic intermediate, and this intermediate targets the mitochondria.²³⁷ The $[\text{Bu}_2\text{Sn(IV)}]^{2+}$ dihydroxybenzoates are also active against different human tumor cell lines.^{232,234}

All dihydroxybenzoates with an *o*-hydroxy group are more active against MCF-7 cells than the substituted salicylates screened previously.²²⁷

The [Bu₂Sn(IV)]²⁺ complexes formed with ligands containing a –COO[–] group(s) are easily prepared by a one-pot method described by Davies et al.²⁰² In first step, tetrabutylldipropoxydistannoxane is prepared from Bu₂SnO and propanol by refluxing in benzene or in toluene. This distannoxane subsequently reacts at room temperature with carboxylates. This method appears to have two advantages over that^{231,238} in which Bu₂SnO reacts with the carboxylic acid in refluxing ethanol/toluene, methanol/toluene; first, as the carboxylic acid is added at room temperature, organotin(IV) carboxylates that are unstable at higher temperature can also be prepared; second, tetrabutylldipropoxydistannolane is synthesized in water-free medium because the H₂O is eliminated through a water/propanol/benzene azeotrope; hence, water-sensitive organotin(IV) carboxylates can conveniently be prepared.

[Ph₃Sn(IV)]⁺ and [Bu₃Sn(IV)]⁺ derivatives of carboxylates could be obtained by the reaction of the latter with Ph₃Sn(OH) and Bu₃Sn(Ac), respectively.^{228,239,240}

Acetate can form only one species, [Me₂Sn(O₂CMe)₂] with [Me₂Sn(IV)]²⁺, while malonate and succinate form a set of species. The thermodynamic parameters confirm the rearrangement of the two methyl groups from the *trans* to the *cis* position during formation of the bis complex.^{76,77} Subsequently, the results of equilibrium studies on the system Me₂Sn(IV)–acetate, –malonate, –1,2,3-propanetricarboxylate, and –1,2,3,4-butanetetracarboxylate have shown that this cation forms quite stable complexes with –COO[–] group containing ligands, with formation constants comparable to those of transition metals (somewhat higher than those of analogous complexes of Cu(II)), except for the hydrolytic species [ML(OH)]^{1–n}. The hydrolytic species and the mixed species have to be taken into account in the course of the curve fitting analysis. For the [Me₂Sn(IV)]²⁺–carboxylate complexes, log *K* is directly proportional to *z*^{2/3}, where *z* is the charge of the ligand. This relation enables to estimate the formation constants of other systems.²⁴¹ The results obtained on the acetate and malonate systems in the same ionic medium are in agreement with previous findings.^{76,77}

The results on the complex formation of [Me₂Sn(IV)]²⁺ with iminodiacetate (idaH₂), oxydiacetate, and thiodiacetate ligands have revealed the conformational flexibility of this cation in its complexes. Such flexibility is manifested not only in the variability of the Me–Sn–Me angle but also in the ability to give rise to unusual asymmetric stereochemistry. In the idaH₂ complex, the skew disposition of the Me groups and different bond lengths of equivalent donor atoms were observed.²⁴² A number of complexes were obtained in the solid state with the same ligand and characterized by different methods.^{243,244} The XRD measurement proved that the structure of [Me₂Sn(ida)(MeOH)]₂ is Centrosymmetric, dinuclear with seven-coordinate tin, similarly to the structure of [Me₂Sn(oda)(H₂O)]₂ (oda = oxydiacetate) (Figure 13).²⁴⁴ By contrast, the crystal structure of [(Et₂SnCl)₂(oda)(H₂O)]_n comprises a zigzag polymeric assembly containing a pair of alternating subunits, [Et₂SnCl(H₂O)] and [Et₂SnCl(oda)(H₂O)], which are connected by way of bridging oda carboxylates, thus giving seven-coordinate tin centers in both components.

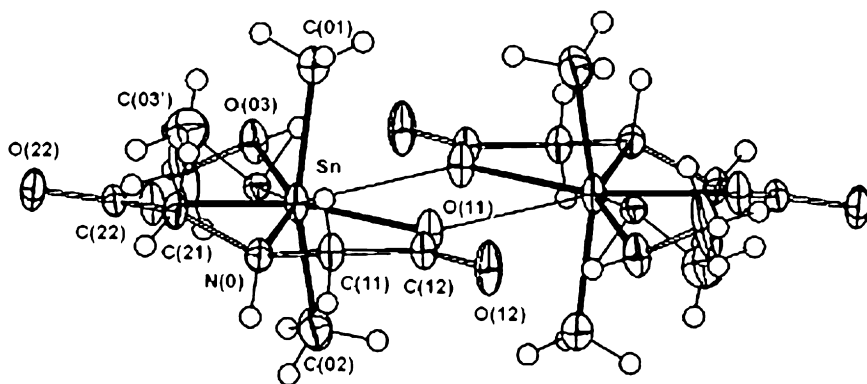


Figure 13 Structure of $[\text{Me}_2\text{Sn}(\text{ida})(\text{MeOH})]_2$.²⁴⁴

Three primary factors are involved: in the structure/activity relationships for organotin(IV) derivatives $(\text{L})_x\text{R}_n\text{SnX}_{4-n}$, the nature of the organic group R, of halide or pseudohalide $\{\text{X}_n\}$, and of donor ligand. Examination of the structures of $\{\text{Sn}\}$ compounds containing a N-donor atom and tested for antitumor activity revealed that in the active $\{\text{Sn}\}$ complexes the average Sn–N bond lengths were >239 pm, whereas the inactive complexes had Sn–N bonds <239 pm, which implies that predissociation of the ligand may be an important step in the mode of action of these complexes, while the coordinated ligand may favor transport of the active species to the site of action in the cells, where they are released by hydrolysis.

About the data published on all these $\{\text{Sn}\}$ derivatives, it can be concluded that $[\text{R}_2\text{Sn}(\text{IV})]^{2+}$ compounds exhibit generally higher antitumor activity than those of corresponding mono-, tri-, and tetraorganotin(IV) or the inorganic $\{\text{Sn}\}$ derivatives, and within the diorganotin(IV) class, the highest activity being exerted by the $[\text{Et}_2\text{Sn}(\text{IV})]^{2+}$ and $[\text{Ph}_2\text{Sn}(\text{IV})]^{2+}$ complexes. In a series of publications, Pettinari et al.^{245–249} investigated a large number of organotin(IV) complexes formed with mono- or bidentate N-donor ligands. The ligands were mainly substituted imidazole derivatives. In some cases, the ligand imidazole-2-thione was also used. The complexes were characterized by their analytical and spectral data. The behavior in solution was investigated by conductivity, molecular weight determinations, and ^1H , ^{119}Sn , and sometimes ROESY NMR experiments. It was found that the reactivities of these imidazoles toward organotin(IV) acceptors depended not only on the electronic and steric features of the groups bound to the $\{\text{Sn}\}$ but also on the position of the R or Ar substituent in the imidazole moiety and on the nature of the counterion. The combined spectral data suggest that the triorganotin(IV) adducts have a T_{bp} structure, whereas a distorted O_h or pseudo- O_h structure is likely for all the other derivatives.

Organotin(IV) derivatives of 2,2'-bisimidazole,²⁵⁰ N-methyl-2,2'-bisimidazole,²⁵¹ and N,N'-dimethyl-2,2'-bisimidazole^{252,253} were studied by Sordo et al. Conductivity measurements in acetonitrile showed that the adducts behave as non-ionogens in this solvent. The spectroscopic data suggest that all the

complexes have analogous pseudo-octahedral geometry, with bidentate ligands, and the R groups are in *trans* positions. The [Bu₂Sn(IV)]²⁺ derivatives proved to be the most active compounds against the well-established cell line KB.

When reacted with tetraalkylammonium halides, hydrated [Me₂Sn(IV)]²⁺, [Bu₂Sn(IV)]²⁺,²⁵⁴ [Ph₂Sn(IV)]²⁺,²⁵⁵ and [EtPhSn(IV)]²⁺,²⁵⁶ ester derivatives of 2,6-pyridinedicarboxylic acid yield tetraalkylammonium diorganohalogeno(2,6-pyridinedicarboxylato)stannates. Both classes of compounds exhibit high *in vitro* antitumor activity.

Bis(dicyclohexylammonium) bis(2,6-pyridinedicarboxylato)dibutylstannate is concluded to have sevenfold coordination at the {Sn} on the basis of its ¹¹⁹Sn CP/MAS NMR chemical shift ($\delta = -424.9$ ppm). The assignment has been corroborated by crystal structure determination of its monohydrate, in which the {Sn} atom has *trans*-C₂SnO₄ PBP geometry (Sn–C = 204.0, 206.7 pm, C–Sn–C = 168.9°). One 2,6-pyridinedicarboxylato group chelates to the {Sn} atom (Sn–O = 223.4, 226.0 pm; Sn–N = 227.9 pm), whereas the other binds through only one carboxyl end (Sn–O = 241.6, 244.1 pm). The anhydrous compound displays higher *in vitro* antitumor activity than those of cisplatin and carboplatin (Table 7).²⁵⁷

Several investigations have shown that the salicylaldimine complexes (Figure 14) with X = H are effective ligands for both inorganic and organotin(IV) species. Replacement of X by a methoxy group radically altered the nature of the metal salicylaldimine complexes as ligands, transforming them from bidentate to extremely effective tetradendate ligands. Much more surprising, however, was the finding that the behavior of the complexes as ligands is markedly and dramatically influenced by the nature of the bridging group in Figure 14. When the number of {C} atoms linking the imine {N} atoms is increased beyond three, the effectiveness of the metal salicylaldimines as ligands is greatly reduced. For example, practically no organotin(IV) Lewis acids react with the complex of *N,N'*-bis(3-methoxysalicylidene)pentane-1,3-diamine (= 3MeO-sal1,3pn),²⁵⁸ *N,N'*-bis(3-methoxysalicylidene)benzene-1,3-diamine and its 1,4-diamine analog.²⁵⁹ ¹¹⁹Sn Mössbauer spectroscopic parameters indicated that all of the adducts of di- and triorganotin(IV) halides are organotin(IV) aqua adducts with the donor water engaged in hydrogen bonding with Schiff base {O} atoms. Ph₃SnCl, Ph₂SnBr₂, and [Bz₂Sn(IV)]²⁺ complexes contained pentacoordinated {Sn}. The $|\Delta_{\text{exp}}|$ value of 3.20–3.29 mm s^{−1} for the Bu₂SnCl₂ adducts may reflect pseudo-O_h coordination geometry around tin central atoms as a result of weak intermolecular Sn–Cl interactions such as those in Me₂SnCl₂ · [Ni(3-MeOsal,salpn)]H₂O.²⁶⁰

Equimolar reactions of Bu₂SnO with Schiff bases derived from amino acids led to the formation of a new series of [Bu₂Sn(IV)]²⁺ complexes of general formula Bu₂SnL (L = dianion of tridentate Schiff bases derived from the condensation of 2-hydroxy-1-naphthaldehyde or acetyl acetone with Gly, L-β-Ala, DL-Val, DL-4-aminobutyric acid, L-Met, L-Leu, and PhGly). The central {Sn} atoms in all these complexes are pentacoordinated with a monodentate –COO[−] group. The complexes have been tested against various bacteria, and exhibited moderate activity. The cytotoxicity of the complexes was higher than those observed for cisplatin and carboplatin.²⁶¹

Table 7 Overview of ID₅₀ values *in vitro* of condensation compounds of Bu₂SnO with F[−]-containing carboxylic acids against MCF-7 and WiDr

Organotin(IV) compound	ID ₅₀ (ng cm ^{−3}) against MCF-7	ID ₅₀ (ng cm ^{−3}) against WiDr	Reference
{[(4-FC ₆ H ₄ CO ₂)SnBu ₂] ₂ O} ₂	81	360	298
[(4-FC ₆ H ₄ CO ₂) ₂ SnBu ₂]	90	309	298
{[(2,3-F ₂ C ₆ H ₃ COO)SnBuR ₂] ₂ O} ₂	9	120	299
(2,3-F ₂ C ₆ H ₃ COO) ₂ SnBu ₂	23	283	299
{[(2,3,6-F ₃ C ₆ H ₂ CO ₂)SnBu ₂] ₂ O} ₂	13	200	300
{[(2,3,4,5-F ₄ C ₆ HCO ₂)SnBu ₂] ₂ O} ₂	35	250	300
{[(2-FC ₆ H ₄ CH=CHCO ₂)SnBu ₂] ₂ O} ₂	28	368	231
{[(4-FC ₆ H ₄ CH ₂ CO ₂)SnBu ₂] ₂ O} ₂	38	268	231
[(1,2-F ₄ C ₆ (CO ₂) ₂ SnBu ₂]	51	68	301
{[(F ₅ C ₆ CO ₂)SnBu ₂] ₂ O} ₂	44	214	231
{[(F ₅ C ₆ CH=CHCO ₂)SnBu ₂] ₂ O} ₂	10	145	231
[Bu ₂ Sn(5-Cl-2-OH-C ₆ H ₃ CO ₂) ₂]	319	89	233
[Bu ₂ Sn(O ₂ CC ₅ H ₃ NCO ₂) ₂]	46	172	257
[2,3-(OH) ₂ -C ₆ H ₃ COO] ₂ SnBu ₂	7	90	232
[2,4-(OH) ₂ -C ₆ H ₃ COO] ₂ SnBu ₂	16	120	232
[2,5-(OH) ₂ -C ₆ H ₃ COO] ₂ SnBu ₂	4	115	232
[2,6-(OH) ₂ -C ₆ H ₃ COO] ₂ SnBu ₂	15	130	232
[3,5-(OH) ₂ -C ₆ H ₃ COO] ₂ SnBu ₂	130	500	232
Salicylaldoxime/Bu ₂ SnO	67	215	302
Salicylaldoxime/ ^t Bu ₂ SnO	49	121	302
Salicylaldoxime/Ph ₂ SnO	1643	4565	302
Et ₂ Sn[2,6-(O ₂ C) ₂ C ₅ H ₃ N] · H ₂ O	822	1290	303
{Et ₂ Sn[2,6-(O ₂ C) ₂ C ₅ H ₃ N]F} [−] [NEt ₄ ⁺]	1002	2495	303
Bu ₂ Sn[2,6-(O ₂ C) ₂ C ₅ H ₃ N] · H ₂ O	54	76	303
{Bu ₂ Sn[2,6-(O ₂ C) ₂ C ₅ H ₃ N]F} [−] [NEt ₄ ⁺]	118	220	303
<i>Etoposide</i>	187	624	304
<i>Mitomycin C</i>	3	17	304
<i>Carboplatin</i>	5500	1500	304
<i>Cisplatin</i>	800	650	304
<i>5-Fluorouracil</i>	210	260	304
<i>Methotrexate</i>	150	140	304
<i>Doxorubicin</i>	8	20	304

The compounds already used in clinical practice are given in italics.

Diorganotin(IV)²⁺ complexes with general formula R₂SnL (R = Ph, Bu and Me) were recently prepared by reacting R₂SnCl₂ and tetradentate Schiff bases (H₂L) containing N₂O₂ donor atoms in the presence of triethylamine (as base) in benzene. In the [Bu₂Sn(IV)]²⁺ complexes formed with 3-methoxysalicylaldehyde derivatives, the {Sn} atom has a distorted O_h structure, where the donor atoms of the Schiff base ligand occupy the four *eq* positions and the organo moieties are in *trans ax* positions.²⁶² Similarly, biologically active, hexacoordinated organotin(IV)

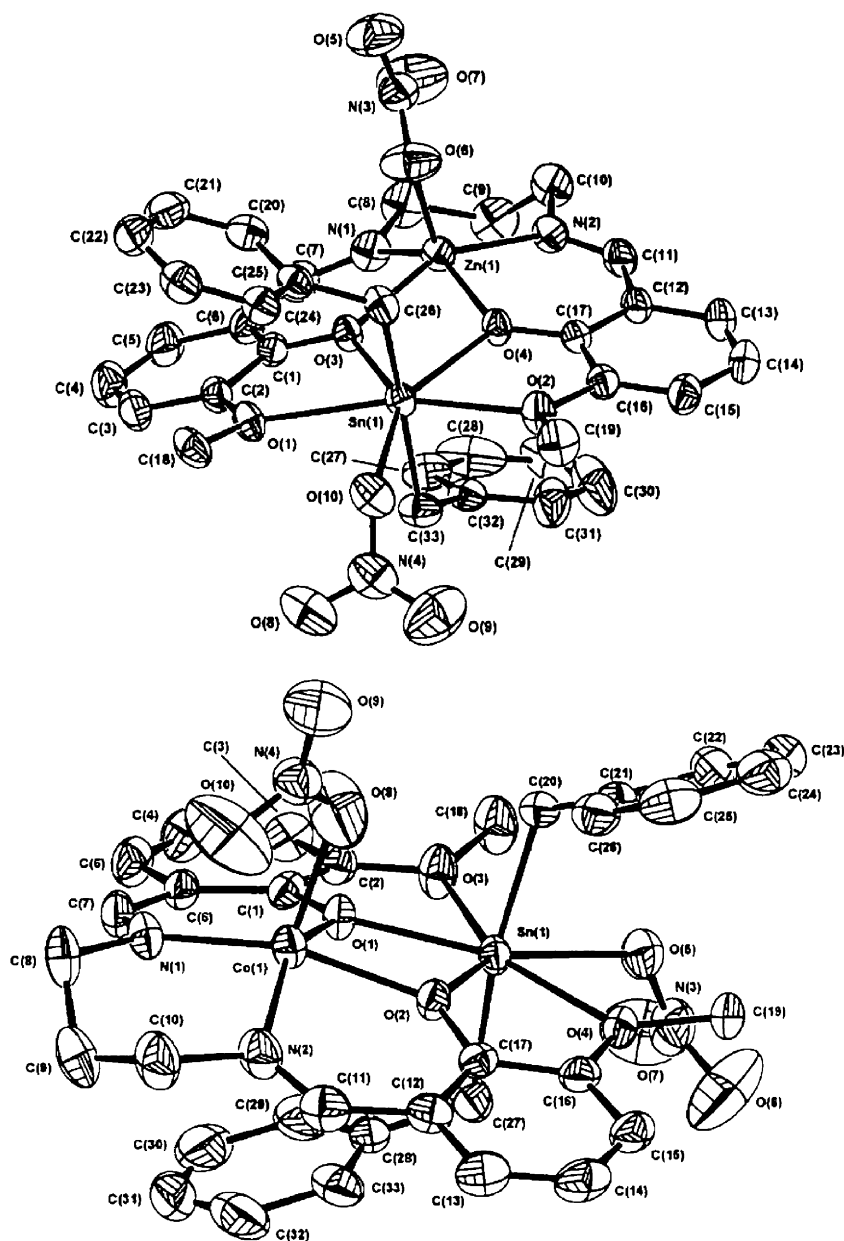


Figure 14 Structures of metal salicylaldehyde complexes.²⁵⁸

complexes, with the two Bu groups in *trans ax* positions are formed with Schiff bases derived from heterocyclic ketones and sulphadiazine drugs.²⁶³

Further results on organotin(IV)-amino acid or 2-amino-2-methyl-1-propanol Schiff base complexes were reported in Refs. (264–271).

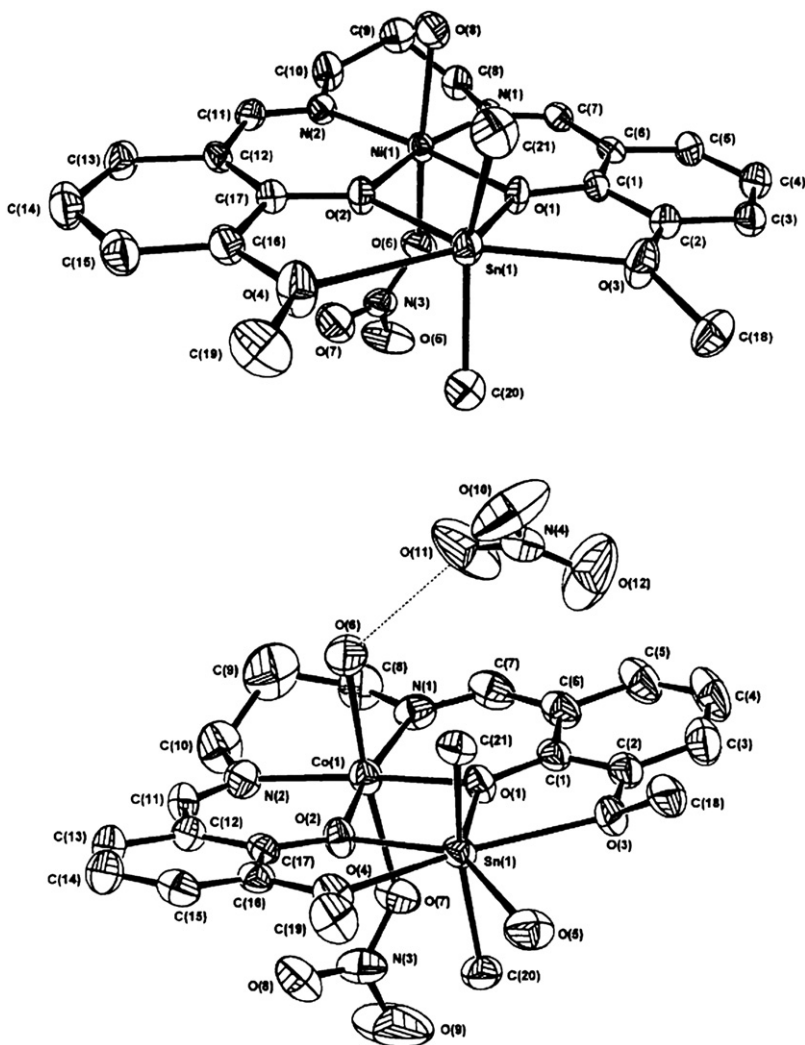


Figure 14 (Continued).

The reactions of mercaptopyrimidine derivatives (HL) with Ph_2SnCl_2 or $\text{Ph}_3\text{Sn}(\text{OH})$ yielded the species Ph_3SnL , Ph_2SnL_2 , or Ph_2SnCIL . The species containing only one anionic ligand are stable in most of the solvents they dissolve in Ph_2SnCIL , whereas complexes interact with strong O-donors, such as DMSO, yielding the corresponding species Ph_2SnL_2 and Ph_2SnCl_2 . Except for two complexes for which an O_h geometry with *trans* arrangement of the phenyl groups was proposed these products, have severely distorted *Tbp* structures (Figure 15).²⁷²

A large number of Ge-substituted $[\text{Bu}_2\text{Sn}(\text{IV})]^{2+}$ dipropionates with the formula $(\text{R}^3\text{GeCHR}^2\text{CHR}^1\text{COO})_2\text{SnBu}_2 \cdot \text{H}_2\text{O}$ ($\text{R}_3 = \text{Ph}_3$, $\text{N}(\text{OCH}_2\text{CH})_3$, $\text{R}^2 = \text{H}$, Me, aryl, $\text{R}^1 = \text{H}$, Me] have been synthesized and characterized by FTIR, NMR,

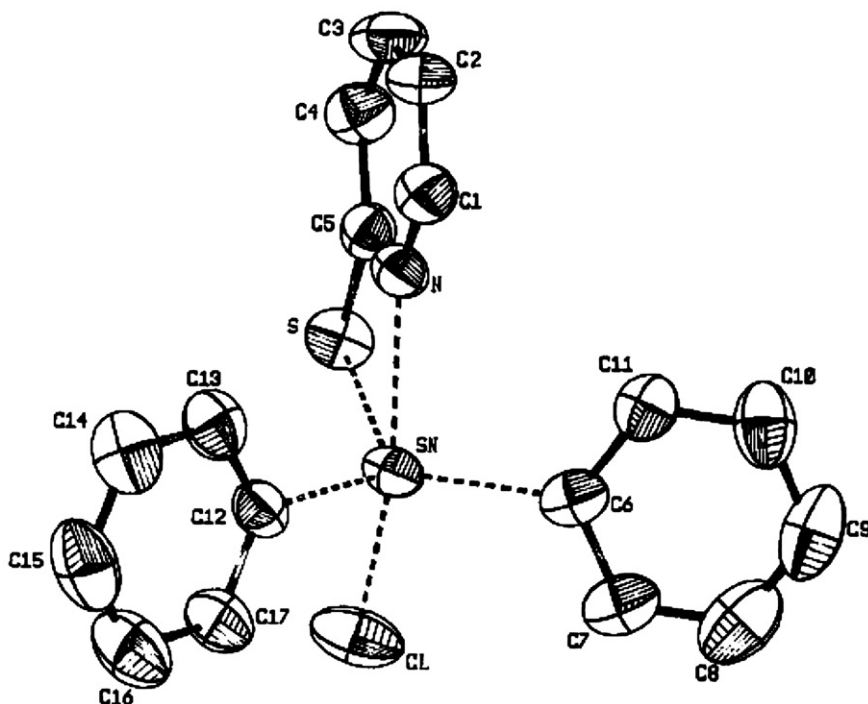
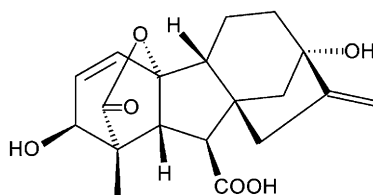


Figure 15 Molecular structure of $\text{Ph}_2\text{SnCl}(\text{MP})$ with the atom numbering scheme, (AMP = 2-mercapto pyridine).²⁷²



Gibberellic acid

Figure 16 The structure of gibberellic acid.²⁷⁸

MS, and in one case XRD. All these compounds display antitumor activity, despite their low solubility in water.²⁷³

Multifunctional di- and triorganotin(IV) carboxylates derived from bioorganic acids such as steroid carboxylic acids,²⁷⁴ terebic acid,²⁷⁵ 2,3:4,6-di-isopropylidene-2-keto-L-gulonic acid,¹³² and gibberellic acid²⁷⁶ (Figure 16) were found to exhibit antitumor properties *in vitro*. On the other hand, numerous other organotin(IV) carboxylates have likewise been shown to exhibit high antitumor activity.^{239,240,277,278} Very recently, the $[\text{Bu}_2\text{Sn}(\text{IV})]^{2+}$, $[\text{Ph}_3\text{Sn}(\text{IV})]^+$, and $[\text{Bu}_3\text{Sn}(\text{IV})]^+$ derivatives of 3S,4S-3-[(R)-1-(*t*-butyldimethylsiloxy)ethyl]-4-[R-1-carboxy ethyl]-2-azetidinone have been synthesized and characterized. They also possess antitumor activity.²⁷⁹

Gibberellic acid (Figure 16) complexes of $[\text{Bu}_2\text{Sn(IV)}]^{2+}$, $[\text{Bu}_3\text{Sn(IV)}]^+$, and $[\text{Ph}_3\text{Sn(IV)}]^+$ have been prepared. The monomeric $[\text{Bu}_3\text{Sn(IV)}]^+$ derivative has the strongest antitumor activity.²⁷⁶

The structure of $[\text{R}_3\text{Sn}(\text{O}_2\text{CCH}_2\text{N}(\text{H})\text{C}(\text{O})\text{NH}_2)]$ [$\text{R} = \text{Ph}$, *c*-Hex (cyclohexyl) or Bu; $\text{HO}_2\text{CCH}_2\text{N}(\text{H})\text{C}(\text{O})\text{NH}_2$ = hydantoic acid] is polymeric as a consequence of the bridging property of the ligand: each ligand coordinates to one {Sn} atom *via* one of the $-\text{COO}^-$ {O} atoms, and to a symmetry-related {Sn} atom *via* a $\text{C}=\text{O}$ group at the other end of the molecule. The structure is distorted *Tbp* around the {Sn} atom, with a *trans*- R_3SnO_2 motif characteristic of triorganotin(IV) complexes. The structure of $[\text{cHex}_3\text{Sn}(\text{O}_2\text{CCH}_2\text{N}(\text{H})\text{C}(\text{O})\text{NH}_2)]$, (*c*Hex = cyclohexyl) by contrast, is monomeric with monodentate carboxylate group. Fungitoxicity and phytotoxicity studies indicate that the butyl derivative is the most active compound.²⁸⁰

Several triorganotin(IV) esters of *N*-arylidene- ω -amino acid complexes have also been prepared. These complexes have a *trans*- R_3SnO_2 pentacoordinated structure with bridging $-\text{COO}^-$ or unidentate $-\text{COO}^-$ and phenolic {O} coordinating the {Sn} atoms. The compounds are active against *Ceratomyces ulmi*.²⁸¹ The $[\text{Bu}_2\text{Sn(IV)}]^{2+}$ complexes of *N*-arylidene- α -amino acid were tested against the panel of 60 cell lines of the National Cancer Institute. The complexes have only moderate activity, probably because of the presence of the N-bearing ligand, which increases the stability of the compounds.²⁸² In the crystal structures of the $[\text{Ph}_3\text{Sn(IV)}]^+$ derivatives of *N*-(2-carboxybenzylidene)aniline, the {Sn} atom in both of the molecules comprising the asymmetric unit exists in distorted T_d geometry owing to an intramolecular acyl $\text{O} \cdots \text{Sn}$ contact. These complexes exhibit high fungicidal activity.²⁸³ Other arylamine complexes of diorganotin(IV) with general formula $\text{R}_2\text{SnCl}_2\text{L}$ ($\text{R} = \text{Me}$, Et, Vin, ^{*t*}Bu, Bu, or Ph; L = *N*-(2-pyridylmethylene)arylamine) have also been prepared. These complexes adopt a distorted *trans*- O_h structure and have a significant cytogenetic effect.²⁸⁴ $[\text{Ph}_3\text{Sn(IV)}]^+$ compounds of *p*-ethoxybenzoic acid and acetylsalicylic acid contain molecular units with Sn–O bonds and distorted T_d {Sn} centers. The phthalic acid derivative contains two tetracoordinated {Sn} atoms with a phthalic acid unit bridging them. The salicylaldehydato compound is polymeric with *Tbp* {Sn} centers in which the Ph groups take *eq* positions. The polymerization occurs *via* the aldehyde {O} atom bonding to a neighboring {Sn} atom.²⁸⁵ These complexes have significant activity against a range of fungi.²⁸⁶

The fungicidal activity of a number of ArSn(IV) compounds, $(p\text{-ZC}_6\text{H}_4)_3\text{SnX}$ (where $\text{X} = \text{OAc}^-$, OH^- , or 0.5 {O}, $\text{Z} = \text{F}$, Cl, CH_3 , CH_3O , C_2H_5 , or $(\text{CH}_3)_3\text{C}$) are reported in Ref. (287); the results are compared with those on the Ph_3SnOAc and Ph_3SnOH archetypes. It was found that, in most cases, *p*-substitution reduces the biocidal activity only slightly, but with *p*- CH_3O the $\text{Ar}_4\text{Sn(IV)}$ is completely ineffective. A model for the fungicidal action was proposed.

In the context of studies on the coordination of organotin(IV) moieties by thiolic {S} and heterocyclic {N} atoms, diorganotin(IV) complexes of 2-mercaptopyridine, $\text{R}_2\text{Sn}(\text{SPy})_2$ and $\text{R}_2\text{SnCl}(\text{SPy})$, have been characterized in the solid state and in solution.²⁸⁸ The structure of the latter complex ($\text{R} = \text{Ph}$) was determined by XRD (Figure 17). The crystal is monoclinic in the space

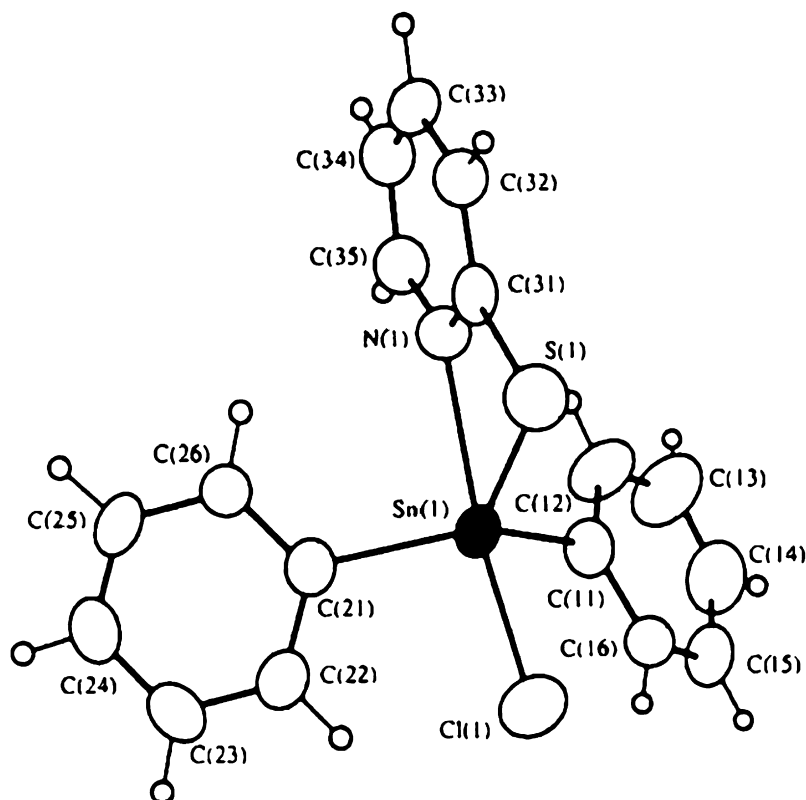


Figure 17 Structure of diphenyl pyridine-2-thiolatochlorotin(IV).²⁸⁸

group $P2_1/m$. With the bidentate ligand SPy, {Sn} forms a four-membered chelate ring with a short N–Sn–N bite angle of $64.8(1)^\circ$, leading to a heavily distorted *Tbp* environment around the {Sn}. The related complexes have analogous structures. The compounds $R_2Sn(SP_y)_2$ are distorted O_h with R in the *trans* position, and {S} and {N} donor atoms in *cis* positions. The solid-state molecular structures are retained in chloroform solution.

The solid-state structures of the complexes $R_2SnHal(SPym)$, ($R = ^iPr, Bu, ^iBu, ^tBu, Cy, Ph, SPym$) are of *Tbp* type, but distorted, with the angles C–Sn–C larger than 120° for the $[R_2Sn(IV)]^{2+}$ and $[Cy_2Sn(IV)]^{2+}$ derivatives. The complexes $R_2Sn(SPyr)_2$ have *trans*- R_2 O_h , or possibly skew-trapezoidal structures, with *cis*-S,S and *cis*-N,N atoms in the *eq* plane. The complex $Me_2SnCl(SPym)$ was assumed to be a monomeric, *Tbp* species with the C–Sn–C angle around $134\text{--}145^\circ$, or a monodimensional polymer with a *trans*- R_2 O_h -type {Sn} environment.²⁸⁹

Monoorganotin(IV) complexes of the above ligands with the compositions $MeSn(SP_y)_3$ and $PhSn(Spy)_3 \cdot 1.5CHCl_3$ are monoclinic. In the discrete monomeric $RSn(Spy)_3$ units, three bidentate SPy ligands together with R form a distorted *PBP* structure around the {Sn}. One {S} and one {C} atom are in the *ax* positions. Two {S} atoms and three {N} atoms form the pentagonal plane.²⁹⁰

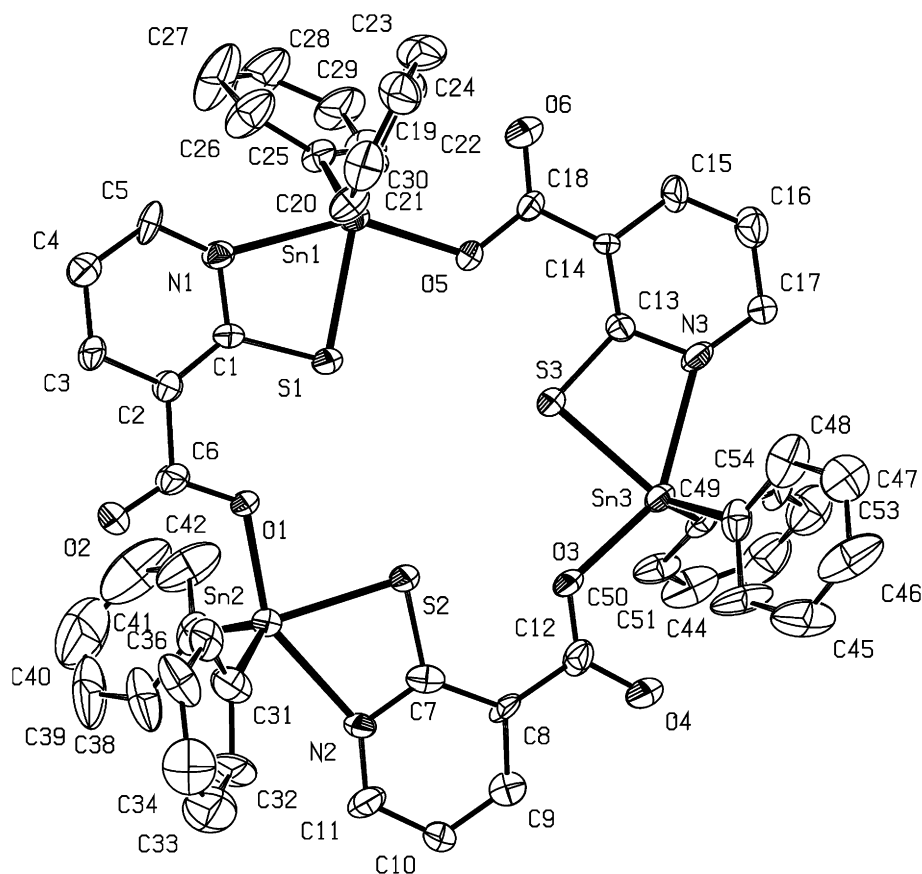


Figure 18 The same molecular structure of complexes 2 and 3 (all solvent molecules omitted for clarity).²⁹¹

Interesting results were published by Ma et al.²⁹¹ on the preparation and structural studies of novel 18-membered stereoregular diphenyltin(IV) macrocycles. The compounds $\{\text{Ph}_2\text{Sn}[\text{S}(\text{C}_6\text{H}_3\text{NO})\text{O}]\}_3$ (1), $\{\text{Ph}_2\text{Sn}[\text{S}(\text{C}_6\text{H}_3\text{NO})\text{O}]\}_3 \cdot 2 \cdot 67\text{H}_2\text{O}$ (2), and $\{\text{Ph}_2\text{Sn}[\text{S}(\text{C}_6\text{H}_3\text{NO})\text{O}]\}_3 \cdot 4\text{C}_6\text{H}_6$ (3) have been synthesized by the reaction of Ph_2SnCl_2 with 2-mercaptitonitonic acid. Single-crystal XRD data revealed that (2) and (3) are highly symmetrical trinuclear cyclic complexes with the ligand bridging the adjacent {Sn} central atoms. The {Sn} environment is distorted *cis-Tbp*. Weak interaction $\text{Sn} \cdots \text{O}$ was recognized between {Sn} and exocyclic-oxygen atoms. The same molecular component of complexes (2) and (3) is depicted in Figure 18.

The structure and dynamics for some representatives of the series of $[\text{Me}_2\text{Sn}(\text{IV})]^{2+}$, $[\text{MeSn}(\text{IV})]^{3+}$, and inorganic Sn(IV) complexes with {S, N}-containing donors have been determined by ^{119}Sn Mössbauer spectroscopy and are reported in Ref. (292).

A series of di- and triorganotin(IV) complexes of 2-thionaphthalene have also been prepared. All the complexes have T_d geometry and moderate biological activities against various bacteria and fungi.²⁹³

The coordination behavior of the diorganotin(IV) compounds R_2SnCl_2 (where $R = Me, Ph$) with 4H-pyrido[1,2-*a*]-pyrimidin-4-one derivatives ($= L$) has been described. The ligands are coordinated in a monodentate fashion, mainly *via* the {O} atom of the 4-one group or possibly *via* the {N} atom of the $C=N$ linkage to give pentacoordinated {S} complexes.²⁹⁴

Bis[3-methoxysalicylatodibutyltin(IV)] oxide, obtained by the condensation of Bu_2SnO and 3-methoxysalicylic acid, exhibits higher antitumor activities *in vitro* against two human tumor cell lines, MCF-7, a mammary tumor, and WiDr, a colon carcinoma, than those of the 5-Me- and 4-MeO analogs.²²⁷ The position of the MeO substituent also influences the antitumor activity of the dibutyltin-bis(methoxysalicylate)s, $(CH_3O-2-OH-C_6H_3COO)_2SnBu_2$: for the 4-MeO derivative, the ID_{50} values are 131 and 1182 ng/ml, whereas for the 5-MeO derivative, they are 54 and 611 ng/ml, respectively. On the other hand, dibutyltin(IV)-bis-(4-hydroxy-3-methoxy-benzoate), $(4-OH-3-CH_3O-C_6H_3COO)_2SnBu_2$ is characterized by excellent ID_{50} values (44 and 82 ng ml⁻¹, respectively),²²⁷ as compared with the former compounds. The dibutyltin(IV)-bis(dihydroxybenzoate)s have skew-trapezoidal bipyramidal or bicapped tetrahedral structures in the solid state ($\Delta = 3.38\text{--}4.66\text{ mm s}^{-1}$),²³² comparable with those of dimethyltin(IV) diacetate²⁹⁵ and dibutyl-bis(o-aminobenzoate)²³³ or dibutyl-bis(5-chloro-2-hydroxybenzoate)tin(IV).²⁹⁶ The much larger $|\Delta_{exp}|$ value (4.7 mm s⁻¹) for $(2,6-(OH)_2C_6H_3COO)_2SnBu_2$ is consistent with a heptacoordinated structure,²³² like that of $[Me_2Sn(IV)]^{2+}$ dipicolinate in the solid state.²⁹⁷ The antitumor activities of these compounds are presented in Table 7.²³²

The substitution of {H} by F^- markedly influences the biological activity of organic molecules. Although the van der Waals radii of F^- (135 pm) and {H} (120 pm) are comparable, the substituent F^- is very resistant to metabolic transformations because of the strength of the C–F bond. The higher electronegativity of F^- also strongly affects the electronic density distribution in the molecule. Accordingly Gielen et al.²³¹ synthesized a series of organotin(IV) carboxylates containing mono- or polyfluorophenyl groups, and screened them for antitumor activity against MCF-7 and WiDr (Table 7).

The dibutyltin(IV) monofluorobenzoates²⁹⁸ are characterized by ID_{50} values roughly half those of etoposide. The 2,6-difluorobenzoates are more active than the 4-monofluorobenzoates, which shows that the activity is enhanced when the number of F^- atoms on the benzoate moiety is increased. The $\{[(2,3-F_2C_6H_3CO_2)Bu_2Sn]_2O\}_2$ compound provides an ID_{50} value against MCF-7 comparable with that of mitomycin C.²⁹⁹ The ID_{50} value of the corresponding 2,3,6-trifluorobenzoate is of the same order of magnitude, while that of the 2,3,4,5-tetrafluorobenzoate is lower.³⁰⁰ Against WiDr, all fluorobenzoates exhibit comparable activities, again except $\{[(2,3-F_2C_6H_3CO_2)Bu_2Sn]_2O\}_2$, which is significantly more active. The activities of dibutyltin(IV) fluorocinnamate and fluorophenylacetate are similar, while dibutyltin(IV) tetrafluorophthalate is characterized by a quite low ID_{50} value against WiDr cells. As far as the cell lines MCF-7 and WiDr are concerned,

the pentafluorobenzoates have activities comparable with those of the tri- and tetrafluorobenzoates and the monofluorophenyl-acetates and -cinnamates.²³¹

The crystal structure of $\text{Bu}_2\text{Sn}(5\text{-Cl-2-OH-C}_6\text{H}_3\text{CO}_2)_2$ [dibutylbis(5-chloro-2-hydroxybenzoato)tin(IV)] shows that in the monomeric species the hexacoordinated {Sn} atom exists in skew-trapezoidal bipyramidal geometry in which the four {O} donor atoms, derived from two asymmetrically chelating carboxylate ligands, define the basal plane. Additionally, the butyl substituents lie over the weaker Sn–O interactions, determining a C–Sn–C angle of 147.6° . The *in vitro* antitumor activity of the compound is shown in Table 7.²³³

The triphenyltin(IV) sarcosine $[\text{Ph}_3\text{Sn(IV)}]^+$ complexes with compositions $[\text{Ph}_3\text{Sn}(\text{OCOCH}_2\text{NH}_2\text{CH}_3)_2]\text{X}$ ($\text{X} = \text{Cl}^-$, SCN^-) were studied by Khoo et al.³⁰⁵ Sarcosine reacts in a zwitterionic form, and behaves as a monodentate ligand *via* coordination through the carboxylate oxygen. All data support the *trans*- R_3SnO_2 *Tbp* structure of the complexes. The cyclosarcosylsarcosine complexes of $[\text{R}_3\text{Sn(IV)}]^{3+}$ and $[\text{R}_2\text{Sn(IV)}]^{2+}$ have also been studied. The $[\text{Ph}_2\text{Sn(IV)}]^{2+}$ derivative forms zigzag polymeric chains of *trans*- $[\text{Ph}_2\text{Sn(IV)}]^{2+}$ bridged by ketonic {O} atoms. Each {Sn} atom is surrounded by two {C} atoms (Sn–C = 212.9 and 214.6 pm, C–Sn–C = 160.1°), two Cl^- (Sn–Cl = 245.5 pm, Cl–Sn–Cl = 98.5°), and two {O} atoms (Sn–O = 237.0 and 246.8 pm, O–Sn–O = 86.1°).³⁰⁶

Triorganotin(IV) and diorganotin(IV) halides and pseudohalides form molecular adducts with zwitterions such as *N*-alkyl and *N*-arylsalicylides,^{307–310} picolinic acid,^{311,312} and quinaldic acid.³¹³ With Schiff bases, the 1:1 and 1:2 adducts normally have *Tbp* and O_h structures, respectively, though some unusual structures have also been reported.^{314,315} With carboxylic acids, hydrated complexes are generally obtained. The acid in its zwitterionic form binds to the $[\text{Ph}_3\text{Sn(IV)}]^+$ moiety and generates *Tbp* geometry around the {Sn} atom. Hydrogen bonding involving noncoordinated water molecules serves to bind the pentacoordinated units together in the form of a dimer. These compounds display a most unusual structure,^{311–315} and show promising fungicidal activity. In [Dimethyl (carboxylatomethyl)ammonium]-chlorotriphenyl stannate, $\text{Me}_2\text{HNCH}_2\text{COOPh}_3\text{SnX}$ ($\text{X} = \text{Cl}$, NCS), the {Sn} atom is also found to be pentacoordinated and the ligand in the form of the zwitterion binds to the metal ion through the monodentate $-\text{COO}^-$ group. Due to the “hard” character of organotin(IV) cations, the NCS^- is bound through the {N} atom. The fungicidal activities are slightly better than that of the parent compound, Ph_3SnCl .³¹⁶ The structure of $[\text{Bu}_3\text{Sn}(\text{N-phthaloylglycinate}) \cdot \text{H}_2\text{O}]$ is similar to the structure discussed above. Instead of a halide ion, a water molecule is coordinated to the {Sn} center. These complexes also have fungicidal activity.³¹⁷ Di- and triorganotin(IV) derivatives of thiophene-2-carboxylic acid and aminobenzoic acid complexes have O_h and *Tbp* geometry.^{318,319}

Diphenic acid (H_2A) also forms diorganotin(IV) complexes, which are T_d with two monodentate $-\text{COO}^-$ groups. On the other hand, soluble dinuclear triorganotin(IV) complexes (where the organo moieties are Me and Ph) contain symmetrically bound carboxylates, while the less-soluble compound (*c*- Hex_3Sn) has two asymmetrically bonded carboxylates. All have *Tbp* structures with $[\text{R}_3\text{Sn(IV)}]^+$ units remote from each other.³²⁰

The preparation and spectroscopic characterization of [R₃Sn(O₂CCH₂SC₅H₄N-4)] (R = Ph, Bz, cHex, and Bu) and [R₃Sn(O₂CCH₂SC₄H₃N₂-2,6)] (R = Me, Ph, Bu) have been reported.³²⁰ The 2-pyrimidyl compounds feature *Tbp* {Sn} centers with *trans*-R₃SnO₃ geometry as confirmed by XRD measurements on [Ph₃Sn(O₂CCH₂SC₅N₂-2,6)]. By contrast, 4-pyridyl complexes have *Tbp* geometry in the solid state (arising from the intermolecular Sn...N interaction) and a *T_d* structure in solution.³²¹

The antitumor activity of salicylaldoxime complexes of [Bu₂Sn(IV)]²⁺, [tBu₂Sn(IV)]²⁺, and [Ph₂Sn(IV)]²⁺ have been tested. The results are collected in Table 7.³⁰²

Ascorbic acid coordinates [Me₂Sn(IV)]²⁺ and [Bu₂Sn(IV)]²⁺ in aqueous solution via O-1, O-2, and O-3 of the lactone ring. Other weak interactions of {Sn} complexes in the solid state are also possible.³²² Due to their practical importance, particular attention has been paid to studies of synthesis, properties, structures, and reactivities of triorganotin(IV) monocarboxylates. Similar triorganotin(IV) di- and polycarboxylates have been studied much less intensively. For triorganotin(IV) carboxylates involving different degrees of the substitution of the -COO⁻ group {H} atoms, it is possible to prepare a diverse palette of mixed esters or ionic salts, in which some {H} atoms are substituted by organic or organometallic groups, and/or by ions. The current knowledge on the crystal and molecular structures of this class of organotin(IV) compounds relates to triorganotin(IV) carboxylates derived from dicarboxylic acids. As far as we are aware, the compounds derived from tricarboxylic acids have not been studied. When dicarboxylic acids react with R₂SnO, they generally lead to a cyclic structure containing one {Sn} atom.^{256,301} The reaction of hexafluoro-2,2-bis(4-carboxyphenyl)propane with tetrabutylldipropoxydistannoxane, formed *in situ* from Bu₂SnO and propanol in benzene, yields a compound whose structure is a strained macrocycle with a single dicarboxylate moiety.³²² The ¹¹⁷Sn NMR spectrum exhibits a single resonance at -142.3 ppm, typical of the usual trapezoidal bipyramidal geometry of diorganotin(IV) dicarboxylate.³²³ Several novel derivatives of 6-[D(-)-β-amino-*p*-hydroxyphenylacetamido]penicillin (amoxicillin),³²³ D(-)-α-aminobenzylpenicillin (ampicillin),³²⁴ 2,6-dimethoxyphenylpenicillin (methicillin),³²⁴ and 4-thia-1-azabicyclo[3.2.0]heptane-2-carboxylate, 3,3-dimethyl-7-oxo-6(2-phenylacetamido)penicillin (penicillin G)³²⁵ with diorgano- and triorganotin(IV) moieties have been prepared. The stoichiometries of the compounds obtained were R₂Sn(IV)Cl(antib)·*n*H₂O, R₃Sn(IV)Cl(antib)Na·*n*H₂O (antib⁻¹ = amoxicillinate, *n* = 2; antib⁻¹ = ampicillinate or methicillinate, *n* = 1; antib⁻¹ = penicillinate, *n* = 0; R = Me, Bu, Ph) and R₂Sn(IV)(antib)₂·2H₂O (antib⁻¹ = amoxicillinate and ampicillinate; R = Me, Bu, Ph). For R₂Sn(IV)Cl(antib)·*n*H₂O and R₃Sn(IV)Cl(antib)Na·*n*H₂O, the IR data suggest pentacoordination around the {Sn} atom, whereas R₂Sn(IV)(antib)₂·2H₂O most probably involves hexacoordination. In all of the compounds, thermogravimetric analysis excludes any coordination of {Sn} of water molecules. On the basis of IR and Mössbauer data, *Tbp* configurations are proposed for both R₂Sn(IV)Cl(antib)·*n*H₂O and R₃Sn(IV)Cl(antib)Na·*n*H₂O (antib⁻¹ = amoxicillinate, ampicillinate, or methicillinate) in the solid state.

FT-IR and Mössbauer spectroscopic measurements lead to T_d structures being proposed for $R_2Sn(IV)Cl$ (chloramphenicol) and $R_2Sn(IV)(chloramphenicol)_2$ in the solid state. In DMSO- d_6 solution, complete or partial dissociation is inferred for the Me and the Ph derivatives, as shown by the 1H and ^{13}C NMR spectroscopic results. Two different {Sn} sites occur. One involves a {Sn} atom tetrahedrally coordinated by a monoanionic monodentate cycloserinate group, through {O} atom of the resonance stabilized hydroxamate anion, furnishing Me_2SnClO and Me_2SnO_2 polyhedra in $Me_2SnCl(D-cycloser)$ and $Me_2Sn(D-cycloser)_2$, respectively. The second site corresponds to {Sn} in a polymeric O_h configuration with Me_2SnCl_2ON and $Me_2SnO_2N_2$ environments in $Me_2SnCl(D-cycloser)$ and $Me_2Sn(D-cycloser)_2$.³²⁶

In diorganotin(IV)chloroproporphyrin IX complexes, with the general formulas $(R_2SnCl)_2$ protoporphyrin IX ($R = Me, Bu, \text{ and } Ph$), the ligand coordinates to the $[R_2Sn(IV)Cl]^+$ moieties *via* bridging $-COO^-$, forming pentacoordinated *cis*- $R_2 Tbp$ structures, as inferred from the FT-IR and Mössbauer spectroscopies data.³²⁷

The spectral features of the complexes $(R_2SnCl)_2$ protoporphyrin IX are in agreement with the monomeric character of protoporphyrin IX.

m-tetra(4-carboxyphenyl)porphine (H_6TPPC) interacts with diorgano- and triorganotin(IV) moieties to afford complexes with the formulae $(R_2Sn)_2H_2TPPC$ and $(R_3Sn)_4H_2TPPC$, respectively. Pentacoordination of the {Sn} atom in both compounds is attained through coordination of the carboxylate {O} of the carboxyphenyl group. In $(R_2Sn)_2H_2TPPC$, two different carboxylate coordination types (bridging and monodentate types) are observed, whereas in $(R_3Sn)_4H_2TPPC$ only bridging carboxylate groups are present, with the {O} atoms in *ax* positions.³²⁸ 1H and ^{13}C NMR data, in DMSO- d_6 solutions, point to the pentacoordinated monomeric structures of the above complexes.

Diorgano and triorganotin(IV) derivatives of *m*-tetra(4-sulfonatophenyl)porphine (H_6TPPS) with formula $(R_2Sn)_2H_2TPPS$ and $(R_3Sn)_4H_2TPPS$ ($R = Me, Bu, Ph$) have been studied by FT-IR and Mössbauer spectroscopy in the solid state, while 1H and ^{13}C NMR spectroscopy have been applied to DMSO- d_6 solutions.³²⁹ The coordination mode of the sulfonate groups toward the organotin(IV) moieties has been established on the basis of S–O vibrations present in the IR spectra of the complexes. In the IR spectrum of the free ligand *m*-tetra(4-sulfonatophenyl)porphine, six S–O vibrations are found (three A_1 and three E). According to Yeats et al.³³⁰ these are due to the RSO_3^- groups present as an ionic species with C_{3v} symmetry in all the complexes. Following coordination and the formation of a more or less covalent bond, the symmetry decreases to C_s , removing the degeneracy of the three modes and increasing the number of fundamentals to nine (six A' and three A''). The preceding findings have been interpreted as reflecting a bidentate bridging behavior of the sulfonate groups. Consequently, in diorganotin(IV) [*m*-tetra(4-sulfonatophenyl)porphinate]s, the {Sn} atom should be hexacoordinated in a polymeric structure, while in triorganotin(IV) [*m*-tetra(4-sulfonatophenyl)porphinate]s, the {Sn} atom should be pentacoordinated in an *eq*- $R_3Sn(IV)$ polymeric configuration with *ax* RSO_3^- groups.³²⁹

The 1H and ^{13}C NMR spectra of the complexes in DMSO- d_6 solution led to the conclusion that the O_h and the *Tbp* configurations of $[R_2Sn(IV)]_2H_2TPPS$ and

[R₃Sn(IV)]₄H₂TPPS, (R = Me, Bu, Ph), respectively, in the solid state, are maintained in solution.³²⁹ Pentacoordination, in a *Tbp* configuration, *eq*-R₃, has been proposed for R₃Sn(IV) derivatives of L-homocysteic acid on the basis of IR and Mössbauer spectroscopy. The SO₃⁻ and NH₃⁺ groups of L-homocysteic acid are not involved in the coordination.

The $\Delta\nu = [\nu_{\text{as}}(\text{COO}^-) - \nu_{\text{s}}(\text{COO}^-)]$ values extracted from the FT-IR data ranged from 117 cm⁻¹ for Ph₃SnL-homocysteate to 140 cm⁻¹ for Me₃SnL-homocysteate, suggesting bidentate bridging behavior of the -COO⁻ group in a polymeric network. Furthermore, the pentacoordination around the {Sn} was preserved in solution, as verified through ¹H and ¹³C NMR in DMSO-d₆. From IR and Mössbauer spectroscopic investigations in the solid state³³¹ it was hypothesized that orotic acid, 6-uracilcarboxylic acid, (H₃Or), coordinates [R₂Sn(IV)]²⁺ moieties to yield two different classes of derivatives with formulas R₂SnHOR · *n*H₂O, and R₂Sn(H₂Or)₂ · *n*H₂O (R = Me, *n* = 0; R = Bu, *n* = 1). In R₂SnHOR · *n*H₂O, the orotic acid behaves as a dianionic tridentate ligand. In R₂Sn(H₂Or)₂ · *n*H₂O, two different {Sn} sites have been evidenced by Mössbauer spectroscopy in the solid state, and by ¹H and ¹³C NMR in DMSO-d₆ solution. Complexes with the formula R₃Sn(H₂Or) (R = Me, Bu) were obtained with the [R₃Sn(IV)]⁺ moieties, in which orotic acid behaves as a monoanionic bidentate bridging ligand and furnishes *Tbp eq*-R₃ complexes.³³¹

Organotin(IV) compounds of the potentially ambidentate ligand *O*-cholesteryl-*O*-phenyl phosphorothioate were prepared according to Ref. (332) and formulated as Me₃SnOSPR'R'', Ph₃SnOSPR'R'', O(CH₂CH₂S)₂Sn(Bu)OSPR'R'', or S(CH₂CH₂S)₂Sn(Bu)OSPR'R'' (where R' = *O*-Ph; R'' = *O*-cholesteryl). The spectroscopic data are consistent with bonding of the phosphorothioate ligand through both {S} and {O} donor atoms to the organotin(IV) center.³³³

A prominent feature of organotin(IV) coordination chemistry is the acceptor property associated with mono-, di-, and triorganotin(IV) compounds containing strongly electron-withdrawing groups such as halide or pseudohalide attached to {Sn}. In contrast, tetraorganotin compounds, R₄Sn, show little tendency to expand their coordination number beyond four. Thus, spectroscopic studies in the solid state of R₄Sn compounds containing intramolecular donor sites attached to the α- or β-carbon atom³³⁴ and in donor solvents of compounds containing relatively electronegative moieties such as furyl,^{335,336} pyridyl,³³⁷⁻³³⁹ perhalogenoaryl,³⁴⁰⁻³⁴² and thienyl^{335,336} have generally not provided unequivocal evidence for higher than tetracoordination at the metal center. However, for one class of tetraorganotins, namely the stannatrane derivatives represented by Me₂Sn(CH₂CH₂CH₂)₂NMe and MeSn(CH₂CH₂CH₂)₃N, a multinuclear (¹H, ¹³C, ¹¹⁹Sn) NMR study has been reported³⁴⁴ which strongly favors transannular N → Sn interactions in these compounds. The pentacoordinated structure of the triptych compound, MeSn(CH₂CH₂CH₂)₃N, has been confirmed.³⁴⁴ The literature also contains two references to isolable pentacoordinated compounds in Me₃SnCF₃ · P(NMe₂)₃³⁴⁵ and lithium 1,1-bis(η¹-cyclopentadienyl)-1-halo-2,3,4,5-tetraphenyl-stannole,³⁴⁶ but the structures have not been rigorously clarified.

Kumar Das et al.³⁴⁷ obtained a unique hexacoordinated tetraorganotin compound, bis[C,N-[3-(2-pyridyl)-2-thienyl]]diphenyltin(IV). The crystal

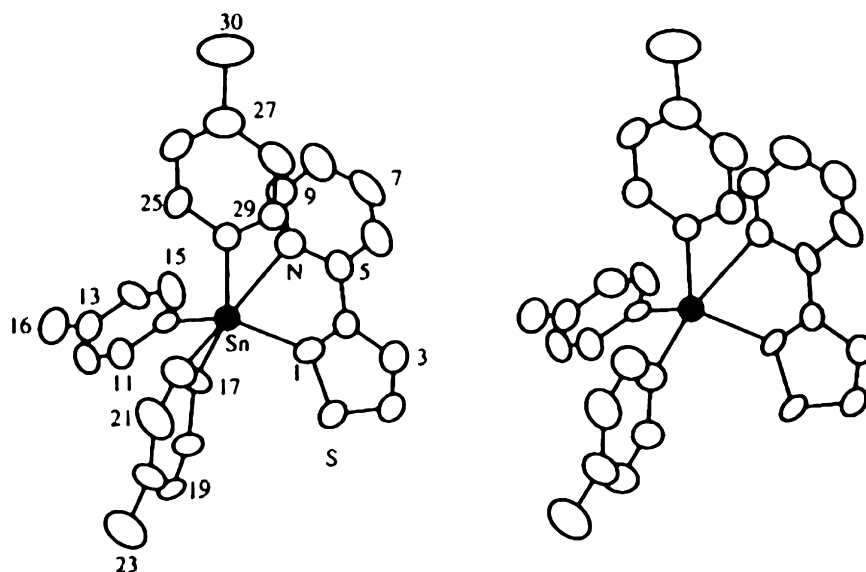


Figure 19 ORTEP diagram (35% thermal ellipsoids) with atom labelling of {C,N-[3-(2-pyridyl)-2-thienyl]}tri(*p*-tolyl)tin(IV).³⁴⁷

structure of this compound revealed the pseudo- O_h environment of the {Sn}, with the coordinating pyridyl nitrogen atoms located *cis* to each other (Sn–N = 256 pm, N–Sn–N = 77.1°) along with the Ph groups (C–Sn–C = 101.9°), and the *ipso*-thienyl {C} atoms arranged approximately *trans* to each other (C–Sn–C = 144.4°). Later, a number of additional R_4 Sn compounds containing the novel 2-(3-thienyl)pyridine ligand as one of the R groups were synthesized.³⁴⁷ X-ray structure analysis of one of the complexes shows a *pseudo-Tbp* arrangement, involving a weak interaction Sn–N bond of distance 284.1 pm (Figure 19). The Mössbauer parameters are in the range $\delta = 1.03$ – 1.35 , $|\Delta_{\text{exp}}| = 0.57$ – 0.96 mm s^{-1} . Further structural data (bond distances and ^{119}Sn NMR data) are summarized in Tables 8 and 9.

Diorganotin(IV) 2,6-pyridine-dicarboxylates exhibit *in vitro* antitumor activities.³⁶⁰ Atassi³⁶¹ assumed that water-soluble organotin(IV) compounds are probably more active than complexes soluble only in organic solvents. Therefore, Willem et al.³⁰³ prepared some tetraethylammonium (diorgano)-halogeno (2,6-pyridinedicarboxylato)-stannates (halogeno = Cl^- , F^-), whose water solubilities under physiological conditions are higher than those of their parent compounds. The desired compounds were obtained by using a similar procedure as in the case of the analogous tetraethylammonium diorgano(halogeno)-thiosalicylatostannates.³⁰¹ The Mössbauer parameters ($|\Delta_{\text{exp}}| = 3.50$ – 4.23 mm s^{-1}) suggested that the heptacoordination around the {Sn} atom in the parent compounds^{254,359} is maintained in the salt.

The inhibition doses, ID_{50} , for the compounds and the parent $[\text{Bu}_2\text{Sn(IV)}]^{2+}$ derivatives are presented in Table 9. These data do not support the hypothesis of Atassi that water-soluble {Sn} compounds might exhibit higher antitumor activity, at least for the cell lines studied. It should be outlined that the

Table 8 Comparison of Sn–N bond lengths in selected organotin(IV) compounds containing (N) donor ligands

No.	Compound	Sn–N (pm)	Reference
1	Me ₃ SnCl.py	226	348
2	(<i>p</i> -ClC ₆ H ₄) ₂ SnCl ₂ .4,4'-Me ₂ bipy	–	
	<i>Cis</i> isomer	229.4, 232.2	349
	<i>Trans</i> isomer	240.6	
3	(<i>p</i> -tolyl) ₂ SnCl ₂ bipy	230.6, 237.4	350
4	Ph ₂ SnCl ₂ · bipy	234.4, 237.5	351
5	ClSn(CH ₂ CH ₂ CH ₂) ₃ NMe	237.2	343
6	Cl ₂ Sn(CH ₂ CH ₂ CH ₂) ₂ Nme	244.0	344
7	¹¹⁹ Pr(Et)Sn(quin) ₂	254.2, 259.7	352
8	Ph ₂ SnCl ₂ · SC ₇ H ₅ N	254.8	353
9	[3-(2-py)-2-C ₄ H ₂ S] ₂ SnPh ₂	256.0	347
10	MeSn(CH ₂ CH ₂ CH ₂) ₃ N	262.0	344
11	Ph ₃ SnSC ₅ H ₄ N	262.0 ^a	354
12	[3-(2-py)-2-C ₄ H ₂ S]Sn(<i>p</i> -tolyl) ₃	284.1	347
13	(Ph ₂ SnCl ₂ · pyz) _n	296.5, 278.2	355
14	(Cys ₃ Sn) ₂ N ₃ (OH)	243.6	357

py, pyridine; bipy, bipyridyl; Hquin, 2-methylquinolin-8-ol; pyz, pyrazine; Cys, cyclohexyl.

^aReported as intermolecular Sn–N distance.**Table 9** ¹¹⁹Sn NMR chemical shifts for organotin(IV) compounds containing different donor atoms

Compound	Concentration (w/w) ^b	δ (ppm) ^a	Reference
[3-(2-py)-2-C ₄ H ₂ S]Sn(<i>p</i> -tolyl) ₃	0.12/1.5	–176.3	347
[3-(2-py)-2-C ₄ H ₂ S]SnPh ₃	0.08/1.03	–181.6	347
[3-(2-py)-2-C ₄ H ₂ S]Sn(<i>p</i> -ClC ₆ H ₄) ₃	0.08/1.3	–180.0	347
[3-(2-py)-2-C ₄ H ₂ S]Sn(cyclo-C ₅ H ₉) ₃	0.4/1.5	–57.8	347
[3-(2-py)-2-C ₄ H ₂ S]Sn(cyclo-C ₆ H ₁₁) ₃	0.11/1.3	–105.9	347
[3-(2-py)-2-C ₄ H ₂ S]SnPh ₂	0.1/1.5	–245.5	347
(3-C ₄ H ₃ S)Sn(<i>p</i> -tolyl) ₃	10 ^c	–157.8	347
(3-C ₄ H ₃ S) ₂ Sn(<i>p</i> -tolyl) ₃	0.1/1.5	–146.3	347
(2-C ₄ H ₃ S)SnPh ₃	0.08/2.0	–135.5	347
(2-C ₄ H ₃ S) ₂ Sn(<i>p</i> -tolyl) ₂	0.07/1.5	–138.0	347
(2-C ₄ H ₃ S) ₂ SnPh ₂	0.13/1.5	–140.8	347
(2-C ₄ H ₃ S) ₂ SnMe ₂	0.4/1.5	–62.7	347
(2-C ₄ H ₃ S) ₄ Sn	7 ^c	–147.0	334
Ph ₄ Sn	Saturated	–128.1	358, 359
(cyclo-C ₅ H ₉) ₄ Sn	0.13/1.5	–18.3	347

^aRelative to Me₄Sn.^bAll measurements were performed in CDCl₃.^cConcentration in w/v (%).

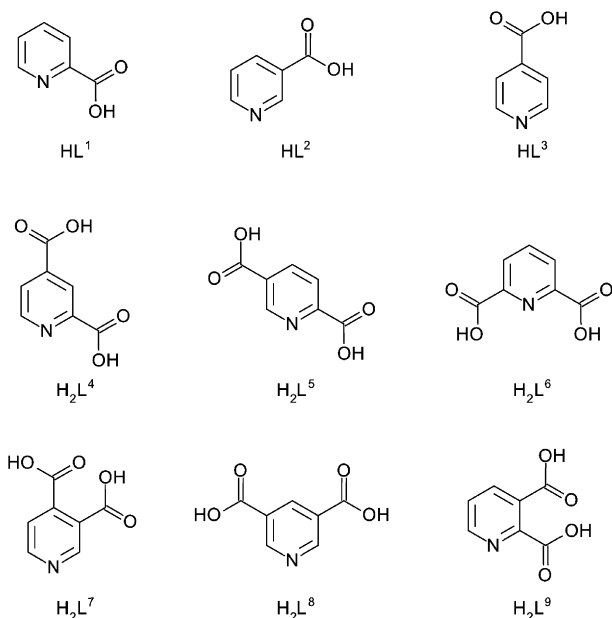


Figure 20 Structure of ligands studied.³⁶³

$[\text{Bu}_2\text{Sn(IV)}]^{2+}$ compounds exhibit a much higher activity than the corresponding $[\text{Et}_2\text{Sn(IV)}]^{2+}$ compounds, in contrast with most {S} compounds tested *in vivo* against P338 mouse leukemia cells.³⁶⁰ Furthermore, the $[\text{Bu}_2\text{Sn(IV)}]^{2+}$ complex is quite active against WiDr cells, which is not the case for most $[\text{Bu}_2\text{Sn(IV)}]^{2+}$ derivatives as they mainly exhibit promising activity against MCF-7 cells.²²⁷

$[\text{Bu}_2\text{Sn(IV)}]^{2+}$ complexes formed for pyridine mono- and dicarboxylic acids (Figure 20) containing $-\text{COO}^-$ group(s) and aromatic {N} donor atom were prepared.

It was found by means of FT-IR measurements that in most cases the $-\text{COO}^-$ groups are bridged to two {Sn} central atoms, and polymeric (oligomeric) complexes are formed. By using this information, the experimental ^{119}Sn Mössbauer spectroscopic data were treated with a pqs approximations. According to the calculation, the {Sn} atoms have O_h and PBP surroundings. Two $[\text{Bu}_2\text{Sn(IV)}]^{2+}$ complexes were obtained as single crystals. The X-ray structural studies showed that the Sn(IV) central atoms are in PBP geometry with bond distances characteristic for organotin(IV) compounds. The two butyl groups are located in *ax* positions (C–Sn–C angle 169°) (Figure 21). ^{119}Sn NMR measurements performed in $\text{DMSO}-d_6$ solution and in the solid state have shown that the polymeric structure of the complexes does neither persist nor remain in solution, and depolymerization occurred. This phenomenon is a characteristic feature for polymeric organotin(IV) complexes.³⁶²

Similar studies on the $^t\text{Bu}_2\text{Sn(IV)}$ complexes formed with the same ligands were performed. The synthetic procedure resulted in the formation of $^t\text{Bu}_2\text{Sn(IV)}$ compounds with a 1:2 metal-to-ligand ratio for pyridinemonocarboxylic acids,

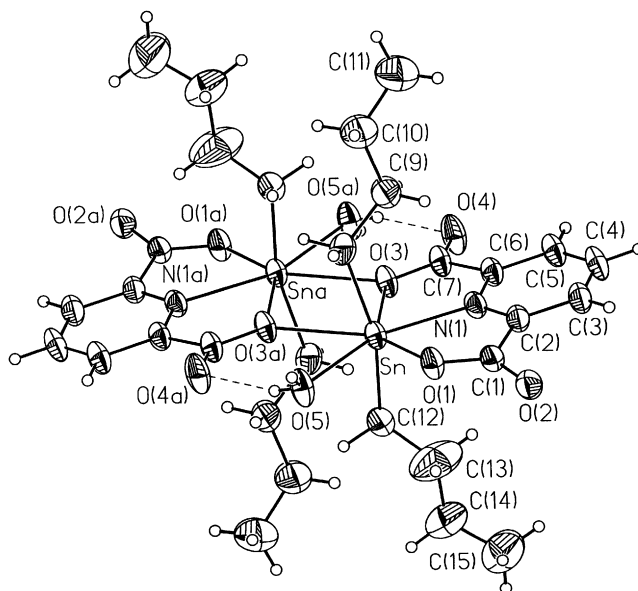


Figure 21 The ORTEP diagram of the $\text{Bu}_2\text{Sn(IV)}$ –2,6-dicarboxylatopyridine complex.³⁶²

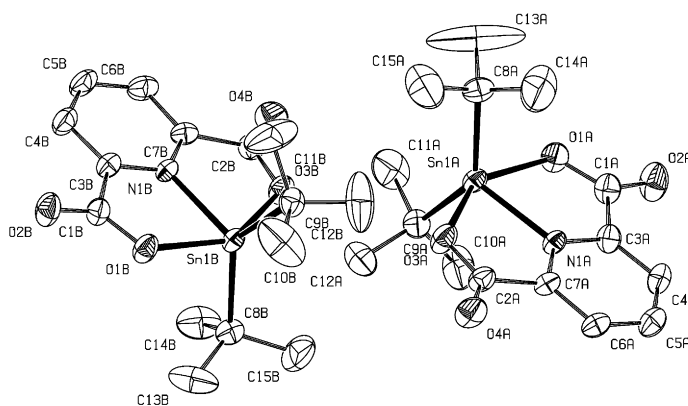


Figure 22 The ORTEP diagram of the $\text{}^t\text{Bu}_2\text{Sn(IV)}$ –2,6-dicarboxylatopyridine complex.³⁶³

and with a 1:1 ratio for the pyridinedicarboxylic acids. In polymeric compounds the polymerization occurred through $-\text{COO}^-$ groups, which bridged two {Sn} central atoms. The molecular structure of one compound was determined by means of XRD measurements, which show a seriously distorted *Tbp* (or *Sp*) coordination sphere with *eq* $\text{}^t\text{Bu}$ groups (Figure 22). The formation of heptacoordinated {Sn} geometry found in $[\text{Bu}_2\text{Sn(IV)}]^{2+}$ complexes is sterically prohibited in $\text{}^t\text{Bu}_2\text{Sn(IV)}$ complexes because of the bulkiness of $\text{}^t\text{Bu}$ groups, supported by a theoretical calculation. The C–Sn–C bond angles obtained from XRD analysis (136.9°) are in good agreement with the values calculated from ^{119}Sn Mössbauer spectroscopic studies (138°). The crystal packing shows a unique

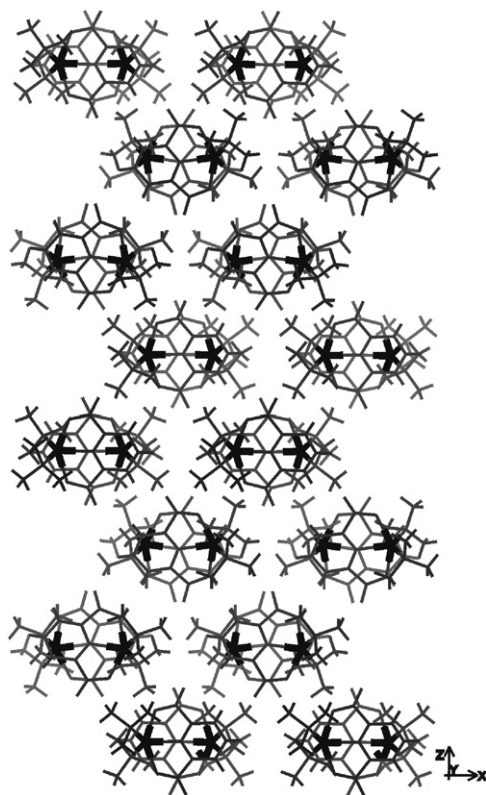


Figure 23 Crystal packing of the $t\text{Bu}_2\text{Sn(IV)}$ -2,6-dicarboxylatopyridine complex.³⁶³

feature (Figure 23). All units contain 16 molecules which are rather far from each other. The two units are held together by a hydrogen bond.³⁶³

A large number $[\text{BuSn(IV)}]^{2+}$ and $[t\text{BuSn(IV)}]^{2+}$ complexes of ligands containing an $-\text{OH}$, $\text{C}=\text{O}$ group or $-\text{OH}$ and $-\text{COOH}$ groups and an aromatic $\{\text{N}\}$ donor atom were prepared by metathetical reactions. On the basis of the FT-IR and Mössbauer spectroscopic data, molecular structures were assigned to these compounds. The binding sites of the ligands were identified by means of FT-IR spectroscopic measurements, and it was found that in most cases the organotin(IV) moiety reacts with the phenolic form of these ligands. In the complexes with $-\text{OH}$ and COOH functions, the $-\text{COOH}$ group is coordinated to the organotin(IV) centers in a monodentate manner. The ^{119}Sn Mössbauer and the FT-IR studies support the formation of Tbp and O_h molecular structures. Furthermore, XRD analysis has been performed on the butyltin(IV)- and $t\text{Bu(IV)}$ -8-quinol 8-olato-O,N single crystals. The hexacoordinated tin centers exhibit $cis\text{-}O_h$ geometry in both complexes (Figure 24a,b).³⁶⁴

A number of $[\text{Ph}_3\text{Sn(IV)}]^+$ complexes formed with ligands containing $-\text{OH}$, $\text{C}=\text{O}$, or $-\text{COOH}$ group(s) and aromatic $\{\text{N}\}$ donor atom have been prepared. The binding sites of the ligands were identified by FT-IR

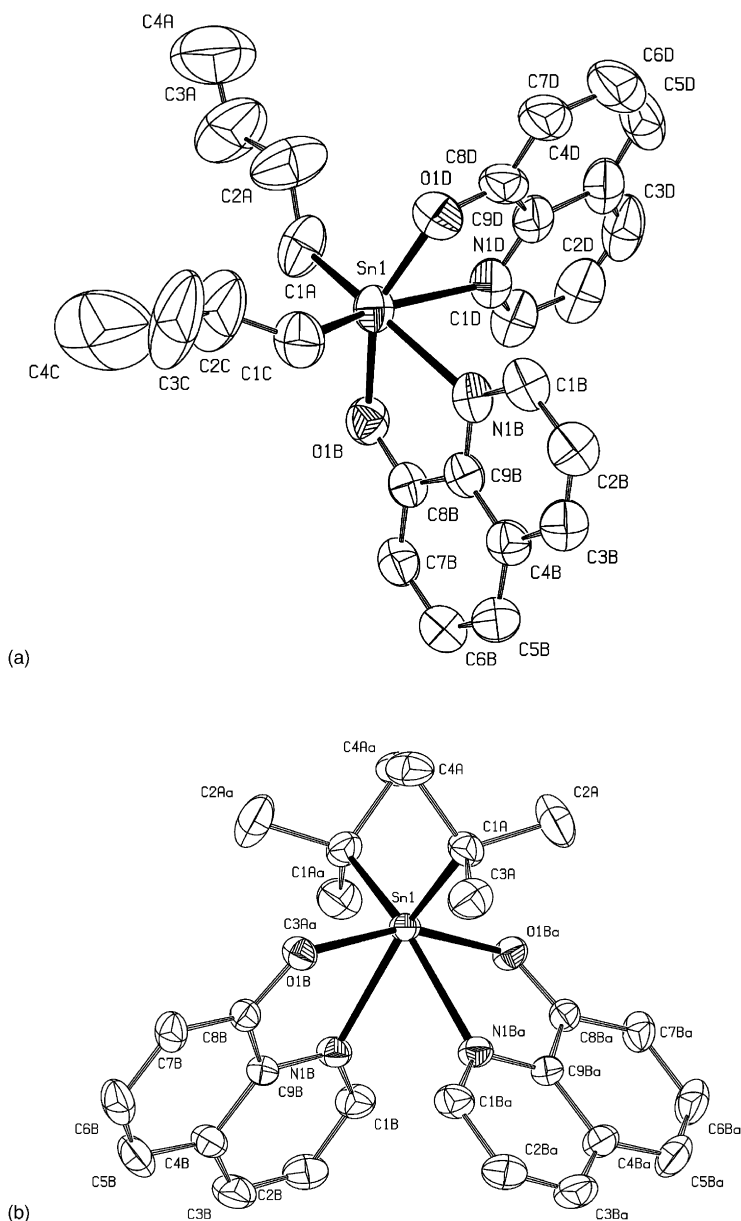


Figure 24 A view of the molecular structures of $\text{Bu}_2\text{Sn}(\text{8-hq})_2$ (a), and $^t\text{Bu}_2\text{Sn}(\text{8-hq})_2$ (b) showing the atom-numbering scheme.³⁶⁴

spectroscopic measurements. In the complexes containing $-\text{OH}$ and $-\text{COO}^-$ functions, the $-\text{COO}^-$ group is coordinated to the organotin(IV) centers in a monodentate or bridging bidentate manner. It was also found that in the hydroxy pyridine and pyrimidine complexes the $[\text{Ph}_3\text{Sn}(\text{IV})]^+$ moiety in most cases reacts

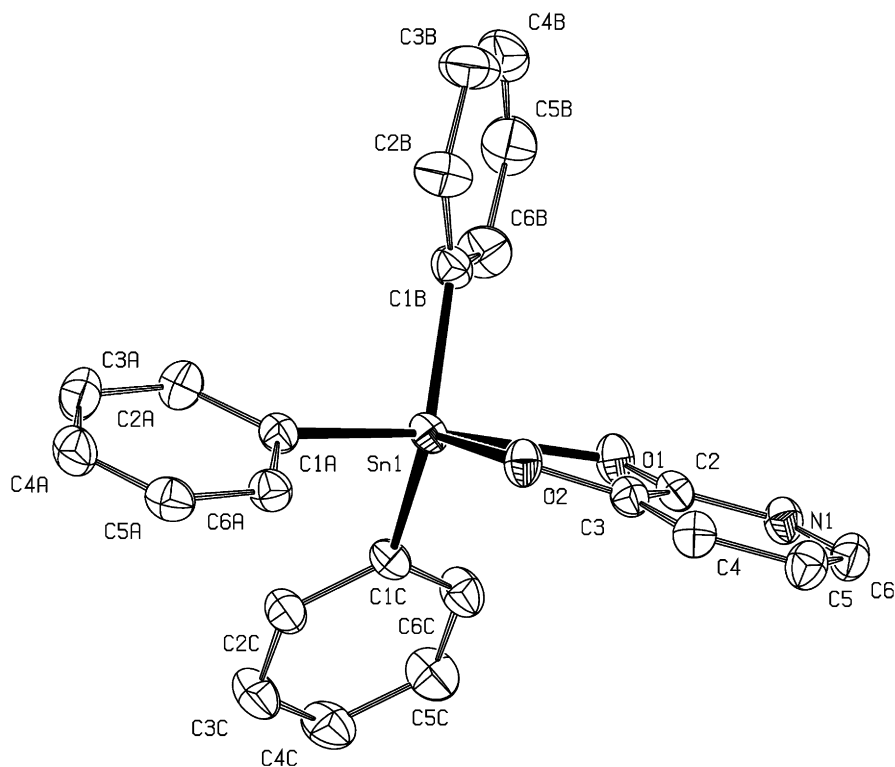


Figure 25 ORTEP diagram of $\text{Ph}_3\text{Sn(IV)}$ -dihydroxypyridine complex.³⁶⁵

with the phenolic form of the ligands. The rationalization of the experimental ^{119}Sn Mössbauer nuclear quadrupole splittings, $|\Delta_{\text{exp}}|$ — according to the point-charge model formalism — together with the FT-IR data, support the formation of Tbp or O_h molecular structures. Furthermore, XRD analysis has been performed on the 2,3-dihydroxypyridine single crystals. The pentacoordinated tin center exhibit a Tbp geometry (Figure 25). In some cases, due to the complexation disproportionation into $[\text{Ph}_2\text{Sn(IV)}]^{2+}$ and $\text{Ph}_4\text{Sn(IV)}$ of the $[\text{Ph}_3\text{Sn(IV)}]^+$ moieties was observed.³⁶⁵

The [2-(dimethylamino)-phenyl] diorganotin(IV) acetates substituted with organophosphorus groups in the α -position of the acetate ligand proved to be monomeric in CDCl_3 solution and in the solid state, with monodentate carboxylate.³⁶⁶ The diorganotin(IV) derivatives of *N*-maleolglycine are hexacoordinated, while the triorganotin(IV) are pentacoordinated in the solid state and T_d in solution. *In vivo* toxicity profiles in mice and antitumor activities in tumor-bearing (colon 26A) mice were obtained. Some of the complexes are active.³⁶⁷

The complexes of four oxime analogs of amino acids (*N*-pyruvoyl amino acid oximes) with Bu_2SnO were prepared. The ligands are coordinated to the tin centers by monodentate $-\text{COO}^-$, and oxime {N} atoms and O_h or Tbp species are formed.³⁶⁸ Similar studies were performed on the MeSn(IV) -SalGly (salicylglycine) system.³⁶⁹

Table 10 Some results of the X-ray diffraction measurements

Compounds	Donor set	Structure	Reference
[Ph ₂ (OH)SnOSnOSn(O ₃ SCF ₃)Ph ₂] ₂	C ₂ O ₃	<i>Tbp</i> (distorted)	356
^t Bu ₂ Sn[4-NC ₅ H ₄ CONN=C(CH ₃)COO]	C ₂ NO ₂	<i>Tbp</i> (distorted)	370
[C ₅ H ₅ NH] ₂ [PhSn(SCH ₂ COO)Cl ₃]	CCl ₃ OS	<i>O_h</i>	380
(4-FC ₆ H ₄ CH ₂) ₃ SnS ₂ -CN(CH ₂ CH ₂)NCH ₃	C ₃ S ₂	<i>Tbp</i> (distorted)	371
(4-FC ₆ H ₄ CH ₂) ₃ SnS ₂ -CNC ₅ H ₁₀	C ₃ S ₂	<i>Tbp</i> (distorted)	372
(4-FC ₆ H ₄ CH ₂) ₃ Sn(Cl)S ₂ -CN(CH ₂ CH ₂) ₂ O	C ₃ S ₂	<i>Tbp</i> (distorted)	373
[Ph ₂ Sn-2-OC ₆ H ₄ CH=NCHCH(CH ₃) ₂ COO]	C ₂ O ₂ N	<i>Tbp</i> (distorted)	374
[Ph ₂ Sn-2-OC ₆ H ₄ C(CH ₃)=NCH ₂ COO]	C ₂ O ₂ N	<i>Tbp</i> (distorted)	375
(PhCH ₂) ₃ Sn(C ₅ H ₃ N ₄ S)Sn(PhCH ₂) ₃ OMe	C ₃ NS, C ₃ NO	<i>Cis-Tbp, trans-Tbp</i>	376
(PhCH ₂) ₂ Sn[S ₂ CN(CH ₂ Ph) ₂] ₂	C ₂ S ₄	<i>O_h</i> (distorted)	377
Ph ₃ SnO ₂ CC ₃ H ₂ NS	C ₃ O	<i>T_h</i> (distorted)	378
(<i>p</i> -C ₆ H ₄ CH ₂) ₂ (S ₂ CNMe) ₂	C ₂ S ₄	<i>O_h</i> (distorted)	379
[C ₅ H ₅ NH] ₂ [PhSn(SCH ₂ COO)Cl ₃]	CCl ₃ OS	<i>O_h</i>	380
MeOCOCH ₂ CH ₂ SnCl ₂ (S ₂ CN(CH ₂ CH ₃) ₂)	CCl ₂ OS ₂	<i>O_h</i> (distorted)	381
CH ₃ OCOCH ₂ CH ₂ SnCl ₂ (S ₂ CN(CH ₃) ₂)	CCl ₂ OS ₂	<i>O_h</i> (distorted)	382
(PhCH ₂) ₂ Sn(phen)CHCl ₃	C ₂ Cl ₂ N ₂	<i>O_h</i> (distorted)	383
(4-Cl-C ₆ H ₄ CH ₂) ₂ Sn[S ₂ CN(CH ₂ CH ₂) ₂ NCH ₃] ₂	C ₂ S ₄	<i>O_h</i> (distorted)	384
(PhCH ₂) ₂ Sn(S ₂ CNC ₅ H ₁₀) ₂	C ₂ S ₄	<i>O_h</i> (distorted)	385
(PhCH ₂) ₂ Sn(S ₂ CNC ₄ H ₈ O) ₂	C ₂ S ₄	<i>O_h</i> (distorted)	386
(2-Cl-C ₆ H ₄ CH ₂) ₂ Sn(ClS ₂ CN(CH ₂ CH ₂) ₂ NCH ₃)	C ₂ ClS ₂	<i>Tbp</i>	387
[(2-Cl-C ₆ H ₄ CH ₂) ₂ Sn(S ₂ CN(CH ₂ CH ₂) ₂ NCH ₃) ₂] ₂	C ₂ S ₄	<i>O_h</i> (distorted)	388
CH ₃ OCOCH ₂ CH ₂ SnCl ₂ [S ₂ COCH(CH ₃) ₂]	CCl ₂ OS ₂	<i>O_h</i> (distorted)	389
Ph ₂ Sn[S ₂ CN(CH ₂) ₅]Cl	C ₂ ClS ₂	<i>Tbp</i>	390
Me ₂ Sn[S ₂ CN(CH ₂) ₅]Cl	C ₂ ClS ₂	<i>Tbp</i>	391

In the recent past a number of complexes were obtained as single crystals. The structures were determined by XRD. Some of the structures and donor sets are collected in Table 10.

E. Some results of biological studies

Organotin(IV) compounds are ecotoxicants whose action depends on their structure. The mechanism of toxic effect of organotin compounds is fairly complicated, and it cannot be regarded as thoroughly studied. It is assumed that these compounds are capable of reacting with cell membranes, finally leading to their decay, accelerating ion exchange processes, and inhibiting oxidative and photochemical phosphorylation. Among R_nSnX_(4-n), (*n* = 1–4) compounds, the most toxic are the R₃SnX.^{392–394}

Organotin(IV) compounds could be involved in other biological processes occurring in cells, specifically in peroxide oxidation of lipids. The latter process is very important from the viewpoint of physiology, and it follows a radical chain mechanism.³⁹⁵

Petrosyan et al.³⁹⁶ studied peroxide oxidation of oleic[(Z)-octadecenoic] acid in the presence of complexes derived from $R_n\text{SnCl}_{4-n}$ and phosphatidylcholine [OP(O)(OH)OCH₂CH₂-N(Me)₃, PChol] which is a short-chain analog of phospholipids, and also compared the effects of the complexes (R₃SnCl)₂-PChol (R = Me, Ph), R₂SnCl₂-PChol (R = Me, Bu), and RSnCl₃-PChol (R = Me, Ph) with that produced by the organotin parents.³⁹⁶

Acceleration of peroxide oxidation of lipids in cells leads to accumulation of hydroperoxides, decay of cell membranes, and various pathologies in living bodies. Insofar as organotin(IV) compounds exhibit electron acceptor properties, it was presumed that their toxicity originates from interaction with electron-donor groups in biomolecules. Reactions of organotin(IV) compounds with phosphorus-containing biomolecules, such as phospholipids, ATP, nucleic acids, etc., were shown to inhibit the synthesis of phospholipids and their intracellular transport, which may be responsible for the antiproliferative activity of organotin(IV) derivatives.^{397,398} It must also be taken into account that organotin(IV) compounds can react with phosphorus-containing fragments of biomolecules in cell membranes to form complexes with dative Sn–O–P bonds. In this case, the mechanism of peroxide oxidation of lipids may change.^{399,400} The health consequences of chronic exposure to low levels of organotin(IV) compounds are unknown, although human and animal studies demonstrate that acute exposures can result in either neurotoxicity or immunotoxicity depending on the specific compound involved. For example, acute human exposure to high doses of trimethyltin(IV) (TMT), due to accidental poisoning, has resulted in memory deficits, seizures, altered emotional affect, hearing loss, disorientation, and death.^{401–404}

1. Biological effects of the parent organotin(IV) compounds

TBT is an agent showing a high toxic effect to aquatic life: even at low (nanomolar) aqueous concentrations it causes chronic and acute poisoning of the most sensitive aquatic organisms, such as algae, zooplankton, mollusks, and the larval stage of some fish.⁴⁰⁵ TBT, used as antifouling agents, is accumulated in aquatic mollusks and it exerts an endocrine-disrupting action on them.⁴⁰⁶ Mollusks, as group, are widely known to exhibit the highest tissue burdens and the highest bioaccumulation factors of TBT among marine organisms. The overall impact of imposex varies among species. In some, such as *Ilyanassa obsoleta*, the imposed male tract does not appear to interfere with the breeding activity nor alter the population ecology of the species. However, in others, such as the muricidae *Nucella lapillus* and *Ocenebra crinacea*, the oviduct structure may become so modified that reproduction is inhibited, resulting in population decline and eventual localized extinctions.^{407,408} Although there has been little evidence of imposex reducing the reproductive capacity in buccinid whelks, imposex has been suggested as a contributing cause to the recent extinction of the common whelk, *Buccinum undatum*, from the Dutch Wadden Sea.⁴⁰⁹ Also the tropical muricidae *Thais distinguenda* develops imposex in a time-dependent manner after transplantation to a TBT contaminated site.⁴¹⁰ The anatomical aberration is

assumed to result from the inhibition by TBT of aromatase cytochrome P450, which catalyzes the aromatization of androgens to estrogens.⁴¹¹

Histone acetylation is important for the regulation of gene expression and is catalyzed by histone acetyltransferase (HAT). Some organotin(IV) compounds — tributyltin (TBT) and triphenyltin (TPT) — enhanced HAT activity of core histones in a dose-dependent way and other endocrine-disrupting chemicals (EDCs) did not affect HAT activity. Organotin(IV) compounds have various influences on physical function including the hormone and immune systems, embryogenesis, and development. Dibutyl- and diphenyltin(IV), metabolites of TBT and TPT, respectively, also promoted HAT activity, but monobutyltin, monophenyltin, and inorganic tin had no effect. Further, TBT and TPT enhanced HAT activity when nucleosomal histones were used as substrates. These data indicate that the organotin(IV) compounds have unique effects on HATs independent of their EDC activities and suggest that the varied toxicities may be caused by aberrant gene expression following altered histone acetylation.⁴¹²

Patricolo et al.⁴¹³ reported endocrine disruption effects of TBT on metamorphosis of ascidian larvae of *Ciona intestinalis*. Triorganotin(IV) compounds appear to inhibit the mitochondrial function in at least three ways: by (1) causing large-scale swelling at high concentrations, (2) mediating Cl[−]/OH[−] exchange across membranes, and (3) inhibiting oxidative phosphorylation or ATP hydrolysis, like oligomycin.⁴¹⁴ The last process is usually assumed to be the most significant one, although binding of [Ph₃Sn(IV)]⁺ to the cell wall was concluded to be responsible for the toxicity of *C. ulmi*.⁴¹⁵ The triorganotin(IV)-mediated anion exchange across the mitochondrial membrane, which is electro-silent, that is, it involves neutral R₃SnX species, may also interfere with ATP synthesis or hydrolysis. Dutch elm disease continues to devastate the diminishing population of American elm trees. The pathogenic fungus responsible for the disease, *C. ulmi* causes a blockage in the vascular tissue, which can lead to the eventual death of the elm. In explorations of the expectation that the incorporation of biologically active entities into a triorganotin(IV) system would lead to the formation of potent biocides,⁴¹⁶ a number of [Ph₃Sn(IV)]⁺ compounds with simple biologically active anionic groups were synthesized and first investigated spectroscopically.⁴¹⁷ The ambiguous spectroscopic data led to further crystallographic investigations on two of the Sn–S bound compounds; these complexes have been shown to be especially active against *C. ulmi*.⁴¹⁸ The results of the studies on the complexes of several [Ph₃Sn(IV)]⁺ carboxylates and of some 1:1 addition compounds of Ph₃SnCl and 2,3-disubstituted thiazolidin-4-ones indicate that the carboxylates in the solid state are monomeric with a T_d {Sn} atom = 2.14–2.54 mm s^{−1} the only exception being the furan-2-carboxylic acid derivative, which is polymeric. The Ph₃SnCl adducts are *Tbp* ($|\Delta_{\text{exp}}|$ = 2.97–3.08 mm s^{−1}) with the three Ph groups in a not coplanar *eq* plane. These complexes are effective inhibitors of *C. ulmi*.⁴¹⁹ The 2,3-disubstituted thiazolidin-4-ones⁴²⁰ are compounds with a wide range of biological activity. Several [Ph₃Sn(IV)]⁺ complexes of these type of ligands have a *Tbp* structure with the three Ph groups in the *eq* plane in noncoplanar positions. These complexes are also effective inhibitors of *C. ulmi*.⁴²¹ Thyroid hormones (THs) are present in ascidian larvae (*Urochordatae*), and their function is related to the control of

metamorphosis. Invertebrates do not have thyroid tissues; nevertheless, some of them possess THs and their precursors.⁴²² Among the invertebrates able to synthesize THs, adult ascidians have phylogenetic importance, as the body plan of their larvae is a basic model of vertebrate morphogenesis.

Ascidians and amphioxys, which are protochordates, together with the ammocoete of the lamprey, a primitive chordate, concentrate iodide and synthesize THs in a subpharyngeal afollicular endostyle. This structure is considered a thyroid homolog. In the larva of the lamprey, the endostyle reorganizes into a follicular thyroid at metamorphosis to the adult, but in protochordates it never transforms into a follicle. A close histological resemblance of the ammocoetes and the protochordates shows the homology of these organs. The endostyle is able to carry out thyroid biosynthesis, and the conclusion is that the characteristic molecules of the thyroid gland are already present in protochordates, the ancestors of vertebrates. Using immunohistochemistry, the presence of tyrosine (T4) in normal larvae of *C. intestinalis* has been localized to mesenchymal cells, many of which will be the future blood cells. It was demonstrated that THs of ascidian larvae are strongly affected by TBT, which not only blocks metamorphosis but also reduces by 70% the amount of the hormone. In vertebrates, EDCs act on thyroid biosynthesis, impairing the production of THs, or blocking hormone-receptor binding. TBT is a compound that can also react directly or indirectly with a hormone in invertebrates, altering its structure or interfering with its biosynthesis; indeed, data indicate that TBT is an ED in ascidians, invertebrates lacking thyroid follicles, which possess, however, THs in larval tissue. This xenobiotic probably alters and destroys almost all T4 molecules present in mesenchymal cells and blocks its neosynthesis. Even in larvae exposed to the lowest TBT concentration used in this study, despite the integrity of all tissues, T4 is found only in a few cells and the content of the hormone is substantially decreased, as independently confirmed by radioimmunological assay RIA even after 3 h of exposure.⁴²²

The negative effects of TBT have been observed in the bivalve larval development of *Crassostrea gigas*,⁴²³ *Mytilus edulis*,⁴²⁴ *Venus gallina*,⁴²⁵ *Sparus aurata*,⁴²⁶ in *Nassarius reticulatus*⁴²⁷ and in the hermaphroditic snails *Physa fontinalis*⁴²⁸ and *Adelomelon brasiliana*.⁴²⁹ Since TBT exerts a variety of toxic actions on some mollusks and fishes⁴³⁰, an adverse effect of TBT on human health is a real threat.⁴³¹

The water pollutant TBT is known to stimulate apoptosis. Induction of apoptosis by TBT has been reported in several species of aquatic organisms such as in the blue mussel *Mytilus galloprovincialis*^{432,433} and in tissues of the marine sponge *Geodia cydonium*.⁴³⁴ It has also been reported that TBT triggers apoptosis in rat hepatocytes⁴³⁵ through a step involving Ca(II) efflux from the endoplasmic reticulum or other intracellular pools and by mechanisms involving cysteine proteases, such as calpains, as well as the phosphorylation status of apoptotic proteins such as Bcl homologs.^{436–438} Orrenius et al.⁴³⁹ hypothesized that in trout hepatocytes the rise in cytosolic Ca(II) level stimulates endogenous endonuclease activity and initiates thymocyte apoptosis. In addition, Chow et al.⁴⁴⁰ invoke a capacitative Ca(II) entry for TBT-induced cell death. Their report shows that the

increase in the cytosolic-free Ca(II) concentration ([Ca(II)]_i) occurs through a three-step mechanism: (i) release of Ca(II) from the intracellular store(s); (ii) inhibition of the Ca(II) extrusion system; and (iii) activation of Ca(II) influx.

Induction of apoptosis has been reported in various mammalian cell lines.^{441,442} In previous studies, it has been reported that TBT induces apoptosis in isolated thymocytes at concentrations which are relevant to those causing thymus atrophy *in vivo*.^{443–446} TBT can also induce apoptosis in PC12 cells, and in human T-lymphoblastoid CEM cells. While the mechanism of TBT-induced apoptosis is still unknown, it has been reported that TBT stimulates thymocyte apoptosis by a mechanism independent of protein synthesis and under conditions where intracellular ATP levels are severely depleted.⁴⁴⁷

Marinovitch et al.⁴⁴⁸ described the events linked to the process in HL-60 promyelocytic cells after triphenyltin chloride treatment: in particular, the increase of intracellular calcium, the alteration of actin polymerization, and the induction of DNA degradation. Cima et al.⁴⁴⁹ revealed apoptosis induced by TBT in hemocytes of the ascidian *Botryllus schlosseri*. The cellular death for apoptosis is an integral part of embryonic development, with organized and regulated biochemical events, as intracellular signal transduction, ordered enzyme cascades, and targeted cell deletion, in response to a variety of stimuli, when various structures are no longer needed and must be removed.⁴⁵⁰ Spontaneous apoptosis in sea urchin larvae of *P. lividus* has been found by Roccheri et al.⁴⁵¹ as a physiological event for the development of the adult.

Recent studies have shown that cysteine and histidine residues are the primary biological ligands for organotin(IV) compounds⁴⁵² and that vicinal dithiols rather than monothiols constitute a general target for organotin(IV).⁴⁵³ Billingsley and coworkers²⁷ have identified a small membrane protein, stannin, containing vicinal dithiols at the membrane interface, which mediates the selective neurotoxic activity of TMT in mammals by triggering neuronal apoptosis in the hippocampus. In fact organotin(IV) possess a high specificity of action as neurotoxins.⁴⁰³ TMT and TET are known to cause damage in the central nervous system. While TMT causes lesions in specific regions of the hippocampus and neocortex, TET damage is localized within the spinal cord.⁴⁵⁴ Interestingly, organotin(IV) compounds have been implicated in their progressive dealkylation in both bacteria and mammals by vicinal cysteine residues.⁴⁵⁵

Aschner and Aschner⁴⁵⁶ suggested that astrocytes may represent an important link in the CNS damage produced by TMT because of evidence of prominently swollen astrocytes without neuronal involvement after *in vivo* exposure. *In vivo* exposure to TMT also produces a transient increase in the specific cell marker glial fibrillary acidic protein (GFAP).⁴⁵⁷ *In vitro* exposure to TMT also disrupts the glutamate transporter associated with astrocytes and stimulate cytokine release from these cells.⁴⁵⁸ DBT has also been shown to be toxic in aggregating brain cell cultures and affecting the myelin content of cholinergic neurons.⁴⁵⁹

The higher molecular weight organotin(IV)s, such as TBT and TPT, are known to be immunotoxic and to cause renal and hepatic damage. TBT at environmentally relevant concentrations increases intracellular concentration of Ca(II) ([Ca(II)]_i) in murine thymocytes by increasing membrane Ca(II) permeability and

releasing Ca(II) from intracellular stores^{440,460} and it induces apoptotic change in plasma membranes.⁴⁶¹

Okada et al.⁴⁶³ examined the effects of TBT on cellular content of glutathione (GSH) in rat thymocytes using a flow cytometer and 5-chloromethylfluorescein diacetate, a fluorescent probe for monitoring the change in the cellular content of GSH. TBT at nanomolar concentrations reduced the cellular content of GSH. There is an important implication on the TBT-induced depletion of cellular GSH since GSH has an important role in protecting the cells against oxidative stress and chemical and metal intoxications. TBT-induced decrease in cellular content of GSH in thymocytes may increase the vulnerability of the immune system.^{460–463}

TBT and TPT are membrane-active molecules, and their mechanism of action appears to be strongly dependent on organotin(IV) lipophilicity.^{464,465} They function as ionophores and produce hemolysis,⁴⁶⁶ release Ca(II) from sarcoplasmic reticulum,⁴⁶⁷ alter phosphatidylserine-induced histamine release,⁴⁶⁸ alter mitochondrial membrane permeability,⁴⁶⁹ and perturb membrane enzymes.^{470,471} Organotin(IV) compounds have been shown to affect cell signaling: they activate protein kinase C⁴⁷² and increase free arachidonic acid through the activation of phospholipase A₂.⁴⁷³

Hydrophobicity of organotin(IV) compounds suggests that their interaction with membranes may play an important role in their toxic mechanism. In this respect, the understanding of the interaction of organotin(IV) compounds with the lipid component of membranes is of considerable interest. Fluorescence polarization measurements suggested that the effect of TBT on liposomal membranes is dependent on the anion moiety.⁴⁷⁴ Studies on the release of liposome bound to organotin(IV) and organolead(IV) compounds indicated that the lipophilicity and polarity of organotin(IV) compounds and the surface potential and environment of the lipid molecules are important factors in their interaction with membranes.⁴⁷⁵ From the study of the interaction of several organotin(IV) compounds (differing in their polar and hydrophobic moieties) with erythrocytes it was concluded that the different effects can result from this effect being more evident in the case of tributyltin(IV) chloride (TBTCl).⁴⁷⁶ In conclusion, organotin(IV) compounds are incorporated into a very important phospholipids of eukaryotic membranes, that is, phosphatidylserine, where they perturb its thermotropic and structural properties.

Organotin(IV) compounds interact in a quantitative different way with phosphatidylserine than with phosphatidylcholine and phosphatidylethanolamine. The evidence supports the hypothesis that organotin(IV) compounds are located in the upper part of the phosphatidylserine palisade. The butyl and phenyl groups intercalate between the initial methylene segments, perturbing their packing and affecting the hydration of the interfacial region.^{477,478} According to the different effects of TBTCl and TPTCl on the fluidity of the acyl chains and the hydration of the interfacial region of phosphatidylserine, it seems that TBTCl is located more deeply in the phospholipid palisade than TPTCl, which is closer to the lipid–water interface. The observed interaction between organotin(IV) compounds and phosphatidylserine promotes physical perturbations,

which could affect membrane function and may mediate some of their toxic effects.⁴⁷⁹

The genotoxic, cytotoxic, and ontogenetic (embryo-larval) or developmental effects of TBT were investigated in various cell lines. Di- and trimethyl-, -butyl and -phenyltin(IV), all as chloride were tested for toxicity toward spindle structure and microtubules in V79 Chinese hamster cells.⁴⁸⁰ All compounds showed a concentration-dependent inhibition of microtubules. An effect on the rate of polymerization was suggested for tributyl- and triphenyltin(IV). The results further indicate that the inhibition of microtubule assembly is through direct interaction with tubulin but does not involve the sulphhydryls of the protein. Thus, the organotin seem to act through two different cooperative mechanisms, inhibition of microtubule assembly and interaction with hydrophobic sites. The latter mechanism might involve Cl⁻/OH⁻ exchange across cellular membranes.

It seems that this anionic exchange would be relevant also to explain interactions of trialkyltin (TAT) compounds (TET, tripropyltin chloride, TBT chloride) with the mitochondria. The current view of this phenomenon is that these compounds, by exploiting the Cl⁻ and OH⁻ gradient in energized mitochondria, behave as electroneutral OH⁻/Cl⁻ exchangers. The crucial point of this new mechanism is that TATs enter the mitochondria as lipophilic cations [R₃Sn(IV)]⁺ and not as electroneutral compounds. The influx is followed by extrusion of the TAT compounds as electroneutral hydroxy compounds R₃SnOH.⁴⁸¹

The embryotoxic effects of both TBT and its degradation products, resulting in altered or blocked embryonic development, have also been observed in the sea urchin *P. lividus*, probably owing to the interference of organotin(IV)s with intracellular calcium homeostasis during skeleton deposition.⁴⁸² The cytotoxic effects of TBTCI, on the neurulation process of the ascidian *C. intestinalis* have been evaluated.⁴⁸³ Exposure of the embryos at early neurula stage in 10⁻⁵ and 10⁻⁷ M TBTCI solutions for 1–2 h provoked the irreversible arrest of their development. Morphological and ultrastructural observations suggested that most probably there are two principal causes determining the neurulation process block. The first is due to the TBT effects of inhibiting the polymerization and/or degradation of microfilaments and microtubules, proteins that constitute the cytoskeleton. The lack of orientation and extension of both microtubules and microfilaments of actin prevent the shape changes and mobility of neural plate blastomeres indispensable to the neurulation process. The second cause is certainly determined by the ultrastructural modification which mitochondria undergo. The ultrastructural anomalies showed by these organelles are so serious as to impede their proper functionality with subsequent inhibition of oxidative phosphorylation and ATP synthesis, remarkable metabolic processes that occur during ascidian neurulation.

Mansueto et al.⁴⁸⁴ suggested that the susceptibility of embryos to toxicants could be first related to their interaction with egg membrane where they could provoke changes of permeability, of transmembrane potential, and of receptors distribution which could in turn drastically interfere with normal cell physiology. Cima et al.⁴⁸⁵ observed that TBT alters, immediately after the entry of

spermatozoon into the cortex of egg, the normal fertilization cytoplasmic movements which are strictly connected to plasma membrane. TBT derivatives alter, also, the intracellular Ca(II) homeostasis through inhibition of the membrane Ca(II) ATPase which activated several processes causing, at first, microfilaments and microtubules disassembly or chromosomal disorders, alteration of cytoplasmic organelles and cell metabolism.⁴⁸⁶

A molecular variation of plasma membrane has been reported by Puccia et al.⁴⁸⁷ Reduction of total lipids (TL) content and significant variations of triglyceride (TG) and phospholipids (PL) fractions were observed as a consequence of exposure of *C. intestinalis* ovaries to TBTCI solutions. In particular, an evident TG decrease and a PL increase were observed, which probably provoked an increment in membrane fluidity, because of the high concentration of long chain fatty acids and, as a consequence, PL. This could be a cell-adaptive standing mechanism toward the pollutants, as observed in *Saccharomyces cerevisiae*. Also the increase in the content of the polyunsaturated fatty acids (PUFA), important in the synthesis of compounds such as prostaglandin which are present in the ovary in a stress situation, was probably a consequence of a defense mechanism to the stress provoked by the presence of TBTCI.

The morphological aspects of *Styela plicata* fertilization after treatment with TBTCI are described by means of scanning SEM and TEM investigations.⁴⁸⁸ Alterations have been shown both on female and male gametes; spermatozoa, all the egg envelopes, and the mitochondria of the egg cortical cytoplasm are modified in relation to incubation time. As a consequence, the damage to gametes blocks sperm-egg interaction and fertilization does not occurs. The ultrastructural aspects of fertilization in *S. plicata* are examined in order to compare the resistance of this species against the pollutant and to extend the study of the fertilization process using SEM. The most relevant alterations, in relation to incubation time, are observed in the follicle cells and the vitelline coat: a few follicle cells are present with a very elongated shape and the vitelline coat is highly damaged until breakage. The vitelline coat shows a different rearrangement: craters, blebs, and holes appear as a new surface organization; also, test cells show signs of degeneration. The mitochondria of the egg cortical cytoplasm start to become damaged after 2 h of incubation in 10^{-5} M TBTCI solution. It is well known that triorganotins can disturb mitochondrial activity, binding to a component of the ATP synthase complex and inhibiting mitochondrial ATP synthesis, and thus disturbing the proton gradient.⁴⁸⁹ It has been suggested that mitochondria serve as mediators of TBT effects and gene-regulatory signaling pathways.⁴⁹⁰

No spermatozoa are seen on the egg surface or on the vitelline coat. After 5 h of treatment with 10^{-5} M TBTCI, a few spermatozoa, with very anomalous heads, have been detected. The absence of spermatozoa on the egg surface or on the vitelline coat could be explained by the absence of the follicle cells, which, in *S. plicata*, primarily play an attracting function.⁴⁹¹ It was previously shown that TBTCI solution, either 10^{-5} or 10^{-7} M, induces anomalies in spermatozoa, unfertilized, and fertilized eggs of *Ascidia malaca*. In particular, the follicle cells detach from eggs and the test cells show anomalies in their nucleus and granules. Moreover, damaged spermatozoa are observed in the vitelline coat, but never in

the egg cortical cytoplasm after incubation for 3 h in 10^{-5} and 10^{-7} M TBTCI. This indicates that fertilization does not occur.⁴⁹²

The reproductive perturbation caused by TBTCI in ascidians resulting in altered functionality or even gametes death, leading to the species being unable to reproduce. As far as the ability of different species to contrast the effects of TBTCI, we can deduce that gametes of *S. plicata* seem to be more resistant than those of *A. malaca*. In fact, in *S. plicata*, a prolonged time of incubation and/or higher concentrations of TBT are necessary to detect the anomalies that prevent the fertilization process. However, in all the cases, fertilization does not occur for at least three reasons: the absence of follicle cells necessary for sperm–egg interaction; the strong anomalies of the vitelline coat, which is considered to be the site of the species-specific binding; and the lack of mobility and alterations of the spermatozoa.^{493,494}

When the antitumor activity of cisplatin was discovered, several research groups started to investigate the possible therapeutic applications of other metal-based, often organometallic, compounds. The organotin(IV) compounds that were first tested were those that were available or easily synthesized, like tri- or diorganotin(IV) halides.

The *in vivo* testing of tetraorganotin(IV) compounds showed that they are inactive, whereas organotin(IV) halides and their complexes with amines and other ligands exhibit borderline activities against P388 or L1210 leukemias.^{235,495–499} The *in vivo* prescreenings against these two leukemias used initially by the National Cancer Institute (NCI) were later replaced by *in vitro* prescreenings against a panel of human tumor cell lines.^{234,500–511} This is also the procedure that was used when organotin(IV) compounds were tested by the Rotterdam Cancer Institute. Seven human tumor cell lines were chosen for the panel that was used: MCF-7 and EVSA-T (two mammary cancers), WiDr (a colon cancer), IGROV (an ovarian cancer), M19 (a melanoma), MEL A498 (a renal cancer), and H226 (a lung cancer).

The main disadvantage of organotin(IV) halides for antitumor testings is that, when they are dissolved in water, the pH of the solution dramatically decreases because the Cl–Sn bonds are converted into water–tin bonds; the formed compounds then lose protons, yielding first organotin(IV) hydroxides that are afterward possibly converted into insoluble bis(triorganotin) oxides or diorganotin(IV) oxides. Because di- or triorganotin(IV) carboxylates do not suffer from the same disadvantage, many series of these compounds were synthesized in order to determine their cytotoxic or antitumor properties. It has been shown that such derivatives, when dissolved in water, remain unaltered for long periods. Several recent reviews and papers have been devoted to the antitumor properties of organotin(IV) compounds.^{15,277,512–515}

2. Biological effects of organotin(IV) complexes

A judicious choice of the ligand coordinated to the organotin(IV) fragment can modulate the activity of the organotin(IV) complexes and minimize its drawbacks. Generally, their mechanism of action is still unknown: some authors proposed that DNA is the probable target for the cytotoxic activity.^{165,193} When DNA undergoes condensation processes, from aqueous solutions, by charge

neutralization of the phosphodiester groups due to addition of cationic species, toroidal structures are detected.⁵¹⁶ DNA condensation is induced also by organotin(IV) derivatives (mono-, di-, triorganotin(IV), salts and complexes).⁵¹⁷

Casini et al. monitored the interactions *in vitro* with DNA of two representative organotin(IV) compounds, the dimer of bis[(dibutyl-3,6-dioxaheptanoato)tin] oxide and tributyltin-3,6,9-trioxodecanoate through various physicochemical techniques.¹⁸⁹ Both investigated organotin(IV)s exhibit strong *in vitro* antitumor activities: the cytotoxic effects were previously analyzed on several tumor cell lines of human origin, MCF-7, EVSA-T, WiDr, IGROV, M19Mel, A498, and H226 and found to be larger than those induced by some classical antitumor drugs. The interactions of these organotin(IV) compounds with DNA were investigated through CD spectroscopy, DNA thermal denaturation analysis, and gel electrophoresis methods. The results suggest that the interaction of organotin(IV) compounds with DNA is not sequence- or diagnostic base-specific and therefore most likely occurs at the level of external phosphate group.

Diorganotin(IV) clinical treatment of certain types of neoplasias placed platinum complexes was reported.⁵¹⁸ Crowe et al.^{519,520} reported the results of the screening of 115 diorganotin(IV) halide in anticarcinogenesis. The most promising development in the field of antitumor-active organotin(IV) compounds has been achieved by the synthesis and testing of organotin(IV) compounds that contain a polyoxaalkyl moiety linked to tin either by a C–Sn or by a C–O bond. Many of these compounds, some of which are very soluble in water, exhibit exceptionally high cytotoxicity against seven human tumor cell lines mentioned above.^{190,521,522} Organotin(IV) complexes of amino acids and their organic derivatives containing the carboxylic O–Sn bond display significant antitumor activity and promising potential in many other fields, like wood preservation, polymer chemistry, pesticidal, bactericidal, and antifouling agents, etc.^{3,523–531} New coordination compounds of some organotin(IV)s with *N*-methylglycine (sarcosine) have been tested for *in vitro* cytotoxic activity against human adenocarcinoma HeLa cells, showing, in some cases, strong activity even at low concentration.⁵³²

Another possibility to constitute a “lead” for a rational development of molecules with antitumor activity, is represented by the organotin(IV)-porphyrin derivatives. In fact, the porphyrin ligands possess all the characteristics of an intercalating agent which, by attachment to the ring of opportune linkers, could selectively bring the organotin(IV) ion on the site where the lesion must be operated. Han and Yang⁵³³ reported the synthesis of organotin(IV)-porphinate based on tris-(4-pyridiniumyl)-porphyrin and tris(*N*-methyl 4-pyridiniumyl)-porphyrin and the activity against P388 and A-549 tumor cell lines and their interactions with DNA. The results show that the antitumor activities of organotin(IV)-porphinate is related to the water solubility of the compounds and the central ion in the porphyrin ring. The interaction between the water-soluble dibutyltin(IV)-porphinate complexes and DNA has been investigated by spectroscopic methods. Electrophoresis test shows that the compound cannot cleave the DNA. According to the electrophoresis test and other results, the cytotoxic activity against P388 and A-549 tumor cells appears not to come from the cleavage of DNA caused by the compounds but from the high affinity of the compounds to DNA.

Bis-[diorganotin(IV)-chloro]-protoporphyrin IX complexes have been investigated and evidence of chromosome damages has been seen in early-developing embryos of *A. physodes* (L.) (Crustacea, Isopoda) following exposure to bis-[dimethyltin(IV)-chloro]protoporphyrin IX.⁵³⁴ The organotin-[*m*-tetra(4-carboxyphenyl)]porphinate, organotin-[*m*-tetra(4-sulfonatophenyl)]porphinate, and diorganotin(IV)chloro protoporphyrin IX derivatives have been tested for their cytotoxicity also toward immortalized mouse cultured embryonic fibroblasts (NIH-3T3) and toward early-developing embryos of *A. physodes* showing that cytotoxicity of the parent organotin(IV) halide may be modulated by using appropriate ligands.^{329,534,535}

Embryos at the two-cell stage were incubated in 10⁻⁵ or 10⁻⁷ M solutions of various compounds. The most toxic among the tested compounds was tributyltin(IV)-[*m*-tetra(4-carboxyphenyl)]porphinate], (Bu₃Sn)₄H₂TPPC, since the fertilized eggs were unable to divide into two cells, even at a concentration of 10⁻⁷ M. This embryonic arrest is correlated with the metabolic pathway. The higher concentration (10⁻⁵ M) reduced the content of ATP, D-glucose (Glu), lipid, protein, and RNA. The cytotoxicity of the (Bu₃Sn)₄H₂TPPC derivative included molecular mechanisms: once the compound migrates inside the cell, it may immediately disrupt the cell metabolism of RNA, proteins, lipids, Glu, and ATP.⁵³⁵

The primary effect seems to be damage to the molecular membrane structure, that is, to the mitochondrial membrane, or cellular membrane, or both. It could be possible that inside the mitochondria, the porphyrin group of (Bu₃Sn)₄H₂TPPC might compete with the porphyrin group of cytochrome and therefore it might damage the H-pump for ATP production.⁵³⁵ In addition, the cytotoxic derivatives diorganotin(IV) and triorganotin(IV)-[*m*-tetra(4-carboxyphenyl)]porphinate], with stoichiometries [R₂Sn(IV)]₄H₂TPPC and [R₃Sn(IV)]₄H₂TPPC [R = Me, Bu, Ph; H₂TPPC⁴⁻ = *m*-tetra(4-carboxyphenyl)]porphinate⁴⁻], namely bis[Me₂Sn(IV)], bis[Bu₂Sn(IV)], bis[Ph₂Sn(IV)], tetra[Me₃Sn(IV)], tetra[Bu₃Sn(IV)], and tetra[Ph₃Sn(IV)] [*m*-tetra(4-carboxyphenyl)]porphinate], have been used to investigate their effects on the cultured human kidney cell-cycle in order to understand further the origin of cell-growth inhibition induced by the above-mentioned chemicals.⁵³⁶

The cell-cycle-dependent DNA content distribution of cultured cells exposed to these compounds has been analyzed through flow cytometry. Cultured human kidney cells have been used as a model system, on the premise of greater physiological similarity to the human situation *in vivo*. The DNA flow histograms represent snapshots of the distribution of nuclei in the various phases of the cell-cycle at the time of fixation. Complexes might synergically interact with DNA, the porphyrin ligand, and the organometallic moieties acting in a concerted fashion and the complex behaving as a pseudo-bifunctional adduct. TBT-PPC is the most toxic of the tested compounds, causing cell death, as indicated by the appearance of a sub-G₁ peak that revealed apoptosis. Pellerito et al.⁵³⁷ showed apoptosis in the sea urchin *P. lividus*, after incubation with four new organotin(IV) chlorin derivatives, [chlorin = chlorin-e₆ = 21H,23H-porphine-2-propanoic acid, 18-carboxy-20-(carboxymethyl)-8-ethenyl-13-ethyl-2,3-dihydro-3,7,12,17-tetramethyl-(2S-*trans*)-]. The results demonstrated that the novel compound (Ph₃Sn)₃chlorin · 2H₂O was the most toxic derivative, by exerting an antimitotic effect very early and by triggering apoptosis in the two-cell stage of sea urchin

embryonic development, as shown by light microscope observations through morphological assays. The apoptotic events in two-cell stage embryos revealed: (i) DNA fragmentation, with the TUNEL reaction (terminal deoxynucleotidyl transferase-mediated dUTP nick end labeling); (ii) phosphatidylserine translocation in the membrane, with Annexin V assay; and (iii) cytoplasm blebbing, with the TUNEL reaction.

Several new organotin(IV) complexes with biologically active ligands have been synthesized and evaluated for cytotoxicity. A number of studies of the triorganotin(IV) compounds, R_3SnX , and diorganotin(IV) compounds, R_2SnXY , indicated that the marked biological activity of the organotins may be due to the transport of either more active species $[R_nSn_{(4-n)}]^+$, $n = 2$ or 3 or the molecule as a whole across the cellular membrane, and the X or XY group influences only the readiness of delivery of the active part $[R_3Sn]^+/[R_2Sn]^{2+}$ into the cell.^{538,539} Furthermore, the studies on structure–activity correlation of organotin(IV) compounds reveal that the biologically active compounds should have coordination positions available at tin and relatively stable ligand–Sn bonds.⁵⁴⁰ These bonds should have low hydrolytic decomposition. The interactions of dibutyltin(IV)–thiaminepyrophosphate (DBTPP) and tributyltin(IV)–thiaminepyrophosphate (TBTPP) complexes with Bluescript KS plasmid and immortalized 3T3 fibroblasts were studied.⁵⁴¹ Both compounds have a clear inhibitory effect on the growth of immortalized mouse embryonal fibroblasts (NIH-3T3), TBTPP being the much more active. No evidence was found, however, for DNA cleavage by the compounds at molar ratios as high as 1:10 (DBTPP, TBTPP/DNA base pairs). The cytotoxicity of TBTPP does not seem to be based on direct interaction with DNA, but in the presence of TBTPP (1:10, TBTPP/DNA bp), plasmid DNA seems to be more susceptible to cleavage by UV.

New organotin(IV) ascorbates of the general formulae $R_3Sn(HAsc)$ (where $R = Me, Pr, Bu,$ and Ph) and $R_2Sn(Asc)$ where $R = Bu$ and Ph) have been synthesized and have been assayed for their anti-inflammatory and cardiovascular activity.⁵⁴² The anti-inflammatory activity of the organotin(IV)–ascorbates is influenced by the nature of ligand environment and organic groups attached to tin. Diorganotin(IV) derivatives have been found to show better activity than the triorganotin(IV) derivatives. The compounds exhibited mild hypotensive activity without affecting the carotid occlusion and noradrenaline response. Such a profile of pharmacological effect is indicative of direct vasodilator action of these compounds.

Biological activity tests on organotin(IV) complexes with a potent anti-hypertensive agent, captopril[(2S)-1-[(2S)-2-methyl-3-sulfanyl propanoyl]pyrrolidine-2-carboxylic acid; cap], were carried toward the embryos of *C. intestinalis*. The main results obtained were as follows:

- (1) The ligand does not affect the embryonic development of *C. intestinalis* significantly.
- (2) $Me_2Sn(cap)$ and $Et_2Sn(cap)$ do not affect the embryonic development; $Bu_2Sn(cap)$ and $tBu_2Sn(cap)$ exert toxic activity on *C. intestinalis* embryos in the early stages of development. This toxicity is concentration-dependent and is related to the lipophilic properties of the complexes.²⁰⁷ Cytotoxic

study on *C. intestinalis* are reported also for organotin complexes with 6-uracilcarboxylic acid (orotic acid = Hor) that plays an important role in pyrimidine biosynthesis in mammalian systems. The compound which exerts the highest cytotoxic effect is Bu₃Sn(H₂or) at 10⁻⁵ M concentration because it blocks embryos development immediately. Me₃Sn(H₂or) at 10⁻⁵ M concentration inhibits cell cleavage in the embryos at the 32-blastomere stage, while Bu₂Sn(Hor) at the same concentration gives rise to abnormal embryos. Me₂Sn(Hor), is less toxic than the trimethyl, dibutyl, and tributyl analogs, since 40% of the total number of treated embryos resulted in normal larvae. The ligand does not affect embryonic development significantly. The results seem to indicate that the chemical species under investigation, especially Bu₃Sn(H₂or), interfere with polymerization of tubulin during the process of cell division in early embryo development.³³¹

Due to the extensive use as pesticides and fungicides, large amounts of organotin(IV) compounds have been introduced into various ecosystems. The current emphasis for chemists is on the production of novel types of pesticide that prevent insect, bacteria, or fungi resistance, and that are environmentally friendly. It has been well established that dithiocarbamates are a group of compounds that are active against fungi and insects.^{392,543,544} A series of triorganotin(IV) dithiocarbamates R₃SnS₂CNR'₂ (R = Cy, Ph; NR'₂ = NEt₂, N(Bu)₂, N(ⁱBu)₂, N(Pr)₂, N(CH₂)₅, NH(Pr), NH(Bu), NH(ⁱBu)) has been synthesized and their insecticidal activities were screened against the second larval instar of the *Anopheles stephensi* Liston and *Aedes aegypti* (L.) mosquitoes that are vectors of human malaria and yellow fever. Results from the screening studies indicated that triorganotin(IV) dithiocarbamates are effective larvicides against both species of larvae.⁵⁴⁵

Organotin(IV) complexes with isatin and *N*-alkylisatin bithiocarbonohidrazones are active against Gram-positive bacteria at concentrations ranging from 0.7 to 50 ng/cm³. None of the tested compounds possess inhibitory properties against fungi up to concentration of 100 ng/cm³. Butyl complexes are detected as broad-spectrum compounds, in fact they inhibit the growth also of *P. vulgaris* and *S. typhimurium* Gram-negative bacteria. It must be noted that, in several cases, their growth-inhibitory effect is better than that of the free ligands. These compounds were tested for mutagenicity in the *Salmonella*-microsome test. Structural factors, including steric and electronic constraints imposed by the organometallic moieties, may be responsible for the absence of activity.⁵⁴⁶

Novák et al. prepared new organotin(IV) compounds containing a {C, N} chelating ligand. These substances represent new types of compound containing a bulky substituent instead of the halogen atom. The *in vitro* antifungal activity of the compounds studied was comparable to similar organotin(IV) compounds and antifungal drugs in clinical use.⁵⁴⁷ Moreover, it was reported that the organotin(IV) steroidcarboxylates are potent and possess *in vitro* cytotoxicity against bacteria and fungi.⁵⁴⁸

Tributyltin(IV) derivatives of six different pharmaceutically active carboxylates were synthesized and their antibacterial activities were tested using 10 different bacteria (*B. cereus*, *C. diphtheria*, *E. C. ETEC*, *K. pneumonia*, *P. mirabilis*, *P. aeruginosa*,

S. typhi, *S. boydii*, *S. aureus*, *S. pyogenes*) relative to the reference drugs ampicillin and cephalixin.⁵⁴⁹ Apparently, the function of the ligand is to support the transport of the active organotin(IV) moiety to the site of action where it is released by hydrolysis. The biocidal activity of triorganotin(IV) carboxylates is also related to their structure; species generating a T_d structure in solution are more active.⁵³³ Due to the emergence of bacterial resistance toward many of the commonly prescribed antibiotics, the development of new antibiotics is urgent.

Many peptide antibiotics have novel structural motifs, such as cyclic structures and are often further modified, (such as in β -lactamic antibiotics) and conjugated with sugars, lipids, and other molecules.

In this perspective, Pellerito et al.³²⁵ designed new complexes of diorganotin(IV) and triorganotin(IV) with peptide antibiotics. It was expected that antibiotic properties of chemiotherapeutic agents may give better properties to organotin(IV) complexes if peptide antibiotics are used as ligands. The fertilized eggs of *C. intestinalis* and *A. malaca* in the 10^{-4} mol dm $^{-3}$ solutions of organotin(IV) chloramphenicol and D-cycloserine derivatives, or incubated 30 min after fertilization, did not cleave into the blastomeres. If they were incubated at the two-cell stage, in the 10^{-4} mol dm $^{-3}$ solutions of organotin(IV) chloramphenicol, and D-cycloserine derivatives, development stopped and the cytoplasm of two blastomeres was fragmented into several parts that often could refuse. The fertilized eggs incubated in 10^{-5} mol dm $^{-3}$ solutions of organotin(IV) chloramphenicol and D-cycloserine derivatives developed into anomalous larvae. They were inside the membrane with an open neural plate lacking sensorial organs and a very short tail. Eggs and embryos incubated for 1 h in 10^{-4} mol dm $^{-3}$ Me $_2$ Sn(chloramph) $_2$ and then transferred into normal seawater originated larvae as the controls, but slightly delayed; those incubated in Me $_2$ Sn(cyclos) $_2$ blocked at the two-cell stage with an anomalous disposition of blastomeres.³²⁶ Penicillins are a very important class of β -lactamic antibiotics used in therapy because of their specific toxicity toward bacteria. From a coordination chemistry perspective it has been demonstrated that all the β -lactamic antibiotics possess a number of potential donor sites and they are known to interact effectively with several metal ions and organometallic moieties, originating complexes.^{550,551}

The cytotoxic activity of dialkyl- and trialkyltin(IV) complexes of the deacetoxy-cephalosporin-antibiotic, cephalixin [7-(D-2-amino-2-phenylacetamido)-3-methyl-3-cephem-4-carboxylic acid (= Hceph)] as well as triorganotin(IV) complexes of 6-[D-(2)-b-amino-*p*-hydroxyphenyl-acetamido]penicillin (5-amoxicillin) and 6-[D-(2)-a-aminobenzyl]penicillin (5-ampicillin) has been tested using two different chromosome-staining techniques Giemsa and CMA3, toward spermatocyte chromosomes of the mussel *Brachidontes pharaonis* (Mollusca: Bivalvia). Colchicized-like mitoses (c-mitoses) on slides obtained from animals exposed to organotin(IV) cephalixinate, amoxicillinate, and ampicillinate compounds, demonstrated the high-mitotic spindle-inhibiting potentiality of these chemicals. Moreover, structural damages such as "chromosome achromatic lesions," "chromosome breakages," and "chromosome fragments" have been identified through a comparative analysis of spermatocyte chromosomes from untreated specimens (negative controls) and specimens treated with the organotin(IV) complexes.^{552,553}

The multidrug resistance (mdr) reversing effect of the new phenothiazine complexes were tested on mouse T cell lymphoma cell lines. Trifluoperazine (TFP) was much more effective at the same concentration than verapamil. The efficacy of some metal coordination complexes [TFP–Cu(II) and TFP–V(IV)] exceeded the action of TFP alone. Chlorpromazine (CPZ) or CPZ–Pt(II) complex had the same or less effect than verapamil or promethazine (Pz) used as a control.

We propose that the compounds mentioned above can form a complex with the regulatory protein or DNA resulting in the inhibition of induction (SOS response). These complexes inhibit the mdr efflux pump by inactivating the P-glycoprotein. We conclude that our data can be exploited in the molecular design of drugs against SOS-related biological function. The results show some interaction between the phenothiazine metal coordination complexes and DNA. The increased melting temperatures of DNA in the presence of metal coordination complexes indicates an interaction with DNA and stabilization of the helix. CPZ and TFP can be seen to stabilize the DNA helix by intercalation causing a slight increase in the thermal denaturation temperature. A similar effect was seen with the TFP–Me₂Sn(IV), the CPZ–Me₂Sn(IV), and the TFP–Cu(II) coordination complexes indicating an interaction with the DNA helix, while metal ions alone showed no significant stabilization of the helix. The chlorides of Pt, Pd, and V degraded the DNA resulting in a linear thermal stability profile. The coordination complexes of these metals with CPZ and TFP however decreased the thermal stability of DNA indicating a destabilization of the DNA helix by weakening the hydrogen bonding between the base pairs. The phenothiazines appear to be exerting a protective effect, protecting the DNA against total degradation caused by the metal ions alone.⁵⁵⁴

V. APPLICATIONS

Organotin(IV) compounds have a range of pharmacological applications. The use of organotin(IV) halides as anti-inflammatory agents against different types of edema in mice is of fundamental interest.^{555,556} Compounds such as Bu₂SnCl₂ or Ph₃SnCl can inhibit edema as effectively as hydrocortisones. Organotin(IV) complexes with Schiff bases are of potential use as amoebicidal agents, displaying activity against axenically grown *Entamoeba histolytica* and *tropozoites*.⁵⁵⁷

Another pharmaceutical application of organotin(IV) complexes is in the chemotherapy of leishmaniasis, a parasitic infection of the skin, where [Oct₂Sn(IV)]²⁺ maleate has shown promisingly high activity.⁵⁵⁸ The [Bu₂Sn(IV)]²⁺ dilaurate, distearate, diolate, phenylethyl acetate, and dipalmitate act as antihelminthic agents in cats suffering from dipylidiosis.

Hyperbilirubinaemia is an abnormality observed mainly in neonates in whom the liver is insufficiently developed to be able to detoxify the bile pigment bilirubin. This situation is known as neonatal jaundice and can sometimes become a serious disease causing neurotoxic symptoms. Bilirubin is produced by the degradation of heme [the Fe(II) complex of protoporphyrin IX] by heme oxygenase to give biliverdin, which is reduced by biliverdin reductase to

Table 11 Antitumor activities of organotin(IV) compounds against two types of leukemia cell lines

Structure	Number of the compounds studied	P338	P338 active (%)	L1210	L1210 active (%)
Altogether	1554	680	25	696	1.0
R ₄ Sn	339	166	2	144	0.4
R ₃ SnX	358	132	9	203	0.0
R ₂ SnX ₂	327	129	48	136	1.0
RSnX ₃	33	11	9	11	0.0
SnX ₄	45	15	7	10	0.0
R ₂ SnX ₃ , R ₂ SnX ₄	160	143	50	35	0.0

Adapted from Ref. (1).

bilirubin. The Sn–heme complex [dichloro(protoporphyrin IX)tin(IV)] is a potential inhibitor of hemoxidase (see e.g., Refs. 559–563). Hyperbilirubinaemia is also a symptom of other diseases such as congenital anemia, thalassemia, and liver abnormalities. Sn–heme has been tested in animals⁵⁶¹ and humans^{564,565} and has been found successful in suppressing formation of the toxic metabolite bilirubin and in curing neonatal jaundice. In extensive toxicological studies on neonates (human or animal) and adults, Sn–heme proved to be essentially innocuous. Pharmacological studies of this therapeutic agent are in progress.

In recent years, the most active bioinorganic chemistry research area concerning organotin(IV) compounds is the investigation of their antitumor activity. It has been established that the [R₂Sn(IV)]²⁺ compounds which exhibit maximum antitumor activity combined with low mammalian toxicity are adducts of the type R₂SnX₂L₂ (X = halogen, pseudohalogen, L = O- or N-donor ligand). Some results are presented in Table 11. A large number of compounds have now been screened against a variety of tumor cell lines, and several reviews have been published as shown above.

Attempts to improve the bioavailability of the organotin(IV) cations by the formation of water-soluble complexes⁵⁶⁶ or by their inclusion into β -cyclodextrin⁵⁶⁷ have also been reported. In spite of their widespread activity, these antitumor organotin(IV) complexes have not yet been subjected to extensive clinical trials in humans.

Organotin(IV) complexes are also used in agriculture. They are efficient fungicides and bactericides. Six triorganotin(IV) compounds are currently marketed. Although these complexes have broad-spectrum activity, in practice their usage is restricted to a limited area. Unfortunately, the high phytotoxicity⁵⁶⁸ of these compounds toward many plants has restricted their practical use. Organotin(IV) compounds are also powerful insecticides, but since the most effective compounds contains the mammalian-toxic [Me₃(IV)]⁺, this property has not been commercialized. The fungicidal properties of [Bu₃Sn(IV)]⁺ compounds have been utilized through their application as wood preservatives since the early 1950s.^{569,570} The details of the action are not well understood and are still under discussion. Some comments on this subject have been made in Section IV.B of this chapter. A complete listing of reports on the evaluation of organotin(IV) chemicals in agriculture is to be found in the two-part review by Crowe.^{5,6}

Marine fouling is the attachment of marine species (animals, plants, etc.) to the surface of immersed structures, mainly ships, hulls, buoys, sonar equipment, or seawater conduits, for example, cooling pipes. The fouling of ships can lead to inefficient travel through the water because of drag, with dramatic increases in fuel consumption. The development of organotin(IV)-based antifouling systems dates back to the early 1960s. The compounds employed for this purpose are usually Ph_3SnX ($\text{X} = \text{OH}^-$, F^- , Cl^- , ^-OAc), Bu_3SnX ($\text{X} = \text{F}^-$, Cl^-), and $(\text{Bu}_3\text{Sn})_2\text{O}$, although many other systems have been developed.^{354,355} It is important that the working life-time of such systems is typically 1–2 years before repainting becomes necessary. Organotin(IV)-based antifouling paints are ca. 10 times more effective than the formerly used conventional Cu_2O -based paints.

Despite the widespread use of organotin(IV)-based antifouling paints, in recent years there has been increasing concern regarding the impact of these chemicals on the environment. Particular concern has been expressed as concerns the effect of aqueous $[\text{Bu}_3\text{Sn}(\text{IV})]^+$ on oyster farming. This topic has been reviewed by Tsangaris et al.⁴

VI. CONCLUSIONS

This survey of the literature data on the interactions of organotin(IV) cations with biologically active ligands demonstrates that this is still a very open field. Above all, it is necessary to emphasize that usage of such complexes to treat humans is not permitted at present. Consequently, all compounds examined and discussed here (although with promising anticancer activity) are in the exploratory research stage.

Equilibrium data on different systems are largely missing. Systematic studies must be undertaken to understand the species distribution in the systems studied or in the environment.

The use of sophisticated experimental methods (e.g., EXAFS, mass spectrometry) or developments in the already used and widespread methods (multi-nuclear ^1H , ^{13}C , and ^{119}Sn , NMR spectroscopy in solution or in the solid state), will greatly accelerate progress. The comparison of solid *versus* solution structures is also needed. The effects of drugs are exerted in biological (mainly in aqueous) systems, and consequently the development of carriers of organotin(IV) cations with relatively high water solubility is at the forefront of recent research. The mode of biological action of organotin(IV) complexes, or even the parent organotin(IV) compounds, has not yet been completely clarified and may vary from one compound to another.

Finally, more and more experimental data must be collected in order to understand the biological (including antitumor) activity of organotin(IV) complexes.^{363,364}

ABBREVIATIONS

5'-AMP	adenosine-5'-monophosphate
5'-ATP	adenosine-5'-triphosphate
<i>ax</i>	axial position in the geometry
cap	captopril <i>N</i> -[(<i>S</i>)-3-mercapto-2-methylpropionyl]-L-proline

CMC	carboxymethyl cellulose
CPZ	chlorpromazine
cupf	<i>N</i> -nitroso- <i>N</i> -phenylhydroxylaminato (PhN_2O_2^-)
<i>eq</i>	equatorial position in the geometry
G-6P	D-glucose-6-phosphate
G-1P	D-glucose-1-phosphate.
GalA	D-galacturonic acid
Glu	D-glucose
GlucA	D-glucuronic acid
GlupA	D-glucopyranosiduronic acid
Gly-Gly	glycyl-glycine
Gly-His	glycyl-histidine
ICP-AES	ion plasma coupled atomic emission spectrometry
NADP	β -nicotinamide-adenine-dinucleotide-phosphoric acid
<i>N</i> -Ac-Gly	<i>N</i> -acetyl-glycine
O_h	octahedral
PHTAc	2-polyhydroxyalkylthiazolidine-4-carboxylic acid
pqs	partial quadrupole splitting
PBP	pentagonal bipyramidal
<i>r</i>	bond distance
R-5P	D-ribose-5-phosphate
Rib	D-ribose
rutin	{3-[6- <i>O</i> -(6-deoxy- α -L-mannopyranosyl)-(β -D-glucopyranosyl)oxy]-2-(3,4-dihydroxyphenyl)-5,7-dihydroxy-4H-1-benzopyran-4-one}
Sal-Gly	salicyl-glycine
S-Me-Cys	S-methyl-cystein
<i>Tbp</i>	trigonal bipyramidal
TBTCl	tributyltin(IV) chloride
TEM	transmission electron microscopy
TFP	trifluoperazine
T_d	tetrahedral
XAFS	X-ray absorption fine structure
XANES	X-ray absorption near-edge structure
δ	Mössbauer isomer shift
Δ	Mössbauer quadrupole splitting
σ	EXAFS Debye-Waller factor

ACKNOWLEDGMENTS

This work was supported financially by the Hungarian Research Foundation (OTKA T043551) and by the Università di Palermo, (ORPA 06K3RK and ORPA 062ELE), Italy.

REFERENCES

- (1) Saxena, A. K.; Huber, F. *Coord. Chem. Rev.* **1989**, 95, 109.
- (2) Holloway, C. E.; Melnik, M. *Main Group Met. Chem.* **1998**, 21, 371.

- (3) Molloy, K. C. In: Hartley, F. R. (Ed.), *The Chemistry of Metal-Carbon Bond: Bioorganotin Compounds*, Wiley, New York, **1989**; Vol. 5, p. 465.
- (4) Tsangaris, J. M.; Williams, D. R. *Appl. Organomet. Chem.* **1992**, 6, 3.
- (5) Crowe, A. J. *Appl. Organomet. Chem.* **1987**, 1, 143.
- (6) Crowe, A. J. *Appl. Organomet. Chem.* **1987**, 1, 331.
- (7) David, S.; Hanessian, S. *Tetrahedron* **1985**, 41, 643.
- (8) Patel, A.; Poller, R. C. *Rev. Sil. Ger. Tin Lead Comp.* **1985**, 8, 263.
- (9) Grindley, T. B. *Adv. Carbohydr. Chem. Biochem.* **1998**, 53, 17.
- (10) Burger, K.; Nagy, L. Metal complexes of carbohydrates and sugar-type ligands, In: Burger, K. (Ed.), *Biocoordination Chemistry*, Chichester, Ellis Horwood, **1990**; Chapter VI, p. 236.
- (11) Gyurcsik, B.; Nagy, L. *Coord. Chem. Rev.* **2000**, 203, 81.
- (12) Verchère, J.-F.; Chapelle, S.; Xin, F.; Crans, D. C. *Prog. Inorg. Chem.* **1998**, 47, 837.
- (13) Nagy, L. *A kémia újabb eredményei, 91 kötet*, **2002**, Akadémiai Kiadó, Budapest; *Novel Results in Chemistry*, **2002**; Vol. 91, Academic Press, Budapest, p. 1.
- (14) Barbieri, R.; Pellerito, L.; Ruisi, G.; Silvestri, A.; Barbieri-Paulsen, A.; Barone, G.; Posante, S.; Rossi, M. ¹¹⁹Sn Mössbauer spectroscopy studies on the interaction of organotin(IV) salts and complexes with biological systems and molecules, In: Gianguzza, A.; Pelizzetti, E.; Sammartano, S. (Eds.), *Chemical Processes in Marine Environments*, Springer Verlag, Berlin, **2000**; Chapter 12, p. 229.
- (15) Gielen, M. *Appl. Organomet. Chem.* **2002**, 16, 481.
- (16) Nath, M.; Pokharia, S.; Yadav, R. *Coord. Chem. Rev.* **2001**, 215, 99.
- (17) Pellerito, L.; Nagy, L. *Coord. Chem. Rev.* **2002**, 224, 111.
- (18) Galbács, G.; Szorcik, A.; Galbács, A. Z.; Buzás, N.; Haraszti, T. *Talanta* **2000**, 52, 1061.
- (19) Wertheim, G. K. *Mössbauer Effect, Principles and Applications*, Academic Press, New York, **1964**.
- (20) Nagy, L.; Yamaguchi, T.; Yoshida, K. *Struct. Chem.* **2003**, 14, 77.
- (21) Nagy, L. *Theoretical Background of EXAFS and XANES Spectroscopies. Application in Inorganic and in Bioinorganic Chemistry. Novel Results in Chemistry*, Akadémiai Kiadó, Budapest, **1999**; p. 63.
- (22) Eastman, A.; Barry, M. A. *Cancer Invest.* **1992**, 10, 229.
- (23) Wyllie, A. H.; Kerr, J. F. R.; Cumi, A. R. *Int. Rev. Cytol.* **1980**, 68, 251.
- (24) Majno, G.; Joris, I. *Am. J. Pathol.* **1995**, 146, 3.
- (25) Wyllie, A. H. *Nature* **1981**, 284, 555.
- (26) Shapiro, H. M. *Practical Flow Cytometry*, Wiley, New York, **1995**; p. 409.
- (27) Thompson, T. A.; Lewis, J. M.; Dejneka, N. S.; Severs, W. B.; Polavarapu, R.; Billingsley, M. L. *J. Pharmacol. Exp. Ther.* **1996**, 276, 1201.
- (28) Ashkenazi, A.; Dixit, V. M. *Science* **1998**, 281, 1305.
- (29) Green, D. R.; Reed, J. C. *Science* **1998**, 281, 1309.
- (30) Earnshaw, W. C.; Martins, L. M.; Kaufmann, S. H. *Annu. Rev. Biochem.* **1999**, 68, 383.
- (31) Fulda, S.; Debatin, K. M. *Curr. Med. Chem. Anticancer Agents* **2003**, 3, 253.
- (32) Schneider, W. C. *J. Biol. Chem.* **1946**, 164, 747.
- (33) Dische, E.; Schawrz, K. *Mickrochim. Acta* **1937**, 2, 138.
- (34) Brown, A. H. *Arch. Biochem.* **1946**, 11, 269.
- (35) Marsh, J. B.; Weinstein, D. B. *J. Lipid Res.* **1966**, 7, 574.
- (36) Lory, J. *J. Biol. Chem.* **1951**, 193, 265.
- (37) Tobias, R. S.; Farrer, H. N.; Hughes, M. B.; Nevett, B. A. *Inorg. Chem.* **1966**, 5, 2052.
- (38) Tobias, R. S. *Organomet. Chem. Rev.* **1966**, 1, 93.
- (39) Buzás, N.; Gajda, T.; Nagy, L.; Kuzmann, E.; Vértés, A.; Burger, K. *Inorg. Chim. Acta* **1998**, 274, 167.
- (40) Natsume, T.; Aizawa, S. I.; Hatano, K.; Funahashi, H. *J. Chem. Soc., Dalton Trans.* **1994**, 2749.
- (41) Arena, G.; Purrello, R.; Rizzarelli, E.; Gianguzza, A.; Pellerito, L. *J. Chem. Soc., Dalton Trans.* **1989**, 773.
- (42) Tobias, R. S.; Yasuda, M. *Can. J. Chem.* **1964**, 42, 781.
- (43) De Stefano, C.; Foti, C.; Gianguzza, A.; Martino, M.; Pellerito, L.; Sammartano, S. *J. Chem. Eng. Data* **1996**, 41, 511.
- (44) Gharib, F.; Amini, M. M.; Haghgou, A. *Main Group Met. Chem.* **2003**, 26, 381.

- (45) Arakawa, Y.; Wada, Y. In: Sigel, H.; Siegel, A. (Eds.), *Metal Ions in Biological Systems: Biological Properties of Alkyltin(IV) Compounds*, Marcel Dekker, Inc., New York, **1993**; Vol. 29, p. 101.
- (46) Thayer, J. S. In: Sigel, H.; Siegel, A. (Eds.), *Metal Ions in Biological Systems: Global Bioalkylation of the Heavy Elements*, Marcel Dekker, Inc., New York, **1993**; Vol. 29, p. 1.
- (47) Hynes, M. J.; Keely, J. M.; McManus, J. J. *Chem. Soc., Dalton Trans.* **1991**, 3427.
- (48) Asso, M.; Carpeni, G. *Can. J. Chem.* **1968**, 46, 1795.
- (49) Hynes, M. J.; O'Dowd, M. J. *Chem. Soc., Dalton Trans.* **1987**, 563.
- (50) Cannizzaro, V.; Foti, C.; Gianguzza, A.; Marrone, F. *Ann. Chim.* **1998**, 88, 45.
- (51) Foti, C.; Gianguzza, A.; Milea, D.; Millero, F. J.; Sammartano, A. *Mar. Chem.* **2004**, 85, 157.
- (52) Barbieri, R.; Silvestri, A. *J. Inorg. Biochem.* **1991**, 41, 31.
- (53) Barbieri, R.; Silvestri, A.; Giuliani, A. M.; Piro, V. S.; Madonia, G. *J. Chem. Soc., Dalton Trans.* **1992**, 85.
- (54) Surdy, P.; Rubini, P.; Buzás, N.; Henry, B.; Pellerito, L.; Gajda, T. *Inorg. Chem.* **1999**, 38, 346.
- (55) Gajda-Schrantz, K.; Nagy, L.; Gajda, T.; Fiore, T.; Pellerito, L. *J. Chem. Soc., Dalton Trans.* **2002**, 152.
- (56) Lockhart, T. P.; Manders, W. F. *Inorg. Chem.* **1986**, 25, 892.
- (57) Barbieri, R.; Musmeci, M. T. *J. Inorg. Biochem.* **1988**, 32, 89.
- (58) Domingos, A. M.; Sheldrick, G. M. *J. Chem. Soc., Dalton Trans.* **1974**, 475.
- (59) Gielen, M.; Sprecher, N. *Organomet. Chem. Rev.* **1966**, 1, 455.
- (60) Kriegsmann, H.; Pauly, S. Z. *Anorg. Allg. Chem.* **1964**, 330, 275.
- (61) Farrer, H. N.; McGrady, M. M.; Tobias, R. S. *J. Am. Chem. Soc.* **1965**, 20, 5019.
- (62) Van den Bergue, E. V.; Van der Kelen, G. P. *Bull. Soc. Chim. Belg.* **1965**, 74, 479.
- (63) Cassol, A.; Magon, L.; Barbieri, R. *J. Chromatogr.* **1965**, 19, 57.
- (64) Cassol, A. *Gazz. Chim. Ital.* **1966**, 96, 1764.
- (65) Luijten, J. O. G. A. *Recueil* **1966**, 85, 873.
- (66) Devaud, M. *J. Chim. Phys.* **1969**, 66, 302.
- (67) Devaud, M. *J. Chim. Phys.* **1970**, 67, 302.
- (68) Devaud, M. *J. Chim. Phys.* **1972**, 69, 460.
- (69) Langlois, M. C.; Devaud, M. *Bull. Soc. Chim. Fr.* **1974**, 5/6, 789.
- (70) Blunden, S. J.; Smith, P. J.; Gillies, D. G. *Inorg. Chim. Acta* **1982**, 60, 105.
- (71) Blunden, S. J.; Hill, R. *Inorg. Chim. Acta* **1990**, 177, 219.
- (72) De Stefano, C.; Foti, C.; Gianguzza, A.; Marrone, F.; Sammartano, S. *Appl. Organomet. Chem.* **1999**, 13, 805.
- (73) Hynes, M. J.; O'Dowd, M. J. *Biochem. Soc. Trans.* **1985**, 13, 490.
- (74) Domazeteis, G.; MacKay, M. F.; Magee, R. J.; Jones, D. B. *Inorg. Chim. Acta* **1979**, 34, L247.
- (75) Buzás, N.; Gajda, T.; Kuzmann, E.; Nagy, L.; Vértes, A.; Burger, K. *Main Group Met. Chem.* **1995**, 18, 641.
- (76) Arena, G.; Gianguzza, A.; Pellerito, L.; Musumeci, S.; Purrello, R.; Rizzarelli, E. *J. Chem. Soc., Dalton Trans.* **1990**, 2603.
- (77) Arena, G.; Cali, R.; Contino, A.; Musumeci, A.; Musumeci, S.; Purello, R. *Inorg. Chim. Acta* **1995**, 237, 187.
- (78) Buzás, N.; Gyurcsik, B.; Nagy, L.; Zhang, Y. X.; Korecz, L.; Burger, K. *Inorg. Chim. Acta* **1994**, 218, 65.
- (79) Gyurcsik, B.; Buzás, N.; Gajda, T.; Nagy, L.; Kuzmann, E.; Vértes, A.; Burger, K. *Z. Naturforsch.* **1995**, 50B, 515.
- (80) Sing, K. H. A.; Sing, G.; Gupta, V. D. *Indian J. Chem., Sect. A* **1988**, 27, 264.
- (81) Mohamed, M. M. A. *J. Coord. Chem.* **2003**, 56, 745.
- (82) Chasapis, C. T.; Hadjikakou, S. K.; Garoufis, A.; Hadjiliadis, N.; Bakas, T.; Kubicki, M.; Ming, Y. *Bioinorg. Chem. Appl.* **2004**, 2, 43.
- (83) Roge, G.; Huber, F.; Preut, H.; Silvestri, A.; Barbieri, R. *J. Chem. Soc., Dalton Trans.* **1983**, 595.
- (84) Ho, B. Y. K.; Zuckerman, J. J. *Inorg. Chem.* **1973**, 12, 1552.
- (85) Hall, W. T.; Zuckerman, J. J. *Inorg. Chem.* **1977**, 16, 1239.
- (86) Ho, B. Y. K.; Molloy, K. C.; Zuckerman, J. J.; Reidinger, F.; Zubieta, J. A. *J. Organomet. Chem.* **1985**, 187, 211.
- (87) Roge, G.; Huber, F.; Preut, H.; Silvestri, A.; Barbieri, R. *Congr. Naz. Chim. Inorg. [ATTI]* **1982**, 15, 241.

- (88) Roge, G.; Huber, F.; Silvestri, A.; Barbieri, R. Z. *Naturforsch. Teil B* **1982**, 37, 1456.
- (89) Huber, F.; Roge, G.; Barbieri, R.; Di Bianca, F. J. *Organomet. Chem.* **1982**, 233, 185.
- (90) Huber, F.; Roge, G.; Carl, G.; Atassi, G.; Spreafico, F.; Filippeschi, S.; Barbieri, R.; Silvestri, A.; Rivarola, E.; Ruisi, G.; Di Bianca, F.; Alonzo, G. J. *Chem. Soc., Dalton Trans.* **1985**, 523.
- (91) Harrison, P. G.; Sharpe, N. W. *Appl. Organomet. Chem.* **1989**, 3, 141.
- (92) Preut, H.; Vornefeld, M.; Huber, F. *Acta Cryst.* **1991**, C47, 264.
- (93) Ruisi, G.; Silvestri, A.; Lo Giudice, M. T.; Barbieri, R.; Atassi, G.; Huber, F.; Gratz, K.; Lamartina, L. J. *Inorg. Biochem.* **1985**, 25, 229.
- (94) Gulì, G.; Gennaro, G.; Pellerito, L.; Stocco, G. C. *Appl. Organomet. Chem.* **1993**, 7, 407.
- (95) Musmeci, M. T.; Madonia, G.; Lo Giudice, M. T.; Silvestri, A.; Ruisi, G.; Barbieri, R. *Appl. Organomet. Chem.* **1992**, 6, 127.
- (96) Jancsó, A.; Henry, B.; Rubini, P.; Vankó, Gy.; Gajda, T. J. *Chem. Soc., Dalton Trans.* **2000**, 12, 1941.
- (97) Gajda-Scrantz, K.; Jancsó, A.; Pettinari, C.; Gajda, T. J. *Chem. Soc., Dalton Trans.* **2003**, 2912.
- (98) Mesubi, M. A.; Eke, U. B.; Bamgboye, T. T. *Appl. Organomet. Chem.* **1988**, 2, 121.
- (99) Ruisi, G.; Lo Giudice, M. T. *Appl. Organomet. Chem.* **1991**, 5, 385.
- (100) Ruisi, G.; Lo Giudice, M. T.; Hubert, F.; Vornefeld, M. *Appl. Organomet. Chem.* **1996**, 10, 779.
- (101) Huber, F.; Vornefeld, M.; Ruisi, G.; Barbieri, R. *Appl. Organomet. Chem.* **1993**, 7, 243.
- (102) Nath, M.; Pokharia, S.; Song, X. Q.; Eng, G.; Gielen, M.; Kemmer, M.; Biesemans, M.; Willem, R.; de Vos, D. *Appl. Organomet. Chem.* **2003**, 17, 305.
- (103) Nath, M.; Yadav, R.; Eng, G.; Nguyen, T. T.; Kumar, A. J. *Organomet. Chem.* **1999**, 577, 1.
- (104) Nath, M.; Pokharia, S.; Eng, G.; Song, X. Q.; Kumar, A. J. *Organomet. Chem.* **2003**, 669, 109.
- (105) Buzás, N.; Nagy, L.; Jankovics, H.; Krämer, R.; Kuzmann, E.; Vértes, A.; Burger, K. J. *Radioanal. Nucl. Chem.* **1999**, 241, 313.
- (106) Koch, J.; Huber, F.; Ruisi, G.; Barbieri, R. *Appl. Organomet. Chem.* **1994**, 8, 113.
- (107) Ho, B. Y. K.; Molloy, K. C.; Zuckerman, J. J.; Reidinger, F.; Zubieta, J. A. J. *Organomet. Chem.* **1980**, 187, 213.
- (108) Ogawa, T.; Takahashi, Y.; Matsui, M. *Carbohydr. Res.* **1982**, 102, 207.
- (109) Patel, A.; Poller, R. C.; Rathbone, E. B. *Appl. Organomet. Chem.* **1987**, 1, 325.
- (110) Jarosz, S.; Fraser-Reid, B. J. *Organic Chem.* **1989**, 54, 4011.
- (111) Pereyre, M.; Quintard, J. P.; Rahm, A. *Tin in Organic Synthesis*, Butterworths, London, **1987**.
- (112) David, S. In: Hanessian, S. (Ed.), *Preparative Carbohydrate Chemistry*, Marcel Dekker, New York, **1996**; Chapter 4.
- (113) Guard, H. E.; Coleman, W. M. III.; Ross, M. M. *Carbohydr. Res.* **1992**, 235, 41.
- (114) Szorcsik, A.; Nagy, L.; Gyurcsik, B.; Vankó, Gy.; Krämer, R.; Vértes, A.; Yamaguchi, T.; Yoshida, K. J. *Radioanal. Nucl. Chem.* **2004**, 260, 459.
- (115) Fiore, T.; Foti, C.; Gianguzza, A.; Orecchio, S.; Pellerito, L. *Appl. Organomet. Chem.* **2002**, 16, 294.
- (116) Bertazzi, N.; Bruschetta, G.; Casella, G.; Pellerito, L.; Rotondo, E.; Scopelliti, M. *Appl. Organomet. Chem.* **2003**, 17, 932.
- (117) Pommier, J. C.; Valade, J. *Bull. Soc. Chim. Fr.* **1965**, 1257.
- (118) Considine, W. J. J. *Organomet. Chem.* **1966**, 5, 263.
- (119) Pommier, J. C.; Valade, J. J. *Organomet. Chem.* **1968**, 12, 433.
- (120) Ogawa, T.; Matsui, M. *Carbohydr. Res.* **1977**, 56, C1.
- (121) Blunden, S. J.; Smith, P. J.; Beynon, P. J.; Gilles, D. G. *Carbohydr. Res.* **1981**, 88, 9.
- (122) Taba, K. M.; Köster, R.; Dahlhoff, W. V. *Synthesis* **1984**, 399.
- (123) David, S.; Thieffry, A.; Vayrieres, A. J. *Chem. Soc., Perkin Trans. 1* **1981**, 1796.
- (124) Tsuda, Y.; Haque, M. E.; Yoshimoto, K. *Chem. Pharm. Bull.* **1983**, 31, 1612.
- (125) Crowe, A. J.; Smith, P. J. J. *Organomet. Chem.* **1976**, 110, C57.
- (126) Köpper, S.; Brandenburg, A. *Liebigs Ann. Chem* **1992**, 933.
- (127) Grindley, T. B.; Curtis, R. D.; Thangarasa, R.; Wasylshen, R. E. *Can. J. Chem.* **1990**, 68, 2102.
- (128) Grindley, T. B.; Thangarasa, R. *Can. J. Chem.* **1990**, 68, 1007.
- (129) Grindley, T. B.; Thangarasa, R. J. *Am. Chem. Soc.* **1990**, 112, 1364.
- (130) Grindley, T. B.; Thangarasa, R.; Bakshi, P. K.; Cameron, T. S. *Can. J. Chem.* **1992**, 70, 197.
- (131) Grindley, T. B.; Wasylshen, R. E.; Thangarasa, R.; Power, W. P.; Curtis, R. *Can. J. Chem.* **1992**, 70, 205.

- (132) Dalil, H.; Biesemans, M.; Willem, R.; Gielen, M. *Main Group Met. Chem.* **1998**, 21, 741.
- (133) Szorcsik, A.; Sletten, J.; Nagy, L.; Lakatos, A.; Kuzmann, E.; Vértés, A. *ACH - Models Chem.* **2000**, 137, 22.
- (134) David, S.; Pascard, C.; Cesario, M. *Nouv. J. Chim.* **1979**, 3, 63.
- (135) Cameron, T. S.; Bakshi, P. K.; Thangarasa, R.; Gridley, T. B. *Can. J. Chem.* **1992**, 70, 1623.
- (136) Holzapfel, C. W.; Kockemoer, J. M.; Marais, C. M.; Kruger, G. J.; Pretorius, J. A. S. *Afr. J. Chem.* **1982**, 35, 81.
- (137) Davies, A. G.; Price, A. J.; Dawes, H. M.; Hursthouse, M. B. *J. Chem. Soc., Dalton Trans.* **1986**, 297.
- (138) Chung, S.-K.; Ryu, Y.; Chang, Y.-T.; Whang, D.; Kim, K. *Carbohydr. Res.* **1994**, 253, 13.
- (139) Chung, S.-K.; Ryu, Y. H. *Carbohydr. Res.* **1994**, 258, 145.
- (140) Lee, S. J.; Cho, S. J.; Oh, K. S.; Cui, C.; Ryu, Y.; Chang, Y. T.; Kim, K. S.; Chung, S. K. *J. Phys. Chem.* **1996**, 100, 10111.
- (141) Donaldson, J. D.; Grimes, S. M.; Pellerito, L.; Girasolo, M. A.; Smith, P. J.; Cambria, A.; Famà, M. *Polyhedron* **1987**, 6, 383.
- (142) Nagy, L.; Korecz, L.; Kiricsi, I.; Zsikla, L.; Burger, K. *Struct. Chem.* **1991**, 2, 231.
- (143) Burger, K.; Nagy, L.; Buzás, N.; Vértés, A.; Mehner, H. *J. Chem. Soc., Dalton Trans.* **1993**, 2499.
- (144) Smith, P. J.; White, R. F. M.; Smith, L. J. *Organomet. Chem.* **1972**, 40, 341.
- (145) Herber, R. H.; Shanzer, A.; Libman, J. *Organometallics* **1984**, 3, 586.
- (146) Buzás, N.; Pujar, M. A.; Nagy, L.; Vértés, A.; Kuzmann, E.; Mehner, H. *J. Radioanal. Nucl. Chem.* **1995**, 189, 237.
- (147) Vértés, A.; Süvegghi, K.; Kuzmann, E.; Burger, K.; Nagy, L.; Schrantz, K.; Buzás, N. *J. Radioanal. Nucl. Chem.* **1996**, 203, 399.
- (148) Nagy, L.; Gyurcsik, B.; Burger, K.; Yamashita, S.; Yamaguchi, T.; Wakita, H.; Nomura, M. *Inorg. Chim. Acta* **1995**, 230, 105.
- (149) Szorcsik, A.; Nagy, L.; Gajda-Schrantz, K.; Pellerito, L.; Nagy, E.; Edelmann, F. T. *J. Radioanal. Nucl. Chem.* **2002**, 252, 523.
- (150) Nagy, L.; Mehner, H.; Christy, A. A.; Sletten, E.; Edelmann, F. T.; Anderson, Q. M. *J. Radioanal. Nucl. Chem.* **1998**, 227, 89.
- (151) Holecck, J.; Lycka, A.; Micak, D.; Nagy, L.; Vankó, Gy.; Ng, S. W.; Brus, J. *Collect. Czech. Chem. Commun.* **1999**, 64, 1028.
- (152) Taylor, O. J.; Wardell, J. L. *Recl. Trav. Chim. Pays-Bas.* **1988**, 107, 267.
- (153) Cox, P. J.; Doidge-Harrison, S. M. S. V.; Howie, R. A.; Nowell, I. W.; Taylor, O. J.; Wardell, J. L. *J. Chem. Soc., Perkin Trans. 1* **1989**, 2017.
- (154) Doidge-Harrison, S. M. S. V.; Nowell, I. W.; Cox, P. J.; Howie, R. A.; Taylor, O. J.; Wardell, J. L. *J. Organomet. Chem.* **1991**, 401, 273.
- (155) Burnett, L. A.; Doidge-Harrison, S. M. S. V.; Garden, S. J.; Howie, R. A.; Taylor, O. J.; Wardell, J. L. *J. Chem. Soc., Perkin Trans. 1* **1993**, 1621.
- (156) Hill, R.; Blunden, S. J. *Appl. Organomet. Chem.* **1988**, 2, 251.
- (157) Barug, D. *Chemosphere* **1981**, 10, 1145.
- (158) Orsler, R. J.; Holland, G. E. *Int. Biodeterior. Bull.* **1982**, 18, 95.
- (159) Cox, P. J.; Howie, R. A.; Melvin, O. A.; Wardell, J. L. *J. Organomet. Chem.* **1995**, 489, 161.
- (160) Richardson, B. A. *Rec. Annu. Conv. Br. Wood Preserv. Assoc.* **1970**, 37.
- (161) Bravery, A.; Parameswaran, N.; Liese, W. *Mater. Org.* **1975**, 10, 31.
- (162) Smith, P. J.; Crowe, A. J.; Allen, D. W.; Brooks, J. S.; Formstone, R. *Chem. Ind.* **1977**, 23, 874.
- (163) Hill, R. International Research Group on Wood Preservation, Doc. No. IRG/WP/3312, **1984**.
- (164) Szorcsik, A.; Nagy, L.; Scopelliti, M.; Pellerito, L.; Sipos, P. *Carbohydr. Res.* **2006**, 341, 2083.
- (165) Nagy, L.; Barátné-Jankovics, H.; Yamaguchi, T.; Yoshida, K.; Scopelliti, M.; Pellerito, L.; Sletten, E. *J. Radioanal. Nucl. Chem.* **2008**, 275, 193.
- (166) Szorcsik, A.; Nagy, L.; Pellerito, L.; Yamaguchi, T.; Yoshida, K. *J. Radioanal. Nucl. Chem.* **2003**, 256, 3.
- (167) Keppler, B. K. *Metal Complexes in Cancer Chemotherapy*, VCH, Weinheim, **1993**
- (168) Allardyce, C. S.; Dorcier, A.; Scolaro, C.; Dyson, P. J. *Appl. Organomet. Chem.* **2005**, 19, 1.
- (169) Fish, R. H.; Jaouen, G. *Organometallics* **2003**, 22, 2166.
- (170) Tullius, A. T. M.; Lippart, S. J. *J. Am. Chem. Soc.* **1981**, 103, 4620.

- (171) Lippart, S. J. *Science* **1982**, 218, 1075.
- (172) Bloemink, M.; Reedijk, J. In: Sigel, A.; Sigel, H. (Eds.), *Metal Ions in Biological Systems: Cisplatin and Derived Anticancer Drugs. Mechanism and Current Status of DNA Binding*, Marcel Dekker, New York, **1996**; Vol. 32, p. 641.
- (173) Crowe, A. J. *Drugs of the Future* **1987**, 12, 255.
- (174) Penninks, A. H.; Seinen, W. Q. *Vet.* **1984**, 6, 209.
- (175) Pellerito, L.; Ruisi, G.; Bertazzi, N.; Lo Giudice, M. T.; Barbieri, R. *Inorg. Chim. Acta* **1976**, 58, L9.
- (176) Cardin, C. J.; Roy, A. *Inorg. Chim. Acta* **1985**, 107, 57.
- (177) Valle, G.; Plazzogna, G.; Ettore, R. J. *Chem. Soc., Dalton Trans.* **1984**, 1271.
- (178) Barbieri, R.; Rivarola, E.; Di Bianca, F.; Huber, F. *Inorg. Chim. Acta* **1982**, 57, 37.
- (179) Barbieri, R.; Di Bianca, F.; Rivarola, E.; Huber, F. *Inorg. Chim. Acta* **1985**, 108, 141.
- (180) Gajda-Schrantz, K.; Nagy, L.; Jankovics, H.; Christy, A. A.; Sletten, E.; Kuzmann, E.; Vértés, A. *J. Radioanal. Nucl. Chem.* **2001**, 247, 79.
- (181) Atkinson, A.; Rodriguez, M. D.; Shewmaker, T. E.; Walmsley, J. A. *Inorg. Chim. Acta* **1999**, 285, 60.
- (182) Barbieri, R.; Silvestri, A.; Piro, V. J. *Chem. Soc., Dalton Trans.* **1990**, 3605.
- (183) Barbieri, R.; Silvestri, A.; Lo Giudice, M. T.; Ruisi, G.; Musmeci, M. T. *J. Chem. Soc., Dalton Trans.* **1989**, 12, 519.
- (184) Piro, V.; Di Simone, F.; Madonna, G.; Silvestri, A.; Giuliani, A. M.; Ruisi, G.; Barbieri, R. *Appl. Organomet. Chem.* **1992**, 6, 537.
- (185) Rekker, R. F. *The Hydrophobic Fragmental Constant: Its Derivation and Application with a Means of Characterizing Membrane Systems*, Elsevier, Amsterdam, **1977**.
- (186) Hansch, C.; Leo, A. *Substituent Constants for Correlation Analysis in Chemistry and Biology*, Wiley, New York, **1979**.
- (187) Gupta, S. P. *Chem. Rev.* **1987**, 87, 1183.
- (188) Barbieri, R.; Huber, F.; Silvestri, A.; Ruisi, G.; Rossi, M.; Barone, G.; Paulsen, A. *Appl. Organomet. Chem.* **1999**, 13, 595.
- (189) Casini, A.; Messori, L.; Orioli, P.; Gielen, M.; Kemmer, M.; Willem, R. J. *Inorg. Biochem.* **2001**, 85, 297.
- (190) Kemmer, M.; Gielen, M.; Biesemans, M.; de Vos, D.; Willem, R. *Met. -Based Drugs* **1998**, 5, 189.
- (191) Ghys, L.; Biesemans, M.; Gielen, M.; Garioufis, A.; Hadjilaidis, N.; Willems, R.; Martins, J. C. *Eur. J. Inorg. Chem.* **2000**, 12, 513.
- (192) Barone, G.; Cotta Ramusino, M.; Barbieri, R.; La Manna, G. J. *Mol. Struct.: Theochem* **1999**, 469, 143.
- (193) Barone, G.; Barbieri, R.; La Manna, G.; Koch, M. H. J. *Appl. Organomet. Chem.* **2000**, 14, 189.
- (194) Jancsó, A.; Nagy, L.; Moldrheim, E.; Sletten, E. J. *Chem. Soc., Dalton Trans.* **1999**, 1587.
- (195) Jankovics, H.; Nagy, L.; Buzás, N.; Pellerito, L.; Barbieri, R. J. *Inorg. Biochem.* **2002**, 92, 55.
- (196) Nagy, L. Unpublished results.
- (197) De Stefano, C.; Gianguzza, A.; Giuffrè, O.; Piazzese, D.; Orecchio, S.; Sammartano, S. *Appl. Organomet. Chem.* **2004**, 18, 653.
- (198) Li, Q.; Yang, P.; Wang, H.; Guo, M. J. *Inorg. Biochem.* **1996**, 64, 181.
- (199) Yang, Z.; Bakas, T.; Sanchez-Diaz, A.; Charalampopoulos, C.; Tsangaris, J.; Hadjilaidis, N. *J. Inorg. Biochem.* **1998**, 72, 133.
- (200) Jankovics, B. H.; Nagy, L.; Longo, F.; Fiore, T.; Pellerito, L. *Magy. Kém. Foly.* **2001**, 107, 392.
- (201) Abdalla, E. M.; Mohamed, M. M. A.; Mahmoud, M. R. J. *Coord. Chem.* **2003**, 56, 691.
- (202) Davies, A. G.; Kleinschmidt, D. C.; Palan, P. R.; Vasistha, S. C. J. *Chem. Soc. C* **1971**, 3972.
- (203) Stapferand, C. H.; Herber, R. H. J. *Organomet. Chem.* **1973**, 56, 175.
- (204) Hager, C. G.; Huber, F.; Silvestri, A.; Barbieri, A.; Barbieri, R. *Gazz. Chim. Ital.* **1993**, 123, 583.
- (205) Sandhu, G. K.; Sharma, N. *Appl. Organomet. Chem.* **1993**, 7, 33.
- (206) Gajda-Schrantz, K.; Nagy, L.; Kuzmann, E.; Vértés, A.; Holecsek, J.; Lycka, A. J. *Chem. Soc., Dalton Trans.* **1997**, 2201.
- (207) Jankovics, H.; Nagy, L.; Kele, Z.; Pettinari, C.; D'Agati, P.; Mansueto, C.; Pellerito, C.; Pellerito, L. *J. Organomet. Chem.* **2003**, 668, 129.
- (208) Jankovics, H.; Pettinari, C.; Marchetti, F.; Kamu, E.; Nagy, L.; Troyanov, S.; Pellerito, L. *J. Inorg. Biochem.* **2003**, 97, 370.

- (209) Gajda-Schrantz, K.; Nagy, L.; Kuzmann, E.; Vértés, A. *J. Radioanal. Nucl. Chem.* **1998**, 232, 151.
- (210) Li, Q.; da Silva, M. F. C. G.; Jinghua, Z.; Pombeiro, A. J. L. *J. Organomet. Chem.* **2004**, 689, 4584.
- (211) Li, Q.; da Silva, M. F. C. G.; Pombeiro, A. J. L. *Chem. Eur. J.* **2004**, 10, 1456.
- (212) Deák, A.; Haiduc, I.; Párkányi, L.; Venter, M.; Kálmán, A. *Eur. J. Inorg. Chem.* **1999**, 1593.
- (213) Deák, A.; Venter, M.; Kálmán, A.; Párkányi, L.; Radics, L.; Haiduc, I. *Eur. J. Inorg. Chem.* **2000**, 127.
- (214) Deák, A.; Radics, L.; Kálmán, A.; Párkányi, L.; Haiduc, I. *Eur. J. Inorg. Chem.* **2001**, 2849.
- (215) Szorcisk, A.; Nagy, L.; Kokeny, I.; Deák, A.; Scopelliti, M.; Fiore, T.; Pellerito, L. *J. Organomet. Chem.* **2007**, 692, 3409.
- (216) Merkord, J.; Henninghause, G. *Pharmazie* **1984**, 39, 572.
- (217) Henninghause, G.; Merkord, J.; Krönig, G. *Plzen. Lek. Sborn. Suppl.* **1988**, 56, 89.
- (218) Kreyberg, S.; Torvik, A.; Bjorneboe, A.; Wiik-Larsen, E.; Jacobsen, D. *Clin. Neuropath.* **1992**, 11, 256.
- (219) Szorcisk, A.; Nagy, L.; Csintalan, G.; Pellerito, C.; Scopelliti, M.; Pellerito, L.; Yamaguchi, T. *Personal communication* **2006**.
- (220) Casas, J. S.; Castellano, E. E.; Condori, F.; Couce, M. D.; Sánchez, A.; Sordo, J.; Varela, J. M.; Zuckerman-Schpector, J. J. *Chem. Soc., Dalton Trans.* **1997**, 4421.
- (221) Casas, J. S.; Castiñeiras, A.; Condori, F.; Couce, M. D.; Russo, U.; Sánchez, A.; Sordo, J.; Valera, J. M. *Polyhedron* **2000**, 19, 813.
- (222) Casas, J. S.; Castaño, M. V.; Garcia-Tasende, M. S.; Perez-Alvarez, T.; Sánchez, A.; Sordo, J. *J. Inorg. Biochem.* **1996**, 61, 97.
- (223) Casas, J. S.; Castiñeiras, A.; Couce, M. D.; Martinez, G.; Sordo, J.; Varela, J. M. *J. Organomet. Chem.* **1996**, 517, 165.
- (224) Narayanan, V. L.; Nash, M.; Paull, K. D. In: Gielen, M. (Ed.), *Tin Based Antitumor Drugs (NATO ASI Series)*, Springer Verlag, Berlin, **1990**; Vol. H37, p. 201.
- (225) Crowe, A. J. In: Gielen, M. (Ed.), *Metal Based Antitumor Drugs*, Freund, London, **1988**; Vol. 1, p. 103.
- (226) Saxena, A. K. *Appl. Organomet. Chem.* **1987**, 1, 39.
- (227) Gielen, M.; Lelieveld, P.; de Vos, D.; Willem, R. In: Gielen, M. (Ed.), *Metal Based Antitumor Drugs*, Freund, Tel Aviv, **1992**; Vol. 2, p. 29.
- (228) Gielen, M.; Willem, R.; Biesemans, M.; Bouâlam, M.; El Khoulfi, A.; de Vos, D. *Appl. Organomet. Chem.* **1992**, 6, 287.
- (229) Bouâlam, M.; Gielen, M.; El Khoulfi, A.; de Vos, D.; Willem, R. (Pharmachemie B.V.), European Patent 91202746.3 (October **1991**).
- (230) Tranter, C. J.; Berners-Price, S. J.; Cutts, J.; Parsons, P. G.; Rintoul, G.; Young, D. J. *Main Group Met. Chem.* **1995**, 1, 165.
- (231) Gielen, M.; Tiekink, E. R. T.; Bouhdid, A.; de Vos, D.; Biesemans, M.; Verbruggen, I.; Willem, R. *Appl. Organomet. Chem.* **1995**, 9, 639 and references therein.
- (232) Gielen, M.; Bouhdid, A.; Kayser, F.; Biesemans, M.; Willem, R.; de Vos, D.; Mahieu, B. *Appl. Organomet. Chem.* **1995**, 9, 251.
- (233) Gielen, M.; Bouâlam, M.; Mahieu, B.; Tiekink, E. R. T. *Appl. Organomet. Chem.* **1994**, 8, 19.
- (234) Gielen, M.; Willem, R. *Anticancer Res.* **1992**, 12, 257.
- (235) Penninks, A. H.; Bol-Schoenmakers, M.; Gillen, M.; Sienen, W. *Main Group Met. Chem.* **1989**, 12, 1.
- (236) Takahashi, M.; Furukawa, F.; Kokubo, T.; Kurata, Y.; Hayashi, Y. *Cancer Lett.* **1983**, 20, 271.
- (237) Ng, S. C.; Parsons, P. G.; Sim, K. Y.; Tranter, C. J.; White, R. H.; Young, D. J. *Appl. Organomet. Chem.* **1997**, 11, 577.
- (238) Gielen, M.; Bouhdid, A.; Tiekink, E. R. T. *Main Group Met. Chem.* **1995**, 18, 199.
- (239) Willem, R.; Bouhdid, A.; Biesemans, M.; Martins, J. C.; de Vos, D.; Tiekink, E. R. T.; Gielen, M. *J. Organomet. Chem.* **1996**, 514, 203.
- (240) Willem, R.; Bouhdid, A.; Mahieu, B.; Ghys, L.; Biesemans, M.; Tiekink, E. R. T.; Gielen, M. *J. Organomet. Chem.* **1997**, 531, 151.
- (241) De Stefano, C.; Gianguzza, A.; Marrone, F.; Piazzese, D. *Appl. Organomet. Chem.* **1997**, 11, 683.
- (242) Cucinotta, V.; Gianguzza, A.; Maccarrone, G.; Pellerito, L.; Purrello, R.; Rizzarelli, E. *J. Chem. Soc., Dalton Trans.* **1992**, 2299.

- (243) Pellerito, L.; Dia, G.; Gianguzza, A.; Girasolo, M. A.; Rizzarelli, E.; Purrello, R. *Polyhedron* **1987**, *6*, 1639.
- (244) Di Nicola, C.; Galindo, A.; Hanna, J. V.; Marchetti, F.; Pettinari, C.; Pettinari, R.; Rivarola, E.; Skelton, B. W.; White, A. H. *Inorg. Chem.* **2005**, *44*, 3094.
- (245) Pettinari, C. *Main Group Met. Chem.* **1999**, *22*, 661.
- (246) Pettinari, C.; Pellei, M.; Marchetti, F.; Santini, C.; Miliiani, M. *Polyhedron* **1998**, *17*, 561.
- (247) Pettinari, C.; Pellei, M.; Santini, C.; Natali, I.; Accorroni, F.; Lorenzotti, A. *Polyhedron* **1998**, *17*, 4487.
- (248) Pettinari, C.; Marchetti, F.; Cingolani, A.; Bartolini, S. *Polyhedron* **1996**, *15*, 1263.
- (249) Pettinari, C.; Marchetti, F.; Pellei, M.; Cingolani, A.; Barba, L.; Cassetta, A. *J. Organomet. Chem.* **1996**, *515*, 119.
- (250) Gonzales, A. S.; Casas, J. S.; Sordo, J. J. *Inorg. Biochem.* **1990**, *39*, 227.
- (251) Boo, P. A.; Casas, J. S.; Couce, M. D.; Freijanes, E.; Furlani, A.; Scarcia, V.; Sordo, J.; Russo, U.; Varela, M. *Appl. Organomet. Chem.* **1997**, *11*, 963.
- (252) Lopez, C.; Gonz  les, A. S.; Garc  a, M. E.; Casas, J. S.; Sordo, J.; Gracianai, R.; Casellato, U. *J. Organomet. Chem.* **1992**, *434*, 261.
- (253) Leal, M. P.; Gonzales, A. S.; Garcia, M. E.; Casas, J. S.; Sordo, J. *Appl. Organomet. Chem.* **1993**, *7*, 421.
- (254) Huber, F.; Preut, H.; Hoffmann, E.; Gielen, M. *Acta Cryst.* **1989**, *C45*, 51.
- (255) Gielen, M.; Acheddad, M.; Mahieu, B.; Willem, R. *Main Group Met. Chem.* **1991**, *14*, 73.
- (256) Gielen, M.; Acheddad, M.; Tiekink, E. R. T. *Main Group Met. Chem.* **1993**, *16*, 367.
- (257) Ng, S. W.; Kumar Das, V. G.; Hole  ek, J.; Ly  ka, A.; Gielen, M.; Drew, M. B. G. *Appl. Organomet. Chem.* **1997**, *11*, 39.
- (258) Boyce, M.; Clarke, B.; Cunningham, D.; Gallagher, J. F.; Higgins, T.; McArdle, P.; Cholch   n, N.; O'Gara, M. *J. Organomet. Chem.* **1995**, *498*, 241.
- (259) Clarke, B.; Clarke, N.; Cunningham, D.; Higgins, T.; McArdle, P.; Cholch   n, M. N.; O'Gara, M. *J. Organomet. Chem.* **1998**, *559*, 55.
- (260) Cunningham, D.; Gallagher, J. F.; Higgins, T.; McArdle, P.; McGinley, J.; O'Gara, M. *J. Chem. Soc., Dalton Trans.* **1993**, 2183.
- (261) Nath, M.; Yadav, R.; Gielen, M.; Dalil, H.; de Vos, D.; Eng, G. *Appl. Organomet. Chem.* **1997**, *11*, 727.
- (262) Dey, D. K.; Saha, M. K.; Das, M. K.; Bhartiya, N.; Bansal, R. K.; Rosair, G.; Mitra, S. *Polyhedron* **1999**, *18*, 2687.
- (263) Sing, H. L.; Varshney, S.; Varshney, A. K. *Appl. Organomet. Chem.* **1999**, *13*, 637.
- (264) Maggio, F.; Bosco, R.; Cefal  , R.; Barbieri, R. *Inorg. Nucl. Chem. Lett.* **1968**, *4*, 389.
- (265) van-der Bergen, A.; Cozens, R. J.; Murray, K. S. *J. Chem. Soc. A* **1970**, 3060.
- (266) Ghose, B. N. *Synth. React. Inorg. Met. -Org. Chem.* **1982**, *12*, 835.
- (267) Nath, M.; Sharma, C. L.; Sharma, N. *Synth. React. Inorg. Met. -Org. Chem.* **1991**, *21*, 807.
- (268) Chaubani, H. P. S.; Bhargava, A.; Rao, R. J. *Ind. J. Chem.* **1993**, *32A*, 157.
- (269) Gopinathan, S.; Degaonkar, M. P.; Hundekar, A. M.; Gopinathan, C. *Appl. Organomet. Chem.* **1993**, *7*, 63.
- (270) Wang, J. T.; Zhang, Y. W.; Xu, Y. M.; Wang, Z. W. *Heteroat. Chem.* **1992**, *3*, 599.
- (271) Teoh, S. G.; Yeap, G. Y.; Loh, C. C.; Foong, L. W.; Teoh, S. B.; Fun, H. K. *Polyhedron* **1997**, *16*, 2213.
- (272) Couce, M. D.; Cherchi, V.; Faraglia, G.; Russo, U.; Sindellari, L.; Valle, G.; Zancan, N. *Appl. Organomet. Chem.* **1996**, *10*, 35.
- (273) Xueqing, S.; Zhiqiang, Y.; Qinglan, X.; Jinshan, L. *J. Organomet. Chem.* **1998**, *566*, 103.
- (274) Willem, R.; Dalil, H.; Broekaert, P.; Biesemans, M.; Ghys, L.; Nooter, K.; de Vos, D.; Ribot, F.; Gielen, M. *Main Group Met. Chem.* **1997**, *20*, 535.
- (275) Gielen, M.; Ma, H.; Bouh  did, A.; Dalil, H.; Biesemans, M.; Willem, R. *Met. -Based Drugs* **1997**, *4*, 193.
- (276) Gielen, M.; Dalil, H.; Mahieu, B.; Biesemans, M.; Willem, R. *Appl. Organomet. Chem.* **1998**, *12*, 855.
- (277) Gielen, M. *Coord. Chem. Rev.* **1996**, *151*, 41.
- (278) de Vos, D.; Willem, R.; Gielen, M.; van Wingerden, K. E.; Nooter, K. *Met. -Based Drugs* **1998**, *4*, 179.
- (279) Gielen, M.; Dalil, H.; Biesemans, M.; Mahieu, B.; de Vos, D.; Willem, R. *Appl. Organomet. Chem.* **1999**, *13*, 515.

- (280) Kamruddin, S. K.; Chattopadhyaya, T. K.; Roy, A.; Tiekink, E. R. T. *Appl. Organomet. Chem.* **1996**, *10*, 513.
- (281) Goh, N. K.; Chu, C. K.; Khoo, L. E.; Whalen, D.; Eng, G.; Smith, F. E.; Hynes, R. C. *Appl. Organomet. Chem.* **1998**, *12*, 457.
- (282) Ogwuru, N.; Khoo, L. E.; Eng, G. *Appl. Organomet. Chem.* **1998**, *12*, 409.
- (283) Khoo, L. E.; Goh, N. K.; Koh, L. L.; Xu, Y.; Whalen, D. J.; Eng, G. *Appl. Organomet. Chem.* **1996**, *10*, 459.
- (284) Basu Baul, S.; Basu Baul, T. S.; Rivarola, E.; Dakternieks, D.; Tiekink, E. R. T.; Syng-Ai, C.; Chatterjee, A. *Appl. Organomet. Chem.* **1998**, *12*, 503.
- (285) James, B. D.; Kivlighon, L. M.; Skelton, B. W.; White, A. H. *Appl. Organomet. Chem.* **1998**, *12*, 13.
- (286) Chandra, S.; Gioskos, S.; James, B. D.; Macauley, B. J.; Magee, R. J. J. *Chem. Tech. Biotechnol.* **1993**, *56*, 41.
- (287) Wharf, I.; Lamparski, H.; Reeleder, R. *Appl. Organomet. Chem.* **1997**, *11*, 969.
- (288) Schmiedgen, R.; Huber, F.; Preut, H.; Ruisi, G.; Barbieri, R. *Appl. Organomet. Chem.* **1994**, *8*, 397 and references therein.
- (289) Schmiedgen, R.; Huber, F.; Silvestri, A.; Ruisi, G.; Rossi, M.; Barbieri, R. *Appl. Organomet. Chem.* **1998**, *12*, 861.
- (290) Huber, F.; Schmiedgen, R.; Schürmann, M.; Barbieri, R.; Ruisi, G.; Silvestri, A. *Appl. Organomet. Chem.* **1997**, *11*, 869.
- (291) Ma, C.; Jiang, Q.; Zhang, R. J. *Organomet. Chem.* **2003**, *678*, 148.
- (292) Barbieri, A.; Giuliani, A. M.; Ruisi, G.; Silvestri, A.; Barbieri, R. Z. *Anorg. Allg. Chem.* **1995**, *621*, 89 and references therein.
- (293) Kalsoom, A.; Mazhar, M.; Ali, S.; Mahon, M. F.; Molloy, K. C.; Chaudry, M. I. *Appl. Organomet. Chem.* **1997**, *11*, 47.
- (294) Al-Allaf, T. A. K.; Al-Bayati, R. I. H.; Rshan, L. J.; Khuzaie, R. F. *Appl. Organomet. Chem.* **1996**, *10*, 47.
- (295) Lockhart, T. P.; Calabrese, J. C.; Davidson, F. *Organometallics* **1987**, *6*, 2479.
- (296) Meriem, A.; Willem, R.; Menuier-Piret, J.; Biesemans, M.; Mahieu, B.; Gielen, M. *Main Group Met. Chem.* **1990**, *13*, 167.
- (297) Lockhart, T. P.; Davidson, F. *Organometallics* **1987**, *6*, 2471.
- (298) Gielen, M.; El Khoulfi, A.; Biesemans, M.; Willem, R. *Appl. Organomet. Chem.* **1993**, *7*, 119.
- (299) Gielen, M.; Biesemans, M.; El Khoulfi, A.; Menuier-Piret, J.; Kayser, F.; Willem, R. *J. Fluorine Chem.* **1993**, *64*, 279.
- (300) Gielen, M.; El Khoulfi, A.; de Vos, D.; Kolker, H. J.; Schellens, J. H. M.; Willem, R. *Bull. Soc. Chim. Belg.* **1993**, *102*, 761.
- (301) Gielen, M.; Bouâlam, M.; Meriem, A.; Mahieu, B.; Biesemans, M.; Willem, R. *Heteroatom Chem.* **1992**, *3*, 449.
- (302) Bouâlam, M.; Biesemans, M.; Menuier-Piret, J.; Willem, R.; Gielen, M. *Appl. Organomet. Chem.* **1992**, *6*, 197.
- (303) Willem, R.; Biesemans, M.; Bouâlam, M.; Delmotte, A.; El Khoulfi, A.; Gielen, M. *Appl. Organomet. Chem.* **1993**, *7*, 311.
- (304) van Lambalgen, R.; Lelieveld, P. *Invest. New Drugs* **1987**, *5*, 161.
- (305) Khoo, L. E.; Goh, N. K.; Eng, G.; Whalen, D. J.; Hazell, A. *Appl. Organomet. Chem.* **1995**, *9*, 699.
- (306) Kovala-Demertzi, D.; Tauridou, P.; Moukarika, A.; Tsangaris, J. M.; Raptopoulou, C. P.; Terzis, A. *J. Chem. Soc., Dalton Trans.* **1995**, 123.
- (307) Srivastava, T. N.; Chauhan, A. K. S.; Kamboj, P. C. *J. Indian Chem. Soc.* **1983**, *60*, 625.
- (308) Lee, F. L.; Gabe, E. J.; Khoo, L. E.; Eng, G.; Smith, F. E. *Polyhedron* **1990**, *9*, 653.
- (309) Khoo, L. E.; Smith, F. E. *Polyhedron* **1985**, *4*, 447.
- (310) Khoo, L. E.; Charland, J. P.; Gabe, E. J.; Smith, F. E. *Inorg. Chim. Acta* **1987**, *128*, 139.
- (311) Prasad, L.; Gabe, E. J.; Smith, F. E. *Acta Crystallogr.* **1982**, *B 38*, 1325.
- (312) Gabe, E. J.; Lee, F. L.; Khoo, L. E.; Smith, F. E. *Inorg. Chim. Acta* **1986**, *112*, 41.
- (313) Gabe, E. J.; Lee, F. L.; Khoo, L. E.; Smith, F. E. *Inorg. Chim. Acta* **1985**, *105*, 103.
- (314) Charland, J. P.; Lee, F. L.; Gabe, E. J.; Khoo, L. E.; Smith, F. E. *Inorg. Chim. Acta* **1987**, *130*, 55.
- (315) Charland, J. P.; Gabe, E. J.; Khoo, L. E.; Smith, F. E. *Polyhedron* **1989**, *8*, 1897.

- (316) Khoo, L. E.; Goh, N. K.; Otieno, M. A.; Lucero, R. A.; Eng, G.; Luo, B. S.; Mak, T. C. W. *Appl. Organomet. Chem.* **1994**, 8, 33.
- (317) Ng, S. W.; Kuthubutheen, A. J.; Kumar Das, V. G.; Linden, A.; Tiekink, E. R. T. *Appl. Organomet. Chem.* **1994**, 8, 37.
- (318) Sandhu, G. K.; Boparoy, N. S. *Synth. React. Inorg. Met.-Org. Chem.* **1990**, 20, 975.
- (319) Sandhu, G. K.; Verma, S. P.; Moore, L. S.; Parish, R. V. *J. Organomet. Chem.* **1987**, 321, 15.
- (320) Sandhu, G. K.; Hundal, R. *Appl. Organomet. Chem.* **1995**, 9, 121.
- (321) Chakrabarti, A.; Kamruddin, S.; Chattopadhyaya, T. K.; Roy, A.; Chakraborty, B. N.; Molloy, K. C.; Tiekink, E. R. T. *Appl. Organomet. Chem.* **1995**, 9, 357.
- (322) Willem, R.; Dalil, H.; Biesemans, M.; Martins, J. C.; Gielen, M. *Appl. Organomet. Chem.* **1999**, 13, 605.
- (323) Pellerito, L.; Maggio, F.; Consiglio, M.; Pellerito, A.; Stocco, G. C.; Grimaudo, S. *Appl. Organomet. Chem.* **1995**, 9, 227.
- (324) Pellerito, L.; Maggio, F.; Fiore, T.; Pellerito, A. *Appl. Organomet. Chem.* **1996**, 10, 393.
- (325) Maggio, F.; Pellerito, A.; Pellerito, L.; Grimaudo, S.; Mansueto, C.; Vitturi, R. *Appl. Organomet. Chem.* **1994**, 8, 71.
- (326) Pellerito, A.; Fiore, T.; Pellerito, C.; Fontana, A.; Di Stefano, R.; Pellerito, L.; Cambria, M. T.; Mansueto, C. *J. Inorg. Biochem.* **1998**, 72, 115.
- (327) Pellerito, L.; Pellerito, A.; Maggio, F.; Beltramini, M.; Salvato, B.; Ricchelli, F. *Appl. Organomet. Chem.* **1993**, 7, 79.
- (328) Mirisola, M. G.; Pellerito, A.; Fiore, T.; Stocco, G. C.; Pellerito, L.; Cestelli, A.; Di Liegro, I. *Appl. Organomet. Chem.* **1997**, 11, 499.
- (329) Pellerito, A.; Fiore, T.; Giuliani, A. M.; Maggio, F.; Pellerito, L.; Mansueto, C. *Appl. Organomet. Chem.* **1997**, 11, 707.
- (330) Yeats, P. A.; Poh, J. R.; Ford, B. F. E.; Sams, J. R.; Aubke, F. *J. Chem. Soc. A* **1970**, 2188.
- (331) Lencioni, S.; Pellerito, A.; Fiore, T.; Giuliani, A. M.; Pellerito, L.; Cambria, M. T.; Mansueto, C. *Appl. Organomet. Chem.* **1999**, 13, 145.
- (332) López-Cardoso, M.; García y García, P.; García-Montalvo, V.; Cea-Olivares, R. *Heteroat. Chem.* **2000**, 11, 6.
- (333) López-Cardoso, M.; García y García, P.; Rogers-Sakuma, A.; Cea-Olivares, R. *Polyhedron* **2000**, 19, 1539.
- (334) Chivers, T.; Sams, J. R. *J. Chem. Soc., Chem. Commun.* **1969**, 249.
- (335) Allen, D. W.; Derbyshire, D. J.; Brooks, J. S.; Blunden, S. J.; Smith, P. J. *J. Chem. Soc., Dalton Trans.* **1984**, 1889.
- (336) Barbieri, R.; Taddei, F. *J. Chem. Soc., Perkin Trans.* **1972**, 2, 1323.
- (337) Philips, J. E.; Herber, R. H. *J. Organomet. Chem.* **1984**, 268, 39.
- (338) Anderson, D. G.; Webster, D. E. *J. Chem. Soc. B* **1968**, 765.
- (339) Anderson, D. G.; Chipperfield, J. R.; Webster, D. E. *J. Organomet. Chem.* **1968**, 12, 323.
- (340) Cordey-Hayes, M. *J. Inorg. Nucl. Chem.* **1964**, 26, 915.
- (341) Cordey-Hayes, M.; Harris, I. R. *Phys. Lett.* **1967**, 24A, 80.
- (342) Parish, R. V.; Platt, R. H. *J. Chem. Soc., Chem. Commun.* **1968**, 1118.
- (343) Jurkschat, K.; Tzschach, A.; Meunier-Piret, J.; van Meerssche, M. *J. Organomet. Chem.* **1985**, 290, 285.
- (344) Tzschach, A.; Jurkschat, K. *Pure Appl. Chem.* **1986**, 58, 639.
- (345) Petrosyan, V. S.; Reutov, O. A. *Pure Appl. Chem.* **1974**, 37, 147.
- (346) Gustavson, W. A.; Principe, L. M.; Min Rhee, W.-Z.; Zuckerman, J. J. *J. Am. Chem. Soc.* **1981**, 103, 4126.
- (347) Kumar Das, V. G.; Mun, L. K.; Wei, C.; Blunden, S. J.; Mak, T. C. W. *J. Organomet. Chem.* **1987**, 322, 163.
- (348) Hulme, R. *J. Chem. Soc., Chem. Commun.* **1963**, 1524.
- (349) Kumar Das, V. G.; Yap, C. K.; Smith, P. J. *J. Organomet. Chem.* **1985**, 291, C17.
- (350) Kumar Das, V. G.; Wei, C.; Keong, Y. C.; Mak, T. C. W. *J. Organomet. Chem.* **1986**, 299, 41.
- (351) Harrison, P. G.; King, T. J.; Richards, J. A. *J. Chem. Soc., Dalton Trans.* **1974**, 1723.
- (352) Kumar Das, V. G.; Wei, C.; Keong, Y. C.; Sinn, E. *J. Chem. Soc., Chem. Commun.* **1984**, 1418.

- (353) Harrison, P. G.; Molloy, K. J. *Organomet. Chem.* **1978**, 152, 63.
- (354) Bokii, N. G.; Struchkov, Yu. T.; Kravstov, D. N.; Rokhlina, E. M. *J. Struct. Chem. (Eng. Transl.)* **1973**, 14, 458.
- (355) Cunningham, D.; Higgins, T.; McArdle, P. J. *Chem. Soc., Chem. Commun.* **1984**, 833.
- (356) Beckmann, J.; Dakternieks, D.; Duthie, A.; Mitchell, C. *Appl. Organomet. Chem.* **2004**, 18, 51.
- (357) Howie, R. A.; Wardell, J. L.; Wardell, S. M. S. V. *Appl. Organomet. Chem.* **2005**, 19, 356.
- (358) Holeček, J.; Nádvorník, M.; Handlír, K.; Lyčka, A. *J. Organomet. Chem.* **1983**, 241, 177.
- (359) Holeček, J.; Nádvorník, M.; Handlír, K.; Lyčka, A. *J. Organomet. Chem.* **1983**, 258, 147.
- (360) Gielen, M.; Joosen, T.; Mancilla, T.; Jurkschat, K.; Willem, R.; Roobol, C.; Bernheim, J.; Atassi, G.; Huber, F.; Hoffman, E.; Preut, H.; Mahieu, B. *Main Group Met. Chem.* **1987**, 10, 147.
- (361) Atassi, G. *Rev. Sil. Ger. Tin Lead Comp.* **1985**, 8, 21.
- (362) Szorcsik, A.; Nagy, L.; Sletten, J.; Szalontai, G.; Kamu, E.; Fiore, T.; Pellerito, L.; Kálmán, E. *J. Organomet. Chem.* **2004**, 689, 1145.
- (363) Szorcsik, A.; Nagy, L.; Deák, A.; Scopelliti, M.; Fekete, Z. A.; Császár, Á.; Pellerito, C.; Pellerito, L. *J. Organomet. Chem.* **2004**, 17, 2762.
- (364) Szorcsik, A.; Nagy, L.; Scopelliti, M.; Deák, A.; Pellerito, L.; Hegetschweiler, K. *J. Organomet. Chem.* **2005**, 690, 2280.
- (365) Szorcsik, A.; Nagy, L.; Scopelliti, M.; Deák, A.; Pellerito, L.; Galbács, G.; Hered, M. *J. Organomet. Chem.* **2006**, 691, 1622.
- (366) Zoufalá, P.; Císařová, I.; Ružička, A.; Štěpnička, P. *Appl. Organomet. Chem.* **2005**, 19, 118.
- (367) Khan, M. I.; Baloch, M. K.; Ashfaq, M. *Appl. Organomet. Chem.* **2005**, 19, 132.
- (368) Szorcsik, A.; Nagy, L.; Pellerito, L.; Lampeka, R. D. J. *Radioanal. Nucl. Chem.* **2003**, 257, 285.
- (369) Jancsó, A.; Gajda, T.; Szorcsik, A.; Kiss, T.; Henry, B.; Vankó, Gy.; Rubini, P. *J. Inorg. Biochem.* **2001**, 83, 187.
- (370) Yin, H. D.; Hong, M. *Appl. Organomet. Chem.* **2005**, 19, 401.
- (371) Yin, H. D.; Xue, S.-C. *Appl. Organomet. Chem.* **2004**, 18, 496.
- (372) Yin, H. D.; Wang, C. H.; Ma, C. L. *Chin. J. Org. Chem.* **2004**, 24, 145.
- (373) Yin, H. D.; Wang, C.-H.; Hong, M.; Wang, D.-Q. *J. Organomet. Chem.* **2004**, 689, 1277.
- (374) Yin, H. D.; Wang, Q. B. *Appl. Organomet. Chem.* **2004**, 18, 493.
- (375) Dakternieks, D.; Basu Baul, T. S.; Dutta, S.; Tiekink, E. R. T. *Organometallics* **1998**, 17, 3058.
- (376) Ma, C.; Sun, J. *Appl. Organomet. Chem.* **2004**, 18, 418.
- (377) Yin, H.-D.; Xue, S.-C. *Appl. Organomet. Chem.* **2004**, 18, 415.
- (378) Yin, H. D.; Wang, C.-H. *Appl. Organomet. Chem.* **2004**, 18, 411.
- (379) Yin, H. D.; Wang, C.-H. *Appl. Organomet. Chem.* **2004**, 18, 409.
- (380) Zhong, G.-Y.; Song, H.-B.; Sun, L.-J.; Xie, Q.-L. *Appl. Organomet. Chem.* **2005**, 19, 388.
- (381) Tian, L.; Shang, Z.; Yu, Q.; Zhang, L. *Appl. Organomet. Chem.* **2005**, 19, 179.
- (382) Jung, Q. S.; Jeong, J. H.; Sohn, Y. S. *Polyhedron* **1989**, 8, 1413.
- (383) Krishnamoorthy, B. S.; Chandrasekar, S.; Arunkumar, P.; Panchanatheswaran, K. *Appl. Organomet. Chem.* **2005**, 19, 186.
- (384) Yin, H. D.; Xue, S. C. *Appl. Organomet. Chem.* **2005**, 19, 187.
- (385) Yin, H. D.; Wang, C. H.; Ma, C. L.; Whang, Y.; Zhang, R. F. *Chin. J. Org. Chem.* **2002**, 22, 183.
- (386) Yin, H. D.; Wang, C. H. Y.; Whang, Y.; Zhang, R. F.; Ma, C. L. *Chin. J. Inorg. Chem.* **2002**, 18, 201.
- (387) Yin, H. D.; Xue, S.-C. *Appl. Organomet. Chem.* **2005**, 19, 193.
- (388) Yin, H. D.; Xue, S.-C. *Appl. Organomet. Chem.* **2005**, 19, 194.
- (389) Tian, L.; Zhang, L.; Liu, X.; Zhou, Z. *Appl. Organomet. Chem.* **2005**, 19, 198.
- (390) Ali, S.; Ahmad, S. U.; Shahzadi, S.; Rehman, S.; Parvez, M.; Mazhar, M. *Appl. Organomet. Chem.* **2005**, 19, 200.
- (391) Ali, S.; Ahmad, S. U.; Shahzadi, S.; Rehman, S.; Parvez, M.; Mazhar, M. *Appl. Organomet. Chem.* **2005**, 19, 201.
- (392) Blunden, S. J.; Chapman, A. Organotin compounds, In: Craig, P. J. (Ed.), *Organometallic Compounds in the Environment*, Wiley, New York, **1986**.
- (393) Attar, K. *Appl. Organomet. Chem.* **1996**, 10, 317.
- (394) Vladimirov, Yu. A.; Archakov, A. I. *Lipid Peroxidation in Biological Membranes (in Russian)*, Nauka, Moscow, **1972**

- (395) Frankel, E. N. In: Simic, M.; Karel, M. (Eds.), *Autooxidation in Food and Biological Systems*, Plenum Press, New York, **1980**; p. 141.
- (396) Petrosyan, V. S.; Gracheva, Y. A.; Tyurin, V. Y.; Grigoriev, E. V.; Milaeva, E. R.; Pellerito, L. *J. Org. Chem.* **2003**, 39, 353.
- (397) Arakawa, Y. *Biomed. Res. Trace Elem.* **1995**, 6, 57.
- (398) Arakawa, Y. In: Kumar Das, V. G. (Ed.), *Main Group Elements and Their Compounds*, Narosa, New Delhi, **1996**; p. 422.
- (399) Barbieri, R.; Ruisi, G.; Silvestri, A.; Giuliani, A. M.; Barbieri, A.; Spina, G.; Pieralli, F.; Del Giallo, F. *J. Chem. Soc., Dalton Trans.* **1995**, 467.
- (400) Barbieri, R.; Silvestri, A.; Giuliani, A. M.; Piro, V.; Di Simone, F.; Madonia, G. *J. Chem. Soc., Dalton Trans.* **1992**, 585.
- (401) Feldman, R. G.; White, R. F.; Eriator, I. I. *Arch. Neurol.* **1993**, 50, 1320.
- (402) Fortemps, E.; Amand, G.; Bomboir, A.; Lauwerys, R.; Laterre, E. C. *Int. Arch. Occup. Environ. Health* **1978**, 41, 1.
- (403) Jiang, G. B.; Zhou, Q. F.; He, B. *Bull. Environ. Contam. Toxicol.* **2000**, 65, 277.
- (404) Jenkins, S. M.; Barone, S. *Toxicol. Lett.* **2004**, 147, 63.
- (405) Gibbs, P. E.; Bryan, G. W. In: Champ, M. A.; Seligman, P. F. (Eds.), *Organotin: Environmental Fate and Effects*, Chapman & Hall, London, **1996**; p. 259.
- (406) Shim, W. J.; Kahng, S. H.; Hong, S. H.; Kim, N. S.; Kim, S. K.; Shim, J. H. *Mar. Environ. Res.* **2000**, 49, 435.
- (407) Gibbs, P. E.; Bryan, G. W. *J. Mar. Biol. Assoc. UK* **1986**, 66, 767.
- (408) Gibbs, P. E.; Bryan, G. W.; Pascoe, P. L.; Burt, G. R. *J. Mar. Biol. Assoc. UK* **1990**, 70, 639.
- (409) Cadee, G. C.; Boon, J. P.; Fisher, C. V.; Mensink, B. F.; Ten Hallers-Tjabbes, C. C. *Neth. J. Sea Res.* **1995**, 34, 337.
- (410) Bech, M.; Strand, J.; Jacobsen, J. A. *Environ. Pollut.* **2002**, 119, 253.
- (411) Bettin, C.; Oehlmann, J.; Stroben, E. *Helgol. Mar. Res.* **1997**, 50, 299.
- (412) Osada, S.; Nishikawa, J.; Nakanishi, T.; Tanaka, K.; Nishihara, T. *Toxicol. Lett.* **2005**, 155, 329.
- (413) Patricolo, E.; Mansueto, C.; D'Agati, P.; Pellerito, L. *Appl. Organomet. Chem.* **2001**, 15, 916.
- (414) Benya, T. *J. Drug Metab. Rev.* **1997**, 29, 1189 and references therein.
- (415) May, L.; Eng, G.; Coddington, S. P.; Stockton, L. L. *Hyperfine Interact.* **1988**, 42, 909.
- (416) James, B. D.; Gioskos, S.; Chandra, S.; Magee, R. J.; Cashion, J. D. *J. Organomet. Chem.* **1992**, 436, 155.
- (417) James, B. D.; Magee, R. J.; Patalinghug, W. C.; Skelton, B. W.; White, A. H. *J. Organomet. Chem.* **1994**, 467, 51.
- (418) Eng, G.; Whalen, D.; Zhang, Y. Z.; Kirksey, A.; Otieno, M.; Khoo, L. E.; James, B. D. *Appl. Organomet. Chem.* **1996**, 10, 501.
- (419) Eng, G.; Whalen, D.; Musingarimi, P.; Tierney, J.; DeRosa, M. *Appl. Organomet. Chem.* **1998**, 12, 25.
- (420) Tierney, J. *J. Heterocycl. Chem.* **1989**, 26, 997.
- (421) Eng, G.; Whalen, D.; Zhang, Y. Z.; Tierney, J.; Jiang, X.; May, L. *Appl. Organomet. Chem.* **1996**, 10, 495.
- (422) Eales, J. G. *Proc. Soc. Exp. Biol. Med.* **1997**, 214, 302.
- (423) His, E.; Robert, R. *Rev. Trav. Inst. Peches Marit.* **1985**, 45, 117.
- (424) Lapota, D.; Rosemberg, D. E.; Platter-Rieger, M. F.; Seligman, P. F. *Mar. Biol.* **1993**, 115, 413.
- (425) Laughlin, R. B. Jr.; Gustafson, R.; Pendoley, P. *Bull. Environ. Contam. Toxicol.* **1989**, 42, 352.
- (426) Dimitriou, P.; Castritsi-Catharios, J.; Miliou, H. *Ecotox. Environ. Safe.* **2003**, 54, 30.
- (427) Sousa, A.; Mendo, S.; Barroso, C. *Appl. Organomet. Chem.* **2005**, 19, 315.
- (428) Leung, K. M. Y.; Morley, N. J.; Grist, E. P. M.; Morritt, D.; Crane, M. *Mar. Environ. Res.* **2004**, 58, 157.
- (429) Goldberg, R. N.; Averbuj, A.; Clédon, M.; Luzzatto, D.; Sbarbati, N. *Appl. Organometal. Chem.* **2004**, 18, 117.
- (430) Reader, S.; Steen, H. B.; Denizeau, F. *Arch. Biochem. Biophys.* **1994**, 312, 407.
- (431) Snoeji, N. J.; Penninks, A. H.; Seinen, W. *Environ. Res.* **1987**, 44, 335.
- (432) Mičić, M.; Bihari, N.; Labura, Z.; Müller, W. E. G.; Batel, R. *Aquat. Toxicol.* **2001**, 55, 61.
- (433) Mičić, M.; Bihari, N.; Jakšić, Ž.; Müller, W. E. G.; Batel, R. *Mar. Environ. Res.* **2002**, 53, 243.
- (434) Batel, R.; Bihari, N.; Rinkevich, B.; Dapper, J.; Schäcke, H.; Schröeder, H. C.; Müller, W. E. G. *Mar. Ecol. Prog.* **1993**, 93, 245.

- (435) Grondin, M.; Marion, M.; Denizeau, F.; Averill-Bates, D. A. *Toxicol. Appl. Pharmacol.* **2007**, 222, 57.
- (436) Nakatsu, Y.; Kotake, Y.; Ohta, S. *Neurotoxicology* **2006**, 27, 587.
- (437) Kawanishi, T.; Kiuchi, T.; Asoh, H.; Shibayama, R.; Kawai, H.; Ohata, H.; Momose, K.; Hayakawa, T. *Biochem. Pharmacol.* **2001**, 62, 863.
- (438) Kawanishi, T.; Asoh, H.; Kato, T.; Uneyama, C.; Toyoda, K.; Teshima, R.; Ikebuchi, H.; Ohata, H.; Momose, K.; Hayakawa, T.; Takahashi, M. *Toxicol. Appl. Pharmacol.* **1999**, 155, 54.
- (439) Orrenius, S.; Zhivotovsky, B.; Nicotera, P. *Nat. Rev., Mol. Cell Biol.* **2003**, 4, 552.
- (440) Chow, S. C.; Kass, G. E. N.; McCabe, M. J. Jr.; Orrenius, S. *Arch. Biochem. Biophys.* **1992**, 298, 143.
- (441) Imreh, G.; Beckman, M.; Iverfeldt, K.; Halleberg, E. *Exp. Cell Res.* **1998**, 238, 371.
- (442) You, R.; Mandlekar, S.; Harvey, K. J.; Ucker, D. S.; Kong, A. N. T. *Cancer Res.* **1998**, 58, 402.
- (443) Bygrave, F. L.; Smith, R. L. *Biochem. J.* **1978**, 174, 1075.
- (444) Raffray, M.; Cohen, G. M. *Arch. Toxicol.* **1993**, 67, 231.
- (445) Raffray, M.; McCarthy, D.; Snowden, R. T.; Cohen, G. M. *Toxicol. Appl. Pharm.* **1993**, 119, 122.
- (446) Zucker, R. M.; Elstein, K. H.; Thomas, D. J.; Rogers, J. M. *Toxicol. Appl. Pharm.* **1994**, 127, 163.
- (447) Viviani, B.; Rossi, A. D.; Chow, S. C.; Nicotera, P. *Neurotoxicology* **1995**, 16, 19.
- (448) Marinovich, M.; Viviani, B.; Corsini, E.; Ghilardi, F.; Galli, C. L. *Exp. Cell Res.* **1996**, 226, 98.
- (449) Cima, F.; Dominici, D.; Mammi, S.; Ballarin, L. *Appl. Organometal. Chem.* **2002**, 16, 182.
- (450) Kerr, J. F. R.; Harmon, B. V. *Apoptosis: The Molecular Basis of Cell Death*. Current Communication in Cell and Molecular Biology, Cold Spring Harbor Laboratory Press, New York, **1991**; Vol. 3.
- (451) Roccheri, M. C.; Tipa, C.; Bonaventura, R.; Matranga, V. *Int. J. Dev. Biol.* **2002**, 46, 801.
- (452) Siebenlist, K. R.; Taketa, F. *Biochem. J.* **1986**, 233, 471.
- (453) Nishikimi, A.; Kira, Y.; Kasahara, E.; Sato, E. F.; Kanno, T.; Utsumi, K.; Inoue, M. *Biochem. J.* **2001**, 356, 621.
- (454) Patanow, C. M.; Day, J. R.; Billingsley, M. L. *Neuroscience* **1997**, 76, 187.
- (455) Buck-Koehntop, B. A.; Porcelli, F.; Lewin, J. L.; Cramer, C. J.; Veglia, G. J. *Organomet. Chem.* **2006**, 691, 1748 and references therein.
- (456) Aschner, M.; Aschner, J. L. *Neurosci. Biobehav. Rev.* **1992**, 16, 427.
- (457) Brock, T. O.; O'Callaghan, J. P. J. *Neurosci.* **1987**, 7, 931.
- (458) Viviani, B.; Corsini, E.; Galli, C. L.; Marinovich, M. *Toxicol. Appl. Pharmacol.* **1998**, 150, 271.
- (459) Eskes, C.; Honegger, P.; Jones-Lepp, T.; Varner, K.; Matthieu, J. M.; Monnet-Tschudi, F. *Toxicol. In Vitro* **1999**, 13, 555.
- (460) Nakata, M.; Oyama, Y.; Okada, Y.; Yamazaki, Y.; Chikahisa, L.; Satoh, M. *Environ. Toxicol. Pharmacol.* **1999**, 7, 267.
- (461) Chikahisa, L.; Oyama, Y. *Pharmacol. Toxicol.* **1992**, 71, 190.
- (462) Chikahisa, L.; Oyama, Y.; Okazaki, E.; Noda, K. *Jpn. J. Pharmacol.* **1996**, 71, 299.
- (463) Okada, Y.; Oyama, Y.; Chikahisa, L.; Satoh, M.; Kanemaru, K.; Sakai, H.; Noda, K. *Toxicol. Lett.* **2000**, 117, 123.
- (464) Cima, F.; Ballarin, L.; Bressa, G.; Martinucci, G.; Burighel, P. *Ecotox. Environ. Safe.* **1996**, 35, 174.
- (465) Tosteson, M. T.; Wieth, J. O. J. *Gen. Physiol.* **1979**, 73, 789.
- (466) Kleszczyńska, H.; Hładyszowski, J.; Puchnik, H.; Przestalski, S. Z. *Naturforsch. C* **1997**, 52, 65.
- (467) Kang, J. J.; Liu, S. H.; Chen, I. L.; Cheng, Y. W.; Lin-Shiau, S. Y. *Pharmacol. Toxicol.* **1998**, 82, 23.
- (468) Iwai, H.; Kurosawa, M.; Matsui, H.; Wada, O. *Ind. Health* **1992**, 30, 77.
- (469) Zarzueta, C.; Reyes-Vivas, H.; Bravo, C.; Pichardo, J.; Corona, N.; Chavez, E. J. *Bioenerg. Biomembr.* **1994**, 26, 457.
- (470) Matsuno-Yagi, A.; Hatefi, Y. J. *Biol. Chem.* **1993**, 268, 6168.
- (471) Celis, H.; Escobedo, S.; Romero, I. *Arch. Biochem. Biophys.* **1998**, 358, 157.
- (472) Pavlakovic, G.; Kane, M. D.; Eyer, C. L.; Kanthasamy, A.; Isom, G. E. J. *Neurochem.* **1995**, 65, 2338.
- (473) Kafer, A.; Krug, H. F. *Environ. Health Perspect.* **1994**, 102, 325.
- (474) Ambrosini, A.; Bertoli, E.; Tanfani, F.; Zolese, Z. *Chem. Phys. Lipids* **1991**, 59, 189.
- (475) Gabrielska, J.; Sarapuk, J.; Przestalski, S. Z. *Naturforsch. C* **1997**, 52, 209.
- (476) Sarapuk, J.; Kleszczyńska, H.; Przestalski, S. *Appl. Organomet. Chem.* **2000**, 14, 40.
- (477) Chicano, J. J.; Ortiz, A.; Teruel, J. A.; Aranda, F. J. *BBA - Biomembranes* **2001**, 1510, 330.
- (478) Chicano, J. J.; Ortiz, A.; Teruel, J. A.; Aranda, F. J. *BBA - Biomembranes* **2002**, 1558, 70.

- (479) Teruel, J. A.; Ortiz, A.; Aranda, F. J. *Appl. Organomet. Chem.* **2004**, *18*, 111.
- (480) Jensen, K. G.; Onfelt, A.; Wallin, M.; Lidums, V.; Andersen, O. *Mutagenesis* **1991**, *6*, 409.
- (481) Bragadin, M.; Marton, D. J. *Inorg. Biochem.* **1997**, *68*, 75.
- (482) Marin, M. G.; Moschino, V.; Cima, F.; Celli, C. *Mar. Environ. Res.* **2000**, *50*, 231.
- (483) Dolcemasclo, G.; Gianguzza, P.; Pellerito, C.; Pellerito, L.; Gianguzza, M. *Appl. Organomet. Chem.* **2005**, *19*, 11.
- (484) Mansueto, C.; Pellerito, L.; Girasolo, M. A. *Acta Embryol. Morphol. Exp.* **1989**, *10*, 237.
- (485) Cima, F.; Ballarin, L.; Bressa, G.; Burighel, P. *Ecotox. Environ. Safe.* **1998**, *40*, 160.
- (486) Vitturi, R.; Zava, B.; Colomba, M. S.; Pellerito, A.; Maggio, F.; Pellerito, L. *Appl. Organomet. Chem.* **1995**, *9*, 561 and references therein.
- (487) Puccia, E.; Messina, C. M.; Cangialosi, M. V.; D'Agati, P.; Mansueto, C.; Pellerito, C.; Nagy, L.; Mansueto, V.; Scopelliti, M.; Fiore, T.; Pellerito, L. *Appl. Organomet. Chem.* **2005**, *19*, 23.
- (488) Mansueto, C.; Villa, L.; D'Agati, P.; Marcianò, V.; Pellerito, C.; Fiore, T.; Scopelliti, M.; Nagy, L.; Pellerito, L. *Appl. Organomet. Chem.* **2003**, *17*, 553.
- (489) Marinovich, M.; Viviani, B.; Galli, C. L. *Toxicol. Lett.* **1990**, *52*, 311.
- (490) Corsini, E.; Viviani, B.; Marinovich, M.; Galli, C. L. *Toxicol. In Vitro* **1998**, *12*, 551.
- (491) Villa, L.; Patricolo, E. Follicle cells of *Styela plicata* eggs (Ascidacea), In: Sawada, H.; Yokosawa, H.; Lambert, C. C. (Eds.), *The Biology of Ascidians*, Springer-Verlag, Tokyo, **2001**.
- (492) Villa, L.; D'Agati, P.; Mansueto, C.; Pellerito, C.; Scopelliti, M.; Fiore, T.; Nagy, L.; Pellerito, L. *Appl. Organomet. Chem.* **2003**, *17*, 106.
- (493) Villa, L.; Patricolo, E. *Anim. Biol.* **1993**, *2*, 175.
- (494) Rosati, F.; De Santis, R. *Exp. Cell Res.* **1978**, *112*, 111.
- (495) Haiduc, I.; Silvestru, C.; Gielen, M. *Bull. Soc. Chim. Belg.* **1982**, *91*, 187.
- (496) Gielen, M.; Jurkschat, K.; Atassi, G. *Bull. Soc. Chim. Belg.* **1984**, *93*, 153.
- (497) Zhang, Z.; Pan, H.; Hu, C.; Fu, F.; Sun, Y.; Willem, R.; Gielen, M. *Appl. Organomet. Chem.* **1991**, *5*, 183.
- (498) Silvestru, C.; Haiduc, I.; Tiekink, E. R. T.; de Vos, D.; Biesemans, M.; Willem, R.; Kovala-Demertzi, D.; Tauridou, P.; Russo, U.; Gielen, M. *Inorg. Chim. Acta.* **1995**, *239*, 177.
- (499) Gielen, M.; de Vos, D.; Meriem, A.; Bouâlam, M.; El Khoulfi, A.; Willem, R. *In Vivo* **1993**, *7*, 171.
- (500) Gielen, M.; Willem, R. *Anticancer Res.* **1992**, *12*, 269.
- (501) Gielen, M.; Willem, R. *Anticancer Res.* **1992**, *12*, 1323.
- (502) Gielen, M.; de Vos, D.; Pan, H.; Willem, R. *Main Group Met. Chem.* **1992**, *15*, 242.
- (503) Gielen, M.; Willem, R. In: Anastassopoulou, J.; Collery, P.; Etienne, J. C.; Theophanides, T. (Eds.), *Metal Ions in Biology and Medicine*, John Libbey Eurotext, Paris, **1992**; Vol. II, p. 186.
- (504) Gielen, M.; Willem, R. In: Anastassopoulou, J.; Collery, P.; Etienne, J. C.; Theophanides, T. (Eds.), *Metal Ions in Biology and Medicine*, John Libbey Eurotext, Paris, **1992**; Vol. II, p. 188.
- (505) Gielen, M.; Willem, R.; Bouâlam, M.; El Khoulfi, A.; de Vos, D. In: Anastassopoulou, J.; Collery, P.; Etienne, J. C.; Theophanides, T. (Eds.), *Metal Ions in Biology and Medicine*, John Libbey Eurotext, Paris, **1992**; Vol. II, p. 190.
- (506) Gielen, M. *Met. -Based Drugs* **1994**, *1*, 213.
- (507) Gielen, M. In: Anastassopoulou, J.; Collery, P.; Etienne, J. C.; Theophanides, T. (Eds.), *Metal Ions in Biology and Medicine*, John Libbey Eurotext, Paris, **1994**; Vol. III, p. 309.
- (508) Gielen, M.; Willem, R. *Main Group Met. Chem.* **1994**, *17*, 1.
- (509) Gielen, M.; Willem, R. In: Kumar Das, V. G. (Ed.), *Main Group Elements and Their Compounds: Perspectives in Materials Science, Chemistry and Biology*, Springer/Narosa, Berlin, **1996**; p. 446.
- (510) Gielen, M.; Willem, R. In: Hadjiliadis, N. D. (Ed.), *Cytotoxic, Mutagenic and Carcinogenic Potential of Heavy Metals Related to Human Environment*, NATO ASI Series 2: Environment, Kluwer Academic, Dordrecht, **1997**; Vol. 26, p. 445.
- (511) de Vos, D.; Gielen, M.; Willem, R.; van Wingerden, K. E.; Nooter, K. *Met. Based Drugs* **1998**, *5*, 179.
- (512) Gielen, M.; El Khoulfi, A.; Biesemans, M.; Mahieu, B.; Willem, R. *Bull. Soc. Chim. Belg.* **1992**, *101*, 243.
- (513) Bouâlam, M.; Willem, R.; Biesemans, M.; Gielen, M. *Appl. Organomet. Chem.* **1991**, *5*, 497.
- (514) Gielen, M.; De Clercq, L.; Willem, R.; Joosen, E. In: Zuckerman, J. J. (Ed.), *Tin and Malignant Cell Growth*, CRC Press, Boca Raton, **1988**; p. 39.

- (515) Gielen, M.; Biesemans, M.; Willem, R. *Appl. Organomet. Chem.* **2005**, *19*, 440.
- (516) Bloomfield V. A. *Curr. Opin. Struc. Biol.* **1996**, *6*, 334; *Biopolymers* **1997**, *44*, 282 and references therein.
- (517) Silvestri, A.; Ruisi, G.; Barbieri, R. *Hyperfine Interact.* **2000**, *126*, 43.
- (518) Narayan, V. L. In: Reinhardt, D. N.; Connors, T. A.; Pinedo, H. M.; Van De Poll, K. W. (Eds.), *Organotin Compound as Antitumor Agents: Structure Activity Relationship of Antitumor Agents (Developments in Pharmacology)*, Springer, Netherlands, **1982**; p. 273.
- (519) Crowe, A. J.; Smith, P. J.; Atassi, G. *Inorg. Chim. Acta* **1984**, *93*, 179.
- (520) Crowe, A. J.; Smith, P. J.; Cardin, C. J.; Parge, H. E.; Smith, F. E. *Cancer Lett.* **1984**, *24*, 45.
- (521) Kemmer, M.; Ghys, L.; Gielen, M.; Biesemans, M.; Tiekink, E. R. T.; Willem, R. J. *Organomet. Chem.* **1999**, *582*, 195.
- (522) Gielen, M.; Willem, R.; Biesemans, M.; Kemmer, M.; de Vos, D.; Pharmachemie B.V. World Patent Publication No. C07F 7/22, A61k 31/32, WO 00/06583, Application No. PCT/NL98/00429, 28/7/98, 10 February 2000.
- (523) Camacho, C. C.; de Dos, D.; Mahieu, B.; Gielen, M.; Kemmer, M.; Biesemans, M.; Willem, R. *Main Group Met. Chem.* **2000**, *23*, 433.
- (524) Ashfaq, M.; Khan, M. I.; Baloch, M. K.; Malik, A. J. *Organomet. Chem.* **2004**, *689*, 238.
- (525) Ashfaq, M. J. *Organomet. Chem.* **2006**, *691*, 2083.
- (526) Kemmer, M.; Dalil, H.; Biesemans, M.; Martins, J. C.; Mahieu, B.; Horn, E.; de Vos, D.; Tiekink, E. R. T.; Willem, R.; Gielen, M. J. *Organomet. Chem.* **2000**, *608*, 63.
- (527) Ashfaq, M.; Majeed, A.; Rauf, A.; Khanzada, A. W. K.; Shah, W. U.; Ansari, M. I. *Bull. Chem. Soc. Jpn.* **1999**, *72*, 2073.
- (528) Nath, M.; Yadav, R.; Eng, G.; Musingarimi, P. *Appl. Organomet. Chem.* **1999**, *13*, 29.
- (529) Pruchnik, F. P.; Bańbula, M.; Ciunik, Z.; Chojnacki, H.; Latocha, M.; Skop, B.; Wilczok, T.; Opolski, A.; Wietrzyk, J.; Nasulewicz, A. *Eur. J. Inorg. Chem.* **2002**, 3214.
- (530) Barbieri, R.; Pellerito, L.; Ruisi, G.; Lo Giudice, M. T.; Huber, F.; Attassi, G. *Inorg. Chim. Acta* **1982**, *66*, L39–L40.
- (531) Chaudhary, A.; Phor, A.; Gaur, S.; Singh, R. V. *Heterocycl. Commun.* **2004**, *10*, 181.
- (532) Ronconi, L.; Marzano, C.; Russo, U.; Sitran, S.; Graziani, R.; Fregona, D. *J. Inorg. Biochem.* **2002**, *91*, 413.
- (533) Han, G.; Yang, P. J. *Inorg. Biochem.* **2002**, *91*, 230.
- (534) Vitturi, R.; Pellerito, L.; Catalano, E.; Lo Conte, M. R. *Appl. Organomet. Chem.* **1993**, *7*, 295.
- (535) Mansueto, C.; Puccia, E.; Maggio, F.; Di Stefano, R.; Fiore, T.; Pellerito, C.; Triolo, F.; Pellerito, L. *Appl. Organomet. Chem.* **2000**, *14*, 229.
- (536) Triolo, F.; Pellerito, C.; Stocco, G. C.; Fiore, T.; Maggio, F.; Pellerito, L.; Triolo, R. *Appl. Organomet. Chem.* **1999**, *13*, 733.
- (537) Pellerito, C.; D'Agati, P.; Fiore, T.; Mansueto, C.; Mansueto, V.; Stocco, G.; Nagy, L.; Pellerito, L. *J. Inorg. Biochem.* **2005**, *99*, 1294.
- (538) Crowe, A. J. In: Gielen, M. (Ed.), *Metal-Based Antitumor Drugs*, Freund, London, **1989**; p. 103.
- (539) Eng, G.; Zhang, Y. Z.; Whalen, D.; Ramsammy, R.; Khoo, L. E.; DeRosa, M. *Appl. Organomet. Chem.* **1994**, *8*, 445.
- (540) Caruso, F.; Giomini, M.; Giuliani, A. M.; Rivarola, E. J. *Organomet. Chem.* **1996**, *506*, 67.
- (541) Fiore, T.; Pellerito, C.; Fontana, A.; Triolo, F.; Maggio, F.; Pellerito, L.; Cestelli, A.; Di Liegro, I. *Appl. Organomet. Chem.* **1999**, *13*, 705.
- (542) Nath, M.; Jairath, R.; Eng, G.; Song, X.; Kumar, A. *Spectrochim. Acta A* **2005**, *61*, 77.
- (543) Ascher, K. R. S.; Nissim, S. *World Rev. Pest Control* **1964**, *3*, 188.
- (544) Davies, A. G.; Smith, P. J. In: Wilkinson, G.; Stone, F. G. A.; Abel, E. W. (Eds.), *Comprehensive Organometallic Chemistry*, Pergamon, New York, **1982**; Vol. 2, p. 519.
- (545) Eng, G.; Song, X.; Duong, Q.; Strickman, D.; Glass, J.; May, L. *Appl. Organomet. Chem.* **2003**, *17*, 218.
- (546) Bacchi, A.; Carcelli, M.; Pelegatti, P.; Pelizzi, G.; Rodriguez-Arguelles, M. C.; Rogolino, D.; Solinas, C.; Zani, F. J. *Inorg. Biochem.* **2005**, *99*, 397.
- (547) Novák, P.; Lycka, A.; Císanova, I.; Buchta, V.; Silva, L.; Kolárová, L.; Růžicka, A.; Holecce, J. *Appl. Organomet. Chem.* **2005**, *19*, 500.

- (548) Gielen, M.; Lelieveld, P.; de Vos, D.; Pan, H.; Willem, R.; Biesemans, M.; Fiebig, H. H. *Inorg. Chim. Acta* **1992**, 196, 115.
- (549) Shahzadi, S.; Bhatti, M. H.; Shahid, K.; Ali, S.; Tariq, S. R.; Mazhar, M.; Khan, K. M. *Monatsh. Chem.* **2002**, 133, 1089.
- (550) Neuman, M. *Vademecum Degli Antibiotici ed Agenti Chemioterapici Anti-Infettivi*, Editrice Sigma Tau, Roma, **1994**; 5th ed., p. 133.
- (551) Neal, M. J. *Medical Pharmacology at a Glance*, Blackwell, Oxford, **1991**; 2nd ed., Chapter 36, p. 78.
- (552) Di Stefano, R.; Scopelliti, M.; Pellerito, C.; Casella, G.; Fiore, T.; Stocco, G. C.; Vitturi, R.; Colomba, M.; Ronconi, L.; Sciacca, I. D.; Pellerito, L. *J. Inorg. Biochem.* **2004**, 98, 534.
- (553) Di Stefano, R.; Scopelliti, M.; Pellerito, C.; Fiore, T.; Vitturi, R.; Colomba, M. S.; Gianguzza, P.; Stocco, G. C.; Consiglio, M.; Pellerito, L. *J. Inorg. Biochem.* **2002**, 89, 279.
- (554) Nacsá, J.; Nagy, L.; Sharples, D.; Hevér, A.; Szabó, D.; Ocsóvszki, I.; Varga, A.; König, S.; Molnár, J. *Anticancer Res.* **1998**, 18, 1373.
- (555) Arakawa, Y.; Wada, O. *Igaku no Ayumi* **1986**, 136, 177.
- (556) Arakawa, Y.; Wada, O. *Biochem. Biophys. Res. Commun.* **1984**, 125, 59.
- (557) Saxena, A. K.; Koacher, J. K.; Tandon, J. P.; Das, S. R. *J. Toxicol. Environ. Health* **1982**, 10, 709.
- (558) Peters, W.; Trotter, E. R.; Robinson, B. L. *Ann. Trop. Med. Parasitol.* **1980**, 74, 321.
- (559) Sardana, M. K.; Kappas, A. *Proc. Nat. Acad. Sc. U. S. A.* **1987**, 84, 2464.
- (560) Kappas, A.; Drummond, G. S.; Manola, T.; Petmezaki, S.; Valaes, T. *Pediatrics* **1988**, 81, 485.
- (561) Emtestam, L.; Angelin, B.; Berglund, L.; Drummond, G. S.; Kappas, A. *Acta Derm-Venerol.* **1993**, 73, 26.
- (562) Cornelius, C. E.; Rodgers, P. A. *Pediat. Res.* **1984**, 18, 728.
- (563) Kappas, A.; Drummond, G. S. *BioEssay* **1985**, 3, 256.
- (564) Kappas, A.; Drummond, G. S.; Simionatto, C. S.; Anderson, K. E. *Hepatology* **1984**, 4, 336.
- (565) Berglund, L.; Angelin, B.; Blomstrand, R.; Drummond, G.; Kappas, A. *Hepatology* **1988**, 8, 625.
- (566) Gielen, M. In: Cardinelli, N. F. (Ed.), *Tin as a Vital Nutrient*, CRC Press, Boca Raton, **1985**.
- (567) Szejtli, J. *Cyclodextrins and Their Inclusion Complexes*, Akadémiai Kiadó, Budapest, **1982**.
- (568) Balabaskaran, S.; Tilakavati, K.; Kumar Das, V. G. *Appl. Organomet. Chem.* **1987**, 1, 347.
- (569) van der Kerk, G. J. M.; Luijten, J. G. A. *J. Appl. Chem.* **1954**, 4, 314.
- (570) van der Kerk, G. J. M.; Luijten, J. G. A. *J. Appl. Chem.* **1954**, 6, 56.

SUBJECT INDEX

- A. fasciatus*, 359
A. malaca, 423, 428
A. physodes, 359, 425
 Acyl radical
 cyclization, 141, 156
 methods of generation, 141, 153, 172
 with tris(trimethylsilyl)silane, 118, 120
 ALD processes, 196, 339–342
 Alkaloid, 143, 149, 156
 Alkoxylamine, 151
 Alkyl radical
 cyclization, 156
 disproportionation, 149
 fluorinated derivative, 118
 primary, 118, 120, 124, 125, 146
 secondary, 118–120, 165
 tertiary, 118
 with poly(phenylhydrosilane) 162
 with silicon hydride, 118
 with silicon surface, 172
 with stable nitroxide radical, 151
 with styrene chromium tricarbonyl, 148
 with silyloxy enamine, 150
 with thiols, 136
 Alkylation
 alkene, 138, 151
 carboxylic imide, 151
 ketone, 150
 Aluminum *tris*(2,6-diphenyl phenoxide)
 (ATPH) 140
 Amino acids, 365–368
 Amidodiarsenes, 223
 Aminopyridinato complexes, 290, 296–297
 Aminyl radical, 120, 136, 137
 AMP, 384
 5'-AMP, 381, 384
 Anilinosilane, 136
Anilocra physodes, *see A. physodes*
 Antibiotics:
 β -lactamic, 385, 428–429
 Amoxicillin, 385, 405, 428
 Ampicillin, 385, 405, 428–429
 Methicillin, 385, 405
 Penicillin G, 385, 405, 428

Aphanius fasciatus, *see A. fasciatus*
 Arene coordination, 195, 210, 244, 282, 317
Ascidia malaca, *see A. malaca*
 (\pm)-Aspidospermidine, 156
 ATP, 360, 384, 417–419, 422–423, 425
 Azabenzonorbornane, 154
 Azabenzonorbornanol, 154
 Azacycle, 154
 Azadirachtin, 139
 aldehydes, 132
 alkenes, 132
 alkyl bromides, 135
 alkynes, 132
 aromatic azides, 136
 aryldiazonium salt, 164
 bromide nucleoside, 126
 dithiane, 127
 dithiolane, 127
 isocyanides, 135
 ketones, 132
 organohalides, 132, 134, 136, 157
 oxathiolane, 127
 oxathiolanone, 127
 phenyl chalcogenides, 135
 phenylselenides, 135
 phosphine selenides, 130
 phosphine sulfides, 130
 radical chain reaction, 125
 thiazolidine derivative, 127
 thiocarbonyl derivative, 134
 4-tert-butyl-cyclohexanone, 132
 water-soluble azides, 136
 water-soluble organohalides, 136
 with silicon hydrides, 125
 xanthates, 135
 1,1'-Azobis(cyclohexane carbonitrile)
 (ACCN) 130
 Azobisisobutyronitrile (AIBN) 126–132, 134,
 135, 139, 142–158, 161

 β -nicotinamide-adenine-dinucleotide-
 phosphoric acid, *see* NADP
B. cereus, 427

- Bacillus cereus*, see *B. cereus*
Barton-McCombie reaction, 134, 154
Benzoyl peroxide, 134, 164
Bicine, 385
Bipyridine, 149
Bisallylamide, 143
Bissallylsulfonamide, 143
Bis(amidinato) complexes;
 aluminum, 206, 319, 324–335
 beryllium, 196–197
 calcium, 201
 chromium, 268–270, 340
 cobalt, 283, 339
 copper, 335–336, 338
 gallium, 209–211, 339
 germanium, 214–215, 217–221
 hafnium, 242
 iron, 275–278, 316, 339–340
 lanthanides, 227–228, 231, 317–319, 333–334
 lithium, 316–318, 325
 magnesium, 197–200
 manganese, 275, 339
 nickel, 287, 293–294, 333, 339
 niobium, 264–265
 osmium, 283
 palladium, 287
 ruthenium, 283
 silicon, 216–217
 tantalum, 264–268
 tin, 218–219, 221–223
 titanium, 242, 247–248, 317, 321–323
 uranium, 241–242
 vanadium, 261–263
 zirconium, 242, 317, 319, 323–324, 331–332
Bis(guanidinato) complexes
 aluminum, 204
 antimony, 225
 calcium, 201
 gallium, 204
 hafnium, 341
 iron, 277–278
 lanthanides, 228, 231–232
 nickel, 287
 niobium, 265–266
 palladium, 287–288
 tantalum, 265–266
 tin, 222
 titanium, 248–249, 319, 340
 zirconium, 243, 252, 319, 341
Bite angles of amidinate and guanidinate ligands, 187
BN₂C heterocycle, 202
Boraamidinate anions, 186
Bond dissociation enthalpy, Si-X, 121–122
Bond formation
 C-C bond, 148, 149, 156
 C-P bond, 152
 C-Se bond, 145
 C-Te bond, 145
 intermolecular, 148, 152
 intramolecular, see Cyclization
 Si-C bond, 164, 166, 172
 Si-Cl bond, 172
 Si-heteroatom, 164
Bromoadamantane, 136
Bromomethylsilyl acetal, 155
Bromopyridine, 149
N-Bromosuccinimide, 164
C. diphtheriae, 427
C. intestinalis, 417–418, 422, 426–427
Calorimetry, 37
Cancer cell lines
 EVSA-T, 367, 368, 424
 H226, 367, 368, 423
 IGROV, 368, 423
 M19, 367, 368, 423
 MCF-7, 367, 393, 403, 410, 423
 MEL A498, 367, 423
 WiDr, 367, 403, 404, 410, 423
Captopril, 386, 426
Carbene insertion reaction, 281–283
Carbocycle, 139
Carbohydrates, 369–380
Carbon nanotubes, 28
 cephalexin, 428–429
 cephalosporines:
 D-cycloserine, 406, 428–429
 chloramphenicol, 406, 428–429
Carbonylation, 153
Carboplatin, 395, 395
Carboxyarylation, 157
Cascade radical reaction, 146, 153, 156, 157
Catalysis, 206, 226, 328–338
 addition of terminal alkynes to carbodiimides, 337
 addition of terminal alkynes to internal alkynes, 338
 C=N metathesis of carbodiimides, 337–338
 cyclotrimerization of arylisocyanates, 337
 fixation of carbon dioxide, 336
 guanylation of amines, 336
 hydroamination/cyclization reactions, 336
 olefin polymerization, 206, 331–333
 polymerization of arylsilanes, 338
 polymerization of carbodiimides, 338

- polymerization of polar monomers, 333–336
- Sonogashira reaction, 337–338
- synthesis of arylisocyanates from nitroaromatics, 336
- Chain reaction, 124, 127, 129, 131, 133–135, 140, 143, 145, 160, 166, 169–171
- Chemical equilibrium, 121
- Chlorodiphenylphosphine, 152
- Chiral amidinate ligands, 292–296
- Ciona intestinalis*, see *C. intestinalis*
- Cisplatin, 367, 380–381, 385, 388, 392, 395, 396, 423–424
- 5'-CMP, 385
- Cobalt catalysis, 146
- Corynebacterium diphtheriae*, see *C. diphtheriae*
- Corey's lactone, 146
- Coupling reaction
 - alkyl bromides to pSi surface, 172
 - cross-coupling two radicals, 145
 - dehydrogenative coupling reaction, 159
 - macroradicals, 152
 - Pd-catalyzed, 131
 - Si-O coupling product, 171
 - three-component reaction, 153
- Cumylperoxyl radical with silicon hydrides, 120, 174
- Cyclic ether, 140
- Cyclization
 - acyl radical, 141, 156
 - alkoxyl radical, 140
 - alkyl radical, 136–138, 146, 148
 - aryl radical, 142, 164
 - 6-endo, 140
 - 5-exo, 140, 146, 147, 156–158
 - 6-exo, 140, 141, 146, 156
 - 7-exo, 156
 - ipso, 143
 - vinyl radical, 140
- Cyclohexadienyl radical, 135, 145, 149
- Cyclohexanone, 161
- Cyclonucleoside, 155
- Cyclooctatetraenyl complexes, 231
- DBT, 419
- 5'-dCMP, 385
- Decarbonylation, 128, 129
- Decarboxylation, 128
- Degradation
 - chain reaction, 160
 - oxidative, 161
 - polyolefins, 161
 - radical-based, 159
- Dehalogenation, 126, 134–136
- Dehydrogenative coupling of silanes, 159
- Dendrimers
 - formation of, 41–43, 62, 74
- Deoxygenation, 128, 130, 134–136, 154
- Desulfurization, 136
- DFT calculations
 - of POSS anions, 6
 - of T8H8, 18
 - of T8Ph8, 31
 - of T12 compounds, 102
- 5'-dGMP, 385
- Diacyl peroxide, 134, 164, 166
- Dialkylaminyl radical, 120
- Diastereoselection, 126, 139, 141, 142, 144, 146, 148, 155–157
- 1,2-Dichlorohexafluorocyclobutane, 134
- Dielectric films, 97
- Diethyl bromomalonate, 150
- Diels-Alder reaction, 146
- 2,6-Diisopropylphenyl substituents, 188, 194, 196, 200–201, 204, 213, 219, 225, 227–228, 232, 237, 242, 244, 259, 273, 309, 333, 336
- Diiminophosphinate anions, 186
- Diiminosulfinate anions, 186
- Dinitrogen complexes, 247–249, 258–259, 262
- Diphenyldisilane, 120
- Diquinane, 139
- 9,10-Disilaanthracene, 134
- Disilane, 120, 122, 148
- Dissociative return electron transfer (DRET) 120
- Di-tert-butyl peroxide, 131
- DNA, 354, 357–360, 380–385
- E. C. ETEC*, see *E. coli*
- E. coli*, 427
- Electroluminescence, 57
- Endohedral complexes
 - of T₈H₈, 29
 - of T₈Ph₈, 32
- Endothermic reaction, 125
- Enterotoxigenic *E. coli*, see *E. coli*
- Enthalpic effect, 118
- Enthalpy of formation
 - silyl radicals, 122
 - trimethylsilyl ion, 122
- Entropic effect, 118
- Epoxidation, 44, 62, 64
- EPR spectroscopy, 50, 121, 123, 159, 161
- Escherichia coli*, see *E. coli*
- ETEC, see *E. coli*
- Exothermic reaction, 174

- Ferrocene derivatives, 57, 62
Ferrocenyl substituents, 188, 189, 202, 275, 283–284, 294–296
5-fluorouracil, 396
Functionalized amidinate ligands, 299–307
Fused cyclic compound, 139, 142, 147, 148
- Germynes, 217–218
5'-GMP, 381, 384, 385
Group migration
 1,2-phenyl, 150
 1,2-silyl, 174
- Heck coupling, 48
Heterocycle
 nitrogen, 139
 oxygen, 139
1,3,4,6,7,8-Hexahydro-2H-pyrimido[1,2-a]pyrimidinato complexes;
 aluminum, 296
 boron, 296–297
 gold, 328
 molybdenum, 328
 niobium, 297–298
 ruthenium, 299
 silver, 328
 tantalum, 298
 titanium, 297
 tungsten, 328
 zinc, 299
N-Heterocyclic carbenes (NHC), 210, 272
Hexamethyldisilane, 122
Hindered amine light stabilizer (HALS) 162
HOMO, 164, 172
Homolytic substitution, 135, 137, 145, 149, 157, 161, 162, 164
Homolytic cleavage
 H-Si bond, 173
 N-O bond, 150
 Si-H bond, 122
 Si-Hg bond, 123
 Si-Si bond, 120
(±)-Horsfiline, 156
Hydrobromination, 44
Hydroformylation, 24, 41
Hydrogen peroxide, 131
Hydrogen-terminated silicon surface
 addition to acetylenes, 167
 addition to olefins, 167, 172
 organic modifications, 163, 176
 oxidation, 173, 174, 176
 structural properties, 163
 with aryldiazonium salt, 173
 with bromoalkanes, 172
 with oxygen, 173, 174, 176
 with water, 173
Hydrogenation, 43, 76, 100
Hydrosilylation
 aldehydes, 132, 171
 alkenes, 132, 137, 166
 alkynes, 131, 132, 166, 167
 C-C multiple bonds, 130
 C-heteroatom multiple bonds, 130
 cyclization combination, 147
 deprotection combination, 144
 diene, 147
 enantioselective, 137
 heteroatom-heteroatom bond, 130
 hydrophobic substrates, 132
 ketones, 132, 162, 171
 methylenelactone, 137
 modification of silicon surface, 167, 171
 olefins, 130, 132, 161, 162, 167, 176
 organohalides, 132
 poly(hydrosilane)s, 161
 thiocarbonyl derivatives, 132
 with thiols as catalyst, 137
Hydrolysis
 of alkoxysilanes, 5, 6, 8, 30, 36, 37, 72, 74, 76, 78, 95, 100
 of chlorosilanes, 5, 36, 37, 72, 83, 95, 100
 of POSS cages, 20
Hydrosilylation
 of T_8H_8 , 20, 22–24, 27
 of $T_8(CH=CH_2)_8$, 20, 48
 of $T_8(OSiMe_2H)_8$, 53, 55, 57
 of $T_8(OSiMe_2CH=CH_2)_8$, 62, 63
 of T_{10} compounds, 97, 99
- ICP-AES, 356, 371
ID₅₀, 367, 396, 403–404, 408
Imido complexes
 indium, 213
 molybdenum, 273
 tantalum, 264–265, 267, 298, 341
 titanium, 247, 249–252, 303, 337
 tungsten, 273–275
 vanadium, 263, 336
 zirconium, 337
5'-IMP, 385
Inelastic neutron scattering, 96
Intramolecular reaction, 133, 139–148, 141, 144, 145, 157, 174
Iodoalkenyl sulfone, 140
Iodoarylazide, 156

- IR spectroscopy
 binding sites of the ligands, 412–414
 FTIR, 172–173
 of T_8H_8 , 16, 17
 of $T_8(CH=CH_2)_8$, 37
 of $T_8(OH)_8$, 78
 of T_8Ph_8 , 31
 of T_{10} compounds, 96
 organotin(IV) derivatives, 365, 368, 380
 Sn compounds, 381, 390, 406
 triorganotin(IV) derivatives, 406
Isomerization cis/trans, 129–132, 140–142, 147, 148
- K. pneumoniae*, 427
Ketene acetal, 142
Klebsiella pneumoniae, see *K. pneumoniae*
(–)-Kumausallene, 141
- Lactam, 129, 142, 143, 149
Lactone, 137, 139, 146, 148
“Lantern”-type complexes, 187, 325–327
Laser flash photolysis, 130
 LD_{50} , 367
Leukemias
 L1210, 423
 P388, 423, 424
Lewis acid, 132, 140
Ligand exchange of guanidinate ligands, 205
Liquid crystal properties
 of T_8R_8 compounds, 24
LUMO, 164, 172
- MALDI-TOF spectrometry, 61, 103
Mesoporous polymers, 28
Metal amidinato complexes
 coordination modes, 186–187
 general synthetic routes, 185
Metal guanidinato complexes
 coordination modes, 186–187
 general synthetic routes, 185
Metallaphosphazenes, 186
Metalsilyl radicals, 123
Methotrexate, 367
2-Methoxypropene, 161
Methyl acrylate, 154
(+)-Methyl nonactate, 140
1-Methylene cyclohexane, 153, 161
Michael additions, 97
MOCVD processes, 196, 240, 339–342
Mono(amidinato) complexes
 alkali metals, 188–196
 aluminum, 206–207, 211, 305
 arsenic, 223–225
 boron, 201–202
 copper, 339, 341–342
 gallium, 207, 209–210
 germanium, 219–221
 gold, 288–289
 hafnium, 242, 244
 indium, 207, 210–211, 213
 iridium, 284
 iron, 277
 lanthanides, 229–231, 300–303, 305, 337
 lithium, 188–192, 196, 293, 299–302, 307, 325
 magnesium, 198–200, 305
 molybdenum, 271–272
 potassium, 192–194, 196
 rhenium, 275
 rhodium, 283–284, 294–296
 ruthenium, 278–283
 silicon, 216–217
 silver, 339
 sodium, 196
 tantalum, 263–264
 thallium, 210
 titanium, 244, 246–247, 249–253, 302–305
 tungsten, 271–273
 vanadium, 261, 305, 332–333
 zinc, 291
 zirconium, 244, 255–260, 292, 305, 331–332
Mono(guanidinato) complexes
 alkali metals, 189, 210
 aluminum, 204–205
 arsenic, 223–225
 gallium, 204
 germanium, 219–221
 hafnium, 259
 iridium, 285–287, 337
 lanthanides, 228–229, 234
 niobium, 264–266
 tantalum, 264–267
 tin, 222
 titanium, 340
 tungsten, 273–275
 zirconium, 243–244
Monte Carlo studies, 64
Montmorillonite clays
 modification of, 69
Mössbauer spectroscopy, 356, 362, 364, 367–372, 374, 377, 380–382, 384–385, 388, 390, 396, 402, 406–408, 410, 412–413
2,2-dibutyl-D-mannose-stannolane, 372
quick-frozen solutions, 369–370
 ^{119}Sn , 356, 364, 368, 371

- partial quadrupole splitting (pqs), 371, 374,
380–381, 384, 390, 410
triorganotin(IV)-amino acid compound,
365
Multiple extrusion, 162
- NADP, 384–385
Nanocomposite materials, 36, 53, 64, 67
Nanoparticles
 of Ag, 67
 of Au, 69, 70
Nanostructure, 171
Neophyl radical rearrangement, 154
Neutron diffraction studies, 17
Nitrogen-centered radical, 120
Nitroxide radicals, 123, 130, 151,
162, 171, 172
NMR
 ¹³C, 406–407
 amine group, 369
 carbohydrate-organotin(IV) complexes, 371
 saccharides, 369
 ¹H, 362, 363–364, 365, 368, 371, 377–378,
 384–385, 387, 392, 395, 406–408, 431
 organotin(IV)ⁿ⁺ complexes, 362–363, 384,
 385, 390
 ¹⁵N, 385–386
 ³¹P, 381, 384–385
 ¹¹⁹Sn, 356, 362, 364, 368, 371, 377–378,
 385–386, 405, 408, 410, 431
N,N'-Diarylformamidinate complexes,
 325–327
 alkali metals, 190–196
 alkaline earth metals, 201
 aluminum, 214
 bismuth, 226
 cadmium, 292
 chromium, 328
 cobalt, 328
 copper, 288
 gallium, 214
 gold, 328
 indium, 213–214
 iron, 328
 lanthanides, 227–228, 232–233
 molybdenum, 272, 328
 palladium, 328
 silver, 288
 titanium, 245
 vanadium, 328
 zinc, 289–290
N,N,N'-Tris(trimethylsilyl)benzamidine, 184
Nucleoside analogue, 126, 128, 144, 145, 155
Nucleic acids, 380–385
¹⁷O NMR chemical shifts, 49
Organic monolayer
 nanopatterning techniques, 172
 pattern by masking procedure, 168,
 169
 photopatterning procedure, 169
 synthesis, 163, 166, 167
Oxalamidinate complexes
 aluminum, 313
 lithium, 307
 lanthanides, 308–312
 nickel, 312–313
 palladium, 313–316
 tantalum, 312
 titanium, 312
 uranium, 308
 zirconium, 312
Oxidation
 one-electron, 123
 photochemical, 120, 173
 radical, 143
 Si-H bond, 173
 silane, 160, 174
 silicon surface, 173, 174, 175
 with hydrogen peroxide, 131
Oxidizability value, 159
Oxime ether, 141, 151
Oxygen-centered radical, 120
Oxygen heterocycle, 140
- P. aeruginosa*, 427
P. lividus, 359, 419, 421, 425
P. mirabilis, 427
P. vulgaris, 427
Paddlewheel-type complexes, 187,
325–327
Palladium catalysis, 131
Paracentrotus lividus, *see P. lividus*
Peptides, 365–368
Peroxyl radical, 174
Phenyl radical, 118
Phenylseleno derivatives, 148, 153, 155, 164,
173
Phenylseleno esters, 128, 141
Phosphaguanidinate complexes, 327
Phosphonation, 152
Phosphination, 152
Phosphine-borane complex, 130
Phosphine sulfide, 152
Photoacoustic calorimetry, 122
Photochemical reaction, 120, 123, 130, 140,
144, 166, 169, 173, 174
Photoelectron spectroscopy
 of T₈H₈, 19

- Photolysis
 dprotection of silyl groups, 132
 1,1-dilithiosilane, 123
 Hg-compounds, 123
 H-Si(111) surface, 173
 laser flash techniques, 130
 UV cleavage of Si-Si bond, 120
- Photoluminescence
 in T_6 compounds, 11
 in T_8H_8 , 19
 in $T_8(OSiMe_3)_8$, 50
 in $T_8(OSiMe_2R)_8$ derivatives, 57
 in T_8R_8 compounds, 74
 in T_{12} compounds, 102
- Photo-oxidation, 120, 173, 174
- Piperidine derivative, 142
- Polarity-reversal catalysis, 125, 136
- Polydispersity index, 152
- Poly(hydrosilane)s, 158–162, 174
- Polymerization, 120, 151, 161, 165
- Poly(phenylsilane)s
 dehalogenation reactions, 134
 oxidation, 160
 oxidized products, 159
 stabilize polypropylene, 162
- Polysilanes, 120, 158–162
- Polysilylene, *see* Polysilane
- Polyurethanes
 hybrids with POSS compounds, 55
- Porphyrine-supported hafnium guanidinate, 259
- Porphyrynes
 protoporphyrin IX, 406, 425, 430
 m-tetra(4-carboxyphenyl)porphine (H_6TPPC), 406, 425–426
 m-tetra(4-sulfonatophenyl)porphine (H_6TPPS), 406
- Propagation step, 124, 133, 138, 160, 162
- Proteus mirabilis*, *see* *P. mirabilis*
- Pseudomonas aeruginosa*, *see* *P. aeruginosa*
- Pseudomonas vulgaris*, *see* *P. vulgaris*
- Pyrazolato complexes, 268–269
- Pyridinium replacement, 129
- Pyrolysis, 122
- Pyrrolidine derivative, 141
- Pyrroline derivative, 142
- Quantum dot materials, 33
- R. rubilio*, 359
- Radical initiators, 126, 130, 132, 134–136, 141, 143, 145, 147, 149, 150, 151, 157, 159, 160, 161, 164, 165, 172
- Radical translocation, 150, 155, 165, 166, 168, 169, 174
- Raman spectroscopy
 of POSS anions, 50
 of T_8H_8 , 17
 of T_8Ph_8 , 31
 of T_{10} compounds, 96
- Rate constant, 118–121, 124, 125, 130, 133, 154, 161, 174
- Rearomatization, 143, 145, 149
- Reducing agents, 118, 120, 124, 125, 134–136, 140, 142, 161, 176
- Reduction
 aldehydes, 132
 alkenes, 132
 alkyl bromides, 135
 alkynes, 132
 aromatic azides, 136
 aryldiazonium salt, 164
 bromide nucleoside, 126
 dithiane, 127
 dithiolane, 127
 isocyanides, 135
 ketones, 132
 organohalides, 132, 134, 136, 157
 oxathiolane, 127
 oxathiolanone, 127
 phenyl chalcogenides, 135
 phenylselenides, 135
 phosphine selenides, 130
 phosphine sulfides, 130
 radical chain reaction, 125
 thiazolidine derivative, 127
 thiocarbonyl derivative, 134
 4-*tert*-butyl-cyclohexanone, 132
 water-soluble azides, 136
 water-soluble organohalides, 136
 with silicon hydrides, 125
 xanthates, 135
- Ring-closure metathesis, 143
- Ring contraction, 143
- Ring formation reaction
 aromatic ring, 143
 four-membered ring, 172
 five-membered ring, 139, 171
 six-membered ring, 142, 171
 eight-membered ring, 171
- Ring-opening reaction, 171
- RNA, 360
- Rutilus rubilio*, *see* *R. rubilio*
- Ruthenium hydride complexes, 143
- S. aureus*, 428
- S. boydii*, 428

- S. plicata*, 422–423
S. pyogenes, 428
S. typhi, 428
Salmonella typhi, see *S. typhi*
Salmonella typhimurium, see *S. typhi*
Scanning tunneling microscope (STM) 17,
165, 169, 171, 172, 174
Selenocarbonate, 127, 128
Selenophene, 145
Shigella boydii, see *S. boydii*
Silanols
 reactions of, 83, 84, 87
 synthesis of, 8, 12, 84
Silicon hydride
 alkyl derivative, 134
 as radical mediator, 148
 chloro derivative, 120
 phenyl derivative, 134
 reducing agent, 136, 140
 with alkoxyl radical, 146
 with polyfluorinated halocarbons, 134
 with primary alkyl radical, 125
 with radical, 118, 124
 with TEMPO, 130
 with thiyl radical, 125, 136
Silicon hydride/thiol couple
 absorption, 164
 alkanethiols, 136
 reactivities, 124
 role of thiol, 125, 137
 silane/thiol, 176
 triethylsilane/1-adamantanethiol, 125
Silicon-hydrogen bond
 bond dissociation enthalpy, 121–122, 167
 bond strength, 122
 oxidation, 173, 174
 substitution, 162
 surface bond, 163
 vicinal, 165
 with acyl radical, 120
 with alkoxyl radical, 119
 with aminyl radical, 120
 with carbon-centered radical, 119, 125,
 172
 with cumylperoxyl radical, 120, 174
 with phenoxyl radical, 120
 with phenyl radical, 119
Silicon-silicon bond
 bond dissociation enthalpy, 122
 cleavage in a concerted mechanism, 167
 homolytic cleavage, 120
 in disilanes, 120
 migration of oxygen, 174
 oxidation, 173
 oxygen insertion, 174
Silicon surface
 Br-Si(111) 164
 Cl-Si(111) 164
 H-Si(100)-2x1 163, 170, 172, 173
 H-Si(111) 118, 163–169, 173, 174
 oxidation, 173, 174
 pSi, 163, 172–173, 176
 pSi_{scr} 172–173
 R-Si(111) 164, 165
 with oxygen, 173
N-Silylaniline, 136
N-Silylarylaminy radical, 136
Silylated cyclohexadienes, 124, 135, 147
Silylation reactions
 of T₈(O[−])₈, 51
Silylative coupling reactions, 40
Silyldesulfonylation, 131
Silylene, 216–217
 dialkylsilylene, 121
 extrusion reaction, 120
 heterocyclic, 121
 stable, 121
 with free radicals, 121
 with nitroxides, 120
Silyl hydroperoxide, 159
Silylium ion, 123
Silyloxy enamine, 150
Silyloxyl radical, 174
Silylperoxyl radical, 133, 160, 172, 174
Silyl radical
 abstraction of hydrogen atom from
 polysilane, 159, 160
 addition of surface silyl radical to a C=C
 double bond, 169
 addition of alkyne to a surface silyl radical,
 166
 as mediator, 150
 cyclization, 159
 dioxirane-like pentacoordinated, 134
 enthalpy of formation, 122
 half-lives, 123
 metalsilyl radicals, 123
 methods of generation, 118, 120, 121, 126,
 145, 150, 158–161, 164, 165, 169, 174
 rearomatization, 135
 stable, 123
 structure, 122–123
 surface-isolated silyl radical on Si(111) 164,
 165
 trialkylsilyl radicals, 122, 134
 with alkene, 165, 172
 with carbon-centered radical, 138
 with halides, 135
 with lithium, 123
 with nitroxides, 120

- with oxygen, 133, 160, 174, 176
- with silanes, 158
- with silicon atom, 159
- with trimethylene sulfide, 171
- with unsaturated bonds, 138, 161
- SiNC inorganic heterocycles, 215
- ²⁹Si NMR chemical shifts
 - of alkenyl substituted POSS cages, 37, 39, 40
 - of alkyl substituted POSS cages, 21, 23, 42, 45, 66, 67, 71, 73, 75, 79–81, 85
 - of aryl substituted POSS cages, 33
 - of silicate anions, 6, 7
 - of Si-substituted POSS cages, 51, 75
 - solid state, 9, 31, 37, 49, 50
 - of T₆ compounds, 9, 11
 - of T₈H₈, 19
 - of T₈(OR)₈ compounds, 26, 52, 53, 54, 57–59, 63, 87
 - of T₁₂ compounds, 101
 - of T₁₄ compounds, 103
- Size exclusion chromatography, 16, 100
- Spirocyclohexadienone, 143
- Spirodihydroquinolone, 143
- Spirooxindole, 143
- Staphylococcus aureus*, see *S. aureus*
- Stereoselection, 126, 131, 138, 139, 142, 144, 145, 147, 156
- Steric cyclopentadienyl equivalents, 188, 242
- Steric effect, 120, 149
- Streptococcus pyogenes*, see *S. pyogenes*
- Styela plicata*, see *S. plicata*
- Sugar derivative, 128, 147, 148, 155
- Sulfido complexes, 222, 247, 337
- Sulfur-centered radical, 169
- Sultam, 143
- Tandem cyclization, 153, 156
- Tantalum η^2 -ketenimine complex, 267
- Tantalum methyldiene complex, 267
- TBT, 416–423, 425
- TBTCl, 420–421, 422–423
- TBTO, 380
- T₂ compounds
 - calculations on, 4–5
- T₄ compounds
 - Calculations, 7
 - Physical properties, 6–7
 - Structural properties, 6–7
 - Synthesis of, 5–6
- T₆ compounds
 - calculations, 9, 11
 - physical properties, 9–11
 - reactions and applications, 11–13
 - structural properties,
 - calculated, 9
 - experimental, 9
 - synthesis of, 7–9,
- T₈ compounds
 - calculations,
 - T₈H₈, 17, 18, 29
 - T₈R₈ compounds, 72
 - physical properties, 16–19, 37, 65
 - reactions and applications, 19–29, 37–48, 66–72, 77, 82
 - structural properties,
 - calculated, 18, 48
 - experimental, 16, 18, 52, 61, 65
 - synthesis of, 15–16, 22–26, 30, 48–49, 52, 61–64, 75, 79–81, 85, 86, 87
- T₁₀ compounds
 - calculations, 96, 97
 - physical properties, 95–97
 - reactions and applications, 97–99
 - structural properties,
 - calculated, 96, 97
 - experimental, 96, 97
 - synthesis of, 92–95
- T₁₂ compounds
 - calculations, 102
 - physical properties, 101
 - reactions and applications, 7, 99–100
 - structural properties,
 - calculated, 99, 102
 - experimental, 99, 102
 - synthesis of, 99, 100
- T₁₄ compounds, 102–103
- T₁₆ compounds, 102–103
- Tellurophene, 145
- TEM, 359–360, 422–423
- Terphenyl substituents, 188, 198, 204, 229, 268, 275, 283, 287, 324
- Tert*-butoxyl radical, 120
- 4-*Tert*-butyl-cyclohexanone, 132
- Tert*-butyl perbenzoate, 134
- Tert*-dodecanethiol, 136
- TET, 419, 421
- Tetraphenylbiphosphine, 152
- 1,1,2,2-Tetraphenyldisilane, 148
- 1,1,2,2-Tetra-*tert*-butyl-1,2-diphenyldisilane 120
- Theoretical study
 - ab initio* calculation Si-H bond dissociation energy, 167
 - DFT metod, 121, 169, 171
 - Empirical calculation, 171

- radical translocation, 165
- reaction of silane with oxygen, 133
- Thermodynamic properties
 - of T_8H_8 , 19
 - of T_8Me_8 , 19
- Thermogravimetric analysis
 - of T_8H_8 , 29
- Thiocarbonate derivative, 128, 157
- Thioglucose tetraacetate, 137
- Thiol catalysis, 125, 136, 137
- Thiyl radical, 136
- Threshold photoelectron-photoion coincidence spectroscopy (TPEPICO)
 - 122
- Titanacarborane guanidinate complex,
 - 261
- Titration
 - pH-metric, 355, 362, 369–370, 384, 385–386
 - NMR, 369, 384
 - Mössbauer, 381
- Transition state, 120, 124, 171, 174
- Triazolato complexes, 268–269
- Trialkylsilane, 134
- Tributyltin hydride, 124, 142
- Tricine, 385
- Triethylborane, 126, 127, 129, 131, 135, 140, 141, 143, 144, 146, 147, 150, 151, 156
- Triethylsilane, 136
- Trimethylsilyl ion, 122
- Trimethylsilyl radical, 122
- Trimethyltin(IV) (TMT), 416, 419
- Triphenylmethyl ion, 123
- Triphenyltin (TPT), 416, 419
- Triphenyltin chloride (TPTCl), 420
- Triplet sensitizer tetrachlorophthalic anhydride (TCPA) 120
- Tris(amidinato) complexes
 - chromium, 268
 - cobalt, 283
 - indium, 212
 - iron, 278
 - lanthanides, 234–241, 335, 339–340
 - titanium, 339
 - uranium, 241
 - vanadium, 339
- Tris(guanidinato) complexes
 - aluminum, 204
 - gallium, 204
 - lanthanides, 234–237
- Tris(trimethylsilyl)silane
 - as mediator, 139, 141, 148, 155
 - oxidation, 155, 160, 174
 - reducing agent, 140, 142
- Si-H dissociation energy, 167
- with acyl chlorides, 128
- with acyl selenides, 149
- with aldehyde, 145
- with alkoxyl radical, 174
- with alkyl halide, 148, 152
- with alkyl radical, 118, 136, 146
- with aryl iodide, 150
- with alkyne, 131
- with azides, 142
- with bromo derivative, 155, 157
- with cumylperoxyl radical, 120, 174
- with dialkylaminyl radical, 120
- with halocarbonyl compound, 146
- with *N*-hydroxypyridine-2-thione esters, 128
- with nitroxide, 130
- with oxygen, 120, 176
- with phenoxyl radical, 120
- with phenylseleno derivative, 128, 148, 153, 155
- with phosphine sulfide, 130
- with phosphine selenide, 130
- with sulfone, 131
- with sulfonyl radical, 131
- with *tert*-butoxyl radical, 120
- with vinyl iodide, 145
- with water, 132
- Tris(trimethylsilyl)silyl radical
 - addition to alkene, 141
 - addition to alkyne, 141
 - addition to a thiocarbonyl function, 157
 - addition to azide, 136
- 2,4,6-Tri-*tert*-butylphenoxyl radical, 120
- Unimolecular reaction, 133, 134
- UV spectroscopy
 - of T_8H_8 , 19
 - of T_8Ph_8 , 31
- Valeraldehyde, 161
- (\pm)-Vindoline, 156
- Vinyl radical, 140, 166
- Vinyl sulfone, 131
- Volatility studies, 198–200, 209, 236–237, 340–342
- Water-soluble
 - aliphatic azides, 136
 - aromatic azides, 136
 - organohalides, 136
 - polysilanes, 161
- XAFS/EXAFS, 356–357

- Xanthate derivative, 154
Xerogels, 25
X-ray crystal structures
 of T_6 compounds, 9, 11
 of T_8 compounds, 17, 31, 32, 36, 37, 38, 49, 52, 53, 61, 62, 72, 88–92
 of T_{10} compounds, 96
 of T_{12} compounds, 102
 of T_{14} compounds, 103
X-ray diffraction, 354, 356–357, 366, 368, 374, 377, 383, 387, 408, 410
X-ray photoelectron spectroscopy, 166
X-ray photoemission spectroscopy,
 of T_8H_8 , 17, 96
 of T_{10} compounds, 96
 of T_{12} compounds, 100
 of T_{14} compounds, 103
X-ray powder diffraction, 17, 65
Zeolite frameworks, 29, 103
Zirconacarboranes, 306
Zirconium diazametallacycles, 252–255
Zirconium η^2 -styrene complexes, 255
Zirconium trimethylenemethane complexes, 256–257

CUMULATIVE LIST OF CONTRIBUTORS FOR VOLUMES 1–36

- Abel, E. W., 5, 1; 8, 117
 Aguiló, A., 5, 321
 Akkerman, O. S., 32, 147
 Albano, V. G., 14, 285
 Alper, H., 19, 183
 Anderson, G. K., 20, 39; 35, 1
 Angelici, R. J., 27, 51
 Aradi, A. A., 30, 189
 Armitage, D. A., 5, 1
 Armor, J. N., 19, 1
 Ash, C. E., 27, 1
 Ashe, A. J., III, 30, 27
 Atwell, W. H., 4, 1
 Baines, K. M., 25, 1
 Barone, R., 26, 165
 Bassner, S. L., 28, 1
 Behrens, H., 18, 1
 Bennett, M. A., 4, 353
 Bickelhaupt, F., 32, 147
 Binningham, J., 2, 365
 Blinka, T. A., 23, 193
 Bockman, T. M., 33, 51
 Bogdanović, B., 17, 105
 Bottomley, F., 28, 339
 Bowser, J. R., 36, 57
 Bradley, J. S., 22, 1
 Brew, S. A., 35, 135
 Brinckman, F. E., 20, 313
 Brook, A. G., 7, 95; 25, 1
 Brown, H. C., 11, 1
 Brmon, T. L., 3, 365
 Bruce, M. I., 6, 273; 10, 273; 11, 447; 12, 379; 22, 59
 Brunner, H., 18, 151
 Buhro, W. E., 27, 311
 Byers, P. K., 34, 1
 Cais, M., 8, 211
 Calderon, N., 17, 449
 Callahan, K. P., 14, 145
 Canty, A. J., 34, 1
 Cartledge, F. K., 4, 1
 Chalk, A. J., 6, 119
 Chanon, M., 26, 165
 Chatt, J., 12, 1
 Chini, P., 14, 285
 Chisholm, M. H., 26, 97; 27, 311
 Chiusoli, G. P., 17, 195
 Chojinowski, J., 30, 243
 Churchill, M. R., 5, 93
 Coates, G. E., 9, 195
 Collman, J. P., 7, 53
 Compton, N. A., 31, 91
 Connelly, N. G., 23, 1; 24, 87
 Connolly, J. W., 19, 123
 Corey, J. Y., 13, 139
 Corriu, R. J. P., 20, 265
 Courtney, A., 16, 241
 Coutts, R. S. P., 9, 135
 Coville, N. J., 36, 95
 Coyle, T. D., 10, 237
 Crabtree, R. H., 28, 299
 Craig, P. J., 11, 331
 Csuk, R., 28, 85
 Cullen, W. R., 4, 145
 Cundy, C. S., 11, 253
 Curtis, M. D., 19, 213
 Darensbourg, D. J., 21, 113; 22, 129
 Darensbourg, M. Y., 27, 1
 Davies, S. G., 30, 1
 Deacon, G. B., 25, 337
 de Boer, E., 2, 115
 Deeming, A. J., 26, 1
 Dessy, R. E., 4, 267
 Dickson, R. S., 12, 323
 Dixneuf, P. H., 29, 163
 Eisch, J. J., 16, 67
 Ellis, J. E., 31, 1
 Emerson, G. F., 1, 1
 Epstein, P. S., 19, 213
 Erker, G., 24, 1
 Ernst, C. R., 10, 79
 Errington, R. J., 31, 91
 Evans, J., 16, 319
 Evan, W. J., 24, 131
 Faller, J. W., 16, 211

- Farrugia, L. J., **31**, 301
 Faulks, S. J., **25**, 237
 Fehlner, T. P., **21**, 57; **30**, 189
 Fessenden, J. S., **18**, 275
 Fessenden, R. J., **18**, 275
 Fischer, E. O., **14**, 1
 Ford, P. C., **28**, 139
 Furniés, J., **28**, 219
 Forster, D., **17**, 255
 Fraser, P. J., **12**, 323
 Friedrich, H., **36**, 229
 Friedrich, H. B., **33**, 235
 Fritz, H. P., **1**, 239
 Fürstner, A., **28**, 85
 Furukawa, J., **12**, 83
 Fuson, R. C., **1**, 221
 Gallop, M. A., **25**, 121
 Garrou, P. E., **23**, 95
 Geiger, W. E., **23**, 1; **24**, 87
 Geoffroy, G. L., **18**, 207; **24**, 249; **28**, 1
 Gilman, H., **1**, 89; **4**, 1; **7**, 1
 Glădfelter, W. L., **18**, 207; **24**, 41
 Gladysz, J. A., **20**, 1
 Glänzer, B. I., **28**, 85
 Green, M. L. H., **2**, 325
 Grey, R. S., **33**, 125
 Griffith, W. P., **7**, 211
 Grovenstein, E., Jr., **16**, 167
 Gubin, S. P., **10**, 347
 Guerin, C., **20**, 265
 Gysling, H., **9**, 361
 Haiduc, I., **15**, 113
 Halasa, A. F., **18**, 55
 Hamilton, D. G., **28**, 299
 Handwerker, H., **36**, 229
 Harrod, J. F., **6**, 119
 Hart, W. P., **21**, 1
 Hartley, F. H., **15**, 189
 Hawthorne, M. R., **14**, 145
 Heck, R. F., **4**, 243
 Heimbach, P., **8**, 29
 Helmer, B. J., **23**, 193
 Henry, P. M., **13**, 363
 Heppert, J. A., **26**, 97
 Herberich, G. E., **25**, 199
 Herrmann, W. A., **20**, 159
 Hieber, W., **8**, 1
 Hill, A. F., **36**, 131
 Hill, E. A., **16**, 131
 Hoff, C., **19**, 123
 Hoffmeister, H., **32**, 227
 Holzmeier, P., **34**, 67
 Honeyman, R. T., **34**, 1
 Horwitz, C. P., **23**, 219
 Hosmane, N. S., **30**, 99
 Housecroft, C. E., **21**, 57; **33**, 1
 Huang, Y. Z., **20**, 115
 Hughes, R. P., **31**, 183
 Ibers, J. A., **14**, 33
 Ishikawa, M., **19**, 51
 Ittel, S. D., **14**, 33
 Jain, L., **27**, 113
 Jain, V. K., **27**, 113
 James, B. R., **17**, 319
 Janiak, C., **33**, 291
 Jastrzebski, J. T. B. H., **35**, 241
 Jenck, J., **32**, 121
 Jolly, P. W., **8**, 29; **19**, 257
 Jonas, K., **19**, 97
 Jones, M. D., **27**, 279
 Jones, P. R., **15**, 273
 Jordan, R. F., **32**, 325
 Jukes, A. E., **12**, 215
 Jutzi, P., **26**, 217
 Kaesz, H. D., **3**, 1
 Kalck, P., **32**, 121; **34**, 219
 Kaminsky, W., **18**, 99
 Katz, T. J., **16**, 283
 Kawabata, N., **12**, 83
 Kemmitt, R. D. W., **27**, 279
 Kettle, S. F. A., **10**, 199
 Kilner, M., **10**, 115
 Kim, H. P., **27**, 51
 King, R. B., **2**, 157
 Kingston, B. M., **11**, 253
 Kisch, H., **34**, 67
 Kitching, W., **4**, 267
 Kochi, J. K., **33**, 51
 Köster, R., **2**, 257
 Kreiter, C. G., **26**, 297
 Krüger, G., **24**, 1
 Kudaroski, R. A., **22**, 129
 Kühlein, K., **7**, 241
 Kuivila, H. G., **1**, 47
 Kumada, M., **6**, 19; **19**, 51
 Lappert, M. F., **5**, 225; **9**, 397; **11**, 253; **14**, 345
 Lawrence, J. P., **17**, 449
 Le Bozec, H., **29**, 163
 Lendor, P. W., **14**, 345
 Linford, L., **32**, 1
 Longoni, G., **14**, 285
 Luijten, J. G. A., **3**, 397
 Lukehart, C. M., **25**, 45
 Lupin, M. S., **8**, 211
 McGlinchey, M. J., **34**, 285
 McKillop, A., **11**, 147
 McNally, J. P., **30**, 1
 Macomber, D. W., **21**, 1; **25**, 317
 Maddox, M. L., **3**, 1
 Maguire, J. A., **30**, 99

- Maitlis, P. M., **4**, 95
 Mann, B. E., **12**, 135; **28**, 397
 Manuel, T. A., **3**, 181
 Markies, P. R., **32**, 147
 Mason, R., **5**, 93
 Masters, C., **17**, 61
 Matsumura, Y., **14**, 187
 Mayr, A., **32**, 227
 Meister, G., **35**, 41
 Mingos, D. M. P., **15**, 1
 Mochel, V. D., **18**, 55
 Moedritzer, K., **6**, 171
 Molloy, K. C., **33**, 171
 Monteil, F., **34**, 219
 Morgan, G. L., **9**, 195
 Morrison, J. A., **35**, 211
 Moss, J. R., **33**, 235
 Mrowca, J. J., **7**, 157
 Müller, G., **24**, 1
 Mynott, R., **19**, 257
 Nagy, P. L. I., **2**, 325
 Nakamura, A., **14**, 245
 Nesmeyanov, A. N., **10**, 1
 Neumann, W. P., **7**, 241
 Norman, N. C., **31**, 91
 Ofstead, E. A., **17**, 449
 Ohst, H., **25**, 199
 Okawara, R., **5**, 137; **14**, 187
 Oliver, J. P., **8**, 167; **15**, 235; **16**, 111
 Onak, T., **3**, 263
 Oosthuizen, H. E., **22**, 209
 Otsuka, S., **14**, 245
 Pain, G. N., **25**, 237
 Parshall, G. W., **7**, 157
 Paul, I., **10**, 199
 Peres, Y., **32**, 121
 Petrosyan, W. S., **14**, 63
 Pettit, R., **1**, 1
 Pez, G. P., **19**, 1
 Poland, J. S., **9**, 397
 Poliakov, M., **25**, 277
 Popa, V., **15**, 113
 Pourrean, D. B., **24**, 249
 Powell, P., **26**, 125
 Pratt, J. M., **11**, 331
 Prokai, B., **5**, 225
 Pruett, R. L., **17**, 1
 Rao, G. S., **27**, 113
 Raubenheimer, H. G., **32**, 1
 Rausch, M. D., **21**, 1; **25**, 317
 Reetz, M. T., **16**, 33
 Reutov, O. A., **14**, 63
 Rijkens, F., **3**, 397
 Ritter, J. J., **10**, 237
 Rochow, E. G., **9**, 1
 Rokicki, A., **28**, 139
 Roper, W. R., **7**, 53; **25**, 121
 Roundhill, D. M., **13**, 273
 Rubezhok, A. Z., **10**, 347
 Salerno, G., **17**, 195
 Salter, I. D., **29**, 249
 Satgé, J., **21**, 241
 Schade, C., **27**, 169
 Schaverien, C. J., **36**, 283
 Schmidbaur, H., **9**, 259; **14**, 205
 Schrauzer, G. N., **2**, 1
 Schubert, U., **30**, 151
 Schultz, D. N., **18**, 55
 Schurnann, H., **33**, 291
 Schwebke, G. L., **1**, 89
 Seppelt, K., **34**, 207
 Setzer, W. N., **24**, 353
 Seyferth, D., **14**, 97
 Shapakin, S. Yu., **34**, 149
 Shen, Y. C., **20**, 115
 Shriver, D. F., **23**, 219
 Siebert, W., **18**, 301; **35**, 187
 Sikora, D. J., **25**, 317
 Silverthorn, W. E., **13**, 47
 Singleton, E., **22**, 209
 Sinn, H., **18**, 99
 Skinner, H. A., **2**, 49
 Slocum, D. W., **10**, 79
 Smallridge, A. J., **30**, 1
 Smeets, W. J. J., **32**, 147
 Smith, J. D., **13**, 453
 Speier, J. L., **17**, 407
 Spek, A. L., **32**, 147
 Stafford, S. L., **3**, 1
 Stańczyk, W., **30**, 243
 Stone, F. G. A., **1**, 143; **31**, 53; **35**, 135
 Su, A. C. L., **17**, 269
 Suslick, K. M., **25**, 73
 Süß-Fink, G., **35**, 41
 Sutin, L., **28**, 339
 Swincer, A. G., **22**, 59
 Tamao, K., **6**, 19
 Tate, D. P., **18**, 55
 Taylor, E. C., **11**, 147
 Templeton, J. L., **29**, 1
 Thayer, J. S., **5**, 169; **13**, 1; **20**, 313
 Theodosiou, I., **26**, 165
 Timms, P. L., **15**, 53
 Todd, L. J., **8**, 87
 Touchard, D., **29**, 163
 Traven, V. F., **34**, 149
 Treichel, P. M., **1**, 143; **11**, 21
 Tsuji, J., **17**, 141
 Tsutsui, M., **9**, 361; **16**, 241

- Turney, T. W., **15**, 53
Tyfield, S. P., **8**, 117
Usón, R., **28**, 219
Vahrenkamp, H., **22**, 169
van der Kerk, G. J. M., **3**, 397
van Koten, G., **21**, 151; **35**, 241
Veith, M., **31**, 269
Vezey, P. N., **15**, 189
von Ragué Schleyer, P., **24**, 353;
 27, 169
Vrieze, K., **21**, 151
Wada, M., **5**, 137
Walton, D. R. M., **13**, 453
Wailles, P. C., **9**, 135
Webster, D. E., **15**, 147
Weitz, E., **25**, 277
West, R., **5**, 169; **16**, 1; **23**, 193
Werner, H., **19**, 155
White, D., **36**, 95
Wiberg, N., **23**, 131; **24**, 179
Wiles, D. R., **11**, 207
Wilke, G., **8**, 29
Williams, R. E., **36**, 1
Winter, M. J., **29**, 101
Wojcicki, A., **11**, 87; **12**, 31
Yamamoto, A., **34**, 111
Yashina, N. S., **14**, 63
Ziegler, K., **6**, 1
Zuckerman, J. J., **9**, 21
Zybill, C., **36**, 229

CUMULATIVE INDEX FOR VOLUMES 37–57

	VOL.	PAGE
Abu Ali, Hijazi, <i>see</i> Dembitsky, Valery M		
Adams, Joanne R., <i>Transition Metal Complexes of Tethered Arenes</i>	54	293
Allan J. Canty, Thomas Rodemann, and John H. Ryan, <i>Transition Metal Organometallic Synthesis Utilising Diorganoiodine(III) Reagents</i>	55	279
Al-Ahmad, Saleem, <i>see</i> Ashe, Arthur J., III		
Andersen, Jo-Ann M., and Moss, John R., <i>Alkyl (pentacarbonyl) Compounds of the Manganese Group Revisited</i>	37	169
Aroop K. Roy, <i>A Review of Recent Progress in Catalyzed Homogeneous Hydrosilation (Hydrosilylation)</i>	55	1
Ashe, Arthur J., III, and Al-Ahmad, Saleem, <i>Diheteroferrocenes and Related Derivatives of the Group 15 Elements: Arsenic, Antimony, and Bismuth</i>	39	325
Aumann, Rudolf, <i>(1-Alkynyl)carbene Complexes (= 1-Metalla-1-buten-3-yne): Tools for Synthesis</i>	41	165
Baines, K. M., and Stibbs, W. G., <i>Stable Doubly Bonded Compounds of Germanium and Tin</i>	39	275
Baker, Paul K., <i>The Organometallic Chemistry of Halocarbonyl Complexes of Molybdenum (II) and Tungsten (II)</i>	40	45
Belzner, Johannes, and Ihmels, Heiko, <i>Silylenes Coordinated to Lewis Bases</i>	43	1
Bennett, Martin A., <i>see</i> Adams, Joanne R.	54	293
Berry, Donald H., <i>see</i> Reichl, Jennifer A.	43	197
Bertrand, Guy, <i>see</i> Bourissou, Didier		
Blom, Burgert, Clayton, Hadley, Kilkenny, Mairi, and Moss, John R., <i>Metallacycloalkanes - synthesis, structure and reactivity of medium to large ring compounds</i>	54	149
Bode, Katrin, and Klingebiel, Uwe, <i>Silylhydrazines; Lithium Derivatives, Isomerism, and Rings</i>	40	1
Bo-Hye Kim and Hee-Gweon Woo, <i>Dehydrocoupling, Redistribute Coupling, and Addition of Main Group 4 Hydrides</i>	52	143
Bok Ryul Yoo, <i>see</i> Il Nam Jung		
Bourissou, Didier, and Bertrand, Guy, <i>The Chemistry of Phosphinocarbenes</i>	44	175
Braunschweig, Holger, <i>Borylenes as Ligands to Transition Metals</i>	51	163
T. Brent Gunnoe, <i>see</i> Marty Lail		
Breunig Hans Joachim and Ghesner Ioan, <i>Coordination Compounds with Organoantimony and Sb_n Ligands</i>	49	95
Brook, Adrian, G., and Brook, Michael, A., <i>The Chemistry of Silenes</i>	39	71
Brook, Michael A., <i>see</i> Brook, Adrian G.		
Brothers, Penelope J., and Power, Philip P., <i>Multiple Bonding Involving Heavier Main Group 3 Elements Al, Ga, In, and Tl</i>	39	1
Brothers, Penelope J., <i>Organometallic Chemistry of Transition Metal Porphyrin Complexes</i>	46	223
Brothers, Penelope J., <i>Organoelement Chemistry of Main Group Porphyrin Complexes</i>	48	289

Bruce, Michael I., and Low, Paul J., <i>Transition Metal Complexes Containing All-Carbon Ligands</i>	50	179
Carty, Arthur J., <i>see</i> Doherty, Simon		
Chatgililoglu, Chrysostomos, and Newcomb, Martin, <i>Hydrogen Donor Abilities of the Group 14 Hyrides</i>	44	67
Chatgililoglu, Chrysostomos, and Timokhin, Vitality, <i>Silyl Radicals in Chemical Synthesis</i>	57	117
Clayton, Hadley, <i>see</i> Blom, Burgert	54	149
Corey, Joyce Y., <i>Dehydrocoupling of Hydrosilanes to Polysilanes and Silicon Oligomers: A 30 Year Overview</i>	51	1
Corrigan, John R, <i>see</i> Doherty, Simon		
Cumulative Subject Index for Volumes 1–44	45	1
Dembitsky, Valery M., Abu Ali, Hijazi, and Stebnik, Morris, <i>Recent Chemistry of the Diboron Compounds</i>	51	193
Doherty, Simon, Corrigan, John P., Carty, Arthur J., and Sappa, Enrico, <i>Homometallic and Heterometallic Transition Metal Allenyl Complexes: Synthesis, Structure, and Reactivity</i>	37	39
Driess, Matthias, <i>Silicon-Phosphorus and Silicon-Arsenic Multiple Bonds</i>	39	193
Dyson, Paul J., <i>Chemistry of Ruthenium–Carbide Clusters $Ru_5C(CO)_{15}$ and $Ru_6C(CO)_{17}$</i>	43	43
Edelmann, Frank T., <i>Advances in the Coordination Chemistry of Amidinate and Guanidinate Ligands</i>	57	183
Eduardo J. Fernández, Antonio Laguna, and M. Elena Olmos, <i>Recent Developments in Arylgold(I) Chemistry</i>	52	77
Eichler, Barrett, and West, Robert, <i>Chemistry of Group 14 Heteroallenes</i>	46	1
Eisch, John J., <i>Boron–Carbon Multiple Bonds</i>	39	355
Erker, Gerhard, Kehr, Gerald, and Fröhlich, Roland, <i>The (Butadiene) zirconocenes and Related Compounds</i>	51	109
Escudie, Jean, and Ranaivonjatovo, Henri, <i>Doubly Bonded Derivatives of Germanium</i>	44	113
Esteruelas, Miguel A. <i>The Chemical and Catalytic Reactions of Hydrido-chloro-carbonylbis (triisopropylphosphine) osmium and its Major Derivatives</i>	47	1
Eva Becker, Sonja Pavlik, and Karl Kirchner, <i>The Organometallic Chemistry of Group 8 Tris(pyrazolyl)borate Complexes</i>	56	155
F. Gordon A. Stone, <i>see</i> Thomas D. McGrath		
Fiore, Tiziana, <i>see</i> Nagy, László		
Fleig, Patrick R, <i>see</i> Wojtczak, William A.		
François P. Gabbai, <i>see</i> Mohand Melaimi		
Frank T. Edelmann, <i>see</i> Volker Lorenz		
Gable, Kevin P., <i>Rhenium and Technetium Oxo Complexes in the Study of Organic Oxidation Mechanisms</i>	41	127
Gauvin, François, Harrod, John F., and Woo, Hee Gweon, <i>Catalytic Dehydrocoupling: A General Strategy for the Formation of Element–Element Bonds</i>	42	363
Georgii I. Nikonov, <i>Recent Advances in Nonclassical Interligand $Si^{\cdots}H$ Interactions</i>	53	217
Gibson, Susan E., and Peplow, Mark A., <i>Transition Metal Complexes of Vinylketenes</i>	44	275
Gulliver T. Dalton, <i>see</i> Jospeh P. Morral		
Hampden-Smith, Mark J., <i>see</i> Wojtczak, William A.		
Hanusa, Timothy P., <i>see</i> Hays, Melanie L.		
Harrod, John K., <i>see</i> Gauvin, François		
Haubrich, Scott, Power, Philip, and Twamley, Brendan, <i>Element Derivatives of Sterically Encumbering Terphenyl Ligands</i>	44	1

Hays, Melanie L., and Hanusa, Timothy, P., <i>Substituent Effects as Probes of Structure and Bonding in Mononuclear Metallocenes</i>	40	117
Helmold, Nina, <i>see</i> Klingebiel, Uwe.	54	1
Hemme, Ina, <i>see</i> Klingebiel, Uwe		
Henderson, William, <i>The chemistry of cyclometallated gold(III) complexes with C,N donor ligands</i>	54	207
Hopkins, Michael D., <i>see</i> Manna, Joseph		
Humphrey, Mark G., <i>see</i> Whittall, Ian R.		
Humphrey, Mark G., <i>see</i> Waterman, Susan M.		
Herrmann, Wolfgang A., Weskamp, Thomas, and Böhm, Volker P. W., <i>Metal Complexes of Stable Carbenes</i>	48	1
Ian R. Crossley, <i>The Organometallic Chemistry of Group 9 Poly(pyrazolyl)borate Complexes</i>	56	199
Ihmels, Heiko, <i>see</i> Belzner, Johannes	43	1
Il Nam Jung and Bok Ryul Yoo, <i>Synthesis of Novel Silicon-Containing Compounds via Lewis Acid Catalyzed Reactions</i>	53	41
Iwamoto, Takeaki, <i>see</i> Kira, Mitsuo	54	73
Jafarpour, Laleh, and Nolan, Steven P., <i>Transition-Metal Systems Bearing a Nucleophilic Carbene Ancillary Ligand: from Thermochemistry to Catalysis</i>	46	181
Jean-Paul Picard, <i>Silylmethylamines and Their Derivatives: Chemistry and Biological Activities</i>	52	175
John, Kevin D., <i>see</i> Manna, Joseph		
John H. Ryan <i>see</i> Allan J. Canty		
Jones, William M., and Klosin, Jerzy, <i>Transition-Metal Complexes of Arynes, Strained Cyclic Alkynes, and Strained Cyclic Cumulenes</i>	42	147
Joseph P. Morrall, Gulliver T. Dalton, Mark G. Humphrey, and Marek Samoc, <i>Organotransition Metal Complexes for Nonlinear Optics</i>	55	61
Jung, IL Nam, <i>see</i> Yoo, Bok Ryul		
Jung, Il Nam, and Yoo, Bok Ryul, <i>Friedel-Crafts Alkylations with Silicon Compounds</i>	46	145
Karl A. Pittard, <i>see</i> Marty Lail		
Karl Kirchner, <i>see</i> Eva Becker		
Kalikhman, Inna, <i>see</i> Kost, Daniel		
Kawachi, Atsushi, <i>see</i> Tamao, Kohei		
Kehr, Gerald, <i>see</i> Erker, Gerhard		
Kilkenny, Mairi, <i>see</i> Blom, Burgert	54	149
Kira, Mitsuo, <i>Progress in the Chemistry of Stable Disilenes</i>	54	73
Klingebiel, Uwe, Helmold, Nina, and Schmatz, Stefan, <i>Intramolecular Interconversions in Cyclosilazane Chemistry: A Joint Experimental-Theoretical Study</i>	54	1
Klingebiel, Uwe, and Hemme, Ina, <i>Iminosilanes and Related Compounds: Synthesis and Reactions</i>	39	159
Klingebiel, Uwe, <i>see</i> Bode, Katrin		
Klosin, Jerzy, <i>see</i> Jones, William M.		
Kost, Daniel, and Kalikhman, Inna, <i>Hydrazide-Based Hypercoordinate Silicon Compounds</i>	50	1
Kühler Thorsten and Jutzi Peter, <i>Decamethylsilicocene: Synthesis, Structure, Bonding and Chemistry</i>	49	1
Kyushin Soichiro and Matsumoto Hideyuki, <i>Ladder Polysilanes</i>	49	133
Lickiss, Paul D., and Rataboul, Franck, <i>Fully Condensed Polyhedral Oligosilsesquioxanes (POSS): From Synthesis to Application</i>	57	1
Lorraine M. Caldwell, <i>Alkylidyne Complexes Ligated by Poly(pyrazolyl)borates</i>	56	1
Lothar Stahl, <i>Pentadienyl Complexes of the Group 4 Transition Metals</i>	55	137

Lotz, Simon, Van Rooyen, Pertrus H., and Meyer, Rita, <i>σ, π-Bridging Ligands in Bimetallic and Trimetallic Complexes</i>	37	219
Low, Paul J., <i>see</i> Bruce, Michael I.		
Low, Paul J., and Bruce, Michael I., <i>Transition Metal Chemistry of 1,3-Diynes, Polyynes, and Related Compounds</i>	48	71
Lucas, Nigel T., <i>see</i> Waterman, Susan M.		
Manna, Joseph, John, Kevin D., and Hopkins, Michael, D., <i>The Bonding of Metal-Alkynyl Complexes</i>	38	79
Manners, Ian, <i>Ring-Opening Polymerization of Metallocenophanes: A New Route to Transition Metal-Based Polymers</i>	37	131
Mark G. Humphrey, <i>see</i> Joseph P. Morrall		
Marek Samoc, <i>see</i> Joseph P. Morrall		
Marty Lail, Karl A. Pittard, and T. Brent Gunnoe, <i>Chemistry Surrounding Group 7 Complexes that Possess Poly(pyrazolyl)borate Ligands</i>	56	95
Mathur, Pradeep, <i>Chalcogen-Bridged Metal–Carbonyl Complexes</i>	41	243
McDonagh, Andrew M., <i>see</i> Whittall, Ian R.		
Meyer, Rita, <i>see</i> Lotz, Simon		
Mohand Melaimi and François P. Gabbaï, <i>Bidentate Group 13 Lewis Acids with ortho-Phenylene and peri-Naphthalenediyl Backbones</i>	53	61
Moss, John R., <i>see</i> Andersen, Jo-Ann M.		
Moss, John R., <i>see</i> Blom, Burgert	54	149
Nagy, Enikő <i>see</i> Nagy, László		
Nagy, László, Pellerito, Lorenzo, Fiore, Tiziana, Nagy, Enikő, Pellerito, Claudia, Szorcsik, Attila, and Scopelliti, Michelangeló, <i>Equilibrium, Structural and Biological Activity Studies on [Organotin(IV)]ⁿ⁺ Complexes</i> . . .	57	353
Nakazawa, Hiroshi, <i>Transition Metal Complexes Bearing a Phosphenium Ligand</i>	50	107
Newcomb, Martin, <i>see</i> Chatgililoglu, Chrysostomos		
Nienaber, Hubert, <i>see</i> Aumann, Rudolf		
Nolan, Steven P., <i>see</i> Jafarpour, Laleh		
Ogino, Hiroshi, and Tobita, Hiromi, <i>Bridged Silylene and Germylene Complexes</i>	42	223
Okazaki, Renji, and West, Robert, <i>Chemistry of Stable Disilenes</i>	39	231
Oro, Luis A. <i>see</i> Esteruelas, Miguel A.		
Peplow, Mark A., <i>see</i> Gibson, Susan E.		
Pellerito, Claudia <i>see</i> Nagy, László		
Pellerito, Lorenzo <i>see</i> Nagy, László		
Power, Philip P., <i>see</i> Brothers, Penelope J.		
Power, Philip P., <i>see</i> Brothers, Penelope J.		
Power, Philip, <i>see</i> Haubrich, Scott		
Pradeep Mathur, Saurav Chatterjee and Vidya D. Avasare, <i>Mixed Metal Acetylides Complexes</i>	55	201
Pülm, Melanie, <i>see</i> Tacke, Reinhold		
Ranaivonjatovo, Henri, <i>see</i> Escudie, Jean		
Rataboul, Franck, <i>see</i> Lickiss, Paul D		
Reichl, Jenifer A., and Berry, Donald H., <i>Recent Progress in Transition Metal-Catalyzed Reactions of Silicon, Germanium, and Tin</i>	43	197
Richard D. Ernst, <i>see</i> Lothar Stahl		
Roland, Fröhlich, <i>see</i> Gerhard, Erker		
Roth, Gerhard, <i>see</i> Fischer, Helmut	43	125
Roundhill, D. M., <i>Organotransition-Metal Chemistry and Homogeneous Catalysis in Aqueous Solution</i>	38	155
Sakurai, Hideki, <i>see</i> Sakiguchi, Akira		
Samoc, Marek, <i>see</i> Whittall, Ian R.		
Sappa, Enrico, <i>see</i> Doherty, Simon		
Saurav Chatterjee <i>see</i> Pradeep Mathur		

Schmatz, Stefan, <i>see</i> Klingebiel, Uwe	54	1
Scopelliti, Michelangelo, <i>see</i> Nagy, László		
Schulz Stephan, <i>Group 13/15 Organometallic Compounds-Synthesis, Structure, Reactivity and Potential Applications</i>	49	225
Sekiguchi, Akira, and Sakurai, Hideki, <i>Cage and Cluster Compounds of Silicon, Germanium, and Tin</i>	37	1
Sita, Lawrence R., <i>Structure/Property Relationships of Polystannanes</i>	38	189
Smith, David J., <i>Organometallic Compounds of the Heavier Alkali Metals</i>	43	267
Smith, Paul J., <i>see</i> Welton, Tom		
Sonja Pavlik, <i>see</i> Eva Becker		
Srebnik, Morris, <i>see</i> Dembitsky, Valery M.		
Stephan, Douglas W., <i>Sterically Demanding Phosphinimides: Ligands for Unique Main Group and Transition Metal Chemistry</i>	54	267
Stibbs, W. G., <i>see</i> Baines, K. M.		
Stumpf, Rüdiger, <i>see</i> Fisher, Helmut	43	125
Sun, Shouheng, and Swelgart, Dwight A., <i>Reactions of 17- and 19-Electron Organometallic Complexes</i>	40	171
Swelgart, Dwight A., <i>see</i> Sun, Shouheng		
Szorcsik, Attila, <i>see</i> Nagy, László		
Tacke, Reinhold, Pülm, Melanie, and Wagner, Brigitte, <i>Zwitterionic Penta-coordinate Silicon Compounds</i>	44	221
Tamao, Kohei, Kawachi, Atsushi, <i>Silyl Anions</i>	38	1
Thayer, John S., <i>Not for Synthesis Only: The Reactions of Organic Halides with Metal Surfaces</i>	38	59
Thomas D. McGrath and F. Gordon A. Stone, <i>Metal Complexes of Monocarbon Carboranes: A Neglected Area of Study?</i>	53	1
Thomas Müller, <i>Cations of Group 14 Organometallics</i>	53	155
Thomas Rodemann, <i>see</i> Allan J. Canty		
Timokhin, Vitality, <i>see</i> Chatgililoglu, Chrysostomos		
Tobisch Sven, <i>Structure-Reactivity Relationships in the Cyclo-Oligomerization of 1,3-Butadiene Catalyzed by Zerovalent Nickel Complexes</i>	49	168
Tobita, Hiromi, <i>see</i> Ogino, Hiroshi		
Twarnley, Brendan, <i>see</i> Haubrich, Scott		
Uhl, Werner, <i>Organoelement Compounds Possessing Al–Al, Ga–Ga, In–In, and Tl–Tl Single Bonds</i>	51	53
Van Rooyen, Petrus H., <i>see</i> Lotz, Simon		
Veith, Michael, <i>Molecular Alumo-Siloxanes and Base Adducts</i>	54	49
Vidya D. Avasare, <i>see</i> Pradeep Mathur		
Volker Lorenz and Frank T. Edelmann, <i>Metallasilsesquioxanes</i>	53	101
Wagner, Brigitte, <i>see</i> Tacke, Reinhold		
Warren E. Piers, <i>The Chemistry of Perfluoroaryl Boranes</i>	52	1
Waterman, Susan M., Lucas, Nigel T., and Humphrey, Mark G., <i>“Very-Mixed” Metal Carbonyl Clusters</i>	46	47
Weber, Lothar, <i>Transition-Metal Assisted Syntheses of Rings and Cages from Phosphaalkenes and Phosphaalkynes</i>	41	1
Welton, Tom, and Smith, Paid J., <i>Palladium Catalyzed Reactions in Ionic Liquids</i>	51	251
Went, Michael J., <i>Synthesis and Reactions of Polynuclear Cobalt-Alkyne Complexes</i>	41	69
West, Robert, <i>see</i> Eichler, Barrett		
West, Robert, <i>see</i> Okazaki, Renji		
Whitmire, Kenton H., <i>Main Group-Transition Metal Cluster Compounds of the group 15 Elements</i>	42	1
Whittall, Ian R., McDonagh, Andrew M., and Humphrey, Mark G., <i>Organometallic Complexes in Nonlinear Optics II: Third-Order Nonlinearities and Optical Limiting Studies</i>	43	349

Whittall, Ian, R., McDonagh, Andrew M., Humphrey, Mark G., and Samoc, Marek, <i>Organometallic Complexes in Nonlinear Optics I: Second-Order Nonlinearities</i>	42	291
Wojtczak, William A., Fleig, Patrick F., and Hampden-Smith, Mark J., <i>A Review of Group 2 (Ca, Sr, Ba) Metal-Organic Compounds as Precursors for Chemical Vapor Deposition</i>	40	215
Woo, Hee Gweon, <i>see</i> Gauvin François		
Yoo, Bok Ryul, <i>see</i> Jung, Il Nam		
Yoo, Bok Ryul, and Jung, Il Nam, <i>Synthesis of Organosilicon Compounds by New Direct Reactions</i>	50	145
Zemlyansky Nikolai N., Borisova, Irina V., and Ustynyuk, Yuri A., <i>Organometallic Phosphorous and Arsenic Betaines</i>	49	35